Executive summary of the "Towards quantum-secured wireless networks" project

Challenge

The dramatic progress of quantum computing capabilities poses a real threat to conventional RSA asymmetric encryption in communication. Quantum computers will be able to break encryption algorithms securing the transfer of data. Low-power devices, such as the Internet of Things that can be responsible for transferring sensitive information may lack the computational resources to maintain security against upcoming threats. Finding new ways to safeguarde information transferred over radio frequency (RF) and wireless networks in general is crucial.

Proposed Project

Within this project, we aim to build a quantum key distribution (QKD) system with auto-tracking capability. The QKD system will be used to secure indoor RF communication links established using universal software radio peripherals (USRPs). The system will use infrared sources (1370 nm) to limit the effect of artificial lighting and ambient sunlight. We will further explore incorporating the orbital angular momentum (OAM) degree of freedom of light to boost the QKD key transfer rate. Other methods to secure RF communication beyond using the shared keys will be explored. Theoretical physical layer security channel modeling will be conducted.

Intended Outcomes

There has been little work on indoor QKD and very little on integrating QKD to secure wireless communication. A successful first demonstration on the topic will lead to further studies that will involve securing THz and even free space optical communication signals. Our main initial focus is to use the QKD system indoors, but further experiments upon successful project completion will involve outdoor tests. We aim to openly share the system design and the generated data to serve as a starting point for other researchers in the field. Any theoretical codes and analysis will be shared with the public.

Towards quantum-secured wireless networks

1 Introduction

Typical wireless communications rely on classical cryptographic methods that are based on mathematical algorithms. With the advances in quantum computing capabilities, these methods will not be enough to ensure security. One potential idea to enhance the security of wireless communication technologies is using quantum key distribution (QKD).

QKD consists of exchanging encryption keys between two parties, commonly known as Alice and Bob. The security of QKD is based on the principles of quantum mechanics. In a typical QKD protocol, Alice prepares a stream of random quantum bits, known as qubits, and sends them to Bob over an unsecured communication channel. These qubits can be encoded using various photon properties, such as the polarization state. Alice and Bob then perform measurements on the received qubits to extract a shared secret key.

The security of QKD lies in the fact that any attempt to intercept or measure the qubits by an eavesdropper, often referred to as Eve, will necessarily disturb the quantum state of the qubits. This disturbance introduces errors in the transmission, which Alice and Bob can detect through error-checking techniques. By comparing a subset of their received bits, they can estimate the noise level or errors in the communication. If the error rate is below a certain threshold, Alice and Bob can proceed to extract a secure key from the remaining error-free bits. If the error rate exceeds the threshold, it indicates the presence of an eavesdropper, and Alice and Bob stop the key exchange.

QKD holds great potential for enhancing the security of wireless communication systems, particularly in scenarios where the long-term security of transmitted information is critical. QKD has been demonstrated over long distances using optical fibers [1]. There are also studies on short-range free space QKD between handheld devices [2, 3]. Earth-Satellite QKD demonstrations over distances beyond 1000 km have been reported [4, 5]. The field of satellite-based QKD is continuously growing [6, 7], and these research and development efforts aim to result in a global QKD network that may enhance the encryption of conventional near-Earth communication.

However, there has been little work on indoor wireless QKD and very little on integrating it with classical communication networks. Our objective is to define how QKD might be used with conventional wireless communication systems. The main focus of our work is to develop a QKD tool capable of securing a conventional wireless communication link. More specifically, we will implement the system to secure an indoor radio frequency (RF) communication link using a pair of universal software radio peripherals (USRPs). A basic concept illustration can be seen in Fig. 1. The transmitter and receiver will be built on two breadboards with tracking features for flexible mobility. The work will involve theoretical channel modeling of physical layer security (PLS) to determine the needed QKD key rate to secure a given RF link. Additionally, we will consider further system improvements by using spatially structured beams, including those carrying orbital angular momentum (OAM), to boost the key rate.

The project will run over two years and has two primary work packages (WP):

WP1: Build a mobile QKD setup with automatic tracking mechanism.

WP2: Test the setup to secure RF data transmissions indoors.

2 Project Objectives and Activities

A. Primary Objective: Building a mobile QKD Setup. Whether in a room or outdoors, a key challenge for QKD links is to mitigate the noise generated by light sources or ambient sunlight. The mobile setup will be built based on a previously developed QKD system at the University of

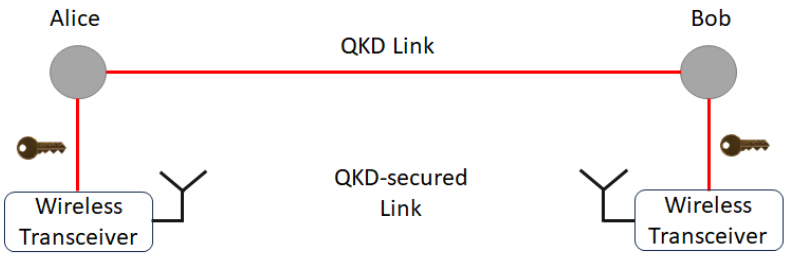

Figure 1: Illustration of a quantum-secured RF link.

Oxford [8]. This operates at a wavelength (1370 nm) outside the visible spectrum and where solar irradiance is at a minimum. The system is based on the BB84 protocol [9]. In this protocol, Alice sends qubits (a series of 0s and 1s) to Bob using polarization (Horizontal, Vertical, Diagonal, and Anti-diagonal) over an insecure channel. Bob randomly chooses a basis horizontal/vertical (H/V) or diagonal/anti-diagonal (D/A) to measure each qubit he receives.
Illustrations of the transmitter and receiver are shown in Fig. 2. The transmitter (Alice) comprises a control board connected to four 1370-nm lasers. A half-wave plate (HWP) and a polarizer are fixed after the output of each laser. When in operation, one of the four lasers sends a light pulse. The receiver (Bob) comprises a spectral filter centered at 1370 nm at the entrance to suppress the ambient light entering the receiver. A non-polarizing 50:50 beam splitter (BS) is used to facilitate Bob's choice of basis pair. One receiver branch consists of a polarizing beam splitter (PBS) to choose between a Horizontal and Vertical basis. The other branch comprises a half-wave plate and a PBS to select between a Diagonal and Anti-diagonal basis.

An automatic tracking mechanism will be used to ease the alignment between the transmitter and the receiver. This will be based on a previous tracking system implemented at Oxford [3]. A theoretical PLS modeling will be conducted to determine the key rate needed to secure a given system.

Within this objective, we will also explore the feasibility of installing an OAM-QKD link within the project time frame to support higher secure key rates. The OAM-QKD link will utilize electronically addressed spatial light modulators (SLMs) available in the host group's laboratory. If successfully built, it will be tested to secure RF communication links.

B. Secondary Objective: Secure wireless RF communication with QKD. The second objective is to use QKD to secure an RF communication link established with USRPs, which are software-defined radio platforms that enable rapid design, prototype, and deployment of wireless systems [10].

A series of experiments using the developed system will be conducted in a room under varying illumination levels and sunlight conditions. The QKD system will be initially used to supply the encryption keys to secure the RF communication. There will be other methods to secure the RF links that we will consider. For instance, it might be possible to harness the exchanged keys through QKD to control frequency hopping between many carrier frequencies to avoid interception in the RF link.

3 Project Impact

As wireless moves to 6G, security requirements are more stringent than previous generations [11]. Energy consumption is a challenge for advanced encryption, and QKD may offer cryptography. A successful demonstration would show that it is possible to use QKD to secure RF links indoors,

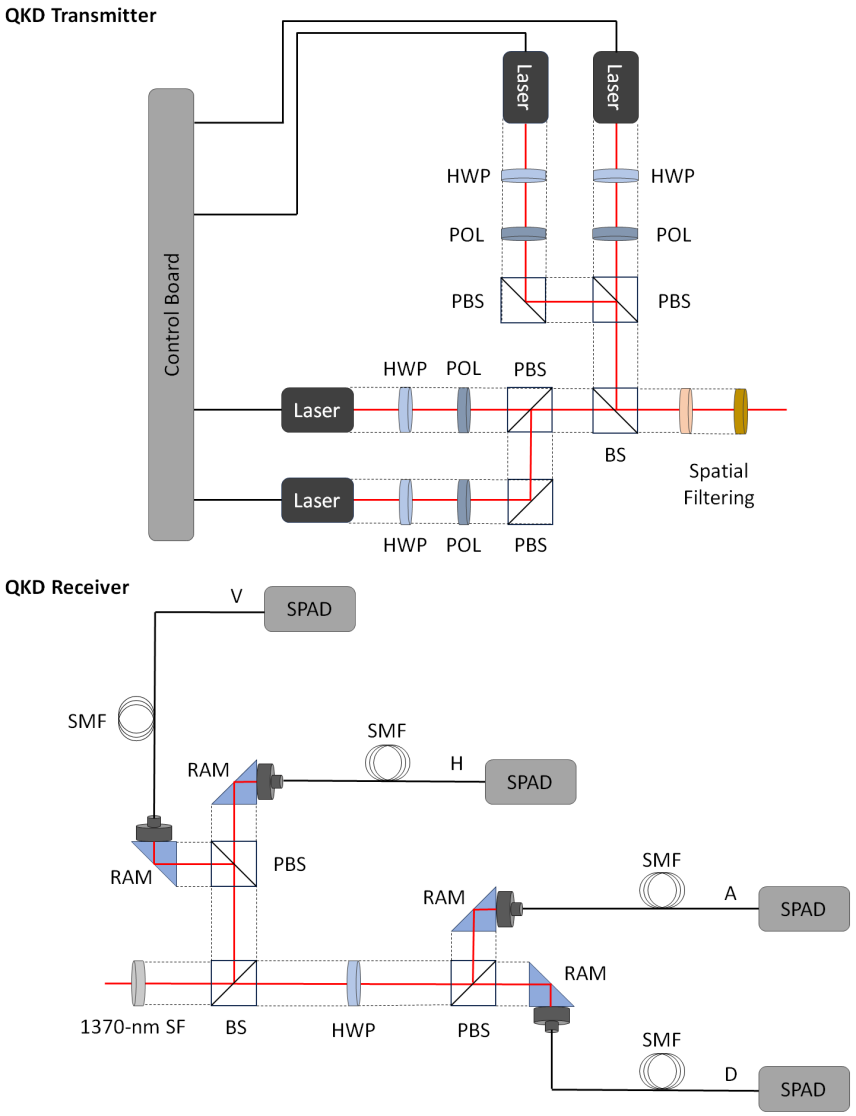

Figure 2: Available QKD receiver. BS; Beam splitter; HWP: Half-wave plate; PBS: Polarising beam splitter; POL: Polarizer; RAM: Right-angle mirror; SF: Spectral filter: SMF: Single mode fiber; SPAD: Single-photon avalanche diode. Polarization states; V: Vertical; H: Horizontal, A: Anti-diagonal; D: Diagonal.

which may lead to further studies in the broad wireless communication, including THz for the upcoming 6G era. Success would also demonstrate a system that is robust to ambient light. Given that QKD is anticipated to secure communications over a wide range of distances, from a few meters [12] to several hundred kilometers [7], the same system can potentially secure short-range indoor and long-range outdoor communications.

Leveraging the OAM degree of freedom enables high-dimensional QKD, potentially achieving higher data rates compared to conventional schemes. This is due to the ability to transmit a larger amount of information per photon [13]. Extensive research has been conducted over the last decade to develop efficient OAM generation and detection devices and understand the propagation of OAM beams. Designing a system with this capability can benefit from recent studies aiming to build structured light links resilient to propagation effects [14] and operating over wavelengths far from the solar spectrum [15].

4 Research Outputs and Outcomes

Journal Papers We plan to publish at least one paper per objective in open-access Optica journals, but more are likely.
Conference Presentations We will present our work at Optica-organized international conferences. Our results will be presented at Frontiers in Optics (FIO 2024) and Optical Fiber Conference (OFC 2025 and OFC 2026).
Data Availability We will openly share the system design, control codes, and generated data with the public by uploading them on GitHub. Manuscripts will be shared on the Oxford University Research Archive (https://ora.ox.ac.uk/).
Outreach Activities We will actively engage in various educational and general-public outreach activities to benefit next-generation scientists and engineers. We will organize demos for high-school and undergraduate students under general-public scientific events in Oxford. We will also create at least one video explaining QKD's fundamental principles and why it is essential for next-generation wireless networks. Additionally, we aim to submit a tutorial proposal to one of the major optical communication conferences where we can present our work to non-experts. We will set master engineering (MEng) projects at the Department of Engineering Science that align with the two project work packages. By involving students in this work, we hope this will motivate them to pursue DPhil degrees focusing on the field of quantum-secured networks.

5 Project Planning

Here, we chronologically summarize the WP milestones:

WP1: Building a mobile QKD setup (12 months Jan.-Dec. 2024)

In WP1, we construct the mobile QKD system with auto-tracking capability, conduct key exchange tests, and perform a PLS analysis.
- Milestone 1, (M1.1, Month 4): Replicating the available QKD setup on breadboards.
- Milestone 2, (M1.2, Month 9): Adding automated alignment capabilities and PLS modeling.
- Milestone 3, (M1.3, Month 12): Incorporate the OAM degree of freedom to the designed QKD link through SLMs.
- Deliverable (D1.1, Month 4): A technical report on the built QKD setup.
- Deliverable (D1.2, Month 10): A technical paper on the designed mobile QKD setup (to be submitted to Optics Express).
-Deliverable (D1.3, Month 12): A report of the PLS analysis and the outcomes of incorporating OAM in the system.
- C1, Month 5: Conference paper submission to FIO-2024 conference
- C2, Month 9: Conference paper submission to OFC-2025 conference.
-S1, Month 11: Online seminar/Conference tutorial.

WP2: Securing wireless RF communication with QKD (12 months: Jan.-Dec. 2025)

In WP2, the QKD system will be used to secure in-lab RF communication.
- Milestone 4, (M2.1, Month 15): Test the QKD setup with an RF link indoors.
- Milestone 5, (M2.2, Month 24): Explore further methods to secure RF using QKD such as controlling frequency hopping.
- Deliverable (D2.1, Month 20): A technical paper on using the QKD system to secure classical

Table 1: Gantt Chart of the project.

Month	1	2	3	4	5	6	7	8	9	10	11	12	13	14	15	16	17	18	19	20	21	22	23	24
Work package	WP1	WP1	WP1	WP1	WP1	WP1	WP1	WP1	WP1	WP1	WP1	WP1	WP2	WP2	WP2	WP2	WP2	WP2	WP2	WP2	WP2	WP2	WP2	WP2
Milestone				M1.1					M1.2			M1.3			M2.1									M2.2
Deliverable				D1.1						D1.2		D1.3								D2.1				D2.2
Conference					C1				C2												C3			
Seminar											S1											S2		

communication (to be submitted to Optica).
- Deliverable (D2.2, Month 24): A technical report containing the obtained results to be shared with the data and system design to the public.
- C3, Month 21: Conference paper submission to OFC-2026 conference.
- S2, Month 22: Seminar as a part of the Optica Traveling Lecturer program.

Gantt Chart: Given in Tab. 1
In terms of risk mitigation, the QKD experimental setup developed in Oxford will be our starting point for building the mobile QKD system. Meetings with experienced researchers will be held for advice and discussions. The host team has experience with QKD, conducting optical wireless experiments, and performing measurements. A handheld free space QKD system using a visible wavelength able to generate a secret rate of more than 30kb/s was demonstrated [3]. The group also has experience in optical beam steering and tracking.

Project Collaborators: Prof. Dominic O'Brien and Dr. James Farmer from the University of Oxford and Dr. Hyunchae Chun from Incheon National University.

References

1. J.-P. Chen et al. "Sending-or-not-sending with independent lasers: Secure twin-field quantum key distribution over 509 km". *Phys. Rev. Lett.* 124.7 (2020).
2. J Wabnig et al. "Demonstration of free-space reference frame independent quantum key distribution". *New J. Phys.* 15 (2013).
3. H. Chun et al. "Handheld free space quantum key distribution with dynamic motion compensation". *Opt. Express* 25.6 (2017).
4. S.-K. Liao et al. "Satellite-to-ground quantum key distribution". *Nature* 549 (2017).
5. J. Yin et al. "Satellite-based entanglement distribution over 1200 kilometers". *Science* 356.6343 (2017).
6. R. Bedington et al. "Progress in satellite quantum key distribution". *npj Quantum Information* 3.30 (2017).
7. D. K. L. Oi et al. "Nanosatellites for quantum science and technology". *Contemp. Phys.* 58.1 (2017).
8. V. Lee and D. O'Brien. "Indoor optical wireless communications using quantum key distribution at 1370 nm". *in 2020 IEEE Photonics Conference (IPC)* (2020).
9. C. H Bennett and G. Brassard. "Quantum cryptography: Public key distribution and coin tossing". *arXiv:2003.06557* (2020).
10. National Instruments. *What Is a USRP Software Defined Radio Device?* `https://www.ni.com/en-gb/shop/wireless-design-test/what-is-a-usrp-software-defined-radio`. (accessed: 07.2023). 2023.
11. L. Mucchi et al. "Physical-layer security in 6G networks". *IEEE Open J. Commun. Soc.* 2 (2021).
12. O. Elmabrok et al. "Quantum-classical access networks with embedded optical wireless links". *J. Opt. Soc. Am. B* 35 (2018).
13. A. Forbes et al. "Structured light". *Nat. Photonics* 15.4 (2021).
14. K Singh et al. "A robust basis for multi-bit optical communication with vectorial light". *Laser Photonics Rev.* 17.6 (2023).
15. K Zou et al. "High-capacity free-space optical communications using wavelength- and mode-division-multiplexing in the mid-infrared region". *Nat Commun.* 13.1 (2022).

Executive summary for

Dynamic nanophotonic trap-release for in-situ regenerative biosensing

Abraham Vázquez-Guardado, Electrical and Computer Engineering, NC State University, USA.

The scope of this research proposal is to design and implement a *dynamic biosensing strategy* that leverages highly sensitive plasmonic devices. The concept relies on dynamic trapping of *functionalized carriers that serve as transient affinity hotspots for in-situ biosensing*, which are subsequently reagent-free eluted via trap release. This approach would permit the prompt sensor regeneration and re-functionalization on demand, with same or different affinity, which are the key ingredients for continuous biosensing.

Biosensing is the fundamental step for interrogating the state of a biological system, including human health. Whether it is a biomarker that indicates the state of a disease, infection, or chronic pathology, or the detection of an infection that can threat the individual or the surrounding population's health. Furthermore, in-line and real time biosensing has been a sought-after technology for biological reactors, such as organs on chip, where not only the sensing of ions is important but cellular byproducts such as proteins, enzymes, antibodies, and other relevant biomolecules indicates the health of the biological model, or which serve as parameters for closed-loop feedback.

Plasmonic devices that support localized plasmonic resonance modes have been extensively studied as potential ultra-sensitive biosensors. Colleagues in the field have demonstrated the *detection of almost any imaginable biomarker of interest to human health* even in scenarios where the concentration suggests an early onset of an acute disease, infection, or chronic pathology. However, the covalent nature of the affinity surfactants limits the use of these *plasmonic biosensors to a single sensing event*. On top of this, high-quality plasmonic biosensors use noble metals and expensive nanofabrication processes, which results as financial burdens that hinders mass production for statistical and clinically relevant validations and its eventual commercial translation.

The solution proposed here aims to develop a strategy that employs the concept of surface trapping and release of off-line functionalized functional carriers (FCs). Using a capture and release approach the high quality plasmonic chips trap and hold the FCs in place using, providing a temporary affinity functionalization. Biosensing occurs via localized plasmonic resonance spectroscopy while the optical trap is still active. Then, the optical trap is released allowing the sensor to elute the FCs without involving harmful reagents that might degrade the quality of the device or the supporting infrastructure. Therefore, multiple sensor regenerations, even with different affinity, will be possible.

Although plasmonic biosensors have found a great appeal as potential biosensing technology for clinical and commercial use, the translation of the technology as continuous or universal sensing platform requires to address a *perennial problem that has prevailed in the field: surface regeneration*. If successful, this proposed research will open the opportunity to translate plasmonics biosensing technologies into practical applications. The direct impact is in applications that require on-demand continuous biosensing such as ions/metabolites in bioreactors, biomarkers at the bedside or operating-room settings, or as a universal sensing platform for points of care/detection solutions at remote locations.

The high-risk factor that this proposed work accompanies makes funding from external sources a challenge, especially in the context of a junior assistant professor. The proposed work seeks to establish the foundations for an active research program in novel nanophotonic biosensing, which leverage the PI's experience in plasmonic biosensing, nanoimprinting technology for mass production of high-quality plasmonic devices, microfluidics integration, and integration with optoelectronic and spectroscopic system. Most importantly, it will reiterate the solid strength of optical technologies as potential disruptors in the market of ultra-sensitive optical biosensors.

Title: Dynamic nanophotonic trap-release for in-situ regenerative biosensing

Abraham Vázquez-Guardado, Ph.D. Assistant Professor of ECE, NC State University
Email: abraham.vg@ncsu.edu | Tel: (919) 515-9592

INTRODUCTION

Biosensing represents one of the most important pieces in understanding and evaluating the health condition of a biological system either in its natural state or during a disease or an infection. In this context, the development of biosensing technologies employed for applications in fundamental biosciences, clinical diagnostics, food safety, infectious disease monitoring, etc., have observed a tremendous worldwide thrust due to its impact in the global health. For instance, the emergence of new unknown infectious diseases represents a global threat and the best line of action is to prevent its dissemination[1]. Furthermore, the prevalence of chronic pathologies requires personalized treatments which is impossible without assessing the progress of the disease and its response to the treatments[2,3]. Thus, the accurate identification and detection of biomarkers remains at the heart of research and development of biosensing technologies across multiple disciplines[4,5].

Biosensing applications consist in the detection, identification, and quantification of biomarkers, which are the routine practice in clinical and research laboratories. In fact, techniques such as the enzyme-linked immunosorbent assay (ELISA), the polymerase chain reaction (PCR), or mass spectroscopy are the gold standards and widely adopted biosensing techniques that come at the cost of expensive instrumentation, slow processing times and biosensing protocols that require trained personnel[6]. Despite the unmatched performances, those constraints hinder the adoption in emergent niches of biosensing applications which as those that require rapid detection of biomarkers at the site of interested, e.g. remote locations, in the field, the community clinic[7]; or continuous biosensing, e.g. bioreactors, organs on chip, pharmaceutical processes, environmental monitoring[8].

The field of biosensors have been extremely active in the past decade[9] with solutions that address the specifications previously described. In general, biosensors leverage two simple elements: a biorecognition element and a transductor. The former provides the biochemical selectivity such as antibodies, proteins, enzymes, single stranded oligonucleotides (e.g. aptamers), whereas the latter translates the biochemical/reaction binding into a readable signal such as in electrochemical, optoelectronic, optical, and plasmonic biosensors. In fact, the detection of almost any imaginable biomarker of interest for human, animal, and environmental health, and food safety has been demonstrated using the appropriate transductor and affinity element[9–11]. Such is the case of plasmonic biosensors, which are at the heart of this proposed work. Plasmonic biosensors, in particular those made up of nanoscale metallic resonators deterministically organized in two-dimension lattices, leverage the strong EM field confinement at the near field, typical tens of nanometers away from the metallic surface, to translate controllable perturbation of the permittivity in the surrounding environment. Such perturbations resulting from electrochemical binding between a bio-molecule analyte target and the complementary affinity receptor produce very sensitive changes in the system characteristics, e.g. its resonance, that is quantized using visible and NIR spectroscopy even at ultra-low concentrations[12]. The use of integrated microfluidic systems for sample preparation or management ultimately uplifted the appeal of plasmonics as analytical biosensors[13]. In fact, the detection of virus, bacteria, proteins, ions, etc., have been demonstrated with comparable performance as bioassay gold standards, even in challenging conditions such as in minimally processed biological fluids[14].

Despite the energetic activity of the plasmonic biosensing community a fundamental challenge prevails, which lays at the soul of the biosensor –the affinity layer that functionalizes the sensor's surface. Several protocols have been proposed to regenerate the surface of the sensor, such as chemical, thermal, electrochemical, enthalpic/entropic interactions[15]. Some of which strip off the entire affinity/analyte complex off the surface which increases the time for a subsequent biosensing event[13] or those that elute only the analyte off the affinity layer which limit the biosensing to the same analyte[16]. Therefore, the scope of this proposed work is to implement a strategy to regenerate the high-quality and expensive plasmonic biosensor for multiple uses of biosensing, even with different affinity elements, which in principle opens the opportunity for translating this technology for applications in the field or continuous biosensing –i.e. a universal biosensing platform.

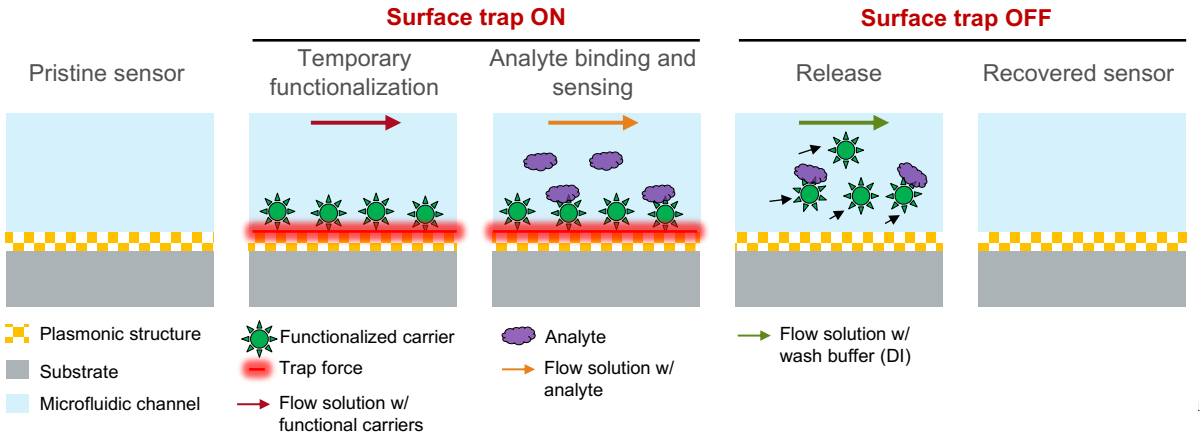

Figure 1. Schematic that demonstrates, from left to right, the trap-release strategy to temporarily functionalize the sensor's surface using functional carriers (LSPR-t ON), perform the biosensing (LSPR-t ON and monitor LSPR-s), and then regenerate the sensor by releasing the used functional carriers (LSPR-t OFF).

PROBLEM STATEMENT AND OBJECTIVES

The translation of plasmonic biosensors as a potential biosensing technology faces multiple challenges that hinders its widespread adoption; primarily because of the following two main reasons: 1) the fabrication of standardized deterministic high-quality 2D plasmonic nanostructures is expensive, 2) surface functionalization employs covalent binding of affinity surfactants that render the sensor useless after the first use. In one hand, plasmonic nanostructures require expensive and slow fabrication techniques such as e-beam lithography, which remains the most challenging and expensive factor for mass production. In the other hand, the single use restriction imposed by covalent surface functionalization and analyte binding strategy limits the efforts in statistically relevant validations. Therefore, applications in reusable or continuous biosensors have remained elusive and demonstrations are primarily limited to proof of concepts[9].

The proposed project aims to increase the utility value of plasmonic biosensors by implementing a reagent-free sensor regeneration scheme for reusable and continuous biosensing. The concept leverages surface micro trapping effect enabled by localized surface plasmons (LSP) on nanoscale apertures, such as nanohole arrays[17,18]. At resonance the incident light excites LSP whose intense electromagnetic field gradients and confinement gives rise to strong potential traps capable of securing dielectric nanospheres down to 50 nm[18]. The optical power requirement can be up to two orders of magnitude lower than traditional lens based optical tweezers that produce detrimental thermal effects on biological specimens or reduce the potential trap due to convection[18].

Dynamic biosensing and trapping in the same system we will possible by exploiting multi resonant plasmonic device such as an elliptical nanoaperture on square lattices[19]. This asymmetric system supports two spectrally separates and polarization dependent LSP resonances (LSPR) along the principal polarizability axes, one which is exploited for trapping (LSPR-t) and the other for sensing (LSPR-s). Using this concept and plasmonic device geometry we propose to implement dynamic functionalization for regenerative biosensing. The working mechanism is as follows, see Figure 1. Polystyrene nanoparticles (~100 nm diameter), called here functional carriers (FCs), are trapped on the sensor's surface by using a pilot polarized laser at the LSPR-t wavelength. These FCs are offline prepared with the affinity layer required for binding the target analyte. Once in place the solution containing the target analyte is delivered to the temporarily functionalized sensor. The binding events on the FCs will then be transferred to the plasmonic device whose LSPR-s shifts. After binding and detection, the FCs are released from the surface by turning off the pilot trap laser and then flowing a neutral buffer such as deionized water or saline, which will leave a clean sensor behind ready for a subsequent functionalization. The most attractive utility of this concept is the fact that the recovered sensor can be re-functionalized with same FC, as in the context of continuous biosensing, or a different FC with different affinity as in the context of generic biosensing for multianalyte detection.

The project leverages the PI's experience in numerical simulations, nanofabrication and optical spectroscopy characterization of plasmonic devices, microfluidic device fabrication and system level integration and automation of the pertaining technologies[20,21]. For instance, the PI has experience in

nanofabrication of plasmonic devices using nanoimprinting technology which has proved robust to mass produce high quality nanostructures for several applications including biosensing[22–25]. In addition, the PI has experience with fabrication of microfluidic chips as well as its integration with microfluidic hardware[20,21]. All these technical skills and the previous experience with plasmonic biosensors will remain an asset to the proposed research program, which suggest a spearheaded focus on the key challenges described in the following specific aims.

Specific aim 1) Design and fabricate an integrated plasmonic device and microfluidic cell for biosensing applications. The design of the asymmetric plasmonic device will be carried our using finite difference in the time domain (FDTD) simulations to produce a system with two polarization dependent resonances frequency in the NIR region (the LSPR-t~780 nm, laser line). The plasmonic device will correspond to an elliptical nano-hole array on a glass substrate (proposed parameter space: period = 400-600 nm, diameter = 100-200 nm, depth = 50-150 nm). Once designed a master pattern will be fabricated using electron beam lithography at NC State Nanofabrication Facility (Raith 150 two). A polymeric stamp, which copies the inverse of the master pattern, will be used to imprint the original pattern on SU-8 epoxy and then metallized using electron beam evaporation (info) of 30 nm of gold. Figure 3 shows an example of a plasmonic devices designed and fabricated using this methodology[20]. The microfluidic channel will be fabricated as follows. The mold is fabricated using standard UV lithography and the microfluidic channels will be fabricated on polymethyl siloxane (PDMS) using soft lithography followed by perforation of inlets and outlets.

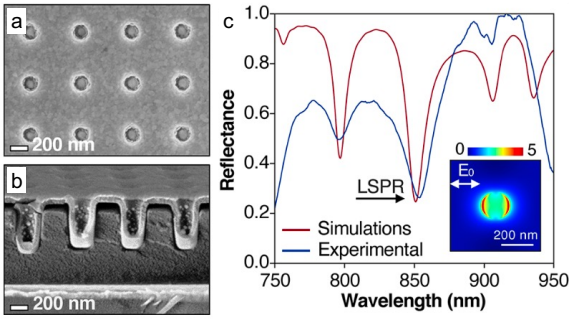

Figure 3. Scanning electron microscopy image of the (a) top and (b) cross sectional views of one plasmonic device fabricated using the nanoimprinting technique. (c) Spectra of the FDTD simulation and experimental reflectance of the plasmonic device. Ref: A. Vazquez-Guardado, et. al. Nano Lett. **21**(18), 7505–7511 (2021).

Potential pitfalls and mitigation strategies: The design and fabrication of plasmonic devices, and other photonic devices is withing the expertise of the PI as observed in the publication record. Although no potential pitfalls are expected, close attention will be paid to maximizing the volumetric field enhancements at the two resonances, so an efficient trapping and nearfield overlaps are available within the sensing and trapping volume of interest.

Specific aim 2) Implementation of an integrated optical setup equipped with microfluidic flow control to implement in-situ trapping on the photonic device's surface. The programable trap is implemented using a fiber coupled tunable CW laser (TLB 6813 Newport) whose controller interfaces via RS232 serial interface and auxiliary TTL inputs for external control and synchronization. Parameters such as central wavelength and power are remotely controlled for the basis of fine and dynamic tunning of the trapping. The laser output is coupled to a microscope, configured in reflection mode, to focus the light at the area of interest on the plasmonic sensor. The microfluidic control system consists of a pressure pump, programable microfluidic valves, flow controller, and multiple reservoirs (e.g. buffer, analyte, FCs) to manage the synchronization of the biosensing protocol (from Fluigent or Elvesys). The system integration is done using Labview (National Instruments) where we will implement a control and a graphic user interface to interface the laser and microfluidic controllers. Figure 4 shows a modular schematic of the integrated setup. With the use of the graphic user interface the user will easily access the operation modalities of the systems, as well as configuration parameters. With this control we will be able to implement autonomous routines for standardizing the biosensing protocol. The integration of the optical components will leverage a microscope coupled UV-Vis-NIR spectrometer with fluorescence measurement capabilities (Horiba),

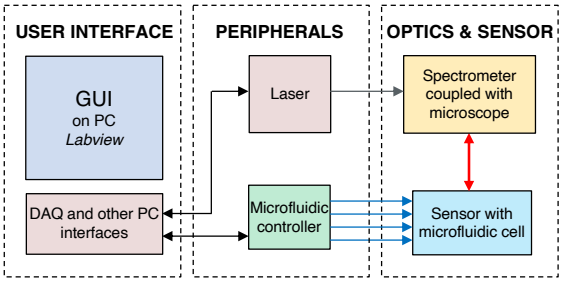

Figure 4. Block diagram that shows the system integration needed to implement this project.

which is currently in the process of procurement by the PI and is expected to be available by the time this program starts. This microscope will be equipped with external input light sources via fiber couplers to deliver the laser source to the sample, compartments for polarizers and filter placement should further light parameters are needed to be modified, manually or automatically.

Potential pitfalls and mitigation strategies: The implementation of these tasks is straightforward from the engineering perspective. The PI has vast experience with automation and system integration; thus, no potential pitfalls are expected.

Specific aim 3) Dynamic trapping of functionalized carriers and biosensing using a standard affinity model. Once the plasmonic biosensor and hardware has been implemented and characterized we will proceed with the practical demonstration of the concept. The first experiment consists of evaluating the trapping efficiency of the functional carriers (FCs) in buffer. For this we will use green fluorescent polystyrene nanoparticles in the order of 50-200 nm. The use of fluorescence microscopy will validate the trapping of the nanoparticles in real time. In addition, the use of in-situ optical spectroscopy will be used to record dynamic changes in the plasmonic resonance as the result of the particle trapping. Here parameters such as temperature, flow rates, trapping optical power, and diameter of beads, concentration of beads, etc., will be optimized.

Potential pitfalls and mitigation strategies: The trapping force might be a challenge and further optimization of the plasmonic system will be needed to make sure surface force is enough to compensate Brownian motion. So, it is typical to implement a plasmonic system with several parametric parameter that will aid the in fine tuning of the device.

The second demonstration consist of employing the FCs, same polystyrene nanoparticles with affinity elements, to produce the same trap-release effect on the optimized system, i.e. FC diameter, geometrical parameter of the plasmonic device, optical power of trap, flow rates, etc. The affinity model to use is the standard biotin/streptavidin couple, which is readily commercially available on multiple platforms including dielectric nanoparticles. Once the biotin-functionalized FCs are held in place the microfluidic system delivers the solution with streptavidin and the plasmonic resonance will be tracked in real-time to characterize the binding dynamics. Once the detection is finished the FCs are released to regenerate the sensor. Special attention will be paid to number of regeneration cycles, as this will indicate the potential lifetime of the use of the sensor and one of the main outcomes of this aim.

Potential pitfalls and mitigation strategies: During the flow of the solution with the analyte (streptavidin in this case) there can be streptavidin adsorption on the sensor's surface which might not be completely removed during the regeneration cycle. In order to minimize this potential problem, we will implement surface passivation strategy, such as a monolayer formation of mercaptoundecanoic acid to block the surface to minimized fouling, which has been demonstrated in several other biosensing experiments[20].

OUTLINE OF TASKS AND WORKPLAN

The proposed one-year research plan is organized as follows.

Aims	Q1	Q2	Q3	Q4
1) Design and fabricate an integrated plasmonic device and microfluidic cell for biosensing applications.				
2) Implementation of an integrated optical setup equipped with microfluidic flow control to implement in-situ trapping on the photonic device's surface.				
3) Dynamic trapping of functionalized carriers and biosensing using a standard affinity model.				

Progress reports will be prepared and submitted to the program committee at 6, 12, and 18 months after the project start date.

OUTCOMES

This project will strongly support the long-term vision of the PI's biosensing research program, which spans over novel biosensing strategies (such as the one proposed here) and novel active plasmonic/photonic devices for biosensing. Although the direct outcomes of this project are

associated to the three main specific aims described above, the most important outcomes will contribute to vision of the PI's research program in the following way:

1. Establish the instrumentation infrastructure for biosensing applications in the PI's laboratory.
2. Establish biosensing and functionalization protocols for diversifying an active biosensing research portfolio that will address specific clinical models and attract collaborators.
3. Train students and postdocs who will be participating in subsequent biosensing projects derived from this project.
4. Gather preliminary data that will help attract medical and clinical collaborators to pursue a more ambitious projects founded by NIH, DARPA, and other agencies that focus on the translation of proven technologies.

IMPACT

This proposal seeks to develop a technology platform that addresses the perennial challenge that have prevailed in the field of highly sensitive plasmonic biosensors and allow continuous biosensing in clinically and commercially relevant use case scenarios. If successful, this proposed research will open the opportunity to translate plasmonics biosensing technologies to more ambitious applications and it will set the technological foundation for modular hardware implementation for use in the field. The direct impact of the concept is in applications that require on-demand continuous biosensing such as ions/metabolites in bioreactors, biomarkers at the bedside or operating-room settings, or as a universal sensing platform for points of care/detection solutions at remote locations.

REFERENCES

1. Y. Rasmi, X. Li, J. Khan, T. Ozer, and J. R. Choi, Anal. Bioanal. Chem. **413**, 4137 (2021).
2. A. Ngo, P. Gandhi, and W. G. Miller, J. Appl. Lab. Med. **1**, 410 (2017).
3. E. R. Kim, C. Joe, R. J. Mitchell, and M. B. Gu, Trends Biotechnol. **41**, 374 (2023).
4. N. L. Henry and D. F. Hayes, Mol. Oncol. **6**, 140 (2012).
5. G. Zanchetta, R. Lanfranco, F. Giavazzi, T. Bellini, and M. Buscaglia, Nanophotonics **6**, 627 (2017).
6. J. Hu, F. Liu, Y. Chen, G. Shangguan, and H. Ju, ACS Sensors **6**, 3517 (2021).
7. D. Liu, J. Wang, L. Wu, Y. Huang, Y. Zhang, M. Zhu, Y. Wang, Z. Zhu, and C. Yang, TrAC Trends Anal. Chem. **122**, 115701 (2020).
8. M. Tric, M. Lederle, L. Neuner, I. Dolgowjasow, P. Wiedemann, S. Wölfl, and T. Werner, Anal. Bioanal. Chem. **409**, 5711 (2017).
9. H. Altug, S.-H. Oh, S. A. Maier, and J. Homola, Nat. Nanotechnol. **17**, 5 (2022).
10. M. Eswaran, B. Chokkiah, S. Pandit, S. Rahimi, R. Dhanusuraman, M. Aleem, and I. Mijakovic, Small Methods **6**, (2022).
11. H. Geng, S. Vilms Pedersen, Y. Ma, T. Haghighi, H. Dai, P. D. Howes, and M. M. Stevens, Acc. Chem. Res. **55**, 593 (2022).
12. P. Zijlstra, P. M. R. Paulo, and M. Orrit, Nat. Nanotechnol. **7**, 379 (2012).
13. H. Im, H. Shao, Y. Il Park, V. M. Peterson, C. M. Castro, R. Weissleder, and H. Lee, Nat. Biotechnol. **32**, 490 (2014).
14. E. Mauriz, P. Dey, and L. M. Lechuga, Analyst **144**, 7105 (2019).
15. J. A. Goode, J. V. H. Rushworth, and P. A. Millner, Langmuir **31**, 6267 (2015).
16. H. E. Indyk and E. L. Filonzi, Int. Dairy J. **15**, 429 (2005).
17. M. L. Juan, M. Righini, and R. Quidant, Nat. Photonics **5**, 349 (2011).
18. M. L. Juan, R. Gordon, Y. Pang, F. Eftekhari, and R. Quidant, Nat. Phys. **5**, 915 (2009).
19. M. Tavakoli, Y. S. Jalili, and S. M. Elahi, Superlattices Microstruct. **130**, 454 (2019).
20. A. Vázquez-Guardado, F. Mehta, B. Jimenez, A. Biswas, K. Ray, A. Baksh, S. Lee, N. Saraf, S. Seal, and D. Chanda, Nano Lett. **21**, 7505 (2021).
21. A. Vázquez-Guardado, S. Barkam, M. Peppler, A. Biswas, W. Dennis, S. Das, S. Seal, and D. Chanda, Nano Lett. **19**, 449 (2019).
22. A. Vázquez-Guardado, A. Smith, W. Wilson, J. Ortega, J. M. Perez, and D. Chanda, Opt. Express **24**, (2016).
23. A. Vázquez-Guardado, A. Safaei, S. Modak, D. Franklin, and D. Chanda, Phys. Rev. Lett. **113**, 263902 (2014).
24. A. Vázquez-Guardado and D. Chanda, Phys. Rev. Lett. **120**, 137601 (2018).
25. A. Vázquez-Guardado, J. Boroumand, D. Franklin, and D. Chanda, Phys. Rev. Mater. **2**, 035201 (2018).

Quantifying gold nanoparticle uptake and aggregation in live cells using nanoparticle plasmon coupling and deep learning.

Dr. Abu S. M. Mohsin, Associate Professor, BracU, EEE, 66 Mohakhali, Dhaka-1212, Bangladesh

Challenges: Gold nanoparticles (AuNPs) have recently become widely used in cellular imaging, single particle tracking, photothermal cancer therapy, surface plasmon resonance based biosensing, disease detection, and drug transport. However, determining AuNP uptake and aggregation without destroying the cell is challenging. The early and critical processes of EGF-induced signal transduction are dimerization and phosphorylation of the epidermal growth factor (EGF) receptor (EGFR). The mechanism by which EGFR ligands cause dimerization and phosphorylation, however, remains unknown. In search of higher-level ordering of receptor clusters, we require a technique that can probe the size regime in 10 –100 nm. Direct microscopic observation of such cluster oligomerization on cell membrane is difficult, because of the resolution limit of light microscopy (250 nm). To address this, we propose to use nanoparticle plasmon coupling and deep learning-based image segmentation technique in human cervical carcinoma (HeLa) cells. Recently Artificial Intelligence (AI) and deep learning methods play a crucial role in understanding, diagnosing, and treating diseases and analyzing cell images. For microscopic image segmentation, Generative Adversarial Networks (GANs) [26] and other image segmentation technique such as UNet, SegFast etc. has been applied to image segmentation, disease detection, cell, or nuclei detection, counting numbers of cells, and cell structure analysis for cancer detection [27]. Plasmonic nanoparticles will be used as multifunctional probes and nano-spacers in a model cell system to investigate the organization of membrane proteins and how receptor spatial arrangement influences cell behavior.

Aim & Objectives The aim of the project is to determine the role of spatial organization on the function of membrane proteins. The objective of the project is as follows: **(a)** Investigate the light matter interaction and determine nanoparticle (NP) Uptake mechanism **b)** Probe the spatial organization of membrane proteins (EGFR). (c)Control the spatial organization of membrane proteins**. (d)** Determine how receptor spatial arrangement influences cell behaviour.

Expected Outcome: Expected outcome from aim 1: Investigate the light matter interaction of single particle and cluster on the 10-100 nm scale. We will provide evidence of how the shape, size and geometry of the particle influence NP uptake. **Likely Impact from aim 1:** The results will be useful to investigate monomer-dimer transitions at the molecular scale. **Expected outcome from aim 2:** We will probe the spatial organization of membrane proteins (EGFR) using nanoparticles as a probe or nanospacer. We will demonstrate perturbation of spatial organization through the creation of clusters of different size, spatial extent, and geometry. **Likely impact from aims 2:** The impact from this study will be high because it will address the issues of creating clusters with defined size and geometry directly. **Expected outcome from aim 3:** We will determine how cellular function is linked to spatial organization of membrane proteins. **Likely impact from aims 3:** The concept of spatial organization appears to be important for polyvalent ligand-receptor interactions where ligand-mediated receptor cross-linking brings components into molecular contact. Additionally, the proposed project will help to address SDG 3 (Good Health and Wellbeing), SDG 4 (Quality Education), and SDG 9 (Industry, Innovation, and Infrastructure), as well as produce a competent workforce to meet the challenges posed by Industry 4.0.

S/L	Task	Facility at BracU	Collaborator
1	Bioconjugation: Nanomaterial & EGF Antibody	Wet chemistry & cell culture laboratory (pharmacy dept.)	Monash University Australia, Swinburne University Australia, Kind Saud University, UAE, University of Central Florida, USA, Coppin State University, USA, Pharmacy, CSE and Biotechnology Dept BracU, BUET, Bangladesh
2	Numerical Simulation-FDTD	Workstation available with Lumerical software	
3	Confocal Scattering Microscopy & Spectroscopy	Fluorescence and Darkfield Confocal Microscopy and Spectroscopy laboratory	
4	Live cell imaging	Biological cell imaging facility	
5	Deep learning	High computing workstation	

The findings of this study will be helpful in spatial structuring, receptor organization and cellular function and drug delivery. Most importantly, we will utilize our expertise and existing microscopy, spectroscopy, and wet chemistry laboratory available at BracU. If needed, we will seek assistance from our collaborators in the United States, Australia, and the United Arab Emirates.

Quantifying gold nanoparticle uptake and aggregation in live cells using nanoparticle plasmon coupling and deep learning

I. INTRODUCTION

Membrane proteins are the first line of communication between the extracellular environment and the cell interior. This communication in cellular systems is largely under the control of complex spatial and temporal networks of macromolecular interactions called signaling pathways [1]. Traditional biochemical tools such as yeast-two-hybrid [2], co-immunoprecipitation [3] together with gene [4] and protein arrays [5] provides critical information on the constituents of interaction networks. Recently it has been known that the activation of epidermal growth factor receptor (EGFR) occurs via dimerization [6,7,8] or higher order oligomerization however the precise geometry, stoichiometry, and relevance to signaling pathways is not known at this time [9].

In search of higher-level ordering of receptor clusters, we require a technique that can probe the size regime in 10 – 100 nm. Direct microscopic observation of such cluster oligomerization on cell membrane is difficult, because of the resolution limit of light microscopy (250 nm). The techniques for investigating oligomerisation, such as Forster resonance energy transfer (FRET), operate on the restrictive 1-10 nm scale. Spatial patterning is one approach to corralling membrane protein clusters into forming patterns of differing morphology and scale, as recently demonstrated by Salaita et al [7]. However, this method interferes with protein dynamics and cellular processes such as internalization. Super-resolution microscopy techniques are promising for sub-diffraction imaging but require complex instrumentation (Stimulated Emission Depletion microscopy [10]) and material characteristics (i.e., blinking or photo activation [11]) that restricts their use in general samples. To address this, we propose to use nanoparticle plasmon coupling and deep learning-based image segmentation technique in human cervical carcinoma (HeLa) cells. Plasmonic nanoparticle will be used as multifunctional probes and nano-spacers in a model cell system to investigate the organization of membrane proteins and how receptor spatial arrangement influences cell behavior. The findings of this study will be helpful in spatial structuring, receptor organization and cellular function and drug delivery. Most importantly, the novelty of our work lies in the presentation of a pioneering technique that allows in-vitro cellular studies of membrane protein interaction in a non-destructive setting under the diffraction limit.

II. LITERATURE REVIEW

The optical properties of plasmonic nanoparticles have fascinated many scientists since ancient times [12-15]. The topic has generated renewed interest among researchers, beginning with the developments of classical electromagnetic theory. Gustav Mie [16] deduced Maxwell's equation to explain the strong absorption of the gold nanosphere (AuNS) while illuminated under plane waves, offering a rigorous scientific foundation for understanding these phenomena. More recently, plasmonic nanoparticle has created a considerable amount of interest in the scientific community due to excellent optical properties, especially for nanoparticle plasmon coupling [12-15].To understand this phenomenon, sufficient knowledge of the electromagnetic properties of interacting metallic nanoparticles at close proximity is required. This property has been introduced in several applications such as solar cells [17], data storage [18], biological imaging, [13] bio labelling and sensing, [19] diagnostics, [20] photo thermal cancer therapy, [21] drug and gene delivery, [22] and probing membrane proteins. [9] Recently, the prospect of these plasmonic particles as therapeutic cancer agents and probing membrane protein has grown enormously, which necessitates the particles to be internalized or uptake by cells. [23] Consequently, the study of AuNP uptake of cells has been a major research focus in which the effect of size, [24] shape, [24] surface coatings [25] and concentration have been intensively studied. Previously several research have been conducted on micrometer scale on ensembles however there have been very few research conducted on single particle at nanometer scale. The main objective of this study is to conduct a systematic study to investigate the oligomerization of membrane protein utilizing plasmon coupling and deep learning-based image segmentation technique. Unlike Forster resonance energy transfer (FRET), there has very few studies conducted to investigate the higher-order spatial organization or oligomerization on the length scale of protein diameters (1 – 10 nm). Therefore, in search of higher-level ordering of receptor clusters, we require a technique that can probe the size regime in 10 – 100 nm. To address such issue, we propose to use plasmonic nanoparticle aided deep learning analysis on nanoparticle (NP)-antibody-EGFR complexes.

Quantifying gold nanoparticle uptake and aggregation in live cells using nanoparticle plasmon coupling and deep learning

Recently Artificial Intelligence (AI) and deep learning methods plays a crucial role in understanding, diagnosing, and treating diseases and analyzing cell images. For microscopic image segmentation, Generative Adversarial Networks (GANs) [26] and other image segmentation technique such as UNet, SegFast etc. has been applied to image segmentation, disease detection, cell or nuclei detection, counting numbers of cells, and cell structure analysis for cancer detection [27]. Kimm et. al used deep learning to segment patches of AuNPs around cancer cells [28]. Oumano and Yu used a custom CNN to classify AuNP concentrations in CT images of AuNPs [29]. Beyond AuNPs, CNN models such as U-Net have been effectively used in other problems in dark-field microscopy [30] such as generating or reconstructing images. Not as much work has been done on the specific problem of AuNP uptake and oligomerization analysis with deep learning. Tangential work to uptake analysis/counting involves instance detection and segmentation. Okunev et al. used a cascade M-RCNN to analyze individual particles in STM microscopy images [31]. While their focus was on calculating the size of the AuNP, instance detection can be extended to counting. For instance, in detection, their accuracy was 0.78. Similarly, Faraz et al instance segmented and tracked palladium oxide nanoparticles using a U-Net model [32].The primary challenge with this domain is the lack of a bulk amount of data for challenging diseases and variety in the quality of images due to the different types of imaging devices involved.

III. AIM & OBJECTIVES

AIM: To determine the role of spatial organization on the function of EGFR membrane proteins.

OBJECTIVES: The objectives are **(a)** Investigate the light matter interaction and determine nanoparticle uptake **(b)**Probe the spatial organization of membrane proteins (EGFR). **(c)** Control the spatial organization of membrane proteins**. (d)** Determine how receptor spatial arrangement influences cell behaviour.

IV. EXPECTED OUTCOMES OF THE RESEARCH

Expected outcome from aim 1: Investigate the light matter interaction of single particle and cluster on the 10-100 nm scale. We will provide evidence how the shape, size and geometry of the particle influence the nanoparticle uptake. **Likely Impact from aim 1:** The results will be useful for understanding the fundamental properties of plasmonic nanoparticles, uptake mechanism and employ them in disease detection, drug delivery etc. This will help to investigate monomer-dimer transitions at the molecular scale. We expect to have one peer reviewed paper from these findings.

Expected outcome from aim 2: We will probe the spatial organization of membrane proteins (EGFR) using nanoparticle as a probe or nanospacer. We will demonstrate perturbation of spatial organization through the creation of clusters of different size, spatial extent, and geometry. **Likely impact from aims 2:** The impact from this study will be high because it will address the issues of creating clusters with defined size and geometry directly. We expect to have one peer reviewed paper from these findings.

Expected outcome from aim 3: We will determine how cellular function is linked to spatial organization of membrane proteins. **Likely impact from aims 3:** The concept of spatial organization appears to be important for polyvalent ligand-receptor interactions where ligand-mediated receptor cross-linking brings components into molecular contact. However, being able to ascertain the role of different sizes and geometries has been challenging because of the numerous species on the cell surface. Our novel approach will provide the link between spatial structuring, receptor organization and cellular function. We expect to have one peer reviewed paper from these findings.

V. RESEARCH DESIGN

Conceptual framework: To utilize gold/silver plasmonic nanoparticle (such as NRs) as both multifunctional probes and nano-spacers of membrane protein (EGFR) organization and combine them with cell biology to determine consequences for cellular function.

Design: The experimental design consists of gold/silver nanorods as probes, nano-spacers and a model cell system for investigating receptor function. ***Nanorods as probes*:** We will create gold/silver plasmonic NRs of varying lengths (tunable between 10 nm -100 nm, width can be fixed at anywhere 10 - 20 nm). The

Quantifying gold nanoparticle uptake and aggregation in live cells using nanoparticle plasmon coupling and deep learning

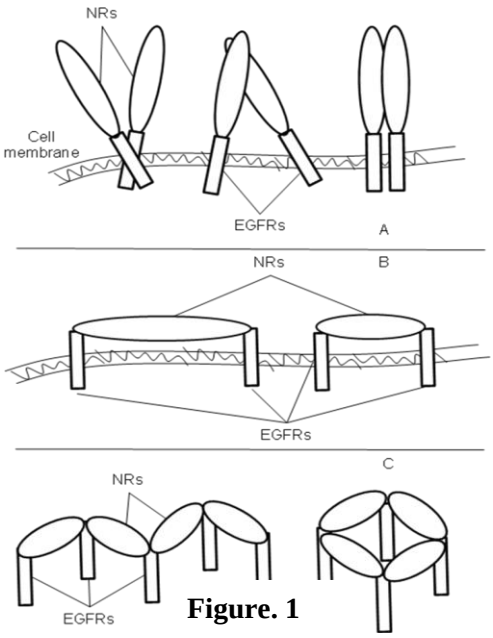

Figure. 1

synthesized NRs will then be conjugated to antibodies specific to the EGFR (clone 29.1.1 Sigma) using available protocol [13] and the resulting conjugates will be added to the surface of intact normal cells expressing the EGFRs. To measure the size (number of receptors) and average distance between receptors (10-100 nm scale) on the surface of intact cells we will deploy plasmon resonance coupling. The separation distance and conformational information will be determined from the shift of the Plasmon resonance from dark field scattering spectroscopy, while the intensity of scattered light will provide information on the number of receptors per cluster. Numerical simulation (finite difference time-domain methods, Lumerical) or analytical Mie–Gans theory on light wave interaction with coupled NRs will be used to calculate SPR shifts with respect to coupling geometries of NRs and subsequent scattering results. Experimental results will then be compared to theoretical simulations to discover conformational geometries of EGFRs. These experiments will be performed on resting (inactivated) cells and cells activated with ligand for the EGFR. **Figure 1.** Schematic depiction of membrane protein (EGFR) organization with plasmonic NRs attached as probe or nano-spacers **A.** Receptor pair attached with NRs, and their possible coupling configuration in oligomerization. The signatory SPR shifts induced from these configurations will be detected to unveil their conformational geometries. **B**. NRs used as variable length nano-spacers (10-100nm) between receptor pair or cluster pair. **C.** Possible higher-level ordering involving 4-5 EGFR monomer/dimer/tetramers with NRs as preset nano-spacers. ***Nanorods as nano-spacers****:* We will then use NRs of specific lengths as steric spacers of receptor-receptor association. We will prepare antibody-nanorod conjugates at low antibody-to-nanorod ratio and add them to cells expressing EGFR with a fluorescent protein tag on the c-terminus as a fluorescence probe of the receptor. We will create NRs of the form antibody-nanorod-antibody to bivalently cross-link receptors at defined spacing. This will enable the effect of space on receptor organization and function.

To create higher-level ordering, we will use the antibody-nanorod-antibody system described above and use secondary antibodies against the primary antibodies. By varying the secondary antibody to antibody-nanorod-antibody concentration ratio, and the nanorod length, clusters with different spatial extents and valency will be able to be produced. Simplistic possible geometric configurations of such higher orderings for 4-5 EGFR receptor monomers or clusters are shown in Figure 1B and Figure 1C. Obviously many different variations in number and configuration are expected. **Model cell system:** We will use a model cell system, Hela cell or A431 cells, which enable the function and biophysics of the EGFR to be studied without the complications of other cell types.

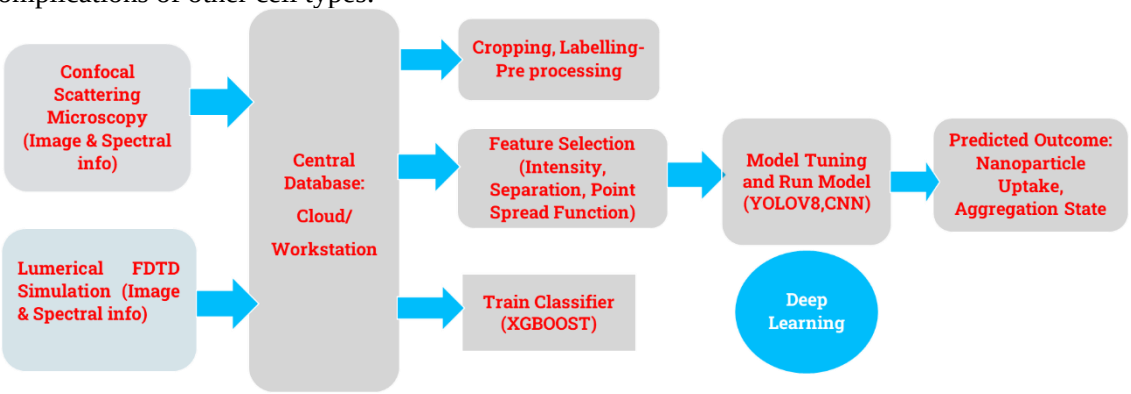

Figure 2: Overall methodology of the proposed study

Here in Fig.2. Image and spectral information stored in cloud server, pre-processing has been performed before testing with developed/available deep learning model for predicting uptake & aggregation.

VI. RESEARCH SCHEDULE AND DELIVERABLES

Specific aim 1: Investigate the light matter interaction and nanoparticle uptake, Year 1,1st half: We will investigate the light matter interaction of Ag, Au, Al, Ge, Si, Ga using available analytical models (such as Mie and Mie Gans theory) and Numerical Simulations (Lumerical-FDTD). We will determine the effect of size, shape, and geometry of plasmonic nanoparticles and structures and determine the optical and electrical property. This will have a huge impact because, specially providing a guideline to functionalize nanoparticle as a probe for drug delivery, molecular tracking and disease detection etc.

Specific aim 2: Probe the spatial organization of membrane proteins (EGFR), Year 1, 2nd half: We will firstly create model clusters of nanoparticles for probing oligomerization. We will vary the concentration of antibodies relative to nanoparticle (nanorod/bipyramid) concentration to control the valancy per nanoparticle (nanorod/by pyramid) and inject the secondary antibodies for cross-linking and clustering nanoparticle in solution. We will use confocal/dark filed micro-spectroscopy (spectrum and polarization selective light scattering) to probe the spatial organization of Nanoparticle-antibody complexes. Electron microscopy will be employed to get a clear geometry of clustering and correlated optical images will be analysed. Dark field imaging will be performed using Nikon trinocular upright LED microscope ready to operate at Brac University, EEE NanoBio photonics lab along with chemical synthesis and bio lab. Nanoparticle precursors, antibodies, EGF ligands and fluorophores will be required.

Specific aim 3: Control the spatial organization of membrane proteins, **Year 2,1st half**: We will perform numerical simulation of various geometry of predetermined nanoparticle cluster by commercial Lumerical (finite difference time domain simulation –FDTD software). For the experimental purpose we will prepare nanoparticle-antibody complex in a model cell system (HeLa/ A431 human epidermoid carcinoma cells), for linking with EGFRs. We will use three types of nano-spacers to perturb the spatial organization of nanoparticle-antibody complex on model cell system. The number of receptors per cluster will be determined from the scattering strength of plasmon resonance. Also the average distance between receptor will be determined from the shift of plasmon resonance as previously identified from numerical simulations. The generative adversarial network (CGAN) or other Deep learning algorithm (SegFast) will be used for probing the spatial organization. For that purpose, we will build our image/spectral library capturing dark field images of nanoparticle-antibody complex, later level the image, test and train the image for further analysis. Consumables such as tissue culture reagents and microscope substrates, immersion oil, coverslip glass and lamp will be required

Specific aim 4: Determine how receptor spatial arrangement influences cell behaviour, Year 2, 2nd half: We will probe and control the spatial organization of the EGFR monomers and clusters in higher-level oligomerization. The dark filed images of nanoparticle-antibody complex will be analysed utilizing plasmon coupling concept. Later the findings will be verified using deep learning algorithm to identify best complex which have effect on spatial organization. Standard cell biological assay will be used to determine the impact on receptor organization, cellular proliferation, and survival.

Execution Plan: Dr. Abu S. M. Mohsin (PI), BracU, BD will lead the project and responsible for nanoparticle cell interaction section, (Aim 1-3), Professor Dr. Mohsin Kazi (CO-PI), King Saud University Professor Dr. Aparna from Biotechnology, BracU will be responsible for bio-conjugation and cell signaling (Aim 3-4). We will also utilize our collaborator from USA, Australia for further investigation purpose.

Aim	Task	GANTT CHART (months)											
		2	4	6	8	10	12	14	16	18	20	22	24
Goal 1	Finding Gap in Literature												
Goal 2	Analytical + Numerical												
Goal 3	Synthesis/Bio conjugation												
Goal 4	Experiment (Dark field)												
Goal 5	Data processing using Deep learning												
Goal 6	Results & Publication												

Quantifying gold nanoparticle uptake and aggregation in live cells using nanoparticle plasmon coupling and deep learning

VII. IMPACT & RELEVANCE TO THE INSTITUTE AND COUNTRY

How the research is significant and how the research addresses an important problem: In addition to nanoparticle uptake mechanism, membrane proteins are significant because (1) They make up 30% of proteins encoded in the human genome, (2) They perform critical functions in normal physiology, (3) They are targets for most drugs in the pharmaceutical industry. EGFR is an archetypical type 1 membrane receptor protein that controls cellular processes such as proliferation, migration and survival. However, the way in which a single receptor can mediate a variety of cell pathways is poorly understood. This research will examine an aspect of membrane-protein structure of EGFR in which the higher-level cluster-cluster oligomerization and 2D spatial organization on a cell surface alters cellular functioning. This is significant because up to relatively recently this aspect of membrane protein structure has been largely explored using methods that destructively extract proteins from the cell surface or imaging methods that don't have the resolution to deal with interactions in the 10-100nm scale.

How the outcomes will advance the knowledge base of the discipline with novel and innovative aims and concepts: The outcomes will advance the knowledge base of the discipline by providing the following novel information; (1) New understanding of nanoparticle uptake mechanism and the association of an important membrane receptor (EGFR) on the 10-100 nm scale. This goal is achievable using our expertise in the exploitation of the novel optical properties of anisotropic plasmonic nanoparticles such as NRs. (2) New understanding on the role of spatial organization with respect to size and geometry of receptor clusters on cellular behavior. This goal is achieved using our expertise in plasmonic NRs, multidimensional microscopy, deep learning, and EGFR biophysics.

Environmental, social or economic benefits: Bangladesh is a developing country, and via this unique effort, Bangladeshi researchers will expand their impact in biological science, structural biology, and immunology. However, there is a need to develop new fundamental technologies based on fundamental physics and biology that can investigate the internal structure and dynamics of live cells. This application spans numerous priority areas and employs cutting-edge technologies (bio) photonics and deep learning to comprehend a fundamental yet challenging problem. The project will provide multidisciplinary training across cell biology, pharmacist, biophysics, biochemistry, nanotechnology, and deep learning for developing researchers such as postgraduate research students.

CONCLUSION: To summarize, the findings of this study will aid in the identification of membrane protein interaction, proliferation, survival, differentiation, nanoparticle uptake and aggregation kinetics, cellular function, and drug administration. Most importantly, it will enable non-destructive in-vitro cellular studies of membrane protein interaction under the diffraction limit.

REFERENCES

[1] Kholodenko BN. (2009). Spatially distributed cell signaling. FEBS Lett. 583(24), 4006-12.
[2] Fields S, Song O (1989). A novel genetic system to detect protein-protein interactions. Nature 340 (6230), 245–6.
[3] Selbach, M., Mann, M. (2006). Protein interaction screening by quantitative immunoprecipitation combined with knockdown (Nature Methods 3, 981–983.
[4] Schena M, Shalon D, Davis RW, Brown PO (1995). Quantitative monitoring of gene expression patterns with a complementary DNA microarray. Science 270, 5235, 467–470.
[5] Gavin MacBeath and Stuart L. Schreiber (2000) Printing Proteins as Microarrays for High-Throughput Function Determination. Science 289, 1760–1763.
[6] D. Sil, J. B. Lee, D. Luo, D. Holowka, and B. Baird, Trivalent ligands with rigid DNA spacers reveal structural requirements for IgE receptor signaling in RBL mast cells, ACS Chem. Biol., 2, 674-684, (2007)
[7] K. Salaita, P. M. Nair, R. S. Petit, R. M. Neve, D. Das, J. W. Gray, J. T. Groves, Restriction of receptor movement alters cellular response: physical force sensing by EphA2, Science, 327, 1380-1385, (2010)
[8] N. C. Hartman, J. A. Nye, J. T. Groves, Cluster size regulates protein sorting in the immunological synapse, Proc. Nat. Acad. Sci. 106, 12729-12734 (2009)
[9] Clayton AH, et. al. (2005). Ligand-induced dimer-tetramer transition during the activation of the cell surface epidermal growth factor receptor-A multidimensional microscopy analysis. J Biol Chem. 280, 30392-9.
[10] S. Bretschneider, C. Eggeling, S. W. Hell, Phys. Rev. Lett., 98, 218103, (2007)
[11] M. J. Rust, M. Bates, X. Zhuang, Sub-diffraction-limit imaging by stochastic optical reconstruction microscopy (STORM), Nature Methods, 3, 793-796 (2006)
[12] Soennichsen, C.; Reinhard, B. M.; Liphardt, J.; Alivisatos, A. P. *Nat.Biotechnol.* 2005, *23* (6), 741–745
[13] J. Aaron, K. Travis, N. Harrison and K. Sokolov, Dynamic imaging of molecular assemblies in live cells based on nanoparticle plasmon resonance coupling, Nano Lett., 9 3612-3618, (2009)
[14] H. Wang, G. Rong, B. Yan, L. Yang and B. M. Reinhard, Nano lett., 11, 498-504, (2011)
[15] J. Perez-Juste, I. Pastoriza-Santos, L. M. Liz-Marzan, P. Mulvaey, *Coord. Chem. Rev.* 249 1870 (2005)
[16] G. Mie, "Beitrage zur Optik truber Medien, speziell kolloidaler Metallosungen," *Annalen der Physik*, vol. 330, no. 3, pp. 377-445, 1908, doi: 10.1002/andp.19083300302.
[17] H. A. Atwater and A. Polman, "Plasmonics for improved photovoltaic devices," *Nature Materials*, vol. 9, no. 3, pp. 205-213, 2010/03/01 2010, doi: 10.1038/nmat2629
[18] Z. Peter, W. M. C. James, and G. Min, "Five-dimensional optical recording mediated by surface plasmons in gold nanorods," *Nature*, vol. 459, pp. 410-413, 2005.
[19] C. J. Murphy *et al.*, "Chemical sensing and imaging with metallic nanorods," *Chemical Communications*, no. 5, pp. 544-557, 2008.
[20] X. Huang, I. H. El-Sayed, W. Qian, and M. A. El-Sayed, "Cancer Cells Assemble and Align Gold Nanorods Conjugated to Antibodies to Produce Highly Enhanced, Sharp, and Polarized Surface Raman Spectra: A Potential Cancer Diagnostic Marker," *Nano Letters*, vol. 7, no. 6, pp. 1591-1597, 2007/06/01 2007, doi: 10.1021/nl070472c.
[21] X. Huang, I. H. El-Sayed, W. Qian, and M. A. El-Sayed,"Cancer cell imaging and photothermal therapy in the near-infrared region by using gold nanorods," *Journal of the American Chem Society*, vol.128, no.6, pp.2115-2120,2006.
[22] N. L. Rosi, D. A. Giljohann, C. S. Thaxton, A. K. R. Lytton-Jean, M. S. Han, and C. A. Mirkin, "Oligonucleotide-Modified Gold Nanoparticles for Intracellular Gene Regulation," *Science*, 10.1126/science.1125559 vol. 312, no. 5776, p. 1027, 2006. [Online].
[23] A. M. Alkilany, P. K. Nagaria, C. R. Hexel, T. J. Shaw, C. J. Murphy, and M. D. Wyatt, "Cellular uptake & cytotoxicity of gold nanorods: molecular origin of cytotoxicity and surface effects," *Small*, vol. 5, no.6, pp.701-708, 2009.
[24] B. D. Chithrani, A. A. Ghazani, and W. C. Chan, "Determining the size and shape dependence of gold nanoparticle uptake into mammalian cells," *Nano letters*, vol. 6, no. 4, pp. 662-668, 2006.
[25] C. Grabinski *et al.*, "Effect of Gold Nanorod Surface Chemistry on Cellular Response," *ACS Nano*, vol. 5, no. 4, pp. 2870-2879, 2011, doi: 10.1021/nn103476x.
[26] Ding, C., Xia, Y., and Li, Y., Supervised segmentation of vasculature in retinal images using neural networks. In: Orange technologies (ICOT), 2014 IEEE International Conference on, IEEE, pp. 49-52, 2014
[27] Humayun Irshad, Antoine Veillard, Ludovic Roux, and Daniel Racoceanu. 2014. Methods for nuclei detection, segmentation, and classification in digital histopathology: A review—Current status and future potential. IEEE Reviews in Biomedical Engineering 7 (2014), 97–114.
[28] Kimm, M. A., Shevtsov, M., Werner, C., Sievert, W., Zhiyuan, W., Schoppe, O., Menze, B. H., Rummeny, E. J., Proksa, R., Bystrova, O., Martynova, M., Multhoff, G., Stangl, S.: Gold Nanoparticle Mediated Multi-Modal CT Imaging of Hsp70 Membrane-Positive Tumors. Cancers, 12(5), 1331 (2020). https://doi.org/10.3390/cancers12051331
[29] Oumano, M., & Yu, H.: A deep learning approach to gold nanoparticle quantification in computed tomography. Physica Medica, 87, 83–89 (2021). https://doi.org/10.1016/j.ejmp.2021.05.036
[30] Meng, Z., Ding, L., Feng, S., Xing, F., Nie, S., Ma, J., Pedrini, G., Yuan, C., Numerical dark-field imaging using deep-learning. Optics Express 28(23), 34266-34278 (2020). https://doi.org/10.1364/OE.401786
[31] Okunev, A.G., Mashukov, M.Yu., Nartova, A.V., Matveev, A.V.: Nanoparticle Recognition on Scanning Probe Microscopy Images Using Computer Vision and Deep Learning. Nanomaterials. 10(7), 1285 (2020).
[32] Faraz, K., Grenier, T., Ducottet, C., Epicier, T.: Deep learning detection of nanoparticles and multiple objects tracking of their dynamic evolution during in situ ETEM studies. Sci Rep 12, 2484 (2022).

Structured light generation and sensing with metasurfaces for THz communications

Optica Foundation Challenge: Information

PI: Ahmed H. Dorrah, Harvard University, 9 Oxford Street, Cambridge, MA 02138;
dorrah@seas.harvard.edu

Introduction: The global free space optical (FSO) communications market is projected to reach 7 billion USD by 20230 with CAGR of 30%. Terahertz (THz) radiation, located in the wavelength range from 3 mm to 30 μm, between the microwave and infrared, holds the promise of hosting a wide range of new communications protocols. It provides larger bandwidth than current microwave wireless standards such as IEEE 802.11b WiFi while imposing minimal effects on the human body (as it is non-ionizing in nature) making it ideal for indoor and short-haul communications. Besides FSO communications, THz waves have been widely utilized in non-invasive imaging, remote sensing, and material identification. However, the widespread use of THz waves has been hindered by the shortage of affordable cameras at room temperature with high sensitivity, fast speed, and broadband operation. Moreover, current THz camera sensors can primarily detect intensity information without retrieving phase and polarization — missing two rich information carriers of light. The goal of this project is to develop efficient schemes for sensing and generating THz beams in order to facilitate their use in free space communications and beyond.

Objective: We propose the use of metasurfaces to convert any 1D THz power detector array to a full 2D wavefront camera. Metasurfaces refer to flat optics made of subwavelength-spaced arrays of patterned structures which can control the phase, amplitude, and polarization of incident light, point-by-point. Our proposed system is composed of a static metasurface and a power detector array (for e.g., Schottky diodes or bolometers). The metasurface performs a discrete set of operations on incoming light and projects the result into diffraction orders which can be captured by the detector. From this discrete set of intensity measurements, the full wavefront of the incident THz beam can be fully retrieved including its 2D intensity, phase, and polarization profiles over a broadband. Besides their use at the receiver end, our metasurfaces can be deployed at the source as a wavefront shaping platform to generate light with complex spatial structures such as vortex and vector beams, unlocking a gamut of structured light modes in the THz regime.

Plan: The duration of this project is 12 months. It combines concepts from signal processing, holography, and nanophotonics. We will utilize the recently developed THz laser source by the group of Prof. Federico Capasso at Harvard University. The wide tunability of this source in the 0.25-0.955 THz range (and beyond) makes it ideal for free space communications. The experiment will be performed in collaboration with Dr. Paul Chevalier who built this laser. The metasurfaces will be fabricated at the Center for Nanoscale Systems (CNS) at Harvard University following standard lithography, deposition, and etching protocols. To build and characterize our setup, we will purchase Schottky diodes, lens kit, polarization optics, and a THz camera. The project will also involve a collaboration with the group of Prof. Nader Engheta from the University of Pennsylvania who will contribute expertise in electromagnetic wave modelling at THz.

Impact: Efficient and versatile detectors and generators of THz waves will facilitate their widespread use in a variety of applications such as free space communications (including 6G and IoT), remote sensing, and non-invasive imaging. Furthermore, owing to their lightweight, our metasurfaces can address many challenges in drone-based sensing and space domain awareness. Lastly, given their CMOS compatibility and compact footprint, our flat optics enable a direct route to integration and large scale. With the abundance of efficient and compact THz sensors and modulators, we will take a key step towards solving one of the open challenges in optics related to affordable, secure, and fast information processing.

Structured light generation and sensing with metasurfaces for THz communications

Optica Foundation Challenge: Information

PI: Ahmed H. Dorrah, Harvard University, 9 Oxford Street, Cambridge, MA 02138

dorrah@seas.harvard.edu

1. Introduction

Terahertz (THz) frequencies are located in the spectral range from 0.1 to 10 THz, and the corresponding wavelengths range from 3 mm to 30 μm, between the microwave and infrared regions. It marks a spectral range with a variety of compelling applications. For example, THz waves can penetrate deep in fabrics and plastics and, hence, have been used in surveillance to uncover concealed weapons [1], as well as in non-invasive imaging and industrial quality control [2]-[3]. The 0.1–10.0 THz range also exhibits spectral signatures of ions, atoms and molecules that are key to material identification and to our understanding of the composition and origin of the Solar System and galaxies. Moreover, with the advent of 6G communications and the pursuit of new spectral windows for high data rate transmission, THz holds the promise of hosting a wide range of new communications protocols as it offers larger bandwidth than current microwave wireless protocols such as IEEE 802.11b [4]. Notably, THz radiation has minimum effects on the human body (as it is non-ionizing in nature) making it ideal for indoor and short-haul communications. **The goal of this project is to develop efficient schemes for modulating and sensing THz beams to facilitate their use in free space optical communications, imaging, and sensing.**

2. Problem Statement

Despite the potential impact of THz radiation on communications and sensing applications, its widespread use has been hindered by the shortage of room temperature cameras with high sensitivity, fast speed, and broadband operation [5]-[6]. More importantly, most existing THz camera sensors can only detect intensity information without retrieving phase and polarization — overlooking two key information carriers of light. Phase information is crucial for sorting vortex beams (i.e., waveforms which carry helical phasefronts and orbital angular momentum [7]), whereas polarization detection is key to resolving vector beams which carry spatially varying polarization profiles [8]. Vortex and vector beams —referred to as structured light [9] — collectively offer additional spatial modes for free space communications which can be (de)multiplexed to expand the channel capacity. However, their generation in THz has been hindered by the lack of spatial light modulators with full $0-2\pi$ phase coverage [10] and the shortage of wavefront sensing modalities.

In principle, 2D phase retrieval can be performed using a Shack Hartman configuration which interfaces a microlens array made of metallic holes with a pyroelectric detector [11]. However, this technique often suffers from low resolution and limited number of pixels, constrained by the pitch and dimensions of the microlens array. Another class of THz wavefront sensing reported recently relies on first converting the incident THz radiation to visible wavelengths which can then be captured with the widely available sensors in that regime [12]. However, this comes with other intrinsic limitations due to the frequency conversion including noise and efficiency degradation. Single pixel intensity imaging has been demonstrated using pump and probe setups which involve an ultrashort laser and a digital micromirror device, introducing more complexity and cost [13]-[14]. Moreover, the vast majority of existing THz detectors are either polarization insensitive or are only sensitive to one linearly polarized component of THz radiation [5]-[6]. **In short, a compact, robust, and high-resolution snapshot THz full wavefront camera sensor remains elusive.**

3. Objective

We propose the use of metasurfaces to convert any 1D THz power detector array to a full 2D wavefront camera. Metasurfaces refer to flat optics made of subwavelength-spaced arrays of patterned structures which can control the phase, amplitude, and polarization of incident light, point-by-point [15]. **Our proposed system is composed of a static metasurface and a power detector array (for e.g., Schottky diodes or bolometers). The metasurface performs a discrete set of operations on incoming light and projects the result onto diffraction orders which can be captured by the detector. From this set of intensity measurements, the full wavefront of the incident THz beam can be fully retrieved including its 2D intensity, phase, and polarization profiles.** In addition, our metasurfaces can be used at the source as a wavefront shaping platform [16] to generate light with complex spatial structures such as vortex and vector beams, providing a rich gamut of communications modes in the THz regime. Notably, metasurfaces can be dispersion engineered for broadband response. Figure 1 illustrates the dual use of our proposed metasurface platform, possibly at the receiver end for full wavefront sensing as depicted in Fig. 1(a), or at the source for complex wavefront shaping as shown in Fig. 1(b). Efficient generation and detection of THz waves represents a key step towards its widespread use in free space communications, sensing, and imaging.

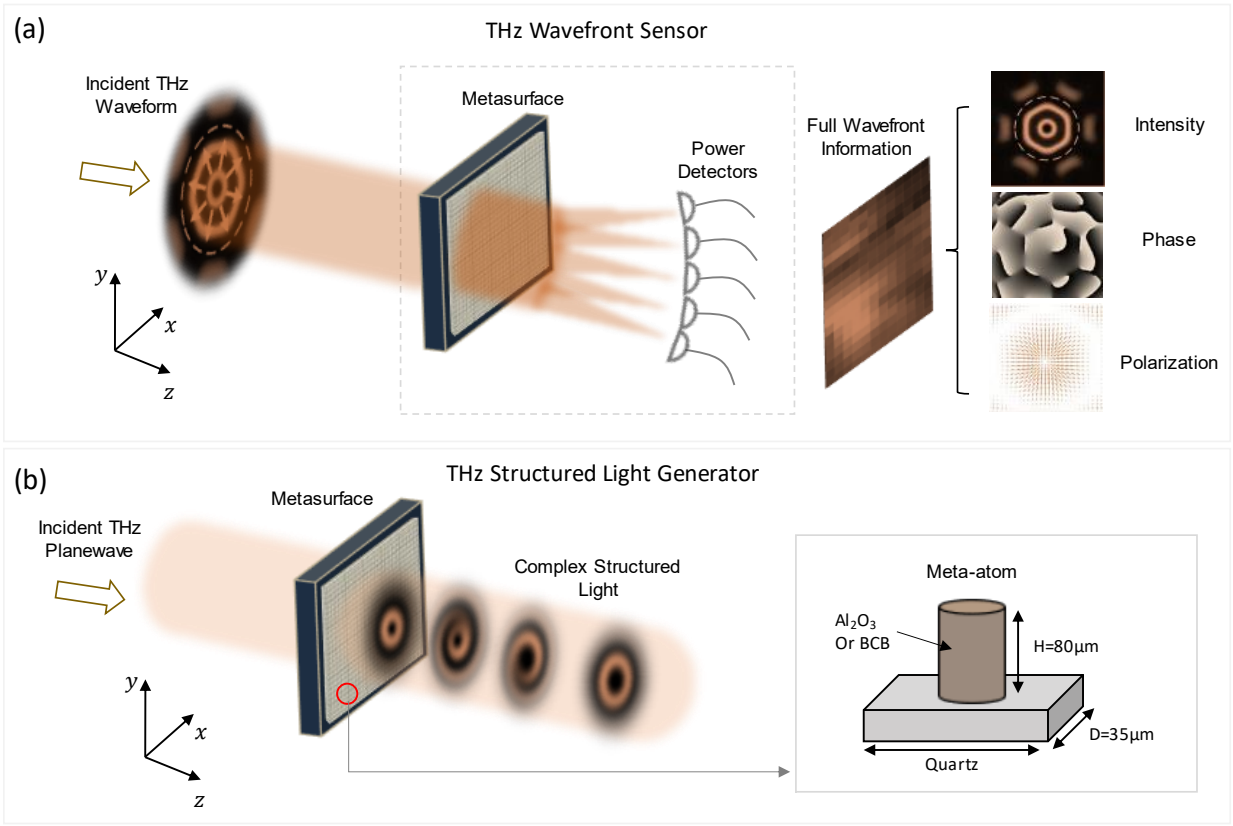

Figure 1: Schematic showing the dual use of the proposed metasurface for THz detection and generation. (a) An incident THz radiation with arbitrary wavefront interacts with a metasurface which encodes a particular computer-generated hologram (CGH). Light projected by the metasurface onto different diffraction orders will then be captured by a power detector array (for e.g., Schottky diode detectors or bolometers). From these intensity measurements, the 2D intensity, phase, and polarization profiles of the incident waveform are fully retrieved. b) Alternative use of metasurfaces at the source for structured light generation. A planewave incident on the metasurface will be transformed into a complex mode with any desired spatial profile (for e.g., an optical vortex with orbital angular momentum) which may vary in phase, amplitude, or polarization. The inset shows a schematic of the metasurface unit cell (i.e., meta-atom); a cylindrical pillar made of aluminum oxide on top of a quartz substrate.

4. Approach and Tasks

4.1 Phase retrieval: Our approach for full wavefront sensing using a conventional THz power detector relies on combining concepts from signal processing, holography, and nanophotonics. Central to our technique is the fact that any arbitrary waveform, given by $\mathbf{U}(\mathbf{r})$, can be decomposed into a superposition of basis functions, Ψ_ℓ, each weighted by a complex coefficient, c_ℓ, such that:

$$\mathbf{U}(\mathbf{r}) = \sum \mathrm{c}_\ell \, \Psi_\ell(\mathbf{r}). \tag{1}$$

Here, $c_\ell = A_\ell e^{i\Delta\phi_\ell}$, where A is a scalar amplitude and $\Delta\phi$ is a relative phase. If the basis functions and their weights are evaluated, then one can determine the resulting ensemble without ambiguity (to a global phase). Variations of this method, known as modal decomposition, have been previously demonstrated at visible wavelengths due to the abundance of spatial light modulators and CMOS cameras [17]. However, to the best of our knowledge, wavefront sensing based on modal decomposition has not been implemented in the THz regime. Modal decomposition relies on projecting an incident waveform of any arbitrary profile onto a set of orthogonal 2D basis functions. The inner product between the incident waveform and a set of matched filters (corresponding to each basis function) will provide the scalar weights, A_ℓ, i.e., the amplitude of the projection. The transmission function of each matched filter at the receiver end is given by:

$$T_\ell = \Psi_\ell^*(\mathbf{r}), \tag{2}$$

where $*$ is a complex conjugate. The key component of this technique is a computer-generated hologram (CGH) that is illuminated by the incident beam. The diffraction pattern of the hologram is then projected in the far field. The amplitudes and phases of all modes, c_ℓ, are determined through a discrete set of intensity measurements which capture the central pixel of each diffraction order. This is equivalent to measuring the correlation signal of the incoming beam with its matched filter inscribed in the hologram — a commonly used inner product measurement. The type of transmission function depends on the quantity to be measured. For instance, to extract the amplitude of one specific mode, the transmission function is chosen to be the conjugate complex of that mode (Eq. (2)). To retrieve the phase component, however, one needs to perform an interferometric measurement with a reference beam, Ψ_0^*. To perform this, two transmission functions are necessary, each representing an interferometric superposition of the two mode fields, and are given by:

$$T_\ell^{cos} = \Psi_0^*(\mathbf{r}) + \Psi_\ell^*(\mathbf{r})/\sqrt{2} \text{ , and } T_\ell^{sin} = \Psi_0^*(\mathbf{r}) + i\Psi_\ell^*(\mathbf{r})/\sqrt{2}. \tag{3}$$

From these two intensity measurements, the relative phase $\Delta\phi_\ell$ of each mode can be retrieved [17]. Hence, by implementing a single CGH which encodes a superposition of all transmission functions $\sum T_\ell$, each weighted by a grating with different blazed angle (for angular multiplexing), one can reconstruct the 2D intensity and phasefront of the incident wave, in single shot, using a metasurface and a power detector array.

4.2 Polarization Imaging: The 2D polarization profile can be retrieved via a Stokes measurement which typically requires at least four intensity measurements (since polarization can be fully characterized by a 4-element Stokes vector) by making use of a linear polarizer and quarter waveplate. Alternatively, these four measurements can be captured in a single shot using metasurfaces with birefringent meta-atoms, i.e., unit cells which are sensitive to the incident polarization. This can be realized by incorporating rectangular fins (instead of the isotropic cylindrical pillars of Fig. 1(b)). A metasurface of this kind can project incoming light into a set of diffraction orders, each analyzing for a distinct polarization state in the far-field, enabling single shot polarimetry, as has been demonstrated at visible wavelengths [18]. This concept, dubbed matrix Fourier optics, will be used here to design and implement a birefringent THz metasurface for polarization imaging. The metasurface will still encode the transmission functions in Eqs. (2-3), $\sum T_\ell$, with one key difference: each function T_ℓ will now be projected onto the far-field four times with different polarization-dependent intensities reminiscent of to the 4 Stokes intensity measurements. **From this set of angularly multiplexed intensity measurements the 2D polarization profile can be fully retrieved in a single shot.**

4.3 Metasurface Library: Our proposed metasurfaces is composed of 80 μm tall micro-patterned pillars of aluminum oxide (Al_2O_3) on a Quartz substrate as depicted in Fig. 2(a). Each metasurface unit cell is 35 μm in size. By changing the pillar's diameter, an incident THz planewave will experience different effective index (i.e., phase delay) as it propagates. A library of meta-atoms is shown in Fig. 2(b) demonstrating the ability of the proposed structure to impart full $0-2\pi$ phase coverage while maintaining high transmission by changing the pillar's diameter. Given the isotropic nature of this cylindrical structure, however, light interacts with it without changing its polarization. A polarization-sensitive metasurface library can, in principle, be realized by making use of the structural birefringence of the meta-atoms. This is depicted in Fig. 2(c) which shows meta-atoms made of rectangular Al_2O_3 micro fins. Light polarized along the major and minor axes of this structure experiences different phase delays, enabling full control over the polarization of the output beam (Fig. 2(d)). This becomes also useful for controlling the polarization, pixel-by-pixel, with subwavelength resolution, at the receiver or at the source; for e.g., to generate vector beams.

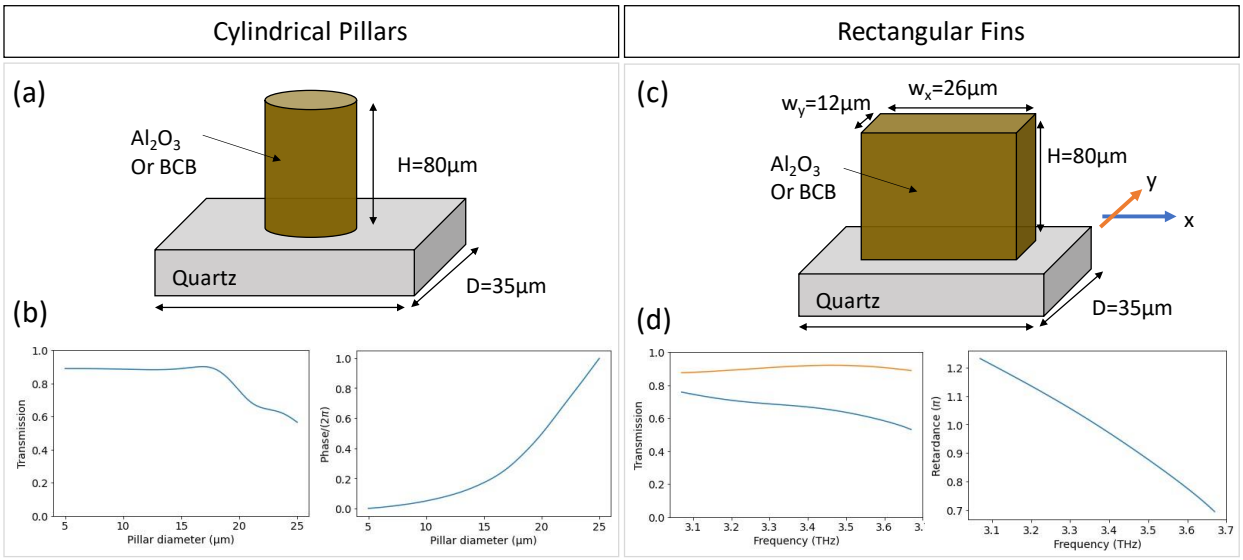

Figure 2: Metasurface libraries for wavefront shaping and detection. a) An isotropic meta-atom unit cell made of an aluminum oxide pillar on top of a quartz substrate. b) By varying the pillar diameter one can impart a phase shift between 0-2π on incident THz beam. c) A birefringent unit cell which can introduce relative retardance on the two orthogonal (x- and y-) polarized components of the incident beam. d) Transmission (along major and minor axis) and retardance for the geometry in (c) as function of frequency. Simulations were carried out using the RCWA method.

5. Work Plan

We will make use of the recently developed THz laser source by the group of Prof. Federico Capasso at Harvard University [19]. The wide tunability of this source in the 0.25-0.955 THz range (and beyond) makes it ideal for free space communications. The experiment will be performed in collaboration with Dr. Paul Chevalier who has built this laser. The Al_2O_3 metasurfaces will be fabricated at the Center for Nanoscale Systems (CNS) at Harvard University following standard lithography, deposition, and etching techniques. Furthermore, new equipment such as Schottky diodes, lens kit, polarization optics (such as retarders and polarizers), and a commercial THz camera will be purchased to demonstrate and benchmark our proposed camera. Simulation and modeling of the metasurfaces will make use of RCWA (rigorous coupled-wave analysis) which can be implemented in MATLAB as well as other commercial Finite-Difference Time-Domain (FDTD) solvers such as Lumerical. We will first build the phasefront sensor then expand it to demonstrate the full polarization sensor. The project will involve an external collaboration with the group of Prof. Nader Engheta from the University of Pennsylvania who will contribute expertise in electromagnetic wave modelling in the THz regime. **The planned duration of this project is 12 months.**

6. Significance

6.1 Outcome: We introduce a new class of cost-effective flat optics which can turn any 1D power detector array to a full wavefront camera. By combining a metasurface with an array of detectors (implemented via Schottky diodes or bolometers) one can image the 2D intensity, phase, and polarization profile of an incoming THz radiation. Since our metasurfaces can impart full $0-2\pi$ phase shift, pixel-by-pixel, and can exhibit form birefringence, they can be exploited in wavefront shaping to generate complex structured light such as vortex and vector beams for free space communications. The dual use of our metasurfaces, at the receiver and at the source, will be demonstrated and benchmarked versus commercially available devices.

6.2 Impact: Efficient and versatile detectors and generators of THz waves at room temperature will facilitate their use in a variety of applications such as free space communications (including 6G and IoT), remote sensing, and non-invasive imaging. Furthermore, owing to their compact form and lightweight, our metasurfaces can address many challenges in drone-based sensing and space domain awareness. Lastly, given their CMOS compatibility, our flat optics enable a direct route to integration and large scale. **With the abundance of these tools, the proposed work takes a key step towards solving one of the open challenges in optics related to affordable, secure, and fast information processing.**

References

[1] I. Duling and D. Zimdars, "Revealing hidden defects," *Nature Photonics* 3(11), 630–632 (2009).

[2] S.-H. Ding, Q. Li, R. Yao, and Q. Wang, "High-resolution terahertz reflective imaging and image restoration," *Applied Optics* 49(36), 6834-6839 (2010).

[3] J. Liu, J. Dai, S. L. Chin, and X.-C. Zhang, "Broadband terahertz wave remote sensing using coherent manipulation of fluorescence from asymmetrically ionized gases," *Nature Photonics* 4(9), 627–631 (2010).

[4] J. Ma, R. Shrestha, J. Adelberg et al., "Security and eavesdropping in terahertz wireless links," *Nature* 563(7729), 89–93 (2018).

[5] F. Sizov and A. Rogalski, "THz detectors," *Prog. Quantum. Electron.* 34(5), 278 – 347 (2010).

[6] R. A. Lewis, "A review of terahertz detectors," *J. Phys. D: Appl. Phys.* 52(43), 433001 (2019).

[7] Y. Shen, X. Wang, Z. Xie et al., "Optical vortices 30 years on: OAM manipulation from topological charge to multiple singularities," *Light Sci. Appl.* 8(1), 90 (2019).

[8] C. Rosales-Guzmán, B. Ndagano and A. Forbes, "A review of complex vector light fields and their applications," *Journal of Optics* 20(12), 123001 (2018).

[9] H. Rubinsztein-Dunlop, A. Forbes, M. V. Berry et al., "Roadmap on structured light," *Journal of Optics* 19(1), 013001 (2017).

[10] L. Wang, Y. Zhang, X. Guo, T. Chen et al., "A Review of THz Modulators with Dynamic Tunable Metasurfaces," *Nanomaterials* 9(7), 965 (2019).

[11] M. Cui, J. N. Hovenier, Y. Ren, A. Polo and J. R. Gao, "Terahertz wavefronts measured using the Hartmann sensor principle," *Optics Express* 20(13), 14380-14391 (2012).

[12] J. Shi, D. Yoo, F. Vidal-Codina et al., "A room-temperature polarization-sensitive CMOS terahertz camera based on quantum-dot-enhanced terahertz-to-visible photon upconversion," *Nat. Nanotech.* 17(12), 1288–1293 (2022).

[13] R. I. Stantchev, D. B. Phillips , P. Hobson et al., "Compressed sensing with near-field THz radiation," *Optica* 4(8), 989-992 (2017).

[14] R.I. Stantchev, X. Yu, T. Blu et al., "Real-time terahertz imaging with a single-pixel detector," *Nature Communications* 11(1), 2535 (2020).

[15] A. H. Dorrah and F. Capasso, "Tunable structured light with flat optics," *Science* 376(6591), eabi6860 (2022).

[16] M. Veli, D. Mengu, N.T. Yardimci, et al., "Terahertz pulse shaping using diffractive surfaces," *Nature Communications* 12(1), 37 (2021).

[17] C. Schulze, D. Naidoo, D. Flamm, O. A. Schmidt, A. Forbes and M. Duparré, "Wavefront reconstruction by modal decomposition," *Optics Express* 20(18), 19714-19725 (2012).

[18] N. A. Rubin, G. D'Aversa, P. Chevalier et al., "Matrix Fourier optics enables a compact full-Stokes polarization camera," *Science* 365 (6448), eaax1839 (2019).

[19] P. Chevalier, A. Amirzhan, F. Wang et al., "Widely tunable compact terahertz gas lasers," *Science* 366(6467), 856-860 (2019).

Multilayer holographic augmented reality with digital micromirror devices: content pipeline and system implementation

Executive summary

Most augmented and virtual reality devices currently available rely on stereoscopy to present 3D information to users. However, stereoscopy has certain limitations, including the issue of vergence-accommodation conflict. On the other hand, holographic displays have the potential to fully control the amplitude and phase of a light field, allowing for visualizations that closely resemble natural vision. Additionally, holographic displays can project multiplane scenes, where different information is presented to the user's eyes depending on their focus position. However, there are several challenges that need to be addressed in order to fully realize this potential.

The main challenges are related to the need for fast and accurate methods to encode a target scene into a hologram, as well as the availability of suitable devices to modulate a light field with the resulting holograms. Current high-performance holographic displays use phase-only holograms combined with liquid crystal on silicon spatial light modulators (LCOS-SLM). However, these devices are expensive and limit the potential applications of holographic display techniques. An alternative option is the use of digital micromirror devices (DMD), which are more affordable but limited to binary amplitude modulation. Due this limitation, most existing high-performance hologram generation methods were developed for phase only holographic displays and are not suitable for projection using a DMD. Despite these limitations, recent advances in fast propagation methods and binary amplitude hologram generation with binarized neural networks show promise in overcoming these challenges.

In this project, we aim to leverage the latest advancements in hologram generation to develop a holographic display based on a digital micromirror device, as well as a binary amplitude hologram generation pipeline that takes advantage of the high speed offered by DMDs compared to LCOS-SLMs. Specifically, our intention is for the prototype system developed during the project to serve as a test platform to demonstrate the capabilities of new binary amplitude hologram generation methods, as well as the potential of holographic augmented reality in general. Moreover, by highlighting the potential of digital micromirror technology in holographic displays, we hope to lower the entry barrier for many applications, such as optogenetics, superresolution microscopy, and holographic tweezers, which have traditionally relied on expensive LCOS-SLM-based solutions.

Multilayer holographic augmented reality with digital micromirror devices: content pipeline and system implementation

Alejandro Velez-Zea

Literature review

Since its discovery by Dennis Gabor in 1948 [1], holography has become the cornerstone of many powerful techniques like metrology [2,3], optical tweezers [4,5], neural optostimulation [6,7] and holographic displays [8,9]. This latest application has become the focus of renewed interest, as holographic displays could enable true high-fidelity 3D visualization by reproducing the full phase and amplitude of a 3D scene. The full reproduction of the phase and amplitude can enable a holographic display to avoid the issues present in common implementations of virtual or augmented reality devices based on stereoscopy, such as the accommodation-vergence conflict [10].

Most modern holographic display setups are designed to work in conjunction with computer-generated holograms (CGH) instead of actual experimental holographic recordings of real scenes. This eliminates the need for large and complex holographic recording setups and enables the generation of holograms from virtual objects. Despite this advantage, the calculation of holograms is a computationally intensive process [11].

To deal with this challenge, many algorithms for computer-generated holography tailored to different scenarios have been proposed. One of the first such algorithms is the Gerchberg-Saxton (G-S) algorithm [12], an iterative method that enables the calculation of a phase connecting two different planes related by a Fourier transform. Other iterative methods for hologram generation have been proposed, where the phase or amplitude is found solving an optimization problem with a well-defined loss function. Amongst these approaches we find both non-convex optimization algorithms [13,14], gradient descent [15], and as a more recent development, the use of deep learning [16,17].

Finally, there are CGH methods based on the use of point clouds or polygon decomposition [18,19]. These methods take advantage of the fact that simple geometric shapes have easily calculated diffraction patterns. These patterns can be pre-generated for different positions and stored in a lookup table (LUT) [20,21]. Then a target scene can be decomposed on a finite number of points, triangles, or lines and the diffraction pattern of each one retrieved from the lookup table, after which a hologram can be acquired by adding all resulting patterns.

Beyond conventional reproduction of 2D and 3D scenes, extended depth multiplane scenes can also be codified into a CGH. In this case, multiple 3D objects can be reproduced along the same optical axis with minimal crosstalk or occlusion. This enables the reproduction of different scenes at different focus depths from a single hologram. This capability is desirable in varifocal displays, since a user can perceive different scenes depending on the focus plane of their eyes [22].

The algorithms used for generation of multiplane holograms are significantly more computationally intensive than those used to generate conventional holograms of 2D or 3D scenes. This is because in addition to encoding each scene into the hologram, they must also be optimized to avoid crosstalk between the information in each plane or focus position. The basic algorithms used to generate these holograms are the global [23] and sequential [24] Gerchberg-Saxton algorithms (GGS and SGS respectively). In particular, the GGS algorithm has demonstrated the capability for generating holograms with a significantly higher reconstruction quality than the SGS. However, both approaches require iteratively projecting each individual plane of the target scenes, making computation very slow [25].

Other approaches used to generate multiplane holograms are the non-convex and gradient descent optimization, which presents better quality than the SGS and GGS but also shows limited computation speed [13,15]. To address this issue, we recently introduced a multiplane hologram generation method based on the singular value decomposition of the Fresnel transform function [26]. This approach makes light propagation computation planes significantly faster, which is a requirement of many iterative 3D hologram generation algorithms. Using this approach, we introduced a modification of the GGS called the two-step global iterative Fresnel algorithm (TGS-IFrTA), which leads to significantly faster hologram generation.

Despite these advances in multiplane hologram generation, there has been limited success in developing a full color multilayer holographic augmented reality display capable of reproducing scenes where several objects can be presented at different distances from the user along the same axis without crosstalk. From the viewpoint of augmented reality displays, the attempts to implement this capability have been limited. For instance, Song et al. [27] recently demonstrated a full-color near eye display by generating a color hologram of a 2D scene using multiplexing encoding and a Maxwellian configuration. Similarly, Lin et al. [28] implemented a binocular full-color near eye display using frequency division multiplexing, where the frequency spectrum of the holograms for each color channel of a 3D scene were tailored to enable color display using a single SLM. Despite the effectiveness of these approaches, they are currently limited to displaying single 2D or 3D scenes. To address this limitation, we implemented a full-color near-eye multiplane augmented reality holographic display based on a single phase-only SLM, that makes use of TGS-IFrTA for efficient generation of multiplane holograms. The implemented display can superpose multiplane scenes composed of multiple 2D and 3D objects placed along the same optical axis with minimal crosstalk and demonstrates that the TGS-IFrTA has superior performance compared with other common multiplane hologram generation techniques [29].
While this setup shows good performance, like most current holographic displays it is based in liquid crystal on silicon (LCOS) SLM, which offer very good performance for phase modulation. However, despite the advantages of phase-only CGH in combination with LCOS-SLM, the cost of these devices is a barrier for their use in many applications. In response to this limitation, other SLM technologies applied to CGH have been explored. Among these, we find digital micromirror devices (DMDs). A DMD is an array of small mirrors that can rotate at certain angles, allowing for binary amplitude modulation of incoming light. DMDs have found broad use in many applications [30–32] and compared to LCOS-SLM offer significant lower cost and higher refresh rates [33]. Since DMDs are only capable of binary amplitude modulation, they must be used in combination with CGH techniques that produce binary amplitude holograms (BAHs) for holographic projection and display applications. BAHs encode holographic information from two-dimensional or three-dimensional objects in binary amplitude-only functions [23]. Although these holograms present low quality and low diffraction efficiency compared to POHs, the inherent speed and cost advantages of DMDs can make these limitations acceptable in many applications [24,25]. Furthermore, recent works using binarized neural networks have demonstrated the capability for generating BAHs of extended depth multilayer scenes with a high level of quality. In our preliminary tests, we have found that the binarization approach used in this last work can be used adapted successfully to common gradient descent optimization algorithms. This, in combination with efficient light propagation approaches like the one we demonstrated in [26], is the key for a high accuracy and fast BAH generation method, which can be the cornerstone of an augmented reality holographic display headset based on digital micromirror devices.

Problem statement

The problem to be addressed with this project is the fact that currently available augmented reality displays rely on stereoscopy, which introduces a series of unwanted effects due the vergence accommodation conflict, limiting their mass adoption. On the other hand, holographic displays

are an option to overcome this issue, and present novel capabilities unavailable to stereoscopic solutions, like the capability for reproducing extended depth multilayer scenes. Despite this advantage, holographic displays are limited the high cost of their components, in particular phase only spatial light modulators, and the complexity of the CGH algorithms needed to produce their content. To solve these issues, we propose integrating digital micromirror devices and binary amplitude hologram generation methods into a full augmented reality display portable solution, capable of reproducing 2D, 3D and extended depth multilayer scenes at high speed with acceptable quality. This includes the optical design of the headset itself, as well as the optimization of a BAH algorithm for multiplane hologram generation, taking advantage of recent advances in fast light propagation computation and binarized gradient descent optimization methods.

Work plan

The work plan for this project is divided into 4 stages or tasks. A breakdown of the expected chronogram can be found in table 1.

1. Optical engine and Micromirror Device: First we will focus on identifying the limitations of current digital micromirror devices, selecting a suitable candidate based on cost, resolution, pixel size, connectivity, and form factor, and then proceeding to the design an adequate optical engine well suited for a headset portable display. This includes minimizing weight and energy consumption of the illumination and associated optics. Expected timeframe: (9 months)
2. Binary Amplitude Hologram Generation: Once the suitable DMD is selected, and in parallel with the optical engine design, we will develop algorithms and techniques to achieve a content generation pipeline, involving the computation of binary amplitude holograms that encode the desired multilayer three-dimensional information. To achieve this, we will deploy state of the art gradient descent optimization algorithms with pass-through binarization, capable of considering the specific parameters of the micromirror device. Expected time frame: 12 months.
3. Holographic Display System Integration: We will integrate the micromirror device, optical engine, and binary amplitude holograms into a comprehensive holographic display system. This integration involves the development of control electronics, optical elements, and software interfaces that enable fast rendering and projection of holographic content. Expected timeframe: 6 months.
4. Performance Optimization: Finally, we will focus on improving the display system's performance parameters, brightness, viewing angle, and measuring and correcting optical aberrations By optimizing the device design, hologram generation algorithms, and system calibration techniques, we aim to deliver a holographic display solution that matches or surpasses current industry standards at lower costs. Expected timeframe: 6 months.

Task\month	*1-3*	*4-6*	*7-9*	*10-12*	*13-15*	*16-18*	*19-21*	*22-24*
1	X	X	X					
2		X	X	X	X			
3					X	X		
4							X	X

Table 1: Task chronogram for the current proposal.

Outcome

As a result of this project, we expect to have developed and advanced key methods necessary for a new generation of portable augmented reality holographic displays based on digital micromirror

devices. In particular, we intend that the prototype system developed during the project to become a test platform intended to demonstrate the capabilities of new BAH generation methods and of holographic augmented reality in general. Furthermore, by highlighting the potential of digital micromirror technology in holographic displays, we hope to contribute to lowering the barrier for entry for many of its applications, like optogenetics, superresolution microscopy and holographic tweezers, which usually have relied on costly LCOS-SLM based solutions. Finally, the knowledge and capabilities developed during the project can help bring attention and empower the applied optics research being conducted in public institutions of less developed countries like Colombia, despite the current limitations in founding.

Impact

The implementation of a holographic display system using micromirror devices and binary amplitude holograms holds significant potential across various industries:

Entertainment and Gaming: The system can revolutionize the gaming and entertainment industry by providing lifelike, immersive 3D experiences. Holographic displays can enhance virtual reality (VR) and augmented reality (AR) applications, enabling users to interact with holographic objects in real-time, without the undesirable effects of the vergence-accomodation conflict found in stereoscopic displays.

Medical Imaging and Education: Holographic displays can find applications in medical imaging, allowing physicians to visualize complex anatomical structures and perform detailed simulations. Medical education and training can also benefit from holographic representations, enhancing the understanding and practical skills of students.

Architectural Visualization: The system can facilitate the visualization of architectural designs, allowing architects and designers to showcase their concepts in 3D. Clients can experience virtual walkthroughs and assess the spatial aspects of a project before construction begins.

Advertising and Retail: Holographic displays can create captivating visual displays for advertising and retail purposes. By leveraging the realism and interactivity of holograms, marketers can engage consumers in unique and memorable ways, driving brand awareness and sales.

References

1. D. Gabor, "A new microscopic principle," Nature **161**, 777–778 (1948).
2. Z. Wang, L. Miccio, S. Coppola, V. Bianco, P. Memmolo, V. Tkachenko, V. Ferraro, E. Di Maio, P. L. Maffettone, and P. Ferraro, "Digital holography as metrology tool at micro-nanoscale for soft matter," Light Adv. Manuf. **3**, 151 (2022).
3. P. Shanmugam, A. Light, A. Turley, and K. Falaggis, "Variable shearing holography with applications to phase imaging and metrology," Light Adv. Manuf. **3**, 16 (2022).
4. J. Abacousnac and D. G. Grier, "Dexterous holographic trapping of dark-seeking particles with Zernike holograms," Opt. Express **30**, 23568–23578 (2022).
5. H. Kim, M. Kim, W. Lee, and J. Ahn, "Gerchberg-Saxton algorithm for fast and efficient atom rearrangement in optical tweezer traps," Opt. Express **27**, 2184–2196 (2019).
6. S. Junge, F. Schmieder, P. Sasse, J. Czarske, M. L. Torres-Mapa, and A. Heisterkamp, "Holographic optogenetic stimulation with calcium imaging as an all optical tool for cardiac electrophysiology," J. Biophotonics **15**, e202100352 (2022).
7. H. Adesnik and L. Abdeladim, "Probing neural codes with two-photon holographic optogenetics," Nat. Neurosci. **24**, 1356–1366 (2021).
8. Y. Duan, F. Zhang, M. Pu, Y. Guo, T. Xie, X. Ma, X. Li, and X. Luo, "Polarization-dependent spatial channel multiplexing dynamic hologram in the visible band," Opt. Express **29**, 18351–18361 (2021).
9. C. Chang, K. Bang, G. Wetzstein, B. Lee, and L. Gao, "Toward the next-generation VR/AR optics: a review of holographic near-eye displays from a human-centric perspective," Optica **7**,

1563 (2020).
10. A. U. Batmaz, M. D. Barrera MacHuca, J. Sun, and W. Stuerzlinger, "The Effect of the Vergence-Accommodation Conflict on Virtual Hand Pointing in Immersive Displays," Conf. Hum. Factors Comput. Syst. - Proc. (2022).
11. D. Blinder, A. Ahar, S. Bettens, T. Birnbaum, A. Symeonidou, H. Ottevaere, C. Schretter, and P. Schelkens, "Signal processing challenges for digital holographic video display systems," Signal Process. Image Commun. **70**, 114–130 (2019).
12. R. W. Gerchberg and W. O. Saxton, "A practical algorithm for the determination of the phase from image and diffraction plane pictures," Optik (Stuttg). **35**, 237–246 (1972).
13. J. Zhang, N. Pégard, J. Zhong, H. Adesnik, and L. Waller, "3D computer-generated holography by non-convex optimization," Optica **4**, 1306–1313 (2017).
14. C. Jin, C. Liu, R. Shi, and L. Kong, "Precise 3D computer-generated holography based on non-convex optimization with spherical aberration compensation (SAC-NOVO) for two-photon optogenetics," Opt. Express **29**, 20795–20807 (2021).
15. C. Chen, B. Lee, N.-N. Li, M. Chae, D. Wang, Q.-H. Wang, and B. Lee, "Multi-depth hologram generation using stochastic gradient descent algorithm with complex loss function," Opt. Express **29**, 15089–15103 (2021).
16. Y. Rivenson, Y. Wu, and A. Ozcan, "Deep learning in holography and coherent imaging," Light Sci. Appl. **8**, 85 (2019).
17. T. Shimobaba, D. Blinder, T. Birnbaum, I. Hoshi, H. Shiomi, P. Schelkens, and T. Ito, "Deep-Learning Computational Holography: A Review (Invited)," Front. Photonics **3**, 1–16 (2022).
18. Y. Yamamoto, H. Nakayama, N. Takada, T. Nishitsuji, T. Sugie, T. Kakue, T. Shimobaba, and T. Ito, "Large-scale electroholography by HORN-8 from a point-cloud model with 400,000 points," Opt. Express **26**, 34259–34265 (2018).
19. Y. Pan, Y. Wang, J. Liu, X. Li, and J. Jia, "Fast polygon-based method for calculating computer-generated holograms in three-dimensional display," Appl. Opt. **52**, A290–A299 (2013).
20. D. Blinder and P. Schelkens, "Accelerated computer generated holography using sparse bases in the STFT domain," Opt. Express **26**, 1461–1473 (2018).
21. H.-K. Cao and E.-S. Kim, "Full-scale one-dimensional NLUT method for accelerated generation of holographic videos with the least memory capacity," Opt. Express **27**, 12673–12691 (2019).
22. D. Dunn, C. Tippets, K. Torell, P. Kellnhofer, K. Aksit, P. Didyk, K. Myszkowski, D. Luebke, and H. Fuchs, "Wide Field of View Varifocal Near-Eye Display Using See-Through Deformable Membrane Mirrors," IEEE Trans. Vis. Comput. Graph. **23**, 1322–1331 (2017).
23. R. Piestun, B. Spektor, and J. Shamir, "Wave fields in three dimensions: analysis and synthesis," J. Opt. Soc. Am. A **13**, 1837–1847 (1996).
24. M. Makowski, M. Sypek, A. Kolodziejczyk, and G. Mikula, "Three-plane phase-only computer hologram generated with iterative Fresnel algorithm," Opt. Eng. **44**, 125805 (2005).
25. A. Velez-Zea and R. Torroba, "Mixed constraint in global and sequential hologram generation," Appl. Opt. **60**, 1888–1895 (2021).
26. A. Velez-Zea, J. F. Barrera-Ramírez, and R. Torroba, "Improved phase hologram generation of multiple 3D objects," Appl. Opt. **61**, 3230–3239 (2022).
27. W. Song, X. Li, Y. Zheng, Y. Liu, and Y. Wang, "Full-color retinal-projection near-eye display using a multiplexing-encoding holographic method," Opt. Express **29**, 8098–8107 (2021).
28. S.-F. Lin, S.-H. Zhang, J. Zhao, L. Rong, Y. Wang, and D. Wang, "Binocular full-color holographic three-dimensional near eye display using a single SLM," Opt. Express **31**, 2552–2565 (2023).
29. A. Velez-Zea and J. F. Barrera-Ramírez, "Color multilayer holographic near-eye augmented reality display," Sci. Rep. **13**, 1–15 (2023).
30. M. Chlipala and T. Kozacki, "Color LED DMD holographic display with high resolution across large depth," Opt. Lett. **44**, 4255–4258 (2019).
31. B. Hellman and Y. Takashima, "Angular and spatial light modulation by single digital micromirror device for multi-image output and nearly-doubled étendue," Opt. Express **27**, 21477–21496 (2019).
32. A. Jaramillo-Osorio, S. Bustamante, B. Munoz, A. Velez-Zea, J. F. Barrera-Ramírez, and R. Torroba, "Experimental Fresnel and Fourier digital holography using a digital micro-mirror device," J. Opt. **23**, 035701 (2021).
33. J.-Y. Son, B.-R. Lee, O. O. Chernyshov, K.-A. Moon, and H. Lee, "Holographic display based on a spatial DMD array," Opt. Lett. **38**, 3173 (2013).

Executive summary

Optica Foundation Challenge – 2023 (Category – Environment)

Sensing trace gases by speckle correlations and adaptive random laser spectroscopy

Sensing of trace gases is crucial for safe and secure environment. Presence of the trace gases above the permissible limit increases the green-house effect and causes serious health risk such as lunge, kidney, and mental diseases. Methane and ammonia are two of the well-known trace gases that have significant contribution in air pollution and are of major concern. Methane is one of the fastest growing green-house gases and has a contribution of around 30% of global warming. Moreover, it has thirty times more potential in global warming than carbon-di-oxide and is responsible for half a million premature death annually due to the air pollution. Most of the developed nations have also acknowledged ammonia as an air pollutant and implemented restrictive measures to control its emission. Ammonia is highly reactive and can form aerosols that contribute in the green-house effect. These two trace gases have a wide range of sources such as agricultural sector, decomposition of manure from wildlife and plants, motor vehicles and fossil fuel, chemical industry, and mining. Optical gas sensors are widely used to detect and monitor the concentration levels of these gases in the environment. However, most of the optical sensors available today for sensing these gases have low sensitivity and gas selectivity. Moreover, the infrared absorption bands of these gases are targeted to detect them and hence, sensing different gases requires sources of corresponding wavelengths. Furthermore, the existing optical gas sensors are complex and expensive. Therefore, developing a chip-scale gas sensor to detect these trace gases is highly demanding, but possess several difficulties due to their small interaction length/area and poor signal to noise ratio. In this respect, a random laser based and laser speckle correlation-based sensing technologies can provide the possible solutions to overcome this problem. Both of these techniques utilize multiple scattering of light in a disordered material: the former uses an active disordered medium, whereas the latter utilizes a passive disordered system. Any change in the scattering environment due to interaction between the analyte trace gases and the selected disordered material alters the random lasing properties and also the speckle pattern which can be exploited to detect and monitor these trace gases.

Therefore, in the proposed project, to the best of our knowledge, we target to develop, for the first time, an adaptive random laser-based ammonia sensor and a speckle cross-correlation based methane gas sensor. Polymer based planar waveguide diffuser will be fabricated to build both of these sensing systems. Adaptive optic control of random lasing modes by wavefront shaping of the excitation beam will be employed for detecting the ammonia gas and measuring its concentration level in the environment. Random lasing in the disordered material will also enhance the gas detection sensitivity. In methane gas sensor, the change in the speckle pattern due to the interaction between the methane gas and a conductive polymer diffuser will be monitored to sense and evaluate the gas concentration. Both of these sensors will work at visible wavelength range. Additionally, these compact, portable, lab-on-a-chip trace gas sensors will find applications in agriculture sector, mining, fertilizer and automobile industries, and disease control in biomedical field. Moreover, they will have less response time, improved sensitivity and gas selectivity compared to the existing optical gas sensors. Precise detection of ammonia and methane gases in the local atmosphere would help to control their possible origins and also save the human and animal lives from the possible health risk. We believe that these new gas sensing technologies can further be used for sensing other trace gases as well and will open up the possibility of remote and real-time sensing. Hence, this work will contribute in detecting the concentration levels of the trace gases in local atmosphere, controlling their emission sources and reducing the green-house effect.

Optica Foundation Challenge – 2023
Category – Environment

Sensing trace gases by speckle correlations and adaptive random laser spectroscopy

Anirban Sarkar, Department of Physics, National Institute of Technology Calicut, Kozhikode 673 601, India

I. Literature Review

Trace gas sensing is important for safe environment and healthy life. Presence of these gases in the atmosphere, above the permissible limit, not only seriously degrades the air quality, but also increases the green-house effect and as well as causes some serious health issues [1]. Ammonia and methane are two well known trace gases that are of major concern. Besides being the second most abundant green-house gas, methane has thirty times more potential in global warming than carbon-di-oxide, whereas ammonia is highly reactive and can form aerosols that contribute in green-house effect [2]. Methane is one of the fastest growing green-house gases and has a contribution of around 30% of global warming since the industrial revolution [3]. Moreover, it is responsible for half a million premature death annually due to the air pollution [4]. Most of the developed nations have also acknowledged ammonia as an air pollutant and put in place restrictive measures to control its emission [5]. Ammonia and methane have a wide range of sources such as agricultural sector [6], decomposition of manure from wildlife and plants [7], motor vehicles and fossil fuel [8], chemical industry [9], and mining [10]. Most of the trace gas sensing techniques available today are mainly based on Raman spectroscopy [11], infrared spectroscopy [12], electrochemical sensing [13], piezoelectric sensing [14], and fluorometric sensing [15] etc. These sensors have low sensitivity and are complex and expensive. Multi-pass passive cavity ring-down spectroscopy is also frequently used to detect these trace gases [16]. However, developing a chip-scale sensor to detect these gases is challenging because of small interaction length/area and poor signal to noise ratio. Scattering of light in certain disordered materials can significantly be modified due to interaction of these trace gases with those respective materials. Multiple scattering of light in passive disordered material generates speckle pattern whereas that in an active disordered medium amplifies the light and produces random lasing. Random lasers (RLs) have high spectral energy density with low coherence and possess many fundamental properties of a conventional lasers e.g. lasing threshold and distinct lasing modes [17]. Although RLs have a wide range of applications such as speckle free imaging [18], super resolution spectroscopy [19], and biomedical sensing [20], but their application in gas sensing has not been explored yet. Despite the development of light scattering based gas sensors, speckle correlation based on-chip trace gas sensors are also unavailable.

In this project, we aim to develop, for the first time, an adaptive random laser-based ammonia sensor and a speckle cross-correlation based methane gas sensor. Controlling the random lasing modes and monitoring them under ammonia gas environment, the concentration level of the ammonia gas will be measured. Additionally, the random lasing action in the disordered material will enhance the sensitivity of sensor. In the other case, tracking the change of the laser speckle due to interaction between methane gas and the passive disordered medium, concentration of the methane gas will be estimated. The proposed work will help us to explore new chip-scale gas sensing technologies based on random lasing and speckle correlation. We believe these new gas sensing technologies can further be used for other trace gases as well and will open up the possibility of remote and real time sensing. Hence, this work will contribute in detecting trace gas level in local atmosphere, controlling their emission sources and reducing the green-house effect.

II. Problem Statement/Objective

Methane and Ammonia gases both play important roles in green-house effect. Besides affecting the environment, they also impact on human health, causing kidney, lung, and mental health related diseases. Hence, sensing these gases is crucial for environmental monitoring, disease control, and industrial emission control. Most of the existing optical sensors for sensing the ammonia and methane gases suffers from low sensitivity. Moreover, they are expensive and complex. Multi-pass passive optical resonators are also used to sense these gases by increasing the interaction length. Additionally, infrared absorption bands of these gases are targeted to detect them and hence, sensing different gases requires respective wavelength sources. Optical sensors, that operate in the visible wavelength range, mainly utilize the change in the fluorescence of the probe material. Their sensing capability can be improved further by developing an intra-laser-cavity sensor. However, it involves multiple sophisticated fabrication techniques and reducing the size affects their sensitivity. Therefore, developing a chip-scale optical sensor for methane and ammonia gases with high sensitivity is challenging.

For this project, we set two major objectives as follows:

- **Objective-I:** developing an adaptive random lasing-based ammonia sensor
- **Objective-II:** developing a speckle-correlation based methane sensor

To the best of our knowledge, we aim to develop for the first time an adaptive random lasing-based ammonia sensor. Here, in objective-I, an organic dye doped polymer based random laser (PRL) will be developed in the visible wavelength range. In the first phase, the PRL will be operated without controlling its lasing modes and change in the random lasing properties will be monitored under ammonia gas environment to detect its concentration. In the next phase, the modes of the PRL will be controlled by adaptive pumping technique.

For the objective-II, we target, for the first time, to build a speckle-correlation based methane gas sensor. In this part, a highly scattering polymer diffuser will be fabricated, which will be capable of generating a fully developed speckle. Monitoring the speckle patterns under methane gas environment, we aim to sense the gas and measure its concentration.

III. Outline of tasks/Work Plan

- **Methodology**

We propose to develop an adaptive random lasing-based ammonia (NH_3) gas sensor under objective-I. For this, an organic dye doped polymer film random laser will be utilised. First, fluorescein doped PMMA polymer (FDPMMA) film will be fabricated by sol-gel process. We have selected fluorescein dye as the absorption and fluorescence emission of the dye changes in ammonia environment [21]. Moreover, it's fluorescence peak changes with concentration level of the ammonia gas. Hence, developing a random laser and exploiting this modification of fluorescence of the fluorescein dye will enhance the sensitivity of the ammonia detection by manifold. The FDPMMA film will be coated on a quartz substrate by spin-coating technique and the film will act as a planar waveguide due to high refractive index of the PMMA film compared the quartz substrate. Finally, to develop an RL, a one-dimensional random grating pattern will be fabricated on the FDPMMA film surface by electron beam lithography. Exciting the RL by a nano-second pulse laser at 532 nm wavelength will give rise to random lasing from the system. The RL will be operated in two modalities: first without controlling the random lasing modes and secondly by controlling the lasing modes. Importantly, the modes of the random laser will be controlled by wavefront shaping of the pump beam using a spatial light modulator as shown in Fig. 1. In both the cases, change in the laser spectra and as well as other random lasing properties of the FDPMMA will be monitored under ammonia gas environment to detect its concentration level.

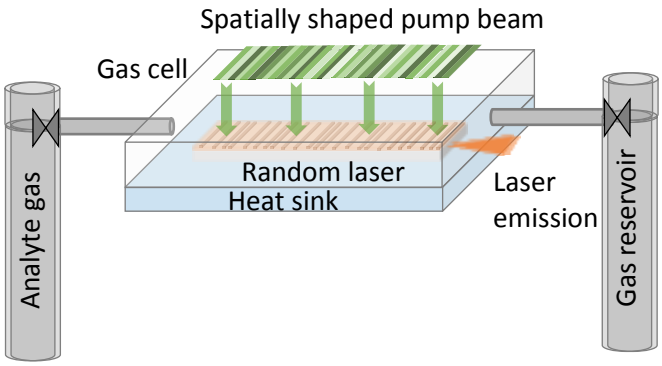

Fig. 1: Schematic of the adaptive pumping of random laser for ammonia gas sensing

For the objective-II, we target to develop a speckle correlation-based methane (CH_4) gas sensor. In this case, we will use a π-conjugated conducting polymer with TiO_2 nanoparticles to fabricate a diffuser film that will generate laser speckle due to multiple light scattering process as shown in Fig. 2. The polymer film will be coated on a quartz substrate by sol-gel and followed by spin coating techniques. Due to the absorption of methane gas, the dielectric constant of the π-conjugated conducting polymers will change [22]. As a result, scattering environment of the film will be altered and consequently, the speckle pattern will also be modified. Evaluating the spatial correlations of the modified speckle patterns under methane gas environment, its detection and concentration evaluation would be possible.

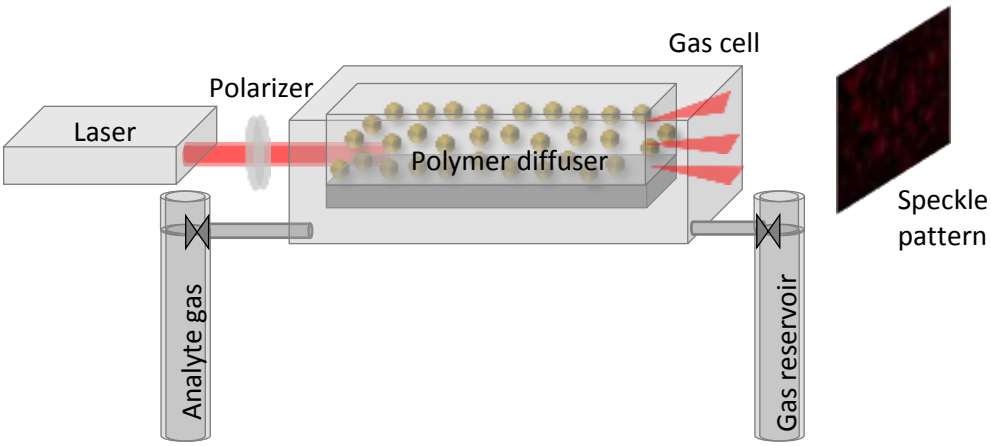

Fig. 2: Schematic of the speckle correlation-based methane gas sensing

- **Work plan/timeline**

A detailed work plan/timeline of the research has been shown in Table 1 based on the objectives of the project. The overall duration of the project has been divided into eight quarters and specific target of each quarter has explicitly been shown by blue shading. To carry out the project, we need to procure some of the major equipment such as a nano-second pulse laser, a spatial light modulator, a table-top optical spectrometer, a He-Ne laser, a CCD camera, a vibration isolation optical table and some consumables. To complete these purchases, first quarter of the project will be utilised. Experimental set up under objective-I and objective-II will be built during the second and third quarters. Additionally, the polymer diffuser and random laser will be fabricated during this time. During the third, fourth, and fifth quarters, random lasing experiment to control the lasing modes will be performed under objective-I. In the timeline from third quarter to seventh quarter, the gas sensing experiments of the objective-I and objective-II will be carried out. Moreover, experimental data obtained in these experiments will also be analysed during this time. Fourth to eight quarter time-frame will be utilised for writing conference proceedings and journal papers with the obtained results, whereas the last two quarters will be utilised to write the final project report.

Table 1: Workplan and timeline of the research project with objective-wise work summary

Activity	1st Year				2nd Year			
	Q1	Q2	Q3	Q4	Q5	Q6	Q7	Q8
Purchasing components and consumables	■							
Objective-I								
(a) Build lasing experimental set up		■	■					
(b) Fabricate polymer random laser		■	■					
(c) Random laser mode selection expt.			■	■	■			
(d) Investigate the ammonia gas sensing			■	■	■	■	■	
Objective-II								
(a) Build speckle experimental set up		■	■					
(b) Fabricate gas adsorbing polymer diffuser		■	■					
(c) Speckle-based methane sensing expt.			■	■	■	■	■	
Analysis of experimental data			■	■	■	■	■	
Writing journal papers and conference proc.				■	■	■	■	■
Writing final project report							■	■

IV. Outcome(s)

Random laser based optical sensor is an emerging area of research and we expect multiple outcomes of the research project, as listed below.

- To the best of our knowledge, we aim to develop for the first time a random laser-based lab-on-a-chip gas sensing technology which will have intellectual property right value.
- Additionally, we target to develop a simple, low cost laser speckle correlation-based gas sensing technology with improved gas selectivity and sensitivity.
- We believe that the gas sensing technologies developed in this project will improve the detection efficiency of trace gases such as ammonia (NH_3) and methane (CH_4). Early detection of these gases in the local atmosphere would help to control their possible sources and also save the human and animal lives from possible health risk. As these gases also contribute in the global warming, more efficient detection by these new sensing technologies would boost our effort to reduce the green-house effect.
- The experimental results of the research project will be presented in national and international conferences. Moreover, the results will be published in high impact Scopus/SCI indexed scientific journals and conference proceedings.
- Furthermore, at least one research student and two master's students will be trained in laser and optical gas sensing technologies.

V. Impact

As the target of the project is to develop new optical sensors for ammonia and methane gases, the outcomes of the proposed work will open up a new avenue in trace gas sensing technology. Random laser and speckle correlation-based sensing techniques developed in

this research work for sensing the ammonia and methane gases respectively will provide us new mechanisms to build a chip-scale optical gas sensor which will find wide range of applications from remote sensing to industrial gas leakage monitoring and trace gas level monitoring in urban areas. Additionally, these compact, portable, lab-on-a-chip trace gas sensors will find applications in agriculture sector, mining, fertilizer and automobile industries, and disease control in biomedical field. Moreover, they will have less response time, improved sensitivity and gas selectivity compared to the existing optical gas sensors. Although we plan to develop ammonia and methane sensors in this project, these technologies can also be used for building optical sensors for detecting other trace gases. Therefore, we believe this study will contribute in monitoring the global green-house balance and reducing air pollution related health issues. This will eventually safeguard the environment, human and wild lives.

References

[1] H. Akimoto, “Global Air Quality and Pollution,” Science **302**, 1716-1719 (2003).

[2] H. O. T. Pye *et al.*, “Effect of changes in climate and emissions on future sulfate-nitrate-ammonium aerosol levels in the United States,” J. Geophys. Res. **114**, D01205 (2009).

[3] https://www.unep.org/news-and-stories/story/methane-emissions-are-driving-climate-change-heres-how-reduce-them

[4] https://www.ccacoalition.org/en/slcps/methane

[5] R. Cisneros *et al*., “Ozone, nitric acid, and ammonia air pollution is unhealthy for people and ecosystems in southern Sierra Nevada, California,” Environmental Pollution **158** 3261-3271 (2010).

[6] S. Saggar *et al*., “A review of emissions of methane, ammonia, and nitrous oxide from animal excreta deposition and farm effluent application in grazed pastures,” New Zealand Journal of Agricultural Research **47**, 513-544 (2004).

[7] D. R. Chadwick, “Emissions of ammonia, nitrous oxide and methane from cattle manure heaps: effect of compaction and covering,” Atmospheric Environment **39**, 787-799 (2005).

[8] A. Thiruvengadam *et al*., “Unregulated greenhouse gas and ammonia emissions from current technology heavy-duty vehicles,” Journal of the Air & Waste Management Association **66**, 1045–1060 (2016).

[9] C. Brinka, C. Kroezeb, Z. Klimontc, “Ammonia abatement and its impact on emissions of nitrous oxide and methane in EuropeFPart 1: method,” Atmospheric Environment **35**, 6299–6312 (2001).

[10] C. O. Karakan, F. A. Ruiz, M. Cote, S. Phipps, “Coal mine methane: a review of capture and utilization practices with benefits to mining safety and to greenhouse gas reduction,” International Journal of Coal Geology **86**, 121-156 (2011).

[11] S. Hanf *et al*., “Fiber-Enhanced Raman Multigas Spectroscopy: A Versatile Tool for Environmental Gas Sensing and Breath Analysis,” Anal. Chem. **86**, 5278−5285 (2014).

[12] T. Töpfer *et al.*, “Room-temperature mid-infrared laser sensor for trace gas detection,” Appl. Opt. **36**, 8042-8049 (1997).

[13] M. D. Steinberg, P. Kassal, and I. M. Steinberg, “System Architectures in Wearable Electrochemical Sensors,” Electroanalysis **28**, 1149 – 1169, (2016).

[14] Y. Ma *et al*., “Trace gas sensing based on multi-quartz-enhanced photothermal spectroscopy,” Photoacoustics **20**, 100206 (2020).

[15] Z. Li, J. R. Askim, and K. S. Suslick, “The Optoelectronic Nose: Colorimetric and Fluorometric Sensor Arrays,” Chem. Rev., **119**, 231−292 (2019).

[16] J. Wojtas *et al*., “Ultrasensitive laser spectroscopy for breath analysis,” Opto−Electron. Rev. **20**, 26–39 (2012).

[17] D. S. Wiersma, “The physics and applications of random lasers”, Nature physics **4**, 359-367 (2008).

[18] B. Redding, M. A. Choma, and H. Cao, “Speckle-free laser imaging using random laser illumination,” Nature photonics **6**, 355–359 (2012).

[19] A. Boschetti *et al*., “Spectral super-resolution spectroscopy using a random laser,” Nature Photonics **14**, 177–182 (2020).

[20] K. Ge *et al*., “Large-Area Biocompatible Random Laser for Wearable Applications,” Nanomaterials **11**, 1809 (2021).

[21] S. Widmer *et al*. "Coumarin meets fluorescein: a Förster resonance energy transfer enhanced optical ammonia gas sensor," Analyst **139**, 4335-4342 (2014).

[22] T. Hong *et al.* "State-of-the-art of methane sensing materials: A review and perspectives," Trends in Analytical Chemistry **125**, 115820 (2020).

Executive Summary of Proposal

Miniaturization of Laser Speckle in Application for Non Invasive Intraocular Pressure (IOP) Monitoring for Glaucoma

Aryan Agarwal (ara005@ucsd.edu)
CEO and Co-Founder at forMED Technologies
Master of Science Student
Department of Electrical and Computer Engineering
University of California, San Diego

Intraocular pressure (IOP) is a physiological parameter that eye care providers measure to monitor and assess the progression of glaucoma, a leading cause of blindness that affects over 100 million people in the world. Since early treatment is imperative to prevent irreversible vision loss, the primary goal behind early glaucoma management is to reduce and control a patient's IOP level using prescribed eye drop medications for an indefinite period. Additionally, patients exhibit diurnal fluctuations of IOP, making the timing and close monitoring of the medication's effects essential to treatment efficacy. Without an optically-based, non-invasive technique to develop a portable solution that captures true IOP, current methods limit the frequency and accuracy of IOP measurement and thus prolongs the treatment process resulting in untimely treatment, disease progression, and financial burdens.

Elevated IOP is characterized by a buildup of aqueous humor in the anterior chamber of the eye due to increased resistance to fluid outflow. Several non-invasive optical techniques have been developed to probe the anterior chamber and extract information from aqueous humor for biomedical diagnostics and monitoring, with laser speckle imaging (LSI) being the most prominent. However, current LSI techniques are unable to measure IOP independent of measuring for the indirect effect of ocular blood flow. As a result, many LSI instrumentations either have not been developed for commercial use or optimized for precisely imaging the anterior chamber. The presence of the light scattering particles in blood also found in aqueous humor allow for the potential to use laser speckle to characterize fluid activity relating to IOP.

In this proposal, we will use optoelectronics such as laser diodes and photodetectors to develop and test an innovative, portable LSI system for measuring changes in IOP in an experimental model of ocular hypertension. The optical components are integrated and miniaturized into a benchtop headset prototype used to control, focus, and align the laser path corresponding to the anterior chamber. We consider that changes in fluid activity from outflow resistance causing pressure differences in the eye will directly impact the observed random interference pixel intensity pattern and generate repeatable speckle behavior related to IOP. As such, our approach involves generating a computational model from a series of speckle contrast values instead of determining conventional 2D maps of fluid flow. To validate this, an *ex vivo* study on enucleated rabbit eyes will be performed to establish technical feasibility followed by an *in vivo* study on live rabbits to demonstrate the accuracy and repeatability of a laser speckle-based method of measuring IOP.

Beyond demonstrating technical feasibility and validation, the proposed project will lead the innovation of traditional IOP monitoring systems and allow further research and development towards a commercially viable product. Our findings will advance the scientific understanding and engineering capabilities of laser speckle technology, broadening perspectives on ocular diseases such as glaucoma. LSI has the potential to extend clinical knowledge by revealing more about the properties of aqueous humor flow that relate to IOP levels. The proposed technology will extend applications towards at-home, remote patient monitoring devices that increase accessibility to eye care, elevate quality of life, and offer peace of mind by limiting the extent of disease progression towards blindness.

Miniaturization of Laser Speckle in Application of Non Invasive Intraocular Pressure (IOP) Monitoring for Glaucoma

Literature Review

Laser speckle imaging (LSI) visualizes the light scattering properties of particles in a moving fluid. A random interference pattern, or speckle pattern, is produced from the coherent light and scattering medium which can be captured with a photodetector. This phenomenon has been adopted to image and characterize blood flow in the skin, brain, and retina where increased flow blurs the speckle pattern and the variations in intensity responsible for speckle contrast correlates to fluid behavior [1]. However, unlike other laser-based technologies, LSI has yet to fully miniaturize and lend itself to a form factor suitable for commercialization and alternative application [2]. Such alternative applications include possible insights into blood pressure and other biomarkers. However, **c**ommon portable LSI setups in literature achieving compact and near-distance imaging are not designed and tested against ANSI laser safety standards for commercial use [3][4]. Further miniaturization of large form factor components such as He-Ne lasers, and photodetectors capable of achieving necessary signal to noise ratio (SNR) have yet to be fully implemented.

Ophthalmology represents the largest research opportunity for laser speckle imaging (LSI). Thus far, LSI has been implemented especially in the development of real-time perfusion measurements and hemodynamic monitoring of choroidal circulation in the eye [5]. A key dynamic fluid within the eye, the aqueous humor causes changes in respect to change in eye pressure. The porous nature of the trabecular meshwork creates resistance to aqueous humor outflow which produces a pressure gradient for fluid movement [6].

Therefore, utilization of laser speckle is feasible in application within the eye, as can be seen in studies primarily focusing on blood supply. One study showcased how the frequency shift of the reflected speckle pattern at the pulsating sclera/iris due to blood supply to the eye is indirectly correlated to IOP changes [7]. Other methods have used laser speckle to determine IOP indirectly from ocular perfusion pressure and mean arterial pressure by evaluating the ocular blood flow in the retina and measuring blood pressure separately [8]. Thus, current LSI techniques are unable to measure IOP independent of the indirect effect of ocular blood flow. Although laser speckle has yet to be fully investigated within the anterior chamber, several non-invasive optical techniques, such as OCT, have been developed to probe the anterior chamber and extract information from aqueous humor for biomedical diagnostics and monitoring [9][10][11]. For instance, glucose is a major optical rotatory component in aqueous humor that has allowed glucose concentration measurements by passing light through the cornea and across the anterior chamber of the eye [11]. As such, the presence of additional light scattering particles also found in blood, such as albumin protein or ascorbic acid, in aqueous humor allow for the potential to use laser speckle to characterize fluid activity relating to IOP [6].

The diagnostic and clinical potential of aqueous humor activity, outflow facility can provide valuable insight into those that suffer from glaucoma, a degenerative eye disease that can be tracked through intraocular pressure (IOP) or eye pressure. In primary open-angle glaucoma (POAG), abnormalities in the drainage pathway increase resistance to fluid outflow, disrupting normal aqueous humor flow in the anterior chamber and elevating IOP [12]. To mediate this, eye drop medications can limit the production or promote the outflow of aqueous humor.

Therefore, it is imperative for any laser eye device to be portable and within a suitable form factor for clinical and patient use. However, infrared laser diodes implemented in the optical designs of commercial LSI products for retinal use exceed the target visible wavelength speculated to image aqueous humor [13][14]. Furthermore, previous work deriving information from aqueous humor activity is limited due to its significantly lower flow rate (3 μL/min) and unknown optical properties compared to conventional fluids such as retinal blood (~45 μL/min) [8]. Although developments towards portable and handheld LSI devices have been made to image blood flow, this project will introduce the first portable, miniaturized LSI system intended for use in clinical and athome settings [15].

Problem Statement and Objective

Glaucoma affects over 100 million people in the world which, when left untreated, leads to irreversible blindness. IOP is the only physiological parameter measured to assess the progression and adjust the treatment of glaucoma. Since early treatment is imperative to prevent irreversible vision loss, the primary goal for glaucoma management is to control IOP levels using prescribed eye drop medications for an indefinite period. However, current methods of IOP measurement are not repeatable outside the clinical setting and patients exhibit diurnal fluctuations of IOP, making the timing and close monitoring of the medication's effects essential to treatment efficacy.

Normal IOP measured with traditional methods ranges between 12-21 mmHg with measurements over 30 mmHg indicating a need for glaucoma treatment [16]. These methods rely on the force needed to flatten a fixed corneal area rather than the balance of aqueous humor production and outflow that is attributed to true IOP. Current IOP measuring devices operate with the assumption that pressure is uniformly distributed in the anterior chamber [17]. As a result, varying central corneal thickness, corneal biomechanical properties, and operator experience have a significant effect on IOP accuracy [18].

With patients experiencing peak IOP outside of the doctor's office, current infrequent IOP monitoring prevents proper assessment of medication efficacy, resulting in untimely treatment, preventable disease progression, and increased financial burdens. For instance, one study showed that 33% of newly diagnosed patients develop blindness when treated with standard methods [19]. Furthermore, medication adjustments delay treatment and increase optic nerve damage by 17% [20]. As a result, annual costs related to glaucoma management, medication adjustments, recurring visits, surgical intervention, and postoperative care increase from $623 to $2,533, on average, per patient [21]. Interviews with eye care professionals further highlight the clinical value daily IOP trends hold for determining the right combination of treatments needed to prevent blindness compared to the single, discrete IOP measurements doctors currently rely on.

Remote digital healthcare, demand for monitoring changes in IOP over a longer duration, and a rising glaucoma population drive the need for a disruptive solution to glaucoma management. The landscape of solutions offering more frequent IOP monitoring include rebound tonometry, microsensor contact lens sensors, and analysis of the ocular vascular pressure response from applying air pressure. However, since only 70-75% of patients successfully complete a single measurement when using rebound tonometry at home, the user-dependency of the HOME increases the difficulty of obtaining diurnal IOP measurements, hindering flexible and frequent monitoring [22]. Furthermore, recurring purchasing of contact lenses can become a financial burden to patients while sensitivity and discomfort levels reduce peace of mind during treatment [23]. Methods requiring external pressure inadvertently create artificial pressures in the eye and provide inaccurate readings [24]. Thus, an optically-based, non-invasive IOP monitoring system will provide patients with an easy-to-use solution that prioritizes patient operability, comfortability, and accuracy with more frequent and flexible monitoring options.

We propose the development of a non-invasive IOP monitoring system using a novel application of LSI optoelectronics that characterizes the fluid activity in the anterior chamber to detect and measure changes in IOP in an experimental model of elevated ocular hypertension. Our innovative approach considers that the changes in the scattering of light from disrupted aqueous humor flow in a glaucomatous eye due to increased outflow resistance will directly impact the observed speckle pattern and generate repeatable speckle behavior that can be directly correlated with different IOP levels. Whereas conventional methods create 2-D maps of fluid flow according to speckle contrast, our approach involves a novel technique of computing a single speckle contrast value from millions of pixel intensity data from a set of images. The innovative LSI system implemented in this proposal consists of a laser diode that outputs a diverging beam through a plano-convex lens for collimation followed by a neutral density filter and two rotating silver right angle prism mirrors. We have reduced risks associated with this challenge by validating proof of concept of the technology in a controlled, *ex vivo* environment. This proposal aims to build upon our preliminary *ex vivo* experiments on rabbit eyes to better understand the relationship between speckle contrast and IOP while evaluating the accuracy and repeatability of a laser-speckle derived model for IOP measurement *in vivo*.

Outline of Tasks and Work Plan

Aim 1

Rationale: To overcome initial challenges associated with precisely imaging the anterior chamber, optically measuring aqueous humor activity, and observing changes in speckle contrast with changes in fluid pressure to validate feasibility and commercial potential. A rabbit eye *ex vivo* system with simulated aqueous humor inflow and natural TM outflow allows for fine and repeatable changes in induced pressure for validating the proposed IOP measurement system. In this controlled environment, adjustments to the optical system can be more easily made to optimize speckle contrast. A rabbit model is considered the standard animal model by the ophthalmic community due to the eyes' similar size and structure to humans, making the results more readily translatable to humans. Additionally, for our purposes, the larger volume of aqueous humor present in rabbit eyes provides a favorable sized region of interest for LSI [25].

Methods: The setup for Aim 1 is adopted from similar IOP measurement experiments [26][27]. Enucleated rabbit eyes are secured to position and align the anterior segment within our prototype headset and with the laser path. A three-way valve is connected to (a) an infusion syringe inserted into the anterior chamber, (b) a variable-height manometer reservoir of artificial aqueous humor, and (c) a pressure transducer measuring IOP in the eye. By raising the reservoir to a known height above the eye and opening the infusion port, the force of gravity allows passive diffusion from the reservoir into the eye, mimicking the natural production and flow of aqueous humor and inducing IOP within the anterior chamber. Data will be collected across 10-50 mmHg to mimic normal and elevated human IOP values.

We have programmed a custom GUI in Python that (1) calibrates the camera's position in the headset to focus the anterior chamber and the center the eye in the field of view, (2) controls the direction and orientation of the optical pathway to enable the laser to illuminate the anterior chamber, (3) adjusts the camera's position to ensure the speckle pattern encompasses the field of view, (4) validates camera settings (i.e. exposure time and frame rate) to ensure the pixel intensities generates a Cauchy distribution, and (5) records IOP measurements from the pressure transducer. The infusion port for aqueous humor is closed when the transducer reading exceeds ±1 mmHg the target setpoint. Once target pressure stabilizes, 10 seconds of laser speckle images (~150 frames) is collected. After collecting 3 additional, independent 10 second image datasets (n=4) at a given pressure, all ports are closed. The process is repeated for each subsequent pressure reading.

Success Criteria: Data analysis will calculate speckle contrast from an aggregate of pixel intensities from each trial and determine statistical significance by a strong correlation with a polynomial fit between speckle contrast and pressure and a Kruskal-Wallis test. A successful Aim 2 identifies a significant statistical relationship ($R^2 > 0.9$) between speckle contrast and IOP at a maximum sensitivity of 3 mmHg according to ANSI Z80.10 and a 5% significance level ($p < 0.05$).

Aim 2

Rationale: To conduct *in vivo* rabbit testing to evaluate the accuracy and repeatability of a laser speckle-derived model for IOP measurements. *In vivo* testing relies on the animal's natural flow patterns while allowing for direct contact tonometry as a reference for IOP accuracy. Rebound tonometry by the iCare TonoVet will be used for initial IOP comparison given its demonstrated accuracy, reproducibility in rabbits, and minimal learning curve [28][29]. This study will offer minute manipulation of IOP by corticosteroid administration to investigate IOP measurement sensitivity, while maintaining relevance to humans. Corticosteroids have previously shown to induce ocular hypertension by altering the cellular structure of the TM which, in turn, increases aqueous humor outflow resistance and IOP, serving as a representative animal model for POAG [30][31]. Betamethasone by subconjunctival injection to the eye offers stable and sustained elevations in IOP amongst rabbits based on prior studies [32][33][34].

Methods: Funding will allow for industry-sponsored research UC Irvine's Dr. Matthew Brenner. We will obtain an approved UCI-IACUC protocol that covers the live rabbit study involving corticosteroid administration and IOP measurements under anesthesia. New Zealand white rabbits

(Charles River Laboratories) will be kept at the UCI vivarium where University Laboratory Animal Resources will be responsible for veterinary and husbandry services. Ten rabbits at the 7-10 week age, the developmental period where prior studies demonstrated effective corticosteroid-induced ocular hypertension, will be used for the study [35][36]. Left eyes of the first group (n=5) will be subconjunctivally injected with 6 mg betamethasone twice a week for 4 weeks to progressively elevate IOP, with untreated right eyes as the control. Prior rabbit studies using the same 12 mg total dosage of betamethasone per week resulted in about 30 mmHg measured IOP by week 4 [32][33]. Lubricating eye drops will be given while rabbits are under anesthesia to avoid corneal dehydration [37]. Body weight will be recorded alongside IOP to monitor the systemic effects of the steroid on the animals.

IOP will be measured every 5 days at 8 AM throughout the 4 week treatment by both the TonoVet and LSI to account for diurnal fluctuations and capture peak IOP after waking. To reduce discomfort during TonoVet measurements, rabbits will be given topical anesthesia (2% lidocaine hydrochloride) on the eyes. Prior to corticosteroid injections and IOP measurements, rabbits will be anesthetized by intramuscular injection of ketamine (10 mg/kg body weight) and xylazine (2 mg/kg body weight) followed by 3% isoflurane inhalation maintenance to limit motion during the procedures [38][39]. The anesthetized rabbits will be placed on a stage for alignment of the anterior chamber with the LSI system. Rabbits will be recovered with atipamezole of equal dosage to ketamine and xylazine. The data collected throughout the treatment period will generate a best fit model correlating LSI speckle contrast to IOP via TonoVet similar to Aim 2. Dr. Brenner's lab personnel will handle rabbit anesthetization, while Aguas will administer the corticosteroid therapy and conduct TonoVet and LSI measurements.

Success Criteria: A second experiment with another set of 5 rabbits will be conducted to assess the accuracy and reliability of the correlation model. Rabbits will be treated with the same betamethasone treatment over 4 weeks, and both TonoVet and LSI measurements will be taken at the same frequency. Using the LSI correlation model, calculated IOP will be compared to measured TonoVet IOP at each timepoint (n=120) and evaluated for statistical significance using a Wilcoxon Signed Rank (WSR) test and intraclass correlation coefficient (ICC). A successful Aim 3 will demonstrate the accuracy of our LSI method in measuring IOP by failing to reject the null hypothesis of zero median at a 5% significance level ($p > 0.05$) and achieving an ICC greater than 0.75 indicating good reliability.

Outcomes

By achieving the objectives detailed here, we will demonstrate the accuracy of our proposed method and the merit of portable optics for at-home, glaucoma management. Our efforts will produce a model to measure IOP in rabbit eyes using an optimized optical design implementing LSI. As a result, the proposed innovation will improve the imaging precision, leverage the simple instrumentation of laser speckle technology, and extend its application to measure high-resolution flow changes in the anterior chamber related to IOP levels. The optical system's specifications will be proven safe for use in humans, allowing for further research and development towards a commercially viable product. The experimental results will showcase how a strong, statistically significant correlation model is generated to determine IOP with clinical accuracy, thus validating the method's technical feasibility. Results from the research will be disseminated through patents, publications in scientific journals, and collaboration with the ophthalmology industry.

Furthermore, completion of the work plan in this proposal will enable us to focus on developing a final prototype that achieves high spatial imaging precision of the anterior chamber. This involves miniaturizing optical components within an enclosed device and automating the measurement process. By incorporating LSI to measure IOP, we will create a portable solution for glaucoma management that provides more accuracy and meaningful information related to eye health for patients and doctors. Obtaining and demonstrating the success criteria to our clinical mentor, Dr. Ken Lin, a board-certified ophthalmologist at the Gavin Herbert Eye Institute and clinical professor at UC Irvine, will garner support for human subject testing for regulatory clearance through the clinic.

Impact

Our findings will advance the scientific understanding and engineering capabilities of laser speckle technology, leading to new and groundbreaking methods in IOP monitoring that broadens perspectives on ocular diseases such as glaucoma. LSI has the potential to extend clinical knowledge by revealing more about the properties of aqueous humor flow that relate to IOP levels. The integrated optical components for which the proposed technology is validated will reflect the final design of an at-home, non-invasive IOP monitoring system. The commercialization of the intended product will increase accessibility to eye care, elevate quality of life, and offer peace of mind for glaucoma patients. The inability to monitor diurnal fluctuations of IOP has inhibited doctors from better understanding its implication on medication efficacy and glaucoma progression, thus preventing effective disease management. A proven functional prototype providing more frequent IOP data will advance the health and welfare of the American public by promoting better health outcomes that limit the extent of disease progression towards blindness.

The commercialization of our product enhances the emerging infrastructure of remote patient monitoring services and virtual care in the American healthcare system and extends healthcare access to underserved populations. Moreover, our product can improve glaucoma management for surgically treated late-stage patients for whom IOP is the only indicator of proper recovery and a successful procedure. These patients are more sensitive to standard, direct contact IOP measuring methods and thus, our non-invasive monitoring method will enable quality care for postoperative treatment. During the postoperative period, frequently measured IOP can provide glaucoma surgeons with early phase success of the procedure and prevent frequent visits to clinics for postoperative evaluation. Additionally, by increasing eye care accessibility while reducing socio-economic burdens, our proposed technology can produce similar positive societal outcomes in the lives of patients in developing countries. We aim to revolutionize the delivery of eye care and impact the lives of those struggling with glaucoma by providing clinicians with the valuable information to enhance the treatment process and make eye care more accessible despite socio-economic burdens.

Another key impact stemming from this project includes the ability to lower the overall cost of optically based medical devices. Normal devices within the clinic, including retinal OCT scanners and fundus cameras, require a high barrier of entry due to initial costs and ongoing maintenance. The ability to leverage the low costs of components for laser speckle imaging, can further improve accessibility and awareness of optically based devices not only within the ophthalmic space, but also in other biomarker areas such as non-invasive blood pressure or hydration studies.

Support for the work outlined in the proposal will enable further seed funding from accelerator programs and angel investors that will aid in reducing associated technical and commercial risks for rapid product development. Furthermore, the success of forMED as a company will have a direct impact on regional economic development in optical ocular technology. Glaucoma currently costs the US healthcare system $2.5 billion annually [40]. By offering an affordable, non-invasive solution, patients reduce healthcare costs related to extra examination visits, medication changes, and surgical intervention.

References

[1] D. A. Boas and A. K. Dunn, "Laser speckle contrast imaging in biomedical optics," *Journal of Biomedical Optics*, vol. 15, no. 1, p. 011109, Jan. 2010.

[2] J. O'Doherty, P. McNamara, N. T. Clancy, J. G. Enfield, and M. J. Leahy, "Comparison of instruments for investigation of microcirculatory blood flow and red blood cell concentration," *Journal of Biomedical Optics*, vol. 14, no. 3, p. 034025, May 2009.

[3] L. M. Richards, S. M. Kazmi, J. L. Davis, K. E. Olin, and A. K. Dunn, "Low-cost laser speckle contrast imaging of blood flow using a webcam," *Biomedical Optics Express*, vol. 4, no. 10, p. 2269, Sep. 2013.

[4] "American National Standard for Safe Use of Lasers." Laser Institute of America, Orlando, 2007.

[5] W. Heeman, W. Steenbergen, G. M. van Dam, and E. C. Boerma, "Clinical applications of Laser Speckle Contrast Imaging: A Review," *Journal of Biomedical Optics*, vol. 24, no. 08, p. 1, Aug. 2019.

[6] D. W. Abu-Hassan, T. S. Scott, and M. J. Kelley, "The Trabecular Meshwork: A Basic Review of Form and Function," *Journal of Ocular Biology*, vol. 2, no. 1, May 2014.

[7] I. Margalit, Y. Beiderman, A. Skaat, E. Rosenfeld, M. Belkin, R.-P. Tornow, V. Mico, J. Garcia, and Z. Zalevsky, "New method for remote and repeatable monitoring of intraocular pressure variations," *Journal of Biomedical Optics*, vol. 19, no. 2, p. 027002, Feb. 2014.

[8] C. Iwase, T. Iwase, R. Tomita, T. Akahori, K. Yamamoto, E. Ra, and H. Terasaki, "Changes in pulse waveforms in response to intraocular pressure elevation determined by laser speckle flowgraphy in healthy subjects," *BMC Ophthalmology*, vol. 21, no. 1, Aug. 2021.

[9] Hwang, Yih-Shiou et al. "Noncontact Optical Measurement of Aqueous Humor Glucose Levels and Correlation with Serum Glucose Levels in Rabbit." Biosensors vol. 11,10 387. 13 Oct. 2021, doi:10.3390/bios11100387

[10] Malik, Bilal H., and Gerard L. Coté. "Characterizing Dual Wavelength Polarimetry through the Eye for Monitoring Glucose." Biomedical Optics Express, no. 5, The Optical Society, Oct. 2010, p. 1247. Crossref, doi:10.1364/boe.1.001247.

[11] John, Pauline, et al. "Glucose Sensing in the Anterior Chamber of the Human Eye Model Using Supercontinuum Source Based Dual Wavelength Low Coherence Interferometry." Sensing and Bio-Sensing Research, Elsevier BV, Apr. 2019, p. 100277. Crossref, doi:10.1016/j.sbsr.2019.100277.

[12] G. Heiting, "What is primary open-angle glaucoma?," *Primary Open-Angle Glaucoma: Causes, Risks, and Treatment*, 15-Sep-2022. [Online]. Available: https://www.allaboutvision.com/conditions/primary-open-angle-glaucoma/.

[13] K.-A. Cho, A. Rege, Y. Jing, A. Chaurasia, A. Guruprasad, E. Arthur, and D. Cabrera DeBuc,

"Portable, non-invasive video imaging of retinal blood flow dynamics," *Scientific Reports*, vol. 10, no. 1, Nov. 2020.

[14] G. Calzetti et al, "Assessment of choroidal neovascularization perfusion: A pilot study with Laser Speckle Flowgraphy," *Translational Vision Science & Technology*, vol. 9, no. 5, p. 9, Apr. 2020.

[15] B. Lertsakdadet, C. Dunn, A. Bahani, C. Crouzet, and B. Choi, "Handheld motion stabilized laser speckle imaging," *Biomedical Optics Express*, vol. 10, no. 10, p. 5149, 2019.

[16] S. S. Ahmad, "Glaucoma suspects: A practical approach," *Taiwan Journal of Ophthalmology*, vol. 8, no. 2, p. 74, 2018.

[17] J. Bader, M. Zeppieri, and S. Havens, "Tonometry," *National Library of Medicine*, Jan-2022. [Online]. Available: https://www.ncbi.nlm.nih.gov/books/NBK493225/.

[18] P. Brusini, M. L. Salvetat, and M. Zeppieri, "How to measure intraocular pressure: An updated review of various tonometers," *Journal of Clinical Medicine*, vol. 10, no. 17, p.3860, Aug. 2021.

[19] K. Mansouri, R. N. Weinreb, and F. A. Medeiros, "Is 24-hour intraocular pressure monitoring necessary in glaucoma?," *Seminars in Ophthalmology*, vol. 28, no. 3, pp. 157–164, 2013.

[20] C. H. Ho and J. K. Wong, "Role of 24-hour intraocular pressure monitoring in glaucoma management," *Journal of Ophthalmology*, vol. 2019, pp. 1–13, 2019.

[21] M. G. Hattenhauer, D. H. Johnson, H. H. Ing, D. C. Herman, D. O. Hodge, B. P. Yawn, L. C. Butterfield, and D. T. Gray, "The probability of blindness from open-angle glaucoma," *Ophthalmology*, vol. 105, no. 11, pp. 2099–2104, Nov. 1998.

[22] S. Nakakura, "Icare® rebound tonometers: review of their characteristics and ease of use," Clinical Ophthalmology, vol. Volume 12, pp. 1245–1253, May 2018.

[23] G. E. Dunbar, B. Shen, and A. Aref, "The sensimed triggerfish contact lens sensor: Efficacy, safety, and patient perspectives," Clinical Ophthalmology, vol. Volume 11, pp. 875–882, May 2017.

[24] N. A. Townsend and J. J. McSoley, "The Do's and Don'ts of measuring IOP," *Review of Optometry*, 15-May-2015. [Online]. Available: https://www.reviewofoptometry.com/article/the-dos-and-donts-of-measuring-iop.

[25] M. Stastna, A. Behrens, P. J. McDonnell, and J. E. Van Eyk, "Analysis of protein composition of rabbit aqueous humor following two different cataract surgery incision procedures using 2-DE and LC-MS/MS," *Proteome Science*, vol. 9, no. 1, p. 8, Feb. 2011.

[26] K. Nagae, H. Sawamura, and M. Aihara, "Investigation of intraocular pressure of the anterior chamber and vitreous cavity of porcine eyes via a novel method," *Scientific Reports*, vol. 10, no. 1, Nov. 2020.

[27] J. C. Millar, A. F. Clark, and I.-H. Pang, “Assessment of aqueous humor dynamics in the mouse by a novel method of constant-flow infusion,” *Investigative Ophthalmology & Visual Science*, vol. 52, no. 2, pp. 685–694, Feb. 2011.

[28] C. J. Bertens et al, “Repeatability, reproducibility, and agreement of three tonometers for measuring intraocular pressure in rabbits,” *Scientific Reports*, vol. 11, no. 1, Sep. 2021.

[29] M. Chen et al, “Comparability of three intraocular pressure measurement: Icare pro rebound, non-contact and Goldmann applanation tonometry in different IOP Group,” *BMC Ophthalmology*, vol. 19, no. 1, Nov. 2019.

[30] D. R. Overby and A. F. Clark, “Animal models of glucocorticoid-induced glaucoma,” *Experimental Eye Research*, vol. 141, pp. 15–22, Jun. 2015.

[31] I. Rybkin et al, “Model Systems for the study of steroid-induced IOP elevation,” *Experimental Eye Research*, vol. 158, pp. 51–58, 2017.

[32] L. Bonomi et al, “Experimental corticosteroid ocular hypertension in the rabbit,” *Albrecht von Graefes Archiv für Klinische und Experimentelle Ophthalmologie*, vol. 209, no. 2, pp. 73–82, 1978.

[33] J. Melena, J. Santafé, and J. Segarra, “Betamethasone-induced ocular hypertension in rabbits,” *Methods Find Exp Clin Pharmacol*, vol. 19, no. 8, pp. 553–558, 1997.

[34] D. E. Hester, P. N. Trites, R. L. Peiffer, and V. Petrow, “Steroid-induced ocular hypertension in the rabbit: A model using subconjunctival injections,” *Journal of Ocular Pharmacology and Therapeutics*, vol. 3, no. 3, pp. 185–189, 1987.

[35] Y. Qin et al, “A rabbit model of age-dependant ocular hypertensive response to topical corticosteroids,” *Acta Ophthalmologica*, vol. 90, no. 6, pp. 559–563, Nov. 2010.

[36] P. A. Knepper, M. Breen, H. G. Weinstein, and L. J. Blacik, “Intraocular Pressure and Glycosaminoglycan Distribution in the Rabbit Eye: Effect of age and dexamethasone,” *Experimental Eye Research*, vol. 27, no. 5, pp. 567–575, Nov. 1978.

[37] V. P. Nguyen, Y. Li, W. Zhang, X. Wang, and Y. M. Paulus, “High-resolution multimodal photoacoustic microscopy and optical coherence tomography image-guided laser induced branch retinal vein occlusion in living rabbits,” *Scientific Reports*, vol. 9, no. 1, 2019.

[38] K. S. Lim, S. S. Wickremasinghe, M. F. Cordeiro, C. Bunce, and P. T. Khaw, “Accuracy of Intraocular Pressure Measurements in New Zealand White Rabbits,” *Investigative Ophthalmology & Visual Science*, vol. 46, no. 7, pp. 2419–2423, Jul. 2005.

[39] J. J. Chae, M. R. Prausnitz, and C. R. Ethier, “Effects of General Anesthesia on Intraocular Pressure in Rabbits,” *Journal of the American Association for Laboratory Animal Science*, vol. 60, no. 1, pp. 91–95, Jan. 2021.

[40] Y. N. Covin, D. Laroche, and M. M. G. Olivier, “The societal costs of blindness from uncontrolled glaucoma,” *Glaucoma Today*, Aug-2014. [Online]. Available: https://glaucomatoday.com/articles/2014-july-aug/the-societal-costs-of-blindness-from-uncontrolled-glaucoma.

Fully-integrated implantable light-sheet microscope

PI: Aseema Mohanty, Tufts University

Challenge: Health Category

High-resolution microscopy currently relies on table-top optics which are large, bulky, slow, and expensive. Light-sheet microscopy belongs to a class of microscopy techniques that decouple the light excitation from the optical readout gaining significant resolution in the axial dimension, less photodamage, and faster imaging of large volumes. However, these techniques require large objectives and beam shaping apparatus including spatial light modulators and galvo-mirrors that ultimately prohibit their use in practical or mobile settings that require portability and lower costs. In addition, these techniques are limited by optical scattering at visible wavelengths which limits specimen that can be studied to transparent, artificially cleared, small volumes and short depths (typically <100 μm). For eventual point-of-care use for medical diagnostics, these systems should ideally be handheld and not rely on expensive, bulky table-top optics and powerful lasers while being compatible with larger scattering tissues.

Objective and Outcomes:

Here we propose a fully-integrated light-sheet microscope based on a hybrid platform combining visible wavelength photonic integrated circuits (PIC), an integrated laser, and 3D polymer micro-optics to extend imaging depths by up to 100 times in scattering tissue. Recent advances in silicon nitride PICs have shown operation down to 400 nm and active control of optical modulators, switching networks, and phased arrays for beam routing and beamsteering. This platform can be thinned down to thicknesses below 50 μm and has been demonstrated for implantable neural probes. Combined with a tunable self-injection locked microresonator-assisted diode laser, we will demonstrate an actively switched light-sheet for multi-plane excitation and detection through a 3D polymer waveguide and lens system all fabricated on the same chip. The implantable microscope will be mechanically and optically tested in brain phantoms of fluorescent bead embedded agarose to demonstrate readiness for scattering brain tissue and in-vivo neuroscience experiments. There will be several key outcomes with the success of the project: 1) fully-integrated biocompatible visible PIC with laser and electrical control, 2) implantable microscope reaching depths beyond multiphoton imaging, 3) low-power optical switching at visible wavelengths, 4) novel device structures for beam shaping.

Capabilities and Applications:

The implantable microscope will be able to measure down to depths of approximately 1 cm, which is 100 times that of a traditional light-sheet microscope in scattering tissue. The chip-generated light-sheet allows for cellular-scale axial sectioning that can be scanned in depth at kHz speeds. The device can be used for time-multiplexed multi-plane imaging. Short-term applications of the device will be for in-vivo deep brain imaging with neuroscience collaborators at Tufts University School of Medicine to study neural circuit dynamics related to mood disorders, epilepsy, and other neuropsychiatric diseases. Many of these disorders are studied in a mouse model, but the brain regions involved lie below what can be reached with multiphoton imaging (<1 mm). The device will be compatible with the open-source Miniscope allowing fast adoption within the neuroscience and biomedical imaging communities. Long-term applications of this type of device will be for point-of-care imaging. Currently, high resolution imaging involves taking a biopsy and sending it out to an imaging specific lab. However, with the move towards portable, handheld, and low-cost technologies such as the proposed device, these imaging devices could be made more accessible to medical facilities and be used in real-time with patients. This would be transformative for healthcare, taking a technique that is typically used in research to understand disease to real-world heath monitoring potentially for medical diagnostics.

Fully-integrated chip-scale light-sheet microscope

PI: Aseema Mohanty, Tufts University

Introduction:

High-resolution microscopy currently relies on table-top optics which are large, bulky, slow, and expensive. Light-sheet microscopy belongs to a class of microscopy techniques that decouple the light excitation from the optical readout gaining significant resolution in the axial dimension, less photodamage, and faster imaging of large volumes[1–3]. However, these techniques require large objectives and beam shaping apparatus including spatial light modulators and galvo-mirrors that ultimately prohibit their use in practical or mobile settings that require portability and lower costs. In addition, these techniques are limited by optical scattering at visible wavelengths which limits specimen that can be studied to transparent, artificially cleared, small volumes and short depths (typically <100 μm). For eventual point-of-care use for medical diagnostics, these systems should ideally be handheld and not rely on expensive, bulky table-top optics and powerful lasers while being compatible with larger scattering tissues.

State-of-the-art light-sheet using table-top optics is limited by scattering of visible light (400-800 nm), where fluorescent probes for imaging lie[1–3]. The imaging field-of-view has been increased to about 2 times using two-photon light sheet reaching depths of about 200-300 μm by leveraging near-infrared excitation wavelengths which have a longer penetration depth[4]. However, the imaging depth here is still limited by the scattering of visible wavelengths that need to be detected by the detection objective (see Fig. 1a). To date, there have been two demonstrations of implantable light-sheet devices using photonic integrated circuits (PICs)[5,6]. These demonstrations show the possibility of having an ultrathin minimally-invasive implantable probe to excite tissue. However, the depth and portability of these devices have been limited because they still require a table-top imaging objective and optical setup for detection. This means the imaging depth is still fundamentally limited by the scattering of light. In addition, the reconfiguration of these devices was limited to table-top optical devices to reconfigure light to an array of emitters on a passive chip. The limitations stem from challenges facing visible PICs in general related to losses, scattering, and reconfigurability as the field is fairly nascent.

There have been advances in the field of active visible PICs by Mohanty and several other groups as emerging applications such as optogenetics neural stimulation, biomedical imaging, and atoms, trapped-ions, and other solid-state quantum information systems require wavelengths down to the ultraviolet range. Mohanty demonstrated the first active switching of blue light using a silicon nitride PIC and used it for deep-brain in-vivo neural stimulation and recording[7]. Since the first demonstration of this platform, Mohanty and collaborators have used this platform to demonstrate wide-angle, high resolution beam steering, low-power optical modulators, and tunable hybrid integrated lasers at visible wavelengths[8–10]. The silicon nitride platform has many advantages useful for useful for future biological devices: 1) foundry-compatible for future widespread dissemination, 2) transparent down to 405 nm with mode engineering covering the typical biological stimulation and imaging spectrum, 3) does not require complex wafer bonding, and 4) kHz reconfiguration speeds by thermos-optic tuning which is 100 times faster than the MHz-to-Hz frame rates of spatial light modulators and galvo-mirrors typically used. Although, the reconfiguration speeds are quite a bit slower than electro-optic platforms such as lithium niobate, the thermo-optic platform has advantages in its CMOS compatibility and simple fabrication methods for low-cost, wide-spread future adoption. A unique issue at visible wavelengths is power handling which is necessary to deliver enough power to a large array of emitters. Silicon nitride is attractive for this reason as it does not suffer from photorefractive effect present in platforms like lithium niobate which limit total optical power to the mW-range[11]. Full system integration and large-scale visible PICs are active areas of research.

Objective:

Here we propose a fully-integrated light-sheet microscope based on a hybrid platform combining visible wavelength photonic integrated circuits (PIC), an integrated laser, and 3D polymer micro-optics to extend imaging depths by up to 100 times in scattering tissue. Recent advances in silicon nitride PICs have shown operation down to 400 nm and active control of optical modulators, switching networks, and phased arrays for beam routing and beamsteering. This platform can be thinned down to thicknesses below 50 µm and has been demonstrated for implantable neural probes[12]. Combined with a tunable self-injection locked microresonator-assisted diode laser, we will demonstrate an actively switched light-sheet for multi-plane excitation and detection through a 3D polymer waveguide and lens system all fabricated on the same chip. Tunable, narrow-linewidth lasers at visible wavelengths are typically bulky and expensive making them difficult to adopt for biological applications. However, our solution allows for low power WDM switching with a cheap Fabry-Perot diode and PIC.

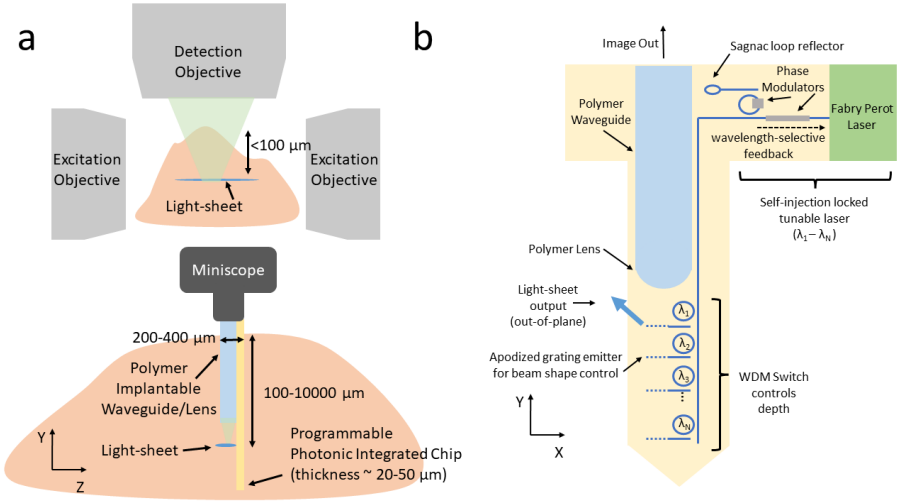

Figure 1 Overview of the fully-integrated implantable light-sheet microscope. a) Comparison of imaging with a traditional light-sheet microscope (top) and the proposed implanted microscope (bottom). The traditional microscope uses orthogonal objectives to generate the light sheet which generates fluorescence that is captured by the detection objective. The proposed microscope uses a visible PIC to switch light-sheets aligned to polymer waveguide and lens system that carries the image to the Miniscope. b) Schematic of visible PIC with self-injection locked tunable laser for sweeping wavelength redirecting light to depth-defined by wavelength-division multiplexing (WDM) switch. Each microresonator redirects light to apodized grating emitters outputting beams shaped for light-sheet generation. The polymer lens and waveguide system detects fluorescence from the light-sheet.

The proposed device uses a visible PIC at 473 nm (key optogenetic stimulation and fluorescent imaging wavelength) to switch light-sheets aligned to a polymer waveguide lens system that transmits the image to a Miniscope (see Fig. 1). For excitation, the visible PIC has two components: 1) a tunable hybrid self-injection locked laser that can sweep wavelength and 2) a microresonator-based wavelength-division multiplexing switch that switches light based on wavelength. This will route light to grating emitters that can produce shaped beams including Gaussian and Bessel-beam light-sheets that will be optimized for highest axial resolution. For detection, the light sheet will be aligned within the depth of focus of the polymer waveguide and lens. The image will be guided through this system to a Miniscope. The Miniscope is a miniaturized microscope that is actively being used by neuroscience researchers to study neural circuit dynamics in-vivo in freely-behaving mice[13]. The Miniscope is open-source, so ensuring compatibility with this technology will allow for easier and more widespread adoption in the neuroscience and biomedical imaging community. Our goal is to image at depths of 1 cm in scattering mediums as this would push the imaging depth beyond what can be done with multiphoton imaging (<1 mm) (see **Impact**)[14]. Further depths may also be possible, but will be limited by mechanical robustness of the device.

Work Plan:
The work plan is divided into three main tasks: 1) switchable light-sheet PIC design, fabrication, and testing, 2) passive 3D polymer implantable lens and laser integration, and 3) preparation and characterization for in-vivo imaging. Below we outline the strategies and risk-management plan for each component. The three tasks will be implemented in parallel (see timeline of tasks at the end of **Work Plan**).

Task 1: Switchable light-sheet PIC design, fabrication, and testing
Subtask 1.1: Light-sheet beam design and fabrication
Light-sheets will be designed to fill the entire field-of-view of the polymer waveguide lens system. Grating emitters with controlled partial-etching and apodization will be used to shape beam outputs. Gaussian and Bessel-beams will be targeted initially to explore tradeoffs in terms of footprint on the chip vs. beam waist characteristics. The beams will be optimized to deliver localized light with minimal out-of-focus light to ensure high resolution. The target beam waists will be from 1-20 μm for cellular and potentially sub-cellular axial resolution. The beam waist and spatial extents will be characterized and optimized to consider scattering cross-sections at visible wavelengths. The fabrication of the silicon nitride PIC will use the processes outlined in previous work and have been successfully transferred to the Harvard Center for Nanoscale Systems cleanroom[7].
Subtask 1.2: Low-power visible microresonator-based WDM switch design and fabrication
The WDM relies on microresonators with slightly different free-spectral ranges that lie within the free-spectral range (FSR) of the laser microresonator. A tunable laser based on self-injection locking of a Fabry Perot to a microresonator will be designed with a large FSR using a vernier ring structures to allow for wide tuning range of the wavelength[10]. WDM rings will be optimized to lower losses to achieve dense wavelength spacing within the range of the wavelength sweep. The electrical power necessary to sweep between all of the rings will be maximum power for a 2π phase shift to cover the free-spectral range of the laser. We leverage adiabatic tapered resonators which have been recently demonstrated to cut thermo-optic modulator powers down to the milliwatt range to sweep through all the switches[9]. Considering ring phase shifter and a maximum 2π on the bus phase shifter. The maximum chip power will be approximately 2-3 mW which is more than 50 times lower than previous demonstrations of active neural probe switching[7].
Risk Management:
The number of light-sheets that can be generated will rely on the density of the resonances and frequency control. The adiabatic tapering allows proper modal control while maintaining low losses and has demonstrated high yield and uniformity spatially over the wafer[9]. We will use a vernier ring approach to increase the free-spectral range to allow for more flexibility in the frequency domain.

Task 2: Passive 3D polymer implantable lens and laser integration
Subtask 2.1: 3D polymer implantable lens design and fabrication
An implantable polymer waveguide and lens will be designed to transmit the image from the light-sheet to the Miniscope. A lens relay will be used to extend the lengths of this system[15]. We have experience fabricating and aligning 3D polymer micro-optics on top of visible PICs using Nanoscribe to develop fiber-to-chip couplers for ease of fiber packaging (CLEO 2023, see Fig. 2). The size of the waveguide and polymer lens will determine the field-of-view achievable. Although we would like to maximize this for higher numerical aperture, considerations for minimal invasiveness will be taken into account. The target diameters will be about 150-250 μm to keep total thickness including the PIC below 300 μm.
Subtask 2.2: Self-aligning polymer packaging of self-injection locked microresonator-assisted laser and testing

We will fabricate a polymer prism coupler lens on the chip to help self-align the Fabry-Perot laser for ease of laser integration. As an alternative strategy, we will fabricate polymer guides on the PCB using nanoscribe for self-aligning purposes of the chip to the laser.

Risk Management:

In parallel to the waveguide and lens relay system, we will develop a GRIN (gradient index) lens holder that can self-align with the micro-optic with a microlens as a backup option. These GRIN lenses are used actively by the neuroscience community for deep brain imaging. However, the sizes are much larger pushing the bounds on what is considered minimally invasive.

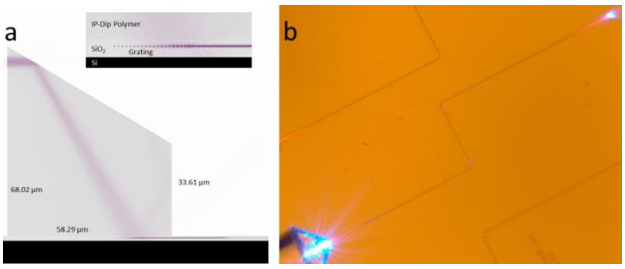

Figure 2 Micro-optics aligned to visible PIC (CLEO 2023). a) FDTD simulation of fiber-to-chip prism polymer coupler for 473 nm. b) Microscope image of fiber prism coupling to SiN PIC.

Task 3: Preparation and characterization for in-vivo imaging

Subtask 3.1: Ultrathin probe fabrication

For PIC device development in Task 1, we will employ standard silicon substrates. For in-vivo imaging, we will use our same silicon nitride process on top of SOI wafers, where the top silicon and oxide layers will be patterned in the shape of the probe and can have thickness between 20-50 µm. This strategy has been employed before for implantable neural probes[16].

Subtask 3.2: Optical and mechanical characterization of probe in agarose brain phantom

Agarose brain phantoms embedded with green fluorescent beads of varying sizes will be used to characterize the light-sheet dimensions. The agarose concentration can be controlled to mimic scattering within brain and other tissues and also the mechanical stiffness[17]. We will evaluate the mechanical stability of our devices by testing with ultrathin probes without PIC, lens, and laser integration to optimize the dimensions of the neural probe.

Risk Management:

The packaging of the PIC with the ultrathin probe and the laser and polymer waveguide lens system will be difficult due to the fragile nature of the probe. We will reserve the final release of the probe tip until the end which will utilize a KOH and HF dip to release the tip from the substrate and any bottom oxide. The top silicon substrate layer will be protected using spray coated resist.

Timeline – Quarters for Year 1	**1**	**2**	**3**	**4**
Subtask 1.1: Light-sheet beam design and fabrication				
Subtask 1.2: Low-power visible microresonator-based WDM switch design and fabrication				
Subtask 2.1: 3D polymer implantable lens design and fabrication				
Subtask 2.2: Self-aligning polymer packaging of self-injection locked microresonator-assisted laser and testing				
Subtask 3.1: Ultrathin probe fabrication				
Subtask 3.2: Optical and mechanical characterization of probe in agarose brain phantom				

Outcomes:

There will be several key outcomes with the success of the project: 1) fully-integrated biocompatible visible PIC with laser and electrical control, 2) implantable microscope reaching depths beyond multiphoton imaging, 3) low-power optical switching at visible wavelengths, 4) novel device structures for beam shaping. The implantable microscope will be able to measure down to depths of approximately 1 cm, which is 100 times that of a traditional light-sheet microscope in scattering tissue with cellular and potentially sub-cellular resolution. The chip-generated light-sheet allows for cellular-scale axial sectioning that can be scanned in depth at kHz speeds. The device can be used for time-multiplexed multi-plane imaging.

Impact:

Short-term applications of the device will be for in-vivo deep brain imaging with neuroscience collaborators at Tufts University School of Medicine to study neural circuit dynamics

related to mood disorders, epilepsy, and other neuropsychiatric diseases[18]. Many of these disorders are studied in a mouse model, but the brain regions involved lie below what can be reached with multiphoton imaging (<1 mm). The device will be compatible with the open-source Miniscope allowing fast adoption within the neuroscience and biomedical imaging communities. Long-term applications of this type of device will be for point-of-care imaging. Currently, high resolution imaging involves taking a biopsy and sending it out to an imaging specific lab. However, with the move towards portable, handheld, and low-cost technologies such as the proposed device, these imaging devices could be made more accessible to medical facilities and be used in real-time with patients. This would be transformative for healthcare, taking a technique that is typically used in research to understand disease to real-world heath monitoring potentially for medical diagnostics.

References:

1. Stelzer, E. H. K. *et al.* Light sheet fluorescence microscopy. *Nat Rev Methods Primers* **1**, 1–25 (2021).
2. Glaser, A. K. *et al.* A hybrid open-top light-sheet microscope for versatile multi-scale imaging of cleared tissues. *Nat Methods* **19**, 613–619 (2022).
3. Bouchard, M. B. *et al.* Swept confocally-aligned planar excitation (SCAPE) microscopy for high-speed volumetric imaging of behaving organisms. *Nature Photon* **9**, 113–119 (2015).
4. Truong, T. V., Supatto, W., Koos, D. S., Choi, J. M. & Fraser, S. E. Deep and fast live imaging with two-photon scanned light-sheet microscopy. *Nat Methods* **8**, 757–760 (2011).
5. Sacher, W. D. *et al.* Implantable photonic neural probes for light-sheet fluorescence brain imaging. *NPh* **8**, 025003 (2021).
6. Lin, N. C. *et al.* Implantable integrated photonic probe for light sheet brain imaging in vivo. in *Biophotonics Congress 2021 (2021), paper BM3B.3* BM3B.3 (Optica Publishing Group, 2021). doi:10.1364/BRAIN.2021.BM3B.3.
7. Mohanty*, A. *et al.* Reconfigurable nanophotonic silicon probes for sub-millisecond deep-brain optical stimulation. *Nature Biomedical Engineering* **4**, 223–231 (2020).
8. Shin*, M. C. *et al.* Chip-scale blue light phased array. *Opt. Lett., OL* **45**, 1934–1937 (2020).
9. Liang, G. *et al.* Robust, efficient, micrometre-scale phase modulators at visible wavelengths. *Nat. Photon.* **15**, 908–913 (2021).
10. Corato-Zanarella, M. *et al.* Widely tunable and narrow-linewidth chip-scale lasers from near-ultraviolet to near-infrared wavelengths. *Nat. Photon.* **17**, 157–164 (2023).
11. Xu, Y. *et al.* Mitigating photorefractive effect in thin-filmlithium niobate microring resonators. *Opt. Express* **29**, 5497 (2021).
12. Segev, E. *et al.* Patterned photostimulation via visible-wavelength photonic probes for deep brain optogenetics. *Neurophotonics* **4**, 011002 (2016).
13. Aharoni, D., Khakh, B. S., Silva, A. J. & Golshani, P. All the light that we can see: a new era in miniaturized microscopy. *Nat Methods* **16**, 11–13 (2019).
14. Horton, N. G. *et al.* In vivo three-photon microscopy of subcortical structures within an intact mouse brain. *Nat Photon* **7**, 205–209 (2013).
15. Tadayon, M. A. *et al.* 3D microphotonic probe for high resolution deep tissue imaging. *Opt. Express, OE* **27**, 22352–22362 (2019).
16. Shim, E., Chen, Y., Masmanidis, S. & Li, M. Multisite silicon neural probes with integrated silicon nitride waveguides and gratings for optogenetic applications. *Scientific Reports* **6**, 22693 (2016).
17. Fain, R., Barbosa, F., Cardenas, J. & Lipson, M. Photonic Needles for Light Delivery in Deep Tissue-like Media. *Sci Rep* **7**, 5627 (2017).
18. Davis, P., Zaki, Y., Maguire, J. & Reijmers, L. G. Cellular and oscillatory substrates of fear extinction learning. *Nat Neurosci* **20**, 1624–1633 (2017).

Executive Summary

Asymmetric wavefront manipulation through all-dielectric passive metasurfaces

Asymmetric transmission (AT) is the intrinsic limitation of electromagnetic waves due to the time reversal property. To address this problem Junus subwavlength engineered structures (metasurface) are explored by stacking the multiple metallic layers. However, they are configured with multi-layered metallic transmissive layers structures for shorter wavelengths. These structures have limitation in higher frequencies due the fabrication difficulties of stacked subwavelength structures as well as ohmic losses. Additionally, the usage of external beam reconfiguration techniques contributes to efficiency loss and difficulty of device integration. Therefore, there is need to realize to subwavelength structures which can realize asymmetric wavefront manipulation in optical frequency regime. In this project, passive dielectric structure will be studied with minimal stacking layers (maximum two) without external parameters (electrical gating, temperature etc.) to realize asymmetric wavefront manipulation such as asymmetric holography, asymmetric orbital angular momentum generation, and asymmetric beam steering. The enhanced signal isolation, increased data capacity, reduced crosstalk, enhanced security, and compatibility with existing infrastructure assisted by AT through ultrathin platform will significantly benefit the several practical fields such as imaging, data storage and communication.

The specific objectives are to realize and **solve following key scientific problems**:

- **AT through Non-interleaved wavefront engineering:** To achieve multiple functionalities by using single cell design meta-structures is key scientific issue to be solved. In multifunctional meta-designs, interleaved meta-design refers to metadesign where one column or row performs one function, and the neighboring column/row/elements performs different function which takes extra space on the metasurface. In this project, by studying the propagation phase and geometric phase simultaneously this issue will be resolved which will lay a foundation to achieve multiple functionalities without using extra space on metasurface.
- **Spin to orbital momentum converter (SOC) assisted by AT:** This project will realize SOC design to decode different orbital angular momentum (OAM) "l" values from back and front side of the metasurface.
- **Information encryption/decryption by utilizing all the transmitted channels for circularly input light:** For circularly input light we have four transmitted channels, however, normally only two channels are utilized. This research problem of utilizing of all the four transmitted channels will be solved and will apply for dynamic holographic display. A unique design by using non-interleaved metasurface will be realized, where for circular polarized input light, both the co and cross polarization transmitted channels will be utilized for holographic images encryption. Specific input polarizing light which will work as an encryption key.
- **Expand the use of Janus metasurfaces in optical frequency regime:** The project will be expanding the utilization of directional metasurfaces to explore the wavefront engineering applications in optical frequency regime through dielectric subwavelength structures.
- **High efficiency:** Efficiency is a key issue at shorter wavelengths e.g., visible and Infrared therefore dielectric metasurfaces will be utilized for our design which exhibit high efficiency.
- **Low fabrication cost:** The non-interleaved metasurfaces designs will not only reduce the complexity but also the cost of microwave systems.
- **Simple compact structure:** In order to easily fabricate, the target metasurfaces aimed to have a simple rectangular structure. Further, the project will not include any active component such as gating which will make the design compact and less complex.
- **Scalability:** As EM characteristics of light are scalable. Therefore, the approach adopted for AT in this project is extendable to any frequency of EM waves spectrum by using dielectric structures.

It is also expected that, upon completion of the project, the future career prospects of the participants will be enhanced. The project is expected to train two (2) MSc and one (1) PhD students. The research team will participate in scientific conferences, symposia and patent submission, publish research findings in peer reviewed journals. Further, the outcome of this project will benefit whole electromagnetic community and will play a vital role to design ultrathin smart optoelectronic devices.

Research Proposal
Asymmetric wavefront manipulation through all-dielectric passive metasurfaces

1. Introduction, Background and Literature Review

Electromagnetic (EM) radiations propagate energy and travel through space in the form of waves [1]. The electromagnetic waves can be divided into different regions based on wavelengths or frequencies. These regions include radio waves, microwaves, infrared radiation, visible light, ultraviolet radiation, X-rays, and gamma rays. Every single component of the electromagnetic spectrum can be utilized for communication, imaging and sensing [Figure 1]. The manipulation of EM waves introduced plethora of research fields since its early invention. Among them electronics and photonics are closely related fields of study that deals with the behavior, manipulation and transmission of information through electronic and optical signals. In terms of application and technologies both have overlaps and interwinds, and they are leading to exciting new opportunities for research and innovation. For the development of ultra-smart devices in these fields, design flexibility, tunability and reconfigurability is of great interest in research.

The EM waves can be manipulated through amplitude, phase, and polarization [2]. The modern trend of technology lies in miniaturization and flexibility, as a result, engineering physical systems that grant full control of the EM waves has been a developing area of research in the past decades. With the ongoing trend toward miniaturization, ever smaller electrical, optical, optoelectronic, and mechanical devices are becoming progressively popular. In more recent years, a keen interest has been bestowed upon the subwavelength engineered materials: called metasurfaces. The ability to control the local response of EM wave through subwavelength thickness has provided a promising platform to numerous novel phenomena, such as, negative index of refraction, subdiffraction imaging, invisibility cloaking, slow and stopped light, and nonreciprocal and extraordinary wave propagation, holographic imaging, surface clocking and lensing [3–9]. Metasurfaces can be fabricated using standard micro- and nanofabrication techniques, such as electron-beam lithography and focused-ion beam milling, which can produce high-resolution patterns over large areas. This makes metasurfaces an attractive technology for a wide range of applications, from consumer electronics to healthcare. Some of the intriguing applications of metasurfaces are shown in Fig. 2.

Besides metasurfces offers several advantages there exists **some limitation** of their usage in practical application due intrinsic property of material and wave nature of EM Waves. One of limitation the metasurfaces' and optical components is the direction dependent asymmetric response [Figure 3] which is beneficial in numerous practical applications, such as dual sided display, and asymmetric data encryption, and communication. In addition, **AT can offer several benefits, few of them are listed below**:

1. **Enhanced signal isolation:** Through AT, by transmitting one signal with a specific polarization and another signal with a different polarization, it becomes easier to separate and distinguish between them, reducing interference and improving signal quality.
2. **Increased data capacity and Enhanced Security:** Asymmetric transmission techniques, such as polarization multiplexing, can increase the data capacity of communication systems. Furthermore, By exploiting the polarization properties of EM waves, polarization-based encryption techniques can be implemented, providing an additional layer of security to protect sensitive information from unauthorized access.
3. **Compatibility with existing infrastructure:** Asymmetric transmission techniques can be integrated into existing communication systems and infrastructure without requiring significant modifications. This compatibility allows for the adoption of asymmetric transmission methods in various applications while leveraging existing resources.

To achieve AT, magneto-optic materials or nonlinear materials have been studied to break the time-reversal symmetry and thus achieve nonreciprocal AT behavior, but they suffer from the bulky dimensions, poor efficiency, and reduced scalability [10–12]. To circumvent these limitations, temporal modulation, space–time phase modulation, and surface plasmon coupling have been developed to achieve AT, and have been applied in coupler, circulators, isolators, directional amplifiers, etc [13,14]. Nevertheless, complicated configuration of these approaches and difficultly in implementation of ultrafast modulation (due to the external stimulation) block the further development in miniaturized and highly integrated AT systems.

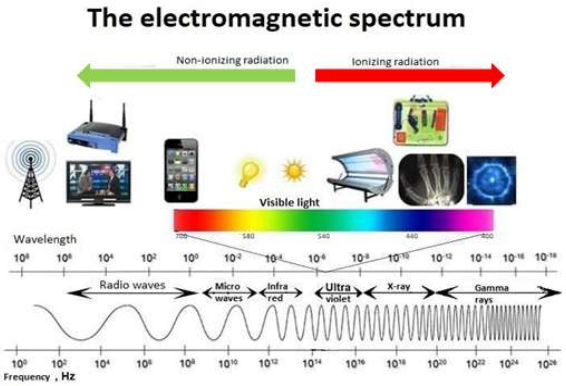

Figure 1 EM Spectrum and its applications

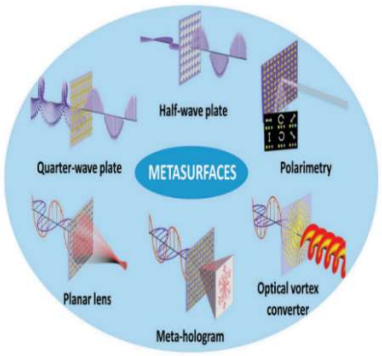

Figure 2 Applications of Metasurfaces

More recently, many attempts have focused on passive Janus metasurfaces, in which the spatial symmetry is broken to achieve the AT, yet reciprocal, behaviour[15–20]. Such metasurfaces generally consist of two orthogonally orientated metallic gratings, serving as top and bottom layers, sandwiching a polarization converting middle layer. Considering the polarization conversion before and after the middle layer, impinging EM waves with an electric field perpendicular to the top grating can pass through the two grating layers successively. Meanwhile, the transmission phase is controlled by the geometry of the polarization converter. Conversely, the incidence with same polarization but opposite direction is completely reflected, owing to the orthogonal polarization selectivity between top and bottom gratings. Consequently, by blocking the wave transmission along one direction [21]. To achieve AT Ref. [22] utilized interleaved metasurfaces for which only half of the unit cells are used for each direction when similar polarized wave is incident from the two opposite directions. However, it is still challenging to achieve asymmetric wavefront manipulation through a non-interleaved metasurfaces through the characteristics of the unit structure in without a special arrangement at shorter wavelengths.

This project is intended to overcome above said limitations by smartly designing the non-interleaved metasurfaces with **minimal stacking layers (maximum two) by using dielectric (silicon or titanium dioxide) engineered structures for visible and infrared region**. Moreover, to avoid the complexity in the designs, active elements such as gating and external tuning mechanism will not be utilized. **The outcome of this project is anticipating following potential designs and resolve key scientific problems:**

(1) **AT through Non-interleaved wavefront engineering:** To achieve multiple functionalities by using single cell design meta-structures is key scientific issue to be solved. In multifunctional meta-designs, interleaved meta-design refers to metadesign where one column or row performs one function, and the neighboring column/row/elements performs different function which takes extra space on the metasurface. In this project, by studying the propagation phase and geometric phase simultaneously this issue will be resolved which will lay a foundation to achieve multiple functionalities without using extra space on metasurface.

(2) **Spin to orbital momentum converter (SOC) assisted by AT:** This project will realize SOC design to decode different orbital angular momentum (OAM) "ℓ" values from back and front side of the metasurface [Figure 4].

(3) **Information encryption/decryption by utilizing all the transmitted channels for circularly input light:** For circularly input light we have four transmitted channels, however, normally only two channels are utilized. This research problem of utilizing of all the four transmitted channels will be solved and will apply for dynamic holographic display. A unique design by using non-interleaved metasurface will be realized, where for circular polarized input light, both the co and cross polarization transmitted channels will $T = \begin{pmatrix} T_{co} & T_{corss} \\ T_{corss} & T_{co} \end{pmatrix}$ be utilized for holographic images encryption. specific

input polarizing light which will work as an encryption key [Figure 5].

(4) **High efficiency:** Efficiency is a key issue at shorter wavelengths e.g., visible, therefore dielectric metasurfaces will be utilized for our design which exhibit high efficiency.
(5) **Low fabrication cost:** The non-interleaved metasurfaces designs will not only reduce the complexity but also the cost of microwave systems.
(6) **Simple compact structure:** In order to easily fabricate, the target metasurfaces aimed to have a simple rectangular structure. Further, the project will not include any active component such as gating which will make the design compact and less complex.
(7) **Scalability:** As EM characteristics of light are scalable. Therefore, the approach adopted for AT in this project is extendable to any frequency of EM waves spectrum.

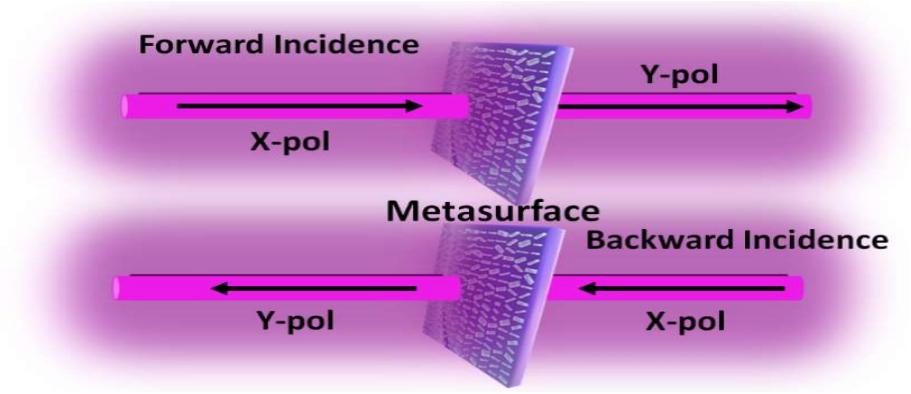

Figure 3 The schematic for AT through All-dielectric metasurface. Under same polarization (pol-x) from backward and front, two different responses will be achieved.

2. Description of the objectives of the Proposal

This proposal is dedicated to realize metasurface based designs with dynamic/flexible functionalities. First of all polarization multiplexing will be considered to achieve multi-functionalities. The transmitted and incident electric fields, are related through transmission matrix in a particular basis: $\begin{pmatrix} Ex \\ Ey \end{pmatrix} = \begin{pmatrix} T_x x & Txy \\ T_y x & Tyy \end{pmatrix} \begin{pmatrix} Ex \\ Ey \end{pmatrix}$, where T_{ij} represents transmission coefficient when the incident linear polarization is 'j' while the transmitted field polarization is 'i'. Similarly, linear transmission coefficients can be used to find transmission coefficients for circular polarized (CP) incident wave. The transmitted and incident electric fields, are related through Jones matrix as:

$$T_{cir} = \begin{bmatrix} T_{++} & T_{\mp} \\ T_{\pm} & T_{--} \end{bmatrix} = 0.5 \begin{bmatrix} T_{xx} + T_{yy} + i(T_{xy} - T_{yx}) & T_{xx} - T_{yy} - i(T_{xy} - T_{yx}) \\ T_{xx} - T_{yy} + i(T_{xy} + T_{yx}) & T_{xx} - T_{yy} - i(T_{xy} - T_{yx}) \end{bmatrix}$$

$T_{\pm}$ &T_{-+} are the cross-CP polarization channels and T_{++} & T_{--} are the co-CP polarization channels. This expression can be further simplified as:

$$T_{cir} = \begin{bmatrix} T_{++} & T_{\mp} \\ T_{\pm} & T_{--} \end{bmatrix} = \begin{bmatrix} T_{co} & T_{cross} \\ T_{cross} & T_{co} \end{bmatrix}$$

The linear and CP AT factor Δ can be written as $\Delta lin^x = \left|T_{yx}^f\right|^2 - \left|T_{yx}^b\right|^2 = \left|T_{yx}^f\right|^2 - \left|T_{yx}^b\right|^2 = -\Delta_{lin}^y$. And, $\Delta_{circ}^+ = \left|T_{-+}^f\right|^2 - \left|T_{-+}^b\right|^2 = \left|T_{+-}^f\right|^2 - \left|T_{+-}^b\right|^2 = -\Delta_{circ}^-$. Here, "f"and "b" represent forward and backward direction, respectively.

The phase is important characteristic to control the EM waves. The common phase control schemes are propagation phase (PP) and geometric phase (GP). The GP values for the cross-polarization channels are 2θ and -2θ, respectively. The PP can be merged with GP values on both cross polarization which gives an extra degree of freedom to realize the dynamic functions. By this approach, several phase relationships can be obtained for one or both cross CP polarization channels to realize dynamic wavefront manipulation functionalities. Here, dielectric rod-shaped meta-element will be utilized whose rotation at $\theta = 0 - 180^{\circ}$ provides high amplitude and full $0 - 2\pi$ phase coverage; therefore, linearly polarized outgoing wavefront can be easily manipulated with high efficiency. Fortunately, by simultaneous exploitation of PP and GP, the CP wavefront can be easily manipulated. Here, GP can be obtained by rotation and PP can be freely adjusted by structuring the side lengths of meta-elements. Hence, the outgoing CP wavefront can be engineered in a desired manner through simultaneous manipulation of GP and PP. To support the conceptualization preliminary simulation results for proposed SOC designs are shown in Fig. 6 which depicts that under the CP-polarized light design 1 and 2 are two different OAM values l according to the Figure 6.

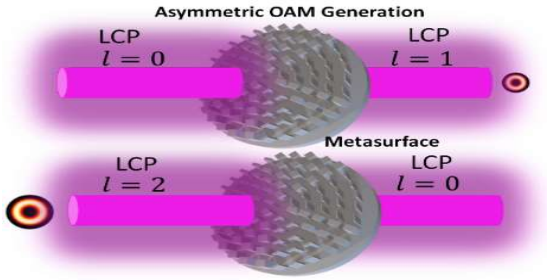

Figure 4 AT assisted OAM generation.

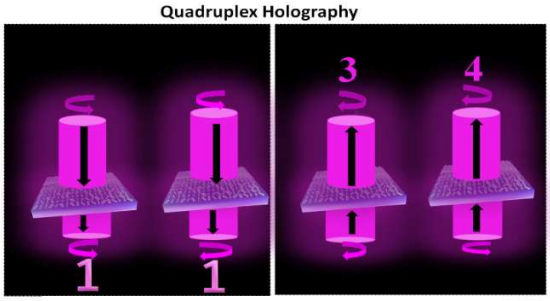

Figure 5 Metasurfaces quadruplex holography

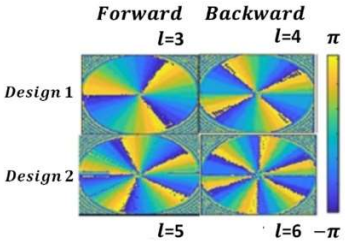

Figure 6 Preliminary simulation results for the proposed SOC designs.

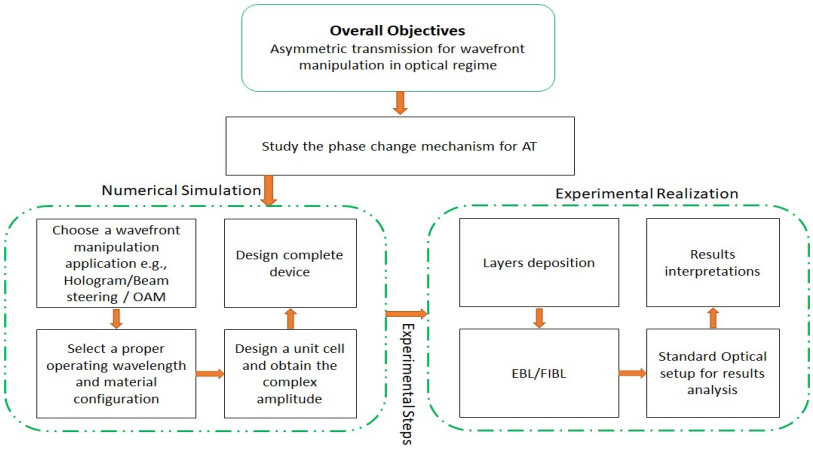

Figure 7 Route to realize the proposed designs.

3.Research approach and methodology, as well as feasibility analysis

The applicant has long been engaged in the theoretical and experimental research for wavefront engineering by using metasurfaces. Closely focusing on the major development of metasurface, the applicant has carried out systematic research work in multiple aspects such as new principles, methods, and devices and has achieved a series of innovative research results. The research works as a first author and with an co-authors has been published in **top journals** such as Optics Express, Journal of Physics D, Photonics Research, IEEE Antennas and Wireless Propagation Letters, and Optics letter. The applicant has also published **more than 15 SCI** academic papers as a coauthor from microwave to visible regime related to wavefront engineering. Incorporating the ideas and expertise from previously published research work will successfully bring our project into reality. **Preliminary** numerical simulation results of some of

proposed designs are presented Figure 7 which need further optimization and experimental realization. The complete feasibility analysis route is illustrated in Fig.7.

(3a) Methodology and Feasibility:

Based on strong theoretical and experimental background, this research will be confidently performed through computer simulations and experimentally. The research methodology is discussed below [Fig. 8]: **(1)** Numerical simulation will be done by CST for a unit cell having TCE engineered structure to obtain high efficiency. Lumerical FDTD simulation tool will be used to get EM response of dielectric unit cells for shorter wavelengths. **(2)** MATLAB tool will be used for OAM generation, hologram generation, and data sorting. **(3)** Mapping of the structures on the substrate and re-simulation of complete device design**. (4)** Analyze near and far-field results of each of the designs. **(5)** Standard fabrication procedures (CVD, EBL, and Lift-off techniques) will be used for the device design. **(6)** Standard detection setup (Light source, waveplate, objective lenses, and CCD) will be used for the outcome validation.

4a. Annual Research Plan:

2024.01-2024.06
Theoretical research and device design stage: In this time frame, phase modulation by using metasurfaces will be studied along with literature review. A unit-cell consists ofdielectric material will be utilized for FDTD simulation to realize the electromagnetic response. From the electromagnetic simulation results, propagation and geometric phase will be studied separately as well as simultaneously.
2024.06-2024.12
Material and device fabrication: For dielectric designs, Chemical vapor deposition, EBL/FIBL and standard fabrication procedures (e.g., lift-off) will be used.
2025.01-2026.12
Experimental results validation and manuscript: Experimental testing, interpretation, compilation of the results, and manuscript submission will be performed in this time period.

5b. Expected results:

In this project, AT devices such as, beam steering, holographic images encryption/decryption, and SOC will be experimentally realized. (2) Apply for one patent; And publish 4-5 high-quality SCI articles. (3). Attend 1-2 domestic and international conferences.

References:

1. R. M. Walser, in *Complex Mediums II: Beyond Linear Isotropic Dielectrics* (2001), **4467**, pp. 1–15.
2. M. G. Kenney, 241 (2015).
3. N. Yu and F. Capasso, Nat Mater **13**, 139 (2014).
4. V. P. Drachev, W. Cai, U. Chettiar, et al, Laser Phys Lett **3**, 49 (2006).
5. G. Li, S. Chen, N. Pholchai, B. Reineke, P. W. H. Wong, etal., Nat Mater **14**, 607 (2015).
6. N. Han, L. Huang, and Y. Wang, Opt Express **26**, 31625 (2018).
7. X. Li, X. Ma, and X. Luo, Guangdian Gongcheng/Opto-Electronic Engineering **44**, 255 (2017).
8. S. J. Byrnes, A. Lenef, F. Aieta, and F. Capasso, Opt Express **24**, 5110 (2016).
9. J. Sung, G. Y. Lee, and B. Lee, Nanophotonics **8**, 1701 (2019).
10. Y. Shi, Z. Yu, and S. Fan, Nature Photonics 2015 9:6 **9**, 388 (2015).
11. N. Shitrit, J. Kim, D. S. Barth, H. Ramezani, Y. Wang, and X. Zhang, Phys Rev Lett **121**, 046101 (2018).
12. L. Fan, J. Wang, L. T. Varghese, H. Shen, B. Niu, Y. Xuan, A. M. Weiner, and M. Qi, Science (1979) **335**, 447 (2012).
13. H. Lira, Z. Yu, S. Fan, and M. Lipson, Phys Rev Lett **109**, 033901 (2012).
14. F. Ruesink, M. A. Miri, A. Alù, and E. Verhagen, Nature Communications 2016 7:1 **7**, 1 (2016).
15. Y. Chen, X. Yang, and J. Gao, Light: Science & Applications 2019 8:1 **8**, 1 (2019).
16. K. Chen, G. Ding, G. Hu, Z. Jin, J. Zhao, Y. Feng, T. Jiang, et al., Advanced Materials **32**, 1906352 (2020).
17. H. X. Xu, C. Wang, G. Hu, Y. Wang, S. Tang, Y. Huang, X. et al., Adv Opt Mater **9**, 2100190 (2021).
18. D. Frese, Q. Wei, Y. Wang, L. Huang, and T. Zentgraf, Nano Lett **19**, 3976 (2019).
19. Z. Tang, L. Li, H. Zhang, J. Yang, J. Hu, X. Lu, Y. Hu, S. Qi, K. Liu, et al., Mater Des **223**, (2022).
20. B. Yao, X. Zang, Z. Li, L. Chen, J. Xie, Y. Zhu, and S. Zhuang, Photonics Res **8**, 830 (2020).
21. B. Chen, S. Yang, J. Chen, J. Wu, K. Chen, et al., Light Sci Appl **12**, (2023).
22. W. Yang, K. Chen, S. Dong, S. Wang, K. Qu, T. Jiang, J. Zhao, and Y. Feng, ACS Appl Mater Interfaces **15**, 27380 (2023).

Executive Summary for: **A Holographic Quantitative Phase Imaging Approach to Mapping the Biochemical Pathway for Synaptic Vesicle Fusion and Neurotransmitter Release**

Atrouli Chatterjee, Department of Cell Biology, Yale University, USA

Challenge. Many processes in biology require the assembly of multiple proteins; however, challenges in characterizing the identity, structure, role, and the dynamic assembly of such heterogeneous protein aggregates poses a severe limitation to our understanding of a wide range of biological processes. As an example, consider information transfer in neurons, where calcium mediates the release of neurotransmitters stored in synaptic vesicles.[1-3] In this case, the key proteins involved in the process of anchoring the vesicle to the target bilayer and inducing fusion in the presence of calcium are known.[1-3] Moreover, a variety of fluorescence-based assays have identified some of the roles that the proteins may play, and electron microscopy-based characterization has identified critical structures[3] that are thought to mediate this biochemical pathway. Nevertheless, ***there is no existing method by which to identify and monitor the dynamics of such large protein clusters*** as they alter the relative position of a synaptic vesicle with respect to a bilayer to ultimately induce vesicle fusion, content release, and therefore enable neuronal information transfer.

Solution. Quantitative phase imaging (QPI) techniques, such as interferometry and holography, enable a label-free, non-destructive approach for studying biological systems. Current state-of-the-art technologies enable vesicle tracking[4] and both custom-built as well as commercially available QPI and holotomography microscopes can be used to monitor refractive index changes in cells and vesicles as well as the self-assembly of high refractive index proteins in solution.[5-8] Herein, I aim to build upon these established technologies to assemble ***a holography system capable of z-resolution ~ 10 nm*** by maximizing the ratio of signal-to-noise and leveraging known geometric constraints to more accurately determine the center of mass and thus the relative position of the point spread function for the scatterers in our system. After assembling the holographic QPI (HQPI) system, I aim to establish, for the first time, a standard method for spatially calibrating the HQPI and other QPI systems. Then, I aim to ***apply HQPI to resolve the biochemical pathway by which synaptic transmission occurs*** with the goal of ultimately being able to monitor the step-by-step proteomic changes that occur between a synaptic vesicle and bilayer during vesicle docking and subsequent fusion. Furthermore, by combining the HQPI system with spectroscopic modalities (*e.g.*, Raman/electrochemical impedance spectroscopy) I aim to provide a more localized understanding of the chemical changes that occur in the active zone of synapses. Altogether, the successful development of the HQPI system will broaden the scope of holography within the context of biological research and for the first time provide an easy-to-translate platform for studying dynamic protein assembly *in vitro* and *in vivo*.

Impact. By leveraging existing technologies, this proposal aims to design a microscopic modality that is able to address a critical need in biomedical research – a way to directly study protein dynamics under conditions that reconstitute the native structures of interest. Moreover, we specifically chose to study synaptic vesicle fusion because the fundamental understanding of this biological phenomenon will not only answer questions in neuroscience but will also provide ***a new basis for understanding information transfer in the brain*** and will likely also lead to significant advances in our understanding and treatment of the severe, often lethal, pathologies caused by key proteins involved in the fusion process[9-11]. Furthermore, given the similarity in the component proteins for neurotransmission, optical signaling in the eye, insulin secretion, as well as cellular signal transduction via exosomes, extracellular vesicles, and multi-vesicular bodies, it is indubitable that the successful utilization of the HQPI system in one field may directly lead to new findings in adjacent fields. Such findings could completely alter our understanding of how our body communicates with itself so rapidly and efficiently, which is ultimately critical for medical, scientific, and technological advancement. Taken together, the development of the HQPI microscope could ***provide a broadly applicable technology that addresses a critical need in biomedical research***.

References:

1. P. S. Kaesar *et al. Annu. Rev. Physiol.* **76**, 333 (2014)
2. J. E. Rothman *et al. FEBS Lett.* **591**, 3459 (2017)
3. K. Gurshin *et al. Proc. Nat. Acad. Sci.* **119**, e2121259119 (2021)
4. A. Witkowska *et al. Biophys. J.* **119**, 2431 (2020)
5. A. Chatterjee *et al. Nat. Commun.* **11**, 2708 (2020)
6. M. J. Umerani *et al. Proc. Nat. Acad. Sci.* **117**, 32891 (2020)
7. A. Chatterjee *et al. ACS Biomater. Sci. Eng.* **9**, 978 (2023)
8. A. G. Engel *et al. Neurol. Genet.* **2**, e105 (2016)
9. H. Melland *et al. J. Neurochem.* **157**, 130 (2020)
10. M. Verhage *et al. Neuron* **107**, 22. (2020)

A Holographic Quantitative Phase Imaging Approach to Mapping the Biochemical Pathway for Synaptic Vesicle Fusion and Neurotransmitter Release

Literature Review: Multimeric protein assemblies play critical roles in physiology and being able to study both their clustering dynamics as well as their function is crucial to our understanding of biological processes. To date, fluorescence-based strategies and electron microscopy (EM) have been the primary methodologies by which proteins have been studied. Fluorescence microscopy is advantageous because it: (i) offers various methods to identify specific proteins (*e.g.*, *via* immunofluorescence); (ii) allows tracking of cells as well as intra- and extra-cellular proteins; (iii) allows evaluation of molecular localization; and (iv) offers a wide range of imaging modalities that enable the multi-scale characterization of protein ensembles.[1-4] However, the utility of such fluorescence-based methods are limited by: (i) the necessity of modifying/labeling the sample; (ii) photobleaching/blinking effects; (iii) variable labeling efficiencies (*i.e.*, the variabilities in the fraction of sample labeled and their relative fluorescence intensity); and (iv) phototoxicity to biological systems can limit the extent of imaging possible. In contrast, EM and more recently cryo-EM, is able to provide structural information about quaternary protein assemblies without the need for modification or labeling of the sample.[5,6] Nevertheless, EM-based methods are critically limited by: (i) the lack of dynamic information; (ii) the requirement for specialized equipment (both EM hardware as well as computational facilities required to deconvolute collected data); (iii) extensive training requirements for users (especially for cryo-EM); and (iv) complex, time-intensive, and chemically harsh methods for staining samples (especially for transmission-EM). As such, there is a need for an alternative optical strategy that is able to capture the biomolecular arrangement dynamics of native, unmodified proteins.

Within the context of label-free imaging technologies, quantitative phase imaging techniques (e.g., interferometry, digital holography, and holotomography) have been gaining significant attention.[7-9] These techniques have several advantages including: (i) no requirements for modifying/labeling samples; (ii) 3D imaging capabilities; (iii) high spatial and temporal resolution; and (iv) they are generally non-destructive strategies for imaging biological samples.[7-9] So far, quantitative phase imaging techniques have been primarily used to study cellular morphology, study live cell dynamics, calculate protein and lipid dry masses, to track particle distributions and motion, track vesicle diffusion, and increasingly to study biomedical/cellular pathophysiology.[7-15] Notably, I have used both a custom-built quantitative phase imaging microscope and a commercial holotomography microscope to (i) characterize proteins that form gradient refractive index particles; (ii) demonstrate that the expression of these proteins in cells enable refractive-index based labeling of cells and vesicles; and (iii) the self-assembly of these proteins after stimulation can be studied in solution.[12-15] Altogether, quantitative phase imaging modalities offer promising approaches to study the dynamic assembly of large heterogeneous protein structures.

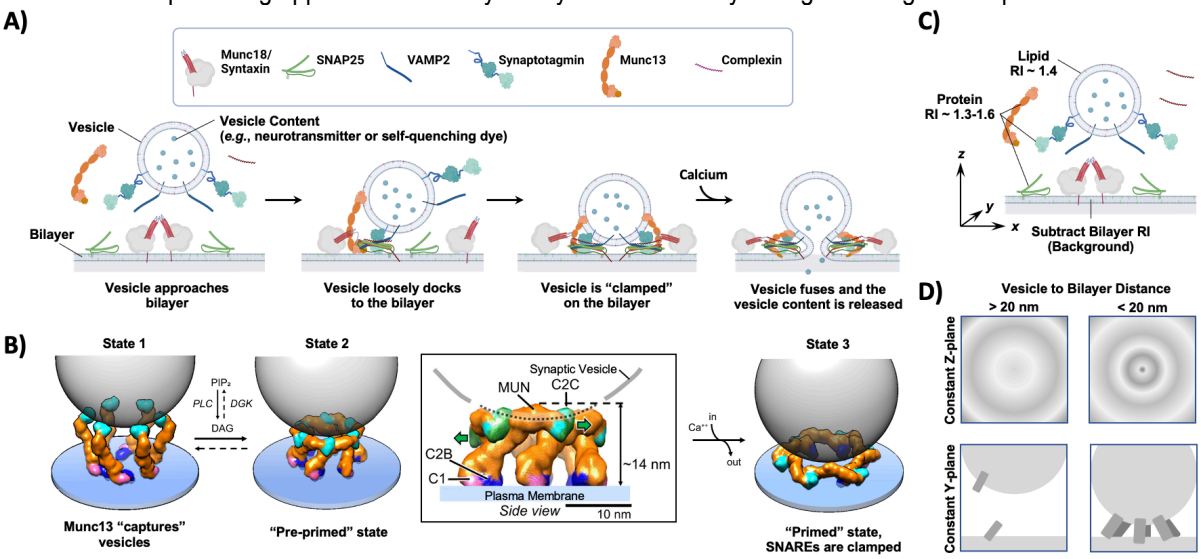

Figure 1: (A) A schematic depicting the generally hypothesized mechanism by which synaptic vesicle docks and fuses onto a bilayer surface. The relevant proteins are shown and labeled in the legend (top). Briefly, a vesicle (with VAMP2 and Synaptotagmin) approaches a bilayer (containing Munc18/Syntaxin complexes and SNAP25) with Munc13 and Complexin in solution (left); the vesicle loosely docks on the bilayer *via* SNARE protein and chaperone interactions (middle left); the vesicle is "clamped" to the bilayer *via* SNAREpins, *i.e.*, stable complexes of SNARE proteins and chaperones (middle right); finally, the addition of calcium induces the vesicle to fuse with the bilayer, releasing the vesicle content (right). Part (A) is adapted from [22]. **(B)** A hypothesized model of how the chaperone Munc13 enables vesicle capture and fusion. Briefly, in state 1 (left), six Munc13 molecules capture the vesicle; interaction with diacylglycerol induce the Munc13s to ratchet and form the pre-primed state 2 (inset and middle); finally, the addition of calcium induces Munc13 into state 3 (right), where the vesicle is now able to fuse. The overall change in z-position of the vesicle during this process is ~ 20 nm. Part (B) is adapted from [5]. **(C)** A schematic of the vesicle and bilayer geometry with lipid and protein refractive indices (RI) indicated. **(D)** A depiction of the expected interference patterns for a constant Z (top) or Y (bottom) plane when the vesicle is far from (left) or near to (right) the bilayer.

A Holographic Quantitative Phase Imaging Approach to
Mapping the Biochemical Pathway for Synaptic Vesicle Fusion and Neurotransmitter Release

One field in which optical methodologies for probing the dynamic assembly and disassembly of multimeric protein ensembles is needed is in neurology, specifically, to study the way in which proteins enable the specific and rapid (< 1ms) transfer of information from one neuron to another.[16-18] In particular, there is significant interest in understanding the mechanism by which proteins involved in synaptic vesicle fusion (which includes SNARE proteins: VAMP2, Synaptotagmin, SNAP25, Syntaxin; Complexin; and the chaperone proteins Munc18 and Munc13) assemble in concert to allow rapid vesicle fusion (Fig. 1A).[16-18] Beyond the fundamental importance of this mechanism to understanding neural function, all of the component proteins involved in this process lead to severe developmental, neuromuscular, and ophthalmic pathologies that are typically lethal (Tbl. 1) and thus understanding the component proteins' precise role and the mechanisms by which they act could be revolutionary in understanding and treating a wide range of diseases.[19-21] Given the inherent complexity of neurons, significant effort has been expended to develop *in vitro* reconstitution assays that can be probed *via* spectroscopy, fluorescence microscopy, and EM.[1-6] Beyond the inherent limitations of fluorescence microscopy and EM-based assays for understanding dynamic protein assembly as discussed above, these assays have typically also used pre-assembled bilayers that circumvent the need for chaperone proteins (Munc18 and Munc13), thereby limiting their interpretation with respect to what is observed *in vivo*. In this regard, we have recently developed a reconstitution assay that requires both chaperone proteins, verified fast fusion (< 20 ms, resolution limited by camera frame rate) *via* content release of a self-quenching dye from the vesicle, demonstrated that the reconstitution assay recapitulated the *in vivo* effects of several known gain- and loss-of-function SNARE protein mutations, and by tracking single vesicle docking and fusion on the bilayer, we have provided new insight into the mechanism by which the SNARE proteins and chaperones work in concert.[22] Nevertheless, neither the function observed in our recent work and previous fluorescence-based functional assays nor previous EM-based studies have been able to capture the dynamic changes in the arrangement of SNARE proteins and the chaperones between the vesicle and bilayer (Fig. 1), leaving the mechanism for fusion unresolved.

Table 1: Pathologies associated with the lack of expression of a single SNARE protein.

SNARE Protein/Chaperone	Pathology	Reference
VAMP2	Neurodevelopmental-disorder, seizures, motor impairments, ophthalmic disabilities	19
Synaptotagmin-1	Baker-Gordon Syndrome (BAGOS), ophthalmic disorders including esotropia, strabismus, nystagmus, delayed visual maturation)	19, 20
Munc18-1 (or Syntaxin binding protein, STXBP)	STXBP1 encephalopathy (with variable motor impairments and some cortical atrophy, thin corpus callosum, hypomyelination)	19
Syntaxin-1	Generalized Epilepsy with Febrile Seizures (GEFS + 9), DEE, Williams syndrome	19, 20
SNAP 25	Developmental and Epileptic Encephalopathy (DEE), intellectual disability with seizures, ptosis	19
Munc13-1	Microcephaly, cortical hyperexcitability, fatal myasthenia, dyskinetic movement disorder (with comorbid ADHD and febrile seizures)	19, 21
Complexin-1	Early Infantile Epileptic Encephalopathy 63 (EIEE)	19

Problem Statement/Objective: Currently, the standing hypothesis in the field is that the chaperone Munc13 effectively helps capture the vesicle, is involved in the formation of SNAREpins and by going through ratcheted transitionary conformations is able to prime the vesicles for rapid fusion upon calcium stimulation (Fig. 1B). Notably, these transition states are thought to involve a ~ 20 nm change in the separation distance between the vesicle and bilayer and comprise of clusters of at least 6 SNAREpins (each comprising at least 7 interacting proteins). Given the high protein density, relatively small change in z-distance, and the fast kinetics of the whole process, fluorescence-based microscopy techniques are unsuited for the purpose and cryo-electron microscopy-based approaches, although ideal for capturing the transition states, do not provide dynamic information regarding the change in architecture and geometry of the protein complex. As such, I propose to leverage the innate optical properties of the protein with holographic quantitative phase imaging (HQPI). Critically, this non-invasive approach has several advantages, including: (i) the ability to minimize imaging time without significant loss of signal as scattering signal is only limited by the incident photon flux unlike fluorescence; (ii) indefinite observation times are possible without photobleaching or blinking effects; (iii) the inherently modular nature of interferometry allows for parallel analysis modalities (*e.g.*, fluorescence microscopy, Raman or electrochemical impedance spectroscopy, multi-spectral imaging); and (iv) straight-forward translation from *in vitro* systems to cell-based systems for *in vivo* testing. ***Herein, we aim to (1) assemble and calibrate a holographic quantitative phase imaging (HQPI) which***

will be used to (2) characterize and (3) stabilize the stages of synaptic vesicle docking and fusion as well as to (4) evaluate the effect of local chemistry on the kinetics protein assembly, synaptic vesicle fusion, and neurotransmitter release in tandem with spectroscopy modules.

Table 2: The tentative timeline to accomplish project goals and the relevant expected deliverables at each stage.

Timeline	Goals	Deliverables
Months 1-3	(1) Set up holographic quantitative phase imaging (HQPI) microscope	• Set up HQPI microscope and develop software interface for data collection and analysis • Demonstrate size resolution of interferometry system with polystyrene beads • Demonstrate z-axis resolution of interferometry system with calibrated DNA tethers
Months 4-6	(2) Demonstrate reconstituted vesicle docking and fusion using HQPI microscope	• Use Munc13-dependent reconstitution assay to confirm vesicle docking and fusion can be monitored using the HQPI microscope • Characterize the change in z-distance at different docking and fusion stages
Months 7-9	(3) Stabilize transition states of synaptic vesicle docking and fusion	• Use mutations that stabilize (gain-of-function) and destabilize (loss-of-function) the SNARE complex to evaluate how the z-distance kinetics are affected • Use "tethers" to stabilize transition states of the SNARE complex to evaluate how the z-distance kinetics are affected • Combine mutations and "tethers" together to establish the role of the proteins involved in the vesicle docking and fusion process
Months 10-12	(4) Combine HQPI with spectroscopy modules to evaluate how local chemistry affects protein assembly, fusion kinetics, and neurotransmitter release	• Combine chemical characterization methods (*e.g.*, Raman spectroscopy) to evaluate how local changes in bilayer/vesicle chemistry affects the kinetics of protein assembly • Combine fluorescence microscopy and electrochemical impedance with HQPI microscopy to evaluate the kinetics of fusion pore opening and neurotransmitter (*i.e.*, fluorescent dye) release

Outline of Tasks/Work Plan: In order to visualize relatively small changes in z-distance at a sufficiently high frame rate, within a small area that will likely have high scattering (due to the high protein density) sandwiched between similar refractive index surfaces (*i.e.*, lipidic bilayers of the surface and vesicle) (Fig. 1C), we plan to use HQPI (Fig. 2). Briefly, we will have a multi-channel laser source (to allow simultaneous interference and fluorescence imaging capabilities), which will pass through a beam expander and an acousto-optic deflector (AOD) to allow precise and rapid control over the angle of incidence light, which will then pass through the sample and will be captured by a CCD camera (Fig. 2). In parallel, the reference beam will have the same path length as the sample beam, but for which the fluorescence wavelength will be filtered out, to complete the interferometer. We will attempt both the 4f and off-axis holography configurations to determine which offers the highest signal-to-noise ratio for our application (Fig. 2i and ii). In general, we expect the irradiance at the detector to follow *Eqn.1*, typical of full-field QPI, whereas with the with the off-axis configuration, the irradiance will follow *Eqn. 2*.[7] By taking an initial measurement prior to vesicle addition, the background intensity of the bilayer can be subtracted (Fig. 1C) and by selecting a constant *y*-plane for our analysis (Fig. 1D), we can extract changes in the protein density between the background and vesicle. The spacing can be further calibrated with commercially available polystyrene or gold nanoparticles and DNA tethers which form rigid, linear spacers and the signal from the vesicle can be further modulated by altering the effective refractive index of the lipids (*e.g.*, by using brominated lipids). Altogether, the successful completion of this stage (Tbl. 2, *Goal 1*) will: (i) lead to the fabrication of our HQPI microscope along with the development of necessary computational tools for data analysis; (ii) establish the size resolution of our microscope and (iii) establish the z-resolution of our microscope.

(Eqn. 1) $$I(x,y) = I_0 + I_1(x,y) + 2\sqrt{I_0 I_1(x,y)}cos\,[\omega\tau + \phi(x,y)]$$

where I_0 and I_1 are the irradiances for the reference phase wave and object field, respectively, ω is the angular frequency of the optical field, τ is the time delay between the two waves, and ϕ is the phase image.

(Eqn. 2) $$I(x,y) = I_0 + I_1(x,y) + 2\sqrt{I_0 I_1(x,y)}cos\,[\alpha x + \phi(x,y)], \alpha = 2\pi\sin(\theta)/\lambda$$

where I_0 and I_1 are the irradiances for the reference plane wave and image field, respectively, α is the spatial frequency and is a function of the off-axis angle (θ) and the wavelength of light (λ), and ϕ is the phase image.

Next, we aim to apply our HQPI system to the problem of synaptic vesicle fusion. Specifically, we will first use our established Munc13-dependent reconstitution assay[22] to confirm that the functional behavior observed with fluorescence-microscopy can be observed with our HQPI system and will then characterize the changes in z-position of the vesicle throughout the docking and fusion process (Tbl. 2, *Goal 2*). We presume that the hypothesized ratcheting-mechanism[5,17] for vesicle fusion (Fig. 1B) will likely require transition states that may not be stable for sufficiently long periods of time for the transitionary arrangements to be captured. As such, we will next use protein mutations as well as additional biomolecular or polymeric "tethers" to stabilize the transition states and evaluate how they change vesicle docking and fusion as well as the relative transitions in the z-positions throughout the process (Tbl. 2, *Goal 3*). Finally, we aim to leverage the modular nature of our HQPI system to further characterize the effect of protein assembly on vesicle docking and fusion(Tbl. 2, *Goal 4*). As one example, we can combine Raman spectroscopy[23,24] with our system to evaluate the role of local lipid domains in vesicle docking and fusion as well as to characterize how changes in vesicle composition affect the kinetics and mechanism of ratcheted vesicle fusion (Fig. 2iv). As another example, we can combine electrochemical impedance microscopy[25-27] in tandem with fluorescence microscopy and HQPI to observe calcium-mediated vesicle fusion pore opening and characterize the release profile of neurotransmitters (*i.e.*, fluorescent dyes in our reconstitution system) (Fig. 2iii). Taken together, the development of the HQPI microscope could provide a broadly applicable technology for studying neurological processes comparable to the utility of patch-clamps in their utility to study fundamental neurophysiology and neuropathies.

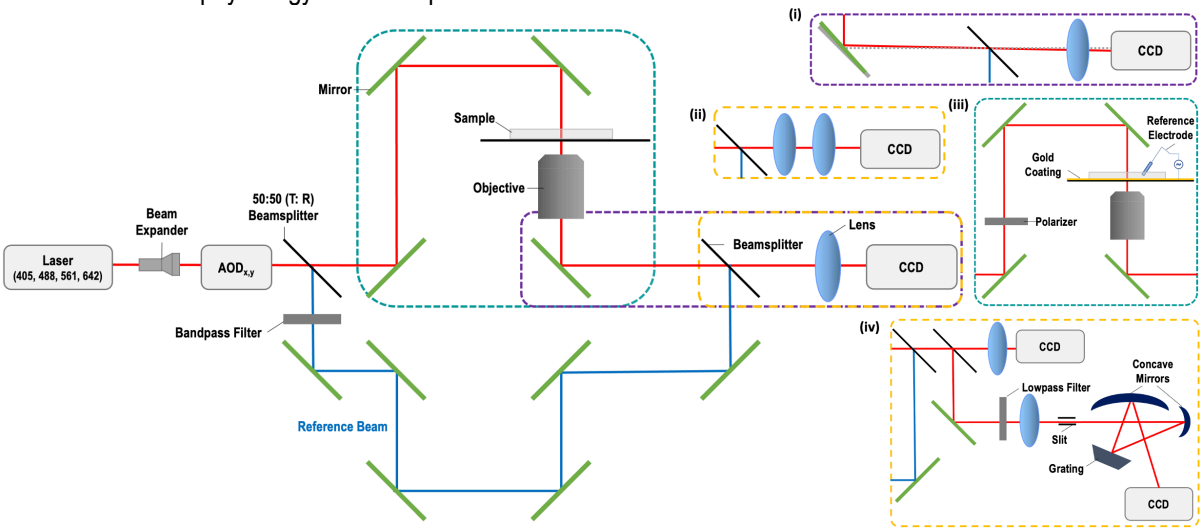

Figure 2: A schematic showing a sample geometry for HQPI. The light path for the sample and reference beams are shown in red and blue, respectively. The area highlighted with a dashed purple line can be modified to have an off-axis configuration with respect to the reference beam as shown in **(i)**. The standard geometry is shown in gray (mirror is a solid line and the light path is a dashed line) for comparison. The off-axis configuration has been used for holography to shift the unwanted signal onto a different axis with respect to the in-focus image. Alternatively, the area highlighted with a dashed yellow line can be modified with two lenses to have a 4f configuration with respect to the input plane of light and the camera as shown in **(ii)**. By effectively using a Fourier transformation, the 4f configuration may be more effective at removing background noise, which we expect due to high protein density and the sandwiched-lipid geometry. In parallel, the area highlighted with a dashed teal line can also be modified to add a polarizer and the relevant electrical components (reference electrode and an AC modulation potentiostat) to enable electrochemical impedance microscopy as shown in **(iii)**. In this case, the sample will need to be on a conductive surface (*e.g.*, gold-coated substrate). Moreover, the area highlighted with a dashed yellow line can also be modified to add in a spectrometer geometry (as an example a simple Raman spectrometer set up is shown here) as shown in **(iv)**.

Outcome(s): We expect that the successful assembly of our HQPI microscope will lead to several advancements in the utility of holography-based systems in general as well as to study synaptic vesicle fusion. First, as yet, there are no standards available to calibrate z-position or size in holography – however, by using commercial polystyrene beads as well as designer DNA tethers, we aim to establish an easily reproducible calibration system that can be used in all holography microscopes. Second, the spatial calibration of our system will be directly applicable to the ratcheted docking of synaptic vesicles and will provide, for the first time, a dynamic view of how a vesicle is captured and is actively "clamped" by neuronal proteins. Furthermore, the subsequent mutational studies in tandem with the addition of spectroscopic capabilities to our microscope will enable precise identification of the functional role of the relevant SNARE proteins and may also shed light on how the local chemistry of the bilayer/vesicle affects synaptic vesicle fusion in a dynamic, native-like fusion-competent system, which has never been done before. Moreover, by using fluorescence in tandem with interferometry and electrochemical impedance, we will be able to

accurately determine how vesicle fusion correlates to the rate at which neurotransmitters are released, enabling a better understanding of the physics of neuronal information transfer. Altogether, our multi-faceted HQPI microscope will broaden the scope of holography within the context of biological research and will provide new outlooks for unravelling questions surrounding the rapid and high-fidelity process of synaptic vesicle fusion.

Impact: HQPI aims to bring together not only multiple facets of microscopy, spectroscopy, and interferometry, but to provide a straightforward platform to utilize these techniques to study the dynamics of multimeric protein assembly, which occupies a scale that falls almost directly between fluorescence microscopy and EM. As a case study, we plan to use HQPI to study the proteins involved in synaptic vesicle docking and fusion. Understanding the way in which the protein machinery works to enable fusion is critical to understanding how it can be compromised and will unfold the precise mechanisms by which the SNARE proteins contribute to severe pathologies. As a result, diagnostic tools to identify these conditions, the pharmacological design of drugs to treat these conditions, and strategies to reduce the lethality of these conditions can be effectively designed. Moreover, the understanding of synaptic vesicle fusion at the biochemical level opens up several parallel paths to unfold similar machineries including signal transduction in the eye[28,29] and insulin secretion[30-31] (both of which use similar SNARE proteins) as well as the way in which extracellular vesicles[32-34] (such as exosomes and multi-vesicular bodies, which have been gaining significant attention for their utility in drug delivery) are able to transport information and cargo with high fidelity. Furthermore, the overall simplicity of the interferometry system will allow easy integration of this technology in other laboratories and clinical facilities that aim to understand similarly complex protein association and dissociation (*e.g.*, understanding protein clustering in other neuronal disease states such as Alzheimer's or Parkinson's, which form large protein aggregates and, in some cases, derive from SNARE protein anomalies[35,36]). Altogether, there is no doubt that the HQPI system will have wide-ranging applications in biomedical research and could make a significant impact in the effective diagnosis and treatment of a variety of severe pathologies.

Why the Optica Foundation Challenge? Despite the promise of the technology and the potential for a large impact on a breadth of fields, the inherently interdisciplinary nature of this project makes funding *via* traditional agencies challenging. As an example, despite relying on the development of an optical technology, a large portion of the project focuses on biochemistry, as such funding programs that focus either only on technology development or fundamental research finds this project unsuitable for funding. Nevertheless, my experience[12-15,22] in optics, protein engineering, and biochemistry provides me with the unique position to pursue such interdisciplinary projects, which I hope to take with me as I look towards establishing my own research laboratory. Critically, the opportunity afforded by the Optica Foundation Challenge provides the perfect avenue by which to initially establish the system design and utility of the HQPI microscope using my current work in synaptic vesicle fusion as a steppingstone to launch this technology. I hope to subsequently leverage the system for other applications, particularly in studying ophthalmic pathologies as well as to further our understanding of neuronal information transfer through more traditional funding agencies and thereby to set up my own independent research direction.

References:

1. S. Ramakrishnan et al. Langmuir 34, 5849 (2018)
2. M. Bera et al. eLife 11, e71938 (2022)
3. F. Li et al. FEBS Lett. 595, 2185 (2021)
4. R. V. K. Sundaram et al. FEBS Lett. 595, 297 (2021)
5. K. Grushin *et al. Proc. Natl. Acad. Sci.* **119**, e2121259119 (2022)
6. A. Radhakrishnan *et al. Proc. Natl. Acad. Sci.* **118**, e2024029118 (2021)
7. Y. K. Park *et al. Nat. Photon.* **12**, 578 (2018)
8. T. Cacace *et al. Opt. Laser Eng.* **135**, 106188 (2020)
9. C. Hu *et al. IEEE J. Sel. Top.* **25**, 6801309 (2019)
10. A. Witkowska *et al. Biophys. J.* **119**, 2431. (2020)
11. E. R. Firdaus *et al. J. Biophotonics* **13**, e202000055 (2020)
12. A. Chatterjee *et al. Nat. Commun.* **11**, 2708 (2020)
13. M. J. Umerani *et al. Proc. Natl. Acad. Sci.* **117**, 32891 (2020)
14. A. Chatterjee *et al. ACS Biomater. Sci. Eng.* **9**, 978 (2023)
15. G. Bogdanov *et al. iScience* (2023) DOI: 10.1016/j.isci.2023.106854
16. P. S. Kaeser *et al. Annu. Rev. Physiol.* **76**, 333 (2014)
17. J. E. Rothman *et al. FEBS Lett.* **591**, 3459 (2017)
18. T. C. Sudhof *Neuron* **80**, 675 (2013)
19. H. Melland *et al. J. Neurochem.* **157**, 130 (2020)
20. M. Verhage *et al. Neuron* **107**, 22 (2020)
21. A. G. Engel *et al. Neurol. Genet.* **2**, e105 (2016)
22. R. V. K. Sundaram *et al. bioRxiv* (2023) DOI: 10.1101/2023.06.05.543781
23. D. Talaga *et al. Angew. Chem.* **57**, 15738 (2018)
24. N. Emmanuel *et al. J. Chem. Educ.* **98**, 2109 (2021)
25. W. Wang *et al. Nat. Chem.* **3**, 249 (2011)
26. C. MacGriff *et al. Anal. Chem.* **85**, 6682 (2013)
27. A. Valiuniene *et al. J. Electroanal. Chem.* **864**, 114067 (2020)
28. A. Lakkaraju *et al. IOVS* **51**, 490 (2010)
29. M. C. M. Kwok *et al. Mol. Cell. Proteom.* **7**, P1053 (2008)
30. H. Y. Gaisano *Diabetes Obes. Metab.* **19**, 115 (2017)
31. M. Barillaro *et al. Endocrinol.* **164**, bqac179 (2022)
32. N. P. Hessvik *et al. Cell. Mol. Life Sci.* **75**, 193 (2018)
33. S. Gurung *et al. Cell Commun. Signal* **19**, 47 (2021)
34. M. Xu *et al. Genes Dis.* **10**, 1894 (2022)
35. M. K. Tobin *et al. Cell Stem Cell* **24**, 974 (2019)
36. S. Majd *et al. BMC Neurosci.* **16**, 69 (2015)

NONLINEAR INTERFEROMETRY FOR ENHANCED OPTICAL SENSING

Metasurfaces have the potential to become the key building block of smart, multi-functional sensing devices. Once integrated with microfluidic technologies, they can be engineered (via geometry) and functionalized (with surface chemistry) to target a broad variety of analytes and address various properties such as concentration, refractive index, chirality. etc. **Plasmonic** metasurfaces (Fig. 1, left) are a particularly attractive platform, due to the ease of functionalization and the strong confinement of the electric field at the surface, enabling **ultra-sensitive** detection of a targeted molecular species with very **small sample volumes**. Most often, sensing relies on the spectral shift of a plasmonic resonance induced by the modification of the local environment of the metasurface upon binding of the target analyte to the metal surface. While in conventional implementations resonances are monitored via refractometry, lately it has been proposed to rely on **nonlinear optical processes**, to benefit from their enhanced surface sensitivity and superlinear dependence on local perturbations of the electric field due to the binding analytes. In principle, this was expected to yield sizable improvements in sensitivity, but in practice such gains have been hindered by the low efficiency of nonlinear conversion, which leads to small signals affected by a comparatively large noise.

In this project, I aim to demonstrate a **phase-sensitive interferometric detection** scheme capable of circumventing the noise limitations of previous reports of static nonlinear sensing. Specifically, I will exploit a **dual-wavelength illumination** scheme whereby a pulse at the telecom frequency ω and the externally-generated replica at the double frequency 2ω excite the metasurface simultaneously. Due to the coherence of the second harmonic generation process, the direction of the energy flow between the two frequencies depends on the relative phase of the two pumps. **High-frequency phase modulation** of one pump has already been shown to implement a phase-sensitive imaging modality. A balanced detection of any two opposite diffraction orders of the metasurface (Fig. 1, right) will also implement a homodyne detection with effective rejection of common-mode laser noise. Application of this innovative nonlinear interferometry to sensing will boost the sensitivity of the plasmonic platform, abating the noise limitations that have so far prevented translating these assets into technology.

The benchmark of the proposed sensing platform will be the label-free detection of small amounts (<pM concentration) of **insulin-autoantibodies**, which are the very first blood indicator of the insurgence of **type 1 diabetes**, a non-preventable autoimmune disease which frequently has its offset during childhood. Such sensitivity is key to an early diagnosis, enabling effective therapeutic interventions, but is hardly achieved with standard immunoassay techniques, such as radioactive tagging or enzyme-linked immunosorbent assays.

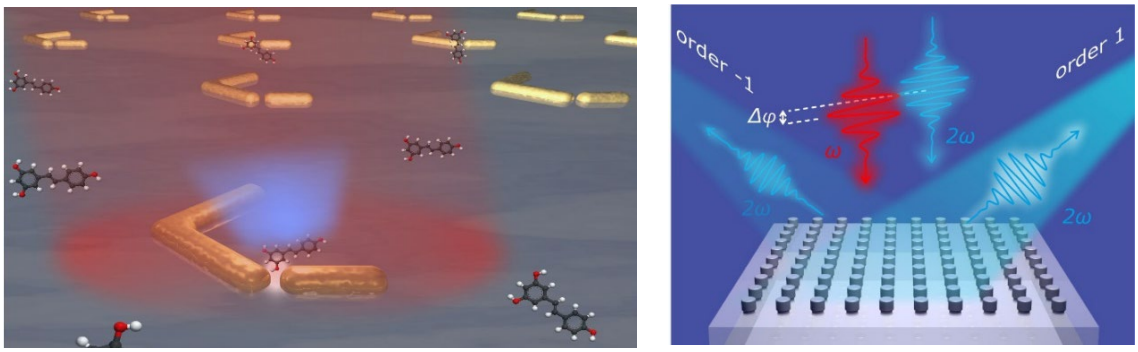

Figure A Artist's impression of the proposed sensing concept. (Left) **Sample**: a plasmonic metasurface whose optically resonant response at ω brings about an enhanced sensitivity to the local chemical environment. (Right) **Experiment**: controlling the relative phase Δφ between pump pulses modulates the nonlinear emission at 2ω, enabling phase-sensitive high-frequency demodulation with balanced photodetection of opposite diffraction orders.

1. INTRODUCTION AND LITERATURE REVIEW

Optical sensing Our ability to detect and identify chemical and biological species in liquid environments—for example for water quality control or blood and urine testing—underpins much of the technological infrastructure that maintains a healthy food supply and effective analytical tools for medical diagnostics. Optical sensing has emerged among the most promising approaches, due to its **non-invasive** character and capability for **high speed** and **sensitivity**. The key physical mechanism enabling sensing is the dependence of many types of optical resonances on the refractive index of the environment: when an analyte adheres to the sensor surface the resulting spectral shift can be monitored e.g., as a reflectivity change.

Optical metasurfaces While some simple optical sensors, such as those based on surface plasmon polaritons propagating on planar metals films, have already been successfully commercialized over two decades ago, there is presently a renewed push to explore more sophisticated architectures incorporating concepts developed in the rapidly advancing field of optical metamaterials. Specifically, optical metasurfaces—namely, planar arrays of particles of subwavelength size—offer ample capability, through a careful engineering of their resonant behavior, to control the radiative in- and out-coupling and to confine the electromagnetic field within micrometric volumes. Therein lies their attractiveness for sensing, allowing a sensitive detection while dramatically **reducing** the required **sample volume**.[1] Moreover, the reduced footprint and versatility of metasurfaces makes them appealing for multi-functional **miniaturized devices**, allowing multiplexing and integration with microfluidics, in view of applications to high-throughput screening and point-of-care real-time diagnostics.

Nonlinear optics (NLO) studies the interaction of multiple photons, that is, the **scattering of light with light**. Perhaps the simplest example of NLO process is second-harmonic generation (SHG), represented in Figure 1a: two photons are converted into one whose energy is the sum of the incident two, namely, without a net energy exchange with matter. **SHG** is a specific case of sum-frequency generation (SFG), where the inputs photons can have arbitrary energies. SFG (and hence SHG) is a second-order NLO, namely mixing three fields. However, higher-order processes involving more photons are also possible, such as third-harmonic generation (THG), whereby three input photons add up their energies. Beyond energy conservation, **coherence** is the other crucial feature of the NLO processes I listed, meaning input and outputs have a definite phase relation. Moreover, the efficiency of SHG depends on the relative amplitude of the second-harmonic (SH) and fundamental-wavelength (FW) fields, but also on their relative phase. This implies that one can control the direction of the energy flow between FW and SH through the relative phase of the inputs. Notably, such modulation concept has already been demonstrated as an interferometric imaging modality.[2] It has also been suggested to use an external beam at the SH frequency as an interferometric control of the SHG emission of a nanostructure.[3]

Interferometric techniques have long been leveraged in the field of biological imaging thanks to their ability to **detect phase shifts** (as in differential interference contrast) and **amplify weak** scattered **fields** to measurable levels (as in iSCAT). Only recently, the sensing community began to realize the opportunities of translating this approach, particularly in conjunction with nanoscale devices, albeit so far only in a liner regime.[1,4] This project puts together, for the first time, interferometry to the concepts introduced above, namely, it aims at demonstrating a **nonlinear optical interferometry** technique for **metasurface-based optical bio-sensing**. The main arguments for exploiting NLO for boosting the sensing performance are: (i) the narrower spectral width of NLO emissions with respect to the FW resonances mediating them; and (ii) the strong surface sensitivity of several second-order nonlinear processes (e.g., SFG in centro-symmetric materials). Partly because of (ii), most attention was

initially devoted to plasmonic nanostructures, that exhibit extreme confinement of the electric field at their surface.[5,6] Another appealing aspect of metal platforms is (iii) the ease of chemical functionalization, that is, attach ligands to their surface for targeting specific molecular species.

2. PROBLEM STATEMENT/OBJECTIVE

2.1. State of the art

My research group, led by Prof. Michele Celebrano and Prof. Marco Finazzi at Politecnico di Milano (**PoliMi**), has an active collaboration with Dr. Anne-Laure Baudrion in the Technical University of Troyes (**UTT**) on the topic of **NLO sensing based on nanoplasmonic devices**. Within this context, a first work[6] demonstrated the sensing capability, but at the same time highlighted the need for cleverer schemes than the simple resonance shift monitorin to take full advantage of the nonlinearity and achieve performances significantly exceeding the linear regime despite a lower signal level and hence a **higher noise** floor.
In the meantime, with my collaborators at PoliMi we have been developing over the last few years a **dual-wavelength nonlinear interferometry** scheme[7,8,9] whereby nanostructures are concurrently excited by a laser pulse (wavelength λ = 1550 nm, duration σ = 160 fs) with angular frequency ω in the telecom C-band and its replica at 2ω, delayed by a time interval τ via a linear translation stage. Importantly, as the latter pulse is generated externally via SHG in a β-barium borate crystal, (BBO) the two pump pulses are coherent mutually and with the resulting NLO emissions. Mixing of ω and 2ω SFG at $3\omega = \omega + 2\omega$ on top of THG (also at $3\omega = \omega+\omega+\omega$) seeded by the sole telecom pulse.[7] As these two are coherent in phase and degenerate in frequency, they can interfere—provided some degree of symmetry breaking is achieved— resulting in an amplitude modulation controlled by the relative phase delay $\Delta\varphi$, that is via τ.8 Finally, we translated this paradigm from a single nanoparticle to an optical metasurface, which allowed us to realize multiplexing and steering of the nonlinear emission through interferometric control.[9]

2.2. Objective of the project

This project proposes to combine the **meta-plasmonic sensing** know-how with **a NLO interferometric control** scheme, aiming in particular at the sensitive detection of small amounts of insulin-autoantibodies for the early diagnosis of Type 1 diabetes—see Sec. 5 for this application. The required sensitivity will be achieved by developing an innovative interferometry technique, retaining the dual-beam $\omega+2\omega$ excitation described in Sec. 2.1, but monitoring with a phase-sensitive coherent detection scheme the NLO signal at 2ω instead of 3ω. Details of the envisaged technical implementation are given in the next section.

3. OUTLINE OF TASKS/WORK PLAN

The proposed project is planned to take place in **PoliMi**, where I hold a Junior Researcher position which allows me to perform self-directed research activity. The $\omega+2\omega$ interferometric set-up which my collaborators and I developed is hosted in the **sNOm Lab**, falling under the responsibility of Prof. Michele Celebrano. Access to the Lab will allow me to use essential pieces of equipment, first and foremost the fs pulsed laser sources (a mode-locked Er:Yb:glass laser at 1550 nm and a tunable Ti:Sa-pumped optical parametric oscillator).

3.1. Demonstration of nonlinear interferometry

I will build a nonlinear microscope based on the dual-beam excitation scheme depicted schematically in Figure 1b. The two coherent pulses at frequency ω and 2ω are generated by SHG as already described in Sec. 2.1. Conversion from ω to 2ω via SHG will occur at the sample, which is a periodic grating—a metasurface—and will therefore diffract light at 2ω (both

SHG from ω and linear scattering from 2ω) into tightly beamed diffraction orders. These are visible as a reciprocal lattice (diamond in the case of a square grating as the metasurface in Figure 1c) in the wavevector (**k**) space, as exemplified by the back focal plane image in Figure 1d. Let me now present the main concepts behind the envisaged experimental realization, whose blueprint is shown in Figure 1e.

Coherent detection Monitoring the (small) SHG signal requires some approach to filter it out from the dominating linear background of diffracted light at 2ω. One can exploit the mechanism anticipated in Sec. 1, whereby the SHG amplitude is modulated by the relative phase of the pumps, Δφ, controlled for example by an electro-optical modulator (EOM). This effectively means implementing a homodyne detection scheme, with the linear scattering acting as the reference (i.e., the *local oscillator*) and demodulation at the EOM frequency performed via **lock-in amplification**. Moreover, scattering constitutes the DC component of the signal and thus can be largely removed via **balanced detection**[10]—an arrangement that offers the advantage of rejecting common-mode noise such as laser power fluctuations. Finally, interferometric detection allows measuring the complex SHG emission, namely, in amplitude (A) and phase (ϕ); and there are good grounds to expect that phase will turn out as a more sensitive probe of the resonance shifts used for sensing.

Common-path interferometer Our current implementation of a ω+2ω excitation relies on a two-arm interferometer for controlling the relative phase and delay of the pump pulses. While this arrangement has demonstrated sufficient interferometric stability,[9] reduction of the noise on the ϕ channel is key to optimizing the sensing performance. I envisage therefore a common-path implementation of the ω+2ω interferometric scheme that would simplify its operation and reduce it to a compact size amenable to a practical sensing device. Importantly, the crystal symmetry of the BBO crystal used for duplication results in a **SHG cross-polarized** to the

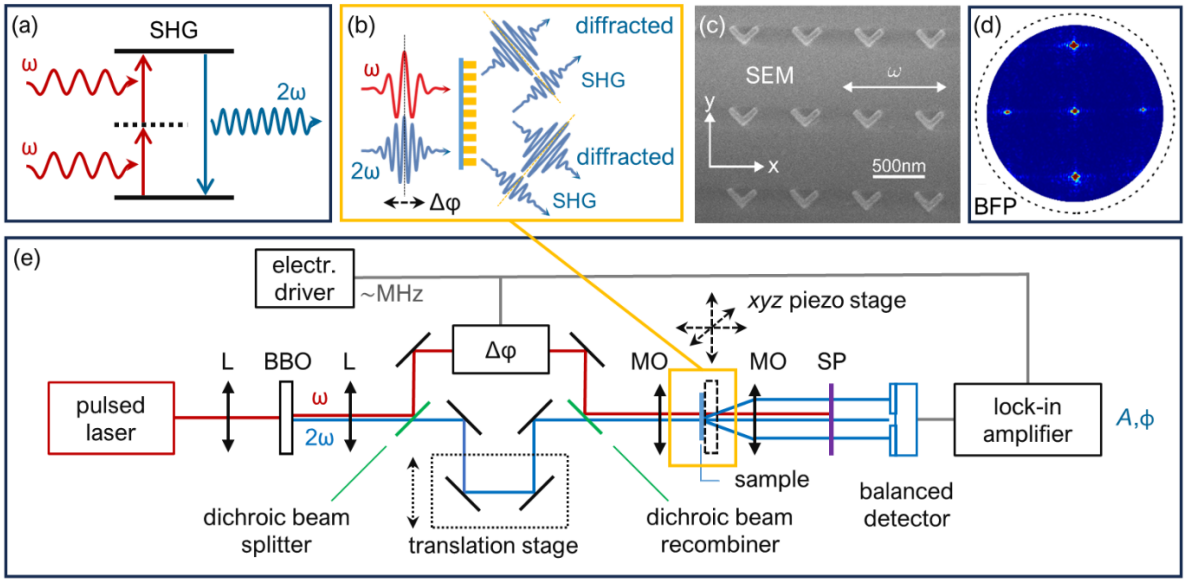

Figure 1 (a) Energy diagram of second-harmonic generation (SHG). (b) Sketch of the envisaged double-pump, phase-modulated excitation scheme. The SHG seeded by the pump at ω is degenerate with the diffracted pump at 2ω, both in wavelength and in wavevector, as both are beamed into the diffraction orders of the metasurface. (c) Scanning electron microscopy (SEM) detail of a representative plasmonic metasurface. (d) Exemplary back focal plane image mapping in the **k**-space the nonlinear emission at 2ω by a plasmonic metasurface excited only at ω. The SHG is channeled into diffraction orders and captured by a CCD camera. (e) Diagram of a realization of a nonlinear interferometry microscope with phase-sensitive balanced detection, described in the text. Acronym key: L = lens (telescope); MO = microscope objective; SP = shortpass filter. Optical elements for beam steering, polarization and power control are omitted from this simplified drawing.

pump at ω. This makes it possible to use **birefringent optical elements** (namely, whose refractive index is different along two perpendicular axes) to control the delay between the two pump pulses. Specifically, the coarse, static temporal superposition between pulses can be controlled using a birefringent slab of variable thickness. This is achieved by sliding two wedges along each other.[11] For the fine, dynamic modulation of Δφ I will use a photoelastic modulator (PEM), namely a transparent bar whose refractive index is modulated along one direction (corresponding to the polarization of the ω beam) via mechanical stress. Typical modulation frequencies ~50 kHz are achieved, corresponding to the transverse vibrational mode of the bar. As discussed above, the phase modulation of the pumps brings about an amplitude and phase modulation of the difference between the 2ω signal collected at opposite diffraction orders. These oscillations at the PEM driving frequency will be then picked up via coherent demodulation by a lock-in amplifier.

3.2. Deployment of a metasurface-based sensing platform

In this section I summarize the practical steps I am planning in order to exploit for sensing the home-built microscope described in Sec. 3.1.

Numerical design Over the last couple of years I have been developing a suite of analytical and numerical methods (mainly **Comsol** models interfaced with **Matlab** scripts) to simulate nonlinear optical processes in individual nanostructures and periodic ensembles; these include rigorous modal decomposition and simulation of far-field coupling, see Ref. [9]. This toolbox will be instrumental for designing the sensing platform, namely adjusting the geometry of the metasurface to achieve a strong resonant behavior at ω and an efficient radiative outcoupling at 2ω. Further down the line, I would like to explore the potential for sensing of collective, delocalized modes such as **surface lattice resonances**, which feature high Q factors (up to thousands)[12] and therefore promise to boost both the nonlinear conversion efficiency (through local field enhancement) as well as the sensing performance.

Samples will be obtained through existing collaborations, as I do not possess the required expertise nor direct access to nanofabrication facilities. For developing and testing the NLO interferometry set-up I will rely on dielectric metasurfaces made by AlGaAs nanocylinders, which are robust and provide a steady SH signal. These are fabricated in the group of Prof. G. Leo at the Université de Paris and are a workhorse of my past and present research activity. For the ensuing demonstration of sensing, I will use **plasmonic metasurfaces** instead, which are provided by Dr. Anne-Laure Baudrion in the Technical University of Troyes—an example is shown in Figure 1c. Plasmonics offers the advantage of a higher sensitivity, given the strong confinement of the electromagnetic field at the metal surface. This comes at the cost of strong dissipation and heating, which makes metallic nanostructures prone to photodamage. Nonetheless, even safely operating at a low power level, our homodyne detection scheme should ensure much lower noise with respect to previous works by the host group.[6]

Sensing We learned in the past[6] how to encapsulate plasmonic metadevices in microfluidic systems, molded by soft lithography in a polydimethylsiloxane (PDMS) slab, which is bonded to the glass substrate after oxygen plasma activation. Initially, a proof-of-principle demonstration of refractive index sensing will be carried out using the standard controlled mixture of ethanol and water. The final goal is to functionalize the gold particles to detect small quantities of biological markers linked to the insurgency of type 1 diabetes, see Sec. 5 below.

4. EXPECTED OUTCOMES

Consistent with the goals laid out in Sec. 2, I aim to progress through the following milestones.

Coherent detection Realization the nonlinear interferometry microscope set-up depicted in Figure 1e and demonstration of a lock-in based, phase-sensitive SHG imaging modality.

Sample Numerical design, nanofabrication, and optical characterization (both linear and nonlinear) of plasmonic metasurfaces optimized for SHG.
Refractive-index sensing Integration of the metasurface in a microfluidic system and determination of the sensitivity to refractive-index variations in homogeneous medium.
Chemical sensing Real-time, label-free detection of small amounts of insulin-autoantibodies produced by patients suffering from type 1 diabetes.
Common-path interferometry Further development of the set-up to a more stable and compact form; comparison of the sensing performance to the previous dual-arm configuration.
Dissemination At the early-stage of technology readiness level (TRL 1 to 3) of this concept and given the academic setting where the work will take place, the expected deliverables are open-access research articles (on Optica journals) as well as contribution to international conferences (including major Optica events such as CLEO).

5. IMPACT

Type 1 diabetes (T1D) is an autoimmune disease, while type 2 diabetes (T2D) results from insulin resistance and pancreatic cell dysfunction. Although T1D was once considered a pediatric disease, approximately one-fourth of affected individuals are now diagnosed during adulthood. Concurrently, the rate of T2D, also called metabolic diabetes, has rapidly escalated in children since the early 1990s, likely linked to the present global obesity epidemic. While T1D and T2D are treated differently, most symptoms overlap so that the two diseases often mask each other, delaying the application of adequate treatment. Indeed, encouraging preliminary studies indicate that immune modulation and antigen-specific therapies can preserve the pancreatic cell functions, but also that these therapeutic interventions are most effective when administered at a very early stage of T1D.[13]
This project aims at demonstrating a NLO biosensing platform for real-time **sensitive detection** of biological markers within **small volumes** of liquid (e.g., blood). The testing ground for such a device will be the detection of the smallest possible amounts of insulin-autoantibodies produced by patients with T1D, allowing an **early diagnosis** of the disease. Such early diagnosis is defined by the detection of two or more autoantibodies against the pancreatic endocrine cells or against specific molecular targets (insulin, glutamic acid decarboxylase and tyrosine phosphatase).[14] Currently, radio-assay, where the target analyte is tagged with a radioactive marker, remains the most common tool to detect these autoantibodies at concentrations down to pM. However, it requires radioactive components, consumes a large blood volume, and presents a long processing time, hence a low throughput.

---

[1] Qin et al., *ACS Nano* **16**, 11598 (2022). DOI: 10.1021/acsnano.2c03310.
[2] Gao et al., *Nano Lett.* **18**, 5001 (2018). DOI: 10.1021/acs.nanolett.8b01827.
[3] Rodrigo et al., *Phys. Rev. Lett.* **110**, 177405 (2013). DOI: 10.1103/physrevlett.110.177405.
[4] Moon et al., ACS Nano **4**, 2070 (2010). DOI: 10.1021/nn901312f.
[5] Mesch et al., *Nano Lett.* **16**, 3155 (2016). DOI: 10.1021/acs.nanolett.6b00478.
[6] Ghirardini et al., *J. Phys. Chem. C* **122**, 11475 (2018). DOI: 10.1021/acs.jpcc.8b03148.
[7] Zilli et al., *ACS Photonics* **8**,1175 (2021). DOI: 10.1021/acsphotonics.1c00112.
[8] Di Francescantonio et al., *Adv. Opt. Mater.* **10**, 2200757 (2022). DOI: 10.1002/adom.202200757.
[9] Di Francescantonio et al., *ArXiv*:2307.01794 (2023). DOI: 10.48550/arXiv.2307.01794.
[10] I earmarked in the budget the price of the Nirvana™ Auto-Balanced Optical Receivers by Newport.
[11] Arrangement marketed as GEMINI by the PoliMi spin-off NIREOS: https://www.nireos.com/gemini/.
[12] Bin-Alam et al., *Nat. Comm* **12**, 974 (2021). DOI: 10.1038/s41467-021-21196-2.
[13] Greenbaum et al., *Diabetes* **61**, 1323 (2012). DOI: 10.2337/db11-1452.
[14] Zhang et al., Nat. Med. **20**, 948 (2014). DOI: 10.1038/nm.3619.

EXECUTIVE SUMMARY

Integrated photonics has led to revolutionary advances in communications, computing, and information processing; however, there is an ever-increasing Challenge to densely encode, manipulate, transmit, and process even more information on a chip. Achieving such integrated photonic devices while maintaining a small size, weight, and power (SWaP) would further augment communications and computing, both classically and in emerging quantum computing and networking infrastructures. The underutilized transverse spatial degree of freedom of multimode waveguides provides a potential route to encoding more information, which can multiplicatively increase the number of information channels carried by a photonic link, i.e., beyond polarization- and wavelength-division multiplexing (WDM). Such mode-division multiplexing (MDM) using just 4 modes has shown promise to massively increase the data capacity of silicon photonic interconnects beyond terabits per second (Tb/s). For example, an MDM x WDM link with 20 wavelengths near 1550 nm, 10 spatial modes per wavelength, and QPSK modulation @ 50 GHz, can achieve high bit rates greater than 20x10x50 = 10 Tb/s, which can be further increased using coherent modulation formats.

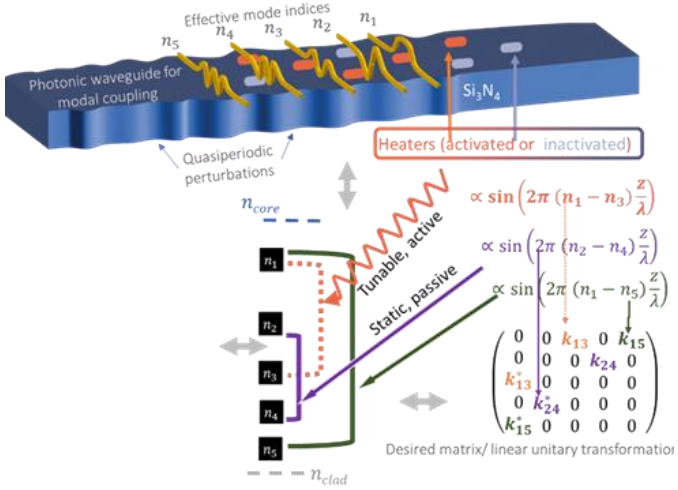

Fig. 1: Multimode photonic waveguide (top) with passive quasi-periodic perturbations and tunable heaters. Bottom: arbitrary engineering of target matrix's coupling amplitude and phase is possible by superimposing subwavelength nanopatterned

However, traditional mode-division multiplexing (MDM) uses each transverse mode as a different information channel, and interference or crosstalk between them is undesirable, hence suppressed. The overarching goal of this Optica Challenge proposal is to explicitly leverage interference between many transverse spatial modes of high-confinement multimode waveguides to build arbitrary scalable photonic circuit topologies for dense classical and quantum information processing with small footprint. This is in striking contrast to existing work which focus on mode conversion, multiplexing and demultiplexing between few modes. A high-contrast multimode waveguide can accommodate many transverse modes (N>10) yet occupy a much smaller footprint than N single-mode waveguides, while still maintaining low-power operation due to SiN's high spatial confinement and ultralow-loss (0.01~0.1 dB/cm), thus improving SWaP. By precisely engineering the amplitude and phase of subwavelength quasiperiodic perturbations to simultaneously couple higher-order modes, we will dramatically scale up the number of modes that can be encoded and processed within a desired footprint, especially within CMOS-compatible silicon-based photonics. In comparison to the predominant technique of creating arbitrary linear transformations or matrix vector multiplications using Mach-Zehnder meshes, our proposal has substantially better scaling with loss, number of modes N, and spatial footprint, especially since it can couple far-off modes in a single shot. If successful, the advance here will be substantial in integrated photonics, comparable to the manipulation and control of free-space orbital angular momentum (OAM) modes through spatial light modulators, but now miniaturized to the chip-scale. Additionally, since our proposed platform uses ultralow-loss silicon nitride waveguides, they are fully quantum-compatible yet possessing low size, weight and power (SWaP). Lastly, since we use high-confinement silicon nitride waveguides for our demonstrations, the proposed approach should be scalable to a wide range of high-confinement platforms like silicon, lithium niobate, diamond and silicon carbide, thus providing a universal tool for ultracompact, dense information processing for emerging technologies such as quantum computing and machine learning hardware.

Title: Integrated mode-multiplexed waveguides with arbitrary connectivity for high-density encoding and processing of information

Introduction, Motivation and Impact

The overarching goal of this Optica Challenge proposal is to explicitly leverage interference between many transverse spatial modes of high-confinement multimode waveguides to build arbitrary photonic circuit topologies for dense classical and quantum information processing with small footprint. This is in striking contrast to existing work which uses transverse waveguide modes as independent information carrier channels, and thus focus on mode conversion, multiplexing and demultiplexing between few modes. By precisely engineering the amplitude and phase of subwavelength perturbations to simultaneously couple higher-order modes, we will dramatically scale up the number of modes that can be encoded and processed within a desired footprint, especially within CMOS-compatible silicon-based photonics. If successful, the advance here will be substantial in integrated photonics, comparable to the manipulation and control of free-space orbital angular momentum (OAM) modes through spatial light modulators[1–3], but now miniaturized to the chip-scale. Additionally, since our proposed platform uses ultralow-loss silicon nitride waveguides, they are fully quantum-compatible yet possessing low size, weight and power (SWaP).

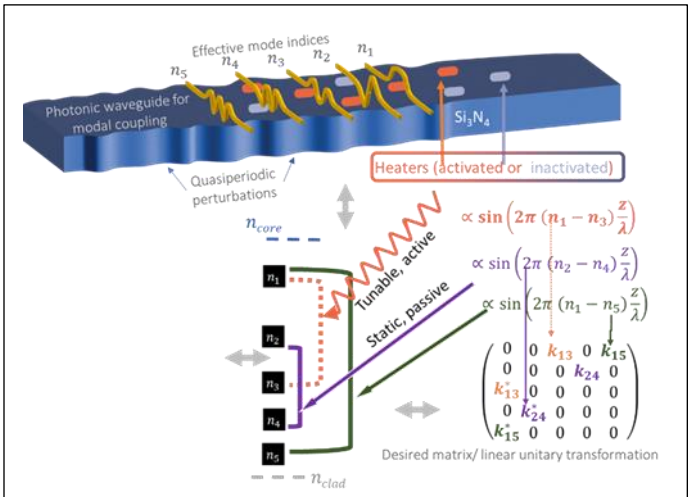

Fig. 1: Multimode photonic waveguide (top) with passive quasi-periodic perturbations and tunable heaters. Bottom: arbitrary engineering of target matrix's coupling amplitude and phase is

Literature Review and Problem Statement

Integrated photonics has led to revolutionary advances in communications, computing, and information processing; however, there is an ever-increasing need to densely encode, manipulate, transmit, and process even more information on a chip. Achieving such integrated photonic devices while maintaining a small size, weight, and power (SWaP) would further augment communications and computing, both classically and in emerging quantum computing and networking infrastructures[4,5]. The transverse spatial degree of freedom[1,5] of multimode waveguides (Fig. 1) provides a potential route to encoding more information, which can multiplicatively increase the number of information channels carried by a photonic link, i.e., beyond polarization- and wavelength-division multiplexing (WDM). Such mode-division multiplexing (MDM) using just 4 modes has shown promise to massively increase the data capacity of silicon photonic interconnects beyond terabits per second (Tb/s)[6]. For example, an MDM x WDM link with 20 wavelengths near 1550 nm, 10 spatial modes per wavelength, and QPSK modulation @ 50 GHz, can achieve high bit rates greater than 20x10x50 = 10 Tb/s, which can be further increased using coherent modulation formats[3,7].

However, traditional mode-division multiplexing (MDM) uses each transverse mode as a different information channel, and interference or crosstalk between them is undesirable, hence suppressed. Here we propose to instead leverage this interference between transverse spatial modes of multimode waveguides to generate any desirable photonic circuit or network with improved SWaP and substantially better scalability compared to existing approaches. We will achieve this controlled interference using precisely engineered wavelength-scale structures on low-loss, high-index-contrast silicon nitride (Si_3N_4 or SiN in

short) waveguides, which are compatible with CMOS silicon-based foundries. A high-contrast multimode waveguide can accommodate many transverse modes (N>10) yet occupy a much smaller footprint than N single-mode waveguides, while still maintaining low-power operation due to SiN's high spatial confinement and ultralow-loss (0.01~0.1 dB/cm), thus improving SWaP.

Note that the PI has previously explored the quantum interference of single photons propagating in two different transverse spatial modes of a single multimode waveguide[8]. For this purpose, an off-chip photon pair source was coupled to two single-mode waveguides and then multiplexed into the multimode waveguide. High-visibility Hong-Ou-Mandel (HOM) interference was observed (**Fig.** Fig. 2), showing the precision with which subwavelength gratings can achieve 50:50 beam-splitters between transverse modes. The generation of maximally entangled N00N states for N=2 was also reported by cascading two 50:50 beam splitters. However, these results were limited to N=2, and the current proposal *dramatically scales this up, aiming to demonstrate a much larger N>10 that can be coupled to create nanopatterned geometries for not only mode conversion but completely arbitrary matrix-vector multiplications*.

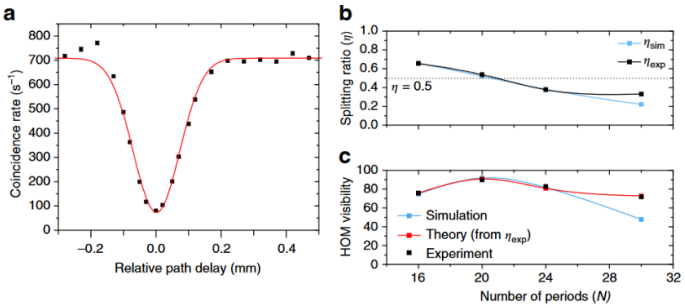

Fig. 2: a. Hong-Ou-Mandel (HOM) quantum interferences between transverse waveguide modes using a 50:50 modal beam splitter showing high visibility >90%. **b.** Control of splitting ratio using the number of periodic gratings, in theory and experiments, and its impact on the HOM visibility.

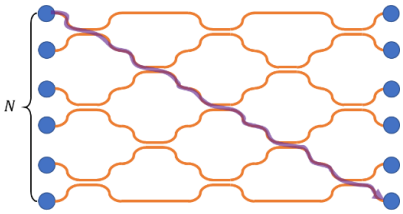

Fig. 3: N × N matrix implementation using a conventional MZI mesh (left). It takes ~N passes to couple the top waveguide mode to the bottom mode in the MZI scheme, as indicated by the purple line. Hence, circuit depth is O(N), spatial footprint is O(N^2), and loss scales exponentially with N. Our proposal has improved scaling (Table 1, Fig. 1) since the top mode can be coupled directly to the bottommost mode.

The network graphs we propose to implement in multimode waveguides have several applications e.g., in optical communications for denser data encoding, optoelectronic computing and photonic machine learning (where they are called matrix-vector multiplications)[9–11] and in quantum computing[12] (where they are termed unitary linear transformations). The prevalent on-chip approach to implement such circuit topologies with N nodes in photonics involves an array of $O(N^2)$ Mach-Zehnder interferometer meshes (MZI) acting on N single-mode waveguides[9] (Fig. 3). Despite impressive demonstrations, this suffers from limitations: only adjacent waveguides can be coupled at a time, and hence a fully arbitrary matrix demands large spatial footprint $O(N^2)$ and insertion loss $O(N)$. The impact of these limitations in comparison to our suggested approach is outlined in Fig. 1, 3 and Table 1.

	Couplings	Spatial Footprint	Loss	Circuit Depth	Reconfigurability
MZI Meshes	Side-by-Side only (adjacent)	$O(N^2)$	$O(N)$	$O(N)$	Easy
Multimode	Arbitrary	$O(N)$	$O(1)$	$O(1)$	Challenging; but possible with PCM/heaters

Table 1: Comparison of the conventional MZI mesh platform for spatially-encoded network graphs to our proposed platform in a multimode waveguide. The ability to implement arbitrary couplings between nodes of the graph enables significantly better scaling in almost all aspects. However, our platform has the drawback that it is not immediately capable of being reconfigured, though we will explore the possibility of using phase-change materials (PCM) or heaters during step IV to add this capability to our platform.

Our proposed multimode implementation resolves these issues since appropriately designed deep-subwavelength perturbations can couple far-separated modes (e.g. TE0 ↔ TE9) directly. ***Multiple superimposed quasiperiodic perturbations can achieve all-to-all arbitrary couplings with desired amplitude and phases, thus implementing the matrix for an arbitrary N-node graph in a single shot.*** Note that this is different from existing mode converters in silicon photonics which use gratings or inverse designed regions to convert an input mode into a desired higher-order mode. Our proposal instead creates any desired topology of coherent coupling between modes with target amplitudes and phases of the coupling through multiple superimposed gratings. Such an approach has sometimes been termed a "synthetic dimension"[13–16], which has shown promise for reconfigurable processing of information in photonics[17].

Work Plan, Outcomes and Impact

We propose the following steps I-V, with I-III being reiterated to achieve optimal metrics (fidelity>95%, loss < 1 dB) for a single waveguide, and IV-V exploring routes for further scaling/reconfigurability.

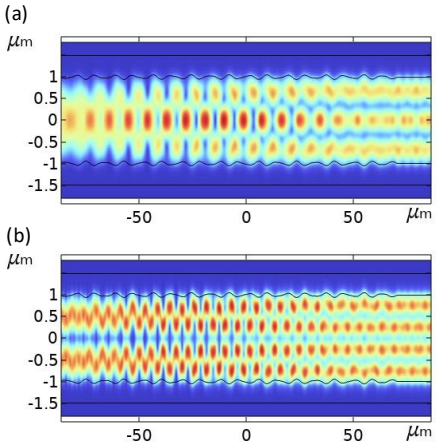

Fig. 4: FEM simulation of a quasi-periodic subwavelength perturbation that couples both TE0 to TE2 and TE1 to TE3 mode with near-unity efficiency. The perturbation is the sum of a sine (period 8.9 μm, amplitude 40 nm) with another sine (period 5.8 μm, and amp. 15 nm).

Task 1. Design deep-subwavelength perturbations for* single-polarization *multimode coupling. By pairing first-principles coupled-mode theory with simulations using finite-element methods (FEM, COMSOL) and finite-difference time domain methods (FDTD, Lumerical), we will design couplings with any desired amplitude and phase between nearby modes (e.g. $TE_0 \leftrightarrow TE_1$) as well as far-separated modes (e.g. $TE_0 \leftrightarrow TE_9$). The coupling between two modes with indices n_{eff1} and n_{eff2} is created by a perturbation with a spatial period $\Lambda=\lambda/\Delta n_{eff}$, where $\Delta n_{eff} = n_{eff1} - n_{eff2}$ (Fig. 1, Fig. 4). We are designing explicit expressions to deterministically couple modes without relying on brute-force 3D propagation simulations, since memory requirements and computation time for such 3D simulations scale unfavorably when long multimode waveguides are involved. Preliminary simulations show that nanoscale perturbations < 5% of the waveguide width (~100 nm for waveguide width of 2 μm) with different periods can simultaneously create the required coupling strengths for nearby and far-off modes while minimizing loss/ backscattering (Fig. 4). We *hypothesize* that linear coupled mode theory, widely used for such purposes, is inadequate, and we will develop semi-analytical expressions to predict the required geometry accounting for nonidealities from (i) field variations across the core-cladding interface, and (ii) the effect of square vs. sinusoidal perturbations, that can design the couplings within seconds, whereas FEM/FDTD simulations take several tens of minutes. PI Dutt has access to university high-performance computing clusters to scale this design to >10 modes and create optimal designs. This task will focus on transverse electric (TE) modes. A symmetric perturbation is needed for coupling modes with the same parity (Fig. 4), while asymmetric perturbations can couple modes with opposite parity (e.g. TE0 to TE3).

Task 2. Fabricate and experimentally characterize single-polarization structures from Task 1: We will fabricate the structures designed above the UMD NanoCenter FabLab facility on 400-nm thick PECVD SiN films grown on oxidized silicon wafers. We chose PECVD as it allows for faster deposition and iteration at CMOS-backend-compatible lower temperatures (<400 °C), but LPCVD films might be chosen later if lower loss is targeted. The deep-subwavelength perturbations (<100nm @ λ=1550 nm) will be patterned through e-beam lithography, which allows for sufficient resolution while maintaining smooth sidewalls. We will measure output mode distributions for various input mode excitations to the multimode waveguide using a fiber-to-chip coupling setup. This is nontrivial since most coupling setups work with

single-mode waveguides. We will use two independent strategies to measure the arbitrary topologies and networks. First, we will fabricate an array of fan-in and fan-out single-mode waveguides that respectively multiplex/demultiplex (mux-demux) a specific mode through phase-matched directional couplers or through inverse-designed multimode interference couplers (Fig. 5)[6,8,18]. Then, we will measure the input-output scattering matrix using lensed-fiber arrays. Second, we will perform spatial homodyne interference of the waveguide's output with a beam of tunable width and phase, followed by imaging of the interference pattern using a CCD camera (charge-coupled device), for single-shot extraction of the complex mode amplitudes without demultiplexing (**Fig.** b).

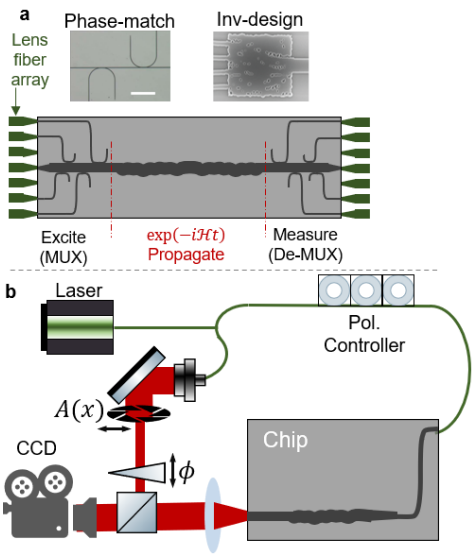

Fig. 5: Two strategies to measure multimode propagation/coupling: **a.** through multiplexing and de-multiplexing such that the I/O waveguides are exclusively single mode. The mux and de-mux structures can be designed using phase matching or inverse design. **b.** through homodyne spatial interference with a reference beam of tunable cross-sectional amplitude A(x) and phase ϕ.

Task 3: Design, fabricate and test dual-polarization coupled multimode structures: Tasks 1 and 2 will focus exclusively on coupling higher-order modes with transverse-electric (TE) polarization. To support multiple transverse magnetic (TM) modes, we will need thick films (> 1 μm) that suffer from high-stress-induced film cracking. We will mitigate this by depositing non-stoichiometric low-stress SiN films with pre-inscribed trenches, as shown by the PI in previous work[19,20].

Task 4: Explore routes to post-fabrication tunability, reconfigurability: The matrix transformations in Tasks 1, 2 and 3 are passive, thus not tunable post fabrication. We will explore the integration of patterned heaters[21,22] atop passive SiN, as shown by PI Dutt earlier, which allows for electrically-induced, index perturbations without increasing the loss of the SiN device layer, thus enabling us to tune or reconfigure the network. The separation between the integrated platinum microheaters and the device layer will be > 2um to prevent such increase in loss.

Task 5: Further scale-up through multiple waveguides: We expect each multimode waveguide to host up to ~15 modes before the index differences between high-order modes become too small and sensitive to fabrication. Next, we will evanescently couple several multimode waveguides, and inverse-design coupling regions which allow a high-order mode (TE7) in the first waveguide to convert into a different high-order mode in the second waveguide (TE9). Although this design does not provide long-range connectivity between non-adjacent waveguides, we anticipate a large subset of network topologies or matrices to be implemented scalably (e.g. 10 waveguides × 15 modes/waveguide = 150×150 matrices).

References

1. Rubinsztein-Dunlop, H. *et al.* Roadmap on structured light. *J. Opt.* **19**, 013001 (2016).
2. Berkhout, G. C. G., Lavery, M. P. J., Courtial, J., Beijersbergen, M. W. & Padgett, M. J. Efficient Sorting of Orbital Angular Momentum States of Light. *Phys. Rev. Lett.* **105**, 153601 (2010).
3. Wang, J. *et al.* Terabit free-space data transmission employing orbital angular momentum multiplexing. *Nat. Photonics* **6**, 488–496 (2012).
4. Awschalom, D. *et al.* Development of Quantum Interconnects (QuICs) for Next-Generation Information Technologies. *PRX Quantum* **2**, 017002 (2021).

5. Nape, I., Sephton, B., Ornelas, P., Moodley, C. & Forbes, A. Quantum structured light in high dimensions. *APL Photonics* **8**, 051101 (2023).
6. Yang, K. Y. *et al.* Inverse-designed multi-dimensional silicon photonic transmitters. *arXiv:2103.14139* (2021) doi:10.48550/arXiv.2103.14139.
7. Liu, X. *et al.* 448-Gb/s Reduced-Guard-Interval CO-OFDM Transmission Over 2000 km of Ultra-Large-Area Fiber and Five 80-GHz-Grid ROADMs. *J. Light. Technol.* **29**, 483–490 (2011).
8. Mohanty, A. *et al.* Quantum interference between transverse spatial waveguide modes. *Nat. Commun.* **8**, 14010 (2017).
9. Shen, Y. *et al.* Deep learning with coherent nanophotonic circuits. *Nat. Photonics* **11**, 441–446 (2017).
10. Wetzstein, G. *et al.* Inference in artificial intelligence with deep optics and photonics. *Nature* **588**, 39–47 (2020).
11. Kudyshev, Z. A., Shalaev, V. M. & Boltasseva, A. Machine Learning for Integrated Quantum Photonics. *ACS Photonics* **8**, 34–46 (2021).
12. Clements, W. R., Humphreys, P. C., Metcalf, B. J., Kolthammer, W. S. & Walmsley, I. A. Optimal design for universal multiport interferometers. *Optica* **3**, 1460–1465 (2016).
13. Lustig, E. & Segev, M. Topological photonics in synthetic dimensions. *Adv. Opt. Photonics* **13**, 426–461 (2021).
14. Ozawa, T. & Price, H. M. Topological quantum matter in synthetic dimensions. *Nat. Rev. Phys.* **1**, 349–357 (2019).
15. Bartlett, B., Dutt, A. & Fan, S. Deterministic photonic quantum computation in a synthetic time dimension. *Optica* **8**, 1515–1523 (2021).
16. Dutt, A. *et al.* Experimental band structure spectroscopy along a synthetic dimension. *Nat. Commun.* **10**, 3122 (2019).
17. Buddhiraju, S., Dutt, A., Minkov, M., Williamson, I. A. D. & Fan, S. Arbitrary linear transformations for photons in the frequency synthetic dimension. *Nat. Commun.* **12**, 2401 (2021).
18. Yang, K. Y. *et al.* Inverse-Designed Optical Interconnect Based on Multimode Photonics and Mode-Division Multiplexing. in *2020 Conference on Lasers and Electro-Optics (CLEO)* 1–2 (2020).
19. Luke, K., Dutt, A., Poitras, C. B. & Lipson, M. Overcoming Si3N4 film stress limitations for high quality factor ring resonators. *Opt. Express* **21**, 22829–22833 (2013).
20. Ji, X. *et al.* Ultra-low-loss on-chip resonators with sub-milliwatt parametric oscillation threshold. *Optica* **4**, 619–624 (2017).
21. Dutt, A. *et al.* On-chip dual-comb source for spectroscopy. *Sci. Adv.* **4**, e1701858 (2018).
22. Dutt, A. *et al.* Tunable squeezing using coupled ring resonators on a silicon nitride chip. *Opt. Lett.* **41**, 223 (2016).

Executive summary

The rise in the rate of plastic waste accumulation currently surpasses the capabilities of recycling technologies and leading towards dangerous concentration of microplastics in the environment. An obvious solution of burning plastics is barred by the toxic chemicals that are produced during the incineration process. The commonly proposed methodologies usually involve large scale and high up-front costs installations, which incentivizes future production of plastics while reduction in plastic consumption is currently promoted. Furthermore, removal of persistent toxic chemicals is an energy intensive process, as high energy bonds must be separated to form new inert compounds. This in turn makes it very efficiency sensitive problem, even more so in face of energy consumption driven climate change. One of the classic approaches to the problem of toxic chemicals is photolysis. However, it is rather limited in terms of energy efficiency due to physical restriction in ultraviolet sources. On the other hand, the efficiency of infrared sources has experienced a steady growth in recent years which has also led to advances of laser sources in this spectral region. If we consider that bond dissociation observed after absorption of ultraviolet photons can also be achieved by simultaneous multiphoton absorption, new possibilities for photolysis arise. Therefore, in this application we propose investigation of laser resonator based nonlinear photolysis as an efficient tool for such toxic molecules accelerated decomposition. However, there is little information on the nonlinear absorption induced dissociation in toxic chemical compounds. Therefore, the investigation begins by characterizing the interaction at various parameters such as incident wavelength, pulse duration, concentration, and intensity. Using this information theoretical design as well as the optimization of the laser resonator and the nonlinear photolysis process will take place. This will be followed by the evaluation of physical as well as economic viability. In case of positive outcome, a construction of a prototype will commence.

Nonlinear laser resonator-based photolysis for accelerated decomposition of dioxins.

One of the many issues that our society is facing right now is the accumulation of plastic pollution. While the preferred method would be to recycle the plastics, as it currently is, the recycling technology cannot keep up with the production. Less than 10% of plastic is recycled on average across the world [1]. Meanwhile the production is expected to grow even further with the world moving to sustainable energy sources and the fossil fuel companies using plastics as an off ramp. Furthermore, not all types of plastics can be recycled and the quality of those that can usually degrades with each recycling cycle eventually becoming unusable [2,3].

An obvious solution to the problem of accumulation would be burning the plastics before they can reach the environment. After all most plastics are just a different state of fossil fuels, and it would be a preferable alternative to poisoning our water supplies and soil with microplastics – the end state of natural decay for most the plastic discards. [4,5,6]. However, proper disposal of plastics via burning requires very specific conditions – if the temperature or the amount of oxygen is insufficient, this could lead to the formation of toxic chemicals such as polycyclic aromatic hydrocarbon, furans, and dioxins [7,8,9] that could potentially cause even more harm than the microplastics.

Solutions for controlled disposal of plastics already exist. For example, high temperature or electric discharge waste incinerators with filtering systems for emission control. However, they are barred behind large upfront costs as to be efficient large plants are necessary. Such also demands high volumes of plastics and leads to complex logistical networks. Therefore, a small and relatively cheap method for removing pollutants from the output streams could provide a localized, maybe even mobile, solution to the already accumulated waste problem while not encouraging prolonged use and, subsequently, production of plastics due to the large upfront investment.

The existing technologies for dealing with toxic emissions can be separated into two sections – capture [10] and degradation [11] of pollutants to inert chemicals. While the primary is usually easier to implement via employment of filtering systems it does not fully address the problem as the toxic pollutants still need to be eventually destroyed. The latter is not always a trivial process – the chemical compounds that escape the incineration process usually exhibit strong chemical bonds, which makes natural decomposition unlikely and leads to the accumulation in the natural environment [12]. A strong bond means that extreme conditions are necessary to decompose the material. There are many ways these can be achieved. These include but are not limited to: Incineration at very high temperatures [13], fragmentation via photolysis [14], chemical decomposition via highly reactive compounds or via catalytical reactions [15], mineralization, irradiation with high energy ionizing particles or decomposition [16,17] via electric discharge [18].

When it comes to photolysis the limiting factor is the efficiency of the process. The prime issue with efficiency arises from the fact that if high energy bonds are to be destroyed light photons with similar energy are necessary. In case of the organic pollutants resulting from plastic incineration, photons in ultraviolet side of the spectrum must be used. However, the current technology can not produce efficient light sources in this spectral diapason. The highest reported efficiency near 250 nm comes from mercury lamps and does not exceed 35% [19]. Furthermore, only a fraction of photon interaction finalizes in the dissociation of the molecular bonds. There is a possibility that the recently separated molecular bonds can still reform by releasing the excess energy via heat

transfer [20]. This can happen if the density is sufficient for efficient energy coupling via molecular impact. On the other hand, optical absorption also depends on the density of the material and this disparity complicates the control of the process. The issue can be remedied to some extent by extending the volume of the sample or using multiple reflections however, the optical elements for UV radiation are known to degrade [21] and typically possess lower values of parameters such as reflection coefficient [22], damage threshold [23] and higher price due to more stringer requirements caused by the shorter wavelengths. In turn this would further reduce the total efficiency of the system.

In this work we explore an alternative approach to photolysis based on infrared radiation. Instead of a single high energy photon multiphoton ionization can be employed to cause molecular dissociation. This is a commonly encountered and well-known phenomena in the field of laser physics [24]. However, it is rarely considered as a driver for photochemical reactions and there are multiple reasons for this. To begin with the conditions necessary to efficiency ionize materials with IR pulses can be relatively hard to achieve. Typically, durations at sub nanosecond scale and intensities in above $10^{12}W/cm^2$ level are required [25]. This means that due to the restriction of optical damage on the optical components in use it is hard to create large volumes of space where such intensities can be maintained which could lead to scaling issues. Furthermore, only a fraction of energy from the pulse can be used in the process – as soon as the light pulse leaves the focal volume and intensity falls below certain value – the multiphoton ionization becomes unlikely and the residual IR photons are wasted. This makes the straightforward approach of irradiating the sample mixture directly rather energy inefficient.

With ultrafast laser technology maturing, the prices for such laser systems and laser components have experienced a steady decline which makes them more than ever competitive with alternative methods for chemical decomposition. In this proposal, we consider the case of multi-pass nonlinear excitation with the photodecomposition taking place within the focal volume. A simplified photoreactor system could consist of a laser resonator supplemented by focusing optics to create a focal spot within this closed loop. High quality and inherently low loss resonator could be achieved by using high reflection mirrors on both ends of the resonator, antireflecting coating and Brewster angle optics within the system. Optical to optical efficiencies for thin disk lasers are reported to achieve close to 80% [26]. Significant loss per round trip would only occur in the focal spot due to nonlinear absorption or ionization. This would only remove a fraction of the energy from the oscillating pulse which in turn could be resupplied in the active laser media via optical pumping. The effectiveness of laser resonator pumping has also experienced steadily improvement over the year with the recent advances in light emitting diode laser for near infrared region pushing for close to 80% [27] efficiencies. In this manner, by applying short laser pulses, we strive for an efficient funnel to transfer energy from the infrared radiation into the target molecule. However, such approach has not been yet investigated so a lot of uncertainties lies ahead. One of which is how selective such nonlinear excitation could be what laser wavelength would be the most energy efficient and similar. Therefore, before such system can be designed and constructed, measurements of nonlinear interaction at various impulse energies, wavelengths, and intensities with toxic elements such as dioxins are required.

Problem statement

Development of small-scale high efficiency nonlinear resonator-based photolysis system for rapid decomposition of toxic chemical compounds resulting from plastic burning.

Work plan

- Since the optimal condition for the nonlinear ionization of the materials is not clear the works begins with measuring the parameters of the interaction by employing variable wavelength ultrafast laser sources and pump-probe methodology.
- The obtained results will be used in the theoretical design of the resonator to minimize the energy loss and optimize wavelength selectivity, pulse duration and beam intensity near the focal volume within the resonator and calculate the necessary flow of compound for optimal decomposition.
- Selection of optical components and laser media, theoretical evaluation of best-case efficiency comparison to available technologies.
- Construction of a prototype, optimization, and laboratory testing.

Outcomes

- Characterization of nonlinear absorption at various infrared wavelengths.
- Selection of suitable laser media for optimal wavelength and minimal loss of energy.
- Theoretical design and optimization of the resonator based photoreactor.
- Evaluation of the viability of the methodology.
- Potential prototype of the photoreactor.

Impacts

- The primary impact would be evaluation of nonlinear photolysis as a tool for dealing with toxic byproducts of plastic burning.
- If successful it could lead to further research on decomposition of other resilient chemical compounds such as PPAS.
- In case of a very high success this could lead to novel small scale photochemical reactor designs enabling efficient processing of chemical compounds with strong bonds into desirable chemical products such as CO2 into CO and O2.
- Potential small-scale energy-based air scrubbers.

Literature

[1] Ellen MacArthur Foundation and McKinsey & Company, The New Plastics Economy: Rethinking the future of plastics. World Economic Forum, 2016.
[2] RAHIMI, AliReza; GARCÍA, Jeannette M. Chemical recycling of waste plastics for new materials production. Nature Reviews Chemistry, 2017, 1.6: 0046.
[3] DORIGATO, Andrea. Recycling of polymer blends. Advanced Industrial and Engineering Polymer Research, 2021, 4.2: 53-69.
[4] DO SUL, Juliana A. Ivar; COSTA, Monica F. The present and future of microplastic pollution in the marine environment. Environmental pollution, 2014, 185: 352-364.
[5] CRAWFORD, Christopher Blair; QUINN, Brian. Microplastic pollutants. Elsevier, 2016.
[6] CHIA, Rogers Wainkwa, et al. Microplastic pollution in soil and groundwater: a review. Environmental Chemistry Letters, 2021, 19.6: 4211-4224.
[7] VERMA, Rinku, et al. Toxic pollutants from plastic waste-a review. Procedia Environmental Sciences, 2016, 35: 701-708.
[8] VALAVANIDIS, Athanasios, et al. Persistent free radicals, heavy metals and PAHs generated in particulate soot emissions and residue ash from controlled combustion of common types of plastic. *Journal of hazardous materials*, 2008, 156.1-3: 277-284.

[9] NAKAO, Teruyuki, et al. Formation of toxic chemicals including dioxin-related compounds by combustion from a small home waste incinerator. Chemosphere, 2006, 62.3: 459-468.
[10] KUO, Jia-Hong, et al. The prospect and development of incinerators for municipal solid waste treatment and characteristics of their pollutants in Taiwan. Applied Thermal Engineering, 2008, 28.17-18: 2305-2314.
[11] VERMA, Sanny, et al. Recent advances on PFAS degradation via thermal and nonthermal methods. Chemical engineering journal advances, 2022, 100421.
[12] MCLACHLAN, Michael S. A simple model to predict accumulation of PCDD/Fs in an agricultural food chain. Chemosphere, 1997, 34.5-7: 1263-1276.
[13] VAN BERKEL, Olga M.; OLIE, Kees; DEN BERG, Martin Van. Thermal degradation of polychlorinated dibenzo-p-dioxins and polychlorinated dibenzofurans on fly ash from a municipal incinerator. International journal of environmental analytical chemistry, 1988, 34.1: 51-67.
[14] MILLER, Glenn C., et al. Photolysis of octachlorodibenzo-p-dioxin on soils: production of 2, 3, 7, 8-TCDD. Chemosphere, 1989, 18.1-6: 1265-1274.
[15] FINOCCHIO, Elisabetta; BUSCA, Guido; NOTARO, Maurizio. A review of catalytic processes for the destruction of PCDD and PCDF from waste gases. Applied Catalysis B: Environmental, 2006, 62.1-2: 12-20.
[16] TROJANOWICZ, Marek. Removal of persistent organic pollutants (POPs) from waters and wastewaters by the use of ionizing radiation. Science of The Total Environment, 2020, 718: 134425.
[17] ZHOU, Y. X., et al. Application of non-thermal plasmas on toxic removal of dioxin-contained fly ash. Powder technology, 2003, 135: 345-353.
[18] YOSHIDA, Keiichiro, et al. Pilot-scale experiment for simultaneous dioxin and NO x removal from garbage incinerator emissions using the pulse corona induced plasma chemical process. Plasma chemistry and plasma processing, 2009, 29: 373-386.
[19] Bright Future of Deep-Ultraviolet Photonics: Emerging UVC Chip-Scale Light-Source Technology Platforms, Benchmarking, Challenges, and Outlook for UV Disinfection
[20] LYMAN, John L.; JENSEN, Reed J. Chemical reactions occurring during direct solar reduction of CO2. Science of the total environment, 2001, 277.1-3: 7-14.
[21] GATTO, Alexandre, et al. Toward resistant UV mirrors at 200 nm for free electron lasers: manufacture, characterizations, and degradation tests. In: Inorganic Optical Materials II. SPIE, 2000. p. 261-275.
[22] https://www.edmundoptics.eu/knowledge-center/application-notes/optics/highly-reflective-coatings/
[23] GALLAIS, Laurent, et al. Wavelength dependence of femtosecond laser-induced damage threshold of optical materials. Journal of Applied Physics, 2015, 117.22.
[24] MAINFRAY, G.; MANUS, G. Multiphoton ionization of atoms. Reports on progress in physics, 1991, 54.10: 1333.
[25] GULLEY, Jeremy R. Frequency dependence in the initiation of ultrafast laser-induced damage. In: Laser-Induced Damage in Optical Materials: 2010. SPIE, 2010. p. 239-252.
[26] ALABBADI, Abdullah; LARIONOV, Mikhail; FINK, Florian. High-power Yb: YAG thin-disk laser with 80% efficiency pumped at the zero-phonon line. Optics Letters, 2022, 47.1: 202-205.
[27] YAMAGATA, Yuji, et al. Highly efficient 9xx-nm band single emitter laser diodes optimized for high output power operation. In: High-Power Diode Laser Technology XVIII. SPIE, 2020. p. 10-15.

Executive Summary of the challenge project

In the low-carbon future, hydrogen plays a vital role as an alternative and sustainable energy carrier that can be stored and used to release its energetic potential, of chemical, electrical, or thermal nature, on demand. Proton exchange membrane water electrolyzer (PEMWE) is the most promising technique for hydrogen production. A variety of different transport processes, such as proton flux and mass (liquid, gas, vapor) diffusion, pressure- or concentration-driven, are involved in the operation of a PEMWE cell; On the anode side, upon applying an electrical current, water is oxidized and releases gaseous oxygen, electrons, and protons; While electrons and protons reach the cathode side, the non-oxidized water and oxygen gas are transferred back to the entrance flow channel; On the cathode side, electrons and protons recombine to form hydrogen. Investigating these processes is crucial for controlling the local concentration and efficient distribution of various species in the reaction sites of the cell.

The PEMWE assembly consists of adjacent compact layers stacked in the cell to provide multiphase (gas, liquid, and ions) permeability, optimize the contact area between the layers, and increase the thermal and electrical conductivity of the device for efficient species transportation. The liquid/gas diffusion layer (LGDL) on the anode side acts as an entrance gateway for controlling the water flow rate from the entrance flow field channel to the rest of the cell while removing the produced oxygen gas bubbles. The access of the reactive sites to the water and the hydration of the membrane while preventing the flooding of the electrodes are crucial for the whole cell's performance. The performance and durability of the cell are also associated with the produced gas density in two-phase regions. For instance, the accumulation of oxygen gas can shield the anode from water and negatively impact cell performance. For these reasons, LGDL significantly influences the performance and efficiency of the PEMWE cell. Therefore, methods that provide new insights into the dynamic behavior and distribution of liquid water as it migrates through LGDL allow an early diagnosis of the faulty states with inefficient access to the water. Moreover, techniques for simultaneous visualization of liquid/gas transfer through this reactive site provide a deeper understanding of the complexity of underlying processes. Particularly, observational methodologies can enable the identification of the connectivity and interdependence of the species in this multiphase region where both the flow field of gas and water need to be analyzed.

Herein, we propose an optical quantitative methodology for the *in-situ* evaluation of water/gas transport in PEMWE cells. The proposed optical system is designed for two-phase visualization of water and gas through LGDL on the anode side of the PEMWE cell. While the available observational diagnostic techniques for PEMWE are mostly *ex-situ,* offering insights into the distribution of the water droplets within the LGDL, our proposed experimental setup allows a simultaneous evaluation of bulk transport of liquid water through LGDL as well as the distribution of oxygen gas bubbles on its surface during the PEMWE operation. Similar to the well-established optical techniques for flow measurements, such as Schlieren Imaging and Mach-Zehnder interferometry, we apply the dependence of the fluid's medium refractive index on its density. The goal is to measure the optical path differences caused by the refractive index nonuniformities due to various water densities through instantaneous recording of the phase variation of the light field as it passes through the LGDL. The recorded interferogram provides spatial information about the water density variation as it flows through different paths in LGDL. In addition, we use the deflection of the light ray traces caused by oxygen bubbles to measure the distribution of gas on the LGDL surface. The present proposal describes in detail the technical and experimental adaptations to apply these concepts for the case of two-phase flow measurement in a PEMWE cell. The viable optical setup will present a diagnostic prototype device capable of simultaneously quantifying the two-phase (gas/water) flow through a delivery channel (LGDL). Ultimately, the results of the experiments provide an in-depth understanding of micro- and macroscale phenomena in the PEMWE cell, helping to develop new materials for multi-phase delivery sites.

Literature Review

Hydrogen production, despite the numerous available amounts of this simple element on earth, has not yet reached a high level. PEM water electrolyzer, one of the most promising techniques for producing hydrogen, covers only 4% of global hydrogen production [1]. To increase the level of hydrogen production and turn it into a frequently used energy source, improvements in production cost, the durability of the PEMWE, and the lifespan of its construction material are necessary. Diagnostic tools can provide profound insights into the operation of this technology and help accelerate its development process.

Several electrochemical techniques, such as polarization measurements, electrochemical impedance spectroscopy (EIS) [2] and concentration alternating frequency response analysis (CFRA) [3], have been developed to study the processes in the PEM fuel cell in detail. PEM fuel cell is a technique for hydrogen storage. It is similar to the PEMWE in construction but functions reversely. In contrast to the PEMWE, for instance, there is no gas production on the electrode sides of the PEM fuel cell. The gas-evolving electrodes have a complex feedback effect on the mass transfer in PEMWE, making it more complicated to be fully understood [4]. A simplified schematic configuration of a PEMWE unit cell is shown in **Figure 1A**. A proton-conductive polymer membrane separates the cell into two halves. The anode and cathode sides of the membrane are attached to a thin catalyst layer. A liquid/gas diffusion layer (LGDL) is placed on both sides of the cell between the membrane electrode assembly and the bipolar plates. Each component acts as a delivery channel or transportation site which controls the various species' transport, allowing some species to permeate while expelling others. Visualization of the transport of different species through these delivery channels can provide more information about the flow dynamics inside the PEMWE cell.

Some optical techniques, jointly with electrochemical devices, were used to characterize the two-phase (water/gas) flow behavior in PEMWE cells [5, 6]. In these in-situ visualization techniques, continuous images of bubbles evolution were acquired by a high-speed camera. These images revealed the two-phase behavior of the anode flow channel while both oxygen gas and water were present. A high-power lighting system illuminated the channel during the measurement. By tracking the movement of bubbles from consecutive images based on the time interval for the bubbles to travel a given distance, the flow velocity could be quantitatively measured [6]. However, an accurate quantitative in-situ visualization of two-phase flow without simultaneously using an electrochemical technique has not been reported yet. In addition to the complexity of processes occurring in micro- and macroscale in PEMWE, the difficulty of integrating an optical setup with a PEMWE cell might be the main reason why in-situ optical techniques have not been used frequently to achieve visualization-based flow measurements within the cell. The layers in a PEM cell are stacked, and the whole system is optically opaque. Therefore, the only access for visualizing the processes in the cell is through bipolar plates. As a result, transparent flow field channels or endplates are used for optical characterization with a camera system [5]. Ex-situ visualization techniques are also capable of overcoming the optical configuration challenge. For instance, fluorescence microscopy was used for the ex-situ visualization of water transport processes in gas diffusion layers. By employing fluorescein dye and using the correlation between local intensity and concentration, various paths of water inside the LGDL and the dynamic interaction between adjacent flow paths could be identified [7]. However, spatially resolving the flow within a single pore, i.e., the through-hole visualization of the water paths along the length of LGDL, needs a resolution beyond the mean LGDL hole size (~35 μm).

The availability of various well-established optical methods for fluid measurements motivates the development of an optical characterization technique for flow visualization in a PEMWE cell. Optical methodologies for fluid dynamic visualization have been used for various purposes. In addition to high-speed imaging systems which aim at obtaining precise information about the position and dimensions of the fluid flow at continuous time intervals [8], other commonly used instruments such as Schlieren

Imaging and Mach Zehnder Interferometer [9, 10] have been developed for flow visualization and measuring fluid density. The exploited effect in these techniques is a produced variable phase distribution of light upon passing through media with different refractive indices. Information about flow density is then provided by continuously measuring the variation of photographic density. Compared to photos, interferometric patterns enable a more accurate evaluation of the phase distribution variation. For quantitative analysis, therefore, a Mach-Zehnder interferometer or its combination with a Schlieren setup is usually preferred [11, 12].

Problem Statement/Objective

A simplified flow field system, as depicted in **Figure 1B**, will be used for preliminary experiments. The goal of these experiments is to focus on examining the two-phase flow field measurement without the complexity of the optical geometry that is needed for the actual PEMWE diagnosis. In addition, the simplified model of the flow field channel is suitable for adding the analytes (water and gas) step by step while evaluating them separately before performing a simultaneous two-phase measurement experiment. A customized glass house made of BK7 with the possibility of vertical installation of LGDL, as depicted in **Figure 1Bb**, will be applied as the flow chamber to provide optical access into the flow field. A syringe pump (**Figure 1Ba**) produces various water flow rates to pass through LGDL. We will use two kinds of LGDL; the conventional model made of porous media such as carbon cloth or carbon fibers (**Figure 1Bc-left**) and the novel thin LGDL made of Titanium (**Figure 1Bc-right**). While the first model is commercially available and widely used in PEMWE, the thin metallic LGDL with customized pore size and morphology has been recently developed for higher-efficiency hydrogen production [13]. The main difference between the two LGDL models is their thickness which is an essential parameter for our study because it affects the water rate along the through-plane height of the LGDL and, consequently, the light-illuminating strategy to have the entire area of the LGDL simultaneously in focus. We will use Bessel beam for this purpose. As the pressure in the syringe pump increases, the path evolves inside the LGDL. A random water path inside a porous media is shown in **Figure 1Bd**. Slowly increasing the pressure controlled by the pumping rate of the syringe pump will allow us to observe and measure the step-by-step evolution of the water path and density.

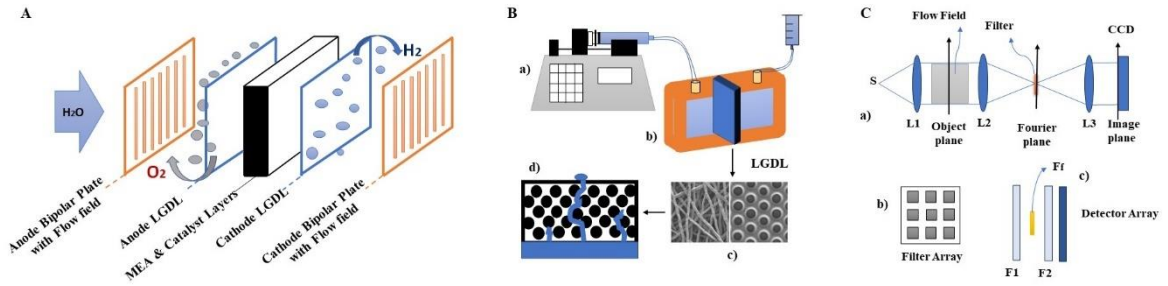

Figure 1: Schematic configurations of PEM water electrolyzer cell (A), simplified model for flow field channel including syringe pump (Ba), BK7 glass chamber (Bb), the conventional LGDL (Bc-left), and the novel thin LGDL (Bc-right) (Figure Bc taken from [13]). The random water path inside a porous media is shown in Bd. The optical concept of the Schlieren system is depicted in Ca. The modulated configuration for the collecting optics (Cc) includes filter arrays (F1 and F2, shown schematically in Cb), disturbance filter (Ff), and CCD detector array.

We choose the Schlieren optical system and adapt it for water density measurements in the anode side of the PEMWE cell. In the available quantitative Schlieren systems, as shown in **Figure 1Ca**, the collimated light, after illuminating the flow field, is brought to the focal plane of a lens. Since various portions of the flow field have different refractive indexes (due to flow density variation), the light possesses the corresponding phase variation. This phase variation can be observed in the image plane by introducing modification into the focal plane. The free-field (undisturbed) light portion will then interfere with the disturbance portion on the image plane. The *Dale-Gladstone Law* defines the relation between phase and flow density distribution. The first challenge for using this usual form of the Schlieren system for the two-phase flow field measurement in a PEMWE cell is the quantitative

analysis of the interference pattern. The optical path differences that occur throughout the entire light path along the length of the LGDL are affected by variations in the random distribution of the water density and the presence of gas bubbles which are also randomly distributed on the surface of the LGDL. The result is a density distribution with a complex function. For simplifying the phase distribution analysis, the refractive index should be separately analyzed in lateral (on the surface of the LGDL) and axial (along the length of the LGDL) directions. In this way, the variation in each part of the interference image can be associated with the density variation of the corresponding portion. The effect of various flow field portions on the light beam, as it passes through different lateral regions, can be differentiated by introducing a substructure to the detection of the measurement volume. On the side of collection optics, the lenses L2 and L3 are replaced by filter arrays (**Figure 1Cb**) attached to a CCD filter array. The disturbance filter is sandwiched between two filter arrays (**Figure 1Cc**). Each array of the filters and their corresponding CCD pixels can be considered as one channel controlling the reaching of the light to the detector based on their transmission function. In this study, the arrays are designed to act as micro diffractive lenses. Using the spatial light modulator (SLM) for F1 and F2 makes it possible to change the focal length, size of the arrays, or even the transmission function of each array during the experiment. For the disturbance filter, we apply a derivative transmission function so that the resulting intensity is proportional to the phase function gradient. Designing a suitable disturbance filter is critical for analyzing the resulting phase distribution. The compact configuration of filters and CCD arrays instead of the bulky feature of the collecting optics is also more suitable for PEMWE cells.

Integrating the optical setup with the optically nontransparent construction of PEMWE in a sealed compartment is another challenge. LGDL is in close contact with the anode catalyst layer and membrane. Therefore, it is not possible to apply the transmissive configuration of the Schlieren system for our experiments. Designing a suitable geometry with practicality for an operating PEMWE system is a foreseen task for work package three. The collecting optic should be placed on the anode side. One possible way is to add a reference beam to the illumination with a small angle relative to the main beam, which is parallel to the flow field, allowing them to interfere inside the LGDL. Unlike the main beam, the reference beam will deflect inside the LGDL at the end of water surface. With this strategy, the contributed light field from each one of the four-interference sentences will be deflected and separated by an angle making it possible to capture the virtual image on the anode side. Moreover, the maximum intensity of interfered light defines the maximum length to which the water is evolved.

Outline of tasks

WP	**Content**	**## PM** **Person-Months**
1	**Preparation:** The first two months are devoted to experimental specifications. This time is especially required for ordering customized materials such as flow-field chamber and LGDL.	1 PM
2	**Proof of Concept (preliminary Experiments)**	4 PM
2.1	Water-flow measurement test	1.5
	The optical setup for water flow measurement through LGDL using the simplified flow field channel is optimized.	
2.2	Gas-density measurement test	1.5
	In this work package, the applicability of the proposed optical setup for measuring the density distribution of gas bubbles on the LGDL surface is tested in a water-free flow field channel.	
2.3	Two-phase measurement test	1
	The two-phase measurement capability of the proposed optical system is investigated by simultaneously using gas and water in the flow field.	

WP	Content	## PM Person-Months
3	**Design and layout of the optical configuration**	5 PM
3.1	Integrating the optical setup with a PEMWE cell – configuration and optimization	2.5
3.2	Integrating the optical setup with a PEMWE cell – Experiments and data analysis	2.5
4	**Communication and Dissemination**	2 PM
	The possible ways of communication and dissemination (open-access publication, patent, industrial prototyping, …) with considering the acquired results and advice from the Challenge Committee are evaluated and executed.	

Work Plan

Work Packages	First Year										Second Year											
	PM1	PM2	PM3	PM4	PM5	PM6	PM7	PM8	PM9	PM10	PM11	PM12	PM13	PM14	PM15	PM16	PM17	PM18	PM19	PM20	PM21	PM22	PM23	PM24
WP 1 Preparation																								
	0.5	0.5																						
WP 2 Proof of concept (preliminary experiments)																								
Water flow measurement test			0.5	0.5	0.5																			
Gas density measurement test						0.5	0.5	0.5																
Two-phase measurement test									0.5	0.5														
WP 3 Design & Layout of the optical configuration																								
Optical setup & PEMWE cell integration-configuration & experiment											0.5	0.5	0.5	0.5	0.5									
Optical setup & PEMWE cell integration-data analysis & optimization																0.5	0.5	0.5	0.5	0.5				
WP 4 Communication & Dissemination																								
																					0.5	0.5	0.5	0.5
										M1										M2				

Outcome(s)

As the worldwide need for renewable energies increases, technical issues for efficient hydrogen production, storage, and transportation (PST) are getting more dominant. Various developments in different fields are crucial in accelerating the process of PST technical improvements, among which is developing suitable diagnostic and measurement techniques. Diagnostic methodologies can help a faster expansion of PST techniques by providing an accurate measure of their functionality. Here, we aim to use the specificity and accuracy of optical methods to monitor the performance of PEMWE as one of the most promising techniques for hydrogen production. The capability of the proposed technique for two-phase monitoring of liquid and gas transport in LGDL will help in understanding the complex processes involved in a PEMWE cell. The ultimate setup will be a prototype for PEMWE cells' diagnosis and development. The host institute can apply the developed method in future research projects that involve hydrogen production techniques. Moreover, the outcome will be a prototype of an optical device with the capacity for further improvement and commercialization through industrial partners in either energy or optics sectors. In addition, the proposed optical technique is not limited to electrolyzer cells but can be adapted for any application involving measuring fluid and gas transportation. In addition to the technical outcomes, expanding the interdisciplinary knowledge by applying optics in the energy sector and the possibility of publishing in open-access journals describes the valuable benefits for the project lead investigator.

Impact

HySON Institute focuses on research activities around technology developments related to hydrogen production, storage, and transportation. Currently, the institute works on expanding the horizon of its activities to other sub-areas of renewable energies with more focus on inter- and cross-disciplinary research topics. Therefore, defining and executing new research developments with long-term goals, the result of which can be applied to current or future planned projects, are among crucial tasks. As for

the current proposed project, the idea of the optical visualization and measurement technique for a PEM electrolyzer has a double-side potentiality for not only diagnosis of the currently available types of PEM cells but also as an evaluation technique that can be used for developing new materials and components to improve PEMWE. As an example, designing new and more efficient materials and structures for LGDL is a foreseen project for the near future in HySON. After successfully developing the optical system for flow visualization through LGDL, we can effectively apply it in the processes associated with material development. In addition, this project can draw the attention of new partners in optics and techniques to the institute, helping to enable more interdisciplinary projects between the fields of optics and energy. As a young institute, HySON is actively involved in research and administrative activities in renewable energies, such as the hydrogen economy and environment. Hence, executing this project will also help the visibility of optics and Optica among research and industrial communities involved in these areas in local, national, and international scope.

References

[1] B. Yodwong, D. Guilbert, M. Phattanasak, W. Kaewmanee, M. Hinaje, and G. Vitale, "Proton Exchange Membrane Electrolyzer Modeling for Power Electronics Control: A Short Review," *C*, vol. 6, no. 2, p. 29, 2020, doi: 10.3390/c6020029.

[2] A. Sorrentino, K. Sundmacher, and T. Vidakovic-Koch, "Polymer Electrolyte Fuel Cell Degradation Mechanisms and Their Diagnosis by Frequency Response Analysis Methods: A Review," *Energies*, vol. 13, no. 21, p. 5825, 2020, doi: 10.3390/en13215825.

[3] A. Sorrentino, K. Sundmacher, and T. Vidakovic-Koch, "Decoupling oxygen and water transport dynamics in polymer electrolyte membrane fuel cells through frequency response methods based on partial pressure perturbations," *Electrochimica Acta*, vol. 390, p. 138788, 2021, doi: 10.1016/j.electacta.2021.138788.

[4] F. Aubras *et al.,* "Two-dimensional model of low-pressure PEM electrolyser: Two-phase flow regime, electrochemical modelling and experimental validation," *International Journal of Hydrogen Energy*, vol. 42, no. 42, pp. 26203–26216, 2017, doi: 10.1016/j.ijhydene.2017.08.211.

[5] J. O. Majasan, J. I. Cho, I. Dedigama, D. Tsaoulidis, P. Shearing, and D. J. Brett, "Two-phase flow behaviour and performance of polymer electrolyte membrane electrolysers: Electrochemical and optical characterisation," *International Journal of Hydrogen Energy*, vol. 43, no. 33, pp. 15659–15672, 2018, doi: 10.1016/j.ijhydene.2018.07.003.

[6] I. Dedigama *et al.,* "In situ diagnostic techniques for characterisation of polymer electrolyte membrane water electrolysers – Flow visualisation and electrochemical impedance spectroscopy," *International Journal of Hydrogen Energy*, vol. 39, no. 9, pp. 4468–4482, 2014, doi: 10.1016/j.ijhydene.2014.01.026.

[7] S. Litster, D. Sinton, and N. Djilali, "Ex situ visualization of liquid water transport in PEM fuel cell gas diffusion layers," *Journal of Power Sources*, vol. 154, no. 1, pp. 95–105, 2006, doi: 10.1016/j.jpowsour.2005.03.199.

[8] M. Versluis, "High-speed imaging in fluids," *Exp Fluids*, vol. 54, no. 2, 2013, doi: 10.1007/s00348-013-1458-x.

[9] P. S. Greenberg, R. B. Klimek, and D. R. Buchele, "Quantitative rainbow schlieren deflectometry," *Applied optics*, vol. 34, no. 19, pp. 3810–3825, 1995, doi: 10.1364/AO.34.003810.

[10] E. B. Temple, "Quantitative Measurement of Gas Density by Means of Light Interference in a Schlieren System," *J. Opt. Soc. Am.*, vol. 47, no. 1, p. 91, 1957, doi: 10.1364/JOSA.47.000091.

[11] W. L. Howes, "Rainbow schlieren vs Mach-Zehnder interferometer: a comparison," *Applied optics*, vol. 24, no. 6, p. 816, 1985, doi: 10.1364/AO.24.000816.

[12] W. L. Howes and D. R. Buchele, "Optical Interferometry of Inhomogeneous Gases," *J. Opt. Soc. Am.*, vol. 56, no. 11, p. 1517, 1966, doi: 10.1364/JOSA.56.001517.

[13] J. Mo *et al.,* "Thin liquid/gas diffusion layers for high-efficiency hydrogen production from water splitting," *Applied Energy*, vol. 177, pp. 817–822, 2016, doi: 10.1016/j.apenergy.2016.05.154.

Executive summary Optica Foundation Challenge

Applicant: Dr. Carlos Doñate Buendía, University of Wuppertal, Germany

Category: Health **Anticipated total duration of the project: 24 months**

Stereolitography 3D printed custom and low-cost bactericidal dentures by laser generated Ag_2WO_4 nanoparticles additivation

The proposed project addresses a fundamental problem in nowadays society, universal health access. Specifically, **dental health costs limit its access to low-income population and countries**, resulting in reduced well-being, sickness, and even death. Implants, crowns, and dentures costs still represent a barrier for their extended employment. One of the sources of the high costs comes from the necessity of fabricating custom dental prosthetics for each patient, not allowing serial production. To overcome this limit, a **photonics-based 3D printing** technique as stereolitography (SLA) is proposed **to produce dentures** with complex custom geometries and low production costs.

Another problem linked to **dental prosthetic** is the proliferation of bacterias and the **risk of infection**. Dentures represent a reservoir of microorganisms that can derive into stomatitis or infections. In fact, 70% of dentures wearers suffer from denture stomatitis. To treat infection problematics, antibiotic protocols are developed. However, this solution is limited due to the emergence of antibiotic resistant superbugs. To address it, the employment of **laser irradiated Ag_2WO_4 particles to provide them bactericidal properties** is proposed.

Overall, in the current project a complete photonics based approach is proposed to produce dentures with bactericidal properties by the formulation and SLA printing of resins containing laser generated Ag_2WO_4 particles with enhanced bactericidal properties.

The proposed methodology can be explained in three steps, represented in the scheme below. First, the **irradiation of Ag_2WO_4 particles dispersed in the dental resin**, a commercial flexible resin to produce dentures. The irradiation is carried out by laser fragmentation in liquids (LFL), it enhances the Ag_2WO_4 bactericidal effects and facilitates the particle dispersion. Then, the **Ag_2WO_4-resin is employed for SLA** after detailed characterization of the Ag_2WO_4 particle stability in the resin, the viscosity and wettability. Finally, the **produced dentures are characterized by tensile, hardness, bactericidal, and biocompatibility** tests to evaluate their suitability for in-vivo applications.

The proposed approach aims to overcome the current main drawbacks of dental prosthetics. On the one side, high costs that difficult general population access to basic dental health treatments. On the other side, infection and bacteria proliferation and the subsequent loss of patient well-being and extra dental health treatment costs.

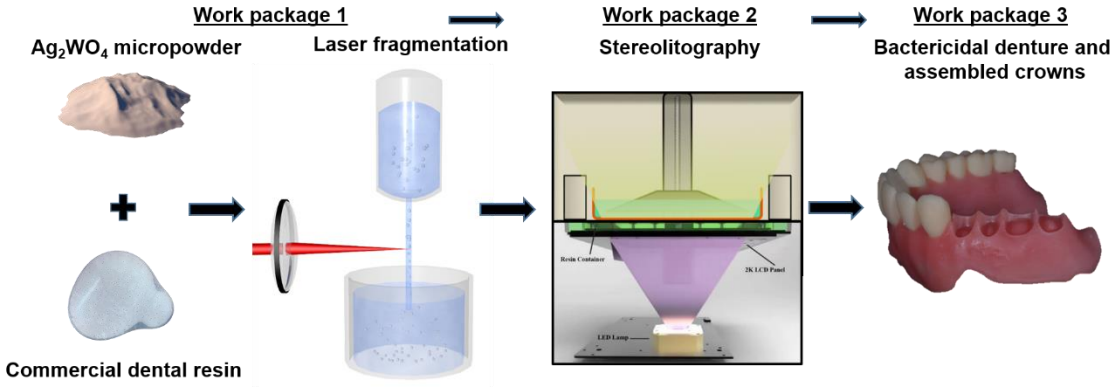

Project Proposal Optica Foundation Challenge

Applicant: Dr. Carlos Doñate Buendía, University of Wuppertal, Germany

Category: Health **Anticipated total duration of the project: 24 months**

Stereolitography 3D printed custom and low-cost bactericidal dentures by laser generated Ag_2WO_4 nanoparticles additivation

1 Literature Review and problem statement

Photonics, nanotechnology and advanced materials are considered by the European Commission as key enabling technologies for the improvement of human society lifestyle in the following decades. These technologies are key to improve imaging and treatments in medicine, material fabrication and processing, or green energy harvesting systems, facilitating a sustainable human development. Pulsed laser ablation in liquids (PLAL), joins Photonics and nanotechnology, representing a green synthesis technique of colloidal nanoparticles with an available broad material and solvent library that allow the straightforward synthesis of metallic, ceramic, organic, and alloy nanoparticles. This versatility is a key feature for the development of advanced materials. The modification of currently existing materials to provide new functionalities represents the best approach to produce cost-effective smart materials for demanding applications. In this context, the production of smart materials with custom geometries and functionalities is a shared goal by researchers and industry. Photonics based additive manufacturing (AM) techniques offer the required design freedom, and represent a growing industrial market. Within this project, photopolymer dental materials will be modified by the addition of laser generated Ag_2WO_4 nanoparticles to provide the AM printed custom dentures bactericidal properties towards mitigation of oral disease complications. Oral diseases are considered by the World Health Organization (WHO) as a major health burden for many countries that affect people throughout their lifetime, causing pain, discomfort, and even death [1]. Diseases as dental caries, periodontal, or dental trauma can lead to tooth loss or gums degradation, reducing the affected person wellbeing, and requiring the employment of prosthesis or implants. This worldwide problematic further affects low- and middle-income countries and society sectors [2] due to the costly access to dental care [3].

The impact of dental implants can be assessed in few numbers, its annual global market is estimated at around 12-18 million implants, with more than 200 million patients having received an implant in the last two decades [4]. However, implants, and dentures costs still represent a barrier for their extended employment in several countries and parts of society [3]. One of the sources of the high costs comes from the necessity to fabricate a custom implant for each patient, not allowing serial production. To overcome this limit, photonics-based 3D printing techniques have been employed to produce dentures, achieving complex geometries and low-cost custom parts [5]. Within the broad spectrum of 3D printing techniques, stereolitography (SLA) provides key advantages for prosthetic manufacturing cost reduction. SLA is based on the photopolymerization of a liquid resin that turns into a solid under UV light illumination. The low energy photopolymerization threshold of the resins allows the employment of low cost UV sources such as LEDs. The light modulator used to spatially control the layer-by-layer photopolymerization of the resin can be a LCD display, reaching resolutions of 20 µm. The employment of general consumer technology reduces the overall cost of standard SLA devices to hundreds of dollars. Besides, there already exist commercial dental resins suitable for dentures [6]. Overall, SLA printing offers an excellent perspective to reduce production costs of dental parts, prospectively facilitating access to such essential goods to a broader worldwide population percentage.

An additional problem arising after incorporation of the dental pieces to the patient are infections resulting in peri-implantitis. It occurs in 3% of the patients [7,8], which results in approximately 6 million people affected in the last two decades. As another example, 70% of dentures wearers suffer from denture stomatitis [9]. To prevent infection problematics, antibiotic protocols have been developed [8]. Nevertheless, this solution presents also limitations when the emergence of antibiotic resistant superbugs is considered. To address it, the employment of inorganic particles exhibiting bactericidal properties such as Ag or Cu has been proposed [10, p1]. However, when incorporated into dentures, the elemental metals can suffer from leaching, increasing their concentration in the media to toxic levels [9]. To control the release of the bactericidal Ag, the employment of Ag_3PO_4 has been proposed, proving that the composite can be integrated in a scaffold providing bactericidal properties without cytotoxicity, and even allowing cell proliferation [11]. Hence, inorganic particles have been shown effective as bactericidal agent [12]. However, the addition of bactericidal particles to SLA dental resins has been only recently tested for elemental metals, and oxides, mostly focusing on their effect over the mechanical properties of the printed parts and not providing extra bactericidal properties [13]. Preliminary work from the applicant [p2,p3] confirmed that high intensity laser irradiation of Ag_2WO_4 microparticles in air leads to the formation of Ag nanoparticles bonded to the original composite [14]. The Ag nanoparticles formed, provide bactericidal, antifungal, and antitumor properties to the irradiated material, with specificity and biocompatibility with healthy human cells (BALB/3T3) [15]. Even SARS-CoV-2 deactivation has been demonstrated by the applicant employing a laser irradiated chitosan/Ag_2WO_4 composite [p2]. Consequently, laser irradiated Ag_2WO_4 represents an interesting material to provide antiseptic properties to denture manufacturing dental resins employed in SLA.

Overall, a complete photonics based approach is proposed to produce dentures with bactericidal properties by the formulation and printing of new SLA resins containing laser generated Ag_2WO_4 particles. This approach aims to overcome the current main drawbacks of dental parts. On the one side, high costs that difficult general population access to these dental health treatments. On the other side, infection and bacteria proliferation and the subsequent patient well-being and health treatment costs.

2 Objectives

The specific objectives are intended to provide broader worldwide access to dental parts by reducing production costs and to address human wellbeing and resources losses arising from bacteria development and infections in dentures. To achieve this, two main objectives are pursued within the current project:

1) The **adaptation of nanoparticle additivated resins** as base materials **in SLA**, allowing the production of **custom dentures with novel functionalities** at reduced costs, making them more accessible for low-income countries.
2) **The production of bactericidal and biocompatible dentures** by the formulation of new Ag_2WO_4-resins printed by SLA.

3 Work Plan

WP1 – Dental resin additivation with laser generated Ag_2WO_4 nanoparticles

In WP1, a laser based procedure to prepare Ag_2WO_4 nanoadditivated dental resins will be studied. The process will be compared with direct mixing of the Ag_2WO_4 micropowder with the SLA resins, and direct mixing of air irradiated Ag_2WO_4 micropowder with the SLA resins. This way, the effect of laser fragmentation of Ag_2WO_4 on the stability of the particles and their bactericidal performance will be evaluated.

Table 1. Planned time flow for the work packages over the two-year project period.

Work packages	1st year				2nd year			
	Q1	Q2	Q3	Q4	Q1	Q2	Q3	Q4
WP1	**Dental resin additivation with laser generated Ag_2WO_4 nanoparticles**							
WP 1.1: Laser fragmentation (LFL) of Ag_2WO_4 microparticles								
WP 1.2: Ag_2WO_4 additivation of the dental resin								
WP1.3: Optical and rheological characterization of additivated resins								
WP2	**Photonics based 3D printing (SLA) of additivated dental parts**							
WP 2.1: SLA printing of test samples for optimization and characterization								
WP 2.2: SLA printing of additivated flexible dentures and dental crowns								
WP3	**Bactericidal and mechanical characterization of the printed dental parts**							
WP 3.1: Hardness and tensile testing of the printed parts								
WP 3.2: Antimicrobial and biocompatibility tests								

The project is divided into 3 main work packages (WPs). The synergies and time flow are depicted in Table 1.

WP1.1 – Laser fragmentation (LFL) of Ag_2WO_4 microparticles

Direct addition of Ag_2WO_4 powders to the SLA resins could result in agglomeration of the material and sedimentation before printing. This would affect the homogeneous distribution of the particles in the printed part, generating local variations of the mechanical and bactericidal properties that can result in the fracture of the part or infection risk increase in specific areas. In order to avoid this problem, the novel procedure proposed in this project is based on the initial mixing of the Ag_2WO_4 microparticles with the dental resins employed, Fig. 1a. The mixture is ultrasonically dispersed, and irradiated in a liquid flow configuration, Fig. 1b. The irradiated particles with increased bactericidal properties will also gain stability in the resin due to the coverage of the particles' surface with the photopolymer functional groups. In order to avoid degradation of the resin (designed for printing at 405 nm) during laser irradiation, the laser source employed will be a 1064 nm ps laser (4 MHz, 10 ps, 120 W).

WP1.2 – Ag_2WO_4 additivation of the dental resin

The in-situ laser irradiated Ag_2WO_4-resins in WP1.1 will be compared in terms of particle stability, and viscosity (WP1.3), as well as mechanical, bactericidal, and biocompatibility properties (WP3), with 1) the base Ag_2WO_4 microparticles added to the resin, and 2) the Ag_2WO_4 powder irradiated in air and mixed with the resin. The mixing process for the initial and irradiated in air Ag_2WO_4 will be performed by direct mixing and ultrasonic dispersion before printing by SLA. This provides a fair comparison in terms of stability and dispersion in the printed parts. A commercial dental resin (DENTURE, Power Resins) will be employed.

WP1.3 – Optical and rheological characterization of additivated resins

The effect of Ag_2WO_4 particles addition to the resin will be evaluated by the influence on its optical and flow properties. The measurements described will be performed for the Ag_2WO_4-resins prepared in WP 1. 1) Denture resin with Ag_2WO_4 particles; 2) Denture resin with Ag_2WO_4 particles irradiated in air; 3) Laser irradiated Ag_2WO_4-resin.

The optical properties will be characterized by UV-Vis spectrophotometry (StellarNet Inc.). The stability of the optical properties, absorption peaks wavelengths, and intensity, provide

information of the laser interaction effect on the resin and the dispersed Ag_2WO_4 particles. The data collected will allow determining the mixing and laser irradiation methodology leading to the optimum dispersion of the Ag_2WO_4 particles without resin degradation.

To evaluate the influence of the Ag_2WO_4 particles and laser irradiation methodology on the flow properties of the resulting additivated resins, contact angle (sessile drop method) and viscosity measurements (rotational rheometry) will be conducted. These parameters are especially relevant for the processability of the resulting resins by SLA keeping the maximum spatial resolution, process reproducibility, and mechanical performance of the printed parts.

WP2 – Photonics based 3D printing (SLA) of additivated dental parts

Within this work package, the prepared Ag_2WO_4 resins will be processed by SLA (Elegoo Mars 2) to produce test samples for characterization, WP 2.1. In WP 2.2, tensile tests, disks, and dentures will be printed employing the Ag_2WO_4-resins produced in WP1, Fig. 1c.

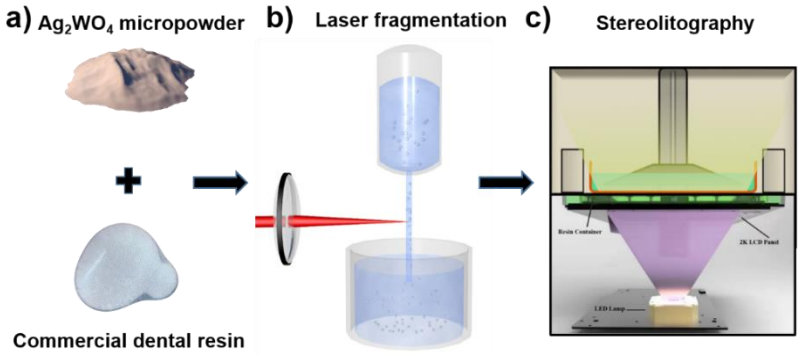

Figure 1. a) Ag_2WO_4 commercially available micropowder and dental resin mixed for laser irradiation in b). b) Laser fragmentation setup in a flow jet configuration to ensure uniform irradiation of the particles and promote a homogeneous bactericidal effect enhancement. c) Stereolitography (SLA) setup with a 405 nm LED and LCD employed to process the laser irradiated Ag_2WO_4-resins, bottom image reproduced from [16].

WP 2.1: SLA printing of tensile tests and disks for optimization and characterization

The influence of the 405 nm LED light employed in the SLA system on the Ag_2WO_4-resins will be evaluated in WP 3.2 to confirm that bactericidal enhancement of the Ag_2WO_4 particles can be achieved in-situ during SLA even if the material has not been previously irradiated. A strong synergy with WPs 1.3 and 3 will be required at this point to optimize the processing parameters and achieve simultaneously high printing spatial resolution, repeatability of the process, high mechanical properties of the printed parts, and maximum bactericidal effect.

WP 2.2: SLA printing of additivated flexible dentures

The flat geometries proposed in WP 2.1 will be replaced by the intended denture models for the additivated flexible resin. Different complete and partial dentures from open 3D repositories will be printed to confirm the advantage that SLA provides for the production of custom parts with complex geometries.

WP 3: Bactericidal and mechanical characterization of the printed dental parts

To quantify the effect of the Ag_2WO_4 particles and the laser irradiation methodology over the performance of the printed dental parts, mechanical and bactericidal characterization of the printed objects is required.

WP 3.1: Hardness and tensile testing of the printed parts

The tensile test printed parts in WP 2.1 will be used for the characterization according to DIN 53504:2017-03, hardness tests will be performed according to DIN ISO 48-4:2021-02. The samples exhibiting hardness or tensile stress values significantly below (<20%) the provider specified range will be discarded. The LFL processed samples are expected to exhibit the lower diminishing due to the size reduction of the Ag_2WO_4 and better dispersion within the printed part, contributing to a reduction of the part porosity and an increase of the density.

WP 3.2: Antimicrobial and biocompatibility tests

The antimicrobial tests will be performed for C. Albicans, E. Coli, and MRSA, the most common bacteria present in dentures. Besides, to be able to prospectively qualify the produced parts for in-vivo employment, biocompatibility with oral cells is required. Hence, alamarBlue™ assay and an MTT assay will be performed to ensure that the printed parts exhibit no toxicity that could damage the denture user.

4 Outcome and impact

The funds required to develop the project include the purchase of the necessary Ag_2WO_4 micropowders, the dental resins, and a SLA processing station fully dedicated to the printing of dental resins. Furthermore, material for analytics and optics are included in the budget. The UV-Vis, contact angle, viscosity, mechanical, bactericidal and biocompatibility tests can be performed with the already available devices in the group and close groups at the University of Wuppertal. The PhD contract is envisioned to produce major evidences of the project outcomes, representing a fundamental advance in the applicant's current early career stage to start his independent career and apply for a 3-year full-time proposal (estimated budget of approximately 400 k€) to the German Research Foundation (DFG) to continue the topic and extend the PhD candidate position until graduation.

The expected outcomes of the project can be summed up as:

1) Qualification of the **laser fragmentation in liquid** approach for the **in situ nanoparticle additivation of SLA resins** with enhanced **bactericidal properties.**
2) Establishment of a photonics-driven printing protocol for the generation of **custom dentures with bactericidal properties and reduced cost.**

The project outcomes address a fundamental problem in nowadays society, universal health care access. Specifically, dental health costs limit the access to low-income population and countries, resulting in reduced well-being, sickness, and even death. The photonics-driven qualification of lower cost approaches to generate dentures offer a possibility to improve dental health for the general population. Furthermore, the bactericidal properties of the generated dentures are envisioned to further reduce health risks as infection, and bacteria proliferation. Overall, it represents a strong benefit for a situation that a significant part of the population faces during their lives, the requirement of a denture.

5 References

[p1] **C. Doñate-Buendia**, A. Ingendoh-Tsakmakidis, …, S. Barcikowski, B. Gökce, Proc. CIRP 111 (2022).
[p2] P. Pereira, …, **C. Doñate-Buendía**, G. Mínguez-Vega, J. Andrés, E. Longo, Sci. Rep. 12 (2022).
[p3] C. dos Santos, …, **C. Doñate-Buendía**, J. Andres, E. Longo, Part. & Part. Syst. Char. 36 (2019).
[1] M.A. Peres, L.M.D. Macpherson, R.J. Weyant, et al., Lancet. 394 (2019) 249–260.
[2] G.H. Gilbert, R. Paul duncan, B.J. Shelton, Health Serv. Res. 38 (2003) 1843–1862.
[3] E. Bernabé, M. Masood, M. Vujicic, BMC Public Health. 17 (2017) 1–8.
[4] B. Klinge, M. Lundström, M. Rosén, et al., Clin. Oral Implants Res. 29 (2018) 145–151.
[5] L. Lin, Y. Fang, Y. Liao, et al., Adv. Eng. Mater. 21 (2019) 1801013.
[6] A. Della Bona, V. Cantelli, V.T. Britto, et al., Dent. Mater. 37 (2021) 336–350.
[7] O. Camps-Font, P. Martín-Fatás, A. Clé-Ovejero, et al., J. Periodontol. 89 (2018) 1165–1173.
[8] R. Tabrizi, F. Mobin, M. Dehghanpour, et al., J. Cranio-Maxillofacial Surg. 50 (2022) 293–297.
[9] P. Ramburrun, N.A. Pringle, A. Dube, et al., Materials (Basel). 14 (2021) 3167.
[10] M. Cao, S. Wang, J. Hu, et al., Adv. Sci. 9 (2022) 2103721.
[11] K. Hayashi, M. Shimabukuro, K. Ishikawa, ACS Appl. Mater. Interfaces. 14 (2022) 3762–3772.
[12] C. Zhao, W. Liu, M. Zhu, et al., Bioact. Mater. 18 (2022) 383–398.
[13] M.M. Gad, A.M. Al-Thobity, Jpn. Dent. Sci. Rev. 57 (2021) 46–53.
[14] N.G. Macedo, T.R. Machado, R.A. Roca, et al., ACS Appl. Bio Mater. 2 (2019) 824–837.
[15] M. Assis, T. Robeldo, C.C. Foggi, et al., Sci. Rep. 9 (2019) 1–15.
[16] A. Al Rashid, S.A. Khan, S. G. Al-Ghamdi, et al., J. Mater. Res. Technol. 14 (2021) 910–941.

Energy-efficient Analog Computing with Simultaneous Photonic and Electronic In-Memory Processing

PI: Carlos A. Rios Ocampo | University of Maryland College Park

Overview

This proposal aims to develop a transformative approach based on optoelectronic multilevel nonvolatile phase-change memories in a co-located photonic and electronic in-memory computing processor. While electronics and photonics have been co-integrated in the same chip die to accelerate digital computing, an analog computing counterpart has not yet been demonstrated, nor is an architecture in which multiplications are also performed in the optical domain, as opposed to only use light for data transfer. This proposal aims to fill this gap by creating an innovative hybrid optoelectronic approach based on photonic integrated circuits (PICs) with embedded phase-change materials (PCMs) and a triple electrical Vertical Interconnect Access (vias) scheme, which enables a fully versatile architecture that can be written and read both optically and electrically. Developing a proof-of-concept computational device with seed funding is the first step towards the long-term vision of building a full in-memory computing processor with dual optical and electrical readout, which we intend to pursue further through NSF or DoD funding. Moreover, this proposal's scope perfectly matches OPTICA's interest in driving new scientific discoveries and breakthroughs to transform our world in the information space by enabling faster and energy-efficient ways to compute large volumes of information.

Problem statement

Unlike current phase-change memory technology operating either optically or electrically, our approach will create innovative systems that **integrate both into a single device**, **merging the best performance metrics from both domains**. Photonic PCM architectures have advantages in bandwidth, throughput, heat dissipation, no drift, and multiplexing over their electronic counterpart. Electronics benefits from mature, scalable, and standardized fabrication and demonstrated memory architectures (exemplified by Micron/Intel's 3D Xpoint), enabling volume manufacturing and interfacing with advanced logic and digital-analog converters inexistent in photonics. This team seeks to validate the central hypothesis by completing three main tasks: **1) optical materials innovation using high-throughput material discovery**: Mapping the Ge-Sb-Te PCMs alloyed with Sn, Ti, or Ag to achieve optimal optical and electrical performance by leveraging the metal content to improve both optical attenuation and electrical conductivity. **2) device engineering, fabrication, and testing:** hybrid memory devices will be home-built using three electrical ports on silicon-on-insulator (SOI) waveguides with embedded PCMs.

Impact

This project pursues a unique cross-disciplinary technology, innovating in fields such as optical material synthesis and processing, device design engineering, system architecture innovation, and photonics manufacturing**.** Our innovation will enable faster and energy-efficient ways to compute large volumes of information by matching the software requirements of the artificial intelligence revolution with hardware that optimizes the arithmetic operation at the core: matrix-vector multiplications. The high-performance computing market is expected to grow from $36.0b in 2022 to $49.9b by 2027, and with that growth also comes a spike in power consumption, already up to 10MW (electricity for ~10,000 homes) per supercomputer. Minimizing energy waste in heat by using hybrid optoelectronic memory while allowing the seamless combination of both domains in a portable device operating in ambient temperature conditions (vs. extreme cold locations) is the major impact we foresee in this critical technology development.

Energy-efficient Analog Computing with Simultaneous Photonic and Electronic In-Memory Processing

PI: Carlos A. Rios Ocampo | University of Maryland College Park

1. Overview and background

This proposal aims to develop a transformative approach based on optoelectronic multilevel nonvolatile phase-change memories in the co-located photonic and electronic in-memory computing processor shown in **Fig. 1**. While electronics and photonics have been co-integrated in the same chip die to accelerate digital computing by moving data at the speed of light,[1] an analog computing counterpart has not yet been demonstrated, nor an architecture in which multiplications are also performed in the optical domain, as opposed to only use light for data transfer. Today's prevailing von Neumann computing architecture is largely non-optimal when handling massive matrix-vector multiplications for machine learning.[2] This limitation has spurred tremendous efforts in developing advanced hardware accelerators capitalizing on the unique benefits of analog electronics[3,4] and optics[5,6] for ultrahigh-speed, low power consumption, and massive parallelism. In-memory computing has emerged as the optimum architecture for high-throughput matrix-vector multiplications—the core operation in machine learning (ML) tasks[7]—given that it allows for performing multiplications in a single time step and directly in the memory. This approach breaks the processor-memory dichotomy in conventional computers by performing computing and data storage in the same device. In-memory computing avoids the bottleneck caused by moving data back and forth between processor and memory units and drastically reduces the complexity of arithmetic operations by computing in the analog domain, as opposed to the digital domain, where many transistors are needed even for a simple scalar-scalar multiplication. The result is a computing architecture capable of reducing the energy consumption of the computations behind the fast-growing ML applications and simultaneously alleviating the need for more transistors to keep up with Moore's law and the growing demand for computing power. While several memristive platforms such as phase-change materials (PCMs),[8] oxides,[9] 2D materials,[10] and others have enabled analog electronic in-memory computing architectures, the optical counterpart is in its infancy.

Performing in-memory computing on a light-based platform furthers the performance by enabling ultra-fast speeds and wavelength multiplexing.[6] This approach has been demonstrated using optical pulses to write the memories and perform scalar-scalar multiplications—work pioneered by the PI.[11] However, this all-optical approach poses serious scalability challenges when considering potential

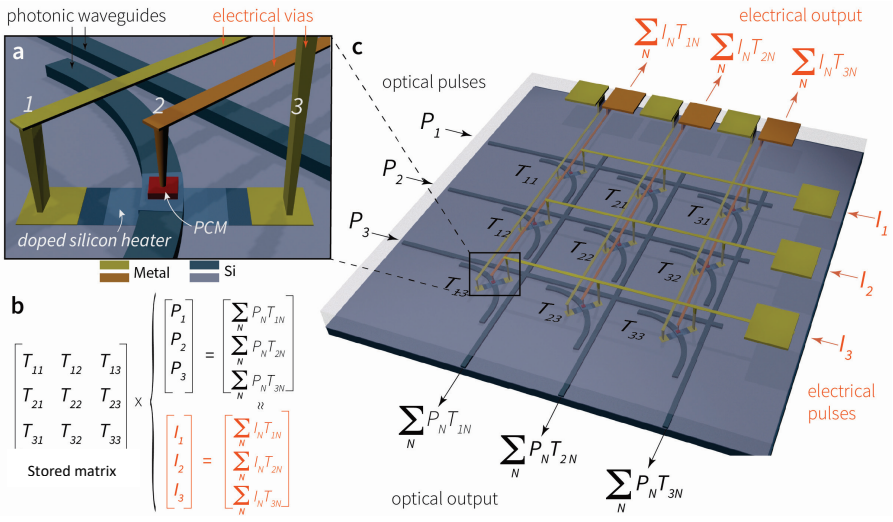

Fig. 1. (a) PCM hybrid memory onto a photonic circuit with a doped-Si heater and 3 electrical vias (labelled 1, 2, and 3). Data is stored in the PCM using heat (passing current 1↔3), electrical signals (passing current 2↔3), or optical pulses within the waveguide. Data is retrieved optically using the waveguide or through conductivity interrogation between 2↔3. **(b)** matrix-vector multiplications performed using the architecture in **(c). (c)** A nonvolatile matrix T_{MN} is codified in the memories. Columns collect and accumulate the light from the multiplications at each intersection between each optical pulse P_i and the memory transmittance. The same array of memories are accessed with two metal vias to perform the same task in the electrical domain by accumulating the output current resulting from an input current I_i and each memory resistance.

architectures with thousands of memory elements due to the complexity of routing optical pulses on-chip. Hybrid optoelectronic multilevel memories that can be written electrically (i.e., leveraging standard electronic packaging) and readout both optically and electrically would guarantee seamless scalability and maximum architecture versatility. This proposal aims to fill the gap by creating an innovative *hybrid optoelectronic approach based on photonic integrated circuits (PICs) with embedded phase-change materials and a triple electrical Vertical Interconnect Access (via) scheme* (Fig. 1).

2. Problem statement

Unlike current PCM-based technology operating either optically or electrically, a hybrid computational memory will create innovative systems that **integrate both into a single device**, **merging the best performance metrics from both domains**. Photonic PCM architectures have advantages in bandwidth, throughput, heat dissipation, no drift, and multiplexing over their electronic counterpart. Electronics benefits from mature, scalable, and standardized fabrication and demonstrated memory architectures (exemplified by Micron/Intel's 3D Xpoint), enabling volume manufacturing and interfacing with advanced logic and digital-analog converters inexistent in photonics. This team seeks to validate the central hypothesis by completing three main tasks: **1) optical materials innovation using high-throughput material discovery**: Mapping the Ge-Sb-Te PCMs alloyed with Sn, Ti, or Ag to achieve optimal optical and electrical performance by leveraging the metal content to improve both optical attenuation and electrical conductivity. **2) device engineering, fabrication, and testing:** hybrid computational memories will be home-built using three electrical ports on silicon-on-insulator (SOI) waveguides with embedded PCMs (Fig. 1).

3. Work Plan

The proposed technology uses the remarkable bistable change in the optical and electrical properties of PCMs upon amorphization and crystallization, which enables nonvolatile reconfiguration of integrated electronic/photonic circuits. This material class succeeds as low-energy nonvolatile multilevel memories for on-chip photonic[11] and electronic[8] in-memory computing, demonstrating thus the fastest and most scalable way to perform matrix-vector multiplications. To demonstrate a hybrid memory in which a single device can perform both optical and electronic computing, we will pursue the following tasks, in parallel:

3.1 Task 1: Optoelectronic material innovation: Using chalcogenide phase-change materials (e.g., $Ge_2Sb_2Te_5$, Sb_2Se_3, etc.) to control optical properties on-chip is a particularly intriguing solution for photonic device tunability due to significant, reversible, and nonvolatile changes in refractive index and electrical conductivity when switched between their amorphous and crystalline states (**Fig. 2a**).[12] The large change in refractive index ($\Delta n = n_{cry} - n_{am}$) significantly reduces the interaction length needed to achieve a π-phase shift, and thus reduces the device footprint by >10× (e.g., a device length of ≤10 μm for non-resonant Sb_2Se_3 phase shifters demonstrated by the PI[13]). In addition, a large extinction coefficient ($\Delta k = k_{cry} - k_{am}$) increases the amplitude modulation upon switching, which can be used to codify multiple transmission levels for data storage and computing, as demonstrated by the PI in the field's pioneering work.[6,11,14] The optimization of either Δn or Δk leads to different photonic devices and applications, and with a growing library of optical PCMs, there are materials available for both phase and amplitude modulation (see **Fig.** 2a). In particular, the alloy $Ge_4Sb_6Te_7$ with outstanding Δk and Δn was discovered at PI's collaborator Prof. Ichiro Takeuchi's group at UMD using machine learning in combinatorial material discovery techniques.[15] Another alloy of interest is $Ge_2Sb_2Se_4Te_1$ or GSST, which offers broadband bi-state transparency.[16] This alloy was demonstrated by the PI and collaborators at MIT (Prof. Juejun Hu) through judicious engineering of the alloy's resonant bonding configuration (to maximize optical contrast) as well as carrier localization (to

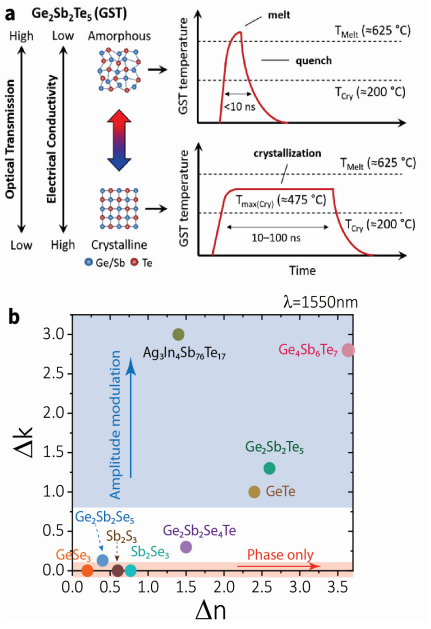

Fig. 2: **a.** reversible switching mechanism between the amorphous and the crystalline states of $Ge_2Sb_2Te_5$ **b.** Overview of change in absorption and refractive index for various optical phase-change materials.

suppress free-carrier absorption). Regarding electrical properties modulation, the community has focused on optimizing the contrast in resistivity: up to five orders of magnitude difference is achieved between insulating amorphous and conductive crystalline states.[16] However, achieving multilevel behavior has proved challenging. The resistivity of PCMs drifts in time, thus losing the stored information. Also, the switching mechanism in the electrical domain relies on a stochastic process that affects the multilevel repeatability required in precise data storage – a task outstandingly done in the optical domain due to the stability of the refractive index.

The nonvolatile nature of PCMs also allows long-term reconfigurability and data storage (>10 years at 85 °C) without needing a continuous electric field or current. Additionally, these PCMs are glassy materials, making them substrate-blind. This provides a direct method to add optical nonvolatile tunability to photonic platforms other than silicon. The nature of these materials also opens many opportunities to engineer their physical properties by varying the atomic composition from a wide variety of possible elements. In this direction, finding a PCM simultaneously claiming significant optical and electrical contrast, fast switching kinetics, and large endurance is central to the project's success. We will leverage our GSST and $Ge_4Sb_6Te_7$ success paradigms combining Machine Learning-enhanced material screening and high-throughput material characterization to facilitate rapid discovery and validation of new optoelectronic PCMs. We will capitalize on a wafer-scale platform we have recently pioneered, which is designed for combinatorial PCM synthesis and integrates device arrays encompassing waveguides, micro-heaters, and electrical probes for automated optical/thermal/electrical PCM characterizations. Since in-memory computing requires amplitude modulation, we will seek to optimize the Δk further. However, our hybrid computational memories also requires simultaneous electrical conductivity optimization, a multi-parameter optimization with no precedent. To do so, we will explore the combinatorial space of Ge-Sb-Se-Te alloys and metal-doped variations such as Sn/Ti/Ag-Ge-Sb-Te to enhance the electrical conductivity further while preserving a large optical modulation. With progress in device manufacturing, we will test the best alloys' performance at attaining multilevel data in both domains.

3.2 Task 2: Device engineering, manufacturing, and testing: Through five years of extensive R&D collaborations with MIT Lincoln Laboratory (LL) first as a postdoctoral associate at MIT and now as PI at UMD, we have successfully integrated PCMs as part of the standard LL's silicon photonics foundry process.[13,17] This important milestone allows manufacturing PCM devices while enabling their seamless integration with mature silicon photonics and nanoelectronics. We will leverage this unique capability, and our previous demonstrated electrothermal device in **Fig. 3**[13] to fabricate the proposed hybrid computational memories using UMD's NanoCenter facilities. With devices shown in **Fig. 3b** as starting point (which already places us in an advantageous position), we propose fabricating the three metal terminals (see **Fig. 4)** following a deposition, lithography, etching, and electro-plating sequence. This process, however, comes with several challenges to be addressed: 1) the contact area between the metal via and PCM needs to be carefully engineered to display electrical conductivity with high signal-to-noise ratio (SNR), yet low optical insertion loss – the larger the contact area, the more metal contributing to propagation loss. 2) Pattern a *via* terminal on top of the PCM cell without causing damage. 3) Finding the optimum thickness of PCM capable of inducing high SNR in both the optical and electrical readouts while allowing for seamless reversible and multilevel switching. We will address these questions and design challenges using finite-element method in COMSOL Multiphysics and finite

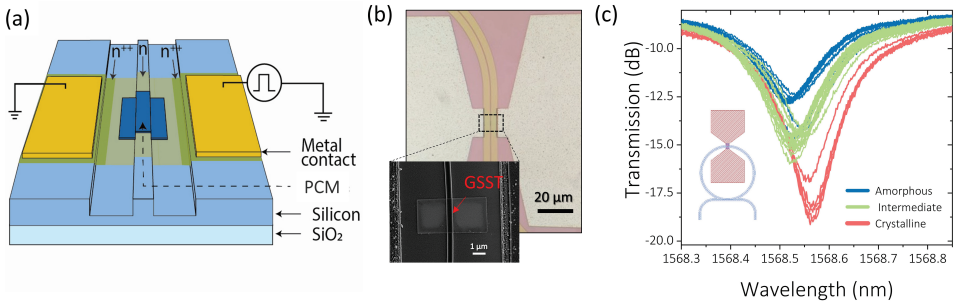

Fig. 3: a 3D sketched waveguide-integrated electrical heater used to switch GSST – this device is equivalent to that in Fig. 1, except for electrical terminal 2. **b** Optical microscope and SEM image of the actual device' top view. **c** Experimental switching of GSST over 50 cycles in a ring resonator for optical readout with electrical switching.

differences in time domain in Ansys Optics (Lumerical). The result of the simulations will provide valuable information on the devices' thermal, electrical, and optical properties, and geometry.

We will use the PI's custom automated electro-optical probe station to perform on-chip photonic testing of our devices. To control nonvolatile memory elements in the devices shown in **Fig. 3**, short electrical pulses with high amplitude (e.g., 400 ns at 21V) were used to increase the heater's temperature and melt-quench the PCM deposited onto the waveguide. A longer low amplitude (e.g., 0.1–1 ms at 3.2V) voltage pulse returns the PCM to its crystalline state to complete the reversible switching – see temperature evolution in **Fig. 2a**.[13] In this manner, high-contrast changes to the optical transmission can be achieved with electrothermal control of the PCM, as shown in **Fig. 3c**. Additional to this electrothermal write and optical-read measurement, we will pioneer a hybrid memory in which we also obtain electrical readout from contact 2 to verify the state of the PCM memory (**Fig. 4**). We expect high conductivity for crystalline PCM, unlike the insulating amorphous state. The electrical readout would enable us to interface the hybrid memory with external electronics (e.g., DAC, ADC, ASICs, etc.) and provide feedback to the system, which is useful in optical neural networks.[7] A clear example of the potential of an electrical read is to measure the weight of each memory cell in real-time for processing in the digital domain, an otherwise difficult task since individual memory information is lost during accumulation. The electrical readout also avoids losing energy to an electro-optical conversion since we will not need photodetectors to convert from the analog optical to the electronic digital domain. Moreover, electrode 2 can induce filamentation through the PCM following a pulse excitation to either electrode 1 or 3, thus enabling electrical Write. A final degree of freedom is optical Write: use a strong optical pulse to switch a lossy (large Δk) PCM, while having both electrical and optical readout. The unprecedented versatility of our hybrid memory will open avenues for inter-domain computing, where the choice of Write and Read operations will ultimately be determined by the nature of the application.

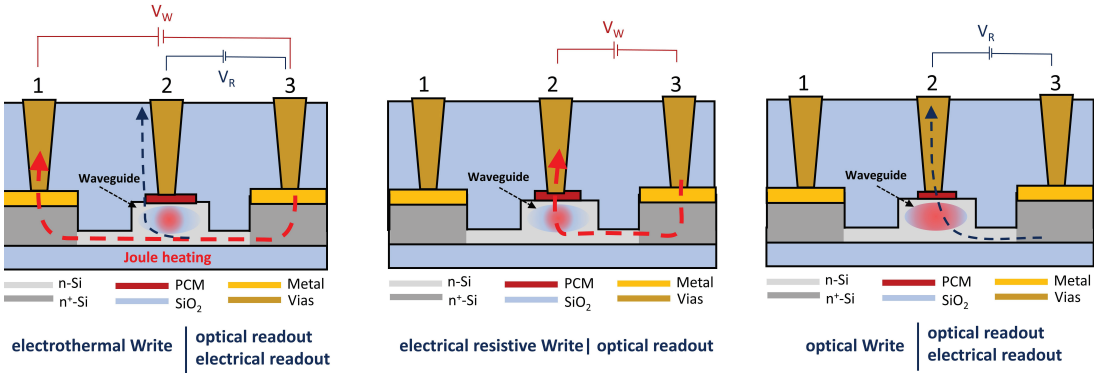

Fig. 4: Write and read possibilities with our Hybrid Optoelectronic Memory. V_W and V_R stand for voltage pulses to write and read, respectively, where $V_W > V_R$. Dashed lines represent electrical current. 1, 2, 3 denote the three vias. For optical write (right), a pump-probe scheme is necessary. A strong optical pump switches using the heat that results from material absorption and a subsequent lower power pulse reads out the state.[12]

4. Expected outcomes

Our expectations for a one-year seed funding are ambitious, given our accumulated experience in this type of device. Our long-term vision, solutions, and risks/mitigation strategies are shown in **Fig. 5**. For the first year under the OPTICA challenge, we anticipate: **1)** finding at least one optimum PCM alloy for simultaneous electrical and optical operation. **2)** demonstrating a high-yield device fabrication process for electrical via 2 (see Fig. 2), the crucial third electrode for electronic readout and biggest challenge. **3)** experimentally demonstrate a functional hybrid computational memory with successful readout in both domains an using the alloy found in (1). Moreover, we expect insightful exchanges and fruitful collaborations from other scientists in the OPTICA network.

5. Impact

This project pursues a unique cross-disciplinary approach spanning optical material synthesis and processing, device design engineering, system architecture innovation, and scalable photonics manufacturing. Unlike existing PCM memories, our hybrid memory design allows cell programming and readout using both electrical and optical channels, which will boost the performance of the current

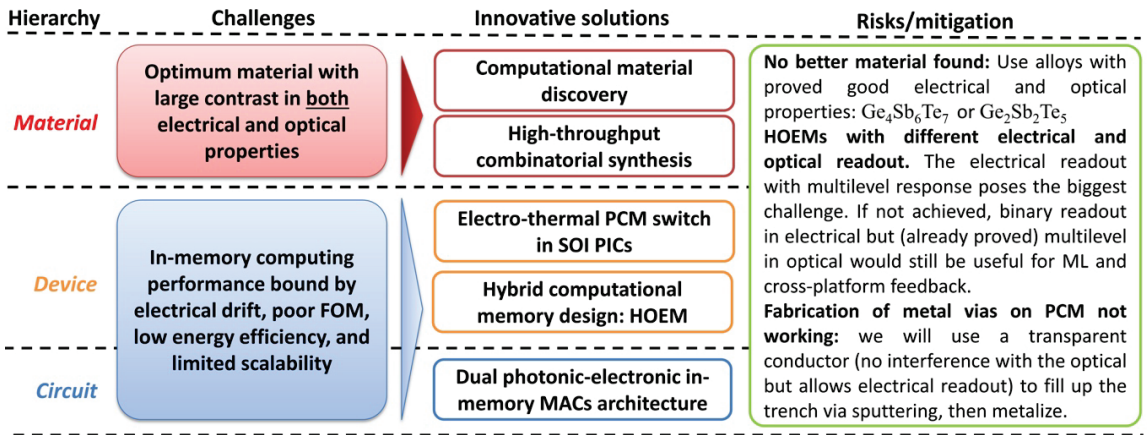

Fig. 5. Summary of proposed research activities.

in-memory processors by providing: **1)** active reconfiguration of the matrix using an optical or electrical signal to provide closed-loop control, which has been predicted to enable the array to perform arbitrary linear operations; **2)** enhanced optical matrix-vector computing by co-integrating with other ASIC carrying out operations, in parallel, that are not available in photonic circuitry such as nonlinear functions, logic, and DAC/ADC; **3)** use of electrical conductivity of the PCM matrix to retrieve the optical baseline and thus speed up the postprocessing and improve the precision of matrix-vector calculations[11], and **4)** a scalable platform for a large volume of computing operations. Therefore, our approach adds unprecedented versatility to optoelectronic in-memory computing architectures for high-throughput data processing, thus enabling faster and more energy-efficient ways to compute large volumes of information. Furthermore, PCMs are a versatile family of materials enabling multiple technological innovations; these hybrid devices will find applications beyond computing, such as optical switching fabrics for data centers and reconfigurable optics for imaging[18] – areas in which the PI actively conducts research.

6. References

1. Atabaki, A. H. *et al.* Integrating photonics with silicon nanoelectronics for the next generation of systems on a chip. *Nature* **556**, 349–354 (2018).
2. Berggren, K. *et al.* Roadmap on emerging hardware and technology for machine learning. *Nanotech.* **32**, (2020).
3. Traversa, F. L. & Di Ventra, M. Universal Memcomputing Machines. *IEEE Trans Neural Netw Learn Syst* **26**, 2702–2715 (2015).
4. Sebastian, A., Le Gallo, M., Khaddam-Aljameh, R. & Eleftheriou, E. Memory devices and applications for in-memory computing. *Nat Nanotechnol* **15**, 529–544 (2020).
5. Shen, Y. *et al.* Deep learning with coherent nanophotonic circuits. *Nat Photonics* **11**, 441–446 (2017).
6. Feldmann, J. *et al.* Parallel convolutional processing using an integrated photonic tensor core. *Nature* **589**, 52–58 (2021).
7. Shastri, B. J. *et al.* Photonics for artificial intelligence and neuromorphic computing. *Nat Photonics* **15**, 102–114 (2021).
8. le Gallo, M. *et al.* Mixed-precision in-memory computing. *Nat Electron* **1**, 246–253 (2018).
9. Li, J., Li, Y., Yang, L. & Miao, X. Memristor-Based In-Memory Computing Architecture for Scientific Computing. in *Memristor Computing Systems* (eds. Chua, L. O., Tetzlaff, R. & Slavova, A.) vol. 1 141–165 (Springer International Publishing, 2022).
10. Yin, L., Cheng, R., Wen, Y., Liu, C. & He, J. Emerging 2D Memory Devices for In-Memory Computing. *Advanced Materials* vol. 33 Preprint at https://doi.org/10.1002/adma.202007081 (2021).
11. Ríos, C. *et al.* In-memory computing on a photonic platform. *Sci Adv* **5**, eaau5759 (2019).
12. Wuttig, M., Bhaskaran, H. & Taubner, T. Phase-change materials for non-volatile photonic applications. *Nat Photonics* **11**, 465–476 (2017).
13. Ríos, C. *et al.* Ultra-compact nonvolatile phase-shifter based on electrically reprogrammable transparent phase change materials. *PhotoniX* **3**, (2022).
14. Rios, C. *et al.* Integrated all-photonic non-volatile multi-level memory. *Nat Photonics* **9**, 725–732 (2015).
15. Kusne, A. *et al.* On-the-fly closed-loop materials discovery via Bayesian active learning. *Nat Comm* **11**, (2020).
16. Zhang, Y. *et al.* Broadband transparent optical phase change materials for high-performance nonvolatile photonics. *Nat Commun* **10**, 2–3 (2019).
17. Hu, J. *et al.* Optical Devices with Phase-Change Materials. (2021).
18. Zhang, Y. *et al.* Electrically reconfigurable non-volatile metasurface using low-loss optical phase-change material. *Nat Nanotechnol* **16**, 661–666 (2021).

Project Title: Development of a polarization-sensitive holographic microscope for point-of-care diagnosis of Malaria in resource-limited settings.

Category: Health

Summary:

The project addresses the pressing need for accurate and accessible diagnostic tools in resource-limited settings for malaria diagnosis. The project aims to develop a submicrometric-resolution, cost-effective, and portable multiparametric optical microscope incorporating polarization-sensitive holographic imaging techniques. This innovative approach will enable point-of-care diagnosis of Malaria in regions with limited resources, where traditional diagnostic methods face significant challenges.

The project will focus on three key objectives. Firstly, we will design and implement the hardware components of the polarization-sensitive holographic microscope, ensuring high spatial resolution and sensitivity to polarization, optical phase changes, and absorption. This device will involve the development of optimized illumination sources and the integration of polarization-sensitive elements.

Secondly, we will develop computationally efficient software algorithms for reconstructing and analyzing holographic images acquired by the microscope. These algorithms will enable rapid and accurate interpretation of the acquired data, facilitating identifying and quantifying malaria parasites and other microorganisms of interest.

Lastly, we will miniaturize the developed system, leveraging 3D printing technologies and compact designs, to create a portable and user-friendly device suitable for point-of-care settings. This miniaturized microscope will be evaluated and validated with medical experts in malaria diagnosis, ensuring its reliability and usability in real-world scenarios.

The successful implementation of this project will have significant outcomes and impact. Firstly, it will lead to the development of an affordable and portable multiparametric optical microscope specifically designed to detect pollutants and microorganisms, particularly for malaria diagnosis accurately. This innovative technology will improve access to timely and precise diagnostic tools in resource-limited settings, reducing malaria morbidity and mortality rates.

This project represents a significant advancement in optical diagnostics for health applications. By developing an affordable and portable multiparametric optical microscope, we aim to address the global challenge of accurate and accessible diagnosis of diseases in resource-limited settings. The project outcomes will directly impact improving public health, enhancing research capabilities, and fostering innovation in the field of optical technologies for healthcare.

Name of Challenge Project: Development of a polarization-sensitive holographic microscope for point-of-care diagnosis of Malaria in resource-limited settings.

Literature Review

Early diagnosis and effective treatment are crucial for reducing malaria morbidity and mortality rates[1]. According to the World Malaria Report[2], there were 247 million malaria cases in 2021 compared to 245 million in 2020. The estimated number of malaria deaths was 619,000 in 2021 compared to 625,000 in 2020. Over the two peak years of the pandemic (2020–2021), COVID-related disruptions led to about 13 million more malaria cases and 63,000 more malaria deaths. The 2022 edition of the report acknowledges that, despite disruptions to prevention, diagnostic, and treatment services during the pandemic, countries worldwide have largely managed to maintain progress in malaria control. However, these statistics highlight the ongoing global burden of Malaria and underscore the urgent need for improved diagnostic tools.

Brightfield microscopy (BM) remains the most commonly used technique for diagnosing and studying Malaria due to its ability to directly visualize the malaria parasite, Plasmodium, and record the kinetics of parasite removal [3]. While other microscopy techniques, such as fluorescence microscopy[3], confocal microscopy [4], and phase contrast microscopy[5], have been employed for P. falciparum detection, BM remains the most affordable and relatively easy-to-use option. However, sustaining microscopy services in resource-limited areas presents a significant challenge due to limited economic resources and a shortage of qualified personnel.

In BM-based malaria diagnosis, considered the "Gold Standard", a blood sample, either in a thin smear or thick drop, is examined using a microscope equipped with a 100X oil immersion objective. The sample is typically stained prior to analysis[6], and a highly-trained microscopist visually quantifies parasitemia and identifies different types of malaria[7]. However, the Gold Standard method's cost and lack of portability hinder its widespread use in regions with limited resources. Furthermore, the staining process, despite its relatively low cost and high sensitivity and specificity, has drawbacks, including potentially contaminating reagents, the need for trained personnel, and the time-consuming sample preparation that can take up to 45 minutes. Inadequate sample preparation can introduce artifacts, fungal contamination, dye residues, dirt, and cell debris, leading to false-positive diagnoses. These limitations underscore the need for alternative diagnostic methodologies.

Polarization-based microscopes have been reported in the literature to address Malaria parasite detection. However, these proposals often rely on using pigments and dyes, which can hinder the possibility of precise diagnosis and diminish the feasibility of implementing such methods in situ within resource-limited areas. For instance, a study [8] presented a cost-effective, optical cell-phone-based transmission polarized light microscope system specifically designed for imaging the malaria pigment, hemozoin. While polarized light microscopy facilitates the observation of hemozoin, existing commercial devices with complicated designs, high maintenance requirements, bulkiness, and cost pose obstacles to widespread adoption. Similarly, another study [9] demonstrated a cell phone-based polarized microscope for diagnosing Malaria through hemozoin recognition. Although these systems offer increased resolving power, wider field-of-view, and portability compared to traditional microscopy, they still rely on pigment identification and may require additional retraining of microscopy technicians.

To improve the accuracy of unstained sample diagnosis and contribute to low-cost technology and ease of operation, several studies in the literature have explored the use of Holographic Microscopy (HM) for Plasmodium detection[10,11]. HM architectures supported by off-axis configurations have demonstrated high sensitivity, but their implementation has limitations in terms of portability and cost [12]. Lensless HM (LHM) techniques have been utilized to develop low-cost systems for inspecting biological samples[13]. Previous reports have focused on sample visualization[10]. In that proposal, the sample is placed directly on the digital sensor and illuminated by a set of 23 point sources generated by optical fibers. Compared to LHM, this configuration offers a larger field of view but requires multiple point sources and imposes a higher computational load. Notably, the system is portable, weighing only 95 grams, although the exact cost is not specified. Based on the technology involved, an estimated cost of around USD 1000 per unit may be expected, which presents a limitation for implementation in certain endemic areas. While this method detects Plasmodium, it operates on samples stained using the Giemsa method, lacks reported sensitivity, and does not explore the possibility of detecting mixed malaria infections.

Therefore, it is evident that there is a need to develop alternative techniques that combine holographic and phase-sensitive methods to create ultra-low-cost tools for Malaria diagnosis. While the existing state-of-the-art solutions based on HM have shown advancements in Plasmodium detection, they do not fully meet the required characteristics for addressing the specific challenges in certain regions. The accurate diagnosis of Malaria with unstained blood samples remains an open research area that necessitates the creation of low-cost platforms supported by digital holographic microscopes. These platforms should offer high sensitivity, ease of use, and portability, serving as effective point-of-care diagnostic tools for this disease in resource-limited settings. By developing such innovative approaches, we can overcome current methods' limitations and significantly improve the accuracy and accessibility of Malaria diagnosis.

Problem Statement/Objective

The problem addressed in this project centers around the scientific challenges and limitations associated with current holographic microscopy (HM) techniques for accurately diagnosing Malaria in resource-limited settings. While HM has shown potential for diagnosing Malaria without needing prior staining of blood samples, the lack of readily available and affordable devices with polarization sensitivity and sufficient spatial resolution to resolve malaria parasites presents a significant obstacle.

LHM offers a simple imaging method for recovering information from microscopic samples[14]. LHM enables the numerical retrieval of the complete optical complex wavefield scattered by the specimens, allowing for the numerical refocusing of individual objects and phase information retrieval from transparent samples[15]. However, developing portable LHM devices with polarization sensitivity remains a critical challenge to expand the use of this imaging technique in point-of-care malaria diagnosis. This research project aims to address these challenges and develop specialized point-of-care platforms for the accurate in-situ diagnosis of Malaria. The specific objectives are as follows:

1. Develop a mechanically stable, low-cost point source LHM illumination system with high spatial coherence using off-the-shelf elements. This will enable the generation of coherent illumination sources for LHM without the need for micrometer pinholes or bulky setups, thereby improving portability and reducing costs.

2. Design and implement a full Muller-matrix polarization-sensitive LHM system with fewer polarizing elements and simple numerical processing. The goal is to develop an affordable solution that can run on embedded computer systems while accurately quantifying the linear diattenuation response of the samples, enhancing disease diagnosis.
3. Create a miniaturized LHM device using 3D printing technology that incorporates the advancements achieved in the first two objectives. This device will be compact, cost-effective, and suitable for point-of-care malaria diagnosis in resource-limited settings.

By addressing the challenges related to LHM's portability, polarization sensitivity, and cost-effectiveness, this research aims to provide a breakthrough in malaria diagnosis. The proposed developments will contribute to the advancement of point-of-care diagnostic tools for accurate and accessible malaria detection, ultimately reducing the burden of the disease in affected regions.

Outline of tasks/Work Plan

The personnel involved in this project and collaborators are listed below:
Dr. Carlos Trujillo, Professor. Principal investigator (EAFIT – Colombia).
Ph.D. Student Maria Josef Lopera Acosta (double degree student in EAFIT and VPHOT, Belgium).
Master student 1 Tomas Velez Acosta (Master in Applied Physics – EAFIT)
Master student 2 Sofia Obando Vasquez (Master in Applied Physics – EAFIT). *Granted with OPTICA's scholarship for undergraduate and master 's-level women 2023.*
Undergraduate students (2) to be defined. (Physic Engineering program – EAFIT)
Dr. Adriana Pabón-Vidal, Universidad de Antioquia, Colombia. Malaria diagnosis expert.
Collaborator 1: Dr. Heidi Ottavaere, Professor, Head of TONA Department. Vrije Universiteit Brussel.
Collaborator 2: Dr. Ana Doblas, Professor. UMass-Dartmouth, USA.

The project has four stages, each with specific activities, timeframes, and responsible personnel.

Hardware implementation (first part):
a. In this stage, we will perform the optical design of the full polarization-sensitive LHM system and its experimental implementation in the laboratory. The known polarizing elements will be inserted into the system, and their full-matrix parameters will be contrasted against the theoretical expectation to ensure proper functioning. This activity will be carried out by a Ph.D. student and the Principal Investigator. The timeframe for this stage is from 0 to 6 months.
b. Concurrently, we will develop holographic point sources with optimized optical diffraction efficiency to achieve state-of-the-art imaging performance, including lateral resolution below 1 μm and λ/10 phase sensitivity. A master student and the principal investigator will be responsible for this task. The timeframe for this activity is also from 0 to 6 months.
Collaborator 1 will participate in this stage by co-directing Ph.D. Student 1, and assisting in the design of the illumination source.

Software implementation:
a. In this stage, we will focus on developing computationally simple numerical propagators to reconstruct the recorded LHM holograms using low-cost embedded systems efficiently. A second master's student and the principal investigator will undertake this task. The timeframe for this stage is from 6 to 11 months.

b. Additionally, we will train learning-based methods for the end-to-end reconstruction of phase maps using datasets acquired with the instruments developed in the first stage. This task will be carried out by the second master's student, in collaboration with the Ph.D. student and the Principal Investigator. The timeframe for this activity aligns with the period from 6 to 11 months. Collaborator 2 will participate in this stage by co-directing Master Student 2 and assisting in the design of the holographic reconstruction methods.

Hardware implementation (second part):
a. In this stage, we will focus on developing a miniaturized version of the LHM platform using dedicated CAD software and incorporating polarization-sensitive elements and the engineered illumination point source. The goal is to achieve a compact imaging device with dimensions of 10cm x 10cm x 10cm. Two undergraduate students and the Principal Investigator will collaborate on this task. The timeframe for this stage is from 12 to 18 months.

Validation with a medical expert:
a. The final stage involves quality control and validation of the developed platform by a professional with expertise in malaria diagnosis. The expert will perform blind readings of sample density and stages, and the platform's performance will be validated through concordance analysis by two additional experts. This validation procedure will be conducted at the Malaria Laboratory of the University of Antioquia in Medellin, Colombia (School of Medicine), in accordance with national guidelines for malaria diagnosis. Malaria Diagnosis Expert and the Principal Investigator will be responsible for this stage, which will take place from 16 to 24 months.

Outcome(s)

1. Development of an affordable and portable platform for point-of-care diagnosis of malaria.
2. Creation of an innovative polarization-sensitive holographic microscope with submicrometric resolution, enabling accurate detection and quantification of malaria parasites.
3. Establishment of a comprehensive database of holographic images and corresponding metadata, facilitating future research and algorithm development in malaria diagnosis.
4. Formation of a collaborative network with malaria experts, clinicians, and researchers for knowledge exchange and further advancements in malaria diagnosis and treatment.
5. Demonstration of the feasibility and effectiveness of the developed platform through extensive validation studies using clinical samples from malaria-endemic regions.
6. Capacity building and training of healthcare professionals in the use and maintenance of the developed platform for point-of-care malaria diagnosis.
7. Dissemination of project findings and methodologies through the publication of two (2) Q1 manuscripts and three (2) Q2 manuscripts in Optica open-access journals.
8. Presentation of two (2) contributions reporting project progress and results in Optica-organized symposiums.
9. Potential for scalability and adaptability of the developed platform to address other infectious diseases and healthcare challenges in resource-limited settings.
10. Contribution to the global fight against malaria by providing an affordable and portable diagnostic tool that aids in early detection and timely treatment, ultimately reducing malaria-related morbidity and mortality rates.

Impact

Short-term impact: Development of low-cost platforms for accurate and precise diagnosis of Malaria, enabling timely treatment and reducing the burden of the disease.
Training and capacity building of specialized and high-level human capital in research and technological developments, contributing to the advancement of scientific expertise in the field of optical diagnostics and healthcare in Colombia.
The contributions made through this project in malaria diagnosis and the validation of its performance will have a significant impact on the national, institutional, and regional academic communities. These developments will provide an innovative strategy for diagnosing Malaria, serving as a model for the production of other diagnostic platforms applicable in diverse fields such as medicine and industry.

Long-term impact: The availability and deployment of the developed technologies in malaria-endemic areas will have a transformative impact on the quality of life for people residing in these regions. By enabling accurate and timely diagnosis of Malaria, the project will contribute to the reduction of malaria morbidity and mortality rates, thereby improving public health outcomes and reducing the associated healthcare costs. This long-term impact will result in healthier communities, enhanced productivity, and a better quality of life for individuals living in malaria-endemic areas. Overall, this project's outcomes and impact will extend beyond immediate scientific advancements, influencing healthcare practices, fostering innovation, and ultimately contributing to the well-being of individuals affected by Malaria.

References

1. W. H. Organization and Others, (2021).
2. World Health Organization, (2021).
3. C. J. Janse and P. H. Van Vianen, in *Flow Cytometry*, Z. Darzynkiewicz, J. P. Robinson, and H. A. B. T.-M. in C. B. Crissman, eds. (Academic Press, 1994), **42**, pp. 295–318.
4. A. Aroonsri, N. Posayapisit, J. Kongsee, O. Siripan, D. Vitsupakorn, S. Utaida, C. Uthaipibull, S. Kamchonwongpaisan, and P. J. Shaw, PeerJ **7**, e6713 (2019).
5. C. Li, S. Chen, M. Klemba, and Y. Zhu, Journal of biomedical optics **21**, 90501 (2016).
6. D. Bibin and P. Punitha, in *Lecture Notes in Electrical Engineering* (2013).
7. J. K. Baird, N. Valecha, S. Duparc, N. J. White, and R. N. Price, Am J Trop Med Hyg **95**, 35 (2016).
8. C. W. Pirnstill and G. L. Coté, Sci Rep **5**, 1 (2015).
9. Z. Yu, Y. Li, L. Deng, B. Luo, P. Wu, and D. Geng, J Biophotonics **16**, (2023).
10. S. Seo, T.-W. Su, D. K. Tseng, A. Erlinger, and A. Ozcan, Lab Chip **9**, 777 (2009).
11. O. Mudanyali, D. Tseng, C. Oh, S. O. Isikman, I. Sencan, W. Bishara, C. Oztoprak, S. Seo, B. Khademhosseini, and A. Ozcan, Lab on a chip **10**, 1417 (2010).
12. A. Anand, V. K. Chhaniwal, N. R. Patel, and B. Javidi, IEEE Photonics Journal **4**, 1456 (2012).
13. C. A. Trujillo and J. Garcia-Sucerquia, Optics Letters, Vol. 39, Issue 9, pp. 2569-2572 **39**, 2569 (2014).
14. H. Tobon-Maya, S. Zapata-Valencia, E. Zora-Guzmán, C. Buitrago-Duque, and J. Garcia-Sucerquia, Appl Opt **60**, A205 (2021).
15. P. Piedrahita-Quintero, C. Trujillo, and J. García-Sucerquia, (n.d.).

Advancing Cancer Diagnostics: Development of a Non-Contact Viscoelastic Imaging System using Nanosecond Laser Pulse-Generated Photoacoustics with Photorefractive Interferometry

Category: Health

Executive summary

The diagnosis of cancer, a leading cause of mortality worldwide, necessitates innovative and non-invasive imaging techniques to improve early detection and personalized treatment strategies. This research proposal presents the development of a groundbreaking diagnostic imaging system based on viscoelastic contrast for tumor tissues, utilizing nanosecond laser pulse-generated photoacoustics (PA) with photorefractive two-wave mixing photorefractive interferometry (TWMPI). The proposed approach seeks to revolutionize cancer diagnostics by providing a truly remote and non-contact imaging modality capable of visualizing viscoelastic properties of tumors without physical contact with the patient's tissue.

The primary goal of this project is to establish an optoacoustic imaging instrumentation modality for non-contact viscoelastic imaging of tumor tissues. By harnessing the unique viscoelastic contrast between tumor and normal biological tissues, this imaging technique aims to facilitate early-stage tumor detection with high sensitivity and specificity. Moreover, the developed imaging system will enable precision medicine by providing valuable insights into the mechanical properties and heterogeneity of tumors at the molecular level, thus optimizing personalized treatment plans for improved patient outcomes.

The proposed research project will consist of three key tasks. Task 1 focuses on laser photoacoustics of biosamples using low and high excitation lasers, integrating the TWMPI method for non-contact detection of ultrasonic displacements on the specimen surface. Task 2 involves the validation of the results with Brillouin spectroscopy, further characterizing the viscoelastic properties of biomaterials. Task 3 is dedicated to the development of a robust image reconstruction and processing technique to convert photoacoustic signals into viscoelastic images of biological materials ex-vivo. The logarithmic PA-BLS pictures will be obtained by scaling the raw data based on histogram distribution, reducing background noise.

The proposed research project's impacts are multifold, ranging from advancing cancer diagnostics and precision medicine to minimizing patient discomfort and health risks associated with traditional imaging modalities. By bridging the gap between research and clinical practice, the successful development of the remote viscoelastic imaging system can catalyze collaborations and inspire future research in medical imaging and beyond.

In conclusion, this research proposal endeavors to introduce a transformative diagnostic imaging system that capitalizes on viscoelastic contrast for tumor tissues, leveraging nanosecond laser pulse-generated photoacoustics with photorefractive interferometry. With the potential to revolutionize cancer diagnostics and enhance patient care, this non-contact imaging modality holds promise for addressing critical challenges in oncology and shaping the future of biomedical imaging technologies.

Advancing Cancer Diagnostics: Development of a Non-Contact Viscoelastic Imaging System using Nanosecond Laser Pulse-Generated Photoacoustics with Photorefractive Interferometry

1. Introduction.

Viscoelastic contrast between tumor and normal biological tissues can be utilized for the diagnostics of cancer. Opto-acoustic techniques such as nanosecond laser pulse photoacoustics (PA) could be utilized to monitor this viscoelastic contrast as non-invasive diagnostics of tumor tissues. We propose the development of **diagnostic imaging** of tumor tissues based on their viscoelastic contrast using opto-acoustics techniques in the time-domain (laser pulse generated photoacoustics). The proposed technique will comprise viscoelastic imaging by nanosecond laser pulse-generated ultrasound to be detected by photorefractive two-wave mixing photorefractive interferometry (TWMPI).

1.1 Project goal

Optoacoustic imaging instrumentation modality for non-contact viscoelastic imaging of tumor tissues.

1.2. Project Objectives

The accomplishment of these objectives is based on experimental and theoretical characterization of biological tissue biomechanics and laser-based imaging instrumentation development. The project will involve:

1) Viscoelastic microscopy and mapping of tumored biological tissues by nanosecond laser pulse photoacoustics with TWMPI.

2) Viscoelastic image reconstruction and processing of photoacoustic mapping data during diagnostics of tumor tissues

2. Literature review and problem statement

Conventional photoacoustic imaging (PAI) is an emerging imaging technique that utilizes optical excitation and acoustic detection. It is based on the photoacoustic effect, where the excitation energy is partially absorbed by molecules and converted into heat [1]. This process leads to thermoelastic expansion and the generation of acoustic waves under pulse laser excitation. Consequently, these acoustic waves are detected on the sample surface using an ultrasound transducer. Conventional PA uses an ultrasound transducer to detect acoustic waves generated by the absorption of a pulsed excitation laser scanned over the sample. PAI is currently widely used in biomedicine. Its main disadvantage is the need for the ultrasound transducer to be placed in direct physical contact with the sample using a coupling medium such as ultrasound gel or water. This condition is not desirable in many clinical applications as it might cause contamination, infection, or harm to delicate tissues [2]. Therefore, researchers are developing various **non-contact** methods to detect acoustic wave signal [3][4]. A photoacoustic imaging modality by non-contact detection of acoustic waves addresses current issues of traditional PAI techniques and opens the door to various exciting biomedical applications. We have taken part in the development of deformable mirror-based photoacoustic remote sensing (PARS) microscopy for depth scanning [4].

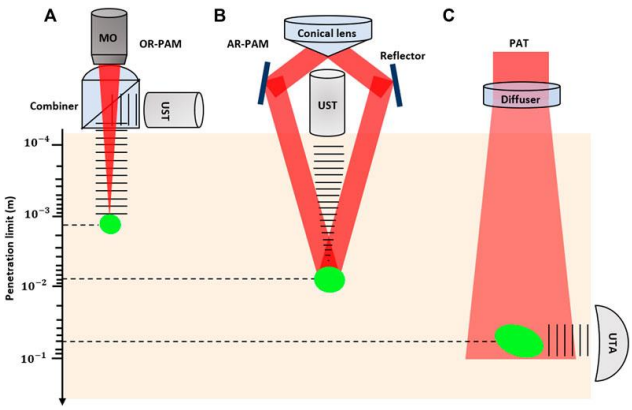

Figure 1. Signal generation and detection in different implementations of PAI and penetration limits in scattering tissue.

PAI can be categorized into two main groups depending on the image formation technique: photoacoustic tomography (PAT) and photoacoustic microscopy (PAM). PAT utilizes reconstruction-based image formation, while PAM utilizes focused-based image formation [1]. In PAT, the excitation beam is usually unfocused on the sample and therefore enables a wide field of view images. This technique has provided great results in imaging small animals [5] and in cancer studies [6]. On the other hand, PAM forms images by raster scanning of optical and acoustic foci. PAM can be categorized into two groups where the excitation beam is focused tighter (optical resolution PAM) or where the acoustic focusing is tighter (acoustic resolution PAM). PAM provides higher-resolution imaging, while PAT has deeper penetration [7]. Figure 1 above demonstrates different types of PAI [8].

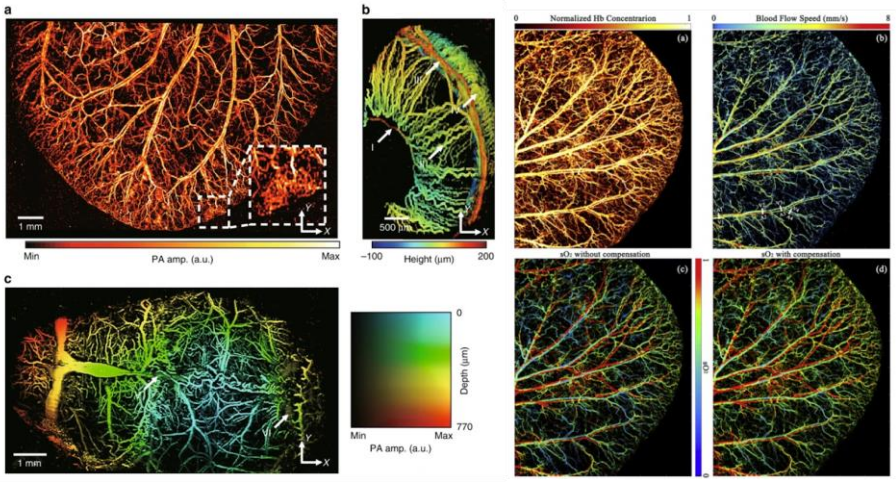

Figure 2. Depth-resolved and functional photoacoustic images of mouse ear, eye, and brain.

Photoacoustic imaging has many advantages such as it is not a non-invasive and non-ionizing imaging technique that allows for deep tissue penetration. Since this imaging modality relies on optical absorption, it has high sensitivity and specificity. As a result, researchers can obtain functional and depth-resolved images as seen in Figure 2 [9,10].

As mentioned earlier, a non-contact method of detecting acoustic waves will expand the range of applications of photoacoustic imaging techniques. One imaging technique for all-optical, non-contact and label-free detection of acoustic signals is called photoacoustic remote sensing (PARS) microscopy first developed in 2017 [11]. In PARS microscopy, a traditional ultrasonic transducer is substituted by a probe beam. The probe beam is usually co-aligned and co-focused with the excitation beam onto a specimen of interest. During the excitation, the tissue goes through thermo-elastic expansion, and the energy absorbed by chromophores is converted to pressure. The rise in pressure causes elasto-optic modulations in the local optical properties within absorbers and results in the intensity change of the back-reflected interrogation beam. PARS imaging modality produced great results when imaging microvasculature of the back and the front of a rat eye [12], functional imaging as seen in Figure 3 [13], combined with other imaging modalities such as optical coherence tomography [14], and H&E-like histology imaging [15].

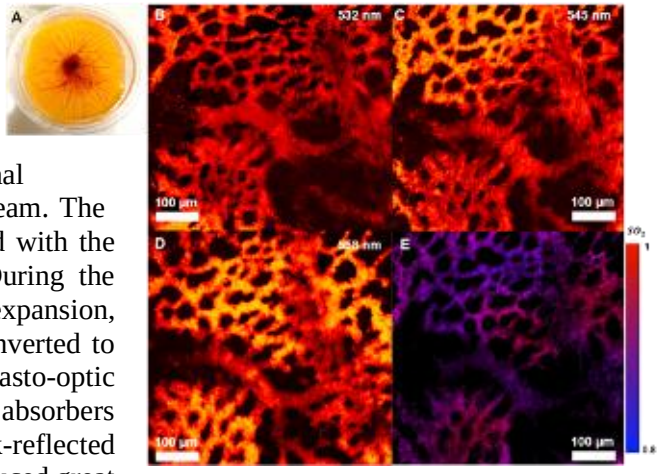

Figure 3. Functional imaging of chicken embryo chorioallantoic membrane (CAM) using PARS

The novelty of this study would be to develop a truly remote (*non-contact) and non-invasive* measurement method that uses nanosecond pulse laser-based PAM with TWMPI sensing for *diagnostic* imaging of biological tissues.

3. Outline of tasks

This project will be carried out through the following three tasks:

Task 1: Laser photoacoustics of biosamples using low and high excitation lasers.

Various researchers have shown successful implementation of optical detection of ultrasonic displacements on the tissue surface using Fabry-Perot interferometry [16] and other interferometric methods [17,18]. However, the Fabry-Perot interferometric detection of ultrasonic displacement is not fully non-contact as it requires foils to be in physical contact with the sample. The other interferometric methods call for a smooth surface such as liquids. Therefore, a TWMPI) method was implemented to enable the detection of ultrasonic displacements even on rough surfaces [19]. This method was used on rough industrial samples [20], but further was altered to image biological samples. In this study, we propose using a TWMPI technique to detect ultrasonic displacements on the specimen surface due to acoustic wave propagation. The proposed optical setup is demonstrated in Figure 4.

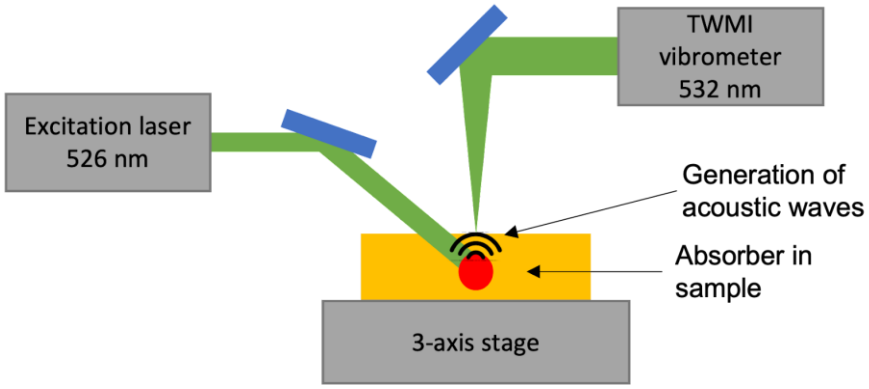

Figure 4. All-optical non-contact detection of ultrasonic displacements using TWMI.

Task 2: Validation of the results with Brillouin spectroscopy for measurement of viscoelastic properties of biomaterials

Preliminary result was obtained by the author and colleagues from AMRELAT (https://www.amrelat.com) to characterize the viscoelastic properties of bovine (BSA) and human albumin proteins (HSA) using Brillouin spectroscopy (BLS) [21]. Brillouin spectroscopy will be applied to measure viscoelastic properties employing six pass Tandem Fabry Perot Interferometry (TFPI) as in [21] for validation of results taken from task 1.

Task 3: Signal mapping, image reconstruction and processing

Viscoelastic properties of biological materials ex-vivo will be determined using our system ascertained in task 1. The co-focused excitation and probe beams will be mechanically traversed over the material to create PA pictures. Pulsed beams from the excitation laser will be used while scanning to probe regularly spaced absorption contrast sites. By altering the mechanical scanning pattern and speed of the stage, the lateral spacing of the interrogation sites will be changed. The majority of the photos that will be used in this task will have a lateral spacing of ~ 500 nm. The PA-BLS signal and interrogation site are noted for each interrogation occurrence. Using a 14-bit digitizer with high bandwidth, these signals will be recorded to computer memory. The time domain data from TWPMI will be processed to reduce it to a single distinctive photoacoustic amplitude and associated position signal. After scanning will be finished, signals will used to create a picture. To convert the PA signals to a decibel scale, the raw data will be first normalized, and log scaled to remove scanning noise. The logarithmic PA-BLS picture will be rescaled based on histogram distribution to get the final image, which lowers background noise.

4. Impact and outcome.

The proposed research project aims to develop a truly remote and non-invasive diagnostic imaging system based on viscoelastic contrast for tumor tissues using nanosecond laser pulse-generated photoacoustics (PA) with photorefractive two-wave mixing photorefractive interferometry (TWMPI). The successful realization of this novel imaging modality is expected to have significant impact in several key areas:

4.1 Advancing Cancer Diagnostics:

The development of a non-contact, non-invasive, and label-free imaging technique capable of visualizing viscoelastic properties of tumor tissues represents a paradigm shift in cancer diagnostics. By harnessing the opto-acoustic capabilities of the proposed system, researchers and clinicians will be empowered with a powerful tool to detect early-stage tumors with high sensitivity and specificity. The ability to identify tumor-specific viscoelastic signatures could lead to more accurate and timely diagnoses, facilitating improved patient outcomes through early intervention and targeted treatment plans.

4.2 Precision Medicine and Treatment Planning:

The remote viscoelastic imaging of tumor tissues will provide valuable insights into the mechanical properties and heterogeneity of tumors at the molecular level. This information is crucial for tailoring personalized treatment strategies based on individual patient characteristics. By understanding the viscoelastic contrast between tumor and normal biological tissues, clinicians can optimize treatment modalities, dose levels, and delivery methods to enhance treatment efficacy while minimizing adverse effects. Ultimately, this will contribute to the advancement of precision medicine in oncology, resulting in better patient responses and prolonged survival rates.

4.3 Minimizing Patient Discomfort and Health Risks:

The proposed truly remote imaging system eliminates the need for physical contact between the imaging apparatus and the patient's tissue, reducing the potential for contamination, infection, or harm to delicate tissues. This non-contact approach enhances patient safety and comfort, mitigating risks associated with traditional imaging methods that require invasive procedures or coupling mediums. By offering a non-ionizing and non-invasive imaging solution, the proposed system provides a safer alternative for patients, especially those who require frequent imaging for monitoring tumor progression or treatment response.

4.4 Advancing Biomedical Imaging Techniques:

The successful implementation of non-contact photoacoustic imaging with photorefractive two-wave mixing photorefractive interferometry (TWMPI) for viscoelastic imaging represents a notable advancement in the field of biomedical imaging. By extending the capabilities of photoacoustic imaging to include non-contact detection, this research project opens the door to various exciting biomedical applications beyond tumor diagnostics. The developed system has the potential to be adapted for investigating other medical conditions, facilitating research in material science, and providing new insights into biological phenomena with unprecedented precision.

4.5 Bridging the Gap Between Research and Clinical Practice:

The proposed research project bridges the gap between innovative research and real-world clinical applications. By developing a functional prototype of the remote viscoelastic imaging system, the study will demonstrate the feasibility and practicality of this cutting-edge technology for diagnostic use. The successful translation of this technology into clinical practice has the potential to revolutionize cancer diagnostics and impact patient care on a global scale, underscoring its significance as a transformative advancement in medical imaging.

4.6 Catalyzing Collaborations and Future Research:

As a pioneering development in the field of photoacoustic imaging, the proposed remote viscoelastic imaging system is expected to attract attention from researchers and clinicians worldwide. The project's success will catalyze collaborations between interdisciplinary teams, fostering knowledge exchange, and encouraging further research and innovation in the domain of photoacoustic techniques, viscoelastic imaging, and beyond. The new opportunities and avenues of research unlocked by this project could lead to breakthroughs in medical imaging and contribute to a vibrant ecosystem of cutting-edge scientific discoveries.

In conclusion, the proposed development of a truly remote diagnostic imaging system based on viscoelastic contrast using nanosecond laser pulse-generated photoacoustics with photorefractive two-wave mixing photorefractive interferometry (TWMPI) holds immense potential for transforming cancer diagnostics, advancing precision medicine, enhancing patient safety, and propelling the field of biomedical imaging to new frontiers. The proposed research project aligns with the critical needs of

improving cancer management and patient outcomes, and its successful implementation could bring about far-reaching impacts in healthcare and scientific communities worldwide.

References:

1. Beard P. Biomedical photoacoustic imaging. Interface Focus. 2011. doi:10.1098/rsfs.2011.0028
2. Zhang HF, Puliafito CA, Jiao S. Photoacoustic ophthalmoscopy for in vivo retinal imaging: current status and prospects. Ophthalmic surgery, lasers & imaging : the official journal of the International Society for Imaging in the Eye. 2011. doi:10.3928/15428877-20110627-10
3. Hosseinaee Z, Le M, Bell K, Reza PH. Towards non-contact photoacoustic imaging [review]. Photoacoustics. 2020. doi:10.1016/j.pacs.2020.100207
4. Mukhangaliyeva L, Kocer S, Warren A, Bell K, Boktor M, Yavuz M, et al. Deformable mirror-based photoacoustic remote sensing (PARS) microscopy for depth scanning. Biomed Opt Express. 2022;13: 5643–5653. doi:10.1364/boe.471770
5. Xia J, Chatni MR, Maslov K, Guo Z, Wang K, Anastasio M, et al. Whole-body ring-shaped confocal photoacoustic computed tomography of small animals in vivo. J Biomed Opt. 2012;17. doi:10.1117/1.jbo.17.5.050506
6. Lin L, Hu P, Shi J, Appleton CM, Maslov K, Li L, et al. Single-breath-hold photoacoustic computed tomography of the breast. Nat Commun. 2018;9. doi:10.1038/s41467-018-04576-z
7. Stein EW, Maslov K, Wang L V. Noninvasive, in vivo imaging of blood-oxygenation dynamics within the mouse brain using photoacoustic microscopy. J Biomed Opt. 2009;14. doi:10.1117/1.3095799
8. Hosseinaee Z, Tummon Simmons JA, Reza PH. Dual-Modal Photoacoustic Imaging and Optical Coherence Tomography [Review]. Frontiers in Physics. 2021. doi:10.3389/fphy.2020.616618
9. Kim J, Kim JY, Jeon S, Baik JW, Cho SH, Kim C. Super-resolution localization photoacoustic microscopy using intrinsic red blood cells as contrast absorbers. Light Sci Appl. 2019;8. doi:10.1038/s41377-019-0220-4
10. Liu C, Liang Y, Wang L. Single-shot photoacoustic microscopy of hemoglobin concentration, oxygen saturation, and blood flow in sub-microseconds. Photoacoustics. 2020;17. doi:10.1016/j.pacs.2019.100156
11. Hajireza P, Shi W, Bell K, Paproski RJ, Zemp RJ. Non-interferometric photoacoustic remote sensing microscopy. Light Sci Appl. 2017;6. doi:10.1038/lsa.2016.278
12. Hosseinaee Z, Pellegrino N, Abbasi N, Amiri T, Simmons JAT, Fieguth P, et al. In-vivo functional and structural retinal imaging using multiwavelength photoacoustic remote sensing microscopy. Sci Rep. 2022;12. doi:10.1038/s41598-022-08508-2
13. Hosseinaee Z, Ecclestone B, Pellegrino N, Khalili L, Mukhangaliyeva L, Fieguth P, et al. Functional photoacoustic remote sensing microscopy using a stabilized temperature-regulated stimulated Raman scattering light source. Opt Express. 2021;29. doi:10.1364/oe.434004
14. Hosseinaee Z, Nima Abbasi, Pellegrino N, Khalili L, Mukhangaliyeva L, Haji Reza P. Functional and structural ophthalmic imaging using noncontact multimodal photoacoustic remote sensing microscopy and optical coherence tomography. Sci Rep. 2021;11. doi:10.1038/s41598-021-90776-5
15. Boktor M, Ecclestone BR, Pekar V, Dinakaran D, Mackey JR, Fieguth P, et al. Virtual histological staining of label-free total absorption photoacoustic remote sensing (TA-PARS). Sci Rep. 2022;12: 1–12. doi:10.1038/s41598-022-14042-y
16. Hou Y, Huang S-W, Ashkenazi S, Witte R, O'Donnell M. Thin polymer etalon arrays for high-resolution photoacoustic imaging. J Biomed Opt. 2008;13. doi:10.1117/1.3042260
17. Payne BP, Venugopalan V, Mikić BB, Nishioka NS. Optoacoustic tomography using time-resolved interferometric detection of surface displacement. J Biomed Opt. 2003;8. doi:10.1117/1.1559727
18. Carp SA, Venugopalan V. Optoacoustic imaging based on the interferometric measurement of surface displacement. J Biomed Opt. 2007;12. doi:10.1117/1.2812665
19. Hochreiner A, Berer T, Grün H, Leitner M, Burgholzer P. Photoacoustic imaging using an adaptive interferometer with a photorefractive crystal. J Biophotonics. 2012;5. doi:10.1002/jbio.201100111

20. Berer T, Hochreiner A, Zamiri S, Burgholzer P. Remote photoacoustic imaging on solid material using a two-wave mixing interferometer. Opt Lett. 2010;35. doi:10.1364/ol.35.004151
21. Kharmyssov C, Sekerbayev K, Nurekeyev Z, Gaipov A, Utegulov ZN. Mechano-Chemistry across Phase Transitions in Heated Albumin Protein Solutions. Polymers (Basel). 2023;15. doi:10.3390/polym15092039

Proposal Title: Green and Affordable Energy Harvesting Using Laser Sculptured Moist-Electric Generators

Category: Environment

This research proposal addresses the urgent global energy problems of greenhouse gas emissions and lack of access to energy. By harnessing the abundant moisture in the atmosphere, this project aims to develop green and affordable energy harvesting technology using laser-sculptured moist-electric generators (MEGs). The proposed MEGs will utilize active materials with abundant channels and functional groups, obtained from lab-free materials such as cloth, paper, wood, food, and cork, through a controllable laser sculpture technique.

The research objectives can be summarized as follows:

1. Develop a laser sculpture technique to fabricate active materials with abundant channels and functional groups from lab-free materials, enabling the conversion of these materials into graphene-like nanomaterials for the development of cost-effective and environmentally friendly MEGs.
2. Investigate the interfacial force-electric-thermal coupling process to gain a deep understanding of the moisture-induced electricity mechanism. The study will involve cross-scale dynamic simulations to simulate charge transfer at the water-material interface and explore influential factors on electricity output. Advanced analytical techniques will be used to characterize the active materials and study their interaction with water molecules.
3. Build generators capable of efficiently harvesting green moisture energy using laser-sculptured active materials in large scale. The generators will be tested in various ambient conditions and geographic locations in China, including deserts, forests, and mountains.

The outcomes of this research program are expected to include the development of cost-effective and environmentally friendly MEGs, capable of efficiently harvesting energy from ambient moisture. The controllable laser sculpture technique will enable the fabrication of scalable generators using lab-free materials, contributing to the affordability and accessibility of green energy solutions. The project aims to achieve milliwatt-level electricity output and demonstrate the feasibility of moisture-electric generation in real-world applications.

The broader impact of this research lies in addressing global energy challenges while promoting collaboration among researchers with diverse expertise. By leveraging advanced optics and photonics, this project underscores the potential for international collaboration and collective efforts in finding solutions to urgent environmental issues the world faced today. The outcomes of this study have the potential to revolutionize energy harvesting technologies, mitigate climate change, and improve energy access for underserved communities worldwide.

In conclusion, the proposed research program combines interdisciplinary knowledge and expertise to develop laser-sculptured moist-electric generators for green and affordable energy harvesting. The project aims to provide novel solutions to the pressing energy problems faced globally, emphasizing the importance of international collaboration and the application of advanced optical technologies.

Green and Affordable Energy Harvesting Using Laser Sculptured Moist-Electric Generators

Introduction and Background

The world faces two energy problems: most of our energy production still produces greenhouse and polluted gas emissions, and hundreds of millions of people lack access to energy entirely [1]. The global harmful emissions, most of which is caused by the production of energy, lead to climate change and further responsible for drought, wildfires, flooding, poverty displacement, food insecurity, health risks, and species loss [2,3]. So far, anthropogenic activities have caused about 1.0 °C of global warming above the pre-industrial level and this is likely to reach 1.5 °C between 2030 and 2052 if the current emission rates persist [4]. In 2018, the world encountered 315 cases of natural disasters which are mainly related to the climate [5]. Approximately 68.5 million people were affected, and economic losses amounted to $131.7 billion, of which storms, floods, wildfires and droughts accounted for approximately 93% [6]. Ongoing increase in temperature and natural disasters cause some species to migrate further inland or upland, resulting in fragmented, isolated populations and local extinctions [7]. To bring emissions down towards net-zero will be one of the world's biggest challenges in the years ahead.

But the world has another global energy problem that is just as big: hundreds of millions of people lack access to sufficient energy entirely, with terrible consequences to themselves and the environment. According to the report by the International Energy Agency (IEA), there are almost one billion of people around the world living without electricity, while they are most affected by climate change [8]. For example, Africa accounts for less than 3% of the world's energy-related carbon dioxide emissions to date and has the lowest emissions per capita of any region [9]. But Africans are disproportionately experiencing the negative effects of climate change, including water stress, reduced food production, increased frequency of extreme weather events and lower economic growth. The world needs solutions for the twin problems by developing green and affordable energy technology.

The atmosphere has long been recognized as a sink of electrical power, as water covers 71% of the Earth's surface, and water vapor or moisture is abundant almost everywhere, even in the very dry area such as desert, no matter day and night [10]. The atmosphere contains approximately 1.3×10^4 cubic kilometers of water, mainly in the form of vapor and droplets. Within a relatively small area, water is evenly distributed in the air. The conversion of water form from one to another involves tremendous energy exchange with environment. Specifically, one single gram of water evaporates or condenses, converting 2.6 kJ of energy, which is equivalent to the energy contained in an AAA battery [11]. And the annual energy power involved in the natural water cycle is up to 6×10^{15} W, three orders of magnitude higher than the annual energy consumption of human beings [12]. As the water vapor (moisture) resource is clean and sustainable, and most importantly, accessible worldwide including undeveloped countries or remote areas, harvesting energy from ambient moisture then shows potential to provide a promising solution for the twin energy problems the world faced today.

Problem Statement

The opportunities for moisture-enabled electricity generation have been usually overlooked for a long time. The possibilities for electricity generation are facilitated by the electrification of water in response to changes in phase but experiments directed toward the harvesting of this charge to generate electrical power from atmospheric water vapor have been only recently been reported [13]. The moisture energy harvesting can be achieved mainly by: 1) doing work driven by reversible deformation of moisture-responsive materials and 2) ion diffusion driven by moisture-induced gradient energy. The first method converts environmental humidity changes into mechanical shifts of moisture-responsive materials, further driving piezoelectric or magnetoelectric generators to output electricity. The latter method is to drive ion migration by moisture-induced gradient energy, in which the chemical potential changes of water from gas to liquid or the phase. Either way the nanomaterials with functional groups are need to yield electricity output because there needs relatively high specific area and active sites to interact with water molecular in ambient moisture [14].

Nanomaterials with high specific area due to reduced size are usually used for constructing moist-electric generator (MEG). Qu's group reported the first graphene-based MEG in 2015 and propelled its development with substantive works[13]. The applicant (Prof. Daozhi Shen) also had made significant

contribution to developing efficient metal-oxide-nanowire-based MEGs for harvesting ambient moisture energy and pioneering their self-powered wearable electronic applications [15–17]. However, the current MEGs fabrication is costly and the materials used are not eco-friendly enough. For example, the graphene materials used were fabricated through strong acid chemical reaction with low productivity [18]. Metal oxide nanowires were grown through dangerous hydrothermal method in sealed autoclave with high inner pressure for days [15]. Some polymer-based MEGs show high output, but the materials synthesis includes serious pollution issues and the devices themselves may be harmful to both humans and environment, which does not meet the requirement of green and sustainable life. In addition, the highest energy conversion efficiency is 1~2%, still low compared with typical energy conversion technologies [19]. The primary reason is the lacked in-depth understanding of the interfacial force-electric-thermal coupling process and mechanism of moisture-induced electricity generation.

Despite the ambient moisture source is green and ubiquitously accessible, the current MEGs for moisture energy harvesting are not yet green and affordable. Thus, in order to let moist-electricity offer a potential solution for two energy problems, cost-effective and lab-free active materials, together with efficient and scalable fabrication method are necessary. Building affordable generators capable of harvesting green moisture energy eventually with fundamental insight of understanding interfacial process is also essential.

Goals

The main goal of this proposal is to establish an effective protocol for addressing two energy problems globally by harvesting green energy from ubiquitous moisture source through low-cost and environmental-friendly generators sculptured by laser from lab-free materials, with three specific objectives to:

(1) Develop controllable laser sculpture technique for generators with active materials containing abundant channels and functional groups from lab-free materials like cloth, paper, wood, food and cork, etc.;

(2) Investigate the interfacial force-electric-thermal coupling process for deeply understanding moisture-induced electricity mechanism in order to guide the materials fabrication and device design for energy conversion efficiency enhancement;

(3) Build prototype of affordable generators capable of harvesting green moisture energy with scalable electricity output based on the low-cost laser sculpture technique from environmental-friendly materials and test the output in different regions of China, including deserts, forests, and mountains, etc.

This research program ultimately aims at the understanding between the feasibility of laser sculptured nanomaterials and the moisture electric generation for affordable and green energy harvesting practice, with possibilities of providing novel solutions for continued growth twin energy problems on the help of advanced optical technology.

Laser sculpture, an advanced photonics-based technology, can provide a unique approach for moisture-electric generators fabrication in a low-cost and environmental-friendly way. Laser shows powerful to sculpture almost any carbon-atom-rich and lab-free materials, including cross-linked polymers, cloth, paper, wood, food and cork, with the capability of converting them into graphene-like nanomaterials [20], which can be further used for efficiency moisture-electric generator construction due to high specific area and active sites. Laser-based processes can largely reduce the fabrication time and simplify the manufacturing process by avoiding two or more steps for manipulation, placement, and integration of materials. Laser engineering can not only use high power irradiation to obtain scalable modification efficiently, but also selectively engrave nanostructured materials with high resolution by providing local high-temperature and high-pressure environments in a controllable way, without additional use of harmful chemical processes. As the affordable energy from clean and sustainable moisture source can be harvested in a low-cost and environmental way, the proposed moisture-electric generators sculptured by laser offers a promising solution to address the two energy problems globally.

Research Design

Task 1. One major task is to develop laser sculpture technique to obtain active materials containing abundant channels and functional groups from lab-free materials. Direct induction of the graphene will

be developed through one-step graphitization process by converting carbon precursors into graphene-like flakes under the irradiation of low-cost lasers such as CO_2 laser. In this context, lab-free materials including cloth, paper, wood, food and cork will be used for providing carbon precursors and directly converted into graphene flakes. To increase the hydrophobic surface states, oxygen plasma may be used for posttreatment. As the graphitization is strong related to thermal process, different laser power densities and photonic energies will be used to tune the graphene transformation and adjust the sheet conductivity. Furthermore, the different graphene structures such as porous sheets and fibers will be obtained by changing the laser focal conditions. High speed scanning will be adopted to patterning the active materials and electrodes in a scalable production way. This task will be done in the first 8 months.

Task 2. To understand the interfacial process for interaction between water molecules and nanomaterials surface, charge transfer at the water-material interface will be stimulated using the cross-scale dynamic simulation method. The influence of various factors including surface properties, channel size, temperature, and humidity on the water molecular migration will be considered in the simulation, together with the influential effects on electricity output will be explored. The active materials characterization and geometrical dimensions before and after interaction with water molecules will be examined by advanced analytical instruments such as Raman spectroscopy, scanning electron microscopy (SEM), transmission electron microscopy (TEM), atomic force microscopy (AFM) and X-ray photoelectron spectroscopy (XPS). Both inert and active electrodes will be used for building device geometry and the electricity output will be compared to check the role of electrochemical reaction during electricity generation. This task will be done in the following 8 months.

Task 3. In the third task, we will use the laser sculptured active materials to build the prototypes of generators that can efficiently harvest ambient moisture energy. Both planner and sandwiched device structures with active materials between two electrodes will be built from the output of Tasks 1 and 2, with electricity generation driven by reversible deformation of moisture-responsive materials and ion diffusion driven by moisture-induced gradient energy, respectively, when interact with moisture. To increase the overall voltage or current output, a number of generators can be connected together in series or in parallel, respectively. The devices will be tested in various ambient conditions including highly moist and dry environment, sunlight, cloudy and night times to show the capability of versatile output. To demonstrate that the device can provide accessible energy in undeveloped regions or remote areas, the output of generators prototype will be also tested in different regions of China, including deserts, forests, and mountains. This task is arranged to be done in the last 8 months.

This project requires a range of skills, tools, and expertise in optics, materials, mechanicals, chemistry and electronics. This project comprises Daozhi Shen (material/electrical scientist, PI), Honghao Zhang (optics/mechanical scientist, PDF), and Linglan Guo (material/chemical developer, PhD student) at the Shanghai Jiao Tong University (SJTU). We have also initiated a collaboration with material/mechanical scientists from (Prof. Norman Zhou and Dr. Xiaoye Zhao) University of Waterloo (UW) for sharing materials and device tests. We have already built the ultrafast laser and CO_2 laser scanning system with micro/nano fabrication capability, as well as the electrical test platform. This concerted effort and multidisciplinary approach provides an excellent starting point for completing this project in two years.

Outcomes

Based on our experience with laser-matter interaction, we expect that the transformation of carbon-rich lab-free materials into graphene-like sheets will occur through the fast scanning of focused high-power lasers. We also expect that the porous sheet or graphite fibers with high specific area will be obtained by changing the laser parameters. By using laser fabricated graphene materials with nanochannels as active layer for constructing generators, we expect that electricity output will occur when exposed in moist environment. Identification of the surface charges distribution in nanomaterials when interacting with water molecules can be used to interpret the diffusive charges. With the high level of details obtained from computational simulations, we should be able to resolve the dynamic behavior of the charges and understand electricity generation mechanism. Finally, we expect that the generators will yield electricity output in milliwatt level from single device by harvesting moisture energy in various geographic locations, including forests, mountains and even remote deserts, in a green and affordable way.

Broader Impact

Problems associated with energy issues including global warming, polluted air and water, poverty displacement, and species loss represent unprecedented challenges to our society and planet. The world needs solutions for the twin energy problems by developing green and affordable energy technology, which requires the strong collaboration between researchers with different expertise including physics, chemistry, material/mechanical/electronic science and engineering, with the global participations. The proposed project helps to cement new collaborative relationship among PIs with different academic backgrounds, institutions, and industries (AquaSensing) and will aid in fostering the broader international collaborative team across different countries. This study will demonstrate the fact that, with the help of advanced optics and photonics, global environmental challenges and threats can potentially be solved by embracing wide collaboration and efforts across countries and regions.

The proposed research will also provide valuable training for an early career PI (Daozhi Shen, the applicant) to support establishing the career in optics and green energy. This is the first grant where PI Shen will take a lead role in the investigations and project managements. Shen will gain experience organizing field campaigns internationally and managing a project involving collaboration among several researchers with different areas of expertise. Moreover, this project will support graduate student (Linglan Guo from SJTU) to gain experience with field work and learn the novel concept of solving global challenging through optics, with participation in gathering, organizing, archiving, and analyzing data. This project will provide Guo with the opportunity to study in UW for 3 months and strengthen the international collaboration aiming at solving global challenges. Furthermore, Dr. Xiaoye Zhao, a female scientist, will benefit from this project by her collaborative work with shared materials and geographic data for pursuing her second PhD degree in UW now.

Reference Cited

(1) The world's energy problem. Our World in Data. https://ourworldindata.org/worlds-energy-problem (Accessed 2023-06-06).
(2) Jansson, J. K.; Hofmockel, K. S. *Nat. Rev. Microbiol.* **2020**, *18* (1), 35–46.
(3) Yue, X.-L.; Gao, Q.-X. *Adv. Climate Change Res.* **2018**, *9* (4), 243–252.
(4) Fawzy, S.; Osman, A. I.; Doran, J.; Rooney, D. W. *Environ. Chem. Lett.* **2020**, *18* (6), 2069–2094.
(5) UNCCS (2019) Climate action and support trends, United Nations Climate Change Secretariat. https://unfccc.int/sites/default/files/resource/Climate_Action_Support_Trends_2019.pdf. (Accessed 2023-06-06).
(6) UNEP (2019) Emissions gap report. UN Environment Program, Nairobi. https://wedocs.unep.org/bitstream/handle/20.500.11822/30797/EGR2019.pdf?sequence=1&isAllowed=y. (Accessed 2023-06-06).
(7) Román-Palacios, C.; Wiens, J. J. Recent Responses to Climate Change Reveal the Drivers of Species Extinction and Survival. *Proc. Natl. Acad. Sci. U.S.A.* **2020**, *117* (8), 4211–4217.
(8) Access to electricity – SDG7: Data and Projections – Analysis. IEA. https://www.iea.org/reports/sdg7-data-and-projections/access-to-electricity (Accessed 2023-06-06).
(9) IEA. https://www.iea.org/news/global-energy-crisis-shows-urgency-of-accelerating-investment-in-cheaper-and-cleaner-energy-in-africa (Accessed 2023-06-06).
(10) Shen, D.; Duley, W. W.; Peng, P.; Xiao, M.; Feng, J.; Liu, L.; Zou, G.; Zhou, Y. N. *Adv. Mater.* **2020**, *32* (52), 2003722.
(11) Stephens, G. L.; Li, J.; Wild, M.; Clayson, C. A.; Loeb, N.; Kato, S.; L'ecuyer, T.; Stackhouse, P. W.; Lebsock, M.; Andrews, T. *Nat. Geosci.* **2012**, *5* (10), 691–696.
(12) Huang, Y.; Cheng, H.; Qu, L. *ACS Mater. Lett.* **2021**, *3* (2), 193–209.
(13) Zhao, F.; Cheng, H.; Zhang, Z.; Jiang, L.; Qu, L. *Adv. Mater.* **2015**, *27* (29), 4351–4357.
(14) Zhao, X.; Shen, D.; Duley, W. W.; Tan, C.; Zhou, Y. N. *Adv. Energy Sus. Res.* **2022**, *3* (4), 2100196.
(15) Shen, D.; Xiao, M.; Zou, G.; Liu, L.; Duley, W. W.; Zhou, Y. N. *Adv. Mater.* **2018**, *30* (18), 1705925.
(16) Shen, D.; Xiao, Y.; Zou, G.; Liu, L.; Wu, A.; Xiao, M.; Feng, J.; Hui, Z.; Duley, W. W.; Zhou, Y. N.

Adv. Mater. Technol. **2020**, *5* (1), 1900819.
(17) Shen, D.; Xiao, M.; Xiao, Y.; Zou, G.; Hu, L.; Zhao, B.; Liu, L.; Duley, W. W.; Zhou, Y. N. *ACS Appl. Mater. Interfaces* **2019**, *11* (15), 14249–14255.
(18) Huang, Y.; Cheng, H.; Yang, C.; Zhang, P.; Liao, Q.; Yao, H.; Shi, G.; Qu, L. *Nat. Commun.* **2018**, *9* (1), 1–8.
(19) Zhang, Z.; Li, X.; Yin, J.; Xu, Y.; Fei, W.; Xue, M.; Wang, Q.; Zhou, J.; Guo, W. *Nat. Nanotechnol.* **2018**, *13* (12), 1109–1119.
(20) Chyan, Y.; Ye, R.; Li, Y.; Singh, S. P.; Arnusch, C. J.; Tour, J. M. *ACS Nano* **2018**, *12* (3), 2176–2183.

Mid-infrared spectroscopy-based breath analysis tool for mass-screening of early cancer diagnosis

This project aims to develop a non-invasive, compact mid-infrared spectroscopy system with artificial intelligence-based statistical analysis to generate extensive patient data for early-stage cancer detection and treatment. The system will continuously monitor metabolic health, disease progression, disease phenotyping, and pharmacokinetics, among other applications. The main objectives include demonstrating the world's first compact mid-infrared system using cutting-edge fiberized supercontinuum light sources, hollow-core optical fiber technology, and up-conversion detectors for online analysis. It also aims to explore high-resolution mid-infrared spectroscopy (2 to 10 μm) to identify and validate biomarkers in human exhaled breath for detecting oesophageal-gastric cancers, lung cancers, and other diseases. The proposal also focuses on standardizing the compact point-of-care (POC) optical spectroscopy system through clinical trials to gather extensive patient data for early oesophageal-gastric cancer detection and cross-platform validation.

The project shows promising expected outcomes and potential applications. It aims to create a non-invasive, patient-friendly alternative to invasive endoscopy/biopsy tests for diagnosis. Additionally, the project seeks to enable cost-effective mass-scale screening for early detection of various cancers and diseases among the general population, ultimately leading to improved treatment outcomes. Another important aspect of the project is the exploration of mid-infrared spectroscopy to gain insights into the biology of different diseases. The development of a compact spectroscopy system will facilitate its easy integration into diverse medical studies, promoting research across various disease domains. Furthermore, the system's versatility allows for the analysis of different bodily fluids, such as saliva, sputum, urine, and blood, expanding its potential diagnostic capabilities. Notably, the project also contributes to advancements in optical technology through the development of novel fiber designs for mid-infrared range spectroscopy, sensing, and beam delivery. To ensure the field's growth and expertise, the project includes manpower training in mid-infrared spectroscopy and diagnostic tools, fostering knowledge dissemination in this cutting-edge area.

In conclusion, this project holds significant promise in revolutionizing early cancer detection and treatment, enabling more accessible and non-invasive diagnostic tools, and enhancing our understanding of various diseases through the novel application of mid-infrared spectroscopy and artificial intelligence.

Mid-infrared spectroscopy-based breath analysis tool for mass-screening of early cancer diagnosis

Aims and Objectives of the Proposal:

This project aims to generate large patient cohorts' data for early-stage cancer detection and treatment by developing insight into patients' metabolism through a non-invasive, online, in-house developed compact mid-infrared spectroscopy system with artificial intelligence-based statistical analysis. This novel system will allow continuous monitoring of metabolic health, disease progression, disease phenotyping, and monitoring of pharmacokinetics, etc. The key objectives of this proposal are:

- To demonstrate the world's first compact mid-infrared system based on current state-of-the-art fiberized supercontinuum light sources, hollow-core optical fiber technology, and up-conversion detectors for online analysis.
- To explore the high-resolution mid-infrared spectroscopy from 2 to 10 μm to identify and validate the biomarkers present in ppm and ppb in human exhaled breath to detect oesophageal-gastric cancers, lung cancers, and other diseases and study pharmacokinetics.
- To standardize the compact point-of-care (POC) optical spectroscopy system with clinical trials to generate large patient cohorts' data and cross-platform validation for early oesophageal-gastric cancer detection.

Specific Technological Questions in the Context of the Unmet Need & its Rationale

The human exhaled breath has been a matter of strong interest for non-invasive diagnosis of several diseases including cancers. More than 3000 Volatile Organic Compounds (VOCs) including CO_2, O_2, H_2O, and N_2 are present in the exhaled breath [1]. The cancer cells and their microenvironment change the composition of exhaled breath. Alkanes and Methylated alkanes are common VCOs in human breath due to the activation of cytochrome p450 via oxidative stress, in case of lung cancer [2]. The exhaled breath in oesophageal-gastric cancer has higher ketones, aldehydes, alcohols, acids, and phenols than normal exhaled breath [3]. However, these VOCs are complex in nature, comprising of multitudes of metabolite compounds, present in picomolar (10^{-12} mol/l) to nanomolar (10^{-9} mol/l) concentrations, such as methane in 2-10 ppm, ethane in 0-10 ppb, nitric oxide 10-50 ppb, and carbon monoxide 1-10 ppm, etc [4]. **An instrument with a broad spectrum, ultra-high sensitivity, precise molecular selectivity, and ultra-high rapidness can detect these biomarkers. Such instruments can be used for mass-scale screening for early-stage cancers and other diseases. The implementation of such a system in hospitals can massively reduce the burden on the healthcare system and increase the prognosis dramatically.**

Figure 1 Schematic of exhaled human breath. Picture Source: ACS Publications.

Gas chromatography and mass spectrometry are golden standards for the analysis of gases; however, sensitivity is fairly poor, and detection time can be as long as 30 minutes to 60 minutes [5]. There are several optical techniques such as Tunable diode laser absorption spectroscopy (TDLS), Cavity Ring-Down Spectroscopy (CRDS), Photoacoustic Spectroscopy (PAS), and Hollow Waveguide (HWG) Absorption Spectroscopy [5]. Among these optical techniques, CRDS is good, as it can increase the interaction time between gases and light. However, it requires optical alignment and suffers from fringes due to the multi-mode behaviour of the light in the cladding. On the other hand, hollow-core fiber offers a high-interaction and low-volume molecular absorption spectroscopy and can offer detection at parts per million and parts per billion by volume in less than a minute with good reproducibility. A low-loss, effective single-mode operation of a large-diameter hollow-core fiber will offer a very high-quality interaction between gases and light. Other than the system, the wavelength spectrum of light is also critical for spectroscopy. The mid-infrared wavelength is of great importance as it offers absorption to the fundamental vibrational transitions of most molecules. However, mid-infrared spectroscopy remains limited due to bulky and highly-temperature sensitive mid-infrared light sources and detectors.

The last decade has seen great progress in terms of the development of compact and reliable fiber-based coherent broadband mid-infrared supercontinuum sources, up-conversion-based mid-infrared detectors, and low-loss hollow-core fibers. Therefore, there is a unique opportunity to develop a compact breath analyzer with high sensitivity and high specificity to generate a large cohort of patients' data with cross-validation with current state-of-the-art invasive techniques.

References

1. Behera *et* al., "Electronic nose: anon-invasive technology for breath analysis of diabetes and lung cancer patients," Journal of Breath Research, 13(2019).
2. Phillips *et* al., "Detection of lung cancer with volatile markers in the breath," Chest, 123(6) (2003).
3. Chung *et* al., "Diagnosis of Volatile Organic Compounds in Exhaled Breath from Patients with Gastric and Colorectal Cancers," Int J Mol Sci. 2023 Jan; 24(1): 129.
4. Murtz *et* al., "Breath Diagnostics using Laser Spectroscopy," Optics & Photonics News, 30 (205).
5. Tobias *et* al., "On-Line Analysis of Exhaled Breath," Chemical Reviews (2019).

Current State of the Proposed Research [Literature Review]:

This has been a hot topic for a long time and a lot of work has been done using three approaches: mass spectrometry, optical spectroscopy, and chemical sensors. In 2013, Kumar *et* al. showed a higher concentration of the four VOCs hexanoic acid, phenol, methyl phenol, and ethyl phenol in patients with oesophageal and gastric cancer compared to the positive control group [1]. In 2018, Shehda *et* al. reported an accuracy larger than 85% to discriminate between gastric cancer and control conditions using a silicon nanowire-based detector [2]. In 2018, Rocco *et* al. conducted a detailed survey on using electronic sensors-based breath analyzers for lung cancer detection [3]. This survey shows that electronic sensors provide 70-93% sensitivity, 73-100% specificity, and 80-100% accuracy over different studies. A combination of electronic sensors and mass spectrometry provides 100% sensitivity, 80-96% specificity, and 88-94% accuracy over different studies.

At the international level, there is a strong interest in optical spectroscopy technology [4]. The optical spectroscopy system offers a compact size with good sensitivity. The interest in optical spectroscopy has emerged since the advancement in mid-infrared supercontinuum light sources in the last decade. In 2019, Nikodem *et* al. demonstrated a quantum cascade laser emitting around 4.53 μm to sense nitrous oxide in a hollow-core fiber at the parts per billion level [5]. In 2020, Jahromi *et* al. demonstrated a combination of a fiber-based supercontinuum source from (2.85 to 3.90 μm), a 30 m multipass absorption cell, and a scanning grating spectrometer to achieve a resolution of 2.5 cm−1 in 100 ms [6]. However, none of these studies explored developed systems for medical applications. Moreover, there is no demonstration of a spectroscopy system based on the current state-of-art all-fiberized supercontinuum light sources, low-loss hollow core fibers, and up-conversion detector.

References

1. Kumar *et* al., "Selected Ion Flow Tube Mass Spectrometry Analysis of Exhaled Breath for Volatile Organic Compound Profiling of Esophago-Gastric Cancer," Analytical Chemistry, 85, 6121-6128, (2013).
2. Shehada *et* al., "Ultrasensitive Silicon Nanowire for real-world gas sensing: non-invasive diagnosis of cancer from breath volatolome," Nano Letters, 15, 1288-1295 (2014).
3. Rocco *et* al., "Breathprinting and Early Diagnosis of Lung Cancer", 13(7), 883-894 (2018).
4. Metsala *et* al, "Optical techniques for breath analysis: from single to multi-species detection," Journal of Breath Research, 12, 027104, 1-6 (2018).
5. Nikodem *et* al., "Demonstration of mid-infrared gas sensing using an anti-resonant hollow core fiber and a quantum cascade laser," 27(25), 36350, Optics Express (2019).
6. Jahromi *et* al., "Sensitive multi-species trace gas sensor based on a high repetition rate mid-infrared supercontinuum source," 28(18), 26091, Optics Express (2020).

The novelty of the Proposal and Outline of Tasks

This project will be executed in two years. The whole project will be divided into three work packages (WPs) with the following novelties as described below:

Work Package (WP) 1: Prototype of novel mid-infrared spectroscopy system and approval for trials (0-6 Months): HR: One PhD student. IIT Delhi allows each faculty to recruit 4 PhD students through Institute fellowships.

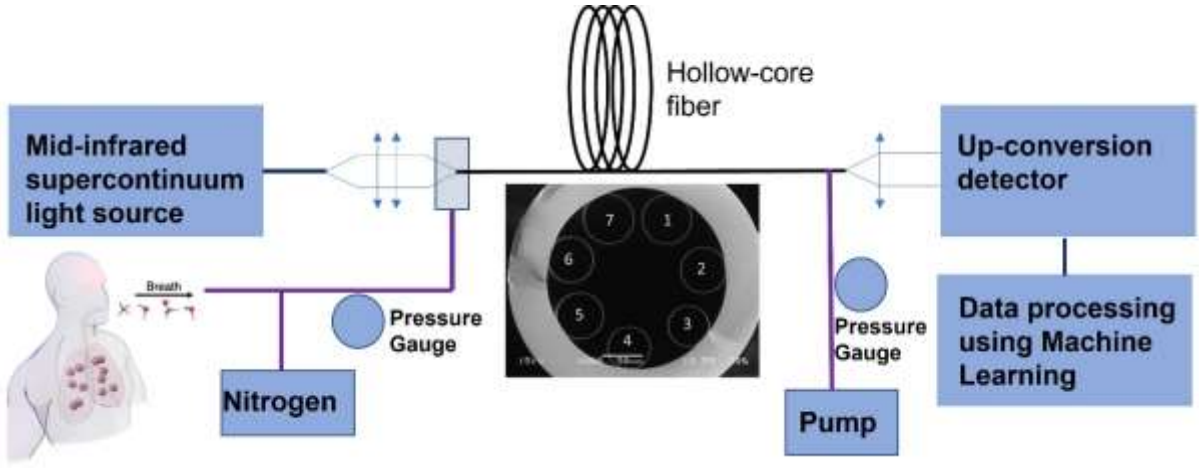

Figure 2 Schematic of a mid-infrared spectroscopy system for exhaled breath.

(a) Light Source: The narrow line-width laser source can detect only small molecules (2-5 atoms). The larger molecules (>6 atoms) have a broader absorption spectrum, which requires

broadband lasers. This project will use a novel optimized broadband all-fiberized supercontinuum source emitting from 2 to 10 μm to allow the detection of multi-species and large molecules. The broad spectrum of the light source will allow the detection of a set of biomarkers for a particular disease. A set of biomarkers statistically boost predictive performance over single markers. Such supercontinuum sources are commercially available from NORBLIS, a Danish company. It is important to note that the PI is capable of constructing such super-continuum source but that may take a long time and delay the project. Though PhD student will be thoroughly trained in supercontinuum numerical modelling to develop next-generation mid-infrared supercontinuum sources better suited for such applications.

(b) Hollow-core fiber cavity: We will employ novel anti-resonant hollow-core fibers offering single-mode operation with ultra-loss allowing a very high interaction length between light and exhaled breath. This will ensure the ultra-low sensitivity of the system. We will also employ gold parabolic mirror-based cavity. A comparison between hollow-core and mirrors-based cavities will also be done to figure out the precise advantages of the hollow-core fibers for such a system. We will buy commercially available hollow-core fibers and will collaborate with Prof. Francesco Poletti, ORC, Southampton, and Prof. Jonathan Knight, Bath to get some pieces of fiber, again to accelerate the process. It is important to note that, there is no single hollow-core fiber that offers low loss over a 2 to 10 μm wavelength, therefore, 2-3 channels of hollow-core fiber will be employed. Prof. Jonathan's group has demonstrated a low-loss (<0.1 dB/m) silica-glass-based hollow-core fiber for a 2.3 to 4.4 μm wavelength range [APLPhoton.4,080803(2019)]. The progress in the 5 to 10 μm wavelength range is limited due to the difficult fabrication process (extrusion process) required for Chalcogenide fibers.

PI has strong expertise in optical fiber design. Attempts will be made to design novel hollow-core fiber design will exotic cladding design based on chalcogenide glasses to achieve a broadband, effectively single-moded, low-loss fiber in 2 to 10 μm wavelength for future research. Students will also be trained in FEM-based Optical fiber design modelling.

(c) **Up-conversion detector:** The detection of mid-infrared wavelength is challenging and limits the mid-infrared spectroscopy applications. HgCdTe detectors suffer from significant amounts of thermal noise due to their low bandgap. This project will employ up-conversion-based compact mid-infrared spectrometers: (1) 2 to 5 um spectral width, up to 130 KHz full-spectrum readout rate, -80 dBm/nm sensitivity, time resolution less than 10 μs, resolution from 3 to 6 cm^{-1}, and (2) 6 to 12 um spectral width, up to 50 Hz full-spectrum readout rate, and -67 dBm/nm sensitivity.

Milestone: M1, Deliverables: One report on the performance of the system (D1).

WP2: Clinical Trials (7-18 Months):

We will run large-scale clinical trials with replicate measurements at the Institute of Liver & Biliary Science (ILBS) (ILBS is India's best research Mono-speciality Research Hospital). A cross-platform validation with respect to endoscopy can also be obtained at ILBS. There is also a need to set up the standardization of data collection to avoid sampling errors. Prof. Vikram Bhatia, MD, DM and A/Professor Sejal Patwardhan, PhD, Advanced Center for Treatment Research & Education in Cancer, Tata Memorial Center, Navi Mumbai, India has kindly

agreed to this collaboration. The light source with a broad spectrum from 1 to 12 μm, will let identify many new biomarkers for different cancers.

Milestone: M2, Deliverables: One report on the clinical trials (D2).

WP3: Artificial Intelligence & Data Analysis (19-24 Months):

A large data set is mandatory for assessing reproducibility and for validation of biomarkers candidates. Moreover, the statistical analysis of such a large data set is a herculean task. We will employ machine learning-based algorithms to analyse and interpret the big dataset resulting from the clinical trials. In order to set up standardization, it is extremely important to estimate the magnitude of the remaining random error. The implementation of ML-based algorithms will dramatically increase our capability for statistical analysis. A collaboration has been established with Prof. Sudipan Saha, Yardi School of Artificial Intelligence, IIT Delhi for this work package.

Milestone: M3, Deliverables: One report (D3).

Expected Outcomes & Their Potential Applications

- To avoid the need for invasive endoscopy/biopsy tests required for diagnosis.
- This system will allow conducting low-cost mass-scale screening of the general population to detect gastric, lung, and oral cancers and other diseases at an early stage.
- This will also open pathways of exploiting mid-infrared spectroscopy in understanding the biology of different diseases. The compact system will ensure easy use of this system in different medical studies.
- This spectroscopy system can also be used for the spectroscopy of saliva, sputum, urine, and blood.
- Novel fiber designs for mid-infrared range suitable for spectroscopy, sensing, and beam delivery.
- Manpower training: Project will train manpower in the area of mid-infrared spectroscopy and diagnostic tools.

Immediate Benefit:

This project will help PI to establish his group at IIT Delhi and convince the funding agencies to establish a current state-of-the-art facility at IIT Delhi. All attempts will be made to raise funds during and after the project through several schemes. If PI wins this grant, PI may get a grant worth 30K US under the category of “equipment matching grant” from IIT Delhi.

Executive summary-health category

Development of an affordable robotic microscope for rapid and stain-free malaria diagnosis

Malaria is one of the most serious public health challenges globally, despite current therapeutics having high efficacy rates when administered timely. Most concerning is that the fight against malaria has stalled. There were 230 million cases in 2015 (the baseline year of the global technical strategy for malaria 2016-2030) and 247 million cases in 2020. The barrier to malaria eradication is the lack of early diagnosis of the infected population. Current malaria diagnostics can be classified into three categories with specific strengths and weaknesses: 1) highly sensitive molecular-based techniques which use PCR. These are slow and demand the use of sophisticated equipment, expensive reagents, and a highly trained workforce; 2) Rapid Diagnostic Tests (RDTs) are relatively fast in comparison to optical microscopy but less sensitive (100-200 parasite μL^{-1}). Besides, the majority of them target the *Plasmodium falciparum* histidine-rich protein 2 *(pfhrp-2*) biomarker, and recent studies have shown the deletion of *pfhrp-2* which causes false negatives and threatens malaria control strategies. 3) Optical microscopy, the gold standard method for diagnosis. This involves examining stained blood smear samples under a microscope. It can detect up to 5-20 parasite μL^{-1}, however, the results vary significantly based on the expertise of the technician or health care provider, and it is labor and time intensive.

None of the three methods offers a definitive solution to early detection. Prompt treatment is crucial in preventing severe illness, complications, and deaths associated with malaria. To boost the fight against malaria, new approaches for diagnostics must be adopted to enhance the sensitivity, accuracy of detection besides being rapid and affordable. While research and development efforts are ongoing to improve and develop these and other malaria diagnostic methods, microscopy is likely to remain a vital tool in malaria diagnosis due to its proven effectiveness, cost-effectiveness, and established specialists in many malaria-endemic regions. Therefore, we think offering a solution within microscopy is key to enhancing early screening and reducing the disease burden.

In this study, we propose to develop an affordable robotic configuration for imaging Malaria by detecting the presence of the parasite waste product, hemozoin (Hz). The affordable OpenFlexure microscope (OFM) will be modified to incorporate polarizing microscopy capability. Leveraging on the magneto-optical physical properties of malaria pigment Hz, we will develop a phase-locked imaging microscope for maximal sensitivity. The microscope will have autofocusing and auto-imaging capability. We will develop a phase-locked mode combining magneto-optical control, thus fully exploiting the Hz features to maximise sensitivity and allow a full automation of the detection assay. We can thus overcome the limitations of traditional microscopy and improve malaria diagnostics in terms of accuracy, efficiency, and accessibility.

Development of an affordable robotic microscope for rapid and stain-free malaria diagnosis

Introduction

Malaria is one of the most serious public health challenges globally. According to World Health Organization (WHO), there were 247 Million reported cases and 625,000 Malaria related deaths in 2020. This was a 10% increase from 2019[1]. Interestingly, current malaria therapeutics have nearly 100% efficacy if administered timely. The barrier to Malaria eradication is the lack of early diagnosis of the infected population.

Malaria diagnostics can be classified into three categories: immunological-based, molecular-based techniques, and optical microscopy [2-4]. Immunological diagnostic kits are commonly referred to as Rapid Diagnostic Tests (RDTs). They are relatively fast, cost-effective, and user-friendly. However, they are less sensitive, and the majority target histidine-rich protein 2 (*pfhrp-2*) [5, 6]. Recent studies have shown the deletion of *pfhrp-2* genes which causes false negatives and threatens malaria control strategies [7-9]. In any case, the use of *pfhrp-2* biomarker limits the use of the RDTs in monitoring disease progression, and evaluating the efficacy of the interventions due to its persistence in the bloodstream long after malarial infection [10-12]. The molecular-based techniques uses Polymerase Chain Reaction (PCR) to probe and amplify the *Plasmodium* parasites' genetic material (either DNA or RNA) present in the blood to detectable levels. The technique is highly sensitive but slow and demands the use of sophisticated equipment, expensive reagents, and a highly trained workforce. Optical microscopy is the gold standard method for the diagnosis of the disease. It involves examining stained blood smear samples under a light microscope. The process is labor and time intensive and the reliability of the results depends on the expertise of the technician or health care provider.

Various methods have been proposed to overcome the challenges of the three methods highlighted above. For example, electrochemical biosensors for Malaria detection which offer high sensitivity [13-16] and have been demonstrated capable of rapid detection [17, 18], allowing timely initiation of treatments. However, electrochemical biosensors often require complex fabrication processes which can increase the cost of production and limit their accessibility [19]. Optical-based techniques have also been proposed for Malaria diagnostics. These techniques leverage optical principles such as fluorescence, luminescence, optical fiber, photonics, and Surface Plasmon Resonance (SPR). Optical techniques offer theoretically higher levels of sensitivity[20]. For example, the cloning and expression of fluorescent Malaria parasite protein probes were shown in the fabrication of fluorescent-based biosensors for measuring the amount of heme in cells[21]. In principle, there is fluorescence quenching during the heme binding[22-24]. Nevertheless, the method is limited by the short life span of the fluorophores and the photostability of the fluorophores[25]. Other methods reported include the use of the FRET-based heme sensor[22] and the noninvasive and rapid photoacoustic technique [26]. The major drawback of the photoacoustic technique is the attenuation of the signal before reaching the transducer, resulting in poor SNR. To suppress the noise and enhance the detected signal, specialized technology must be employed, which makes the setup complex and expensive.

The SPR technique relies on the variations in the refractive index of the plasma resonance material, in the SPR angle. This is coupled with the reflectance intensity, caused by the interaction between the biomaterial targets[27-30]. Briand *et al.*[27] used hemoglobin-polyacrylic acid as a bio-recognition target for a gold-coated SPR based sensor for rapid heme detection. This

biosensor acted by extracting the heme, followed by heme-free hemoglobin exposure to samples containing heme that interact with the bio recognition element. Though the SPR-based Malaria biosensors are highly sensitive, have high resolution and can allow real-time measurements, they are motion-sensitive and depend on the development of light detectors with a high signal-to-noise ratio[31, 32].

Various configurations of polarizing optical microscopy have been proposed to leverage on the optical birefringence of hemozoin (Hz) [33-37]. Hemozoin is accumulated in blood cells by all malaria species. Cellphone based methods are particular appealing because of their portability. For example, the two mobile phones configuration has demonstrated similar sensitivity comparable to microscopy with advanced lab instruments. In addition, it demonstrated four times improvement in field of view and better imaging quality compared to other mobile-optical-polarization imaging device [34]. However, the methods fail to account for all Hz due to the random orientation of the Hz crystals. Besides, examples published so far depend on phones with advanced cameras imaging capabilities, making them expensive and requiring regular charging in continuous use. Since Hz also exhibits strong paramagnetic behavior, responding to low magnetic field strengths, magneto-optic-based techniques have also been proposed [38-40]. The method can detect parasite densities as low as less than 10 parasites/mL [41]. Majority of the studies using this method were done under laboratory conditions. However, recent studies by Arndt *et al* [42] has shown the method has great potential as a malaria biosensor with 82% and 84% sensitivity and specificity respectively. Importantly, the parasite density correlated well with the quantitative magneto-optical signal.

While research and development efforts are ongoing to improve and develop alternative malaria diagnostic methods such as new RDTs, affordable molecular-based techniques, and optical methods, microscopy remains a vital tool in malaria diagnosis due to its proven effectiveness, cost-effectiveness, and established specialist in many malaria-endemic regions. In addition, the limit of detection of malaria parasites is among the best (5-20/microliter) [42]. But light microscopy is time and labor-intensive. Nevertheless, offering a solution within microscopy is key to enhancing early screening and reducing the disease burden.

We propose to develop an affordable robotic microscope to leverage on the magnetic and optical features of Hz. We will adopt the openhardware OpenFlexure microscope (OFM) configuration [43-45] on which we have previous experience, and develop it for affordable polarized microscopy by incorporating polarizers and cellophane sheet half waveplate (HWP). Motorization of magnets will allow for the rotation of the aligned Hz crystals to vary the contrast, and this will be done in a phase-locked configuration with detection, for maximal sensitivity. We hypothesize that the integration of phase-locking will enhance the contrast of the sample making it easy for the health professional to detect and quantify the parasite load, hence increasing the accuracy of detection and reduce the time required to scan the sample. The development of this biosensor will be key to early, affordable, and accurate diagnosis of Malaria. Accurate diagnosis promotes more tailored treatments that lead to better disease management resulting in efficient use of limited resources in low-income setups[46]. Overall, this supports the provision of quality health services and is essential for attaining universal health care as envisioned in the Vision 2030[47], the Bottom – Up Economic Transformation Agenda for Inclusive Growth in Kenya[48] and the Sustainable Development Goals (SDGs)[49].

Problem Statement

Current Malaria therapeutics have high efficacy rates, with some demonstrating nearly 100% effectiveness. However, according to the 2020 World Health Organization (WHO) report, there were 247 Million reported cases of infections and 625,000 deaths [1]. Of concern is that progress against malaria fight has stalled since 2015 (the baseline year of the global technical strategy for malaria 2016-2030). In that year, there was an estimated 230 million Malaria cases [50, 51]. The barrier to malaria eradication being the lack of early diagnosis of the infected population. Early detection and prompt treatment are crucial in preventing severe illness, complications, and deaths associated with malaria. To boost the fight against malaria, new approaches for diagnostics must be adopted to enhance the sensitivity, accuracy of detection besides being rapid and affordable. In addition, standardization is very key to reducing human error and variability in the interpretation of the results. In this study we propose to develop a robotic configuration for imaging Malaria by detecting the presence of Hz.

Aim of Study

To develop an affordable robotic microscope to leverage on the magnetic and optical features of Hz for rapid and stain-free malaria diagnostics. The specific objectives will be:

(i) Design an imaging phase-locked system integrated with a time-dependent magnetic field.
(ii) Redesign and fabricate a modified OFM to incorporate the additional components.
(iii) Test and compare the performance of the setup with standard methods.
(iv) Conduct a clinical trial in small populations in Nyanza region, Kenya (Migori Teaching and Referral Hospital, and Jaramogi Oginga Odinga Teaching and Referral Hospital).

Outline of tasks/Work Plan

Table 1 shows the work plan of the research. The task highlighted in grey will be done under the mentorship Prof Pietro Cicuta of the Biological and Soft Systems group at the Cavendish Laboratory, University of Cambridge (see appendix B) given his vast experience in developing low-cost biomedical solutions including the OpenFlexure Microscope (OFM) [52-55]. The last three activities will be done at Kirinyaga University-Kenya and two Masters level student will be involved for training. A brief description of the activities are highlighted below:

Table 1: Work Plan

	YEAR 1			YEAR 2			
Month 1	4	9	12	1	3	8	12
|→ Hardware development							
Automation system |→							
Testing using controlled samples |→							
Clinical trials				|→			
Performance evaluation and optimization					|→		
Dissemination of research findings						|→	

a. Designing of a phase-locked system and integration with a time-dependent magnetic field:

The main design of the setup will based on the OFM platform by incorporating a polarizer followed by a cellophane HWP as shown in **Figure 1 (a)**. Another polarizer at cross polarization

(analyzer) will be mounted behind the objective lens. The cellophane will be used as a cheap HWP to rotate the polarization of the incident light to optimize the detection contrast. Previous studies by our group and others have shown the ability of a cellophane sheet as a purpose built HWP [56-58]. The redesigning of the microscope frame and mounting will be done using open source computer aided design (CAD) software.

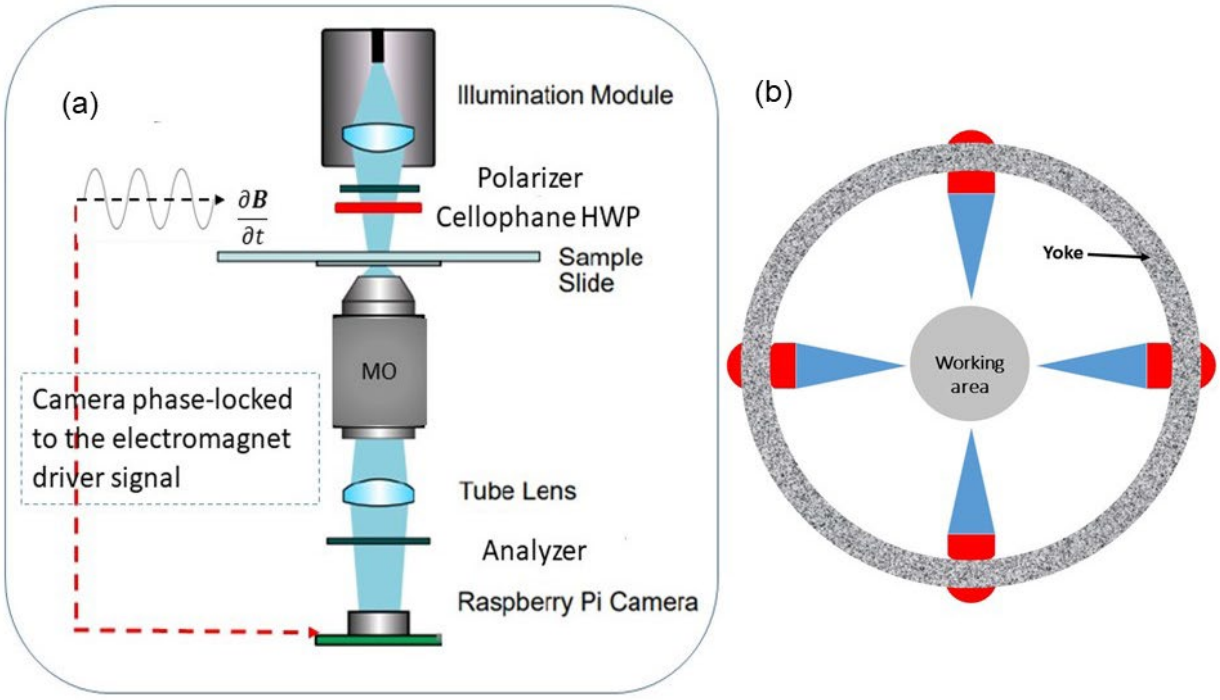

Figure 1: (a). Schematic of the proposed phase locked image acquisition setup based on the OFM platform, where MO is the microscope objective. **(b).** Shows the quadruple design for generating a uniform time dependent magnetic field (in red is the coil and blue is the magnetic pole tips)

The quadrupole design concept [59] is illustrated in **Figure 1(b).** Four magnetic poles connected to a magnetic yoke will be placed in a quadrupole configuration to generate an efficient and uniform magnetic field. Each magnetic pole will have an actuating coil. Applying an electric current to the coil, magnetic flux is generated and permeated through to the pole tip resulting in a strong flux diverging outward from the pole tip to the workspace. By applying a time-varying sine wave a rotating magnetic field will be generated. When Hz is suspended in a fluid, the crystals are randomly orientated implying that optical absorption using linearly polarized light expresses no preferred direction. But, with the introduction of a magnetic field, the paramagnetic crystals become weak bar magnets and uniformly orient along the field. Optically this manifests as induced dichroism and the orientation of the Hz crystals orthogonal to a polarized light leads to maximum absorption of incident the beam [60]. When the field is rotated the resulting torque forces make the crystal reorient to the field. At high frequencies, the crystals have increased angular delay relative to the field resulting in a decreasing amplitude of the optical signal [61]. Therefore, the time-dependent magnetic field will be optimized at frequencies

between 0.1-1 Hertz. The camera will be phase-locked in reference to the electromagnet signal driver to acquire images at the maximum contrast (Hz crystals orthogonal to polarized light) ensuring maximal sensitivity.

b. Algorithm for image extraction in the Phase-locked configuration

Briefly, the following procedure will be followed: First, the sampling rate of the camera will be synchronized with the signal generator frequency through an external triggering. The sampling rate will coincide with maximum input signal attenuation at the cross polarization. Second, the system will run for 10 cycles. This will be followed by a computation of the average image from the *n*-number phase locked images.

c. Testing and comparison of the performance of the setup with a standard methods

Plasmodium falciparum parasites (laboratory adapted strain) will be cultured following a modified method of Trager and Jensen [62]. For the preparation of the blood lysates, whole blood will be mixed with lysis solution in the ratio of 1:9 and allowed to stand for at least 10 min to ensure complete lysis. The lysate will be transferred the concave microscope slides and measurements performed.

d. Clinical trials in small populations in Nyanza region, Kenya

Samples will be collected in three clinics in Nyanza region Kenya, a Malaria endemic area [63]. A written informed consent will be obtained from participants before sample collection. A comparison will be done using the gold standard microscope. Ethical approval of the study will be obtained from NACOSTI-Kenya.

Outcome(s)

(i) Developed protocols and designs for imaging magnetic-optical properties in biomedical probes
(ii) Fabrication of rapid, stain-free and accurate robotic microscope malaria diagnosis platform for Malaria.
(iii) Report on the performance of the device both in the lab and clinical trials.
(iv) Enhanced capacity for Kenyan researchers on designing and fabrication of affordable biosensors.
(v) Dissemination of research findings

Impact

The development of the robotic microscope will lead to the creation of a new diagnostic platform for Malaria by providing rapid, stain-free and accurate diagnosis. This will significantly reduce the time the health care personnel requires for staining the samples and scanning for parasites using a light microscope. Meaning, more patients could be tested at the same time. Besides, microscopy is the gold standard method for malaria diagnosis, and offering affordable and rapid solutions within the platform will be very appealing to policymakers and biomedical companies. This can generate significant revenue from the sale of these products and encourage more research on expanding the robotic microscope for other applications. Finally, the collaboration with Prof. Pietro Cicuta and colleagues in the Cavendish Laboratory at the University of Cambridge UK will help build capacity for Kenyan researchers in designing and fabrication of affordable biosensors.

Appendix A

References

1. Organization, W. H., *World malaria report 2022*. World Health Organization: 2022.
2. Makler, M. T.; Palmer, C. J.; Ager, A. L., A review of practical techniques for the diagnosis of malaria. *Annals of tropical medicine and parasitology* **1998,** *92* (4), 419-434.
3. Vo, Q. H.; Le, X.-H.; Le, T.-H., A deep learning approach in detection of malaria and acute lymphoblastic leukemia diseases utilising blood smear microscopic images. *Vietnam Journal of Science, Technology and Engineering* **2022,** *64* (1), 63-71.
4. Wongsrichanalai, C.; Barcus, M. J.; Muth, S.; Sutamihardja, A.; Wernsdorfer, W. H., A review of malaria diagnostic tools: microscopy and rapid diagnostic test (RDT). *Defining and Defeating the Intolerable Burden of Malaria III: Progress and Perspectives: Supplement to Volume 77 (6) of American Journal of Tropical Medicine and Hygiene* **2007**.
5. Sivaradjy, M.; Hamide, A.; Krishnamoorthy, S.; Rajkumari, N.; Mohan, V.; Sharmila, F. M., Assessment of Plasmodium falciparum histidine rich protein 2 and/3 (pfhrp 2&/pfhrp 3) gene deletion or mutation in Plasmodium falciparum positive blood samples in a tertiary care centre in South India. *Journal of Parasitic Diseases* **2022,** *46* (3), 729-743.
6. Kaaya, R. D.; Kavishe, R. A.; Tenu, F. F.; Matowo, J. J.; Mosha, F. W.; Drakeley, C.; Sutherland, C. J.; Beshir, K. B., Deletions of the Plasmodium falciparum histidine-rich protein 2/3 genes are common in field isolates from north-eastern Tanzania. *Scientific reports* **2022,** *12* (1), 5802.
7. Molina-de la Fuente, I.; Pastor, A.; Herrador, Z.; Benito, A.; Berzosa, P., Impact of Plasmodium falciparum pfhrp2 and pfhrp3 gene deletions on malaria control worldwide: a systematic review and meta-analysis. *Malaria Journal* **2021,** *20* (1), 1-25.
8. Gatton, M. L.; Chaudhry, A.; Glenn, J.; Wilson, S.; Ah, Y.; Kong, A.; Ord, R. L.; Rees-Channer, R. R.; Chiodini, P.; Incardona, S., Impact of Plasmodium falciparum gene deletions on malaria rapid diagnostic test performance. *Malaria journal* **2020,** *19* (1), 1-11.
9. Mukkala, A. N.; Kwan, J.; Lau, R.; Harris, D.; Kain, D.; Boggild, A. K., An update on malaria rapid diagnostic tests. *Current infectious disease reports* **2018,** *20*, 1-8.
10. Piper, R.; Lebras, J.; Wentworth, L.; Hunt-Cooke, A.; HouzÃ, S.; Chiodini, P.; Makler, M., Immunocapture diagnostic assays for malaria using Plasmodium lactate dehydrogenase (pLDH). *The American journal of tropical medicine and hygiene* **1999,** *60* (1), 109-118.
11. Krampa, F. D.; Aniweh, Y.; Kanyong, P.; Awandare, G. A., Recent advances in the development of biosensors for malaria diagnosis. *Sensors* **2020,** *20* (3), 799.
12. Markwalter, C. F.; Davis, K. M.; Wright, D. W., Immunomagnetic capture and colorimetric detection of malarial biomarker Plasmodium falciparum lactate dehydrogenase. *Analytical Biochemistry* **2016,** *493*, 30-34.
13. Jain, P.; Das, S.; Chakma, B.; Goswami, P., Aptamer-graphene oxide for highly sensitive dual electrochemical detection of Plasmodium lactate dehydrogenase. *Analytical Biochemistry* **2016,** *514*, 32-37.
14. Figueroa-Miranda, G.; Feng, L.; Shiu, S. C.-C.; Dirkzwager, R. M.; Cheung, Y.-W.; Tanner, J. A.; Schöning, M. J.; Offenhäusser, A.; Mayer, D., Aptamer-based electrochemical biosensor for highly sensitive and selective malaria detection with adjustable dynamic response range and reusability. *Sensors and Actuators B: Chemical* **2018,** *255*, 235-243.
15. Dutta, G.; Nagarajan, S.; Lapidus, L. J.; Lillehoj, P. B., Enzyme-free electrochemical immunosensor based on methylene blue and the electro-oxidation of hydrazine on Pt nanoparticles. *Biosensors and Bioelectronics* **2017,** *92*, 372-377.
16. Hemben, A.; Ashley, J.; Tothill, I. E., Development of an Immunosensor for PfHRP 2 as a Biomarker for Malaria Detection. *Biosensors* **2017,** *7* (3), 28.

17. Singh, P.; Chatterjee, M.; Chatterjee, K.; Arun, R. K.; Chanda, N., Design of a point-of-care device for electrochemical detection of P.vivax infected-malaria using antibody functionalized rGO-gold nanocomposite. *Sensors and Actuators B: Chemical* **2021,** *327*, 128860.
18. Dutta, G.; Lillehoj, P. B., Wash-free, label-free immunoassay for rapid electrochemical detection of PfHRP2 in whole blood samples. *Scientific Reports* **2018,** *8* (1), 17129.
19. Fan, R.; Andrew, T. L., Perspective—Challenges in developing wearable electrochemical sensors for longitudinal health monitoring. *Journal of The Electrochemical Society* **2020,** *167* (3), 037542.
20. Zherebtsova, A. I.; Dremin, V. V.; Makovik, I. N.; Zherebtsov, E. A.; Dunaev, A. V.; Goltsov, A.; Sokolovski, S. G.; Rafailov, E. U., Multimodal optical diagnostics of the microhaemodynamics in upper and lower limbs. *Frontiers in physiology* **2019,** *10*, 416.
21. Wißbrock, A.; Imhof, D., A tough nut to crack: intracellular detection and quantification of heme in malaria parasites by a genetically encoded protein sensor. *ChemBioChem* **2017,** *18* (16), 1561-1564.
22. Abshire, J. R.; Rowlands, C. J.; Ganesan, S. M.; So, P. T.; Niles, J. C., Quantification of labile heme in live malaria parasites using a genetically encoded biosensor. *Proceedings of the National Academy of Sciences* **2017,** *114* (11), E2068-E2076.
23. Ragavan, K.; Kumar, S.; Swaraj, S.; Neethirajan, S., Advances in biosensors and optical assays for diagnosis and detection of malaria. *Biosensors and Bioelectronics* **2018,** *105*, 188-210.
24. Xu, S.; Liu, H.-W.; Chen, L.; Yuan, J.; Liu, Y.; Teng, L.; Huan, S.-Y.; Yuan, L.; Zhang, X.-B.; Tan, W., Learning from artemisinin: bioinspired design of a reaction-based fluorescent probe for the selective sensing of labile heme in complex biosystems. *Journal of the American Chemical Society* **2020,** *142* (5), 2129-2133.
25. Villena Gonzales, W.; Mobashsher, A. T.; Abbosh, A., The progress of glucose monitoring—A review of invasive to minimally and non-invasive techniques, devices and sensors. *Sensors* **2019,** *19* (4), 800.
26. Lukianova-Hleb, E. Y.; Campbell, K. M.; Constantinou, P. E.; Braam, J.; Olson, J. S.; Ware, R. E.; Sullivan, D. J.; Lapotko, D. O., Hemozoin-generated vapor nanobubbles for transdermal reagent-and needle-free detection of malaria. *Proceedings of the National Academy of Sciences* **2014,** *111* (3), 900-905.
27. Briand, V. A.; Thilakarathne, V.; Kasi, R. M.; Kumar, C. V., Novel surface plasmon resonance sensor for the detection of heme at biological levels via highly selective recognition by apo-hemoglobin. *Talanta* **2012,** *99*, 113-118.
28. Chaudhary, V. S.; Kumar, D.; Kumar, S., Gold-immobilized photonic crystal fiber-based SPR biosensor for detection of malaria disease in human body. *IEEE Sensors Journal* **2021,** *21* (16), 17800-17807.
29. Wu, F.; Singh, J.; Thomas, P. A.; Ge, Q.; Kravets, V. G.; Day, P. J.; Grigorenko, A. N., Ultrasensitive and rapid detection of malaria using graphene-enhanced surface plasmon resonance. *2D Materials* **2020,** *7* (4), 045019.
30. Sikarwar, B.; Sharma, P. K.; Srivastava, A.; Agarwal, G. S.; Boopathi, M.; Singh, B.; Jaiswal, Y. K., Surface plasmon resonance characterization of monoclonal and polyclonal antibodies of malaria for biosensor applications. *Biosensors and Bioelectronics* **2014,** *60*, 201-209.
31. Piliarik, M.; Homola, J., Surface plasmon resonance (SPR) sensors: approaching their limits? *Optics express* **2009,** *17* (19), 16505-16517.
32. Caucheteur, C.; Guo, T.; Albert, J., Review of plasmonic fiber optic biochemical sensors: improving the limit of detection. *Analytical and bioanalytical chemistry* **2015,** *407* (14), 3883-3897.

33. Pirnstill, C. W.; Coté, G. L., Malaria diagnosis using a mobile phone polarized microscope. *Scientific reports* **2015,** *5* (1), 13368.
34. Yu, Z.; Li, Y.; Deng, L.; Luo, B.; Wu, P.; Geng, D., A high-performance cell-phone based polarized microscope for malaria diagnosis. *Journal of Biophotonics* **2023**, e202200290.
35. Maude, R. J.; Buapetch, W.; Silamut, K., A simplified, low-cost method for polarized light microscopy. *The American journal of tropical medicine and hygiene* **2009,** *81* (5), 782.
36. Gordon, P.; Venancio, V. P.; Mertens-Talcott, S. U.; Coté, G., Portable bright-field, fluorescence, and cross-polarized microscope toward point-of-care imaging diagnostics. *Journal of Biomedical Optics* **2019,** *24* (9), 096502-096502.
37. Cho, S.; Kim, S.; Kim, Y.; Park, Y., Optical imaging techniques for the study of malaria. *Trends in biotechnology* **2012,** *30* (2), 71-79.
38. McBirney, S. E.; Chen, D.; Scholtz, A.; Ameri, H.; Armani, A. M., Rapid diagnostic for point-of-care malaria screening. *ACS sensors* **2018,** *3* (7), 1264-1270.
39. Kumar, R.; Verma, A. K.; Shrivas, S.; Thota, P.; Singh, M. P.; Rajasubramaniam, S.; Das, A.; Bharti, P. K., First successful field evaluation of new, one-minute haemozoin-based malaria diagnostic device. *EClinicalMedicine* **2020,** *22*, 100347.
40. Valdivia, H. O.; Thota, P.; Braga, G.; Ricopa, L.; Barazorda, K.; Salas, C.; Bishop, D. K.; Joya, C. A., Field validation of a magneto-optical detection device (Gazelle) for portable point-of-care Plasmodium vivax diagnosis. *Plos one* **2021,** *16* (6), e0253232.
41. Orbán, Á.; Butykai, Á.; Molnár, A.; Pröhle, Z.; Fülöp, G.; Zelles, T.; Forsyth, W.; Hill, D.; Müller, I.; Schofield, L., Evaluation of a novel magneto-optical method for the detection of malaria parasites. *PloS one* **2014,** *9* (5), e96981.
42. Arndt, L.; Koleala, T.; Orbán, Á.; Ibam, C.; Lufele, E.; Timinao, L.; Lorry, L.; Butykai, Á.; Kaman, P.; Molnár, A., Magneto-optical diagnosis of symptomatic malaria in Papua New Guinea. *Nature Communications* **2021,** *12* (1), 969.
43. Board, S. A., OpenFlexure: an open-source 3D printed microscope.
44. Grant, S. D.; Cairns, G. S.; Wistuba, J.; Patton, B. R., Adapting the 3D-printed Openflexure microscope enables computational super-resolution imaging. *F1000Research* **2019,** *8*.
45. Stirling, J.; Sanga, V. L.; Nyakyi, P. T.; Mwakajinga, G. A.; Collins, J. T.; Bumke, K.; Knapper, J.; Meng, Q.; McDermott, S.; Bowman, R. In *The OpenFlexure project. the technical challenges of co-developing a microscope in the UK and Tanzania*, 2020 IEEE Global Humanitarian Technology Conference (GHTC), IEEE: 2020; pp 1-4.
46. Moturi, A. K.; Robert, B. N.; Bahati, F.; Macharia, P. M.; Okiro, E. A., Investigating rapid diagnostic testing in Kenya's health system, 2018–2020: validating non-reporting in routine data using a health facility service assessment survey. *BMC Health Services Research* **2023,** *23* (1), 1-14.
47. David, N.; Wanjala, P., A case for increasing public investments in health. 2020.
48. The National Treasury and Economic Planning, R. O. K., Bottom – Up Economic Transformation Agenda for Inclusive Growth in Kenya. 2023.
49. Spencer, G.; Corbin, J. H.; Miedema, E., Sustainable development goals for health promotion: a critical frame analysis. *Health promotion international* **2019,** *34* (4), 847-858.
50. Organization, W. H., *Global technical strategy for malaria 2016-2030*. World Health Organization: 2015.
51. World Health, O., *World malaria report 2015*. World Health Organization: Geneva, 2015.
52. Han, J.; Xia, T.; Spathis, D.; Bondareva, E.; Brown, C.; Chauhan, J.; Dang, T.; Grammenos, A.; Hasthanasombat, A.; Floto, A.; Cicuta, P.; Mascolo, C., Sounds of COVID-19: exploring realistic performance of audio-based digital testing. *npj Digital Medicine* **2022,** *5* (1), 16.

53. McDermott, S.; Ayazi, F.; Collins, J.; Knapper, J.; Stirling, J.; Bowman, R.; Cicuta, P., Multi-modal microscopy imaging with the OpenFlexure Delta Stage. *Optics Express* **2022,** *30* (15), 26377-26395.
54. Knapper, J.; Collins, J. T.; Stirling, J.; McDermott, S.; Wadsworth, W.; Bowman, R. W., Fast, high-precision autofocus on a motorised microscope: Automating blood sample imaging on the OpenFlexure Microscope. *Journal of Microscopy* **2022,** *285* (1), 29-39.
55. McDermott, S.; Kim, J.; Leledaki, A. A.; Parry, D.; Lee, L.; Kabla, A.; Mkindi, C.; Bowman, R.; Cicuta, P., autohaem: 3D printed devices for automated preparation of blood smears. *Review of Scientific Instruments* **2022,** *93* (1).
56. Kinyua, D. M.; Rurimo, G. K.; Karim, P. M.; Maina, S. N.; Ominde, C. F., Interferometry analysis of cellophane birefringence. **2013**.
57. Juárez-Ramírez, J. C.; Ortiz-Gutiérrez, M.; Salgado-Verduzco, M. A.; Pérez-Cortés, M.; Olivares-Pérez, A.; Ordoñez-Padilla, M. J.; Ibarra-Torres, J. C. In *Birefringence measurement of the cellophane film*, Practical Holography XXVIII: Materials and Applications, SPIE: 2014; pp 354-359.
58. Pabón, J.; Salazar, K.; Torres, R., Characterization method of the effective phase retardation in linear birefringent thin sheets. *Applied Optics* **2021,** *60* (14), 4251-4258.
59. Sokolich, M.; Rivas, D.; Yang, Y.; Duey, M.; Das, S., ModMag: A modular magnetic micro-robotic manipulation device. *MethodsX* **2023,** *10*, 102171.
60. Newman, D. M.; Heptinstall, J.; Matelon, R. J.; Savage, L.; Wears, M. L.; Beddow, J.; Cox, M.; Schallig, H. D.; Mens, P. F., A magneto-optic route toward the in vivo diagnosis of malaria: preliminary results and preclinical trial data. *Biophysical journal* **2008,** *95* (2), 994-1000.
61. Butykai, A.; Orbán, A.; Kocsis, V.; Szaller, D.; Bordács, S.; Tátrai-Szekeres, E.; Kiss, L. F.; Bóta, A.; Vértessy, B. G.; Zelles, T., Malaria pigment crystals as magnetic micro-rotors: key for high-sensitivity diagnosis. *Scientific reports* **2013,** *3* (1), 1431.
62. Trager, W.; Jensen, J. B., Human malaria parasites in continuous culture. *Science* **1976,** *193* (4254), 673-675.
63. Amboko, B.; Stepniewska, K.; Macharia, P.; Machini, B.; Bejon, P.; Snow, R.; Zurovac, D., Trends in health workers' compliance with outpatient malaria case-management guidelines across malaria epidemiological zones in Kenya, 2010–2016. *Malaria Journal* **2020,** *19*, 406.

Appendix B:

University of Cambridge
Cavendish Laboratory

Professor Pietro Cicuta
Tel: +44 1223 337462
Fax: +44 1223 337000
E-mail: *pc245@cam.ac.uk*
http://people.bss.phy.cam.ac.uk/~pc245

JJ Thomson Avenue
Cambridge CB3 0HE, UK

13th July, 2023

To: Dr Dickson Kinyua
Kirinyaga University
School of Pure and Applied Sciences
Kerugoya – Kenya

Dear Dickson,
It is my pleasure to absolutely support your application to the Optical Foundation Challenge 2023 call.

The discussion with you around the proposed project has been extremely exciting. I think you have carefully considered what aspect of new technology you can develop and deploy, taking account of the specific challenges in your local area, and the impact that your work would have globally. The device you describe for the affordable monitoring of malaria will have both great scientific value and a significant impact on the way diagnostics is performed, especially in the rural areas that do not have regular access to sophisticated medical centers.

Last year in Summer 2022 you visited my lab for a couple of months and that time was very useful to test out preliminary imaging of red blood cells in the conditions you want to develop in the project. We also discussed the potential to use phase-locked approaches, which you had suggested, and I think the way you propose to phase-lock between the magnetic field orientation and optically polarized imaging is a powerful and new technique.

I will be very happy to host you and work with you for 12 months at the start of the grant, and to continue collaborating with you and your team on your return to Kenya. Whilst in Cambridge you will be a visiting researcher in the department, and you will be integrated with my research team.

Yours sincerely,

Prof. Pietro Cicuta
Professor of Biological Physics
Head of Group – Biological and Soft Matter Systems
Fellow of Corpus Christi College

e-CoMet: **E**nergy **E**fficient 5G/6G **Co**mmunications with Optically Transparent, Multifunctional **Met**asurfaces

Executive Summary

This aspiring project will focus on designing and implementing **high-efficiency transparent multifunctional metasurfaces** with particular emphasis on their potential to revolutionize the **environmental impact of 5G/6G telecommunication** technologies.

Our ambitious approach will prioritize the development of transparent, multifunctional, and reconfigurable metasurfaces to overcome the efficiency limitations observed in current examples, where efficiency often falls below 50%. Therefore, the main objective will be **to create (design, implement, and characterize) efficient metasurfaces made from transparent conductors.** To achieve improved efficiency, we will explore innovative design techniques, such as **inverse-design** methodologies, combined with advanced 3D printing approaches fused with **highly efficient transparent conductors**. These will allow us to create **the first-of-its-kind multifunctional transparent metasurface** with **enhanced efficiency**.

Incorporating transparent surfaces into buildings can significantly enhance the energy consumption and efficiency of 5G devices. Meta Materials Inc. and other companies are working diligently to achieve this goal, but producing highly effective transparent metasurfaces is still challenging. Our proposed approach aims to lead the way in achieving groundbreaking advancements in technology, particularly in the field of communication and beyond.

The **e-CoMet** project aims to provide various benefits to both the Optica society and the telecommunications industry, including research innovations and patents. The expected technological advancements can bring advantages with impact in both academic and industrial settings. By improving and extending the concept of transparent metasurfaces concept, we can move closer to a more sustainable and efficient future for telecommunications.

e-CoMet: **E**nergy **E**fficient 5G/6G **Co**mmunications with Optically Transparent, Multifunctional **Met**asurfaces

Literature Review: As 5G and future 6G technologies evolve, the demand for power in telecommunications networks increases significantly due to advanced antenna systems, network densification, and additional processing requirements [1,2]. To ensure sustainable and energy-efficient solutions, innovative approaches in hardware design, network planning, renewable energy utilization, and energy-efficient algorithms are being explored [1,2].

Utilizing metasurfaces consisting of optically transparent conductors is an emerging paradigm in this context [3,4]. These metasurfaces offer passive and active elements that can efficiently redirect and control incoming radiation, optimizing power allocation toward more personalized, on-demand telecommunication functionalities and modalities [3,4]. Therefore, integrating metasurfaces into network planning becomes a promising approach to tackling the challenges posed by power-hungry 5G and future 6G technologies [1,2]. By dynamically modifying the propagation environment, metasurfaces can enhance signal transmission, beamforming calculations, and synchronization, all while mitigating power consumption [1-3]. The intelligent use of transparent conductors in the design of multifunctional telecommunication devices further contributes to energy-efficient solutions.

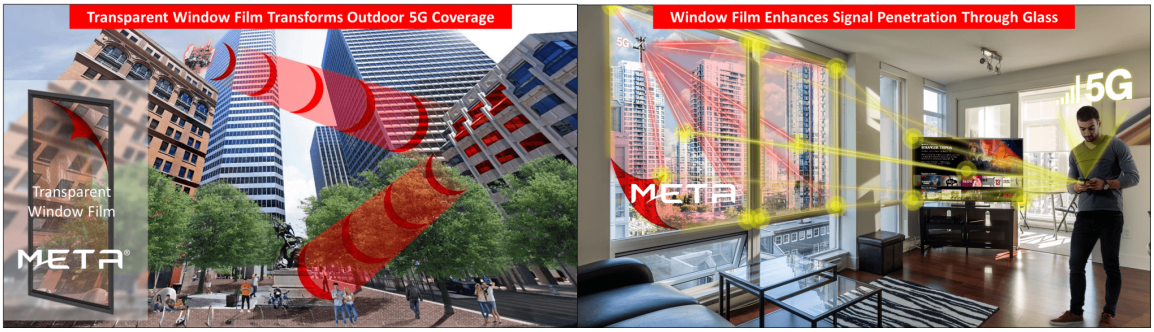

***Figure 1**: Potential uses for multifunctional transparent metasurfaces in an urban environment. For example, these surfaces could be installed in windows and buildings to improve outdoor coverage as needed, as shown in the picture on the **left**. On the **right**, a similar approach could be used to boost and redirect indoor signals. **e-CoMet** aims to create reliable and efficient versions of these transparent metasurfaces. (Pictures adapted from Meta Material Inc. - https://metamaterial.com/industries/5g-communications/ - retrieval date 07.18.2023)*

The advent of multifunctional metasurfaces presents an opportunity to develop green and sustainable telecommunication networks. By leveraging the capabilities of metasurfaces, it becomes possible to strike a delicate balance between high-performance networks and minimized power consumption. As the telecommunication industry moves towards a more energy-efficient future, integrating these technologies is expected to play a pivotal role in meeting the rising demand for data and network capacity while mitigating the environmental impact.

The focus of this ambitious proposal will be **to exploit transparent multifunctional metasurfaces** for revolutionizing their **environmental impact** in an industrial setting by addressing central features such as energy efficiency, functionality, cost reduction, and design robustness.

Problem Statement and Objectives: The proposed metasurfaces promise to be a game-changing passive component that can be widely used for the on-demand control of E/M waves, assuming a real-life scenario. The main functionalities of these metasurfaces lie typically in the following three categories:

1. Control of E/M radiation, e.g., reflection, transmission, absorption [4]
2. Harvest of E/M radiation [5]
3. Other functionalities, such as edge detection, image processing, and analog optical computing [6]

The concept of transparent metasurfaces can already be found in experimental implementations [5]. However, the main bottleneck is their poor/moderate efficiency, stemming mainly from transparent conductors exhibiting very high resistivity, which limits their overall efficiency relative to conventional conductors.

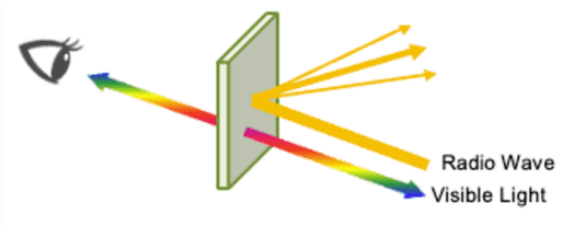

Figure 2: *This proposal aims to create transparent metasurfaces that can efficiently control and manipulate radio waves (RF) without compromising their high transparency. The goal is to use inverse design and other constrained optimization techniques to design and implement multifunctional and reconfigurable metasurfaces with maximum efficiency. (Figure adapted from Meta Material Inc. - https://metamaterial.com/industries/5g-communications/ - retrieval date 07.18.2023)*

Our ambitious project prioritizes the development of disruptive transparent, multifunctional, and reconfigurable metasurfaces to overcome efficiency limitations observed in current examples of antennas and metasurfaces utilizing transparent conductors, where efficiency often falls below 50%. Therefore, the main **problem is creating (designing, implementing, and characterizing) efficient metasurfaces made from transparent conductors.** This efficiency improvement will try to maintain the basic two modalities, i.e., transparency and efficient radio wave manipulation. To achieve improved efficiency, we will explore innovative design techniques, such as inverse-design methodologies, combined with advanced 3D printing (and other open and proprietary) approaches and highly efficient transparent conductors. These will allow us to create **the first-of-its-kind multifunctional transparent metasurface with enhanced efficiency**.

Two key approaches allow us to attack the problem. **First**, the choice of a **highly efficient transparent conductor** is of paramount importance. To this end, Meta Materials Inc. (the hosting company/entity) is actively developing NANOWEB, a transparent conductor with unprecedented features, such as very low resistivity (<2 ohm/square) with very high transparency (>95%). Therefore, all metasurfaces will be designed using high-quality NANOWEB.

The **second key approach** will be at the design and optimization stage. Since transparent conductors exhibit some intrinsic features, it is apparent that a non-intuitive constrained design is required. Inverse design is one of the best options for approaching such a problem, widely used in fields such as photonics. Despite limitations in materials and processes, this technology has delivered efficient photonic devices with quite strict constraints [7]. Here, we plan to use inverse design to tailor the near-field interactions of the periodic cells for high-efficiency metasurface design. The envisioned transparent metasurfaces will be designed, implemented, characterized, and demonstrated using first-principle approaches. The project will proceed toward evaluating the

link budget through ray tracing methods and measurements. Finally, a demo case will be measured where the transparent metasurface will be placed in realistic 5G/6G communication scenarios. This final phase will assess and demonstrate the effectiveness of the metasurfaces in a realistic environment, with the specific goal of improving 5G coverage.

Overall, the **e-CoMet** project seeks to unleash the full potential of transparent metasurfaces by leveraging inverse design techniques and photonic approaches, aiming to significantly improve the efficiency of components made from transparent conductors. The multifunctional, transparent, and reconfigurable nature of these metasurfaces will pave the way for transformative advancements in various technological applications, especially in the realm of communication and beyond.

Outline Tasks/Work Plan: The main work plan includes the inverse design of optically transparent multifunctional metasurfaces for 5G/6G applications. It will be divided into four tasks. The first task (**T.1**) will be the detailed identification of the targeted study (frequency range, bandwidth, functionality) and the main key performance indicators (KPIs), such as efficiency and cost. The second task (**T.2**) will focus on optimizing the **1st Gen** design of the metasurface. Emphasis will be given to the main functionalities and the characterization of such a device. A second iteration, i.e., **2nd Gen**, (**T.3**), will further optimize the 1st Gen design towards multifunctionality, transparency, and efficiency. Finally, the fourth task (**T.4**) will test the **1st Gen** and **2nd Gen** designs deployed into a realistic scenario for demonstrative purposes (demo showcase).

	Gantt Diagram of Work Plan & Tasks	**Q1**	**Q2**	**Q3**	**Q4**	**Q5**	**Q6**	**Q7**	**Q8**
WP	**Inverse design of optically transparent multifunctional metasurfaces for 5G/6G applications**			**M.1**		**M.2**		**M.3**	
T.1	Detailed **identification** of the target study (Demo) and the KPIs								
T.2	**1st Gen metasurface**: design, implementation, characterization performance assessment								
T.3	**2nd Gen metasurface**: emphasis on transparency, multifunctionality, efficiency, and other KPIs.								
T.4	**Demo** showcase of the proposed case study								

For all tasks, we will utilize cutting-edge inverse design techniques, algorithms, and workstations, in tandem with advanced manufacturing techniques (3D printing, laser cutting etc.) and other implementation processes, to create transparent metasurfaces with exceptional efficiency. We will conduct both full-wave simulations and thorough ray-tracing analysis to verify and evaluate their performance both in ideal and in realistic scenarios. The project will be spearheaded by the author (Senior R&D engineer), with the help of one or more junior engineers at the R&D premises of Meta Materials Europe (a subsidiary of Meta Materials Inc.) in Athens, Greece. The largest portion of the grant will be used for covering (either partially or in total) the salary of one leading and one assisting engineer/scientist. The remaining funding sum will be allocated towards procuring

software licenses, improving our current design infrastructure, and covering other expenses, e.g., consumables. The main testing facilities, e.g., VNAs, waveguides, horn antennas, anechoic chamber, etc., will be provided by the hosting entity, i.e., the Meta Material Europe labs in Athens, Greece.

Outcomes: In this project, we aim to design and fabricate proof-of-concept metasurfaces for 5G/6G telecom bands, which will have multiple functionalities such as optical transparency, reflection, transmission mode, and reconfigurability. The goal is to efficiently combine these features into a metasurface design. We plan to implement two different metasurfaces designs (1st and 2nd Gen) and characterize their overall performance (demo).

Based on the Optica Foundation Challenge directions, we identify three milestones that follow the three stages of the study. The first milestone (**M.1** – 6-month summary) involves reporting on the target study and the 1st-gen metasurface. We will identify key performance indicators of the demo case study and the metasurface while testing the first metasurface design. The focus here is on verifying the extent of the desired functionalities. The second milestone (**M.2** – 12-month summary) involves optimizing the 2nd Gen metasurface to meet the identified main performance goals. The emphasis will be on multifunctionality and optical transparency. Finally, the third milestone (**M.3** – 18-month summary) will include deploying the metasurfaces on a real 5G/6G coverage improvement example, showcasing their essential efficiency. In terms of reporting, the main outcomes will be:

1. Scientific reports/articles: Our design process and implementations will be thoroughly documented in scientific articles and reports, focusing on transparent components with multiple functionalities/modalities. We anticipate publishing at least one to two papers in relevant journals such as Optics Letters, Optical Material Express, and Optica and presenting at corresponding conferences like CLEO and Fi-OS/LS.
2. Patents and IP: Regarding patents and **potential commercialization** of the results, it is anticipated that Meta Materials Inc., where the study and implementation will occur, will assist in developing a plan for intellectual property protection, licensing, and other necessary actions. After the completion of the project, the focus will be on achieving a high TRL level (4 or higher) to rapidly facilitate any potential commercialization of the proposed technology.

Impact: The use of transparent intelligent surfaces and metasurfaces on buildings has the potential to greatly improve the energy consumption and efficiency of various 5G devices. To this end, a highly efficient transparent metasurface will drive the penetration of metasurfaces to the realm of the necessary 5G/6G telecommunication components. Many deep tech companies, such as Meta Materials Inc. and others, are currently conducting orchestrated efforts in this area since a solution that can optimize the power management of wireless networks is of paramount importance for both the end users and the providers. Through this new technology, it is hoped that higher TRL levels can be achieved, ultimately bridging the cap towards a possible market availability of transparent metasurfaces.

The project being proposed has the potential to provide immense benefits to both Optica society and the telecommunications industry. This technological advancement offers numerous advantages, from academic to industrial outcomes. By further developing this concept, we can move towards a more sustainable and efficient future of telecommunications for everyone.

Reference list

1. University of Oulu, “Key drivers and research challenges for 6G ubiquitous wireless intelligence,” http://jultika.oulu.fi/files/isbn9789526223544.pdf.
2. C. -X. Wang et al., “On the Road to 6G: Visions, Requirements, Key Technologies, and Testbeds," in IEEE Communications Surveys & Tutorials, vol. 25, no. 2, pp. 905-974, 2023, doi: 10.1109/COMST.2023.3249835.
3. M. Di Renzo, F. H. Danufane and S. Tretyakov, "Communication Models for Reconfigurable Intelligent Surfaces: From Surface Electromagnetics to Wireless Networks Optimization," in Proceedings of the IEEE, vol. 110, no. 9, pp. 1164-1209, Sept. 2022, doi: 10.1109/JPROC.2022.3195536.
4. Tsilipakos, O., Tasolamprou, A. C., Pitilakis, A., Liu, F., Wang, X., Mirmoosa, M. S., **Tzarouchis, D. C.**, Abadal, S., Taghvaee, H., Liaskos, C., Tsioliaridou, A., Georgiou, J., Cabellos-Aparicio, A., Alarcón, E., Ioannidis, S., Pitsillides, A., Akyildiz, I. F., Kantartzis, N. V., Economou, E. N., Soukoulis, C. M., Kafesaki, M., Tretyakov, S., “Toward Intelligent Metasurfaces: The Progress from Globally Tunable Metasurfaces to Software-Defined Metasurfaces with an Embedded Network of Controllers.” Adv. Optical Mater. 2020, 8, 2000783. https://doi.org/10.1002/adom.202000783
5. Daisuke Kitayama, Yuto Hama, Kenta Goto, Kensuke Miyachi, Takeshi Motegi, and Osamu Kagaya, "Transparent dynamic metasurface for a visually unaffected reconfigurable intelligent surface: controlling transmission/reflection and making a window into an RF lens," Opt. Express 29, 29292-29307 (2021)
6. V. Nikkhah*, **D. C. Tzarouchis***, A. Hoorfar, and N. Engheta, “Inverse-Designed Metastructures Together with Reconfigurable Couplers to Compute Forward Scattering” ACS Photonics 2023 10 (4), 977-985, DOI: 10.1021/acsphotonics.2c00373 (*equal contribution)
7. Molesky, S., Lin, Z., Piggott, A.Y. et al. “Inverse design in nanophotonics.” Nature Photon 12, 659–670 (2018). https://doi.org/10.1038/s41566-018-0246-9

2023 Optica Foundation Challenge
Category: Environment
Title: Spectral radiance mapping to characterize the ecological impacts of light pollution
Name: Dorukalp Durmus
Affiliation: Pennsylvania State University

Executive summary:

The challenge

The accessibility and growing demand for electric lighting have a large-scale impact on natural habitats. Unfortunately, the electric light at night (LAN) can cause negative consequences, such as disrupting ecosystems, confusing migratory patterns, altering predatory-prey relations, causing stress, and interrupting the entrainment of circadian rhythms of many species. The negative effects of LAN (aka "light pollution") is often quantified using photometric and colorimetric measures. Despite the complexity of spectral impact of light sources on the environment, research suggests that light source spectra influences arachnida, aves, instecta, mammalia, and reptiles in predictable manners. However, ecological research studies still use photometric (i.e., illuminance, luminance) and colorimetric (i.e., correlated color temperature) measures, which are based on human visual sensitivity. In addition, photometric and colorimetric measurements are performed using either spot measurements or satellite images. While these measurement methods have merits, they have limitations in accurately evaluating the ecological impacts of light pollution.

Proposed project

Characterizing the impacts of light pollution on several species requires a holistic measurement approach in spectral and spatial dimensions. The proposed research project aims to characterize optical radiation using a spectral imaging radiance colorimeter and assess the outcomes compared to spot (e.g., handheld spectroradiometer) and remote (satellite) measurements. A test field in central Pennsylvania will be identified, and light pollution of a large field of view will be characterized using radiance imaging colorimeter to simulate realistic field conditions. The variation between the traditional and proposed measurement methods will be evaluated, and a new metric for light pollution will be developed using the data generated in this project.

Intended outcomes

The results of this project will help characterize the unintended consequences of light pollution that captures the effects on the environment beyond just humans. New light pollution metric and measurement methods comparison will be disseminated to relevant bodies, such as the Council for Optical Radiation Measurements, the International Commission on Illumination, and International Dark-Sky Association. The project aims to reach a transformative impact on project development where designers and engineers can quantify the impact of lighting systems and mitigate any potential offence. The development of a holistic light pollution metric will also help ecological researchers find acceptability thresholds and guide outdoor lighting standards and recommendations, such as Model Lighting Ordinance (MLO), LEED Sustainable Sites program, the International Commission on Illumination (CIE) recommendations, and standards, such as the Australian New Zealand Standard AS/NZS 4282:2019 Control of the obtrusive effects of outdoor lighting.

1. Literature review

1.1 Negative impacts of light pollution

Light is imperative to achieve viable conditions for human activity at night, such as transportation, work, commerce, and leisure. The use of outdoor lighting is beneficial for commercial and cultural endeavours, especially in urban environments, but electric light at night (LAN) also reduces darkness which may be necessary for the ecology and some animals. For the outdoor lighting to be sustainable it should fulfil the functional needs of the users, be cost- and energy-efficient, and result in minimal environmental impact. The use of outdoor lighting during night-time can result in various unwanted and harmful side-effects (often collectively referred to as light pollution). The unwanted effects of the use of outdoor LAN include:

- Increase in human-made sky glow (the diffuse luminance of the night sky),[1]
- Degradation of ground-based astronomical observatories operating in the optical range and a decreased ability to observe the stars due to the brightening of the night sky,[2]
- Increase in obtrusive light causing nuisance and discomfort glare for humans,
- Adverse health outcomes, such as circadian disruption, mood effects, and increased breast cancer incidence risk in humans,[3]
- Disturbances and negative impacts on species, ecosystems, and wildlife.[4]

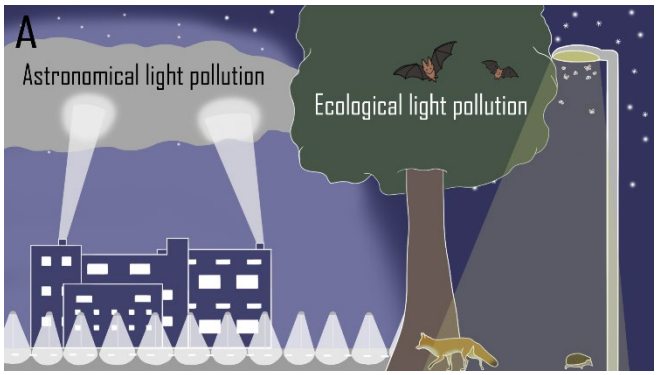

Fig. 1. Electric light at night can cause astronomical and ecological light pollution.[5]

The unwanted side-effects are measured through response variables and vary significantly depending on the research discipline and the study objects. In astronomy, the response variable can be sky brightness or upward emitted light. For impacts on human health, the response variable can be human behaviour or various health outcomes (e.g., sleep quality, melatonin suppression or risk of cancer). In ecology, the response variable is usually restricted to appropriate study variables for the specific species, the spatial scale or ecosystem of the investigation. Characterizing the ecological impacts of light pollution requires considering species' spectral sensitivity to optical radiation. The spectral sensitivities can help characterize

[1] Kyba, C., Tong, K. P., Bennie, J., Birriel, I., Birriel, J. J., Cool, A., ... & Gaston, K. J. (2015). Worldwide variations in artificial skyglow. *Scientific Reports*, 5(1), 1-7.
[2] Riegel, K. W. (1973). Light Pollution: Outdoor lighting is a growing threat to astronomy. *Science*, 179(4080), 1285-1291.
[3] Durmus D., Tengelin, M. N., & Jägerbrand, A. K. (2022) Investigating the methods and health outcomes of research studies on light pollution and human physiology and behaviour: a systematic review, 17th International Symposium on Science & Technology of Lighting, Toulouse, France.
[4] Sanders, D., Frago, E., Kehoe, R., Patterson, C., & Gaston, K. J. (2021). A meta-analysis of biological impacts of artificial light at night. *Nature Ecology & Evolution*, 5(1), 74-81.
[5] Jägerbrand, A. K., Tengelin, M. N., & Durmus, D. (2022) An overview of the adverse effects of outdoor light at night and the research methods used in different areas. 2022 Conference Proceedings of Lux Europa. Prague.

their visual response (i.e., brightness perception) to natural and electrical lighting. Some species may require darkness to hunt or hide from predators, find mating partners, or forage. Electric light at night with spectral distributions that are different than natural light sources (e.g., moonlight) may cause disruption to biological cycles of many species.

1.2 Light pollution measurement methods

Methods used in ecological light pollution studies are plentiful because of the large number of organisms that are studied. For example, LAN impact on birds have been studied through observational studies in the field that correlated bird responses (e.g., migration) to satellite-based light measurements or to ground-based measurements, but also through controlled indoor experiments or through experiments using bird enclosures outdoor. Bio-loggers attached on birds can help correlated exposure of LAN to movement patters. The effects of LAN on insects (or invertebrates) have been studied in observational studies, often by comparing the number of trapped insects, with and without lighting (often using light as a source of attraction for the insects), or by introducing different kinds of interventions in unlit or lit areas. Insect responses have also been studied by introducing LAN in previously unlit areas in manipulative field experiments and observing the responses.

Bats have only been studied through field experiments. Observational studies have been performed that compares bat movements and frequency of activity without any intervention. Field experiments varies much in their design, but some use already lit areas for introducing interventions (e.g., altered light sources, light intensity, or light distribution) and others use previously unlit areas to introduce LAN and study impacts on behaviour. Fish responses to LAN can be studied in field experiments, mesocosms, enclosures or in laboratory studies. Field experiments can be conducted to study both lit or unlit conditions with or without interventions. Use of mesocosms, enclosures or laboratory environments can improve the scientific reliability of the study since it is more controlled, and the influence of external factors can be minimized.

Responses of plants can be investigated through controlled field experiments manipulating various lighting conditions. Studies can also be performed as observations in unlit or lit areas with or without interventions. Tree phenology can be correlated with satellite-based measurements or with ground-based measurements. Similarly, turtles have mainly been studied in their natural habitats and in the field. Studies are often observations of behaviour before/after interventions have been introduced. Studies focuses on hatchlings, but adult turtles have also been under investigation. On the other hand, responses of rats, mice and rodents have been investigated in controlled laboratory studies where lighting manipulations can be fully controlled and measured. Field experiments of mice and rats in natural environments or in more controlled enclosures have also been performed. Response variables includes behaviour, ecological relevant variables and physiological measurements.

Many ecological studies are conducted without including data on environmental factors that may influence the results. Especially field experiments are very poor in reporting the lighting condition, for example light source, light intensity, and light distribution.[5] Only a few studies report enough information on light distribution to be able to repeat the study. Light sources are often mentioned but rarely with enough information to replicate the study. For example, the spectral power distribution (SPD) of the light sources are rarely reported. Even during controlled conditions, measurement details are not often clearly stated or reported. In addition, exposure levels for organisms are rarely reported.

These ecological studies often characterize the lighting conditions using photometric measures, such as illuminance (unit: lux). Illuminance, the total luminous flux incident on a surface per unit area, does not quantify the light reflected from surfaces and it is based on human visual sensitivity to optical radiation. The human spectral sensitivity to optical radiation is assessed using the photopic luminous efficiency function, which peaks at 555 nm. However,

most other animals (e.g., mammals except old and new world monkeys, insects, birds) have different photoreceptor spectral sensitivities due to evolutionary reasons, such as detecting flowers or fruits.[6] Some animals can even detect optical radiation beyond light, such as ultraviolet and infrared radiation. Therefore, the use of photometric measures (i.e., illuminance, luminance) is limited at best, and might mislead researchers, conservators, and lighting designers in their efforts in protecting natural habitats. In addition, the typical illuminance and luminance meters can only perform point measurements (a single point in time). A single point measurement does not fully characterize the visual scene in an outdoor setting but taking more measurements can be cumbersome and time intensive with these devices. Therefore, alternative methods should be used to characterize the lighting conditions of a field of view of a large area.

1.3 Satellite images

An alternative approach to photometric spot-measurements is extracting light exposure information from satellite images. Ground-based measurements include astronomical photometry and spectroscopy at large observatories, wide-field photometry using all-sky cameras with fish-eye lenses, narrow angle measurements (typically in only one band) using sky quality meters. Naked eye observations of stellar objects where citizen observations can be used to get large coverage of the observations. For light emitted through the earth atmosphere, remote sensing is carried out with radiance measurements by satellite-based sensors and photographs taken from NASA's International Space Station.

In earlier studies, mostly telescopes and naked eye observations were used in ecological research. From the year 2000 and onwards satellite-based radiometry has been used in the studies of light pollution, starting with the Defense Meteorological Satellite Program (DMSP) Operational Linescan System and later with the higher resolution of the monthly cloud-free night-time imagery from the Suomi National Polar-Orbiting Partnership (Suomi NPP), Visible Infrared Imaging Radiometer Suite (VIIRS) Day/Night Band, and most recently the Chinese satellite Jilin-1, claiming to have a spatial resolution below 1 m. With the development of wide-angle photometry, from 2010 and onwards the number of studies using camera-based measurements have increased.[5]

LAN measured by satellite is often correlated to urbanization, noise levels, and air pollution. In outdoors, it was found that satellite-based radiance measurements were useful when estimating the ground exposure, although luminance values from The New World Atlas had a better correlation with ground measurements considering the full sky. However, both the satellite image composites, and the estimated zenith brightness levels were found to smooth out local spatial variations as measurements performed on the ground have shown a much larger variation between high and low exposure sites when total exposure is considered.[7]

Although, satellite measurements of sky brightness can provide a broad analysis of a larger geographical area, it has limitations. For example, the process of sky glow and the measurement of the sky brightness is highly influenced by meteorological conditions. In astronomical studies, different units are used depending on the experimental technique. It is common to report the sky brightness in the astronomical magnitude system mag/arcsec^2. This can be approximately compared to luminance in mcd/m^2, but the different measurement techniques and bands used make it difficult to compare results from different studies. Another important limitation of the satellite images is the spectral sensitivity of the radiometers in the satellite (i.e., between 500 nm and 900 nm), which does not include a substantial portion of short wavelength energy that animals, including humans, are sensitive.

---

[6] Osorio, D., & Vorobyev, M. (2008). A review of the evolution of animal colour vision and visual communication signals. *Vision Research*, *48*(20), 2042-2051.

[7] Simons, A. L., Yin, X., & Longcore, T. (2020). High correlation but high scale-dependent variance between satellite measured night lights and terrestrial exposure. *Environmental Research Communications*, 2(2), 021006.

1.4 Spectral radiance imaging

The limitations of photometric and satellite measures can be balanced by utilizing spectral radiance measurements captured through imaging systems. Spectral radiance imaging is the method of collecting radiometric data from a scene using a calibrated camera. Spectral radiance imaging is a subset of remote imaging, where electromagnetic radiation emitted or reflected from surfaces are measured. This method enables large field-of-view scanning and imaging for remote sensing and surveillance, with early applications focusing on the relationship between electromagnetic radiation and water,[8] complex vegetation,[9] and climate variability.[10] Today, spectral imaging cameras can be purchased to measure the radiometric quantities that are far more relevant for ecological and environmental research.

2. Problem statement / objective

The growing population and the increase in urbanization has rapidly expanded the human reach into the natural habitats. This increase comes at a price for the ecological environments and its inhabitants. Light, a key factor for human vision, can disrupt other species' biological cycles. Current methods of quantifying the negative impacts of light pollution is limited. The objective of this project is to evaluate the performance of spectral radiance imaging for a faster and accurate measurement of the lit night environment. The data collected in this study will be also used to develop new metrics to quantity the ecological impacts of light pollution.

3. Outline of tasks/work plan

The tasks of the proposed project is shown in Table 1.

Table 1. The outline of tasks for the proposed research project

Task	**Q1**	**Q2**	**Q3**	**Q4**
1. Identify test site				
2. Data collection from satellite images				
3. Field measurements with photometers and spectroradiometers				
4. Spectral characterization with spectral radiance colorimeter				
5. Data analysis				
6. Report, dissemination, outreach				

Task 1. Identifying a test site to conduct light pollution measurements: An outdoor area in central Pennsylvania (Centre County) will be identified to perform light pollution measurements. The outdoor area will include a rural access to a road, light installations (street lighting), and natural habitat to replicate a broad set of ecological research studies. The availability of the satellite images for this area will also be required before confirming the site.

Task 2. Data collection from satellite images: The lighting exposure in the test field will be evaluated using satellite information downloaded from DMSP Operational Line-Scan System (OLS) Nighttime Lights Time Series Version 4. For accurate satellite image analysis, World

[8] Curran, P. J., & Novo, E. M. M. (1988). The relationship between suspended sediment concentration and remotely sensed spectral radiance: a review. *Journal of Coastal Research*, 351-368.
[9] Goward, S. N., Cruickshanks, G. D., & Hope, A. S. (1985). Observed relation between thermal emission and reflected spectral radiance of a complex vegetated landscape. *Remote sensing of Environment*, *18*(2), 137-146.
[10] Iacono, M. J., & Clough, S. A. (1996). Application of infrared interferometer spectrometer clear sky spectral radiance to investigations of climate variability. *Journal of Geophysical Research: Atmospheres*, *101*(D23), 29439-29460.

Bank's Open Night Lights[11] tutorial will be utilized. Open Night-time Lights program offers open source tools (Python-based code) and basic operations for processing composite night-time images. A reference grid will be established, light sources will be identified and geolocated, and digital values will be established to the radiance scale.

Task 3. Field measurements with photometers and spectroradiometers: Photometric and radiometric measurements will be conducted in the field using calibrated Konica Minolta T-10A illuminance meter, LS-150 luminance meter, and Gigahertz BTS256 spectroradiometer. In addition, luminance maps will be created using state-of-art high-dynamic range (HDR) luminance mapping techniques[12] for an alternative fast and cost-effective measure.

Task 4. Spectral characterization with spectral radiance colorimeter: The spectral properties of the visual scenes of the test field will be characterized using a spectral imaging radiance colorimeter, which will be purchased with funds provided by this grant.

Task 5. Data analysis: The data points in each scene taken by imaging colorimeter will be matched with the data from the spectroradiometer and luminance meters. Radiometric quantities will be calculated for each pixel, and the variation between measurements methods will be quantified, and a regression model will be developed to use RGB values from a simple camera.

4. Outcomes

The primary outcome of this project is the development and confirmation of novel method to accurately assess the impact of light pollution. A mathematical model will be developed that can best estimate radiometric quantities. In addition, a new light pollution metric will be develop considering light source spectra and irradiance of a visual scene. The data will be made available online for other researchers to develop their own approaches and evaluate the proposed metrics and measurement methods.

5. Impact

The project outputs will directly impact the practice of lighting design and illumination engineering. There are currently several outdoor lighting standards that aim to limit the light exposure on unwanted areas to limit the negative consequences of light pollution. The International Commission on Illumination (CIE) "CIE 150:2017 Guide on the limitation of the effects of obtrusive light from outdoor lighting installations," the Model Lighting Ordinance (MLO) published jointly by the International Dark Sky Association and the Illuminating Engineering Society (IES), Leadership in Energy and Environmental Design (LEED) Light pollution reduction Sustainable Sites (SS8), and Australian and New Zealand Standards (AS/NZS) 4282:2019 Outdoor Lighting Obtrusive Effects are some of the most prominent examples. However, these standards still utilize photometric measures and are often limited to negative impacts on humans (e.g., glare). The PI Durmus has connections to many of these organizations and will work with the committees to improve the existing guideline to incorporate the metrics developed using outcomes of this research proposal. For example, Dr. Durmus is a member of two IES technical committees, was a member of CIE Australia and was a presentative, and worked in the AS/NZS standards committee previously. Through dedicated service work, the results will be metallized into reality to ensure immediate real-world impact.

[11] https://worldbank.github.io/OpenNightLights/welcome.html

[12] Pierson, C., Cauwerts, C., Bodart, M., & Wienold, J. (2021). Tutorial: luminance maps for daylighting studies from high dynamic range photography. *Leukos*, *17*(2), 140-169.

2023 Optica Foundation Challenge

Name of Challenge Project: Artificial Intelligence enabled smart Optical Absorption Point-of-Care device for Malaria screening.

Executive summary:

Background: For the larger interest of the needy design and development of Point-of-Care (PoC) diagnostics is the critical requirement of the health care industry. The requirement of rapid, sensitive detection and reliable solution with minimal human intervention is the front runner objectives of the research and innovation. The aim of the present research proposal is to develop an indigenous smart PoC instrument for screening/ detection of the malaria. The monitoring and screening of malaria transmission is possible with the advancement of the technology in view of malaria eradication.

Scientific Rationale: The microvascular system is responsible for the transfer of oxygen and nutrients and the removal of the waste products generated by the tissue it serves. Here, the main role of the erythrocyte/ Red Blood Cells (RBCs) is the transmission of hemoglobin (oxygenated) and nutrients through microvascular system. As we know that the malarial parasite targets RBCs such as infect inside the RBCs and reduce the hemoglobin concentration by degrading it as hemozyme. As a result, there will be changes in the level of hemoglobin present in normal RBC and malarial infected RBCs. So, this information can be utilized to develop a point of-care device to differentiate between malarial infected and normal RBCs at single-cell high-throughput by differential light absorption in microfluidic channel as observed in any flow cytometry. The proof-of-concept and primary results shown briefly in the figure below.

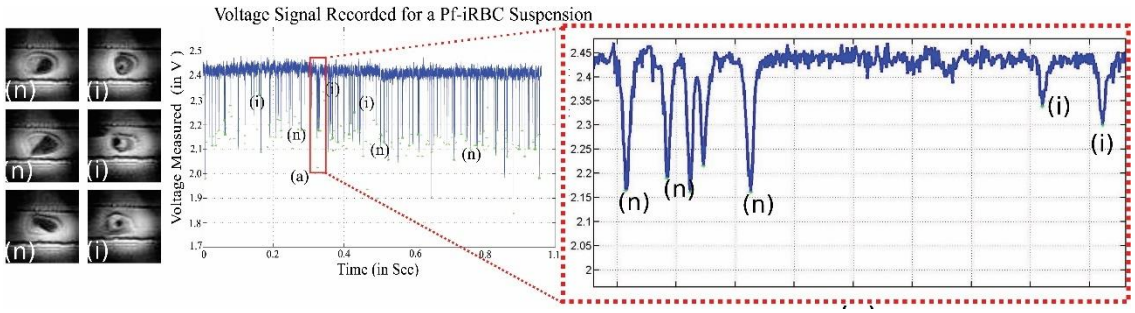

Novelty: The present malaria diagnosis instruments including clinical microscopy, PoC, Rapid (**qualitative info**.) testing devices use standard signal/image processing algorithms. PoC devices integration with AI models for automatic malaria screening/ testing may give more promising results. Current proposal aims in development of an AI-enabled PoC device for Realtime analysis at single-cell high-throughput (quantitative info.). The primary objective of the study involves development of smart PoC device for malaria screening. The secondary objective of the study includes proper design of experiments for clinical validation and testing, Develop the novel AI based algorithm and comparison with state-of-the-art techniques

Methods: The major principle involved in development of device is to study the light (near UV) absorption properties of malaria infected and healthy/normal blood cells. Predominant features are automatically extracted from the output signal of the sensor using signal processing algorithms and trained with artificial intelligence algorithms for classifying malaria and non-malaria cells. Novel reinforcement learning techniques will be incorporated and further tested.

Expected outcome: Low cost and portable Smart point-of-care Instrument for malaria screening and research publications in high reputed journals along with patents. Custom design and developments of flow-focusing microfluidic devices which are used for identifying cell morphology, deformability, blood flow velocity. Development of GUI based algorithm for malarial parasite detections, finding the stages of infection, quantitative information of infected cells from overall assessed sample. Development of this type of product help in early screening of malaria endemic zone which help towards the eradication of malaria.

Name of Challenge Project: Artificial Intelligence enabled smart Optical Absorption Point-of-Care device for Malaria screening.

Malaria is one of the deadliest, sometimes fatal diseases caused by infection of red blood cells with a malarial parasite. Majorly, the transmission of malaria occurs through a parasite that infects female misquotes which feed on the blood of humans and animals. In a regular day-to-day basis, we witness the spread of mosquitoes in almost every season. The seriousness of the infection depends on the types and stages of the parasite infection in humans. It insists on the need to develop medical devices, a potential tool for screening/ detection of the malaria parasite in patients' blood, and take the necessary steps in the treatment. The scheme of malaria eradication in developing and underdeveloped countries would be successful, if the more and more invention of novel, enhanced, and high-efficient screening and detection instruments are in practice. Further, the success of these advanced instruments in screening and detection should be robust and could be reached the remote location where the actual need lies. In the present three years research proposal, I propose to develop a novel high throughput single-cell detection Point-of-Care Device (PoCD) for malaria screening. *The realization of PoCD will be achieved through the synergetic integration of optics, microfluidics, and simple electronics*. The advancement of AI will facilitate the automation of the proposed PoCD to smart and real-time point-of-care screening/ detection. My current experience in the design and development of point-of-care devices will help in the realization of the present novel work. As my past work involves evaluating the hemoglobin content present in normal, single RBC, and malaria-infected RBCs. The work done so far in the realization of absorption flow-cytometer for point-of-care detection/ screening of malaria is reported in the methodology section. The significant features from the signal (output of optical device) will be extracted automatically and trained with different ML and AI models (SVM, Gradient boost, Decision Tree, ANN, etc.). Individual modules will be developed for each AI model with a user-friendly GUI to analyze the results.

Literature Review: Despite of the severity of Malaria like life-threatening diseases transmission and spread across the globe, there has been a limited effort to curb malaria. However, the good sign is that the world progressively making efforts towards the elimination of malaria, a disease of tropical countries. Every year, the overall cases are reducing as per the reports of World Health Organization (WHR2019) [1]. Worldwide, over *228* million cases were estimated in 89 countries and about 0.5 million death cases in 2018. As per the World Malaria Report (WMR) 2019, over a 3% of malaria cases were reported in India and it was around 49 % reduction compared to WMR-2018. However, the recent report of WMR 2021 shows the statistics of sudden raise of the estimated cases in parallel of COVID pandemic [2]. Globally over 258 million cases and 627000 deaths were estimated in 2020. It shows over 12% increase due to the various reasons including COVID pandemic, neglecting measuring constraint, treatments and controlling precautions. Specific to South-East-Asia, over 82% cases were reported in India. These data shows that the efforts put in towards malaria elimination needs to improve to achieve the success in the challenge of malaria eradication. The necessary steps in the eradication of the malaria involve precaution steps to avoid the spread/ transmission, screening of malaria within the transmission zone and detection/diagnosis followed by the treatment. Medical devices are the instruments for screening and detection/ diagnosis of any diseases [3]. The diagnosis of malaria involves the process of identifying the parasite in the blood cells or finding the protein content through an antigens test in blood sample. The diagnosis of malaria efficacy relies on many factors which include the form of malaria species, level of infections, immunity level of the infected individual, drug resistivity and region-based population density and mosquito's transmission within the location and others. The most conventional methods used for malaria diagnosis/detection include clinical diagnosis, which is the symptomatic signs of patients and physical findings of the pathologist. This method is more helpful in region specific and transmission of malaria in localities. The limitation includes the possibilities of misdiagnosis in asymptomatic patients [4] Laboratory diagnosis is the most effective method for diagnosis of malaria. These techniques help from over-treatment of symptomatic signs and effective diagnosis. Laboratory diagnosis comprisses of "Gold-stranded" clinical microscopy, rapid diagnostic test (RDT), QBC, ParaScreen, Paracheck, Flow-Cytometry (FCM), Imaging FCM and molecular diagnostic methods like RT-PCR. Clinical microscopy is

labor intensive method and RDT is used in inaccessible places in absence of clinical microscopy. However, the accuracy of RDT is less than 70 % and it gives qualitative information only. Since RDTs is an antigen test, and provides qualitative information of malaria positive or negative, it requires clinical microscopy to reconfirm the severity of the infection [5-10]. Other techniques like fluorescent microscopy and polymerase chain reaction (PCR) are useful for malaria detection but due to the limitations of resources at ground settings inhibit the widespread usage of these techniques. Testing of RT-PCR, FCM and Imaging FCM is hardly performed in pathological laboratories due to expense and high expertise of manpower involved. In the recent past several attempts have been made for cost-effective, point-of-care devices for malaria detection, such as magnetic resonance relaxometry, recording absorption spectrum has been reported. In addition, several optical detection techniques have been demonstrated [11-19]. Overall, optics-based approaches have high sensitivity and single-cell level findings, enable by microfluidics- high throughput and on-chip sample handling. The present advancement in the healthcare sector is a smart move towards PoCD from proof-of-concept. There are some rapid and qualitative diagnostic devices available for the diagnosis of malaria and other diseases at PoC diagnosis [20-25]. In the process of adopting new techniques, the initial stage needs to address its own constraints and come up with advanced and highly sensitive PoC diagnostics. Hence, there is a need to develop a simple, user-friendly, battery-operated, stand-alone device that can quick and quantitatively screen/detect/ diagnose the patients and direct them towards proper medication. Such advancement will increase the reach of diagnostic services to people living in rural, hilly, and remote location in both developing and underdeveloped countries.

Problem Statement/Objectives: The present research work aims to develop the indigenous single-cell high throughput microfluidic Absorption flow-cytometer for rapid screening/ detection of endemic diseases like malaria at Point-of-Care (POC). Integration with AI models for automatic malaria screening/testing may augment the impact of the device. To the best of the PI's knowledge, malaria is an endemic disease, spread across half of the world every year over 3.3 billion population undergoes screening/ testing for malaria and over 1.2 billion people are at high-risk areas and India is one among those countries where the prevalence of malaria and dengue is high. Further, in region-specific, Odisha (PI state) is one of the states which is having high-risk areas accounting for over 26 % of malaria infection cases reported in India [26-28]. Moreover, as it evident that diseases affect children under the age of 5 and pregnant women, POC screening for early detection will help in the prevention and control of the transmission of malaria. Below are the objectives towards better way to address the problem:

The primary objectives of the study involve:

- To develop a smart point-of-care instrument for malaria screening.
- Development of AI based framework for high throughput analysis.

The secondary objectives of the study involve:

- Design of experiments (DoE) for clinical validation of developed POC device
- Validation and comparison of developed AI-based framework with the state-of-the-art techniques.

Outline of tasks/ Work Plan: In the present research proposal, aimed to develop a Point-of-Care Device for malaria screening. The diagnostic instrument would be working on the principle of absorption properties of malaria infected and uninfected blood cells. Initial study is the development of standalone system for the characterization of the chemical and morphological features of blood cells using both the bulk as well as a single-cell analysis at high throughput as shown figure 1. Though it has many applications like malaria, cancer cells, stem cells, DNA/ RNA analysis, drug discovery and drug screening but the implementation of single-cell technique is beset with problems. Ascertaining accurate information of single-cell from a whole sample mean response is near-impossible. To address the single-cell characterization, the experimental setup has been developed in my previous work shown in Figure 1. Which work for the simultaneous imaging and detection. A laser diode (near-UV 405 nm, 10 mW used for a particular application), and 4-f lens system was used as the precisely illuminate tiny spot. In the beam path, the collimated beam was focused as a tiny spot on the sample plane by using another biconvex

lens. A polydimethylsiloxane (PDMS) microfluidic device was placed in the sample plane. The micro channel developed inside the microfluidic device was used as a sample-carrier to flow the sample, the design and development of which is discussed in the fabrication section. The micro-objective 40X is placed immediately after the microfluidic channel to collect the light transmitted through the sample. A beam splitter (BS) was placed in the same path in-between the micro-objective and the tube lens. The transmitted and reflected light path directly reaches the camera through the tube lens and photodetector. A condenser lens f = 40 mm was used to focus a tiny spot on the active area of the detector. The photodetector is connected to a microcontroller which records the optical signal. The data recorded here is through the manual synchronization of camera and detector. *In the present work, much valuable progress would be initial characterization and setting-up of absorption thresholds for malaria infected and uninfected blood cells.* Moreover, the image and signal acquired would be analyzed with a new AI-based framework. The exemplified threshold is implemented in the redesigned user-friendly handheld device (Figure 2).

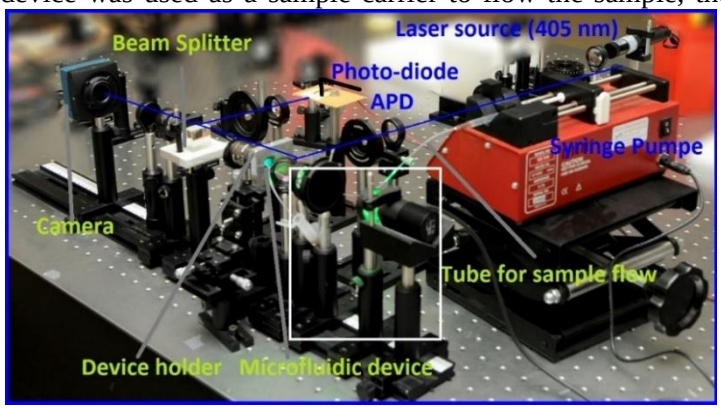

Figure 1 Experimental setup for characterization of malaria infected and healthy RBC high throughput microfluidic system

Project Implementation Plan: Smart Point-of-Care Device development for malaria screening

This project proposal main aim is for the Re-Engineer the current lab-based absorption flow-cytometer that has been developed for malaria detection in the previous work shown in Figure. 2 with industrial component and incorporate additional features like AI-enabled analysis in the current AFCM. It involves a novel microfluidic design to perform the sorting of blood cells automatically and enable single cell flow. As we knew, single-cell analysis offers huge advantages over whole sample assays like single-cell analysis offers precise information of the molecular and optical properties of individual cells. More details of schematic and preceding work are available in my previous research articles references [26-28]. The overall cost of the present basic laboratory is around 1000 USD. However, the final prototype cost may reduce while mass production takes place. **Sample Size:** Sample collection will be taken from Ispat General Hospital, Rourkela. The sample size would be 400 (Normal and infected). Statistical analysis will be performed on the signal data received from PoC device.

Figure 2: Developed Lab type prototype for same analysis using simple source, microfluidic device and simple electronics for malaria diagnosis at Point-of-Care (27)

AI based framework: The focus of the work is to deploy the advancements in an optofluidic instrument to detect/ screen and classify malaria at point-of-care from a small drop (5 to 10 µl) of whole blood. An automated algorithm would be developed using AI/ ML algorithms for screening malaria positive or negative quantitatively from the subject. This will facilitate the automated count of hundreds of thousands of normal and infected cells and the test case is ***plasmodium falciparum*** samples. More explicitly, the goal is to introduce time-based denoising and drift removal techniques to enable better identification of cell-specific peaks in the signal. Mean-centering will be used for removing overall DC level and drift in the detector signal. Following this, the signal will be normalized, and peaks will be detected. The signal will be partitioned into small temporal windows which will be averaged and filtered to remove high-frequency noise. Handcrafted features will be automatically extracted from the filtered

sample signal. These features will be fed to Machine learning models for classification.

Algorithm and technique involved: In the current project, we are interested to extensively use RL algorithms for automatic screening of malaria using **signal data**. This environment and agent interaction is considered as Markov Decision Process (MDP). Here, we are going to study different Markov models and compare the results with state-of-the-art machine learning and deep learning algorithms. Steps involved in the implementation of the policy gradient reinforcement algorithm is given below: Hand crafted feature extraction from the data is helpful for training. Development of an Agent and creation of an objective function based on the influencing parameters. Strength of the algorithm depends on the optimal selection of Agent and the objective function (Policy).

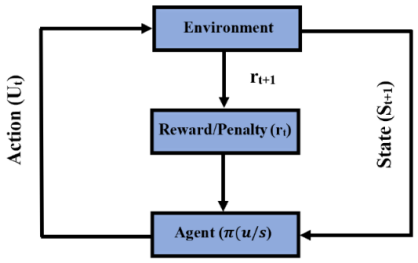

Figure 3: Flow diagram of Reinforcement Learning

- Assigning formal work to Agent through a well-known framework known as Markov Decision Process (MDP) which helps in taking the decision to be made at each state. This gives rise to sequence of states, actions and rewards, known as trajectory.
- The gradient of the rewards is determined such as derivative of expected reward is expectation of product of reward and gradient of log of policy
- The optimized path is determined using the policy gradient algorithm for automatic classification of malaria infected and uninfected cells.

Outcome(s): The proposed work plan is for three years: the vision and excepted outcomes are portrayed as following:

- The work proposal brings a compact, battery-operated, Low-cost smart AI enabled PoCD instrument for malaria screening and this would be implemented for limited clinical trials.
- Development of GUI based algorithm for malarial parasite detections, stages of infection, quantitative information of infected cells from overall assessed sample.
- The vision of research will bring high impact factor publications on developed AI algorithms and developed device and filing national and international Patents on the developed technology.
- The most important outcome is creating a research and development platform at NIT Rourkela, in the department of Biotechnology and Medical Engineering.
- Of course, this work generates employment and provides the necessary training to individuals.
- The complete reports and user manual will be prepared for further use and commercial enhancement.

Impact of Research proposal/significance and clinical applications:

This research will be conducted on the custom developed hyper Imaging system where morphological and optical properties of cells can be characterized at single cell level. Owing to its capabilities of capturing morphological and analytical properties of cells at different length scale, it could be used for studying sub-cellular interaction withs drugs, nanoparticles etc. to facilitate drug/nanoformulation discovery. The design and development of novel blood cells separation microfluidic channel will enable it to be fitted with hyper Imaging system like a USB. This will enable identifying cell morphology, deformability, blood flow velocity in a microfluidic platform. Further, this information can be analyzed by in-built AI/ML algorithm for rapid malaria screening in resource limited settings. The portable design of absorption flow cytometry can be deployed in any primary healthcare centers in developing and underdeveloped countries. Development of this type of product helps in early screening of malaria endemic zones which helps towards the eradication of malaria in these countries. The microfluidic USB could be fitted with portable absorption flow cytometer by any non-expert professional and could record and execute the data easily for malaria screening. The POC could be tailored to screen other diseases like dengue and anemia by modification in the microfluidic chip and algorithm.

Gantt chart for the execution of the Project

S No	Activity /Milestone	Months							
		01 – 12				13 – 24			
	Purchase of essential components and development of the experimental setup								
1.	**Primary objectives: develop a smart point-of-care instrument for malaria screening**								
Sub-objectives	Design and development of microfluidic device								
	-Microfluidic device design and Fabrication								
	- Optimization & Computational analysis								
	Development of setup Hyper-Imaging phase lock system for characterization								
	Re-design and fabrication of lab-based prototype to industry-grade prototype.								
	Testing and validation of the device in the lab setting and clinical validation.								
2.	**Development of AI-based framework for high throughput analysis**								
Sub-objectives	AI-based algorithm development for robust identification of biological cells in the sample								
	1. Design of experiments (DoE) for clinical validation of developed POC device								
	2. Validation and comparison of developed AI-based framework with the state-of-the-art techniques								
	3. Draft report on completion of project work, Possible patents and SCI publications								

References:

1. Programme GM. World Malaria report 2019. 232
2. Programme GM. world Malaria report 2021. WHO. 2021:322.
3. Medical Devices and Systems [Internet]. (2006).
4. Amexo M, Tolhurst R, Barnish G, Bates I. Malaria misdiagnosis: effects on the poor and vulnerable. Lancet (London, England). 2004;364(9448):1896-8.
5. Endeshaw T, Gebre T, Ngondi J, Graves PM, Shargie EB, Ejigsemahu Y, et al. Evaluation of light microscopy and rapid diagnostic test for the detection of malaria under operational field conditions: a household survey in Ethiopia. Malaria journal. 2008;7:118.
6. Mukry SN, Saud M, Sufaida G, Shaikh K, Naz A, Shamsi TS. Laboratory Diagnosis of Malaria: Comparison of Manual and Automated Diagnostic Tests. Canadian Journal of Infectious Diseases and Medical Microbiology. 2017;2017:9286392.
7. Moody A. Rapid diagnostic tests for malaria parasites. Clinical microbiology reviews. 2002;15(1):66-78.
8. Lee SW, Jeon K, Jeon BR, Park I. Rapid diagnosis of vivax malaria by the SD Bioline Malaria Antigen test when thrombocytopenia is present. J Clin Microbiol. 2008;46(3):939-42.
9. Vo TK, Bigot P, Gazin P, Sinou V, De Pina JJ, Huynh DC, et al. Evaluation of a real-time PCR assay for malaria diagnosis in patients from Vietnam and in returned travellers. Transactions of the Royal Society of Tropical Medicine and Hygiene. 2007;101(5):422-8.
10. Padial MM, Subirats M, Puente S, Lago M, Crespo S, Palacios G, et al. Sensitivity of laser light depolarization analysis for detection of malaria in blood samples. Journal of medical microbiology. 2005;54(Pt 5):449-52.
11. Peng WK, Kong TF, Ng CS. Micromagnetic resonance relaxometry for rapid label-free malaria diagnosis. 2014;20(9):1069-73.
12. Chen L, Huang Y, Bhagat AA, Nguyen NT.
13. Kozicki M, Creek DJ, Sexton A, Morahan BJ, Wesełucha-Birczyńska A, Wood BR. An attenuated total reflection (ATR) and Raman spectroscopic investigation into the effects of chloroquine on Plasmodium falciparum-infected red blood cells. Analyst. 2015;140(7):2236-46.
14. Breslauer DN, Maamari RN, Switz NA, Lam WA, Fletcher DA. Mobile phone based clinical microscopy for global health applications. PloS one. 2009;4(7):e6320.
15. Bishara W, Sikora U, Mudanyali O, Su T-W, Yaglidere O, Luckhart S, et al. Holographic pixel super-resolution in portable lensless on-chip microscopy using a fiber-optic array. Lab on a Chip. 2011;11(7):1276-9.
16. Wood BR, Bambery KR, Dixon MW, Tilley L, Nasse MJ, Mattson E, et al. Diagnosing malaria infected cells at the single cell level using focal plane array Fourier transform infrared imaging spectroscopy. Analyst. 2014;139(19):4769-74.
17. Cojoc D, Finaurini S, Livshits P, Gur E, Shapira A, Mico V, et al. Toward fast malaria detection by secondary speckle sensing microscopy. Biomed Opt Express. 2012;3(5):991-1005.
18. Pai NP, Vadnais C, Denkinger C, Engel N, Pai M. Point-of-care testing for infectious diseases: diversity, complexity, and barriers in low- and middle-income countries. PLoS medicine. 2012;9(9):e1001306.
19. Palmer T, Aiyenigba AO, Bates I, Okyere DD, Tagbor H, Ampofo GD. Improving the effectiveness of point of care tests for malaria and anaemia: a qualitative study across three Ghanaian antenatal clinics. BMC Health Services Research. 2020;20(1):444.
20. Zhu H, Mavandadi S, Coskun AF, Yaglidere O, Ozcan A. Optofluidic Fluorescent Imaging Cytometry on a Cell Phone. Analytical Chemistry.2011;83(17):6641-7.
21. Pirnstill CW, Coté GL. Malaria Diagnosis Using a Mobile Phone Polarized Microscope. Scientific Reports. 2015;5(1):13368.
22. Gopakumar GP, Swetha M, Sai Siva G, Sai Subrahmanyam GRK. Convolutional neural network-based malaria diagnosis from focus stack of blood smear images acquired using custom-built slide scanner. Journal of biophotonics. 2018;11(3).
23. Patankar S, Sharma S, Rathod PK, Duraisingh MT. Malaria in India: The Need for New Targets for Diagnosis and Detection of Plasmodium vivax. Proteomics Clinical applications. 2018;12(4):e1700024.
24. Sahu SS, Gunasekaran K, Jambulingam P. Field performance of malaria rapid diagnostic test for the detection of Plasmodium falciparum infection in Odisha State, India. The Indian journal of medical research. 2015;142 Suppl (Suppl 1):S52-8.
25. Siwal N, Singh US, Dash M, Kar S, Rani S, Rawal C, et al. Malaria diagnosis by PCR revealed differential distribution of mono and mixed species infections by Plasmodium falciparum and P. vivax in India. 2018;13(3):e0193046.
26. Banoth E, Jagannadh VK, Gorthi SS. Single-Cell Optical Absorbance Characterization With High-Throughput Microfluidic Microscopy. IEEE Journal of Selected Topics in Quantum Electronics. 2016;22(3):111-6.
27. Banoth E, Kasula VK, Gorthi SS. Portable optofluidic absorption flow analyzer for quantitative malaria diagnosis from whole blood. Applied optics. 2016;55(30):8637-43.
28. Banoth E, Kasula VK, Jagannadh VK, Gorthi SS. Optofluidic single-cell absorption flow analyzer for point-of-care diagnosis of malaria. Journal of biophotonics. 2016;9(6):610-8.

Proposal Title: A Laser Helmet Device for Transcranial Infrared Laser Stimulation: A Home-Based Approach for the Treatment of Dementia

Research Category: Biomedical Optics, Therapeutic Laser Applications

EXECUTIVE SUMMARY

A little boy's response to the question, "What is the scariest thing in the world?" was, "The unstoppable nature of time, which slowly leads us all to an inevitable death." Surprisingly, this is quite accurate, despite coming from a little child. Our bodies age and become less functional over time until their ultimate demise. Nonetheless, though the ultimate demise is inevitable, certain comorbidities associated with old age are somewhat avoidable and/or reversible. A considerable proportion of elderly individuals, for instance, are afflicted by a group of disorders that cause progressive deterioration in cognitive function, despite having many more years to live. These disorders, collectively called "dementia," are neurologic dysfunctional diseases characterized by variable degrees of cognitive impairment and other neurologic functional insufficiencies that diminish the quality of life (QoL) in old age. Medical professionals, as directed by allopathic medicine, have sought effective therapies for these conditions for many years with very limited success, and to date, approximately 50 million people are afflicted with dementia on a global scale, with projections indicating that this number will nearly triple by 2025 (Arvanitakis et al. 2019). How, then, can we combat dementia so that our journey through life is enjoyable even in old age?

This work aims to build a home-use-compatible bioactive laser device for transcranial infrared laser stimulation (TILS) as a method of treating dementia. TILS is a form of photobiomodulation in which bioactive, frontal lobe-penetrating lasers are utilized to stimulate the proliferation and regeneration of neuronal cells and neural vascular tissue. It uses near-infrared light to enhance the proliferation of cells, improve circulation, and reduce inflammation (Caldieraro and Cassano 2019). Two arguments support the use of TILS to treat dementia. First, because the various types of dementia involve either one or a combination of cellular degeneration of brain cells, impairment of vascular tissue, and/or the occurrence of diffuse inflammation; and second, because the pathological mechanisms associated with dementia indicate that cognitive decline is acquired rather than developmental. Hence, TILS could efficiently reverse degeneration. In this project, therefore, a laser gadget will be constructed, housed for both clinical and home usage, and utilized in a Johannesburg population of dementia-stricken adults. *In vitro* performance evaluation will be followed by *in vivo* administration of diverse dosages and fluencies of TILS. Measures of brain activity, including the psychomotor vigilance task (PVT) and delayed match-to-sample (DMS) memory task, will be conducted on all experimental and placebo groups after dose administration to determine the effect of this laser device.

This study's primary outcome is a potentially efficacious and cost-effective alternative therapy for treating dementia. The device developed in the study will be patented, and subsequent studies and prospective phases of clinical trials will be done with the ultimate goal of establishing this therapeutic alternative as a clinically authorized treatment. Besides, to ensure accessibility, the design of this product is intended to be convenient for home use, allowing people with dementia to be treated at home without making random visits to a clinic where a stationary laser device is held.

TITLE: A Laser Helmet Device for Transcranial Infrared Laser Stimulation: A Home-Based Approach for the Treatment of Dementia

PI: Elvin Peter Chizenga, PhD Health Sciences (Biomedical Science)

1. BACKGROUND

Dementia is the most prevalent disease of old age, but no one expects to develop it because there are no reliable predictors. According to the World Health Organization (WHO), more than 55 million people worldwide have dementia, with nearly 10 million new cases as of 2023 (WHO factsheets, 2023). It is currently one of the leading causes of disability and dependence among older people worldwide, resulting in a significant decline in quality of life (QoL) and death. Despite having distinct causes, the pathology of the different types of dementia is remarkably similar, involving mechanisms that are acquired and amenable to reversal using an innovative photobiomodulation (PBM) technique called Transcranial Infrared Laser Stimulation (TILS), a technique in which light is irradiated through the frontal bone, resulting in neural tissue's absorption of photons that influences biological functions including gene expression, signaling pathway activation, chemical synthesis, and influence on molecular metabolic mechanisms. Hence, due to the fact that the pathologic mechanisms of dementia involve a decline in function, the photobiomodulatory effect of TILS may be able to reverse dementia, as suggested by a small number of pre-clinical and clinical studies. Below is a brief description of the proposed study, outlining the current state of the literature, the desired objectives, the proposed methodology, and the potential outcomes and impact of the study.

2. LITERATURE REVIEW

2.1 Dementia

Dementia includes a group of disorders involving a major neurocognitive deficiency that affects memory, cognitive abilities, and behavior, ultimately interfering with one’s ability to perform daily activities (Raz et al. 2016). The variety of dementia subtypes and other dementing conditions are described on the basis of etiology, clinical presentation, and/or pathologic findings, regardless of the fact that the different subtypes frequently co-occur, rendering their classification somewhat impractical for intervention purposes. Nonetheless, Alzheimer's disease (AD) is the most prevalent form of dementia, accounting for over 60 percent of all cases, followed by other less prevalent types, including vascular dementia (VD) and Lewy body disease (LBD). Less common neurodegenerative dementias, including frontotemporal dementia, prion disease, and pick disease, also occur in other populations. Despite these classifications, and though aetiologies and severity may differ, all types of dementia share common molecular mechanisms, which may include either one or a combination of hypoxia and oxidative stress, neuroinflammation, accumulation of misfolded proteins, mitochondrial insufficiencies, neural tissue degeneration, and blood-brain barrier permeability. To date, approximately 55 million people worldwide suffer from dementia, a number that, without intervention, is expected to triple by 2050 (Raz et al., 2016, WHO Factsheets, 2023).

2.2 Laser physics and biological interactions

In the absence of effective dementia treatments and interventions, light has emerged as a possible game-changer. The interaction of light with biological tissues is very intricate, resulting in measurable effects in tissues after they absorb photons of light. PBM involves the utilization of light from the visible and near-infrared portions of the spectrum at a relatively low power density that is insufficient to heat or burn tissue but capable of instigating biological reactions when the photons themselves stimulate chemical changes within the cells (de Freitas & Hamblin 2016). On top of that, light absorption by ion channels forces the release of Ca^{2+}, a cation that stimulates both the activation of transcription factors and the expression of genes in the nucleus. In the end, this interaction affects cell metabolism and cell growth kinetics.

Additionally, the level of cellular function is influenced by and limited by the amount of energy available at any given time. An important enzyme called cytochrome c oxidase (COX), along with other factors, is responsible for oxygen consumption in the cells, which initiates processes that ultimately produce adenosine triphosphate (ATP), the primary fuel for every cell (Kadenbach 2018). The mechanism of energy production involving COX in the mitochondrial respiratory chain can be stimulated by red or NIR light during PBM. Moreover, increasing the perfusion of blood and tissue oxygenation provides enough raw material for metabolism. Therefore, PBM stimulates not only neural cell proliferation but also the proliferation of cells in blood vessels, causing angiogenesis. Other processes stimulated by PBM include the activation of anti-inflammatory processes, anti-apoptotic mechanisms, and antioxidant responses. Besides, evidence of psychomotor changes after brain irradiation with suitable light suggests the existence of additional intracellular and extracellular signaling mechanisms that have not yet been identified.

2.3 Transcranial infrared laser stimulation as a therapeutic option for dementia

PBM is therefore be a better alternative to treating dementia because the common feature in all forms of dementia is cellular degeneration, involving the neural cells, vascular tissue or surrounding connective tissue stroma, besides the accumulation and infiltration of misfolded proteins i.e., amyloids. Therefore, a regenerative, photobiomulatory effect is required to reverse dementia. TILS uses longer wavelengths of laser light preferably in the far red or near infrared region (NIR) to stimulate the functional ability of the brain by irradiation through the frontal bone (Holmes et al. 2019). Though transmittance is never 100%, the amount of light that reaches the brain tissue has enough photons to cause the biological effects of PBM resulting in effective reversal of cellular degeneration and possibly increased regeneration of functional cells and stem cells. Ultimately, TILS enhances metabolism, induces neuroprotective responses, increases blood flow and neurogenesis, and reduces inflammation and oxidative stress. Until now, the beneficial effects of TILS have been reported in numerous practical cases, and measures of brain activity such as psychomotor vigilance task (PVT) and delayed match-to-sample (DMS) memory task have demonstrated this effect (Holmes et al. 2019). To date, TILS is the most promising therapeutic option for dementia because living tissue is essentially permeable to light in the red and NIR regions, and second because dementia is a disease that affects the frontal lobe of the brain, both these making the penetration of light through the frontal bone a brilliant non-invasive, safe and efficacious treatment for the disease.

3 PROBLEM STATEMENT AND OBJECTIVES

The incidence of dementia is exponentially increasing, and projected to triple by 2050. To date, there is no curative therapy for dementia, other than symptom management using allopathic medicines and remedial approaches. The introduction of newer technologies is therefore not only necessary, but critical. In addition, human diversity involving varying skin profiles, bone and tissue thickness, which are significant biological properties with varying optical densities, requires an inclusive approach in the design of light therapies. Besides, new approaches need not only to be efficacious, but also accessible and cost-effective. The aim of this study is therefore to design, construct and assess the usability of a novel helmet laser device comprising of multiple light parameters of compatible semi-conductor diode lasers, assembled for home use, which can potentially be used for TILS to treat dementia, in different populations. The objectives are set out as follows:

- Construction of a multi-channel laser helmet of class-IV lasers with three wavelengths
- *In vitro* assessment of the prototype on commercial cell lines and bioinformatics studies
- Performance of a first-in-human medical device trial at three sites in Johannesburg
- Assessment of treatment using psychological screening, metabolic assessment, and determination of molecular patterns
- Study close-out procedures, and regulatory affairs for medical device registration or continuation to a larger trial, depending on the significance of the first trial results

4 OUTLINE OF TASKS/WORK PLAN

4.1 Study plan, design and location

The research is a multi-disciplinary approach comprising of mixed-methods research design including a pre-clinical experimental analytical study and a follow up first-in-human medical device trial, which will be conducted in partnership with participating collaborators including Corning Inc. for helmet fabrication and the African clinical research organization (ACRO), a certified commercial contract research organization (CRO). The prototype design and laboratory work will be conducted at the university of Johannesburg, departments of biomedical engineering and biomedical sciences, respectively. The first-in-human medical device trial will be conducted at three trial approved sites in Johannesburg, South Africa, which will be confirmed after a feasibility study within the research period.

4.2 Timelines

The research will be conducted over a period of five years, from January 2024 to December 2029, divided into two research periods with definite conclusions and outcomes. Period one (January 2024–December 2025), indicated elsewhere as P1, will be used for development, in vitro investigation, and site feasibility, followed by period two (January 2026–December 2029), indicated elsewhere as P1, which is allocated for the first-in-human medical device trial of the laser helmet device. The actual trial in period two will be conducted over a period of no more than 14 months: 3 months start-up; 6 months from First Patient In (FPI) to Last Patient In (LPI); 2–3 months from LPI to Last Patient Visit (LPV); and up to 6–8 weeks (1–2 months) from LPV for database lock, study close-out, and notification of the end of the study. The extra time is allocated for regulatory affairs and waiting periods.

4.3 Laser optimization, prototype design and fabrication (P1)

To construct the custom helmet device, three wavelengths that have been widely investigated in both animal and clinical models will be purchased from Thorlabs. The optimization of PBM parameters and dosimetry to maximize effectiveness and tolerability will be conducted before fabrication. Final fabrication onto the custom helmet device will be done in collaboration with Corning Inc. The final product will hold a multi-channel module combining three class-IV lasers, single and multiple switch modes, and three wavelengths including 1064, 960 and 830 nm, with the following details:

- A 1064 nm, 110 mW, Butterfly DBR Laser, PM Fiber, FC/APC, Internal Isolator (Thorlabs)
- A 960 nm, 250 mW, Ø9 mm, H Pin Code, Laser Diode (Thorlabs)
- An 830 nm, 300 mW, Butterfly Laser Diode, PM Fiber, FC/APC (Thorlabs)

The single and multiple switch options will enable irradiation of each wavelength singularly or combined for varying therapeutic plans and doses. This form of fabrication will allow for multiple therapeutic options for different skin types, i.e., melanin content, hydration, i.e., normal, dry, or oily, and anatomical variations, e.g., thick, wrinkled, etc.

4.4 Assessment of product properties and *in vitro* cellular responses (P1)

Assessment of the laser's biological properties will be done using *in vitro* cell culture, irradiation, and analysis of cellular responses post-irradiation. Neural progenitor cells derived from XCL-1 GFAPp-Nanoluc-Halotag, (ATCC) for assessment of neuronal differentiation, and HPAEC-BMI1 (ATCC), a primary human pulmonary endothelial cell to be used for investigation of the pro-angiogenic effects of irradiation, will be cultured in treated in cell culture dishes (Corning Inc.) and irradiated. Cellular responses, including the CellTiter-Glo luminescent cell proliferation assay (Promega), the CytoTox 96® non-radioactive cytotoxicity assay (Promega), and Trypan blue viability assays, will be used for post-irradiation.

4.5 First-in-human medical device trial operation (P2)

This part of the research will be conducted in collaboration with ACRO for trial regulatory affairs and trial motoring. A total of 20 participants, i.e., the maximum for this type of study, including experiment and placebo groups, will be invited to participate in the study. Participants for TILS will be recruited from trail-approved sites, as determined after a site feasibility study, in Johannesburg, South Africa. The CRO will handle most aspects of this phase, as South African regulation requires only certified organizations to register and conduct human trials. The results of the in vitro experiments and bioinformatics studies will influence the course of the trial.

4.6 TILS Procedures (P2)

The device will be designed to target the dorsolateral prefrontal cortex, i.e., Brodmanns' area 9, and the anterior prefrontal cortex, i.e., Brodmanns' area 10, and the light will be delivered using two to three sessions of TILS, delivering an adjustable dosimetry including an option for single or multiple wavelengths, varying power outputs per wavelength, and a fluence that will be determined in the pre-clinical assessment, which could be anything between 10 and 90 J/cm^2. The time of irradiation will be determined from the fluence used and calculated based on the estimated transmittance and amount of light reaching the tissue surface. A test of function will be conducted before, during, and after treatment at varying dose intervals. The following tests will be conducted to assess the effect of TILS:

- PVT
- DMS memory task
- Positive and Negative Affect Schedule (PANAS)
- Psychology experiment building language (PEBL),
- Sensation-seeking scale (SSS)
- Tri-Dimensional Personality Questionnaire (TPQ),

Measures of metabolic function will also be performed before, during, and after treatment using diffuse optical spectroscopy (DOS) to determine oxygen saturation, blood flow, and any significant anatomical variations induced by therapy.

4.7 Ethical considerations (P1 & P2)

All relevant Institutional Review Boards (IRB), including the University of Johannesburg's research ethics committee and national regulatory bodies, will be consulted, and ethical clearance will be sought to ensure that the risks are reduced and are outweighed by potential benefits. All participating old-age homes should be consulted and given the details of the study to give consent and clearance to conduct research. The following ethical principles The study will include adults aged 55 and above who will take part in the study on their own volition. In the case of cognitive incapacitation (i.e., severe dementia), approval from a legal relative or guardian will be solicited, and participation will be approved after clinical assessment by the collaborating neurologist. A unique digital identifier will be assigned to each participant to protect their privacy, confidentiality, and anonymity. All files harboring names will be stored securely in a locked cabinet on password-protected computers, as required by law. The researchers do not anticipate any risks to participants from participating in this study. Only participants with an approved clinical report by a neurologist will be recruited. Clinical assessment will be done by an experienced neurologist certified by the Health Professionals Council of South Africa (HPCSA). The lasers used in this study are safe and have not been linked to any health disruption based on previous clinical studies in a similar context. A direct benefit to participants will be the free consultation, disease assessment, and therapy, which may influence their health outcomes.

5 OUTCOMES

5.1 Research Findings

The main outcomes of this present study are: first, a prototype of the laser helmet device that is intended for use in TILS; and second, proof of concept and medical application of the newly fabricated laser device. The two research periods are distinct but sequential, with each period dependent on the outcome of period one. Similarly, the conclusion of the first in-human medical device trial will depend on the significance of the results. In the end, the results of this study will largely be suggestive of the way forward before possible mass production of the confirmed device.

5.2 Academic Outputs and publications

		Study Period
Year one:	Prototype laser helmet device Patent application	Jan 2024-Dec 2025
Year two:	*In vitro* studies complete 2 MSc dissertations 1 journal publication	Jan 2025-Dec 2026
Year three to five:	Proof of concept of medical device In-human evidence Product registration or larger study 1 journal publication Conference presentation and proceeding	Jan 2027-Dec 2029

6 IMPACT

This research will alter the global trajectory of dementia interventions. The WHO global action plan on the public health response to dementia 2017–2025 has given theoretical focus to the public health management plan for dementia but lacks the inclusion of a permanent solution to treating the condition. Hence, this research is an initiative for a permanent solution, and the success of this study will introduce an innovative therapeutic technique that is safer, more convenient, more cost-effective, more efficacious for dementia, and more inclusive for diverse population groups. Note that the end point of research could either be medical device registration and approval or the requirement for a larger study, depending on the significance of the outcome of the in-human therapeutic evidence. In the end, end-of-life years should be enjoyable with sound cognitive ability and pleasant experiences.

References

I. de Freitas, L. F., & Hamblin, M. R. (2016). Proposed mechanisms of photobiomodulation or low-level light therapy. IEEE Journal of selected topics in quantum electronics, 22(3), 348-364.
II. Holmes, E., Barrett, D.W., Saucedo, C.L., O'connor, P., Liu, H. & Gonzalez-Lima, F., (2019). Cognitive enhancement by transcranial photobiomodulation is associated with cerebrovascular oxygenation of the prefrontal cortex. Frontiers in Neuroscience, 13, 1129.
III. Kadenbach, B., (2018). Regulation of mitochondrial respiration and ATP synthesis via cytochrome c oxidase. Rendiconti Lincei. Scienze Fisiche e Naturali, 29(2), 421-435.
IV. Raz, L., Knoefel, J., & Bhaskar, K. (2016). The neuropathology and cerebrovascular mechanisms of dementia. Journal of cerebral blood flow and metabolism : official journal of the International Society of Cerebral Blood Flow and Metabolism, 36(1), 172–186.
V. WHO fact sheets (2023). Dementia, updated on.15 March 2023. Available at: https://www.who.int/news-room/fact-sheets/detail/dementia#:~:text=Key%20facts,injuries%20that%20affect%20the%20brain. Accessed on 28 June 2023.

Democratizing Shortwave Infrared Imaging with Avalanching Nanoparticles

Executive Summary – Information Challenge

Emma Xu, Columbia University, NY, emma.xu@columbia.edu

The challenge: Shortwave-Infrared (SWIR) refers to wavelengths between approximately 1 and 2um. Imaging in SWIR can provide crucial information about systems that cannot otherwise be obtained with visible light. Thus, SWIR is vital to many industries, including semiconductor, agriculture, and healthcare.

Despite its wide range of potential uses and impact, commercially available SWIR cameras are extremely costly relative to visible ones ($20k+), dramatically limiting their accessibility. The key component within a SWIR camera is the photodetector (PD). Most of these cameras use Indium Gallium Arsenide (InGaAs) for the PD. While it has very high quantum efficiencies (QE) in the SWIR range, it is expensive, complicated to manufacture, and must be cryogenically cooled to reduce background noise. More recently, Colloidal Quantum Dots (CQD) have been demonstrated as a cheaper alternative PD material system; however, due to difficulties in controlling uniformity during synthesis, their tendency to degrade in air, and low QE, CQDs are still a long way from delivering a robust SWIR solution.

Proposed project: we propose to build a robust, high pixel density, highly sensitive, affordable, easy to manufacture SWIR camera with avalanching nanoparticles (ANPs) and Silicon sensors. Invented during my PhD, ANPs are nanocrystals that exhibit photon upconversion and photon avalanching (PA) phenomena. ANPs can not only convert SWIR photons into ones detectable by Silicon (Si), but the PA property also boosts the QE of this process to up to 40%. The inherent high nonlinearity of this material enables an ultra-high photon sensitivity. Importantly, ANP-based SWIR imaging circumvents the need for InGaAs and is compatible with Si-based complementary metal-oxide semiconductor (CMOS) sensors: a film of ANPs is simply deposited onto a substrate above a Si sensor, which upconverts SWIR light directly to Si-detectable wavelengths. The advantage is multifold: much lower noise can be achieved without cooling, and as a much more mature technology, the manufacturing of Si CMOS is cheaper, the pixel sizes are smaller, and the quality is higher. Compared to CQD, ANPs are also superior because they are extremely air- and photo-stable, and the synthesized uniformity is well-controlled. In terms of fabrication, InGaAs and CQD PDs require 10+ layer semiconductor deposition and lithography processes in the cleanroom. In contrast, ANP-based PDs just require spin-coating a layer of ANP onto a substrate.

	InGaAs	CQD	ANP
Signal-to-noise ratio	Low	Low	High
Uncooled	✗	✗	✓
Pixel density	Low	High	High
Photo- & air-stability	High	Low	High
Quantum efficiency	High	Medium	Medium
Fabrication	Hard	Hard	Easy
Cost	$$$$	$$$	$

Chart: side-by-side comparison of InGaAs, CQD, and ANP-enabled photodetectors across multiple performance factors.

This project has three major tasks: (1) investigate the ANP deposition. Because it is the first of its kind, we will develop a recipe for the concentration and layer thickness of ANPs needed for optimal SWIR photon detection; (2) optimize the coupling of light from the substrate into the Si imager; we will then characterize key performance parameters of this system, including its responsivity, QE, and signal-to-noise ratio; (3) finally, we will retrofit our ANP-based PD into a commercial camera and demonstrate SWIR imaging.

Intended outcomes: My ultimate goal is to commercialize this technology, and my near-term career plan is to graduate with a PhD from Columbia University in the Fall of 2023, and continue to develop this project as an Associate Research Scientist in 2024. The funding of the Optica Foundation Challenge will provide me with the capital needed to develop a first prototype of an ANP-based SWIR camera. This opportunity is pivotal because, with it, I can de-risk this game-changing technology and raise future funds to continue on the commercialization path, thus providing affordable, high-performing SWIR cameras to all.

Democratizing Shortwave Infrared Imaging with Avalanching Nanoparticles

Emma Xu, Columbia University, NY, emma.xu@columbia.edu

Literature Review

Shortwave Infrared (SWIR) refers to a range of wavelengths spanning roughly 1 to 2um. This region lies slightly beyond the wavelengths visible to the human eye. By capturing images in SWIR, valuable chemical and environmental data can be obtained for various systems that are not accessible using visible light alone. Consequently, SWIR imaging is critical in many industries, such as semiconductor manufacturing, agriculture, and healthcare. Its applications include inspecting wafers, sorting food products, conducting deep tissue imaging, and numerous others.

The key component of a SWIR camera is its photodetector (PD). The PD is made up of many pixels; they are arranged in 1D or 2D arrays. Each pixel is composed of two major parts: a photodiode layer that collects the incoming photons and subsequently converts them into electrical signals; then that signal is sent to a complimentary metal-oxide semiconductor (CMOS) readout integrated circuit (ROIC), which is coupled to the photodiode via different methods.

Indium Gallium Arsenide (InGaAs): While Silicon (Si) is the preferred material for most semiconductor applications, it falls short when it comes to SWIR because it is photosensitive to wavelengths only up to 1000nm. The incumbent SWIR technology uses InGaAs for the photodiode layer. InGaAs is a semiconductor compound engineered specifically to be sensitive in the SWIR region, with a quantum efficiency (QE) of 60-80% between 950 and 1650nm. This high QE, coupled with an extremely fast response time (ns), has made InGaAs the dominant SWIR detection solution on the market.

However, InGaAs also come with several major drawbacks. Intrinsic to its low bandgap, which makes it photosensitive to SWIR, it also has a higher dark noise. Compared to a Si camera, an InGaAs camera has dark current 6 orders of magnitude higher. The most prominent method to limit this adverse effect is to cryogenically cool the system with liquid nitrogen. Depending on the setup, the dark current can reach levels that are “only” 1-2 orders of magnitude higher than Si. [2] The cooling also comes at a spectral cost: as the temperature decreases, the photosensitive SWIR wavelength range shrinks. Hence, it loses the ability to detect the longer SWIR wavelengths. Another major disadvantage of InGaAs is the complicated nature of the PD fabrication. InGaAs photodiodes are produced with photolithography processes on 3- or 4-inch Indium Phosphide (InP) wafers in cleanrooms. They are then bonded to CMOS ROIC with indium (In) bumps. This process is complicated and costly; moreover, it limits the pixel size to ~20um to preserve the fidelity of the pixel quality. InGaAs image sensor chips, therefore, cost $10-20k a piece, and a full camera with built-in cooling and other add-ons costs in the $20-50k range.

Colloidal Quantum Dots (CQDs): In the past decade, researchers have exploited a new design for SWIR photodiodes using CQDs. A few startups have recently commercialized this technology. CQDs are semiconducting nanostructures that can respond to different wavelengths at different physical sizes. Compared to InGaAs, one major advantage of a CQD PD is its fabrication process. While ~10 layers of CQDs, transport, and electrode layers are needed, and the patterning of the pixels still needs to be done in the cleanroom, the process can be done on a CMOS ROIC monolithically. This reduces the pixel size (down to the length of SWIR waves), hence increasing the pixel density compared to InGaAs sensors.

However, CQD cameras also come with their own disadvantages. CQD systems tend to have QEs much lower than those of InGaAs PDs (<15% in SWIR), limiting their performance. There are multiple reasons for this: 1. QDs have low carrier mobility; 2. the size uniformity of QDs can be hard to control at the atomic scale during the synthesis, directly impacting the wavelengths they absorb; 3. QDs also are prone to degradation in air and moisture. Notably, the cost of commercially available CQD cameras remains high because of a. complicated fabrication, b. cooling is still needed to improve the signal-to-noise ratio, and c. an active illumination system is required to compensate for the low QE.

	InGaAs	CQD	ANP
Signal-to-noise ratio	Low	Low	High
Uncooled	✗	✗	✓
Pixel density	Low	High	High
Photo- & air-stability	High	Low	High
Quantum efficiency	High	Medium	Medium
Fabrication	Hard	Hard	Easy
Cost	$$$$	$$$	$

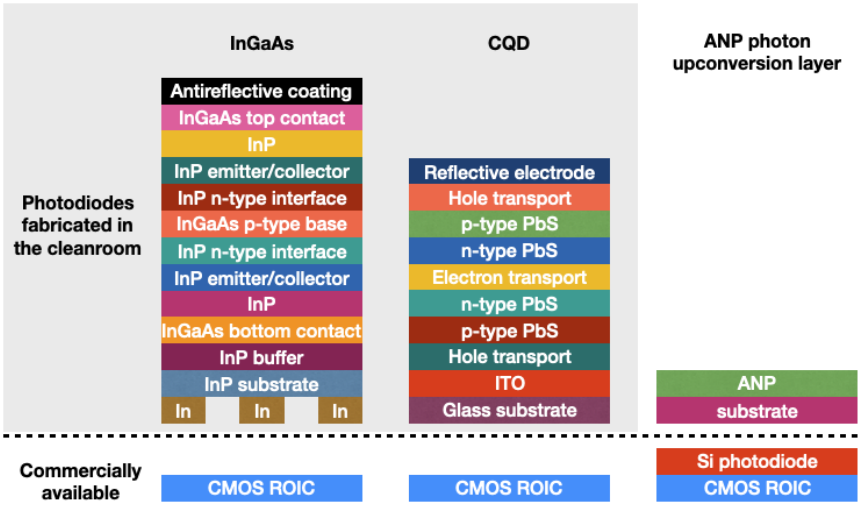

***Chart 1 (left)**: side-by-side comparison of InGaAs, CQD, and ANP-enabled photodetectors across multiple performance factors. **Figure 1 (right)**: the fabrication process of the three types of photodetectors. Note that in contrast to the ANP layer, which is simply spin-coated onto a substrate, both the InGaAs [3] and CQD [4] photodiodes need to be fabricated in the cleanroom.*

Avalanching Nanoparticles (ANPs): invented during my PhD, ANPs are nanocrystals that exhibit exceptional photon upconversion (UC) and photon avalanching (PA) properties. With UC, ANPs can convert SWIR wavelengths between 1 and 1.8um into wavelengths detectable by Si (<1um). With PA, ANPs can dramatically increase the historically inefficient UC process (usually 1%) up to 40%. [5] This giant leap in QE invites ANPs to be a serious contender in SWIR imaging. There are several other competitive advantages of ANPs: **I**. Compared to its colloidal counterpart CQD, the synthesis of ANPs is **highly uniform**, and the ANPs have **exceptional air- and photo-stability** over long periods of time (years). **II**. Instead of inventing a new PD device, we can simply couple ANPs to a commercially available Si CMOS imager (Si photodiode & CMOS ROIC in one product). The benefit of leveraging Si imagers is multifold: **(1), easy fabrication**: ANPs can simply be spin-coated onto a substrate, without needing cleanroom access; **(2), low cost**: the cost of ANP for the amount needed is negligible, and the Si imagers are very affordable compared to InGaAs (~ $100); **(3), low noise without cooling**: Si is an inherently low-noise system (due to a larger bandgap than InGaAs and SWIR CQDs), so no cooling is required to achieve the low-noise-level, which the other two systems cannot approach, even with cooling; **(4), saturation resistant**: in low light conditions when longer integration times are needed, the best InGaAs cameras saturate with dark noise after 2 minutes, while CMOS cameras can go for hours; **(5), high-quality pixels and high pixel density** have already been perfected over the decades of R&D efforts poured into Si semiconductor development. Of course, there are inevitably risks and limitations to this design, and I will address them in the following sections.

Objective

In this project, I propose to build the first ANP-enabled SWIR camera. Unlike all previous research on SWIR imaging that makes incremental advancements in InGaAs and CQD systems, this project is a paradigm shift in this field, as it will be the first system to combine efficient photon upconversion and Si-based imagers to achieve an affordable and highly functional SWIR imaging system.

Experiment Design

ANPs are ceramic nano-particles doped with rare-earth elements. The most common host matrix is $NaYF_4$. While several elements have been identified to exhibit the PA behavior, for this project, we will investigate Thulium (Tm)-based ANPs, since they have absorption peaks covering most of the SWIR band.

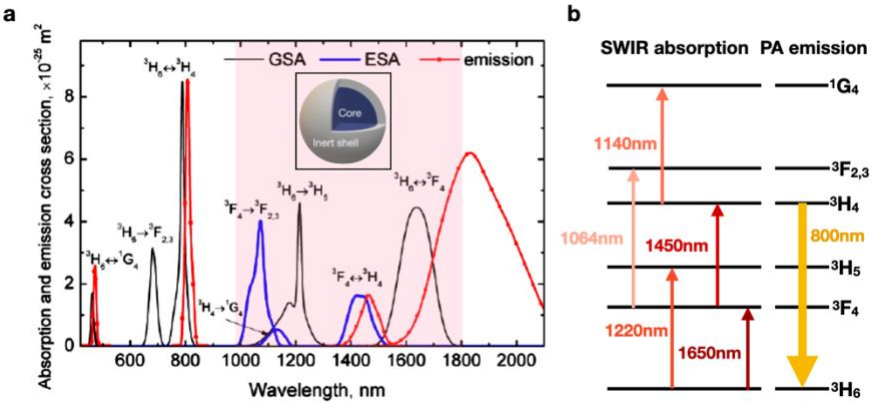

*Figure **2**: **a**, the absorption and emission spectrum of Tm.* [1] *GSA: ground state absorption; ESA: excited state absorption; shaded area: SWIR wavelengths ranging 1-1.8um. **Inset**:* the *core-shell structure of an ANP. **b**, the energy level diagram of Tm, the upward arrows are its absorption in SWIR, and the downward arrow is the PA emission.*

During PA, a population inversion is created at the excited state. That is, the number of Tm ions in an excited state exceeds that in the ground state. This phenomenon is responsible for the bright emission and the high QE of ANPs. To enable specific absorption peaks (the black and blue curves in Figure 2a) to benefit from PA, we will provide a seed excitation at the PA threshold intensity of the ANPs (dotted line in Figure 3a). The threshold intensity is on the order of a few kW/cm^2; this can be achieved with standard IR laser diodes (~100mW) and sheet illumination techniques. Moreover, the seed excitation also serves to speed up the detection process. ANPs usually have a long rise time, on the order of a few hundred milliseconds, to achieve population inversion. The introduction of the seed shrinks that time to <50ms [5], rendering them suitable for imaging applications. We have already established the viability of the seed approach in our lab (prelim. data not shown), measuring >100x enhancement in SWIR detection sensitivity.

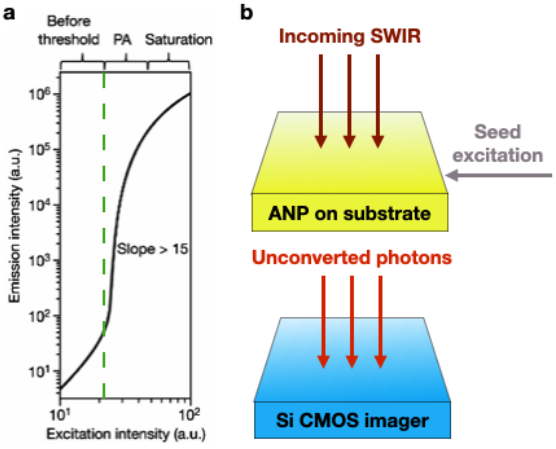

***Figure 3**: **a**, the s-shaped, high-slope curve of PA. Dotted line: PA threshold intensity. **b**, the schematic of SWIR detection with ANP and Si CMOS.*

The design of the ANP-enabled SWIR imager is the following (Figure 3b): a substrate with a deposited ANP film is mechanically fixed above a Si imager in close proximity; both elements have the same area. A seed excitation laser beam (e.g., 1450nm) enters the substrate from the side; it is guided via total internal reflection (TIR). The ANP layer thus gets excited to its PA threshold. Owing to their high nonlinearity, once seeded, ANPs are extremely sensitive to even a tiny amount of incoming SWIR photons. Upon external SWIR illumination, they

immediately absorb those photons and emit 800 nm light detectable by the Si imager. This seeding approach upgrades a slow multiphoton process (non-linear) into an efficient single-photon (linear) process.

Work Plan

While the fabrication process of making the photon upconversion layer can be straightforward, several engineering challenges must be addressed to build a working device.

1. Determine optimal ANP layer thickness and structure. It is important to systematically study ANP layer thickness and uniformity, optimizing for high absorption of the incoming SWIR photons, low scattering of the upconverted photons as they travel through the layer to the Si imager, and waveguiding properties of the seed illumination. This will be achieved through an iterative process of varying deposition parameters and performing spatially resolved characterization measurements (e.g., atomic force microscopy, optical absorption measurements) across the layer area (0.25-1cm^2).

2. Select the optimal seed excitation wavelength and intensity. There are two candidate seed wavelengths that lead to PA in our materials: 1064nm and 1450nm. We will begin by investigating 1450nm, which is promising because it is transparent to Si, and thus will not contribute any background noise. However, as I reported in our *Nature* paper on ANPs, the PA threshold intensity for 1450nm is more than a factor of 2 higher than that for the 1064nm excitation [5]. Thus, I will also study 1064nm as a seed, and carefully experiment with TIR conditions and the distance of the substrate to the Si imager to minimize noise. This will allow me to select an optimal seed wavelength after understanding the tradeoffs.

3. Optimally couple the seed excitation into the substrate. One major challenge is establishing a critical power density of the seed excitation as it enters the substrate. A 100mW laser diode, with a beam size of 10 mm^2 matched to the PD area, has a power density of only 1W/cm^2, well below the PA threshold. This will be overcome by condensing the beam in one dimension and illuminating it from the side using a cylindrical lens to achieve light sheet illumination. [6] This technique will result in power densities of 1-10kW/cm^2 that reach the PA threshold intensity. If further enhancement is required, the addition of mirrors on the sides of the substrate can be investigated, which creates an optical cavity.

4. Select the substrate material. The substrate is critical because it will need to support TIR of the seed illumination. We will explore transparent materials with different (wavelength-dependent) refractive indices (RI), ranging from silica glass (RI = 1.45), quartz (RI = 1.55), to dense optical flint glass (RI = 1.65).

Milestones:

i. By the mid-point of the project (middle of 2024), I will have made significant progress in the four tasks detailed above; I will have demonstrated basic SWIR detection with optical components in the lab.

ii. By the end of the project (end of 2024), I will have completed all the listed tasks. I will also have incorporated this design onto a commercial Si CMOS camera, performed SWIR imaging with it, and characterized initial performance factors.

I am currently a Ph.D. student at Columbia University, scheduled to graduate in the Fall of 2023. Beginning in January 2024, with the funding of the Optica Foundation Challenge, I will continue as an Associate

Research Scientist, and serve as the PI for this project. During my years as a Ph.D. student, I have successfully mentored high school, college, and MS students to complete research projects in the lab, as well as collaborated with scientists from all over the world. As the co-founder and CEO of a startup commercializing ANP-enabled novel technologies, I have also been leading a team of former postdocs to carry out business development activities. I firmly believe in the value of teamwork; thus, I will recruit 1-3 undergraduate and/or graduate students, whom I will mentor and lead for the project.

Outcomes

There are multiple expected outcomes: **(1)**, this project will be the basis for a publication and a patent, both of which are expected to be high-impact as they will serve as the foundation for all future ANP-based SWIR works. **(2)**, at the end of the project, we will have completed a **prototype of an ANP-enabled SWIR camera** and demonstrated its imaging capabilities. This prototype will enable me to raise future funding to continue the R&D and commercialization of this invention. **(3)**, it will become the thesis project for one or more students. The students will have gained hands-on experience solving problems ranging from optics to chemistry to engineering, they will thus be able to pursue a wide range of career paths after graduation.

Impact

The success of this project will have a significant impact on both research and industry. The utilization of ANPs for technological applications is quickly accelerating, as evidenced by a large number of citations (>135) already garnered by our ANP *Nature* paper published just 2 years ago. This project will represent the pioneering work demonstrating the feasibility of using ANP (and photon upconversion technology in general) for SWIR detection and imaging, forming the foundation of a new research discipline.

Moreover, there is a high demand for affordable SWIR cameras both commercially and scientifically. ANP-enabled SWIR cameras will be the first to offer affordability without compromising on performance. As mentioned earlier, by efficiently converting SWIR into Si-detectable wavelengths, we can reap the benefits of Si CMOS imagers for free, and access certain performance factors that are superior to the InGaAs counterpart: **significantly lower noise, no cooling needed, saturation resistant, high-quality pixels and high pixel density (high resolution).** These properties could render ANP-enabled SWIR cameras advantageous for many applications: silicon wafer inspection, plastic and glass sorting, defense and surveillance, etc. We will thus not only capture a sizeable segment of the current market, but also open up new markets that previously avoided SWIR due to its prohibitively high cost and other undesirable properties associated with InGaAs. In this sense, we will democratize SWIR sensing and imaging for all.

1. Peterka, P., et al., *Theoretical modeling of fiber laser at 810 nm based on thulium-doped silica fibers with enhanced 3H4 level lifetime.* Optics express, 2011. **19**: p. 2773-81.
2. Instruments, T.P. *Introduction to Scientific InGaAs FPA Cameras*. July 12, 2023]; Available from: https://www.princetoninstruments.com/learn/swir-nirii/intro-to-scientific-ingaas-fpa-cameras.
3. Wang, Z. and W.E. Nuri, *InP/InGaAS Symmetric Gain Optoelectronic Mixers*, in *Optoelectronics*, L.P. Sergei and M.B. John, Editors. 2013, IntechOpen: Rijeka. p. Ch. 4.
4. Vladimir, P., et al. *Switchable dual-band photodetector based on PbS colloidal quantum dots for multispectral short-wavelength infrared imaging*. in *Proc.SPIE*. 2021.
5. Lee, C., et al., *Giant nonlinear optical responses from photon-avalanching nanoparticles.* Nature, 2021. **589**(7841): p. 230-235.
6. Stelzer, E.H.K., et al., *Light sheet fluorescence microscopy.* Nature Reviews Methods Primers, 2021. **1**(1): p. 73.

Volcano-in-a-chip: Simulating CO_2 Uptake of Thermophiles under Extreme Conditions for Industrial Implementation

As carbon dioxide (CO_2) levels in the atmosphere continue to rise, new carbon-negative technologies are required to keep global warming well below the critical 2°C threshold. To achieve net-zero targets and foster circular economies, industries generating flue gases must adopt direct CO_2 capture mechanisms.
While engineered direct air capture system are still under development, natural systems are already well adapted for sequestering CO_2 from the environment, converting it into biomass or minerals. Bioreactors, equipped with precise control over light and CO_2 conditions, have shown potential for achieving high conversion efficiencies required at industrial scales. Nevertheless, existing bioreactors can only operate at ambient conditions, constrained by the requirements of the organisms involved. This limitation becomes apparent when dealing with industrial flue gases, which can reach temperatures as high as 100°C.
Recently, thermophile bacteria have been rediscovered thanks to their exceptional ability to sequester CO_2 at high temperatures. These microorganisms thrive near hydrothermal vents of volcanoes, having evolved to withstand extreme environments. Consequently, their implementation at industrial processing sites holds significant promise.
Incorporating thermophiles into current bioreactor designs presents significant technological challenges due to the need for precise environmental control. Conventional techniques like resistive heating are limited to broad and uniform heating, thus can not realistically simulate dynamic thermal conditions required by such microorganisms. Conversely, light-to-heat conversion offers a fast, easily implementable solution that enables precise localization of thermal conditions, making it a promising approach for addressing this issue.

This research project aims to explore the CO_2 sequestration capabilities of thermophiles under extreme conditions within a highly controlled microenvironment. To achieve this, we propose an advanced optofluidic system integrating digital holography, optical diffraction tomography, spatial light modulation and the efficient light-to-heat conversion via plasmonics, into a state-of-the-art optofluidic system with unprecedented thermal control. The system will facilitate precise thermal control, enabling the creation of spatially confined temperature gradients of up to 100°C, which closely mimic the complex environmental conditions encountered near volcanoes and within industrial processes.
By applying specifically designed optical fields on plasmonic nanostructures, we can induce and measure temperatures in situ with high accuracy through tomography. This feature will allow us to fine-tune our experimental protocols to identify the optimal growth conditions for thermophiles. Notably, the extended depth of field provided by digital holographic microscopy will enable us to monitor thermophile movement and growth in 3D while simultaneously measuring the induced temperatures.
Through careful control of the temperature landscape, we will guide thermophiles into desired structures, promote clustering, and thereby stimulate their growth. Further optimization of these protocols could potentially enhance the efficiency of CO_2 sequestration under less-than-ideal environmental conditions.
Assessing CO_2 sequestration of thermophiles under extreme conditions is a crucial first step in evaluating their performance in industrial settings. To achieve this, we will develop a miniature bioreactor prototype that enables exceptional optothermal control while precisely monitoring CO_2 conditions. This on-chip setup will facilitate the measurement of the CO_2 sequestration efficiency and allow for a direct comparison between ideal growth and simulated industrial conditions. The findings from this research will shed light on the potential of thermophiles as a viable solution for CO_2 capture in industrial applications.

This project holds the potential to yield significant insights into CO_2 sequestration using biological systems as an alternative pathway towards climate neutrality. On-site CO_2 capture directly at the site of emissions will provide the industry a quantitative tool for direct sequestration and storage, leading to more sustainable practises.
Advancing our understanding of thermophiles as key species in CO_2 sequestration will provide critical insights into the fundamental carbonic anhydrase process to enhance the efficiency of synthetic biofuel production and foster the development of alternative food and animal feed resources.
The significance of optics and photonics in the sustainable transformation of societies becomes apparent when considering their capacity to control microenvironments of biological systems. By promoting the broader utilization of optical tools across various industries, this research will enhance accessibility to these cutting-edge technologies for an interdisciplinary community, contributing to the broader goal of promoting sustainable solutions.

Volcano-in-a-chip: Simulating CO2 Uptake of Thermophiles under Extreme Conditions for Industrial Implementation

1. Literature Review

With continuously increasing carbon dioxide (CO_2) concentrations in the atmosphere, the development of CO_2 sequestration technologies are crucial to effectively limit global warming below the 2°C target. In industrial processing sites, the direct capture of CO_2 from flue gases before their emission into the atmosphere is particularly important. However, current direct air capture systems are inadequate for flue gas purification due to high concentrations of CO_2 and temperatures exceeding 100°C[1].

Alternatively, biological CO2 sequestration via enzymatic carbonic anhydrase (CA) offers a promising, cost-effective, and scalable approach. Certain thermophile bacteria are able to sequester CO_2 by binding it with metal ions to form carbonate, which permanently sediments to the ocean floor[2]. These thermophiles thrive in high temperature environments (>50°C) near underwater hydrothermal vents of volcanoes[3], where they have evolved to withstand extreme temperature variations. The remarkable heat resistance of thermophiles' carbonic anhydrase process is thus of particular interest for their application in industrial processes.

Notably, thermophile research has predominantly focused on studying them in non-ideal conditions such as bulk measurements, fixed temperatures and low CO_2 concentrations[4]. Such an approach overlooks their natural ability to navigate significant thermal gradients, which is a critical survival strategy[5,6]. To fully harness the potential of thermophiles for CO_2 sequestration, it is essential to provide them with the most suitable conditions and control their behaviour, including motility. The integration of optics and microfluidics in a unique optofluidic platform offers a viable solution. Whereas **microfluidics** provide the necessary microenvironment and better CO_2 control, **optics** allow for to real-time monitoring of thermophile behaviour and for precise manipulation of the local temperature landscape. This beneficial combination allows for the **induction and monitoring of local temperature changes** while **simultaneously tracking the entire thermophile population**.

Such an optofluidic platform could potentially enable **highly efficient CO_2 sequestration in bioreactors**[7] compared to conventional systems relying on large-scale reactor tubes with nonuniform CO_2 perfusion[8,9].

2. Problem Statement/Objective

2.1 Current limitations in the study of Thermophiles

Understanding the proliferation of thermophiles in complex environments is a crucial first step towards harnessing their CO_2 sequestration capabilities in bioreactors. So far, research on thermophiles has focused on studying their growth under bulk conditions, which can only simulate homogeneous temperature conditions and obscures individual responses to dynamic stimuli[4]. Moreover, creating the required high temperature environments is challenging, particularly in microscopy setups limited to temperatures below 50°C to prevent damage to the optical system. However, the biggest current limitation for studying the motility of thermophiles is the lack of fast and localised control over temperature and CO_2 concentrations.

We will first describe each individual challenge in more detail, before demonstrating how we can address each of them using a comprehensive optical tool box within a highly controlled microfluidic environment.

Bulk conditions: The growth of thermophiles has traditionally been studied under bulk conditions using large flasks or tubes placed in incubators at fixed temperature and CO_2 concentration[10]. This, however, neglects their ability to quickly adapt to changing environmental conditions by navigating strong temperature gradients[11]. Consequently, the inability to observe the motility of individual organisms hinders the understanding of their complex behavior under stress, which cannot be adequately addressed in bulk studies.

---

[1] Ma et al., Carbon Dioxide Sequestration by Microbial Carbonic Anhydrases From Submarine Hydrothermal Systems, *Front. Marine Sci.* **9**, 908818 (2022)
[2] De Luca et al., An *α*-carbonic anhydrase from the thermophilic bacterium Sulphurihydrogenibium azorense is the fastest enzyme known for the CO2 hydration reaction. *Bioorg. Med. Chem.* **21**, 1465-1469 (2013).
[3] Dick, The microbiomes of deep-sea hydrothermal vents: distributed globally, shaped locally, *Nat. Rev. Microbiol.* **17**, 271-283 (2019)
[4] Ahring and Westermann, Isolation and characterization of a thermophilic, acetate-utilizing methanogenic bacterium, *FEMS Microbiol. Lett.* **25**, 47-52 (1984)
[5] Demir and Salman, Bacterial thermotaxis by speed modulation, *Biophys. J.* **103**, 1683-1690 (2012).
[6] Dubay et al., Quantification of Motility in *Bacillus subtilis* at Temperatures Up to 84C Using a Submersible Volumetric Microscope and Automated Tracking, *Front. Microbiol.* **13**, 836808 (2022).
[7] Pasirayi et al., Microfluidic bioreactors for cell culturing: A review, *Micro and Nanosyst.* **3**, 137-160 (2011).
[8] Naderi et al. Investigating and modelling of light intensity distribution inside algal photobioreactor, *Chem. Eng. Proc.* **122**, 530-537 (2017).
[9] Huang et al. Novel flat-plate photobioreactors for microalgae cultivation with special mixers to promote mixing along the light gradient, *Bioresour. Technol.* **159**, 8-16 (2014).
[10] Ahring and Westermann, Isolation and characterization of a thermophilic, acetate-utilizing methanogenic bacterium, *FEMS Microbiol. Lett.* **25**, 47-52 (1984)
[11] Mehta et al., Insight into thermophiles and their wide-spectrum applications, *3 Biotech.* **6**, 81 (2016).

High temperatures: Studying individual organism requires high magnification microscope setups, which limits the maximum applied temperature to prevent permanent damage to optical elements. Although high temperature microscopy utilizing resistive heaters has expanded the temperature range[12,13] and demonstrated high heating rates (up to 100°C/s)[14], it lacks the ability to create localised heating or precise temperature gradients. The growth of thermophiles not only depends on the absolute surrounding temperature (which, for hyperthermophiles exceeding 70°C, surpasses current experimental realizations) but also on the precise spatial control of temperature.

Temperature gradients: The investigation of thermophiles under fluctuating temperature fields remains largely unexplored. While some early studies have demonstrated their ability to sense and move along stationary temperature gradients[11], harnessing this thermotactic behaviour to guide them in real time is yet to be demonstrated. Such guidance could provide unprecedented control over their localisation solely through temperature manipulation. The formation of localized clusters of cells is known to enhance survivability[15], suggesting that such controlled localization may lead to increased efficiency in CO_2 sequestration over extended periods.

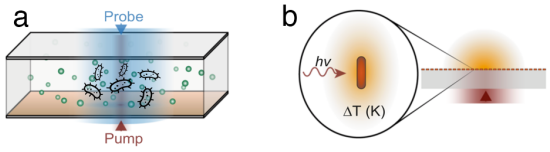

Figure 1: **Optothermal control** (a) Microfluidic chamber including bacteria and CO_2 control. (b) Light-to-heat generation with gold nanorods (adapted from Ref. 20).

The goal of this project is to **develop a microscopic system that allows for unprecedented high temperature control** with respect to its uniformity, temperature range, local confinement, and time. It allows us to monitor temperature while simultaneously observing thermophile behaviour at both an individual and population level. To address all of the above mentioned challenges, we propose a unique experimental setup comprising a microfluidic chip within an optical microscope.

We will employ four distinct optical methods - *digital holographic microscopy, plasmonics*, *spatial light modulation*, and *optical diffraction tomography* - synergistically within a single powerful setup. Utilizing digital holographic microscopy (DHM)[16], we can track individual cells in three dimensions despite cells moving out of focus under high magnification, thanks to its extended depth of field. This capability allows us to monitor the motility of the entire population, while observing their growth over time (Fig. 1a). For generating localized spots of high temperature, we will utilise a uniform coating of gold nanorods deposited on a cover slip. Upon irradiation with light, these nanorods produce localised surface plasmon resonances (LSPR), resulting in increased temperatures up to 100°C[17] (Fig. 1b). This approach enables selective heating of specific regions of interest, confining thermophiles locally and thus allow for longer observation of their growth without affecting equipment. The exact size and shape of the induced temperature fields can be precisely controlled via spatial light modulation of a single beam[18] (see Fig. 2). By splitting the beam into multiple ones, we can induce more complex temperature patterns including temperature gradients, which can be dynamically adjusted over time. Optical diffraction tomography (ODT) allows us to quantitatively assess the light-induced temperature maps in situ with high accuracy[19].

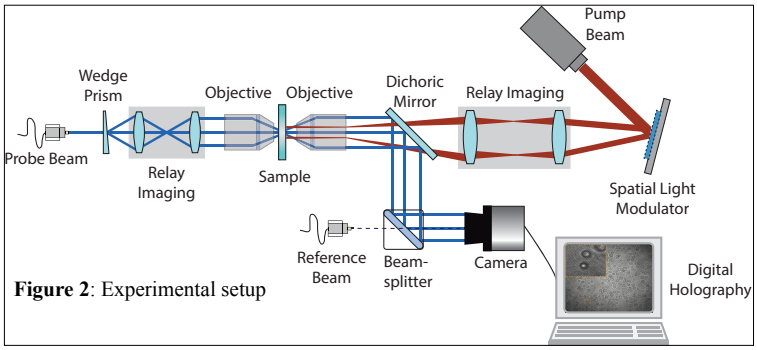

Figure 2: Experimental setup

Our research group has already developed a working experimental setup incorporating all mentioned[20], as depicted in Figure 2. With our existing expertise we are well-equipped to modify and adapt this setup to fulfil the requirements outlined in WP1.2.

Our system **addresses major limitations** of previously developed systems for studying thermophiles, **in a single, compact setup** enabling growth, motility and CO_2 sequestration on chip. It allows us to recreate natural volcanic conditions within a controlled microfluidic environment to determine the ideal conditions for efficient CO_2 sequestration. Importantly, we expect to **find significant improvements of their growth** when employing locally distributed

[12] Gluch et al. Motility and thermotactic responses of Thermotoga maritima. *J. Bacteriol.* **177**, 5473–5479 (1995).
[13] Herzog & Wirth Swimming behavior of selected species of Archaea. *Appl. Environ. Microbiol.* **78**, 1670–1674 (2012).
[14] Icha et al., Precise and Dynamic Temperature Control in High-Resolution Microscopy with VAHEAT, *Microscopy Today* **30,** 34-41 (2022).
[15] O'Toole et al., Biofilm formation as microbial development, *Ann. Rev. Microbiol.* **54**, 49-79 (2000).
[16] Kim, Principles and techniques of digital holographic microscopy. *SPIE reviews* **1.1**, 018005 (2010).
[17] Hutter and Fendler. Exploitation of localized surface plasmon resonance, *Adv. Mater.* **16**, 1685-1706 (2004).
[18] Molinaro et al., Life at high temperature observed in vitro upon laser heating of gold nanoparticles, *Nat. Commun.* **13**, 5342 (2022).
[19] Sung et al., Optical diffraction tomography for high resolution live cell imaging. *Opt. Express* **17**, 266-277 (2009).
[20] Ciraulo, Bernard, et al., Long-range optofluidic control with plasmon heating, *Nat. Commun.* **12**, 2001 (2021).

temperatures as opposed to bulk heating, which is a crucial step towards developing bioreactors for industrial processes.

Our objectives for understanding the behaviour of thermophiles inside a microfluidic environment are:

1. **Find the optimal growth conditions of 3 thermophiles under constant temperature and CO_2 conditions.** Under uniform temperatures inside our microfluidic chip we will investigate the growth of three species of thermophiles, Sulfurihydrogenibium azorense Az-Fu1[3], Thiomicrospira crunogena XCL-2[21], and Thermovibrio ammonificans HB-1[22], which have been selected for their fast replication rate, ability to sequester CO_2 and motility. The precise CO_2 control in microfluidics, combined with our digital holography, allows us to monitor the doubling of the organism and optically measure their biomass over time. This will enable us to identify the optimal parameter range before proceeding to more complex scenarios.
2. **Investigate the adaptability of thermophiles in a dynamically changing environment.** By introducing temperature gradients and fluctuations over time, we will monitor the real-time response of thermophiles to unfavorable conditions, measuring their motility in three dimensions. We will investigate how the motion of individual organisms could be guided with spatiotemporal control of temperature to form clusters, potentially leading to more optimal aggregation strategies. We anticipate minimal impact of the high-power near-infrared beams used for heat generation on bacteria, considering the optical transmission window of water in this spectrum.

2.2 The need for microfluidic bioreactors with CO_2 monitoring

Microfluidic bioreactors offer numerous advantages for cell culturing, such as reduced reagent volume, improved data quality, and seamless integration compared to conventional macroscale systems[10]. Moreover, they provide superior control over parameter such as temperature and CO_2 distribution throughout the system, which is challenging to achieve in conventional systems[23,24].
Having established the ideal growth conditions in section 2.1, we will design a specific **miniature bioreactor featuring precise CO_2 and pH control** under high temperatures. Moreover, we will add CO_2 and pH monitoring to our chip to assess successful CO_2 sequestration into carbonate. To develop specific biological assays for thermophile sequestration, we will collaborate with the microbiology group of Prof. Jörn Piel at ETH Zurich, experts in microbial interactions and metabolism. They also possess the necessary analytical instruments to detect bacterial metabolites. **Measuring CO_2 sequestration on-chip** will allow us to make first estimates on conversion efficiencies enabling a direct comparison between sequestration under ideal growth and simulated industrial conditions. Such insights are critical for evaluating if thermophiles could **potentially be applied for CO_2 removal in flue gases of industrial processes**.

The objective for our on-chip bioreactor is:

3. **Measure thermophiles' CO_2 sequestration under ideal and simulated industrial conditions.** Building on the tools developed in WP1, we will closely monitor changes in CO_2 and pH values to estimate the efficiency of the sequestration process. Under simulated near-industrial conditions, encompassing higher temperatures and larger fluctuations over time, we will estimate real-world efficiency rates for CO_2 sequestration.

3. Outline of tasks

3.1 Timeline

Gantt chart for Volcano-in-a-chip		Months											
Task		2	4	6	8	10	12	14	16	18	20	22	24
WP1	**Simulations of volcanic conditions on-chip**												
	Pre-Growth of thermophiles												
	Develop optical protocols for thermophile studies			D									
	Study thermophile growth and mobility under varying environmental conditions			M			D						
WP2	**CO_2 sequestration inside microbioreactor**												
	Add CO2 monitoring capabilities to microfluidic chip									D			
	Measure CO_2 sequestration in simulated industrial conditions								M				D

[21] Menning et al., Dissolved inorganic carbon uptake in *Thiomicrospira crunogena* XCL−2 is Δp− and ATP−sensitive and enhances RubisCO−mediated carbon fixation, *Arch. Microbiol.* **198**, 149-159 (2016).
[22] Gionavelli et al., Complete genome sequence of *Thermovibrio ammonificans* HB-1, a thermophilic, chemolithoautotrophic bacterium isolated from a deep-sea hydrothermal vent, *Stand. Genom. Sci.* **7**, 82-90 (2012).
[23] Naderi et al. Investigating and modelling of light intensity distribution inside algal photobioreactor, *Chem. Eng. Proc.* **122**, 530-537 (2017).
[24] Huang et al. Novel flat-plate photobioreactors for microalgae cultivation with special mixers to promote mixing along the light gradient, *Bioresour. Technol.* **159**, 8-16 (2014).

3.2 Work Plan

WP 1: Simulation of volcanic conditions on-chip (months 1-12)

Description: The goal of this WP is to investigate thermophiles under extreme environmental conditions. We will study their growth and motility under local and dynamic temperature maps.

Task 1.1 Pre-Growth of Thermophiles

We will start by growing three types of thermophiles (Sulfurihydrogenibium azorense, Thiomicrospira crunogena, Thermovibrio ammonificans) in bulk conditions inside an incubator. The measured growth rates at given temperature and CO_2 values will set the baseline with which we can compare our on-chip measurements with.

Task 1.2 Develop optical protocols for thermophile studies

Here, we develop specific spatial light modulation protocols for local temperature generation. The desired heat distributions can directly be tested via optical diffraction tomography. To benchmark the uniform heating induced through light modulation, we will employ an on-stage resistive heating element (VAHEAT, Interherence) comparing their responses. We will further optimise our holographic tracking methods for bacteria and incorporate the measurement of biomass growth.

Task 1.3 Study thermophile growth and mobility under varying environmental conditions

In this task, we start by observing thermophile growth under high, but constant, temperatures. Comparing them with those of task 1.1 will allow us to further optimise our protocols until optimal growth conditions are found. Next, we will create local temperature gradients to explore their motility response. At last, time-varying temperature fields are added to achieve optimal control over their aggregation behaviour. For this task, a simple microfluidic device with CO_2 control will suffice, whereas precise monitoring will be added later on in WP2.

Deliverables: **D-1.1 Report on bulk growth** (month 3). **D-1.2 Optical Setup with spatiotemporal temperature control** (month 6). **D-1.3 Report on spatiotemporal control** (month 12) to be considered for a scientific article.

Milestones: **M-1.1 Constant biomass growth on chip** (month 6). We will access whether we are able to recreate the ideal growth conditions of thermophiles within a microfluidic chip. Based on these results, we will alter their local environment to precisely control their temporal and spatial behaviour.

WP 2: CO_2 sequestration inside microbioreactor prototype (months 11-24)

Description: In this WP, we will develop a simple bioreactor prototype capable of monitoring CO_2 sequestration of thermophiles in real-time.

Task 2.1 Add CO_2 monitoring capabilities to microfluidic chip

Here, we will focus on adding CO_2 and pH monitoring capabilities to our previous microfluidic chip (WP1). This allows us to track the conversion of CO_2 in real time. If needed, we will add other functionalities to the chip that can track the thermophiles' metabolic activities more accurately.

Task 2.3 Measure CO_2 sequestration in simulated industrial conditions

We will introduce the fastest growing thermophile from task 1.3 into our microfluidic bioreactor. We will compare CO_2 sequestration under optimal conditions established in task 1.3 with conditions resembling industrial flue gases of industrial processes.

Deliverables: **D-2.1 Bioreactor prototype with CO_2 monitoring** (month 24) as test platform for industrial sequestration. **D-2.2 Report on CO_2 sequestration on-chip** (month 24) to be considered as scientific article.

Milestones: **M-2.1 Ability to measure CO_2 sequestration on-chip** (month 16) We will access whether we can accurately measure sequestration directly on chip.

3.3 Risk Mitigation

Risks (Likelihood, Impact)	WPs	Risk Mitigation Strategy
Bacteria can not be properly tracked as they frequently exit the field of view (Low, Low).	1	Match the microfluidic compartment with the field of view or use smaller magnification objective.
Growth or CO_2 uptake of thermophiles is found to be low (Low, Low).	1,2	Choose alternative thermophiles such as Persephonella marina EX-H1 or Sulfurihydrogenibium yellowstonense.
CO_2 sequestration can not be properly addresses on-chip (Low, Medium).	2	Assess sequestration a posteriori using analytical instruments in the microbiology lab of Prof. Jörn.

4. Outcomes

The primary objective of this project is to demonstrate the potential of thermophiles in sequestering CO_2 under extreme conditions prevalent in industrial processing sites. Leveraging the high environmental control enabled by optics and microfluidics, we will construct a bioreactor prototype capable of accurately measuring CO_2 sequestration under simulated industrial conditions. The outcomes of this study will not only enhance our fundamental understanding of CO_2 sequestration in natural systems but also constitutes a crucial step for its practical implementation in industries.

4.1 Determining optimal growth conditions of three types of thermophiles in CO_2 sequestration

This project will significantly advance current digital holography and thermometry techniques, facilitating comprehensive studies of thermophiles through a versatile optical setup. By dynamically controlling temperature with high spatial resolution using light and simultaneously monitoring 3D bacterial movement, we will unveil, for the first time, the impact of varying temperature fields on thermophile proliferation. Moreover, we will demonstrate how these optothermal techniques can be utilized to develop experimental protocols that can enhance control over bacteria localisation and growth.

4.2 A mini bioreactor prototype for purification of industrial flue gases from CO_2

Upon completion of the project, we will present a functional miniaturised bioreactor in a microfluidic chip. It will provide a suitable platform for the efficient growth of thermophiles at high temperatures and under CO_2 influx. Rigorous monitoring of on-chip conditions will assess the bioreactor's efficiency in sequestering CO_2 under optimal growth conditions compared to its performance when simulating industrial conditions. These results will show if future implementation in industrial processing sites is feasible and if, how such implementation could look like.

4.3 Strengthening the applicants profile

This project will allow me to execute one of my first self-funded research projects to become a more independent researcher. During this project, I will acquire important technical skills on digital holography and thermometry, which will further boost my expertise and help me building up my own research niche. Securing successful funding, is one of the important skills in becoming a principle investigator, which I strive to achieve in the next three years.

5. Impact

This research project holds the potential to yield significant insights into CO_2 sequestration using biological systems as an alternative pathway towards climate neutrality. Advancing our understanding of thermophiles as key species in CO_2 sequestration will further drive sustainable development of alternative food and fuel resources. The pivotal role of optics and photonics will be underscored through their capabilities in controlling microenvironments of biological systems.

5.1 Advancing on-site CO_2 capture for net-zero targets

This project paves a promising path for on-site CO_2 capture directly at the site of emissions, such as power plants, thus mitigating the exacerbation of greenhouse effects. The ability to capture CO_2 at its point of origin will offer a quantitative tool for sequestration and storage, leading to better regulation of industrial processes. This will facilitate transitions towards more sustainable practises in industry, ultimately aiding them to reach net-zero targets.

5.2 Harnessing thermophile's carbon anhydrase process in other organisms

The advancement of optical tools for precise thermophile control will provide crucial insights into the underlying CO_2 sequestration process, particular the role of carbonic anhydrase (CA), within realistic environmental conditions. Gaining control over the most suitable conditions for CA represents a fundamental step toward its future genetic implementation in other organisms, such as *Escherichia coli*, better suited for industrial scalability. Furthermore, beyond sequestration, CA offers substantial potential to enhance the efficiency of synthetic biofuel production and foster the development of alternative food and animal feed resources[5].
Notably, several recent breakthroughs have been achieved by studying thermophiles in thermal gradients, including their role in the origin of life[25]. The findings of this project might lead to further insights in these areas, while the here developed optical tools are universally applicable.

5.3 Photonics as enabling technology for environmental control

This project will effectively demonstrate that optics and photonics technologies are ideally suited to control the environment of biological organisms through optothermal processes, not only limited to thermophile bacteria, but also encompassing archaea and algae (the latter being commonly used in applications described in 5.2). By further promoting the utilization of optical tools in various industries, this research will enhance accessibility to these technologies for an interdisciplinary community.

[25] Baaske, et al. Extreme accumulation of nucleotides in simulated hydrothermal pore systems., *Proc. Nat. Acad. Sci.* **104**, 9346-9351 (2007).

Low-Cost Stain-free Computational Spectral Fluorescence Imager for Diagnosis of Diseased Tissues

Effective and timely diagnosis is critical for successful disease treatment. Yet, conventional diagnostic methods often involve invasive procedures, high costs, and limited accessibility, particularly in resource-restricted areas. One promising alternative to traditional invasive diagnostic methods is optical biopsy. Unlike conventional biopsy techniques that require tissue extraction, optical biopsy allows for real-time, non-invasive visualization of tissue morphology and pathology. It provides immediate and accurate results, greatly reducing patient discomfort and the risk of complications, as well as overall healthcare costs. However, current optical biopsy methods, reliant on contrast agents and requiring expensive equipment and skilled personnel, are challenged by potential inaccuracies, slow operation speeds, and high costs. Fluorescence microscopy could potentially overcome these limitations. This technique offers high specificity and sensitivity in visualizing cellular components, yet traditional fluorescence microscopy requires tissue labeling with dyes and lacks the necessary spectral information to identify specific disease markers, compromising the accuracy of diagnosis. To address these challenges, we propose the low-cost Computational Spectral Fluorescence Imager. This innovative technology combines the benefits of label-free fluorescence microscopy and optical biopsy, offering three key features:

1. **Multiplex Color Imaging**: The proposed system is designed for direct compressive imaging of multiple fluorescence contrasts, facilitating multiplex color imaging. This design will potentially overcome the limitations of current color imaging techniques, offering the capability to simultaneously image multiple fluorescence contrasts. This feature will greatly enhance the system's ability to differentiate and classify multiple entities in complex tissue environment.
2. **Rapid Optical Biopsy**: The proposed work will also enable rapid compressive imaging of autofluorescence images. By leveraging cutting-edge data compression techniques, we aim to significantly increase the speed of optical biopsy procedures. This will streamline data acquisition and processing, making the procedure more efficient and accessible while maintaining high diagnostic accuracy.
3. **Advanced Signal Analysis**: Lastly, the unique feature of the system will allow for higher-level analysis of detected signals that mix the multidimensional information of the tissue of interest, enabling applications such as classification of tissue types, disease types, and more.

By providing an affordable, non-invasive diagnostic tool, this proposal has the potential to democratize healthcare, particularly in low-resource areas, while serving as a precise, cost effective, and non-invasive imaging tool for broad biomedical research.

Backing this proposal signifies support for meaningful health advancements in underserved areas and for advancing biomedical research. The Computational Spectral Fluorescence Imager, at the intersection of optics, biotechnology, and information theory, is a practical, cost-effective solution to enhance disease diagnostic quality and to catalyze advances in global health.

Low-Cost Stain-free Computational Spectral Fluorescence Imager for Diagnosis of Diseased Tissues

Literature Review and Problem Statement

1. Autofluorescence Microscopy for Diseased Tissue Diagnosis: Current Status and Challenges

Accurate disease diagnosis forms the bedrock of effective therapeutic intervention and shapes patient prognosis. While traditional pathological techniques remain indispensable, they often entail invasive procedures, posing a risk of patient discomfort, elevated costs, and potential limitations in accessibility. More critically, these techniques require tissue alteration, which may disturb the native state of the tissue and potentially compromise diagnostic precision [1]

Optical biopsy, a groundbreaking advancement, promises non-invasive visualization of tissue morphology and pathology in real-time. Delivering immediate and precise results, it mitigates patient discomfort, reduces the risk of complications, and potentially lowers healthcare costs [2]. Its potential to increase diagnostic accessibility, particularly in resource-limited settings, represents a significant stride forward [3]. Within the umbrella of optical biopsy, autofluorescence-based techniques exploit intrinsic light emission from biological structures upon light absorption, thereby providing molecular specificity without necessitating extrinsic labeling [4].

In biological tissues, various endogenous biomolecules such as coenzymes, pigments, vitamins, lipids, and bilirubin, exhibit autofluorescence, emitting light at specific wavelengths when excited. These biomolecules are key markers in a range of biological and pathological processes [5]. However, a significant challenge arises in the form of spectral overlap between these biomolecules. Advanced techniques, such as fluorescence lifetime imaging (FLIM) or hyperspectral imaging, attempt to navigate these challenges. However, despite these advancements, these techniques still face limitations. For biopsies, the time of diagnosis is critical for efficient and improved healthcare. In the context of intraoperative optical biopsy, doctors require imaging times ranging from seconds to minutes for a large field of view tissue. This timing is crucial to inform the next-step surgical procedure. In non-intraoperative cases, a faster biopsy can inform a quicker diagnosis, which is often crucial for diseases like cancer where early diagnosis is key to curing. These processes, however, are often slow and generate large datasets. This makes diagnosis time-consuming and places significant demands on expensive computing and hardware resources. Such limitations hinder wider applications, particularly in low-resource settings where these capabilities may not be readily available, potentially compromising the accuracy of diagnosis. Therefore, despite the strides made in autofluorescence-based imaging techniques, there remains a critical need for the development and refinement of methodologies that can overcome these challenges to enhance diagnostic capabilities.

2. Compressed Sensing in Imaging Towards Microscopy: Opportunities and Challenges

Compressive Sensing (CS), a signal processing paradigm that recovers a signal or image from significantly fewer samples or measurements than traditional methods, harnesses the sparsity or compressibility of signals in a certain domain. Compressive Sensing (CS) has already shown considerable promise in the field of medical imaging, particularly with respect to Magnetic Resonance Imaging (MRI). Leveraging the inherent sparsity of MRI images, CS has been instrumental in facilitating high-resolution reconstructions from significantly fewer data samples. Empirical evidence suggests this method has led to an acceleration of imaging periods by factors ranging from 4 to 10 in commercial MRI systems [8].

In microscopy, CS has primarily been deployed in the spatial domain. This technique harnesses the sparsity of images, enabling high-resolution reconstruction from fewer samples and speeding up the imaging process. For instance, CS has led to notable improvements in electron microscopy, where it has reduced data acquisition times by factors of up to 3 [6]. Similarly, in optical microscopy, CS has yielded speed increases by factors of up to 5 [7]. A promising area for the application of CS is in the spectral domain of hyperspectral microscopy [9]. Hyperspectral imaging, which captures both spatial and spectral information simultaneously, has traditionally been limited by the high-dimensional nature of the data. This necessitates extensive data acquisition and processing times. By employing CS in the spectral domain, we could dramatically accelerate imaging speeds. This is due to the fact that CS can

exploit the inherent sparsity within the spectral data, allowing for fewer measurements and thus reducing the requirement for subsequent processing.

Building on these foundations, our proposal aims to design an imager that integrates both spatial and spectral compressive sensing. This imager would leverage the advantages of CS in both domains, significantly speeding up data acquisition and processing times, thereby enabling real-time, high-resolution spectral imaging. This innovative approach holds substantial potential to advance the field of spectral imaging and promises to bring about a transformative change in healthcare diagnostics.

Project Objectives, Key Innovations, and Expected Outcomes

The proposed project will address the limitations of current diagnostic methods and develop an new Compressive Spectral Fluorescence Imager for efficient, affordable, and non-invasive optical biopsy. We aim to achieve the following objectives and bring about crucial advancements in the field:

- The Compressive Spectral Fluorescence Imager will be capable of direct multiplex color imaging of multiple fluorescence contrasts, overcoming the limitations of current color imaging techniques. This innovative feature will enhance the system's capacity to differentiate and classify various entities within a complex tissue environment.
- The system will enable rapid compressive imaging of autofluorescence images, streamlining data acquisition and processing, while maintaining a high level of diagnostic accuracy. By leveraging cutting-edge data compression techniques, we aim to significantly increase the speed of optical biopsy procedures, making them more efficient and accessible.
- The proposed system will employ a minimal number of pixels at the backend, transforming the device into an efficient optical encoder. This distinctive feature will facilitate advanced signal analysis of the detected spatial-spectral information from the tissue of interest, enabling applications such as classification of tissue types, disease types, and more.

We will design, optimize, and test the Compressive Spectral Fluorescence Imager during the funded period. We will build an optical biopsy testbed to evaluate the performance and reliability of the system through rigorous experiments. We aim to demonstrate a significant improvement in imaging speed, diagnostic accuracy, and cost-effectiveness compared to existing methods in both theory and practice. The successful completion of this project will serve as a funding step for the applicant to start her career in designing hardware together with software optimization to improve healthcare, particularly in resource-limited areas, by providing an affordable, non-invasive diagnostic tool. Furthermore, it has the potential to serve as a precise, cost-effective, and non-invasive imaging tool for a broad range of biomedical research.

Technical Rationale and Approach

1. Computational fluorescence imager design for label-free fluorescence microscope. Existing microscope designs predominantly rely on two illumination methodologies: laser scanning and widefield illumination/excitation. The associated detection elements incorporate either a single-detector, such as a photomultiplier tube (PMT), or a camera. These conventional designs, conceived for general applications, often lack the necessary adaptability for specialized use-cases demanding superior imaging performance. This limitation becomes particularly acute for fast multi-contrast autofluorescence imaging for biopsy, which requires a large field of view and stringent photon budget management. One significant challenge in this context is the relatively weak autofluorescence signals compared to traditional labeled fluorescence imaging. This limitation calls for a more innovative design enabling efficient photon collection compared to conventional microscopes. We propose a key solution in the form of a

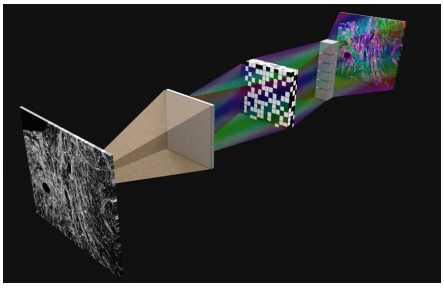

Fig. 1 concept figure of computational fluorescence imager: stain-free sample is imaged through a diffractive element and compressed into a few pixels to get information of biomarkers

programmable spatio-spectral imager with a programmable fluorescence filter. This design allows signal collection across the entire bandwidth of emitted autofluorescence signals, surpassing the restricted bandwidth of physical filters commonly used to prevent cross-talk between channels. This programmable fluorescence imager, incorporated into the detection arm of the microscope, would enable the collection and utilization of all emitted photons for imaging and data analysis. Central to our proposed design is a Digital Micromirror Device (DMD), a programmable intensity modulator. Positioned after a grating that spatially splits the light spectrum, the DMD modulates the light's intensity, facilitating adaptability to both laser scanning and widefield imaging systems. The rapid response times of DMDs, typically in the microsecond range, allow for fast, dynamic adaptive filtering. This high-speed updating capability is critical for spatio-spectral multiplexing, where multiple filter patterns are implemented within a single camera exposure. To further reduce the time required for full-spectral sampling in conventional imaging, a process that can be time-consuming and computationally intensive, we introduce the concept of compressive sampling. This technique allows signal reconstruction from considerably fewer samples than dictated by the traditional Nyquist-Shannon sampling theorem, assuming signal sparsity or compressibility in the spatio-spectral domain. By combining compressive sampling with the programmable fluorescence imager design, we can enhance signal detection and accelerate data acquisition, leading to a more efficient method of capturing and processing spatio-spectral data in microscopy.

Preliminary demonstrations of this design, compatible with both laser scanning and widefield detection systems, have been built in the applicant's lab [see preliminary result]. Future work will focus on refining the optical elements and advancing signal processing techniques for better co-design of DMD patterns with information retrieval for diseased tissue diagnosis. This novel approach could dramatically broaden the scope and versatility of microscope systems, enabling more specialized and effective imaging solutions. Moreover, it could instigate a paradigm shift in how we capture and process image data for specialized optical biopsy, promoting faster data acquisition, more efficient spectral imaging, and leading to more accurate and detailed examinations of samples.

2. Algorithm design for adaptive filter design, diseased tissue classification and segmentation. Taking inspiration from the highly successful end-to-end design paradigm in computer science, we propose a synergistic approach to designing the protocol, integrating programmable filters with the data processing algorithm. Our proposal concentrates on the design of modulation patterns for the DMD, which would facilitate spatial-spectral modulation of fluorescence signals, effectively functioning as an optical encoder. For the decoding process, we leverage our prior experience using a matrix completion algorithm for spatial-spectral reconstruction. Our intention is to bolster the robustness of these algorithms, especially in scenarios with considerable spectral overlap and low signal-to-noise ratios, utilizing machine learning techniques. Specifically, we propose the use of proven decoder architectures, such as the CNN decoder part of U-net and Multilayer Perceptrons (MLPs), renowned within the computer vision community. These machine learning architectures, lauded for their proficiency in processing spatial information and identifying intricate patterns, are ideally suited for reconstructing images from our spectrally modulated signals. Once trained on the spectral data captured using our programmed imager, we anticipate that our algorithm will assist in denoising, enhancing, and interpreting the resulting images.

For more complex tasks, such as disease diagnosis, we envisage the use of machine learning for direct diagnosis without the need for image reconstruction. This approach could further expedite the process for doctors and reduce the waiting time for patients. Specifically, we aim to train neural networks, which excel at classification tasks. When trained on spectrally encoded data with disease labels, they could provide highly precise diagnostic predictions, along with quantified confidence levels, within well-defined application regimes.

In summary, our innovative design marries sophisticated optical hardware with cutting-edge computational methods, synergistically optimizing the collection and processing of vital image data. This end-to-end solution aims to significantly improve both efficiency and accuracy in microscopy imaging, opening new avenues for scientific and medical research.

3. Preliminary results in hardware implementation and simulation.

Hardware: A compressive detection system for laser scanning microscope and widefield microscope In our lab, we have established compressive detection systems, all equipped with key components such as spectral splitting grating and a DMD for spectral modulation and encoding. For detectors, we have incorporated three different versions, ranging from single pixel to large pixel array: 1) PMT [11, 12] 2) SPAD array [10] and 3) an sCMOS camera. This wide range allows us to demonstrate possibilities from single-to-high dimensional spatio-spectral signal mixing spaces, all with ultrahigh sensitivity. Two of our previous designs have been published as prototypes for laser scanning microscopy [11, 12], and an additional new design, featuring an sCMOS camera, was recently developed by the applicant. We plan to mainly explore ways to exploit the spatio-spectral mixed states of fluorescence signals for information retrieval, aiming for two goals: (1) multiplex color imaging for fast imaging of multiple stain-free fluorescence biomarkers and (2) information processing for higher-level analysis for disease tissue diagnosis, such as diseased tissue classification.

Software: In our quest to reconstruct multiple color imaging, we initially explored an algorithm centered on matrix completion, where the forward model of the imaging procedure is constructed simply as the linear combination of fluorescence spectra and their corresponding spatial distributions. While these algorithms were sufficient in retrieving spatial and spectral information from our system, they were unable to fully tap into the potential of our hardware and the complexity of spatial-spectral data. To overcome this, we started the development of programmable filters for spectrally-overlapping cases and our preliminary results have been promising, indicating a significant potential for enhancing the quality and quantity of information derived from each scan. Simultaneously, we embarked on crafting more sophisticated image reconstruction algorithms, leveraging recent advancements in machine learning and compressed sensing. Our initial tests reveal that these improvements markedly reduce reconstruction errors and expedite image generation, paving the way for real-time image reconstruction. This not only enables us to provide high-resolution, multi-color imaging at faster speeds and with richer information, but also boosts our capability to study complex diseased tissues thereby supplying a powerful tool for clinicians in disease diagnosis and treatment planning.

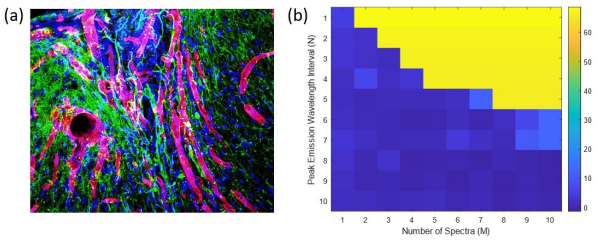

Fig. 2 (a) reconstruction of images of at least 6 colors from tissue in simulation with proposed method (b) reconstruction errors (in log scale) at different colors and emission peaks.

Outline of tasks

The project will be organized as three separate work packages:

Work Package I: Development of low-cost computational fluorescence imager for color-multiplexed fluorescence Imaging. This package involves creating and optimizing a low-cost computational fluorescence imager for color-multiplex fluorescence imaging. The system will be designed to simultaneously capture multiple autofluorescence contrasts. We'll first add 3 more laser lines (405 nm, 488 nm, and 635 nm) based on our current system that only has 532 nm laser, this will allow excitation of fluorescence signal ranging from 400-800 nm. An essential aspect of this package will be the incorporation of compressive sensing principles into the system. This incorporation will ensure that the system can generate large field-of-view and high-resolution imaging rapidly. A DMD will be used as an optical encoder to modulate light patterns to capture the most information-rich measurements. The DMD modulation patterns will be optimized to match the constraints of the optical setup and the spectral characteristics of the sample. Autofluorescence biomarkers like NAD(P)H, flavins, lipofuscins, retinoids, porphyrins, bilirubin, and lipids will serve as the primary markers for autofluorescence. These markers, which are inherent to various tissues, emit light upon absorption and carry valuable diagnostic information. The optimization phase of this work package involves testing the system using standard

fluorescence samples such as beads and dyes with the aim of simultaneous imaging of over 5 colors that break the limitation of multicolor fluorescence imaging. This testing phase will provide valuable insight into the system's performance and highlight areas requiring further optimization. The feedback from this testing will be used to refine the system continually.

Work Package II: Advanced signal analysis for disease diagnosis. The second work package primarily focuses on developing machine learning algorithms specifically tailored for spectral imaging data, thereby enabling effective disease diagnosis. By identifying unique patterns and features in the processed spatio-spectral multiplexed data, the machine learning model will be trained to classify abnormalities and will be optimized to accurately classify diseased tissue regions.

We plan to collaborate with L'Oreal Research in Paris, where we will utilize cultured skin tissues for various skin disease diagnoses. The ground truth of diseased areas and labels will be provided. Auto-fluorescence spectral data will be pre-processed using a programmable fluorescence filter, which will adjust the spatio-spectral filtering pattern to minimize the error between the desired output and the ground truth. We will include an additional output representing the confidence level with each diagnosis, through multiple runs of the trained model with variations in the signal-to-noise ratios of the input data. This addition will provide clinicians with a quantitative measure of prediction certainty.

This process aims to transform traditional pathological diagnosis methods by enabling rapid, quantitative, and potentially early detection of diseases. It will streamline the process from raw spectral data acquisition to high-level data interpretation, offering a significant boost to the efficiency and accuracy of fluorescence microscopy.

Work Package III: Optimize the system and algorithm for rapid optical biopsy through computational fluorescence imager. The final work package will involve optimizing our computational fluorescence imager with optical data compression capability, along with its downstream algorithm design, to enable quick and accurate optical biopsy procedures. Autofluorescence-based optical biopsy is a non-invasive technique that can potentially provide real-time visualization of tissue morphology and pathology, significantly reducing patient discomfort, risk of complications, and overall healthcare costs. We aim to optimize our imaging protocol and method for applications in in vivo imaging, where there could be sample motion. The challenge lies in designing the encoding process in such a way that it achieves optimal compression without losing significant diagnostic information when the sample may have motions, typically around ~Hz from breathing. We will mainly optimize our imaging system for even faster imaging, meaning a higher compression ratio, to directly overcome the motions. To manage risks, in case a severe compression ratio is needed, we will explore optimization with custom-engineered diffractive elements with Prof. Rajesh Menon at the University of Utah, who has extensive experience in engineering diffractive elements for incoherent hyperspectral fluorescence imaging. At the same time, we will work on optimizing algorithms that include a registration process to compensate for potential artefacts in spatial and spectral information extraction.

Outcome and Impact

A breakthrough accomplishment of our project will be the development of a computational fluorescence imager that transcends existing limitations in multicolor fluorescence imaging. By enabling the simultaneous imaging of over five colors, we stand to transform the depth of diagnostic and research data available from biological samples. The optimization of this system is set to pave the way for real-time, non-invasive optical biopsy procedures. This cutting-edge tool will provide instant visualization of tissue morphology and pathology, significantly reducing patient discomfort, potential complications, and healthcare costs. Complementing this, the machine learning algorithms developed will revolutionize disease diagnosis, shifting from the subjective, labor-intensive procedures to an objective, quantitative approach. This will not only enhance diagnostic accuracy but also provide a measure of prediction certainty, giving clinicians a reliable decision-making tool. Simultaneously, this project's multi-disciplinary nature will offer invaluable cross-disciplinary training to students and engineers, and the techniques and knowledge generated could find broad applications in domains such as deep learning and AI. Through these advancements, we're pushing the boundaries of fluorescence microscopy and redefining what is achievable across various scientific and technological realms.

References:

1. Braakhuis, B. J. M., Tabor, M. P., Kummer, J. A., Leemans, C. R., & Brakenhoff, R. H. (2004). A genetic explanation of Slaughter's concept of field cancerization: evidence and clinical implications. Cancer research, 64(18), 6455-6460.

2. Lovat, L. B., Johnson, K., Mackenzie, G. D., Clark, B. R., Novelli, M. R., Davies, S., ... & Thorpe, S. M. (2006). Elastic scattering spectroscopy accurately detects high grade dysplasia and cancer in Barrett's oesophagus. Gut, 55(8), 1078-1083.

3. Fatakdawala, H., Poti, S., Zhou, F., Sun, R., Bec, J., Liu, J., ... & Marcu, L. (2014). Multimodal in vivo imaging of oral cancer using fluorescence lifetime, photoacoustic and ultrasound techniques. Biomedical optics express, 5(9), 3254-3267.

4. Monici, M. (2005). Cell and tissue autofluorescence research and diagnostic applications. Biotechnology annual review, 11, 227-256.

5. Croce, A. C., & Bottiroli, G. (2014). Autofluorescence spectroscopy and imaging: a tool for biomedical research and diagnosis. European Journal of Histochemistry, 58(4).

6. Binev, P., Dahmen, W., DeVore, R., Lamby, P., Petrova, G., & Wojtaszczyk, P. (2011). Compressed sensing and electron microscopy. In: Model and Data Analysis. Radon Series Comp. Appl. Math., vol 2. De Gruyter, Berlin, Boston.

7. Tian, L., & Waller, L. (2015). 3D Intensity and Phase Imaging from Light-Field Measurements in an LED Array Microscope. Optica, 2(2), 104-111.

8. Lustig, M., Donoho, D., & Pauly, J. M. (2007). Sparse MRI: The application of compressed sensing for rapid MR imaging. Magnetic resonance in medicine, 58(6), 1182-1195.

9. Gehm, M. E., John, R., Brady, D. J., Willett, R. M., & Schulz, T. J. (2007). Single-shot compressive spectral imaging with a dual-disperser architecture. Optics express, 15(21), 14013-14027.

10. Gentner, C., Burri, S., Charbon, E., Bruschini, C., & de Aguiar, H. B. (2023). Compressive Raman microspectroscopy parallelized by single-photon avalanche diode arrays. arXiv preprint arXiv:2301.07709.

11. Sturm, B., Soldevila, F., Tajahuerce, E., Gigan, S., Rigneault, H., & de Aguiar, H. B. (2019). High-sensitivity high-speed compressive spectrometer for Raman imaging. ACS photonics, 6(6), 1409-1415.

12. Soldevila, F., Dong, J., Tajahuerce, E., Gigan, S., & de Aguiar, H. B. (2019). Fast compressive Raman bio-imaging via matrix completion. Optica, 6(3), 341-346.

Proposal title: Development of a clinical multi-excitation optical coherence elastography system to interrogate corneal biomechanics for the detection and staging of normotensive glaucoma.

Category: Medicine

Abstract:

In Peru, Glaucoma is the first cause of irreversible blindness characterized by progressive optic nerve damage and visual field loss. It is estimated that 50% of Glaucoma Peruvian patients are not aware they carry such a disease. The primary risk factor for Glaucoma detection is elevated intraocular pressure (IOP). However, normotensive Glaucoma (NTG) is a form of Glaucoma that develops in the eye despite its IOP being within the normal range of 12 to 21 mmHg. Therefore, early detection of NTG becomes a challenging task and it is crucial for timely intervention and preservation of vision. Currently, NTG diagnosis relies on IOP measurements through the cornea and visual field testing, which may miss the early stages of the disease. Corneas with abnormal (softer) biomechanics and topography (high astigmatism) may lead to inaccurate readings of IOP which, added to the assumptions made by each clinical tonometer, results in high variability in the estimation of IOP. Moreover, there is scientific evidence reporting that patients with NTG tend to have softer corneas compared to control patients. We propose the development of a clinical multi-excitation optical coherence elastography system to interrogate corneal biomechanics for the detection and staging of normotensive glaucoma. This system will be capable of measuring the topography of the cornea (structural B-mode frame information) and the corneal dynamic response (biomechanical information) from two simultaneous excitation sources: air-pulse macro deformation (AP-MD), and air-couple ultrasonic wave excitation (AC-US). The innovative integration of both excitation technologies together with a finite element model (FEM) of the eye will allow us to probe not only the shear modulus of the cornea through the propagation of Lamb waves, but the calculation of a true-biomechanically corrected IOP. The accuracy of the estimations of shear modulus and corrected IOP using measurements from the clinical system and the outcomes of the inverse FEM simulations will be tested using ex vivo animal models of the eye by modulating IOP with an artificial pressure-control system, and corneal stiffness with collagen enzymes. After a safety validation of the system in terms of acoustics, photonics, and air pressure for human use, a preliminary patient study will be carried out with 20 control patients, 20 patients with NTG, and 20 patients with high-tension Glaucoma (HTG). These measurements and estimations will be used to generate biomechanically inspired biomarkers of the corneal to detect early and advanced stages of NTG. We expect that shear modulus and the true-biomechanically correlated IOP can separate NTG from control and HTG patients. The impact of this research on the Peruvian ophthalmology healthcare system is fundamental since our proposed solution could catch NTG earlier and enable patient treatment to avoid further optical nerve damage and vision loss. This represents more than 80% in savings in the application of more invasive (costly) treatments and preserving vision quality. Finally, this technology can be used to understand the impact of unusual corneas (i.e., high astigmatism, low rigidity, and thin corneas) in the estimation of IOP, treatment monitoring, and the evaluation of other ocular diseases such as keratoconus.

Project title: Development of a clinical multi-excitation optical coherence elastography system to interrogate corneal biomechanics for the detection and staging of normotensive glaucoma.

1. Literature review:

In Peru, Glaucoma is the first cause of irreversible blindness characterized by progressive optic nerve damage and visual field loss according to the National Institute of Ophthalmology. The National Ministry of Health estimated that 50% of Glaucoma Peruvian patients are not aware they carry such disease. The primary risk factor for Glaucoma detection is elevated intraocular pressure (IOP). However, normotensive Glaucoma (NTG) is a form of Glaucoma that develops in the eye despite its IOP being within the normal range of 12 to 21 mmHg. In the USA, NTG could account for up to 40% of the patients with open-angle Glaucoma [1], and there is no evidence that this percentage could strongly differ in Peru. Therefore, early detection of NTG becomes a challenging task and it is crucial for timely intervention and preservation of vision.

Currently, NTG diagnosis relies on IOP measurements through the cornea and visual field testing, which may miss the early stages of the disease [2]. Corneas with abnormal (softer) biomechanics and topography (high astigmatism) may lead to inaccurate readings of IOP [3]. This problem added to the assumptions made by each clinical tonometer about corneal biomechanics and thickness results in high variability in the estimation of IOP [4]. Moreover, there is scientific evidence reporting that patients with NTG tend to have softer corneas compared to control patients [5]. This tendency could explain the underestimation of IOP due to the abnormally softer corneas in NTG when using clinical systems such as rebound tonometer, air-puff deformation system (e.g. Corvis and the Oculus Response Analyzer), and Goldman tonometry. Other research reports the possibility of monitoring NTG progression by measuring biomechanical parameters of the cornea using ORA [6].

Optical coherence elastography (OCE) based on the propagation of mechanical waves has been successfully applied for probing the biomechanics of the eye [7]. Recent studies made by our group [8, 9] demonstrated the capability of non-contact air-coupled ultrasound (ACUS) excitation co-focused with a phase-sensitive optical coherence tomography (OCT) system to generate elasticity maps of the cornea for the detection of early stages of keratoconus. Even though this technology does not alter the IOP of the eye during the measurement of shear modulus (unlike air-puff techniques), it is not possible to obtain IOP measurements only based on these measurements. On the other hand, air-puff macro deformation (APMD) of the cornea has been successfully implemented for the measurement of IOP and IOP-corrected versions to biomechanics and corneal thickness [10]. However, due to the lack of independent measurements of corneal elasticity, IOP estimations among different commercial systems remain highly variable. Recently, air-puff excitation technology has been coupled with an OCT system for the estimation of corneal biomechanics and structure [11]. This system allows for the fast monitoring of corneal deformation which can be potentially integrated with the ACUS technology.

We propose the development of a clinical multi-excitation optical coherence elastography system to interrogate corneal biomechanics for the detection and staging of normotensive glaucoma. This system will be capable of measuring the topography of the cornea (structural B-mode frame information) and the corneal dynamic response (biomechanical information) from two simultaneous excitation sources: air-pulse macro deformation, and air-couple ultrasonic wave excitation. The innovative integration of both excitation technologies under the same clinical OCE system could potentially provide accurate estimations of the shear modulus of the cornea and the true-biomechanically corrected IOP using a finite element model (FEM) of the eye. The use of FEM for modeling the cornea has been successfully applied for surgery planning during LASIK by generating a digital twin of the patient's eye using personalized topographical information [12]. However, these models do not contemplate the variability of corneal elasticity within patients and the impact it could have during the simulated outcomes. Therefore, we propose a FEM model that leverages measurements of elasticity, topography, and corneal deflection for IOP estimations. We

expect that shear modulus and the true-biomechanically corrected IOP can be used as integrated biomarkers to separate NTG from control and high-tension Glaucoma (HTG) patients. The impact of this research on the Peruvian ophthalmology healthcare system is fundamental since our proposed solution could catch NTG earlier and enable patient treatment to avoid further optical nerve damage and vision loss.

2. Problem statement:

There is not a clinically available medical device capable of detecting early onsets of NTG due to the limitations and assumptions of corneal rigidity in the commercial tonometers during IOP measurements. Moreover, there is scientific evidence that shows NTG patients having abnormally softer corneas [5] which may lead to erroneous estimations of IOP if not taken into account. This technological problem avoids the early detection and prompt treatment application of NTG patients that may result in vision loss and the application of highly invasive interventions. In Peru, Glaucoma is the first cause of irreversible blindness characterized and the National Ministry of Health estimated that 50% of Glaucoma Peruvian patients are not aware they carry such disease. Therefore, the development of new medical-imaging ophthalmic solutions accounting for corneal biomechanics is fundamental for the advancement in detecting early onsets of NTG.

3. Objectives:

General objective: The development of a clinical multi-excitation optical coherence elastography system to interrogate corneal biomechanics for the potential detection and staging of normotensive glaucoma.

Specific objectives:

- The development of a clinical Swept-Source OCT system integrated with two excitation modules: ACUS and APMD, capable of measuring the structural and biomechanical properties of human subjects.
- The development of a FEM simulation based on a digital twin of a patient eye and integrating the system human measurements for the calculation of shear modulus of the cornea and the true-biomechanically corrected IOP.
- The proposal of biomarkers and preliminary tests to separate NTG patients from control and HTG patients based on shear modulus and IOP measurements.

4. Methodology:

The proposed system for mapping the biomechanics of the cornea and calculating the biomechanically corrected IOP includes: a) a confocal air-couple ultrasonic transducer focused on the corneal apex to generate elastic wave propagation in the cornea; b) an air-puff pneumatic module capable of generating central macro deformation in the corneal apex; c) high-speed phase-sensitive OCT for measurements of the wave propagation and corneal macro deformation; d) spatial reconstruction of the biomechanical properties of the cornea and IOP based on a FEM of patient's eye incorporation wave velocity, corneal deflection, and thickness. The research plan has been divided into three specific aims.

- **<u>Work Package 1. Clinical translation of multi-excitation OCE technique for biomechanical mapping of human corneal elasticity and IOP:</u>**

Rationale. The faster acquisition speed enables a significant reduction in the acquisition time required to reconstruct corneal biomechanical properties, sufficient to overcome eye motion artifacts *in vivo*. We will leverage our previous research-based table-dependent OCE system setup [13] to build a clinical stand-alone prototype. We will build an excitation module that integrates ACUS and APMD technologies. Shear modulus will be derived by quantifying depth-resolved Lamb wave propagation and validated by mechanical testing of the gelatin phantoms.

Research Design:

Improving OCT imaging speed: We expect that elastic wave velocities in normal, NTG, and HTG human corneas will be in the range of 5 to 15 m/s. That means that the minimal time for the wave to travel over, e.g., 5 mm distance is ~0.3 ms. Therefore, in order to image the wave propagation with acceptable spatial resolution (e.g. 100 µm or 50 samples along 5mm) the OCT frame rate of 150 kHz is required. Thus, in order to maintain the same lateral resolution in the B-mode image (100 µm), an A-scan of 200 kHz will be required. To achieve this speed, we will purchase a commercially available 200 kHz swept laser source (Thorlabs Inc.).

Building a clinical prototype: We are going to implement a system prototype based on the OCE technology able to operate in clinical environments. Therefore, the stand-alone system will be compact, portable, easy to operate, and will have mechanical and robotics components that will allow for the stable acquisition in patients by using (1) a head holder; (2) a visualization target mounted in a Badal system to stabilize the voluntary movements of the eye, and (3) a 3D motorized stage to align the OCT acquisition arm to the patient's cornea.

Building multi-excitation module: A spherical air-coupled 500 kHz ultrasonic transducer will be custom designed to host pneumatic methacrylate-based conduct in the center of the transducer for the release of the air-pulse (~2.5 mm diameter air release hole). The positioning and material of the conduct will allow for OCT imaging while the tissue is excited. The distance between the corneal apex and the conduct should not be greater than 10 mm, while the distance between the corneal apex and the acoustic focusing point of the transducer should not be greater than 30 mm to ensure proper excitation magnitude and avoid attenuation. Both excitation systems will be controlled by the same PC unit for synchronized acquisition.

Potential Problems & Alternatives: Eye blinking is a potential problem during corneal measurements in the blocking of the OCT signal in short periods of time (~0.2 sec) due to the patient's blinking. We propose to acquire multi-meridian corneal signals crossing the corneal apex (between 16 to 32 meridians) for 1 to 2 seconds. The repetition of these measurements (at least 3 times) will enable discarding and replacing corrupted signals at specific meridians due to the blinking effect.

- **Work Package 2. Design of FEM and evaluate the sensitivity of measurements and suitability for human clinical studies:**

Rationale: These studies are designed to create the FEM simulation to determine shear modulus and biomechanically corrected IOP, and to test determine the accuracy, precision, and safety of our system and serve as an important transitional step toward clinical studies.

Research Design:

FEM analysis: Generation of a digital twin of the patient's eye using the topographical information of the cornea and average human measurements of the eyeball. The dynamic FEM simulation will recreate the ACUS and APMD excitation of the cornea and how wave propagation and corneal deflection change as IOP, shear modulus, and corneal thickness are varied. This sensitivity analysis will serve to create a model for the proper estimation of corneal shear modulus and the true-biomechanically corrected IOP. We will take the work by [14] as the reference of the constitutive model of the cornea.

Accuracy and precision: Measurements of the multi-excitation system will be acquired in animal models of the cornea in order to estimate shear modulus and IOP. Both biomechanics and IOP will be modulated using collagenase (and/or gelatinase), and a pressure-control system, respectively. The FEM model will be used to calculate the shear modulus and corrected IOP and it will be compared with the ground truth corneal stiffness (measured with a linear stretcher device) and IOP (measured by the pressure sensor). The FEM-based parametric model will be adjusted in order to obtain the highest accuracy a precision of the estimations.

Safety evaluation: Measurements of laser intensity and exposure time will be conducted using a power-meter device to calculate if values are within permissible safety requirements for ocular tissue [15]. Similarly, values of spatial-peak temporal-average intensity and Mechanical Index for the acoustic exposure in the cornea will be calculated in compliance with the safety standards in ocular tissues [16].

Potential Problems & Alternatives: Extensiometry measurements are notoriously variable and it may still limit our ability to provide meaningful benchmarks without very large subject numbers. We will evaluate alternative measurement methods, e.g. indentation testing that may be more reliable and comparable to elastography.

- **Work Package 3. Perform preliminary clinical studies in humans with our system for the detection of different stages of NTG**

Rationale. The ultimate goal of this research is to enable the detection of subclinical NTG. The objective of these clinical pilot studies will be to determine the sensitivity and specificity of the system for NTG detection through the development of biomechanically inspired biomarkers.

Research Design:

Measurement of human subjects: A cohort of normal and NTG subjects will be recruited from the clinical service of the National Institute of Ophthalmology – INO from the Spanish acronym – (Lima, Peru) following the approved research protocol adhered to the tenets of the Declaration of Helsinki. The developed system will be relocated to INO for these clinical studies. NTG subjects will be medically diagnosed as such by doctors at INO and will be further divided by severity into the following groups: subclinical, mild, moderate, and advanced. Subjects will be evaluated clinically to determine eligibility and testing include visual acuity, slit-lamp biomicroscopy, Scheimpflug videokeratography, and ocular wavefront sensing. A group of normal subjects will receive the same clinical evaluation for the generation of a baseline of normal corneal biomechanics.

Biomarker development: We will propose a number of biomarkers based on the directional-dependent wave speed, corneal thickness, and corneal deflection in order to classify subclinical and other stages of NTG. These results will be compared against medical diagnosis and other clinical instruments (ORA/CorVis). This will then be compared with the subject's actual class assignment to compute the following classification metrics: sensitivity (true positive rate), specificity (true negative rate), accuracy (total true classifications), and the area underneath the receiver-operator characteristic (ROC) curve.

Potential Problems & Alternatives: Motion artifacts: As stated previously we are informed about this potential problem and our current strategy is to increase our imaging speed to defend against this potential confounder. We will investigate the feasibility and necessity of passive and active eye-tracking methods as an alternative strategy.

5. **Expected outcomes:**

- A non-contact and non-invasive multi-excitation system capable of imaging Lamb wave propagation and corneal macro deflection for the mapping of cornea biomechanical properties both in vitro and *in vivo* with lateral and axial resolutions of 100 µm and 16 µm, respectively, in clinical environments.
- A FEM package capable of simulating a patient's cornea integrated with the experimental measurements for the accurate calculation of the shear modulus of the cornea and the true-biomechanically corrected IOP.
- A set of potential biomarkers using the previous estimations for the detection and staging of NTG using a cohort of control, NTG, and HTG patients.

6. **Viability:**

The principal investigator (PI) of this proposal is an expert in optical coherence elastography as demonstrated by his trajectory in multiple institutions of high-level research in the USA and Europe. Moreover, the PI had the experience of implementing functional air-coupled ultrasonic transducers and an air-puff excitation module in separate projects and institutions. The host institution has the infrastructure and experience of fabricating medical devices and translating them into the clinic from a technological readiness level (TRL) 2 to TRL 9. Finally, the clinical partner in this project is the National Institute of Ophthalmology (Lima, Peru) which is currently collaborating with the host institution on other projects. Therefore, the academic trajectory of the PI, the capabilities of the host institution, and the collaboration with the clinical partner make this project viable and increases the chances of success.

7. Impact:

The impact of this research on the Peruvian ophthalmology healthcare system is fundamental since our proposed solution could catch NTG earlier and enable patient treatment to avoid further optical nerve damage and vision loss. This represents more than 80% in savings in the application of more invasive (costly) treatments and preserving vision quality. Finally, this technology can be used to understand the impact of unusual corneas (i.e., high astigmatism, low rigidity, and thin corneas) in the estimation of IOP, treatment monitoring, and the evaluation of other ocular diseases such as keratoconus. Finally, this project represents one of the first stones in the development of the areas of Biomedical Optics and Biophotonics in Peru which will allow the involvement of a new generation of students in this discipline and the collaboration with the local industry, health companies, and ophthalmology clinics.

References:

1. M. R. Razeghinejad and D. Lee, "Managing normal tension glaucoma by lowering the intraocular pressure," Survey of Ophthalmology **64**, 111-116 (2019).
2. S. Drance, D. R. Anderson, and M. Schulzer, "Risk factors for progression of visual field abnormalities in normal-tension glaucoma," American Journal of Ophthalmology **131**, 699-708 (2001).
3. J. Liu and C. J. Roberts, "Influence of corneal biomechanical properties on intraocular pressure measurement: quantitative analysis," J Cataract Refract Surg **31**, 146-155 (2005).
4. P. Brusini, M. L. Salvetat, and M. Zeppieri, "How to Measure Intraocular Pressure: An Updated Review of Various Tonometers," Journal of clinical medicine **10**(2021).
5. Y. Xu, Y. Ye, Z. Chen, J. Xu, Y. Yang, Y. Fan, P. Liu, I. T. Chong, K. Yu, D. C. C. Lam, and M. Yu, "Corneal Stiffness and Modulus of Normal-Tension Glaucoma in Chinese," American Journal of Ophthalmology **242**, 131-138 (2022).
6. H. Helmy, M. Leila, and A. A. Zaki, "Corneal biomechanics in asymmetrical normal-tension glaucoma," Clin Ophthalmol **10**, 503-510 (2016).
7. F. Zvietcovich and K. V. Larin, "Wave-based optical coherence elastography: the 10-year perspective," Progress in Biomedical Engineering **4**(2021).
8. F. Zvietcovich, A. Varea, N. Alejandre-Alba, J. Merayo-Lloves, J. Birkenfeld, and S. Marcos, *Detecting subclinical keratoconus by mapping corneal biomechanics using wave-based optical coherence elastography*, SPIE BiOS (SPIE, 2023), Vol. PC12360.
9. F. Zvietcovich, A. Varea, N. Alejandre-Alba, J. Merayo, J. Birkenfeld, and S. Marcos, *Optical coherence elastography for customized eye care: a success case of clinical translation (Conference Presentation)*, SPIE BiOS (SPIE, 2023), Vol. PC12381.
10. A. Eliasy, K.-J. Chen, R. Vinciguerra, B. T. Lopes, A. Abass, P. Vinciguerra, R. Ambrósio Jr., C. J. Roberts, and A. Elsheikh, "Determination of Corneal Biomechanical Behavior in-vivo for Healthy Eyes Using CorVis ST Tonometry: Stress-Strain Index," Frontiers in Bioengineering and Biotechnology **7**(2019).
11. A. Curatolo, J. S. Birkenfeld, E. Martinez-Enriquez, J. A. Germann, G. Muralidharan, J. Palací, D. Pascual, A. Eliasy, A. Abass, J. Solarski, K. Karnowski, M. Wojtkowski, A. Elsheikh, and S. Marcos, "Multi-meridian corneal imaging of air-puff induced deformation forimproved detection of biomechanical abnormalities," Biomed. Opt. Express **11**, 6337-6355 (2020).
12. A. Sinha Roy and W. J. Dupps, Jr., "Patient-specific modeling of corneal refractive surgery outcomes and inverse estimation of elastic property changes," J Biomech Eng **133**, 011002 (2011).
13. F. Zvietcovich, J. Birkenfeld, A. Varea, A. M. Gonzalez, A. Curatolo, and S. Marcos, "Multi-meridian wave-based corneal optical coherence elastography in normal and keratoconic patients," Investigative Ophthalmology & Visual Science **63**, 2380 – A0183-2380 – A0183 (2022).
14. M. Xu, A. L. Lerner, P. D. Funkenbusch, A. Richhariya, and G. Yoon, "Sensitivity of corneal biomechanical and optical behavior to material parameters using design of experiments method," Comput Methods Biomech Biomed Engin **21**, 287-296 (2018).
15. F. C. Delori, R. H. Webb, and D. H. Sliney, "Maximum permissible exposures for ocular safety (ANSI 2000), with emphasis on ophthalmic devices," J. Opt. Soc. Am. A **24**, 1250-1265 (2007).
16. F. a. D. Administration, "Guidance for Industry and Food and Drug Administration Staff," in *Marketing Clearance of Diagnostic Ultrasound Systems and Transducers*, U. S. D. o. H. a. H. Services, ed. (Center for Devices and Radiological Health, Rockville, MD, USA., 2019).

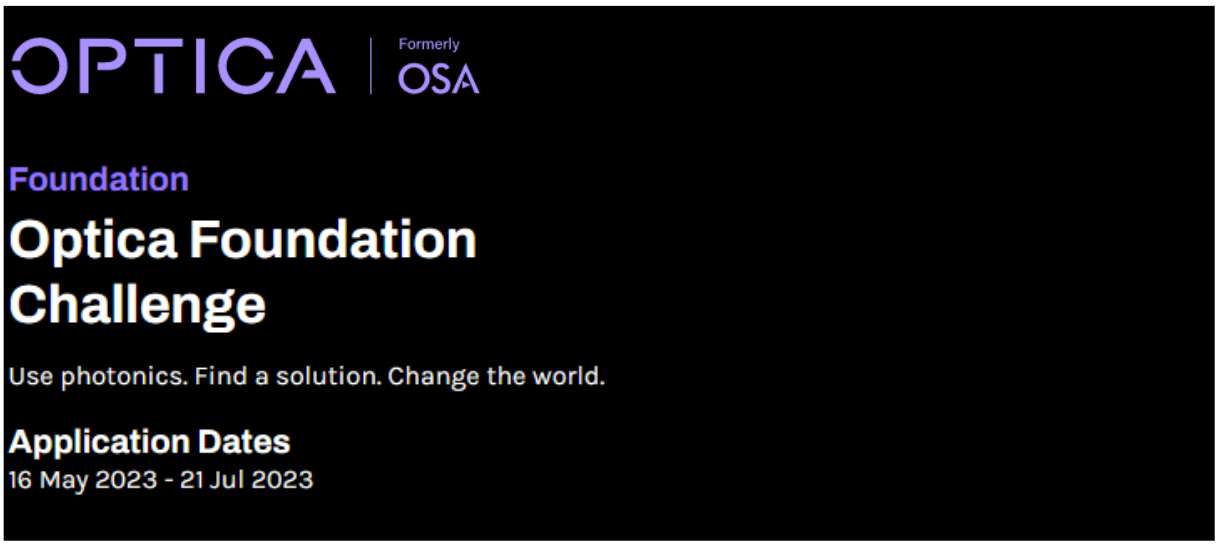

Executive Summary of "Hardware and Software Enablers for Future Optical Access Networks"

Contact: Gaël Simon, Philippe Chanclou

The access network recently witnessed an important increase, through the massive deployment of Fiber To The Home (FTTH). The industry is already working on the definition of the optical technologies which will replace the currently deployed technology, the G-PON (gigabit passive optical network) standard, offering higher than ever throughputs. Those future technologies will enable, beside the throughput increase, to answer the constantly evolving customers' uses.

The success of G-PON and the coming XGS-PON technologies and similar permitted to imagine new use cases for those technologies, in taking advantage of their robustness, their low energy consumption, or their low-cost for mass production in other network segments. This is the objective of the "ETSI-F5G" organism, which aims to "extend the FTTH paradigm to a Fiber to Everywhere".

In parallel, the rapid development of mobile networks (5G's deployment started; 6G's main directions emerge) requires the fiber infrastructure to evolve toward antenna sites. Mobile network transport and associated specifications induce important constraints on optical segments in terms of throughput (10x more in 6G than 5G), and latency (10x less in 6G than 5G). This is emphasized by the interest in solutions as "Cloud Radio Access Network". The later splits the radio network functions and creates new interfaces, often requiring high bitrates, as the x-Haul.

The objective of this project is to identify technological solutions allowing to answer to previously presented stakes, and to identify their strength and weaknesses, while insuring interoperability of the future systems working at 100Gbit/s. The current optical transmission technologies for access network employ Non-return to Zero modulation format, for the sake of simplicity and cost. However, the need for high bitrate interface come at a price, which imposes to reevaluate the solutions and to assess the need for a technological rupture. It could mean to choose PAM4, coherent detection "regular" or simplified, the use of Frequency Division Multiplexing, Wavelength Division Multiplexing, NRZ at higher bitrate,… In any case, those solutions must adapt to the multiple access topology of the FTTH. The energy consumption must also be carefully monitored, and so must be the ability to maintain interface's interoperability, avoid the dependency to a vendor, and make the optical fiber passive infrastructure viable.

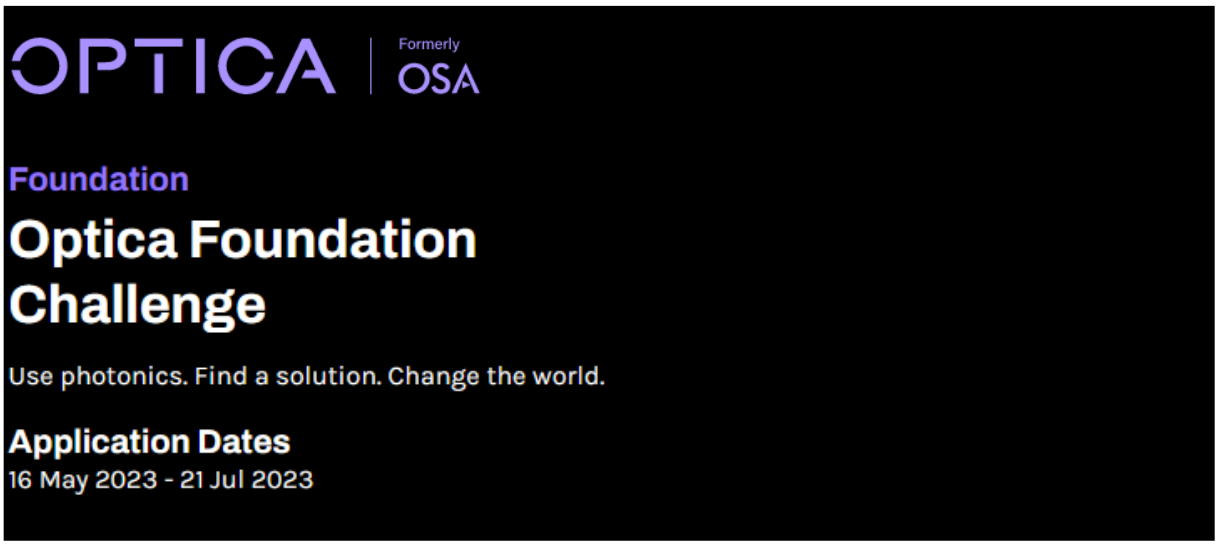

Proposal “hardware and software enablers for future optical access networks”

Contact: Gaël Simon, Philippe Chanclou

Literature review for Fiber to the Home:

The ITU-T has been preparing for several years the successor of Gigabit Passive Optical Networks (G-PON) and 10G Symmetrical (XGS-PON): Higher Speed PON (HS-PON). It already provides consolidated standards, even if several parameters remains for further study, particularly in upstream. It aims to provide 50Gb/s in downstream with a Non-Return to Zero (NRZ) modulation format. The upstream must be single wavelength and NRZ, and several bitrate options exist, namely 12.5Gb/s, 25Gb/s, or 50Gb/s, to enable wider applications than FTTH, such as high throughput gold offers for enterprises. HS-PON is the first PON standard to enable the use of Digital Signal Processing (DSP) in order to meet high bitrate performances. While DSP is more and more used in other network segments, it presents strong disadvantages, such as added costs and complexity and can be prohibitive for broadband applications. For example, solutions such as Feed-Forward Equalizers (FFEs) present several “taps” to manage, which should be adapted to the different electro-optical path to be crossed by the signal: with different lasers or receivers with limited bandwidths, optical paths subject to chirp, radio frequency reflections, … Also, the point-to-multipoint nature of HS-PON induces the use of various transceivers from many vendors and different generations, making the correct management of DSPs more complex.

Now in research, we have to define the next PON generation working at 100Gbit/s line rate supporting the existing fiber infrastructure and the coexistence with previous PON systems.

Literature review for Fiber to the Antenna:

After the commercial deployment of the 5th generation of mobile network (5G), the work on the 6th generation (6G) has begun. To handle new usages unlocked by future 6G networks, the future optical access network needs to be capable to transport the great amount of data that 6G will lever. Mobile Back/Mid/Fronthaul optical links capable to transport 100 Gbit/s to up to 1 Tbit/s are required [1] on a point-to-point topology (PtP). New usages such as industry 4.0 and metaverse should also benefit from these future high bitrate fiber links. The current PtP standards [2] used for mobile X-haul use intensity modulation and direct detection (IM/DD) with the Non-Return to Zero On-Off Keying (NRZ-OOK) modulation format and provide up to 25 Gbit/s per wavelength. Coherent technologies intend to meet the requirements for such transmission systems [3] but the added complexity and cost compared to an IM/DD system remains a drawback. Standardisation bodies like the Institute of Electrical and Electronics Engineers (IEEE) have already edited specification on 100 Gbit/s links [4]. For these links, the targeted channel insertion losses must be above 15 dB and the optical budget (OB) must reach to 21.5 dB.

[1] N. Rajatheva, “White paper on broadband connectivity in 6G,” 2020. Accessible online: https://www.6gflagship.com/white-paper-on-broadband-connectivity-in-6g/
[2] IEEE Standard for Ethernet -- Amendment 14: Bidirectional 10 Gb/s, 25 Gb/s, and 50 Gb/s Optical Access PHY, IEEE 802.3cp-2021, 2021.
[3] N. Suzuki, H. Miura, K. Mochizuki, and K. Matsuda, “Simplified digital coherent-based beyond-100G optical access systems for B5G/6G [Invited],” Journal of Optical Communications and Networking, vol. 14, no. 1, pp. A1–A10, Jan. 2022, doi: 10.1364/JOCN.438884.

Problem Statement/Objective:

The objective of this proposal is to identify technological solutions allowing to answer to previously presented stakes, and to identify their strength and weaknesses, while insuring interoperability of the future systems. The current optical transmission technologies for access network employ Non-return to Zero modulation format, for the sake of simplicity and cost.
However, the need for high bitrate interface come at a price, which imposes to reevaluate the solutions and to assess the need for a technological rupture. It could mean to choose PAM4, coherent detection “regular” or simplified, the use of Frequency Division Multiplexing, Wavelength Division Multiplexing, NRZ at higher bitrate,… In any case, those solutions must adapt to the multiple access topology of the FTTH. The energy consumption must also be carefully monitored, and so must be the ability to maintain interface’s interoperability, avoid the dependency to a vendor, and make the optical fiber passive infrastructure viable.

Outline of tasks/Work Plan:

The main direct output of this proposal is to lead three PhD students towards their PhD defense during this three years project. Being part of a wider research team, the work in which the student will participate will include the following technical task:

- Assessment of 100Gbit/s or more based on NRZ modulation with DSP
- Evaluation of new optical access transmission supporting multiple access function
- Feasibility study to support existing optical fiber infrastructure and new fiber (multi-core and hollow core) and coexistence with legacy optical access solutions
- Feasibility to support interoperability (physical layer and MAC layer) to have open access systems

Outcome(s):

The expected outcomes are :

- Addressing disruptive research for complementary technologies enabling to support the full potential of future FTTH wired and 6G wireless communications and service infrastructure
- Availability of fixed xHaul networks with performance levels compatible with 6G KPI’s in terms of bandwidth, capacity, latency, and flexibility
- Foster capabilities in key technologies and notably advanced signal processing for optical communications
- Trustworthy and energy-efficient network and infrastructures
- Offering increased network resilience, openness, and transparency

Impact:

Given the disruptive and ambitious nature of this proposal research and the potential of its ultimate deployment to break existing technological barriers enabling the sustainable growth of the internet into the 6G era, it can have a multi-dimensional, positive and long-lasting impact across many sectors.
The research proposal is primarily concerned with the generation of new high-quality knowledge that will play a central role in the development of next generation FTTH and 6G networks, and this will be created through practice, collaboration, interaction, and education, generated thanks to the complementary know-how provided by the scientific dissemination. In particular, this proposal is proposing a set of new advancements covering different scientific areas which are imperative for future optical access networks:

· High performance transceivers: Scientific impact here will be related to the development of proof-of-concept systems that can support up to Terabit/s capacity for short reach optical fiber communication. Additional impact in this area will be concerned with the development of components (photonic chips) for transceivers.
· Bespoke architectures for 6G services: Based on the novel optical transceiver, the research plan will design a truly converged and flexible mobile transport network architecture featuring ultra-high throughput, energy efficient and low latency optical communication, providing secure and reliable optical only pathways from remote antenna sites back to the network core. The establishment of a new network architecture offering unprecedented levels of network flexibility while ensuring the evolution to 6G connectively is a key scientific impact of the work.

This proposal will embrace the *Open Science practice*, sharing the knowledge and data generated in the RD&I process, through contributions in key scientific journals, conferences, and workshops, granting full and immediate Open Access to the project outcomes. This will increase the openness, quality and performance of the research, sharing with the scientific community and general public the new knowledge generated in the optical and 6G domain. The key results will be promoted also on social and popular science media to increase understanding and engagement of society in optical fiber capabilities and advantages.

PLASMONIC SENSORS FOR MONITORING WATER CONTAMINANTS

In rural zones of Northeast Mexico

Category: Health

The goal of wastewater quality monitoring is to obtain quantitative information about the physical and chemical characteristics of the water, such as color, refractive index, acidity, and salinity, to mention a few. Due to in *rural areas*, especially in the *north of Mexico*, obtaining fresh water is complex and is getting harder to obtain; usually, access to water in these areas is through subsoil water wells and then purified using artisanal water filters. Therefore, to improve human health in the community, it is necessary to monitor the quality of water from these artisanal filters, which are handmade using local resources.

The refractive index (RI) is a generic indicator of water quality, as any substance dissolved in water will change the refractive index of the water matrix. Its advantage is that it includes consistent sensitivity for all substances, response linear with concentration, and high resistance to matrix interference. Surface plasmon resonance (SPR) senses the refractive index changes near the surface layer and is extremely sensitive to detecting minimal refractive index changes. By angular scanning reflectivity, the SPR angle occurs at the minimum reflectivity. The SPR angle changes with the solution's refractive index at the interface, and the latter changes with the mass, density, and refractive index of foreign items attached to the surface of the metallic film. We use the transfer matrix method for a multilayer system to simulate numerically the reflectivity intensity of the p-polarized incident beam.

The general objective is to design and optimize a portable plasmonic sensor in the Kretschmann configuration for monitoring the water quality of artisanal filters in rural zones based on refractive index changes using the matrix transfer method.

Participants will focus activities to achieve the following specific objectives: 1) to achieve the relationship between the ratio of containments presented in a water sample with the refractive index, 2) to prepare solutions for different molarities of different contaminants and measure the refractive index of the solution for each concentration, 3) to propose a n-layers Kretschmann configuration sensitive to water contaminants, 4) to simulate numerically the reflectivity angular scanning for each concentration and achieve the resonance angle, 5) to use the Taguchi´s method to determine the best performance of the sensor from the control factors (wavelength, metal film, thickness) and 6) to implement the experimental prototype for monitoring the quality water from the artisanal filter.

The quality of water for human consumption depends on the area's environmental conditions. In urban areas with seismic fractures, such as Mexico City, wastewater is enriched with sulfates, nitrates, arsenic, manganese, lead, and iron. In contrast, in rural areas in the northeast of Mexico, wells are contaminated with coliform organisms due to fecal contamination of warm-blooded animals. Particularly, in the northeast of Mexico, the presence of dissolved solids is related to the surroundings of the Sierra Madre Oriental, as it comes from the dissolution of minerals that form subsoils and rocks. Along the Santa Catarina River, the concentration varied from 500 to 600 ppm, and this can be attributed to the flow that carries groundwater through the subsoil, dissolving salts such as chlorides, sulfates ($CuSO_4$), and the higher the content of dissolved solids there are, the greater the possibility of taste problems, laxative effects, etc. Thus, preserving and keeping the natural space that provides the water source free of contaminants is necessary. Plasmonic sensors can improve community health through real-time measurements of filtered water quality from subsoil wells and artisanal filters in rural areas.

PLASMONIC SENSORS FOR MONITORING WATER CONTAMINANTS

In Rural Communities of Northeast Mexico

Introduction

Commercial wastewater comes from non-domestic sources, such as industrial processes, where wastewater can be incredibly harmful [1]. Wastewater quality monitoring is a public health tool essential for effective pandemic management [2]. The objective of wastewater quality monitoring is to obtain quantitative information on the physical and chemical characteristics such as color, refractive index, acidity, and salinity, to mention a few [3]. Domestic water is another of the leading causes of wastewater pollution. The house wastewater is water generated after using fresh water. The source of wastewater in homes, residential and domestic, comes from bathing, toilet flushing, laundry, and dishwashing, to mention someone [4]. Besides, there are non-residential areas, such as rural areas, where access to fresh water is difficult [5]. The access to water in these areas is through subsoil water wells purified using artisanal water filters. Then, to improve human health through access to clean water in the community, it is necessary to monitor the quality of water from the artisanal filters [6, 16]. An artisanal or handmade water filter is a water filtration system made using a few essential items such as activated carbon, Tenzontle stone, marvel gravel, natural coarse silica sand, and fine-grained silica sand. In this filtering method, the bed of activated carbon removes the impurities from a fluid by adsorption mechanism. After passing through the activated carbon, it flows through the Tenzontle stone, a reddish-colored porous stone. At this stage, the water is filtered through the holes, reducing impurities and contaminants. Marble gravel, coarse and fine silica are materials based on crushing, screened for the necessary grain distribution. They serve as a support, aiming to eliminate salts, metals, and minerals. Measurement devices for various chemical and physical parameters facilitate us in monitoring the water quality of artisanal filters, such as pH [7], electrical conductivity (EC) [8], redox potential (ORP), dissolved oxygen (DO), turbidity [9] and refractive index [10].

Typically, the Refractive Index (RI) of water is approximately 1.333 at 20 degrees Celsius (nD20) and is a valuable indicator of water quality because when any substance is mixed, the refractive index changes. The Abbe refractometer is the standard instrument for measuring the refractive index [11]. The Abbe refractometer has a wide range (nD = 1.3 to 1.7) and requires a minimal sample, its accuracy is about ±0.0002.

Problem statement

In this project, we propose designing and optimizing a portable plasmonic sensor for monitoring the water quality of artisanal filters in rural zones based on refractive index changes. This phenomenon uses the surface plasmon polariton (SPP) excitation on the interface metal/dielectric of our device to sense the refractive index in each stage of the artisanal filter.

Literature review

Surface plasmons are electromagnetic waves propagating along the surface at the interface metal/dielectric [12] as the core of the sensor device. Surface plasmon resonance (SPR) senses the refractive index changes near the surface layer and is extremely sensitive to detecting minimal RI changes [13]. By angular scanning reflectivity, the SPR angle occurs at the minimum reflectivity. The SPR angle changes with the solution's refractive index at the interface, and the latter changes with the mass, density, and refractive index of foreign items attached to the surface of the metallic film. SPR angle changes provide information about mass, density, and refractive index change on the metallic surface. The Kretschmann configuration is a setup to excite surface plasmon polaritons (SPPs) in thin metal films [14]. The Kretschmann configuration consists of a thin metal film deposited on a high-index prism. Under total internal reflection, the incident light at the interface glass-metallic film, an evanescent wave, excites the electrons metal producing an SPP. Theoretically, only the

parallel-polarized light is practical in the SPR sensing techniques. Thus, we use the transfer matrix method for a multilayer system to simulate numerically the reflectivity intensity of the p-polarized incident beam [15]. A specific thickness characterizes each layer of the structure (stratified medium) d with a complex refractive index $N = n + ik$. Furthermore, each layer of a multilayer coating has its transfer matrix, and the overall transfer matrix of the system is the product of individual transfer matrices, taken in the order in which the light propagates through the multilayer stack for each incident angle θ_i.

$$M_i = \prod_{j=1}^{n} M_{j-1,j} = \begin{pmatrix} m_{11,i} & m_{12,i} \\ m_{21,i} & m_{22,i} \end{pmatrix}.$$

The interference matrix of the jth layer is expressed by

$$M_{j-1,j} = \begin{pmatrix} \dfrac{\exp(i\varphi_j)}{t_{j-1,j}} & \dfrac{\exp(-i\varphi_j)\, r_{j-1,j}}{t_{j-1,j}} \\ \dfrac{\exp(i\varphi_j) r_{j-1,j}}{t_{j-1,j}} & \dfrac{\exp(-i\varphi_j)}{t_{j-1,j}} \end{pmatrix},$$

where

$$r_{j-1,j} = \frac{n_{j-1}^2 k_x^j - n_j^2 k_x^{j-1}}{n_{j-1}^2 k_x^j + n_j^2 k_x^{j-1}},\ t_{j-1,j} = \frac{n_{j-1}}{n_j}\left(1 + r_{j-1,j}\right) \text{ and } \varphi_j = \frac{2\pi}{\lambda_0} n_j d_j \cos(\theta_j)$$

For each incident angle θ_i, the total reflectance R_{θ_i} is calculated by $R_{\theta_i} \sim |R_i|^2$, where $R_i = \frac{m_{21,i}}{m_{11,i}}$.

Objectives

- To develop a protocol to evaluate the quality of an artisanal water filter.
- To design a prototype of a plasmonic sensor in the Kretschmann configuration for monitoring well water quality in artisanal filters located in rural areas. The sensor will detect contaminants using changes in the refractive index using the matrix transfer method.

Work plan

The work plan is presented in the next table.

Activity/Month	1	2	3	4	5	6	7	8	9	10	11	12	13	14	15	16	17	18
Purchases of laboratory equipment and materials: • Review of suppliers • Administrative process for the purchases • Shipment and imports																		
Numerical analysis: • Software development in Python • Definition of control factors and variables • Proposal of multiple layer arrays for the sensors • Statistics analysis to determine the best arrays																		
Collection of **water samples**:																		

• Visiting different rural communities to collect water samples. • Characterization of water samples at the "Environmental Bioremediation Laboratory" of the Medical Faculty – UANL.																		
Artisanal filters construction																		
Design and fabrication of thin films: • Installation of the evaporator • Training of the research team members to use the evaporator. • Creation of different thin films • Characterization of thin films to prove the quality at CIMAV – Unidad Monterrey.																		
1st Report																		
Experiments: • Assembling the experimental arrangements • Automation in the handling of the experimental arrangement and the data collection of the sensors in collaboration with the Instituto Tecnológico Superior del Sur de Guanajuato. • Conducting the experiments and comparison between numerical and experimental results • Improvement of experiments																		
2nd report																		
Proof of concept: • Selecting the best experimental setup • Prototype design • Prototype construction • Testing																		
Bachelor thesis[1]																		
Field testing																		
3rd report																		

[1] The bachelor Physics students will collaborate since the begging of the project but as part of their academic activities they must prepare their thesis during their last semester and participate in different academic activities.

Outcomes

- Involve at least two undergraduate physics students to work on the project, expecting to have a bachelor thesis by the end of their participation.
- Increase the available literature about water pollution in the northeast of Mexico by reviewing the contaminants found and the efficiency of the artisanal filters used in the region.
- It is expected to obtain the relationship between the concentration of different contaminants in water solution with the refractive index, design the experimental setup of a plasmonic sensor, to generate a statistics analysis of the main factors that contribute to increase the sensor quality, among other scientific results that will be presented at national/international conferences and publish in OPTICA journals.
- Develop a protocol that will be used to determine contaminants in water and evaluate the efficiency of artisanal water filters.
- The project's main outcome will be the creation of an experimental prototype. This prototype will gather angle scans of the reflectance for each concentration. The SPR angle for each concentration will also be calculated. Samples will be taken using water from wells and an artisanal filter with various stages.
- In addition, this project will have these secondary outcomes:
    - The strengthening of the recently created "Plasmonic Sensors Laboratory", which will increase the research capacity of UANL (Universidad Autónoma de Nuevo León), my research group, and myself.
    - The research group that will help me during the project, integrated by Dr. Rodolfo Cortés-Martínez from Centro de Investigación Científica y de Educación Superior de Ensenada – Monterrey (CICESE) and my partners Dr. Edgar Martínez-Guerra and Dr. Perla Viera-González, begin new collaborations:
        - Dr. Karim Acuña-Askar from the Medical Faculty of the Universidad Autónoma de Nuevo León.
        - Dr. Eduardo Martínez-Guerra from the Centro de Investigación en Materiales Avanzados – Unidad Monterrey (CIMAV).
        - Dr. Carlos Alberto Fuentes-Hernández from Instituto Tecnológico Superior del Sur de Guanajuato

Impact

The quality of water that humans consume is influenced by the environmental conditions of the area where the water sources are located. In rural northeast Mexico, well contamination occurs due to fecal matter from animals, dissolved solids from minerals in the subsoil, and rocks related to the surroundings of the Sierra Madre Oriental are also present in water sources, causing taste and laxative issues. Ensuring the quality of natural water in rural areas is needed, so a portable device is necessary to help communities' well-being. Developing a portable plasmonic sensor can be a valuable aid in achieving this goal. By detecting contaminants in real time, this technology can help ensure that the water supply remains safe and healthy for consumption.

References

[1] Moore, J.W. (1989). Industrial Wastewater Management. In: Balancing the Needs of Water Use. Springer Series on Environmental Management. Springer, New York, NY. https://doi.org/10.1007/978-1-4612-3496-8_6.

[2] Quevauviller, Philippe & Thomas, Olivier & A., Van. (2006). Wastewater Quality Monitoring and Treatment. 10.1002/9780470058725.

[3] Omer, Nayla. (2020). Water Quality Parameters. 10.5772/intechopen.89657.

[4] Cominola, A., Preiss, L., Thyer, M. *et al.* The determinants of household water consumption: A review and assessment framework for research and practice. *npj Clean Water* **6**, 11 (2023). https://doi.org/10.1038/s41545-022-00208-8.

[5] Silva Rodríguez de San Miguel, Jorge Alejandro. (2016). Rural Water Supply in Mexico. Cuadernos de Desarrollo Rural. 13. 123-141. 10.11144/Javeriana.cdr13-78.rwsm.

[6] Silva, Jhon Lennon Bezerra Da & Oliveira, J & Miranda, E & Oliveira, Emanuele & Ortiz, Pedro Francisco & Lins, Frederico. (2019). EFFICIENCY OF ARTESIAN FILTERS TO ELIMINATE SOLIDS PRESENT IN IRRIGATION WATER.

[7] Yiheng Qin, Arif U. Alam, Si Pan, Matiar M.R. Howlader, Raja Ghosh, Nan-Xing Hu, Hao Jin, Shurong Dong, Chih-Hung Chen, M. Jamal Deen, Integrated water quality monitoring system with pH, free chlorine, and temperature sensors, Sensors and Actuators B: Chemical, Volume 255, Part 1, 2018, Pages 781-790, ISSN 0925-4005, https://doi.org/10.1016/j.snb.2017.07.188

[8] Ramos, P.M.; Pereira, J.M.D.; Ramos, H.M.G.; Ribeiro, A.L. (2008). A Four-Terminal Water-Quality-Monitoring Conductivity Sensor., 57(3), 577–583. doi:10.1109/tim.2007.911703.

[9] Mulyana, Y; Hakim, D L (2018). Prototype of Water Turbidity Monitoring System. IOP Conference Series: Materials Science and Engineering, 384(), 012052–. doi:10.1088/1757-899X/384/1/012052.

[10] Van den Broeke, J. The Benefits of Using Refractive Index for Water Quality Monitoring in Distribution Networks; Optiqua Technologies: Richmond, VIC, Australia, 2014.

[11] Rheims, J & Köser, Jan & Wriedt, Thomas. (1999). Refractive-index measurements in the near-IR using an Abbe refractometer. Measurement Science and Technology. 8. 601. 10.1088/0957-0233/8/6/003.

[12] Zhang, Junxi & Zhang, Lide & Xu, Wei. (2012). Surface plasmon polaritons: Physics and applications. Journal of Physics D-applied Physics - J PHYS-D-APPL PHYS. 45. 10.1088/0022-3727/45/11/113001.

[13] J. Divya, S. Selvendran, A. Sivanantha Raja, A. Sivasubramanian, Surface plasmon based plasmonic sensors: A review on their past, present and future, Biosensors and Bioelectronics: X, Volume 11, 2022, 100175, ISSN 2590-1370, https://doi.org/10.1016/j.biosx.2022.100175.

[14] Vinogradov, A. & Dorofeenko, Alexander & Pukhov, A. & Lisyansky, Alexander. (2017). Exciting of surface plasmon polaritons in the Kretschmann configuration. Physical Review B. 97. 10.1103/PhysRevB.97.235407.

[15] Gwon, Hyuk & Lee, Seong. (2010). Spectral and Angular Responses of Surface Plasmon Resonance Based on the Kretschmann Prism Configuration. Materials Transactions - MATER TRANS. 51. 10.2320/matertrans.M2010003.

[16] M. de los A. Ayala Cruz, “Calidad Fisicoquimica y Bacteriologica de un Acuifero de Cadereyta Jimenez, nuevo leon,” Universidad Autónoma de Nuevo León, 1996.

Background – Quantum information processing (QIP) takes advantage of quantum mechanical resources like superposition and entanglement, leading to groundbreaking advancements in computational efficiency, communication security, and sensing/imaging resolution. Various systems, from single atoms to macroscopic objects such as superconducting circuits, have demonstrated quantum effects. Among the many potential quantum platforms, photon-based optical systems stand out as prime candidates due to their exceptional qualities: ultimate propagation speed, immunity to decoherence and crosstalk, and low power consumption. Despite the recent attention to photonic QIP schemes, there is a fundamental hurdle in achieving scalable photonic QIP. This obstacle arises from the requirement of strongly enhanced photon interaction and/or high nonlinearities, which have proven challenging to attain. Despite efforts to improve nonlinearities in traditional materials, the achieved interaction falls far short of the single-photon nonlinearity necessary for a practical and scalable quantum photonic platform.

Project goals – To address the significant challenges in achieving robust photon-photon interactions at the single-photon level through a scalable approach, our endeavor focuses on developing the first *nonlinear quantum nanophotonics* platform. We will leverage the recently discovered strongly interacting Rydberg excitons in cuprous oxide (Cu_2O) thin films and microcrystals for this innovative platform. By combining nanophotonics as a controllable, low-loss, and scalable foundation with extraordinary quantum properties and strong single-photon level interaction of Rydberg atoms, we aim to create a novel quantum material-based system. Our project will begin by establishing a CMOS-compatible and easily integrable growth method to produce thin films and microcrystals of Cu_2O, a quantum material uniquely known for its highly-excited Rydberg states. Through detailed high-resolution laser spectroscopy, we will thoroughly investigate the properties of these excitonic levels, including their coherence and optical characteristics. The ultimate objective is to realize the Rydberg photonics platform by effectively coupling strongly interacting Rydberg excitons in Cu_2O with specially designed and optimized nanophotonic structures. To achieve this, we will study the mutual coupling between the Rydberg exciton and engineered nanostructures. By examining the dynamics of this hybrid system and assessing the impact of Rydberg excitons in facilitating strong photon-photon interaction and generating substantial optical nonlinearities, we seek to overcome the existing limitations and unlock the potential for scalable quantum nanophotonics.

Broader Impact – By gaining fundamental insights into Cu_2O Rydberg excitons and their exciton-photonic hybrids, we have the potential to usher in the next generation of powerful quantum optics methodologies, which were previously limited mostly to atomic systems. The results of this endeavor will push the boundaries of light-matter interactions in solid states, transcending conventional excitonic schemes that rely on ground-state excitons. The proposed novel platform presents an exciting opportunity to explore quantum optics at the *single-photon level*, capitalizing on the concept of Rydberg blockade and forming strongly interacting photons. They could enable the realization of photonic quantum simulators and facilitate progress in quantum nonlinear optics, nanophotonics, and QIP. The outcomes of this project would not only hold great significance for the fundamental understanding of quantum phenomena but also carry substantial implications for technological applications. This research has the potential to unlock new possibilities in quantum optics and solid-state physics, bringing us closer to the practical implementation of quantum-enhanced technologies and furthering our exploration of the quantum world.

Nonlinear Quantum Optics at the Ultimate Limit: The Intersection of Rydberg Physics with Nanophotonics

A. Motivation and Statement of Objectives

Quantum information processing (QIP) exploits quantum mechanical resources, such as superposition and entanglement, to achieve advancements in computational efficiency, communication security, imaging resolution, and metrology. Quantum effects have been observed in diverse systems, from single atoms and molecules to larger objects like superconducting circuits. Photons, among numerous potential quantum platforms, offer advantages such as high propagation speed, immunity to decoherence and crosstalk, and low power consumption. These attributes make photons a competitive choice for harnessing quantum effects. However, the inherent minimal interaction of photons in a vacuum limits optical nonlinearities, impeding the emergence of photonic quantum many-body effects and the realization of photonic quantum gates. Efforts to enhance optical nonlinearity using nonlinear materials or mediated interactions in cold atomic ensembles face challenges, including weak interaction strength and practicality issues, respectively.

To address the challenge of achieving robust on-chip photon-photon interactions at the *single-photon level*, my research group focuses on utilizing *Rydberg excitons in cuprous oxide* (Cu_2O) thin films and microcrystals. Leveraging the unique properties of Rydberg states that can be obtained in this material, we aim to enhance our understanding of strongly-correlated photon states, enabling exploration of wide arrays of problems ranging from fundamental questions in quantum non-equilibrium phases of driven-dissipative systems to applications in quantum sensing and imaging. Our research has broad implications for quantum information science and engineering (QISE), as summarized in **Fig. 1(a)**. Our long-term research goal is to develop an integrable nonlinear quantum optics platform, as depicted in **Fig. 1(b)**. In this one-year project, we will take three critical steps toward achieving our long-term goals:

1. Develop CMOS-compatible fabrication of Cu_2O thin films and microcrystals exhibiting highly excited Rydberg excitons and investigate their optical and quantum coherence properties (cf. **C.1.**)
2. Develop a model and perform numerical simulations for nanophotonic devices such as waveguides and ring resonators integrated with Cu_2O microcrystals to obtain the optimal design parameters that maximize the coupling (cf. **C.2.**)
3. Realize integrated photonic devices that are coupled to the Rydberg excitons to conduct detailed studies of the exciton-device optical properties and how the Rydberg properties can be controlled via nanophotonic structures (cf. **C.3.**)

The outcomes of this research are expected to have significant fundamental and technological implications in quantum nonlinear optics, nanophotonics, photonic quantum information processing, Rydberg sensing and metrology, and quantum photonics simulators.

B. Background and State-of-the-art

Photons have played a crucial role in the advancement of quantum science and technology. They can transmit information over long distances and serve as the foundation for current telecommunication networks, making them a vital infrastructure component for future quantum internet applications. Furthermore, photons can be manipulated within sophisticated photonic circuits, enabling the scalability of photonic quantum computing. However, the development of more advanced devices and protocols relies on the utilization of multi-photon states with specific forms of entanglement, which necessitates strong photon-photon interactions, a crucial element that is currently lacking. As a result, there is an ongoing pursuit to discover efficient light-matter interfaces that can increase the photon-photon interaction and hence, reliably generate quantum many-body resource states. In solid-state platforms, the strong coupling

regime has been achieved using ground-state excitons in various materials such as bulk semiconductors, quantum wells and dots, 2D materials, and organic molecules [1],[2]. Despite significant progress in these areas, none of these platforms have achieved the level of few-photon nonlinearity required for photonic QIP. In the quest for new platforms to enhance this interaction, it has been demonstrated in atomic systems that highly excited Rydberg states hold great promise for achieving this goal [3]-[7].

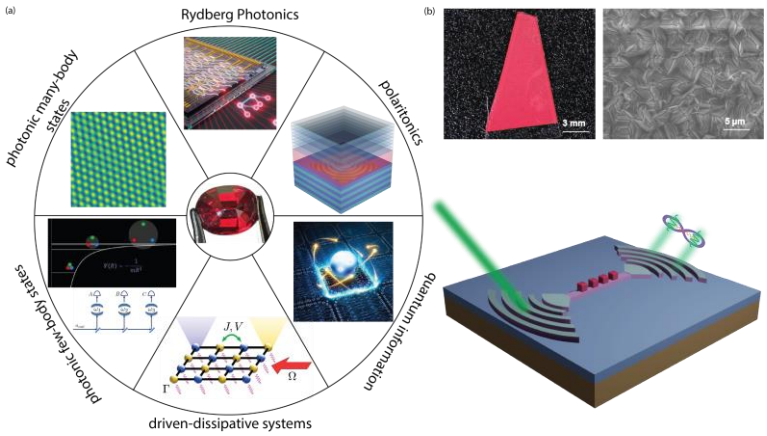

Figure 1. **Vision.** (a) My long-term scientific vision and the wide array of single-photon non-linearity applications in QISE. (b) Schematics of Rydberg photonics of this proposal.

Rydberg physics is a field of study that focuses on highly excited electronic states denoted by a principal quantum number, n, possessing unique properties due to their extended electronic wavefunction and low binding energy. Notably, Rydberg atoms exhibit a van der Waals interaction that scales as n^{11}, making it significantly stronger than the interaction between ground-state atoms [8]. This interaction can lead to the *Rydberg blockade* phenomenon, where the energy level of a double-excited state is shifted, preventing the simultaneous excitation of nearby atoms, as shown in **Fig. 2**. The Rydberg blockade has enabled coherent control of Rydberg atoms, on-demand, and deterministic single-photon sources, strong optical nonlinearities, and photon correlations. Ongoing research aims to utilize Rydberg atoms in sensing, quantum optics, and quantum simulations [9]-[13]. However, a fundamental question remains: *Can these exceptional capabilities be achieved in the solid-state realm, which offers advantages in scalability and robustness*?

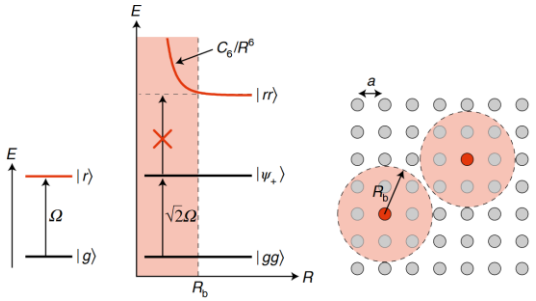

Figure 2. Rydberg blockade. Large energy shift due to the strong Rydberg-Rydberg interaction leads to the blockade effect (middle panel) where the number of excitations in a sphere of blockade radius, R_b, is limited to only one, as depicted in the right panel.

Semiconductors present an opportunity for integrating Rydberg physics into nanostructures, benefiting from controllability and scalability. Moreover, semiconductors bridge the gap between quantum photonics and solid-state systems. Rydberg exciton interactions in semiconductors are remarkably strong, leading to significant optical nonlinearities at the single-photon level. This characteristic makes Rydberg excitons in semiconductors promising candidates for various quantum photonic applications, such as on-demand single-photon sources and single-photon transistors. Considerable exploration has been conducted thus far, resulting in the observation of excitonic states beyond the ground state in a few material systems, such as two-dimensional transition metal dichalcogenides. Among these materials, Cu_2O stands out as the only semiconductor capable of hosting giant Rydberg excitons. Excited excitonic states in cuprous oxide share many similarities with Rydberg atoms, with principal quantum numbers reaching up to n = 29 for Rydberg excitons in Cu_2O, surpassing the excitation levels observed in any other solid-state systems [14],[15].

C. Technical Approach

C.1. *This Task develops CMOS-compatible fabrication of Cu_2O thin films and microcrystals exhibiting highly excited Rydberg excitons and investigates their Rydberg properties.*

To date, the research on Rydberg excitons in Cu_2O has primarily focused on bulk samples obtained from the Tsumeb mine in Namibia. These samples underwent mechanical polishing and chemical treatment to achieve smooth surfaces. However, obtaining high-quality synthetic samples is crucial for practical applications. Natural crystals have limitations in scalable technologies due to random impurities, defects, and their incompatibility with existing nanophotonics and integrability. Therefore, developing a robust fabrication method for synthetic films and crystals is essential. This approach offers several advantages: 1) *Scalability*: A reliable fabrication recipe for synthetic Cu_2O films and crystals allows control over various optical properties and facilitates the mass production of high-purity crystals. This approach has the potential to realize Cu_2O's scalability. 2) *Site-controlled growth*: Synthetic films and crystals enable precise placement of excitons, allowing for their coupling to on-chip nanophotonic circuits. It also offers a wide range of applications in quantum sensors, quantum sources, and QIP units. 3) *Extreme nonlinearity*: Thin-film samples and microcrystals with thicknesses comparable to the blockade radius can selectively excite only one Rydberg exciton, leading to extreme nonlinearity at the single-photon level. Their integration with nanophotonic devices enables the realization of various hybrid systems with implications for fundamental research and applications.

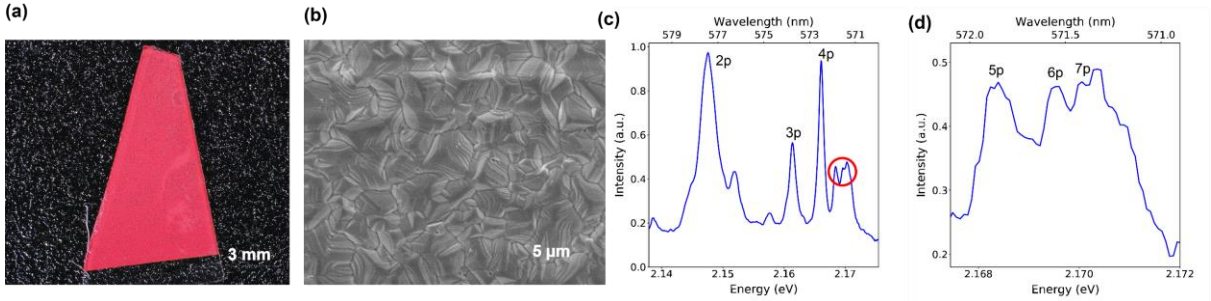

Figure 3. Results from PI's lab. (a) An optical microscope image and (b) SEM image of the grown synthetic Cu_2O film in my lab. (c) Excited Rydberg states up to (n = 8) in a non-resonant PL spectroscopy.

In our laboratory, we have recently implemented a CMOS-compatible method based on thermal oxidation to grow high-purity synthetic Cu_2O [16]. We have successfully observed Rydberg excitons up to n = 8 [17], as shown in **Fig. 3**. In this proposal, we aim to optimize the growth method further. We will focus on controlling the film's thickness within the range of 0.5-10 µm, comparable to the Rydberg blockade radius. Additionally, we will explore site-controlled growth techniques for efficient coupling to nanophotonic circuits. We will employ a home-built high-resolution cryo-spectroscopy setup, as schematically depicted in **Fig. 4**, to investigate the optical properties of the sample. Besides, both resonant and non-resonant photoluminescence (PL) spectra of Rydberg states will be studied.

C.2. *This Task develops a model and performs numerical simulations for nanophotonic devices such as waveguides and ring resonators integrated with Cu_2O microcrystals to obtain the optimal design parameters that maximize the coupling.*

In structured systems, the discrete energy spectrum of excitons can lead to efficient modification of relaxation processes between energy levels, and hence the excited state's lifetime. Previous studies have shown that the radiation rate of a quantum emitter can be noticeably controlled in the plasmonic mode of a single plasmonic nanoparticle or photonic structure, reaching frequencies in the terahertz range. In this Task, we will systematically study and optimize SiN nanophotonic devices including *waveguides* and *ring resonators* to couple the photonic modes to Rydberg excitons and control their radiative emission rate, respectively. **Figure 5** schematically depicts the heterogeneous Rydberg photonic platform with exemplary nanophotonic devices such as waveguides, ring resonators, and a *Mach-Zehnder interferometer*, which will be considered and optimized within the scope of this proposal.

The coupling between the optical mode of the device and Rydberg excitons depends on various parameters such as device geometry, the position of Rydberg excitons relative to the device, and the polarization of

photons in the optical mode. Controlled tuning of these parameters enables strong coupling between Rydberg excitons and the device, making this system a suitable platform for exploiting *strong light-matter interactions*. Using the same coupling scheme, we will couple Rydberg excitons to ring resonators, allowing specific coupling to transitions and enabling control through Purcell modifications. To study the collective phase shift of this ensemble on the photonic modes, we will also design an interferometer to directly investigate the dispersive effect of the interaction. Numerical simulations will be performed to find optimal geometries for achieving maximal enhancement at various emission wavelengths within the range of 570 nm to 615 nm. To obtain the best designs with the desired figure of merits, topology optimization methods in photonics will be leveraged for optical structure designs [18]. Special attention will be given to accounting for inevitable experimental imperfections, especially defects in fabrication, such as bumps and holes in Cu_2O films or nanoparticles.

C.3. *This Task will realize integrated photonic devices that are coupled to the Rydberg excitons and conduct detailed studies of the exciton-device optical properties and how the Rydberg properties can be controlled via nanophotonic structures.*

In this Task, we will integrate Cu_2O thin films and localized microcrystals developed in **Task 1** into the designed SiN devices in **Task 2** and experimentally realize the heterogeneous Rydberg photonics platform. However, stoichiometric SiN often exhibits high autofluorescence in the yellow exciton series, which hinders the observation of photoluminescence from the yellow and green Rydberg series. To overcome this limitation, we will employ non-stoichiometric nitrogen-rich SiN grown via high-density plasma chemical vapor deposition (HDPCVD), which substantially suppresses autofluorescence [19]. The SiN waveguide fabrication process involves patterning the waveguide on the substrate using e-beam lithography, followed by reactive ion etching (RIE) and lift-off processes.

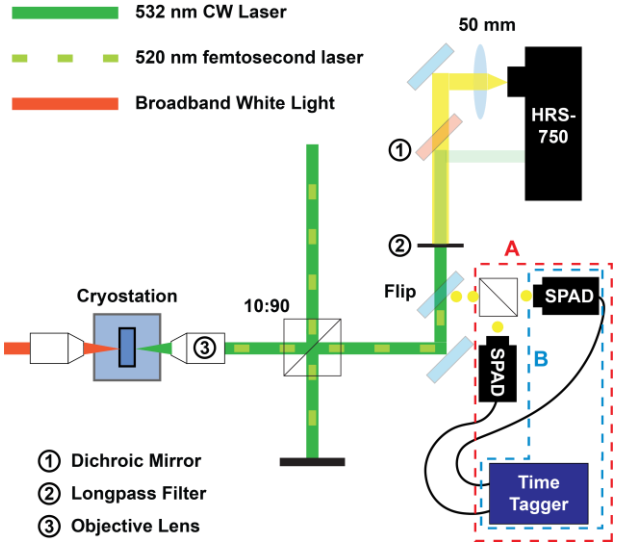

Figure 4. Home-built setup. Schematics of the home-built high-resolution laser spectroscopy setup for optical density, photoluminescence, and quantum correlation measurements at cryogenic temperatures.

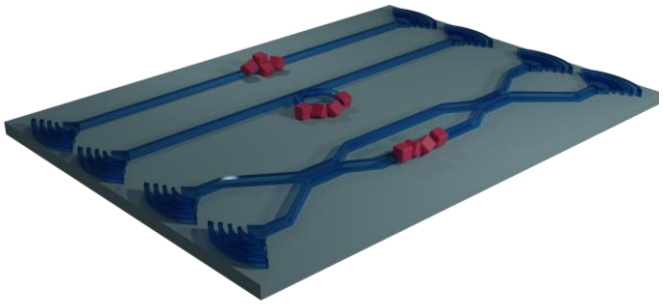

Figure 5. Rydberg photonics. Schematics of on-chip nanophotonic devices, e.g., waveguides, ring resonators, or interferometers, coupled to Cu_2O thin films or microcrystals (red parts in the middle of each device) hosting high-lying Rydberg excitons (not drawn to the scale).

After device fabrication, microcrystal Cu_2O will be grown on top of the SiN waveguides, resonators, and interferometers via the thermal oxidation method. The goal is to develop Cu_2O Rydberg excitons fully integrated with SiN-quantum photonic circuitry. Initially, high-resolution absorption spectroscopy will be performed to verify the coupling of Rydberg excitons within the wavelength range of 570 - 580 nm to the waveguides. By systematically studying the transmitted spectrum as a function of exciton density, we will map the effect of the blockade on the waveguide modes. Next, the developed time-correlated single-photon spectroscopy setup will be employed to resolve photoluminescence processes and the coupling dynamics on a scale of a few picoseconds. Low-jitter silicon

single-photon avalanche diode detectors and femtosecond-scale excitation will be used to accurately measure the Purcell enhancement due to nanophotonic cavities and optimized ring resonators. Additionally, a Mach-Zehnder interferometer will be used to measure the phase shift induced by Rydberg-mediated photon-photon interaction. At the extreme limit of the blockade, a π-phase shift is expected using only one photon, enabling the realization of a *deterministic photonic CNOT gate*. All experimental data will be carefully analyzed and compared to numerical simulations from **Task 2**.

D. Broader Impact

Our approach for achieving robust photon-photon interaction is distinctive and novel due to its utilization of the powerful and long-range interaction of highly-excited Rydberg states, combined with the unique quantum properties of Cu_2O as a solid-state host for such states. By working with Rydberg excitons in Cu_2O, we aim to apply advanced atomic physics techniques that were traditionally limited to actual atoms, thereby pushing the boundaries of light-matter interactions in solid-state materials beyond conventional excitonic schemes that primarily focused on ground-state excitons. This innovative platform opens up exciting opportunities for exploring quantum optics at the individual photon level, harnessing the concept of Rydberg blockade, and enabling the generation of strongly interacting photons [20]-[22]. The impact of this work extends across diverse fields, offering promising avenues for advancements in quantum science and technology.

Bibliography

[1] D. Ballarini and S. De Liberato, *Nanophotonics* **8**, 641-654 (2019).

[2] S. Haroche and M. Brune and J. M. Raimond, *Nat. Phys.* **16**, 243-246 (2020).

[3] J. D. Thompson et al., *Nature* **542**, 206-209 (2017).

[4] C. G. Wade et al., *Nat. Photonics* **11**, 40-43 (2017).

[5] D. Tiarks, S. Schmidt-Eberle, T. Stolz, G. Rempe, and S. Dürr, *Nat. Phys.* **15**, 124-126 (2019).

[6] H. Levine et al., *Phys. Rev. Lett.* **121**, 123603 (2018).

[7] Q. -Y. Liang et al., *Science* **359**, 783-786 (2018).

[8] T. F. Gallagher, *Rep. Prog. Phys*. **51**, 143 (1998).

[9] H. Bernien et al., *Nature* **551**, 579 (2017).

[10] A. Browaeys and T. Lahaye, *Nat. Phys*. **16**, 132-142 (2020).

[11] G. Semeghini et al., *Science* **374**, 1242 (2021).

[12] G. Giudici, M. D. Lukin, and H. Pichler, *Phys. Rev. Lett*. **129**, 090401 (2022).

[13] F. B. Dunning et al., *J. Phys. B: At. Mol. Opt. Phys.* **42**, 022001 (2009).

[14] T. Kazimierczuk, D. Fröhlich, S. Scheel, and M. Bayer, *Nature* **514**, 343-347 (2014).

[15] M. Aßmann, M. Bayer, *Adv. Quantum Technol*. **3**, 1900134 (2020).

[16] S. Steinhauer et al., *Comm. Mater.* **1**, 11 (2020).

[17] J. DeLange, K. Barua, V. Zwiller, S. Steinhauer, and H. Alaeian, *arXiv*:**2210.16416v1** (2022).

[18] R. E. Christiansen and O. Sigmund, *J. Opt. Soc. Am. B* **38**, 496 (2021).

[19] A. Senichev et al., *ACS Photonics* **9**, 3357-3365 (2022).

[20] V. Walther, S. O. Krüger, S. Scheel, and T. Pohl, *Phys. Rev. B* **98**, 165201 (2018).

[21] M. Khazali, K. Hashemi, and C. Simon, *J. Phys. B: At. Mol. Opt. Phys*. **50**, 215301 (2017).

[22] V. Walther, R. Johne, and T. Pohl, *Nat. Commun.* **9**, 1309 (2018).

Handheld MEMS-SOA Silicon Based Gas Analyzer for Real-time, Cumulative and Wide-Band Environmental Monitoring in Smart Cities

Assoc. Prof. Dr. Eng. Haitham Omran

Laboratory of Micro Optics, Faculty of Information Engineering and Technology (IET), German University in Cairo, Egypt

Human activities are the main cause of Earth's environmental changes [1]. Effects like global warming caused by increasing carbon dioxide (CO_2) and methane (CH_4) emission from fossil fuel, human waste and agricultural activities have disastrous effect on humankind [1, 2]. Rising see levels and extreme weather triggered by environmental changes affects the existence of many communities and even nations across the globe [3, 4]. Limiting the global warming and pollution to the target levels requires continuous, wideband, cheap and accumulative monitoring solutions for CO_2, CH_4 and other climate forcing emissions [1-4].

This proposal aims at contributing to achieve the global warming 2°C target limit implying a cumulative carbon emission limit of the order of 500 GtC [1]. The target limit is to be achieved by continuous, cumulative and smart monitoring of climate forcing gas emissions (e.g. CO_2, CH_4) using a flexible use case handheld micro-electro-mechanical-system semiconductor-optical-amplifier (MEMS-SOA) Silicon based gas analyzer with cloud connectivity for Internet of things (IoT) smart cities. The analyzer core engine is an experimentally verified MEMS-SOA swept laser source connected to a small gas cell [5-7]. The MEMS is constructed from two deeply-etched Si/Air Bragg mirrors attached to an electrostatic comb actuator allowing the tuning of the swept laser over 100 nm bandwidth with up to 0.2nm resolution depending on sweep speed [6, 7]. The absorption spectrum of gases in the near-infrared is used for quantitative and qualitative monitoring of the environment climate forcing emissions [5]. The device smart IoT and cloud connectivity allow real-time and accumulative monitoring which is crucial for correct environmental assessment and decision-making. The device will have a flexible use case by working in two gas sampling modes; an in-device near gas cell mode and long-fiber far gas cell mode for difficult to access locations (e.g. factories, mining cites and gas pipelines) enabled by a detachable gas cell head.

At the end of the project, the team will demonstrate a working prototype of a packaged handheld MEMS-SOA gas analyzer in the near-infrared spectrum. The package is to include all functional parts including the MEMS-SOA swept laser core module, control electronics, power supply, gas flow control and detachable gas cell head. We will demonstrate practical sensing of climate forcing gas emissions (e.g. CO_2, CH_4) in the range (1500 nm – 1600 nm) with up to 0.2nm resolution. The device will have IoT connectivity for smart cities environmental monitoring. We will develop a mobile app with cloud connectivity allowing device control, real-time monitoring and cumulative data logging for fast and accurate analysis and long-term decision-making based on cumulative sensing in smart cities.

Handheld MEMS-SOA Silicon Based Gas Analyzer for Real-time, Cumulative and Wide-Band Environmental Monitoring in Smart Cities

Assoc. Prof. Dr. Eng. Haitham Omran

Laboratory of Micro Optics, German University in Cairo

- **Literature Review**

Human induced climate changes are severely affecting and even threating the existence of the humankind. Global warming is mainly attributed to increased carbon dioxide (CO_2) emission from fossil fuels [1]. This emission have long lasting effects as they remain in the atmosphere for millennia affecting balanced echo systems [8]. A very dangerous consequence is the lock-in of these long lasting responses. European Union in 1996 proposed to limit global warming to 2°C [9] and the target was reaffirmed in the 2009 ‘‘Copenhagen Accord’’ [10]. Achieving the 2°C target converts to a fossil fuel emissions target using climate-carbon-cycle models. These models depends on cumulative emission data and not on temporal emission data [11]. Other human induced gas emissions like methane contribute to the global warming crisis [2]. Methane emission harms human and ecosystem health by contributing to the formation of ground-level ozone [2]. Limiting the global warming and pollution to the target levels requires multifold treatment with innovative systems and solutions enabling continuous, wideband, cumulative, cheap, and smart monitoring for climate forcing gas emissions. CO_2 monitoring is also very important in the safety of natural gas pipelines [1] and in the quality control of agri-food industry [12].

Gas chromatography [13] and mass spectroscopy [14] are famous techniques for gas detection but are not suitable for real-time and low cost environmental monitoring. Gas chromatography cannot work in real-time while mass spectroscopy is very expensive and bulky.

Sensing mechanisms of CO_2, methane and other climate forcing gases can be broadly classified as optical and electrochemical mechanisms [12]. The main optical mechanism depends on bulky and expensive mono-chromators and mid infrared optical detectors or high resolution but very expensive tunable laser sources [15, 16]. Optical MEMS based FT-IR spectrometers were demonstrated for gas sensing but they suffer from low resolution and low signal to noise ratio (SNR) attributed to the small travel range of the miniaturized MEMS interferometer [17]. On the other hand, electrochemical sensors depends on the chemical reactions that occur on the sensing surface. They have low cost and high sensitivity but suffer from limited measurement accuracy, problems of long-time stability, cross-response issues and limitation to an individual type of gas [12, 16].

- **Problem Statement/Objective**

In this project, we propose a solution to real-time, cumulative, high resolution, high signal to noise ratio (SNR) and multiple gas environmental monitoring using a handheld MEMS-SOA Silicon based gas analyzer for IoT smart cities. A high-resolution optical MEMS-SOA based swept laser core module would concurrently; harness the merits of mass production – low cost and small size of silicon integration technology compared to bulky expensive techniques - and

overcome limitations of miniaturized structures in gas sensing. The handheld analyzer would be an enabling technological tool to limit global warming to less than 2 ºC above pre-industrial values and achieve other industrial and environment monitoring requirements including agri-food industry.

The handheld MEMS-SOA gas analyzer is based on an experimental verified proof of concept of a MEMS-SOA swept laser spectroscopic gas analyzer presented in [5-7]. The core engine of the analyzer is a micro-electro-mechanical system (MEMS) tunable optical filter and a semiconductor optical amplifier (SOA) in a MEMS-SOA swept laser configuration as shown in Figs. 1a and 1b. The MEMS filter is fabricated using deep reactive ion etching (DRIE) of silicon on insulator wafer (SOI) [6]. It consists of two deeply etched Si/Air Bragg mirrors and fiber grooves with 90 um depth as shown in Fig. 1a. Light propagates in plane in the MEMS structure, which acts like a micro optical bench. One of the Bragg mirrors is movable and attached to an electrostatic comb actuator allowing tuning of the MEMS filter. The in-plane propagation allows hybrid integration of the MEMS with an SOA chip and micro collimation optics in a small package. The MEMS-SOA, is then inserted in a swept ring fiber laser configuration to be tuned by the in-loop MEMS filter as soon in Fig. 1b. A small size gas cell and a detector attached to the MEMS-SOA laser as shown in Fig. 1c allow absorption spectroscopy of gases over 100 nm tuning range with up to 0.2nm resolution depending on sweep speed.

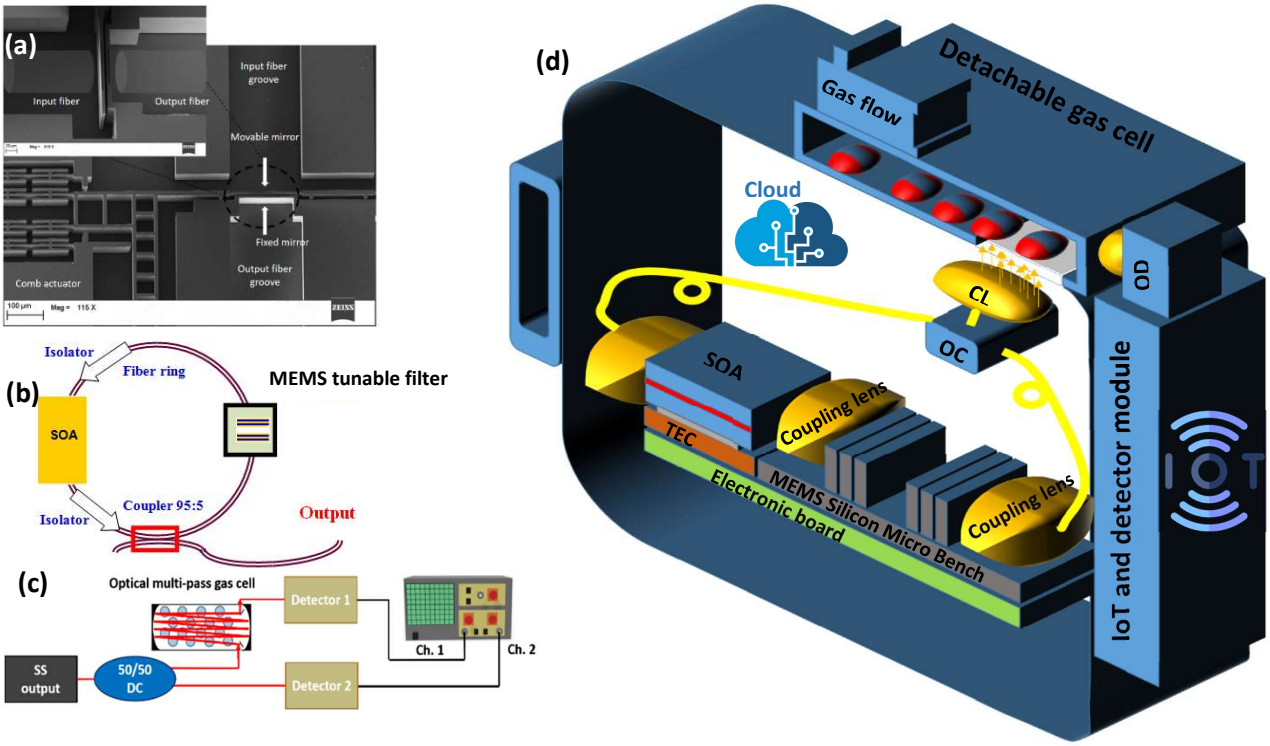

Fig. 1. (a) SEM photo of optical MEMS tunable filter. (b) Schematic of a basic MEMS-SOA swept laser. (c) Typical laboratory setup for swept source spectroscopic gas sensing. (d) Proposed Handheld MEMS-SOA Gas Analyzer. SS: Swept source, CL: Coupling lens, OC: Optical coupler, OD: Optical detector.

The device will have a flexible use case by working in two gas sampling modes; an in-device near gas cell mode and long-fiber far gas cell mode for difficult to access locations (e.g. factories, mining cites and gas pipelines) enabled by a detachable gas cell head as shown in Fig. 1d. The device will be equipped with smart IoT module and cloud connectivity to allow real-time and accumulative monitoring which is crucial for correct environmental assessment and decision-making on the long term.

The MEMS-SOA core engine is to be packaged together with electronic circuitry, micro gas cell, detachable gas sample collection head and IoT cloud connectivity module as a flexible use case handheld device as proposed in Fig. 1d.

- Outline of tasks/Work Plan

	Task	Description	Expected Duration
1	MEMS and System design	- Design and FDTD simulation of a deeply-etched filter using Si/Air layers - System design to achieve target specs	2 months
2	MEMS-SOA coupling optics	Design and simulation of MEMS-SOA coupling optics	1 months
3	- MEMS Fabrication - Core module electronics	- MEMS Fabrication at ESIEE, Paris - MEMS electronic circuitry design and fabrication - SOA current driver and TEC system design and fabrication	3 months
4	Assembly of MEMS-SOA and coupling optics	- MEMS-SOA assembly - Assembly of coupling optics for MEMS-SOA and SOA-optical fiber	3 months
5	Packaging and testing of swept laser core module	- Swept source core module packaging - Testing to achieve target specs for core module	3 months
6	Design and implementation of gas sampling head	- Gas sampling system - Gas flow control - Detachable head design and implementation	4 months

7	IoT and cloud connectivity	- Design and implementation of IoT module - Cloud connectivity and Mobile app	4 months
8	Full system assembly and testing on use cases	- Assembly of swept core module, detachable gas cell head and IoT module - Testing on practical use cases	4 months
	Total Duration		24 months

- **Outcome(s)**

  At the end of the project period, the project team will deliver a prototype of a novel handheld MEMS-SOA Silicon based gas analyzer for real-time, cumulative and wide-band environmental monitoring in IoT smart cities including the following subsystems:

  - Wide bandwidth tunable optical MEMS filter
  - MEMS-SOA swept laser core module
  - Detachable gas sampling head
  - Electronic control system
  - IoT connectivity module.
  - Mobile app for system control and cloud connectivity.
  - Handheld package for the whole system.

- **Impact**

  We expect the handheld MEMS-SOA gas analyzer to have a multifold impact:

  Climate impact: The device will contribute to achieve the 2°C target limit of global warming crisis by providing real-time and cumulative monitoring of pollution levels in smart cities and industrial complexes.

  Market impact: The device will introduce a novel technology in the gas sensing market estimated to reach 2.1 Billion USD by 2027.

  National impact: The device will have a huge impact in Egypt. It would foster the idea of technological industries based economy. It will attract investors to new technological sectors. It will foster Egyptian researchers to address demanding environment and economic problems using Hi-Tech technology. It will contribute to achieve sustainability and green economy targets of developing Egyptian economy.

- **References**

[1] Hansen, James, Pushker Kharecha, Makiko Sato, Valerie Masson-Delmotte, Frank Ackerman, David J. Beerling, Paul J. Hearty et al. "Assessing “dangerous climate

change": Required reduction of carbon emissions to protect young people, future generations and nature." PloS one 8, no. 12 (2013): e81648.
[2] United Nations Environment Programme and Climate and Clean Air Coalition (2021). Global Methane Assessment: Benefits and Costs of Mitigating Methane Emissions. Nairobi: United Nations Environment Programme.
[3] Zhang, Keqi, Bruce C. Douglas, and Stephen P. Leatherman. "Global warming and coastal erosion." Climatic change 64, no. 1 (2004): 41-58.
[4] DeConto, R.M., Pollard, D., Alley, R.B. et al. The Paris Climate Agreement and future sea-level rise from Antarctica. Nature 593, 83–89 (2021). https://doi.org/10.1038/s41586-021-03427-0
[5] John O. Gerguis, Yasser M. Sabry, Haitham Omran, and Diaa Khalil, "Spectroscopic Gas Sensing Based on a MEMS-SOA Swept Fiber Laser Source," J. Lightwave Technol. 37, 5354-5360 (2019).
[6] Haitham Omran, Yasser M. Sabry, Mohamed Sadek, Khaled Hassan, and Diaa Khalil, "Wideband Subwavelength Deeply Etched Multilayer Silicon Mirrors for Tunable Optical Filters and SS-OCT Applications", IEEE Journal of Selected Topics in Quantum Electronics, vol. 21, no. 4, July-Aug. 2015.
[7] Haitham Omran, Yasser Sabry, Mohamed Sadek, Khaled Hasan, Mohamed Shalaby, and Diaa Khalil, "Deeply-Etched Optical MEMS Tunable Filter for Swept Laser Source Applications", IEEE Photonic Technology Letters PTL, Vol. 26, No.1, pp37-39, January 1, 2014.
[8] Archer, David. "Fate of fossil fuel CO2 in geologic time." Journal of geophysical research: Oceans 110, no. C9 (2005).
[9] Randalls, Samuel. "History of the 2 C climate target." Wiley Interdisciplinary Reviews: Climate Change 1, no. 4 (2010): 598-605.
[10] Accord, Copenhagen. "United Nations Framework Convention on Climate Change, Draft decision 2/CP." (2009).
[11] Matthews, H. Damon, Nathan P. Gillett, Peter A. Stott, and Kirsten Zickfeld. "The proportionality of global warming to cumulative carbon emissions." Nature 459, no. 7248 (2009): 829-832.
[12] Neethirajan, Suresh, D. S. Jayas, and Shashikant Sadistap. "Carbon dioxide (CO2) sensors for the agri-food industry—a review." Food and Bioprocess Technology 2, no. 2 (2009): 115-121.
[13] McNair, Harold M., James M. Miller, and Nicholas H. Snow. Basic gas chromatography. John Wiley & Sons, 2019.
[14] Karasek, Francis W., and Ray E. Clement. Basic gas chromatography-mass spectrometry: principles and techniques. Elsevier, 2012.
[15] Lee, Duk-Dong, and Dae-Sik Lee. "Environmental gas sensors." IEEE sensors journal 1, no. 3 (2001): 214-224.
[16] Hodgkinson, Jane, and Ralph P. Tatam. "Optical gas sensing: a review." Measurement science and technology 24, no. 1 (2012): 012004.
[17] Erfan, Mazen, Yasser M. Sabry, Mohammad Sakr, Bassem Mortada, Mostafa Medhat, and Diaa Khalil. "On-chip micro–electro–mechanical system Fourier transform infrared (MEMS FT-IR) spectrometer-based gas sensing." Applied spectroscopy 70, no. 5 (2016): 897-904.

Executive summary of

Scalable room-temperature quantum computing based on nonlinearity in microcavities

Quantum computing promises an exponential speedup on some special tasks over classical computers. However, most of quantum computing systems, such as superconducting qubit, trapped ions, neutral atoms, silicon quantum dots, etc, have to be cooled to cryogenic temperature to reduce the relentless deleterious influence of the environment. Photon, a quanta of light, is naturally decoupled with environment thus provides a promising approach to realize universal quantum computing [1] working at room temperature under atmospheric condition. Nevertheless, the lack of photon-photon interaction at a single-photon level [2] hinders the realization of this enormous goal in the last decades.

In this project, we proposed that a set of coupled optical microcavities with strong $\chi^{(2)}$ nonlinearity provides a solid-state system to implement a high-precision room-temperature quantum computing. Owing to the strong nonlinearity in the materials [2-5], the harmonicity of cavity energy levels can be broken so that all requirements—a well-defined qubit with a long coherent time, initialization of qubit, single- and two-qubit operations, readout of qubit—can be realized with high efficiency and fidelity, simultaneously. This is the first macroscopic qubit working at room temperature, containing more than 10^{10} atoms in a single qubit. This CMOS-compatible scalable scheme can be carried out within next few years in view of rapid development of high-Q cavity fabrication on nonlinear materials.

Given the current state of quantum control technologies, achieving this ambitious goal requires substantial technological accumulation and simplification of theoretical approaches in order to develop this direction into a competitive research field in quantum computing. As this project spans two years, it is expected to achieve two milestone objectives: room-temperature single-photon source based on photon blockade, and strong coupling between microcavity modes.

References:

1. E. Knill, R. Laflamme, and G. J. Milburn, Nature 409, 46 (2001).
2. D. E. Chang, V. Vuletić, and M. D. Lukin, Nat. Photon. 8, 685 (2014).
3. N. K. Langford, S. Ramelow, R. Prevedel, W. J. Munro, G. J. Milburn, and A. Zeilinger, Nature 478, 360 (2011).
4. M. Heuck, K. Jacobs, and D. R. Englund, Phys. Rev. Lett. 124, 160501 (2020).
5. M. Li, Y.-L. Zhang, H. X. Tang, C.-H. Dong, G.-C. Guo, and C.-L. Zou, Phys. Rev. App. 13, 044013 (2020).

Scalable room-temperature quantum computing based on nonlinearity in microcavities

Introduction

Quantum computing harnesses the rule of quantum mechanics to deliver a huge leap forward in computation to solve certain problems. Very recently, we have witnessed the strong supports of quantum supreme by quantum sampling tasks [1,2], multipartite entanglement preparation [3-6] for noisy intermediate-scale quantum (NISQ) applications, etc. However, unrelenting hazardous effect of environment grievously hinders the scalability and development of quantum computing. To combat it, most of the physical system must be cooled to cryogenic temperature to protect the coherence of quantum hardware, either by sophisticated laser cooling [7,8] or by expensive refrigerators [9,10]. This makes quantum computers costly and impractical for future's applications.

A long sought-after goal here is to directly realize a universal quantum computer at room temperature. Extensive efforts have been devoted into this direction [11-19]. Among all candidates, photon [11-15] is a prominent alternative to realize this enormous goal since it perfectly decouples with environment and thus is potentially free from decoherence at room temperature. However, this also prohibits an interaction between photons, while such an interaction is essential for scalable quantum computing. The lack of high-fidelity photon-photon gate is the main bottleneck of current photonic quantum computing with single photons.

Literature brief review

In 2001, a pioneering work by Knill, Laflamme, and Milburn (KLM) [20] demonstrated that single photons, linear optical elements and projective measurements are sufficient for universal quantum computing. However, the prohibitively large overhead of a nondeterministic two-photon gate renders KLM scheme daunting for physical implementation [21]. For a deterministic photon-photon logic gate, it's strongly believed that nonlinearity should be added to linear optics for scalable quantum computing. To this end, several alternative ways are developed to obtain strong nonlinearity for deterministic two-photon gate, including electromagnetically induced transparency (EIT) using atomic ensembles [22], strongly coupled atom-cavity system (also called Duan-Kimble scheme) [23], Rydberg blockade [24,25], chiral quantum optics in waveguide [15], and natural occurring nonlinearities in materials [11-13,26].

Nevertheless, all previous methods face a number of limitations to make two-photon quantum gate with high efficiency and fidelity simultaneously. For example, EIT faces

a great challenge to realize photon-photon interaction at a single-photon level [27]. An experiment based on Duan-Kimble scheme showed a photon-photon gate with an efficiency of 4.8% and a fidelity of 76.2% [28], which suffers from inefficient photon storage and retrieval during whole process, and the gate fidelity is limited by precision of spin characterization. Same issues happen to several recent experiments utilizing Rydberg blockade [29-31]. By storing single photons to a long-lived Rydberg state, the efficiency of single-photon storage and retrieval has been improved to 39% [30]. Even so, the average efficiency is only ~40%, which is far away from the threshold of quantum error correction. Until now, the former four approaches are unrealistic to realize quantum computing at room temperature. For the latter one, it has been commented that realizing high-fidelity two-photon gate faces many challenges due to causal, noninstantaneous nature of the nonlinear response both in second- and third-order nonlinear medium.

Problem statement & Objectives

In this project, we propose that a series of coupled microcavities with strong second-order nonlinearity provide a reliable and realistic physical system to implement a scalable room-temperature quantum computing. Owing to the strong $\chi^{(2)}$ nonlinear susceptibility, the harmonicity of microcavity can be broken so that one and only one photon can inject in. This so-called photon blockade in strong coupling regime enables all key elements for scalable quantum computing—well-designed qubit with long coherent time, qubit initialization, single- and two-qubit logic gates, and high-fidelity readout. The distinctive features of our work include (i) this is the first solid-state qubit based on macroscopic quantum effects meanwhile working at room temperature, (ii) the dominant error in our system—loss—can be detectable and erased, (iii) the final qubits can be measured by a nondemolition mean, and (iv) all elements can be integrated on a single chip working at room temperature under atmospheric condition.

For the second-harmonic generation (SHG) in a microring, the Hamiltonian of the system can be written as $H = \omega_a a^\dagger a + \omega_b b^\dagger b + g(a^2 b^\dagger + a^{\dagger 2} b)$, where ω_a and ω_b are the frequency of pump light and its second harmonic generation, the photon-photon interaction strength is denoted as g. If g is larger than the loaded dissipation rate κ of the microcavity, the harmonicity will be broken such that a two-level system formed by vacuum and the first excited state is well isolated (see Fig. 1a). This effect is very similar in superconducting qubits, both are based on the anharmonicity of cavities due to the strong nonlinear effects of devices. the main difference is that superconducting qubits works at microwave frequency while our system is for optical wavelength. This brings a remarkable advantage of our system over superconducting qubits---free from decoherence at room temperature.

Based on this two-level system, we can realize room-temperature quantum computing with either flying photon qubits or solid-state qubits. Here, we do not intend

to provide any further details on this. However, it is worth noting that this project explores a completely new field of physics, named as **quantum nonlinear optics** [32]. Compared to traditional linear optics and nonlinear optics, quantum nonlinear optics allows photon-photon interaction at single photon level, without neither post-selections in linear optics nor strong pumping of light field.

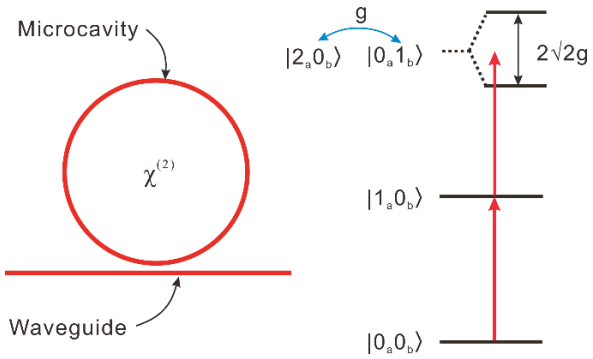

Figure 1. A microring cavity with strong $\chi^{(2)}$ nonlinearity can break the harmonicity of the cavity, thus forms a two-level system for quantum computing.

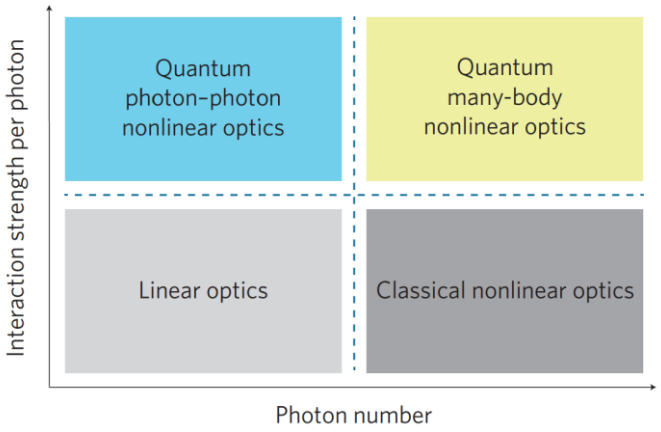

Figure 2. Comparison of quantum nonlinear optics and conventional linear optics, nonlinear optics. From [32].

This is the first macroscopic qubit working at room temperature, containing more than 10^{10} atoms in a single qubit. This CMOS-compatible scalable scheme can be carried out within next few years in view of rapid development of high-Q cavity fabrication on nonlinear materials. Given the current state of quantum control technologies, achieving this ambitious goal requires substantial technological accumulation and simplification of theoretical approaches in order to develop this direction into a competitive research field in quantum computing. As this project spans two years, it is expected to achieve two milestone objectives:

1. room-temperature single-photon source based on photon blockade, and
2. strong coupling between microcavity modes.

Outline of tasks

This project will span two years. The main focus of the first year's work is to mature and streamline the nano fabrication process. This process will take around seven months to optimize all parameters to improve the quality factor of microrings. After that, we will develop various quantum control technologies to achieve controllable cavity modes and develop a cavity-cavity coupling system. The assessment criteria include observing unconventional photon blockade phenomena in the weak coupling regime with high Q-factor and high nonlinear coefficients, as well as preparing single-photon sources.

The focus of the second year's work is primarily centered around achieving a strong coupling system with high Q-factor and high nonlinear coefficients through technological innovation and iteration. Based on this system, the objectives include demonstrating single-photon source experiments and two-qubit gate operations using different encoding schemes. Further experiments aim to enhance the scalability of the system and demonstrate error-correcting codes and scalable quantum computing achieved through optical nonlinear systems.

Impact

The deterministic interaction between single photons is recognized as a great challenge in the field of photonic quantum computing. The breakthrough of this project will not only hold the potential to revolutionize the field of optical quantum computing but also paves the way for a new discipline called quantum nonlinear optics, which will have a profound impact on fundamental research. In some sense, this project's room-temperature optical quantum computing can be considered as "room-temperature superconducting quantum computing," with similarities both in principles and performance. In the future, room-temperature quantum computing will undoubtedly become an important branch, not only contributing to fundamental research but also providing a more feasible and cost-effective research path for quantum computing.

References:

1. H.-S. Zhong, H. Wang, *et al.*, *Science* **370**,1460 (2020).
2. F. Arute *et al.*, *Nature* **574**, 505 (2019).
3. X.-L. Wang, *et al*., *Phys. Rev. Lett*. **120**, 260502 (2018).
4. C. Song, *et al*., *Science* **365**, 574 (2019).
5. A. Omran, *et al*., *Science* **365**, 570 (2019).
6. I. Pogorelov, *et al*., *PRX Quantum* **2**, 020343 (2021).
7. D. Leibfried, R. Blatt, C. Monroe, and D. Wineland, *Rev. Mod. Phys*. **75**, 281 (2003).
8. C. Gross and I. Bloch, *Science* **357**, 995 (2017).
9. J. Clarke and F. K. Wilhelm, *Nature* **453**, 1031 (2008).
10. F. A. Zwanenburg, *et al*., *Rev. Mod. Phys.* **85**, 961 (2013).
11. N. K. Langford *et al*., *Nature* **478**, 360 (2011).

12. M. Heuck, K. Jacobs, and D. R. Englund, *Phys. Rev. Lett.* **124**, 160501 (2020).
13. M. Li *et al*., *Phys. Rev. Appl.* **13**, 044013 (2020).
14. S. Krastanov *et al*., *Nat. Commun.***12**, 1 (2021).
15. Z. Chen *et al*., *Phys. Rev. A* **103**, 052610 (2021).
16. G. Balasubramanian *et al*., *Nat. Mater.* **8**, 383 (2009).
17. K. Bader *et al*., *Nat. Commun*. **5**, 1 (2014).
18. N. Y. Yao *et al*., *Nat. Commun*. **3**, 1 (2012).
19. E. Herbschleb *et al*., *Nat. Commun*. **10**, 1 (2019).
20. E. Knill, R. Laflamme, and G. J. Milburn, *Nature* **409**, 46 (2001).
21. P. Kok *et al*., *Rev. Mod. Phys.* **79**, 135 (2007).
22. M. Fleischhauer, A. Imamoglu, and J. P. Marangos, *Rev. Mod. Phys.* **77**, 633 (2005).
23. L.-M. Duan and H. Kimble, *Phys. Rev. Lett.* **92**, 127902 (2004).
24. A. V. Gorshkov *et al*., *Phys. Rev. Lett.* **107**, 133602 (2011).
25. S. Das *et al*., *Phys. Rev. A* **93**, 040303 (2016).
26. I. L. Chuang and Y. Yamamoto, *Phys. Rev. A* **52**, 3489 (1995).
27. M. Bajcsy *et al*., *Phys. Rev. Lett.* **102**, 203902 (2009).
28. B. Hacker, S. Welte, G. Rempe, and S. Ritter, *Nature* **536**, 193 (2016).
29. D. Tiarks *et al*., *Nat. Phys.* **15**, 124 (2019).
30. T. Stolz *et al*., *Phys. Rev. X* **12**, 021035 (2022).
31. J. Vaneecloo, S. Garcia, and A. Ourjoumtsev, *Phys. Rev. X* **12**, 021034 (2022).
32. D. E. Chang, V. Vuletić, and M. D. Lukin, *Nat. Photon.* **8**, 685 (2014).

Development of Spatial Heterodyne Atmospheric Carbon-Dioxide Spectrometer (SHACS)

Executive Summary

Finding solutions to the continuous concerns over climate change has been of increased interest in recent times with efforts targeted at mitigating its effects. Satellite observations and *in-situ* terrestrial networks play key roles in the understanding and management of the problem. Whilst detecting carbon-dioxide (CO_2) optically is relatively straightforward, and has been achieved with small satellites, accurate quantitative mapping of CO_2 requires very high precision (~1 ppm uncertainty or better) measurements of the gas concentration. This normally requires high-performance, large and complex instruments whose high cost, mass, volume, and power requirements preclude their use on small satellites.

To provide a low-cost solution for the global monitoring of atmospheric CO_2, we propose the development of a Spatial Heterodyne Atmospheric Carbon-Dioxide Spectrometer (SHACS). SHACS is a robust, no-moving-part, compact precision atmospheric CO_2 monitoring instrument that is suitable for deployment for both space-based and *in-situ*-based observations. It provides a cost-effective and affordable means of monitoring atmospheric CO_2 levels globally. SHACS comprises of two interferometer channels (1 & 2) and an O_2 A-band Channel. Channel-1 was developed and tested during my PhD and Postdoctoral research. Both Channels will be redesigned and developed with improvements for the 2023 Optica Foundation Challenge Program at the Institute of Space Science and Engineering (ISSE) in Nigeria. Due to its compact configuration, the instrument fits into a microsatellite-size platform and is capable of tackling the concerns of climate change by providing high-quality hourly measurements of atmospheric CO_2 concentration when launched in constellation.

It is vital to ascertain the levels of atmospheric CO_2 since it is the most anthropogenic (manmade) greenhouse gas constituent responsible for increase in global temperatures which leads to global warming that causes climate change. Therefore, there is a crucial need for effective monitoring of CO_2 especially along the tropics where there are sparse terrestrial observatories and nondedicated satellites for monitoring CO_2 in the Sub-Saharan African (SSA) region. The ability to effectively monitor CO_2 sustainably in this region, will assist in ascertaining the uncertainty surrounding the annual net increase of global atmospheric CO_2 and provide solutions to Climate Change. This information will enable policymakers to enact policies that promote clean air, good health and wellbeing.

Having a constellation of satellites and a network of cost-effective *in-situ* measurement hubs in Nigeria and across the SSA regions using the SHACS instrument, which is designed for both terrestrial and space-based observations, would vastly promote economic development and welfare of countries across the region through job creation, capacity building, collaboration, innovative solutions, good health and wellbeing, whilst providing carbon flux data to offer solutions to issues surrounding climate change and mitigating its effects.

Apart from benefits obtained from mitigating the effects of climate change, the outcome of this project also features added value through advancement in technology by development of spin-offs. By caring for the environment and combating climate change, investors would be attracted from both local and international communities to utilize our products and services which cuts across key sectors that promote sustainable economic growth such as agriculture (for food security), health and education. Furthermore, the outcome of this project develops knowledge, collaboration and expands its benefits to schools/colleges, higher institutions, research institutes, space-related institutions, government and non-governmental organizations etc. The establishment of regional hubs across Sub-Saharan Africa, would promote regional collaborations, reduced inequalities and provide a platform for technological growth in this region thereby addressing 13 UN Sustainable Development Goals (SDGs).

2023 Optica Foundation Challenge Proposal for the

Development of Spatial Heterodyne Atmospheric Carbon-dioxide Spectrometer (SHACS)

Literature Review

With the global concern over climate change in recent years, the key to understanding the problem is the characterization of the sources, sinks and transportation of greenhouse gases (GHGs) such as atmospheric carbon-dioxide (CO_2). Atmospheric CO_2 remains the main anthropogenic greenhouse gas and the primary atmospheric component of the global carbon cycle, contributing about 2.14 Wm^{-2} to the global radiative forcing as of 2021 [1]. Its concentration has increased from a preindustrial value of about 280 parts per million (ppm) to about 420 ppm as of April 2023 [2] mainly due to fossil fuel combustion, land-use change (LUC), and biomass burning [3]. Studies have shown that the terrestrial biosphere carbon fluxes cannot be fully resolved, and the identification and determination of the extent of atmospheric carbon dioxide (CO_2) fluxes in the tropics, especially in regions around the equatorial zone, has been difficult due to the sparseness of *in-situ* terrestrial CO_2 measurement networks [4-5]. Knowledge of these regional fluxes and processes can be greatly improved by providing precise, accurate, and reliable CO_2 measurement data through additional space-based and *in-situ*-based observations [6] focusing primarily on the tropics, especially Sub-Saharan Africa (SSA).

Monitoring of atmospheric CO_2 from space often requires the identification of CO_2 in its Short-Wave Infra-red (SWIR) spectral absorption bands of 1.56 µm - 1.62 µm and 1.92 µm - 2.06 µm wavelengths (Figure 1(a)). The CO_2 absorption bands around 1.6 µm and 2.0 µm are important, since absorptions in these bands provide information on the near-surface concentrations, while the absorption band around 14 µm is used for obtaining information mainly at altitudes above 2 km [7]. Therefore, it is essential to monitor the lower troposphere where the greenhouse effect mainly occurs. The O_2 A-band channel at 760 nm shown in Figure 1(b) is required to correct for air mass and identify cloud effects [6,8].

Terrestrial-based monitoring networks for CO_2 do not have the spatial coverage needed to identify the natural sinks responsible for absorbing CO_2, or the processes that control how their efficiency changes from year to year. Most spaceborne CO_2 monitoring instruments offer a global view but are limited in their temporal resolution due to their large size and high cost, and so as yet, there is no operational system which can meet the demands of climate-change scientists [3].

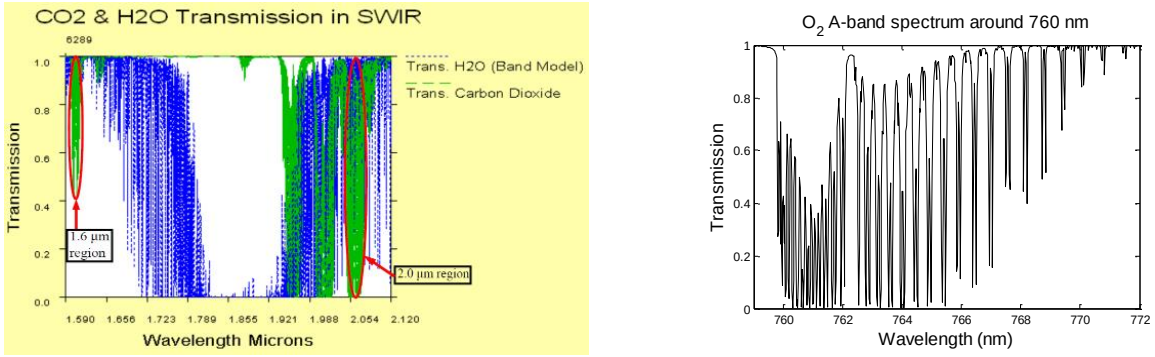

(a) (b)

Figure-1. (a) Simulated CO_2 and H_2O transmission covering 1.6 µm and 2.0 µm spectral regions. Red arrow identifies the spectral region of interest (b) Simulated O_2- A-band spectrum around 760 nm.

Hence, having a compact but efficient CO_2 monitoring instrument with low cost, power and mass, which fits into a microsatellite platform, could enable the feasibility of a constellation, thereby providing frequent monitoring and measurements of precise CO_2 flux data.

The Spatial Heterodyne Atmospheric Carbon-dioxide Spectrometer (SHACS) – a low-cost, robust and solid-state instrument that utilises the Spatial Heterodyne Spectroscopy (SHS) technique [9-10], is proposed for the 2023 Optica Foundation Challenge program. SHACS is comprised of two interferometer channels (Channel-1 and Channel-2), an oxygen (O_2) A-band channel and a telescope module. In its novel application, this compact instrument uses low groove density gratings on a standard SHS to record interferograms on 2-dimensions of an array detector for broadband absorption spectroscopy applications. It is designed to operate as both a terrestrial and a space-based instrument.

Although CO_2 mainly occurs around the 1600nm and 2000nm spectral regions following the spectral transmission model [9], the 2000nm region is greatly characterised by the presence of water vapour and is complemented by the 1600nm region (Figure-1(a)). Therefore, the implementation makes use of two optical benches each tuned to one of the key CO_2 absorption bands. The first channel covers the 1599nm to 1605nm band, while the second channel covers 2045nm to 2060nm. Both benches share a common receiver three-mirror-reflector telescope which splits the incoming signal with the aid of a dichroic beam-splitter for the two channels.

The complete optical model of SHACS instrument comprising a three-mirror telescope, Channel-1 and Channel-2 has been performed using ZEMAX® optical design software and is shown in Figure-3. With the successful development of a bench-top prototype demonstrator of Channel-1 in a laboratory environment using Quartz-Halogen lamp as the input light source (Figure-4), qualitative (CO_2 spectrum) and quantitative (CO_2 concentration and precision) was obtained. It was then followed by the development and testing of a moveable bench-top prototype of this channel in open-air environment using sunlight as the input light source (Figure-5). The testing of this moveable bench-top platform for daily Total Column CO_2 ($TCCO_2$) measurements was done at Surrey Space Centre (SSC), University of Surrey, UK [6]. A fast-processing algorithm based on Inverse Fourier Transforms and Inverse Model [9,10,11] was developed for the retrievals of measured CO_2 spectra and concentrations obtained by SHACS Channel-1. Having recorded significant achievement with SHACS Channel-1 instrument, the next research progression is the redesign, development and testing of Channels-1 and 2 in Nigeria, which the Optica Foundation Challenge program will enable if provided the opportunity to carry out this project. The redevelopment of Channel-1 will feature state-of-the-art detector that supports seamless and efficient data acquisition and retrieval. SHACS Channels-1 and 2 will be integrated and tested at this phase of the project. This work will be based at the Institute of Space Science and Engineering (ISSE), NASRDA, Nigeria.

Problem Statement

As an efficient greenhouse gas with an increasing concentration in the atmosphere since the beginning of the industrial age, CO_2 remains the principal man-made greenhouse gas and the primary atmospheric component of the global carbon cycle [10]. However, a large uncertainty is associated with the quantification of global carbon fluxes as well as the precise locations of the regional carbon surface sources and sinks.

This is largely due to the sparseness of the *in-situ* networks and the inability to resolve the regional carbon fluxes and processes through space-based observations owing to the lack of the needed temporal resolution requirement which cannot be provided by either the surface networks or existing space-based atmospheric CO_2 monitoring instruments. Therefore, it has

become increasingly difficult to resolve the “missing carbon sink” due to the underestimation of CO_2 uptake (sink) by the terrestrial biosphere.

Having a robust and compact instrument that fits into a microsatellite to provide high-quality precision measurements of CO_2 concentration from clear-sky soundings with hourly revisit capability if used in a constellation and focused on the SSA, ultimately provides the solution.

Objectives

The objective of this project is to redesign, develop and test a compact, low cost, volume, mass and power instrument suitable for both terrestrial and space-based applications and fits into a microsatellite platform to enable constellations of microsatellites monitor atmospheric CO_2, thus providing higher spatial and temporal resolution measurements of sufficient scientific quality useful for the study of climate change. This objective can be grouped into two categories: the primary and secondary objectives.

The primary objectives of this research are:

a) To build and test the two spectrometer channels of SHACS instrument (Channel-1 and Channel-2) prototype using Commercial-Off-The-Shelf (COTS) state-of-the-art components
b) To obtain daily terrestrial measurements of Total Column Carbon-dioxide (TCCO2) data in Nigeria thereby providing CO_2 flux data within the Sub-Saharan African (SSA) region
c) To monitor and accurately analyse the net yearly subtle change of atmospheric CO_2

The secondary objectives of this research are:

a) To develop enhanced capacity for space research innovations in Africa through the Institute of Space Science and Engineering (ISSE), National Space Research and Development Agency (NASRDA), Nigeria
b) To acquire and disseminate timely CO_2 data for the scientific community and provide solutions towards improvement of our environment, health and wellbeing through air quality, policy management and technological advancements in SSA

Outline of tasks/Work Plan

There are three main Work Packages (WP) itemised in this project as shown in Figure-2. It covers a period of 24 months from the 1st of September 2023 to the 31st of October 2024. The WP are:

- **WP-1:** This work package oversees the management and build of SHACS Channel-1 module. It includes processing and purchasing of orders for Channel-1, building and testing of prototype module, measurement campaign and processing of measured data and conference presentation.
- **WP-2:** This work package follows a similar workflow as WP-1. It focuses on the development of SHACS Channel-2 module.
- **WP-3:** This work package is responsible for the assembly, integration and testing (AIT) of the SHACS spectrometer channels. It offers a general review of the results obtained from the instrument built. It also ensures the publication of papers and showcasing the product in workshops and conferences.

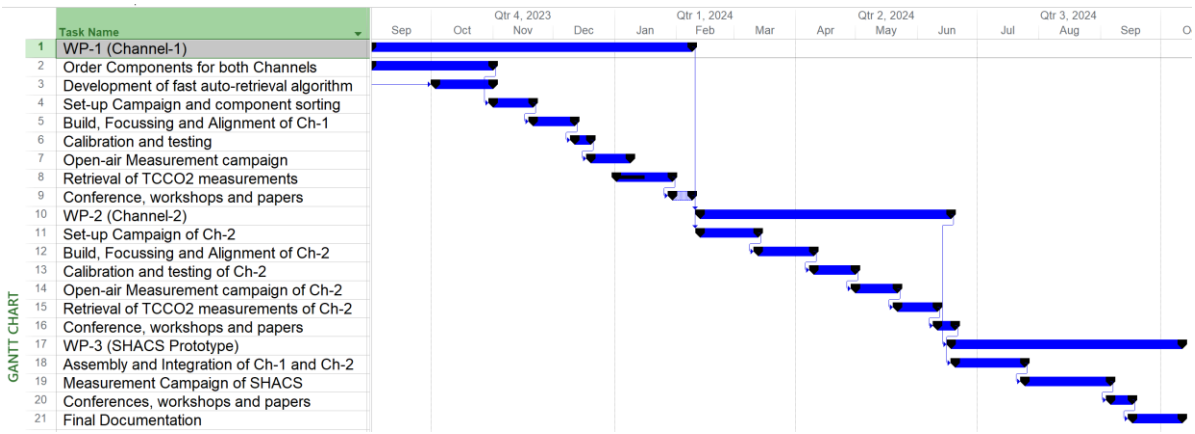

Figure-2: Work plan for the proposed project

Outcomes

Having a network of cost-effective in-situ instrument hubs in Nigeria and across regions in Sub-Saharan Africa using the SHACS instrument, which is designed for both terrestrial and space-based observations of atmospheric carbon-dioxide (CO_2), would vastly promote economic development and welfare of the country through job creation, capacity building, collaboration, good health and wellbeing, innovative solutions, whilst providing carbon flux data to offer solutions to the issues surrounding climate change and mitigating its effects.

Also, apart from the benefits obtained from mitigating climate change effects, the outcome of this research activities features added value to promote optical engineering research and advancement in technology by development of spin-offs such as sun trackers, spaceborne imagers and portable CO_2 sensors. Another outcome of this project is the capability of developing a small size instrument that competes favorably with large traditional ones in terms of performance. This outcome makes it feasible for SHACS to be launched in constellation at low-cost, thus providing frequent data to the scientific community.

Impact

The impact of this research cannot be over-emphasised especially when the effects of climate change are clearly visible globally. This project is poised to address the issues of climate change and provide the needed solutions for policymakers to ensure compliance by all parties. This project addresses and impacts positively on 13 UN SDGs (Goals 1, 2, 3, 5, 7, 8, 9, 10, 11, 12, 13, 15 and 17) with a direct contribution to Goals 3, 10, 13 and 17.

The anticipated development impact of this research cuts across multi-disciplines such as environment, health and wellbeing through air quality, policy management and technological advancements. With various countries poised to address the global effect of climate change by setting targets to reduce carbon emissions within their regions; SHACS instrument will provide a cost-effective and affordable means for monitoring atmospheric CO_2 levels globally if launched in constellation. It further provides checks and balances on air quality thereby improving on health and general wellbeing. With resolutions reached at the Conference of Parties (COP), the data provided from the end product of this project further assist policy drivers to ensure strict compliance.

The set-up of CO_2 measurement hubs across Sub-Saharan Africa using SHACS would also bring economic growth and collaboration in this region and assist in reducing inequality within and among countries thereby having a positive impact on SDG: 10.

References

[1] Montzka, S.A., The NOAA Annual Greenhouse Gas Index (AGGI). National Oceanic and Atmospheric Administration, Global Monitoring Laboratory, Earth System Research Laboratories (NOAA/GML/ESRL), (Apr. 4, 2023).

[2] Tans, P. “Trends in atmospheric carbon dioxide”, Carbon Cycle Greenhouse Gases, National Oceanic and Atmospheric Administration, Global Monitoring Laboratory, Earth System Research Laboratories, (NOAA/GML/ESRL), (Apr. 4, 2023)

[3] Ikpaya, I. O. and Underwood, C. I., "Development of SHACS: Progress on Channel-1 Prototype Demonstrator," in IEEE TGRS, 60(1001115), (2022).

[4] Kuang, Z., et al., “Spaceborne measurements of atmospheric CO2 by high-resolution NIR spectrometry of reflected sunlight: An introductory study,” Geophys. Res. Lett., 29(15), 11-1–11-4 (2002).

[5] O’Brien, D. M., et al, "Airborne Measurements of Air Mass from O2 A-Band Absorption Spectra," J. Atmos. Ocean. Technol., 15(6), 1272-1286 (1998).

[6] Ikpaya Ikpaya and Craig Underwood, “Towards high-temporal-resolution global monitoring of atmospheric carbon-dioxide using a compact spaceborne spatial heterodyne SWIR spectrometer – SHACS”, Proc. SPIE 12534, Infrared Technology and Applications XLIX, 1253422 (13 June 2023)

[7] I. Morino, et al., "Preliminary validation of column-averaged volume mixing ratios of carbon dioxide and methane retrieved from GOSAT short-wavelength infrared spectra," Atmos. Meas. Tech., (4), pp. 1061–1076, 2011.

[8] I. Ikpaya and C. I. Underwood, "SHACS: Spatial Heterodyne Atmospheric Carbon-Dioxide Spectrometer," in 12th IAA Symposium on Small Satellites for Earth Observation, Berlin, 2019.

[9] I. Ikpaya and C. I. Underwood, "Design Analysis of Compact Short-Wave Infrared Spatial Heterodyne Fourier Transform Spectrometer for an Atmospheric CO2 Monitoring Micro-Satellite Constellation," in 9th IAA Symposium on Small Satellites for Earth Observation, International Academy of Astronautics (IAA), Berlin, Germany, 2013.

[10] I. O. Ikpaya, "Compact Spatial Heterodyne SWIR Spectrometer for Atmospheric CO2 Monitoring," PhD Thesis, Surrey Space Centre, University of Surrey, Guildford, 2013.

[11] C. D. Rodgers, Inverse Methods for Atmospheric Sounding: Theory and Practice, (2), F. W. Taylor, Ed., New Jersey: World Scientific Pub. Co. Pte. Ltd, USA, 2000, p. 238.

Appendix

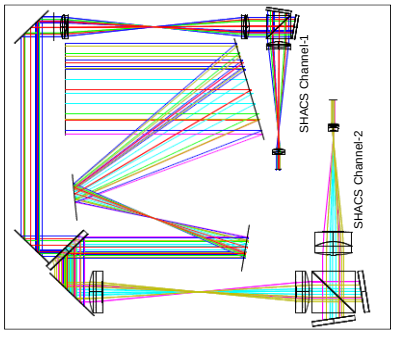

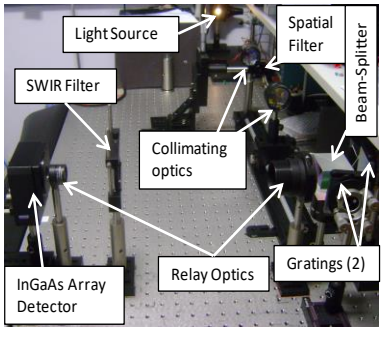

Figure-3: SHACS Payload design with two optical benches and TMA Telescope	Figure-4: SHACS Channel-1 Lab set-up using Halogen lamp as input light source at SSC, UK	Figure-5: Moveable SHACS Channel-1 obtaining TCCO2 measurements at SSC, UK

Jhonattan Cordoba Ramirez
Universidade Federal de Minas Gerais (UFMG)

Executive Summary

Highly efficient all-optical isolators on silicon-based Brillouin platform for modern communications systems

The proposed research project aims at addressing the challenges associated with developing highly efficient all-optical isolator systems in integrated photonics. The current state of non-reciprocal devices, particularly optical isolators, has hindered their integration into photonic systems due to limitations such as bandwidth constraints, reliance on magnetic fields, and sensitivity to nonlinear effects. The proposed research presents an innovative approach that harnesses the power of Brillouin scattering, space-time modulation, and waveguide-based designs. In addition, this study explores the vast potential of using highly versatile 2D materials, such as graphene and/or twisted bilayer graphene, to integrate them seamlessly into structures with the previously described characteristics. By leveraging the exceptional physical properties of these proposed materials and structures, we aim to significantly enhance the expected effects, thereby opening new possibilities in the field. The anticipated outcomes of this research include developing highly efficient all-optical isolator systems with broadband operation, reducing power consumption, improving performance compared to existing solutions, reducing signal loss, and increasing network efficiency. Overcoming bandwidth limitations, addressing nonlinear absorption effects, and enhancing conversion efficiencies are among the key goals. This research is significant for advancing integrated photonics by developing more reliable and efficient photonic systems for modern communication networks.

By successfully bringing this proposal to fruition, we aim to significantly contribute to developing this technology, propelling it forward, and pushing the boundaries of the state-of-the-art. The integrated-photonics-based isolators allow the integration of this technology with other integrated photonics components, systems, and technologies. The alignment of this proposal with Sustainable Development Goals (SDG) and Environmental, Social, and Corporate Governance (ESG) principles emphasizes the responsible and ethical advancement that we aim to have in developments related to new technologies based on integrated photonics.

Overall, the proposed research has the potential to significantly impact the field of integrated photonics by advancing optical isolator technology, improving performance and efficiency in communication networks, enabling integration with other photonic components and technologies, and promoting sustainable and responsible practices. The outcomes of this research can benefit various sectors, including telecommunications, data centers, and optical sensing applications, with significant implications for researchers, industry professionals, communication network providers, end users, environmental advocates, and government/regulatory bodies.

Highly efficient all-optical isolators on silicon-based Brillouin platform for modern communications systems

Jhonattan Cordoba Ramirez – Universidade Federal de Minas Gerais (UFMG) – Brazil
jcordoba@cpdee.ufmg.br – +55 (31) 3409 - 3449

1. Literature review

The fundamentals and applications of Stimulated Brillouin Scattering (SBS) derived from Townes' pioneer experiments in nonlinear light-scattering impacted several research fields, mainly due to the importance of this matter in early experiments on optical fibers and planar waveguides. For example, the vast and narrow-band optical gain available through the Brillouin interaction has enabled efficient fiber-optic-based slow transmission, fast light, nanosecond storage of optical pulses, and radio frequency (RF) tunable filters with an unprecedented narrow band, extinction, and tunability. Other technological breakthroughs enabled by the recent advances in Brillouin optomechanics are the generation of high spectral purity RF sources, distributed strain and temperature sensors, high-resolution spectrometers, liquid-compatible sensors, gyroscopes, and narrow linewidth Brillouin lasers. Following the growth and availability of advanced top-down nanofabrication tools in the last ten years, several research advances have occurred within the classical and quantum realms. The advancement of these integrated photonic structures also affected backward Brillouin scattering, especially after the landmark demonstration on-chip of SBS, demonstrated by Pant et al., [1] which caused a convergence of traditional waveguide-based Brillouin concepts with those of cavity optomechanics. One clear outcome of this convergence was the prediction and subsequent demonstration of significant gain Brillouin scattering in a CMOS-compatible platform [2], which culminated in the first generation of on-chip Brillouin lasers [3], and on-chip signal processing devices [3, 4]. In the context of these recent demonstrations, drawing a line dividing the fields of Brillouin scattering in wave-guiding photonic structures and the area of cavity optomechanics is more complex. One of the main problems in integrated-photonics Brillouin applications, which demand a definitive solution, is the simultaneous confinement of optical and acoustic waves. In this sense, research aiming at this solution has emerged recently, which can be concentrated into three main groups. The first solution to the confinement problem, and the first demonstration of SBS in an integrated photonic environment, was found on the chalcogenide soft glass platform [5], where, thanks to the high refractive index of said material, it is possible to achieve strong confinement. A second option is the mechanical isolation of the waveguides from the substrate, where the suspended silicon waveguides stand out [6]. A third strategy is to manage without acoustic confinement, an approach that has been demonstrated using ultra-low-loss waveguide systems [7].

All these developments have contributed significantly to the scientific progress of this field in various areas of knowledge and multiple applications. However, there is still a long way to go.

2. Problem statement: A clear description of the issues to be examined in the proposed research, originality, outcomes, and significance for the advancement of the research field

Multiple developments in integrated photonics have led to highly relevant devices for modern communication systems, such as modulators, switches, frequency shifters, lasers, and photodetectors,

among others. These devices rely on integrated optical waveguides for guidance, offering improved performance and compactness. However, while significant progress has been made, there are certain components, including non-reciprocal devices like optical isolators, that have not yet reached an acceptable level of development. Optical isolators are crucial in photonic systems to enable directional signal routing and protection functions.

From the perspective of sustainable development goals (SDGs) and Environmental, Social, and Corporate Governance (ESG), it is essential to ensure that technological advancements align with principles of sustainability and responsibility. As we strive for a more sustainable future, it is crucial to address challenges and opportunities in the field of integrated photonics in a manner that promotes environmental stewardship, social well-being, and ethical corporate practices.

In theory, achieving non-reciprocal operation in optical isolators is straightforward: break the symmetry of time inversion in the medium. However, practical implementation presents complexities that involve the use of magnetic fields, temporal variation of material properties, or nonlinearity. While different options have shown promise, the magneto-optical approach faces challenges in terms of manufacturing processes and the availability of suitable materials for this application. Additionally, traditional nonlinear effects for achieving non-reciprocity typically operate in a narrow bandwidth, and their effectiveness depends on the signal's power. This poses significant challenges in integrated photonics due to potential high losses, whether linear or non-linear, in such devices.

These limitations have spurred researchers to explore alternative solutions, with Brillouin scattering emerging as a viable approach. Brillouin-based isolators offer several advantages. They can achieve broadband operation, exhibit linear dependence on pump power (which can be independently adjusted from the signal), and work effectively with a wide range of dielectrics. Moreover, Brillouin-based isolators are compatible with integration technologies like CMOS, which allows for the full integration of a range of optoelectronic functions.

Breaking the time reversal symmetry in a medium can be accomplished through space-time modulation of the local susceptibility. This process mimics a momentum bias, which can be obtained using the Brillouin scattering phenomenon. Two alternatives for achieving this momentum bias exist. One approach involves generating acoustic waves that propagate and interact with the electric field in a waveguide, where non-reciprocal optical gain naturally occurs in Stimulated Brillouin Scattering (SBS) due to phase matching dictated by the pump direction.

However, a limitation of this configuration is its bandwidth, which is restricted by the linewidth of the SBS gain and typically falls in the tens of MHz range. Such bandwidth is inadequate for high-speed signal processing applications. To address this limitation, researchers have explored other alternatives, including the implementation of whispering-gallery-mode cavities that provide low-power operation in a compact footprint but are limited to ultra-narrow bandwidths. Additionally, an acoustically excited optical waveguide enables interband or intermodal optical coupling over a broad frequency range, provided appropriate visual mode spreads are achieved. Importantly, this scattering is highly non-

reciprocal due to the Brillouin phase matching rules [8]. Integrating a mode splitter with the waveguide facilitates mode separation and serves as a basis for obtaining optical isolators.

Recent research has focused on on-chip architectures, examining the feasibility of dispersion engineering to extend bandwidth [9]. Notably, direct acoustic pumping in an aluminum nitride resonator and optically pumped SBS in a silicon waveguide have demonstrated on-chip non-reciprocity [10]. The waveguide method utilizes long propagation lengths to achieve high-contrast non-reciprocal light propagation at very high bandwidths. However, addressing two-photon absorption and free-carrier dispersion effects in silicon-based Brillouin devices requires innovative strategies to improve conversion efficiencies towards unity, which is a primary objective for developing highly efficient optical isolators.

In this proposal, given the high non-linear refractive index of silicon, a two-pump system aims to excite acoustic modes in the integrated photonic system while generating parametric amplification. This compensates for the optical power loss due to non-linear absorption effects intrinsic to silicon while maintaining phase matching along the photonic component controlling the optical path's width. Resonator devices, which trade bandwidth for compactness, can significantly reduce optical insertion loss when used in bypass or induced-transparency configurations, making them attractive for implementation. Additionally, the generation of acoustic waves through a piezoelectric system will be investigated, as it reduces the length of the integrated photonic device while achieving the desired phenomena [11, 12]. However, this alternative may introduce additional losses due to absorption caused by the presence of conductive materials. To mitigate losses resulting from waveguide-conductive material interaction, a capacitive structure based on graphene or twisted bilayer graphene can be implemented. This structure allows for control of the Fermi energy level, ensuring the generation of acoustic waves in the proposed capacitive structure while reducing optical losses in the optical waveguide [13].

These approaches aim to solve the problem of non-linear absorption effects in silicon-based photonic platforms and contribute positively to the development of highly efficient all-optical isolator systems. By aligning these research efforts with SDGs and ESG principles, we can ensure that technological advancements in integrated photonics are not only innovative and functional but also environmentally sustainable, socially responsible, and ethically governed, fostering a more sustainable and equitable future for all.

3. Scientific methodology

We will develop the proposal through the following methodology, divided into three work packages (WP1 to WP3), each aimed at achieving specific objectives.

WP1: Design, simulation, and optimization of silicon-based Brillouin devices: In this WP, we will design and optimize photonic components for efficient optical isolators based on stimulated Brillouin scattering. The optimization process will involve analyzing parameters such as geometry, dimensions, material distribution, and operational wavelength. The components will be designed to initially operate

in the C-Band range with minimal losses while ensuring high stability and low signal-to-noise ratio. Numerical simulations using finite element, finite-difference time-domain, and beam propagation (BPM) methods will guide the design process and help achieve optimal optical and acoustic performance.

WP2: Fabrication of proposed devices: The fabrication and characterization process will occur at the Laboratory of Characterization and Processing of Nanomaterials at UFMG and the Microscopy Center at UFMG. The chosen materials in the previous WP will undergo deposition using techniques such as Electron Beam Evaporation to achieve precise thickness control. For nanometer-scale layers, Atomic Layer Deposition can be employed. Lithography techniques such as conventional photolithography (AutoStep200, MJB3, or MJB4), Direct Laser Writer or Electron Beam Lithography will be used depending on the device dimensions. Etching processes, such as Inductively Coupled Plasma-Reactive-ion Etching, will provide an excellent component finish, particularly reducing roughness-induced losses. Additional steps will be implemented if suspended or capacitive structures are required. The characterization will be performed through lateral light coupling or Bragg Gratings, depending on the chosen method. Specific device characteristics will be achieved, such as inverted couplers or Bragg-gratings.

WP3: Acousto-optic characterization process: This WP focuses on constructing an experimental setup for acousto-optic characterization of the fabricated devices. The setup will include laser light in-coupling from monochromatic semiconductor diodes operating in the IR wavelength range, a temperature control unit, photo-detectors or Optical Spectrum Analyzers for read-out, control electronics, and accompanying software for system usability. In-coupling can be accomplished through end-fire or grating couplers, optionally incorporating micro-lenses or fiber-pigtailed components. Strict control of vibration and humidity will be maintained during characterization to ensure accurate measurements and observe the intended effects on the waveguides.

By following this methodology, we aim to develop highly-efficient silicon-based Brillouin devices with optimized performance characteristics, successfully fabricate them, and carry out accurate acousto-optic characterizations.

Activities / Quarterly	1	2	3	4	5	6	7	8
Work Package – WP1								
Work Package – WP2								
Work Package – WP3								
Dissemination								

Table 1. Gantt Chart

4. Impact

The proposed research aims to significantly impact integrated photonics by overcoming challenges and limitations in developing efficient all-optical isolator systems. The research can lead to the following outcomes: **1)** Advancement of Optical Isolator Technology: By addressing limitations like narrow

bandwidth and sensitivity to nonlinear effects, the research can advance the state-of-the-art in optical isolator technology. Novel approaches based on Brillouin scattering, space-time modulation, and waveguide-based designs can result in more efficient and high-performance optical isolators, meeting the demands of modern communication systems. **2)** Broadband Operation and Improved Performance: The research targets achieving broadband operation in optical isolators, overcoming existing bandwidth limitations. Innovative techniques and materials like graphene or twisted bilayer graphene can enhance isolator performance, allowing a wider range of frequencies for signal routing and protection. This can lead to improved data transmission, reduced signal loss, and increased network efficiency. **3)** Reduction of Power Consumption: The research aims to develop all-optical isolators with reduced power consumption compared to current technologies. By optimizing the design and using efficient materials, the proposed isolators can contribute to the overall energy efficiency of photonic systems, promoting sustainable practices. **4)** Integration with Integrated Photonics Platforms: The proposed isolators are compatible with integration technologies like CMOS, allowing seamless integration with other photonic components. This enhances the functionality and performance of photonic systems, enabling the development of compact and versatile photonic devices and circuits for various applications. **5)** Alignment with Sustainable Development Goals (SDGs) and ESG Principles: The research emphasizes alignment with SDGs and ESG principles, demonstrating a commitment to sustainability and ethical governance. Responsible technological advancements ensure positive contributions to society and the environment.

In summary, the proposed research can advance optical isolator technology, improve communication network performance and efficiency, enable integration with integrated photonics platforms, and align with sustainable development goals and ESG principles. These outcomes benefit sectors like telecommunications, data centers, and optical sensing applications, leading to more reliable, efficient, and sustainable photonic systems.

5. References

[1] R. Pant, et al., Opt. Lett. 36, 3687 (2011).

[2] R. Van Laer, et al., Nat. Photonics 9, 199 (2015).

[3] B. Morrison, et al., Optica 4, 847 (2017).

[4] E. Giacoumidis, et al., Optica 5, 1191 (2018).

[5] Pant, R. et al., Opt. Express 19, 388–392 (2011).

[6] Shin, H. et al., Nat. Commun. 4, 1944 (2013).

[7] Gundavarapu, S. et al., Nat. Photon. 13, 60–67 (2019).

[8] Huang, X. and Fan, S., J. Light. Technol. 29, 2267–2275 (2011).

[9] Poulton, C. G. et al., Opt. Express 20, 21235–21246 (2012).

[10] Kittlaus, E. A., et al., Nat. Photon. 12, 613–619 (2018).

[11] Nadas, RB, Gadelha, **Ramirez, JC**, et al. Nano Letters,**2023**. 10.1021/acs.nanolett.3c00851.

[12] Ohlberg, D. A. A., **Ramirez, J. C.**, et al., Nat. Comm., 12, 8–13. 10.1038/s41467-021-23253-2.

[13] **Ramirez, J. C.**, and Dagli, N. (2021). CLEO, STh4B.4. DOI: 10.1364/CLEO_SI.2021.STh4B.4.

Multi-gas sensing with ultralow-loss hollow-core fibers

Jonas H. Osório

Federal University of Lavras, Lavras, Brazil

Category: Environment

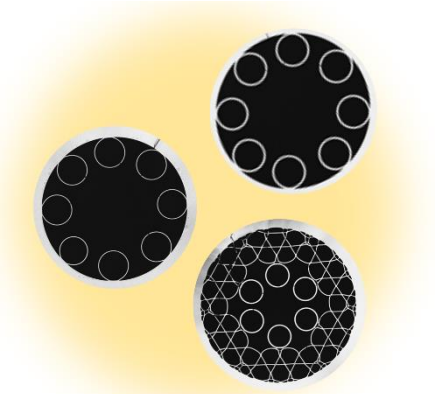

The development of devices able to monitor multiple gas species is a pressing need in environmental science. Although it motivated the study of a great set of gas sensors, selectively and remotely detecting multiple gas species using a single platform lingers as a challenging task. This project proposes the realization of multi-gas fiber-enhanced Raman spectroscopy (FERS) with newly demonstrated hollow-core photonic crystal fibers (HCPCFs) displaying ultralow loss in the short-wavelength range. Performing FERS with such new fibers, which stand nowadays as the lowest loss fiber optics guiding in the visible range, will allow enlarging the interaction lengths to potentially achieve lower detection limits for greenhouse gases and gaseous pollutants sensing. Additionally, this platform will enable the realization of remote multi-gas sensing as the sensor head can be deployed at the application site while the measurement apparatus can be kept away from the measurement locus.

The outcomes of this project will encompass both scientific and practical achievements. From the scientific viewpoint, the activities to be developed within this project will allow delving into HCPCF properties – modal content, polarization characteristics, and sources of loss –, to identify the most suitable configuration for the sensors' operation. From the practical point of view, the development and application of the sensors will allow demonstrating devices able to detect and quantify greenhouse emissions and gaseous pollutants. This in turn will contribute to the broad community efforts towards a better future for humanity by providing the social actors involved in productive, monitoring, and controlling actions with an effective means for assessing multi-gas environments using a simple and cost-effective configuration.

The development of the proposed multi-gas HCPCF sensors will impact the scenario of environmental monitoring systems and, therefore, significantly contribute to the efforts regarding environment preservation. This, together with other techniques, has the potential of supplying information on the environmental conditions capable of providing guidance for strategic discussions on environmental conservation and climate change assessment.

Additionally, being Brazil, due to its wide availability of natural resources and need for environmental monitoring, a country with strategic importance to world's environmental issues, I highlight that the development of this project has the potential of having amplified repercussions of its gas sensing results, as the developed devices will be, after laboratory characterization, employed in on-the-field applications in areas of interests such as urban and rural environments, plantations, livestock production sites, and forests.

Optica Foundation Challenge – Proposal

Category: environment

Multi-gas sensing with ultralow-loss hollow-core fibers

Prof. Jonas Henrique Osório

Federal University of Lavras, Lavras, Brazil

The development of devices able to monitor multiple gas species is a pressing need in environmental science. Although it motivated the study of a great set of gas sensors, selectively and remotely detecting multiple gas species using a single platform lingers as a challenging task. This project proposes the realization of multi-gas fiber-enhanced Raman spectroscopy (FERS) with newly demonstrated hollow-core photonic crystal fibers (HCPCFs) displaying ultralow loss in the short-wavelength range. Performing FERS with such new fibers, which stand nowadays as the lowest loss fiber optics guiding in the visible range, will allow enlarging the interaction lengths of the current systems and achieve lower detection limits for greenhouse gases and gaseous pollutants sensing. Additionally, this platform will enable the realization of remote multi-gas sensing as the sensor head can be deployed at the application site while the measurement apparatus can be kept away from the measurement locus.

Literature review

Bountiful results have been achieved by the gas sensors research community in the latest years regarding the demonstration of the sensing schemes and their corresponding performances. Indeed, these efforts have been highly motivated by the pressing need for the development of such devices, which became of paramount importance to medical and industrial applications, as well as to environmental science (*e.g.*, for the detection of greenhouse emissions and gaseous pollutants).

Among the different gas sensing approaches, optical methods appear as highly promising ones as they afford excellent selectivity, sensitivity, and very low detection limits whilst keeping the possibility of being set in compact, lightweight, and electromagnetic interference-immune setups. Thus, techniques such as laser absorption and photothermal spectroscopies [1, 2] have been investigated and successfully applied

to the detection of different gas species. Although these techniques can provide superior performances, they are typically designed to probe single gas molecules. Alternatively, if one wishes to perform multiple gas sensing using the latter, the complexity of the experimental setups can rapidly increase, as multiple optical sources might be needed to assess the different absorption lines of the gases under study.

In this context, Raman spectroscopy [3] emerges as a potent alternative to the realization of multi-gas sensing as it is able to detect the molecules' spectral fingerprints and, hence, afford a highly selective measurement for the study of complex gas mixtures while using a single optical source. Despite its potentialities for the detection of multiple gases, the Raman scattering cross-sections of gases are diminutive (typically in the order of 10^{-27} cm^2), hence entailing feeble Raman signals. To circumvent this limitation, resonant or multi-pass configurations have been approached [4].

Hollow-core photonic crystal fibers (HCPCFs), in turn, appear as an excellent alternative for the realization of Raman scattering-based gas sensing. This is so because HCPCFs, special optical fibers exhibiting an internal microstructure that defines a void core, can simultaneously act as performant waveguides and hosts for gas molecules. This capability readily allows to significantly increase the interaction length between the optical fields and the analyte gas molecules, hence heightening the Raman signals and enabling the development of sensors with smaller detection limits. Due to the latter, one typically refers to the Raman spectroscopy experiments using HCPCFs as fiber-enhanced Raman spectroscopy (FERS). Similarly to free-space configurations, FERS has allowed the development of gas sensors with sub-ppm detection limits [5, 6]. Noteworthily, as they rely on fiber optics, FERS sensors enable the realization of remote gas detection measurements, an advantage over free-space setups.

In this framework, we observe that HCPCF technology has experienced intense development in recent years. Amid the important results in the area, one finds ***my recent work that demonstrated the fabrication of record low-loss HCPCFs guiding in the short-wavelength range [7]***. The reported fibers display, in fact, the lowest loss figures in the visible and ultraviolet considering *all fiber optics* as they lie below the silica Rayleigh scattering limit (a fundamental hindrance for loss decreasing in solid-core fibers). The availability of these new-generation ultralow-loss HCPCFs, therefore, stands as the core of this grant proposal since the application of such fibers as a platform for FERS opens a promising path for demonstrating gas sensors with better performances. This is so because their ***reduced loss enables the utilization of longer fibers*** to enhance the measured signals and ***potentially reduce the detection limits***.

Ergo, the efforts to be devoted to this project will pursue the demonstration of multi-gas sensors with better performances than those reported hitherto. Additionally, this project's endeavors will aim at applying the studied sensors to greenhouse gas emissions and gaseous pollution detection. The development of this project in Brazil, a country with salient importance to climate change scenario due to its great availability of natural resources and the critical need for environment preservation, will enhance the impact of the efforts to be devoted to this research. Finally, considering the broader impact of such advancements, one can cite the possibility of applying the developed gas sensors in industry, agriculture, and livestock production. Moreover, future applications might also encompass the characterization of liquid samples, with potential use in water quality monitoring, for example.

Problem statement/Objective

The development of multi-gas sensors for environment monitoring is a pressing need for environmental science. In this framework, ***this project's objective is to develop multi-gas sensors based on Raman spectroscopy and new-generation HCPCFs with ultralow loss in the short-wavelength range***. The devices to be developed within the context of this project will therefore be applied in monitoring greenhouse gas emissions (*e.g.*, methane and carbon dioxide) and gaseous pollution detection, such as hydrogen sulfide.

Fig. 1 displays a representative diagram of this project's aims and actions. As indicated in the introduction, my recent work [7] demonstrated HCPCFs with record low-loss figures in the visible and ultraviolet ranges (typical HCPCFs cross-sections are shown in Fig. 1). The availability of such new-generation HCPCF allows proposing the realization of Raman spectroscopy of gaseous samples to attain multi-gas sensors with better performance than those reported up to date. I mention that I keep with me several samples of these fibers, which have been fabricated in France, XLIM Institute, University of Limoges. Additionally, I mention the collaboration channel with the French group is absolutely open and allows for additional samples to be sent if needed.

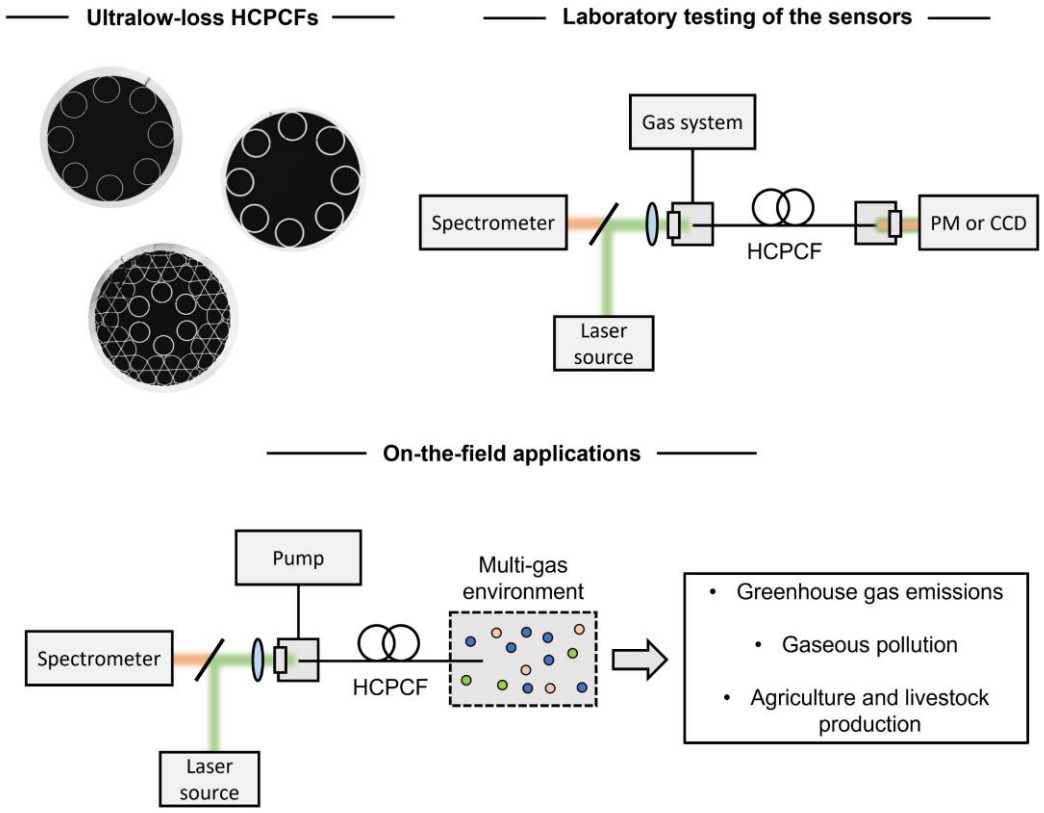

Fig. 1. *Diagram of the project activities, which will encompass the use of ultralow-loss HCPCFs for the development of multi-gas sensors based on Raman spectroscopy. The initial tests will evaluate the sensor response under laboratory-controlled conditions so that the platform can act in on-the-field applications involving greenhouse gas emission and gaseous pollution monitoring, as well as gas sensing within agriculture and livestock production.*

As represented in Fig. 1, the initial tests will take place in a laboratory environment by accounting for the Raman spectra of known gas species at known concentrations (in single-gas and multi-gas scenarios) so as to determine the response of the sensors and obtain an adequate calibration of the latter. In this context, one will study the proposed platform using different fiber lengths and light coupling conditions to evaluate the optimum configuration for the sensor operation.

Following the laboratory testing of the sensors, on-the-field applications will be approached. In this context, one of the HCPCF ends will be placed into real-world environments of interest (*e.g.*, urban environment, agriculture, and livestock production sites) and a pump will be used to fill the fiber with the gaseous sample to be assessed. It is expected that the developed sensors will enable remote detection and quantification of gaseous pollution and greenhouse gas quantities in the studied environments.

Outline of tasks/Work plan

The activities to be developed within this project and the corresponding timeline are appended below:

1) Purchase of equipment and consumables;
2) Identification and hiring of students;
3) Construction of the Raman spectroscopy and gas handling setup;
4) Laboratory-controlled experiments for single-gas detection;
5) Laboratory-controlled experiments for multi-gas detection;
6) Deployment of the sensors in real-world applications and on-the-field detection of greenhouse gas emissions and gaseous pollution.

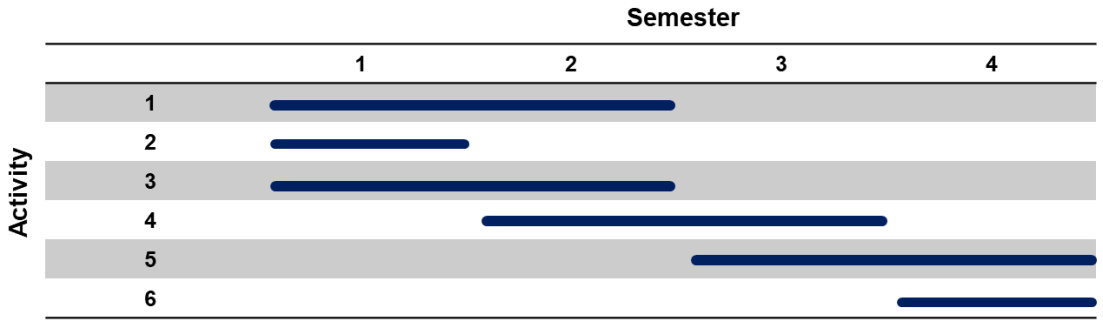

Outcomes

The outcomes of this project will encompass both scientific and practical achievements. From the scientific viewpoint, the activities to be developed within the scope of this project will allow delving into HCPCF properties – modal content, polarization characteristics, and sources of loss –, to identify the most suitable configuration for the sensors' operation. Indeed, although there are previous studies in the literature regarding FERS in HCPCF, the latter are mostly related to the applications themselves. Thus, more comprehensive studies on the impact of HCPCF properties on sensing performance are highly desirable. Hence, one can expect that the efforts to be dedicated to this project will generate scientific papers on the subject.

From the practical point of view, the development and application of the sensors will allow demonstrating devices able to detect and quantify greenhouse gases and

gaseous pollutants. This in turn will contribute to the broad community efforts on environment preservation towards a better future for humanity and will provide the society actors involved in productive, monitoring, and controlling actions with an effective means for assessing multi-gas environments using a simple and cost-effective configuration.

Additionally, this grant will act as ***seed funding*** for the establishment of the research line proposed in this project at the University of Lavras, Brazil. This is highly beneficial as obtaining substantial financial resources for initiating a research line in Brazil is very challenging due to strict economic conditions. The funding by Optica Challenge, therefore, will allow consolidating of the infrastructure for the development of HCPCF-based multi-gas sensors in Brazil and enable future advancements via local funding.

Impact

The development of the multi-gas HCPCF sensors proposed herein will impact the broad scenario of environmental monitoring systems and supply the social actors with an efficient means for remotely assessing multi-gas compositions in environments of interest. The endeavors to be devoted to this project will, therefore, significantly contribute to community efforts regarding environment preservation by providing a means for attaining data on greenhouse emissions and gaseous pollution. This, together with other techniques, has the potential of supplying information on the environmental conditions hence providing guidance for discussions on the strategies for environmental conservation and climate change assessment.

Additionally, being Brazil, due to its wide availability of natural resources and need for environmental monitoring, a country with strategic importance to world's environmental issues, I highlight that the development of this project has the potential of having amplified repercussions of its gas sensing results, as the developed devices will be, after laboratory characterization, employed in on-the-field applications in areas of interests such as urban and rural environments, plantations, livestock production sites, and forests.

References

[1] C. Liu & L. Xu, "*Laser absorption spectroscopy for combustion diagnosis in reactive flows: a review*," Applied Spectroscopy Reviews 54, 1 (2019).

[2] S. E. Bialkowski *et al.* "*Photothermal spectroscopy methods*," John Wiley & Sons (2019).

[3] E. Smith & G. Dent, "*Modern Raman spectroscopy: a practical approach*," John Wiley & Sons (2019).

[4] M. Hippler, "*Cavity-enhanced Raman spectroscopy of natural gas with optical feedback cw-diode lasers*," Analytical Chemistry 87, 15, 7803-7809 (2015).

[5] A. Knebl *et al.* "*Fiber enhanced Raman gas spectroscopy*," TRAC 103, 230-238 (2018).

[6] T. W. Kelly *et al.* "*Sub-ppm gas phase Raman spectroscopy in an anti-resonant hollow core fiber*," Opt. Express 30, 43317-13329 (2022).

[7] **J. H. Osório** *et al.* "*Hollow-core fibers with reduced surface roughness and ultralow loss in the short-wavelength range*," Nat. Commun. 14, 1146 (2023).

Title: Diffractive Optical-Computational Imaging for Deep Learning-Based Depth Estimation of Skin Chronic Wounds

Abstract: Skin chronic wounds pose a serious health problem, especially in patients with diabetes or Hansen's disease, as their healing capacity is limited, leading to significant healthcare and socioeconomic repercussions. An early treatment of these chronic wounds can prevent up to 80% of amputations. To achieve effective monitoring and control of patients with chronic wounds, it is essential to determine various wound characteristics, such as area, perimeter, and depth. These parameters help to determine the precise amount of medical products needed for treatment in each evaluation and monitor the evolution of skin tissue, being the depth the most decisive parameter. However, current depth calculation methods involve invasive techniques with direct contact with the ulcer, making precise measurement difficult and potentially interrupting the healing process. Therefore, there is a need to develop non-invasive and accurate technological solutions for the depth estimation of skin chronic wounds.

Computer vision systems are experiencing growing popularity in the field of medicine, thanks to image processing and the use of artificial intelligence algorithms, which have enabled the development of various applications in the healthcare sector, such as action recognition, patient monitoring, and hygiene protocol control, among others. However, conventional cameras only capture a 2D spatial projection of scenes, losing depth information. Although techniques such as structured light or stereo vision exist for depth estimation in images, they have limitations for use in healthcare due to high costs, sensitivity to lighting, and adaptation difficulties and calibration. Recently, a new methodology has been proposed that utilizes optical-computational diffractive systems to encode depth optically and subsequently estimate it using computational algorithms. Diffractive elements are optical devices capable of custom encoding the amplitude or phase of light waves passing through them by modifying their height map. The advantage of this methodology is its lower cost compared to structured light and stereo vision systems, as it does not require expensive or complex devices.

The present project, led by researcher Jorge Bacca, aims to address the need for an innovative approach to estimate ulcer depth in images of patients from the Sanatorio de Contratación E.S.E. in Santander, Colombia. The project spans a duration of 2 years and encompasses various stages, starting from establishing the acquisition requirements in Colombian patients, followed by the creation of a dataset using structured light systems used only for training, verification, and comparison. The project further involves utilizing deep learning techniques to develop an optical-computational diffractive system for accurately estimating ulcer image depth. The final stages of the project entail the implementation and validation of the proposed system. Collaboration between Dr. Jorge Bacca, experts from the HDSP research group at Universidad Industrial de Santander, and the Computational Imaging group at Stanford University has contributed valuable knowledge for designing and assembling the proposed diffractive camera, with the potential to significantly enhance ulcer medical diagnosis. By providing healthcare professionals with quantitative criteria, this technology enhances diagnostic accuracy and reduces the burden on the healthcare system.

The intended outcomes of this project are:

1. Development of an optical-computational diffractive system for depth estimation in ulcer images.
2. Construction of a database of ulcer images using structured light systems.
3. Utilization of deep learning algorithms to improve the accuracy of ulcer depth estimation.
4. Enhanced medical diagnosis of ulcers, through training/awareness-raising session with medical staff.

1. **Title:** Diffractive Optical-Computational Imaging for Deep Learning-Based Depth Estimation of Skin Chronic Wounds

2. Literature Review:

Chronic wounds image processing: Image processing algorithms for ulcers are based on detecting the region of interest that contains the wound known as the segmentation task. Among these methods used are spatial gradients and fully convolutional networks [1]. For instance, a semi-automatic measurement of lesions has been developed, which includes the calculation of perimeter, area, length, and maximum width of ulcers through segmentation and detection of digital images [1], as shown in Figure 1.

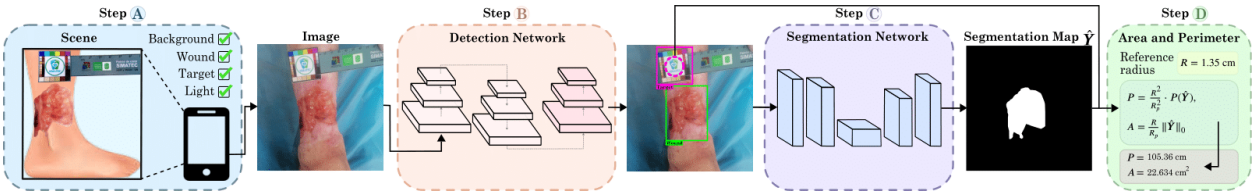

Figure 1. Area and perimeter estimation through segmentation and detection of ulcers in images [1].

Depth estimation based on structured light: Structured light estimates depth by actively illuminating a spatially varying 2D pattern specifically designed for this purpose, as shown in Figure 2. The goal of structured light is to encode and extract the shape of the 3D surface based on the deformations of the light patterns. This information can be calculated using algorithms based on phase recovery and unwrapping [2], which are ideal for small scenes.

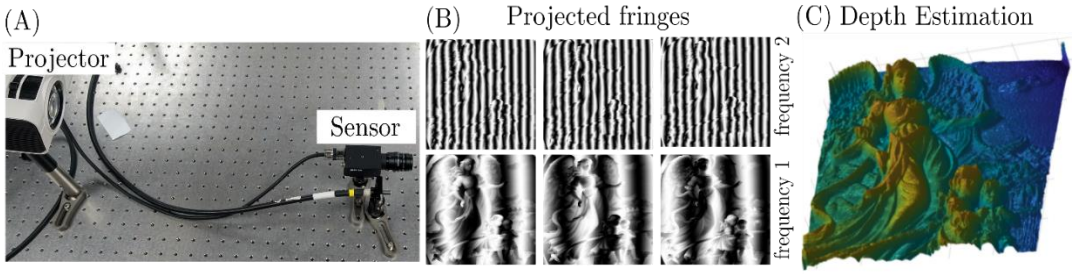

Figure 2. (A) Composite structured light optical system. (B) Projected fringes. (C) Depth estimation.

Depth estimation based on defocus using diffractive elements: Diffractive lenses have been employed to reduce the size of conventional optical systems and improve depth estimation [3,4], as shown in Fig 3. Diffractive lenses modify their height to design point-spread function (PSF) at different depth levels of the scene [4]. The height map can be modeled using Zernike polynomials, which have enabled the application of diffractive lenses to tasks such as super-resolution and extended field of view [5].

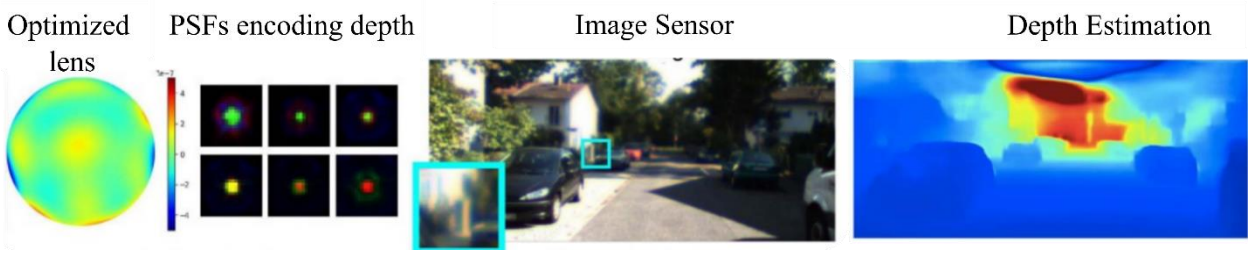

Figure 3. Diffractive lens for depth estimation in outdoor scenes [3].

Diffractive optical design using end-to-end estimation: Recent advancements in optical systems have shifted focus towards utilizing image databases and developing robust algorithms for tasks such as depth estimation, rather than relying on a priori assumptions about optical elements [6]. One approach that has emerged is the joint utilization of deep learning and end-to-end models, where optical elements are modeled as layers of neural networks coupled with artificial intelligence models [5]. These interpretable optical layers learn optimal parameters along with neural network weights to achieve optimal inference results. Figure 4 illustrates the training process using deep learning techniques. Once optical parameters are optimized, real optical systems can be constructed and assembled to acquire encoded images, as depicted in the lower part of Figure 4, where the trained neural network serves as the inference operator. This allows better estimates in inference tasks. This training paradigm has been effectively employed in designing diffractive elements for spectral imaging [7] and compressive sampling [6]. Specifically, the end-to-end approach has inspired the design of diffractive lenses that encode blur in terms of depth to be estimated by a neural network [8].

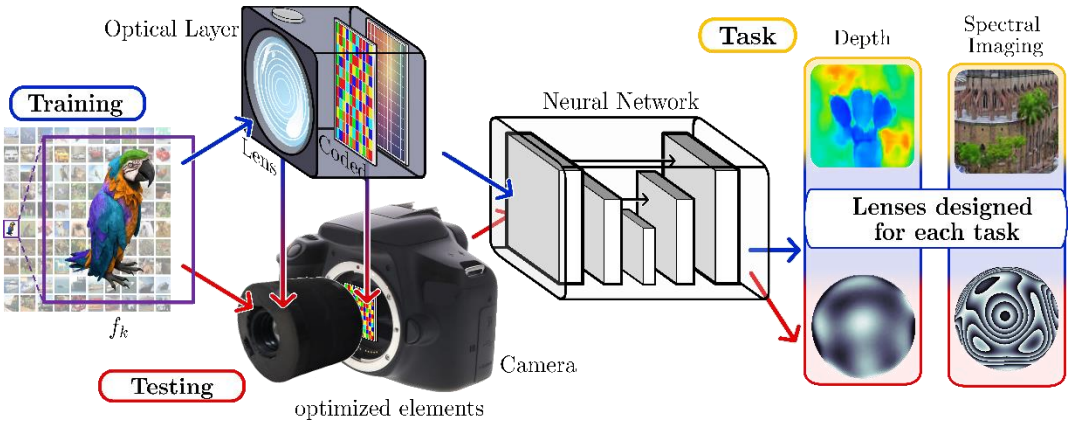

Figure 4. Visual representation of an end-to-end model. The blue arrows represent the training step where the camera is modeled as neural network layers. The red lines depict the evaluation scheme where optimal parameters are fabricated, and the neural network is trained to perform the task. [5].

3. Problem Statement:

According to the World Health Organization, there were 6.7 million deaths related to ulcers worldwide in 2021, and it is estimated that this number will reach 23.6 million by 2030 [9], with 80% of these cases occurring in countries with low or middle economic development [9,10]. For instance, in Contratación, a town in Santander, Colombia, there is a medical center that cares for patients with Hansen's disease. However, due to heavy rainfall, the city occasionally experiences road closures, making it difficult for patients with ulcers to receive timely treatment (See Figure 1). Recently, new treatment schemes have been developed to promote faster and more effective wound healing [11]. In this context, the measurement of depth has emerged as a crucial parameter for evaluating patient progress and evolution, enabling the precise determination of medical product requirements for treatment, and facilitating the monitoring of skin tissue evolution. However, the current methods for measuring depth are invasive and potentially detrimental to the patient's treatment [11], leading to subjective assessments by physicians being a problem for people who live far from medical centers. Although advanced techniques such as structured light or stereo vision can estimate depth in images, they have limitations for use in medical settings due to their high cost, sensitivity to lighting conditions, and challenges in adaptation [9,10].

A recently proposed methodology utilizes computational imaging systems to encode depth information optically and subsequently estimate it using computational algorithms [5]. This approach incorporates diffractive elements, optical devices capable of encoding the amplitude or phase of light waves passing through them [5]. The advantage of this technology lies in its cost-effectiveness compared to structured light and stereo vision systems, as they reduce the need for active illumination or additional cameras. Consequently, the research proposal poses the following question: How can a low-cost optical-computational diffractive system be designed to enable computational depth estimation of ulcer images?

Figure 5. Representation of the problem in Colombian towns where it is difficult to travel to the medical center (Images of the Bucaramanga-Contratación Road).

4. General Objective:

To design an optical-computational diffractive system for depth estimation in ulcers using deep learning algorithms.

Specific Objectives:

1. Establish the requirements of healthcare professionals for ulcer image acquisition.
2. Build an ulcer image database with depth information using structured light.
3. Develop a deep learning algorithm that combines the optimization of a diffractive lens and depth estimation for ulcer image acquisition.
4. Implement and evaluate a prototype of the diffractive optical-computational system for ulcer image acquisition, enabling depth estimation.

5. Outline of tasks/Work Plan:

Schedule: The activities and the work plan are designed to meet the objectives established above.		**Meses**											
		Year 1						**Year 2**					
		Months						Months					
		2	4	6	8	10	12	14	16	18	20	22	24
Obj 1	**Act. 1.1** Sociodemographic characterization of patients with ulcers in medical centers near the department of Santander.												

	Act. 1.2 Definition of protocols for RGB image acquisition and structured light techniques.	
Obj 2	**Act. 2.1** Implementing and calibrating a structured light optical system for depth determination. An optical fringe projector and a conventional RGB camera will be used, along with a phase unwrapping algorithm.	
	Act. 2.2 Building an anonymized depth image database of skin ulcers using the system and algorithm from activities 2.1.	
Obj 3	**Act. 3.1** Design of the diffractive system and mathematical modeling of the light propagation process through the imaging formation system. The height map of a diffractive lens will be parameterized and modeled using Zernike polynomials.	
	Act. 3.2 Designing a deep learning algorithm to jointly optimize the diffractive lens and a neural network model for depth estimation.	
Obj 4	**Act. 4.1** To build, assemble, and calibrate the designed diffractive lens.	
	Act. 4.2 Experimental validation of the proposed computational model for ulcer depth estimation by comparing it with depth measurements obtained by a specialist physician using conventional methods.	

6. Outcome (s)

1. Protocol for acquiring ulcer images using the computational imaging system.
2. Database of image pairs of ulcers and their respective estimation of Depth.
3. Deep computational model for depth estimation based on measurements acquired by the designed diffractive camera.
4. Diffractive Optical-Computational Imaging system.
5. Training/awareness-raising session with medical staff
6. Two (2) submitted scientific articles in Optica magazines.
7. Two (2) presentation of the results in Optica Conferences.

7. Impact

Expected impact	Time	Verifiable indicator	Assumptions
Image acquisition for depth estimation in clinical settings using the proposed optical system.	3 years - short	Image data set in clinical settings preserved under the proposed computational system.	They will continue to implement the computer system in the department.
Improvement and implementation of the proposed system to other health areas.	6 years - medium	Number of medical specialties used to estimate the depth under the proposed computational system.	The advantages of applying the methods developed in other areas of health and of high impact for the country are exploited.
Implementation of the optical computational system making the technology accessible for Colombia	8 years - long	Number of cities or towns other than the study, where the proposed system is in use.	The industrial sector will support the commercialization of this type of optical systems to reach clinical environments in Colombia.

Bibliography:

[1] Monroy, B, et al (2021). Two-step deep learning framework for chronic wounds detection and segmentation: A case study in Colombia. *In 2021 XXIII Symposium on Image, Signal Processing and Artificial Vision (STSIVA)* (pp. 1-6). IEEE.

[2] Pineda, et al. (2020). SPUD: simultaneous phase unwrapping and denoising algorithm for phase imaging. *Applied Optics*, 59(13), D81-D88.

[3] Chang, J et al. (2019). Deep optics for monocular depth estimation and 3d object detection. In *Proceedings of the IEEE/CVF International Conference on Computer Vision* (pp. 10193-10202).

[4] Masoumian, A., et al. (2022). Monocular depth estimation using deep learning: A review. Sensors, 22(14), 5353.

[5] Arguello H, et al. (2023). Deep Optical Coding Design in Computational Imaging: A data-driven framework. *IEEE Signal Processing Magazine*, *40*(2), 75-88.

[6] Bacca, J., et al. (2021). Deep coded aperture design: An end-to-end approach for computational imaging tasks. IEEE Transactions on Computational Imaging, 7, 1148-1160.

[7] Arguello H, et al. (2021). Shift-variant color-coded diffractive spectral imaging system. Optica, 8(11), 1424-1434.

[8] Masoumian, A., et al. (2022). Monocular depth estimation using deep learning: A review. Sensors, 22(14), 5353.

[9] Jin, Q., et al (2021). Metabolomics in diabetes and diabetic complications: *Insights from epidemiological studies*. Cells, 10(11), 2832.

[10] World Health Organization and UNAIDS, *Prevention of Cardiovascular Disease*. World Health Organization, 2007.

[11] L. Atkin and A. Critchley, "The leg ulceration pathway: impact of implementation," Wounds UK, vol. 13, 2017.

Clinically validated equitable polarization pulse oximetry

Increasing access to reliable pulse oximeters worldwide remains a challenge as there is an unprecedented need for creating new and effective standards and technologies for oximetry validation accounting for all skin complexions. A 2020 retrospective study carried out at the Univ. of Michigan and published in the *N Engl J Med* found that Black patients with critically low SaO_2 levels were 3X more likely than White patients to suffer from *hidden hypoxemia* (SpO_2 of 92 – 96% on pulse oximetry, but an SaO_2 < 88%) [1]. The following year, Wong ***et al*** determined that all racial and ethnic patient groups with *hidden hypoxemia* experienced higher in-hospital mortality. These shortcomings have been recognized by the FDA and identified as a major issue to address shared during the Pulse Oximetry Forum, a joint meeting of experts and the ISO Oximeters Joint Working Group, held at UCSF by the Open Oximetry project in March.

Today, it is commonly believed that mitigating this problem boils down to incorporating real-time skin-tone detection and by calibrating for a more diverse distribution of skin tones using better instruments and procedures than current practice. However, to-date, there are no published studies showing that spectral calibration procedures improve the accuracy of pulse oximetry, yet alone in a clinical setting. Moreover, the purported model to correct for skin tone still assumes that subsurface optical scattering in skin by melanosomes changes slowly or not at all with respect to wavelength and can be effectively ignored. Crucially, this model has yet to be vetted and is at the crux of purely optical-based approaches by others to arrive at an equitable pulse oximeter.

Recently, our group at Brown University led by Prof. Kimani Toussaint has developed an alternative approach based on a novel single-wavelength polarization pulse oximeter (PPO) that has the potential to correct for melanated skin tones (See Fig. 1 for approach comparison) [2]. Following the proof-of-concept demonstration on healthy patients, our team swiftly partnered with expert clinicians and pulmonary physicians to complete a pilot study on critically-ill patients with arterial lines at the Miriam Hospital ICU. With this on-going 24-patient study, we aim to benchmark the PPO accuracy for hypoxic patients representing diverse skin complexions. Our initial results from 12 patients on supplemental oxygen indicate that both the medical-grade pulse oximeter and PPO oximeter fall within 3% of the SaO_2 ranging between 96 – 98%. However, the PPO suffers from limited polarization contrast thus leading to poor signal-to-noise ratio (SNR) below 96%.

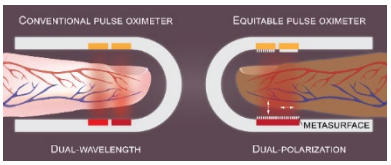

Fig. 1 | Conceptual diagram comparing conventional (left) to a novel single-wavelength (right) pulse

The **outcome of this proposal is expected to be an improved portable polarization-based pulse oximeter**. The envisioned compact, single-wavelength, polarization pulse oximeter will feature enhanced SNR and dynamic range of the reflected photoplethysmogram (PPG) signal with extended polarization contrast. This project will evaluate the accuracy of medical grade and polarization pulse oximeters in a clinical study on diverse populations. Importantly, the new reduced fill-form prototype design would account for patient comfortability and clinical accessibility.

Our proposed equitable technology will potentially diminish the global health gap disparity, especially in emerging global economies where there is a growing prevalence of respiratory diseases. By leveraging eccentric degrees-of-freedom of light and novel metasurface platforms, our interdisciplinary team of engineers, physicists, clinicals and statisticians will validate the accuracy of a novel approach for PPG-based sensing technologies and outline a viable path toward commercialization by partnering with companies and under the advisement of local biomedical technology business experts.

[1] Sjoding MW, et al., Racial bias in pulse oximetry measurement. N Engl J Med. 383(25):2477-2478. (2020)
[2] Jakachira, R. et al, “Single-wavelength, single-shot pulse oximetry using an LED-generated vector beam.” Opt. Express 30, 27293-27303 (2022).

Introduction & Literature Review

Inaccuracies in pulse oximetry have come under immense scrutiny over the past 3 years, as a 2022 study showed that inaccurate blood-oxygen readouts from Hispanic and Black Patients cause them to be 25% less likely to be recognized as eligible for COVID-19 treatment [1]. Irregularities in pulse oximetry accuracy have been known since its inception by Aoyagi in 1974 [2,3], but was still rapidly adopted as a clinical standard to avoid using the invasive and time-consuming arterial blood gas (ABG) alternative. However, in 2005, Bickler *et al*., concluded in a perspective deliberate desaturation study that biases in pulse oximetry stem from skin pigmentation. Each of the three pulse oximeters under investigation overestimated SaO_2 during hypoxemia in dark-skinned individuals [4]. Furthermore, pigment-related bias increased approximately proportional to desaturation. Hence, darker-skinned patients are more likely to experience *hidden hypoxemia* (SaO_2 < 88% when SpO_2 was 92% – 96%) which can lead to delayed medical treatment thereby resulting in unfavorable clinical outcomes [5]. In 2021, Wong and colleagues demonstrate the consequences of underdetection of hypoxemia among a diverse (Asian, Black, Hispanic and White) population of patients with respiratory disease [6]. In this multicenter, retrospective, cross-sectional study using data from 3 publicly available databases that included 215 hospitals and 382 intensive care units, the authors associated higher odds of hospital mortality, elevated lactate, and high sequential organ failure assessment scores with a higher prevalence of hidden hypoxemia among Asian, Black, and Hispanic patients compared with White patients. Since SpO_2 is widely used to inform early clinical decisions for patients, the inaccuracies from skin pigmentation in pulse oximetry, especially over-the-counter (OTC) devices, further widens the health disparity gap, as racial and ethnic marginalized groups are typically of darker-skin hues.

One issue with retrospective studies is that melanin content of an individual is not accurately captured as part of the medical record, thus retrospective studies differ to race and ethnicity as surrogates, which ultimately will not fully reflect the skin tone diversity within each patient group or other differences that contribute to pulse oximetry bias. Recently, Ajizian *et al*. assessed the pulse oximetry performance across varying skin pigmentations for SaO_2 between 80 – 92% in a limited sample size study [7]. Contrary to the reported hidden hypoxemia rates of 3.6 – 6.6% by Henry and Medtronix colleagues in 2022, the results showed no statistical bias observed between lighter and darker skin patients. As reported by the authors, the discrepancies may have been due to differences in patient type, timing between SpO_2 and SaO_2 readings, the amount of motion noise across studies, and the limited sample size in this analysis. Furthermore, and arguably most important, clinicians either rely on self-reported race and ethnicity or at best subjective skin color assessment approaches, as opposed to quantitative approaches using spectroscopy. Recently, the FDA has recognized this issue and has convened publicly with researchers, scientists, public health specialists, and pulse oximetry manufacturers to address this stagnation [8].

A combination of Monte Carlo optical transport models and clinical findings will ultimately strengthen our understanding of the convoluted issues posed by pulse oximetry; these include the effects of pigmentation, as well as those of low perfusion of blood through a person's tissue, carbon monoxide poisoning and anemia. The success of pulse oximetry as a real-time low-cost tool for monitoring a person's cardiorespiratory status has led to its widespread use, and the technique's prevalence has, in turn, highlighted situations in which inaccuracies occur. Clearly, clinical findings from the past few years provide an imperative for developing and validating oximeters without a fundamental dependence on pigmentation. These studies also highlight the importance of using quantitative measurements (i.e. spectroscopy, CIE chromaticity and perception) to evaluate skin pigmentation rather than or in addition to current qualitative and subjective approaches (Martin & Massey, and Monk perception-based scales).

Problem Statement/Objectives

Photoplethysmography (PPG) is an optical technique where fluctuations in light intensity reflected or transmitted through microvascular bed of tissue are related to volumetric variations

in blood circulation. The non-invasive approach has led to a ubiquitous tool for continuous physiological sensing (e.g. heart rate monitoring, instantaneous respiratory rate extraction, and pulse oximetry), especially with the rising popularity of smartwatches and similar wearable technologies. Pulse oximeter technologies, enabled by PPG, have been rapidly adopted as a clinical standard in anesthesiology and used for early diagnosis of hypoxemia. Despite the advancement of instrumentation over the years, the operation principle of pulse oximetry has remained largely the same, namely that oxyhemoglobin (HbO_2) absorbs light of red (e.g., 660 nm) and IR (e.g., 940 nm) wavelengths differently as compared with deoxyhemoglobin (Hb). The ratio of HbO_2 and Hb concentrations can hence be extracted by examining the ratio of time-varying pulsatile signals at the two wavelengths, upon which SpO_2, the blood-oxygen-saturation level in peripheral capillaries, can be determined [9]. The conventional approach however often relies on empirically determined correction factors obtained by in vivo comparison of oximeter readings with arterial oxyhemoglobin saturation (SaO_2) of volunteer subjects. One could imagine that other non-pulsatile such as the abundance of melanin could adversely affect these correction factors if such confounders are not accounted for and the volunteer patient population is not diverse in skin tones.

Sources of biases, that is differences in SpO_2 and SaO_2, include motion artifacts, low perfusion, ambient lighting, dyes (intravenous), carboxy- (HbCO) and methemoglobin (MetHb). Skin pigmentation and other surface light absorbers should, in theory, not cause errors in SpO_2 readings IF the absorber rate is equal for red and IR light. Secondly, this notion assumes the scattering rates are consistent for both optical frequencies.

In 2022, we presented a novel polarization imaging-based technique to measure SpO_2 in five healthy volunteers carried out using a radially polarized vector beam. For the case of PPO, SpO_2 can be determined by

$$SpO_2 = \left(1 - \frac{I_{par} - I_{per}}{I_{par} + I_{per}}\right) \times 100\% = \frac{R_d}{R_d + R_s} \times 100\% \quad (1)$$

where R_d and R_s are the components of the incident reflected light from the deep layers (arteries predominantly containing oxyhemoglobin) and superficial layer (veins predominantly containing deoxyhemoglobin). The I_{par} and I_{per} are the time-varying intensities for orthogonal eigen polarization projections.

Figure 1 depicts the experimental setup, radially polarized vector beam and comparison between our device and a Masimo finger-tip pulse oximeter described in our recent work [10]. We transformed our tabletop device into a robust mobilized prototype permitting single-shot data acquisition at a single wavelength in a clinical study with critically-ill patients. The results curated from the 75% complete clinical study have revealed the need for technological adjustments and to improve clinical protocol for ancillary melanin quantification.

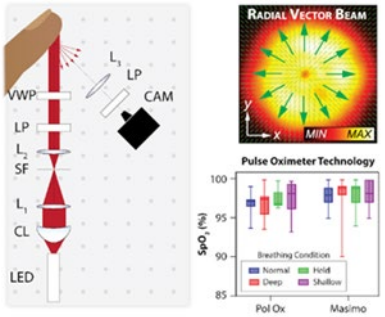

Fig. 2 | (Left) Free space experimental setup, (Top-right) quasi-coherent vector beam generated by vortex waveplate, and (Bottom-right) pulse oximetry testing on healthy volunteers under varying breathing conditions.

The objectives of the proposed collaborative effort are to (1) determine the absorption contributions due to skin pigmentation and scattering associated with melanin and (2) evaluate the polarization-based approach to pulse oximetry in a clinical setting and upon validation, design a miniaturized plug-and-play on-chip device. Our technology intellectual property was filed on 8/11/21 under the following ID number (PCT/US2022/04/0020) describing a new system for detecting cardiovascular parameters independent of the relative absorption contribution of melanin in biological tissues. Our proposed project will design, develop and validate a smaller and more modular portable pulse oximeter, as well as set a pathway toward a truly integrated miniaturized device enabled by meta-optics. The collaborative project will be conducted with a team of physicists, optical, mechanical and electrical engineers, statisticians, and clinicals and pulmonary physicians.

Outline of tasks/Work Plan

The project will comprise the following three major tasks: 1) optimization (wavelength, polarization, wavefront, etc) stage, 2) prototype (re) design and development, and 3) clinical testing. Leveraging the outcomes of the current pilot clinical study underway at the Miriam Hospital (Providence, RI), we will take the opportunity to optimize all aspects (user experience, size, weight, and accuracy) of our portable oximeter.

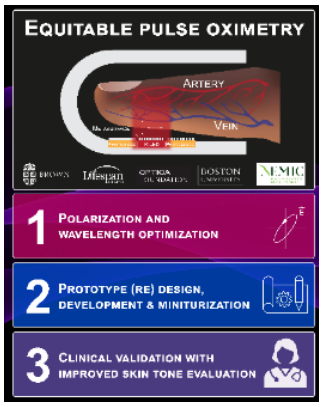

(1) Polarization and wavelength optimization. The polarization model for pulse oximetry permits cancelation of the absorption coefficient by ratiometric analysis provided that the measurement is carried out at a single illumination wavelength and in a single shot. However, to increase the dynamic range for SpO_2 measurements (polarization contrast of at least 10%) obtained in this manner, a wavelength range should be determined that allows for maximum contrast in the polarization response from veins and arteries. To achieve this, the extinction coefficient (absorption plus scattering) of the tissue will be obtained, which will also help clarify which wavelengths might dominate the specular and diffusely reflected polarization responses. A bench-top high-speed polarization spectrometer will be developed to evaluate the PPG from polarization channels on 50-100 volunteers. Information on which wavelength to use for maximum polarization contrast will facilitate clinical testing as the complexity of the setup will be reduced.

Similar to the need to optimize wavelength, it is not clear whether there are preferred eigenstates of polarization in the tissue (finger) for optimizing light throughput. Thus, a more detailed polarimetric mapping of the finger using a single-shot Mueller calculus approach will provide an analysis of the illuminated region on the finger. This type of analysis will offer more precise control for optimizing the contrast between the response from Hb and HbO_2. The optimal polarization will subsequently be used to engineer vector-beam (VB) generating metasurfaces to reduce the size and weight of the redesigned prototype in collaboration with Prof Abdoulaye Ndao (Boston University). Currently, a first-generation vector-beam generating meta-axicon has been fabricated and characterized in free-space over 3 cm propagation distance. Moreover, the information will also significantly help the development of a simulation model based on a modified Monte Carlo approach for optical diffusion in turbid tissues developed by 2022 Optica Amplify Scholar and 2023 Google Fellow, Ms. Rutendo Jakachira.

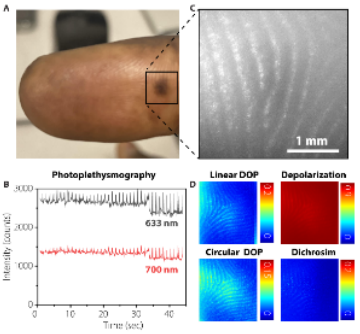

Fig. 4 | Polarization response at 780 nm (A) Image of a volunteer's finger, and (B) displayed two spectral channels from PPG waveform recorded by a spectrometer. (C) Region of interest of finger, and (D) corresponding polarization analysis. (unpublished results)

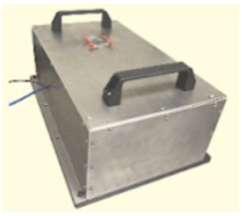

Fig. 3 | Photo of our current pulse oximeter prototype. The size of the entire unit is 18" x 12" x 8".

(2) Prototype (re) design and development. With the knowledge learned from our ongoing pilot clinal study, we are in a unique position to improve the design, speed, and performance of the pulse oximeter. Importantly, the new prototype design would account for patient comfort and clinical accessibility. Currently, two summer undergraduate Electrical Engineering students (one of whom will attend the 2023 Amplify Optics Immersion Program) will work on the Interfacing of a Miniaturized Prototype Pulse Oximeter and Optimization of Signal Process for Physiological Monitoring. Students currently work under the advisement of both myself and Toussaint on the hardware and software components of the prototype device, along with Ph.D. Physics Student, Rutendo Jakachira. These summer efforts coupled with our keen clinicians (Lifespan) and entrepreneurial advisors (NEMIC and Brown Innovations) place our interdisciplinary team in a unique position to expedite the project to meet the urgency of the matter from both a health disparity and commercialization point of view.

(3) Clinical testing with improved skin pigment evaluation. Our final stage for this 1-year project will be to return to a revised clinical study with our clinical collaborators (at the Miriam Hospital) to test our next-generation prototype. The new clinical study will be carried out to ensure that oxygen saturation levels are also acquired in the hypoxic regime, which was unable to be captured when critically-ill ICU patients are on supplemental oxygen.

In our ongoing clinical study, visual surveys are performed and enrolled patients are assigned a visual color scale value at the volar and dorsal side of the distal phalanx. While visual color scales are cost-effective and potentially reliable means of measuring skin undertones in diverse populations, they can be prone to inconsistencies and variation. Hence, further improvements to our clinical study design include quantitative skin-tone metrics. Spectroscopic-based approaches are more reliable than perception-based color scales due to inherent subjectivity in the latter approach. Thus, in our new study, each patient will also be categorized based on reflection-based spectrophotometer measurements, to which our statisticians will draw accurate and unbiased inferences from the collected information. Last, the study will be designed to incorporate simultaneous blood oxygen measurements by SpO_2 and SaO_2, measurement of patients' peripheral perfusion, type of pulse oximeter, probe and site of probe placement, among different patient populations.

The table below shows the proposed timeline along with projected tasks, subtasks and milestones of the effort.

Task	Description of task	Fall 2023				Spring 2024				Summer 2024			
		Sep	Oct	Nov	Dec	Jan	Feb	Mar	Apr	May	Jun	Jul	Aug
1	**Polarization distribution and wavelength selection optimization**												
1.1	Spectroscopic characterization of PPG signals in a diverse population of 25 – 50 volunteers												
1.2	Polarization characterization via high-speed Mueller Matrix polarimetry of tissue scattering for various skin tones												
1.3	Validation with polarization-sensitive Monte Carlo-based numerical model												
Milestone 1	Optimum wavelengths and polarization eigenstates identified and applied												
2	**Prototype (re) design and development**												
2.1	Design new portable prototype with improved interfacing and reduced footprint												
2.2	Engineer new portable PPO with optimal wavelength and polarization distribution												
2.3	Render architecture for the miniaturized prototype PPO enabled by metasurfaces												
Milestone 2	Develop new, portable prototype with optimized components												
3	**Clinical testing and validation**												
3.1	Summarize results of pilot ICU clinical study #1 and submit results for journal publication in Optica Publishing												
3.2	Improve clinical study design in collaboration with clinicians and statisticians												
3.3	IRB submission for clinical study #2												
3.4	Conduct pilot clinical study #2												
Milestone 3	Validate our technology with other medical grade pulse oximeters and submit results for journal publication												

Outcome(s)

The outcomes of the project are to develop and validate the first polarization-based pulse oximeter based on vector beams. The proposed project ultimately aims to demonstrate improved accuracy over standard pulse oximetry irrespective of skin tone. Detailed descriptions of several outcomes are listed below:

[1] Development of a wavelength and polarization optimized, small-footprint second-generation PPO with SpO2 dynamic range above 4%

[2] Compare skin pigment-dependent pulse oximeter accuracy in a subsequent clinical study using quantitative skin tone assessment (i.e. hand-held spectrophotometer or colorimeter)

[3] Undergraduate and graduate level training of two Optica Amplify Immersion Program Attendees in spectroscopy, polarimetry, numerical modeling of optical transport in turbid media, and science communication

[4] Create a polarization-based Monte Carlo simulation model for photon transport using wavelength-dependent import parameters obtained from 50 – 100-person database

[5] 2+ invited talks at Optica events and historically black colleges and universities (HBCUs) that has been established by Burrow as a 2023 Optica Ambassador
[6] Establish a black-owned start-up company, co-founded by Burrow, on photonics-based technology, under the advisement of Brown Innovations and the NEMIC program

Impact

Medical practitioners use readings from prescription pulse oximeters as one factor to inform patient triaging and critical care decisions that will ultimately improve clinical outcomes. Anesthesiologists employ them to monitor respiratory status and prescribe accurate amounts of supplemental oxygen in surgical procedures. Additionally, clinicians may prescribe a pulse oximeter for home use by patients with asthma, lung cancer, influenza, COVID-19, sleep apnea, pneumonia, and carbon monoxide poisoning. Most people resort to non-FDA cleared, OTC pulse oximeters and wearable technologies (e.g. Apple Watch, Fit Bit, etc) intended for fitness and general wellness. In all cases, these monitoring techniques for blood oxygen transport are viable alternatives to the more invasive gold standard, arterial blood gas (ABG) test administered by medical experts. Thus, it is imperative to improve the accuracy and reliability of pulse oximetry, as this stagnation contributes to the health disparity gap.

The patient population is most directly impacted by non-equitable pulse oximeters, we can consider that in American, 40% of the population are non-white (Census 2020), with over half of the population under 16 years identifying as a racial or ethnic minority. Hence, the future US demographics are trending toward are darker-skinned population, and thereby indicating a trend of increasing need for a device that is not designed for white skin. From a global perspective, roughly 85% of the world is non-white which opens are broad landscape for universal impact and additionally multiple market entry points. In summary, if pulse oximeters are less accurate and robust for darker skin-tone individuals then this impacts BILLIONS of people around the globe. Moreover, it is imperative to develop commercially viable solutions in emerging global economies, especially with the growing prevalence of target diseases such as asthma, hyperlipidemia, hypertension, diabetes, ischemic conditions, cardiac arrhythmia, sleep apnea, and COPD is expected to increase over the coming years.

References

[1] Fawzy, A. et al. “Racial and Ethnic Discrepancy in Pulse Oximetry and Delayed Identification of Treatment Eligibility Among Patients With COVID-19”. JAMA Intern Med 187(2) 730-738 (2022)
[2] Aoyagi T. Pulse Oximetry: its invention, theory, and future. J. Anesth 17 pp 259-266 (2003)
[3] Severinghaus, J.W. “Takuo Aoyagi: Discovery of pulse oximetry. Anesth Analg (Philadelphia, PA, US) 105(6 Suppl) S1-S4 (2007)
[4] Bickler et al., “Effects of skin pigmentation on pulse oximeter accuracy at low saturation.” Anesth 102(4) pp 715-719 (2005)
[5] Keller et al., “Skin colour affects the accuracy of medical oxygen sensors” *Nature* 610 pp 449-451 (2022)
[6] Wong, AL. et al, Analysis of Discrepancies Between Pulse Oximetry and Arterial Oxygen Saturation Measurements by Race and Ethnicity and Association with Organ Dysfunction and Mortality, *JAMA Netw Open.* 4(11):e2131674 (2021)
[7] Ajizian, S. Occult hypoxemia and pulse oximetry performance across skin pigmentation group 51(1) pp 509 (2023)
[8] Pulse Oximeter Accuracy and Limitations: FDA Safety Communication. June 21, 2022, https://www.fda.gov/medical-devices/safety-communications/pulse-oximeter-accuracy-and-limitations-fda-safety-communication.
[9] Nitzan, M. et al., Puulse oximetry: fundamentals and technology update. Med Devices (Auckl) 7, 231-239 (2014).
[10] Jakachira, R. et al, “Single-wavelength, single-shot pulse oximetry using an LED-generated vector beam.” Opt. Express 30, 27293-27303 (2022).

Name of the project proposal: Development of optical fiber based portable device for drug-free sustainable cancer therapy

Category: Health

Cancer is one of the most serious diseases that is severely threatening the health of human beings. Worldwide, an estimated 19.3 million new cancer cases and almost 10.0 million cancer deaths occurred in 2020, being the first or second leading cause of death before the age of 70 years in 112 of 183 countries. Therefore, the development of novel therapeutic modalities with concurrent high efficacy and largely diminished side effects in combating cancer is urgently required to save millions of lives worldwide. The surgery, radiotherapy and chemotherapy are three main treatment strategies for cancer. There are several limitations to use these three techniques. Surgery is effective only in early stage of cancer when it is very much localized. Radiation therapy is very much slow process to cure cancer. It also damages healthy cells. Chemotherapy is a systemic medication which uses anti-cancer drugs to kill cancer cells. However, the poor aqueous solubility and permeability of these drugs have resulted in low bioavailability and decreased treatment efficiency. Chemotherapy can cause side effects like hair loss and nausea. Recently, a number of emerging therapeutic modalities such as photodynamic therapy and photocatalytic therapy, have shown high performance for cancer treatment, but they are still undergoing basic research and have not been extensively used in the clinic.

To address this serious issue, I am proposing to develop a portable device based on laser or LED coupled optical fiber. The light can be driven to cancer tumor through the fiber. Because of high flexibility and durability of the fiber it can be placed anywhere in the body easily. The end of the fiber will be activated with nano-photocatalysts which will generate ROS on excitation of light and the ROS will kill the cancer cells. There is very less probability that healthy cells are damaged using this technique as the fiber can reach exact location of the tumor or cancer cells. This device may bring revolution in cancer therapy as the proposed device is associated with sustainable, effective and side-effects free cancer treatment. Moreover, the cost to fabricate this device is not expensive and it is reusable after sterilization, and does not require any drugs. Therefore, this device will reduce the cost of cancer treatment significantly and it will prevent the death of a cancer patient because of poverty.

Development of optical fiber based portable device for drug-free sustainable cancer therapy

Joy Sankar Roy
Center for Optics, Photonics, and Lasers
Laval University, 2375 rue de la Terrasse, Quebec, G1V 0A6, QC, Canada
Email: joy-sankar.roy.1@ulaval.ca
Ph: +1 5814439695

1. Introduction and Justification:

Cancer is one of the most serious diseases that is severely threatening the health of human beings. Worldwide, an estimated 19.3 million new cancer cases and almost 10.0 million cancer deaths occurred in 2020, being the first or second leading cause of death before the age of 70 years in 112 of 183 countries [1]. Therefore, basic and clinical research on efficient cancer treatment is still highly urgent.

The surgery, radiotherapy and chemotherapy are three main treatment strategies for cancer [2]. There are several limitations to use these three techniques. Surgery is the oldest process to treat cancer. Surgery is the most effective in early stage of cancer when it is very much localized. But, sometimes it is not possible to remove all of the cancer cells. This can happen when the tumour is in a place where it's too hard to remove without damaging other organs or cells. It is also risky for some cancer in sensitive organs. There may be several side effects for cancer surgery. Radiation therapy kills cancer cells or slows their growth by damaging their DNA. Cancer cells whose DNA is damaged beyond repair stop dividing or die. But, radiation therapy does not kill cancer cells right away. It takes days or weeks of treatment before DNA is damaged enough for cancer cells to die. Then, cancer cells keep dying for weeks or months after radiation therapy ends. Radiation not only kills or slows the growth of cancer cells, it can also affect nearby healthy cells. Damage to healthy cells can cause side effects. Chemotherapy is a systemic medication which uses anti-cancer drugs to kill cancer cells. However, the poor aqueous solubility and permeability of these drugs have resulted in low bioavailability and decreased treatment efficiency [3-4]. Moreover, the drugs travel through the bloodstream and reaches all parts of the body, and hence it can also damage healthy cells as they go through their normal cell cycle. This is why chemotherapy can cause side effects like hair loss and nausea. In combating

cancer, one of the most critical challenges for successful chemotherapy are the undesirable toxic side effects of chemotherapeutic agents delivered to normal cells, tissues and organs due to their non-specificity.

The development of novel therapeutic modalities with concurrent high efficacy and largely diminished side effects in combating cancer is therefore urgently expected. Recently, a number of emerging therapeutic modalities such as photodynamic therapy and photocatalytic therapy, have shown high performance for cancer treatment, but they are still undergoing basic research and have not been extensively used in the clinic.

As a non-invasive cancer therapeutic technique, photodynamic therapy provides spatiotemporal control over drug activation, overcoming the problems of chemotherapeutic drugs such as severe side effects and acquired drug resistance [5-6]. Traditionally, phototherapy uses light activation of an organic photosensitizer (PS) to react with tissue oxygen for the generation of reactive oxygen species (ROS) which induce cytotoxicity to the targeted cells. However, a few factors such as low aqueous solubility and oxygen dependent mechanism of action limit their application. To overcome the limitations of organic PSs, photoactive metal complexes are under investigation as next generation PSs for phototherapy [7-8].

Very recently, the researchers found that the photocatalysis process can damage cancer cells very quickly using nano-photocatalysts [9-11]. Huang et al reported photocatalytic cancer therapy of highly bio-compatible Iridium [9]. There are many bio-compatible photocatalysts like TiO_2 and ZnO, that can be used for PCT. But, still there is several problems with delivery of photocatalysts to cancer location specially for effected interior organ. It is also difficult to deliver light there. Hence, emerging technology is needed to overcome these problems for sustainable drug-free cancer therapy.

2. Objectives of the proposed project

The development of novel therapeutic modalities with concurrent high efficacy and largely diminished side effects in combating cancer is urgently required. The photocatalytic therapy has shown high performance for cancer treatment, but they are still undergoing basic research and have not been used in the clinic. To address this serious issue, I am proposing to develop a portable device based on laser or LED coupled optical fiber. The light can be driven to cancer tumor through the fiber. Because of high flexibility and durability of the fiber it can be placed

anywhere of the body easily. The end of the fiber will be activated with nano-photocatalysts which will generate ROS on excitation of light and the ROS will kill the cancer cells. There is very less probability that healthy cells are damaged using this technique as the fiber can reach exact location of the tumor or cancer cells. There will be no headache to remove nanoparticles from the body after treatment alike conventional photocatalytic therapy using direct nanoparticles which are injected to the tumor or locality of cancer cells. This device may bring revolution in cancer therapy as it is the most sustainable, drug free and safe treatment process.

3. Work Plan

The main objective is to develop portable device for cancer therapy and to achieve the goal following procedure will be executed:

- The pure silica optical fiber (SOF) having core size between 200 and 300 microns with acrylic cladding will be drawn using 10-meter drawing tower. The SOF will be used because of its negligible loss in transmission of light.
- The acrylic cladding will be removed from the top of the fiber (about 3 to 4 cm) and will be coated with nanoparticles to prepare photocatalytic optical fiber (PCOF).
- A small fiber bundle will be fabricated using 10 to 20 pieces of PCOF.
- A portable laser source or a high-power LED will be coupled with the fiber bundle to inject light into the fibers.
- The performance of the device will be tested for in-vivo and in-vitro cancer treatment.

The schedule with work plan of the proposed project is summarised in following table.

Activities	**6 months**	**12 months**	**18 months**	**24 months**
Preparation SOF and PCOF				
Characterization of PCOF				
Photocatalysis activity study of PCOF				
Development of device				
Cancer therapy trial with device				

Group meeting and discussions				
Report/Research articles writing				

4. Expected outcomes and impact of the project

The development of novel technology with high efficacy and largely diminished side effects in combating cancer is urgently expected to save millions of lives. From this perspective, this project may bring revolution in cancer therapy as the proposed device is associated with sustainable effective and side-effects free cancer treatment. Moreover, the cost to fabricate this device is not expensive and it is reusable after sterilization, and does not require any drugs. Therefore, this device will reduce the cost of cancer treatment significantly and it will prevent the death of a cancer patient because of poverty. The specific outcomes can be summarised below:

- Very much cost-effective portable device that may cure cancer very easily and effectively, which can save millions of lives worldwide. Cancer patients will recover quicker than conventional treatment methods.
- Presentation of this new technology to international audience in conference and seminars.
- Publications of patents and good research articles in reputed international journals.

References

[1] Sung et al. Global cancer statistics 2020: GLOBOCAN estimates of incidence and mortality worldwide for 36 cancers in 185 countries. CA Cancer J Clin 2021; 71: 209. https://doi.org/10.3322/caac.21660.

[2] Debela et al. New approaches and procedures for cancer treatment: current perspectives. SAGE Open Med 2021, 9. https://doi.org/10.1177/20503121211034366.205031212110343.

[3] Tran et al. Recent advances of nanotechnology for the delivery of anticancer drugs for breast cancer treatment. J Pharm Investig 2020, 50, 261–70. https://doi.org/10.1007/s40005-019-00459-7.

[4] Din et al. Effective use of nanocarriers as drug delivery systems for the treatment of selected tumors. Int J Nanomedicine 2017, 12, 7291. https://doi.org/10.2147/IJN.S146315.

[5] Cao et al. Adv. Healthcare Mater. 2018, 7, 1701357. Intraparticle FRET for Enhanced Efficiency of Two-Photon Activated Photodynamic Therapy. DOI: 10.1002/adhm.201701357.

[6] Correia et al. Pharmaceutics 2021, 13, 1332. Photodynamic Therapy Review: Principles, Photosensitizers, Applications, and Future Directions. https://doi.org/10.3390/pharmaceutics13091332.

[7] Chen et al. Advances in nanomaterials for photodynamic therapy applications: Status and challenges. Biomaterials 2020, 237, 119827.

[8] Zhao et al. Recent progress in photosensitizers for overcoming the challenges of photodynamic therapy: From molecular design to application. Chem. Soc. Rev. 2021, 50, 4185.

[9] Huang et al. In-vitro and In-vivo Photocatalytic Cancer Therapy with Bio-compatible Iridium (III) Photocatalysts. Angew. Chem. 2021, 133, 9560. https://doi.org/10. 1002/anie.202015671

[10] Zhao et al. Nature communications 2021, 12, 1345. Photocatalysis-mediated drug-free sustainable cancer therapy using nanocatalyst. https://doi.org/10.1038/s41467-021-21618-1.

[11] Kang et al. Mater. Horiz., 2021, 8, 2273. Piezo-photocatalytic effect mediating reactive oxygen species burst for cancer catalytic therapy. https://doi.org/10.1039/D1MH00492A

深圳国际量子研究院
Shenzhen International Quantum Academy

Prof. Dr. Junqiu Liu
Principal Researcher,
Director of Integrated Photonics Lab,
International Quantum Academy, Shenzhen,

No.10 Binglang Rd, Futian District,
518208 Shenzhen, China
E-mail: liujq@iqasz.cn

Excutive Summary: Photonic Quantum Computing and Phase-Sensing Using Ultralow-Loss Silicon Nitride Integrated Circuits

Exploiting the quantum superposition, quantum information processing (QIP) greatly complements the conventional concept of computer and information science, providing computational ability overwhelmingly exceeding state-of-the-art classical computers for specific problems. Among its multiple physical realizations, photonic systems feature extremely weak interaction with environment and are free from decoherence. This unique property allows photon manipulation at room temperature.

As entering the noisy intermediate-scale quantum (NISQ) computing era, manipulation of more than 50 qubits becomes the central goal. For photonic systems, the continuously improving quantum light sources significantly boosts the number of manipulable photons. Combining with state-of-the-art optical interferometers, a large-scale experimental "*Gaussian Boson Sampling*" (GBS) has been reported recently, showing evidence for quantum computational advantages. Meanwhile, there has been equal endeavor on developing quantum sensors using photons, critical to metrology applications and precision measurement. By introducing squeezed light into the interferometer's dark port, one can surpass the quantum noise limit (QNL) of $1/\sqrt{N}$, and potentially achieve Heisenberg scaling of $1/N$ sensitivity, with N being the photon number. Progress has been achieved in designing squeezed light sources and applying them in gravitational wave detection, which ultimately surpasses the QNL and achieves quantum-enhanced sensitivity exceeding 2 dB.

However, currently almost all the high-performance quantum photonic systems are based on bulky, table-top experimental setups. In comparison, chip devices using *photonic integrated circuits* (PIC) can potentially provide a robust way to perform sophisticated and versatile quantum tasks within a much smaller footprint. They can prominently boost the programmability and reconfigurability of photonic systems for QIP.

In the last decade, based on PIC, multiple works concerning QIP have been carried out, including high-dimensional quantum state manipulation, chip-to-chip quantum teleportation, and squeezed states generation. However, extensive demonstrations have been performed on the silicon-on-insulator (SOI) platform. Due to the high optical loss in SOI waveguides (>1 dB/cm), the number of useful quantum bit and the squeeze factor of squeezed states are severely limited. To build large-scale quantum PIC of high-performances, programmability, and – particularly – ultralow loss, silicon nitride (Si_3N_4) PIC technology will be the material of choice.

In this proposal, we aim to develop heterogeneous, programmable, ultralow-loss Si_3N_4 PIC for photonic quantum computing architectures and squeezed-light-based sensors with sensitivity beyond the QNL. We will develop an advanced CMOS-compatible Si_3N_4 PIC fabrication technology with optical loss below 0.005 dB/cm – 200 times smaller than that of the commonly employed SOI waveguides. In addition, we will develop a complete Si_3N_4 quantum photonic design kit, numerical simulation models, and a standard set of building blocks. We will apply this Si_3N_4 quantum PIC technology to demonstrate chip-scale GBS and precise phase sensors.

Our proposed research promises to advance integrated quantum processors and sensors, and will open new avenues for quantum computation and precision metrology, as well as other domains such as telecommunications, LiDAR, imaging and environmental monitoring.

深圳国际量子研究院
Shenzhen International Quantum Academy

Prof. Dr. Junqiu Liu
Principal Researcher,
Director of Integrated Photonics Lab,
International Quantum Academy, Shenzhen,
No.10 Binglang Rd, Futian District,
518208 Shenzhen, China
E-mail: liujq@iqasz.cn

Proposal for 2023 Optica Foundation Challenge: Photonic Quantum Computing and Phase-Sensing Using Ultralow-Loss Silicon Nitride Integrated Circuits

Literature review and background: Exploiting the quantum superposition, quantum information processing (QIP) greatly complements the conventional concept of computer and information science, providing computational ability overwhelmingly exceeding state-of-the-art classical computers for specific problems. The realization of QIP relies on specific physical systems including ultracold atoms, trapped ions, superconducting circuits, and photons. Among these, photonic systems feature extremely weak interaction with environment and are free from decoherence. This unique property allows photon manipulation at room temperature.

The pursue of noisy intermediate-scale quantum (NISQ) computing is the central goal of quantum computation community [1]. The demonstration of NISQ computing requires manipulation of more than 50 qubits. For photonic systems, the continuously improving spontaneous parametric down-conversion (SPDC) light sources [2] significantly boost the number of manipulable photons. In a typical continuous-variable quantum computing setup, squeezed photons are fed into a linear optical network. One can directly sample photon distribution at the output of the network, known as "*Gaussian Boson Sampling*" (GBS). Combining with state-of-the-art optical interferometers, a large-scale experimental GBS has been reported in 2020, showing evidence for quantum computational advantages [3]. Recently up to 255 photon-click events have been observed [4]. Equally important effort has been made on a hybrid photonic system with 216 modes [5].

Interestingly, GBS is linked to several potential applications such as quantum chemistry [6], graphic optimization [7], and quantum machine learning [8]. In these applications, a programmable optical network is required. Recently, a GBS-based NISQ device has been reported that can solve graph problems [9], paving a way towards testing real-world problems. However, the programmability is still limited, since only the squeezing parameters and the phases of the input states are controlled by changing the pump power and stretching the fibers. In fact, while advanced optical coating offers free-space optics with ultralow loss and complex functions, almost all the reported large-scale photonic quantum systems are realized with bulky, free-space and fiber elements on optical tables.

In addition, there has been equal endeavor on developing quantum sensors using photons, critical to metrology applications and precision measurement. Classical interferometry is limited by photon shot noise, following the quantum noise limit (QNL) of $1/\sqrt{N}$ with N being the photon number. Increasing signal-to-noise ratio within the QNL typically requires high optical power or long measurement time. On the other hand, introducing squeezed light into the interferometer's dark port can surpass the QNL and achieve Heisenberg scaling of $1/N$ sensitivity [10-12]. Progress has been achieved in designing squeezed light sources and applying them in gravitational wave detection, which ultimately provides quantum-enhanced sensitivity exceeding 2 dB [13,14]. The advantages of squeezed light have also been shown in distributed phase sensing [15], biological sensing [16], and microscopy [17].

Compared to bulky, table-top optical systems, *integrated photonic chip devices* provide a robust way to perform versatile quantum tasks within a much smaller footprint. In the past two decades, *integrated photonics* has evolved into a mature technology enabling the generation, modulation, and detection of optical signals on-chip. Devices have already been transferred from academic research to high-volume commercial deployment in datacenter interconnects.

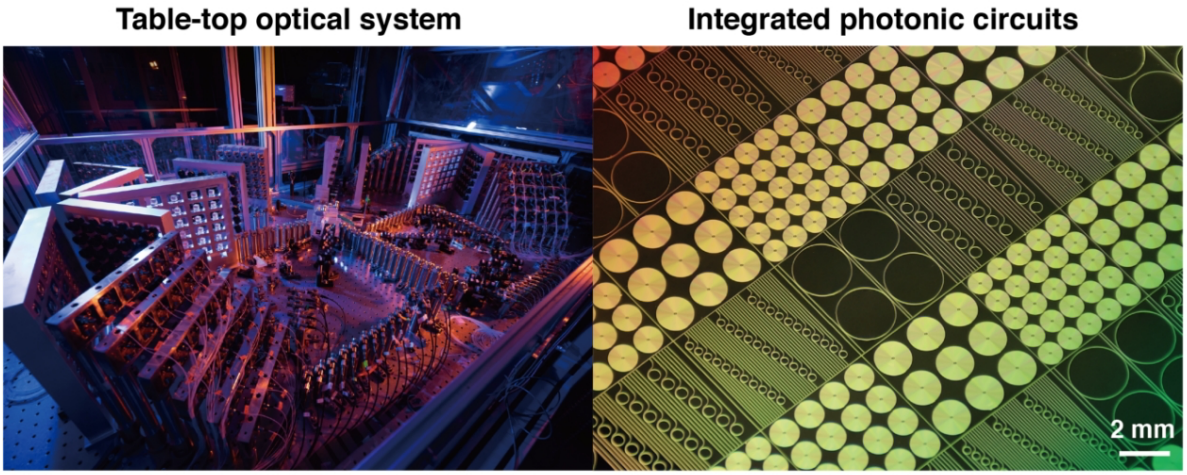

Figure 1. Comparison of a meter-scale table-top optical systems (source: courtesy of Prof. Chaoyang Lu, USTC) and millimeter-scale chips containing complex photonic integrated circuits.

Using CMOS fabrication technology to create *photonic integrated circuits* (PIC), today it is possible to combine narrow-linewidth pump lasers, modulators, nonlinear frequency converters and large-scale programmable circuits on the same chip via heterogeneous integration [18]. This technology has been driving not only the progress of linear and nonlinear optics, but also a comprehensive exploration of quantum computing and sensing applications. For example, with PIC, one can also generate the Gottesman-Kitaev-Preskill (GKP) code [19] that can be used for fault-tolerant quantum computation [20]. An integrated Mach–Zehnder interferometers (MZI) enables phase-variant detection by converting phase variations to amplitude variations. The integration of squeezed light sources using integrated nonlinear microresonators with MZI-based phase sensors has the potential to revolutionize quantum sensing by replacing expensive elements commonly used in table-top setups.

Problem statement: In the last decade, based on PIC, multiple works concerning QIP have been carried out, including high-dimensional quantum state manipulation [21] and chip-to-chip quantum teleportation [22]. For two-level systems, a qubit can be realized in the propagation path of a single photon and freely manipulated with an MZI. On-chip nonlinearity further extends the toolbox for photon manipulation. Enhanced by a high-*Q* microresonator, optical nonlinearities can provide an appealing solution to construct high-quality single-photon sources [23] and to implement deterministic quantum gates between photons [24]. Therefore, integrated photonic systems have the potential to execute complicated qubit operation at room temperature. Besides, the photon path state is not limited to two-dimensional Hilbert space. High-dimensional quantum states can be conveniently generated and manipulated within programmable PIC, representing an ideal workhorse for Bell test and quantum protocols concerning high-dimensional entanglement states.

In all examples mentioned above, as well as others, programmable, ultralow-loss, heterogeneous PIC is the foundation. Previously, extensive QIP have been performed on the silicon-on-insulator (SOI) platform [25]. However, due to the high optical loss in SOI waveguides (>1 dB/cm), the number of useful qubits – inversely proportional to the linear optical loss – is limited to only a few [26]. Therefore, these SOI-based chips cannot prove quantum advantages over classical methods, which would require tens of useful qubits.

Therefore, optical loss reduction in PIC is critical. Lower loss means higher efficiency to generate exotic quantum light sources and more freedoms to perform sophisticated operation. To build integrated quantum PIC featuring sufficient number of qubits, programmability, and – particularly – ultralow loss, silicon nitride (Si_3N_4) is the material of choice [27, 28]. The 5-eV bandgap of Si_3N_4 makes it transparent from ultraviolet to mid-infrared, and immune to two-photon absorption in the telecommunication band. Meanwhile, Si_3N_4 has a dominant Kerr nonlinearity but negligible Raman and Brillouin nonlinearities (which often add excessive

noises). In addition, with advanced CMOS fabrication techniques, linear optical loss down to 1 dB/m or even lower has been only achieved in Si_3N_4 among all integrated platforms [29]. All these advantages have triggered the rapid development of Si_3N_4 integrated photonics [30], and have enabled key advances such as the generation of frequency combs [31], supercontinua [32], and quantum light sources [33].

In addition, active functions such as light sources and optical phase tuners can be naturally added to Si_3N_4 PIC via heterogeneous integration, enabling hybrid quantum systems [34]. The light sources and phase control endow programmability and reconfigurability for universal algorithms. The light source can be III-V quantum dots or color centers added on Si_3N_4 via wafer-bonding or transfer [35]. The phase tuners can be $LiNbO_3$ electro-optic modulators [36] or aluminum-nitride MEMS actuators [37]. Nearly all these key techniques to create hybrid quantum chips are being developed worldwide, as well as in my research group.

Objective and work plan: Here we aim to develop heterogeneous, programmable, ultralow-loss Si_3N_4 PIC for photonic quantum computing architectures and squeezed-light-based sensors with sensitivity beyond the QNL. In fact, high-*Q* Si_3N_4 microresonators and spiral waveguides have already demonstrated remarkable efficiency to generate entangled photon pairs and squeezed light [38-40]. By leveraging the ultralow loss and Kerr nonlinearity, one can employ the spontaneous four-wave mixing (SFWM) to generate high-rate photon pairs and pure squeezed light. Besides, high-*Q* microresonators enable operation at optical power level compatible with commercial chip-scale diode lasers. In details, we will do the following:

1. We will develop a foundry-level Si_3N_4 PIC fabrication technology based on 6- or 8-inch wafers. We target to reach 0.5 dB/m optical loss (physical length). In fact, we have already made preliminary results of Si_3N_4 PIC with 2 dB/m loss [41].
2. We will develop a quantum photonic design kit (QPDK) for Si_3N_4 PIC, allowing automatic generation of chip layout. We will also improve the fiber-to-chip coupling efficiency, with targeted insertion loss below 1 dB per facet.
3. We will investigate entangled quantum light sources based on zero-dispersion waveguides for high-rate photon pair generation, which is suitable for integrated quantum key distribution. For spirals, pulsed laser pumps will be adopted. Meanwhile, the waveguides geometric parameters will be optimized to eliminate spectral correlation, a basic requirement for multi-photon entanglement and GBS.
4. After a few iterations of simulation, design, fabrication and characterization, we will finally obtain the proper Si_3N_4 quantum chips for experiments.
5. We will combine the entangled photon-pair sources and passive elements on a monolithic chip, to generate GHZ state consisting at least 6 photons. Then we will construct programmable quantum PIC, supporting programmable GBS of more than 30 photons.
6. We will use a SFWM technique, MZI filters and high-*Q* microresonators to convert the pump laser into single-mode squeezed light of synchronized phase, enabling quantum interference. The squeezing parameter will be optimized to above 10 dB.
7. For quantum phase sensing with squeezed light, we will use a low-noise pump laser and a homodyne measurement setup. A portion of the pump light is split to create a local oscillator (LO) laser. The LO laser acts as a reference and undergoes phase sweeping using a phase shifter. The squeezed light interferes with the LO laser, and the degree of squeezing is measured by the fluctuations in the photocurrent difference in the RF domain. We will compare our results with existing techniques and validate the sensing performance.
8. Finally, we will also develop heterogeneous integration of other materials and active functions on Si_3N_4. For example, a low-noise pump can be made by integrating laser diodes with high-*Q* Si_3N_4 microresonators using laser self-injection locking [35, 42]. The MZI can be implemented by heterogeneous integration of $LiNbO_3$ electro-optic modulators [38] or aluminum nitride piezoelectric modulators [39] on Si_3N_4 waveguides.

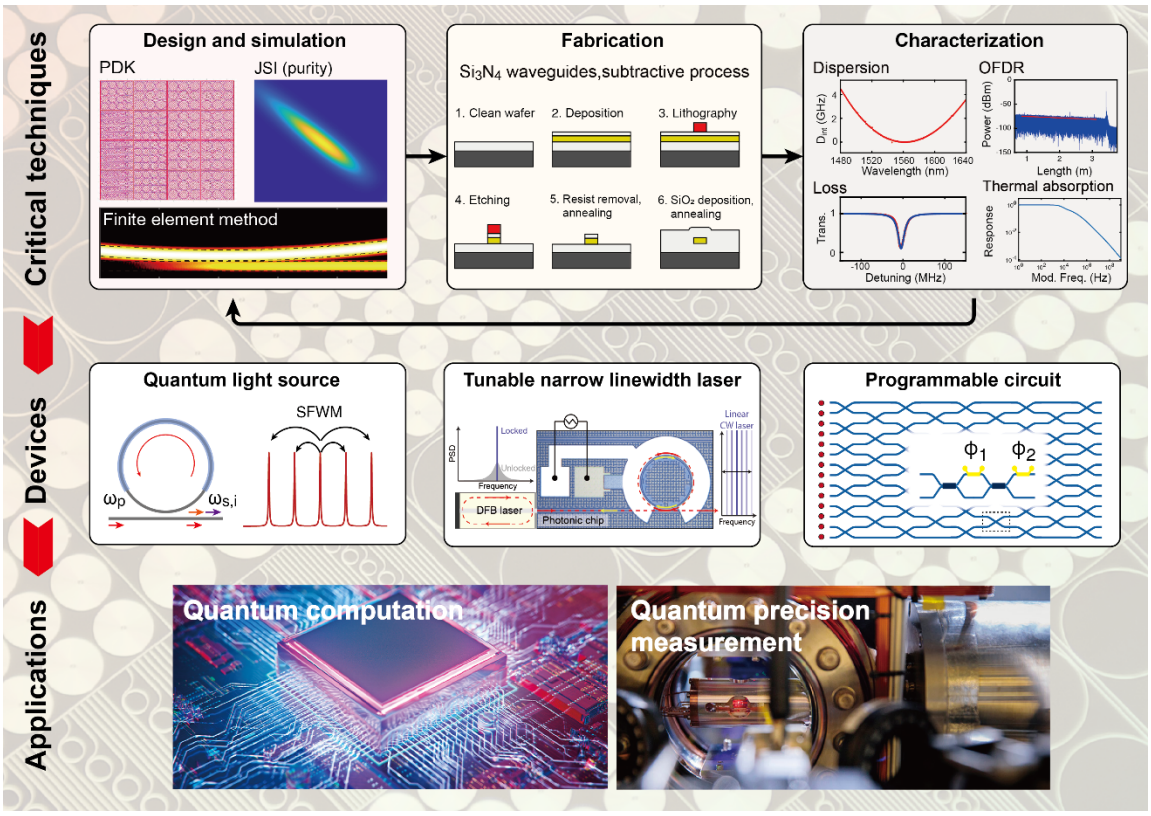

Figure 2. Summary of the work plan and outcomes of this proposal.

Outcome: By the end of the project, we expect the following outcomes:

1. An advanced ultralow-loss Si_3N_4 PIC fabrication technology based on 6- or 8-inch wafers will be established. Heterogeneous integration of III-V semiconductors, silicon, $LiNbO_3$, aluminum nitride, and lead zirconate titanate (PZT) on Si_3N_4 PIC will be established.
2. A Si_3N_4 QPDK will be developed for automatic generation of chip layout including inverse tapers, grating couplers, microresonators, spirals, MZI, multimode interferometers (MMI), arrayed waveguide gratings (AWG), heaters, modulators, etc.
3. Comprehensive numerical simulation tools and models will be established, allowing simulation and optimization of insertion loss, waveguide dispersion, optical coupling strength, modulation efficiency, mode mixing, etc.
4. A standard set of building blocks for Si_3N_4 quantum PIC will be established, including optimized microresonators for entangled photon pair and squeezed light generation with maximum fidelity and squeezing parameters, MZI for efficient filtering of the residual pump and quantum interference of squeezed light with LO laser for phase measurement, etc.
5. Finally, package and deliver few chip-scale GBS chips and phase sensors.

I believe the proposed research will have profound implications for quantum computing, sensing and precision measurement. The results and findings will be shared through peer-reviewed publications and conference presentations. We will also patent particular inventions and techniques arising from this research, and pursue possibilities to commercialization.

Impact: The endless quest for transmitting light with minimum loss has shaped our information society. Charles Kao identified and solved the major reasons of optical loss in glass, thus laid the foundation to optical fibers as we all know – with 0.2 dB/km optical loss, optical fibers and amplifiers form today's global telecommunication network.

I believe our endeavor on heterogeneous ultralow-loss Si_3N_4 PIC and its applications in QIP can have a similar impact. The proposal aims to revolutionize the field of quantum computing

and sensing via integration of entangled photon pairs, squeezed light sources and linear processing units using ultralow-loss S_3N_4 PIC. This integration promises to enable the development of practical quantum processors and highly sensitive optical sensors, addressing the limitations associated with complex and bulky experimental setups.

This research will open new avenues for QIP and precision metrology. For example, semiconductor chip lasers integrated with high-*Q* Si_3N_4 microresonators can achieve ultralow phase noise on par with fiber lasers [47], a key component for coherent LiDAR and optical atomic clocks. Complex photonic linear network made of Si_3N_4 PIC can be used for photonic neuromorphic computing [48]. Combining integrated Si_3N_4 photonics and ultrafast electron microscopy, continuous-beam electron phase modulation [49] and electron-photon pair generation [50] have been realized. The development of Si_3N_4 quantum PIC has the potential to drive quantum information science and substantially contribute to various domains.

References:

1. J. Preskill. Quantum 2, 79 (2018).
2. H.-S. Zhong *et al*. Phys. Rev. Lett. 121, 250505 (2018).
3. H.-S. Zhong *et al*. Science 370, 1460 (2020).
4. Y.-H. Deng *et al*. arXiv: 2304.12240 (2023).
5. L. S. Madsen *et al*. Nature 606, 75 (2022).
6. J. Huh *et al*. Nat. Photon. 9, 615 (2015).
7. J. M. Arrazola and T. R. Bromley. Phys. Rev. Lett. 121, 030503 (2018).
8. M. Schuld and N. Killoran. Phys. Rev. Lett. 122, 040504 (2019).
9. Y.-H. Deng *et al*. Phys. Rev. Lett. 130, 190601 (2023).
10. U. L. Andersen *et al*. Phys. Scr. 91, 053001 (2016).
11. V. Giovannetti, S. Lloyd, and L. Maccone. Science 306, 1330 (2004).
12. V. Giovannetti, S. Lloyd, and L. Maccone. Phys. Rev. Lett. 96, 010401 (2006).
13. K. Goda *et al*. Nat. Phys. 4, 472 (2008).
14. J. Aasi *et al*. Nat. Photon. 7, 613 (2013).
15. X. Guo *et al*. Nat. Phys. 16, 281 (2020).
16. M. A. Taylor *et al*. Nat. Photon. 7, 229 (2013)
17. C. A. Casacio *et al*. Nature 594, 201 (2021).
18. T. Komljenovic *et al*. J. Light. Technol. 34, 20 (2016).
19. D. Gottesman, A. Kitaev and J. Preskill. Phys. Rev. A 64, 012310 (2001).
20. D. Su, C. R. Myers and K. K. Sabapathy. Phys. Rev. A 100, 052301 (2019).
21. J. Wang *et al*. Science 360, 285 (2018).
22. D. Llewellyn *et al*. Nat. Phys. 16, 148 (2020).
23. J. Lu *et al*. Optica 7, 1654 (2020).
24. M. Li *et al*. Phys. Rev. Appl. 13, 044013 (2020).
25. J. Wang *et al*. Nat. Photon. 14, 273 (2020).
26. X. Qiang *et al*. Nat. Photon. 12, 534 (2018).
27. C. Xiang *et al*. Photon. Res. 10, A82 (2022).
28. E. Pelucchi *et al*. Nat. Rev. Phys. 4, 194 (2022).
29. J. Liu *et al*. Nat. Commun. 12, 2236 (2021).
30. D. J. Moss *et al*. Nat. Photon. 7, 597 (2013).
31. T. J. Kippenberg *et al*. Science 361, eaan8083 (2018).
32. A. L. Gaeta *et al*. Nat. Photon. 13, 158 (2019).
33. M. Kues *et al*. Nat. Photon. 13, 170 (2019).
34. A. W. Elshaari *et al*. Nat. Photon. 14, 285 (2020).
35. C. Xiang *et al*. Science 373, 99 (2021).
36. M. Churaev *et al*. Nat. Commun. 14, 3499 (2023).
37. J. Liu *et al*. Nature 583, 385 (2020).
38. A. Dutt *et al*. Phys. Rev. Appl. 3, 044005 (2015).
39. V. D. Vaidya *et al*. Sci. Adv. 6, eaba9186 (2020).
40. Y. Zhang *et al*. Nat. Commun. 12, 2233 (2021).
41. Z. Ye *et al*. Photon. Res. 11. 558 (2023).
42. N. M. Kondratiev *et al*. Front. Phys. 18, 21305 (2023).
43. G. Lihachev *et al*. Nat. Commun. 13, 3522 (2022).
44. J. Feldmann *et al*. Nature 589, 52 (2021).
45. J.-W. Henke *et al*. Nature 600, 653 (2021).
46. A. Feist *et al*. Science 377, 777 (2022)

Executive Summary

Next-Generation High Throughput Plasmonic Nanotweezers for Nanoplastics Analysis

The contamination of the environment by plastic waste has become a pressing global challenge, with an alarming projection that there will be more plastics in the ocean than fishes by 2050. Understanding the properties and potential health impacts of plastic nanomaterials, specifically nanoplastics (1 nm to 100 nm), is crucial. However, analyzing nanoplastics remains a significant challenge due to their small size. Current analytical tools are limited, hindering our comprehensive understanding of nanoplastic exposure and its consequences.
To address this critical need, this research project aims to develop a groundbreaking technology for the rapid characterization of nanoplastics with single-particle resolution. We propose a high throughput plasmonic nanotweezers approach, merging plasmon-nano-optics and microfluidics, to enable stable trapping and enhanced Raman spectroscopy of individual nanoplastic particles.

Our research objectives are to develop plasmonic optical nanotweezers for high throughput nano-optical trapping (within seconds) and enhanced Raman spectroscopy of single nanoplastics. By controlling the nanogap spacing of the central plasmonic cavities, we will stably trap and analyze a wide range of nanoplastic sizes, from 5 nm to 100 nm.
We will also utilize engineered and natural nanoplastics to experimentally validate the technology's ability to trap and perform enhanced Raman nanoplastics at various concentrations. By analyzing the enhanced Raman signals, we will determine the chemical composition of trapped nanoplastics.

The completion of this research will yield a transformative technology that overcomes the limitations of conventional optical tweezers and current nanoplastic analysis methods. It will allow for rapid and precise characterization of nanoplastics, enabling more comprehensive assessments of nanoplastic pollution levels and potential impacts on ecosystems and human health. The research findings will be shared through scientific publications in leading journals and conferences, facilitating knowledge dissemination, and encouraging the adoption of this technology by other researchers. Moreover, the technology will help offer new insights into nanoplastic degradation and breakdown processes, contributing to effective strategies and policies to combat plastic contamination.

The potential impacts of this research are significant, and they include:
Environmental monitoring: The technology could be adapted to detect nanoplastics at extremely low concentrations, making it ideal for identifying leaching from infant plastic feeding bottles and evaluating suitable materials. It will aid in assessing nanoplastic pollution in water bodies, and air, supporting targeted cleanup efforts.
Industry motivation: The accurate measurement of nanoplastic pollution will incentivize industries to develop sustainable alternatives, fostering innovation in eco-friendly materials and packaging solutions.
Ecological consequences: The high-throughput detection technology can help assess the ecological impact of nanoplastic pollution, helping conservationists and biologists design appropriate conservation strategies.
In conclusion, our research project holds significant promise for advancing nanoplastic analysis, addressing an important timely grand challenge, and contributing significantly to global efforts to combat plastic pollution and safeguard the health of our planet and its inhabitants.

Next generation high throughput plasmonic nanotweezers for nanoplastics analysis

1. Literature Review:

One of the most pressing challenges facing our global society is the contamination of our environment by plastic wastes. Currently, about 20 million metric tons of plastic wastes are discharged in the ocean annually. Alarmingly, if the current rate of plastic contamination continues, it is projected that by 2050, there will be more plastics than fishes in the ocean by weight [1]. To mitigate this growing concern, urgent action is required to identify efficient strategies and implement new policies aimed at reducing plastic contamination.

Furthermore, it is of immense importance to characterize plastic nanomaterials to better understand their properties and their potential impact on human health. Plastic wastes range from macroplastics to microplastics and nanoplastics (Fig. 1). Microplastics range in size from several mm to about 1 um. In comparison, nanoplastics are considerably smaller, measuring from 1 nm to 100 nm. Plastics are ubiquitous and have been found to leach from diverse sources including coffee cups and infant feeding bottles during sterilization, leading to their consumption by infants[2]. This raises concerns about the potential health impact of these plastics on organs and human health in general.

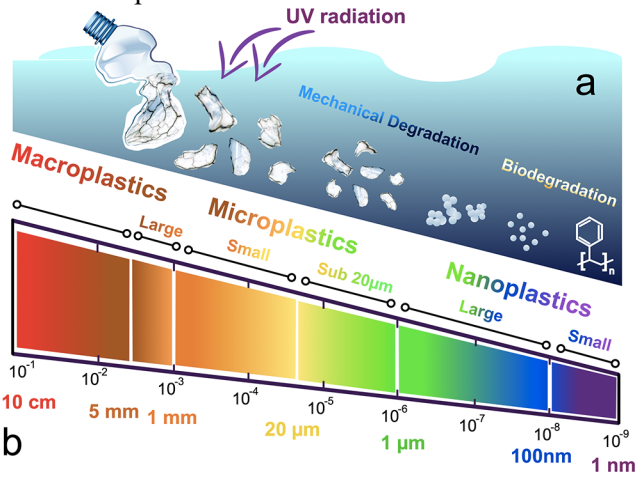

Figure 1: Degradation process and size-based definition of plastics. Small nanoplastics are extremely difficult to manipulate and analyse. (Adapted from ref. 10)

Over the years, most studies have focused on understanding the impact of microplastics, while research on nanoplastics and their health impacts remains limited.[3,4] The primary reason is due to the considerably smaller size of nanoplastics, which makes them challenging to manipulate and characterize using currently available tools. Analyzing nanoplastics at very low concentrations, such as those found from the leaching of infant feeding bottles, is particularly crucial. Assessing the impacts of nanoplastics on environmental systems is fundamentally different from assessing the impacts of macro- or microplastics, and current methodologies for measuring particulate plastic in environmental samples mostly focus on microplastics. On the other hand, nanoplastics pose serious health concerns because particles that small are prone to uptake by cells[5] and able to cross biological barriers such as human placenta [6].

Current analytical tools have limitations in measuring nanoplastics in samples[7]. While electron microscopy can characterize the size of nanoplastics, it does not provide information on their chemical composition. On the other hand, Fourier Transform Infrared (FTIR) spectrometry can provide chemical information but it is only limited to particles greater than 10 um in size. Consequently, the scientific community is far from fully understanding nanoplastics exposure in most environments due to these analytical limitations. Urgent efforts are needed to develop methodologies to accurately measure and characterize nanoplastics, allowing us to assess their impact more comprehensively. Only through a thorough understanding of nanoplastics and their potential consequences can we develop effective strategies and policies to mitigate plastic contamination and safeguard the health of our planet and its inhabitants.

Towards meeting the need for single plastic analysis, the use of optical tweezers for trapping single plastics and performing Raman analysis, a technique also referred to as laser trapping Raman spectroscopy (LTRS) [8–10] has been explored and is increasingly gaining attention. Raman analysis is a label-free technique for analyzing materials based on the inelastic scattering of light by molecules. The Raman scattering spectrum directly depends on the molecules that the material is composed of, and thus Raman scattering can provide information about the chemical composition of plastics. LTRS is a promising approach for providing information on the global biomolecular composition of single

particles in solution non- destructively and as a result can help unravel the chemical heterogeneity of plastic particles. To acquire the Raman signals nondestructively, it is important to trap the particles in solution so that they do not escape the interrogation area. In LTRS, this is performed using an optical tweezer. Optical tweezer[11,12] recently recognized with a 2018 Physics Nobel Prize, uses a tightly focused laser beam to stably trap micron-scale and sub-micron particles in solutions such as microplastics. Unfortunately, due to the diffraction limit that precludes focusing light to nanoscale volumes, optical tweezers cannot be used to trap nanoplastics below 100 nm in size. To date, there has not been any known experimental demonstration of optical trapping of single nanoplastics below 50 nm. Attempts to trap nanoscale particles require substantial laser powers that causes photo-induced damage, a process also referred to as opticution[11]. Another limitation of LTRS is that the spontaneous Raman signal is not enhanced, and it is usually a very weak signal, thus necessitating long exposure times to collect the Raman signals. In summary, LTRS are lacking in their application for nondestructive analysis of single nanoplastics because of the inability to stably trap nanoscale plastics, and the inability to provide enhancement of the weak spontaneous Raman signals. Hence there is a need for another innovative technology that overcomes the limitations of existing optical tweezers, by enabling to stably trap nanoplastics, while also dramatically boosting the Raman signals from single nanoplastics.

To overcome the diffraction- limited issue of optical tweezers, the use of plasmonic nanostructures[13] to confine light to nanoscale volumes well below the diffraction limit to generate strong optical forces for stably trapping nanoscale objects have also generated substantial interests. A plasmonic cavity can confine light to nanoscale spots and increase the light intensity by 700 times or more as shown in the preliminary design of Fig. 2f, permitting the use of low optical powers for particle trapping. This plasmonic field enhancement also provides strong excitation and emission of Raman signals enabling the enhancement of the Raman scattering of even single molecules[14]. Thus, a plasmonic nanostructure could be harnessed to simultaneously perform stable nano-optical trapping in solution combined with Raman enhancement of trapped nanoplastics in one platform. However, a long-standing issue that has limited the applications of plasmonic tweezers for nanoplastics analysis is the low throughput. The existing plasmonic tweezers rely on slow Brownian diffusion to deliver particles to the region of highest plasmonic field enhancement, a process that is non-deterministic and could take anywhere from several tens of minutes to an hour before trapping can occur.

I have recently addressed this long-standing challenge for the first time by developing an original geometry-induced electrohydrodynamic tweezer (GET) that places single nanoscale objects in parallel near plasmonic cavities within seconds thus enabling instantaneous plasmonic-enhanced optical trapping (in less than one second) when any GET site is illuminated with a laser beam without heat generation as depicted in Fig. 2. A manuscript describing preliminary data on this breakthrough achievement is in the process of being accepted in Nature Communications (pending minor editorial revisions request) and it is available on arXiv[15].

2. Research Objectives:

The objective of this grand challenge proposal is to develop a high throughput plasmonic nanotweezer technology to stably trap and characterize nanoplastics with single particle resolution using enhanced Raman spectroscopy, a capability that has remained elusive.

To achieve high throughput plasmon-enhanced optical trapping of nanoplastics, we will investigate a plasmonic optical nanotweezers approach that leverages our GET platform to enable parallel placement and trapping of single nanoplastics within seconds. GET traps are scalable and the number of single-particle GET traps depends on the number of trap sites defined on-chip via lithographic fabrication and can range from thousands to millions as desired to enable high throughput parallelized trapping of thousands or millions of single nanoplastics within seconds. By controlling the nanogap spacing of the central plasmonic cavities, we will control the confinement of the enhanced light field and achieve the trapping of nanoplastics across a wide range of sizes from 5 nm to 100 nm.

The proposed high throughput plasmonic nanotweezer approach will combine the advantages of optical tweezers and plasmonic nanostructures to overcome existing limitations, allowing for stable trapping and Raman signal enhancement of single nanoplastics. Through the proposed highly innovative technology, we aim to demonstrate the rapid characterization of nanoplastics at the single particle level paving the way to advancing our understanding of nanoplastic contaminants.

These objectives will be met through the following research tasks.

3. Outline of Research Tasks:

Task 1: Development of optical nanotweezers for high throughput nano-optical trapping and enhanced Raman spectroscopy of single nanoplastics:

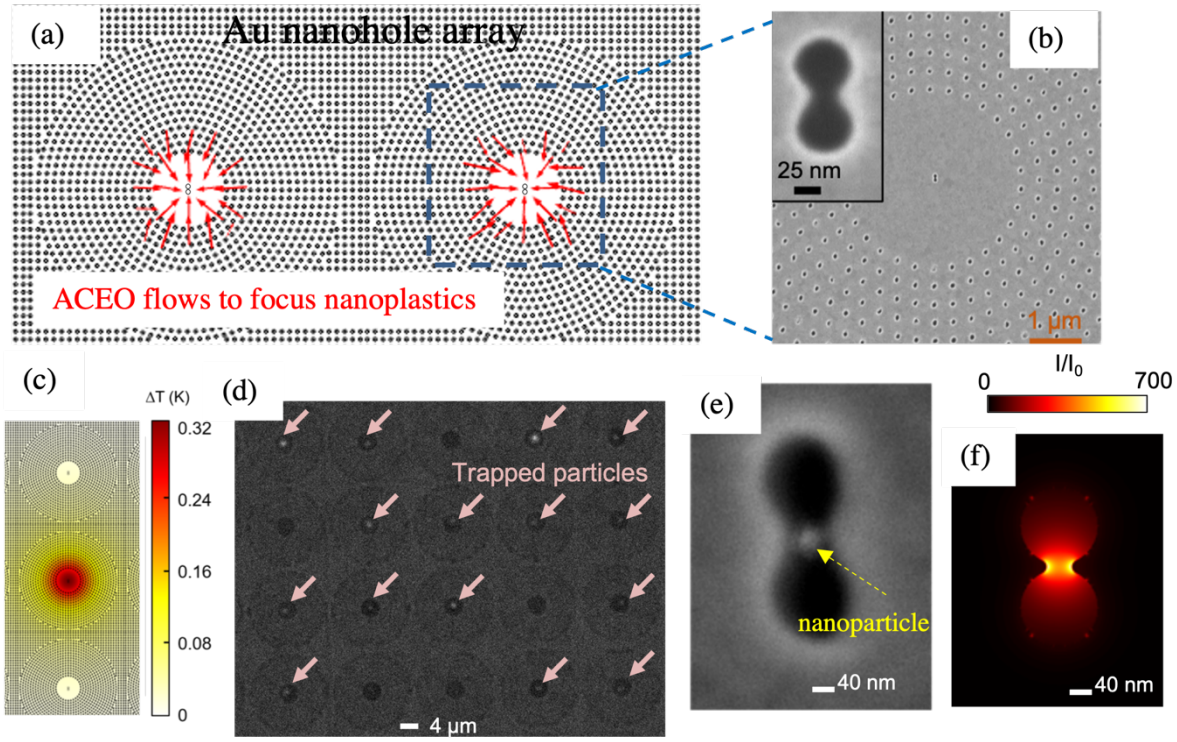

Figure 2: Preliminary data. Geometry-induced Electrohydrodynamic Tweezer (GET) for scalable placement of single nanoplastics to plasmonic cavities for Raman enhancement. (a) AC electro-osmotic flow is induced for focusing single particles in parallel near each plasmonic cavity. Figure shows only two such traps. Tens of thousands of such GET trap sites can be readily fabricated on-chip. (b) SEM image showing plasmonic aperture cavity where trapping and Raman enhancement occurs. (c) simulation showing negligible temperature rise achieved by placing the structured gold film on a high thermal conductivity substrate. (d) optical images demonstrating the trapping of particles in parallel near plasmonic cavities within seconds using GET. (e) SEM image showing a single nanoparticle placed at the center of a plasmonic cavity with 35 nm gap within seconds. (f) simulation showing enhancement of local light intensity using a plasmonic cavity. Trapping and Raman enhancement occurs at the high intensity region.

In this project, we will investigate a high throughput plasmonic optical nanotweezers approach that can confine light to the nanoscale well below the diffraction limit and enhance the Raman signal of trapped nanoplastics at the single particle level. To achieve rapid trapping with high throughput, we will build on our recent development of geometry-induced electrohydrodynamic tweezers (GET)[15]. In the GET platform, we introduce an array of gold nanoholes with a microscale void region. Each void region contains a plasmonic cavity at the center where nanoscale optical trapping of single nanoplastics and enhancement of Raman signal is achieved. The application of an a.c. field will result in a.c. electro-osmotic flows that focus single nanoplastics at the center of the void regions in parallel within seconds as depicted in the preliminary data of Figure 2d. The nanoplastics can be released by turning OFF the a.c. field. Since the nanoplastics are already placed at the center of the void regions in parallel, which also corresponds to the location of the plasmonic cavities, the illumination of any of the plasmonic cavities at the void regions results in instantaneous plasmonic-enhanced trapping of the nanoplastic at the illuminated plasmonic hotspot. Preliminary data in Figure 2e shows that a single particle can be precisely placed at the highest field enhancement region (i.e. nanogap spacing) of the plasmonic cavity where the highest Raman enhancement can be achieved. The preliminary design has a local light intensity enhancement of approximately 700 times.

Task 2: Experimentally demonstrate the high throughput plasmon-enhanced trapping and Raman spectroscopy of nanoplastics and establish the size limits and concentrations that can be characterized:

We will conduct experiments to demonstrate the ability to rapidly trap and characterize nanoplastics using Raman spectroscopy with the proposed high throughput plasmonic nanotweezers. The fabricated sample will be packaged into a PDMS-based microfluidic chip for efficient delivery of the sample solution containing the nanoplastics into the chip. To characterize, the device, we will perform experiments using both engineered nanoplastics comprising of polystyrene and PMMA nanoparticles with known size as well as nanoplastics derived from natural plastic materials. Engineered nanoplastics such as polystyrene and Poly(methyl methacrylate) (PMMA) beads of varying sizes ranging from 5 nm to 100 nm will be purchased from commercial vendors such as Thermofisher. To prepare the natural nanoplastics from different plastic materials, we will start with cm-scale plastic fragments extracted from a plastic bottle (Polyethylene terephthalate, PET), plastic cup (PMMA), and credit card (Polyvinyl chloride, PVC). The plastic will be rubbed against a grinding stone and then the grinding stone will be repeatedly rinsed with denoised water. The process will be repeated for about three times. The solution will be passed through a filter with a 100 nm cut-off to exclude bigger particles such as microplastics. We will introduce the sample solutions containing the nanoplastics into the plasmonic nanotweezer device. The plasmonic nanoantenna gap spacings will be tuned to enable the trapping of nanoplastic samples of varying sizes. Subsequently, we will trap the nanoplastics at the plasmonic hotspots and collect the enhanced Raman signals at each trapping site. Chemical component analysis[16] will be performed to analyze the data and determine the chemical constituents corresponding the Raman peaks. We will perform experiments to determine the limits on the concentration of nanoplastics that can be trapped and analyzed using the proposed high throughput plasmonic nanotweezer technology. The concentration of nanoplastics will be varied from 10e2 particles per ml to 10e10 particles per ml.

4. Outcomes:

Upon completion, the proposed research project will yield a groundbreaking technology, combining plasmon-nano-optics and microfluidics, for rapid characterization of nanoplastics below 100 nm. This innovative technology overcomes the limitations of conventional optical tweezers, enabling high throughput analysis and reducing analysis time by three orders of magnitude compared to traditional LTRS systems that rely on slow Brownian diffusion for particle trapping and lack Raman enhancement. The research findings will be disseminated through leading peer-reviewed scientific journals and conference presentations, making the technology accessible to other researchers for nanoplastic characterization. This advancement will also provide a new tool for studying the degradation of nanoplastics in the presence of chemical enzymes and understanding the breakdown of microplastics into nanoplastics. The developed technology will address a critical gap in nanoplastic research by offering reliable accounts of nanoplastic concentrations in various environmental settings. This knowledge will be invaluable in assessing nanoplastic pollution levels and its potential impacts on ecosystems and human health. In summary, the successful completion of this research project will lead to a transformative technology that enables rapid and precise analysis of nanoplastics, contributing significantly to the understanding and management of nanoplastic pollution in diverse environments.

5. Impacts:

The technology proposed in this research can efficiently trap and characterize nanoplastics at extremely low concentrations, making it ideal for detecting nanoplastics leaching from infant feeding bottles and identifying suitable materials. Moreover, it enables the selection of specific nanoplastics for further analysis, offering new opportunities to study their impact on human health and the environment. Additionally, the technology can shed light on the degradation of microplastics into nanoplastics, which remains an open question. The ability to analyze nanoplastics with single particle resolution enhances environmental monitoring efforts. Researchers and environmental agencies can utilize this technology to assess nanoplastic pollution in various ecosystems, leading to targeted and efficient cleanup efforts. This technology could also incentivize industries to develop more sustainable alternatives, knowing that nanoplastic pollution can now be accurately measured. This, in turn, may drive innovation in eco-friendly materials and packaging solutions. Finally, as nanoplastics can harm marine life and terrestrial

ecosystems, the proposed high-throughput analysis technology can aid in assessing the ecological consequences of nanoplastic pollution. Overall, the technology has the potential to significantly improve our understanding of nanoplastic pollution and its effects on the environment and human health.

6. References:

1. More Plastic Than Fish in the Oceans - Plastic Soup Foundation. Available at: https://www.plasticsoupfoundation.org/en/plastic-problem/plastic-soup/more-plastic-than-fish/. (Accessed: 22nd July 2023)
2. Li, D. *et al.* Microplastic release from the degradation of polypropylene feeding bottles during infant formula preparation. *Nat. Food 2020 111* **1**, 746–754 (2020).
3. Gigault, J. *et al.* Nanoplastics are neither microplastics nor engineered nanoparticles. *Nat. Nanotechnol. 2021 165* **16**, 501–507 (2021).
4. Allen, D. *et al.* Microplastics and nanoplastics in the marine-atmosphere environment. *Nat. Rev. Earth Environ. 2022 36* **3**, 393–405 (2022).
5. Geiser, M. *et al.* Ultrafine Particles Cross Cellular Membranes by Nonphagocytic Mechanisms in Lungs and in Cultured Cells. *Environ. Health Perspect.* **113**, 1555–1560 (2005).
6. Wick, P. *et al.* Barrier Capacity of Human Placenta for Nanosized Materials. *Environ. Health Perspect.* **118**, 432–436 (2010).
7. Ivleva, N. P. Chemical Analysis of Microplastics and Nanoplastics: Challenges, Advanced Methods, and Perspectives. *Chem. Rev.* **121**, 11886–11936 (2021).
8. Zhang, S., Sun, Y., Liu, B. & Li, R. Full size microplastics in crab and fish collected from the mangrove wetland of Beibu Gulf: Evidences from Raman Tweezers (1–20 μm) and spectroscopy (20–5000 μm). *Sci. Total Environ.* **759**, 143504 (2021).
9. Schwaferts, C. *et al.* Nanoplastic Analysis by Online Coupling of Raman Microscopy and Field-Flow Fractionation Enabled by Optical Tweezers. *Anal. Chem.* **92**, 5813–5820 (2020).
10. Gillibert, R. *et al.* Raman tweezers for small microplastics and nanoplastics identification in seawater. *Environ. Sci. Technol.* **53**, 9003–9013 (2019).
11. Ashkin, A., Dziedzic, J. M., Bjorkholm, J. E. & Chu, S. Observation of a single-beam gradient force optical trap for dielectric particles. *Opt. Lett.* **11**, 288 (1986).
12. Neuman, K. C. & Block, S. M. Optical trapping. *Rev. Sci. Instrum.* **75**, 2787 (2004).
13. Schuller, J. A. *et al.* Plasmonics for extreme light concentration and manipulation. *Nature Materials* **9**, 193–204 (2010).
14. Le Ru, E. C. & Etchegoin, P. G. Single-molecule surface-enhanced raman spectroscopy. *Annual Review of Physical Chemistry* **63**, 65–87 (2012).
15. Hong, C. & Ndukaife, J. C. Scalable trapping of single nanosized extracellular vesicles using plasmonics. (2023).
16. Kuzmin, A. N., Pliss, A. & Kachynski, A. V. Biomolecular component analysis of cultured cell nucleoli by Raman microspectrometry. *J. Raman Spectrosc.* **44**, 198–204 (2013).

Meta-optics for high-dimensional coherent detections in optical communications

Traditional incoherent modulation techniques face limitations due to the dispersion of optical fibers, which hinders bandwidth expansion in optical communications. To overcome this bottleneck, people seek to harness the two critical advantages of light: coherence and multiple degrees of freedom. Coherent optical communication enables the transmission of multiple bits per symbol, significantly increasing data capacity. At the same time, mode division multiplexing allows independent data streams to be transmitted through different spatial modes simultaneously, further boosting bandwidth. However, there remain many challenges to the large-scale applications of these techniques.

A key bottleneck is the precise and efficient detection and measurement techniques. Such measurements are highly challenging because they require detection of not only amplitude but also phase and coherence of light across many modes. The number of unknown variables scales quadratically with the mode number. Conventional detection methods, such as direct heterodyne detection, are either unsuitable or limited to very few degrees of freedom. Moreover, the typically used reconfigurable systems are bulky and slow, suffering from poor scalability. New paradigms of coherent measurement devices are thus highly desirable to overcome these challenges and unleash the full potential of these technologies.

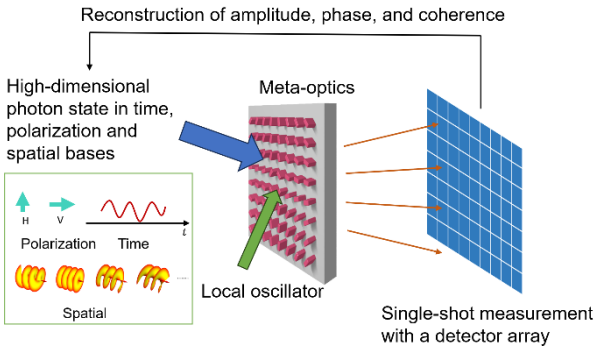

This proposal aims to develop inverse-designed nanostructured meta-optics elements and systems to enable coherent, single-shot, and highly efficient measurement of high-dimensional states encoded in various degrees of freedom of classical and non-classical light in optical communication channels. Meta-optics will be used as an unconventional "camera lens" in conjunction with photodiode arrays or image sensors to achieve a massively parallel interferometric measurement at once. The project focuses on highly transmissive meta-optics designs with no moving parts that can efficiently utilize light with no extra post-selection. This approach ensures robust and scalable measurement capabilities while enabling miniaturization of the detection systems.

The key objectives of the project include the **design** and **experimental realizations** of:

- Nonlocal meta-optics structure for efficient single-shot retrieval of spatial states.
- Meta-optics for single-shot imaging-based measurement of polarization & spatial states
- Meta-optics for compressed sensing of high-dimensional states encoded in time, polarization, and spatial modes.

The project's outcomes are expected to have significant impacts on optical communication and quantum communication technologies:

- **Enhanced efficiency and scalability**: The measurement process is highly efficient and scalable by utilizing dielectric meta-optics with optimized diffraction efficiency and no moving parts. The incorporation of compressed sensing approaches further enhances scalability, making it applicable to large-scale communication networks.
- **Single-shot measurement**: The proposed meta-optics designs enable single-shot measurements, eliminating the need for post-selection and improving measurement accuracy and reliability.
- **Miniaturization**: The miniaturization potential of meta-optics elements ensures that the coherent measurement devices can be integrated into compact communication systems, reducing the overall footprint and resource requirements.
- **Straightforward extension to quantum communications**: The proposed project's advancements in coherent measurement techniques promise extensions to quantum communication technologies, enabling high-speed and secure transmission of quantum information.

Overall, the proposed project aims to revolutionize the optical and quantum communication field by developing advanced nanostructured meta-optics for coherent single-shot measurements. The project's focus on efficiency, scalability, and miniaturization will have far-reaching implications for optical communication networks and potential applications in quantum communication.

Meta-optics for high-dimensional coherent detections in optical communications

This project aims to develop nanostructured meta-optics elements and systems designed using advanced nonlocal simulation and inverse design techniques for the coherent, fast, and robust measurement of high-dimensional states encoded in various degrees of freedom of both classical and non-classical light in optical communication channels.

Background/Problem Statement

Nowadays, the demand for bandwidth in optical communication has skyrocketed due to the exponential growth of data-intensive applications such as streaming services, cloud computing, and the Internet of Things (IoT). However, the dispersion of optical fibers imposes a limitation on the bandwidth of optical communications with conventional incoherent modulation techniques. Therefore it becomes extremely essential to use the two key advantages of light, i.e., coherence and the many degrees of freedom in optical communication systems. On the one hand, coherent optical communication can enable the transmission of multiple bits per symbol, significantly increasing the data capacity. On the other hand, mode division multiplexing (MDM), which leverages the multiple spatial modes supported by optical fibers or free space, allows independent data streams to be transmitted through different modes simultaneously. A combination of coherent communication and MDM promises a drastic boost in the bandwidth of optical communication systems.

A critical bottleneck in implementing coherent MDM is the precise and efficient detection and measurement techniques. Such measurements are highly challenging because they require detection of not only amplitude but also phase and coherence of light across many modes. The number of unknown variables scales quadratically with the mode number. Conventional detection methods, such as direct detection or heterodyne detection, are either unsuitable or limited to very few degrees of freedom. Moreover, the typically used reconfigurable systems are bulky and slow, suffering from poor scalability. New paradigms of coherent measurement devices are thus highly desirable to overcome these challenges and unleash the full potential of these technologies.

Recent advances in nanotechnology are leading to transformative provides new opportunities to revolutionize the way we make coherent measurement devices for optical communication, in particular using the powerful concept of meta-optics that uses metasurfaces and metamaterials to design entirely new types of optical elements composed of subwavelength nanostructures [1]. With meta-optics, one or a few layers of tailored nano-resonators (also known as meta-atoms) offer unprecedented flexibility in controlling light in all degrees of freedom, combining high efficiency, miniaturization, stability, and scalability. Meta-optics elements are particularly suitable for manipulating classical and non-classical light in free space and across various interfaces [2], as they have the most direct access to all the internal degrees of freedom of photons, such as polarization, spatial modes, and frequency. Compared to integrated photonic circuits based on a limited number of spatial modes that are extremely difficult to scale, meta-optics enables a massively parallel approach to transforming high-dimensional quantum information encoded in different degrees of freedom. Together with advanced image sensors, meta-optics can enable fast and efficient readout of quantum information.

Meta-optics provides a new opportunity for the detection and measurement of coherent mode-division multiplexed optical signals in communication channels. Designing simple and static meta-optics elements that can be used together with an array of photodiodes or various types of image sensors for the one-shot retrieval of amplitude, phase, and coherence of optical modes will provide a solution to this challenge with unprecedented simplicity, miniaturization, robustness, and scalability.

Furthermore, such advancements will also have far-reaching implications for quantum communication. Unlike incoherent communications based on optical amplifiers and wavelength-division multiplexing, advanced techniques established for coherent optical communication and MDM are directly transplantable to quantum communications. Moreover, MDM techniques can provide higher data rates and improved noise resilience. Therefore, such newly developed meta-optics elements can also play an enabling role in implementing quantum key distribution (QKD) protocols, offering unbreakable encryption based on the fundamental principles of quantum mechanics.

Literature review

Meta-optics, especially metasurfaces, have been widely used in the coherent measurement of photon states for both classical and non-classical light, most typically in the polarization degree of freedom [1]. However, it remains largely an open question on if a single piece of metasurface can be used as an

unconventional "camera lens" that enables the measurement of high-dimensional photon states encoded in several degrees of freedom. This was considered particularly challenging with the conventional metasurfaces based on sweeping parameters of periodic single nano-resonators and search for desired ones, which cannot correctly capture the nonlocal interactions of light across different nano-resonators. Local metasurface limits the range of transformations a metasurface can achieve, and therefore the design is highly limited. Recent advances in full-wave simulation have dramatically reduced the time and computational resources needed to perform large-area meta-optics stimulations, such as augmented partial differentiation [3] and graphics processing unit (GPU) accelerated finite-difference time-domain (FDTD) methods [4]. These simulations can be combined with advanced optimization algorithms with reduced iterations [5], allowing for the free-form engineering of each meta-atom. The meta-optics designed by this means can operate in highly nonlocal regimes among the meta-atoms, allowing for the combination of direct manipulation in k-space in addition to real space. However, it remains unclear what simulation and optimization strategy can be best used for designing high-dimensional photon state reconstructions.

I have done several impactful works in designing meta-optics for the measurement of quantum states of light, with its earliest effort dating to my work in 2018 [6]. We used metasurfaces to convert multiphoton polarization-entangled states to several judiciously designed spatial outputs for optimized measurements of the quantum-polarization state. We had recent progress on meta-optics for performing non-unitary transformations of polarization-entangled photon pairs [7] and for quantum state measurements based on general positive operator-valued measures (POVMs). These works are highly relevant to the proposed project since the classical photon state coherent measurement problem is inherently a measurement of a density matrix in the representation of the degrees of freedom.

Objectives

The proposed research program has a *long-term vision* to revolutionize the coherent measurement technology in optical communications using scalable and efficient nanostructured meta-optics. Meta-optics will be used as an unconventional "camera lens" together with photodiode arrays or image sensors for the coherent detection of information encoded in various degrees of freedom, including time, polarization, and spatial mode. Such meta-optics will also be used for state tomography of non-classical high-dimensional states encoded in various degrees of freedom. The long-term outcome of this research program will deliver a toolbox that can readily analyze the number of resources (such as thickness, layers, and size) to realize a specifically given detection and then provide a design with the minimized resource that is practical to fabricate.

The *short-term objectives* for the next two years focus on the following three thrusts:

1) Nonlocal meta-grating for spatial mode retrieval.
2) Metasurfaces for the imaging-based measurement of multidimensional spatial & polarization states.
3) Metasurfaces for compressed sensing of high-dimensional states encoded in time, polarization, and spatial modes.

Outline of tasks/Work Plan

Objective 1: Nonlocal meta-grating for spatial state retrieval

In this objective, we will use efficient numerical techniques (temporal coupled-wave analysis and/or augmented partial factorization) combining advanced optimization algorithms (gradient descent and adjoint optimization) to inversely design a two-dimensional nonlocal meta-optics structure (i.e., meta-grating) optimized for the retrieval of spatial states described as Hermite Gaussian functions.

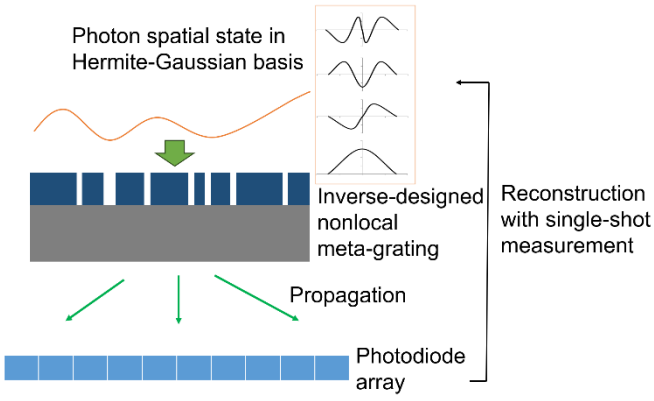

Figure 1 Illustration of Objective 1

Task 1.1: Developing a numerical design framework for two-dimensional nonlocal meta-optics simulation and end-to-end optimization. We will develop a physics-oriented tailored design strategy combining the latest simulation and

optimization techniques. In particular, we aim to design structures that are highly resonant across many meta-atoms nonlocally. We will capitalize on the latest computationally inexpensive simulation tools for such nonlocal structures (e.g. augmented partial factorization) to base our inverse design on the simulation of the entire structure at tens or hundreds of micro-meter size. The nonlocal properties can expand the range of possible transformations that the dielectric metasurface performs on the input spatial state and thereby lead to a better-conditioned reconstruction. The optimization will be an end-to-end approach that takes the reconstruction into account. Inherently we will optimize the condition number of the instrument matrix of this system.

Task 1.2: Design an example meta-grating for one-dimensional Hermite-Gaussian state retrieval and compare the performance with local meta-optics structures. Using the framework established in Task 1.1, we will design an example meta-grating using amorphous silicon. We will compare the reconstruction condition to the inverse-designed local metasurface (that treats the transformation as a phase mask) and showcase the strength of the nonlocal meta-grating.

Task 1.3: Testing relevant fabrication capabilities for our designed meta-optics. We have already started to test fabrication processes in the McGill Nanotools Micro and Nanofabrication Facility and Institut national de la recherche scientifique (INRS). We are focusing on meta-optics based on amorphous silicon that is suitable for mass production and typical telecom wavelengths. The main techniques will include plasma-enhanced chemical vapor deposition to deposit thin-film amorphous silicon or silicon nitride, electron beam lithography for patterning the nanostructures, and reactive-ion etching to obtain the structures. If there are unexpected delays, we will get samples from foundries.

Task 1.4: Experimental realization of the representative design described in Task 1.2. We will fabricate the nonlocal meta-grating described in Task 1.2 and experimentally demonstrate its strength in the one-shot measurement of photon spatial states, including the information of amplitude, phase, and coherence in the mode space of encoding (here being Hermite-Gaussian). A spatial light modulator will generate the spatial states. The metasurface will be first calibrated and then be used for the measurements and reconstructions.

Objective 2: Metaurfaces for the imaging-based measurements of multidimensional polarization & spatial states

This objective brings the design to a complete three-dimensional (3D) structure (i.e., nonlocal metasurface instead of nonlocal meta-grating). Such an extension will enable the single-shot coherent measurement of photon states encoded in both spatial and polarization degrees of freedom, further expanding the dimensionality of the measured state. Notably, we will explore the use of image sensors for such measurements taking advantage of the large number of pixels and the no need for fast time-resolved detection. Specific tasks for this objective are:

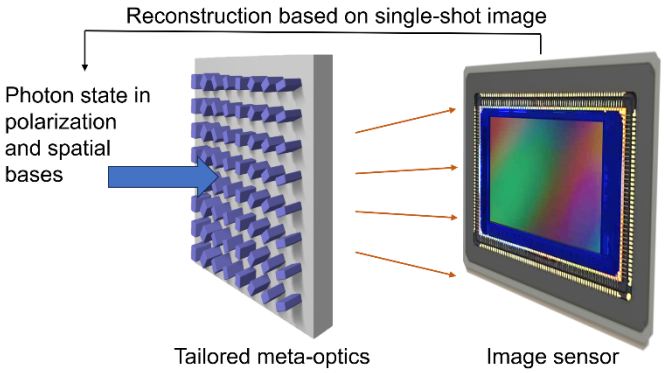

Figure 2 Illustration of Objective 2

Task 2.1: **Extending the design framework established in Task 1.1 to three-dimensional structures and adding image sensors into the modeling.** The key step in this task is to develop a three-dimensional computationally inexpensive 3D full-structure meta-optics simulation code. We will base it on the augmented partial factorization approach, which currently only works for 2D. We will also insert the image sensor specifications into the simulation, such as readout noise and dark counts.

Task 2.2: **Designing a metasurface for measuring polarization & spatial states.** By combining the simulation code developed in Task 2.1 with our existing optimization code based on gradient descent, we will aim to inversely design a nonlocal metasurface with good condition numbers for the

reconstruction of polarization & spatial states. The spatial degree of freedom can be in the basis of either Lagurre-Gaussian or Hermite Gaussian.

Task 2.3: **Experimental realization of the metasurface designed in Task 2.2.** Based on the design in Task 2.2, we will fabricate the metasurface and demonstrate its capabilities in polarization-spatial state measurements based on an image sensor. Importantly, since no polarizer exists between the metasurface and the image sensor, each pixel's signal involves an incoherent mixture of the two polarization components. Thus, it is necessary to use a general positive operator-valued measure (i.e., projection to mixed states) instead of a projective measurement (to pure states) to characterize the metasurface. We will develop the necessary calibration formalisms and test the feasibility of such metasurfaces.

Task 2.4: Extending the design to multiphoton quantum states encoded in polarization-spatial bases considering click detectors (single-photon avalanche photodiode array, SPAD). We will also explore how we further optimize the metasurface designed in Task 2.2 to make it suitable for multiphoton states encoded in the same degrees of freedom. While for a quantum state encoded in the same bases with a known and fixed photon number N, the classical design should also work as one changes the spatially-resolved intensity measurements to N -fold photon spatial correlation measurements. However, if the pixels of the image sensor (such as SPAD cameras) cannot resolve the photon number, one would lose information from unresolved local coincidence events. It is, therefore, necessary to run the optimization based on the actual multiphoton and image sensor scenario to further optimize the metasurface design.

Objective 3: Metasurfaces for compressed sensing of high-dimensional state encoded in time, polarization, and spatial modes

In this part, we will design a metasurface capable of measuring high-dimensional photonic states encoded in time, polarization, and spatial degrees of freedom. Importantly, this step brings in the time degree of freedom, which is the most commonly used degree of freedom in optical fiber-based communications. More specifically, the measurement will be achieved by interfering the measured light with a local oscillator (a continues-wave laser at the carrier frequency of the measured state) at the metasurface and by performing time-resolved detections 2D photodiode arrays and time-to-digital conversion for each photodiode in the array. Due to the high-dimensional nature of the measured state and the relatively small number of photodiodes, for this objective, we will assume sparsity for the measured state and apply compressed sensing principles for the design and reconstruction. The specific tasks for this objective include:

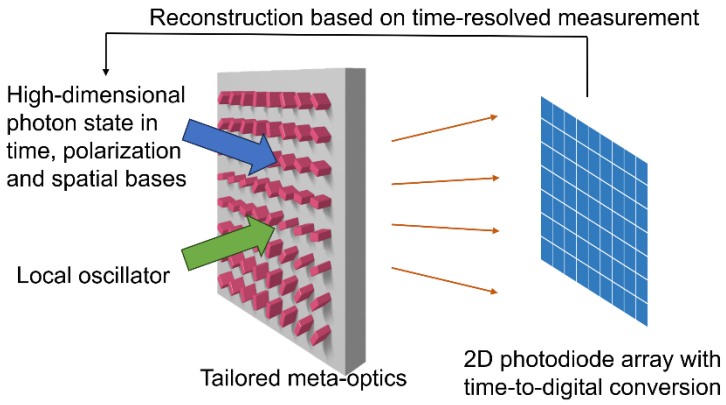

Figure 3 Illustration of Objective 3

Task 3.1: Designing a metasurface that can be used with a local oscillator input for time-polarization-spatial state measurement based on compressed sensing. The key to this objective in the design is to judiciously combine a local oscillator on the metasurface that effectively performs optical heterodyne detection and can convert the time-varying phase information in the signal to intensity measurements while preserving the optimized reconstruction conditions for the polarization and spatial degrees of freedom. Another key is to use sparsity as *a priori* knowledge and base our design and reconstruction on an L^1 norm approach since the number of measurements, in this case, becomes smaller than the unknowns.

Task 3.2: Experimental realization of the metasurface designed in Task 3.1. After the metasurface is designed, we will fabricate it and experimentally demonstrate its capabilities. We will prepare high-dimensional states combining electro-optic phase&intensity modulators, spatial light modulators, and polarization optics to prepare a high-dimensional state. We will develop experimental approaches to

calibrate the transformation associated with the fabricated metasurface and perform high-dimensional state measurements with fabricated metasurfaces.

Outcomes

The proposed project holds great promise for playing a transformative role in the field of optical communication by achieving several key outcomes:

Enhanced data capacity and speed: By leveraging coherence and high-dimensional states encoded in various degrees of freedom, the project will enable the coherent and fast detection of optical signals. This breakthrough will significantly enhance data capacity and speed in optical communication channels, meeting the escalating bandwidth demands of data-intensive applications. The suitability for massive production will make such meta-optics devices a game-changer in coherent and MDM optical communications.

Scalability and adaptability: The development of nanostructured meta-optics elements will not only provide immediate benefits to optical communication but also pave the way for future scalability and adaptability. These elements can be integrated into existing communication infrastructures and extended to handle higher-dimensional quantum states, ensuring that the research remains relevant in the long term.

Technological advancements: The project's focus on cutting-edge meta-optics technologies will stimulate advancements in numerical simulation and inverse design techniques. As the research progresses, it may lead to breakthroughs in other areas of photonics and optical engineering, expanding the applications of meta-optics beyond communication to imaging, sensing, and computing.

Quantum communication advancements: High-dimensional coherent detection is vital for the secure and high-speed transmission of quantum information. As quantum communication technologies continue to mature, the project's outcomes will play a critical role in establishing a quantum internet and facilitating secure quantum key distribution (QKD) protocols.

Impacts

Revolutionizing communication networks: The outcomes of the research will lead to the deployment of advanced coherent optical communication systems with unprecedented data capacity and speed. This transformative upgrade will revolutionize communication networks, facilitating seamless data-intensive applications such as high-definition video streaming and cloud computing.

Enabling quantum-secured communication: Quantum communication is the future of secure data transmission. The project's impacts on quantum communication technologies, such as QKD, will enable a class of important devices for secure communication channels, benefitting sectors dealing with sensitive information, such as finance, defense, and healthcare.

Socio-economic growth: The project's technological advancements will foster innovation and competitiveness in the photonics industry, leading to economic growth and job creation. Companies involved in the development and commercialization of meta-optics components and systems will flourish, contributing to the overall socio-economic landscape.

Scientific advancement: The research will contribute significantly to the scientific community's understanding of high-dimensional photon states and their interaction with complex nanostructured meta-optics. The knowledge gained from this project will open new avenues driving fundamental scientific advancements.

Technological advancements and industry relevance: The outcomes will be relevant not only to academia but also to industry sectors, potentially leading to the development of novel products and applications in the field of optical communications and quantum technologies.

References

[1] Z. Bomzon et al. Opt. Lett. 26, 1424–1426 (2001); P. Lalanne, P. Chavel, Laser Photonics Rev. 11, 1600295 (2017); Yu and Capasso, Nat.Mater. 139(2014).
[2] K. Wang, et al., Physics Today 75, 38 (2022).
[3] H.-C. Lin, et al. Nature Computational Science 2, 815 (2022).
[4] T. W. Hughes, et al., Applied Physics Letters 119, 150502 (2021).
[5] M. Zhou, et al., ACS Photonics 8, 2265 (2021).
[6] K. Wang et al., Science 361, 1104 (2018).
[7] S. Lung, et al. ACS Photonics 7, 3015 (2020).

Immune Cell Tracking with Adaptive Illumination

Highly motile immune cells actively migrate in various organs and tissues in normal and disease states to initiate efficient immune response. Understanding how the immune cells migrate in various organs under various conditions is important for finding disease treatments. The major technology used for immune cell tracking in intact, living tissue is multiphoton fluorescence microscopy. As a nonlinear process, however, multiphoton excitation generates an inherently weaker signal than one-photon excitation, and high excitation power is typically required for fast tracking deep within intact tissues. Because multiphoton microscopes typically operate at the photon shot-noise limit, the maximum number of cells that can be tracked at high spatial and temporal resolution is fundamentally limited by the number of signal photons, which in turn is determined by the maximum permissible average and peak power in biological specimens. Therefore, the fundamental limit for technologies aimed at measuring real-time immune cell migration in intact tissues is the photon budget: the number of signal photons obtainable from the sample within a given period of time. Simply scanning fast, while necessary, is not sufficient for high speed and large volume imaging. This proposal will create new imaging technologies to address this fundamental challenge in dynamic immune cell imaging.

To address the fundamental limit of the photon budget, we will develop adaptive cell tracking (ACT) that will illuminate only the ROIs. A one to two orders of magnitude gain in photon budget can be achieved by ACT because the ROIs usually only occupy a small fraction of the imaging volume (1-10%). This gain in photon budget can directly translate to an increase in imaging volume or imaging speed (or a combination of the two), without increasing the excitation power on the sample or sacrificing signal-to-noise ratio (SNR). (1) To demonstrate the concept of ACT, we will image T cell migration in a live mouse by using 3D ROI localization algorithms and direct modulation of the laser output to illuminate only the ROIs. This demonstration will show how much photon budget can be saved with ACT when compared to that without ACT. However, the direct modulation of the laser output wastes a large fraction of the laser output power and is impossible to achieve the optimum performance when imaging deep. (2) Next, we will combine the ACT with the adaptive excitation source (AES) that reduces the required output power of the excitation source and ensures every photon emitted from the laser is directed towards the ROIs. To do this, we will significantly reduce the time required for the gain equalization in the AES by obtaining a good initial guess of the input pulse train with a machine-learning approach. (3) In addition, we will develop photon efficient scanning and localization algorithms to further reduce the excitation and emission photons required for cell tracking.

Through the development of imaging methods, lasers, photon efficient scanning and object localization algorithms, this work will increase the fluorescence signal by one to two orders of magnitude without increasing the excitation power in the specimen or the laser output power. While we will focus on immune cells, the technologies developed in this program are applicable for tracking any cells or molecules deep within intact tissues. The gain in photon budget will proportionally increase the tracking speed or volume (or a combination of speed, depth and volume), and ultimately enable dynamic, real-time tracking at the cellular and sub-cellular levels deep within intact tissues or organs that are completely beyond the reach of any existing techniques.

Immune Cell Tracking with Adaptive Illumination

Literature Review

Highly motile immune cells are actively recruited to the sites where infection or other diseases (autoimmune disease, tumor, etc.) occur to protect our body from invading pathogens (bacteria or virus) or to attack our body when they lose control. They are also continuously migrating even in normal state to search potential antigens in various organs and tissues for immune surveillance. The efficient recruitment or efficient antigen searching of immune cells is critical to initiate effective immune response at an early time of disease. Therefore, understanding how the immune cells migrate in various organs under various conditions is important for finding disease treatments. During the last 20 years, two-photon microscopy (2PM) have been utilized to visualize immune cell migration in various organs of live animal with sub-micron resolution and 4D resolution (x, y, z, and t)[1]. However, the imaging volume at sufficient temporal resolution to track the cells is limited, which makes it difficult to obtain long-term cell tracks (> 1 hour) because the cell can rapidly disappear from the imaging volume. In particular, thin volume imaging (e.g., 492x492x40 μm^3 with 20.3 s interval) due to slower scanning along z-axis than xy-axis can lead to skew the interpretation of the migration data[2].

2PM technique has been improved for fast thicker imaging: simultaneous multiplane imaging[3] and fast z-scanning by remote focusing[4]. These techniques allow to visualize 690x675x600 μm^3 volume at 16.7 Hz with single-neuron resolution (~5 μm for lateral, ~15 μm for axial) in a mouse brain cortex[5]. However, for more opaque organs than the brain cortex (e.g., lymph nodes densely packed with immune cells) the thick volume imaging has been challenging because conventional 2PM with 920nm excitation can penetrate only 300 um depth of lymph node. Recently, we demonstrated that three-photon microscopy (3PM) with 1300 nm excitation can visualize a mouse popliteal lymph node through its entire depth (600-900 μm)[6], but only a small volume (~ 50 cells within 300x300x100 μm^3) can be tracked at a low temporal resolution (30 s/volume) when imaging 500-600 μm deep into the lymph node (Fig. 1)[6] because the maximum permissible average power (< 80 mW)[6] limits the rate of signal photons obtainable from the sample.

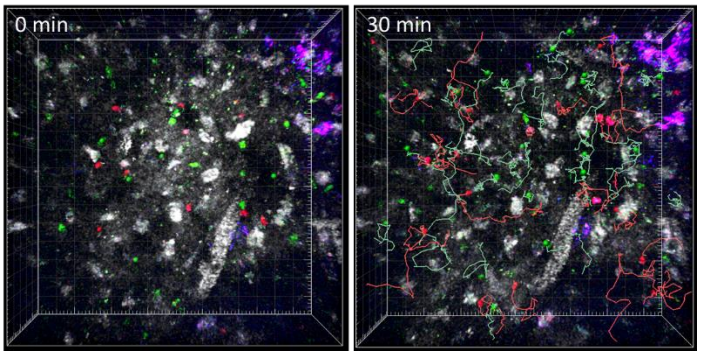

Fig. 1 Intravital 3P imaging of immune cell migration at 500-600 um depth in a mouse lymph node. CD4+ T cell (green) and CD8+ T cell (red) were labeled with CFSE and CMRA fluorescent dyes, respectively. Green and red lines in right figure show tracks of the cells for 30 min. White and magenta are third-harmonic generation (THG) signal and eFluor615-labled LYVE-1+ lymphatic sinuses, respectively. Imaging volume (300x300x100 μm^3, 256x256 pixels and 25 planes) was acquired every 30 s with ~70 mW of average laser power. The pulse repetition rate was 0.654 MHz.

Problem Statement

A critical concern in large scale imaging for immune cell tracking is the photon budget. Because multiphoton microscopy typically operates at the photon shot-noise limit, the maximum volume where cells can be imaged and tracked at high spatial and temporal resolution is fundamentally limited by the rate of signal photons, which defines the signal-to-noise ratio (SNR), and in turn is determined by the maximum permissible average and peak power in biological specimens. For example, in multiphoton brain imaging over a large field of view[7] the SNR is currently limited by the total laser power that can be delivered to the mouse brain (< 250 mW)[8]. On the other hand, the regions of interest (ROIs), e.g., user defined cells and molecules, typically only occupy a small fraction of the volume. With standard raster scanning, a large fraction of excitation is therefore wasted on non-informative parts of the sample outside the ROIs. Therefore, there is an urgent need to create the most photon-efficient excitation scheme to enable dynamic

cell tracking with high spatial and temporal resolution over a large volume.

Objective

The research proposed here directly addresses the challenges of large-scale, fast dynamic tracking at the cellular or sub-cellular level. To address the fundamental limit of the photon budget, we will develop adaptive cell tracking (ACT) that will illuminate only the ROIs. In principle, ACT is analogous to spotlight tracking of ballet dancers on a stage: each dancer is illuminated and tracked by one spotlight while the rest of the stage remains in the dark. ACT thereby dramatically improves the photon efficiency for dynamic cell tracking, i.e., every photon on the sample is used to record the cellular motion. A one to two orders of magnitude gain in photon budget can be achieved by ACT because the ROIs usually only occupy a small fraction of the imaging volume (e.g., the fluorescent-labeled T cells occupy < 1% of the volume imaged in Fig. 1). This gain in photon budget directly translates to an increase in imaging volume or imaging speed (or a combination of the two), without increasing the excitation power on the sample or sacrificing SNR.

While the concept of ACT can be demonstrated by direct modulation of the excitation source, direct modulation wastes a large fraction of the laser output power (e.g., >99% of the power will be wasted when imaging the T cells shown in Fig. 1) and is impractical to implement for imaging at the shallow depths and impossible to achieve the optimum performance when imaging deep. We will combine ACT with the concept of the adaptive excitation source (AES)[9], which was developed recently by our group for imaging stationary ROIs (e.g., neurons in the mouse brain). AES reduces the required output power of the excitation source and ensures every photon emitted from the laser is directed towards the ROIs. The combination of ACT and AES will create the most photon efficient system for dynamic imaging: every photon from the laser which enters the specimen is used for dynamic tracking of the ROIs. The photon efficiency of AES and ACT will be further enhanced by exploring smart scanning patterns and object localization algorithms. The ultimate goal of this program is to create a new, readily deployable technology platform that uses the minimum number of excitation and/or emission photons for real-time tracking of cells or molecules in intact tissues.

Work Plan

<u>Aim 1: Demonstrating the concept of adaptive cell tracking (ACT).</u>

The concept of ACT is schematically illustrated in Fig. 2. ACT starts with conventional raster scanning of a 3D volume capturing the cells to be tracked and their environment (e.g., using different colors to label the cells and their environment, such as shown in Fig. 1). Via real-time image processing, the ROIs will be defined by determining the cell boundaries and adding a user defined “guard region” to ensure that the cells will not move out of the ROIs before the next imaging volume is acquired. The ROIs define the pulse sequence of the excitation beam in the time domain (i.e., adaptive excitation). Synchronization of the pulse sequence and the beam scanner ensures that only the ROIs will be illuminated by the excitation beam. To track the new cells entering the imaging volume, the borders of the volume can be labeled as ROIs as well. Multiple cell types can be tracked simultaneously by labeling them with different colors and performing multiphoton multi-color imaging with a single excitation wavelength[10,11]. The 3D environment can be re-captured by imaging the entire volume as needed.

3D ROI localization and adaptive excitation generation (steps 2 to 6 in Fig. 2a) form an automatic adaptive loop to continuously image and track cells; however, the time required (Δ) to perform these steps represents a “dead time” between two image acquisitions. We will leverage the rapidly expanding field of computer vision that has created a plethora of image segmentation algorithms[12,13]. Determining ROIs is an image-specific task and therefore the best image segmentation technique can vary greatly depending on the cells imaged. For the T cells (Fig. 1), for example, we found an algorithm based on image erosion and Otsu’s method to be sufficient[14]. For other cell types, an extensive list of options utilizing state-of-the-art deep learning techniques

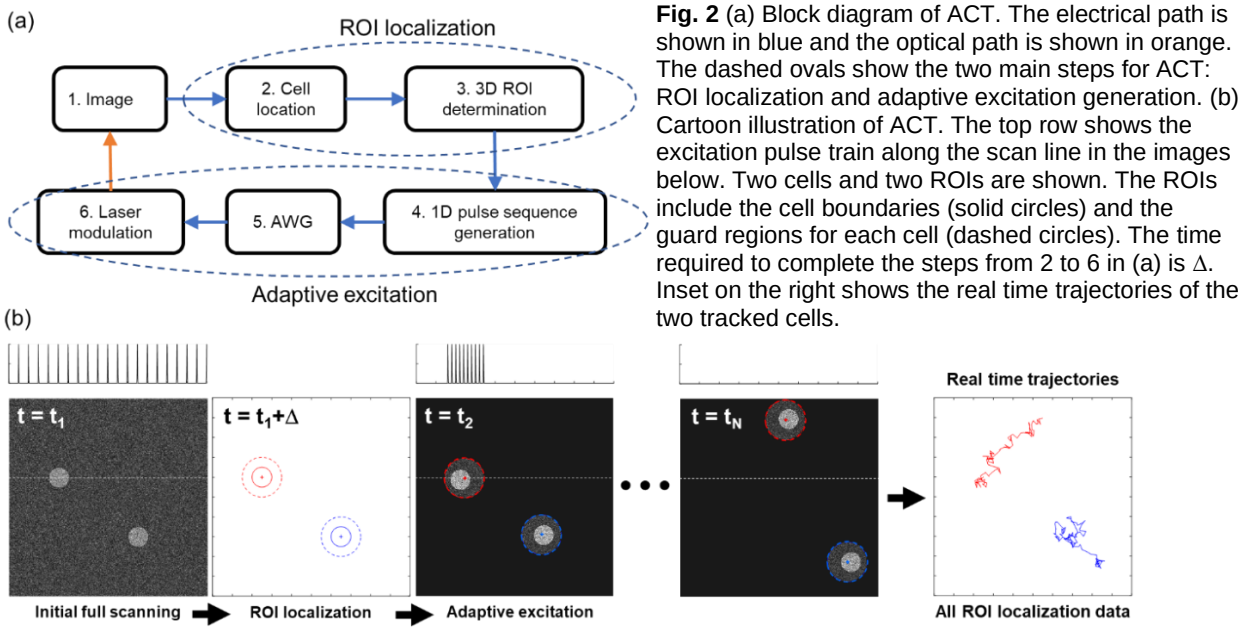

Fig. 2 (a) Block diagram of ACT. The electrical path is shown in blue and the optical path is shown in orange. The dashed ovals show the two main steps for ACT: ROI localization and adaptive excitation generation. (b) Cartoon illustration of ACT. The top row shows the excitation pulse train along the scan line in the images below. Two cells and two ROIs are shown. The ROIs include the cell boundaries (solid circles) and the guard regions for each cell (dashed circles). The time required to complete the steps from 2 to 6 in (a) is Δ. Inset on the right shows the real time trajectories of the two tracked cells.

exist[13,15,16]. Our current estimate is that Δ < 70 ms is achievable, which is sufficiently short for the concept demonstration.

We will directly modulate the laser output using an electro-optic modulator for 2PM and 3PM to demonstrate the ACT concept. To confirm if cell tracks obtained with ACT are same as that without ACT, we will image same T cell migration in a mouse lymph node simultaneously with and without ACT by simultaneous 2P and 3P imaging[17]. The $CFP^{+}DsRed^{+}$ double-labeled T cells can be imaged by 2P excitation of CFP at 860 nm without ACT and 3P excitation of DsRed at 1650 nm with ACT.

Aim 2: Combining ACT with an adaptive excitation source (AES).

We recently demonstrated an AES for imaging stationary ROIs (e.g., neurons in the mouse brain) for 2PM and 3PM[9]. Because the on-demand pulse train is not periodic in time, a key feature of the AES is pre-compensation of the gain transient from the fiber amplifiers[9]. Such gain transients are well-known in burst-mode amplification in fiber-optic telecommunications, and a closed-form solution of the inverse problem does not exist. Therefore, we used a feedback loop, which takes ~ 30 iterations (~ 15 s) to equalize the gain for one frame (512x512 pixels)[9] (Fig. 3a and 3b). While such a time delay is inconsequential when imaging non-moving objects, it is incompatible for tracking fast moving cells. We propose to employ machine-learning to provide an intelligent initial guess of the pre-compensation for a given pulse sequence. Our aim is not to replace the feedback loop but to vastly reduce the number of iterations (e.g. < 10). In addition, we will further reduce the time by increasing scanning speed and reducing pulse number

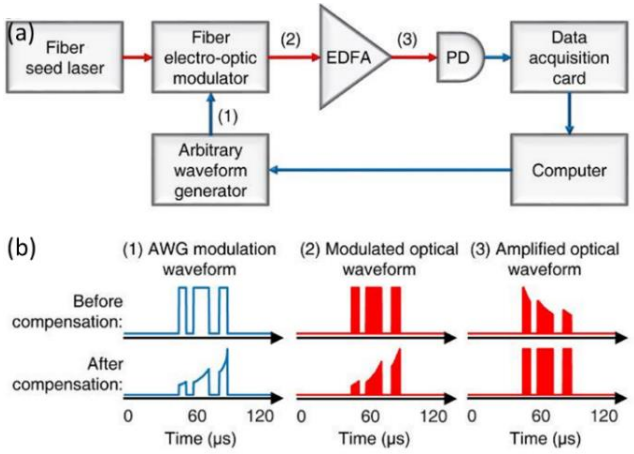

Fig. 3 (a) AES gain equalization using a feedback loop (see ref. 9). The electrical and optical paths are indicated in blue and red, respectively. PD: photo diode. EDFA: erbium doped fiber amplifier. (b) Schematic illustration of gain transient and equalization of the AES (see ref. 10). The electrical (blue) and optical (red) waveforms at three positions indicated by (1), (2), and (3) in (a) are shown.

per pixel during the iterations so that the time required for gain equalization for one volume is smaller than a volume acquisition time (e.g., 1 to 10 s). We will then eliminate the dead time by using two AWGs to alternately drive the intensity modulator, with AWG1 for the odd imaging volumes (t1, t3, ..) and AWG2 for the even imaging volumes (t2, t4, ..).

Aim 3: Developing photon efficient scanning and localization algorithms to improve ACT.

Since for tracking applications it is only necessary to determine the cell location, it is possible to consider alternative scanning strategies that would use fewer excitation and/or emission photons, ultimately allowing for a further reduction in illumination power and an increased tracking time. We propose a strategy inspired by MINFLUX[18,19] for super-resolution microscopy. The MINFLUX technique tracks single emitters by using an intensity minimum. Intuitively, if one can exactly match the intensity minimum to the emitter location, then the emitter location is known without any photons being received. Similarly, we consider just illuminating the guard region (Fig. 4). Any cell that does not move can in principle be found without any emission photons. To test this idea, we have performed 1D simulations and back-of-the-envelope calculations for localizing a rigid 10 μm cell which is allowed to move up to ± 5 μm between two imaging frames. We then considered scanning the entire region and just the guard regions, while keeping the total number of received photons (on average) the same. Comparing the root-mean-squared error (RMSE) of both cases, we find that if the cell does not move much and the received photon number is low (which is likely the case for most practical applications), the RMSE is lower when scanning just the guard region, indicating a possible saving of emission photons. For example, if the cell takes random walk with a standard deviation of 0.5 μm, with 16 received photons the guard region RMSE is better on average by a factor of 2. We also considered the same analysis but kept the total input power the same and found similar results. This preliminary analysis showed that for the same number of emission or excitation photons, scanning just the guard regions is a promising approach to further improve the photon efficiency. While generating arbitrary illumination patterns (e.g., generating an intensity minimum at the center of a point-spread function) in intact tissue is challenging in super-resolution microscopy, the various scanning patterns proposed here can be conveniently obtained from the AES by time-domain modulation. We will explore similar improvements in 3D volume by testing various scan patterns, e.g., a 3D shell around the cell instead of uniformly illuminate the entire ROI. We will further investigate the impact on cell localization by changes in cell morphology during the movement. Our ultimate goal is to use the minimum number of excitation and/or emission photons for real-time tracking of cells in intact tissues.

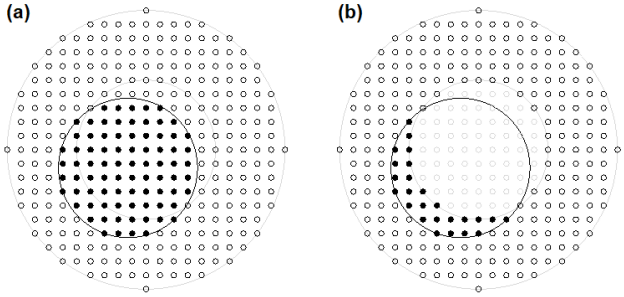

Fig. 4 Illustrated is a cell (large dark grey circle) which has moved off center and is to be scanned by (a) full ROI scan, and (b) guard-region-only scan. The small black circles (both open and filled) indicate the voxels to be scanned, i.e., the laser is on at these locations, with open circles indicating no signal is produced and filled circles indicating signal is produced. The small grey open circles in (b) show voxels that the laser would be on in the full ROI scan but isn't for the guard-region-only scan.

Outcomes & Impact

ACT will improve the cell tracking speed or volume by 10 to 100x, which will enable T cell tracking over the entire volume of mouse popliteal lymph node (~ 1000x1000x600 μm^3). Although the entire volume is ~ 67x of the imaging volume in Fig.1, the required average power is well within the permissible range because the ROIs are ~ 1% and the required power exponentially decreases as the depth approaches the surface. The T cell tracking in the entire volume will allow us to observe T cell migration in all directions over a long period of time (> 1 hour), for the first

time. Our proposed imaging method will be powerful tool for uncovering many unresolved questions related fundamental physiology and dynamic cellular immune response to many diseases. In addition, the smart localization developed in Aim 3 represents a totally new direction for cell tracking that will provide the most photon-efficient tracking strategy. While we will focus on immune cells, the technologies developed in this program are applicable for tracking any cells or molecules deep within intact tissues. In addition, an important practical feature of the proposed imaging method is that it can be implemented with current multiphoton imaging systems without any modification of the microscope hardware.

References

1. Germain, R. N., Robey, E. A. & Cahalan, M. D. A Decade of imaging cellular motility and interaction dynamics in the immune system. *Science (80-.).* **336**, 1676–1681 (2012).
2. Textor, J. *et al.* Defining the quantitative limits of intravital two-photon lymphocyte tracking. *Proc. Natl. Acad. Sci. U. S. A.* **108**, 12401–12406 (2011).
3. Amir, W. *et al.* Simultaneous imaging of multiple focal planes using a two-photon scanning microscope. *Opt. Lett.* **32**, 1731 (2007).
4. Botcherby, E. J. *et al.* Aberration-free three-dimensional multiphoton imaging of neuronal activity at kHz rates. *Proc. Natl. Acad. Sci. U. S. A.* **109**, 2919–2924 (2012).
5. Weisenburger, S. *et al.* Volumetric Ca2+ Imaging in the Mouse Brain Using Hybrid Multiplexed Sculpted Light Microscopy. *Cell* **177**, 1050-1066.e14 (2019).
6. Choe, K. *et al.* Intravital three-photon microscopy allows visualization over the entire depth of mouse lymph nodes. *Nat. Immunol.* **23**, 330–340 (2022).
7. Sofroniew, N. J., Flickinger, D., King, J. & Svoboda, K. A large field of view two-photon mesoscope with subcellular resolution for in vivo imaging. *Elife* **5**, 1–20 (2016).
8. Podgorski, K. & Ranganathan, G. Brain heating induced by near-infrared lasers during multiphoton microscopy. *J. Neurophysiol.* **116**, 1012–1023 (2016).
9. Li, B., Wu, C., Wang, M., Charan, K. & Xu, C. An adaptive excitation source for high-speed multiphoton microscopy. *Nat. Methods* **17**, 163–166 (2020).
10. Xu, C., Zipfel, W., Shear, J. B., Williams, R. M. & Webb, W. W. Multiphoton fluorescence excitation: new spectral windows for biological nonlinear microscopy. *Proc. Natl. Acad. Sci.* **93**, 10763–10768 (1996).
11. Hontani, Y., Xia, F. & Xu, C. Multicolor three-photon fluorescence imaging with single-wavelength excitation deep in mouse brain. *Sci. Adv.* **7**, eabf3531 (2021).
12. Zaitoun, N. M. & Aqel, M. J. Survey on Image Segmentation Techniques. *Procedia Comput. Sci.* **65**, 797–806 (2015).
13. Mary, S. P., Ankayarkanni, Nandini, U., Sathyabama & Aravindhan, S. A Survey on Image Segmentation Using Deep Learning. *J. Phys. Conf. Ser.* **1712**, (2020).
14. Otsu, N. A Threshold Selection Method from Gray-Level Histograms. *IEEE Trans. Syst. Man. Cybern.* **9**, 62–66 (1979).
15. Pachitariu, M. *et al.* Suite2p: beyond 10,000 neurons with standard two-photon microscopy. *Bioarxiv* **20**, 2017 (2017).
16. Upschulte, E., Harmeling, S., Amunts, K. & Dickscheid, T. Contour proposal networks for biomedical instance segmentation. *Med. Image Anal.* **77**, 102371 (2022).
17. Ouzounov, D. G. *et al.* In vivo three-photon imaging of activity of GCaMP6-labeled neurons deep in intact mouse brain. *Nat. Methods* **14**, 388–390 (2017).
18. Balzarotti, F. *et al.* Nanometer resolution imaging and tracking of fluorescent molecules with minimal photon fluxes. *Science (80-.).* **355**, 606–612 (2017).
19. Gwosch, K. C. *et al.* MINFLUX nanoscopy delivers 3D multicolor nanometer resolution in cells. *Nat. Methods* **17**, 217–224 (2020).

Summary:

Time Crystal Dynamics and Entropy in Periodically Driven Quantum Systems

Krzysztof Giergiel
Swinburne University of Technology

Categories:

Quantum Information, Ultracold Quantum Gases, Condensed Matter Physics, Many-Body Physics

Intended Outcomes:

1. **Detection of Momentum Transfer**: The project aims to detect the tiny change in momentum of the Bose-Einstein condensate (BEC) as it bounces on the vibrating atomic mirror in the time crystal experiment.
2. **Understanding Information and Entropy**: The investigation of time crystal dynamics will provide insights into how information and entropy flow in periodically driven closed quantum systems.
3. **Characterization of Periodically Pulsed Quantum Systems**: The research will contribute to characterizing big periodically perturbed quantum systems using ultracold atoms, helping understand macroscopic laws emerging from quantum descriptions. Investigating the back-reaction of time crystals to periodic drives may reveal periodic drives' role as an entropy sink.
4. **Validation of Time Crystal Dynamics**: By observing clean non-dissipative time crystals, the project aims to validate and explore the dynamics of time crystals.
5. **Development of Experimental Techniques**: Techniques to analyze light profiles affected by atom reflection and monitor laser light fluctuations will be developed, aiding future experiments.
6. **Advancement in Optical Fiber Optics**: Collaboration with fiber optics specialists will lead to advancements in storing high-power visible light using hollow-core optical fibers.
7. **Contributions to Scientific Literature**: The project's findings will contribute valuable data and insights to the scientific literature on time crystals, quantum matter, and periodically driven quantum systems.
8. **Importance for General Public**: Working with visible light storage in fiber optics is of general importance and relevant to various technological applications.

The research on time crystal dynamics and entropy has significant implications for the development of future quantum technologies, including quantum computing and quantum communication. By understanding how information and entropy flow in periodically driven quantum systems, the project contributes to the creation of energy-efficient and robust quantum systems. This is of paramount importance as global energy consumption from digital devices continues to rise. The insights gained from this study will contribute to advances in quantum simulation, sensing, and inertial navigation, positioning Australia at the forefront of ultracold quantum gas research. Furthermore, the project's findings will be of broader importance to condensed matter physics and many-body physics, fostering a better understanding of macroscopic laws emerging from quantum descriptions. The potential advancements in fiber optics for storing visible light have practical implications in various fields, including electronics, computing, communications, imaging, sensing, timing, and navigation.

Overall, the research holds significant promise in advancing our knowledge of time crystals and periodically driven quantum systems, while also having broad applications in quantum technologies and related scientific disciplines.

Time Crystal Dynamics and Entropy in Periodically Driven Quantum Systems

LITERATURE REVIEW

Time crystal is a name for the unexpected spontaneous breaking of discrete time translation symmetry. Following the 2012 [1] and 2015 [2] theoretical proposals and the 2017 [3,4] experiments a new field of research regarding this phenomenon was born. The first time crystals were observed just 6 years ago. Since then more than 8 experiments have been performed in different settings advancing the field exponentially (see review [5]). Still, the immense potential of time crystals remains to be exploited. The Australian time crystal experiment [6] I helped to design and build will be the first to produce clean non-dissipative time crystals of size up to about 100 unit cells. I have shown that this experimental platform can be a tool to investigate the physics of crystalline systems with long-range interactions not possible in conventional crystals [7]. The dressed atom is a special case of a dressed source in Quantum Field Theory, which finds application in diverse branches of physics. Recently, it reappeared in studies of Quantum Jumps and the Quantum Zeno Effect. In Quantum Zeno's paradox the field observes the atom and dresses its states. The change of energy of the dressed states moves them away from the resonant transition, thus stopping state changes. The bouncing of a Bose-Einstein condensate (BEC) of ultra-cold atoms on an oscillating atom mirror dresses the mass degrees of freedom, with the quanta of vibration playing the role of photons. It is in itself an interesting theoretical and experimental challenge. The mass degrees of freedom are relatively slow, compared to the internal structure of an atom, which places this system in its own class in terms of stability and what we can measure. The dressing by the vibrations can cause the atoms to obtain the temporal analogue of momentum and kinetic energy. I have shown different periodic drivings leading to dressed systems corresponding to a very broad front of hot research topics [7–12]: from Anderson's localisation in the temporal domain, including many-body localisation, through time-quasi-crystals, up to topologically protected temporal order and phase transitions associated with it and even crystallisation on a Möbius strip.

REFERENCES

[1] F. Wilczek, Phys. Rev. Lett. 109, 160401 (2012).
[2] K. Sacha, Phys. Rev. A 91, 33617 (2015).
[3] J. Zhang, P. W. Hess, A. Kyprianidis, P. Becker, A. Lee, et al., Nature 543, 217 (2017).
[4] S. Choi, J. Choi, R. Landig, G. Kucsko, H. Zhou, et al., Nature 543, 221 (2017).
[5] K. Sacha, Time Crystals, Springer Series on Atomic, Optical, and Plasma Physics (2020).
[6] **K. Giergiel**, T. Tran, A. Zaheer, A. Singh, A. Sidorov, et al., New J. Phys 22, 085004 (2020).
[7] **K. Giergiel**, A. Miroszewski, and K. Sacha, Physical Review Letters 120, 140401 (2018).
[8] **K. Giergiel**, A. Dauphin, M. Lewenstein, J. Zakrzewski, and K. Sacha, New J. Phys 21, 052003 (2019).
[9] **K. Giergiel**, A. Kuroś, and K. Sacha, Phys. Rev. B 99, 220303 (2018).
[10] **K. Giergiel**, A. Kuroś, A. Kosior, and K. Sacha, Phys. Rev. Lett. 127, 263003 (2021).
[11] M. Mierzejewski, **K. Giergiel**, and K. Sacha, Phys. Rev. B 96, 140201 (2017).
[12] **K. Giergiel** and K. Sacha, Phys. Rev. A 95, 063402 (2017).

PROBLEM STATEMENT

This project aims to investigate Discrete Time Crystals in the context of their effects on the periodic driving and lay the foundation for the possibility of reusing this driving for the purpose of creating an almost energy-free, robust, infinitely oscillating, large interacting quantum system.

Quantum communication and quantum information is bringing quantum physics into our everyday world. It promises quantum computing advantage in the speed of certain computational problems and absolute security of communications. These advancements are crucial as the energy required by digital devices is predicted to rise to about 21% of global energy consumption by 2030. Studying periodically

pulsed quantum systems is of utmost importance as these will be the building blocks of all emerging quantum technologies. On the other hand, characterising big periodically perturbed quantum systems is essential to understanding how the macroscopically observed laws of nature and thermodynamics emerge from a microscopic quantum description of the universe. This can be effectively probed by performing experiments with ultracold atoms, i.e., atoms cooled to temperatures near absolute zero. At these temperatures the quantum mechanical features of atoms become very apparent.

Time Crystals are a new dynamical state of quantum matter, which may provide a platform for future quantum technology. The use of quantum devices based on space-time crystals is enticing with the possibility of creating crystalline structures with an additional dimension — time. The usual approach to time periodic systems is based on Floquet theory - but the main results of analysis of periodic differential equations were described in many forms by George William Hill, Alexander Lyapunov and lastly by Felix Bloch, whose formulation of the theorems is most widely known to physicists. In these time-dependent systems energy is no longer a conserved quantity; instead one uses the concept of quasi-energy much like in spatial crystals one deals with quasi-momenta. The quasi-energy is bounded from above and below, and the width of this interval is associated with the period of the drive, just like the Brillouin zone is associated with a spatial crystal's unit cell.

The recent time crystal discovery has unexpectedly shown us that periodic driving not only does not necessarily mean a transfer of energy and heating of the system, but also that the symmetry of the periodic driving can be spontaneously broken (see Fig. 1), leading to systems with much richer structures (spanning multiple Brillouin zones) than those restricted by the symmetry rules imposed by the drive (a single Brillouin zone). This happens because we departed the region of applicability of Floquet theory, which deals only with systems with a finite number of states. Instead, we are looking at a thermodynamic (infinite) limit of particles. With this new class of periodically driven systems we have an opportunity to investigate physics from a new perspective.

In the long term we will start changing our point of view and attempt to prepare the ground to understand physics in which entropy and information flow are playing a central role. The energy is still extremely relevant as it sets the time scales of interest associated with any experiment we want to perform. This project will do just that by studying the back-reaction of the time crystal on the periodic drive used in its creation. Although no net energy is transferred between the time crystal and the drive it should be possible to see that the periodic driving, with its perfect repeating structures might be acting as an entropy sink for the time crystal. In doing so it will help in understanding these fascinating systems.

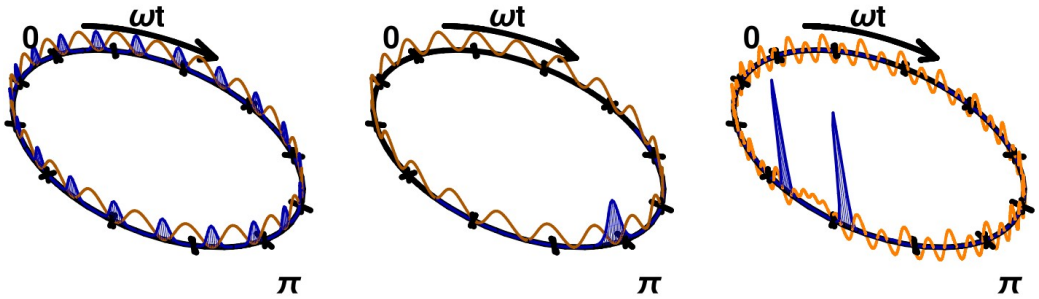

(a) Superfluid in a Temporal Lattice (b) Discrete Time Crystal (c) Edge state of the temporal Su-Schrieffer-Heeger model

Figure 1. The ring in time corresponding to a single characteristic period of the system. Effective potential in a time lattice - orange lines - and the sample eigenstate probability density - blue filled-in areas - are shown. Choosing a harmonic mirror vibration driving one can obtain a symmetry unbroken phase - all points shifted by the time translation of the mirror drive are equivalent (a). This symmetry is spontaneously broken by sufficiently strong interactions and the system now evolves on a stable periodic trajectory with a multiple of the drive frequency (b). Using a more complex vibration protocol with multiple harmonics, one can blanket the periodic orbit with an almost arbitrary potential making this a promising universal experimental platform (c).

OUTLINE OF TASKS

In the Time Crystal experiment Bose-Einstein Condensate (BEC) bounces on the vibrating atomic mirror, without heating and in a state evolving with a multiple of the drive frequency. No energy is transferred but it is clear that the reflection of the BEC off the mirror requires transfer of momentum of the condensate (see Fig. 2). Comparing the momentum of an atomic cloud to the momentum carried by an entire Gaussian profile of a light-sheet mirror beam gives a relative change of 10^{-11}. Detecting this tiny change is the challenge of this project, as this is where the information and entropy might leave the so-called periodically driven *closed* quantum system.

A commercially available Fabry-Pérot interferometer can be obtained with a relative resolution of about 10^{-9} for 532 nm light. First, we do not need or want to analyse the entire high power beam of laser light. We can only select the part of the profile most affected by the reflection of atoms easily bridging the required accuracy gap. That is, discard the part of the Gaussian beam that did not originate from the atom mirror interaction site.

Second, the mirror oscillations will not be generated by changing the mirror's position, but instead I intend to investigate changing just the light's power. This makes the mirror profile softer or harder effectively changing the position of where the atoms are reflected. This will mitigate the problem of changes of the light path geometry with respect to the created wavefront analysis device.

Third, the mirror laser light will be monitored for small fluctuations, while another beam will bypass the experimental cell and be used as a reference source and interfere with the light experiencing interactions. As a homodyne detection scheme this will improve the system sensitivity vastly.

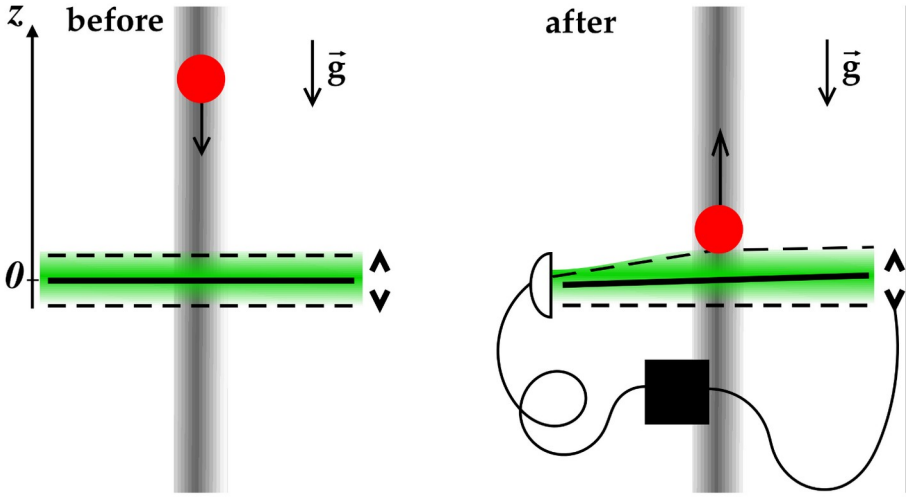

Figure 2. On the left, the current semi-classical setup. The quantum particles are confined in a vertical tube (grey) and bounce on a vibrating mirror driven (green) by a classical external source. Attractive particle interactions in this system can lead to spontaneous formation of time crystals. On the right, a schematic of momentum transfer, as the condensate is reflected the light-sheet mirror has to be deflected. By comparing the state of light before and after interacting with atoms the momentum transfer can be measured. This is a departure from the classical drive assumption underlying the current theoretical understanding of time crystals.

From the start we will work with a hollow-core optical fiber-optics specialist to be able to store the light in a couple kilometers of fiber, which will correspond to a single mirror oscillation time. This technology is able to store high power light and is rapidly growing, as it seems as the peak of silica fiber efficiency is now very close. Especially for visible light, the solid core fibers are fundamentally limited by attenuation due to Rayleigh scattering. This last step should allow us to interfere light from the mirror interacting with the system at two different points in time – spaced by the time crystal's unit cell. The fiber length accuracy is not as important here, as instead we should be able to readily prepare time crystals with the fundamental frequency matching the time retardation of the fiber.

All of these are steps of building a machine that should be able to expose the momentum transfer from the bounces of the time crystal and analyse the results to gain information that is revealed by the system interacting with a realistic periodic drive.

OUTCOMES

Detection of Momentum Transfer: The project aims to successfully detect the tiny change in momentum of the Bose-Einstein condensate (BEC) as it bounces on the vibrating atomic mirror in the time crystal experiment. By comparing the momentum of the light-sheet mirror with after the bounce with the reference.

Understanding Information and Entropy in Periodically Driven Quantum Systems: Through the investigation of the time crystal experiment, the project intends to shed light on how information and entropy flow in periodically driven closed quantum systems. The analysis of the momentum transfer and its connection to information and entropy will contribute to a deeper understanding of the system's behavior.

Characterization of Periodically Pulsed Quantum Systems: The project will contribute to the characterization of big periodically perturbed quantum systems using ultracold atoms. Studying these systems is crucial for understanding how the macroscopic laws of nature and thermodynamics emerge from microscopic quantum descriptions.

Validation of Time Crystal Dynamics: By observing clean non-dissipative time crystals of sizes up to about 100 unit cells, the project aims to validate and explore the dynamics of time crystals. This research will contribute to the field of dynamical quantum matter and potentially pave the way for future quantum technologies.

Development of Experimental Techniques: The development of techniques to analyze the part of the light profile most affected by the reflection of atoms and to monitor small fluctuations in the mirror laser light will be valuable for future experiments in the field. Measurments of changes to the wavefront are an important imaging resource.

Advancement in Optical Fiber Optics: Collaborating with hollow-core optical fiber optics specialists will help develop and utilize cutting-edge technology to store high-power light. The use of optical fibers to store light for a single mirror oscillation time will enable the examination of the mirror interacting with the system at different points in time, contributing to deeper insights into the time crystals' behavior.

Potential Implications for Thermodynamics and Entropy: The project's investigation of the periodic driving's back-reaction on time crystals may reveal the role of periodic drives as entropy sinks

for time crystals. This understanding could have broader implications for thermodynamics and the role of entropy in quantum systems.

New Perspectives in Physics: By departing from the region of applicability of Floquet theory and classical drive approximation and investigating thermodynamic limits of particles in periodically driven systems, the project opens up new perspectives in physics. It offers an opportunity to explore physics from a fresh viewpoint and potentially uncover novel phenomena.

Contributions to the Scientific Literature: The project's findings will be valuable contributions to the scientific literature on time crystals, quantum matter, and periodically driven quantum systems. The outcomes may lead to further research and advancements in the field of quantum physics and quantum technologies.

IMPACT

The research described in this project is at the forefront of the highly competitive field of ultracold quantum gases and is expected to significantly enhance the international reputation of Australian research. The outcomes will also impact on the fields of condensed matter physics and many-body physics and are likely to lead to a series of high quality publications in high-impact journals.

The scientific knowledge gained from analysis of this light will add new experimental data on time crystals based on closed quantum systems. Such time crystals are in the theoretical limit an infinitely oscillating system, which is protected from heating and absorbs no energy. While it is expected that the energy is conserved, it is crucial to understand entropy flow in these systems, if they are to play a role in the future low energy quantum circuitry. The basic science insights gained from this project are of importance in a large area of research topics.

Working with 532nm light used as the blue-detuned repulsive lightsheet creating the mirror is of interest to the general public, as this is a frequency doubled light of 1064 nm standard Ytterbium fiber lasers. Storing green light in standard fiber materials is about 10 times more lossy than for the 1550 nm light used in communications technology. Thus, working with the storage of visible light in different designs of fibers is of general importance.

It is widely recognised that the next major technological advances this century will come from harnessing the quantum world, e.g., solving problems in electronics, computing, communications, imaging, sensing, timing and navigation. This is evident from the miniaturization of electronic devices and computer chips towards the atomic scale. Heavily funded programs to exploit quantum phenomena for future technologies are ongoing in the UK (£270M Quantum Technologies Program), Europe (1B EUR Quantum Technology Flagship), USA and China. Ultracold atom physics is central to all of these programs, particularly in quantum simulation, sensing and inertial navigation.

Project Title: "Photonics-Driven Solutions for Sustainable Solar Energy: Research, Education, and Outreach Initiatives"

Category: Environment

This project seeks to establish a state-of-the-art Optics & Photonics Laboratory at NTU "KhPI" focused on advancing sustainable solar energy solutions. By leveraging photonics technologies, the project aims to optimize the conversion of solar energy into electrical and thermal energy, specifically in the context of hybrid solar installations. The project's key objectives include conducting cutting-edge scientific research, fostering the education of students and young researchers, and promoting solar energy awareness through various outreach initiatives. Through the acquisition of necessary equipment, participation in conferences and workshops, and organization of educational events, the project aims to contribute to the growth of solar energy research and its practical implementation, while inspiring the next generation of scientists and engineers in the field of optics and photonics.

My active work is focused on scientific research in the field of solar energy and the use of solar radiation and on their popularization among schoolchildren and young people. For this, the Department of Micro- and Nanoelectronics of NTU "KhPI" was equipped with an Optics & Photonics Laboratory, the equipment of which included optometric devices as well as solar radiation simulators and measuring devices for research aimed at increasing the conversion of solar energy into electrical and thermal energy. In addition to purely scientific research, the laboratory was a base for conducting introductory workshops and STEM events aimed at encouraging school-age children to engage in science. Based on this laboratory, I conducted research in the field of thermophotovoltaic solar energy conversion systems as the basis of my doctoral dissertation. This year, two new post-graduate students are to join the research, whose scientific work is also planned to be aimed at optimizing the processes of simultaneous production of thermal and electrical energy by hybrid solar installations.

However, during the war, Kharkiv suffered significant destruction, in particular, a direct missile hit practically destroyed the educational building in which the department and the actual laboratory are located. The premises were severely damaged; some of the equipment was lost. Currently, we have a new premises and have begun to actively work on the restoration of the laboratory, the purpose of which is aimed at scientific research and raising awareness of the processes related to the production of electricity at photovoltaic power plants, the creation of photovoltaic systems, thermophotovoltaic systems and other design solutions, as well as motivation young people to choose this direction as a future profession and specialty.

The opportunity to equip a new laboratory will be the basis for continuing my scientific work, the work of my graduate students, and conducting activities to popularize solar energy and the physical principles of using solar radiation (trainings, master classes, STEM events).

The importance of my work is due to the fact that in recent years Ukraine has gone through a rapid path of development of alternative energy, business began to rapidly enter the field of renewable energy, due to which large capacities of solar and wind power plants were built. Now the emphasis on the development of alternative energy has changed and the greatest attention has begun to be paid to compact solutions aimed at providing not only electrical energy, but also thermal energy, and optical solutions for such projects are decisive for their success - first of all, we are talking about the study of solar radiation concentration processes in order to reduce the number of used solar cells. Receiving the grant will allow our team to accelerate research into optical elements for such photo-energy systems.

Thanks to the Grant, we will be able to conduct optical experiments involving licensed software packages and accelerate work on equipping the Optics & Photonics Laboratory for the manufacture and testing of experimental samples. As part of the Grant, we will pay attention to marketing research and participation in conferences and workshops, which will ensure active promotion of the results of our research among representatives of the business community. With the involvement of domestic business, we will achieve a truly broad introduction of research results at the Optics & Photonics Laboratory into the life of our country. Particular attention is planned to be given to the participation of the newly equipped laboratory in educational projects such as master classes, STEM events to spread the ideas of renewable energy among schoolchildren and involve young people in research in the field of optics and photonics.

The presence of an Optics & Photonics Laboratory with appropriate equipment on the campus of our university will expand the participation of our team in borderline research of colleagues from other fields in order to strengthen the role of optical sciences in the general spectrum of university research.

Project Title: "Photonics-Driven Solutions for Sustainable Solar Energy: Research, Education, and Outreach Initiatives"

Category: Environment

- **Literature Review**

The research and development of photonics-driven solutions for sustainable solar energy have gained significant attention in recent years. This literature review aims to provide an overview of key studies and advancements in this field, highlighting the role of photonics technologies in optimizing the conversion of solar energy into electrical and thermal energy. It explores research efforts, educational initiatives, and outreach activities that have contributed to the growth and implementation of sustainable solar energy solutions.

Photonics Technologies for Solar Energy Conversion:

Photonics technologies, including optics and photonics-based devices, play a crucial role in enhancing the efficiency and performance of solar energy conversion systems. One of the key areas of research is the development of photovoltaic (PV) systems. Researchers have explored various techniques to improve light absorption, charge carrier generation, and collection efficiency in solar cells. Nanostructured materials, such as quantum dots and plasmonic nanoparticles, have shown promise in enhancing light absorption and reducing reflection losses.

Furthermore, researchers have focused on novel approaches to concentrate and manage solar radiation for more efficient energy conversion. Concentrated photovoltaics (CPV) systems, which utilize optical elements to focus sunlight onto high-efficiency solar cells, have demonstrated higher energy conversion efficiencies compared to conventional PV systems. Advances in optical design, such as nonimaging optics and micro-optical elements, have contributed to the development of efficient CPV systems.

In addition to photovoltaics, solar thermal technologies have also benefited from photonics-driven solutions. Concentrated solar power (CSP) systems utilize mirrors or lenses to concentrate sunlight onto a receiver, which generates heat for power generation or other applications. Optical elements, such as Fresnel lenses and parabolic trough reflectors, have been studied to optimize light concentration and improve the overall efficiency of CSP systems.

Educational Initiatives and Outreach:

The promotion of solar energy awareness and education plays a vital role in the adoption of sustainable energy solutions. Many research institutions and organizations have initiated educational programs and outreach activities to engage students, young researchers, and the general public in the field of solar energy.

These initiatives often include hands-on workshops, seminars, and training sessions focused on the principles of solar energy, photovoltaic technologies, and optical design for solar applications. Such programs aim to inspire the next generation of scientists and engineers, nurturing their interest in sustainable energy research and technology development.

Collaborations between research institutions, industry partners, and educational institutions have also been instrumental in providing practical training opportunities for students. Internships, research projects, and joint ventures allow students to gain firsthand experience in working with photonics technologies and their application in solar energy systems.

Research and Development Collaborations:

Collaborative efforts between researchers, industry stakeholders, and policymakers have been crucial in advancing photonics-driven solutions for sustainable solar energy. International conferences, workshops, and symposiums provide platforms for knowledge exchange, showcasing the latest research findings, and fostering collaborations.

These collaborations have led to advancements in materials science, optical design, and manufacturing techniques for solar energy systems. Multidisciplinary research teams bring together experts from various fields, including physics, engineering, materials science, and optics, to address the complex challenges associated with solar energy conversion.

Furthermore, collaborations between academia and industry facilitate the transfer of research outcomes into practical applications. Industry partners provide valuable insights into market requirements and help bridge the gap between laboratory-scale innovations and commercial viability.

The literature review highlights the significance of photonics technologies in optimizing the conversion of solar energy into electrical and thermal energy. Research efforts have focused on enhancing the efficiency of photovoltaic and solar thermal systems through advanced optical design, novel materials, and light management strategies. Educational initiatives and outreach activities have played a crucial role in raising awareness, inspiring young researchers, and promoting the adoption of sustainable solar energy solutions. Collaborative efforts between research institutions, industry partners, and policymakers have accelerated the development and implementation of photonics-driven solutions for sustainable solar energy.

- **Problem Statement/Objective**

Problem Statement:

The conversion of solar energy into electrical and thermal energy is a key component of sustainable energy solutions. However, the efficiency and cost-effectiveness of current solar energy systems can be improved. There is a need to optimize the conversion processes, particularly in the context of hybrid solar installations, which combine photovoltaic and solar thermal technologies. Additionally, there is a lack of awareness and understanding among the general public about solar energy and its potential benefits. There is a need to address these challenges through research, education, and outreach initiatives.

Objective:

The objective of this project is to establish a state-of-the-art Optics & Photonics Laboratory at NTU "KhPI" focused on advancing sustainable solar energy solutions. The project aims to optimize the conversion of solar energy into electrical and thermal energy using photonics technologies, specifically in the context of hybrid solar installations. The project has three main objectives:

- Research: The project aims to conduct cutting-edge scientific research to enhance the efficiency, durability, and cost-effectiveness of solar energy conversion. The focus will be on developing innovative solutions for hybrid solar installations through the exploration of novel materials, device designs, and optical systems. The research outcomes will contribute to the growth of solar energy research and its practical implementation.
- Education: The project aims to foster the education of students and young researchers in the field of optics and photonics. The Optics & Photonics Laboratory will provide a platform for hands-on experiments, theoretical lectures, and collaborative projects, equipping students with practical skills and knowledge related to solar energy technologies. The goal is to inspire and cultivate the next generation of scientists and engineers in the field of sustainable solar energy.
- Outreach: The project aims to promote solar energy awareness and engagement among the general public. Various outreach initiatives, such as workshops, seminars, and public lectures, will be organized to disseminate knowledge about solar energy technologies, their advantages, and their societal impact. Partnerships with schools, environmental organizations, and industry stakeholders will be established to foster collaborations and share expertise, thereby expanding the reach and impact of the project.

By achieving these objectives, the project will contribute to the optimization of solar energy conversion, the growth of solar energy research, and the practical implementation of sustainable solar energy solutions. It will also inspire and educate students, researchers, and the wider community about the benefits and possibilities of solar energy, fostering a more sustainable future.

- **Outline of tasks/Work Plan**

Year 1:

1. Laboratory Setup and Equipment Acquisition:

- Identify and procure necessary equipment for the Optics & Photonics Laboratory, including optometric devices, solar radiation simulators, and measurement instruments.
- Set up the laboratory space, ensuring proper infrastructure and safety measures.

Research Initiation and Collaboration:

- Formulate research objectives and identify key areas of focus, such as optimizing solar energy conversion in hybrid solar installations.
- Establish collaborations with other research institutions and industry partners to leverage expertise and resources.
- Conduct a comprehensive literature review to identify gaps in the field and determine research directions.

2. Experimental Design and Data Collection:

- Design experiments and methodologies to investigate photonics-driven solutions for sustainable solar energy.
- Set up experimental setups, ensuring accurate measurements and reliable data collection.
- Collect experimental data on solar energy conversion efficiency, thermal management, and optical design parameters.

3. Analysis and Results:

- Analyze experimental data using appropriate statistical and analytical tools.
- Evaluate the performance and efficiency of different photonics technologies and approaches.
- Identify key findings, insights, and areas for improvement.

4. Education and Outreach Initiatives:

- Organize workshops, seminars, and training sessions to educate students and young researchers on solar energy technologies and photonics principles.
- Conduct introductory programs and STEM events for schoolchildren to raise awareness and interest in solar energy.
- Collaborate with schools, environmental organizations, and industry partners to expand outreach efforts.

Year 2:

1. Research Refinement and Optimization:

- Based on the findings from Year 1, refine research approaches and methodologies.
- Explore advanced materials, device designs, and optical systems to optimize solar energy conversion.
- Investigate novel approaches for concentration, light management, and heat management in hybrid solar installations.

2. Data Analysis and Publication:

- Complete the analysis of experimental data and generate meaningful conclusions.
- Prepare research papers and manuscripts for publication in reputable scientific journals.
- Present research findings at national and international conferences, fostering collaborations and knowledge exchange.

3. Education Enhancement and Mentorship:

- Expand educational initiatives by developing advanced training modules and practical sessions.
- Mentor students and young researchers, providing guidance and support in their research endeavors.
- Encourage student participation in research projects and facilitate their professional development.

4. Industry Collaboration and Technology Transfer:

- Strengthen collaborations with industry partners to bridge the gap between research outcomes and practical applications.

- Conduct market research and identify potential commercialization opportunities for photonics-driven solar energy solutions.
- Facilitate technology transfer through licensing agreements, patents, or industry-sponsored projects.

5. Continued Outreach and Dissemination:

- Organize public lectures, symposiums, and exhibitions to promote solar energy awareness among the general public.
- Collaborate with media outlets to disseminate research findings and increase public understanding of solar energy technologies.
- Engage in community outreach activities, fostering sustainable energy practices and inspiring future generations.

Throughout the two-year work plan, regular project monitoring and evaluation should be conducted to assess progress, identify challenges, and make necessary adjustments. Flexibility and adaptability in the work plan will allow for incorporating emerging research trends and industry developments to maximize the impact of the project.

- ***Outcome(s)***

1. Enhanced Efficiency of Solar Energy Conversion:

Through the research conducted in the Optics & Photonics Laboratory, the project aims to achieve advancements in the efficiency of solar energy conversion. This includes optimizing the conversion processes in hybrid solar installations, improving the performance of photovoltaic and solar thermal systems, and exploring novel materials and optical designs. The project aims to demonstrate improved conversion efficiencies and cost-effectiveness of solar energy systems, contributing to the development of sustainable energy solutions.

2. Cutting-Edge Scientific Research:

The project will contribute to the body of scientific knowledge in the field of photonics-driven solutions for sustainable solar energy. By conducting cutting-edge research, publishing research papers, and presenting findings at conferences, the project aims to advance the understanding of solar energy conversion processes and the role of photonics technologies. The research outcomes will provide insights into optimal design strategies, materials, and system configurations for maximizing solar energy utilization.

3. Education and Capacity Building:

The establishment of the Optics & Photonics Laboratory will provide a platform for education and capacity building in the field of optics, photonics, and solar energy. Through workshops, seminars, and training sessions, students and young researchers will gain practical skills and knowledge in solar energy technologies, photonics principles, and experimental techniques. The project aims to inspire and cultivate a new generation of scientists and engineers who are well-equipped to contribute to the field of sustainable solar energy.

4. Increased Solar Energy Awareness and Outreach:

The project recognizes the importance of raising public awareness about solar energy and its potential benefits. Through various outreach initiatives, including workshops, seminars, public lectures, and collaborations with schools and environmental organizations, the project aims to promote solar energy literacy among the general public. Increased awareness and understanding of solar energy will encourage wider adoption and implementation of sustainable energy practices.

5. Collaboration and Industry Engagement:

The project aims to foster collaborations with industry stakeholders, research institutions, and policymakers. These collaborations will facilitate the transfer of research outcomes into practical applications, bridging the gap between laboratory-scale innovations and commercial viability. By engaging with industry partners, conducting market research, and exploring potential

commercialization opportunities, the project aims to contribute to the growth of the solar energy industry and the implementation of photonics-driven solutions.

Overall, the preliminary outcomes of the project encompass advancements in solar energy conversion efficiency, scientific research contributions, education and capacity building, increased solar energy awareness, and collaboration with industry stakeholders. These outcomes will collectively contribute to the development and practical implementation of sustainable solar energy solutions, fostering a more sustainable and energy-efficient future.

- **Impact**

1. Advancement of Sustainable Energy Solutions: The project's impact lies in its contribution to the advancement of sustainable energy solutions, specifically in the field of solar energy. By optimizing the conversion of solar energy into electrical and thermal energy using photonics-driven approaches, the project aims to increase the overall efficiency and cost-effectiveness of solar energy systems. This impact extends to both residential and industrial applications, fostering a transition towards cleaner and more sustainable energy sources.

2. Environmental Benefits: The project's focus on sustainable solar energy solutions directly contributes to environmental benefits. By improving the efficiency of solar energy conversion, the project reduces reliance on fossil fuels and decreases greenhouse gas emissions. Increased adoption of solar energy systems, facilitated by the project's research, education, and outreach efforts, can lead to a significant reduction in carbon dioxide emissions and mitigate the impact of climate change.

3. Economic Growth and Job Creation: The project has the potential to stimulate economic growth and job creation in the renewable energy sector. As solar energy systems become more efficient and cost-effective, there is an increased demand for their installation and maintenance. This creates opportunities for the growth of solar energy businesses, job creation in manufacturing and installation, and the development of local supply chains. The project's collaboration with industry partners also fosters technology transfer and commercialization, contributing to the growth of the solar energy industry.

4. Education and Skill Development: The project's educational initiatives have a lasting impact on students and young researchers. By providing practical training, hands-on experience, and knowledge in optics, photonics, and solar energy technologies, the project equips individuals with the skills and expertise needed for careers in the renewable energy sector. This contributes to human capital development and empowers the next generation of scientists and engineers to tackle complex challenges related to sustainable energy.

5. Increased Public Awareness and Engagement: Through its outreach initiatives, the project raises public awareness about solar energy and its potential benefits. By organizing workshops, seminars, public lectures, and collaborations with schools and environmental organizations, the project educates and engages the general public in sustainable energy practices. This increased awareness leads to greater public support for renewable energy policies, encourages individual adoption of solar energy technologies, and promotes a more sustainable and energy-conscious society.

6. Scientific and Technological Advancement: The project's cutting-edge scientific research contributes to the broader field of optics, photonics, and solar energy. By generating new knowledge, innovative solutions, and research publications, the project strengthens the scientific community's understanding of solar energy conversion processes and photonics technologies. This advancement facilitates further research and technological developments, paving the way for future breakthroughs and discoveries in the field.

Overall, the project's impact encompasses environmental benefits, economic growth, education and skill development, increased public awareness and engagement, and scientific and technological advancement. By addressing the challenges in solar energy conversion and promoting sustainable practices, the project contributes to a more sustainable and resilient energy future.

Summary: Optical techniques are valuable for diagnosing and treating disease because optical spectroscopic interactions with molecules confer specificity with regard to target biochemical information and quite favorable spatial resolution. Yet, tissues strongly scatter light, making tissue opaque within tens to hundreds of μms of propagation depth, moderating the success of optical biomedical imaging.

Some cancers are very difficult to detect with current technologies. As early detection leads to much better outcomes and lower mortality rates, new diagnostics technologies could profoundly impact our ability to detect and successfully treat disease. I am motivated by ovarian cancer, which is extremely difficult to detect and is usually detected at a late stage where treatments suffer from low efficacy.

I am focusing second harmonic generation (SHG) microscopy which is already established as a powerful tool for biological imaging. SHG has proven diagnostic and prognostic capabilities for a wide range of diseases. Of prominence is the use of SHG imaging to grade cancerous tumors by quantifying the type of organization of collagen around tumors. Moreover, cancers tend to reorganize collagen to present a spiral structure that aids in differentiating healthy tissues, benign tumors, and cancers. Despite this potential, SHG imaging is limited in imaging depth. As a result, non-invasive biological imaging (e.g., optical pathology without the need for surgery) is restricted to superficial tissues or through endoscopy and current SHG microscopy technology is extremely limited in its potential for use with *in-vivo* optical biopsies.

I propose a new approach to rendering opaque tissue effectively transparent using both advanced data science tools and wavefront control to sidestep the current limitations that restrict the SHG imaging depth. This is a radical departure from the conventional paradigm for nonlinear microscopy that relies on scanning a ballistic focus in the specimen and forming an image from the measured power from each focal point. Depth imaging is severely limited because the ballistic light intensity decays exponentially with depth.

This proposal seeks to remedy the deficiency in the limited imaging depth by posing the question: rather than throwing away multiply scattered (MS) light, can we redirect it into image formation? I will explore two methods of harnessing MS light for SHG imaging (e.g., collagen in the extracellular matrix around tumors) at unprecedented imaging depths in tissues. In Aim 1, I will unscramble the SHG light exiting the tissue to remap that information into an image deep within tissue. SHG fields exiting the tissue will be recorded with nonlinear holography. Since the SHG field propagates through tissue, the field is spatially randomized (exits as speckle). The speckle field is a distinct fingerprint of each SHG scattering source point. With a set of measurements that vary the SHG signal brightness spatially, the mapping between the SHG source points and the measured speckle will be uncovered. Armed with the random SHG speckle fingerprint for each point in the object field, the SHG image will be revealed by unscrambling the SHG light that was randomized with propagation through the tissue. Thus, I will break free from relying on image formation by scanning a ballistic focus. In Aim 2, the data will be used to estimate the transmission matrix for the fundamental field. This matrix operator describes the distortion of the input fundamental field at the image plane. This information will be used to focus the wave in the object plane through wavefront shaping to further improve the SHG image quality and enable deeper imaging depths.

This new approach to *in-situ* fundamental transmission matrix estimation opens new avenues of imaging by avoiding the need for a detector in the tissue (not possible) or relying on the accidental existence of a nonlinear guide star. Moreover, the wavefront reshaping increases the SHG signal power, and thus the image quality, and allows for increasing imaging depth. This could change the landscape for deep tissue imaging. Simulations will be employed to study the limits of imaging depth. Data from these experiments will be combined with simulation results to seek additional funding for pushing this new imaging approach to unprecedented imaging depths.

Project outcomes: A) Demonstrate unscrambling of measured SHG speckle fields to obtain an SHG image field deep in tissue. B) Demonstrate estimation of the transmission matrix of the fundamental field to the SHG image plane and use that transmission matrix to generate a brighter focus and a higher quality SHG image. C) Enable deeper imaging by pushing the depth where bright SHG imaging can be accomplished. D) Capture a set of data that will be used for papers, talks, and as preliminary data for future funding.

Re-purposing multiply scattered light for early ovarian cancer diagnostic with deep tissue second harmonic generation

Annually, more than 200,000 women succumb to death by ovarian cancer, with nearly 13,000 of those deaths occurring in the United States alone. Ovarian cancer is the most lethal gynecological malignancy due in large part to a lack of methods for early-stage detection[1]. Typically, ovarian cancer is detected at a later stage where 5-year survival rates hover at $\sim 39\%$ because, at the later stages, the tumor has metastasized and likely spread throughout the body. Early detection through routine screening is a potent tool in our arsenal to fight cancer. This benefit is evidenced by the fact that when detected in stage I, the 5-year survival rate jumps to 94%. Unfortunately, the early-stage diagnosis rate is below 16% due to the lack of effective screening methods. *We propose to pave the way for the use of second harmonic generation (SHG) microscopy as a minimally invasive early diagnostic tool for ovarian cancer (and other cancers in the future) by developing an approach to mitigate the fundamental barrier for deep nonlinear microscopy imaging.*

The two standard methods used in ovarian cancer screening provide early detection only in one out of six patients, accounting for the high mortality rate. The serum cancer antigen 125 levels assay has limited sensitivity, while transvaginal ultrasound provides limited resolution and contrast. Optical imaging has been recognized as an invaluable tool for observing and diagnosing diseases with higher sensitivity and resolution. Yet to date, optical diagnostic methods are not capable of detecting early ovarian cancers. Optical methods are limited by the fact that variations in the refractive index (RI) present in tissues scramble the propagation of light. This multiple scattering (MS) causes a loss of image information when light propagates through tissue.

Several standard imaging methods are impressively wielded to improve imaging depth by exploiting a mechanism that separates the light that has *only* interacted with the desired object (single scattering, SS, the events that carry image information) from the MS light that has completely scrambled image information. Confocal imaging isolates SS from MS light spatially with a pinhole, optical coherence tomography separates SS light through interference with a coherent reference, and nonlinear microscopy relies on intensity-dependent nonlinear excitation to preferentially probe the object with ballistic light and reject MS light. Until recently, these techniques represented the state-of the art.

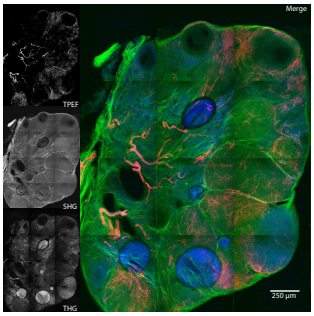

Figure 1: Two-photon excited fluorescence (TPEF), second- and third-harmonic generation (SHG, THG) images of fixed murine ovarian tissue, acquired in the Bartels laboratory circa 2012. Each image represents a maximal projection through 250 μm of tissue.

We focus on SHG imaging, a form of nonlinear microscopy that can be used to take advantage of optical physics principles that remain unexplored for deep imaging in tissues. SHG imaging is powerful as a non-invasive, label-free screening method for ovarian cancer and diagnostic potential in general[2,3]. SHG imaging uses collagen, a structural network protein in the tissue extracellular matrix (ECM), as a biomarker. The lateral and axial resolution of ovarian cancer samples by SHG imaging can approach $< 1\,\mu$m laterally and $< 3\,\mu$m axially[4]. Imaging collagen using SHG could distinguish ovarian cells as normal, malignant, benign, or borderline[5]. A machine-learning-enabled polarimetric SHG microscopy method was reported to enable label-free diagnosis of breast cancer tissues with an accuracy $> 90\%$ [6]. *Due to the limitations of optical scattering in state of the art in SHG microscopy, optical diagnostics based on SHG are restricted to invasive biopsies that study tissue removed from the patient.*

It is recognized that the tissue microenvironment – that is the milieu of cells, ECM, signaling molecules, nutrients, and vasculature surrounding cells within a cancerous tumor – drastically modulates the behavior of the cancer cells that one wishes to eliminate with treatments. While many studies and diagnostic tools avoid the issue of optical scattering by using cells or tissues extracted from patients, tissues and cells out of the body exist in a manifestly different environment than that within the host body. Access to optical

biopsies inside of tissue is critical for both disease diagnosis and for the monitoring of treatment efficacy. As a consequence, there is a pressing need for *in-vivo* optical diagnostics of tumors. Although the infiltration depth of SHG imaging is $200\,\mu$m, MS renders tissue opaque for the imaging depths where subsurface stage I ovarian cancers arise within an inclusion cyst (usually detectable at the depth of a few millimeters).

A. New strategies to exploit optical physics to push SHG microscopy deep into tissues. In the past few years, new strategies have emerged to improve imaging depth. These strategies rely on the random variation of RI that causes scattering remaining stationary (i.e., not moving) on some timescale over which imaging is performed. Treating tissue as such a disordered system admits the ability to unscramble multiple scattering (MS) effects. Light propagation, even though a disordered system, is linear. As a result, the disordered medium can be characterized by a (very complicated) linear transfer matrix, **T**. Many clever strategies have enabled the use of wavefront shaping of light incident on the disordered tissue to undo the multiple scattering[7]. Still, aside from a few cases, a detector must be placed behind the tissue through which imaging occurs This requirement severely limits the usefulness of standard wavefront shaping strategies.

A few years ago new innovations emerged for exploiting the disorder of a random RI distribution while not requiring a detector to be placed behind the section of tissue that is to be imaged through. The idea is simple: in a thin object, transverse scattering vectors are preserved when the incident angle on the object is changed due to the single scattering (SS) angular memory effect (SAME)[8,9]. This scattering conservation can be retained when using a short longitudinal source (broad optical bandwidth) in holographic imaging. By measuring the output *field*, rather than the intensity, and noting that the input and output spatial frequencies can be related to the object spectrum with SAME, summation of the coherent scattered light is constructive. By contrast, summation of the MS field is characterized by a random walk, and the coherent sum averages to zero. The result is a new method to reject the MS field and preserve the SS field, improving image quality by a factor of N over the same number of intensity averages.

To date, only methods that exploit linear scattering for coherent field enhancement have been demonstrated. My postdoctoral research is aimed at exploiting the coherent field summation demonstrated for linear scattering (as described above) with coherent nonlinear scatting, e.g., SHG. This strategy isolates only the SS events – requiring that light be ballistic on the way in and on the way out of the tissue.

Optical physics problem: All of these methods for pushing imaging depth deep into tissues rely on a critical limitation: separating SS from MS light. This requirement suffers from a fundamental limitation that the SS light extracted for imaging also requires that the light used for imaging is unscattered (ballistic) both on the way into and out of the tissue.

B. Proposed work: Coherent SHG imaging with MS light. We propose to bypass the conventional depth limitations of nonlinear optical microscopy by harnessing, rather than suppressing MS light. To demonstrate this new paradigm, I will focus on coherent SHG imaging. The approach is broken into two Aims: 1 seeks to unscramble the SHG signal light as it exits the tissue, and 2 seeks to harness information obtained from 1a to use wavefront shaping to undo the scattering of fundamental light as it propagates into the tissue. The conceptual shift is illustrated in Fig. 2. I propose to explore new strategies that will redirect MS light for SHG imaging, rather than the standard approach of using ballistic light, which decays exponentially with propagation depth. Significant increases in imaging depth will be possible by using, rather than discarding, MS light. This task is complicated by the fact that I cannot place a detector on the distal side of the section of scattering tissue that I wish to image through. I propose two Aims:

Aim 1. Direct SHG imaging in scattering media by unscrambling MS of the SHG field optically scattered as it exits the tissue. Current nonlinear optical microscopy methods rely on the propagation of ballistic light into the tissue to produce an image. The ballistic focus is scanned in three dimensions to form an image (Fig. 1). Unfortunately, ballistic light intensity decays exponentially with propagation depth into the tissue. This decay is the primary limit on the imaging depth. A new strategy for imaging is proposed that will circumvent this limit. The idea is to unscramble the coherent nonlinear scattered light by developing a strategy inspired by the use of non-negative matrix factorization (NMF) for fluorescent imaging[10].

The challenge in this approach is that NMF has not been developed for complex-valued matrices, which must be used to describe coherent light. To tackle this problem, I propose to measure the coherent SHG field with the epi-holography setup and then use the field to estimate the output speckle fields for each scattering point from the object that generates the SHG signal. The SLM in the system will be modulated to sweep through illumination field perturbations that will vary the excitation amplitude and thus the brightness of the SHG scattering spatially. With a suitably large set of measurements, i.e., larger than the number of independent spatial points that I wish to resolve, the measured field data matrix can be factored into a product of low-rank matrices. However, the data matrix will be complex and thus I require a strategy for separating the speckle patterns for the measured SHG field. This will be accomplished using emerging algorithms for complex NMF. Once the output speckle fields are obtained for each SHG image point, the images will be obtained by decorrelation with the speckle fields. In addition, I will be able to extract the illumination field transmission function, which will give us access to information needed for improved SHG signal generation and imaging depth with wavefront shaping.

This approach is inspired by a recent strategy for fluorescent microscopy that avoids the need for a detector behind the scattering medium. The key idea is that an image of a single-point fluorescent emitter will produce an intensity speckle pattern that is unique to that fluorescent source. Because of the spatial incoherence, the image intensity for multiple fluorescent sources is a sum of the speckle intensity patterns from each source. The recorded fluorescent image is a linear sum of the speckle intensity patterns weighted by the brightness of each source. The clever approach is to cycle through a sequence of random illumination patterns that vary the brightness of the fluorescent sources. Applying NMF to a large set of intensity images, the speckle patterns for each source, images, and the illumination transmission matrix can all be extracted.

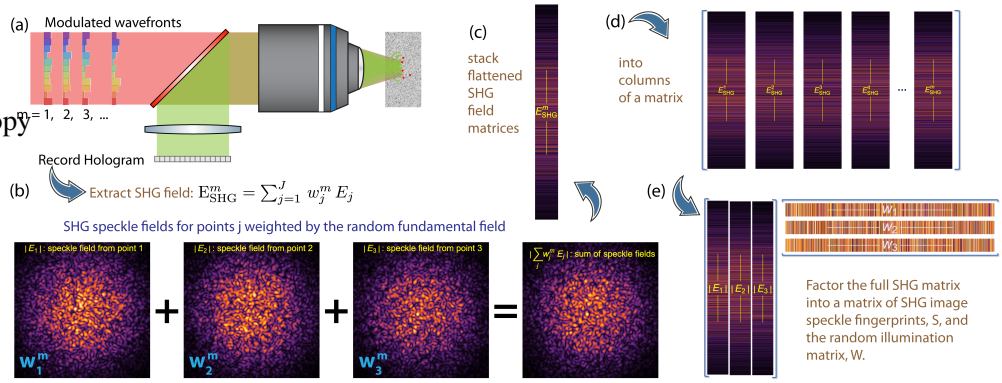

Figure 2: Concept for using MS light for SHG microscopy (described in text).

Figure 2 shows the concept for unscrambling MS SHG light exiting tissue. The approach revolves around epi-SHG holographic imaging of objects embedded in tissue. SHG holography allows for quantitative extraction of the SHG field. Because the SHG light generated by the object must pass through a large section of tissue, MS scrambles the image information. A single-point SHG scatterer will produce a speckle SHG field that is extracted from the hologram. The total recorded field is a sum over all SHG speckle patterns from each object point. The key observation is that each speckle field $\mathbf{E}_j$ does not change when the fundamental illumination light is changed.

However, for a given measurement, there is no way to disentangle the SHG image field produced by the object and the randomization of that field as it passes through the tissue before being captured in the hologram. While SHG scales nonlinearly with the illumination light, the propagation of the SHG field out of the can be modeled with a linear operator $\mathbf{T}_{\mathrm{SHG}}$, that maps the SHG field in the object plane $\mathbf{E}_{\mathrm{obj}}$ to the camera plane $\mathbf{E}_{\mathrm{SHG}} = \mathbf{T}_{\mathrm{SHG}}\,\mathbf{E}_{\mathrm{obj}}$. Written as a matrix equation, $\mathbf{E}_{\mathrm{obj}}$ and $\mathbf{E}_{\mathrm{SHG}}$ are column vectors (flattened images) and $\mathbf{T}_{\mathrm{SHG}}$ is a matrix. Our goal is to estimate $\mathbf{T}_{\mathrm{SHG}}$ so that image information can be recovered.

To obtain the image, more information is needed. This can be accomplished by exploiting the fact that $\mathbf{T}_{\mathrm{SHG}}$ remains unchanged while $\mathbf{E}_{\mathrm{obj}}$ is varied. Additional information is injected by modulating the input fundamental beam wavefront (Fig. 2a). As the object field is modulated, a variation of a complex weight, w_j^m, for each SHG scattered point in the object is produced. The SHG field extracted from the hologram (for

the m$^{\text{th}}$ modulation pattern) can be expressed as $\mathbf{E}^m_{\text{SHG}} = \sum_j w^m_j \mathbf{E}_j$, (Fig. 2b). To extract useful information, many modulated wavefronts are cycled through, leading to random variations of w^m_j. Each extracted SHG field, $\mathbf{E}^m_{\text{SHG}}$, is flattened (Fig. 2c) and stacked into columns of an SHG field matrix (Fig. 2d). Because of the limited information in this matrix (i.e., that speckle fields $\mathbf{E}_j$ are invariant to the modulation variation of the fundamental illumination wave), the matrix is low-rank (rank is determined by the number of SHG image points in $\mathbf{E}_{\text{obj}}$). Thus the matrix can be factored as: $\mathbf{A}_{\text{SHG}} = \mathbf{T}_{\text{SHG}}\,\mathbf{W}^T$ (see Fig. 2e). Here $\mathbf{T}_{\text{SHG}}$ is constructed from columns of the flattened speckle fields $\mathbf{E}_j$ and $\mathbf{W}$ is the set of columns given by the vector w^m_j that is formed from the sequence of modulated fundamental wavefronts at each point j. I hypothesize that the factorized matrix product to obtain $\mathbf{S}$ and $\mathbf{W}$ can be computed from a complex NMF (CNMF) of the data matrix $\mathbf{A}_{\text{SHG}}$. Note that CNMF is a generalization of NMF that is widely used in data science and has been demonstrated for extraction of speckle fingerprints for incoherent light scrambled by a scatterer.

The goal is then to use $\mathbf{T}_{\text{SHG}}$ to estimate the object by inverting the equation $\mathbf{E}^m_{\text{SHG}} = \mathbf{T}_{\text{SHG}}\,\mathbf{E}_{\text{obj}}$. Although a direct inverse is not possible, $\mathbf{E}_{\text{obj}}$ can be estimated using a regularized inverse problem approach. This approach will enable nonlinear imaging in tissue to break free from the limitation of requiring ballistic light to extract the coherent image. In addition, the set of M modulations can be used to coherently sum the SHG field measurements, resulting in a boost of M in the coherent sum of the SHG fields over simple averaging of image intensities.

Aim 2. Increased SHG brightness and imaging depth using $\mathbf{E}_{\text{obj}}$ obtained from Aim. 1. As light propagates in tissue, scattering distorts the light, spreading out the beam spatially and stretching pulses in time. Both of these effects decrease the intensity of the beam in the sample. The drop in intensity decreases nonlinear scattering (such as SHG). While an increase in incident beam energy can compensate for the pulse broadening, even this standard tactic for imaging deep with nonlinear signals is severely limiting. Initial work has shown that by shaping the input wavefront, a beam focus in space and time can be attained by driving constructive interference between sets of scattering paths. Wavefront shaping can increase the beam intensity by orders of magnitude, thereby enabling nonlinear signal increases by orders of magnitude. Yet this strategy is limited because these methods largely rely on measurement of the transmission matrix, which has relied on the placement of a camera on the other side of the tissue.

The goal of Aim 2 is to to boost the SHG signal and penetration depth by unscrambling the illumination (fundamental) light using the transmission matrix estimated in Aim 1. Shaping the wave entering tissue can produce a focused beam (in both space and time) deep inside the tissue that can boost nonlinear signal generation[11]. So far, this has only been accomplished with either a detector must be placed on the far side of the tissue or a nonlinear guide star (a bright, isolated point nonlinear object). Neither approach is practical in situations for non-invasive biomedical imaging. I propose to use the estimate of the transmission matrix $\mathbf{T}_{\text{fund}}$ from Aim 1 to pre-compensate for the scrambling of incident fundamental beam by the tissue. The incident fundamental field at the object plane is given by the linear mapping $\mathbf{E}_{\text{fund}} = \mathbf{T}_{\text{fund}}\,\mathbf{E}_{\text{in}}$. Here, $\mathbf{E}_{\text{in}}$ is the input fundamental field and $\mathbf{T}_{\text{fund}}$ is the linear scattering transmission matrix for the incident field. The object SHG field is then generated by $\mathbf{E}_{\text{obj}} = \chi^{(2)}\,\mathbf{E}^{\odot 2}_{\text{fund}}$. The operator $\odot$ in the square of the fundamental field is an element-wise squaring operation. Observing that the weight in the SHG field at an image point j is simply given by $w^m_j = \chi^{(2)}\,\mathbf{E}^{\odot 2}_{\text{fund}}$, one may use the W matrix obtained from the CNMF algorithm to solve for the input transmission matrix by solving the equation $\mathbf{W} = (\mathbf{T}_{\text{fund}}\,\mathbf{E}_{\text{in}})^{\odot 2}$. Again, this will be treated as an inverse problem from which I will obtain an estimate of $\mathbf{T}_{\text{fund}}$. Armed with $\mathbf{T}_{\text{fund}}$, a spatial frequency phase mask that is applied to the SLM can be used to focus the fundamental field onto the object, producing a brighter SHG field that is extracted from the hologram. Using the estimate of the $\mathbf{T}_{\text{SHG}}$, the SHG object field can be extracted from the complex field obtained from the SHG hologram.

Going deeper: This strategy for deeper imaging will be pursued iteratively. Confidence in the iterative approach is high because I have observed in simulations that a wavefront correction persists over some range of optical depth in the tissue. Thus, I can shift to deeper imaging depths by controlling the arrival

time of the reference beam on the camera, which determines the depth form which $\mathbf{E}_{\text{obj}}$ is extracted. Aims 1 and 2 can be repeated deeper into the tissue to iteratively push to deeper imaging depths. This strategy will be explored more extensively theoretically using scattering propagation codes developed in the Bartels laboratory.

C. Tasks and work plan. All of the major equipment required for the proposed project exists in the Bartels laboratory, which will be at my disposal. These resources include scattering models and a full nonlinear SHG epi-holographic imaging system equipped with a high pixel density spatial light modulator (SLM), which was constructed for the aforementioned CZI project.

Aim. 1a (months 1-2): Develop simulations for CNMF of SHG field data to yield T_{SHG} and W matrices and obtain an SHG object field. **Aim. 1b (months 3-6):** Take data for a variety of samples (SHG-active objects) and scattering media (diffusers, tissue simulating phantoms, tissues) and process them to extract images with CNMF. **Aim. 2a (months 4-6):** Develop simulation for extracting T_{fund} from W. **Aim. 2b (months 7-12):** Take additional data and use those data to control the focused fundamental wavefront to improve the SHG image field brightness by using a wavefront-shaped field and image estimation from the previously obtain T_{SHG}.

D. Outcomes. A new approach to deep imaging by harnessing, rather than rejecting, MS light. Simulations that study the limits of imaging depth and validated with data. Preliminary results will use used to seek additional funding for pushing SHG imaging to unprecedented imaging depths, for clinical ovarian caner screening.

E. Impact. By making use of physics of optical scattering, we will open new avenues for deep tissue imaging. This work will prove the principles and feasibility of an imaging method that may allow for minimally invasive imaging of the ECM around tumors for expanded early screening of cancers, with a particularly high possible impact of detecting ovarian and possibly pancreatic cancers at early stages, which could save the lives of a majority of patients who now succumb to these diseases.

References

1. Huang J, et al., Worldwide Burden, Risk Factors, and Temporal Trends of Ovarian Cancer: A Global Study, Cancers 29, 2230 (2022).

2. Qian, S., et al., Identification of human ovarian cancer relying on collagen fiber coverage features by quantitative second harmonic generation imaging. *Optics Express* **30**(14), 25718, 7 (2022).

3. Campagnola, P. J. and Dong, C. Y. Second harmonic generation microscopy: Principles and applications to disease diagnosis. *Laser and Phot. Rev.* **5**(1), 13–26, 1 (2011).

4. Gant,K.L., et al., Evaluation of collagen alterations in early precursor lesions of high grade serous ovarian cancer by second harmonic generation microscopy and mass spectrometry. Cancers 13(11), 2794, 6 (2021).

5. Huttunen, M. J., et al., Automated classification of multiphoton microscopy images of ovarian tissue using deep learning. Journal of Biomedical Optics 23(06), 1, 6 (2018).

6. Mirsanaye, et al., Machine learning-enabled cancer diagnostics with widefield polarimetric second-harmonic generation microscopy. Scientific Reports 12(1), 1–14, 6 (2022).

7. Rotter, S. and Gigan, S. Light fields in complex media: Mesoscopic scattering meets wave control. Reviews of Modern Physics 89(1), 015005, 3 (2017).

8. Kang, S., Kang, P., Jeong, S. et al., High-resolution adaptive optical imaging within thick scattering media using closed-loop accumulation of single scattering. Nat. Commun. 8, 2157 (2017).

9. Badon, A., et al., Smart optical coherence tomography for ultra-deep imaging through highly scattering media. Science Advances 2, 1600370, (2016).

10. Zhu, L., Soldevila, F., Moretti, C. et al. Large field-of-view non-invasive imaging through scattering layers using fluctuating random illumination. Nat. Commun. 13, 1447 (2022).

11. de Aguiar, Hilton B., et al., Enhanced nonlinear imaging through scattering media using transmission-matrix-based wave-front shaping, Phys. Rev. A, 94 043830 (2016).

A low-cost integrated hyperspectral monitoring device for environmental pollution

Category: Environment

Environmental pollution poses serious threats to human health and well-being. It is crucial to assess the health of ecosystems and detect environmental changes for ecological protection and resource optimization. Current methods of monitoring environmental pollution rely on in-situ sampling, which is inefficient and limited in capturing the spatial and temporal variation of pollutants. Therefore, alternative methods are needed to address this global problem.

Hyperspectral imaging acquires spatial, temporal and spectral information of the physical world, characterizing the intrinsic optical properties of each location. It has been widely applied in environmental pollution monitoring which requires lightweight integration and superior spectral imaging performance. Most of the existing hyperspectral imaging systems employ individual optical elements and mechanical components to scan the dense spatial-spectral data cube, resulting in bulky configuration, low resolution, and high cost. The recent trials of on-chip spectral acquisition apply narrow-band filtering on different pixels, suffering from low light throughput, low resolution, and few channels. To sum up, there still exists a gap towards practical applications of lightweight high-resolution hyperspectral imaging.

To monitor the spatial and temporal variation of environmental pollution, we develop a novel on-chip computational imaging device capable of acquiring tens of hyperspectral images with full temporal and spatial resolution over a wide range.

We will report a novel on-chip computational imaging scheme for high-dimensional vision, providing details of hardware fabrication, optical calibration, and computational reconstruction. This technique integrates innovations from multiple fields, including materials, integrated circuit, computer science and optics. It transforms the common challenges of high-dimensional imaging, which are associated with the physical constraints of high-cost optical fabrication and complex system design, into challenges that can be solved by agile computation. Meanwhile, we will conduct a series of application experiments, including regional monitoring of water and air pollution. For the existing version of our device, the spectral response range covers from 400 nm to 1700 nm, with an average light throughput of 71.8%. It outperforms mosaic multispectral cameras and scanning hyperspectral systems in low-light conditions. The device has an average spectral resolution of 2.65 nm (400-1000 nm) and 8.59 nm (1000-1700 nm), with the ability to differentiate monochromatic light with a peak-to-peak spacing of 10 nm. The peak signal-to-noise ratio (PSNR) of spectral reconstruction achieves 32.5 dB tested on the ColorChecker Classic chart. Each channel consists of 2048 $\times$ 2048 pixels at a frame rate of 47 fps, maintaining 3.43 arc minute optical resolving ability at a 39-degree field of view. The high frame rate allows for the capture of fast-moving objects, facilitating dynamic imaging.

The demonstrated hyperspectral imaging sensor maintains great application potentials in off-of-the-shelf platforms such as unmanned aerial vehicle and nano satellite, as well as consumer electronic products such as smart phones and digital cameras. We anticipate that this technique to open a new venue for the next generation imaging sensor with higher information dimension, imaging resolution, and integration level. In this context, we are applying for the 2023 Optica Foundation Challenge to support our work to contribute to environmental protection.

A low-cost integrated hyperspectral monitoring device for environmental pollution

1 Background

With the rapid development of industrialization and urbanization, environmental pollution represents unprecedented challenges to humans. Good environmental conditions are a necessity for human survival and sustainable development. The study of ecosystem health and the identification of patterns in environmental changes are critical in protecting the ecological environment and optimizing resource allocation. Meanwhile, numerous contemporary studies have demonstrated that environmental pollution, particularly air pollution and water pollution, is a significant contributor to various illnesses in human beings. Hazardous compounds can be transferred to the human body through life activities such as breathing, eating, and drinking, thus causing major health issues. Air pollution has emerged as a global problem in recent years. It has been a primary cause of cardiovascular and chronic respiratory diseases, especially even the malfunctioning of the lungs. Similarly, water pollution is also a severe environmental and public problem. Continuous pollution has resulted in various water-associated disease epidemics, including gastrointestinal infections such as viral diarrhea, cholera, and salmonellosis. Prolonged consumption of water containing high concentrations of toxic substances such as mercury, chromium, and cadmium can also lead to neurological disorders, kidney disease, and cancer.

Fig. 1 Environmental pollution

Therefore, action is needed to create a safer, cleaner, and more comfortable future. Monitoring of specific regions is an effective measurement to address and alleviate the continued growth of these issues. Most of the current methods use the in-situ sampling approach to extract the air and water from the surroundings to check for the contaminants present in them. It is labor-intensive and time-consuming, and cannot easily be employed to monitor the spatial and temporal variation of environmental pollution.

Spectral imaging captures spatial and spectral information of a target, characterizing the intrinsic optical properties of each location. Combining the unmanned aerial vehicle (UAV) and the spectral camera, remote sensing can provide a reliable and effective tool for area monitoring and management of the environment, which is significant for long-time series and large-scale

monitoring. Differing from ocean water estimation and meteorological monitoring, the regional environment estimation is usually small, so the sensor used for data acquisition requires high spatial-spectral resolution. Multispectral and high-resolution remoting sensing sensors are commonly used for local environmental monitoring. Compared to multispectral imaging, airborne hyperspectral remote sensing acquires a significantly large number of wavelength channels ranging from tens to hundreds, and maintains a superior spatial mapping capability compared to spectrometry. Such great high-dimensional information can help us to identify detailed surface information and extract optical features, and allows us to estimate the concentrations of water quality or air quality parameters and trace the source of pollution. As a result, airborne hyperspectral remote sensing possesses the potential to be used for environmental monitoring and estimation, especially in rivers, lakes, reservoirs, and industrial plants.

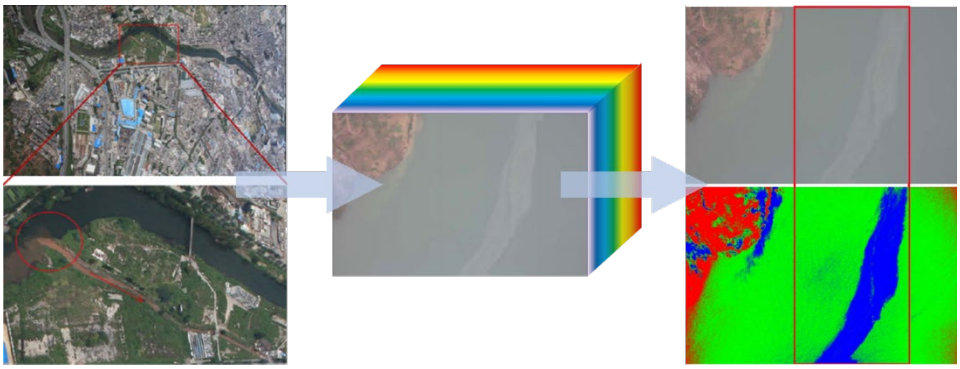

Fig.2 Multispectral images of an example area

2 Literature review

The most severe challenge to realizing hyperspectral imaging is how to efficiently acquire the dense spatial-spectral data cubes. Traditional spectral imaging systems, which employ individual optical and mechanical elements to broaden the dimension of information, include frequency scanning, push broom scanning, and wavelength scanning. Such a working principle is intuitive, and has led to mature market products such as AVIRIS, EnMAP, and AHSI. Such systems have been widely applied in various fields such as remote sensing (GISAT, PRISMA, and GaoFen-5 satellites). However, this scanning mechanism requires a complicated design with inevitable mechanical errors to a certain degree (especially for the cases such as distributed large arrays and vibrating platforms), and results in a long acquisition time for each frame with low temporal resolution.

With the advancement of the compressive sensing theory and computational photography technique, computational snapshot hyperspectral imaging techniques can capture distinctive information in spatial, temporal, and spectral domains simultaneously. Many computational snapshot hyperspectral imaging systems have been developed, such as computed-tomography imaging system (CTIS), coded aperture snapshot spectral imagers (CASSI) and prism-mask multispectral video imaging system (PMVIS). The principle lies in the intrinsic statistic that hyperspectral images exhibit strong redundancy and sparsity in different signal dimensions. The uniform working principle of these systems is first encoding multi-dimensional information into single-shot measurements, and then decoding the data cube via compressive

sensing or deep learning algorithms. Although these systems effectively improve temporal resolution, they still require individual optical elements for explicit light modulation that takes a heavy load for lightweight integration.

3 Problem Statement

Aiming for integrated hyperspectral imaging, there have been several trials for on-chip acquisition. The most intuitive routine is to extend the classic Bayer pattern of RGB color cameras by introducing more narrow-band filters, which has led commercial multispectral imaging sensors with spectrum channels ranging from 4 to 16. However, it suffers from a significant tradeoff between spatial and spectral resolution, and it also significantly reduces light throughput for narrow-band filtering. Benefiting from finely tunable spectrum filtering ability, nano-fabricated metasurface, photonic crystal plate arrays, and Fabry–Pérot filters have also been employed for channel selection. However, for these kinds of filters, the tunning precision is inversely proportional to the spectral range. Experimentally, most of the existing prototypes cover 200 nm at most in the visible range, with only 20 channels at most. Quantum dots have also been applied for spectral modulation, whose self-luminescence is a challenging obstacle that degrades spectral resolution a lot. Most recently, the scattering medium has been studied for spectral encoding, which would also introduce spatial scattering that reduces imaging resolution. Besides, due to the memory effect of scattering correlation, the modulation contrast is also limited and relies only on post-calibration without prior design. Despite the above various on-chip techniques for spectral modulation, most of them suffer from the intrinsic tradeoff between spatial and spectral resolution, which prevents their practical applications towards high-resolution hyperspectral imaging.

4 Work plan

This proposal presents a low-cost integrated hyperspectral imaging sensor with high spatial-temporal-spectral resolution at visible and near-infrared ranges (Vis-NIR). The image acquired by the drone equipped with the sensor is endowed with hyperspectral information. We will study the comprehensive framework of hardware fabrication, optical calibration, and computational reconstruction and conduct experiments for environmental pollution monitoring.

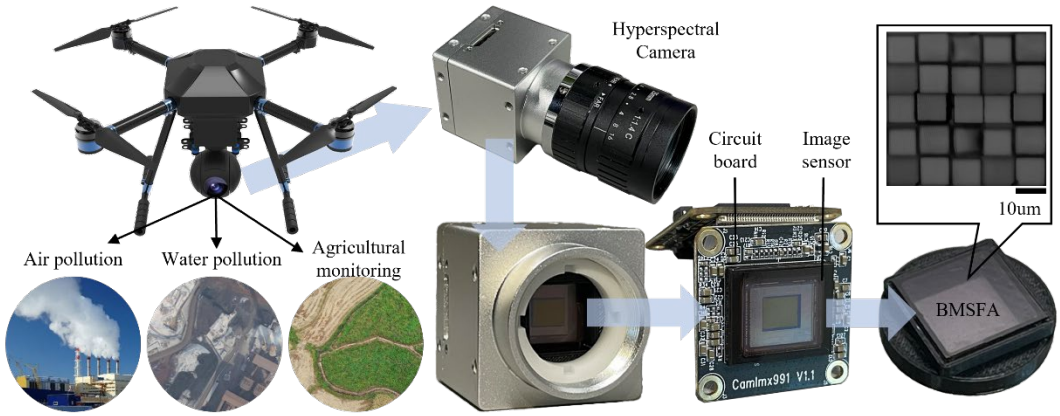

Fig. 3 Integrated hyperspectral monitoring device for environmental pollution

First, to effectively capture both spatial and spectral information, we develop the broadband multispectral filter array (BMSFA) fabrication technique using photolithography. The BMSFA is composed of different broadband spectrum-modulation materials at different spatial locations. Different from the common narrow-band filters, the broadband BMSFA is able to modulate incident light at the entire spectral range, allowing much higher light throughput that benefits low-light and long-distance imaging applications. The modulated information is then intrinsically compressed and acquired by the underlying broadband monochrome image sensor, allowing for spatial-spectral compression with full temporal resolution.

Second, to restore the hyperspectral data cube from the BMSFA compressed measurements, we derive a Transformer-based spectral reconstruction network (SRNet). The network consists of specially-designed spectral attention modules, enabling to compute cross-covariance across spectral channels and create attention feature maps with implicit knowledge of the spectral information and global context, which has more precise feature extraction and fuse ability than the conventional model-based reconstruction methods and convolutional neural networks. Consequently, we can reconstruct hyperspectral images with high spatial and spectral resolution from each frame, realizing real-time hyperspectral imaging.

Finally, prototypes will be designed to monitor different environmental pollution. The flow of data acquisition control and data processing will be determined. Equipment calibration, such as geometric registration, ration calibration, and concentration inversion of the collected data, will be performed many times for different regions. The existing problems and application potential of the integrated hyperspectral monitoring device in environmental pollution alerting will be further investigated.

5 Existing research achievement

Following the above framework, a Vis-NIR hyperspectral imaging device will be integrated. For the existing version of our sensor, the spectral response range covers from 400 nm to 1700 nm, with an average light throughput of 71.8%. In low-light conditions, the hyperspectral device outperforms mosaic multispectral cameras and scanning hyperspectral systems. The average spectral resolution achieves 2.65 nm at 400-1000 nm and 8.59 nm at 1000-1700 nm (calibrated under narrow-band monochromatic light). Experimentally, it can differentiate monochromatic light with a peak-to-peak spacing of 10 nm in the presence of multi-peak monochromatic light. As for the hyperspectral imaging performance, the experiments demonstrated 89 wavelength channels with a 10 nm interval within the range of 400-1000 nm and a 25 nm interval within the range of 1000-1700 nm. The peak signal-to-noise ratio (PSNR) of spectral reconstruction achieves 32.5 dB tested on the ColorChecker Classic chart. Each channel consists of 2048 $\times$ 2048 pixels at a frame rate of 47 fps, maintaining 3.43 arc minute optical resolving ability at a 39-degree field of view. The high frame rate allows for the capture of fast-moving objects, facilitating dynamic imaging.

If sponsored by the foundation, we will further optimize the performance of the sensor and conduct experiments on environmental pollution, such as regional inland water sources and local air pollution to meet current and future challenges affecting our world.

6 Outcomes

1. Active participation in academic conferences organized by OSA to share the latest progress of the project.
2. A complete technical report.
3. Submit results/progress more than three for publication published by OSA.

7 Impact

This scheme integrates innovations from multiple fields of material, integrated circuits, computer science, optics, and so on. It transforms the general challenge of high-dimensional imaging from one that is coupled to the physical limitations of the system's optics to one that is solvable through computation. By leveraging high-cost hardware manufacture and complex system design with agile computational imaging, the remaining cost of monitoring device mainly lies on the underlying broadband sensor. As broadband imaging sensor technology is gradually matured and widely used, the cost of device would be directly decreased, making it priced competitively. This advantage is particularly significant in remote sensing applications, especially in area monitoring devices.

What's more, such an integrated computational sensor framework can be applied to other information dimensions such as phase, polarization, and light field. We anticipate that this scheme may open a new venue for the next-generation imaging sensor of higher information dimension, imaging resolution, and integration level.

Microcomb-based, energy-efficient optical communication

Optica 20th Anniversary Challenge: Information
Lin Chang, School of Electronics, Peking University, Beijing 100871, China;
linchang@pku.edu

The ever-growing data traffic of the internet, fueled by recent advancements in AI and big data, is imposing significant challenges on optical communication infrastructures. Over the last few years, remarkable efforts have been dedicated to increase the capacity of communication links, particularly exploring the massively parallel wavelength division multiplex (WDM) communications. However, conventional approach employing laser arrays as the light source suffers from drawbacks in stability and coherency, resulting in substantial power consumption in both wavelength multiplexing and digital signal processing (DSP).

Recently, microcomb has attracted a lot of attentions as a promising candidate to overcome this problem. One microcomb can provide hundreds of equally-spaced wavelengths, which can support high-capacity communication. However, previous microcomb-based communications rely on bulky and power-hungry pump lasers, thereby causing a disadvantage in terms of energy efficiency.

In this project, we propose to develop a fully chip-based and power-efficient microcomb to drive communication links. We will leverage self-injection locking technology, which enables coherent microcomb generation by laser-diode pumping, without relying on any bulky equipment or auxiliary electronics. Based on ultra-high Q S_3N_4 microresonators ($Q > 2.6 \times 10^8$) manufactured by CMOS foundry, we can achieve high coherence between each comb line, whose linewidth can reach Hz level. Furthermore, the self-injection locking technique enables the generation of a dark pulse, allowing for a conversion efficiency exceeding 50%, which can overcome the energy efficiency problem of microcombs used in previous communication systems.

At the system level, we propose a novel WDM coherent communication architecture that fully leverages the advantage of microcombs in massive parallelization and high coherence. This communication system will incorporate over 150 channels, with each channel capable of supporting high-order coherent modulation formats, leading to beyond 100 Tbps aggregate data rate. Importantly, such high capacity will be achieved with much lower power consumption: the equal spacing of comb lines eliminates the need for wavelength control; more importantly, the constant phase relation among different comb lines can significantly reduce the requirements for two major parts of DSP, carrier recovery and phase estimation. With these advantages, we envision a high-capacity, power-efficient communication system which should have a profound impact on the future of the telecom and datacenters.

Microcomb-based, power-efficient optical communication

Literature Review

The ever-growing data traffic of the internet, fueled by recent advancements in AI and big data, is imposing significant challenges on optical communication infrastructures. Over the last few years, remarkable efforts have been dedicated to increasing the capacity of communication links, including the exploration of massive wavelength division multiplex (WDM) systems, higher channel bandwidths, as well as higher-order communication modulation formats. However, these approaches come at the expense of increased hardware requirements and power consumption: For WDM systems, expanding the channel number often involves adding more individual lasers, which makes precise wavelength control a critical task [1]; for an individual channel, high-bandwidth and high-format transmission requires extensive digital signal processing (DSP), particularly for coherent communications [2].

One promising solution to address the energy-efficiency problem of high-capacity communication is using an optical frequency comb to drive the communication link. A comb consists of multiple equally distributed frequency lines, which can support the massive parallelization for WDM in a single source. Importantly, the recent development of microcomb provides a path to achieve OFC generation on a chip [3], leading to numerous demonstrations of microcomb-driven, high-capacity communication systems. In 2014, Joerg Pfeifle et al. reported the first experimental demonstration of coherent data transmission using 20 microcomb channels, achieving a total data stream of 1.44 Tbit s^{-1} [4]. In 2017, by interleaving two dissipative Kerr solitons (DKS) combs, Pablo Marin-Palomo et al. used a total of 179 comb line carriers to achieve an aggregate line rate of 55.0 Tbit s^{-1} transmitted over a distance of 75 km [5]. In 2020, a high spectral efficiency of 10.4 bits/Hz was realized by using a high modulation format of 64 QAM with a low comb-free spectral range (FSR) spacing of 48.9 GHz in the report of Bill Corcoran et al. [6]. In 2022, Yong Geng et al. used coherence-cloned Kerr soliton microcombs to show the ability of the DKS microcomb coherence to simplify traditional digital signal processing algorithms [7]. In 2022, our group demonstrated a microcomb-driven silicon photonic link with 50 Gbaud PAM4 format and an aggregate bit rate of 2 Tbit s^{-1}[8].

Problem statement/Objective

Despite remarkable progress, the practical implementation of microcombs for real-world applications remains elusive. One big challenge is the integration. Although microresonators for comb generation can be integrated on-chip nowadays, their pumping lasers are usually bench-top ones. Particularly, for coherent communication, a narrow linewidth pump laser is essential, which is usually bulky and expensive. Additionally, the conversion efficiency poses another difficulty. The most commonly used coherent comb state, bright soliton, exhibits a conversion efficiency of around 1-2%, resulting in a main disadvantage in energy efficiency. Meanwhile, the converted power is distributed to combs lines unevenly, which further degrades the effective wall plug efficiency.

To address these challenges, we propose to develop WDM coherent communication technologies based on fully chip-based, power-efficient microcombs. We will use our recently developed self-injection locking technology, which enables coherent microcomb generation by laser-diode pumping, without relying on any bulky equipment or auxiliary electronics. Moreover, to further improve energy efficiency, we will leverage the highly coherent nature of comb lines to reduce the DSP consumption. This combination will lead to a high-capacity, energy-efficient communication system, as shown in Fig.1A.

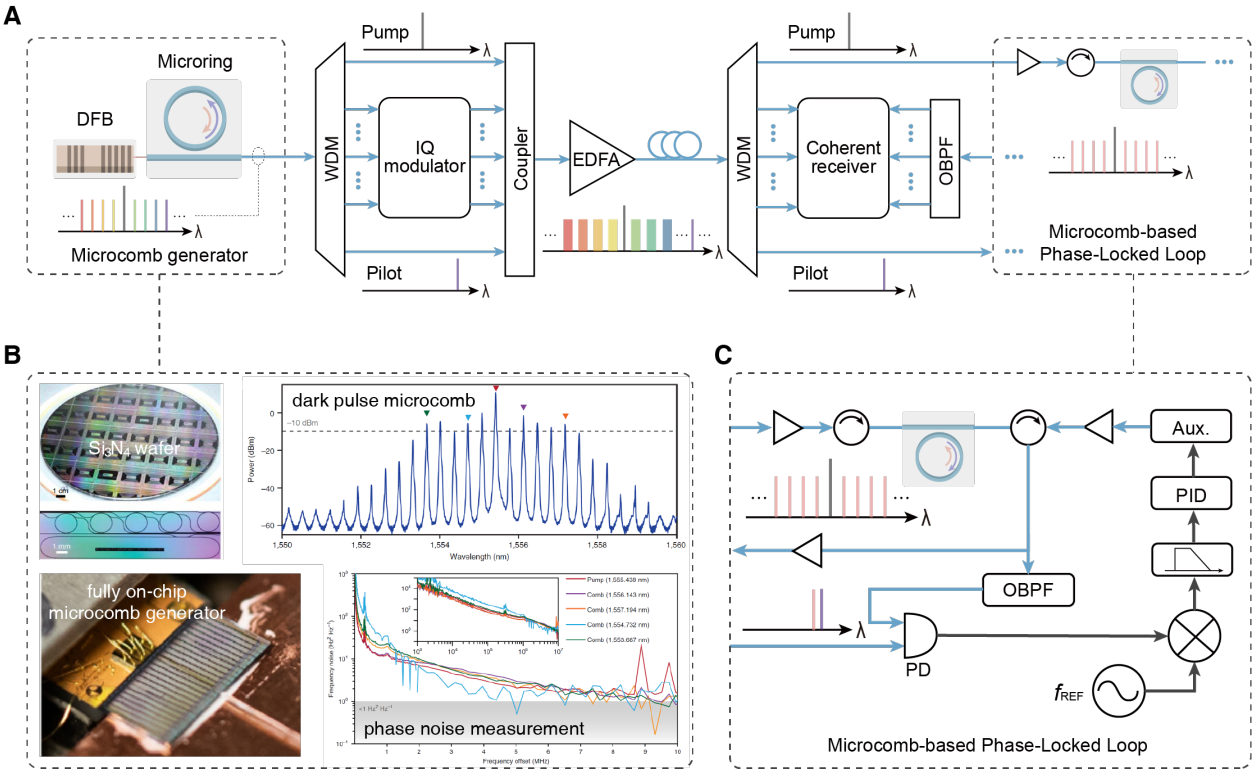

Fig. 1 (A) Proposed microcomb-based, power-efficient coherent communication link; (B) Fully on-chip, energy-efficient coherent microcomb generation based on wafer-scale CMOS Si_3N_4 production; (C) Microcomb-based phase locked loop for reducing DSP consumption.

Outline of tasks

This project comprises two main tasks. At the device level, we will develop a fully chip-based microcomb generator that has a high conversion efficiency and flat envelope. At the system level, we will construct a new microcomb-based coherent communication architecture, characterized by high compacity and significantly reduced DSP consumption. A detailed description is given below:

Fully chip-based, power-efficient microcomb generation

To achieve an operationally simple, fully chip-based microcomb, there are two challenges to overcome: the complexity of tuning schemes and feedback loops used in conventional microcomb pumping setups, and the high-power requirement for the pump laser. In this work, we will address this problem by using an ultra-high-Q microresonator and applying

the self-injection locking strategy for microcomb generation (Fig.1B) based on the technologies recently developed by our team.

Microresonators with ultra-high Q are based on a wafer-scale, CMOS foundry fabrication process for Si_3N_4 [9]. The thickness of Si_3N_4 will be selected to achieve the balance between high Q and dispersion engineering flexibility for broad-band comb generation. In fabrication, advanced lithography and etching have been well developed, ensuring low scattering loss from the sidewall of waveguides. The Si_3N_4 is deposited by low pressure chemical vapor deposition (LPCVD) and later treated by high temperature annealing to outgas the N-H for absorption reduction. Combining these strategies, we have demonstrated a Q factor of microresonator beyond 2.6×10^8, which is one of the highest numbers achieved in integrated photonics. Such high Q characteristic dramatically relieves the pump power requirement: for a 30 GHz microcomb, the power to generate a coherent comb is below 20 mW, a level well within the capabilities of commercial distributed feedback (DFB) lasers.

To get rid of the complex control/feedback procedures for microcomb generation, we will adopt the self-injection locking scheme here[10]. The laser diode will be directly coupled to the microresoantor without an isolator in between. Under the reflection from the high Q resonator induced by Rayleigh scattering, the pump laser can be locked to the resonance of the cavities automatically when the laser frequency and the resonance mode are within a certain bandwidth. This mechanism enables the direct generation of coherent microcomb by simply powering the laser on, making it a turnkey operation. Moreover, the self-injection locking scheme significantly reduces the linewidth of the pump laser, whose coherence can be transferred to all comb lines. Through the ultra-high-Q resonator, we have successfully achieved Hertz-level linewidth for all comb lines, surpassing the performance of commercial bench-top narrow linewidth lasers.

Another critical challenge to overcome is conversion efficiency. In this project, instead of using well-studied bright solitons, we will explore the generation of a dark pulse state. Since the dark pulse is operated at the blue detuning side of the resonance of the cavity, it can support more effective pump coupling and therefore higher conversion efficiencies. Through proper dispersion engineering by tailoring the geometry, the generated comb spectrum can have a flat plateau covering the tens of nm range, which is suitable for WDM purposes by eliminating the spectrum shaping filters.

Power efficient coherent communication link

The self-injection locked microcomb source provides hundreds of comb lines for a WDM communication link, while the high coherence of each comb line allows for higher order modulation formats compared with widely used DFB laser. Since the spacing between comb lines is equal, microcomb gains a significant advantage in massive parallelization without wavelength control, leading to considerable power saving than the DFB arrays. The stable repetition frequency between comb lines also enables a smaller guard band, further improving the efficiency of spectrum utilization. Furthermore, the constant phase

relation among comb lines provides the opportunity to significantly reduce the DSP resources, which previously was a power-intensive part in communication links.

Fig. 1A shows the architecture of our system, we employ a WDM to separate comb lines into different channels as hundreds of carriers, which are further encoded by different IQ modulators. A WDM coupler combines these modulated signals with an uncoded pump laser signal and a pilot tone. All of them are transmitted to the receiver through fiber. By leveraging the phase stability and coherence among different wavelengths, we can achieve significant power savings in digital signal processing (DSP) while maintaining a high-order coherent modulation format, without incurring any noticeable increase in bit error rate.

At the receiver, we clone a microcomb as the local oscillator (Fig.1C): the conveyed pump signal is amplified through a low-noise Erbium-doped fiber amplifier (EDFA) to generate a dark pulse in the receiver microresonator, which may have a slightly different soliton repetition rate compared with the transmit microresonator. The transmitted pilot comb line and the corresponding mode index comb line from the receiver resonator are filtered out and directed to a fast photodiode to be phase-locked using an optical phase-lock loop (OPLL). The resulting error signal is sent back to the auxiliary laser, allowing for feedback control of the laser power. Consequently, this process synchronizes both the pump laser wavelength and the repetition rate. All symbols are decoded by beating different comb lines with corresponding data channels.

By utilizing coherence-cloned microcombs to generate local oscillator (LO) lasers, we eliminate the need for frequency offset estimation in the digital signal processing (DSP) process, as the optical phase-lock loop (OPLL) provides a reliable reference clock. Additionally, all cloned microcombs maintain low phase noise characteristics, simplifying carrier phase estimation in each individual channel. By capitalizing on the coherence among microcombs, we can minimize the carrier phase estimation to only one channel, benefiting all carriers collectively. This strategy will save most of the DSP consumption for coherent communication.

Outcome

This project is expected to have the following outcomes:

At the device level, we will achieve fully on-chip, energy-efficient microcomb generation. The expected pump-to-optical conversion efficiency will be higher than 50%, and the overall wall plug efficiency will exceed 10%. The generated spectrum of the comb will cover the C+L+S band, leading to more than 100 nm span and more than 150 comb lines.

At the system level, we will achieve a communication link with more than 150 channels, and the single channel rate is more than 700 Gbps. The expected aggregate rate will reach 100 Tbps. The DSP consumption will be 90% smaller compared with those of coherent links using DFB arrays.

Impact

This project will lead to a profound impact on future communication technologies. It will bring microcomb to wide deployment for practical use in communications and thus revolutionize the existing WDM architectures. By significantly improving the channel numbers and reducing the DSP power consumption, this strategy will pave the way for high-capacity, energy-efficient communications in future telecom and data-centers.

[1] R. Nagarajan et al., "InP Photonic Integrated Circuits," in IEEE Journal of Selected Topics in Quantum Electronics, vol. 16, no. 5, pp. 1113-1125, Sept.-Oct. 2010, doi: 10.1109/JSTQE.2009.2037828.

[2] M. Yoshida, T. Kan, K. Kasai, T. Hirooka, K. Iwatsuki and M. Nakazawa, "10 Channel WDM 80 Gbit/s/ch, 256 QAM Bi-Directional Coherent Transmission for a High Capacity Next-Generation Mobile Fronthaul," in Journal of Lightwave Technology, vol. 39, no. 5, pp. 1289-1295, 1 March1, 2021, doi: 10.1109/JLT.2020.3034417.

[3] Chang, L., Liu, S. & Bowers, J.E. Integrated optical frequency comb technologies. Nat. Photon. 16, 95–108 (2022). https://doi.org/10.1038/s41566-021-00945-1

[4] Pfeifle, J., Brasch, V., Lauermann, M. et al. Coherent terabit communications with microresonator Kerr frequency combs. Nature Photon 8, 375–380 (2014). https://doi.org/10.1038/nphoton.2014.57

[5] Marin-Palomo, P., Kemal, J., Karpov, M. et al. Microresonator-based solitons for massively parallel coherent optical communications. Nature 546, 274–279 (2017). https://doi.org/10.1038/nature22387

[6] Corcoran, B., Tan, M., Xu, X. et al. Ultra-dense optical data transmission over standard fibre with a single chip source. Nat Commun 11, 2568 (2020). https://doi.org/10.1038/s41467-020-16265-x

[7] Geng, Y., Zhou, H., Han, X. et al. Coherent optical communications using coherence-cloned Kerr soliton microcombs. Nat Commun 13, 1070 (2022). https://doi.org/10.1038/s41467-022-28712-y

[8] Shu, H., Chang, L., Tao, Y. et al. Microcomb-driven silicon photonic systems. Nature 605, 457–463 (2022). https://doi.org/10.1038/s41586-022-04579-3

[9] Jin, W., Yang, QF., Chang, L. et al. Hertz-linewidth semiconductor lasers using CMOS-ready ultra-high-Q microresonators. Nat. Photonics 15, 346–353 (2021). https://doi.org/10.1038/s41566-021-00761-7

[10] Shen, B., Chang, L., Liu, J. et al. Integrated turnkey soliton microcombs. Nature 582, 365–369 (2020). https://doi.org/10.1038/s41586-020-2358-x

Agriphotonic Technique for Sustainable Agriculture: Reducing Human Footprint through Whitefly Pest Management

Author: Luis Miguel Gomes Abegão, Ph.D. || **Category:** Environment

The use of insecticides and pesticides in crop production can significantly impact environmental pollution. Water pollution, soil contamination, non-target species, residue accumulation, and resistance development are examples of the human footprint consequences of controlling crop pests. This real-world issue is among the highest challenges the science community must solve. On one hand, one must provide food for an increasing world population; on the other hand, humanity must drastically decrease its footprint. A solution for this real-world issue is replacing pesticides with novel biocompatible techniques to control crop pests. An agriphotonic technique, based on laser, able to control crop pests without harming the plant's development or affecting non-target species can help tackle this global problem.

Several species of whiteflies are considered pests in agriculture. For example, the whitefly *Bemisia tabaci* (biotype MEAM1) is one of the most relevant insect pests of crops worldwide once it is present in all continents. *Bemisia tabaci* can colonize plants belonging to many plant families and adapt highly to different environments. Moreover, they have a rapid selection of insecticide-resistant populations, which makes them a threat to food security, especially in developing countries.

The main objective of this proposal is to develop a prototype of a future commercial agriphotonic device for pest control. This device will use a novel biocompatible technique based on a laser. Such a technique has already been tested in the laboratory, showing that it is able to achieve 100% mortality of *Bemisia tabaci* without affecting the plant's development [1].

The proposal's objective will be achieved concurrently by conducting a science investigation and technology implementation, as illustrated in Figure 1. The first will focus on how different optical parameters will affect the mortality of whitefly species not yet studied and the plant's development after laser irradiation, and the latter will focus on the prototype development. It is important to emphasize that the strong collaboration between the author's proposal and the Brazilian Agricultural Research Corporation (Embrapa) will trigger a high-level success for the proposed strategy.

In summary, this proposal intends to develop a prototype of a future commercial agriphotonic device, based on a laser, for whitefly pest management. The success of this proposal will be capable of providing a new biocompatible technique for pest control to small- and large-scale farmers, which can decrease environmental pollution by reducing the usage of conventional pesticides. Moreover, if accepted, this proposal will unlock new possibilities and perspectives, paving the way for a new startup company in Agriphotonics.

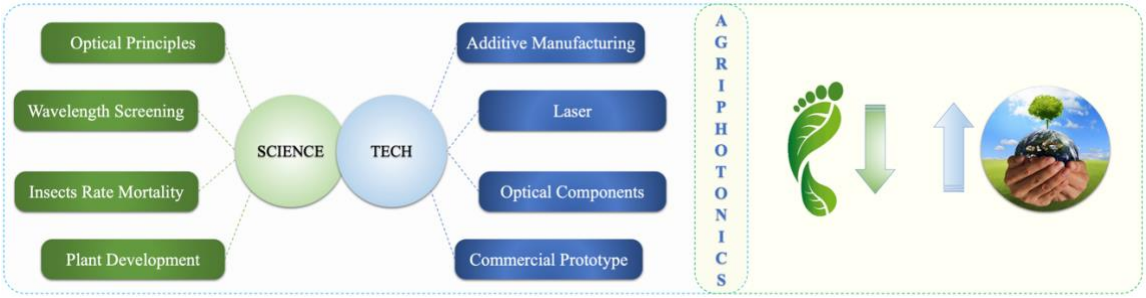

Figure 1. Diagram showcasing the proposal's integration. The left side represents the science and technology elements needed to develop the photonic device prototype. The right side illustrates the proposal's goal, i.e., reducing the human footprint and pursuing a better, more sustainable world using Agriphotonics.

[1] Zaidem, A., Silva, L., Ferreira, A., Carvalho, M., Ragni, M., **Abegão, L.**, & Pinheiro, P. (2023, May). New Biocompatible Technique Based on the Use of a Laser to Control the Whitefly Bemisia tabaci. In *Photonics* (Vol. 10, No. 6, p. 636). MDPI.

PROPOSAL SUBMISSION

Title: Agriphotonic Technique for Sustainable Agriculture: Reducing Human Footprint through Whitefly Pest Management

Author: Luis Miguel Gomes Abegão, Ph.D.

Category: Environment

---

1. Literature Review

The use of insecticides and pesticides in crop production can significantly impact environmental pollution. Water pollution, soil contamination, residue accumulation, non-target species, and pest resistance development are examples of the human footprint consequences of controlling crop pests, which have been pointed out, discussed, and reported since 1986 [1-7]. The economic impact of using insecticides and pesticides in crop production is also a complex issue with both positive and negative implications. On one hand, the chemicals used are essential for protecting crops from pests and diseases, thereby ensuring higher yields and greater economic returns for farmers. On the other hand, the negative environmental impact is enormous. In fact, pesticides increased agricultural productivity and reduced crop losses in the United States, as reported in 2005 by Pimentel et al. [8]. However, the same study also highlighted the environmental and health costs associated with pesticide use, which can result in additional economic burdens in the long term. Therefore, a balance between maximizing crop productivity and minimizing the negative externalities of pesticide use is crucial for achieving sustainable agricultural practices that consider economic and environmental factors. This real-world issue is among the most significant challenges humanity must solve [9-12], and Optica will have the chance to help significantly with this proposal's approval, which proposes a photonics-based prototype to decrease environmental pollution by reducing the usage of conventional pesticides.

There is a multitude of insect pest species encompassing many insects' orders, such as Acari (Mites), Coleoptera (beetles), Diptera (flies), and Hemiptera (True Bugs). The latter order contains several whitefly species that threaten different types of crops [13-16]. For example, the whitefly *Bemisia tabaci* (biotype MEAM1) [17] is one of the most relevant insect pests of crops worldwide once it is present in all continents, particularly in the Americas [18]. This insect species belongs to the Aleyrodidae family and is known for its ability to infest a wide range of host plants, including many economically important crops. The biotype MEAM1, also known as the "Middle East-Asia Minor 1" or the "*Bemisia B*" biotype, is particularly noteworthy due to its invasiveness and adaptability, making it a significant concern for agricultural systems globally. This whitefly species is known to transmit numerous plant viruses, including begomoviruses, criniviruses, and torradoviruses [19]. These viruses can cause devastating crop diseases, leading to reduced yields and significant economic losses. For example, in the United States, was reported losses of over 200 million dollars yearly in cotton production caused by this whitefly biotype [20]. Similarly, in the Andes, substantial yield losses and

economic damages were caused by *Bemisia tabaci* MEAM1 in yellow potatoes and tomato crops [21]. In Brazil, common bean crops are also strongly affected by *Bemisia tabaci* [22].

Sustainable agriculture urges reducing insecticide applications as a pest control method; therefore, insect control methods based on innovative and clean tools such as electromagnetic (EM) radiation can be a valuable option to reduce the human footprint. Ultraviolet (UV) light is the best-known EM radiation to have lethal effects on most organisms. However, it is well known that UV light is highly damaging to biological systems because it can induce various mutagenic and cytotoxic DNA alterations. For example, in 2014, Dáder et al. showed that UV-B (~280-315 nm) radiation might have lethal effects on plants, so they decided to work with UV-A (~315-400 nm), which is not absorbed by native DNA but can still damage cell constituents, such as lipids, proteins, and even DNA, by increasing the synthesis of reactive oxygen species (ROS). There are few reports with precise data on the effect of EM radiation within the visible (VIS) spectral window on insect mortality. In 2021, Gaetni et al. showed that laser emission in the VIS and IR spectral regions could be a potential biocompatible technique for pest control [23]. And the most recent study (2023) was made by Zaidem et al., demonstrated that a laser emission center at 445 nm can achieve 100% mortality on the 3rd instar nymphs of *Bemisia tabaci* without harming the plants' development [24]. These two particular and recent studies have shown the massive potential of VIS light emitted by a laser to become an agriphotonic technique for sustainable agriculture, with excellent chances to reduce the human footprint.

2. Problem Statement/Objective

As described in the previous section, the problem is that using insecticides and pesticides in crop production can significantly impact environmental pollution. Conventional pest control methods often involve applying chemical substances that can adversely affect the ecosystem. These chemicals can seep into the soil, contaminate water sources, harm non-target organisms, and contribute to the development of pesticide resistance in pests. A sustainable and environmentally friendly alternative to pest control methods is vital to ensure agricultural ecosystems' long-term health and balance.

The main objective of this proposal is to consolidate the feasibility and effectiveness of using laser technology as an alternative approach for pest control in crop production, i.e., as an agriphotonic technique for sustainable agriculture. By employing lasers, it is possible to target specific pests without harming beneficial insects, birds, or other organisms within the ecosystem. This approach aims to minimize environmental collateral damage while effectively managing pest populations. Therefore, the proposal's objective will be achieved concurrently by conducting a science investigation (basic research) and technology implementation (product development), as illustrated in Figure 1. The first will focus on how different optical parameters will affect the mortality of whitefly species not yet studied and the plant's development after laser irradiation, and the latter will focus on the prototype development, generating a portable photonic prototype to be used in the field. It is important to emphasize that this proposal's author built a simplified bench version (hardware and software) of the

photonic prototype version proposed in this project, as depicted in Figure 3 of the published work by Zaidem et al. [24]. The strong collaboration between the author's proposal and the Brazilian Agricultural Research Corporation (Embrapa) will trigger a high-level success for the proposed strategy due to knowledge synergy. Finally, the proposal's project also will focus on advancing scientific and technological knowledge and provides a valuable opportunity to prepare and train undergraduate personnel in optics and photonics.

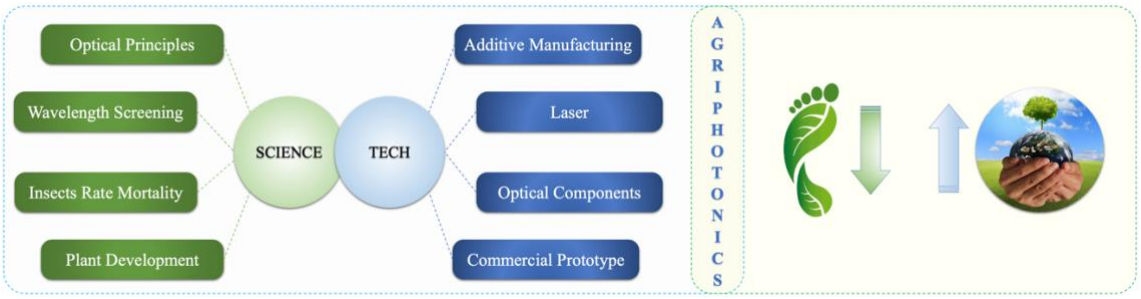

Figure 1. Diagram showcasing the proposal's integration. The left side represents the science and technology elements needed to develop the photonic device prototype. The right side illustrates the proposal's goal, i.e., reducing the human footprint and pursuing a better, more sustainable world using Agriphotonics.

3. Outline of Tasks/Work Plan

The tasks associated with the proposed project plan are described in Table 1. The tasks are distributed over trimestral periods, providing a clear timeline for the execution of activities and milestones.

Table 1. Timeline for the execution of activities/tasks and milestones associated with the project's proposal.

TASKS	Period (months)					
	1-3	3-6	6-9	9-12	12-15	15-18
Tech: Resources selection to develop the portable (field) and the bench (lab) photonic prototypes.						
Science: Resources selection for pest control and insect introduction.						
Tech: Design, manufacture, and assembly both photonic prototypes (portable and bench versions).						
Science: Optimization of optical parameters to increase the prototype's effectiveness.						
Tech: Prototypes testing, characterization, and iterative refinement.						
Science: Irradiation experiments, wavelength screening, data collection, and statistical analysis.						
Tech: Drafting the portable photonic prototype patent application and filling.						
Science: Writing and submitting scientific articles						
Science & Tech: Providing knowledge and training in the photonics field to undergraduate personnel.						

4. Outcome

This proposal aims to address the critical issue of environmental hazards caused by the intense use of pest chemical control, e.g., pesticides. The anticipated outcome of this proposal is to develop a photonic-based prototype to become a commercial agriphotonic device, based on a laser, for pest management, without harming the plant's development. From a practical point of view, this proposal will initially focus on controlling *Bemisia tabaci* insect species on common bean crops via a photonic-based prototype.

The submitted proposal will deliver the intended results in a potential patented photonic-based prototype and scientific papers published in Optica journals. This proposal will also deliver knowledge, learning, and training for the undergraduate students directed and undirected involved in the proposal.

Moreover, Optica's Student Chapter of Goiás, of which this proposal's author is the current chapter's advisor, will diffuse the Agriphotonics concept to society, through several activities, such as seminars and elementary and high school visits, to explain how optics and photonics could be one of the solutions for sustainable agriculture.

5. Impact

The anticipated significant impact of an Agriphotonic technique for pest control is the environmentally sustainable change that will produce long-term changes in the agroindustry and agribusiness, leading to an ultra-positive effect on every chain of the agricultural ecosystem, consequently, in the day life of all humankind. Undoubtedly, it will be an enormous step forward for all agroindustry agents once most seek high productivity yield, i.e., high profit, regardless of the means to achieve it. However, the proposed photonics-based prototype, based on laser for pest control, will benefit small- and large-scale farmers. A successful low-cost, effective, and easy-to-use system is usually well accepted by small farmers, who can use it to prove its performance to large farmers in a practical way.

Developing and promoting the adoption of an Agriphotonic technique for sustainable agriculture will significantly and positively impact the environment, reducing reliance on harmful chemicals. Moreover, this project seeks to foster ecological balance, preserve biodiversity, and safeguard the health of ecosystems. Also, this proposal envisions a transformative shift towards a more sustainable and resilient agricultural sector, with far-reaching benefits that extend to farmers, consumers, and the overall well-being of our planet. Finally, this proposal will unlock new possibilities and perspectives, fostering the potential to create a startup company in Agriphotonics.

References

1. Papendick, R.I., L.F. Elliott, and R.B. Dahlgren, *Environmental consequences of modern production agriculture: How can alternative agriculture address these issues and concerns?* American Journal of Alternative Agriculture, 1986. **1**(1): p. 3-10.
2. Holden, P.W. and N.R. Council, *Pesticides and groundwater quality: Issues and problems in four states*. 1986: National Academies Press.
3. Iyaniwura, T.T., *Non-target and environmental hazards of pesticides.* Reviews on environmental health, 1991. **9**(3): p. 161-176.
4. Krieger, R.I., J.H. Ross, and T. Thongsinthusak, *Assessing human exposures to pesticides.* Reviews of environmental contamination and toxicology, 1992: p. 1-15.
5. Edwards, C.A., *The impact of pesticides on the environment*, in *The pesticide question: Environment, economics, and ethics*. 1993, Springer. p. 13-46.
6. Koh, D. and J. Jeyaratnam, *Pesticides hazards in developing countries.* Science of the total environment, 1996. **188**(1): p. S78.
7. van der Werf, H.M., *Assessing the impact of pesticides on the environment.* Agriculture, Ecosystems & Environment, 1996. **60**(2-3): p. 81-96.
8. Pimentel, D., *Environmental and economic costs of the application of pesticides primarily in the United States.* Environment, development and sustainability, 2005. **7**: p. 229-252.
9. Özkara, A., D. Akyıl, and M. Konuk, *Pesticides, environmental pollution, and health*, in *Environmental health risk-hazardous factors to living species*. 2016, IntechOpen.
10. Carvalho, F.P., *Pesticides, environment, and food safety.* Food and energy security, 2017. **6**(2): p. 48-60.
11. AL-Ahmadi, M.S., *Pesticides, anthropogenic activities, and the health of our environment safety*, in *Pesticides-use and misuse and their impact in the environment*. 2019, IntechOpen.
12. Boudh, S. and J.S. Singh, *Pesticide contamination: environmental problems and remediation strategies.* Emerging and eco-friendly approaches for waste management, 2019: p. 245-269.
13. Martin, J., *An identification guide to common whitefly pest species of the world (Homopt Aleyrodidae).* International Journal of Pest Management, 1987. **33**(4): p. 298-322.
14. Morales, F.J., *Tropical whitefly IPM project.* Advances in virus research, 2006. **69**: p. 249-311.
15. Horowitz, A.R., Y. Antignus, and D. Gerling, *Management of Bemisia tabaci whiteflies*, in *The Whitefly, Bemisia tabaci (Homoptera: Aleyrodidae) interaction with geminivirus-infected host plants: Bemisia tabaci, host plants and geminiviruses*. 2011, Springer. p. 293-322.
16. Shah, M.M.R., S. Zhang, and T. Liu, *Whitefly, host plant and parasitoid: A review on their interactions.* Asian Journal of Applied Science and Engineering, 2015. **4**(1): p. 48-61.
17. LIU, S.-s., J. Colvin, and P.J. De Barro, *Species concepts as applied to the whitefly Bemisia tabaci systematics: how many species are there?* Journal of Integrative Agriculture, 2012. **11**(2): p. 176-186.
18. Barbosa, L.d.F., et al., *Indigenous American species of the Bemisia tabaci complex are still widespread in the Americas.* Pest Management Science, 2014. **70**(10): p. 1440-1445.
19. Fiallo-Olivé, E., et al., *Transmission of begomoviruses and other whitefly-borne viruses: Dependence on the vector species.* Phytopathology, 2020. **110**(1): p. 10-17.
20. Naranjo, S.E., *Impacts of Bt transgenic cotton on integrated pest management.* Journal of agricultural and food chemistry, 2011. **59**(11): p. 5842-5851.
21. Rincon, D.F., et al., *Economic injury levels for the potato yellow vein disease and its vector, Trialeurodes vaporariorum (Hemiptera: Aleyrodidae), affecting potato crops in the Andes.* Crop Protection, 2019. **119**: p. 52-58.
22. Inoue-Nagata, A.K., M.F. Lima, and R.L. Gilbertson, *A review of geminivirus diseases in vegetables and other crops in Brazil: current status and approaches for management.* Horticultura Brasileira, 2016. **34**: p. 8-18.
23. Gaetani, R., et al., *Sustainable laser-based technology for insect pest control.* Scientific Reports, 2021. **11**(1): p. 11068.
24. Zaidem, A., et al. *New Biocompatible Technique Based on the Use of a Laser to Control the Whitefly Bemisia tabaci*. in *Photonics*. 2023. MDPI.

Title of the proposal:

3D Optogenetics for Functional Brain Mapping and Parkinson's Disease Therapy

The objective of the research proposal is to develop a new framework of three-dimensional (3D) optogenetics combined with computational modeling for *in vivo* functional brain mapping and to improve the treatments for neurological diseases including the Parkinson's disease.

The field of applied optics in neuroscience has been profoundly influenced by optogenetics. However, there are multiple challenges in optogenetics for the investigations of structural and functional information of brain. **This project aims to develop a next-generation 3D optogenetics tool aiming to overcome the technological hurdles and close all those gaps to enable *in vivo* optical investigations of brain cell morphology and function**, in the following directions:

1. Development of a 3D multi-spot illumination system realizing the computer-generated holograms [**AIM 1**],
2. Functional observation and computational modeling of neural activity [**AIM 2**],
3. Record the activity of the neurons by 3D fluorescence imaging technology based on metasurface systems [**AIM 3**] to collectively generate the 3D brain mapping, and
4. Utilization of the developed system for the improved treatment of Parkinson's disease [**AIM 4**]

Category it seeks to address:

Health

Intended outcomes, capabilities and applications to real-word issues:

This research work will contribute to the development of new research achievements and activities in the field of **3D optogenetics, 3D imaging, and simultaneous investigations of models of neurological disease**. The proposed research proposal could be beneficial for the imaging tool in the field of neuroscience to uncover the fundamental aspects and pathologies that have been beyond reach and reveal useful neural activity and their behavior and mental states. Since different sets of neurons are associated with different functions, and if the activity of each set of neurons is analyzed then it would be possible to understand how they work together. By analyzing the activity of different neurons, various brain disorders such as depression, Parkinson, etc. can be evaluated. **The proposed system would allow modulating, controlling, and monitoring of manifold neuronal activities with cellular and millisecond-temporal precision and resuscitating the physiological patterns of brain activity**. In optogenetics, various systems have been developed for photo-stimulation. However, none of them is capable of simultaneous 3D stimulation and 3D observation of neural activity. Moreover, the system will be developed with single-neuron (cellular) spatial resolution across a large volume without compromising temporal precision. **Such efforts in the field of 3D brain mapping may provide the necessary evolutions and exciting achievements in the field of neuroscience**. As an excellent tool for studying the brain's development, computation, and adaptation, *in vivo* imaging of brain cells is becoming increasingly popular. It would play an important role in a deeper understanding of brain activity, and helps in the improvement of diagnosis by monitoring disease progression. The health care devices and systems will be developed that may promote several collaborations and receive strong interest from research labs, hospitals, and companies. Being a multidisciplinary research proposal, I will work closely with a team of biologists (**Prof. Prof. Mitsuhiro Morita**, Department of Biology, Kobe University),), optical engineers [**Prof. Osamu Matoba** (Kobe University) and **Prof. Yasuhiro Awatsuji** (Kyoto Institute of Technology)], to develop the state-of-art 3D optogenetics tools and use it for the PD therapy and other neurological investigations. **Upon successful completion, this study will generate sufficient data to determine the feasibility of optogenetic therapy as a potential treatment for Parkinson's disease and may facilitate recovery from several neurological diseases**. It is expected that the success of the proposed project will open new research fields in neuroscience and the biomedical imaging field where **watching brain cells in action is possible**.

Title: 3D Optogenetics for Functional Brain Mapping and Parkinson's Disease Therapy

The objective of the research proposal is to design and develop a new framework of three-dimensional (3D) optogenetics combined with computational modeling for *in vivo* functional brain mapping to improve the treatments for Parkinson's disease.

1. Research Plan: Background

For centuries, researchers have been captivated by the structural and functional information of the brain, and to date, it remains challenging to investigate functional brain mapping on the cellular level in intact brains. **About 15% of the population suffers from mental illness including Parkinson's disease**, chronic pain, dementia or epilepsy, etc. Worldwide, Parkinson's disease (PD) ranks second among neurodegenerative diseases [1]. PD is caused by the degeneration of dopamine neurons in the midbrain, which erodes the neural circuits that control movement. The transplants of fetal neurons in the brain of PD patients and switching on and off their electrochemical activity can modulate the behavior of downstream neurons. For many years, electrophysiology was the only technique for studying transplanted dopamine neurons, including recording and stimulating neuronal activity through electrodes in the brain [e.g., see Fig. 1(a)], which has several drawbacks, such as it requires careful insertion otherwise it may damage the brain; targeted or recognized only for specific cell types, and it activates all the neurons close to the stimulation site in non-selective ways. Moreover, due to the fact that neurons belonging to the same cell class and brain region may show diverse response patterns using this technique, it provides limited insight into the functioning of the brain. Neurobiologists have access to a new set of tools with **optogenetics** to selectively excite or inhibit discrete areas of the brain using a beam of light [2,3]. The hurdles of electrophysiology have been overcome in recent years after the development of optogenetics. In addition to being able to quickly modulate and monitor a large number of neuronal events, it also allows to recreate brain activity in space, time, and physiological terms. The stimulation of user-defined specific neurons or neural circuits in the brain by using light can be realized by modulating the incident light in such a way that it can incident only specific neurons to activate them only and leave others unaltered [e.g., see Fig. 1(b)]. Optogenetics facilitates active control of the genetically defined neurons, which are employed with fluorescent ion indicators and/or light-triggering actuators microbial opsins that either generate or suppress neuronal activity in response to illuminated light.

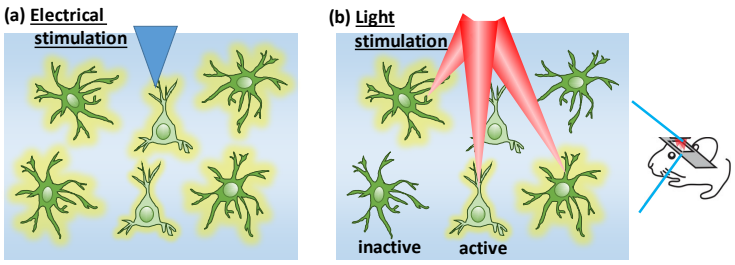

Fig. 1: (a) Electrical stimulation, where all cells close to the stimulation site are also activated and (b) light stimulation, where only specific cells are activated.

2. Problem Statement and Objectives

The field of applied optics in neuroscience has been profoundly influenced by optogenetics [4-6]. However, there are **multiple challenges in optogenetics** for the investigations of structural and functional information of brain. **First**, by incident light, neurons need to be accessible and efficient approaches should be implemented to overcome light scattering of tissues which precludes optical imaging of the intact brain at cellular and subcellular levels. **Second**, for neuronal stimulation to mimic the ensemble of activity patterns that neural networks naturally experience, the time scales and spatial ranges of light-triggering must be maintained with sufficient accuracy. **Third**, more efficient optical methods for photo-stimulation need to be established and optimized for a description of the photophysical properties of fluorescent ion indicators

and light-triggering molecules. **Fourth**, there requires a high light intensity efficiency with equal light distribution in each light pattern that illuminates targeted neurons and zero light intensity in the zeroth order and the regions of no interest. **Fifth**, as the neural circuits lie and operate in a 3D spatial environment, therefore, there require to transform existing scans as well as imaging technologies to 3D. **Furthermore**, the traditional approaches for the treatment of neurological disease (e.g. PD) lack in discrimination of different cell activities, strict eligibility criteria, limited to cell-type specific recognition, and surgical invasiveness.

In general, the majority of optogenetics investigations leverage genetic specificity rather than perfect optical characteristics and designs, such as low cellular/subcellular resolution spatial control due to the tissue scattering and difficulties of accurately focusing light in brain tissue. **I have pioneered a string of optical imaging techniques for bio-imaging and applications** [7-19]. **In this project, I shall develop a next-generation 3D optogenetics tool aiming to overcome the aforementioned technological hurdles and close all these gaps to enable *in vivo* optical investigations of brain cell morphology and function,** in the following directions (see a scheme in Fig. 2):

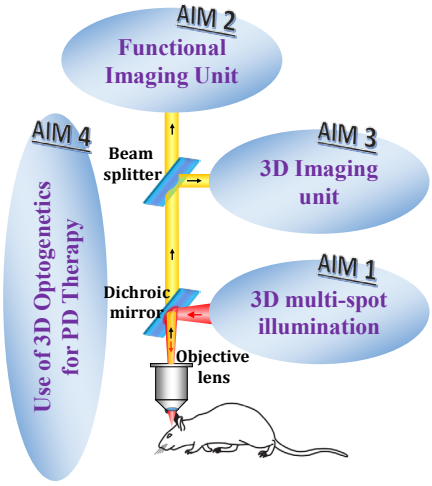

Fig. 2: Schematic of the objectives

1) Design and develop a **3D multi-spot illumination system** realizing the computer-generated holograms [AIM 1],
2) **Functional observation and computational modeling** of neural activity [AIM 2],
3) Record the activity of the neurons by **3D imaging technology based on metasurface systems** [AIM 3] to collectively generate the 3D brain mapping, and
4) Utilization of the developed system for the **improved treatment of Parkinson's Disease** [AIM 4].

3. Outline of Tasks/Work Plan

3.1 *3D Multi-spot Illumination System:*

This part of the project aims to shape illumination laser light in 3D space by designing phase-only modulation-based computer-generated holograms. The purpose of developing multi-spot illumination in 3D volume is to target a predefined set of interests only. Therefore, the light intensity and/or phase of the incident light needs to be spatially modulated for achieving simultaneous stimulation of multiple sites over the sample with arbitrarily-defined illumination patterns. Based on this concept, an efficient phase modulation technique termed computer-generated hologram (CGH) by introducing a flexible method based on the modified **3D Gerchberg–Saxton algorithm** (GSA), will be elaborated to develop a scanless photo-stimulation approach. Thus, the multi-spot illumination patterns, as shown schematically in Fig. 3, are realized by modifying the spatial phase of light in a plane conjugated to the sample plane with the generated CGH and displayed on the spatial light modulator. Though, **several limitations** should be addressed while implementing the technique due to the non-perfect nature of SLM. One of the limitations is the **unmodulated light energy**, termed zero-order light, which is located at the center of the excitation field. This zero-order light has to be rejected and researchers use a mechanical method such as blocking it at the conjugate plane to the objective lens. However, it also blocks a portion of the region-of-interest. New strategies to suppress the zero-order will be implemented by **wavefront-shaping and numerical methods**, and by modifying the optical configurations such as introducing the cylindrical lens in front of the SLM to

disseminate the zero-order intensity over a large area hence reducing its effect. Another limitation is the **speckle pattern**, creating a problem when stimulating a subcellular region [20]. Therefore, there is a need to develop new methods to overcome this issue. I will develop new modified optical configurations and optimized algorithms **to generate speckle-free phase patterns**, enabling the use of low excitation light energies. The optimized speckle-free phase patterns are expected to avoid out-of-focus glare and acknowledge remarkable accuracy for the particular excitation of subcellular activities together with preserving high lateral and axial resolution. There is a huge possibility of developing different illumination strategies to photo-stimulate opsin-expressing neurons to actively produce neuronal events as well as perturbing neural signaling.

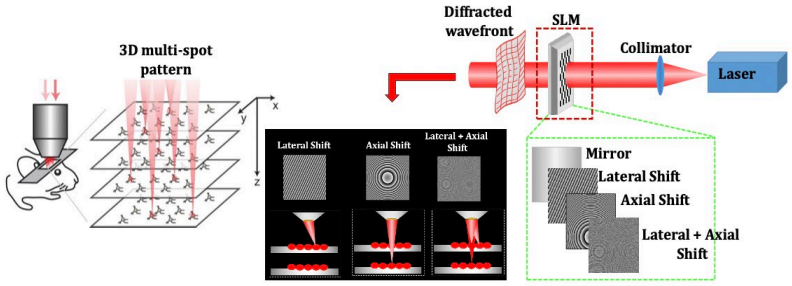

Fig. 3: Schematic of 3D multi-spot illumination system

3.2 ***Functional Observation System:***

The goal of functional imaging is to identify neuronal subpopulations that are associated with specific behavioral outcomes. The fluorescent calcium indicators are enforced in neurons to interrogate **several cellular signaling aspects** as neurons **communicate and process information** through them. The time-lapse studies are created to provide a fluorescent readout (**Ca^{2+} imaging**) for changes in biological activities by the illuminated light, which allows manipulating the morphological changes of neurons in both normal and disease conditions. The obtained traces of the calcium signal from the time-lapse images describe the activities of the neuronal circuits and they are generally associated with **behavior, emotions,** and **other pathological states** and, therefore, **helpful for the simultaneous controlling, monitoring, and perturbation of individual/integrated neuronal activity in the brain**. By analysis of the tuning peak, a mechanistic understanding of network dynamics and behavior can be revealed by identifying neurons and their morphologies and connectivity. Several studies have been reported, including specific behavior investigations of neuronal circuits [21], respiration regulation examination [22], circuits activity analysis [23], and pathological diagnosis of neuronal circuits [24], to name a few.

Research in neuroscience is currently focused on understanding how neuronal circuit activity affects behavior and pathology. To unraveling of this link requires **specific experimental strategies** that enable simultaneous monitoring and perturbing neuronal activity during behavior. As a result, a model of neural circuit mechanism must be developed that takes into account not only the accuracy of biological recordings but also the relationships between the neural circuits and their anatomical organization. With the collaboration of the neuroscientist [**Prof. Mitsuhiro Morita, Department of Biology, Kobe University**], a method should be devised for labeling cells of interest and preserving their basic morphology after functional characterization.

3.3 ***Single-shot Common-path 3D Imaging System based on Meta-surfaces:***

A 3D fluorescence imaging system based on **incoherent holographic principle** will be developed simultaneously to observe the response of the activated neuronal populations *in vivo* in 3D volume by employing the **meta-surfaces** and **diffractive optical elements**. The major focus will be developing the 3D imaging system with the **single-shot acquisition,** and **common-path configuration** as such systems

are of growing interest because they overcome the limitations of the two- or multi-channel optical systems and make the systems simple in geometry, compact in size, inexpensive by reducing the number of optical components, and less prone to environmental vibrations/perturbations. Furthermore, these frameworks provide high spatial and temporal phase stability, therefore these features make them suitable for biological inspection and optical imaging applications. **So, in line with the objective, I plan to design and develop a new framework of the 3D imaging system with single-shot and common-path configuration based on the metasurface**, in which a single recorded image (incoherent hologram), of the biological specimen, is sufficient to retrieve specimen information at different axial positions (see Fig. 4**). It is noteworthy that metasurface phase profiles can encode multiple optical functions** and the optical systems comprising such surfaces have revolutionized the ways with which electromagnetic waves can be **controlled and manipulated**.

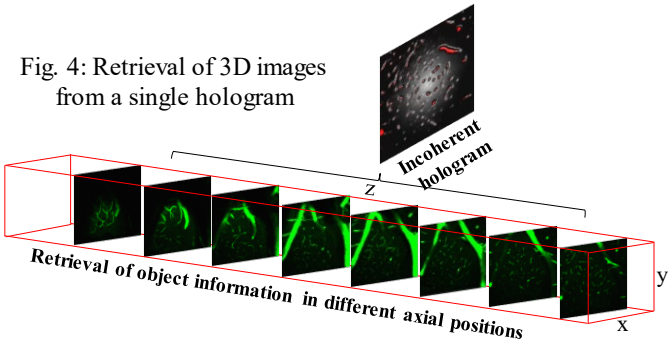

Fig. 4: Retrieval of 3D images from a single hologram

3.4 *3D Optogenetics for Parkinson's Disease Therapy:*

It is not far off to think that optogenetics could offer a more refined approach to the treatment of neurodegenerative disorders including Parkinson's disease (PD). The treatment of PD with deep brain stimulation (DBS) is an alternative method, however, it targets a small population of neurons, together with several other limitations. **The second major objective of the proposal is to use the developed 3D optogenetics system for PD therapy to elucidate neuronal function.** To alleviate the PD symptoms, the fetal brain cells are transplanted into the patient's brain, and traditional procedures such as DBS can damage the grafted cells. Also, the traditional approaches lack in discriminating different cell activities, for example, dopamine release, and secretion of immunomodulatory or paracrine factors. On the contrary, the proposed 3D optogenetics system could be investigated to control the spatial and temporal structures of the individual neurons and their neural activity including dopamine release, and investigate independently the other possible functions of these neurons by excluding the opportunity of useful contribution through other neuronal cell sorts. The brain regions with dysfunction in PD are first delivered by the genes for light-sensitive proteins and then activate the neurons which are blocked by dopamine to restore motor functions with the use of the developed optogenetics system. The precision of 3D optogenetics has the potential to improve the normalization of dysfunctional circuits in PD. Furthermore, using light instead of electricity may also lessen the chance of damaging outcomes because of non-specific influences on unintended targets. **Nevertheless, several other neuronal models of cell therapy can be examined with the developed system for graft function together with graft-to-host connectivity.**

4. Expected Outcomes and Prospects

This research work will contribute to the development of new research achievements and activities in the field of **3D optogenetics, 3D imaging, and simultaneous investigations of models of neurological disease**. The spatial and temporal structure of the complex neural system controls the brain functions and behaviors which can be investigated by the proposed system. Since different sets of neurons are associated with different functions, and if the activity of each set of neurons is analyzed then it would be possible to understand how they work together. By analyzing the activity of different neurons, various brain disorders

such as depression, Parkinson, etc. can be evaluated. **The proposed system would allow modulating, controlling, and monitoring of manifold neuronal activities with cellular and millisecond-temporal precision and resuscitating the physiological patterns of brain activity**. In optogenetics, various systems have been developed for photo-stimulation. ***However, none of them is capable of simultaneous 3D stimulation and 3D observation of neural activity***. Moreover, the system will be developed with single-neuron (cellular) spatial resolution across a large volume without compromising temporal precision. For a large field of view, the imaging speed can be improved by combining multiplexing technologies. Such efforts in the field of 3D brain mapping may provide the necessary evolutions and exciting achievements in the field of neuroscience. As an excellent tool for studying the brain's development, computation, and adaptation, *in vivo* imaging of brain cells is becoming increasingly popular. The health care devices and systems will be developed that may promote several collaborations and receive strong interest from research labs, hospitals, and companies.

5. Impact

The proposed research proposal could be beneficial for the imaging tool in the field of neuroscience to uncover the fundamental aspects and pathologies that have been beyond reach and reveal useful neural activity and their behavior and mental states. Furthermore, it would play an important role in a deeper understanding of brain activity, and helps in the improvement of diagnosis by monitoring disease progression. Being a multidisciplinary research proposal, I will work closely with a team of biologists (Prof. Prof. Mitsuhiro Morita, Department of Biology, Kobe University),), optical engineers [Prof. Osamu Matoba (Kobe University) and Prof. Yasuhiro Awatsuji (Kyoto Institute of Technology)], to develop the state-of-art 3D optogenetics tools and use it for the PD therapy and other neurological investigations. **Upon successful completion, this study will generate sufficient data to determine the feasibility of optogenetic therapy as a potential treatment for Parkinson's disease and may facilitate recovery from several neurological diseases.** It is expected that the success of the proposed project will open new research fields in neuroscience and the biomedical imaging field where **watching brain cells in action is possible.** Further, being an interdisciplinary research proposal, there is a huge possibility to carry out fruitful collaborative work with a team of neurologists, and electrical, and optical scientists.

6. Bibliography

1). Hague, S.M., et al. *Journal of Neurology, Neurosurgery & Psychiatry* 76.8 (2005): 1058-1063. **2).** Deisseroth, Karl, et al. *Journal of Neuroscience* 26.41 (2006): 10380-10386. **3).** Boyden, Edward S., et al. *Nature Neuroscience* 8.9 (2005): 1263-1268. **4).** Dal Maschio, Marco, et al. *Neuron* 94.4 (2017): 774-789. **5).** Ronzitti, Emiliano, et al. *Frontiers in Cellular Neuroscience* 12 (2018): 469. **6).** Yang, Weijian, and Rafael Yuste. *Current Opinion in Neurobiology* 50 (2018): 211-221. **7).** Quan, Xiangyu, Kumar, Manoj, et al. *Optics Letters* 43.21 (2018): 5447-5450. **8).** Kumar, Manoj, et al. *Scientific Reports* 10.1 (2020): 1-13. **9).** Kumar, Manoj, et al. *Journal of Biomedical Optics* 25.3 (2020): 032010. **10).** Rajput, Sudheesh K., et al. *Journal of Biomedical Optics* 25.3 (2020): 032004-032004. **11).** Kumar, Manoj, et al. *Optics and Lasers in Engineering* 151 (2022): 106887. **12.)** Kumar, Manoj, et al. *Applied Optics* 59.24 (2020): 7144-7152. **13).** Kumar, Manoj, and Osamu Matoba. *Optics Letters* 46.23 (2021): 5966-5969. **14).** Kumar, Manoj, et al. *Optics and Lasers in Engineering* 163 (2023): 107452. **15).** Rosen, Joseph, et al. *Advances in Optics and Photonics* 11.1 (2019): 1-66. **16).** Kumar, Manoj, et al. *Scientific Reports* 7.1 (2017): 11555. **17).** Kumar, Manoj, et al. Optics and Lasers in Engineering 160 (2023): 107306. **18).** Kumar, Manoj, et al. *Applied Optics* 59.24 (2020): 7321-7329. **19).** Kumar, Manoj, et al. *Scientific Reports* 12.1 (2022): 16462. **20).** Amako, Jun, et al. *Applied Optics* 34.17 (1995): 3165-3171. **21.)** Adamantidis, Antoine R., et al. *Nature* 450.7168 (2007): 420-424. **22.)**. Iwai, Youichi, et al. *Neuroscience Research* 70.1 (2011): 124-127. **23).** Tsai, Hsing-Chen, et al. *Science* 324.5930 (2009): 1080-1084. **24).** Domingos, Ana I., et al. *Nature Neuroscience* 14.12 (2011): 1562-1568.

OPEN-MED-ACT, **O**ptimization of **P**hotonic **E**quipment with **N**ovel **ME**dical **D**evice design based on optical properties: **A**ccelerating **C**linical **T**ranslation of biophotonics

Category: Health

What is the problem? Despite the potential to translate optical technologies, new spectroscopy/imaging systems and accurate treatment approaches have been slow to emerge. This slow uptake is partly due to the lack of tools to design and optimize optical instruments and treatment dosimetry. Designing medical devices starts with simulating potentially captured signals and/or treated tissue volumes based on instrument specifications and light propagation in the targeted samples (e.g., tissues and biofluids). Since simulations provide the **ground work of any medical device design** as well as **device fine tuning during clinical testing**, it is important that optical properties are reliable, accessible to instrument designers and available at wavelengths used by next-generation devices. However, limitations on the availability of optical properties and the disagreement within the research community slows down the development and clinical translation of optical technologies.

What is the solution? This project aims to accelerate the **clinical translation of biophotonics technologies** by providing an open **database** of optical properties of tissues (including skin, oral subsites, teeth, bone, brain, heart, kidney, liver and lung) and biofluids (including saliva, urine, blood) over a **wide range of wavelengths** (from 350-1900 nm and from 2500-25000 nm). For this purpose, we aim to build tools to extract optical properties based on diffuse reflectance, fluorescence, FT-IR and Raman spectra in a **more reliable** way compared to previous studies. The database will be available to the public as a website enabling quick assessment of optimized parameters for optical instrument design for specific applications. Finally, we intend to include Irish and Brazilian populations in our studies.

Why is this important? Until a reliable database of tissue and biofluid optical properties becomes publicly available, the clinical translation of optical technologies will be hindered by research, commercial and clinical barriers. Most industries typically prioritize application-specific research with shorter term outcomes and benefits to particular institutions and/or nations. That makes building an open database unfeasible and hinder international collaborations that are necessary to quantify variations of biological tissues and biofluids across different populations. **Funding the development of such a database is a rare opportunity to bring the biophotonics community together and encourage data sharing with intent of future standardization of optical properties**.

Why should this proposal be granted? By granting the funding to the Applicant, the database can be built in a research group having current and/or past collaborations with prominent MedTech companies such as Stryker, Medtronics, Raydiant and Rockley Photonics, and where expertise to extract tissue optical properties is already well established. Moreover, the development of such a database represents a critical first step to put the Applicant's long-term research vision into practice. Consolidating a basis for biophotonics medical device design would enable him to apply for follow up funding in collaboration with partner institutions of this project, and world-leading MedTech companies.

What is the impact on global challenges? In terms of applied research and commercial perspective, this database is essential for comparability of studies and multicenter initiatives to **translate biophotonics innovations** for **endoscopes, wearable devices, smartphones, imaging devices, personalized medicine devices, implantable devices** and others. The design of novel biophotonics instruments includes those for **real-time disease screening, diagnostics, staging, monitoring, treatment** and p**rediction of treatment outcomes**, as well as **surgical or therapeutic guidance.** From a fundamental research perspective, this database will be useful to evaluate the feasibility of "omics" studies (including **metabolomics, proteomics, lipidomics**, etc) which target the concentration of tissue constituents reported in the database. Since **translating cellular-level research findings to 3D cell culture models/tissues** may be hindered by light scattering and absorption effects, applications include advances in **tissue engineering, pharmacology, treatment dosimetry** and other fields.

Marcelo Saito Nogueira | marcelo.nogueira@tyndall.ie | IPIC & Tyndall, UCC

OPEN-MED-ACT, **O**ptimization of **P**hotonic **E**quipment with **N**ovel **ME**dical **D**evice design based on optical properties: **A**ccelerating **C**linical **T**ranslation of biophotonics

1. Literature Review

Healthcare economics: Optical technologies have the largest share on the medical imaging market, surpassing the radiological imaging sector with a 64% of the total medical imaging marketing (i.e. 2015-2017 estimated valuation of $72 billion per year, and $90.7 billion if including the home healthcare and wearable devices markets [1]. Current widespread technologies involve endoscopic imaging, optical coherence tomography (OCT), and pulse oximetry. Despite the potential to translate optical technologies, new spectroscopy/imaging systems and accurate light treatment approaches have been slow to emerge. For example, no wearable devices are currently commercialized for widespread hydration monitoring, despite technological proof of concept having been shown more than 30 years ago [2]. The same is valid for photodynamic therapy (PDT) protocols of head and neck surgery [3], colorectal cancer [4], and other diseases. Even biofluid-based diagnosis of brain tumors have not been widely implemented despite the promising approach for cost savings in health systems worldwide [5].

Need for a database of optical properties: A typical route to design medical devices starts with simulating potentially captured signals and/or treated tissue volumes based on instrument specifications and light propagation in the targeted samples (e.g., tissues and biofluids). In screening and diagnostics, simulations indicate whether it is possible to detect the expected biomarker concentration and the optimal instrument specifications for such detection. In therapeutics, simulations provide the light dose threshold to treat the desired tissues. All simulations require accurate values of sample optical properties in order to optimize instruments and protocols of light delivery. Since simulations provide the *ground work of any medical device design* as well as *device fine tuning during clinical testing*, it is important that optical properties are reliable, accessible to instrument designers and available at wavelengths used by next-generation devices. However, optical properties are currently not openly available as part of a database. Most of tissue optical properties have not been measured at both *body temperature* and at a *broad range of wavelengths*. Differences in measurement methods lead to up to ~3664% of discrepancies found in literature values of optical properties [9]. Limitations on the availability of optical properties and the disagreement within the research community slows down the development and clinical translation of optical technologies, as it is uncertain which values are reliable. No community effort has been made to standardize optical properties and make them openly available. In this context, risk for healthcare investors is seen as much greater and the community would highly benefit from an *open database of optical properties*.

Wavelength ranges and measurement reliability: Currently, absorption and scattering properties have been extracted by using three main measurement methods. First, optical properties have been extracted by using integrated sphere setups that require thin tissue slices, which dehydrate faster than bulk tissue and cannot be easily kept at body temperature. The second method is time-of-flight spectroscopy (TOFS), which enables decoupling absorption and scattering coefficients as long as light propagates through sufficiently long pathlengths in tissue and enough photons can be collected to surpass its poor signal-to-noise ratio (limited photons are collected at high absorption and scattering coefficients). Because of this TOFS measurements take longer, cannot be performed at all wavelengths and have been typically performed in bulk tissue only. The third method is reflectance spectroscopy (RS), which enables real-time measurements of tissues and biofluids including samples at body temperature. RS instruments have smaller footprint, are relatively less expensive, can measure

[1] https://spie.org/news/spie-professional-magazine-archive/2018-january/optics-of-medical-imaging?SSO=1
[2] Walling, PRISCILLA L., and JACQUELYN M. Dabney. J. Soc. Cosmet. Chem 40.3 (1989): 151-171 and Matcher, S. J., M. Cope, and D. T. Delpy. Physics in Medicine & Biology 39.1 (1994): 177.
[3] Keller, Gregory S., Daniel R. Doiron, & George U. Fisher. Archives of Otolaryngology 111.11(1985):758-761.
[4] Barr, H., N. Krasner, P. B. Boulos, P. Chatlani, and S. G. Bown. British Journal of Surgery 77.1 (1990): 93-96
[5] Gray, E., Butler, H.J., Board, R., Brennan, P.M., Chalmers, A.J., Dawson, T., Goodden, J., Hamilton, W., Hegarty, M.G., James, A. and Jenkinson, M.D. BMJ open 8.5 (2018): e017593

a wide range of wavelengths can be combined with fluorescence spectroscopy (FS) and Raman spectroscopy (RS), and can be used for sample biochemical characterization with miniaturized probes. In tissues, keeping samples at body temperature is important not to measure unreliable variations of water absorption, which fluctuate with temperature. In biofluids, not keeping body temperature to concentrate analytes during biofluid evaporation may denaturate peptides and proteins and change solvatation states. That means bound water and the spatial distribution of analytes in the concentrated biofluid sample may be different and keeping body temperature during evaporation is important. For both tissues and biofluids, RS (including ATR-FTIR spectroscopy; ATR: Attenuated total reflection) is currently the most reliable method to measure optical properties for our database.

Measurement reproducibility: Studies using biophotonics technologies have been standardized by using phantoms as well as estimating tissue optical properties and the interrogated volume by using analytical or probabilistic models of light propagation in complex media. Although standardization methods are available and multicentre studies have been carried out to develop protocols to standardize optical systems at EU level (21 European laboratories included in the MEDPHOT study)[6], they are mostly used by few research groups with expertise in optical standards [7] and computer simulations [8]. Since each measurement method has different sources of errors and research groups are constantly upgrading their equipment, the consequence is a discrepancy of up to 512 cm^{-1} (~52% discrepancy for dentin) for tissue absorption coefficients, up to 403 cm^{-1} for scattering coefficients (~3664% discrepancy for white matter at 1064 nm) [9], up to 0.72 ns (~44.7% discrepancy for cardiac myocytes) for fluorescence lifetime [10] (pages 58-61) and up to 6.8 μM (~6182% discrepancy for malignant breast lesions) for oxyhaemoglobin concentrations [11]. System calibration with optical phantoms still did not solve the problem of non-comparability between studies. Therefore, no standardization of optical properties has been achieved within the biophotonics community.

2. Problem statement: Until a reliable database of tissue and biofluid optical properties becomes publicly available, the clinical translation of optical technologies will be hindered by research, commercial and clinical barriers. Most industries typically prioritize application-specific research with shorter term outcomes and benefits to particular institutions and/or nations. That makes building an open database unfeasible and hinder international collaborations that are necessary to quantify variations of biological tissues and biofluids across different populations. Funding the development of such a database is a rare opportunity to bring the biophotonics community together and encourage data sharing with intent of future standardization of optical properties.

Why should this proposal be granted? By granting the funding to the Applicant, the database can be built in a research group having current and/or past collaborations with prominent MedTech companies such as Stryker, Medtronic, Raydiant Oximetry and Rockley Photonics, and where expertise to extract tissue optical properties is already well established. Moreover, the development of such a database represents a critical first step to put the Applicant's long-term research vision into practice. Consolidating a basis for biophotonics medical device design would enable him to apply for follow up funding in collaboration with strategic partners of the host organisation, and MedTech companies among the 32 life sciences companies geographically close to Tyndall National Institute. Future partnerships are promising to accelerate the clinical translation of biophotonics technologies.

3. Objectives: In this project, the Applicant aims to accelerate the clinical translation of biophotonics technologies by developing a database of optical properties and biochemical profiles of tissues and biofluids. OPEN-MED-ACT aims to build a database which will contain optical properties measured over a *wide range of wavelengths* (from 350-1900 nm and from 2500-25000 nm) and in *more reliable*

[6] Pifferi, A., Torricelli, A., Bassi, A., Taroni, P., Cubeddu, R., Wabnitz, H., Grosenick, D., Möller, M., Macdonald, R., Swartling, J. and Svensson, T., Appl. Opt., 44, 2104 (2005).
[7] Pogue, Brian W., and Michael S. Patterson. Journal of biomedical optics 11.4 (2006): 041102.
[8] Alerstam, Erik, Tomas Svensson, & Stefan Andersson-Engels.Journal of biomedical optics 13.6(2008): 060504
[9] VV Tuchin. SPIE, 2007 (pages 145-191)
[10] Marcu, Laura, Paul MW French, and Daniel S. Elson, eds. CRC Press, 2014
[11] Grosenick, D., Rinneberg, H., Cubeddu, R. and Taroni, P. Journal of biomedical optics 21.9 (2016): 091311

ways compared to previous studies. Biological tissues will be measured at body temperature. Biofluids will be measured by ATR-FTIR spectroscopy after evaporating water at body temperatures to avoid denaturation of peptides and proteins and avoid changing their solvation states. Keeping body temperature constant during evaporation is important to keep the natural bound water to biochemical constituents of biofluids, as well as keep their spatial distribution of analytes in the concentrated sample. In addition, we intend to include sample measurements of at least Irish and Brazilian populations in our study.

The long-term goal of OPEN-MED-ACT is to provide open source tools for quick assessment of optimized parameters for spectroscopy, imaging and phototherapeutic instruments based on the specific sample targeted by the desired application. These tools consist of website functions capable of quickly displaying sample spectra to users at the desired range of wavelengths or wavenumbers required. Our goal will be reached by accomplishing the following research objectives (ROs):

RO1. Build a database of tissue and biofluid characteristics based on experimental measurements and simulation of light propagation into tissues.
RO2. Implementation of open source tools for access to relevant parameters for instrument design.
RO3. Accelerate the clinical translation by partnering with companies interested in de-risking medical device projects.

4. Outline of tasks/Work plan

Research methodology and approach: In order to address each of the ROs, the OPEN-MED-ACT project combines technical and project management tasks of 5 work packages (WP). **RO1** will be explored as a result of simulations, analysis and experimental measurements performed at WP1, WP3 and WP4. A first version of the database will be built with the data in the current literature and will be upgraded upon processing the data from *ex vivo* and *in vivo* studies. **RO2** will be exploited by developing open source tools in WP1 based on the data analysis in WP4, which will reveal the relevant parameters to be targeted for instrument optimization. Once these parameters are determined,

Gantt chart		Months																	
WP	Title	1	2	3	4	5	6	7	8	9	10	11	12	13	14	15	16	17	18
WP1	**Simulations and open-source tools**																		
T1.1	Literature review																		
T1.2	Simulations									M1.1									
T1.3	Development and update of LUTs																M1.2		
WP2	**Optical systems**																		
T2.1	Build optical systems																		
T2.2	Probe designs and study protocols									M2.1									
T2.3	Adaptation for tissue and biofluid measurements											M2.2							
WP3	***Ex vivo* and *in vivo* studies**																		
T3.1	System calibration																		
T3.2	Phantom validation											M3.1							
T3.3	Laboratory risk assessments																		
T3.4	Clinical research ethics documents												M3.2						
T3.5	*Ex vivo* tissue studies																		
T3.6	*Ex vivo* biofluid studies																		
T3.7	*In vivo* tissue studies																M3.3		
WP4	**Data analysis & database of tissue characteristics**																		
T4.1	Spectral processing algorithms														M4.1				
T4.2	Extraction of relevant tissue characteristics																		
T4.3	Website for the database											M4.2					M4.3		
T4.4	Website user interface																		
WP5	**Project management**																		
T5.1	Supervision & management		M5.1																
T5.2	Project reporting and communication						D5.1						D5.2						D5.3

equipment specifications will be changed as part of WP3. The Applicant will fulfil the requirements for **RO3** by exploiting the network built in University of Sao Paulo (USP), University of Taubate (UNITAU) and the industrial connections Tyndall has with medical device companies for accelerating the clinical translation in biophotonics. To this intent, the Candidate will be consistently trained to acquire sufficient technical knowledge for all the tasks of the OPEN-MED-ACT project, expand his network and industrial collaborations. In addition, the knowledge about the database will be communicated via different channels (including dissemination in scientific journals, social media, etc)

Table 1: **Description of** t**ask allocation and work flow. Acronyms:** m: months, M: milestones, WP: work package, RS: reflectance spectroscopy, FS: fluorescence spectroscopy, ATR-FTIR: Attenuated total reflection (ATR) Fourier-transform infrared spectroscopy, TOF: time-of-flight spectroscopy.

	Description of work
WP1	**Simulations and open-source tools.** In WP1, the tissue optical properties (OPs) listed in the current literature will be investigated until **m5.** These OPs and those obtained through *ex vivo* and *in vivo* tissue measurements and used for Monte Carlo and/or NIRFAST simulations of light propagation in biological tissues until **M1.1 (m9)**. Based on the available OPs, we will evaluate the fluence rate distribution in complex media to build lookup tables (LUTs) associating measured variables (e.g. reflectance and fluorescence) with tissue OPs. We aim to provide an early-stage database for optical designers by **m11** and a second version of the database once we obtain results of the *in vivo* studies **M1.2 (m16).** Simulations will continue until the end of the project (**m1-m18**) to constantly update the LUTs.
WP2	**Optical systems.** Optical systems will consist of (1) a RS system measuring samples from 350-1900 nm, (2) a FS system with excitation at 340 nm, 405 nm, 470 nm, 505 nm, 532 nm, 660 nm and emission from 350-1100 nm, (3) a Raman spectroscopy with excitation at 730 nm, 785 nm, and 830 nm to measure both fingerprint and high-wavenumber regions of the spectra, (4) a portable ATR-FTIR spectroscopy system with temperature control, and (5) a TOF spectroscopy system to compare the extraction of optical properties with RS at particular wavelengths and aid system calibration with tissue-mimicking phantoms. Each system will have different holders for tissue and biofluid samples, depending on their volume and measurement protocols. We aim to build optical systems by **m6** and complete probe designs and study protocols up to **M2.1 (m9)**. Protocols will be adapted throughout measurements performed in WP3. Similarly, system will be adapted as measurements are carried out. We aim to have all optical systems adapted by **M2.2 (m11)**.
WP3	***Ex vivo* and *in vivo* studies.** Optical systems will be calibrated and measurements validated in phantoms throughout the whole study. By **M3.1 (m11)**, we aim to fix the phantoms to be measured at each combination of samples and optical systems. From the beginning of the project, documents for laboratory risk assessments and clinical research ethics approval for all experiments will be sent institutionally. We expect to have approval of these documents by **m6** for the *ex vivo* tissue measurements, by **m9** for the *ex vivo* biofluid measurements and by **M3.2 (m12)** for the *in vivo* tissue measurements. The approval for *in vivo* tissue measurements will be sought at University College Cork (UCC) and at USP, whereas approval for *ex vivo* biofluid measurements will be sought at UCC and at UNITAU in order to cover measurements of Irish and Brazilian populations. Measurements will be taken at both institutions as part of a collaboration. *Ex vivo* tissue measurements will be performed in animal tissues including bone, brain, bladder, heart, kidney, liver, lung, muscle, pancreas and spine. We aim to measure e*x vivo* biofluids including saliva, urine, blood, breast milk, tears, semen and sweat. *In vivo* tissue measurements to be performed at UCC and USP include measurements of normal patient tissues such as skin, oral subsites, teeth, breast and indirect measurement of internal organs by placing probes on the patient skin. Tissue measurements performed only at UCC may include normal and diseased colorectal tissue and oral tissue measurements. We aim to write publications and transfer the collected data to the database by **m10** for *ex vivo* tissue measurements**,** by **m13** for *ex vivo* biofluid measurements**,** and by **M3.3 (m16)** for *in vivo* tissue measurements. Measurements may continue afterwards and the database updated accordingly.
WP4	**Data analysis & database of tissue characteristics.** Reflectance and transmittance data will be used to calculate absorption and reduced scattering coefficients, as well as the biomolecule concentrations associated with the absorption by tissue chromophores. Fluorescence data will be used to compute fluorescence properties and fluorophore concentrations upon prior knowledge of the absorption and reduced scattering coefficients. Tissue optical properties will be determined by using an experimental lookup table based on the calibration with optical phantoms or by using spectral fitting algorithms based on the output of computer simulations of light propagation in complex media. For the systems based on experimental lookup tables (LUT), the validation will be performed simultaneously to acquiring measurements to build LUTs. We aim to finalize the vibrational spectral processing algorithms (for

	ATR-FTIR and Raman) by **m6** including data pre-processing and semi-quantitative analysis only. Since quantitative analysis would require LUTs based on simulations, our preliminary algorithm to extract tissue characteristics should be ready by **m9** and a more sophisticated algorithm should be finalized by **M4.1 (m14)**. The website development will follow the development and update of LUTs with an early-stage database available by **M4.2 (m11)** and a more sophisticated version by **M4.3 (m16).**
WP5	**Project management.** Management activities will consist of a career development plan at **M5.1 (m2)**, review meetings, and reporting schedules. Reports for periodic evaluation of progress will be delivered at **D5.1 (m6)**, **D5.2 (m12)** and **D5.3 (m18).** Training will be provided by the host institutions.

5. Outcomes: we aim to extract optical properties of at least 5 *ex vivo* tissues of internal animal organs, *in vivo* skin and oral subsites, and at least 2 biofluids. OPEN-MED-ACT aims to communicate the existence of the database to the community via the website, 3 journal publications and at least 2 conference presentations. Publications and presentations will be based on the knowledge added through the database as well as topics following the Applicant's expertise (outlined in the Applicant's CV) including: (i) Simulations & retrieval of tissue characteristics, (ii) Phantom validation, animal and human studies, (iii) Tutorials of optimization of optical systems using the database. To promote project visibility, we aim to disseminate the generated knowledge to the widest audience including researchers, physicians, industry partners, policy makers and general public.

6. Impact: Once the optical properties database is completed, there will be endless opportunities to evaluate the *feasibility of biomarker detection* by photonic devices and to *optimize treatment planning*. The first outcome is strategically partnering with research and industry to accelerate the clinical translation of their research-stage devices. For instance, interstitial PDT companies on clinical trials could use the database and the Applicant's expertise on Monte Carlo simulations of light propagation in tissues to set thresholds of light dose to treat the diseased tissue volumes without compromising surrounding normal tissues. Similarly, the same database and expertise can be used to assess the detectability of biomarker (e.g., collagen) concentration in bone fractures located at a certain tissue depth, as well as the optimal instrument specifications for such detection. This extends to any optical instrument including *treatment, imaging, wearable and implantable devices*.

A second outcome is the development of *novel technologies and protocols* to solve global health problems. For example, the current photobiomodulation therapy for oral mucositis involves shining light directly on lesions. However, direct irradiation is not possible for patients who cannot open their mouth because of severe pain. If irradiation is performed from outside the oral cavity, skin color needs to be taken into account in order to deliver the correct light dose to the targeted lesion. The Candidate aims to use the database to extract correction factors for photobiomodulation in various applications including the treatment of oral mucositis, since he already has collaborations for that in University of Sao Paulo (USP; one of the partners in this project).

Finally, the database would enable the Applicant to *quantify tissue and biofluid biomarkers and evaluate their detectability in novel applications*. To be closer to the actual clinical scenario, the ATR-FTIR spectroscopy system aims to be used for clinical applications in which biofluids are measured as they are collected instead of after freezing and thawing as in current measurement protocols. Similarly, technologies built as part of this project will be translated to the clinic. Clinical translation will be enabled by research conducted in collaboration with Mercy University Hospital (MUH), Cork University Hospital (CUH), University of Taubate (UNITAU), USP, and strategic industry partners.

Any future research and industrial projects are paths for the consolidation of the Applicant's research career, as well as ways to solve global health challenges by accelerating the clinical translation of biophotonics technologies. The database is essential for comparability between studies and start multicentre initiatives. Applications include real-time *disease screening, diagnostics, staging, monitoring, treatment, dosimetry, prediction of treatment outcomes, as well as surgical or therapeutic guidance*, as well as evaluation of the feasibility of "omics" studies (including *metabolomics, proteomics, lipidomics*, etc) which target the *concentration of tissue constituents* for tissue engineering, pharmacology, treatment dosimetry and other fields. The open-source tools developed can be used as education resources for biophotonics programs worldwide and open new opportunities for *interdisciplinary education*. The success of the project will be driven by the Applicant's experience with many of the medical applications listed above, biophotonics education, as well as various optical spectroscopy techniques outlined in his CV.

Executive Summary

Artificial Lighfe: Bridging AI and optical lifeforms

Prof. Marco Piccardo
Técnico Lisboa and INESC Microsystems and Nanotechnologies, Portugal
Harvard University, USA

Artificial Intelligence (AI) has revolutionized many areas of information technology, such as data analysis, automation, predictive modeling, and decision-making processes. However, as we continue to generate and process an ever-growing tsunami of data, the global electricity consumption associated with these operations is becoming a significant concern. Photonics, the science of light generation, detection, and manipulation, offers a promising approach to augment or even replace traditional electronic architectures for AI. Photonic systems are renowned for their parallelism, high-dimensionality, and low-power consumption, making them ideal for handling the increasing demands of AI applications. They can help make AI faster, more efficient, and more sustainable, thereby addressing the pressing need for energy-efficient data processing. Despite these advantages, the mutual influence of AI and optics has so far been mainly confined to the realm of deep learning inference in computer vision, microscopy and other visual computing tasks. While these fields have seen significant advancements, there is a vast, unexplored potential for further integration of AI and optics.

This project aims to transcend the boundaries of existing optical architectures and propose a novel optical system rooted in the principles of Artificial Life. This innovative approach opens new horizons in the interplay of AI and optics, pushing the limit of what is currently achievable. Our objective is to implement an analog all-optical system based on continuous cellular automata, which will generate optical lifeforms capable of self-organization, evolution, complex interactions, and dynamic adaptation. We refer to this as "Artificial Lighfe".

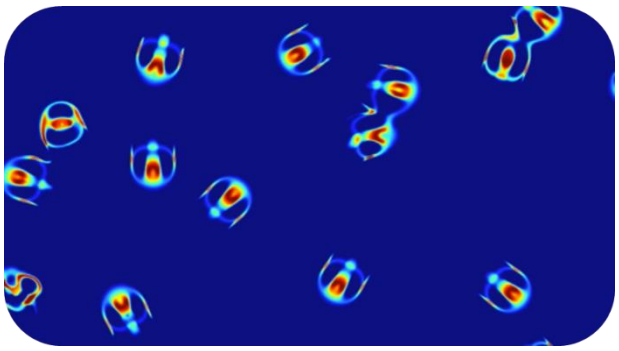

Artificial Lighfe represents a natural, eminently scalable form of optical computing, involving recurrent computation performed entirely with light, with no electronic intermediary. This system will diversify AI by opening the possibility of analog implementation of recurrent residual convolutional neural networks, open-endedness, and generative art via optics. Simultaneously, Artificial Lighfe will serve as a playground for AI, providing a unique platform for the deployment of exploratory, genetic and novelty search algorithms, and enabling the testing of pattern recognition, generation and encoding techniques. The computational capacity of the prototype is estimated to be over 5×10^{16} operations/s, with a power consumption of approximately 10 W. This translates to an energy efficiency better than 0.2 fJ per operation, which is about 5000 times better than a GPU.

By creating a symbiotic relationship between AI and optics, we aim to unlock new possibilities in both fields, paving the way for a more sustainable, efficient, and innovative future in information technology.

Proposal

Artificial Lighfe: Bridging AI and optical lifeforms

Prof. Marco Piccardo
Técnico Lisboa and INESC Microsystems and Nanotechnologies, Portugal
Harvard University, USA

Artificial Lighfe seeks to intertwine the realms of artificial intelligence (AI) and photonics, thereby broadening the scope of AI applications and establishing a unique platform for AI exploration and development. Our primary objective is to engineer an innovative optical system that leverages continuous cellular automata (CA) to generate optical lifeforms exhibiting complex behaviors for efficient and scalable optical computing. We start by examining the existing landscape of photonics within AI, subsequently delving into the relatively unexplored domain of CA. Our focus will be on the potential of continuous CA systems, their optical implementation, and the transformative implications they hold for the future of AI.

Literature Review

The current pinnacle of photonics in artificial intelligence (AI) is represented by photonic deep neural networks [Wetzstein2020, Shastri2021]. These networks, either all-optical or hybrid electro-optical, excel in AI tasks related to imaging and computer vision. They perform key operations, such as creating convolutions, executing Fourier transforms, and projecting randomly, at the speed of light, potentially with minimal power requirements [Chang2018, Lin2018, Saade2016]. However, implementing optical nonlinear activation functions at low optical signal intensities remains a significant challenge. Despite this, recent advances, including nonlinear thresholders, saturable absorbers, and electro-optical approaches, have shown promise in overcoming this hurdle.

Building on this foundation, our focus shifts to an underexplored area in optics for AI: cellular automata. CA, an abstract computational model introduced in the 1940s, were designed to create a self-replicating machine that evolves over time. In their most elementary form, CA are one-dimensional array of cells that can assume only two states and evolve according to a basic set of rules involving only local interactions and giving rise to incredibly complex behaviors [Wolfram2002]. More sophisticated, two-dimensional realizations of CA include the popular Game Of Life. In terms of optical implementations of CA, previous attempts at AT&T Bell Laboratories in the late 1980's faced challenges due to the limitations in manipulating light and the use of inadequate electronic feedback circuits [Murdocca1987, Taboury1988]. More recently, an interesting demonstration of optical CA was achieved using a time-multiplexed photonic network, where the cells are represented by pulses of light in a mode-locked laser, the cell states are encoded by an electro-optical modulator, the neighborhood coupling is carried out by optical summation and the nonlinear feedback is implemented by optoelectronic thresholding and a field-programmable gate array [Li2023]. This approach, while effective in demonstrating the optical CA concept, incurs additional overhead due to the optoelectronic and digital-to-analog conversions performed and was limited to the elementary, discrete CA.

Problem Statement and Objectives

Our work aims to go beyond these limitations by implementing continuous CA systems, which can be more naturally implemented using optics. These models, which include the software-based artificial life simulators demonstrated in the Google project Lenia [Chan2019], Larger-than-Life [Evans2001], and SmoothLife [Rafler2011], extend the Game of Life to a continuum, resulting in far richer and more complex behavior. In particular, the lifeforms discovered in Lenia exhibit a spectacular variety of properties, such as self-organization, self-replication, evolution, division of labor, polymorphism, and behaviors categorized based on their locomotive modes and symmetries (Fig. 1). Despite these patterns not being physical entities, they exhibit many features of lifeforms and can thus help examine systems related to natural life, thus addressing some of the most important problems in Artificial Life, such as determining whether fundamentally novel living organizations can exist [Bedau2000].

In Artificial Lighfe, we aim to bridge these continuous CA with new frontiers in AI by implementing them in innovative optical systems. Our approach—fundamentally different from other optical neural networks—involves recurrent computation performed entirely with light, without an electronic intermediary. This allows for high-speed, energy-efficient computations. The 3D nature of our device makes it scalable in a way that strictly 2D devices are not. This will represent a significant leap beyond the current state of the art in photonics for AI. Our goal is to harness the uncharted territory of optical lifeforms to expand the field of AI, making it more sustainable and efficient through a new form of natural and scalable optical computing.

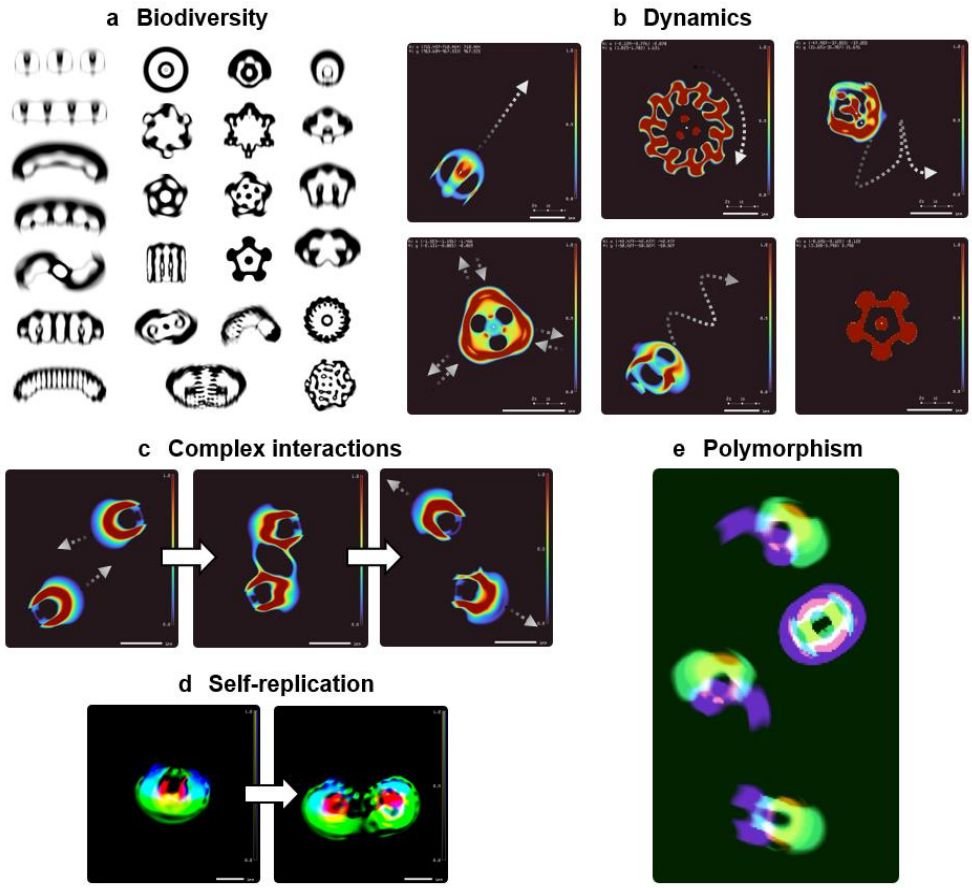

Fig. 1: Artificial lifeforms emerging in the continuous cellular automata model Lenia. a, Diversity of lifeforms obtained with different evolution rules. **b**, Examples of dynamics of some lifeforms (from top row to bottom): linear, rotating, chaotic, oscillating, zig-zag, and stationary. **c**, Two individual lifeforms interacting through attractive and repulsive forces. **d**, Reproduction of a lifeform by binary fission. **e**, Same rule parameters (i.e. same genotype) leading to polymorphism (i.e. multiple phenotypes).

Objective 1: Optical Implementation of Artificial Lighfe

Our first major objective is to implement a Lenia-like continuous CA model using optics. This involves creating a continuum of states, space, and time. The richness of lifeforms that will be produced depends on the number of modes available in the system, requiring the use of a multimode photonics platform [Piccardo2021] with many degrees of freedom. For this, we will develop a modified self-imaging laser cavity [Nixon2013, Piccardo2022] hosting a very large number of transverse modes. In the future other multimode implementations can be considered, such as time bins [Li2023] or frequency combs [Feldmann2021].

The key steps underlying the evolution of artificial life in Lenia are: convolution of the space ("world") with a kernel, nonlinear mapping (i.e. the CA rule) and iterative updating. All these operations will be implemented in our envisioned laser (Fig. 2). Convolutions are very conveniently implemented with free-space optics [Chang2018] as matrix multiplications at the Fourier plane between the optical beam and a mask (corresponding to the Fourier transform of the kernel). The nonlinear mapping will be realized by developing a new type of physical neural network [Wright2022] embedding a spatial light modulator (SLM), gain and saturable absorber nonlinearity. The iterative update will be naturally implemented in the resonator, and an imaging port will allow monitoring the system evolution [Sephton2019]. A preliminary numerical study modeling the system has shown promising results with the emergence of optical lifeforms (Fig. 2b).

Objective 2: Artificial Lighfe for AI

The second major objective is to use Artificial Lighfe as an analog optical platform for implementing and testing AI algorithms. This includes the analog implementation of open-ended algorithms, recurrent residual convolutional neural networks, and generative

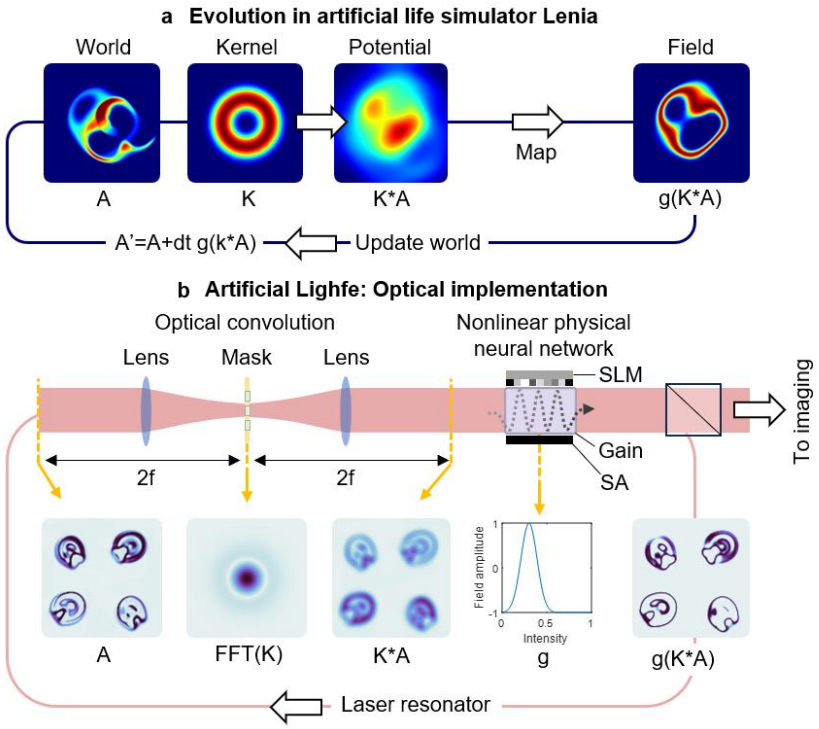

Fig. 2 Optical implementation of Artificial Lighfe: a, The key operations involved in the evolution of the continuous cellular automata model Lenia. **b,** Modified self-imaging laser cavity including a nonlinear physical neural network envisioned to implement an analog Lenia-like artificial life simulator. The images are results of preliminary computational study of the system (confidential).

art. The optical system could serve as a unique environment for AI development and experimentation, providing a rich, dynamic, and interactive platform for testing and refining AI techniques. This will involve using the laser to simulate complex systems or processes and to generate data for training AI models. The unique properties of optical lifeforms, such as their self-organization, evolution, and complex interactions, could also provide valuable insights for the development of new AI techniques.
To highlight the potential of our approach, let us consider the computational capacity of our prototype, assuming we have 10^5 spatial modes [Cao2019] and a cavity length of 60 cm. Each round trip, at 500 MHz, involves a convolutional neural network. Assuming the neighborhood is up to 10^3 sites (pixel modes), we have $N\times10^3\times10^5$ operations per round trip, where N~1-100 is a prefactor depending on the effective number of layers in the physical neural network, roughly considered to be the number of bounces off the SLM. Taking N=1 conservatively, we get 5×10^{16} operations/s. With a typical of laser power consumption of 10 W, we get 0.2 fJ/operation, being about 5000 times better than a GPU. For N=10, the value improves to 20 aJ/operation, underscoring the efficiency of our device. Harnessing this computational power will be a software challenge, akin to how AI engineers learned to exploit GPUs [Hooker2021].

Outline of Tasks

1. Optical Implementation of Artificial Lighfe
    i. Develop a physical neural network implementing nonlinear maps
    ii. Design and fabricate Fourier masks for optical convolutions
    iii. Build the multimode laser cavity
    iv. Set up a fast imaging system for time-resolved characterization
    v. Conduct studies on system's error tolerance and robustness
2. Artificial Lighfe for AI
    i. Establish efficient methods for data input/output and integration with AI
    ii. Train deep learning models using analog artificial life data
    iii. Adapt nonlinear maps for simulating complex systems
    iv. Leverage the platform for the development of new recurrent neural network architectures, generative art, generative models (e.g., stable diffusion).

The laser experiments will be conducted at Técnico Lisboa under the PI's guidance, leveraging his expertise in self-imaging resonators. Fabrication processes will take place at INESC Microsystems and Nanotechnology, where the PI leads nanophotonic research. The development of the nonlinear physical neural network will be in collaboration with Logan Wright's group at Yale University, pioneer in the field. The prize funds will be allocated towards equipment for the construction of the laser cavity and the remuneration of a dedicated postdoctoral researcher.

Outcomes

- Demonstration of a natural computing platform with light based on continuous CA rules enabling complex, self-assembling light structures, such as the solitonic CA [Tokihiro1996];
- Development of a nonlinear physical neural network, providing a practical solution for all-optical implementations of AI and advancing the vision of an energy-efficient and high-speed alternative to traditional electronic computing;
- Connection with generative models through our system's optical diffusion process, enabling tasks like image and video synthesis or reconstruction;
- Scaling up of our system to other multimode systems, such as fiber lasers with 10^{10} modes [Senanian2023], to increase complexity and energy efficiency.

Impact

- Enabling high-speed, energy-efficient AI computations, for real-time responses in high-data scenarios;
- Make information transfer and storage more energy-efficient, enhancing existing technologies in the information sector;
- Enhancement of the efficiency of data transmission in telecommunications through advanced all-optical logic operations enabled by nonlinear physical neural networks;
- Serving as an experimental platform for simulating various natural phenomena, exploring cellular automata principles, and studying complex systems behavior;
- Potential to reshape fields from telecommunications to AI, opening new avenues for fundamental research.

In conclusion, Artificial Lighfe presents a pioneering venture that bridges the realms of artificial intelligence and photonics. By implementing continuous cellular automata in an optical system, we aim to generate complex optical lifeforms, advancing the field of AI, and making it more sustainable and efficient. The potential outcomes and impacts of this project are vast, ranging from high-speed, energy-efficient AI computations to reshaping fields from telecommunications to image processing. This project represents a significant opportunity to support a blue sky idea for the pioneering of new concepts in Portugal—a country lacking specific funding for optics—while expanding the geographical diversity of the Optica Foundation.

References

[Bedau2000] M. A. Bedau *et al*., Open problems in artificial life, Artificial life 6, 363 (2000)
[Cao2019] H. Cao *et al*. Complex lasers with controllable coherence. Nat Rev Phys 1, 156 (2019)
[Chan2019] B. W.-C. Chan, Lenia: Biology of Artificial Life, Complex Systems, 28, 251 (2019)
[Chang2018] J. Chang *et al*., Hybrid optical–electronic convolutional neural networks with optimized diffractive optics for image classification, Sci. Rep. 8, 12324 (2018)
[Evans2001] K. M. Evans, Larger than Life: Digital Creatures in a Family of Two-Dimensional Cellular Automata, Discrete Models: Combinatorics, Computation, and Geometry (2001).
[Feldmann2021] J. Feldmann *et al*., Parallel convolutional processing using an integrated photonic tensor core, Nature 589, 52 (2021)
[Hooker2021] S. Hooker, The hardware lottery, Communications of the ACM 64, 58 (2021)
[Li2023] G. H. Y. Li *et al*., Photonic elementary cellular automata for simulation of complex phenomena, Light: Science & Applications 12, 132 (2023)
[Lin2018] X., Lin *et al*., All-optical machine learning using diffractive deep neural networks, Science 361, 1004 (2018)
[Murdocca1987] M. J. Murdocca, Digital optical computing with one-rule cellular automata, Appl. Opt. 26, 682 (1987)
[Nixon2013] M. Nixon *et al*., Observing geometric frustration with thousands of coupled lasers, PRL 110, 184102 (2013)
[Piccardo2021] M. Piccardo *et al*., Roadmap on multimode light shaping, Journal of Optics 24, 013001 (2021)
[Piccardo2022] M. Piccardo *et al*., Vortex laser arrays with topological charge control and self-healing of defects, Nature Photonics 16, 359 (2022)
[Rafler2011] S. Rafler, Generalization of Conway's" Game of Life" to a continuous domain-SmoothLife, arXiv:1111.1567 (2011).
[Saade2016] A. Saade *et al*., Random projections through multiple optical scattering: approximating kernels at the speed of light, IEEE Intl Conf. Acoustics, Speech and Signal Processing (ICASSP) 6215 (2016)
[Senanian2023] A. Senanian *et al*., Programmable large-scale simulation of bosonic transport in optical synthetic frequency lattices, Nature Physics 1 (2023)
[Sephton2019] B. Sephton *et al*., A versatile quantum walk resonator with bright classical light, PLoS One 14, e0214891 (2019)
[Shastri2021] B. J. Shastri *et al*., Photonics for artificial intelligence and neuromorphic computing, Nature Photonics 15, 102 (2021)
[Taboury1988] J. Taboury *et al*., Optical cellular processor architecture 1: Principles, Appl. Opt. 27, 1643 (1988)
[Tokihiro1996] T. Tokihiro *et al*., From soliton equations to integrable cellular automata through a limiting procedure, PRL 76, 3247 (1996)
[Wetzstein2020] G. Wetzstein *et al*., Inference in artificial intelligence with deep optics and photonics, Nature 588, 39 (2020)
[Wolfram2002] S. Wolfram, A new kind of science (Wolfram media Champaign, IL, 2002)
[Wright2022] L. G. Wright *et al*., Deep physical neural networks trained with backpropagation, Nature 601, 549 (2022)

Enabling Equitable Communication: Next-Generation Connectivity using Neural Network Trained Reconfigurable Intelligent Surfaces to Bridge Urban-Rural Digital Divide

The global climate change has led to an increase in extreme weather events, disproportionately affecting remote areas with limited internet access. Rural communities in the northern territories of Canada, facing severe weather conditions, struggle with their communication infrastructure during crises. Current communication methods, such as satellite and mobile wireless services, are expensive and insufficient to meet the demands of these challenging environments. This situation calls for improved and resilient communication solutions to bridge the urban-rural digital divide and mitigate the impacts of climate change on vulnerable populations.

The advent of 6G communication promises higher data rates and improved connectivity. To counteract the higher propagation losses of 6G millimeter waves, new transmission technologies are needed. Reconfigurable Intelligent Surfaces (RIS) offer a potential solution. RIS consists of passive reflection elements that can dynamically adjust incident signals, enhancing wireless communication performance. Integrating RIS with neural networks enables intelligent adaptation to changing weather conditions, further optimizing signal propagation.

The challenge’s objectives are threefold: (1) Develop a cost-effective and energy-efficient RIS system using printed electronics for remote and rural areas, with a focus on the northern territories of Canada. (2) Integrate neural networks with the RIS system to optimize its performance in extreme weather conditions, allowing real-time adjustments based on meteorological data. (3) Conduct field tests in harsh weather conditions in Arviat, Nunavut, Canada, to evaluate the RIS system's effectiveness in enhancing communication and maintaining reliable connectivity.

In the first year, the focus will be on fabricating and validating the RIS system. The metasurface, a crucial component of the RIS, will be designed and fabricated using two approaches: conventional lithography (RIS-1) and printed electronics (RIS-2). These prototypes will be integrated with a control board and tested in the lab to evaluate their performance in manipulating electromagnetic waves.

The second year of the project will be centered around integrating neural networks with the RIS system and conducting real-world tests. Data on RIS performance under varying weather conditions will be collected, and relevant features will be extracted to establish the relationship between weather and optimal RIS configurations. A neural network will be trained to adaptively optimize the RIS settings based on real-time meteorological data. The final phase involves deploying the RIS system in Arviat, Nunavut, Canada, to evaluate its effectiveness in maintaining reliable communication in adverse weather conditions.

The expected outcomes include a scalable and innovative RIS system, intelligent and weather-aware through neural network integration for real-world deployment. The project's impact reaches beyond the northern territories, empowering vulnerable communities worldwide with improved communication services during extreme weather events. Through multidisciplinary research and cutting-edge technology, this project strives to bring reliable, energy-efficient, and resilient communication infrastructure to remote and rural areas, contributing to a more equitable and connected global society.

LITERATURE REVIEW:

The global climate change has resulted in an increase in extreme weather occurrences, including hurricanes, snowstorms, or extreme heat. These weather events disproportionately impact remote geographic areas, where nearly 3 billion people around the world have limited access to the internet [1]. The effects of extreme weather can be devastating for local communities leading to potential loss of life and severe impacts on local businesses and economies. In the framework of the current challenge, the northern territories of Canada will be studied as a specific case of rural areas facing extreme weather conditions, ranging from snowstorms during the winter season with temperatures as low as -60°C to wildfires in the summer with temperatures exceeding 30°C with 287 mm of precipitation per year [2].

During times of extreme weather, access to reliable and high-speed communication becomes crucial for these vulnerable communities. However, the current communication infrastructure heavily relies on landline telephone, satellite, and mobile wireless service with limited access to fiber-to-home internet [2, 3]. Moreover, geostationary satellites can barely serve areas in the high latitudes. This results in constrained communication bandwidth (800 MHz, 900 MHz, 1800 MHz, 2600 MHz) and low throughput (below 500 kbps) leading to slow and unreliable connectivity for essential applications, e.g., email or Internet, while paying high rates (~ 70 USD/month) [2-4]. Additionally, the weather affects drastically communication, for example, the satellite's signal can cause interference, or the proper maintenance of the satellite is very challenging. Hence, these ways of communication are insufficient in effectively reaching and supporting these communities during times of crisis. The combination of extreme weather events and limited access to reliable communication exacerbates the challenges faced by these remote communities, underscoring the urgent need for improved and resilient communication infrastructure to mitigate the impacts of climate change on vulnerable populations [3].

Northern territories of Canada have limited access to 2G and 3G communication. The development of 6G communication will bring the base station to those areas and will be used as an extension of satellite signals. In general, 6G promises significantly higher data rates, lower latency, and improved connectivity compared to existing networks. Hence, the introduction of 6G communication in the northern territories of Canada can bring transformative benefits to communication infrastructure [2, 5]. However, millimeter waves used for 6G suffer from higher propagation losses compared to lower frequency. Hence, to proactively counteract these losses, improve signal's propagation and increase the overall coverage range, new transmission technologies are needed. One of the potential solutions is implementing the Reconfigurable Intelligent Surfaces (RIS).

RIS typically comprises numerous passive reflection elements that can be dynamically adjusted to reflect incident signals in desired ways, aiding signal alignment at the receiver [6]. RIS technology has been utilized to improve various aspects of wireless communication, such as enhancing differential privacy [7], performance robustness [8], energy efficiency [9], and spectrum efficiency [10]. By equipping RIS with programmable elements like sensors or reflectors, wireless communication can be enhanced through active adjustment of the electromagnetic environment. The primary goal is to optimize signal transmission and reception for improved communication performance. In the context of bridging the urban-rural digital divide, RIS could potentially play a crucial role being cost-effective and energy-efficient solution [11]. Even though RIS is typically used for short-distance communication, its strategic deployment in rural areas with challenging terrain or limited line-of-sight to satellites can greatly improve mobile wireless service signal coverage [12]. By intelligently redirecting and extending signals, RIS ensures that the signals are steered to desired locations, improving the signal strength and quality for rural areas. Furthermore, the programmable capabilities of RIS enable it to intelligently manipulate signals, effectively reducing signal interferences, enhancing overall signal quality, and significantly increasing data throughput.

When it comes to RIS in extreme weather conditions, the continuous advancement of artificial intelligence (AI) particularly neural networks plays a crucial role in optimizing the performance and adaptability of the RIS system. Neural networks can be trained on historical weather data and real-time meteorological information to learn and predict how weather conditions affect signal behavior [13]. By leveraging this knowledge, the neural network can dynamically adjust the configurations of the RIS elements to optimize signal propagation and maintain reliable communication in adverse weather [14]. Additionally, neural networks can help preprocess weather-related data and extract relevant features that impact the RIS system's performance in extreme weather conditions. For example, they can identify patterns in temperature, humidity, or precipitation data that correlate with signal degradation or interference. This information can guide the RIS in adapting its behavior to counteract the weather-related challenges. As well as it can improve the decision-making capabilities of the RIS system by rapidly processing and analyzing complex weather-related data. They can detect sudden weather changes and respond promptly to adjust the RIS configurations accordingly. This adaptability enables the RIS to maintain optimal signal performance despite unpredictable weather fluctuations.

PROBLEM STATEMENT/OBJECTIVE:

The main objective of this challenge is to overcome the digital divide by introducing a new generation of reconfigurable intelligent surfaces (RIS) in communication paths to connect urban and northern rural areas. A new class of lightweight flexible RIS produced at low cost, which will uniquely facilitate future applications in 6G communications. The focus of this challenge is to be on the forefront of the fabrication of printed electronics RIS. In progressing towards the main goal, the challenge program will be segmented into the following short-term objectives:

1. Develop a cost-effective and energy-efficient Reconfigurable Intelligent Surface (RIS) system using printed electronics to improve communication infrastructure in remote and rural areas, specifically targeting the northern territories of Canada.
2. Integrate neural networks with the RIS system to optimize its performance in extreme weather conditions, dynamically adjusting the RIS configurations based on real-time meteorological information.
3. Conduct field tests in harsh weather conditions in Arviat, Nunavut, Canada, to evaluate the effectiveness and adaptability of the RIS system in enhancing communication and maintaining reliable connectivity.

OUTLINE OF TASKS/WORK PLAN:

The proposed solution is based on multidisciplinary research including the advanced fabrication using printed electronics for communication devices and neural network computation. The summarized tasks are presented in the Table 1.

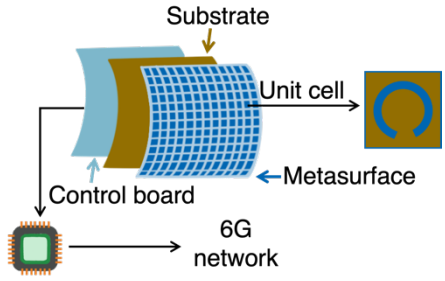

Figure 1 Schematic design of RIS

1. RIS fabrication: The proposed design of RIS is shown in Figure 1. The first layer is made from metasurfaces structure. During this challenge, we propose to fabricate two prototypes of the first layer of RIS. The first prototype will be done using traditional lithography (RIS-1) by depositing metals. This prototype will be used as a reference.

During the second step, RIS-2 will be fabricated using printed electronics (PE) which is additive manufacturing method. Recently, PE have shown their ability for low-cost mass production of lightweight and flexible Internet of Things (IoT) devices for 5G [15]. Currently, the resolution of PE techniques has reached tens of micrometers; hence, it is an attractive solution for the fabrication of 6G RIS [16 - 18]. **This simple fabrication process will provide a new opportunity for large volume**

production of RIS, reducing the devices' cost from ~$2,000 to ~$0.50. RIS-2 will be made from silver ink onto heat-treated polyethylene terephthalate (PET) using screen printing process. This method allows for high-resolved deposition of 5 um thick metallic ink.

Metasurface consists of 16x16 unit cells (256-units) where each unit will be integrated a PIN diode to provide different phase response to the incoming wave. The proposed layout does not require vertical connections, e.g., vias and demand a biasing network in integrated on the same plane. In order to fight extreme cold conditions, RIS will contain the printed heating element to maintain its operation during snowstorm or heavy rainfall. The control mechanisms and electronics components will be integrated into control PCB, as well as temperature and humidity sensor to maintain the operation of RIS in any conditions. Then, communication interface will be established to adjust the properties and behavior of the RIS elements. Since RIS and heated element do not require high-power, a simple 9V battery will be used in the framework of this challenge. Finally, to ensure RIS performance, the initial test will be performed with a single 290 GHz source and detector from TeraSence. This testing will involve signal measurements and evaluation of the RIS's ability to manipulate electromagnetic waves.

Table 1 Challenge activities

	2024				2025			
Steps & Activities	Q1	Q2	Q3	Q4	Q1	Q2	Q3	Q4
1. RIS fabrication								
1.1 Design of metasurface (MS)								
1.2 Fabrication of MS by conventional lithography (RIS-1)								
1.3 Fabrication of MS by printing electronics (RIS-2)								
1.4 Assemble on the control board								
1.5 Validation of the performance in the lab environment								
2. Neural network integration								
2.1 Data collection								
2.2 Features extraction								
2.3 Neural network training								
2.4 Adaptation and prediction								
3. Test in the real-weather conditions								
3.1 Setting up experiment in Arviat, Nunavut, Canada								
3.2 Data collection, analysis and processing								
3.3 Necessary configuration adjustments								
4 Project management								
4.1 Meetings								
4.2 Students supervision								
4.3 Publish and disseminate results								

2. Neural network integration: The last step on the RIS fabrication, it will be the characterization of the beamforming capabilities in an outdoor environment. The line-of-sight path between base station (300 GHz emitter) and end-user (detector) will be blocked by an obstacle. This test will be conducted daily to adapt fabricated RIS to different weather conditions. Here we will apply neural networks to train RIS. This step will be split in the 4 subtasks.

1. The data about the performance and behaviour of RIS system will be collected at different weather conditions with varied temperature, humidity, precipitation and wind speed. This will involve measurements of signal strength and quality as a function of meteorological variables.

2. Once the data is collected, the next step will be to extract relevant features or characteristics that will be used to describe the relationship between the weather conditions and the RIS performance. This may involve preprocessing the data, selecting appropriate features, and normalizing the data to ensure compatibility with the neural network model.
3. The collected dataset and extracted features, a neural network will be trained to learn the relationship between the weather conditions and the optimal configurations or adaptations of the RIS system. The neural network will be designed as a regression model, with the weather conditions as inputs and the desired RIS settings or adaptations as outputs. The training process involves feeding the network with the weather data and corresponding RIS configurations, allowing it to learn the patterns and relationships within the data.
4. Once the neural network is trained, it will be used to predict the optimal RIS configurations or adaptations for new weather conditions. Given the input of current weather data, the network can provide the corresponding RIS settings or adaptations that would be most suitable for the given conditions. This enables the RIS system to dynamically adjust its behavior based on real-time weather information.

3. Field Test in the real-weather conditions: The last step of this challenge will be real-world deployment. In the framework of this challenge, we propose to travel to Arviat, Nunavut, Canada. The temperature in this region is varied from -48.3°C to 33.9°C. Hence, installing our unit there will help us to collect the data and pursued the further improvement of further RIS development. Using neural network, it will dynamically adjust the RIS elements' configurations to optimize the signal propagation environment based on the current conditions.

OUTCOME(S):

This project aims to develop an innovative and scalable RIS system for improving communication in remote and rural areas. The three key objectives will be accomplished:

1. A novel and scalable RIS system fabricated using printed electronics, providing a low-cost, lightweight, and flexible solution for improving communication in remote and rural areas.
2. An intelligent RIS system integrated with neural networks, capable of adapting to changing weather conditions and optimizing signal propagation for enhanced communication performance.
3. Real-world deployment of the RIS system in Arviat, Nunavut, Canada, demonstrating its ability to maintain reliable communication in adverse weather scenarios and bridging the digital divide in the northern territories.
4. Empowerment of vulnerable communities in remote areas, enabling them to access essential communication services during extreme weather events and improving their overall resilience to the impacts of climate change.

Successful implementation of this project will empower RIS to maintain reliable communication and maximize performance even in adverse weather scenarios, making it a valuable tool in challenging environments, offering faster, more reliable, and energy-efficient communication technologies.

IMPACT:

Modern humanity and the global economy depend on optical infrastructures and technologies to drive our digital society, necessitating more energy-efficient approaches and innovations to accommodate the growing data traffic. 6G technologies will revolutionize communication bridging the digital divide between urban and rural areas. It is an important step towards achieving equitable access to technology and communication services and provide an immense impact on citizens, consumers, and businesses towards a future society of fully intelligent and autonomous systems. **The 6G market is expected to reach 4.1B by 2030 with a 70% CAGR [19]**. **Hence,** the interest in areas tied to this **challenge is paramount to achieving societal and governmental goals. The advanced fabrication of RIS devices**

developed within the proposed challenge **will be** become an enabling technology for the rural northern territories. Based on the obtained knowledge, RIS will be further studied for extreme heat conditions, which will allow to improve communication in rural areas in Africa, India and Brazil. By leveraging innovative technologies and embracing a forward-thinking approach, the significant difference in the lives of people living in these regions can be employed have the potential to help thousands of people access the educational, business, and communication benefits of the web. **This program will prepare two high quality professionals with multidisciplinary and marketable experimental, technical, and soft skills. These will be in areas expecting significant growth from technological revolutions that will require supplying 6G IoT with big data at high repetition rates, which can be achieved through creating extensive sensor networks of RIS.**

REFERENCES:

1. “Broadband Commission for Sustainable Development (ITU, UNESCO),” ‘State of Broadband Report 2019’, 2020.
2. McMahon, R. and Akçayir, M., “Voices from Northern Canada: Integrating stakeholder expectations in telecommunications policy for rural, remote and Northern regions,” Telecommunications Policy, 46(9), p.102402, 2022.
3. “Arctic Council Task Force on Telecommunications Infrastructure in the Arctic (TFTIA), Telecommunications Infrastructure in the Arctic”; A Circumpolar Assessment, 2017.
4. Saarnisaari, H. et *al.* “A 6G white paper on connectivity for remote areas,” 2020.
5. Chowdhury, M. Z., et al. “6G wireless communication systems: Applications, requirements, technologies, challenges, and research directions.” *IEEE Open Journal of the Communications Society* 1, 2020.
6. Liu, R., et *al.* “A path to smart radio environments: An industrial viewpoint on reconfigurable intelligent surfaces.” *IEEE Wireless Communications* 29(1): 202-208, 2022.
7. Yang, Y., et *al.*, “Differentially private federated learning via reconfigurable intelligent surface,” IEEE Internet Things J., 9 (20): 19 728 – 19 743, 2022.
8. Samarakoon, S., et *al.*, “Robust reconfigurable intelligent surfaces via invariant risk and causal representations,” in Proc. IEEE SPAWC, pp. 301–305, 2021.
9. Huang, C., et *al.*, “Holographic MIMO surfaces for 6G wireless networks: Opportunities, challenges, and trends,” IEEE Wireless Commun., 27 (5): 118–125, 2020.
10. Wang, Z., et *al.*, “A graph neural network learning approach to optimize RIS-assisted federated learning.” IEEE Transactions on Wireless Communications, 2023.
11. Tran, N. M., et *al.*, “Multi-device charging RIS-aided wireless power transfer systems,” In 2021 International Conference on Information and Communication Technology Convergence (ICTC): pp. 839-844, 2021.
12. Du, H., et *al.*, “Reconfigurable intelligent surface-aided joint radar and covert communications: Fundamentals, optimization, and challenges.” IEEE Vehicular Technology Magazine, 17(3), pp.54-64, 2022
13. Wang, Z., et *al.* “A graph neural network learning approach to optimize ris-assisted federated learning. ” *IEEE Transactions on Wireless Communications*, 2023.
14. Xu, Meng, et *al.* “Deep learning-based time-varying channel estimation for RIS assisted communication. ” IEEE Communications Letters 26.1: 94-98, 2021.
15. J. Gubbi, et al. “Internet of Things (IoT): A vision, architectural elements, and future directions,” Futur. Gener. Comput. Syst. 29 (2013).
16. Ahmad, R., et *al.*, “Reconfigurable terahertz moiré frequency selective surface based on additive manufacturing technology”, Applied Science, 13(5), 2022
17. Zhuldybina, M. et *al.*, “Printing accuracy tracking with 2D optical microscopy and super-resolution metamaterial-assisted 1D terahertz spectroscopy”, npj Flexible electronics 21(4), 2020.
18. Zhuldybina, M. et *al.*, “Contactless In-Situ Electrical Characterization Method of Printed Electronic Devices with Terahertz Spectroscopy”. *Sensors,* 19 (3), 444, 2019.
19. “On the horizon: Several perspectives on Canada's technology future - 2030–35”, Report of the Working Group on Horizon Scanning, Press rel., 2022

Executive summary

Electro-magnetic information theory of Photonic Integrated Curcuits with Fabrication and environmental UNcertainties (EPIC-FUN)

Applicant:
Metodi P. Yankov
Associate professor, PhD
Department of Electrical and Photonics Engineering, Technical University of Denmark

Photonic integrated circuits (PICs) will be the key enabler of the urgently needed sustainable growth in data rates in worldwide communication networks. PICs have the potential to replace a variety of their electronic counterparts in data centers and communications transceivers by providing *higher throughput and lower energy consumption at the same time.* The energy consumption of a PIC is a function of its physical parameters as topology, material composition and parameters of its active components, e.g. lasers and thermal elements used for stabilization. Unlike digital electronics, variations in these parameters across devices due to fabrication tolerances, as well as within each device due to laser stability and environmental factors inevitably impose a stochastic nature on the PIC as a communication channel and affect its information carrying capabilities.

An information theoretic framework can provide the link between signal uncertainty, information capacity and energy. Optimization of the PIC communication channel using such a framework can make it robust to the uncertainties, thereby decreasing energy consumption, increasing yield, improve reliability and increase capacity. Such a framework, while highly desired for widespread PIC deployment, is currently an open research problem.

In this project, I will lay the ground works for deriving an electro-magnetic information theory of photonic devices and the fundamental relation between the energy consumption and information capacity of PICs. This relation will drive the next generation of research into energy-efficient, PIC-dominated networks.

In particular, we will derive Green's functions of PICs with selected functionality, e.g. a ring resonator, and extend it to the general case of a network of resonators which can potentially serve as a switch. Complimentary to that, we will use data driven and machine learning modeling of components in order to capture their fabrication and environmental uncertainty. This uncertainty will then be translated to statistics of signal waveforms propagating through the component and the network, which allows for the optimization of the waveforms for increased robustness and maximized capacity. Constraining this optimization to the maximum required thermal tuning will result in a Pareto front of the information capacity and energy consumption of the component or the network, which can be used for future designs.

This work has the potential to unify the information theoretical modeling and simulation of discrete photonic components with the general optical communication systems and networks. Ultimately, it carries the key to designing PIC-based devices and networks of high-throughput and low energy consumption to be applied in future telecommunication systems.

Project proposal

1. Introduction and motivation

The optical fibre network is the key infrastructure enabling our digital information society. Vast amounts of information driven by 5G mobile communications, internet of things and streaming services are being transported on the core network, which is composed of long-haul fibre links interconnecting end users and data centers (DCs). The latter are also known as 'the Cloud' in popular literature and are one of the fastest growing parts of the Internet. The expected data traffic growth trends are exponential, further exacerbated by the unexpected traffic demands driven by the global COVID-19 pandemic, which has put an unprecedented stress on the optical network infrastructure since 2019. To this day, many businesses continue to focus on 'working from home' methods as a way to decrease cost and improve efficiency. This enormous traffic comes with a price. Information and communication technologies are today responsible for 9% of the global electricity consumption [1], projected to increase to nearly 20% by 2030 [1].

Classically, optical networks have operated using the very basic of communication principles, with extremely low spectral efficiency and capacity. Only in the last decade has Shannon's information theory (IT) [2] been incorporated in network design, leading to dramatically increased capacity limits assessment, as well as practical waveform optimization that approach that capacity, e.g. through constellation shaping and advanced forward error correction [3] [4].

On the other hand, photonic integrated circuits (PICs) have the potential to realize all basic components of such networks at greater energy efficiency, e.g. switches, filters, (de)multiplexers, splitters [5], making them a vital element in solving the global energy crisis. This potential can only be fulfilled if the problem of PIC fabrication and environmental variability is solved [6] [7] [8]. Electromagnetic IT (EIT) [9] [10] can provide a link between Shannon's work and the fundamental description of the PIC communication channel given by Maxwell's equations.

In this project, we will develop the EIT of PICs. Then, we will use EIT to dramatically increase the PIC capacity, yield and energy consumption by optimization of communication waveforms robust to the inherent PIC statistical variations.

2. Goals

The purpose of the project is to provide an assessment of the feasibility of fundamentally relating IT and optical wave propagation through a nonlinear integrated device. The goal of this project is to develop an EIT for photonic devices so that similar to current fiber optic networks, the PIC-dominated segment of the telecommunication infrastructure can be optimized for near-capacity performance at a constrained energy consumption.

Goal 1: Complimentary analytical and data driven frameworks for estimating the information capacity of a PIC and PIC-dominated networks, which take into account all sources of uncertainties due to fabrication tolerances, design imperfections and environmental factors.

Goal 2: Information theoretic link between the signal-carrying waveform and physical device parameters, so that the energy consumption can be linked to the information capacity.

Goal 3: Optimization of waveforms for reduced energy consumption and maximized capacity.

3. State of the art in IT for photonics

As an example, consider the all-optical network in Figure 1 that could potentially replace the current Ethernet-based network in DCs. It is composed of interconnected add-drop components, each of which is realized by e.g. a ring resonator [11]. The necessity for optical-electrical-optical conversion at the switch edges is thus lifted, dramatically decreasing the energy consumption from 68 pJ/bit at 25.6 Tbps in the electrical domain [12] to e.g. 0.29 pJ/bit at 81.9 Tb/s throughput [13] in the optical domain. The

basic component of any PIC is the waveguide, which can in the simplest manner be described as a communication channel with an optical data input, an optical data output, and in some cases an electrical control signal input and a non-data optical signal (e.g. pump laser) input. The signals which propagate through the integrated waveguide are subject to variations and uncertainties across devices (due to e.g. fabrication tolerances), as well as when communicating through an isolated device (due to e.g. laser stability, temperature drifts and other environmental factors). Consider the study in [14], where uncertainty was studied by measuring the parameters of 1600 filters fabricated using an identical process. The slight geometry variations and roughness of the waveguides resulted in resonance wavelength deviation of $\Delta\lambda_{res} = 2.8$ nm, leading to power losses and throughput penalties easily reaching 50% by our preliminary assessments. Compensating the variability can be approached by e.g.

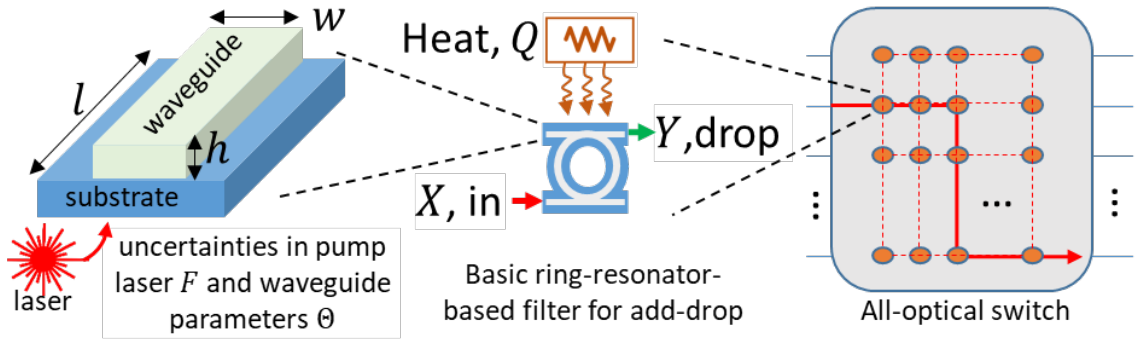

Figure 1. An example of a basic photonic waveguide, applied for the fabrication of a basic filter, which is then used as a component in a multi-radix switch in a DCI network.

thermal tuning [15] [8], which offsets the energy efficiency potential of the PIC altogether and is currently one of the main challenges towards widespread integration of PICs in data networks. Alternatively, devices with sub-optimal characteristics can be rejected at the fabrication stage, leading to yield degradation. *The solution to both of those problems is to communicate through the device in a manner, robust to the statistical variations imposed on the waveforms by the statistical variations of the fabrication process and the environment*. The link between those is currently unknown.

The information capacity C of a component, or in fact, a whole system of components is a fundamental limit on the supported data rate and can be expressed using the mutual information (MI)

$$C = \max_{P_X,Q} \mathbb{E}_{F,\Theta,Q}[\mathcal{I}(X;Y|\Theta = \theta, F = f, Q = q)]. \quad (1)$$

Here, $\mathcal{I}$ is the MI between the input X and output Y, F represents all optical sources, i.e. lasers with uncertainty in their phase, frequency and amplitude, Θ represents the effect of the device(s)' geometry and physical parameters (see Figure 1) and Q represents the effect of the heating elements. The former two are distributed according to the distributions $p_F(F)$ and $p_\Theta(\Theta)$, respectively, while Q has the function of minimizing their uncertainty at the expense of energy. The maximization in (1) is over all possible probability distributions of the signal X, also known as signal (or constellation) shaping. The energy consumption $E(F, Q)$ is in general a function of the active elements F and Q.

For an electronic implementation of the switch example, X and Y are discrete, quantized *bits* (assumed error free from input to output), the distributions of F and Θ in (1) are replaced by delta functions, and the switch capacity is therefore a deterministic function of the number of ports and the data rate per port (25.6 Tbps at 68 pJ/bit energy consumption in state of the art applications [12]).

Applying an IT analysis implies computing the MI and performing the maximization in Eq. (1). Both require a mathematically, or at least computationally tractable expression for the probability distribution of the output Y

$$p_{Y,F,X,\Theta|Q=q} = p_F(F) \cdot p_\Theta(\Theta) \cdot p_X(X) \cdot p_{y|F,X,\Theta,H}(Y|F, X, \Theta, Q = q). \quad (2)$$

Waveform propagation through a waveguide (or any other photonic circuit) is almost entirely described by Maxwell's equations [16], which are too complex to solve analytically. Instead, finite difference

methods are applied [16], e.g. the finite difference time domain (FDTD) method, which is today found in most software for PIC analysis. Finite difference methods can also be adopted to include the effects not directly captured by Maxwell's equations, such as thermal, electro-optic or general dissipative effects [17]. The FDTD method only allows for estimating the relation $(f, x, \theta, q) \rightarrow y$ for a *given realization* of the inputs F, X, Θ, Q. This method generally does not capture the uncertainties and is furthermore too computationally complex to be used for optimization. Uncertainty studies are limited to expectation of physical dimensions, yield and at best – high-level device properties [18] [15] [14].
The field of EIT [9] [10] studies the potential benefits of combining Shannon's theory capacity estimation and Maxwell's equations for channel modeling. Some studies [19] have found that for example antenna design and channel characterization can be approached by employing the fundamental relation between these theories. In wireless channels, the uncertainties are mostly related to temporal variations in the channel. Optical channels, where fabrication uncertainties are also present, are yet to be analyzed using EIT. Green's function applied in the wireless channel [10] has been studied for photonics as well [20]. However, not in the context of capacity estimation, thereby overlooking a potentially powerful method for PIC description. The IT analysis of the system and optimization of signal shaping distributions P_X are currently restricted to the long-haul fibre link [3] [21] [22] [23] [3], including our studies [24]. Optimization of a communication system employing PICs is in its infancy, for example our previous analysis of a link employing a PIC for nonlinearity compensation [25].

4. Methodology and work plan

Hypothesis 1: The uncertainty $p_{F,\Theta}(F, \Theta)$ of the basic parameters can be related in a mathematically tractable way to the uncertainty $p_{y|F,X,\Theta,Q}(Y|F, X, \Theta, Q = q)$ of the waveform and thereby to tractable expressions of MI and throughput of PIC devices and networks.
Hypothesis 2: The MI optimization w.r.t. the signal input can be constrained such that a certain energy consumption is not exceeded. This allows the construction of a Pareto front of the PIC w.r.t. its most important characteristics: its energy consumption and information capacity.

4.1. WP1: Deriving the conditional waveform distribution (Test Hypotheses 1), achieve Goals 1), 2).

In this work package (WP), I will translate the fabrication uncertainties in terms of maximum allowed tolerances in the composition, etching and topology to signal uncertainty and information parameters. The distribution of the uncertainties will be governed by the degree to which thermal stabilization is applied. In particular, this entails using models for the material uncertainties, e.g. [18] and applying them to Maxwell's equations e.g. through deriving Green's functions for PICs of interest or by using FDTD methods to develop models for the conditional distribution in Eq. (2). For standard distributions on Θ and F, e.g. Gaussian, Kalman filter-like methods may be used to propagate the distributions of the parameters to output waveforms. Complimentary to the purely analytical estimation of $p_{Y|F,X,\Theta,H}(Y|F, X, \Theta, Q = q)$, we will apply particle filter methods similar to [26] and machine learning (ML) as in [27]. Training data for the ML models will be generated by propagating the waveforms using a software simulator for given realizations of the parameters, where every time a waveform is propagated, the waveguide composition and topology is drawn from its stochastic model. The two approaches can be explored concurrently to obtain the empirical and/or analytical expression for $p_{y|F,X,\Theta}(Y|F, X, \Theta)$ for several PICs of interest, enough to demonstrate the applicability of the methodology to other types of devices.

4.2. WP2: Constrained input optimization (Test Hypothesis 2), achieve Goal 3)).

Optimization can be approached by using autoencoders (AE). An AE is a mathematical tool which embeds a channel model in between an encoder and a decoder which are optimized together to improve a cost function. This cost function can directly be the MI. The AE framework is currently getting traction in telecommunications [28] for its versatility. Recently, we were able to design such a framework to

perform optimization of an optical fibre system employing a specific discrete optical component, namely a photonic lantern multiplexer for multiple-input multiple-output few-mode fiber transmission [29]. We were able to achieve a dramatic improvement of 5 dB in the cross-talk tolerance of the transmission by a simple pre-coder at the transmitter. This tolerance is directly related to robustness to fabrication uncertainties. Applying the same method to PIC-based multiplexers can be expected to provide the same. This may in turn be translated to increased fabrication yield, lower power consumption of active elements, and to increased throughput of the PIC and therefore the system. In this WP, optimization will be applied to specific devices of interest: e.g. a ring resonator, a multiplexer and/or an entire switch, with the target of obtaining their corresponding Pareto fronts.

5. Feasibility and planning

The nature of the project is in semi-theoretical modeling of the response of PICs to telecommunication signals. The main activities are related to the tasks in WP1. I will spend 2/3 of my time on the project for 1.5 years, of which approx.. 80% on WP1. This includes an already planned 1-month research visit to the Photonics Research Group at Ghent University and IMEC, hosted by prof. Wim Bogaerts, where world-leading expertise exist on modeling of PICs, especially their variations. I intend to capitalize on this collaboration as much as possible in order to maximize the feasibility of WP1. On the other hand, I am an expert in the field of constellation shaping for data rate optimization, including shaping for nonlinear photonic platforms [25], AEs [29] and in general IT for photonics. My unique combination of expertise thus renders the feasibility of WP2 very high and its risk (conditioned on WP1) very low.

6. Impact

A practically usable theoretical model for the PIC capacity as a function of the fabrication process and employed hardware components will have an enormous impact on the way future communication networks are designed. Current solutions for the simulation of PICs can be completely replaced and their simulation completely integrated in the general communication network simulation software. Researchers working in the fields of telecommunication, PIC fabrication and computer scientists will be able to use simulation tools like this in order to find space for improvement in current technologies and processes, as well as to design completely new components and systems *with lower energy consumption at higher throughput*.

Nonlinear photonic devices find themselves in a plethora of applications, where uncertainty analysis plays an important role [5]. For example, the fields of fiber sensing, quantum communication and photonic computing accelerators are currently gathering a lot of research traction and will greatly benefit from uncertainty analysis of the detector and signal processing elements.

In general, extending the field of EIT to photonics, as with any other theoretical work, may further affect future technologies, research and development. This additional impact is difficult to foresee.

Finally, the fundamental limits obtained in this project, specifically Goal 3) will be of great importance to us as a society and will inform us on potential hard choices and tradeoffs we must make in the future regarding energy consumption and our exponential data rate growth trends.

I expect the following research activities to follow the proposed project: 1) experimental validation of the uncertainty analysis by fabricating and testing a sufficiently large sample of a selected PIC, e.g. a ring resonator; 2) developing domain-specific optimization strategies and focus on the energy aspect.

7. Bibliography

[1] A. S. G. Andrae, "Total Consumer Power Consumption Forecast," in *The Nordic Digital Business Summit*, 2017.

[2] C. Shannon, "A mathematical theory of communication," in *The Bell System Technical Journal*, vol. 27, 1948, p. 379–423.

[3] R. J. Essiambre and others, "Capacity Limits of Optical Fiber Networks," *Journal of Lightwave Technology,* vol. 28, p. 662–701, 15 February 2010.

[4] G. Böcherer, P. Schulte and F. Steiner, "Probabilistic Shaping and Forward Error Correction for Fiber-Optic Communication Systems," in *Journal of Lightwave Technology*, vol. 37, 2019, p. 230–244.

[5] P. Minzioni and others, "Roadmap on all-optical processing," *Journal of Optics,* vol. 21, May 2019.

[6] W. Bogaerts, M. Fiers and P. Dumon, "Design Challenges in Silicon Photonics," *IEEE Journal of Selected Topics in Quantum Electronics,* vol. 20, p. 1–8, August 2014.

[7] N. Margalit, C. Xiang, S. Bowers, A. Bjorlin, R. Blum and J. Bowers, "Perspective on the future of silicon photonics and electronics," *Appl. Phys. Lett,* vol. 118, p. 220501, 2021.

[8] X. Chen and others, "Simultaneously Tolerate Thermal and Process Variations Through Indirect Feedback Tuning for Silicon Photonic Networks," in *IEEE Transactions on Computer-Aided Design of Integrated Circuits and Systems*, vol. 40, 2021, p. 1409–1422.

[9] S. Loyka, "Information theory and electromagnetism: Are they related?," in *10th International Symposium on Antenna Technology and Applied Electromagnetics and URSI Conference*, Ottawa, 2004.

[10] J. Zhu and others, "Electromagnetic Information Theory: Fundamentals, Modeling, Applications, and Open Problems," 6 December 2022. [Online]. Available: https://arxiv.org/abs/2212.02882. [Accessed Feb. 2023].

[11] A. Joshi, "Silicon-photonic CLOS networks for global on-chip communication," in *3rd ACM/IEEE International Symposium on Networks*, 2009, p. 124–133.

[12] C. Minkenberg, R. Krishnaswamy, A. Zilkie and D. Nelson, "Co-packaged datacenter optics: Opportunities and challenges," *IET Optoelectron,* vol. 15, p. 77–91, 2021.

[13] R. Matsumoto and others, "Fully-Loaded Operation of 0.29-pJ/bit Wall-plug Efficiency, 81.9-Tb/s Throughput 32 × 32 Silicon Photonics Switch," in *Optical Fiber Communication Conference (OFC) 2021*, Optica Publishing Group, 2021.

[14] Z. Lu and others, "Performance prediction for silicon photonics integrated circuits with layout-dependent correlated manufacturing variability," *Opt. Express,* vol. 25, p. 9712–9733, 2017.

[15] B. Ouyang, Y. Xing, W. Bogaerts and J. Caro, "Silicon ring resonators with a free spectral range robust to fabrication variations," *Opt. Express,* vol. 27, p. 38698–38707, 2019.

[16] K. Kawano and T. Kitoh, Introduction to Optical Waveguide Analysis: Solving Maxwell's Equation and the Schrödinger Equation, Wiley, 2004.

[17] L. Lugiato and others, "the Lugiato-Lefever equation to microresonator-based soliton Kerr frequency combs," *Phil. Trans. R. Soc. A,* vol. 376, p. 20180113, 2018.

[18] W. Bogaerts and others, "Layout-Aware Variability Analysis, Yield Prediction and Optimization in Silicon Photonic Circuits," *IEEE Journal on Selected Topics in Quantum Electronics,* vol. 25, p. 6100413, 2019.

[19] R. Li and others, "An Electromagnetic-Information-Theory Based Model for Efficient Characterization of MIMO Systems in Complex Space," *IEEE Transactions on Antennas and Propagation,* p. 1–1, 2023.

[20] S. Tan and L. Tsang, "Green's functions, including scatterers, for photonic crystals and metamaterials," *Journal of the Optical Society of America B,* vol. 34, p. 1450, 20 June 2017.

[21] G. Kramer, "Autocorrelation Function for Dispersion-Free Fiber Channels With Distributed Amplification," *IEEE Transactions on Information Theory,* vol. 64, pp. 5131-5155, 2018.

[22] M. Secondini and E. Forestieri, "Scope and limitations of the nonlinear Shannon limit," *Journal of Lightwave Technology,* vol. 35, p. 893–902, 2017.

[23] R. Dar, M. Feder, A. Mecozzi and M. Shtaif, "On shaping gain in the nonlinear fiber-optic channel," in *2014 IEEE International Symposium on Information Theory*, 2014, p. 2794–2798.

[24] M. Yankov and others, "Constellation Shaping for Fiber-Optic Channels With QAM and High Spectral Efficiency," *IEEE Photonics Technology Letters,* vol. 26, p. 2407–2410, 2014.

[25] M. P. Yankov and others, "Probabilistic Shaping for the Optical Phase Conjugation Channel," *IEEE Journal of Selected Topics in Quantum Electronics,* vol. 27, p. 1–16, 2019.

[26] N. Irukulapati, H. Wymeersch, P. Johannisson and E, "Stochastic Digital Backpropagation," in *IEEE Transactions on Communications*, vol. 62, 2014, p. 3956–3968.

[27] C. Häger and H. Pfister, "Deep Learning of the Nonlinear Schrödinger Equation in Fiber-Optic Communications," in *International Symposium on Information Theory (ISIT)*, 2018.

[28] T. Shea and J. Hoydis, "An introduction to deep learning for the physical layer," *IEEE Transactions on Cognitive Communications and Networking,* vol. 3, p. 563–575, 2017.

[29] M. P. Yankov and others, "Capacity and Achievable Rates of FadingFew-mode MIMO IM/DD Optical Fiber Channels," in *International Conference on Communications (ICC)*, 2022.

Virtual staining of virtually cleared unlabeled tissue images via deep learning and autofluorescence microscopy

Optica Foundation Challenge, Category: Health

Executive Summary

Challenge:

Traditional tissue clearing and staining methods for pathology assessments present several challenges, including long processing times, uneven tissue penetration, alteration of tissue structure, high costs, and labor-intensive protocols. These limitations hinder the acquisition of accurate three-dimensional (3D) visualizations of tissue biopsies, therefore impeding the comprehensive understanding of tissue structure and cellular organization. Moreover, certain diagnostic scenarios often necessitate invasive excisional biopsies due to the limitations of current 2D imaging techniques, consequently leading to increased patient discomfort and potential risks.

Proposed Project:

We propose the development of a cascading, deep learning-based model, called **ClariGAN**, in order to virtually clear and stain tissue samples, therefore bypassing the physical and chemical procedures involved in traditional techniques. ClariGAN can leverage advanced computing and deep learning methods, transforming 3D (~500 μm) scans of unlabeled samples into virtually stained versions that mimic traditional 2D fluorescent stained thin tissue sections. This model will be based on conditional Generative Adversarial Networks (GANs) and trained on paired confocal microscopy images of tissue samples, before (autofluorescence) and after the clearing and staining procedures.

Intended Outcomes:

Enhanced Pathology Assessments: By digitizing the preparatory workflow of pathology specimens, ClariGAN would enable the acquisition of 3D visualizations of tissue biopsies, thereby capturing certain unique features and preserving interconnections among tissue components. This approach provides a more comprehensive understanding of tissue structure and cellular organization compared to traditional 2D histology.

Time and Cost Efficiency: This proposed model offers a time-efficient alternative to lengthy tissue processing methods. It eliminates the need for laborious clearing and staining procedures, accordingly reducing processing times and associated costs.

Minimally Invasive Diagnostics: ClariGAN's ability to obtain virtually stained 3D scans from minimally invasive core needle biopsies could improve diagnostic accuracy and reduce the need for invasive excisional procedures.

Automation and Standardization: The implementation of ClariGAN in standard pathology workflows can streamline and standardize the staining and clearing process, thus reducing manual handling and limiting potential variations between technicians.

Future Adaptability: Once validated for use with human samples, the ClariGAN model can extend its benefits to a broader range of tissue types and applications, further enhancing pathological tissue examination.

Virtual staining of virtually cleared unlabeled tissue images via deep learning and autofluorescence microscopy

A. Literature Review

Tissue Clearing

Tissue clearing is a process used to render biological specimens transparent, therefore allowing for deep tissue imaging and three-dimensional (3D) visualization of cellular structures. This technique has enhanced our understanding of the spatial organization and function of various tissues and organs[1].

Tissue Clearing for Pathology

The thickness of pathology specimens can vary depending on the type of tissue and the specific application, but most biopsy samples will be within 1-5 millimeters, while a surgical resection specimen may be several centimeters thick or more. To obtain high-quality images using traditional microscopy, the thickness of specimens must usually be reduced by sectioning, which will result in samples that are several micrometers thick. For traditional bright-field microscopy, the thickness of a sample should generally not exceed 10 microns to avoid significant light scattering and absorption. However, other microscopy techniques, such as confocal microscopy, are capable of imaging thicker samples due to their ability to reject out-of-focus light using a pinhole aperture. For optimal confocal imaging, the thickness of a sample should still not exceed 50-100 microns, with the exact limit depending on the specific confocal microscope and objective lens used. **Tissue clearing techniques, however, can breach this thickness restriction by reducing light scattering and increasing tissue transparency**. This can allow for deeper penetration of light into the tissue, enabling imaging of structures further within the sample[2].

There are thus multiple benefits to clearing a tissue sample prior to imaging as it pertains to pathological diagnosis. First, the technique allows for the **visualization of tissue biopsies in three dimensions.** This can provide a more accurate understanding of their structure and cellular organization than traditional two-dimensional histology[3] (which often excludes pertinent diagnostic details). Second, cleared samples can be used to visualize **multiple levels of tissues** within a single sample, which can be particularly useful in complex and heterogeneous cases where clinically relevant changes can be identified only in some tissue areas. Third, 3D imaging preserves **the complex interconnections between various tissue components** and circumvents the laborious sectioning needed to achieve a similar but compromised result via separate (successive) 2D images[4].

Several tissue-clearing methods have been successfully developed in the past decade, including the popular techniques of CLARITY and Scale[1]. These chemical methods involve removing lipids or other cellular components that contribute to light scattering, and replacing them with a refractive index-matching solution (that reduces scattering and improves transparency). Using these techniques, researchers have been able to image samples that are several millimeters thick using confocal microscopy[5].

B. Problem Statement

Although tissue-clearing techniques have revolutionized the field of neuroscience by enabling researchers to visualize intact biological samples at the cellular level, these methods still present several challenges that researchers must overcome to obtain meaningful results and achieve clinical implementation.

The following are a few of the difficulties involved in clearing tissues:

1. Long processing times: Some tissue clearing techniques, such as SCALE, can take several weeks to complete, which can limit their practicality for time-sensitive experiments[5].
2. Even tissue penetration: One of the most significant challenges in tissue clearing is achieving uniform penetration of the clearing agent throughout the tissue. This is particularly challenging in thicker samples, as the clearing agent may not diffuse evenly throughout the entire sample[6].
3. Alteration of tissue structure: Many tissue clearing techniques involve the use of harsh chemicals, such as detergents or organic solvents, which can alter the structure of the tissue. This can lead to changes in the morphology of cells and tissues, which may affect the accuracy of the resulting images[5].
4. Expense: Tissue clearing is a technique used to make biological tissues transparent by removing lipids, pigments, and other light-scattering molecules, which can be costly, as it involves specialized equipment, chemicals, and technical expertise[6].
5. Industry: The clearing process involves multiple steps of tissue preparation, which require manual handling of tissues, incubation in clearing agents, and imaging. Additionally, the size and complexity of the tissue can also contribute to the level of physical effort required for tissue clearing, leading to convoluted, elaborate and tiresome protocols[8].

These downsides establish an incentive to reproduce the results of tissue clearing without undertaking the physical and chemical procedures involved, that is, by building neural networks to digitally accomplish the "tissue clearing" transformation.

C. Objective

We propose to create **a cascading, deep learning-based virtual tissue clearing and staining model** using conditional **GANs** (Generative Adversarial Networks)[9] for facilitating and enhancing pathology examinations of tissue samples.

This innovative concept, termed **ClariGAN**, will leverage advanced computing and deep learning techniques to supersede the current standard of tedious (often inconsistent) and expensive tissue preparation protocols (Figure 1). To achieve our goal, we aim to collect and train pairs of autofluorescence confocal microscopy images of thick tissue samples (100-500 μm) before and after chemical clearing and staining procedures. To ensure a stationary orientation of the three-dimensional sample, we propose to fix our specimens to 35 mm glass bottom dishes with 14 mm micro-well #1.5 cover glass. This will allow us to clear and stain the samples in their imaging container without altering their placement. We will begin with murine lymph node, heart, and appendicular skeleton specimens (which will be fixed to stabilize the tissue structure and be more compatible with clearing and staining techniques) and then tailor the model to other organ types. Once our models are extended and validated for use with human samples, they could provide more comprehensive and accurate pathological tissue examination. Additionally, the ability to obtain 3D scans from minimally invasive biopsies could spare patients from undergoing more intrusive procedures involving larger tissue extractions. This new approach could thus significantly improve the histological assessment of unstained tissue slides for various tissue types.

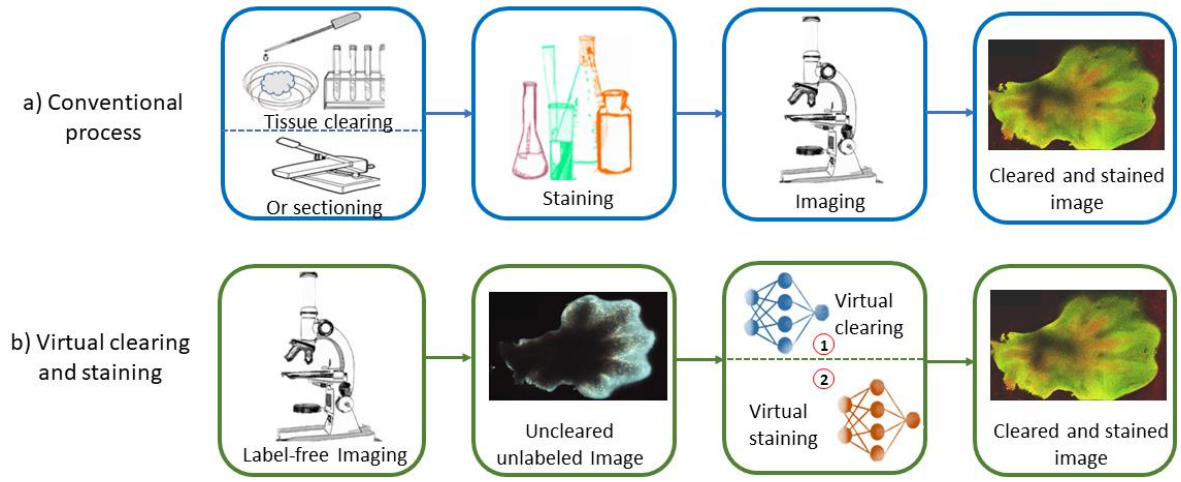

Figure 1. Schematic diagram demonstrating the conventional (top) and virtual tissue clearing+staining (bottom) histological preparation procedures for 3D imaging. The images are preliminary murine limb samples.

D. Outline of Tasks

In this proposal, we aim to create a deep learning-based, virtual tissue clearing and staining method that can be used for enhanced pathology assessments.

The following are the tasks required for this proposed project:

I. Data Acquisition: We will use confocal microscopy to achieve precise 3D scans of murine extremity, lymph node, and heart samples with 100-500µm thickness in (1) unlabeled and uncleared, (2) unlabeled and cleared, and (3) cleared and stained conditions.

II. Sample preparation: The clearing method (to be used as our learning ground truth) will follow the CUBIC protocol[10], and staining will include fluorescent SYTOX and Alexa647 dyes to highlight cell nuclei and membranes, respectively.

III. Model Development: The deep learning models will be based on conditional GANs, as detailed in Figure 2, which can rapidly transform cross-registered pairs of autofluorescence images of uncleared and unstained tissue samples (to be used as inputs during training) into images that mimic traditional 2D fluorescently stained tissue sections.

IV. Data Prepossessing: The registration of paired images is achieved by first finding the best matching z planes in corresponding 3D scans, and then applying algorithms to align the samples' orientation and correct for nonlinear deformations with pixel-level accuracy[11], as outlined in Figure 3.

V. Result Assessment: Evaluation measures will include structural similarity indices to compare model outputs with ground truth images[12], as well as quantitative examinations by board-certified pathologists[13].

D. Discuss future possibilities and potential advancements in the field

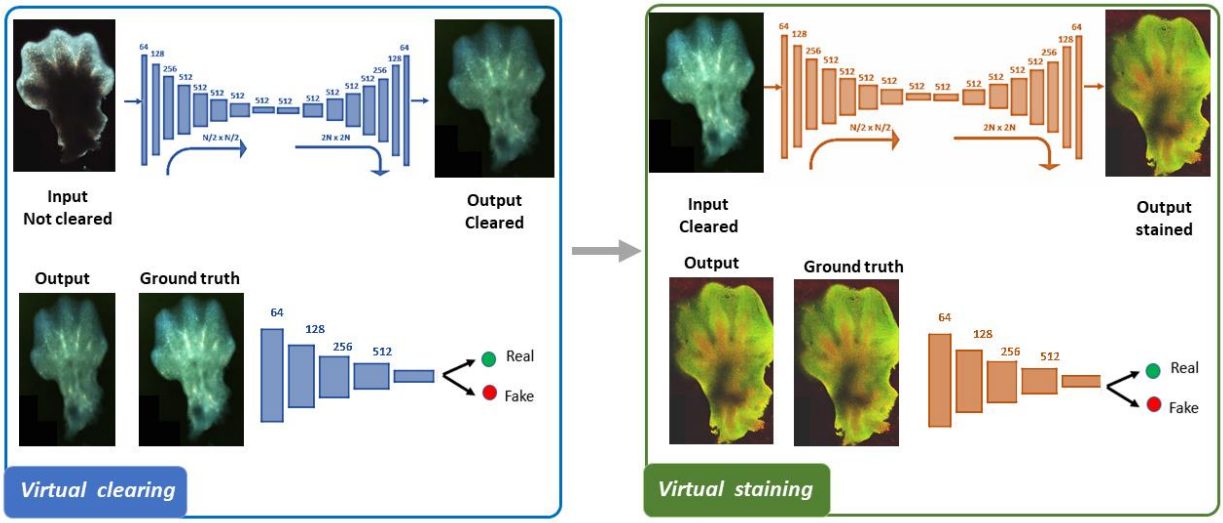

Figure 2. Model architectures for the consecutive virtual clearing and staining processes. Each network consists of a generator and a discriminator model, competing with one another, as part of the conditional GAN training method. The images are preliminary murine limb samples.

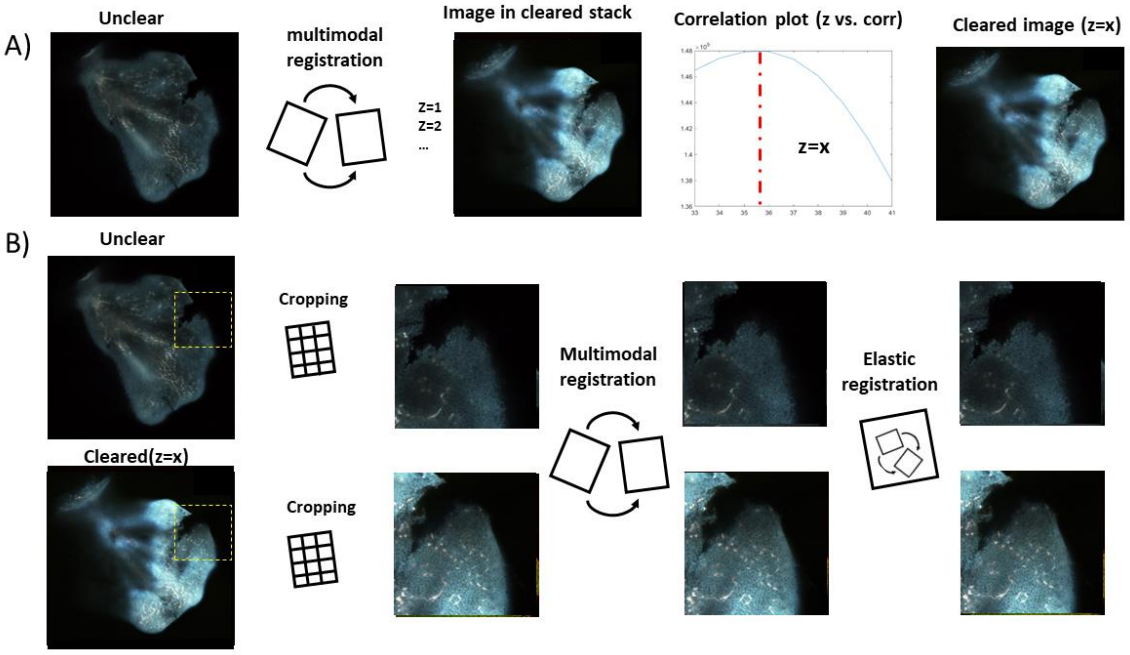

Figure 3. Registration scheme. A) First corresponding z-planes in unclear and cleared image stacks are paired using a correlation algorithm. B) Cropped images of these two image sets are then orientated in the same way (multimodal) and stretched (elastic) to optimize the pixel overlap.

E. Outcomes and Impact

Digitizing the preparatory workflow of pathology specimens through virtual clearing and staining would facilitate the acquisition of three-dimensional visualizations of tissue biopsies, capturing unique features that may only appear on a single plane, while simultaneously preserving the intricate interconnections among tissue components. A cascading virtual clearing and staining model would allow one to forgo the limitations and drawbacks of clearing and staining procedures and achieve the same results through neural networks applied to unlabeled sample images, as illustrated in Figure 4.

In the eventuality that our models are paired with synthetic standard histochemical staining (by training on co-registered 2D stained sections of our samples), they could be implemented in standard pathology workflows. Such network models may be especially useful for pathologists in specific situations that currently **require additional sample excisions**. For instance, core needle biopsies, which are minimally invasive and can be performed bedside with local anesthesia[14], are usually insufficient for diagnosing low-grade lymphoma. This is because the obtained 2D image of the noodle-shaped tissue often fails to reveal most of the tissue architecture[15]. As a result, pathologists frequently cannot reach a definitive diagnosis and consequently, an excisional biopsy of the entire lymph node is recommended, which is an invasive surgical procedure that typically takes place in an operating room and often requires general anesthesia. Obtaining a 3D image from the core needle biopsy that is virtually stained may therefore prove beneficial in such cases, potentially leading to superior diagnosis, intervention, and improved patient outcomes.

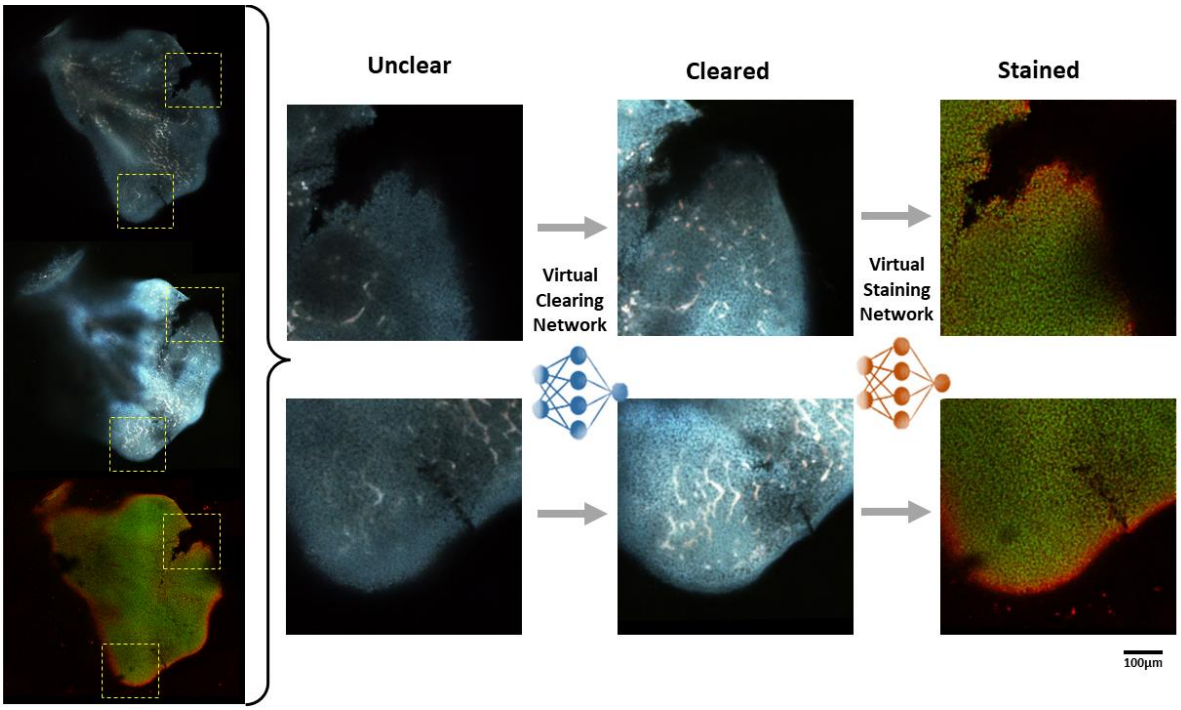

Figure 4. Network Objectives: autofluorescence microcopy fields of view of an uncleared sample can be passed through a deep learning network to first clear the tissue digitally, and then a virtual staining network, to synthetically apply fluorescent stains.

References

1 Richardson, D. S. *et al.* Tissue clearing. *Nature Reviews Methods Primers* **1**, 84 (2021).

2 Chung, K. *et al.* Structural and molecular interrogation of intact biological systems. *Nature* **497**, 332-337 (2013).
3 Nojima, S. *et al.* CUBIC pathology: three-dimensional imaging for pathological diagnosis. *Scientific reports* **7**, 9269 (2017).
4 Delle Cave, D. *et al.* The revolutionary roads to study cell–cell interactions in 3d in vitro pancreatic cancer models. *Cancers* **13**, 930 (2021).
5 Hama, H. *et al.* Sca l eS: an optical clearing palette for biological imaging. *Nature neuroscience* **18**, 1518-1529 (2015).
6 Richardson, D. S. & Lichtman, J. W. Clarifying tissue clearing. *Cell* **162**, 246-257 (2015).
7 Ertürk, A. *et al.* Three-dimensional imaging of solvent-cleared organs using 3DISCO. *Nature protocols* **7**, 1983-1995 (2012).
8 Tomer, R., Ye, L., Hsueh, B. & Deisseroth, K. Advanced CLARITY for rapid and high-resolution imaging of intact tissues. *Nature protocols* **9**, 1682-1697 (2014).
9 Creswell, A. *et al.* Generative adversarial networks: An overview. *IEEE signal processing magazine* **35**, 53-65 (2018).
10 Susaki, E. A. *et al.* Advanced CUBIC protocols for whole-brain and whole-body clearing and imaging. *Nature protocols* **10**, 1709-1727 (2015).
11 Li, J. *et al.* Biopsy-free in vivo virtual histology of skin using deep learning. *Light: Science & Applications* **10**, 233 (2021).
12 Bai, B. *et al.* Label-free virtual HER2 immunohistochemical staining of breast tissue using deep learning. *BME Frontiers* **2022** (2022).
13 Bai, B. *et al.* Deep learning-enabled virtual histological staining of biological samples. *Light: Science & Applications* **12**, 57 (2023).
14 Johl, A., Lengfelder, E., Hiddemann, W., Klapper, W. & Group, G. L.-g. L. S. Core needle biopsies and surgical excision biopsies in the diagnosis of lymphoma—experience at the Lymph Node Registry Kiel. *Annals of hematology* **95**, 1281-1286 (2016).
15 Frederiksen, J. K., Sharma, M., Casulo, C. & Burack, W. R. Systematic review of the effectiveness of fine-needle aspiration and/or core needle biopsy for subclassifying lymphoma. *Archives of Pathology and Laboratory Medicine* **139**, 245-251 (2015).
16 Cang, S., Mukhi, N., Wang, K. & Liu, D. Novel CD20 monoclonal antibodies for lymphoma therapy. *Journal of hematology & oncology* **5**, 1-9 (2012).

Ultra-high Resolution Computational Fundus Camera for Chronic Retinal Disease Detection

Age-Related Macular Degeneration (AMD) is a major issue and the leading cause of blindness in the developed world. According to the World Health Organization, the affected population in 2020 was approximately 200 million people. Limited treatment options, combined with technological barriers against monitoring and early detection of the disease make battling AMD a major challenge.

Early stage AMD is characterized by the gradual deterioration of the retinal pigment epithelium (RPE) layer which sits beneath the photoreceptor cells. As the RPE cells become less efficient in their functions, the photoreceptor cells gradually degenerate, leading to progressive vision loss.

Challenges with imaging the RPE cells are multi-fold: Firstly, the transverse resolution of conventional retinal imaging systems is generally limited to around 20 microns due to intrinsic aberrations of the ocular media (in particular the lens and cornea); second, most of the imaging light entering the pupil is either absorbed or reflected at the interface of photoreceptor segments, overwhelming the weak signal backscattered from the neuronal or RPE cells; and finally, the RPE cells are transparent to visible light, and therefore suffer from low contrast and signal to noise ratio.

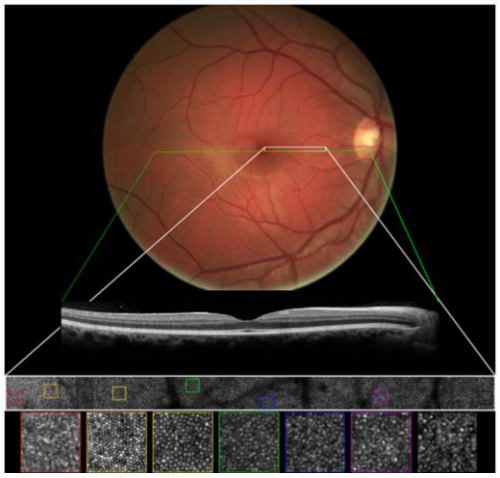

Fig. 1. Sample multi-modal retinal image, demonstrating the trade-off in the FOV, resolution, and information content between wide-field fundus image, OCT B-Scan, and a state-of-the-art, flood illuminated AO retinal image.

To address the limitations in the cellular resolution, the ophthalmic systems have incorporated adaptive optics (AO) techniques which rely on wavefront sensing, and manipulation technologies in order to estimate and correct for optical aberrations. Despite continuous advancements in speed, resolution, and capabilities, conventional AO systems are cumbersome to operate, optically complex, and expensive. Moreover, practical wavefront sensing and correction is only achieved over a very small field of view (FOV) (see Fig. 1 for example).

In this application, we propose to develop a new class of retinal cameras which we term complex field fundus imager. Our technology which combines advances in Fourier Ptychography, Pupil Modulation, and trans-palpebral illumination ***overcomes the limitations faced by the current state of the art in imaging the sub-surface retinal layers while achieving an order of magnitude improvement in the SBP compared to the existing technologies***.

In order to de-risk achieving the greater goal outlined above, we intend to follow three complementary, yet incremental specific aims:

In **Specific Aim 1**, we design, build and optimize a computational retinal camera that recovers complex field from a series of intensity images of a model eye. One of our primary objectives is to develop a cost-effective solution that can be designed and disseminated in the developing world.

In **Specific Aim 2**, we will leverage multiplexed image acquisition and computational reconstruction in order to improve the SNR, and frame rate of our proposed imager.

Finally, in **Specific Aim 3**, we will carry out *in-vivo* imaging studies in order to validate the system performance in presence of motion artefacts and ocular movements.

PROBLEM STATEMENT AND SPECIFIC AIMS

Age-Related Macular Degeneration (AMD) is a major issue and the leading cause of blindness in the developed world. According to the World Health Organization, the affected population in 2020 was approximately 200 million people. Limited treatment options, combined with technological barriers against monitoring and early detection of the disease make battling AMD a major challenge [1-2].

Early stage AMD is characterized by the gradual deterioration of the retinal pigment epithelium (RPE) layer which sits beneath the photoreceptor cells. As the RPE cells become less efficient in their functions, the photoreceptor cells gradually degenerate, leading to progressive vision loss.

Challenges with imaging the RPE cells are multi-fold: Firstly, the transverse resolution of conventional retinal imaging systems is generally limited to around 20 microns due to intrinsic aberrations of the ocular media (in particular the lens and cornea); second, most of the imaging light entering the pupil is either absorbed or reflected at the interface of photoreceptor segments, overwhelming the weak signal backscattered from the neuronal or RPE cells; and finally, the RPE cells are transparent to visible light, and therefore suffer from low contrast and signal to noise ratio [3].

To address the limitations in the cellular resolution, the ophthalmic systems have incorporated adaptive optics (AO) techniques which rely on wavefront sensing, and manipulation technologies in order to estimate and correct for optical aberrations. Despite continuous advancements in speed, resolution, and capabilities, conventional AO systems are cumbersome to operate, optically complex, and expensive. Moreover, practical wavefront sensing and correction is only achieved over a very small field of view (FOV) (see Fig. 1 for example) [4].

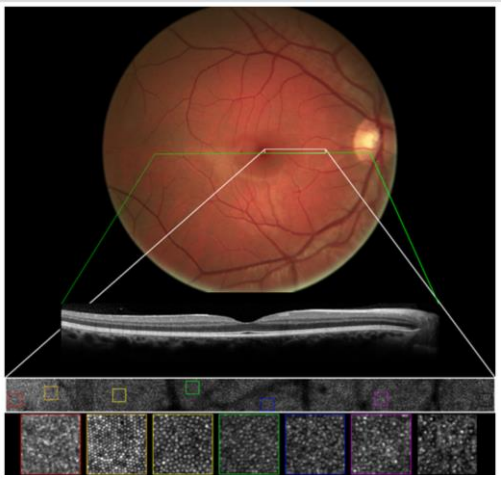

Fig. 1. Sample multi-modal retinal image, demonstrating the trade-off in the FOV, resolution, and information content between wide-field fundus image, OCT B-Scan, and a state-of-the-art, flood illuminated AO retinal image.

In this application, we propose to develop a new class of retinal cameras which we term complex field fundus imager. Our technology which combines advances in Fourier Ptychography, Pupil Modulation, and trans-palpebral illumination ***overcomes the limitations faced by the current state of the art in imaging the sub-surface retinal layers while achieving an order of magnitude improvement in the SBP compared to the existing technologies***.

In order to de-risk achieving the greater goal outlined above, we intend to follow three complementary, yet incremental specific aims:

In **Specific Aim 1**, we design, build and optimize a computational retinal camera that recovers complex field from a series of intensity images of a model eye. One of our primary objectives is to develop a cost-effective solution that can be designed and disseminated in the developing world.

In **Specific Aim 2**, we will leverage multiplexed image acquisition and computational reconstruction in order to improve the SNR, and frame rate of our proposed imager.

Finally, in **Specific Aim 3**, we will carry out *in-vivo* imaging studies in order to validate the system performance in presence of motion artefacts and ocular movements.

INNOVATION, APPROACH AND WORKPLAN

In this proposal we leverage the following key innovations in order to realize an optically simple, high resolution fundus imager for application in early diagnosis of chronic ocular impairments:

1) **Use of reflection-mode, spatially incoherent Fourier Ptychography for sensor-less, computational aberration characterization and correction**

2) **Use of trans-palpebral illumination for overcoming low contrast and SNR**

3) **Use of multiplexed illumination and coded sampling for increased image acquisition rate**

AIM 1. Complex Field Retinal Imager Design **[Months 1 - 6]**

Mathematically, aberrations are described as variations in the spatial phase of the pupil function of a given optical system. AO systems strive to flatten the pupil function by estimating and inverting the wavefront distortions. Here we propose to leverage a technique known as Fourier Ptychography (FP) to circumvent the challenges of wavefront sensing and correction by computational reconstruction of the complex field [5]. Rather than striving to get the highest-quality images possible through an AO corrected imaging system, FP dynamically determines the system's aberrations computationally. An aberration free, high SBP image is then reconstructed by solving an ill-posed problem computationally.

FP is particularly attractive since it overcomes two issues inherent to the traditional AO systems:

1) The typical integration of the AO with an ophthalmic imaging system results in a relatively large and complicated optical setup that uses a Hartmann-Shack Wavefront Sensors placed at an image plane that is optically conjugated to the pupil of the eye. Due to the high sensitivity of the HS-WFS to the back-reflections, the optical system is commonly constructed with concave mirrors instead of lenses. Moreover, in order to reduce the aberrations from the off-axis use of spherical mirrors, long focal lengths are desired, consequently increasing the size of the system.

2) Practical AO systems suffer from relatively small FOV since the wavefront correction is only valid in a small region in the vicinity of a guide star. This region is known as the isoplanatic patch, and its size varies depending on the severity of aberrations. To image a larger area beyond the isoplanatic patch, AO systems need to be raster-scanned which further adds to their complexity.

While conventional FP architectures are limited to optical setups with a well-defined, spatially coherent field on the sample plane, Chung et. al. recently developed a generalized FP system which overcomes the spatial coherence requirement of the original pupil function recovery. In their approach which they termed CACAO-FB, they scan a series of circular and coded masks via a spatial light modulator (SLM) in order to estimate the distortions in the pupil function [6].

While a significant milestone towards extending the FP technique to spatially incoherent sources, their approach suffers from a few major drawbacks: first, use of a mask in the Fourier plane discards a significant amount of precious photons. Second, spatial light modulators (SLMs) add a significant cost to the overall system, and also suffer from polarization dependent losses which

further reduces the SNR; and third, pupil scan is done sequentially, resulting in slow image acquisition and motion artefacts in live imaging.

While the limitations above are applicable to all use cases of the CACAO-FB technique, the most significant drawback for applications in imaging the RPE layers is the flood illumination of the scene though the system's pupil (i.e. cornea and interocular lens in the eye). In addition to the back-reflection artefacts by the cornea and interocular lens, most of the light that impinges on the photoreceptor layer with small incident angle gets absorbed or reflected by these cells. By contrast photoreceptors become less responsive to oblique illumination and light entering the eye at large incident angles penetrates past these cells. This angular reflection dependent of the retina is known as the Stiles-Crawford and it was recently leveraged by Laforest et. al. in their widefield, AO imaging system to image the RPE layers with high contrast and SNR [3]. While this work is a major step forward, the system still suffers from some of the fundamental bottlenecks in terms of cost, and system complexity, which have hindered wide-spread adoption of the AO ophthalmic systems in clinics.

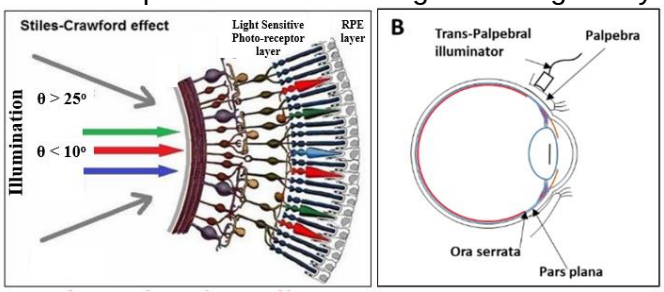

Fig. 2. Directionality of photoreceptor cells is known as Silles-Crawford effect. By illuminating the eye at large incident angles (through the palpebra) we expect to achieve high contrast imaging of the sub-surface layers [7-8].

Proposed Optical Design

As it was mentioned above our proposed design is backed by advances in Fourier Ptychography. Successful implementation, and phase retrieval requires partial overlap of the low SBP scene in the pupil domain (i.e. Fourier domain). In order to capture the high spatial frequencies we propose to use an LED ring array in conjunction with a parabolic mirror. This is similar to conditions used in dark field and phase contrast microscopy, and the i^{th} LED position with respect to the optical axis, d_i, has the following relationship with the illumination angle, θ_i [9]:

$$\sin(\theta_i) = -\frac{d_i}{\sqrt{\left(d_i^2 + \left(-\frac{d_i^2}{4f_p} + f_p\right)^2\right.}}$$

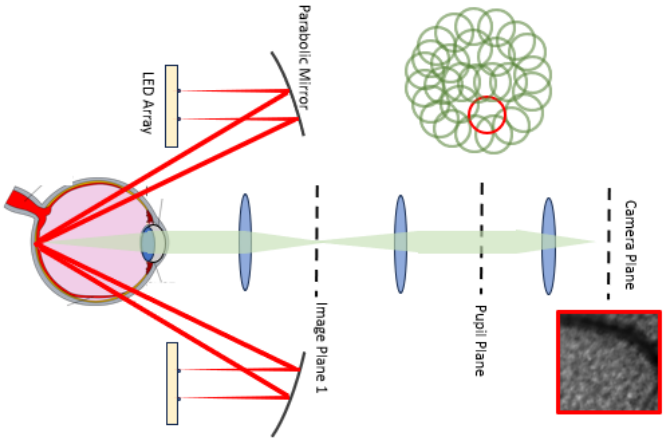

Fig. 3. Conceptual block diagram of our high resolution, trans-palpebral Fourier Ptychography retinal imager. Each LED samples an overlapping fraction of the spatial frequencies. Aberrations are computationally calculated and corrected for using phase retrieval algorithms.

In the interest of brevity, we avoid detailed derivation/ mathematical justification of the complex field recovery process here and instead provide a brief explanation of the underlying mechanisms. The images captured with each LED encode the local aberration of the unknown pupil function (i.e. cornea and interocular lens) in their point spread functions (PSF). We will use a blur

estimation algorithm to extract these PSFs. We then us an FP-based alternating projections algorithm to synthesize the spatially filtered pupil functions into the full pupil function.

Challenges, limitation, and alternative strategies

The main challenge in successful application of our proposed technique in live imaging is the limitation in the SNR caused by the safe exposure limit of the eye. On the hardware side we intend to optimize the optical configuration in order to minimize the overall system loss. Additionally, for the proof of concept demonstration we will use a high sensitivity sCMOS camera. Nevertheless, despite the hardware optimizations, we may have to acquire and average a sequence of low exposure frames in order to enhance the SNR. This is a strategy that is commonly used in the current AO systems. In order to overcome the effect of motion artefacts, industry standard image registration and transform will be performed prior to averaging.

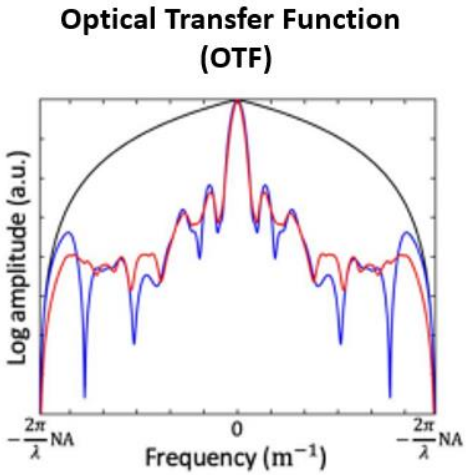

Fig. 4. Comparison of an ideal Optical Transfer Function (OTF) in black with an aberrated transfer function in blue. Inserting a coded phase mask in the pupil plane smooths out the nulls in the aberrated transfer function (red)

AIM 2. Multiplexed Illumination and Coded Sampling **[Months 6 - 15]**

As it was discussed above, FP sequentially illuminates the object (i.e. the retina) using an LED array and collects intensity patterns corresponding to different spatial frequency components. The requirement to acquire 10s of images corresponding to different illumination conditions hinders the effectiveness of the technique in imaging dynamic objects. Here we propose to leverage multiplexed illumination, and coded sampling to achieve single shot acquisition.

Use of multiplexed measurement in Ptychography is quite well established. Lee et. al. demonstrated a single shot FP system by using a micro-lens array in order to capture multiple images corresponding to different illumination conditions [10]. While remarkable in their performance, Lee's solution faces challenges in the presence of severe aberrations, where the Optical Transfer Function (OTF) may have values at or close to zero for many spatial frequency regions within the bandpass of individual lenslets. These nulls are due to the phase gradients with opposite slopes found in an aberrated pupil function [6]. To overcome this limitation we propose to create a coded aperture microlens array. Fig. 4 shows the smoothing effect of using a coded phase mask which provides a transfer function with reasonable signal quality across the spatial bandwidth of the individual lenslets.

The phase mask will be fabricated using standard lithographic techniques. The PI has extensive experience with computational imaging systems using coded aperture technologies.

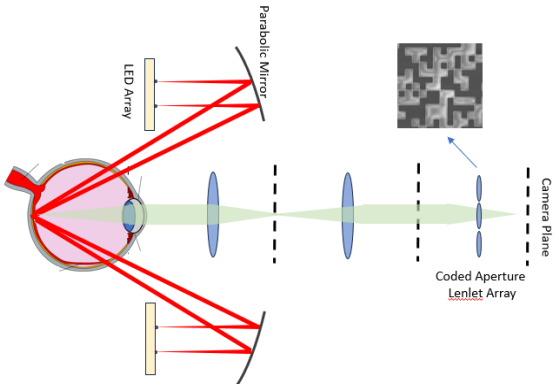

Fig. 5. Proposed coded aperture fundus camera. A lithographically produced pseudo-random phase mask modulates the pupil function of individual lenslets.

Challenges, limitation, and alternative strategies

While the proposed combination of a lenslet array and a coded phase mask is untested, there is a comprehensive body of literature to support our proposed solution. One alternative to this solution is to utilize compressive sampling and coded illumination [11-16]. This is a established solution, and Tian ei. al. demonstrated that a coded illumination can be used in conjunction with phase retrieval algorithms to recover the high resolution object with far fewer number of measurements compared with the conventional FP systems [15].

AIM 3. In-vivo validation **[Months 15 - 18]**

In order to minimize the technical risks, the first two Aims will be completed using phantom objects and eye models. This gives us the flexibility to explore the required photon budget, signal to noise ratio, as well as alignment tolerances prior to live imaging. In our third and final Aim we will attempt to test our hardware performance in vivo. This will require additional expansion of the optical design to incorporate a fixation targets, as well as a secondary infrared imaging arm to assist with pupil tracking and subject alignment. These are challenges we are well versed to tackle at Cambridge Vision Technology (CVT) where we currently develop low cost retinal imaging solutions for use by at risk patients.

Challenges, limitation, and alternative strategies

It may be necessary to dilate the subject's pupil. We do have the in-house expertise and we benefit from our close collaborations with ophthalmologists in Cambridge and London area. In case of severe motion artifact we will investigate utilizing image registration and image transform algorithms which are commonly used in the industry in order to co-align the low SBP images prior to FP based reconstruction. Image registration algorithms are often used in dynamic AO systems.

OUTCOMES AND IMPACT

Chronic retinal diseases are expected to impact an estimated 700 Milion people worldwide by 2040. Early diagnosis and intervention is key to improving the patient's outcome. Unfortunately, OCT and wide-field fundus imaging, do not have the lateral resolution to detect early onset of these diseases. While AO systems have been around for the past 3 decades, their adoption has been hindered by the system bulk and complexity.

Computational imaging solutions overcome the challenges in designing, highly customized, high performing optical solutions by transferring the high bandwidth information recovery to the software domain. Thanks to advances in cloud based computing, and hardware accelerations, computational imaging solutions are becoming more and more mainstream.
If successful, the proposed system will have a significant impact on the early diagnosis and management of many chronic retinal diseases. When combined with advanced machine learning tools, output from our high bandwidth fundus imager will allow the ophthalmologists to detect small anomalies in the retail structure at the single cell level.

This is a very ambitious project. This grant will enable the PI to acquire the preliminary data needed in order to secure larger translational funding through the UK Government for application in early disease detection and patient monitoring.
Results obtained through this project will be shared with the greater scientific community through conferences and OSA publications.

REFERENCES

[1] Wong WL, Su X, Li X, Cheung CMG, Klein R, Cheng CY, et al. Global prevalence of age-related macular degeneration and disease burden projection for 2020 and 2040: a systematic review and meta-analysis. Lancet Glob Health. 2014;2:e106–e116.

[2] Pascolini D, Mariotti SP. Global estimates of visual impairment: 2010. Br J Ophthalmol. 2012;96:614–618.

[3] Laforest, Timothé, et al. "Transscleral optical phase imaging of the human retina." *Nature photonics* 14.7 (2020): 439-445.

[4] Booth, Martin J. "Adaptive optical microscopy: the ongoing quest for a perfect image." *Light: Science & Applications* 3.4 (2014): e165-e165.

[5] Zheng, Guoan, et al. "Concept, implementations and applications of Fourier ptychography." *Nature Reviews Physics* 3.3 (2021): 207-223.

[6] Chung, Jaebum, et al. "Computational aberration compensation by coded-aperture-based correction of aberration obtained from optical Fourier coding and blur estimation." *Optica* 6.5 (2019): 647-661.

[7] Pallikaris, A., Williams, D. R. & Hofer, H. The reflectance of single cones in the living human eye. *Invest. Ophthalmol. Vis. Sci.* **44**, 4580–4592 (2003).

[8] Gao, W., Cense, B., Zhang, Y., Jonnal, R. S. & Miller, D. T. Measuring retinal contributions to the optical Stiles–Crawford effect with optical coherence tomography. *Opt. Express* **16**, 6486–6501 (2008).

[9] Lee, Hwihyeong, Byong Hyuk Chon, and Hee Kyung Ahn. "Reflective Fourier ptychographic microscopy using a parabolic mirror." *Optics Express* 27.23 (2019): 34382-34391.

[10] Lee, Byounghyo, et al. "Single-shot phase retrieval via Fourier ptychographic microscopy." *Optica* 5.8 (2018): 976-983.

[11] Shin, Jaewook, et al. "A minimally invasive lens-free computational microendoscope." *Science advances* 5.12 (2019): eaaw5595.

[12] Shin, Jaewook, et al. "Lens-Free Computational Epi-Fluorescence Microendoscopy." *Optics and the Brain*. Optica Publishing Group, 2020.

[13] Antipa, Nick, et al. "DiffuserCam: lensless single-exposure 3D imaging." *Optica* 5.1 (2018): 1-9.

[14] Asif, M. Salman, et al. "Flatcam: Thin, lensless cameras using coded aperture and computation." *IEEE Transactions on Computational Imaging* 3.3 (2016): 384-397.

[15] Dong, Siyuan, et al. "Spectral multiplexing and coherent-state decomposition in Fourier ptychographic imaging." *Biomedical optics express* 5.6 (2014): 1757-1767.

[16] Tian, Lei, et al. "Multiplexed coded illumination for Fourier Ptychography with an LED array microscope." *Biomedical optics express* 5.7 (2014): 2376-2389.

Executive Summary - Topic Environment

TITLE: Unveiling Optical Properties and Degradation Mechanisms in Emerging Multijunction Solar Cells through Advanced Spectroscopy

Solar power is crucial for addressing global energy and environmental challenges, and multijunction solar cells have gained attention for their ability to achieve higher efficiencies compared to single-junction cells. Unveiling Optical Properties and Degradation Mechanisms in Emerging Multijunction Solar Cells through Advanced Spectroscopy is a proposal that addresses the challenges in the stability and performance optimization of emerging multijunction solar cells. The proposal focuses on optoelectrical characterization, as understanding the underlying mechanisms is essential for optimizing the performance of multijunction solar cells. Traditional techniques provide limited information, but intensity modulated photocurrent spectroscopy (IMPS) has emerged as a powerful tool for characterizing multijunction solar cells. IMPS involves modulating incident light and measuring the photocurrent response, providing insights into charge carrier dynamics and material properties. IMPS has various applications, including evaluating individual subcells within a multijunction architecture, determining the influence of boundary conditions, and studying the stability and degradation of solar cells. However, IMPS still faces challenges in accurately determining optical properties and extracting key parameters from the data. Additionally, it has limitations in measuring only the stability of small-area devices, up to a few cm^2. Further research is needed to develop robust modeling approaches and analysis methods for both small and large-area (> 400 cm^2) devices.

The proposal highlights the advantages of using IMPS for studying the stability and degradation of emerging multijunction solar cells, particularly perovskite-based or tandem solar cells. IMPS offers non-destructive characterization, sensitivity to interface and bulk properties, fast and efficient measurements, quantitative analysis, versatility and compatibility with other techniques, and real-time monitoring capabilities.

The project has two main objectives. Firstly, it aims to develop an improved IMPS technique for identifying degradation mechanisms in large-area multijunction PV devices. This technique will assess the stability of these devices by monitoring changes in charge carrier dynamics and performance degradation over time. The goal is to create a robust and integrated system capable of accurately assessing the optical characteristics of multijunction solar cells. Secondly, the proposal aims to provide crucial information to develop effective strategies for enhancing the performance of emerging multijunction solar cells. By doing so, the project aims to advance the practical viability of these devices for real-world applications.

To achieve these objectives, the proposal outlines a work plan with several interrelated work packages. These work packages include tasks such as defining and selecting experiment parameters, conducting measurement characterization and validation, developing an enhanced IMPS setup, and optimizing the design and fabrication processes of tandem and perovskite solar cells to achieve high performance and extended lifetime. This last task will culminate into the definition of guidelines for the design of highly efficient, stable and long-lasting multifunction solar cells. As a case study, the clean room of Delft University of Technology's photovoltaic materials and devices group will be used to fabricate tandem/perovskite solar cells following the developed guidelines.

The intended outcomes of the research include (i) the development of an advanced IMPS system, (ii) improved stability and reliability, enhanced performance, cost reduction, and technological advancement in multijunction solar cell technology, and (iii) improvement of perovskite solar cell processes.

The impact of the research is significant and aligns with UN initiatives for sustainable development. The outcomes contribute to the transition towards clean and efficient energy, sustainable cities and communities, and affordable and clean energy. The findings will be disseminated through scientific publications, conference presentations, and engagement with industry stakeholders.

By addressing the challenges in multijunction solar cell characterization, stability, and optimization, the proposal aims to advance the field and contribute to the development of sustainable and clean energy solutions. The research outcomes have the potential to support the widespread adoption of solar energy, reduce greenhouse gas emissions, and promote a cleaner and more sustainable future for society.

In addition to addressing the Challenge, the research results obtained will serve as a catalyst for future research activities. The project will also offer valuable mentorship opportunities for two (2) Master's students and one (1) PhD student. Furthermore, there will be an exploration of collaborations, licensing, and start-up creation to foster development and maximize impact. This includes conducting comprehensive customer analysis, crafting a compelling value proposition, determining market sizing, creating a minimum viable product (MVP), and developing a robust business canvas.

Topic Environment, Proposal of interest: Enhancing the technology used on solar farms to reduce greenhouse emissions.

TITLE: Unveiling Optical Properties and Degradation Mechanisms in Emerging Multijunction Solar Cells through Advanced Spectroscopy

Literature Review

Renewable energy sources like solar power are here to save the day, tackling our planet's energy and environmental dilemmas head-on. Ever wondered how we can harness the power of the sun to create electricity? That's where solar cells, also known as photovoltaic (PV) cells, come into play! They're like magical energy transformers, converting sunlight into clean, sustainable electricity that can power our homes, schools, and cities. Let's embrace this incredible technology and pave the way for a more sustainable and eco-friendly world! This is the topic of the proposal. By combining multiple semiconductor materials with different bandgaps, so-called multijunction solar cells can capture a broader range of the solar spectrum and therefore they are able to achieve higher efficiencies compared to traditional single-junction solar cells (1) (2). For this reason, multijunction solar cells have gained significant attention of PV research and development aiming at green energy transition and **reduction of greenhouse gas emissions** (3) (4). An exemplary case of building upon the success of multijunction solar cells, emerging perovskite technology amplifies their efficiency and paves the way for an even greater energy harvest (5).

In this context, the **optoelectrical** characterization of multijunction solar cells is essential for optimizing their performance by understanding the underlying mechanisms for an energy-efficient operation (6). Traditional characterization techniques, such as current-voltage (I-V) measurements (7) and steady-state photocurrent spectroscopy, provide valuable information about the overall performance of solar cells (8). However, they often provide limited information and insights into the carrier dynamics (generation/recombination processes), energy states profiles, interface dynamics, and charge transfer mechanisms occurring within the device (9). Accurately characterizing and testing the performance of multijunction solar cells is a complex task that requires advanced measurement techniques (10). One such technique that has emerged as a powerful tool for evaluating multijunction solar cells is intensity modulated photocurrent spectroscopy (IMPS) (11) (12) (13), **which links the electrical and optical responses of the device.**

IMPS is a non-destructive technique used to investigate the electrical and photoelectric properties of PV devices (14). It involves modulating the intensity of incident light on a solar cell at a certain frequency and measuring the corresponding photocurrent response. The IMPS technique provides valuable information about the charge carrier dynamics, recombination processes, and material properties of solar cells (15) (16).

IMPS has found numerous applications in the characterization of PV devices (17). It allows researchers to evaluate the performance and efficiency of individual subcells to be used as baseline for multijunction structures (8). IMPS can also be used to determine the influence of PV devices' boundary conditions such as illumination intensity, temperature, and bias voltage on the performance of multijunction solar cells (17).

Over the years, several advancements have been made in IMPS techniques (18) to enhance their capabilities for testing multijunction solar cells. For instance, frequency-resolved IMPS (8) has been developed to analyze the spectral response of different subcells within a multijunction solar cell, providing insights into their individual contributions to the overall device performance. So far, IMPS typically operates in the frequency range of a few hertz to several kilohertz, hindering the capture of either metastable or ultrafast processes. Capacitive effects and inductive effects in solar cells can distort impedance response, affecting measurement accuracy (19). Higher frequencies lead to reduced signal amplitude and increased noise contribution, challenging the reliability of IMPS measurements. Additionally, the combination of IMPS with other characterization techniques, such as impedance spectroscopy (20) or transient photocurrent measurements (21), has enabled a more comprehensive understanding of the charge transport and recombination processes in multijunction solar cells.

Despite the advantages and advancements, IMPS for multijunction solar cells still faces numerous challenges. One such challenge is the accurate determination of optical properties and extraction of key parameters from IMPS data such as the effect of doping, dimensionality, morphology, and interface (18). Further research is needed to develop robust modeling approaches and analysis methods to extract accurate information about PV devices' inner physics (22). Moreover, the application of IMPS to emerging optoelectronic device technologies, such as perovskite-based or tandem solar cells (23) and LED, presents exciting opportunities for future research and development. Indeed, IMPS offers several advantages for studying the stability and degradation of perovskite solar cells (24). Here are some key advantages:

- Non-destructive characterization: IMPS is a non-destructive technique for monitoring the stability and degradation of perovskite solar cells over time.
- Sensitivity to interface and bulk properties: IMPS reveals charge transport and recombination processes at interfaces and within the perovskite solar cell bulk.
- Fast and efficient measurements: IMPS enables rapid measurements, suitable for high-throughput screening and evaluating perovskite solar cell stability.
- Quantitative analysis: IMPS allows extracting key parameters like charge carrier lifetimes and recombination rates, providing insights into perovskite solar cell stability.
- Versatility and compatibility: IMPS can be combined with other techniques for a comprehensive analysis of perovskite stability.
- Real-time monitoring: IMPS enables in-situ monitoring of perovskite solar cells under various conditions, offering insights into their stability and performance limitations.

Problem Statement/Objective

The stability and degradation of emerging multijunction solar cells pose significant challenges in achieving long-term performance and reliability (25) (26). Available tools are limited to measuring only the stability of small-area devices, up to a few cm^2 (27). However, the instability of perovskite solar cells and the challenge of scaling up from small to large areas pose significant obstacles to industrial production (28). Therefore, there is a need for advanced optical-electrical characterization techniques that can provide insights into the underlying **degradation** mechanisms to assess the **stability** of standard size large-area PV devices, such as G12 cells (210mm × 210mm). The objective of this project is twofold. On the one hand, the project aims **to develop an improved IMPS technique to identify degradation mechanisms for assessing the stability of emerging large-area multijunction PV devices** by evaluating changes in charge carrier dynamics and monitoring the performance degradation over time. By developing and implementing the proposed IMPS, this research will provide a robust and integrated system capable of accurately assessing the optical characteristics of multijunction solar cells. The improved IMPS combines a multispectral optical light source, lock-in amplifiers for precise signal detection, a custom electronic bias driver capable of handling high currents – up to 10A, and dedicated software for streamlined data acquisition. A first prototype of the proposed IMPS system is shown in Figure 1 and the preliminary version of the custom bias driver is shown in Figure 2. This system will be improved and it will enable comprehensive analysis of multijunction solar cells, providing valuable insights into their optical behavior and allowing for more accurate parameterization.

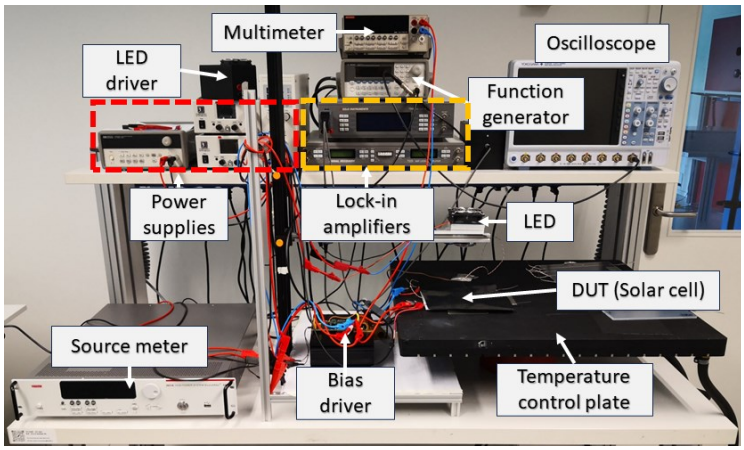

Figure 1: The first prototype of the proposed improved IMPS system. It is composed by an LED driver, different spectral LEDs, source meter for I-V trace, lock-in amplifiers for current and voltage sensing, function generator for the modulated signal, custom bias driver and temperature control plate.

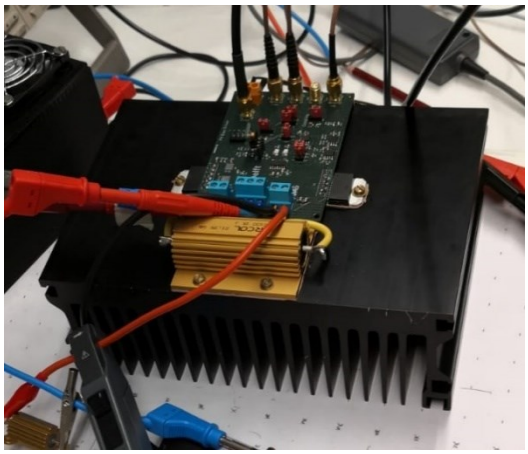

Figure 2: Custom bias driver that can handle high currents – up to 10A – and set the solar cell DC voltage from -5V up to 20V.

On the other hand, this proposal aims at providing crucial information for the **development of effective strategies for improving the performance of emerging multijunction solar cells**, ultimately advancing the viability of these devices for practical applications.

Specifically, this research aims to:

- Determine the correlation between IMPS measurements and the degradation mechanisms in multijunction solar cells: By subjecting the solar cells to various degradation stress factors such as temperature, humidity,

and light exposure, this study will analyze the changes in IMPS parameters and their relationship to degradation mechanisms, such as interface degradation, material degradation, and carrier trapping.

- Evaluate the temporal evolution of charge carrier dynamics during degradation: IMPS allows for the investigation of charge carrier lifetime, recombination rates, and transport properties. By monitoring these parameters over time under different degradation conditions, this research aims to identify the key factors contributing to performance degradation and quantify the degradation kinetics in multijunction solar cells.
- Assess the predictive capability of IMPS for long-term stability: Through an extended degradation study, this research will investigate the ability of IMPS to predict the long-term stability of emerging multijunction solar cells. By correlating IMPS measurements with the observed degradation trends, this study aims to establish a predictive framework for assessing the device lifetime and reliability based on IMPS data.

The applicant needs to realize the following sub-objectives to achieve the main research objective:

- O1: **Determine and analyze the correlation between IMPS measurements and degradation mechanisms** in multijunction solar cells (interface degradation, material degradation, and carrier trapping) under various degradation stress factors (temperature, humidity, light exposure).
- O2: **Evaluate the temporal evolution of charge carrier dynamics and identify the key factors contributing to performance degradation** and quantify the degradation kinetics in multijunction solar cells by monitoring charge carrier lifetime, recombination rates, and transport properties over time under different degradation conditions.
- O3: **Assess the predictive capability of IMPS for long-term stability** in multijunction solar cells.
- O4: **Establish a predictive framework** for assessing the device lifetime and reliability based on IMPS data by correlating measurements with observed degradation trends.
- O5: **Develop and implement an integrated IMPS system** combining a multispectral optical light source, lock-in amplifiers, a custom electronic bias driver, and dedicated software for streamlined data acquisition in order to overcome limitations of existing measurement setups and provide a robust and accurate method for assessing the optical characteristics and stability of large-area multijunction solar cells.
- O6: **Develop guidelines for the design of stable multifunction solar cells with longer lifetime,** based on the newly acquired knowledge and parameters extracted using our improved IMPS technique.

Outline of tasks/Work Plan

This project integrates theoretical study, simulations, design, and fabrication of solar cells and optical-electronic circuits, culminating in the development of a physical demonstrator. To effectively accomplish the stated objectives, a comprehensive research methodology will be employed, establishing connections between these diverse activities and strategically combining theoretical and experimental approaches. The research is structured into interrelated work packages (WPs) that are designed to collectively address the research objectives and sub-objectives outlined earlier.

Work Package 1 (**WP1**) will focus on **Experiments Definition and Parameters Selection**, with the primary objective of establishing the correlation between IMPS measurements and degradation mechanisms in multijunction solar cells. To achieve this, relevant parameters for investigation will be identified, and measurement protocols will be designed to capture data related to degradation mechanisms (Objective O1). (**1 month**)

WP2 will deal with **Measurements, Characterization and Validation**, with the goal of evaluating the temporal evolution of charge carrier dynamics during degradation using IMPS (Objective O2). This involves conducting IMPS measurements on multijunction solar cells under different degradation conditions, collecting data, and analyzing the temporal behavior of charge carrier dynamics. (**1-2 months**)

WP3 will focus on **Enhanced IMPS Setup** to overcome the limitations of existing measurement setups (Objective O5). This includes enhancing the current IMPS setup by integrating advanced components such as a multispectral optical light source, lock-in amplifiers, a custom electronic bias driver, and dedicated software for improved data acquisition and accurate assessment of the optical characteristics and stability of multijunction solar cells. (**2-3 months**)

WP4, titled **Measurements, Characterization, and Validation of the Enhanced IMPS Setup**, focuses on utilizing the improved IMPS setup **to evaluate its predictive capability for long-term stability in multijunction solar cells** (Objective O3) and establishing a framework for assessing device lifetime and reliability based on IMPS data (Objective O4). This involves conducting thorough characterization of

multijunction solar cells, monitoring charge carrier lifetime, recombination rates, and transport properties over time under various degradation conditions**. (2-3 months)**
Finally, in **WP5**, the project focuses on the **Development of guidelines for the design of stable and long-lasting Multijunction Solar Cells** (Objective 6). Leveraging the knowledge and extracted parameters obtained from the improved IMPS technique, the objective is to optimize the design and fabrication processes of tandem and perovskite solar cells to achieve high performance and longer lifetime. Tandem/perovskite solar cells according to the developed guidelines will be fabricated in the clean room of the photovoltaic materials and devices group at Delft University of Technology as a case study. (**3-4 months**).
Through the interplay of these work packages, the project aims to advance the understanding of multijunction solar cells and enhance their stability and performance.

Outcomes
The outcomes of this research will help in advancing the field of multi-junction solar cells and contribute to the broader goal of achieving sustainable and clean energy solutions. The findings will contribute to the development of advanced characterization methods and inform the design and optimization of multijunction solar cells for enhanced stability and improved lifetime in real-world applications. Furthermore, the funding will cover the salary and material costs for the applicant. Additionally, Delft University of Technology will provide extra funds through Dutch funding for research in the field of **Photovoltatronics**. The original and innovative outcomes of the project are enlisted below:

1. Development of an advanced IMPS system to overcome limitations in multijunction solar cell characterization and provide precise and reliable data for performance evaluation and optimization.
2. Improved longevity and reliability of multijunction solar cells through a comprehensive understanding of their stability and degradation behavior over time.
3. Enhanced performance optimization by utilizing insights from stability and degradation studies to optimize the design, materials selection, and manufacturing processes of multijunction solar cells.
4. Cost reduction through the development of more stable and long-lasting cells, reducing maintenance and replacement expenses for solar farm operators.
5. Technological advancement in multijunction solar cell technology through continuous monitoring and analysis, leading to the development of more stable and durable cells and supporting the transition to a low-carbon economy.
6. Lay the foundation for the development of highly efficient emerging solar cell technologies.

Impact
The development of an advanced IMPS system for multijunction solar cell characterization enables informed decision-making in solar cell design, manufacturing, and deployment, supporting the growth of renewable energy sources and promoting a sustainable future. This technology optimizes solar panel manufacturing by automating quality control processes, reducing costs, and enhancing product quality in the production line.
Understanding the stability and degradation behavior of multijunction solar cells improves their longevity and reliability. Longer-lasting and more efficient solar cells in solar farms reduce the need for additional energy generation from fossil fuels, resulting in decreased greenhouse gas emissions and mitigating environmental harm. The development of stable multijunction solar cells leads to cost reduction for solar farm operators, making solar energy economically viable and encouraging wider adoption. As solar power becomes increasingly cost-effective, it becomes a competitive alternative to traditional energy sources, accelerating the transition to a low-carbon economy. Insights gained from IMPS measurements can enhance the perovskite process, facilitating the creation of high-efficiency perovskite solar cells. These cells offer low-cost and highly efficient solar energy conversion. Optimizing fabrication techniques, materials composition, and device architectures based on IMPS data accelerates the development and commercialization of these next-generation solar cells, contributing to a cleaner energy mix.
In light of the aforementioned factors, the outcomes of this project will significantly contribute to the attainment of key United Nations (UN) initiatives aimed at facilitating the transition toward a secure, clean, and efficient energy policy. Specifically, our project aligns with and positively impacts the "Sustainable Cities and Communities," "Affordable and Clean Energy," and "Industry, Innovation and Infrastructure" focus areas of the UN's 17 Sustainable Development Goals. By addressing the challenges related to multijunction solar cell characterization, stability, and optimization, we will actively support the UN's global agenda and promote sustainable development in these crucial areas.

The dissemination of project results will involve publication in renowned scientific journals such as the *IEEE Journal of Photovoltaics*, *Progress in Photovoltaics* and *Solar Energy*. Additionally, results related to IMPS performance and system integration will be published in Optica Publishing Group's journals, including Applied Optics, as well as the Energy and Environmental Optics Express section of Optics Express.
The research findings will be presented at conferences focusing on photovoltaic technology, including the *IEEE Photovoltaic Specialists Conference (IEEE PVSC).* Conferences with a broader focus on sustainable technologies, optical characterization, and symposia organized by Optica will also serve as platforms for sharing results. Regular meetings with the Challenge Committee will be conducted to seek advice and guidance. The host institution's Open Access policy and online repository, compliant with OpenAIRE, will ensure accessibility to the applicant's scientific publications. To foster interaction and promote the project's outcomes, social media platforms such as Twitter, Facebook, YouTube, and LinkedIn will be utilized. Moreover, targeted magazine articles in publications like PV magazine and Optics and Photonics News will be prepared to extend the project's reach and impact.
Beyond the Challenge, the obtained research results will fuel future research activities. The project's research will offer **mentorship** opportunities for two (2) Master's students and one (1) PhD student. Discussions and evaluations will be conducted to devise strategies for utilizing the findings in both research and industrial contexts. Potential industrial applications may include IMPS setup or Perovskite/tandem process line. Through collaborations with industry and licensing of research results, the applicant will explore potential avenues for further development and impact, including the creation of a start-up. The applicant will conduct a comprehensive customer segment analysis, craft a compelling value proposition, determine the market size, create a minimum viable product (MVP) based on the data output, and develop a robust business canvas for optimal growth and success.

References

1. *Multi-junction solar cells paving the way for super high-efficiency.* Yamaguchi, M., et al. 2021, Journal of Applied Physics.
2. *Advanced solar cell concepts.* Solanki, C.S. and Beaucarne, G. 3, 2007, Energy for Sustainable Development, Vol. 11, pp. 17-23.
3. *Considerations for the calculation of greenhouse gas reduction by photovoltaic solar energy.* Krauter, S' and Rüther, R'. 3, 2004, Renewable Energy, Vol. 29.
4. *Life-cycle greenhouse gas emissions and energy payback time of current and prospective silicon heterojunction solar cell designs.* Louwen, A., et al. 10, 2014, Progress in Photovoltaics: Research and Applications, Vol. 23, pp. 1406-1428.
5. *Perovskites: The Emergence of a New Era for Low-Cost, High-Efficiency Solar Cells.* Snaith, H. J. 21, 2013, The Journal of Physical Chemistry Letters, Vol. 4, pp. 3623–3630.
6. *A comparative study of subcell optoelectronic properties and energy losses in multijunction solar cells.* Chavali, S. M., Roller, J. and M. Dagenais, B. H. Hamadani. 2022, Solar Energy Materials and Solar Cells, Vol. 236.
7. *Current-voltage dynamics of multi-junction CPV modules under different irradiance levels.* Fernández, E. F., et al. 2017, Sol. Ener., Vol. 155.
8. *Frequency response of the external quantum efficiency in multijunction solar cells.* Peraca, N. M., Bilir, D. T. and Hamadani, B. H. 16, 2017, Optics Express, Vol. 25, pp. 709-721.
9. *Status and challenges of multi-junction solar cell technology.* Baiju, A. and Yarema, M. 2022, Frontiers in Energy Research, Vol. 10.
10. *Monolithic Perovskite Tandem Solar Cells: A Review of the Present Status and Advanced Characterization Methods Toward 30% Efficiency.* Jošt, M., et al. 26, s.l. : Advanced Energy Materials, 2020, Vol. 10.
11. *The effect of luminescent coupling on modulated photocurrent measurements in multijunction solar cells.* Peraca, N. M., Haney, P. M. and Hamadani, B. H. 8, s.l. : Applied Physics Letters, 2019, Vol. 115.
12. *Space degradation of multijunction solar cells: An electroluminescence study.* Zazoui, M. and Bourgoin, J. C., s.l. : Appli. Phy. Lett., 2002, Vol. 80.
13. *Modulated photocurrent measurements in double junction solar cells.* Peraca, N. M. and Hamadani, B. H. Washington, DC, USA : IEEE 44th Photovoltaic Specialist Conference (PVSC), 2017.
14. *Intensity-modulated photocurrent spectroscopy: reconciliation of phenomenological analysis with multistep electron transfer mechanisms.* Peter, L. M., Ponomarev, E. A. and Fermín, D. J. 1-2, 1997, Journal of Electroanalytical Chemistry, Vol. 427, pp. 79-96.
15. *An intensity-modulated photocurrent spectroscopy study of the charge carrier dynamics of WO3/BiVO4 heterojunction systems.* Rodríguez-Gutiérrez, I., et al. 2020, Solar Energy Materials and Solar Cells, Vol. 208.
16. *Intensity modulated short circuit current spectroscopy for solar cells.* Kavasoglu, N., et al. 2, 2011, Solar Energy Materials and Solar Cells, Vol. 95.
17. *Intensity-Modulated Photocurrent Spectroscopy and Its Application to Perovskite Solar Cells.* Ravishankar, S., et al. 41, 2019, The Journal of Physical Chemistry , Vol. 123.
18. *Recent Progress of Light Intensity-Modulated Small Perturbation Techniques in Perovskite Solar Cells.* Parikh, N., et al. 2022, Phys. Status Sol. RRL, Vol. 16.
19. *Capacitive and Inductive Effects in Perovskite Solar Cells: The Different Roles of Ionic Current and Ionic Charge Accumulation.* Filipoiu, Nicolae, et al. 6, 2022, Physical Review Applied, Vol. 18.
20. *Impedance Spectroscopy for Emerging Photovoltaics.* Hauff, Elizabeth von. 18, 2019, The Journal of Physical Chemistry C, Vol. 123.
21. *Transient analysis of luminescent coupling effects in multi-junction solar cells.* Tayagaki, Takeshi, et al. 18, 2018, Journal of Appl. Phys., Vol. 124.
22. *Robust code-based modeling approach for advanced photovoltaics of the future.* Ogbonnaya, C., et al. 2020, Sol. Ener., Vol. 199.
23. *Perovskite Solar Cell Modeling Using Light- and Voltage-Modulated Techniques.* Ravishankar, Sandheep, et al. 11, 2019, The Journal of Phy. Chemistry C, Vol. 123, pp. 6444–6449.
24. *Impedance Spectroscopy Measurements in Perovskite Solar Cells: Device Stability and Noise Reduction.* Pitarch-Tena, Didac, et al. 4, 2018, ACS Energy Letters, Vol. 3, pp. 1044–1048.
25. *Performance and degradation analysis for long term reliability of solar photovoltaic systems: A review.* Sharma, Vikrant and Chandel, S.S. 2013, Renewable and Sustainable Energy Reviews, Vol. 27, pp. 753-767.
26. *Stability challenges for the commercialization of perovskite–silicon tandem solar cells.* Duan, Leiping, et al. 2023, Nature Reviews Materials, Vol. 8.
27. https://www.fluxim.com/paios-features. [Online] Fluxim AG. [Cited:]
28. *Recent Issues and Configuration Factors in Perovskite-Silicon Tandem Solar Cells towards Large Scaling Production.* Elsmani, Mohammed Islam, et al. 2021, Nanomaterials, Vol. 11.

Multimode fibre based “adaptive optic” for long range free-space optical communications

Mitchell A. Cox

Executive Summary

This research project aims to bridge the digital divide in peri-urban areas through innovative free-space optical communication technology. With two-thirds of the world’s population projected to live in urban areas by 2050, improving access to vital resources like internet, education, healthcare becomes crucial. However, rapid urbanisation in developing nations creates informal settlements with limited infrastructure, hindering digital inclusion.

To tackle this pressing issue, our work in general is focused on the development of low-cost free-space optical communication systems which can be used as a form of "fibre", before the fibre in these areas. Low-cost fibre hardware can be used to avoid expensive custom electronics and signal processing, however the challenge is coupling light efficiently into these transceivers, which were not intended for free-space use. Multi-mode fibres (MMFs) can be used at the receiver for efficiency, with two caveats: Light from high order optical modes may still be lost, and modal dispersion limits the possible capacity (speed) of a system.

The focus of this project is thus to thoroughly investigate using a dynamically actuated MMF to "reshape" the incoming, distorted light into a Gaussian, thus increasing the amount of light impinging on the receiver photodiode and possibly even combating the modal dispersion within the fibre. This "MMF-based adaptive optic" has the potential to significantly enhance the range and speed of communication systems in these peri-urban areas while keeping costs to a minimum, ultimately helping bridge the digital divide. The project is organised into five objectives:

1. Design and construct the necessary electronics and 3D-printed components, incorporating stepper or servo motors for dynamic bending of the fibre.
2. Output beam shaping: Demonstrate the generation of structured light beams using the system, verified with modal decomposition and off-axis interferometry to measure output wavefront characteristics in terms of amplitude and phase.
3. The MMF "adaptive optic": Investigate transforming turbulence-distorted beams back into Gaussian-like beams, optimising the number of actuators for cost-effectiveness.
4. Faster optimisation strategy: Explore machine learning and Bayesian optimisation algorithms to towards real-time adaptive optic control, as opposed to slow population based methods (currently used in literature).
5. The effect on modal dispersion: In parallel, we will study the device’s impact on modal dispersion within the multimode optical fibre, crucial for future high-speed optical communication systems.

Throughout the two-year project, we aim to publish at least four journal papers and present our work at local and international conferences. Additionally, we will provide an open-source design on GitHub, ensuring accessibility to the wider scientific community.

The potential impact of this research is substantial. The developed technology can help bridge the digital divide in peri-urban areas, providing longer range and higher speed FSO systems that are still affordable and use predominantly off the shelf hardware. Moreover, the dynamically actuated multimode fiber technology holds promise for ultra-high-speed optical communications using space division multiplexing and all-optical reservoir computing, making it a disruptive advancement for various applications.

With its scientific rigour, societal relevance, and transformative potential, this research project offers an opportunity to leverage optics and photonics to drive impactful scientific discoveries, transforming the way we address global challenges and creating a more inclusive digital society.

Multimode fibre based “adaptive optic” for long range free-space optical communications

Mitchell A. Cox*

School of Electrical and Information Engineering, University of the Witwatersrand, Johannesburg, South Africa

mitchell.cox@wits.ac.za

1. Introduction and Literature Review

As projected by the United Nations in 2014, by 2050, two-thirds of the world’s population will inhabit an urban environment. Such swift urbanization can potentially bolster individuals’ access to vital resources such as education, infrastructure, and health care, especially if planned meticulously. Unfortunately, the challenges posed by rapid urbanisation, particularly in developing nations, are formidable. Informal settlements often spring up with minimal or no prior infrastructure for utilities like electricity, water, or communications.

These informal settlements become low-income "suburbs", and are frequently located just a few kilometers, and sometimes merely across the road, from areas with superior infrastructure. The striking question, therefore, is how can we start bridging this substantial peri-urban digital divide? A significant impact on education and job opportunities could be made by bringing digital inclusion to people residing in these areas (1). One potentially swift and effective solution is the implementation of free-space optical communications (FSO) (2), anticipated to be a crucial component of future 6G deployments (3).

However, there are multiple hurdles associated with the implementation of commercial FSO solutions, primarily affordability. Striking a balance between the data rate, range, and cost of an FSO system is complex and challenging. Commercial systems are often not designed with the digital divide in mind, making them economically unfeasible for many in the affected areas.

Most commercial wireless optical communication systems leverage technologies similar to fibre-Ethernet - practically "fibre without the fibre". This approach reduces resilience to the adverse effects of atmospheric propagation, thus limiting the range of most commercial systems to about five kilometres at gigabit speeds (Fig. 1) (2). Despite these limitations, such systems hold potential for addressing the digital divide.

For example, at our lab (specialising in structured light FSO communications (4)), we have constructed a low-cost FSO system using off-the-shelf fibre hardware, such as SFP (Small Form-factor Pluggable) transceivers. We successfully demonstrated its capability to deliver 1 Gbps over a distance of 400 m, relying solely on off-the-shelf and 3D printed components. However, one major challenge lies in efficiently coupling light into a receiving fibre, particularly in the presence of atmospheric turbulence.

This challenge has been investigated in several works. Refs. (5, 6) demonstrated the use of SFP modules in cost-effective FSO systems spanning 125 m and 500 m respectively, with fibre cables guiding light into and out of the modules. In Refs. (7, 8), a 1 Gbps FSO system was developed using a 1550 nm SFP module, tested through a 7.2 m atmospheric chamber, emphasising the power loss from coupling light into the fibre cable. Data centres using optical communication for high-speed data transmission have incorporated SFP modules into FSO systems, as seen in ref. (9, 10). These references propose a steerable system and a short-range FSO system, respectively, achieving 10 Gbps across 20m and 200 m distances.

Even if we assume that light can be collected by a multimode fiber (MMF), it is important to note that not all of the light is in the lower-order modes, which means it may not necessarily illuminate the photodiode inside an SFP, leading to potential signal-to-noise ratio issues. This project aims to address this specific challenge, presenting a novel approach. Additionally, we intend to avoid costly custom digital signal processing, modulation schemes, forward error correction, and complex high-bandwidth mechanical arrangements for auto-alignment and conventional adaptive optics. Further details on our approach are provided in the following section.

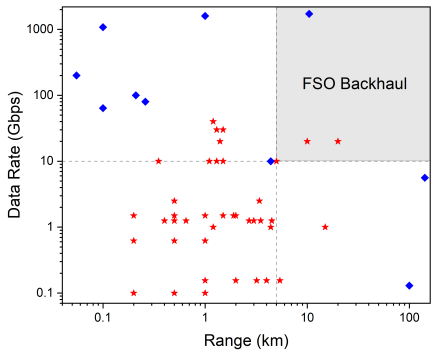

Fig. 1. Range versus data rate of commercial FSO systems (red stars) and some noteworthy experimental systems. Note that these are typically under favourable atmospheric conditions.

2. Problem Statement

A common solution to efficiently coupling incoming, turbulence abberated light into a receiver fibre is to simply use a large-core multi-mode fibre (MMF). This is generally a good solution to capture the most light in the presence of slight misalignment, tilt, and other aberrations. However, this method has limitations. Higher order modes within the fibre may still not efficiently shine on the receiver photodiode, and more importantly for high speed use, the modal dispersion in the MMF constrains the potential data rate of the system to 10 Gbps or less for a practical fibre length inside the receiver. As faster Ethernet hardware becomes increasingly available and affordable (e.g., 100 Gbps, requiring single mode fibre which is nearly impossible to couple into at range), the question arises: how can we adapt a similar low-cost methodology to these higher data rates?

Adaptive optics offer a potential solution, as exemplified in the Taraa (previously Google X) FSO system. However, the mechanical complexity and cost of high-speed tip and tilt compensation mirrors make them impractical. Deformable mirrors are even less feasible given the stringent low-cost requirement.

In this project, we propose an innovative system that retains the use of the multi-mode fibre, thus maintaining relatively efficient coupling. The novelty of our approach lies in using the MMF to "reshape" the incoming, distorted light into a Gaussian, thus increasing the amount of light impinging on the receiver photodiode and possibly even combating the modal dispersion within the fibre. Specifically, we propose placing several 3D-printed actuators along the fibre's length and connecting them to a control system. This system would bend the fibre to mix the modes propagating through the fibre in a controlled way, as well as to potentially compensate for the modal dispersion within it. In principle, these actuators could be dynamically controlled to adjust for turbulence in real time.

Essentially, this system would operate as an adaptive optic by modifying the transmission matrix of the fibre in real time to "distort" the incoming aberrated beam back into a Gaussian-like beam. As demonstrated in (11, 12), such a methodology is capable of shaping the light's amplitude at the output of a multi-mode fibre. The approach has also been used to "shape" non-linear effects in a MMF (13). Nevertheless, further research is needed to fully exploit this technique. We need to shape not only the output wavefronts amplitude, but also its phase, as well as investigate the resulting impact of dispersion within the fibre. Naturally, there is much scope to this and so we detail our specific objectives in the following section.

3. Project Objectives

The project is centred around using a mechanically actuated MMF as an optical signal processor to compensate for the effects of turbulence (i.e. as an "adaptive optic"). As such, the primary aim of the project is to design, build and characterise the capabilities of the system for complex wavefront shaping (amplitude, phase and possibly even polarisation - although this is through a different mechanism). As a secondary aim, we plan to investigate the potential for using the device to compensate for modal dispersion to allow very high data rates. Specifically, our objectives are:

1. Design and build a working device which is controllable by a computer in real-time. The device should have at least 50 actuators to extend the state of the art which is 33. This will enable greater control of the output, which is necessary for the additional degree of freedom (i.e. phase).
2. Implement a standard population-based optimisation algorithm (genetic, swarm, etc.) as used in existing literature to control the device to produce arbitrary amplitude and phase profiles at the output of the MMF.
3. Investigate the device performance as an "adaptive optic" to transform a turbulence-abberrated input beam into a Gaussian. What is the relationship between the number of actuators and the device performance?
4. Work towards a faster optimisation strategy, which will be required if the device is used as an adaptive optic in a real system.
5. Investigate the device's ability to control and affect the modal dispersion in a MMF. (This objective is expected to have large scope and is more exploratory in nature for the purposes of this project)

4. Project Activities (Plan)

The project activities below are numbered according to the objectives above. The project will run over two years, and so the expected timing is divided into four semesters. Note that the PI is an implied key person for the supervision and steering of each activity, but is explicitly specified when there is a more hands-on role for the PI in that activity.

1. **Objective: Design and build the device.**
   Description: We will design and build the electronics and 3D printed components. Firmware will need to be developed to control the many actuators (likely stepper or servo motors) required by the system.
   Time frame: Semester One
   Key people: MSc student A, PI
   Anticipated outputs: Working prototype
   Risks and contingencies: The PI is an expert in electronic engineering and his involvement in this crucial step will ensure success. This activity is actually already underway and is likely to be completed sooner, allowing for slip in other activities.
2. **Objective: Output beam shaping (amplitude and phase).**
   Description: Using modal decomposition and off-axis interferometry we will measure the output wavefront in terms of amplitude and phase (phase has not been done before in literature). We will implement a "standard" population-based optimisation algorithm to shape the output.
   Time frame: Semester Two
   Key people: MSc student A
   Anticipated outputs: 1x journal paper, conference presentation
   Risks and contingencies: It is possible that this activity will take longer than expected. As a contingency, the PI has reached out and developed a relationship with Prof Yaron Bromburg, the author of (11). There is an opportunity to share experience and even send the student to Yaron's lab for troubleshooting.
3. **Objective: The MMF "adaptive optic".**
   Description: Given that we can transform an input Gaussian into arbitrary outputs (Activities 1 and 2, as well as literature), can we transform a turbulence aberrated beam back into a Gaussian? Since the number of actuators increases cost and complexity, what is the fewest number of actuators that can do this?
   Time frame: Semester Three
   Key people: MSc/PhD student B (possibly MSc student A, upgraded to PhD)
   Anticipated outputs: 1x journal paper, conference presentation
   Risks and contingencies: We don't expect any major challenges for this activity except time, as it builds on the previous activity. Simulating turbulence and other structured light work is a day-to-day activity in our lab.

4. **Objective: Faster optimisation strategy.**
   Description: Population based optimisation algorithms are expected to work (as they have been used in literature for this purpose) but are known to be slow. If the device is to be used as a true adaptive optic, control needs to be much faster. Here we work towards a faster control and optimisation strategy and plan to investigate the use of machine learning, bayesian optimisation and other algorithms.
   Time frame: Semester Four
   Key people: MSc/PhD student B, Prof Ling Cheng and Prof Turgay Celik (optimisation expert collaborators)
   Anticipated outputs: 1x journal paper, conference presentation
   Risks and contingencies: This is perhaps the most difficult (but highest reward) activities in the project. The PI has had discussion with several experts in machine learning and optimisation and we will bring them on board as collaborators to ensure success.
5. **Objective: The effect on modal dispersion.**
   Description: In theory, if we are able to control the wavefront of the output then we are by definition affecting the propagation of modes within the MMF, changing the dispersion characteristics. We plan to insert the device into a high-speed optical communication system and measure the devices effect on inter-symbol interference (using an eye diagram for example), and attempt to control it. This objective is open ended and research is expected to continue beyond the formal end of the project.
   Time frame: Semester Three/Four
   Milestones: Working prototype with actuators controllable from MATLAB or Python.
   Key people: MSc/PhD student C, Prof Andrew Ellis (collaborator with high-speed equipment)
   Anticipated outputs: 1x journal paper, conference presentation
   Risks and contingencies: The major challenge in this activity is sending signals fast enough for modal dispersion to affect them, and measuring the effect. Andrew Ellis is a distinguished researcher and an existing collaborator (on past projects) who has an established lab equipped for high-speed optical communications. He has agreed to collaborate on this aspect of the work.

5. Project Impact

The primary driver of this project is the need to find viable, affordable technologies to help bridge the digital divide, a challenge we unfortunately experience on a daily basis in South Africa. Signal processing is required to extend the range of FSO communication systems beyond a few kilometres. However, digital signal processing can be expensive.

We believe that a dynamically actuated multimode optical fibre can achieve similar gains, without requiring advanced and costly digital processing on the received signal, and with low energy consumption (although energy conservation is not the main focus of our research). Over the course of the project, we plan to publish several journal papers and publicise our work at conferences, along with issuing some press releases towards the end. These press releases are designed to raise public awareness about our work at the university, attract talented students to our group in the future, and potentially establish new relationships with industry, funders, and fellow academics.

Additionally, we believe our work has patentable elements; we will explore this avenue, as it could facilitate access to startup funding should we decide to commercialise in the future.

Assuming our new approach to a dynamically actuated multimode optical fibre is viable, the technology could disrupt applications and communities beyond conventional long-range FSO (as described elsewhere in this proposal), which is our immediate focus. We can foresee two other significant and impactful applications:

The first is ultra-high-speed optical communications using space (or mode) division multiplexing. We have reached the so-called Shannon Limit in optical fibre, implying that we can no longer increase the data rate more than linearly (insufficient for the demands of rapid internet growth) without adding additional degrees of freedom. The spatial degree of freedom has proven to be very effective, but it is impractical in real-world systems due to the immense processing power required to untangle the signals at the receiver

in real-time (MIMO). A dynamically actuated multimode optical fibre could, in principle, perform this task to some extent and act as a so-called mode sorter or mode-conditioner.

Another exciting potential application (which we also plan to study in a separate project) of dynamically actuated multimode optical fibre technology could be in all-optical reservoir computing. Reservoir computing is a novel approach to recurrent neural network training, with the "reservoir" referring to a network of randomly connected nodes, which is capable of transforming the input into a higher dimensional space. When dynamically actuated multimode optical fibres are used in this context, light passing through these fibres can effectively act as the reservoir. The dynamic actuation of the fibre facilitates a complex transformation of the input light signals, which can then be linearly read out at the output, facilitating the implementation of machine learning algorithms directly in the optical domain. This all-optical implementation could offer massive speed and energy efficiency improvements over traditional, electronic neural networks. This is due to light's fast propagation speed and the potential for parallel processing in the spatial, wavelength, and polarization domains. Furthermore, such a system could be particularly useful in real-time data processing tasks, such as dynamic pattern recognition or time-series prediction, where the high-speed operation of all-optical networks would be most advantageous.

6. Research Outputs and Outcomes

Journal Papers (4). We plan to publish at least one paper per objective over the course of the project (subject to suitable results, of course!). Preliminary titles: "Arbitrary structured light generation using a MMF", Optics Express; "Modal dispersion compensation using a mechanically actuated MMF", Journal of Lightwave Technology; "Using a MMF as an adaptive optic for FSO turbulence compensation", Optics Letters; "Real-time control of the MMF adaptive-optic", Optics Express.

Conference Presentations (4). We will present our work at both local and international conferences. Locally, the students working on the project will present at SAIP 2024, 2025 (a local physics conference). Internationally we plan to present our published work at conferences such as Photonics West, Frontiers in Optics and OFC, but this is dependant on the timing of the publications.

Artefacts. We will deliver an open-source design on GitHub for the system hardware at the end of the project. This will include the CAD files for the 3D printable components and custom electronics, as well as firmware required for the control of the system.

Outreach Activities. We will be engaged in several educational and general-public outreach activities to benefit next-generation scientists and engineers. Jointly with the Wits Optics student chapter, we will organise demos for high-school and undergraduate students. We will also endeavour to release a series of videos to explain the basic principles behind the developed tool and its mode of operation.

A. Finances. The project finances/budget are given separately on the requested template. Dominant costs are student funding, travel (for student exchange lab visits and conferences) and supplies (optics, mounts, electronics).

References

1. MPJ Lavery, et al., Tackling Africa's digital divide. *Nat. Photonics* **12**, 249–252 (2018).
2. A Trichili, MA Cox, BS Ooi, MS Alouini, Roadmap to free space optics. *J. Opt. Soc. Am. B* **37**, A184 (2020).
3. S Dang, O Amin, B Shihada, MS Alouini, What should 6g be? *Nat. Electron.* **3**, 20–29 (2020).
4. MA Cox, et al., Structured Light in Turbulence. *IEEE J. Sel. Top. Quantum Electron.* **27**, 1–21 (2021).
5. L Mustafa, B Thomsen, Reintroducing free-space optical technology to community wireless networks in *19th Americas Conference on Information Systems, AMCIS 2013, Chicago, Illinois, USA, August 15-17, 2013*. (Association for Information Systems), (2013).
6. C Sekhar, J Agrawal, O Farook, Designing a free space optical/wireless link. pp. 1–13 (2005).
7. MM Abadi, et al., A space division multiplexed free-space-optical communication system that can auto-locate and fully self align with a remote transceiver. *Sci. Reports* **9**, 1–8 (2019).
8. MM Abadi, et al., Implementation and evaluation of a gigabit ethernet fso link for 'the last metre and last mile access network' in *2019 IEEE International Conference on Communications Workshops (ICC Workshops)*. (Institute of Electrical and Electronics Engineers, Shanghai), (2019).
9. N Hamedazimi, et al., Firefly: A reconfigurable wireless data center fabric using free-space optics in *Computer Communication Review*. (Association for Computing Machinery), Vol. 44, pp. 319–330 (2015).
10. M Curran, et al., Fsonet: A wireless backhaul for multi-gigabit picocells using steerable free space optics in *Proceedings of the Annual International Conference on Mobile Computing and Networking*. (Association for Computing Machinery), pp. 154–166 (2017).
11. S Resisi, Y Viernik, SM Popoff, Y Bromberg, Wavefront shaping in multimode fibers by transmission matrix engineering. *APL Photonics* **5**, 036103 (2020).
12. Z Finkelstein, K Sulimany, S Resisi, Y Bromberg, Spectral shaping in a multimode fiber by all-fiber modulation. *APL Photonics* **8**, 36110 (2023).
13. T Qiu, et al., Spatiotemporal control of nonlinear effects in multimode fibers for two-octave high-peak-power femtosecond tunable source. *arXiv* pp. 1–31 (2023).

Executive Summary

Proliferating Radiative Cooling: From Aesthetics to Nonreciprocal Thermal Emission

Challenge: As the global demand for cooling increases, it becomes imperative to explore sustainable alternatives to traditional compression-based cooling that represent 20% of the total electricity usage in buildings. One such alternative is radiative cooling, an energy-efficient and passive cooling process. However, challenges surrounding its efficiency, cost, aesthetic integration into architectural designs, and limited applicability under diverse environmental conditions hinder its adoption.

Proposed Project: This proposal aims to proliferate the usage of radiative cooling by focusing on enhancing its efficiency, reducing its cost, improving its aesthetics, and broadening its applicability under various environmental conditions. The primary tasks of the project include:

Enhancing Efficiency of Radiative Cooling in Humid Environments through Angular Selectivity: This task will focus on developing and testing angularly selective thermal emitters that can cool efficiently in humid conditions.

Photonic crystal-based radiative air conditioning: We will improve radiative cooling-based air conditioning by utilizing a photonic crystal to reflect the solar spectrum and capitalizing on the intrinsic thermal emissivity of water, the coolant, increasing the overall efficiency. The device design relies on scalable and inexpensive nanofabrication methods.

Structural coloring of thermal emitters using Transverse Kerker Effect: The goal is to color radiative cooling panels to blend into various architectural designs, thereby facilitating their adoption. This task will involve exploiting the transverse Kerker effect in dielectric Mie resonators to introduce a color without degrading the radiative cooling performance.

Nonreciprocal and nonlinear photonic cooling: This task will rigorously study the potential of electromagnetic non-reciprocity in overcoming the limits on passive cooling imposed by Kirchhoff law of radiation. Breaking these limits opens the door towards novel niche applications of radiative cooling. In addition, we will debunk existing claims that simple transmission asymmetry is sufficient to overcome Kirchhoff's law of radiation.

Intended Outcomes: Through these initiatives, we intend to overcome the barriers to the adoption of radiative cooling. By improving the cooling efficiency, reducing the costs, introducing aesthetically pleasing designs, and ensuring performance under diverse conditions, we expect to increase the integration of radiative cooling devices into building designs. This will mitigate the impacts of global warming by reducing reliance on energy-intensive cooling methods. We also anticipate opening novel applications such as passive cooling of high-temperature superconductors, thereby further driving the proliferation of radiative cooling technology.

Proliferating Radiative Cooling: From Aesthetics to Nonreciprocal Thermal Emission

Literature Review

Cooling consumes nearly 20% of the total electricity used in buildings globally and represents one of the fastest-growing electricity end uses. The increased demand on cooling is due to escalating global temperatures, urbanization, population growth, and economic development[1]. One often-overlooked factor contributing to the increase in building cooling demands is architectural design [2]. Modern designs tend to prioritize aesthetics over natural ventilation, given the widespread availability of artificial air conditioning[2]. The ever increasing fossil fuel consumption for cooling has rekindled research interest in sustainable cooling alternatives, such as radiative cooling[3].

Radiative cooling is a passive cooling procescs involving the emission of thermal radiation by a surface, which results in heat loss to the surrounding environment and, more significantly, the cold outer space[3]. As a sustainable and energy-efficient method of heat dissipation, radiative cooling can help mitigate global warming effects by reducing the reliance on energy-intensive compression-based air cooling. Recently, numerous nanophotonic-based approaches have been developed to enhance the performance of radiative cooling devices and extend their application beyond traditional air conditioning[3].

Daytime subambient radiative cooling was demonstrated through spectral engineering of thermal emitters[4,5]. This engineering is based on Kirchoff's law of radiation, which states that at equilibrium, the emissivity and absorptivity of a material at a given wavelength and angle are identical. Ignoring parasitic heating due to convection and conduction, an effective radiative cooling material minimizes its absorptivity/emissivity across all wavelengths, except within the atmospheric transparency window. Here, the emitter effectively 'sees' the cold space through the transparent atmosphere. Engineering the angular dependence of emissivity has been recently identified as a crucial design parameter because absorbed radiation from the atmosphere increases at larger angles, where the atmosphere is effectively much thicker[6,7].

Prototypes of air conditioning systems that leverage radiative cooling have been demonstrated, using indirect cooling of a fluid (usually water) that serves as a heat transfer medium[8]. Cooling to deep subfreezing temperatures through spectral selectivity and controlling parasitic heating (conductive and convective) was demonstrated as a potential technology for energy-efficient cooling of vaccines and medications[9]. Since the efficiency of photovoltaic cells declines with temperature, engineering the thermal emission of PV cells has been shown to enhance their efficiency. Furthermore, radiative cooling has been used as a direct source of clean energy by cooling the cold end of a thermoelectric generator[10,11].

Problem Statement/Objective

Despite numerous advances, radiative cooling is not yet a well-established technology. For these devices to gain widespread adoption, they must meet several criteria. Firstly, they should be designed to operate continuously under a wide array of environmental conditions, including cloudy and humid conditions[12] . Many studies have indicated that the remarkable results often highlighted in radiative cooling research are only valid under ideal conditions, where the sky is clear and humidity is low (precipitable water ~ 10 mm-30 mm)[12,13]. Angular selectivity has been

identified as a crucial factor in minimizing the adverse effects of humidity on radiative cooling[6,7]. Secondly, to increase the adoption of radiative cooling devices, it is crucial to optimize their cooling efficiency, while ensuring the use of affordable materials and scalable manufacturing technologies. This will help overcome cost-related barriers to adoption. Thirdly, if radiative cooling solutions can be designed to be aesthetically appealing, their integration into modern building designs could be greatly enhanced. The aesthetic factor is often a major consideration in the architectural design process. Lastly, expanding the range of applications where radiative cooling is an enabling technology can further drive the proliferation of these devices. The objective of this proposal, therefore, is to develop innovative nanophotonic approaches that will facilitate the widespread adoption of radiative cooling. Ultimately, the goal is to establish it as a reliable, sustainable alternative to traditional compression-based cooling.

Outline of tasks/Work Plan

The following research plan pursues novel nanophotonic approaches to overcome these obstacles and presents first steps towards the proliferation of sustainable and clean cooling systems.

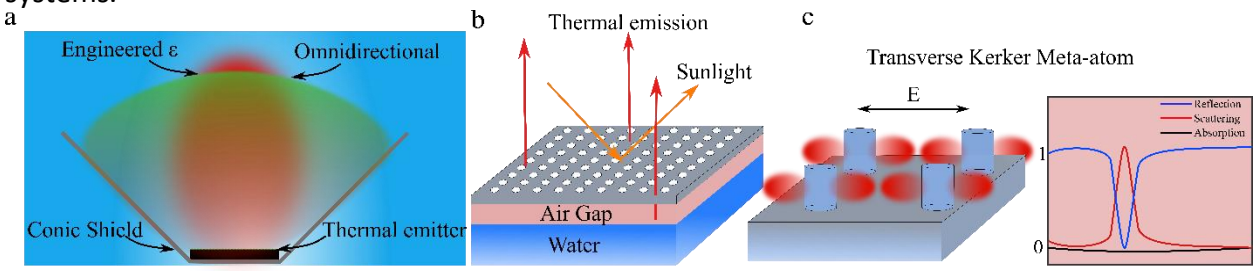

Figure 1: a, Schematics of an angularly selective thermal emitter that either has an engineered emissivity $\varepsilon\,(\lambda, \theta)$, or is omnidirectional but placed inside a conic shield. **b,** A photonic crystal imprinted on a polymer is used to reflect sunlight and transmit thermal radiation from water for air-conditioning based on radiative cooling. **c,** Transverse Kerker meta-atom scatters light in a direction transverse to the incident light to introduce a color without affecting radiative cooling performance. The expected spectrum, in the visible wavelength range, would look like the right panel in **c,** where resonant transverse scattering leads to a dip in reflection which generates a color by subtraction.

Aim 1. Enhancing Efficiency of Radiative Cooling in Humid Environments through Angular Selectivity:

We introduced and studied two approaches for angular selective thermal emission: (i) the engineering of spectral and angular emissivity using a thin-film-based iridescent thermal emitter [7], and (ii) the utilization of optimized conic shields with omnidirectional and spectrally selective thermal emitters[6]. **Figure 1a** is a schematic illustration of these angular selectivity methods. The thermal emitter, depicted in black, either exhibits an angularly dependent emissivity or operates omnidirectionally with angular emissivity achieved through a conic shield. We showed that while the former thrives under humid conditions, the latter is more efficient when parasitic heating is problematic. The objective of this aim is to experimentally investigate these proposed methods and assess their performance across a range of environmental conditions. Our first demonstration will entail the fabrication of a spectrally and angularly selective thermal emitter, followed by the measurement of its radiative cooling performance under varying ambient

conditions and levels of parasitic heating. Similar measurements will be conducted on an omnidirectional, yet spectrally selective, thermal emitter embedded within a conic shield. Our prior work has shown that the angle of the conic shield directly impacts the net radiated power[6].

Aim 2. Photonic crystal-based radiative air conditioning:

Recently, radiative cooling-based air conditioning has been proposed as an energy-efficient, green cooling alternative[8]. These methods depend on a thermal emitter that facilitates heat exchange with a fluid, typically water, which is subsequently used to cool air for air conditioning. However, some cooling power is lost during this heat exchange process. In contrast, using water as a thermal emitter can make radiative cooling air conditioning more efficient, as water itself is an excellent thermal emitter. We will first inverse designed 2D photonic crystal[14] to reflect the solar spectrum and provide spectral selectivity at IR wavelengths (see **Fig. 1b**). Then we will fabricate the photonic crystal via nano-imprint lithography on a polymer sheet, like polyethylene, that is transparent within the solar spectrum wavelength range and the atmospheric window of interest[15]. Water will flow through a serpentine channel directly exposed to the sky, while the gap between the polymer sheet and the water surface minimizes convective heating. We will also introduce angular selectivity with a conic shield to enhance cooling performance.

Aim 3. Structural coloring of thermal emitters using Transverse Kerker Effect:

Modern architecture heavily emphasizes sustainability, which includes integrating clean energy sources into their designs. Several companies have created colorful photovoltaic panels designed to blend into various environments, promoting mass adoption of solar panels in homes[16]. The structural coloring of radiative cooling panels has been a largely unexplored area, primarily because it's challenging to color a panel meant to reflect sunlight fully. A structural coloring platform compatible with radiative cooling would utilize an optical element that scatters light transverse to light propagation at a specific wavelength range, providing color without degrading cooling performance. This can be realized using the transverse Kerker effect in dielectric Mie resonators[17], which can be large-scale fabricated through nanoimprinting (see **Fig. 1c**). Scattered light in the transverse direction would lead to a dip in reflectance within a narrow wavelength range generating a color. The goal of this aim is to implement the transverse Kerker effect using materials compatible with radiative cooling and to demonstrate the color range and purity of structural coloring based on the Transverse Kerker Effect[18].

Aim 4. Nonreciprocal and nonlinear photonic cooling:

Several studies assert that utilizing an asymmetric transmission thermal emitter effectively breaks the reciprocity of thermal emission, as outlined by Kirchoff's third law of radiation, thereby improving radiative cooling efficiency[19,20]. However, these studies are scientifically flawed, as they mistakenly equate nonreciprocity with asymmetric transmission. Asymmetric transmission simply performs mode conversion and does not break time reversal symmetry, a necessary condition for non-reciprocity[21]. The **first objective** of this aim is to debunk these approaches through rigorous numerical and theoretical analysis by considering thermal radiation across all relevant modes. Notably, even if we could achieve true electromagnetic isolation, such as through the magneto-optic effect, it wouldn't result in cooling, as this would contradict the second law of thermodynamics [22]. The only radiative cooling approach that could potentially violate reciprocity requires a nonlinear interaction, such as frequency conversion[23]. Therefore, the **second objective** of this aim is to explore energy-efficient frequency conversion in the mid-infrared wavelength range with the aim of enhancing radiative cooling efficiency. Breaking

thermal emission reciprocity can open the door to novel niche applications, e.g., passive cooling of high temperature superconductors, by overcoming the bounds of deep subfreezing radiative cooling.

Outcomes:

Aim 1. The outcomes of this aim will be the successful experimental demonstration of angular selectivity for efficient radiative cooling in humid environments. By engineering the spectral and angular emissivity of thermal emitters, we expect to create devices that outperform current radiative cooling technologies under a wider range of environmental conditions.

Aim 2. The outcomes of this aim will be the development of a photonic crystal-based radiative air conditioning system. The photonic crystal will be inverse designed to reflect the entire solar spectrum. By using water as a thermal emitter and using a 2D photonic crystal to reflect sunlight and provide spectral selectivity at IR wavelengths, we expect to achieve a more efficient radiative cooling air conditioning system. Large scale nanofabrication through nanoimprint lithography along with the improved cooling efficiency will increase the commerciality of the proposed cooler.

Aim 3. The outcomes of this aim will be the creation of structurally colored radiative cooling panels using the transverse Kerker effect in dielectric Mie resonators. This could help to integrate radiative cooling technologies into modern building designs by providing an aesthetically pleasing cooling solution.

Aim 4. The outcomes of this aim will include the debunking of certain misconceptions in the field and the investigation of energy efficient frequency conversion in the mid infrared wavelength range to increase radiative cooling efficiency. This could potentially lead to overcoming the cooling limits imposed by Kirchoff's law of radiation.

Impact:

The increasing reliance on fossil fuel-powered cooling systems contributes to a vicious cycle of escalating climate temperatures and cooling demands – a cycle that urgently needs interruption. Radiative cooling represents a key technology to break this cycle, yet several challenges prevent it from becoming a household staple. The impact of this proposal lies in addressing these challenges, thus paving the way for wider adoption of radiative cooling devices.

Technological advancements from this project will enhance the efficiency of radiative cooling devices, particularly under diverse environmental conditions, thereby increasing their commercial viability and regional applicability. Further, the development of aesthetically pleasing radiative cooling panels will not only facilitate their integration into modern architecture but also foster acceptance and increased usage in residential and commercial buildings.

From a scientific perspective, our proposal aims to explore theoretical methods to break thermal emission reciprocity genuinely. Successful investigation in this area can unlock new applications for radiative cooling, stimulating its more widespread adoption and contributing to a more sustainable future.

References:

1 Laine, H. Laine, Hannu S.; Salpakari, Jyri; Looney, Erin E.; Savin, Hele; Peters, Ian Marius; Buonassisi, Tonio Meeting global cooling demand with photovoltaics during the 21st century.

2 Ford, B., Schiano-Phan, R. & Vallejo, J. A. *The architecture of natural cooling*. (Routledge, 2019).
3 Zhao, B., Hu, M., Ao, X., Chen, N. & Pei, G. Radiative cooling: A review of fundamentals, materials, applications, and prospects. *Applied energy* **236**, 489-513 (2019).
4 Raman, A. P., Anoma, M. A., Zhu, L., Rephaeli, E. & Fan, S. Passive radiative cooling below ambient air temperature under direct sunlight. *Nature* **515**, 540-544 (2014).
5 Zhai, Y. *et al.* Scalable-manufactured randomized glass-polymer hybrid metamaterial for daytime radiative cooling. *Science* **355**, 1062-1066 (2017).
6 ElKabbash, M. Radiative Cooling with Angular Shields: Mitigating Atmospheric Radiation and Parasitic Heating. *arXiv preprint arXiv:2208.03797* (2022).
7 Chamoli, S. K., Li, W., Guo, C. & ElKabbash, M. Angularly selective thermal emitters for deep subfreezing daytime radiative cooling. *Nanophotonics* **11**, 3709-3717 (2022).
8 Zhao, D. *et al.* Subambient cooling of water: toward real-world applications of daytime radiative cooling. *Joule* **3**, 111-123 (2019).
9 Chen, Z., Zhu, L., Raman, A. & Fan, S. Radiative cooling to deep sub-freezing temperatures through a 24-h day–night cycle. *Nature communications* **7**, 13729 (2016).
10 Mu, E. *et al.* A novel self-powering ultrathin TEG device based on micro/nano emitter for radiative cooling. *Nano energy* **55**, 494-500 (2019).
11 Raman, A. P., Li, W. & Fan, S. Generating light from darkness. *Joule* **3**, 2679-2686 (2019).
12 Tso, C. Y., Chan, K. C. & Chao, C. Y. A field investigation of passive radiative cooling under Hong Kong's climate. *Renewable energy* **106**, 52-61 (2017).
13 Liu, J., Zhou, Z., Zhang, J., Feng, W. & Zuo, J. Advances and challenges in commercializing radiative cooling. *Materials Today Physics* **11**, 100161 (2019).
14 Boutami, S. *et al.* Broadband and compact 2-D photonic crystal reflectors with controllable polarization dependence. *IEEE Photonics Technology Letters* **18**, 835-837 (2006).
15 Harrison, A. & Walton, M. Radiative cooling of TiO2 white paint. *Solar Energy* **20**, 185-188 (1978).
16 Li, Z. *et al.* High-Efficiency, Mass-Producible, and Colored Solar Photovoltaics Enabled by Self-Assembled Photonic Glass. *ACS nano* **16**, 11473-11482 (2022).
17 Shamkhi, H. K. *et al.* Transverse scattering and generalized kerker effects in all-dielectric mie-resonant metaoptics. *Physical review letters* **122**, 193905 (2019).
18 ElKabbash, M. *et al.* Fano resonant optical coatings platform for full gamut and high purity structural colors. *Nature Communications* **14**, 3960 (2023).
19 Wong, R. Y., Tso, C. Y., Chao, C. Y., Huang, B. & Wan, M. P. Ultra-broadband asymmetric transmission metallic gratings for subtropical passive daytime radiative cooling. *Solar Energy Materials and Solar Cells* **186**, 330-339 (2018).
20 Wei, M. *et al.* Universal strategy for all-weather and all-terrain radiative cooling with non-reciprocal mid-infrared windows. *Solar Energy* **207**, 471-478 (2020).
21 Caloz, C. *et al.* Electromagnetic nonreciprocity. *Physical Review Applied* **10**, 047001 (2018).
22 Wood, R. W. *Physical optics*. (Macmillan, 1905).
23 Hovhannisyan, A., Stepanyan, V. & Allahverdyan, A. Photon cooling: linear vs nonlinear interactions. *arXiv preprint arXiv:2203.14116* (2022).

Optica Foundation Challenge Proposal - Health category

Integration of a microcomb-based mid-infrared spectrometer with microfluidics towards biomedical applications

Nathalia Beretta Tomazio
Experimental Physics Department - Institute of Physics of University of Sao Paulo, Brazil

Microfluidics technology has become a mature and ubiquitous tool for many fields, including environmental science, analytical chemistry and biomedicine. Despite the significant progress in microfluidics, strategies for analyte detection and quantification that offer high acquisition rates, sensitivity, and selectivity are still scarse. To this end, optical spectroscopy techniques, encompassing fluorescence, Raman, and UV-visible to infrared spectroscopies, are a remarkable solution. The mid-infrared (mid-IR) spectral range, from 2 to 20 μm, is particularly important since most molecules have intense fundamental vibrational bands there, including the biochemical building blocks of life: proteins, lipids and DNA.

One of the most promising techniques for mid-IR spectroscopy is the dual-comb spectroscopy (DCS), which allows to acquire broadband absorption spectra by measuring the time-domain interference between two frequency combs of slightly different line spacings. Unlike a conventional Fourier-transform IR spectrometer, DCS requires no moving parts, which allows for fast acquisition times with high resolution and signal-to-noise ratio using a single photodetector. DCS in the mid-IR have traditionally been realized with bulky setups based on femtosecond mode-locked lasers, and more recently, it has been realized using chip-scale photonic devices. Although there have been some advances on the use of microcomb-based DCS as an analysis tool for microfluidics, their integration on the same chip has not been demonstrated.

In this project, we will design and develop a microcomb-based mid-IR (2 - 4 μm) DCS integrated with a microfluidics system on the same chip. We intend to fabricate the photonic chip, which will be based on silicon photonics materials, through a foundry run. Our major challenge would be to fabricate a microfluidic device that can be directly integrated with the photonic chip. For that, we propose to use the technique of two-photon polymerization (TPP), a laser writing fabrication technique that leverages the nonlinear nature of two-photon absorption to fabricate 3D microstructures with arbitrary geometries and sub-diffraction features. The mild processing conditions of the TPP technique, combined with its geometry flexibility, makes it suitable for this task. By using TPP, we will fabricate a simple microfluidic scheme on top of the photonic chip and characterize the sensitivity achieved in the DCS system by interfacing waveguide structures with microfluidic channels in the hybrid chip. Our proposal may unlock an *in-situ* strategy for the detection and quantification of biochemical materials with a high acquisition rate and sensitivity. Overall, this proposal takes steps towards a fully integrated optofluidic platform that is scalable and readily deployable to needed places outside a controlled laboratory environment, such as medical settings. If successful, this project will benefit various microfluidic applications, especially those in the biomedical field. Examples of applications that can potentially benefit from our proposed technology include the synthesis of nanoparticles for the treatment and diagnosis of cancer and pharmacodynamics studies.

Optica Foundation Challenge Proposal
Health category

Integration of a microcomb-based mid-infrared spectrometer with microfluidics towards biomedical applications

Candidate: Nathalia Beretta Tomazio
Experimental Physics Department - Institute of Physics of University of Sao Paulo, Brazil

Project Duration: Two years
Keywords: Integrated Photonics, Dual-comb Spectroscopy, Mid-infrared, Microfluidics

Literature review and Problem Statement

Microfluidics technology comprises miniaturized devices that can perform multiple tasks, such as detection, analysis, separation and synthesis of biochemical materials, with high efficiency, high sensitivity and low reagent consumption. [1] It has become a mature and ubiquitous tool for many fields, including environmental science, analytical chemistry and biomedicine [2,3]. For example, microfluidic devices capable of realizing high-throughput DNA sequencing have been speeding up advances in the field of DNA analysis, which plays a pivotal role in life sciences and healthcare [4]. Polymerase chain reaction (PCR), electrophoresis, and cell counting, sorting, and culture are other remarkable examples of established uses of microfluidics [5].

Despite the significant progress in microfluidics, strategies for analyte detection and quantification that offer high acquisition rates, sensitivity, and selectivity are still scarse. To this end, optical spectroscopy techniques, encompassing fluorescence [6], Raman [7], and UV-visible to infrared spectroscopies [8], are a remarkable solution. Fluorescence, although most often used, is limited to the analysis of molecules compatible with fluorescent labeling [9]. The mid-IR spectral range, from 2 to 20 μm, is of fundamental importance since most molecules have intense fundamental vibrational bands there, including the biochemical building blocks of life: proteins, lipids and DNA [8,10]. One of the most promising techniques for mid-IR spectroscopy is the dual-comb spectroscopy (DCS), which allows to acquire a broadband absorption spectra by measuring the time-domain interference between two frequency combs of slightly different line spacings [11]. Unlike a conventional Fourier-transform IR spectrometer, DCS requires no moving parts, which allows for fast acquisition times with high resolution and signal-to-noise ratio using a single photodetector [12].

DCS in the mid-IR have traditionally been realized with bulky setups based on femtosecond mode-locked lasers [13, 14]. More recently, it has been reported using chip-scale photonic devices [15–18], where the frequency comb is generated via optical parametric oscillation in a high Q-factor microresonator pumped with a continuous-wave (CW) laser [19]. In one of these works, the DCS was realized by generating mode-locked frequency combs in a silicon-on-insulator (SOI) platform, as shown in Fig. 1. With this system, a proof-of-principle experiment of DCS in the liquid phase was performed by acquiring the spectra of acetone over the range of 2.9 to 3.1 μm at 127 GHz (4.2 cm^{-1}) resolution and with 2 μs of acquisition time [16]. In a follow-up work, a SOI microcomb-based DSC in the mid-IR was used to dynamically probe the absorption of acetone in a microfluidic channel [17]. Nevertheless, the integration of microcomb-based DCS with microfluidics on the same chip has not been demonstrated. This optofluidic integration would

represent a significant step towards the scalability and applications of these systems outside a controlled laboratory environment, which have an enormous impact for microfluidic applications, especially in the biomedical field. Moreover, by interfacing waveguide structures with microfluidic channels, this strategy could yield a boost of sensitivity by significantly increasing the interaction length of light with the analyte.

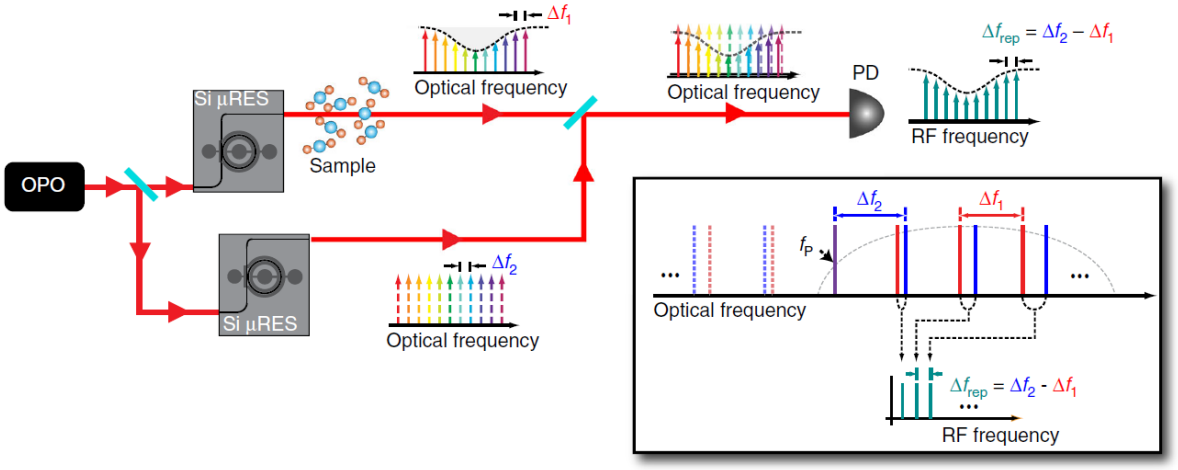

Figure 1: Schematic for microcomb-based mid-IR DCS. A CW OPO pumps two separate silicon microresonators, which generate two mode-locked frequency combs. One of them interrogate the sample and the other is directed to a reference arm. The output is combined in a beam splitter and directed to a photodiode for RF characterization. Inset: Mapping from optical to RF domain. Δf_1 and Δf_2 are the line spacings of two optical frequency combs. $\Delta f = \Delta f_2 - \Delta f_1$ is the difference in the line spacings. PD: photodiode; Si μRES: silicon microresonator; OPO: optical parametric oscillator. Image extracted from Ref. [16]

The major challenge delaying the progress in this direction is the need to match fabrication constraints of both integrated photonics and microfluidics. Although both systems are traditionally fabricated by lithographic techniques, their processing conditions are very different. This is particularly critical for microfluidics applications requiring a biocompatible and gas-permeable material, for which PDMS is the material of choice [1]. In this case, the harsh processing conditions required to etch photonic materials, such as silicon, silicon nitride and lithium niobate, are not compatible with the microfluidic material [20]. One alternative would be to assemble the separate systems together, but this comes at the expense of meeting alignment requirements, which might be equally challenging.

Research goal

The major goal of this project is to provide a proof-of-principle demonstration of the integration of a microresonator-based mid-IR DCS with microfluidics on the same chip. This optofluidic integration can potentially be used as a real-time analysis tool in microfluidic systems for biochemical syntheses and pharmacodynamics studies.

Work Plan and Outline of tasks

In this project, we will work towards a proof-of-principle demonstration of the integration of a microresonator-based mid-IR DCS with microfluidics on the same chip. To this end, we have to tackle two major challenges: (1) To enable two mutually coherent mode-locked Kerr frequency combs spanning a wide range in the mid-IR; (2) To fabricate a microfluidic device that can be directly integrated with the photonic chip.

To design the photonic chip and therefore meet the first challenge, we will build upon previous contributions. For example, Alexander Gaeta' and Michal Lipson's groups at Columbia University, USA, have successfully generated two mutually coherent mode-locked Kerr frequency combs in silicon microresonators, with a span from 2.6 to 4.1 μm. By measuring their time-domain interference, they were able to acquire the spectra of acetone over the range of 2.9 to 3.1 μm at 127 GHz (4.2 cm^{-1}) resolution and with 2 μs of acquisition time [16]. The same groups developed a strategy based on dispersion engineering to counteract the lack of broad transparency beyond the near-IR range of the typical cladding materials used in silicon photonics, making it possible to produce even wider frequency combs across the mid-IR [21]. Other photonic materials, such as lithium niobate whose transparency window extends up to 5 μm, have also been employed for the development of integrated DCS [18]. Due to time contraints and the absence of a complete nanofabrication facility in the University of Sao Paulo, the fabrication of our photonic chip will rely on a foundry multi-project wafer run (e.g., in IMEC - Belgium). We will also develop a strategy to interface waveguide structures in the photonic chip with a microfluidic channel, maximizing the interaction length between the evanescent field of the propagating modes with the analyte.

As for the second challenge, we propose to use the technique of two-photon polymerization (TPP) to fabricate the microfluidic platform directly on top of the photonic chip. TPP is a laser writing fabrication technique that leverages the nonlinear nature of two-photon absorption to fabricate 3D microstructures with arbitrary geometries and sub-diffraction features [22, 23]. A large variety of materials can be employed as photoresist, or be incorporated into it, which allows customizing the microstructures' physical, chemical or biological properties to meet specific applications [24]. For example, TPP can be performed with biocompatible photoresists, which enables its use for biomedical applications [24]. Moreover, the TPP technique uses mild processing conditions that allow its integration with the photonic chip without damaging it. At the present moment, we are about to implement a home-built TPP setup in the laboratory of my research group. We already have assigned a PhD student starting his fellowship on August-2023 to work towards this goal. This setup will comprise a high-precision 3D linear stage capable of scanning up to 170 mm in the lateral dimensions with around 1 nm of minimum step and 600 mm/s of maximum scanning speed, which will be ideal to meet the demands of this proposal. Besides, a microscope system used to monitor the fabrication process in real-time will assist in the alignment of the photonic and microfluidics pieces.

By using TPP, we will fabricate a simple microfluidic scheme on top of the photonic chip and verify the sensitivity achieved with the strategy to interface the waveguide structures with the microfluidic channel in the hybrid chip. For this task, we will use conventional solvents in organic chemistry, such as choroformium, methanol and dimethyl sulfoxide. A next step could involve designing a more sophisticated microfluidic scheme, including T-shape junctions to produce oil-in-water emulsions. The optical characterization will require a high-power laser ($\sim$ 100 mW), a fast detector (100s of MHz - 1 GHz) and fiber-based devices operating in the mid-IR (within the 2-4 μm range), which we plan to purchase within the scope of this project. To speed up the project, we intend to use part of the project‘s budget to hire a post-doctoral fellow.

The 2-year project will be developed according to the following schedule:

Action plan	1st sem.	2nd sem.	3rd sem.	4th sem.
Design and purchase of the photonic chip				
Implementation of the TPP setup				
Fabrication of the microfluidic platform				
Optical characterization of the micromb-based mid-IR DCS				

Outcomes and Impact

The outcome of our proposal is expected to be a microfluidic platform integrated with a microcomb-based mid-IR DCS to enable an *in-situ* detection and quantification strategy offering a high acquisition rate and sensitivity. Overall, this proposal takes steps towards a fully integrated optofluidic platform that is scalable and readily deployable to needed places outside a controlled laboratory environment, such as medical settings. If successful, this project will benefit various microfluidic applications, especially those in the biomedical field.

One application that can potentially benefit from our proposed technology is the synthesis of nanoparticles for the treatment and diagnosis of cancer. For example, it has been shown that an artificial nanoparticle named low density emulsion (LDE), that resembles the low-density lipoprotein (LDL) present in the bloodstream, is substantially taken up by malignant cells, thus making it possible to use it as a selective drug carrier in cancer therapy [25]. Despite the significant progress on the use of LDEs for therapeutic purposes, their production still relies on bulky methods that lack control over the particle size and composition. Microfluidics-based synthesis, which enables more efficient mixing and manipulation of fluids, may be a promising solution to produce the nanoparticles in a controllable manner [1]. In these platforms, the LDEs could be produced following a droplet-making strategy [26, 27], which can both encapsulate active materials and serve as templates on which to build new structures. In this direction, our proposed technology would be useful as an analysis tool to dynamically verify whether the synthesized nanoparticles match the expected result.

Another field where our optofluidic integration technology may have disruptive consequences is in biochemical analysis. Cardiovascular diseases (CVDs), such as hypertension, diabetes and subclinical atherosclerosis, are diseases of severe morbidity worldwide [28]. Although multiple lab-on-a-chip devices have been reported to investigate the pathogenesis, diagnosis and treatment of CVDs [28], the development of compact strategies offering high specificity and detection range to evaluate the effectiveness of certain drugs for the treatment and prevention of CVDs are still on demand. In this direction, our platform can be used to detect drugs largely prescribed to prevent hypertension (e.g., metoprolol succinate and candesartan) and subclinical atherosclerosis (e.g., rosuvastatin and ezetimibe) and track their concentration in blood samples for pharmacodynamics/pharmacokinetics studies.

References

[1] Sia, S. K. & Whitesides, G. M. Microfluidic devices fabricated in poly (dimethylsiloxane) for biological studies. *Electrophoresis* **24**, 3563–3576 (2003).

[2] Yager, P., Domingo, G. J. & Gerdes, J. Point-of-care diagnostics for global health. *Annu. Rev. Biomed. Eng.* **10**, 107–144 (2008).

[3] Agresti, J. J. *et al.* Ultrahigh-throughput screening in drop-based microfluidics for directed evolution. *Proceedings of the National Academy of Sciences* **107**, 4004–4009 (2010).

[4] Paegel, B. M., Blazej, R. G. & Mathies, R. A. Microfluidic devices for dna sequencing: sample preparation and electrophoretic analysis. *Current opinion in biotechnology* **14**, 42–50 (2003).

[5] McDonald, J. C. & Whitesides, G. M. Poly (dimethylsiloxane) as a material for fabricating microfluidic devices. *Accounts of chemical research* **35**, 491–499 (2002).

[6] Rodríguez-Ruiz, I., Ackermann, T. N., Muñoz-Berbel, X. & Llobera, A. Photonic lab-on-a-chip: Integration of optical spectroscopy in microfluidic systems (2016).

[7] White, I. M., Yazdi, S. H. & Yu, W. W. Optofluidic sers: synergizing photonics and microfluidics for chemical and biological analysis. *Microfluidics and nanofluidics* **13**, 205–216 (2012).

[8] Picqué, N. & Hänsch, T. W. Mid-ir spectroscopic sensing. *Optics and Photonics News* **30**, 26–33 (2019).

[9] Lichtman, J. W. & Conchello, J.-A. Fluorescence microscopy. *Nature methods* **2**, 910–919 (2005).

[10] Rodrigo, D. *et al.* Mid-infrared plasmonic biosensing with graphene. *Science* **349**, 165–168 (2015).

[11] Coddington, I., Newbury, N. & Swann, W. Dual-comb spectroscopy. *Optica* **3**, 414–426 (2016).

[12] Dutt, A. *et al.* On-chip dual-comb source for spectroscopy. *Science advances* **4**, e1701858 (2018).

[13] Schliesser, A., Picqué, N. & Hänsch, T. W. Mid-infrared frequency combs. *Nature photonics* **6**, 440–449 (2012).

[14] Link, S. M. *et al.* Dual-comb modelocked laser. *Optics Express* **23**, 5521–5531 (2015).

[15] Suh, M.-G., Yang, Q.-F., Yang, K. Y., Yi, X. & Vahala, K. J. Microresonator soliton dual-comb spectroscopy. *Science* **354**, 600–603 (2016).

[16] Yu, M. *et al.* Silicon-chip-based mid-infrared dual-comb spectroscopy. *Nature communications* **9**, 1869 (2018).

[17] Yu, M., Okawachi, Y., Griffith, A. G., Lipson, M. & Gaeta, A. L. Microfluidic mid-infrared spectroscopy via microresonator-based dual-comb source. *Optics Letters* **44**, 4259–4262 (2019).

[18] Bao, C. *et al.* Architecture for microcomb-based ghz-mid-infrared dual-comb spectroscopy. *Nature communications* **12**, 6573 (2021).

[19] Gaeta, A. L., Lipson, M. & Kippenberg, T. J. Photonic-chip-based frequency combs. *nature photonics* **13**, 158–169 (2019).

[20] Bogdanov, S., Shalaginov, M., Boltasseva, A. & Shalaev, V. M. Material platforms for integrated quantum photonics. *Optical Materials Express* **7**, 111–132 (2017).

[21] Miller, S. A. *et al.* Low-loss silicon platform for broadband mid-infrared photonics. *Optica* **4**, 707–712 (2017).

[22] Fatkullin, N. *et al.* Two-photon photopolymerization and 3d lithographic microfabrication. *NMR• 3D Analysis• Photopolymerization* 169–273 (2004).

[23] LaFratta, C. N., Fourkas, J. T., Baldacchini, T. & Farrer, R. A. Multiphoton fabrication. *Angewandte Chemie International Edition* **46**, 6238–6258 (2007).

[24] Carlotti, M. & Mattoli, V. Functional materials for two-photon polymerization in microfabrication. *Small* **15**, 1902687 (2019).

[25] Maranhao, R. C. *et al.* Plasma kinetics and biodistribution of a lipid emulsion resembling low-density lipoprotein in patients with acute leukemia. *Cancer Research* **54**, 4660–4666 (1994).

[26] Amstad, E. *et al.* Robust scalable high throughput production of monodisperse drops. *Lab on a Chip* **16**, 4163–4172 (2016).

[27] Abate, A. R., Hung, T., Mary, P., Agresti, J. J. & Weitz, D. A. High-throughput injection with microfluidics using picoinjectors. *Proceedings of the National Academy of Sciences* **107**, 19163–19166 (2010).

[28] Ma, Q., Ma, H., Xu, F., Wang, X. & Sun, W. Microfluidics in cardiovascular disease research: State of the art and future outlook. *Microsystems & Nanoengineering* **7**, 19 (2021).

Title: Development of a Wearable Multiwavelength NIR Spectroscopy Module for Diabetes and Cardiovascular Risk Factors Monitoring

Summary:
Diabetes and cardiovascular diseases (CVDs) are two of the most prevalent and significant health challenges facing the global population. Both conditions have reached epidemic proportions, leading to substantial economic burdens, loss of productivity, and increased mortality rates. These diseases are chronic and requires long term monitoring. The proposed project aims to develop a NIR (Near-Infrared) spectroscopy module, wearable and equipped with multiwavelength capabilities, for non-invasive detection of diabetes and cardiovascular diseases. This technology will significantly impact healthcare by enabling mass screening, timely diagnosis, and proactive management of these prevalent diseases.

Objective:
The NIR spectroscopy module will interact with the skin's surface, and underlying tissues and blood vessels. The device will be optimized to capture and analyze the specific spectral patterns indicative of glucose and cardiovascular disease biomarkers. The spectral patterns will be a combination of both chemical changes like glucose, cholesterol levels, etc., and physical changes in blood pressure and heart rate.

Intended Outcomes:

1. **Compact and Wearable Design:** The primary objective is to design a compact and user-friendly NIR spectroscopy module that can be easily worn on the skin and monitor chemical and physical parameters associated with diabetes and cardiovascular diseases. The device will be non-intrusive and comfortable, allowing for continuous monitoring and seamless integration into users' daily lives.
2. **Multiwavelength Functionality:** By integrating multiwavelength capabilities, the module will be able to interact with specific biomarkers relevant to diabetes and cardiovascular diseases. This enhanced specificity will enable accurate detection and differentiation of these conditions, leading to better management and control of the disease. It will also help with incorporating the effects of local environment and skin conditions in the analysis.
3. **Database development:** One of the major challenges with success of such non-invasive devices is unavailability of good reference data. The work will help in creating a database which will be helpful for future researchers.

Applications to Real-World Issues:

1. The device will help end-users with improved diabetes management. It will provide real-time glucose insights, helping users make informed decisions about insulin dosing, diet adjustments, and lifestyle modifications. Timely intervention based on the Cardiovascular risk factor level can prevent or delay the progression of heart-related issues.
2. Overall, the device with help user with enhanced lifestyle choices. Users will be motivated to adopt healthier lifestyle choices based on real-time health data. It also helps with mobile health screening.
3. The portable and user-friendly nature of the wearable module makes it suitable for mobile health screening initiatives. It can be deployed in community health programs to conduct screenings for diabetes and cardiovascular disease risk factors in remote or underserved areas.

Title: Development of a Wearable Multiwavelength NIR Spectroscopy Module for Diabetes and Cardiovascular Risk Factors Monitoring

Section 1: Background and Literature Review

Two of the most common chronic diseases in the world, diabetes and cardiovascular conditions, affect millions of people and present serious healthcare issues. According to International Diabetes Association, there are 537 million diabetic people worldwide and around 7 million deaths due to diabetes [1]. Among these, 75% of diabetic people are from low and medium-income countries (LMIC). In the current setup, one in two diabetic people goes undiagnosed. It is estimated that countries like India will have up to 30% of their population suffering from diabetes in less than 20 years. [2]. Diabetes is a chronic disease that requires management throughout the duration of life and can affect various organs in due course if not adequately controlled. For proper management, regular monitoring is needed. Regular monitoring helps understand the effect of diet, lifestyle, and medication on glucose levels, thereby helping users take appropriate care to keep their glucose levels under control.

Like diabetes, cardiovascular diseases are the leading cause of increased medical costs and death worldwide. Cardiovascular diseases encompass a range of conditions affecting the heart and blood vessels, including coronary artery disease, heart failure, and stroke. A majority of cardiovascular diseases are associated with lifestyle. There are various chemical and physical indicators for monitoring cardiovascular risk. Cholesterol and triglycerides are some of the chemical indicators, and blood pressure and heart rate variability are the physical indicators of cardiovascular diseases. Both diabetes and CVD share several risk factors, including unhealthy diets, physical inactivity, tobacco use, and excessive alcohol consumption. Early detection and management of these diseases are crucial to reducing the associated healthcare costs, improving patients' quality of life, and ultimately decreasing the mortality rates related to these conditions.

The conventional gold standard monitoring method is primarily invasive and requires trained personnel in a laboratory to test the blood. There are point-of-care kits like glucometer, which can be self-administered by the end-user. They are invasive and can have high variability due to storage and temperature affecting the enzymes in the cartridge [3]. The current trend is continuous glucose monitoring devices like Abbott Freestyle Libre, which can be attached to the body and sample interstitial fluids using a micro-needle for monitoring the glucose concentration continuously. But, they are expensive and requires care to keep the needle and the device intact while doing daily activity. There is no continuous monitoring device for chemical biomarkers for CVD. There are many fitness bands and smartwatches that help with continuously monitoring physical parameters like Heart rate variability.

To make chemical biomarker monitoring non-invasive, various researchers have explored monitoring fluids like sweat [4], breath [5], and tears [6] for the detection of various chemical biomarkers. A promising method for non-invasive, continuous monitoring of blood glucose levels and cardiovascular markers is NIR spectroscopy. Some researchers have explored NIR spectroscopy for monitoring chemical biomarkers from the surface of the skin and have got decent accuracy for glucose and cholesterol detection [7-9]. One of the limitations of such a method is it either focuses on only glucose or only cholesterol due to overlap in spectra and completely ignores physical parameters for tracking. For physical parameters monitoring, IR wavelengths can help understand the blood pressure from the PPG signals and the heart rate variability. But care has to be taken that one measurement is not affecting the reading of the

other parameter. For this, the selection of appropriate wavelengths and tuned algorithms or models are needed for calibration.

This project aims to combine multi-wavelength to make multiplexing of both chemical and physical biomarkers feasible, as well as compensate for variations due to sweat, skin type, and local environment. A reliable reference database and real-time algorithms are needed to achieve the required specificity.

References:

1. https://idf.org/about-diabetes/facts-figures/ (Accessed on 2nd July 2023)
2. https://diabetesatlas.org/data/en/country/93/in.html (Accessed on 2nd July 2023)
3. D. Klonoff, *"Point-of-Care Blood Glucose Meter Accuracy in the Hospital Setting",* Diabetes Spectrum, 27 (3): 174, 2014. https://doi.org/10.2337%2Fdiaspect.27.3.174.
4. H. Zafar *et al, "Comprehensive Review on Wearable Sweat-Glucose Sensors for Continuous Glucose Monitoring",* Sensors, 22(20:638, 2022. https://doi.org/10.3390/s22020638.
5. S. Mansouri *et al, "Non-invasive Measurement of Blood Glucose by Breath Analysis",* IEEJ Transaction on Electrical and Electronic Engineering, 15(10):1457, 2020. https://doi.org/10.1002/tee.23216.
6. S. Kim *et al, "Tear Glucose Measurement by Reflectance Spectrum of a Nanoparticle Embedded Contact Lens",* Scientific Reports, 10:8254, 2020. https://doi.org/10.1038/s41598-020-65103-z.
7. H. Cano-Garcia *et al, "Enhancing the Accuracy of Non-Invasive Glucose Sensing in Aqueous Solutions Using Combined Millimeter Wave and Near Infrared Transmission",* Sensors, 21:3275, 2021. https://doi.org/10.3390/s21093275.
8. Srichan *et al, "Non-invasively accuracy enhanced blood glucose sensor using shallow dense neural networks with NIR monitoring and medical features",* Scientific Reports, 12:1769, 2022. https://doi.org/10.1038/s41598-022-05570-8.
9. I. Yusoff *et al, "Non invasive cholesterol meter using Near Infrared sensor",* 2015 Innovation & Commercialization of Medical Electronic Technology Conference (ICMET), https://doi.org/10.1109/ICMETC.2015.7449581.

Section 2: Problem Statement/Objective

The prevalence of diabetes and cardiovascular diseases has reached alarming levels worldwide, leading to significant economic burdens and increased mortality rates. Despite advances in medical technology, early and non-invasive detection methods remain limited.

- The primary objective of our project is to design and create a compact, wearable NIR spectroscopy module with multiwavelength capabilities. This module will continuously monitor diabetes-related biomarkers, such as glucose levels and cardiovascular risk factors, including cholesterol and triglycerides, and the measurement of physical parameters like HR variability and blood pressure. The device aims to improve disease management, reduce healthcare costs, and enhance overall patient outcomes by providing real-time health insights.
- The secondary objective is to create a database of signals from the skin at various NIR wavelengths and standard values to help the global research community use it to build new algorithms with better accuracy.

Section 3: Outline of Tasks/Work Plan for 18 Months

The proposed work plan is divided into distinct stages, each with specific tasks and milestones:

1) **Research and Development Phase (I):** This phase would involve understanding the interaction throughout the NIR range from different skin types, environmental conditions, etc.
    a) Conduct an in-depth study of the interaction of NIR light with skin and blood vessels to identify suitable wavelengths for glucose, cholesterol, and triglycerides detection.
    b) Checking for the selection of wavelengths for physical parameters like HR and blood pressure. In the initial stages, standard HR measurement chest traps, cuff-based blood pressure monitors, and PPG modules will be used for collecting reference data.
    c) The blood glucose levels will be co-related with continuous data available from CGM and point data from blood tests.
    d) Identify the best position to take measurements.
    e) Develop the hardware and software architecture to achieve the requirement. At this phase, the device may not be in a wearable and wireless form factor.
2) **Prototype Development (II):** Design and fabricate a wearable NIR spectroscopy module prototype with multiwavelength capabilities. Conduct initial testing to ensure accurate spectral data acquisition.
    a) Once the acceptable range of wavelength, position, and power is known, an appropriate prototype will be developed to suit the form factor of the wearable device.
    b) Acquisition of data with the developed prototype.
3) **Calibration and Validation (III):** In this phase, calibration models will be defined and validated.
    a) Establish calibration models based on a diverse dataset of known glucose, cholesterol, and triglyceride levels.
    b) Validate the accuracy and reliability of the module's measurements against traditional laboratory methods.
4) **Machine Learning Integration (IV):** In this phase, machine learning models will try to incorporate data from chemical and physical biomarkers and other information to provide better insight. This phase may go in parallel to the calibration and validation phase.
    a) Implement machine learning algorithms to analyze real-time spectral data and provide instant health insights to users.
    b) Merge acquired data from the device to the patient-entered information to check for improvement in prediction and feedback.
5) **User Interface and Optimization (V):** In this phase, the app's user interface and design must be fine-tuned.
    a) Develop a user-friendly interface to display health information and recommendations to individuals.
    b) Optimize the module's design for comfortable and continuous wear.

6) **Clinical Validation (VI):** This phase will involve giving devices to collaborating doctors at healthcare institutions to conduct clinical validation to further validate the module's performance in real-world settings.
   a) Provide training and five pilot devices to doctors for their evaluation.
   b) Getting feedback from volunteers/doctors regarding the results and the sources of error or inconvenience to the end-user to further develop it.
   c) Analysis to verify the accuracy based on Clark Error Grid Analysis or Parkes Error Grid.

At the end of all phases, we will make the design open-source for the benefit of the research community. Being a not-for-profit/non-profit organization, we will share the data with the research community.

The tentative timelines of the different phases can be seen in the chart below:

Phases\Time	Start - 3rd month	4th – 6th month	7th – 9th month	10th - 12th month	13th - 15th month	16th – 18th month
I						
II						
III						
IV						
V						
VI						
Making data/ design open-source						

Section 4: Outcomes

The expected outcomes of the project include:

1. **Compact and Wearable NIR Spectroscopy Module:** The primary objective is to design a compact and user-friendly NIR spectroscopy module that can be easily worn on the skin and monitor chemical and physical parameters associated with diabetes and cardiovascular diseases. The device will be non-intrusive and comfortable, allowing for continuous monitoring and seamless integration into users' daily lives.
2. **Multiwavelength Functionality:** By integrating multiwavelength capabilities, the module will be able to interact with specific biomarkers relevant to diabetes and cardiovascular diseases. This enhanced specificity will enable accurate detection and differentiation of these conditions, leading to better management and control of the disease. It will also help incorporate the effects of the local environment and skin conditions in the analysis.
3. **Database development:** One of the significant challenges with the success of such non-invasive devices is good algorithms. But, that is dependent on the unavailability

of good reference data. The work will help create a database that will be helpful for future researchers in further developing such NIR-based non-invasive devices.

4. **Real-Time Health Monitoring:** Integration of machine learning algorithms to provide real-time health insights, empowering users to manage their conditions proactively.
5. **Validated Calibration Models:** Calibration models are based on extensive datasets validated against traditional laboratory measurements for robust and accurate results.

Section 5: Impact

The proposed technology has the potential to make a significant impact:

1. **Improved Disease Management:** Early and non-invasive detection will allow for timely intervention and personalized treatment plans, leading to better management of diabetes and cardiovascular diseases.
2. **Economic Benefits:** The wearable module can reduce healthcare costs by minimizing complications, hospitalizations, and the need for frequent clinic visits.
3. **Enhanced Quality of Life:** Continuous health monitoring will enable users to make informed lifestyle choices, improving overall well-being.
4. **Accessible Healthcare:** In many parts of the world, healthcare is not easily accessible due to a limited number of doctors in the population or the far-off or few healthcare centers from the villages or countryside. The proposed continuous wearable device can help track chronic diseases which require care and monitoring. The data can be shared with the doctor to decide about the further course of treatment.
5. **Screening Device:** The device can also be used for screening purposes for public health monitoring purposes.
6. **Helps in further research:** The database and open-source design will help enhance the accessibility and accuracy of such devices and support a global support environment.

Section 6: Conclusion

The development of a wearable multiwavelength NIR spectroscopy module for diabetes and cardiovascular disease monitoring can revolutionize healthcare by providing a cost-effective, non-invasive, and real-time monitoring solution. The proposed project aims to build upon the existing literature and address the limitations of previous research, ultimately leading to better disease management and improved health outcomes for individuals worldwide. Also, the database of responses of different NIR wavelengths generated would be a valuable resource for the global research community.

Capturing Cancer's in It's Early Glow: Pioneering Early Detection Strategies using Light Based Biomarkers (Health Challenge) – *Executive Summary*

The Challenge – Cancer is unique among all global health challenges as it is one of the only diseases that will become *more common* as biomedical innovations eradicate other diseases and extend lifespan. As a leading cause of death worldwide, 2 in 5 people will develop cancer in their lifetime and most surviving patients will experience life altering, negative side effects from current anti-cancer treatments. One unfortunate consequence of such anti-cancer treatment, like chemotherapy, is a syndrome of cognitive impairment that has been colloquially termed "Chemo-Brain" (CB), which remains as the leading source of decreased quality of life amongst the increasing number of cancer survivors. Without predictive and early-detection diagnostic tools, clinicians cannot anticipate which patients are most at-risk of developing CB, thus delaying mitigating interventions. Like the early detection of cancer, without an early diagnosis of CB, the mental health and quality of life of cancer patients declines insidiously, leaving both patients and clinicians with diminishing options. Unfortunately, current cancer diagnostics rely on costly and invasive assays of molecular biomarkers that are highly variable across individuals and must be sufficiently concentrated to achieve detection thresholds, leading to diagnoses at later stages and increased patient mortality. **Thus, there are two challenges that require immediate attention: *ultra early detection of cancer and the early detection cancer-related cognitive impairments like CB*.** Earlier, non-invasive detection is crucial for improved patient survival as current treatments are proving to be much less effective at later stages with known racial disparities of outcomes. Again, what is urgently needed are safe, affordable, and scalable diagnostic tools to detect cancers at earlier stages and monitor side effects of therapies to enhance patient outcomes and quality of life for survivors.

Proposed Project – The main objective of the project is to develop a novel diagnostic imaging platform and signal classification algorithm to non-invasively detect early-stage cancer and chemotherapy-related cognitive impairments, with the ***ultimate goal of reducing mortality rates and enhancing the quality of life for cancer survivors***. We will realize this vision by isolating and characterizing light-based biomarkers of cancer that are naturally emitted from cancerous tissues. While it is well established that all cells continuously emit low-intensity light (10^{-15} W/cm^2), termed ultraweak photon emissions (UPE), their use in biomedicine and early detection technologies is only now being realized. UPEs are a consequence of cellular metabolism, resulting from the oxidation of biomolecules such as lipids, nucleic acids, and proteins. Our group demonstrated that UPE signatures, which span the visible and near-visible electromagnetic spectrum are linked to molecular activity within the cell and can be used as readouts of cell state and behaviour, especially in dysfunctional states like cancer. Advances in single-photon detectors (SPDs) have enabled the unprecedented measurement UPEs from cancer cells at high spatiotemporal resolutions. Our published research indicates that cancer cells express fingerprint-like UPE patterns, and our preliminary data indicate functional brain states correlate with UPE fluctuations. Therefore, ***light-based biomarkers of cancer and CB could represent major breakthroughs toward ultra-early detection***. In Aim 1, we will use in vitro methods to identify light-based biomarkers of proliferation and migration of brain and breast cancer cells. In Aim 2, we will use an array of head- mounted UPE detectors to establish a novel method ("photoencephalography") of predicting cognitive symptoms associated with CB.

Intended Outcomes – The project will deliver a fully non-invasive and affordable biomedical imaging platform and classification algorithm that passively senses naturally emitted light patterns to detect cancer earlier than molecular tests and predict chemobrain before the onset of cognitive symptoms. Unlike current imaging tools (MRI, PET, CT), UPE-based diagnostics use inexpensive and portable optical sensors to capture light-based biomarkers of cell state and fate without the use of external magnetic fields or ionizing radiation. Light-based biomarkers of breast and brain cancer-related proliferation and migration as well as chemotherapy-related cognitive impairment will be characterized. The techniques that we will develop can be applied to detect stroke, metabolic disorders, and many other medical conditions at earlier stages of disease progression. The novelty of the research and its appeal as a biomedical advance will be an important factor in recruiting highly qualified trainees and driving accessible and inclusive scientific innovation. Our team of world-renowned experts will use this opportunity to train the next generation of frontier-pushing scientists to explore equally exciting questions and innovate toward a better world.

Capturing Cancer's in It's Early Glow: Pioneering Early Detection Strategies using Light Based Biomarkers - *Proposal*

Literature Review – Cancer is a leading cause of death worldwide, accounting for approximately 10 million deaths per year and nearly twice as many new cases annually[1]. As biomedical research continues to innovate toward the eradication of disease and the extension of lifespan, cancers will become *more common* as they are the inevitable consequence of an accumulation of cellular dysfunction over time[2]. One of the hallmark dysfunctions of cancer is the gradual breakdown of cellular communication underlying essential processes such as proliferation, migration, differentiation, and programmed cell death[3]. Without the ability to tightly regulate signaling thereof, tissue plasticity becomes unrestrained[4], leading to the formation of tumors that can only be treated or surgically removed if they are detected sufficiently early[5]. In search of early-stage biomarkers for cancer diagnostics, researchers have identified many key molecular pathways that indicate tumor growth[6]. However, in recent years, an emerging field of biophysical signaling in cancer[7,8] has inspired new directions for diagnostics that overcome limitations of existing detection technologies such as the variable involvement of specific genes and proteins in diverse cancer subtypes. Several authors have pointed to endogenous optical signaling as a novel source of disease-specific biomarkers[9-11]. Indeed, ***light-based biomarkers may represent the next major advance in biomedical imaging for precision oncology***.

Until recently, cellular communication was thought to emerge from the actions and kinetics of biomolecules; however, emerging discoveries in biophysics have pointed to the role of light as an important non-chemical mediator of information transfer across cells and tissues[9,10]. All cells continuously generate low-intensity (10^{-15} W/cm^2) ultraweak photon emissions (UPEs) which arise from oxidation reactions of lipids, nucleic acids, and proteins, mediated by reactive oxygen and nitrogen species (ROS/RNS)[12,13]. As electrons from proteins and lipids return to the ground state following biochemical reactions, photons are released with emission frequencies and patterns reflective of molecular events within the cell[14]. These reactions and their paired light emissions are intimately associated with metabolism, microtubule function[10], and mitochondrial states[15,16], which have been established as one of the major initiators of carcinogenesis[17,18] . It is noteworthy that UPEs are not mere byproducts of cell physiology; but are involved in signaling pathways, in that biologically generated light emissions can induce tumor-promoting cell functions including rapid mitosis[12]. Several types of human cells express non-visual opsins (e.g., OPN3, OPN5) or other light-sensitive molecules such as cryptochromes, porphyrins, and tryptophan-derivatives such as the neurotransmitter serotonin. This equips the cells to detect a subset of the electromagnetic (EM) spectrum which several studies validated and have demonstrated that UPEs play a role in cellular communication[19,20]. Because UPE profiles reflect a cell's physiological state, and not just a single molecule readout, ***we can now overcome the current diagnostic limitation of inconsistent molecular biomarker expression, toward early-stage cancer diagnoses with light-based biomarkers of disease***.

Current cancer diagnostics that assay molecular biomarkers require the collection of solid or liquid biopsies including cells, blood, saliva, urine, or cerebrospinal fluid, which often cause tissue damage and carry a risk of infection[21,22]. While they do provide diagnostic information, molecular biomarkers must overcome active metabolization and become sufficiently saturated within the sample to achieve detection thresholds, delaying time-to-diagnosis. Unfortunately, imaging-based alternatives carry their own risks[23,24]. However, unlike existing imaging technologies, which require the use of DNA-damaging radiation (PET, SPECT, CT) or prohibitively intense magnetic fields (MRI), light-based biomarkers such as UPEs can be non-invasively sensed as naturally occurring optical emissions from tumors using inexpensive, commercially available optical detectors and wavelength filters. UPEs pass through biological tissues, overcoming metabolic bottlenecks associated with molecular diagnostics. Because abnormal light emissions from biological tissues predict cell cycle progression, stress, senescence, and increased metabolic activity[25-27] there is evidence that UPEs can be used to predict tumor growth before the amplification of cancer-linked molecular pathways.

<u>Preliminary Findings:</u> We have built a UPE-based imaging system for both in vitro and in vivo (animal, human) studies. Our devices leverage optical technologies such as photomultiplier tubes and superconducting nanowire single-photon detectors (SNSPD) to build on existing scientific findings that UPEs can be used as light-based biomarkers for cellular readouts. Our own research suggests that cancer cells emit fingerprint-like UPEs within the ultraviolet (UV), visible, and infrared (IR) ranges of the EM spectrum (i.e., 200 – 1300 nm) that can be detected by non-invasive imaging techniques using commercially available photon detectors[28] (**Figure 1**). Notably, due to the low noise floor/high quantum efficiencies of these detectors, we have been able to use wavelength-dependent UPEs isolated with narrow-band optical filters, including the ratio of infrared-to-ultraviolet emission counts, to discriminate and classify malignant and non-malignant cancer cells[29]. For example, we can discriminate cancerous and non-cancerous cells by filtering UPEs within a narrow band of wavelengths approximating 500 nm [30]. Further, when melanoma cells initiate apoptotic pathways, the spectral characteristics of their UPEs shift markedly and track the expression of specific molecular profiles, coupling cell biology and optical physics[30]. As UPEs are coupled to oxidative stress, rapid cell division, cytoskeletal polymerization, and tissue damage, chemotherapy-induced neurotoxicity among cancer patients and related cognitive impairments associated with the "chemobrain" syndrome (i.e., impaired executive function, memory, and attention)[15,31] may also be non-invasively detected for mitigation of symptoms. Indeed, our preliminary data suggests that brain function is systematically related to UPEs from the head with region-specific activation profiles that correlate with electroencephalographic (EEG) data (**Figure 2**). Together, these findings suggest UPE patterns represent strong candidates as light-based biomarkers for cancer diagnostics and for monitoring treatment-induced neurotoxic and cognitive side effects. Combined with the latest machine learning tools, classification of cancer with UPE data promises to greatly improve cancer diagnostics. Thus, <u>improved UPE detection methods and light-based biomarker classification algorithms will address the related challenges of providing earlier cancer diagnoses and improving quality of life among survivors</u>.

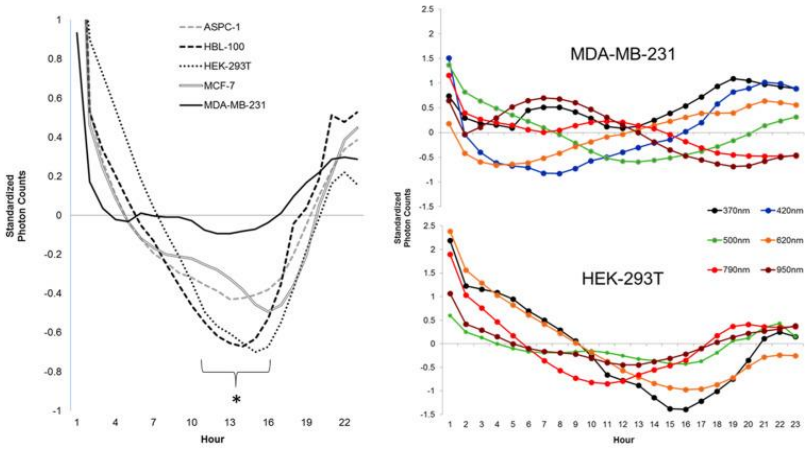

Figure 1: Cancer and non-cancer cells display fingerprint-like UPE signatures that are wavelength- and time-dependent. Adapted from our previously published work[28].

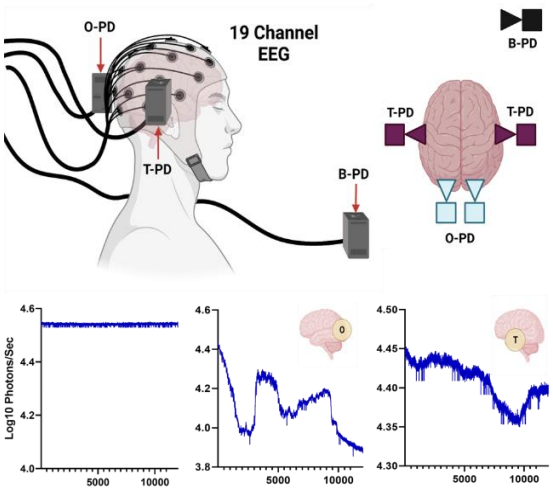

Figure 2: Unpublished preliminary data suggest background photons (bottom left) differ greatly from UPEs obtained over different brain regions including occipital (bottom center) and temporal (bottom right) lobes, which correlate with change sin neural oscillations (via electroencephalography).

Problem Statement and Objective – The evidence is clear that earlier detection of cancer significantly improves patient survival[32]; however, molecular tests are unresponsive to the earliest physiological changes associated with tumorigenesis and current screening strategies have contributed to racial disparities in cancer outcomes. Compounding this problem, existing diagnostics are too invasive and expensive to justify routine screening for otherwise healthy individuals who have not already been identified as uniquely high-risk. Because 2 in 5 people will be affected by cancer in their lifetime[33], there is a timely need to develop highly sensitive, non-invasive, and inexpensive diagnostic techniques to detect ultra-early biomarkers of cancer cell proliferation, tissue invasion, and metastasis. Similarly, there is a timely need to develop optical methods of assessing cancer treatment (chemotherapy) responsiveness to mitigate side effects including chemobrain. To extend life and greatly improve its quality among cancer patients, we will develop our existing technology and methods to engineer an advanced biomedical imaging technique that will detect and classify cancer and related sequelae at earlier stages, enabling precision medicine to save lives and reduce suffering through diagnostics. **The proposed project will address two global health challenges: (1)** Detecting malignancies before the growth of palpable tumours to reduce the likelihood of late-stage cancer diagnoses and mobilize early treatment to maximize survival. (**2)** Detecting early signs of chemotherapy-induced cognitive impairments before the onset of cognitive symptoms to enable early interventions to improve mental health for cancer survivors. The **main objective** of the project is to develop a diagnostic imaging technique and signal classification algorithm to non-invasively detect early-stage cancer and chemotherapy-related cognitive impairment. The proposed research realizes this vision by isolating and characterising light-based markers of cancerous cell states that precede pro-tumorigenic molecular pathways (Aim 1, see Workplan). Because the same technique can be used to measure neurotoxic injuries caused by anti-cancer treatments like, we will also develop methods to predict "chemobrain" among cancer patients before the onset of cognitive impairment (Aim 2, see Workplan).

Workplan

Aim 1: Identifying light-based biomarkers of cancer proliferation and migration

The Goal of Aim 1 is to isolate and characterize UPE patterns associated with cancer cell division and migration as light-based biomarkers that can discriminate and classify cancer cell lines and healthy controls. **Rationale:** Diagnosing cancer at earlier stages than is currently possible will require the identification of novel biomarkers that are detectable before significant volume of tumor growth or metastasis. Ideally, novel biomarkers should also be resistant to metabolic degradation, thus significantly reducing detection thresholds and time-to-diagnosis. In this regard, UPEs represent promising candidates as light-based biomarkers of cancer because their wavelengths and emission intensities vary as a function of DNA damage, mitochondrial respiration, and microtubule polymerization[13-34] but are not subject to metabolic clearance. We hypothesize that that cancer cell lines will display UPE patterns that correlate with molecular markers of cancer and differ significantly from those of healthy cells, thus representing putative light-based biomarkers of cancer for diagnostic applications. **Methods and techniques:** In Aim 1, we will measure UPE markers of cancer with brain and breast cancer cell lines (with tissue-matched healthy controls) using *in vitro* cultures. Using photon detectors positioned over cell cultures in light-shielded incubators, optical filters between 200 nm and 900 nm with narrow-band wavelength transmission (+/- 10 nm) will enable the identification and characterization of light emissions within subsets of the EM spectrum. Building on our seminal results[28-30], we will extend the characterization of cancer-related UPE biomarkers with measures of cell behaviour and molecular profiles. To isolate light-based markers of rapid cell division, we will conduct timed proliferation assays while measuring filtered UPEs from cells at baseline and when exposed to drugs that promote or inhibit mitosis. To isolate light-based markers of cell migration, transwell migration and invasion assays[35] will be performed with or without the presence of microtubule-stabilizing taxanes that are common chemotherapy drugs and known to inhibit migration. We will also use mitochondrial inhibitors to modulate UPE intensity and pattern by suppressing metabolic activity and the production of UPE-linked biomarkers such as ROS/RNS and superoxide[13,34] during the assays. Molecular correlates of UPE patterns,

including malondialdehyde (MDA), which is a product of fatty acid peroxidation and common marker of oxidative stress in cancer patients[36], will be measured by collecting media and lysates from cultures to perform quantitative colorimetric assays and enzyme-linked immunosorbent assays (ELISAs). **Data analysis:** Analyses will be performed on UPE data to discriminate and classify cells by cancer status (i.e., cancer or non-cancer) and tissue origin (e.g., breast or brain). Time-series data collected from photon detectors will be processed using our existing pipelines (e.g. deep learning classification) to remove background variation (noise subtraction), normalize the data, and bin values for analysis. We will use Fourier transformations to derive spectral density values indicative of frequency-specific UPE count peaks that can then be linked to cell behaviour as a function of experimental manipulations. Regression models will be generated to predict specific molecular correlates of cancer as a function of photon emission frequency peaks. Using UPE datasets, we will train machine learning algorithms to classify cancer status and tissue origin and test their sensitivity and specificity on novel UPE datasets (blind validation of training). **Pitfalls and alternative solutions:** Because monolayer *in vitro* cell cultures do not fully recapitulate the three-dimensional (3D) nature of *in vivo* tumor formation and growth, we will further validate the proposed work with experiments involving 3D bioengineered tumor microenvironment models. The 3D tissue models will be adapted from existing protocols[37-39]; however, briefly, we will leverage the expertise of our longstanding collaborator (Dr. Nicolas Rouleau, Assistant Professor of Health Sciences at Wilfrid Laurier University, expert in bioengineered tissue models of disease and biomaterials) to seed cell lines in Matrigel-collagen hydrogels to simulate the extracellular matrix (ECM) of the tumor microenvironment. The models will provide additional tissue depth and heterogeneity to assess optical transmission efficiency and filtration. In addition, we will validate cancer classification algorithms by measuring UPEs from primary brain and breast cancer tissues supplied by our collaborator (Dr. Ioannis Voutsadakis, Oncologist with the Algoma District Cancer Program and Assistant Professor of Internal Medicine at the Northern Ontario School of Medicine University).

Aim 2: Identifying light-based biomarkers of "chemobrain" before cognitive impairment

The Goal of Aim 2 is to isolate and characterize UPE patterns that predict cognitive impairments in cancer patients and survivors with a history of exposure to chemotherapy treatments (i.e., "chemobrain" syndrome). **Rationale:** Despite their effectiveness as anti-cancer treatments, chemotherapies are highly cytotoxic with well-documented side effects that include pain, hair loss, infections, fatigue, anemia, nausea, constipation, and loss of appetite[40,41]. Though often overlooked, significant side effects of chemotherapy exposure also include chronic impairments of cognitive function. Patients that suffer from the "chemobrain" syndrome experience lapses of concentration, impaired memory, mental fog, and confusion[42]. While neuropsychological tests are performed to diagnose chemotherapy-related cognitive impairments, symptoms only emerge after considerable disruptions to neural physiology and, consequently, treatment effectiveness is typically poor. While strategies to predict chemobrain using EEG and fMRI are being investigated, we hypothesize that light-based biomarkers, which are intrinsically linked to chemotherapeutic mechanisms of action (e.g., UPE emission profiles from ROS/RNS production, cell injury/death, microtubule dynamics, etc.), are more likely to provide a robust indication of neurotoxicity and enable the earliest possible intervention. **Methods and techniques:** In Aim 2, based upon the technology developed within our preliminary study of brain UPEs, we will assemble a multi-sensor photon detector array that will be positioned over the heads of human participants undergoing chemotherapy treatment for cancer to non-invasively detect UPE signatures of chemobrain during the premorbid phase. UPE data obtained over the left and right occipital, parietal, temporal, and frontal regions, which we have termed "photoencephalography", will be passively recorded in a dark room with different wavelength filters placed between the photon detector apertures and participant's head. Neuropsychological assessments of cognitive function and impairment will be performed at fixed times following the initiation of chemotherapy (pre-chemotherapy baseline, 1-week post-chemotherapy, 3-weeks post-chemotherapy, and 3-months post-chemotherapy). Importantly, brain tumors will be a major exclusion criterion to eliminate confounding effects of space-occupying brain lesions on cognitive function. Memory and attention subtest

scores will be correlated with UPE measures obtained before, during, and after the onset of symptoms. Patients will also complete standardized, self-report questionnaires to report "chemobrain" symptoms and subjective experiences of severity (with visual analogue scales). MDA levels will be measured from blood samples of patients and correlated with UPE measurements and cognitive scores over time. **Data analysis:** Similar to the approach described in Aim 1, UPE data will be used to discriminate and classify chemobrain status (positive or negative) as a function of self-reported symptom severity, cognitive impairment indices, and oxidative stress markers. As described previously, time-series data will be processed and segmented using our existing deep learning classification pipelines. Spectral analyses (Fourier transformation) will be performed to characterize photon emission frequency profiles across several bands from 200 nm to 900 nm (+/- 10 nm). Multiple regression analyses and machine learning procedures described previously will be used to generate predictive models of UPE generation associated with the course of "chemobrain". **Pitfalls and alternative solutions:** While up to 75% of patients receiving chemotherapy will experience and report "chemobrain" symptoms during treatment, 35% will experience symptoms post-treatment[43]. To account for the expected prevalence and avoid the possibility of limited cases, we will recruit a minimum of n=60 patients and target of n=100 to ensure a sufficient sample size to perform planned analyses. Our collaborator (Dr. Ioannis Voutsadakis, oncologist) will ensure steady recruitment of patients for the purposes of our study.

Expected Outcomes – The main outcome of the proposed work will be the development of a fully non-invasive diagnostic imaging technique and signal classification algorithm to non-invasively detect early-stage cancer and chemotherapy-related cognitive impairment. We anticipate identifying pathognomonic optical biomarkers of specific cancer types that can be discriminated from each other at very low densities and obtain optical signatures of dimensions of proliferation and migration. We will also identify signals that are unique to neurotoxic insults associated with chemotherapy treatment exposures, coupled to elevated oxidative stress, dysfunctional microtubules, and cell cycle disruptions. We will generate powerful classification algorithms using machine learning that will combine many signal parameters (e.g., frequency of photon emissions, wavelength of photons, regularity of UPE signal, entropy, etc.) to automatically detect early-stage cancer cell populations or brain dysfunctions predictive of cognitive impairment following chemotherapy treatment. ***Solving these challenges will****, in turn, result in 1) less advanced stage cancer diagnoses, 2) less aggressive treatments for patients, 3) improved survival, 4) improved quality of life, 5) reduced economic burden associated with incurred costs of treating severe illness or iatrogenic complications, 6) greater access to diagnostic instruments among rural and disadvantaged communities due to the relative low cost of photon detectors, filters, and related technologies*.

Impact – Photonic technologies are advancing rapidly and are poised to become the new biomedical standard due to their multiple advantages such as miniaturization, high speed transmission, low thermal effects, and large integration capacity that allow for high yield, volume manufacturing, and lower cost. In these regards, the proposed technological innovations are timely. ***Knowledge generated from the proposed research will inform approaches to early cancer diagnostics, but lead to cancer prevention strategies, increase patient survival, and significantly improve quality of life among survivors***. Our study on novel biomedical imaging and state-of-the-art classification algorithms for precision oncology, will have a significant impact on multiple stakeholders. Patients, survivors, and caregivers will benefit from reduced personal and economic burdens through the ultra early non-invasive cancer detection and detection of early neurotoxicity and resulting cancer related cognitive impairment. Moreover, this advanced imaging technique can be applied to detect light-based biomarkers associated with various pathologies, enabling early disease detection and improved patient outcomes across a wide range of conditions, such as neurodegenerative disorders, brain injuries, metabolic disorders, and cardiovascular disease. By integrating the light-based biomarkers with artificial intelligence, we can develop smarter tools to detect health changes as early as possible, enabling swift intervention and improved outcomes for patients. Therefore, **the proposed research will provide a foundation for the use of endogenously generated light-based biomarkers for early disease detection and the careful monitoring of treatment effectiveness.**

References

1. Sung, H., Ferlay, J., Siegel, R. L., Laversanne, M., Soerjomataram, I., Jemal, A., & Bray, F. (2021). Global cancer statistics 2020: GLOBOCAN estimates of incidence and mortality worldwide for 36 cancers in 185 countries. CA: a cancer journal for clinicians, 71(3), 209-249.
2. Beerenwinkel, N., Antal, T., Dingli, D., Traulsen, A., Kinzler, K. W., Velculescu, V. E., ... & Nowak, M. A. (2007). Genetic progression and the waiting time to cancer. PLoS computational biology, 3(11), e225.
3. Trosko, J. E., & Ruch, R. J. (1998). Cell-cell communication in carcinogenesis. Frontiers in Bioscience-Landmark, 3(4), 208-236.
4. Molinolo, A. A., Amornphimoltham, P., Squarize, C. H., Castilho, R. M., Patel, V., & Gutkind, J. S. (2009). Dysregulated molecular networks in head and neck carcinogenesis. Oral oncology, 45(4-5), 324-334.
5. Grass, F., Behm, K. T., Duchalais, E., Crippa, J., Spears, G. M., Harmsen, W. S., ... & Larson, D. W. (2020). Impact of delay to surgery on survival in stage I-III colon cancer. European Journal of Surgical Oncology, 46(3), 455-461.
6. Mantovani, A. (2010). Molecular pathways linking inflammation and cancer. Current molecular medicine, 10(4), 369-373.
7. Sheth, M., & Esfandiari, L. (2022). Bioelectric dysregulation in cancer initiation, promotion, and progression. Frontiers in Oncology, 12, 846917.
8. Suresh, S. (2007). Biomechanics and biophysics of cancer cells. Acta biomaterialia, 3(4), 413-438.
9. Popp, F. A. (2003). Properties of biophotons and their theoretical implications. Indian Journal of Experimental Biology, 41, 391-402.
10. Rahnama, M., Tuszynski, J. A., Bokkon, I., Cifra, M., Sardar, P., & Salari, V. (2011). Emission of mitochondrial biophotons and their effect on electrical activity of membrane via microtubules. Journal of integrative neuroscience, 10(01), 65-88.
11. Takeda, M., Kobayashi, M., Takayama, M., Suzuki, S., Ishida, T., Ohnuki, K., ... & Ohuchi, N. (2004). Biophoton detection as a novel technique for cancer imaging. Cancer science, 95(8), 656-661.
12. Bókkon, I., Salari, V., Tuszynski, J. A., & Antal, I. (2010). Estimation of the number of biophotons involved in the visual perception of a single-object image: Biophoton intensity can be considerably higher inside cells than outside. Journal of Photochemistry and Photobiology B: Biology, 100(3), 160-166.
13. Pospíšil, P., Prasad, A., & Rác, M. (2014). Role of reactive oxygen species in ultra-weak photon emission in biological systems. Journal of Photochemistry and Photobiology B: Biology, 139, 11-23.
14. Popp, F. A., Nagl, W., Li, K. H., Scholz, W., Weingärtner, O., & Wolf, R. (1984). Biophoton emission: New evidence for coherence and DNA as source. Cell biophysics, 6, 33-52.
15. Burgos, R. C. R., Červinková, K., van der Laan, T., Ramautar, R., van Wijk, E. P., Cifra, M., ... & van der Greef, J. (2016). Tracking biochemical changes correlated with ultra-weak photon emission using metabolomics. Journal of Photochemistry and Photobiology B: Biology, 163, 237-245.
16. Burgos, R. C. R., Schoeman, J. C., Winden, L. J. V., Červinková, K., Ramautar, R., Van Wijk, E. P., ... & Greef, J. V. D. (2017). Ultra-weak photon emission as a dynamic tool for monitoring oxidative stress metabolism. Scientific Reports, 7(1), 1229.
17. Parker, A. L., Kavallaris, M., & McCarroll, J. A. (2014). Microtubules and their role in cellular stress in cancer. Frontiers in oncology, 4, 153.
18. Wallace, D. C. (2012). Mitochondria and cancer. Nature Reviews Cancer, 12(10), 685-698.
19. Prasad, A., Rossi, C., Lamponi, S., Pospíšil, P., & Foletti, A. (2014). New perspective in cell communication: Potential role of ultra-weak photon emission. Journal of Photochemistry and Photobiology B: Biology, 139, 47-53.
20. Tang, R., & Dai, J. (2014). Biophoton signal transmission and processing in the brain. Journal of Photochemistry and Photobiology B: Biology, 139, 71-75.
21. Loeb, S., Vellekoop, A., Ahmed, H. U., Catto, J., Emberton, M., Nam, R., ... & Lotan, Y. (2013). Systematic review of complications of prostate biopsy. European urology, 64(6), 876-892.

22. Pentsova, E. I., Shah, R. H., Tang, J., Boire, A., You, D., Briggs, S., ... & Berger, M. F. (2016). Evaluating cancer of the central nervous system through next-generation sequencing of cerebrospinal fluid. Journal of clinical oncology, 34(20), 2404.
23. Al-Sharify, Z. T., Al-Sharify, T. A., & Al-Sharify, N. T. (2020, June). A critical review on medical imaging techniques (CT and PET scans) in the medical field. In IOP Conference Series: Materials Science and Engineering (Vol. 870, No. 1, p. 012043). IOP Publishing.
24. Panych, L. P., & Madore, B. (2018). The physics of MRI safety. Journal of Magnetic Resonance Imaging, 47(1), 28-43.
25. Guo, J., Zhu, G., Li, L., Liu, H., & Liang, S. (2017). Ultraweak photon emission in strawberry fruit during ripening and aging is related to energy level. Open Life Sciences, 12(1), 393-398.
26. Jiin-Ju, C. (2008). Physical properties of biophotons and their biological functions. Indian journal of experimental biology, 46(5), 371.
27. Zhao, X., van Wijk, E., Yan, Y., van Wijk, R., Yang, H., Zhang, Y., & Wang, J. (2016). Ultra-weak photon emission of hands in aging prediction. Journal of Photochemistry and Photobiology B: Biology, 162, 529-534.
28. Murugan, N. J., Rouleau, N., Karbowski, L. M., & Persinger, M. A. (2018). Biophotonic markers of malignancy: Discriminating cancers using wavelength-specific biophotons. Biochemistry and biophysics reports, 13, 7-11.
29. Murugan, N. J., Karbowski, L.M., Dotta, B.T., Vares, D.A.E., Saroka, K.S., Lafrenie, R. M., & Persinger, M. A (2016). Differentiation of Malignant Compared to Non-Malignant Cells by Their Bio-Photon Emissions May Only Require a Specific Filter around 500 nm. J Cancer Sci Ther 8: 170-171.
30. Dotta, B. T., Murugan, N. J., Karbowski, L. M., Lafrenie, R. M., & Persinger, M. A. (2014). Shifting wavelengths of ultraweak photon emissions from dying melanoma cells: their chemical enhancement and blocking are predicted by Cosic's theory of resonant recognition model for macromolecules. Naturwissenschaften, 101, 87-94.
31. Sordillo, P. P., & Sordillo, L. A. (2020). The mystery of chemotherapy brain: Kynurenines, tubulin and biophoton release. Anticancer Research, 40(3), 1189-1200.
32. Crosby, D., Bhatia, S., Brindle, K. M., Coussens, L. M., Dive, C., Emberton, M., ... & Balasubramanian, S. (2022). Early detection of cancer. Science, 375(6586), eaay9040.
33. Sasieni, P. D., Shelton, J., Ormiston-Smith, N., Thomson, C. S., & Silcocks, P. B. (2011). What is the lifetime risk of developing cancer?: the effect of adjusting for multiple primaries. British journal of cancer, 105(3), 460-465.
34. Van Wijk, R., Van Wijk, E. P., Pang, J., Yang, M., Yan, Y., & Han, J. (2020). Integrating ultra-weak photon emission analysis in mitochondrial research. Frontiers in physiology, 11, 717.
35. Senger D, Perruzzi C, Streit M et al. (2002). The alpha(1)beta(1) and alpha(2)beta(1) integrins provide critical support for vascular endothelial growth factor signaling, endothelial cell migration, and tumor angiogenesis. Am J Pathol. 160(1):195-204.
36. Jelic, M. D., Mandic, A. D., Maricic, S. M., & Srdjenovic, B. U. (2021). Oxidative stress and its role in cancer. Journal of cancer research and therapeutics, 17(1), 22-28.
37. Agrawal, A., Shahreza, S., Javanmardi, Y., Szita, N., & Moeendarbary, E. (2022). The tumour microenvironment modulates cancer cell intravasation. Organs-on-a-Chip, 4, 100024.
38. Anguiano, M., Morales, X., Castilla, C., Pena, A. R., Ederra, C., Martínez, M., ... & Ortiz-de-Solorzano, C. (2020). The use of mixed collagen-Matrigel matrices of increasing complexity recapitulates the biphasic role of cell adhesion in cancer cell migration: ECM sensing, remodeling and forces at the leading edge of cancer invasion. PloS one, 15(1), e0220019.
39. Lin, C. C., & Korc, M. (2018). Designer hydrogels: Shedding light on the physical chemistry of the pancreatic cancer microenvironment. Cancer letters, 436, 22-27.
40. Basch, E., Artz, D., Dulko, D., Scher, K., Sabbatini, P., Hensley, M., ... & Schrag, D. (2005). Patient online self-reporting of toxicity symptoms during chemotherapy. Journal of clinIcal oncology, 23(15), 3552-3561.

41. Harrington, C. B., Hansen, J. A., Moskowitz, M., Todd, B. L., & Feuerstein, M. (2010). It's not over when it's over: long-term symptoms in cancer survivors—a systematic review. The International Journal of Psychiatry in Medicine, 40(2), 163-181.
42. Taillibert, S., Voillery, D., & Bernard-Marty, C. (2007). Chemobrain: is systemic chemotherapy neurotoxic?. Current opinion in oncology, 19(6), 623-627.
43. Janelsins, M. C., Kesler, S. R., Ahles, T. A., & Morrow, G. R. (2014). Prevalence, mechanisms, and management of cancer-related cognitive impairment. *International review of psychiatry*, *26*(1), 102-113.

QUARTZ-BASED OPTICAL WAVEGUIDE SENSOR FOR MICROPLASTICS DETECTION IN WATER

PROJECT LEADER

- NUR NAJAHATUL HUDA SARIS (Universiti Teknologi Malaysia, UTM)

MEMBER:

- NAZIRAH MOHD RAZALI (Universiti Teknologi Malaysia, UTM)

KEYWORD: Quartz, Optical Waveguide, Optical Sensing and Sensor, Waveguide Sensor, Microplastics, Water

EXECUTIVE SUMMARY

Nowadays, the sizeable number of microplastics pollution has become a global and societal concern that needs to be addressed. Not only does this endanger the ecology and marine animals, but it can also cause health threats to human beings. Moreover, microplastics are optically difficult to be detected especially in water bodies such as rivers, oceans and tap water due to its density, size, shape, morphology, and transparency. This has led to an expansion of studies on microplastics detection methods in water. However, most of the methods introduced to date is rather time-consuming, expensive, and complicated. To overcome this issue, this research aims to develop a compact optical waveguide refractive index sensor by employing the quartz as a main material. In this research, the objectives are to design and model the quartz-based optical waveguide sensor using Ansys Lumerical software for microplastics detection in water as refractive index sensor and to fabricate quartz-based optical waveguide sensor by using moulding and etching fabrication techniques. Note the range of the refractive index used in this research are from 1.30 up to 1.53 which reflect the refractive index of microplastics that commonly found in polluted water. Therefore, to understand the performance of quartz-based optical waveguide sensor, optimisation on the waveguide's geometric parameters will be conducted. These parameters, which include waveguide length and dimension, thickness, refractive index profile as well as variation of coating material will essentially be varied to attain the best sensitivity and linearity performance of the waveguide sensor for microplastics detection in water. Overall, it is believed that this research is beneficial to researchers, government and environmental agencies which provide a better understanding about the technology of microplastics detection in water. With the development of the quartz based optical planar waveguide sensor, new substantial impact could be achieved in water environment sustainability which aligned with SDG 3, SDG 6 and SDG 14 which are good health and wellbeing, clean water, and life below water. The preliminary result from this research will be the early step towards advanced technology in preserving nature.

Quartz-Based Optical Waveguide Sensor for Microplastics Detection in Water

Nur Najahatul Huda Saris
Faculty of Electrical Engineering,
Universiti Teknologi Malaysia,
81310 Johor Bahru, Malaysia.
nurnajahatulhuda@utm.my

Over the past century, there has been a dramatic increase in plastics production especially for textiles, packaging, and automotive industries for its convenience due to versatility [1, 2]. Nevertheless, these industries contribute an exorbitant number of pollutants that end up in water and landfills [3-5]. The breakdown of plastic wastes over time will create different forms of microplastics with various sizes and shape distribution, which can directly damage the environment, ecosystem, and food chain [6]. Numerous studies have shown that microplastics like transparent polyethylene terephthalate (PET), translucent low-density polyethylene (LDPE) and other types of plastic in water resources can cause various human health problems through ingestion and consumption such as reproductive abnormalities, asthma, obesity, gastritis, skin irritation and cancer [7-12].

Accordingly, a number of research on microplastic detection methods in water have been studied and reported based on optical, visual and chemical inspections such as Raman, infrared (IR), and Fourier transform infrared (FTIR) spectroscopy, besides integrated optical waveguide sensors [13-25]. However, the methods introduced to date is time-consuming, expensive, and complicated. The spectroscopic methods suffer from limitations including complicated processing steps that produce low yield with extortionate cost and are time consuming. In fact, it is arduous to differentiate microplastic sizes in water using Raman and FTIR spectroscopy since its detection capability is limited up to 1 μm and 25 μm, respectively. In contrast, integrated optical waveguide sensors is a promising candidate for microplastics detection in water based on its sensitivity towards the difference of refractive index changes according to Fresnel's law and evanescent field wave theory.

Therefore, this research aims to develop a compact optical waveguide sensor with high sensitivity and linearity performance operating at visible wavelength regions – fabricated by using moulding technique to ascertain the presence of microplastics in water. The quartz with 1.544 refractive index is explored extensively in this work. Note that a wide refractive index range of microplastics from 1.3 to 1.53 will be used in this research to investigate the potential of the proposed sensor. To achieve this, a few objectives have been outlined to guide the research route:

1. To model the quartz-based optical waveguide sensor using Ansys Lumerical software.
2. To fabricate the quartz-based optical waveguide sensor using moulding and etching techniques.
3. To evaluate the sensitivity and linearity performance of the quartz-based optical waveguide sensor for microplastics detection in water.

In this research, three work stages will be implemented to ensure all research objectives are met. **Stage 1** is concerned with the simulation for design parameter optimisation of quartz-based optical waveguide such as shape of waveguide, coating material for detection enhancement and dimension as well as length the waveguide —which are considered the fundamental parameters to assess the sensitivity and linearity performance of the waveguide sensor for microplastics detection. By using Ansys Lumerical software, the interaction of light propagation through the waveguides formed according to the evanescent field waves and also the waveguide itself with respect to the microplastics in water can be well analysed. In other

words, once it comes in contact with the respective measured analyte, i.e., the microplastics, the light reflected into the waveguide due to the difference in refractive index can be studied extensively based on the Fresnel reflection law by using Ansys Lumerical software.

Accordingly, **Stage 2** will be focused on the waveguide fabrication using moulding and etching technique. Also, the material's spectroscopic characterization physically, elementally, and optically will take place in Stage 2**.** In this research, Stage 2 is the most crucial step because it is where all the results based of varying parameters are analyzed thoroughly to achieve the best optical sensitivity performance of the optical waveguide sensor in **Stage 3**. In addition, the work towards the enhancement of the waveguide performance is also dedicated in Stage 2. The flowchart of this research project can be found in Figure 1.

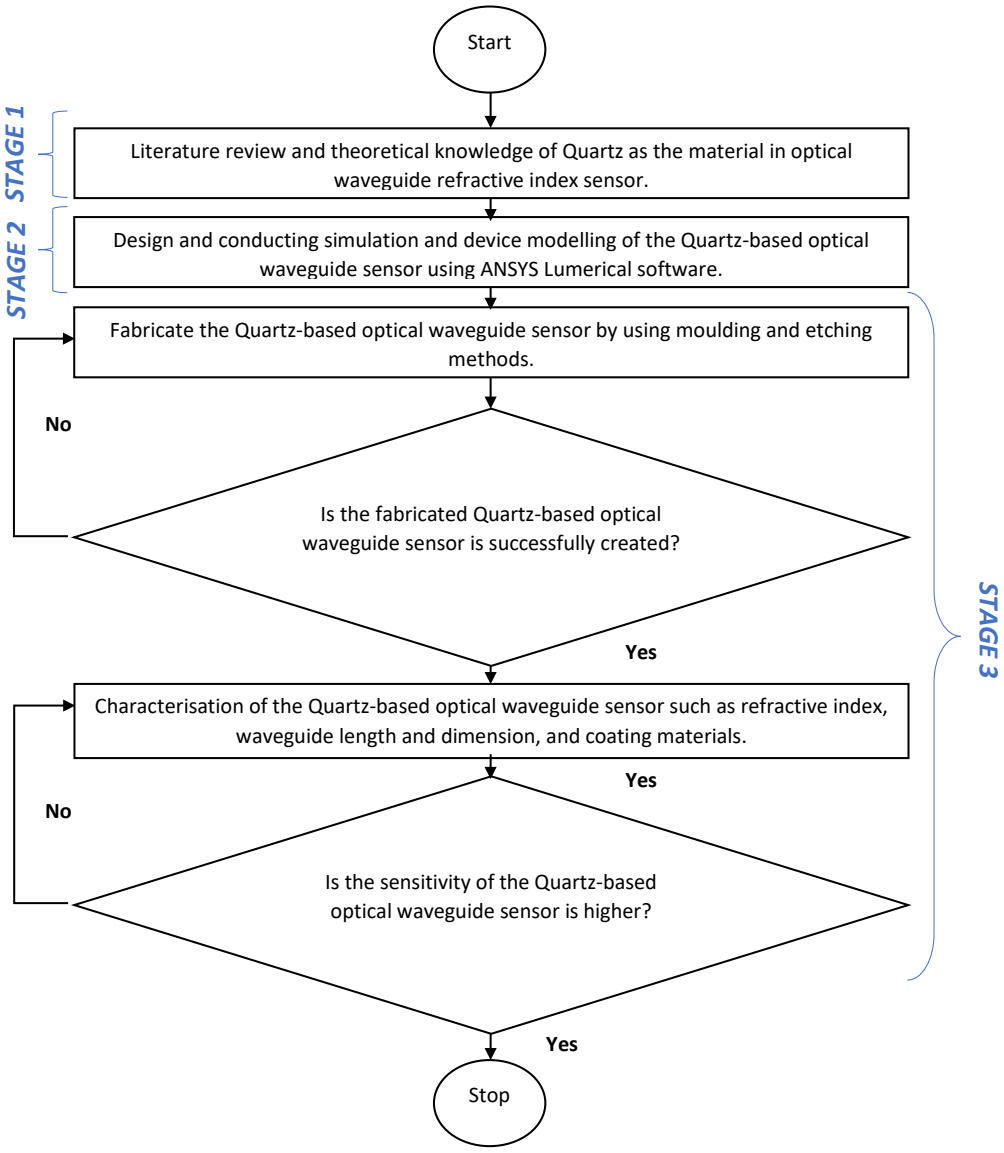

Figure 1: Research Flowchart

Applying this grant will serve as a complementary and matching component to my current research on microplastic detection by using the material namely Europium-Aluminum doped Benzyl Methacrylate (Eu-Al/BzMA). I am now seeking to apply for an additional grant from Optica Foundation to explore a different material rather than Eu-Al/BzMA which is quartz. This endeavour aims to provide a comprehensive comparison and analysis of the various

materials involved in my project. It is believed by investigating potential materials of optical waveguide sensor will unlock new paradigm of sensing application for microplastic detection in which are previously limited to the in-lab equipment such as Raman spectroscopic and FTIR. The refractive index of the material enable the device to sense microplastics with high degree of accuracy which are previously unattainable. With proper optimization on various parameters (physical, elemental, and optical), the device will lead to better performance in terms of sensitivity towards microplastics in water. With the development of the optical waveguide sensor, new substantial impact could be achieved in water environment sustainability. The preliminary result from this research will be the early step towards advanced technology in cleaner drinking water, preserving nature and better human health.

Overall, I really hope that Optica Foundation would give me the opportunity to grow and develop my career to be more successful women in science as an academician and also researcher. This award will a steppingstone for me to contribute to the society through science and technology. My aspiration is to have a future where mothers and children have free access to clean and unpolluted drinking water as they are the cradle of our civilization.

References

[1] T. D. Moshood, G. Nawanir, F. Mahmud, F. Mohamad, M. H. Ahmad, and A. AbdulGhani, "Sustainability of biodegradable plastics: New problem or solution to solve the global plastic pollution?," *Current Research in Green and Sustainable Chemistry,* vol. 5, p. 100273, 2022/01/01/ 2022, doi: https://doi.org/10.1016/j.crgsc.2022.100273.

[2] G. Gourmelon, "Global plastic production rises, recycling lags," *Vital Signs,* vol. 22, pp. 91-95, 2015.

[3] S. J. Barnes, "Understanding plastics pollution: The role of economic development and technological research," *Environmental Pollution,* vol. 249, pp. 812-821, 2019/06/01/ 2019, doi: https://doi.org/10.1016/j.envpol.2019.03.108.

[4] N. P. Ivleva, A. C. Wiesheu, and R. Niessner, "Microplastic in aquatic ecosystems," *Angewandte Chemie International Edition,* vol. 56, no. 7, pp. 1720-1739, 2017.

[5] A. M. Lechner *et al.*, "Challenges and considerations of applying nature-based solutions in low-and middle-income countries in Southeast and East Asia," *Blue-Green Systems,* vol. 2, no. 1, pp. 331-351, 2020.

[6] S. Karbalaei, P. Hanachi, T. R. Walker, and M. Cole, "Occurrence, sources, human health impacts and mitigation of microplastic pollution," *Environmental science and pollution research,* vol. 25, no. 36, pp. 36046-36063, 2018.

[7] S. D'Angelo and R. Meccariello, "Microplastics: a threat for male fertility," *International Journal of Environmental Research and Public Health,* vol. 18, no. 5, p. 2392, 2021.

[8] S. L. Wright, R. C. Thompson, and T. S. Galloway, "The physical impacts of microplastics on marine organisms: a review," *Environmental pollution,* vol. 178, pp. 483-492, 2013.

[9] P. Kolandhasamy, L. Su, J. Li, X. Qu, K. Jabeen, and H. Shi, "Adherence of microplastics to soft tissue of mussels: a novel way to uptake microplastics beyond ingestion," *Science of the total environment,* vol. 610, pp. 635-640, 2018.

[10] S. A. Mason, V. G. Welch, and J. Neratko, "Synthetic polymer contamination in bottled water," *Frontiers in chemistry,* p. 407, 2018.

[11] D. Schymanski, C. Goldbeck, H.-U. Humpf, and P. Fürst, "Analysis of microplastics in water by micro-Raman spectroscopy: release of plastic particles from different packaging into mineral water," *Water research,* vol. 129, pp. 154-162, 2018.

[12] W. C. LI, H. Tse, and L. Fok, "Plastic waste in the marine environment: A review of sources, occurrence and effects," *Science of the total environment,* vol. 566, pp. 333-349, 2016.

[13] B. O. Asamoah, B. Kanyathare, M. Roussey, and K.-E. Peiponen, "A prototype of a portable optical sensor for the detection of transparent and translucent microplastics in freshwater," *Chemosphere,* vol. 231, pp. 161-167, 2019.
[14] M. Wohlschläger and M. Versen, "Detection of plastics in water based on their fluorescence behavior," *Journal of Sensors and Sensor Systems,* vol. 9, no. 2, pp. 337-343, 2020.
[15] M. Wohlschläger, M. Versen, and H. Langhals, "A method for sorting of plastics with an apparatus specific quantum efficiency approach," in *2019 IEEE Sensors Applications Symposium (SAS)*, 2019: IEEE, pp. 1-6.
[16] O. Malyuskin, "Microplastic detection in soil and water using resonance microwave spectroscopy: A feasibility study," *IEEE Sensors Journal,* vol. 20, no. 24, pp. 14817-14826, 2020.
[17] A. Luqman *et al.*, "Microplastic Contamination in Human Stools, Foods, and Drinking Water Associated with Indonesian Coastal Population," *Environments,* vol. 8, no. 12, p. 138, 2021.
[18] V. Hidalgo-Ruz, L. Gutow, R. C. Thompson, and M. Thiel, "Microplastics in the marine environment: a review of the methods used for identification and quantification," *Environmental science & technology,* vol. 46, no. 6, pp. 3060-3075, 2012.
[19] V. Balestra and R. Bellopede, "Microplastic pollution in show cave sediments: First evidence and detection technique," *Environmental Pollution,* vol. 292, p. 118261, 2022.
[20] A. Scircle, J. V. Cizdziel, K. Missling, L. Li, and A. Vianello, "Single-pot method for the collection and preparation of natural water for microplastic analyses: Microplastics in the Mississippi River system during and after historic flooding," *Environmental toxicology and chemistry,* vol. 39, no. 5, pp. 986-995, 2020.
[21] M. G. Löder and G. Gerdts, "Methodology used for the detection and identification of microplastics—a critical appraisal," *Marine anthropogenic litter,* pp. 201-227, 2015.
[22] L. Zada *et al.*, "Fast microplastics identification with stimulated Raman scattering microscopy," *Journal of Raman spectroscopy,* vol. 49, no. 7, pp. 1136-1144, 2018.
[23] L. Cabernard, L. Roscher, C. Lorenz, G. Gerdts, and S. Primpke, "Comparison of Raman and Fourier transform infrared spectroscopy for the quantification of microplastics in the aquatic environment," *Environmental science & technology,* vol. 52, no. 22, pp. 13279-13288, 2018.
[24] A.-K. Kniggendorf, C. Wetzel, and B. Roth, "Microplastics detection in streaming tap water with Raman spectroscopy," *Sensors,* vol. 19, no. 8, p. 1839, 2019.
[25] B. O. Asamoah, E. Uurasjärvi, J. Räty, A. Koistinen, M. Roussey, and K.-E. Peiponen, "Towards the development of portable and in situ optical devices for detection of micro and nanoplastics in water: A review on the current status," *Polymers,* vol. 13, no. 5, p. 730, 2021.

Executive Summary - Health category

Real-time brain Tumor border visualization with imaging Partial Mueller Polarimetry (TurboPMP)

Dr. Omar Rodríguez Núñez
Department of Neurosurgery, Inselspital, University Hospital Bern, UHB, Switzerland
omar.rodrigueznunez@insel.ch

Surgery remains the decisive treatment step for most patients with brain tumors, particularly life-threatening gliomas. A visualization of the precise border between a tumor and healthy brain tissue is crucial for the complete excision of the tumor and preservation of neurological function, because not always a neurosurgeon can perform resection with a wide safety margin without damaging eloquent areas of the brain. Despite the recent advances in intra-operative imaging modalities, e. g. the use of ultrasound, ALA-5 fluorescence and magnetic resonance imaging (MRI), tumor tissue shows low contrast compared to white matter of healthy brain tissue during neurosurgery.

The densely packed and highly aligned fiber tracts of the white matter of healthy brain tissue exhibit uniaxial linear birefringence with an optical axis oriented along the direction of fiber bundles. Brain tumor tissue, whose cells grow in largely chaotic way, should lose this optical anisotropy. To address the limitation of current tumor visualization strategies, the IP research group recently proposed to visualize the microstructure of the brain, through its fiber tracts during tumor surgery, since the absence of fiber would imply tumor tissue. The results using the complete multi-spectral wide-field imaging Mueller polarimetry (IMP) system are promising for both ex and in vivo brain tissue differentiation and diagnosis. However, the complete IMP system realies on the sequential acquisition of the intensity images for each pair of probing and analyzing polarization state at each wavelengths. Moreover, the system uses averaging of 8 up to 16 measurements of the intensities for each pair of polarization states to reduce the noise in the images. These limitations are not compatible with the ultimate goal of real-time polarimetric imaging during neuro surgery.

*My TurboPMP proposal suggest a solution to visualize and segment accurately the border between healthy and brain tumor tissue in the polarimetric images acquired under in vivo neurosurgery conditions, using a real-time partial **V**ideo-**R**ate **I**maging **M**ueller **P**olarimeter (VRIMP).* The new method I propose will be based on the measurements of the partial Mueller matrix (MM) at video-rate, while extracting the same diagnostic information as from the complete MM. It will be a significant breakthrough towards the next generation of intraoperative polarimetric imaging, thus paving the way to the implementation of this imaging modality in clinical settings. The TurboPMP project is realistic and interdisciplinary, as this combine two fields, namely, the IMP instrumental development and the intra-operative neurosurgical imaging. Moreover, their merging for brain tumor neurosurgery is completely new and was not achieved yet.

The creation of an ergonomic VRIMP prototype applicable for use in OR and well adapted for clinical practice, will be the main output of the TurboPMP project. The VRIMP system will have integrated polarimetric images post-processing and interpretation algorithms, the latter will be validated for *in vivo* brain tissue imaging and optimized for running real-time measurements. The versatile design of the final VRIMP system allowing its integration in both a standard commercial microscope and an exoscope which could facilitate the implementation of the VRIMP in OR settings

Successful completion of the TurboPMP project will demonstrate the relevance of the partial IMP technique for the i*n vivo* identification of healthy brain fiber tracts and their orientation at crucial time points of brain surgery. I expect that the implementation of the VRIMP system for a non-contact and real-time visualization of fiber tracts in the tissue-at-sight would be a breakthrough for brain tumor surgery. It will reduce postoperative neurological deficits that have devastating effects on the patient's quality of life and survival time. Hence, the TurboPMP project approach has the potential to significantly improve the patients' outcome and reduce surgical morbidity.

Real-time brain Tumor border visualization with imaging Partial Mueller Polarimetry (TurboPMP)

Dr. Omar Rodríguez Núñez
Department of Neurosurgery, Inselspital, University Hospital Bern, UHB, Switzerland
omar.rodrigueznunez@insel.ch / omarquez300788@hotmail.com

1. Literatura Review

Significance. Malignant tumors of the brain, especially high-grade gliomas [HGG], are among the deadliest tumors known, and survival rates are low despite decades of intensive research[1]. According to the AWMF guide lines[2] for clinical decision-making, complete resection of the enhancing tumor should be attempted as the first-line therapy in patients with HGG. While some well-delineated tumors such as metastases can be removed in-bloc, most gliomas are removed piece by piece, because them tend to grow infiltrative in the white matter inside the brain. A complete resection is of paramount importance in most cases and remains the neurosurgeon's ultimate goal. However, overly aggressive resection of peritumors tissue is prone to cause additional and long-lasting or permanent damage to patients' neurological functions, with a negative impact on the patient's quality of life and the prognosis. Hence, performing surgery on brain tumor patients remains a challenge between too extensive and too little resection. Moreover, the clear identification of brain tumor tissue as well as the surrounding healthy tissue including its potentially eloquent fiber tracts is essential to achieve an optimal clinical outcome. Current limitations of modern brain surgery include a poor contrast between tumor tissue and the surrounding healthy brain, as well as the lack of clear intraoperative segmentation of gray and white matter tissue, observed through a white light neurosurgical microscope[3].

Sophisticated methods addressing this challenge are used in standard neurosurgical practice today, such as neuronavigation, fluorescence staining, intraoperative magneto resonance imaging (MRI), and ultrasound[4,5]. Despite their clear respective benefits, these techniques remain either to some extent prone to inaccuracy, inapplicable to all tumor types or costly in use, making precise and high contrast intraoperative identification of healthy and diseased brain tissue an open challenge in modern neurosurgery[4,5]. This emphasizes the clinical need to improve technological solutions that overcome the aforementioned limitations.

State-of-the-art. Optical imaging has already become a reliable technique for medical diagnosis. The classical intensity images taken with either an endoscope or a binocular microscope provide visual information about the biological tissue, such as its color, vascularization, surface texture, presence of lesions, etc. For example, these imaging modalities are routinely used for the characterization of superficial tissue layers in gynecology, dermatology, and gastroenterology[6-8]. Confocal microscopy and optical coherence tomography make use of ballistic photons to produce microscopic depth-resolved images of tissue. For both modalities, the field of view is typically less than a few square millimeters and the penetration depth does not exceed a few hundred microns[9]. Hyperspectral images (HSI), can be acquired with a snapscan camera operating in a visible wavelength range, in order to build a deep-learning-based diagnostic tool for cancer resection with a potential for intra-operative guidance[10]. However, the main limitation of the HSI snapscan camera is the duration of data acquisition and post-processing for all spectral channels, that limit its widespread deployment in the operation theater.

Polarimetric studies of the thin sections of brain tissue in transmission configuration have confirmed that fiber bundles in white matter cause optical anisotropy of brain tissue[11]. It was possible to obtain the orientation of the fibers by measuring the linear birefringence, which is mainly caused by the regular arrangement of lipids and proteins in the myelin sheath of the axons[11-12]. The high degree of structure within the healthy brain white matter differs strongly from brain tumor tissue that grows in a chaotic way and erase this optical anisotropy of healthy brain white matter. In order to study the structure of the

[1] N.A. Bush, *et al*., Mayo Clin. Proc., **40**(1), 1-14 (2017).
[2] Association of the Scientific Medical Societies (AWMF) online, Clinical Practice Guidelines, https://www.verwaltung.awmf.org/en.html
[3] J.K.W. Gerritsen, *et al.*, Neuro-Oncology Practice **9**(5), 364-379 (2022).
[4] I.J Gerard, *et al.*, Med. Image Anal., **35**, 403-420 (2017).
[5] M.S. Eljamel, *et al.*, Photodiagn. Photodyn. Ther., **16**, 35-43 (2016).
[6] T. Novikova, J. Nanotechnol., **8**, 1844-1862 (2017).
[7] E. Errichetti, *et al.*, Dermatol Ther (Heidelb), **6**, 471-507 (2015).
[8] M. Akarsu, *et al*., J Soc Laparosc. Robotic Surg., **22**, e2017.00053 (2018)).
[9] J. Jonkman, *et al.*, Nat. Proc, **15**, 1585-1611 (2020).
[10] T. Giannantonio, *et al*., arXiv, eess.IV 2302.*02884 (2023).*
[11] M. Menzel, *et al*., Biomed. Opt. Express, **8**, 3163-3197 (2017).
[12] M. Koike-Tani, *et al.*, Mol. Reprod. Dev., **82**(7-8), 548-562 (2015).

fiber tracts of the human brain, it is necessary to resort to specific imaging techniques that resolve the orientation of the fibers not only in high spatial resolutions images but also in the wide-field images of up to several square centimeters.

Recently the PI's research group has shown that the complete multi-spectral wide-field imaging Mueller polarimetry (IMP) system is a promising tool for both *ex* and *in vivo* brain tissue differentiation and diagnosis[13-17]. This polarimetric imaging modality detects accurately the in-plane orientation of brain white matter fiber tracts of a flat formalin-fixed (FF) thick brain specimen measured in reflection geometry[13]. The data acquired on fresh animal brain tissue with the IMP system working in a reflection configuration are robust and stable under the adverse conditions inherent to brain surgery, such as complex surface topography, presence of blood, and tilt[14]. The IMP system detects consistently the orientation of the white matter fiber tracts before and after the removal of a thin brain tissue layer with the ultra-sonic aspirator instruments commonly used in neurosurgery[15]. In addition, the polarimetric properties of FF brain tissue are close to those of fresh brain tissue, thus, allowing the generation of large data sets of polarimetric images required for training of the machine learning (ML) models for automated differentiation of brain tissue[16,17].

The current IMP system design relies on the sequential acquisition of the intensity images for each pair of probing and analyzing polarization states at each wavelengths. Moreover, the system uses averaging of 8 up to 16 measurements of the intensities for each pair of polarization states to reduce the noise in the images. **These limitations are not compatible with the ultimate goal of real-time polarimetric imaging during neurosurgery.** PI's research group is making significant efforts to address these limitations. Computational tools based on ML perform the numerical denoising of single-shot intensity images and partially address the limitation of long acquisition time[18].

The complete IMP approach is widely used in both clinical and pre-clinical studies of biological tissues. However, the utility of polarimetric information acquired via each of 16 measurement channels is difficult to assess because of non-linear data compression of the complete Mueller matrix(MM) commonly used for the meaningful physical interpretation of tissue polarimetric properties. Several studies have reported the results on using the reduced number of MM elements (e.g. 3x4 MM) for the analysis of tissue[19,20]. The obvious advantage of extracting the same diagnostic information while doing fewer measurements consists in reducing the measurement time.

Approach. The TurboPMP proposal suggests a solution for the real-time brain polarimetric system imaging. Using polarization-sensitive camera as a detector that operates at video-rate. We can obtain maps of common parameters of interest: linear depolarization, linear retardance, and azimuth of optical axis, with 3x4 MMs measured at the incidence close to normal with the new generation of imagers with integrated linear polarization selectivity. It opens the window for addressing the time limitations of *in vivo* polarimetric imaging during neuro-oncological surgery, as we will need to perform 4 measurements only. Moreover, using the left- and right- circularly polarized probing light beam we can obtain the exact value of the azimuth of the optical axis of uniaxial linear birefringent medium and fused value of linear depolarization and scalar linear retardance by performing two measurements only.

2. Problem Statement/Objectives

The goal of the TurboPMP project is to visualize and segment accurately the border between healthy and brain tumor tissue in the polarimetric images acquired under *in vivo* neurosurgery conditions, using a real-time partial video-rate imaging Mueller polarimeter (VRIMP). The new method I propose will be based on the measurements of the partial MM at video-rate, while extracting the same diagnostic information as from the complete MM. It will be a significant breakthrough towards the next generation of intraoperative polarimetric imaging, thus, paving the way to the implementation of this imaging modality in clinical settings. The core objectives of TurboPMP project are listed below:

• **O1.** Design, construction, calibration and testing of a real-time wide-field VRIMP based on the new generation of linear polarization sensors. I will develop a versatile system for its easy integration both

[13] P. Schucht, *et al*,. IEEE Trans. Med. Imaging, 39(12), 4376-14382(2020).
[14] O. Rodríguez-Núñez, *et al.*, Biomed. Opt. Express, **2**(10) 6647-6685 (2021).
[15] L. Felger *et al.*, Biomed. Opt. Express, **14**(5), 2400-2415 (2023).
[16] R. Gros, *et al*., Neurophotonics, **10**(2), 025009 (2023).
[17] R. McKinley, *et al.*, SPIE Unvonventional Optical Imaging III, **12136**,93-98, (2022).
[18] S. Moriconi, *et al.*, SPIE Proceedings Volume PC**12382**, PC123820H (2023).
[19] T. Novikova and J. C. Ramella-Roman, *et al*., Opt Lett. 1;**47**(21):5549-5552 (2022).
[20] M. Gonzalez, et al. *J. Phys. D: Appl. Phys.* **54**(42) 424005(1-9) (2021).

on a surgical microscope and on the exoscope head, depending on the operation room (OR) settings.

• **O2.** Implementation of the preprocessing and post-processing chain for the acquisition, visualization and segmentation of polarimetric images. First, I will focus on the Mueller algebra framework for the extraction of the relevant parameters from the acquired partial MM. Then, I will implement robust supervised ML algorithms to assess the capability of the VRIMP to visualize, segment, and track the fibers in the images of both fixed and fresh brain specimens.

• **O3.** Running an *ex vivo* measurement campaign on: a) 200 FF thick brain slices, b) 50 fresh cadaveric animal brains, and c) 50 fresh tumor specimens to create the large data set of polarimetric images that will be annotated by a neuropathologist. First, I will perform the measurements of all samples with the complete IMP, and then I will validate them against the measurements with a new VRIMP.

• **O4.** Integration of the real-time VRIMP system into a mechanical arm, and assessment of its performance under *in vivo* measurements conditions. A feed-back loop with neurosurgeons will help me to understand and improve the requirements and needs for the potential implementation of the VRIMP in a surgical microscope or exoscope for using it in clinical settings.

The proposed objectives are realistic and interdisciplinary, as they combine two fields, namely, the IMP instrumental development and the intra-operative neurosurgical imaging. Moreover, their merging for brain tumor surgery is completely new and was not achieved yet. Indeed, the proposed approach draws on a unique combination of the available expertise. I have been working on the conceptualization designs and construction of polarimetric instruments for biomedical applications, while the neurosurgeons, neuropathologists and mathematicians at the UHB have a longstanding history of translational research on diagnostic, treatment and visualization technologies for brain surgery.

3. Outline of task/Work Plan

To achieve the goal of implementing the VRIMP prototype in clinical settings under *in vivo* measurement conditions, through the development of a wide-field, visible-wavelength, label-free, non-invasive imaging, polarimetric system working in real-time, automatically identifying and segmenting healthy and tumor tissue zones I propose to structure the research into 4 work packages (WPs).

WP1. VRIMP prototype development. This WP aims to generate the optical, mechanical and electronic design of the VRIMP prototype. The designed system should be flexible and movable for using it in OR, well adapted to the established medical practice.

• First, I will design an independent, compact, and ergonomic VRIMP system with the flexibility to add-on onto an exoscope head. This system has the advantage that it would not disturb the well-established workflow during surgery, and would only be used at critical moments to assist the surgeon. Particular attention will be paid to the electronics to control the polarization state generator (PSG), and to synchronize it with the polarization sensitive camera, targeting for a fast acquisition (<100 ms). A detailed examination of different optical components and lighting sources (Xenon, LED or Halogen) will be carried out to maximize the amount of light captured, reduce local heating, improve the signal to noise ratio for the preservation of high quality images. The optical design will be characterized to display images of the brain, simultaneously through a binocular magnifier and through a computer screen connected to a polarimetric imaging system, displaying the parameters of interest to the surgeon.

• A second VRIMP prototype will be designed, adapting the optical and mechanical design appropriately to work into a second-hand commercial neurosurgical microscope. The way to generate the states in the PSG to be measured with the polarization sensitive camera will work analogously for both VRIMPs. Multiple approaches for the PSG will be evaluated, the first PSG design is based on ferroelectric liquid crystals (FLC), the second one will use 4 polarization states (horizontal linear, vertical linear, linear +135 and circular polarization) using a modulated source without FLC or rotating elements, finally a probe light beam with left- and right- circular polarization will be evaluated.

The next step will be to assemble the VRIMP as a fixed experimental system working in ideal laboratory conditions. I will set up a new image acquisition structure for the calculation of the partial MM, particular attention will be paid to the efficiency and speed of data streaming of the polarization sensitive camera, as well as to the synchronization of the acquired image for each polarization state required, aiming for an optimized processing. The implementation of an appropriate calibration method will be essential to increase the precision of the VRIMP. I will assess the experimental fixed VRIMP measuring

the partial MM of well-known reference samples such as polarizers, retarders, etc.

WP2. Data acquisition and validation of the VRIMP approach. Working at the Department of Neurosurgery of UHB, that specializes on intra-operative tumor visualization and resection, I will have access to 300 both FF and fresh brain specimens for testing the ability of VRIMP to visualize fiber tracts in white matter and to detect the exact tumor border. Together with the medical team, we will formalize a protocol of sample handling including the creation of post-operative marks for a specimen orientation, polarimetric measurements at different wavelengths, different sample sides, and cross-validation of polarimetric data with histology analysis.

A proof-of-concept of the performance of reduced Lu-Chipman decomposition to generate polarimetric maps using data from complete IMP has shown promising results[19]. I will massively test the reduced Lu-Chipman decomposition in available 200 images of the fixed human brain already measured with the complete IMP. Then I will measure the 300 brain specimens provided by the UHB, with both partial and complete IMP instruments, to compare the polarimetric maps extracted from data recorded with both systems corresponding non-linear decompositions.

WP3. Implementation of the data post-processing workflow. The images acquired in WP2, together with the associated reduced MM post-processed output, will be curated into a dataset suitable for training of ML algorithms (logistic regression, support vector machine, random forest). The ML image post-processing algorithms should identify robustly both gray matter of brain tissue and specular reflection zones and remove the corresponding pixels from subsequent analysis and visualization. The intensity and depolarization maps have shown to be good indicators to differentiate between white and gray brain tissue[16], but the thresholds may vary from image to image. It is expected that ML methods will allow for providing clear and suitable threshold. Finally, the imaging diagnostic segmentation will be assessed to identify healthy white matter and different types of tumors, as well as tumor cell density related to the degree of tumor infiltration. Special attention will be paid to the studies of polarimetric signatures of different types of tumors (e. g. glioma, meningioma, metastatic tumors, etc.).

WP4. Real-time *in vivo* VRIMP prototype for assessment in OR settings. The multiplatform VRIMP, that can be integrated into an exoscope head or into a classical surgical microscope will be tested and mounted to a mechanical arm first. The VRIMP surgical system will undergo advanced tests in the Near *in vivo* Lab at Department of Neurosurgery, UHB before going to the final set of *in vivo* tests. The Lab is located and adapted to carry out measurements next to OR. The end user requirements will be validated at this stage, and a feed-back process to correct, adapt and optimize the real-time VRIMP for clinical settings will be carried out. Near to *in vivo* measurements will help to refine the efficiency of the data post-processing algorithm for diagnostic image segmentation by validating it against histopathological analysis. A segmentation based on ML approach and subsequent diagnosis by a pathologist will be compared. A blind test of the polarimetric diagnostics will be implemented, including the processing and assessment of the polarimetric images acquired on the specimens with unknown pathological status. The *in vivo* tests will include the measurements of a surgical cavity at an intermittent time-points during the neurosurgery with the *in vivo* VRIMP prototype. Data post-processing workflow will be optimized for real-time performance and tested on *in vivo* data in the final series of tests.

The time schedule for the 24-month research project is shown in a Gantt Chart.

Work Packages - Due date month	**Deliverables - Due date**
WP1. VRIMP prototype development - Months 1-12	**Month 12**
T.1.1 Optical, mechanical and electronic design of the VRIMP. ***T.1.2*** PSG set up and data acquisition structure. ***T.1.3*** Experimental fixed VRIMP assembly and testing on reference samples. ***T.1.4*** Optoelectronics synchronization and data streaming for real-time acquisition. ******* *A master's student will help with the design the opto-mechanical system.* ** Electronics Engineer for the automation of the device.*	**D1** Experimental prototype of a functional VRIMP system. **D2** Scientific publication on the optimized partial IMP prototype. **D3** Conference attendance to present the VRIMP
WP2. Data acquisition and validation or VRIMP approach - Months 6 - 14	**Month 14**
T.2.1 Creation of a measurement protocol based on the previous studies with the complete IMP ***T.2.2*** Generation of a database with polarimetric images of 200 FF thick brain slices, 50 fresh healthy, and 50 fresh tumor brain specimens, using both partial and complete IMP systems ***T.2.3*** Teaching MD Ph.D. to use the VRIMP system to conduct the measurements campaign. ***T.2.4*** Validation of the reduced Lu-Chipman decomposition on a generated dataset.	**D4** Protocol and database: >300 polarimetric images near to *in vivo*. **D5** Validation of the task T.2.2. **D6** Figure of merit for the validation of the partial MP (~200)

WP3. Implementation of the data post-processing workflow - Months 13-20	**Month 18**
T.3.1 Optimization of data processing algorithms and reduced MM decomposition methods. ***T.3.2*** Implementation of the ML-based algorithms image segmentation to the generated. ***T.3.3*** Database (WP2) for the differentiation of healthy and cancerous brain tissue. ***T.3.4*** ML-based algorithm optimization and full integration into the VRIMP workflow. ******* *A master's student will work on the implementation of the ML algorithms*	**D7** Scientific publication on the identification of fiber tracts *ex vivo* using the VRIMP. **D8** Set of data compression algorithm and computational tools for tissue differentiation. **D9** Conference attendance to present.
WP4. Real-time *in vivo* VRIMP prototype for assessment in OR settings- Months 18-24	**Month 24**
T.4.1 Mounting of the multiplatform VRIMP on a mechanical arm for using in OR settings ***T.4.2*** Adjustment and application of the measurement protocol created in WP2 to collect 50 near-*in-vivo* images of healthy brain tissue and brain tumor specimens (specimens with different histological types of tumor) that may include safety margin – the excised healthy tissue zones). ***T.4.3*** *In vivo* proof of concept of the VRIMP systems. ******* *A MD PhD student will help to coordinate the measurement into OR conditions*	**D10** Operational *in vivo* VRIMP system **D11.** In vivo data and scientific publication of the results of post-processing of polarimetric **D12.** Protocol for VRIMP use in clinical settings

4. Outcomes

The creation of an ergonomic VRIMP prototype applicable for use in OR and well adapted for clinical practice, will be the main output of the TurboPMP project. The VRIMP system will have integrated polarimetric images post-processing and interpretation algorithms, the latter will be validated for *in vivo* brain tissue imaging and optimized for running real-time measurements.

Performance assessment of **partial against complete IMP** will allow me to ensure that the approach to data analysis and the corresponding data post-processing algorithm for diagnostic segmentation of polarimetric images of brain tissue, which help delineate the borders between the tumor and the healthy tissue, **is achievable and transferable for the *in vivo* application.**

Finally, the expected results of proof-of-concept *in vivo* studies with VRIMP system would kick start the potential collaboration with the industrial partners equipment (Leica, Zeiss, etc.) for instrument integration into commercial system, and translation to the neurosurgical operation routine.

I plan to publish the results of the TurboPMP project in at least three journals with high impact factor: Biomedical Optics, IF=3.921, IEEE Transactions on Biomedical Imaging, IF=11.034 and Neuroimage, IF=7.4, making them accessible to a broader audience. I am targeting to attend at least two conferences for the fast dissemination of our results: 1) Clinical and Translational Biophotonics, Florida, US, and 2) Optica BioPhotonics Congress: Optics in the Life Sciences, Coronado, California US.

5. Impact

The Optical Foundation Challenge grant will boost my research career and it will allow me to consolidate my interdisciplinary network of collaborators. The successful completion of my proposal will provide me scientific independence in the field of biophotonics and optical biomedical diagnostics. The new knowledge that I will acquire and create during the TurboPMP will allow me to exploit it in my future research projects.

• **Expected scientific impacts**. The flexible and movable VRIMP prototype and the multiple polarimetric data post-processing algorithms for the visualization of brain fiber tracts and the differentiation of healthy and tumor brain tissue, will provide a new synergetic approach and significant breakthrough that links polarimetric imaging and neurosurgery, a connection not explored in depth but with enormous potential. The expected publications will validate the translation of imaging polarimetry into clinical practice.

• **Expected economic/technological impacts**. The versatile design of the final VRIMP system allowing its integration in both a standard commercial microscope, and an exoscope at the end of the TurboPMP project will have a considerable impact on the envisaged technology transfer. It is expected that the optimal VRIMP prototype will have the elements to be protected by a patent, the Technology Transfer Office at UHB will support me to manage the intellectual property portfolio resulting from TurboPMP work which could facilitate potential negotiations with the leading industrial manufacturers of optical medical on the commercialization of the VRIMP for the OR implementation.

• **Expected societal impacts**. Successful completion of the TurboPMP project will demonstrate the relevance of the partial IMP technique for the i*n vivo* identification of healthy brain fiber tracts and their orientation at crucial time points of brain surgery. I expect that the implementation of the VRIMP system for a non-contact and real-time visualization of fiber tracts in the tissue-at-sight would be a breakthrough for brain tumor surgery. It will reduce postoperative neurological deficits that have devastating effects on the patient's quality of life and survival time. Hence, the TurboPMP project approach has the potential to significantly improve the patients' outcome and reduce surgical morbidity.

Design of an Optical Brain Interface: Bio-Neural Dust

CHALLENGE

The field of optogenetics has undergone significant development in recent years. One of its applications is stimulation of neurons with light. However, when coming to stimulating the actual brain, using optical fiber inserted through the skull is not practical. To achieve neural stimulation wirelessly, the concept of neural dust was introduced. Neural dust is a type of brain-computer interface, which uses devices the size of a millimeter as wireless nerve sensors to remotely monitor neural activity. However, despite of their small size, these devices are still very large compared to the size of a neuron, making it impossible to achieve stimulation and monitoring at the granularity level of a single neuron; it is also impossible to achieve very localized brain stimulation/monitoring. In addition, CMOS technology is reaching its limits in terms of miniaturization due to quantum phenomena, making the control of CMOS sensors at the nano level very challenging. The brain stimulation at a single neuron precision level is faced with two problems; size miniaturization and biocompatibility. In the optogenetics literature, we either find miniaturized systems with no biocompatibility, or biocompatible systems but very large compared to the size of neurons.

PROPOSED PROJECT

One promising solution in designing wireless nanosensors is to use bioluminescence and biological agents such as bacteria and viruses. Besides their biocompatibility inside the human body, bio-inspired systems are stable, inexpensively manageable, their tiny size allows them to be injected noninvasively inside the brain and they are easily controlled with genes and enzymes. The goal of this project is to design and implement bio-nanosensors that can monitor and stimulate neurons at nano level by using optogenetics. The proposed bio-nanosensor contains two biosystems. The first uses the piezoelectric properties of M13 virus to harvest the mechanical energy of ultrasonic waves, converting it to electricity. The second biosystem uses a photo-protein called *Aequorin*, which generates bioluminescent blue light in the presence of Ca^{2+} ions. Both biosystems will be placed inside a transparent nanosphere creating a bio-nanosensor, which detects ultrasonic waves, converts them to electricity, which triggers release of Ca^{2+} ions in the pool where *Aequorin* is located. The reaction generates blue light emission. A network of these bio-nanosensors creates the Bio-Neural Dust that will be used as an optical brain interface to stimulate neurons *in vitro* by using optogenetics.

INTENDED OUTCOMES

The project is divided into an analytical study and an experimental study. The intended outcomes of the analytical study are journals, conference publications and a patent of the designed bio-nanosensor. The intended outcomes of the experimental study are testbed, in vitro prototype and a patent of the constructed bio-optical brain interface. The project will involve 4 graduate students (2 PhD and 2 Master), who will acquire multidisciplinary expertise and research training. We have secured use the laboratories required for our research. This project will have a significant scientific and technological impact, especially in the field of medical applications and neuroscience.

Design of an Optical Brain Interface: Bio-Neural Dust

RESEARCH CONTEXT AND LITERATURE REVIEW

The rapid and impressive advancements in nanotechnology have paved the way for new emerging applications in medicine, biosensing and nanonetwork design, which were previously impossible. One of these new emerging applications is the use of light to communicate at the nanoscale. Compared to radio-frequency radiation, light is characterized by high photon energy, very high frequency and very small wavelength, which makes nanoscale interactions feasible. The design of a nanonetwork that can broadcast information optically can lead to very interesting applications, especially in neuroscience by using optogenetics. Optogenetics has the potential not only to realize the dream of understanding neural circuits at single-cell precision level, but also to provide insights into new regenerative medicine protocols, new molecular targets for drug development and other strategies targeting the repair of the brain [1].

Size miniaturization of optical technologies has been one of the current trends in the photonics field. Recent fabricated micro-/nanofibers (MNFs) have aroused great interest. Intensive work has been published related to the design and evaluation of these tiny fibers that are having diameters close to or below the wavelength of the guided light [2]. However, despite the very attractive properties of MNFs, their precision and sensitivity need to be improved and they still have significant challenges to resolve related to both theoretical research and their use in practical applications. Environmental contamination is another challenge that needs to be tackled, because ultrasensitive sensors require extreme cleanness, especially when designed for long-term operations [3]. These remaining challenges make use of these tiny fibers impractical, especially *in vivo* (inside the body) medical applications and for neuro-stimulation. The design of beamforming optical antenna arrays for use in nano-bio sensing was proposed recently [4]. The authors designed a bow-tie optical antenna that uses plasmonic waves and active phase control to allow dynamic beamforming. Nonetheless, the materials used to fabricate such antenna arrays are not biocompatible, which limits their use *in vivo* applications. In addition, the antenna array is fixed in space, which makes it more suitable for usage for *in vitro* than *in vivo*.

Neural dust is a promising technology for achieving wireless neuro-stimulation at single neuron precision level. It is called dust because it contains thousands of independent, floating, small-scale sensor nodes that detect and report local extracellular data. The neural dust system proposed in [5] consists of three communication layers: an external transceiver with a long-range transmitter inserted from the outside, an ultrasound sub-dural transceiver implanted under the skull and independent neural dust sensing nodes dispersed throughout the brain. However, this system is only limited to monitoring neurons and transmitting reports to the sub-dural transceiver via backscattering. The study in [6] proposed an enhancement to the system proposed in [5] by integrating the wireless optogenetic component to the neural dust. The wi-opt neural dust in [6] added a Light Emitting Diode (LED) unit and piezoelectric nanowires allowing the system to stimulate neurons with light and harvest energy generated by ultrasound waves. Nevertheless, despite their small size, these devices are still very large compared to the

size of a neuron (they are at millimeter level vs the nanometer/micrometer level of cells), which makes their use in monitoring and stimulation at single-neuron precision level or placement within the brain at very high granularity level practically impossible. In addition, CMOS technology is reaching its limits in terms of miniaturization due to quantum phenomena, making the control of CMOS sensors at the nano level very challenging.

PROBLEM STATEMENT AND OBJECTIVES

The brain stimulation at single neuron precision level faces two problems; size miniaturization and biocompatibility. In the optogenetics literature, we either find systems with no biocompatibility [5], [6], or biocompatible systems but with size considerably larger compared to the size of neurons [7].

Aim of this project is to design, evaluate and implement an optogenetics-based bio-optical brain interface at the nano level, which can be used non-invasively inside the human body and is capable of monitoring and stimulating neurons at single cell precision level. The proposed optical brain interface can be very useful to many medical applications such as treating Parkinson's disease and neutralizing epileptic seizures as well as offering a new way to kill pain rapidly at specific and very localized areas of the body, without use of drugs. The project will follow the objectives below:

- Design and evaluate a single nanosensor capable of emitting light, receiving light and be powered using ultrasonic waves.
- Study the optical connection between two nanosensors, a source and an actor.
- Study and evaluate a network of optical nanosensors, which will construct the optical brain interface.
- Implement simulators, testbeds, and produce a prototype of the proposed bio-optical brain interface.

Outcomes will be published in patents and academic research papers published in highly reputable journals and conferences.

OUTLINES OF TASKS

Analytical Study:

- First, we will design a biosystem capable of harvesting mechanical energy, converting it into electricity using the piezoelectric properties of M13 virus. Initially we will implement a 3D model of the virus in order to study its mechanical and piezoelectric parameters. We will convert the mechanical process to an equivalent circuit and approximate the values of its components based on the simulation results.
- Second, we will design a biosystem that uses photoproteins, which generate bioluminescent blue light in the presence of Ca^{2+} ions. The Ca^{2+} ions release is triggered by electrical inputs. We will model the system with an equivalent circuit and derive the expressions for the circuit's components. We will analyze the circuit and calculate the intensity of the emitted light that is necessary to stimulate a neuron. This

analysis will allow us to make accurate estimates for the bio-components involved in the implementation of the prototype.

- Third, we will merge the two proposed equivalent circuits into a single one, which models the proposed bio-nanosensor. We will study the equivalent circuit analytically and numerically as well as study the output response and behavior of the bio-nanosensor for a variety of different inputs. We will then use the resulting output as input to a neuron model and study the generated action potential.
- Fourth, after studying the response and behavior of a single bio-nanosensor with a single neuron, we will increase the complexity of the system and study the interaction between multiple bio-nanosensors in order to understand its behavior when stimulating multiple neurons. We will also study the behavior of the system in three scenarios; 1) wired stimulation of neurons by using actin filaments as nanowires between nanosensors, 2) wireless stimulation with optogenetics and 3) a combination of wired and wireless stimulations.

Construction of the system and Experimental Study

- First, we will construct bacteriophage M13 in the laboratory with its PVIII coat major proteins. We attach the constructed M13 with electrodes using gold coated flexible substrates. Then, we will test the piezoelectric properties of M13 *in vitro*. We will measure the obtained current when stimulating M13 mechanically with ultrasound waves. If the constructed bacteriophage uses malign substances, a toxicity test will be conducted and the results will be made public.
- Second, we will construct a transparent nanosphere using polymers and inject calcium ions and photo-proteins into it to generate a bioluminescent reaction. We will place an endoplasmic reticulum (ER) inside the nanosphere, which functions as storage space for calcium ions as shown in Fig. 1. We will measure *in vitro* the light intensity emitted by the engineered transparent nanosphere.
- Third, we will connect the constructed M13 and ER with a nano-wire (materialized using actin filaments) inside the engineered nanosphere. We will generate an ultrasonic signal which will be converted to electricity by M13 and stimulate the ER. The stimulated ER secretes calcium ions triggering the bioluminescent reaction between calcium ions and photoproteins. We will measure the intensity of emitted light for different ultrasonic intensities. Finally, we will stimulate a neuron *in vitro* using optogenetics and the emitted light by the transparent nanosphere (bio-nanosensor), then, several neurons will be stimulated by a network of bio-nanosensors and we will study the behavior of the group.

WORK PLAN AND OUTCOMES

The proposed research is divided into 4 work packages (WPs). WPs will be completed within the following time intervals. WP1: Jan. to April 2024. WP2: May to Aug. 2024. WP3 Sept. to Dec. 2024. WP4: Jan. to Nov. 2025.

- **WP1:** Design and evaluate a single nanosensor by modeling it as an equivalent circuit. The designed nanosensor contains a piezoelectric part that harvests the energy of ultrasonic waves and a bioluminescent part that receives electricity and emits light.

Outcomes: Patent, journal and conference papers reporting on the designed bio-nanosensor.

- **WP2:** Study the optical connection between two nanosensors by deriving the expression of the energy transfer rate, which is influenced by the calcium concentrations inside/outside the nanosensors, the number of photoproteins inside the nanosensor and bound to its membrane. Derive the expression of the energy transfer efficiency of the optical connection, which is influenced by the distance between the two nanosensors, the refractive index of the medium and the absorption of ChR2.
  Outcomes: Journal and conference papers reporting on the optical connection between two designed nanosensors and its rate and efficiency.
- **WP3:** Design the structure and evaluate the performance of a network formed by the proposed optical bio-nanosensors. The transmission of information between sources and actors in the proposed system is a birth-death process, which can be modeled by a Markov chain. We will also derive a closed form expression for the probability of successful triggering of light emission throughout the whole entire optogenetics nanonetwork.
  Outcomes: Journal and conference papers reporting on the optical nanonetwork, its behavior and performance.
- **WP4:** Implement a laboratory testbed and produce an actual prototype of the proposed system. Produce a bio-nanosensor (containing both its piezoelectric and optical parts). Then, test the connection between two nanosensors *in vitro* in a Lab-On-a-Chip and extend the system to become a network of these bio-nanosensors. We will genetically modify a neuron by adding opsins to its membrane, extract it and stimulate it *in vitro* with one bio-nanosensor. Then, we will stimulate several neurons with the extended network of bio-nanosensors (Bio-Neural Dust). We will also implement a wired network with self-assembled actin filaments, which we proposed in our recent studies, and evaluate the performance of a combination between wired and optical nanonetworks.
  Outcomes: Patent, journal and conference papers reporting on the experimental study. Testbed and a prototype of the optical brain interface.

IMPACT

Optogenetics has a critical place in neuroscience and brain related medicine. The development of optics and molecular genetics has provided breakthroughs in our ability to detect and manipulate neural activity and has enhanced immensely our understanding of brain operation. Claiming that optogenetics has the potential to revolutionize neuroscience and brain medicine is far from an overstatement.

The outcomes of this project will lead to the development of new diagnostics techniques and treatments. The proposed optical brain interface will be useful to the treatment of several medical conditions such as Parkinson's disease and epilepsy as well as fast, localized, drugs free pain relief. The project will involve 2 PhD and 2 Master graduate

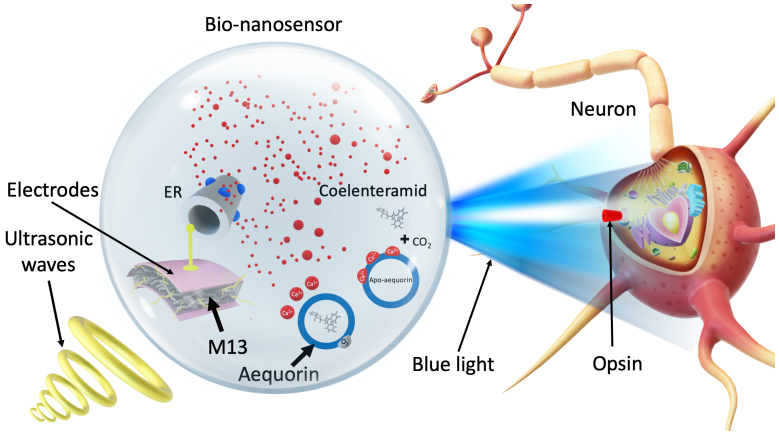

Fig. 1. Design of a bio-nanosensor in the proposed optical brain interface.

students. The PhD students will be funded from the project. The project's nature is multidisciplinary. It requires skills from the electrical and computer engineering, biology and neuroscience. The applicants' graduate and undergraduate studies enable them to have skills in the mentioned areas. We have already secured the right to use the electrical/electronic and biology laboratories we need to carry out our research. It should be noted that the multidisciplinary nature of the project will provide the students with multidisciplinary training, thus enhancing their marketability in all sectors of the high-tech work market; academia, private and public sectors. Therefore, this project will have a significant scientific and technological impact, especially for medical applications in the field of neuroscience. We will also provide several graduate students to acquire unique multidisciplinary knowledge and research skills. Journals and conference publications are anticipated. Also, as mentioned earlier, patents (to secure intellectual property) are expected as well.

REFERENCES

[1] Boyden, Edward S. "Optogenetics and the future of neuroscience." Nature Neuroscience 18 (2015): 1200-1201.
[2] Hironaga Maruya, Yasuko Oe, Hideaki Takashima, Azusa N. Hattori, Hidekazu Tanaka, and Shigeki Takeuchi, "Non-contact detection of nanoscale structures using optical nanofiber," Opt. Express 27, 367-376 (2019).
[3] Lei Zhang, Yao Tang, Limin Tong, "Micro-/Nanofiber Optics: Merging Photonics and Material Science on Nanoscale for Advanced Sensing Technology", iScience, Volume 23, Issue 1, 2020.
[4] Amit Sangwan, Josep M. Jornet, "Beamforming optical antenna arrays for nano-bio sensing and actuation applications," Nano Communication Networks, Volume 29, 2021.
[5] Seo, Dongjin et al. "Neural Dust: An Ultrasonic, Low Power Solution for Chronic Brain-Machine Interfaces." arXiv: Neurons and Cognition (2013).
[6] Wirdatmadja, Stefanus A. et al. "Wireless optogenetic neural dust for deep brain stimulation." 2016 IEEE 18th International Conference on e-Health Networking, Applications and Services (Healthcom) (2016): 1-6.
[7] K. Laursen, A. Rashidi, S. Hosseini, T. Mondal, B. Corbett and F. Moradi, "Ultrasonically Powered Compact Implantable Dust for Optogenetics," in IEEE Transactions on Biomedical Circuits and Systems 14 (2020): 583-594.

EXECUTIVE SUMMARY

We write to propose the integration of ultraviolet (UV) light sources into compact, energy-efficient devices for water treatment. This innovative approach utilizes optics and photonics to address the global challenge of providing clean and safe drinking water to regions facing water scarcity or contaminated water sources. In underdeveloped nations like Ghana, the majority of the people reside in rural areas where it is challenging to find clean and portable drinkable water. The water is drawn from river water which is contaminated with many dirty particles including animal and human excreta. The river water or contaminated water is infected with dangerous bacteria, protozoa, or viruses, and is highly unhygienic. The issue is that these rural settlers lack a developed infrastructure such as electricity. The continuous drinking of unhygienic has resulted in a lot of infectious ailments among the people in rural areas. The main objective of this research is to find a solution that provides people in deprived nations with portable drinking water. In this regard, it is especially important to design portable and effective water purifying systems for rural residents in selected rural communities in Ghana. The project will be piloted in six (6) communities and thirty (30) households in Ghana. The solution describes the steps involved in the proposed water purification system that uses a UV-LED source as a disinfectant and automated solar energy equipment. The proposed solution will provide users with refreshing clean purified water that has gone through treatment with the UV-LED source and a solar energy system. The system will be named 'nsupa UV-LED water purification system'. The simplified design of the nsupa UV-LED water purification system will allow for easy deployment in remote or disaster-stricken areas, ensuring access to clean drinking water in emergency situations. The treated water would be tested by a qualified microbiology and chemical scientist to confirm the quality of the water to ensure it is good for human consumption. After the successful completion of the pilot, the project could be rolled out in other rural communities and nations.

Proposal for the Integration of Ultraviolet (UV) Light Sources into Compact, Energy-Efficient Devices for Water Treatment

Proposed Title: nsupa UV-LED water purification system

Project Team

i. Dr. Owusu Nyarko-Boateng [University of Cincinnati, Ohio, USA]
ii. Dr. Isaac Kofi Nti [University of Cincinnati, Ohio, USA]
iii. Ing. Dr. Danlard Iddrisu [Sunyani Technical University, Sunyani, Ghana]
iv. Dr. Bernice Yram Danu [University of Energy and Natural Resources, Sunyani, Ghana]
v. Eng. Frimpong Kyeremeh [Sunyani Technical University, Sunyani, Ghana]

LITERATURE REVIEW

This project aims at using a UV-LED source to purify contaminated water. This process, according to the literature [1], [2], [3] has been deployed in various forms where the contaminated water runs through UV-integrated tubes for disinfection. In our project, we introduce energy-efficient UV-LED bulbs which receive a power supply from a solar energy system. For easy usage and handling of the proposed system, the UV-LED source would be embedded in a water storage container for thorough purification.

According to research [2], [4], [5], [6], a fixed percentage of the living population of microorganisms that are exposed to UV radiation is rendered inactive with each passing period of time. In their experiment, [4,7,8] said that the impact of the dose of germicidal high-intensity UV light delivered briefly to treat contaminated water would be equally effective at killing as lower-intensity UV energy delivered over a proportionately longer length of time. Site-specific information on the required log removal and water quality is used to calculate the UV dose needed for efficient inactivation [2], [5]. Microorganism survival can be estimated as a function of dose and contact time [2].

In contrast to most disinfectants, UV radiation does not trigger a chemical response that would make microorganisms dormant. UV radiation makes organisms inactive by making them absorb light. The molecular foundation of the components that make up the cell's function is impacted by this photochemical process [7].

The cell wall of a microorganism is permeable to UV rays, which interact with nucleic acids and other vital components of the organism to harm or kill exposed cells. Ultraviolet illumination functions very similarly to fluorescent lighting. The lamp differs from the other two lights in that it has a fluorescent bulb and is covered with phosphorous, which converts UV energy into visible light. Because the UV lamp is exposed, ultraviolet radiation from the arc is transmitted. With the help of photovoltaic systems and ultraviolet light radiation, this study verifies the efficacy of a design for an autonomous device for water purification [2].

PROBLEM STATEMENT/OBJECTIVES

Access to clean water is a pressing issue affecting millions of people globally. Traditional water treatment methods often fall short of effectively eliminating pathogens, bacteria, viruses, and organic pollutants, thereby compromising the safety and quality of drinking water. By leveraging the power of UV light, we can achieve highly efficient and environmentally friendly water purification [2], [3].

Over 2 billion people, or almost half of the population of the world, live in water-stressed nations, a situation that is even projected to get worse in some of these nations due to population increase and climate change. According to World Health Organization (WHO), at least 2 billion people across the globe consume water that has been contaminated with human and animal feces. The biggest threat to drinking water in these rural communities is the presence of these microbial organisms in the water bodies. Some emerging pollutants such as pesticides, medicines, detergents, and polyfluoroalkyl substances (PFASs), as well as microplastics, are major causes of water pollution in these nations. Illegal mining and other small-scale mining activities in developing nations are also a major threat to water pollution [1], [4], [5].

The primary objective of this proposal is to develop compact, energy-efficient devices that utilize UV-LED light sources for water treatment. By integrating advanced optics and photonics technologies, we aim to enhance the disinfection process and ensure the delivery of safe drinking water to communities in need of portable drinking water.

OUTLINE OF TASKS/WORK PLAN

Negative health impacts from waterborne infections result from polluted water exposure. Diarrhea, giardiasis, dysentery, typhoid sickness, and salmonellosis are a few frequent ailments that affect people as a result of drinking contaminated water. Aside from other symptoms, adverse health impacts might include discomfort in the nervous, reproductive, and gastrointestinal systems. Long-term health effects may result from repeated exposure [1], [2]. People in these communities need portable and clean water for cooking, washing, and drinking. The proposed solution will provide users with refreshing clean purified water that has gone through treatment with the nsupa UV-LED water purification system. The name ‘nsupa’ is a Ghanaian Akan language that literally means ‘good water’.

Compact and Portable Design

The proposed solution will use state-of-the-art UV light sources from light-emitting diodes (LEDs) embedded into a solar-powered lid of a water container designed to disinfect water from stored contaminated water. The designed LED bulbs emit UV radiation with germicidal properties, that is able to effectively inactivate microorganisms and destroy contaminants. Advanced optical components, including reflectors and diffusers, will be integrated into the devices to optimize UV light distribution and enhance energy efficiency. These components will be designed and engineered to maximize the exposure of water to UV radiation, ensuring thorough disinfection throughout the treatment process. The proposed nsupa UV-LED water purification system is shown in Figure 1.

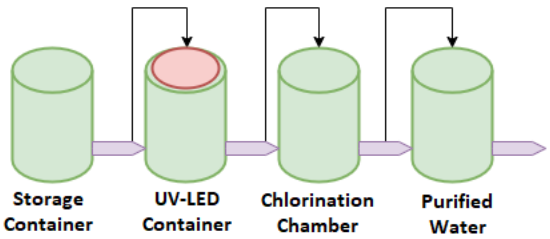

Figure 1: proposed water purification process

Storage Container

The container will store 275 gallons of contaminated water for a specified time so that dirt and other particles can settle at the bottom of the storage container before the water is transferred into the UV-LED container. Ideally, water in this container must be stored for 12-24 hours. All containers must be thoroughly washed and cleaned in 3 storage and purification process.

UV-LED Container

Water stored in the storage chamber for 12-24 hours will be released through a valve into the UV-LED chamber. The UV-LED container comprises an open-top 55-gallon (208 liters) plastic drum with a lid. The Energy-efficient UV light sources, called UV-LEDs, will be employed to minimize power consumption while maintaining high disinfection performance. Additionally, advanced control systems will be implemented to optimize UV light output and distribution on water to further reduce energy requirements.

To have purified clean water, the UV-LED source will be distributed to reach all parts of the water in the container to destroy every organism in the water. UV irradiation may undoubtedly disinfect the water to any necessary level of disinfection if it is able to reach the organisms with a sufficient amount of UV energy. The ultraviolet energy nsupa UV-LED device will be able to disinfect microorganisms such as bacteria, viruses, and large "protozoa" such as Giardia and Cryptosporidium in the water. The UV-LED bulbs have low-pressure and germicidal properties which emit energy at a wavelength range of 245–285nm. The UV dose has a direct correlation to the level of microorganism inactivation or destruction by UV light. The UV dosage [1] is determined by:

$$D = It$$

where D is a UV dose, mW s/cm2, I is intensity, mW/cm2, t is exposure time, s.

Energy efficient system

In order to have a continuous supply of efficient energy systems, a solar power system has been proposed. The solar power system will comprise a photovoltaic cell, cables, inverter, and a battery. This solution will ensure that rural communities can use the nsupa UV-LED water purification device at any time of the day. The purpose of nsupa UV-LED water purification solution is to purify contaminated water for the selected rural communities.

Using the UV- LED bulb for:

i. 1 hour per day uses 0.07 kWh per week, 0.30 kWh per month, and 3.65 kWh per annum of electricity.
ii. 2 hours per day results in the use of 0.14 kWh in a week, 0.61 kWh in a month, and 7.30 kWh per annum.
iii. 3 hours per day use 0.21 kWh per week, 0.92 kWh per month, and 11.0 kWh per annum.

Safety features, such as automatic shut-off mechanisms and fail-safe systems, will be incorporated to prevent any potential risks associated with UV radiation exposure and ensure the devices operate at optimal performance.

Chlorination Chamber

Water treated from the UV-LED chamber is expected to be clean and safe for consumption but to ensure quality drinking water, the water from the UV-LED chamber will further go through a chlorination process. Chlorination is the process of adding chlorine to drinking water to kill parasites, bacteria, and viruses [8]. The appropriate measurement of chlorine would be applied to achieve safe levels of chlorine in the treated water.

Purified Water Chamber

This chamber is the final stage of the UV-LED water purification process. The purified water chamber will store water that has been processed to remove impurities like chemicals and other contaminants by the UV-LED solar-powered device.

BUDGET

A detailed budget outlining the required funds to cover the research including the designing, development, testing, fabrication, and community deployment of the project has been attached to this document.

No	item	Description	Cost ($)	Total cost ($)
i	Photovoltaic panel, inverter, battery, and cables.	The items will be used for the energy-efficient system (40 pieces will be made).	15,000.00	**15,000.00**
ii	Drums	200 drums for the purification process. Valves, connectors, and PVC pipes.	12,000.00	**12,000.00**
iii	UV-LED bulbs	Design and manufacturing of the proposed UV-LED bulbs	16,000.00	**16,000.00**
iv	UV-LED and storage drum fabrication	Fabrication and embedding UV-LED bulbs onto the lid.	10,000.00	**10,000.00**
v	Transportation and flight	Cost of traveling to manufacturing and sales points	12,000.00	**12,000.00**
vi	Allowance for the research team		20,000.00	**20,000.00**
vii	Miscellaneous		5,000.00	**5,000.00**
viii	Institutional overhead cost		10,000.00	**10,000.00**
ix	**Total**			**100,000.00**

Timelines

The proposed duration of the project will be eight (8) months. From the day the selection committee announces that this project has been selected, the team will kick the process started.

OUTCOME(S)

The integration of UV-LED light sources will enhance the disinfection process, effectively eliminating pathogens, bacteria, viruses, and organic pollutants, resulting in cleaner and safer drinking water. The use of energy-efficient UV-LED light sources and advanced control systems will minimize power consumption, reduce operational costs, and environmental impact, which will result in improved health conditions in rural communities.

IMPACT

The project seeks to purify contaminated water in rural communities where access to clean and portable water is not available. The project will target about 6 communities and 30 households. Bringing portable water so such people will bring huge relief and save them from waterborne diseases. In addition, the integration of UV-LED light into water treatment devices promotes sustainable quality health among rural settlers.

CONCLUSION

The integration of UV light sources into compact, energy-efficient devices for water treatment in rural communities in deprived nations is a life-saving innovation. The simplified design of the nsupa UV-LED water purification system will allow easy deployment in remote or disaster-stricken areas, ensuring access to safe drinking water in emergency situations. The treated water would be tested by a qualified microbiological and chemical scientist to confirm the quality of the water to ensure it is good for human consumption.

REFERENCES

1. Radjabov, A., Berdishev, A.S. & Mussabekov, A.T. Autonomous Complex for Water Disinfection in Rural Areas of Uzbekistan. *Appl. Sol. Energy* **55**, 113–118 (2019). https://doi.org/10.3103/S0003701X19020087
2. Heyi, M.H., Patrissi, D. & Khan, B. Small scale automated water disinfection system for rural areas. *Int. J. Environ. Sci. Technol.* (2023). https://doi.org/10.1007/s13762-023-04760-9
3. Amin N, Crider YS, Unicomb L, Das KK, Gope PS, Mahmud ZH, Islam MS, Davis J, Luby SP, Pickering AJ (2016) Field trial of an automated batch chlorinator system at shared water points in an urban community of Dhaka, Bangladesh. J Water Sanitation Hygiene Develop 6 (1):32–41. 1 Mar 2016. https://doi.org/10.2166/washdev.2016.027
4. Berdyshev, A.S., Anarbaev A.I., et al., Autonomous installation for water purification, RUz Patent IAP no. 05371, 2017.
5. Berdyshev, A.S., Radzhabov, A., and Ibragimov, M., *Obezzarazhivanie podzemnykh pit'evykh vod impul'snymi ehlektromagnitnymi polyami* (Disinfection of Underground Drinking Water by Pulsed Electromagnetic Fields), Tashkent: 2008.
6. Berdyshev, A.S., Radzhabov, A., Ibragimov, M., and Anarbaev, A.I., Energy efficient method of disinfecting water by ultraviolet radiation, *Probl. Energo Resursosberezh.*, 2012, no. 3–4, pp. 115–120.
7. Berdyshev, A.S., Use of alternative energy sources for water disinfection using ultraviolet installations, *Irrigats. Meliorats.*, 2016, vol. 3, no. 1, pp. 41–44.
8. Gámiz J, Grau A, Martínez H, Bolea Y (2020) Automated chlorine dosage in a simulated drinking water treatment plant: a real case study. Appl Sci 10:4035. https://doi.org/10.3390/app10114035

Germicidal UV Dosage Index Levels (GUV-DIL) for UV-C LEDs based Photonic Disinfectants, Sustainable Solution Again Diseases Transitions in Healthcare Facilities on the Hearth now and on the Spaces Villages Tomorrow

Dr. Ing. Pablo Fredes[1]

Executive Summary

Resume

The use of mercury (Hg) free germicidal UV sources are increasing every day. The Hospital Acquired Infections (HAIs) on Hearth and the Infection Prevention and Control during Prolonged Human Space Travels, and inhabiting Spaces Villages is a great challenge, that's we are boarding supporting by the new LEDs germicidal UV sources and the Germicidal UV Dosage Index Levels (GUV-DIL). Our main beneficiaries will be users, professionals and staff of the Healthcare Services now, and the space travelers in the near future, they are hiring us to make improvements in the cleaning and disinfection practices in Healthcare Facilities and in the space shuttles, spatial Stations and in the future Spatial Villages.

Introduction

Of all preventable infections on the Hearth, the one that causes the most concern is the Hospital Acquired Infections (HAIs), there as the eighth leading cause of death in the United States, just after diabetes (79,535 deaths in 2015). The two main causes of the appearance of HAIs have relation with the thoroughness of the cleaning and disinfection processes, applied for the surfaces and the airborne transitions. Every year more and more studies appear providing strong evidence supporting the effectiveness of the Photonic Disinfection (UV disinfection technologies) improving the Indoor Air Quality (IAQ) and the cleaning and disinfection levels of the surfaces. Photonic Disinfectants are being a key tool in the fight against HAIs, especially those caused by Antibiotic Resistant Microorganisms. On the other hand, the UV LEDs based emitters appears as a sustainable and mercury (Hg) free option to provide the appropriated UV light source for the innovative photonics disinfectant systems, that's are an indispensable tool again HAIs, and will be indispensable for the prolonged human spaceflight, and the development and building of the future Space Village Projects. To take optimal advantage of the disinfectant capacity of UV LED based photonic solutions, an Germicidal UV Dosage Index Levels (GUV-DIL) is need. We propose a simple and fast reading dosage scale that's relates the applied photonics dose by the devices (or systems) with the desired sanitation level. The top index level of GUV-DIL will be relate with the Spatial Sanitation index level. This index level of sanitation will be needed in the prolonged human spaceflight, in the Spatial Stations and for the future Spatial Villages.

Outcomes: Germicidal UV Dosage Index Levels (GUV-DIL) and Level of sanitation achieved.

Accurate UV light validation plays a crucial role in effective sanitization practices, particularly in the healthcare industry and in Space travels, Spatial Stations and Spatial Villages. By understanding the importance of UV light in eliminating pathogens, we can ensure a safe environment for the patients, healthcare professionals and spaces travelers. By incorporating Germicidal UV Dosage Index Levels (GUV-DIL) into the sanitization protocols, you can confidently monitor and validate the applied germicidal UV dose, thereby enhancing the safety and well-being of patients, professionals and staff.

[1]Acknowledgments to: Dr. Ulrich Raff, Prof. Blanca Troncoso form University of Santiago, Chie, and Mr. Cristobal Rios Director of Hydraluvx, Chile to its valuable comments, suggestions and corrections.

Germicidal UV Dosage Index Levels (GUV-DIL) for UV-C LEDs based Photonic Disinfectants, Sustainable Solution Again Diseases Transitions in Healthcare Facilities on the Hearth now and on the Spaces Villages Tomorrow

Dr. Ing. Pablo Fredes[1]

All things are poison, and nothing is without poison;
the dosage alone makes it so a thing is not a poison.
Paracelsus, 1538

...It's all about saving lives.
Troy Cowan
IUVA Healthcare Working Group. 2020

...It's all about safe the life on hearth and Space
Pablo Fredes 2023

Abstract

The use of mercury (Hg) free germicidal UV sources are increasing every day. The Hospital Acquired Infections (HAIs) on Hearth and the Infection Prevention and Control during Prolonged Human Space Travels, and inhabiting Spaces Villages is a great challenge, that's we are boarding supporting by the new LEDs germicidal UV sources and the Germicidal UV Dosage Index Levels (GUV-DIL). Our main beneficiaries will be users, professionals and staff of the Healthcare Services now, and the space travelers in the near future, they are hiring us to make improvements in the cleaning and disinfection practices in Healthcare Facilities and in the space shuttles, spatial Stations and in the future Spatial Villages.

1. Introduction

Of all preventable infections on the Hearth, the one that causes the most concern is the Hospital Acquired Infections (HAIs), there as the eighth leading cause of death in the United States, just after diabetes (79,535 deaths in 2015). The two main causes of the appearance of HAIs have relation with the thoroughness of the cleaning and disinfection processes, applied for the surfaces and the airborne transitions. Every year more and more studies appear providing strong evidence supporting the effectiveness of the Photonic Disinfection (UV disinfection technologies) improving the Indoor Air Quality (IAQ) and the cleaning and disinfection levels of the surfaces. Photonic Disinfectants are being a key tool in the fight against HAIs, especially those caused by Antibiotic Resistant Microorganisms. On the other hand, the UV LEDs based emitters appears as a sustainable and mercury (Hg) free option to provide the appropriated UV light source for the innovative photonics disinfectant systems, that's are an indispensable tool again HAIs, and will be indispensable for the prolonged human spaceflight, and the development and building of the future Space Village Projects. To take optimal advantage of the disinfectant capacity of UV LED based photonic solutions, an Germicidal UV Dosage Index Levels (GUV-DIL) is need. We propose a simple and fast reading dosage scale that's relates the applied photonics dose by the devices (or systems) with the desired sanitation level. The top index level of GUV-DIL will be relate with the Spatial Sanitation index level. This index level of sanitation will be needed in the prolonged human spaceflight, in the Spatial Stations and for the future Spatial Villages.

[1]Acknowledgments to: Dr. Ulrich Raff, Prof. Blanca Troncoso form University of Santiago, Chie, and Mr. Cristobal Rios Director of Hydraluvx, Chile to its valuable comments, suggestions and corrections.

2. The Hearth: Public Health´s Big Challenge

2.1. The global healthcare system is under tremendous pressure.

One thing all healthcare stakeholders agree on is that our global health systems are near breaking point. The aging population and increasing incidence of chronic disease, in combination with innovative, but high cost technologies and new powerful drugs, have led to an unsustainable cost explosion in healthcare, and it is not surprising that the pressure is mounting [1].

Preventing healthcare-associated infections (HAIs) has been declared as a top priority for CDC and its partners in public health and healthcare [2]. HAIs, also known as nosocomial infections, are those that are not initially present or incubating when healthcare is initiated but that subsequently develop in relation to healthcare exposure. The most recently published numeric data, estimated that the number of HAIs in U.S. hospitals achieve to 687,000, and the number of deaths remained high at 72,000 [3], [4]. This placed HAIs as the eighth leading cause of death in the United States, just after diabetes (79,535 deaths) [5]. The HAIs rates is even higher in third world countries.

The cost estimates for hospital-onset HAIs from varying cost perspectives, including the economic burden to the U.S. healthcare system and excess payments made by insurers such as Medicare, are enormous [6]. While previous studies by healthcare providers have estimated an economic burden of approximately $10 billion annually for HAIs, a more contemporary examination of the impact of societal costs included the economic value of mortality risk reductions, thereby giving an estimate for the total economic burden to society in excess of $200 billion annually, only in USA [5].

2.2. Indoor Air Quality, Surface Sanitation and its relation with HAIs

Figure 1 illustrates different pathways of virus transmission classified into two distinct categories: (1) air transmission of viruses in droplets exhaled by infected individuals and inhaled by healthy individuals; and (2) surface transmission of viruses deposited on surfaces from either exhalations or hand contact. Infected individuals may spread viruses through coughing and sneezing but also through breathing and speaking in the presence of healthy, susceptible individuals [7].

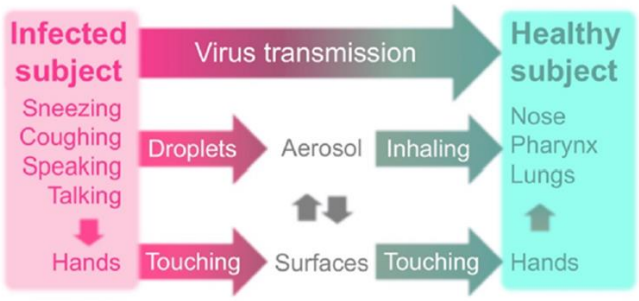

Figure 1, Pathways of viral infection in everyday life in indoor spaces [7].

2.2.1. Surface diseases Transmission

The transmission HAIs by factors related to patient contact with contaminated surfaces has a higher incidence than previously believed. Surfaces such as furniture, doors, and portable and touch-controlled devices are being now considered as potential sources of nosocomial infections, and, consequently, new methods have been sought for surface disinfection [8]–[13]. Improper disinfection of rooms and corridors puts patients at risk. Pathogens can remain on surfaces and be transmitted from one person to another through surface contact. Results from a study carried out in 23 hospitals

in the United States showed that between 40 % and 50 % of the surfaces of the patients' rooms, which must be disinfected by cleaning staff, are not adequately sanitized [14]. The characteristics of a health center, plus the recent incorporation of portable monitoring devices, including mobile phones, mean that there is always the possibility of exchanging microbial agents, as has been demonstrated in outbreaks associated with failures in the sterilization process and disinfection [15].

2.2.2. Airborne diseases Transmission

According to the work of Wang et al. entitled "Airborne transmission of respiratory viruses", which has been published by Science in August of 2021 it can be claimed that Airborne transmission of pathogens has been vastly underappreciated, while we must acknowledge that airborne transmission is much more prevalent than previously recognized and eventually understood. Given all that we have learned about SARS-CoV-2 infection, the aerosol transmission pathway needs to be reevaluated for all respiratory infectious diseases implying long and complex experimental procedures. Additional precautionary measures must be recognized and implemented for mitigating aerosol transmission, with particular attention inter alia, to ventilation, airflows, air filtration and UV LED based photonic solutions for air disinfection [16].

3. UV LEDs a mercury free germicidal radiation source

The Ultraviolet light emitting diodes (UV-C LEDs) are solid-state semiconductor devices. With an applied voltage, electrons are 'pushed' across an energy barrier (band gap) separating differently charged layers within the LED crystal structure. Once across the barrier, these electrons can lose the energy gained in the transition and emit a photon. Commercial UV LEDs are formed with thin crystalline aluminum gallium nitride (AlGaN) layers deposited onto a substrate (sapphire or aluminum nitride); while the ratio of aluminum to gallium in the thin layers determines the band gap and therefore the emission spectrum emitted by the LED [17], [18].

4. Infection Prevention and Control during Prolonged Human Space Travel and inhabiting Spaces villages

Prolonged human spaceflight to another planet or an asteroid will introduce unique challenges of mitigating the risk of infection.

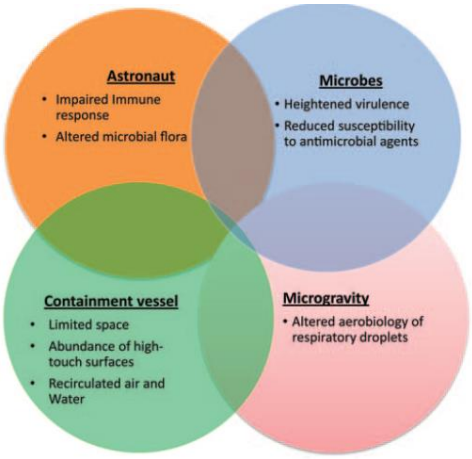

Figure 2, Variables that impact the risk of infectious diseases and their transmission during space travel[22].

During space travel, exposure to microgravity, radiation, and stress alter human immune regulatory responses, which can in turn impact an astronaut's ability to prevent acquisition of infectious agents or reactivation of latent infection [19], [20]. In addition, microgravity affects virulence, growth kinetics, and biofilm formation of potential microbial pathogens [21]. These interactions occur in a confined space in microgravity, providing ample opportunity for heavy microbial contamination of the environment. In addition, there is the persistence of aerosolized, microbe-containing particles. Any mission involving prolonged human spaceflight must be carefully planned to minimize vulnerabilities and maximize the likelihood of success [22].

5. Germicidal UV Dosage Index Levels (GUV-DIL) and Level of sanitation achieved.

Accurate UV light validation plays a crucial role in effective sanitization practices, particularly in the healthcare industry and in Space travels, Spatial Stations and Spatial Villages. By understanding the importance of UV light in eliminating pathogens, we can ensure a safe environment for the patients, healthcare professionals and spaces travelers.

By incorporating Germicidal UV Dosage Index Levels (GUV-DIL) into the sanitization protocols, you can confidently monitor and validate the applied germicidal UV dose, thereby enhancing the safety and well-being of patients, professionals and staff.

6. Outline of tasks/Work Plan

For the creation of the standard GUV-DIL is needed a work plan to follow, that's is composed by 3 stages of implementation

Stage 1: Identification of the State of the art of each discipline related with its multidisciplinary challenge. (Photonics, engineering, medical care, epidemiology, microbiology, pharmacology, infectology, nursing, etc.)

Stage 2: Establishment of an Official research group as a work force for the creation of the GUV-DIL.

Stage 3: Development of official White Papers publications, and peer reviewed publications. In parallel the creations of an integration web platform and were the disciplines identified on the previous stage and the stakeholders, can find all technical and scientific information required to support the criteria used in the new Germicidal UV Dosage Index Levels (GUV-DIL).

7. Outcomes declared

The outcomes will be an standardized germicidal UV dose index levels, inspired in the previous UV index scale for sunlight protection. This previous index scale, define eleven no dimensional energy levels of UV from the sunlight. The UV index relates the UV energy with the levels of protection needed, stablishing actions to protect our health from the UV rays from the sun.

Figure 3, UV Index scale and its relation with safety and preventive action required.

Finally, our project will introduce the new GUV-DIL concept, to make simple, understandable, safe and effective the use of the UV LED based photonic solutions for surface and air disinfection, in a Healthcare environments and for the prolonged human spaceflight, and the development and building of the future Space Village Projects.

References

[1] Y. Jia, "Designing a project selection toolkit for Philips ' value based care studios," Delft University of Technology, 2019.

[2] Centers for Disease Control and Prevention (CDC), "2021 National and State Healthcare-Associated Infections Progress Report," 2021. [Online]. Available: https://www.cdc.gov/hai/data/portal/progress-report.html.

[3] Centers for Disease Control and Prevention (CDC) and National Center for Emerging and Zoonotic Infectious Diseases (NCEZID), "Healthcare-Associated Infections (HAIs) Data Portal," 2022. https://www.cdc.gov/hai/data/portal/index.html.

[4] S. S. Magill *et al.*, "Changes in Prevalence of Health Care–Associated Infections in U.S. Hospitals," *N. Engl. J. Med.*, vol. 379, no. 18, pp. 1732–1744, 2018, doi: 10.1056/nejmoa1801550.

[5] D. L. Poster *et al.*, "Ultraviolet radiation technologies and healthcare-associated infections: Standards and metrology needs," *J. Res. Natl. Inst. Stand. Technol.*, vol. 126, no. 126014, pp. 1–33, 2021, doi: 10.6028/JRES.126.014.

[6] R. D. Scott, S. D. Culler, and K. J. Rask, "Understanding the Economic Impact of Health Care-Associated Infections: A Cost Perspective Analysis," *J. Infus. Nurs.*, vol. 42, no. 2, pp. 61–69, Mar. 2019, doi: 10.1097/NAN.0000000000000313.

[7] F. J. Garciá De Abajo, R. J. Hernández, I. Kaminer, A. Meyerhans, J. Rosell-Llompart, and T. Sanchez-Elsner, "Back to Normal: An Old Physics Route to Reduce SARS-CoV-2 Transmission in Indoor Spaces," *ACS Nano*, vol. 14, no. 7, pp. 7704–7713, 2020, doi: 10.1021/acsnano.0c04596.

[8] D. L. Poster, R. A. Martinello, C. C. Miller, Y. Obeng, M. T. Postek, and T. E. Cowan, "Innovative approaches to combat healthcare-associated infections using efficacy standards developed through industry and federal collaboration," *Proceeding SPIE Int Soc Opt Eng. 2018*, p. 55, 2018, doi: 10.1117/12.2500431.

[9] J. Boyce, "Use of Light for HAI Reduction," 2020, [Online]. Available: https://www.nist.gov/document/john-boycelight-hai-reduction.

[10] C. C. Tseng and C. S. Li, "Inactivation of viruses on surfaces by ultraviolet germicidal irradiation," *J. Occup. Environ. Hyg.*, vol. 4, no. 6, pp. 400–405, 2007, doi: 10.1080/15459620701329012.

[11] M. Nottingham *et al.*, "Ultraviolet-C light as a means of disinfecting anesthesia workstations," *Am. J. Infect. Control*, vol. 45, no. 9, pp. 1011–1013, 2017, doi: 10.1016/j.ajic.2017.02.016.

[12] M. M. Nerandzic, J. L. Cadnum, M. Pultz, and C. J. Donskey, "Evaluation of an automated ultraviolet radiation device for decontamination of Clostridium difficile and other healthcare-associated pathogens in hospital rooms," *BMC Infect. Dis.*, vol. 12, no. 197, pp. 1–8, 2010, [Online]. Available: http://www.biomedcentral.com/1471-2334/10/197.

[13] J. H. Yang, U. I. Wu, H. M. Tai, and W. H. Sheng, "Effectiveness of an ultraviolet-C disinfection system for reduction of healthcare-associated pathogens," *J. Microbiol. Immunol. Infect.*, vol. 52, no. 3, pp. 487–493, 2019, doi: 10.1016/j.jmii.2017.08.017.

[14] P. C. Carling, M. F. Parry, and S. M. Von Beheren, "Identifying Opportunities to Enhance Environmental Cleaning in 23 Acute Care Hospitals," *Infect. Control Hosp. Epidemiol.*, vol. 29, no. 1, pp. 1–7, 2008, doi: 10.1086/524329.

[15] D. Lia and M. Richard, "Movilde Device Use in Healthcare: New Opportunities for UV Disinfection," *Q1*, 2020.

[16] C. C. Wang *et al.*, "Airborne transmission of respiratory viruses," *Science (80-.).*, vol. 373, no. 6558, 2021, doi: 10.1126/science.abd9149.

[17] I. Gaska, O. Bilenko, S. Smetona, Y. Bilenko, R. Gaska, and M. Shur, "Deep UV LEDs for public health applications," *Int. J. High Speed Electron. Syst.*, vol. 23, pp. 1–10, 2014, doi: 10.1142/S0129156414500189.

[18] M. Shatalov *et al.*, "High power AlGaN ultraviolet light emitters," *Semicond. Sci. Technol.*, vol. 29, no. 8, pp. 8–13, 2014, doi: 10.1088/0268-1242/29/8/084007.

[19] G. Sonnenfeld, "The Immune System in Space, Including Earth-Based Benefits of Space- Based Research," *Curr. Pharm. Biotechnol.*, vol. 6, no. 4, pp. 343–349, 2005, doi: 10.2174/1389201054553699.

[20] N. Guéguinou *et al.*, "Could spaceflight-associated immune system weakening preclude the expansion of human presence beyond Earth's orbit?," *J. Leukoc. Biol.*, vol. 86, no. 5, pp. 1027–1038, 2009, doi: 10.1189/jlb.0309167.

[21] R. Ramamurthy *et al.*, "Space flight alters bacterial gene expression and virulence and reveals a role for global regulator Hfq," *Proc. Natl. Acad. Sci. U. S. A.*, vol. 104, no. 41, pp. 16299–16304, 2007.

[22] R. Weinstein and L. A. Mermel, "Infection prevention and control during prolonged human space travel," *Clin. Infect. Dis.*, vol. 56, no. 1, pp. 123–130, 2013, doi: 10.1093/cid/cis861.

NASCENT: **N**on-G**A**us**S**ian **C**ontinuous Variable Quantum N**E**ural **N**e**T**works

Executive Summary – Information Challenge

Despite being extremely promising emerging technologies, quantum computers face significant challenges in their development and implementation. Inter-disciplinary teams worldwide are dedicated to overcoming these hurdles. However, progress is hindered by fundamental issues such as scalability, end-user friendliness, certification of components and algorithms, and the limited applicability to real-world problems. Photonics simulators have emerged as a highly promising candidate in the realm of quantum computing and quantum simulation, drawing significant attention in fundamental and applied physics and engineering. Machine learning (ML), a highly successful technology of the current era, is focused on tasks such as classification, clustering, and pattern recognition for extensive datasets. The performance of deep learning and many ML architectures, is constrained by the available computing power, which, in turn, is restricted by energy consumption. Optics has the potential to enhance neural networks, enabling faster and more efficient operations.

NASCENT aims to combine the two fields and explore how quantum optical phenomena, such as non-Gaussianity, can significantly enhance classical Machine Learning (ML) techniques to address problems in both quantum physics and classical applications. The project has two main objectives. The first objective is to develop and assess continuous variable non-Gaussian variational quantum simulation, demonstrating its utility in studying the static properties of various quantum many-body systems, ranging from quantum chemistry to lattice field theories. The second objective is to leverage entanglement in non-Gaussian systems as a resource to enhance Quantum Machine Learning (QML) models.

To achieve these objectives, the project will be divided into two working packages. The first working package will focus on demonstrating the performance of a variational quantum eigensolver (VQE) in the continuous variable form with non-Gaussian operation. The novelty of this project lies in the variational ansatz that is scalable, hardware efficient, and can be already included in modern-day technology. The VQE will be applied to bosonic systems, relevant for strongly correlated quantum matter physics, and to high-energy physics models, that can be naturally formulated in the Continuous variable formalism. The second working project will focus on the implementation of a Quantum Neural Network in the continuous variable formalism. Quantum photonic systems present promising potential to enhance the performance of ML architectures. This project will investigate how quantum entanglement can provide an advantage in classification tasks for classical and quantum data.

This is an exceptionally thrilling moment to delve into these subjects, given the increasing efficiency and scalability of quantum devices based on photonics. As hardware capabilities advance, it becomes imperative to progress in the algorithmic aspects of quantum computers, particularly focusing on algorithms suitable for near-term devices

NASCENT: **N**on-G**A**us**S**ian **C**ontinuous Variable Quantum N**E**ural **N**e**T**works

NASCENT aims to explore the connection between photonic quantum systems and machine learning (ML). *The performance of deep learning is constrained by the available computing power, which, in turn, is restricted by energy consumption. Optics has the potential to enhance neural networks, enabling faster and more efficient operations. Furthermore, in the realm of quantum computing, quantum machine learning (QML) seeks to explore how quantum mechanics can enhance the performance of classical machine learning architectures. NASCENT will bridge the two fields and investigate how quantum optical phenomena, such as non-Gaussianity, which are not efficiently simulatable classically, can improve classical ML to solve problems in both quantum physics and classical applications.*

I. State of the art

Classical and Quantum simulations with Photons

The idea to simulate a complex quantum system with another well controllable one was originally proposed by Feynman [1] by suggesting that a 'computer' built of quantum mechanical elements is needed to simulate highly complex quantum systems.

Photonics simulators have emerged as a highly promising candidate in the realm of quantum computing and quantum simulation [2], drawing significant attention in fundamental and applied physics and engineering. Numerous experimental devices and theoretical tools have been developed within the field [3, 4, 5, 6].

With their ability to provide accurate manipulation of light, photonic systems are well-suited for the implementation of quantum algorithms. Moreover, photons exhibit long coherence times and can be, in some cases, effortlessly manipulated using established photonic technologies. It is worth highlighting that two experiments that claimed quantum advantage have been carried out using photonic systems [7, 8, 9, 10].

Quantum information can be encoded in physical systems using either discrete variables, such as photon polarization, or continuous variables (CV), such as electromagnetic field quadratures. CV quantum information processing serves as a compelling alternative to discrete variable approaches, as it enables the deterministic generation of highly entangled states and offers high-efficiency measurement options using existing technologies [11].

Within this framework, the focal points of attention are typically the states and operations related to CV systems, particularly those associated with field amplitudes. These states are commonly described using mathematical techniques derived from quantum optics, such as the quantum harmonic oscillator model. CV systems, such as optical modes, have the potential to demonstrate entanglement in high dimensions (many modes CV entanglement has been demonstrated in quantum optics [12]) and can be effectively manipulated using diverse tools such as passive optics, non-linear crystals, single photon detectors, and homodyne detectors [13].

In continuous variable quantum information, quantum states are described mathematically by vectors in a separable Hilbert space of infinite dimension. Alternatively, phase-space formalism allows to describe quantum states conveniently using generalised quasi probability distributions, like the Wigner function. States possessing a Gaussian

Wigner function are classified as Gaussian states, while all other states are referred to as non-Gaussian. Gaussian states and processes exhibit an elegant mathematical representation through the symplectic formalism, making them valuable for various quantum information protocols. However, computations involving only Gaussian components, including input Gaussian states, Gaussian operations, and Gaussian measurements, can be efficiently simulated using classical methods [11]. Conversely, non-Gaussian states are necessary and have practical applications in achieving universal quantum computing with continuous variables [14]. Having access to non-Gaussian entanglement is a key ingredient for devising quantum protocols spanning quantum computing, entanglement distillation, and quantum simulations. Moreover, non-Gaussian quantum states are intricately linked to remarkable quantum phenomena, such as contextuality, that are accompanied by the presence of negative values in the Wigner function [15].

Machine Learning, Neural Network and Quantum Machine Learning

Machine learning (ML), a highly successful technology of the current era, is focused on tasks such as classification, clustering, and pattern recognition for extensive datasets [16]. Accompanying the advancements in ML, learning theory has been developed in parallel to comprehend and enhance its achievements. Concepts like support vector machines, neural networks, and generative adversarial networks have made a significant impact on science and technology. ML has become deeply rooted in society to such an extent that any fundamental improvement in ML yields substantial economic benefits. Neural networks, which are also referred to as artificial neural networks (ANNs) or simulated neural networks (SNNs), form a subset of machine learning and serve as the foundation for deep learning algorithms.

The integration of ML and photonic system has been explored providing extraordinary results. More precisely, a fully-optical neural network, using unique advantages of optics, promises a computational speed enhancement of at least two orders of magnitude over the state-of-the-art and three orders of magnitude in power efficiency for conventional learning tasks [17]. ML can be incorporated within the framework of quantum mechanics. This field is called quantum machine learning (QML) [18]. Quantum computation and simulation harnesses the power of entanglement, superposition, and interference to carry out specific tasks with the aim of reaching significant speed advantages over classical computing. Although such speed improvements have already been theoretically demonstrated for specific problems, achieving them in the realm of data science remains uncertain, even at the theoretical level. However, this serves as one of the primary objectives for QML. In recent times, there has been a growing fascination towards exploring hybrid quantum-classical algorithms, also known as quantum-enhanced algorithms, wherein a portion of the algorithm is executed on a quantum device [18]. As new experimental platforms for quantum computation continue to emerge, researchers are actively seeking applications that are well-suited for these hybrid algorithms. While obtaining quantum advantage would be a groundbreaking achievement, the investigation of quantum-enhanced algorithms operating on these hybrid devices is a captivating problem in its own right, and it has the potential to uncover fascinating physics. Even though a quantum advantage in the sense of speed up is not guaranteed, an energetic quantum advantage can be the right goal for this architectures.

II. Research Project

Goal: Combining Non-Gaussian CV States and Neural Networks

NASCENT aims to propose, study and demonstrate the feasibility of the combination of hardware efficient non-Gaussian and Gaussian operation to create a CV Quantum Neural Network (CVQNN). The basic non-Gaussian operation in the network is a simple photon addiction (subtraction) on a mode that, is the simplest non-Gaussian operation currently available in quantum photonic platforms. This is equivalent to apply creation (annihilation) operator $a^\dagger$ (a) to a quantum state ρ. The Gaussian part is formed of beam splitters and squeezing operation the can be realized in platform directly on chips [19]. This is a major advancement to the previous works that has been done in this direction. In [20], the author have studied a non-Gaussian QNN that has cubic operations that are not feasible experimentally. Moreover, **NASCENT** goes beyond [20] considering different and more complex applications. The basic idea is the following. Let us start from the vacuum state. We then apply a generic unitary Gaussian operation constructed via beam splitters and squeezing operations. As mentioned above the parameters of this gaussian operation can be efficiently and rapidly controlled. This creates a unitary operation that can be tuned in our quantum neural network. A second layer is composed of some non gaussian operation. This is the second layer of the QNN. A hardware efficient non-gaussian operation is the annihilation operation, applied using single photon detector on a mode. The operator a can be applied to a superposition of different modes. These constitute a non-Gaussian layer in our QNN. This two layers are then alternated to construct a hardware-efficient CV-QNN architecture. The following subsections will describe two different work packages of **NASCENT** based on the application of the CV-QNN described above.

WP1: Variational quantum algorithm with CV-QNN

The Variational Quantum Eigensolver (VQE) [5] is a quantum algorithm designed for finding the ground state energy of a given Hamiltonian. It utilizes a hybrid approach, combining classical and quantum computation.

In VQE, a quantum computer is used to prepare a trial wavefunction that depends on a set of variational parameters. The energy of this trial wavefunction is then estimated by measuring it on the quantum computer. By iteratively optimizing the variational parameters using classical optimization techniques, VQE aims to find the set of parameters that minimizes the energy, providing an approximation of the ground state energy of the target Hamiltonian. VQE holds promise for solving problems in quantum chemistry, materials science, condensed matters and High energy physics, where finding the ground state energy is crucial for understanding fundamental properties of the Systems. **I propose to study different models in condensed matter system and high-energy physics** [21]. Since our framework already work naturally in a local Hilbert space that is infinite dimensional, it can be straightforwardly applied to lattice field Theory, that naturally has a infinite dimensional local Hilbert space and, usually, needs to be regularised (e.g. putting a cut-off in the local Hilbert space dimension). Simulating lattice field enhances our understanding of fundamental physics by providing a framework to study the behavior of elementary particles and their interactions. Moreover, it enables exploration of complex phenomena that arise from the interactions of multiple particles, including phase transitions, confinement, and symmetry breaking.

WP2: Quantum machine learning with NG-CV-QNN

A non trivial task in QML is to insert non linearities with respect to the input state in the QNN. Let us assume we have classical data (e.g. pictures) and we want to perform a classification task. One straightforward approach would be to encode the classical data into the input state, the applying a global unitary to the input state (the QNN), and measure the output. The cost function can be the cross entropy or the mean square error between the exact and predicted results. This approach would not give meaningful results [22]. This problem is given by the no-cloning-theorem in quantum information. While quantum computers are unable to duplicate data, classical devices possess this capability [23]. To illustrate this difference, in a neural network, the input is repeatedly utilized in the hidden layer neurons during data processing. Conversely, a quantum neural network can only employ quantum data once, lacking the ability to replicate it. The Universal Approximation Theorem (UAT) states that a neural network with a single hidden layer containing a sufficient number of neurons can approximate any continuous function to arbitrary accuracy, given appropriate activation functions and network parameters. In other words, it demonstrates the capability of neural networks to approximate a wide range of complex functions, making them powerful tools for learning and modeling various types of data. With the simple quantum classifier described above, we do not fulfill the UAT. One way to circumvent this is to alternate layers of uploading data and processing layers in the QNN. It is demonstrated in [22] that the re-uploading procedure is equivalent to the UAT if enough re-upload layer are present in the QNN. The authors of [22] considered a one an multiple quibit classifier. **The scope of this work-package is to extend the demonstration to infinite dimensional local Hilbert space on a theoretical level.** Moreover, levereging on the results of WP1, **WP2 will explore how entanglement and non-gaussianity play a role in the expressively and the learning capabilities of the QNN**. The project will focus on two main application: the classification of phases of matter (quantum data, for example the phase diagram of the Bose-Hubbard model) and the classification of classical pictures (e.g. MNIST datasets [24]). The effect of entanglement in the learning capabilities of QNN is still a open question also in Discrete Variable QNN [25].

III. Outcome and Impact

NASCENT seeks to make significant contributions to the field of QML and quantum simulation by introducing and demonstrating the potential of this innovative paradigm. The project has two main objectives. Firstly, it aims to **develop and evaluate continuous variable non-Gaussian variational quantum simulation**, demonstrating its usefulness in studying the static properties of various quantum many-body systems, from quantum chemistry to lattice field theories. The second goal is to explore how **entanglement in non-Gaussian systems can enhance QML models**.

With the rapid growth of quantum technologies in recent years, the advancement of new paradigms and architectures is crucial to propel the field forward Notably, **NASCENT**'s goals will also contribute to quantum energetic advantages. Traditional neural network architectures consume a vast amount of energy during training. As demonstrated in [17], photonic systems can offer an energy advantage of multiple orders of magnitude. This ambitious project marks just the beginning of a series of exciting future endeavors. One such application involves **designing efficient quantum circuits tailored to specific problems**. By leveraging the findings from Project **NASCENT**, I will form my own research group and embark on a path as an autonomous researcher.

Building on the findings from Project **NASCENT**, I aspire to establish my own re-

search group and embark on an autonomous path as a researcher. My expertise spans classical machine learning [26], quantum machine learning [27], and quantum computing [28]. Additionally, I have cultivated an international network of theoretical and experimental collaborators, both within ICFO The Institute of Photonic Sciences and beyond, collaborating with esteemed professors such as Prof. Philipp Haucke from the University of Trento, Prof. Valentina Parigi from Sorbonne University Paris, and Prof. Ulysse Chabaud from Ecole Normale Supérieure. With my diverse skill set and successful collaborations, I am confident that I am the ideal candidate to lead this challenging research endeavor.

References

[1] R. P. Feynman *Int J Theor Phys* **21** no. 6, (1982) 467–488.

[2] M. J. Hartmann *Journal of Optics* **18** no. 10, (Sep, 2016) 104005.

[3] A. Aspuru-Guzik and P. Walther *Nature Phys* **8** no. 4, (2012) 285–291.

[4] C. Sparrow *et al.* *Nature* **557** no. 7707, (2018) 660–667.

[5] A. Peruzzo *et al.* *Nat Commun* **5** no. 1, (2014) 4213.

[6] F. H. B. Somhorst *et al.* *Nat Commun* **14** no. 1, (Jul, 2023) .

[7] S. Aaronson and A. Arkhipov *Proceedings of the Forty-Third Annual ACM Symposium on Theory of Computing* (2011) 333–342.

[8] H.-S. Zhong *et al.* *Science* **370** no. 6523, (Dec, 2020) 1460–1463.

[9] H.-S. Zhong *et al.* *Phys. Rev. Lett.* **127** no. 18, (Oct, 2021) .

[10] L. S. Madsen *et al.* *Nature* **606** no. 7912, (2022) 75–81.

[11] S. L. Braunstein and P. van Loock *Rev. Mod. Phys.* **77** no. 2, (Jun, 2005) .

[12] S. Yokoyama *et al.* *Nature Photon* **7** no. 12, (2013) 982–986.

[13] J. E. Bourassa *et al.* *Quantum* **5** (Feb, 2021) 392.

[14] Y.-S. Ra *et al.* *Nature Phys* **16** no. 2, (Dec, 2019) 144–147.

[15] R. I. Booth, U. Chabaud, and P.-E. Emeriau *Phys. Rev. Lett.* **129** no. 23, (Nov, 2022) .

[16] I. Goodfellow, Y. Bengio, and A. Courville, *Deep Learning*. MIT Press, 2016. `http://www.deeplearningbook.org`.

[17] Y. Shen *et al.* *Nature Photon* **11** no. 7, (Jun, 2017) 441–446.

[18] J. Biamonte *et al.* *Nature* **549** no. 7671, (2017) 195–202.

[19] J. M. Arrazola *et al.* *Nature* **591** no. 7848, (Mar, 2021) 54–60.

[20] N. Killoran, T. R. Bromley, J. M. Arrazola, M. Schuld, N. Quesada, and S. Lloyd *Phys. Rev. Research* **1** no. 3, (Oct, 2019) .

[21] M. C. Bañuls *et al.* *The European Physical Journal D* **74** no. 8, (Aug, 2020) .

[22] A. Pérez-Salinas, A. Cervera-Lierta, E. Gil-Fuster, and J. I. Latorre *Quantum* **4** (Feb, 2020) 226.

[23] W. K. Wootters and W. H. Zurek *Nature* **299** no. 5886, (1982) 802–803.

[24] L. Deng *IEEE Signal Processing Magazine* **29** no. 6, (2012) 141–142.

[25] A. Abbas *et al.* *Nat Comput Sci* **1** no. 6, (Jun, 2021) 403–409.

[26] K. A. Nicoli, C. J. Anders, L. Funcke, T. Hartung, K. Jansen, P. Kessel, S. Nakajima, and P. Stornati *Phys. Rev. Lett.* **126** (Jan, 2021) 032001.

[27] L. Funcke, T. Hartung, K. Jansen, S. Kühn, and P. Stornati *Quantum* **5** (Mar., 2021) 422.

[28] L. Funcke, T. Hartung, K. Jansen, S. Kühn, P. Stornati, and X. Wang *Phys. Rev. A* **105** no. 6, (Jun, 2022) .

Title: **Robust and reliable mid-infrared pulsed fiber laser as a laser scalpel**

Category: **Health**

Lasers are the surgical tool of the 21st century. They are intrinsically sterile, do not blunt or deform tissue, and present an opportunity for inhuman precision in the depth and positioning of cuts. However, current laser technologies still face a number of challenges that limit their widespread adoption as a substitute to the regular scalpel, among them the difficulty of controlling thermal damage, the inconvenience of their maintenance and their limited capabilities in processing hard tissue such as bone and teeth. CO_2 lasers operating near 10 µm are cheap and robust, but their delivery method (articulated arms with guided mirrors), limited tissue absorption and large spot size limit their effectiveness in the operation room. Flash-lamp-pumped Er:YAG lasers at 2.94 µm have higher absorption in biological tissue, but their low repetition rate, limited pulse length control, frequent need for maintenance and poor beam quality make them a slow, rigid platform that cannot be precisely tailored to specific applications. There is a need for a new, 21st-century laser platform that simultaneously addresses all the constraints of legacy laser technologies and opens the way to the democratization of laser surgery: the high energy pulsed mid-infrared fiber laser.

This proposal for the Optica Foundation Challenge in the health category aims to develop a field-deployable gain-switched all-fiber laser that generates pulses shorter than 100 ns with a power density of up to 2 GW/cm² (a fluence of up to 200 J/cm²). The operation wavelength near 2.8 µm, adjustable repetition rate and near perfect beam quality make it suitable for efficient precision surgery on soft and hard biological tissues. The project is divided into two objectives. The first one focuses on developing a gain-switched mid-IR all-fiber laser system that can be industrialized for soft tissue processing such as arteries or cartilage. The second objective is to build an amplified version capable of generating larger energy pulses at higher average power to ultimately deliver efficient ablation of hard biological tissues such as bones and teeth. These new fiber laser systems offer an excellent beam quality and divergence, and shorter pulses to increase the biological tissue ablation efficiency while also reducing the damage to surrounding tissues compared to current Er:YAG and CO_2 lasers. Achieving these performances with a simple and cost-effective design makes this technology appealing for high-volume markets and has the potential to revolutionize the biomedical industry, just as the adoption of the fiber laser did for the material processing industry.

The main outcome expected from this project is the development of a pre-production prototype suitable for the start of clinical trials and experiments by medical device partners. Moreover, the achievement of an all-fiber mid-IR laser system producing highly energetic pulses with durations in the range of a few tens of nanoseconds would represent a scientific advance that would be worth publishing in highly ranked peer-reviewed journals like *Optics Letters* and *Optics Express* as well as in renowned conferences such as *CLEO*. The application of such laser sources as a novel laser scalpel adapted for efficient biomaterial processing will also be investigated by the medical partners of *LumIR Lasers* and will lead to advances in our understanding of laser-tissue interactions.

The impact of the novel biomedical laser system will be to increase the cutting efficiency while also reducing the surrounding area damage to biological tissues compared to the current laser scalpel technologies. Moreover, these improvements will also enhance the healing process and reduce the pain experienced by the patients of such surgery. The CW mid-IR fiber lasers commercialized by *LumIR Lasers* are already making waves in the biomedical industry and a gain-switched fiber laser adapted to cut through harder biological tissues would open a whole new sector of applications for this “cutting edge” technology while also improving the quality of life of many patients worldwide. Given enough time to complete clinical phases, the flexibility and optical properties of this laser technology will allow dramatic improvements to difficult surgical procedures such as for the treatment of endometriosis, ovary cancer and several bone and teeth conditions.

Robust and reliable mid-infrared pulsed fiber laser as a laser scalpel

Literature Review

A significant effort is currently underway to develop coherent radiation sources emitting between 3 µm and 5 µm for various applications [1–3], including biomedical [4–6], spectroscopy [7], sensing [8], material processing [9,10], and countermeasures [11]. Most existing mid-infrared (mid-IR) laser technologies suffer from issues like a lack of reliability and robustness or insufficient power to meet application requirements. However, mid-IR fluoride fiber lasers have emerged as strong contenders due to their compactness, robustness, tunability and high brightness in both continuous (CW) and pulsed operation modes. Recent advances in high-quality fluoride glass fibers with low optical losses and high dopant concentrations, along with fiber components like fiber Bragg gratings (FBGs) and all-fiber pump combiners have been instrumental in this regard [12,13].

This proposal is based on the expertise and knowledge on mid-IR fiber lasers acquired over the last decade at the Center for Optics, Photonics and Lasers (COPL) of Laval University [3], which has now been transferred to and further developed by *LumIR Lasers*, the industrial start-up partner of this project. Several powerful CW mid-IR fiber lasers in the 2.8 µm to 4 µm spectral range have been achieved, such as 41.6 W at 2.8 µm [14], 10.1 W at 3.24 µm [15], 14.9 W at 3.55 µm [16], and 200 mW at 3.92 µm [17]. These were made possible through expertise in FBG writing, thermal management, and fiber tip end-capping to prevent catastrophic failure of high-power fluoride fiber lasers [18,19]. The all-fiber design employed in most of these demonstrations makes them more reliable and compact compared to hybrid fiber lasers that involve a combination of optical fibers and free-space optics.

High-power lasers operating near 2.9 µm are particularly interesting for biomedical and precision surgery applications due to the strong water absorption related to the O-H fundamental vibrational resonance at 2.94 µm. While *LumIR Lasers* already commercializes CW and quasi-CW mid-IR fiber lasers for the biomedical sector, certain applications such as dental and bone surgery require pulsed operation modes and beam properties that are not currently available commercially from fiber or solid-state lasers. The commonly used 2.94 µm Er:YAG solid-state laser generates millijoule-level pulses with a duration of 200 µs but suffers from its poor beam quality (M^2 typically in the range of 10–100) and low repetition rate [20–22]. There are also a few demonstrations of Q-switched Er:YAG or Er:YSGG systems generating 100 ns pulses at higher repetition rates that showed better hard dental tissue ablation efficiency compared to the low repetition rate lasers [23,24]. Such high-energy, high-peak-power pulses are typically used in combination with a water spray to cool down the treated area and minimize thermal damage. On the other hand, longer pulses from such lasers with relatively low energy and peak power are typically used to cut soft tissues while using some thermal damage to cauterize blood vessels to limit the bleeding. CO_2 lasers operating near 10 µm are also commonly used for surgery since they are reliable and offer high power [25]. However, the guiding of laser beams from Er:YAG or CO_2 lasers to the treated surface often involves multimode fibers or complex free-space optics, resulting in lower overall laser efficiency compared to all-fiber laser systems [22]. Hence, an all-fiber laser operating in the mid-IR range could provide versatile pulses with higher repetition rates, improved precision, and a single-mode beam profile, thereby generating the required laser intensity in a smaller focal area than the established laser technologies.

The research scientist leading this proposal has extensive experience in pulsed mid-IR fluoride fiber lasers, including the demonstration of a high-power soliton source tunable between 2.8 µm and 3.6 µm in 2016 [26]. However, these bulky laser designs are not robust and cost-effective enough for biomedical applications, and the pulse energy is limited to nanojoule levels, unsuitable for tissue processing. Recent studies have explored picosecond pulse amplification, but the extra energy is shifted to longer wavelengths outside the biomaterial absorption band at 2.9 µm due to nonlinear propagation inside the optical fiber [27]. Although a supercontinuum generation scheme enabled laser emission from 2.6 µm to 4.1 µm, most of the pulse energy cannot be efficiently harvested for biomedical processing.

Furthermore, amplifying picosecond pulses to millijoule-level energies with an average power of 5 W has been achieved using multiple amplification stages with fluoride fibers having larger cores, but this approach remains somewhat complex and relies on cumbersome free-space optics [28].

In 2018, the research scientist leading this proposal demonstrated a robust and high-power mid-IR gain-switched laser source generating 170 ns and 80 µJ pulses using the same simple and robust optical architecture as CW fiber lasers [29]. Such gain-switched mid-IR fluoride fiber lasers show promise for hard tissue processing, including bone and tooth tissues. However, there is still room for improvement in the design of gain-switched mid-IR fiber lasers to meet the requirements of the biomedical industry and challenge established Er:YAG and CO_2 laser devices. Further research is needed to determine the ideal pulse duration, peak power, and pulse energy for efficient hard tissue processing.

Problem Statement and Objectives

Lasers are intrinsically sterile, do not blunt or deform tissue, and present an opportunity for inhuman precision in the depth and positioning of cuts. However, current laser technologies still face a number of challenges that limit their widespread adoption as a substitute to the regular scalpel. CO_2 lasers operating near 10 µm are cheap and robust, but their delivery method (articulated arms with guided mirrors), limited tissue absorption and large spot size limit their effectiveness in the operation room. Flash-lamp-pumped Er:YAG lasers at 2.94 µm have higher absorption in biological tissue, but their low repetition rate, limited pulse length control, frequent need for maintenance and poor beam quality make them a slow, rigid platform that cannot be precisely tailored to specific applications. There is a need for a new, 21st-century laser platform that simultaneously addresses all the constraints of legacy laser technologies and opens the way to the democratization of laser surgery: the high energy pulsed mid-infrared fiber laser.

The main goal of this project is to develop a field-deployable gain-switched all-fiber laser that generates pulses shorter than 100 ns with a power density of up to 2 GW/cm². The operation wavelength near 2.8 µm and adjustable repetition rate make it suitable not only for efficient biomedical material processing but also for other applications such as glass and semiconductor processing. The project is divided into two objectives: Objective 1 focuses on developing an all-fiber gain-switched laser system, while Objective 2 aims to build an amplified version delivering larger pulse energies. While the first objective is the industrialization of a first pulsed all-fiber laser system by *LumIR Lasers*, the ultimate goal of this project is to fulfill the requirements of the most demanding biomedical applications [24], particularly the efficient processing of hard biological tissues (bones and teeth) [22]. The advantages of these new laser systems compared to Er:YAG lasers currently used in most biomedical applications are their excellent beam quality and divergence, and their capacity to generate shorter pulses to increase the biological tissue ablation efficiency while also reducing the damage in surrounding tissues. Achieving these performances with a simple and cost-effective design makes this technology appealing for high-volume markets and have the potential to revolutionize the biomedical industry in just the same way that 1 µm ytterbium fiber lasers have revolutionized the metal-processing industry.

Objective 1

This objective is to design and develop a low-cost gain-switched all-fiber laser that can generate pulses with a duration of less than 100 ns and a peak irradiance of around 500 MW/cm² (pulse fluence around 50 J/cm²). These pulse parameters will meet the requirements of intermediately demanding biomedical applications such as soft tissue ablation, including angioplasty [30].

Objective 2

This objective aims to develop a rugged two-stage all-fiber system that can produce pulses shorter than 100 ns with a fluence higher than 200 J/cm² in a near perfect quality single-mode beam. The gain-switched laser developed in Objective 1 will serve as the seed for the amplified system.

Outline of tasks and Work Plan

The work plan is described hereafter followed by a Gantt chart summarizing the tasks and milestones.

Objective 1

Objective 1.1 involves numerically modelling the optimum fiber laser design using codes previously developed by the research scientist. The design will be based on a gain-switched fluoride fiber laser that can generate pulses with a duration of the order of 100 ns. The research scientist will optimize the 2.8 µm signal pulses by adjusting the pump's repetition rate, pulse duration, peak power, as well as the laser cavity's length and output coupler's reflectivity. High-performance computing facilities will be utilized for this numerical optimization. The research scientist's programming and numerical skills will be crucial in generating, processing, and analyzing the data required for optimizing the design of the new all-fiber laser emitting record-breaking gain-switched pulses at 2.8 µm. The design will be based on commercially available or custom-made components, taking advantage of advances in pump lasers, lower losses in erbium-doped fluoride fibers, and improved assembly and thermal management techniques.

Objective 1.2 focuses on the experimental optimization of the laser cavity based on the results obtained from numerical modelling. The gain-switched fiber laser will utilize a low-loss 7 mol.% erbium-doped fluoride fiber from *Le Verre Fluoré* and in-house fabricated fiber Bragg gratings (FBGs). The optical design will be based on *LumIR Lasers*' all-fiber design used for continuous wave (CW) mid-IR lasers. However, a more powerful pump diode and a fast modulation driver will be required to generate the required pulses. *LumIR Lasers*' expertise in building robust and reliable high-power CW all-fiber lasers will be utilized to achieve the desired peak power and energy per pulse. Collaborative efforts will ensure optimal mechanical and electrical designs for the laser cavity, including state-of-the-art thermal management and the manufacturing of an essential end cap for the protection of the fiber output tip.

Objective 1.3 involves characterizing the performance of the pulsed laser. Key parameters such as temporal stability, pulse duration, average power, and laser emission spectrum will be thoroughly characterized using available instruments. Long-term stability tests will be conducted to ensure reliable operation for commercial purposes. These measurements will be performed at repetition rates ranging from 1 Hz to 500 kHz, with optimized pump pulses to achieve optimum 2.8 µm laser performance.

Objective 2

Objective 2.1 focuses on developing the amplifier stage using a large mode area (LMA) single-mode erbium-doped fluoride fiber. Preliminary studies will be conducted to determine the optimal core and cladding diameters for the fiber. They will also include parasitic feedback and different fiber lengths to achieve the desired performance. The optimized LMA fiber will be fabricated, and the amplifier will be assembled in collaboration with *LumIR Lasers*' technical team. To mitigate parasitic feedback, a novel saturable absorber developed by the research scientist will be integrated in an all-fiber format between the seed and the amplifier. The performance of the amplified system will be characterized and further optimized based on experimental data, in order to generate short pulses with energy exceeding 1 mJ while maintaining a cost-effective and robust all-fiber design.

Objective 2.2 involves designing and assembling a pre-production prototype based on the accumulated experimental data from the project. A new packaging solution will be developed to facilitate deployment in key biomedical sectors. Further optimization of the pulse generation control scheme, electronics, and software will be performed to enhance the user-friendliness and operational efficiency of the laser system. Prospective biological tissue ablation tests will be conducted with the help of *LumIR Lasers*' partners to validate the capabilities of the new pulsed system for the biomedical market.

ID	Task Name
1	**Development of the gain-switched mid-IR fiber laser for biomedical applications**
2	**Objective 1: Development of the gain-switched all-fiber laser**
3	Find and purchase suitable high power 976 nm laser diodes for the pulsed laser cavities and amplifiers
4	Find and purchase a versatile and suitable fast modulation drivers for the laser diodes
5	Delivery delay and optimization of the drivers' circuitry for the specific diodes to generate clean short pulses at 976 nm
6	**Objective 1.1**
7	Numerical simulations based on known physical properties to decide the peak reflectivity of the FBGs and the laser cavity's length.
8	**Objective 1.2**
9	Mechanical and electrical design for the pulsed fiber laser
10	Realization of the experimental packaging of the pulsed fiber laser
11	Assembly of the first iteration of the laser device
12	**Objective 1.3**
13	Characterization of the pulses' parameters (pulse shape, duration, peak power, energy, repetition rate, pulse-to-pulse stability)
14	Longterm stability test at high power to verify the reliability of the whole system
15	**Objective 2: Development of the pulsed amplifier**
16	**Objective 2.1: Large mode area single-mode erbium-doped fluoride fiber amplifier**
17	Numerical simulations to determine the best fiber length, core diameter and cladding diameter and pump pulse duration based on the available peak power to optimized the output pulse energy and duration
18	Ordering the optimized LMA fiber to Le Verre Fluoré
19	Mechanical and electrical design for the pulsed amplifier
20	Realization of the experimental packaging of the pulsed amplifier
21	Assembly of the pulsed fiber amplifier
22	Characterization of the amplified pulses parameters
23	Long term stability test
24	**Objective 2.2: Preproduction prototype / technology transfer**
25	Design based on experimental data
26	Development of a ruggedized packaging
27	Assembly of the laser
28	Optimization of the electronics and software
29	Characterization of the laser performances
30	Preproduction prototype

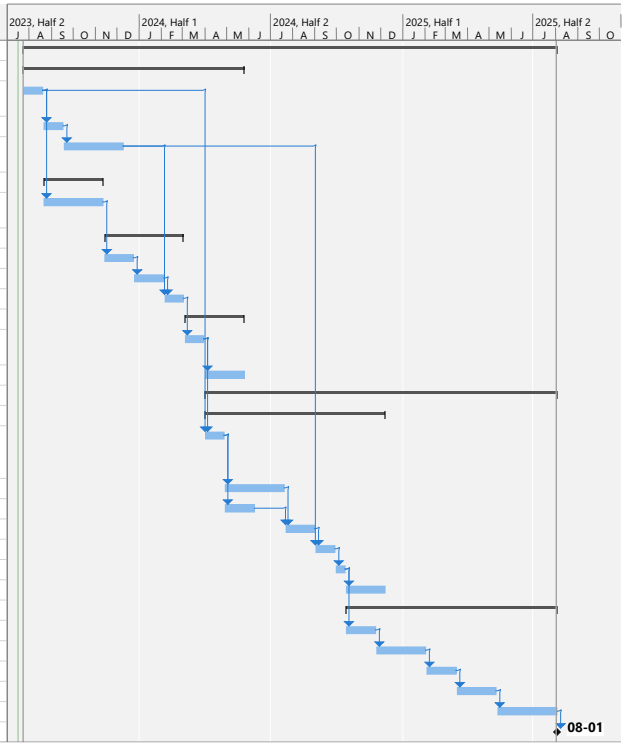

Figure 1: Work plan of this research project

Outcomes

The main outcome expected from this project is the development of a pre-production prototype specially designed for *LumIR Lasers.* Moreover, the achievement of an all-fiber mid-IR laser system producing highly energetic pulses with durations in the range of a few tens of nanoseconds would represent a scientific advance that would be worth publishing in highly ranked peer-reviewed journals like *Optics Letters* and *Optics Express* as well as in renown conferences such as *CLEO*. The application of such laser sources as a novel laser scalpel adapted for efficient biomaterial processing will also be investigated by the medical partners of *LumIR Lasers*. This will lead to advances in our understanding of laser-tissue interactions to be published in specialized biomedical journals such as *Lasers in Surgery and Medicine*. Given enough time to complete clinical trials, the laser developed by this project is poised to birth a new generation of dentistry and surgical laser medical devices, as the CW lasers from *LumIR Lasers* have done before it for dermatology.

Impact

The development of mid-IR sources, especially pulsed laser sources, being currently of great practical relevance, this project is likely to have a great impact on the photonics industry in general. More specifically, this research project will provide a novel biomedical laser system that will improve the cutting efficiency while also reducing the surrounding area damage to biological tissues compared to the current laser scalpel technologies—the first major paradigm shift in medical mid-IR laser sources in several decades. Moreover, these improvements will also enhance the healing process and reduce the pain experienced by the patients of such surgery. The CW mid-IR fiber lasers commercialized by *LumIR Lasers* are already making waves in the biomedical industry for its performances in skin resurfacing. Thus, a gain-switched fiber laser adapted to cut through harder biological tissues would open a whole new sector of applications for this “cutting edge” technology while also improving the quality of life of many patients worldwide. Moreover, its simple and cost-effective design makes this technology appealing for high-volume markets and have the potential to revolutionize the biomedical industry. A growing coalition of renowned doctors and medical device manufacturers is already assessing that the optical properties of mid-IR fiber lasers, combined with their inherent flexibility and convenience, will

be at the epicentre of a brand-new wave of surgical tools targeted at improving the outcome of high-risk surgical operations, such as that of endometriosis and ovaries cancer, as well challenging laser operations on teeth and bone.

References

1. S. D. Jackson and R. K. Jain, Optics Express **28**, 30964 (2020).
2. S. Jackson, M. Bernier, and R. Vallée, eds., First, Woodhead Publishing Series in Electronic and Optical Materials (Elsevier, 2022).
3. F. Jobin, P. Paradis, Y. O. Aydin, T. Boilard, V. Fortin, J.-C. Gauthier, M. Lemieux-Tanguay, S. Magnan-Saucier, L.-C. Michaud, S. Mondor, L.-P. Pleau, L. Talbot, M. Bernier, and R. Vallée, Optics Express **30**, 8615 (2022).
4. B. Jean and T. Bende, in *Solid-State Mid-Infrared Laser Sources*, I. T. Sorokina and K. L. Vodopyanov, eds. (Springer Berlin Heidelberg, 2003), pp. 530–565.
5. H. Jelínková, ed., (Woodhead Publishing, 2013).
6. V. A. Serebryakov, É. V. Boĭko, N. N. Petrishchev, and A. V. Yan, Journal of Optical Technology **77**, 6 (2010).
7. F. K. Tittel, D. Richter, and A. Fried, in *Solid-State Mid-Infrared Laser Sources*, I. T. Sorokina and K. L. Vodopyanov, eds. (Springer Berlin Heidelberg, 2003), pp. 458–529.
8. C. Wang and P. Sahay, Sensors **9**, 8230 (2009).
9. C. Frayssinous, V. Fortin, J.-P. Bérubé, A. Fraser, and R. Vallée, Journal of Materials Processing Technology **252**, 813 (2018).
10. J. L. Koenig, Second (Elsevier, 1999).
11. H. H. P. T. Bekman, J. C. van den Heuvel, F. J. M. van Putten, and R. Schleijpen, in *Technologies for Optical Countermeasures*, D. H. Titterton, ed. (SPIE, 2004), **5615**, pp. 27–38.
12. M. Bernier, D. Faucher, R. Vallée, A. Saliminia, G. Androz, Y. Sheng, and S. L. Chin, Optics Letters **32**, 454 (2007).
13. S. Magnan-Saucier, S. Duval, C. Matte-Breton, Y. O. Aydin, V. Fortin, S. LaRochelle, M. Bernier, and R. Vallée, Opt. Lett. **45**, 5828 (2020).
14. Y. O. Aydin, V. Fortin, R. Vallée, and M. Bernier, Optics Letters **43**, 4542 (2018).
15. V. Fortin, F. Jobin, M. Larose, M. Bernier, and R. Vallée, Optics Letters **44**, 491 (2019).
16. M. Lemieux-Tanguay, V. Fortin, T. Boilard, P. Paradis, F. Maes, L. Talbot, R. Vallée, and M. Bernier, Optics Letters **47**, 289 (2022).
17. F. Maes, V. Fortin, S. Poulain, M. Poulain, J.-Y. Carrée, M. Bernier, and R. Vallée, Optica **5**, 761 (2018).
18. Y. O. Aydin, F. Maes, V. Fortin, S. T. Bah, R. Vallée, and M. Bernier, Optics Express **27**, 20659 (2019).
19. N. Caron, M. Bernier, D. Faucher, and R. Vallée, Optics Express **20**, 22188 (2012).
20. C. Bader and I. Krejci, American journal of dentistry **19**, 178 (2006).
21. B. D. sek-Olup and B. Vedlin, Lasers in Surgery and Medicine **21**, 13 (1997).
22. A. Urich, R. R. J. Maier, B. J. Mangan, S. Renshaw, J. C. Knight, D. P. Hand, and J. D. Shephard, Optics Express **20**, 6677 (2012).
23. Q. Cui, M. Wei, Z. Xiong, S. Hu, J. Jiang, L. Wang, T. Cheng, X. Wu, and H. Jiang, Photobiomodulation, Photomedicine, and Laser Surgery **39**, 390 (2021).
24. J. Yang, L. Wang, X. Wu, T. Cheng, and H. Jiang, Opt. Express **22**, 15686 (2014).
25. D. C. Dumitras, (IntechOpen, 2012).
26. S. Duval, J.-C. Gauthier, L.-R. Robichaud, P. Paradis, M. Olivier, V. Fortin, M. Bernier, M. Piché, and R. Vallée, Optics Letters **41**, 5294 (2016).
27. J.-C. Gauthier, V. Fortin, S. Duval, R. Vallée, and M. Bernier, Optics Letters **40**, 5247 (2015).
28. Y. O. Aydin, S. Magnan-Saucier, D. Zhang, V. Fortin, D. Kraemer, R. Vallée, and M. Bernier, Optics Letters **46**, 4506 (2021).
29. P. Paradis, V. Fortin, Y. O. Aydin, R. Vallée, and M. Bernier, Optics Letters **43**, 3196 (2018).
30. R. F. Bonner, L. G. Prevosti, M. B. Leon, K. Levin, and D. Tran, in *Optical Fibers in Medicine III*, A. Katzir, ed. (SPIE, 1988), **0906**, pp. 288–295.

EXECUTIVE SUMMARY

Silicon photonics and printable photonic ink for an affordable medical sensor platform

Optica Foundation Challenge Category: Health

The Challenge: Traditional medical sensors consisting of discrete optics cannot keep pace with patients' needs and the growing demand for wearable sensors. These limitations were highlighted during the COVID-19 pandemic when the standard pulse oximeters used to measure blood oxygen levels yielded incorrect diagnoses for people with dark skin pigmentation. New devices needed to be developed with even more wavelengths (LEDs) at increased cost to reach the required accuracy for all skin colors. The core issue is that traditional devices based on discrete optics require separate components to be sourced from different supply chains and individually packaged, resulting in complex products. While the individual components are sometimes inexpensive, the true cost driver is the required packaging of each LED. As another example, commercial carbon monoxide poisoning detectors made by the company Nonin require eight or more LEDs and are niche as a result. To advance beyond the current state-of-the-art, Iris Light is pioneering the development of an affordable medical sensor platform based on silicon photonic chips (SiP). A SiP chip requires only a single packaging step and can obtain a bounty of data from densely-packed, on-chip integrated components. Based on direct customer contact with leading Fortune 500 medical companies, Iris Light is targeting hydration sensors as the first application. An optical hydration sensor uses near-infrared wavelengths to accurately measure the water content in skin. Our SiP based optical medical sensor platform will enable the collection of more health data per dollar leading to improved patient outcomes. Looking to the future, the $20 billion medical sensor industry needs a way to achieve accuracy, complexity, and versatility while maintaining a low cost to expand global access to healthcare.

Proposed Project: *This Optica Foundation Challenge will provide critical seed funding for demonstrating the viability of optical medical sensors based on SiP*. The specific challenge addressed here is the printing of LEDs directly onto a SiP chip to improve performance compared to the discrete optics approach. To achieve this, our company is pioneering a new class of printed photonic inks for light sources and detectors (actives) based on nanoscale black phosphorus (BP), a material that exhibits desirable opto-electronic properties including direct-gap light emission and high conductivity. BP is a 2D semiconductor that can be tuned to emit over a broad spectrum from visible to infrared based on the number of atomic layers. **Here, we will achieve an electrically driven BP LED emitting at 1450 nm for water absorption measurements in skin.**

Intended Outcomes: This project will leverage key results from our company's work on BP over the last several years including world-record conductivity for semiconductor ink, and demonstration of printed photodiodes with state-of-the-art performance. Here, the main outcome will be an LED consisting of a BP-based P-N junction that emits at 1450 nm. Towards this goal, we recently demonstrated a new nanomaterial *synthesis* recipe where we isolated a single spectral band (monodisperse) for the first time. The specific band we isolated was of 4-atomic layer BP (4L BP) that covers the desired spectral range for this project. Three major milestones are targeted by this proposal: First, we will improve the yield of our 1450 nm ink. Next, we will optimize the ink for emission at 1450 nm. Finally, we will print the ink onto pre-patterned substrates to form the LED and verify emission at 1450 nm. **This advance will represent the first ink-printed light-emitters on silicon chips.**

New Capabilities: The success of this project will illustrate how printed photonic inks can enable SiP to reach its full potential as a transformative technology. A wearable hydration monitor will be a major step toward sophisticated optical medical sensors that will improve patient outcomes. At scale, our new photonic chip medical sensor platform will enable access to affordable, state-of-the-art medical care for people all over the world. More broadly, printable photonic inks solve one of the most important outstanding problems for the entire silicon photonics industry: namely, the need for an on-chip light-source covering multiple spectral bands. Beyond medical sensors, the impact of this new on-chip ink-printed LED platform will enable SiP to expand its reach into applications in environmental monitoring, communications, quantum photonics, and beyond. Further, the photonic inks will foster growth in the *printed electronics* industry to open the way for applications in *printed opto-electronics*.

Pradeep Subedi, Ph.D. Iris Light Technologies, Inc.

Problem Statements

The 'why' for societal benefit: improved public health

Imagine a world where your current health is visible on your wrist. **Silicon photonics (SiP) has the potential to revolutionize the medical industry with sophisticated monitoring devices that collect more health data per dollar for improved patient outcomes.** This Optica Foundation Challenge will provide critical seed funding to demonstrate *the world's first* ***affordable*** *optical medical sensors based on silicon photonic chips*. To illustrate the broader nature of the challenge, we first consider a medical application that uses *discrete* optics, the pulse oximeter. This well-known example illustrates simultaneously the importance of current optical medical sensors, as well as the future potential of wearable medical sensors based on SiP (integrated optics). Pulse oximetry, which measures oxygen in the blood, has reached the level of 'standard of care' and is one of the five vital signs measured at every doctor's visit [1]. Before this invention, patients had to endure a blood draw to measure their blood oxygen saturation levels. The issue of invasive measurement persists for many ailments such as diabetes. Wearable medical devices not only eliminate painful poking but will also enable monitoring of important vital signs and alert people about their health to prevent serious health complications.

Beyond diabetes, there are a significant number of additional health issues that require constant monitoring today. Optical medical sensors are one class of 'non-invasive sensors' employed by the medical industry to provide maximum health data with minimal patient impact. Through our commercial engagement with the industry in over 100 customer interviews, our company uncovered a first target application in *continuous hydration measurement*. As the Head of Open Innovation at one major Fortune 500 medical device company framed it, "***Though it sounds simple, measuring water in the body is still done by pushing on the skin and watching it recoil, which is an unreliable, non-quantitative method. If a quantitative, affordable solution were available, it would be a game changer."*** The impact of having patient hydration data is significant as hydration is a leading indicator of damaging, even fatal, conditions such as organ failure and sepsis. Future wearable medical sensors based on SiP hold the potential to expand access to improved healthcare at affordable price points and empower patients to measure their own vital signs with the help of a clinician, and possibly at home.

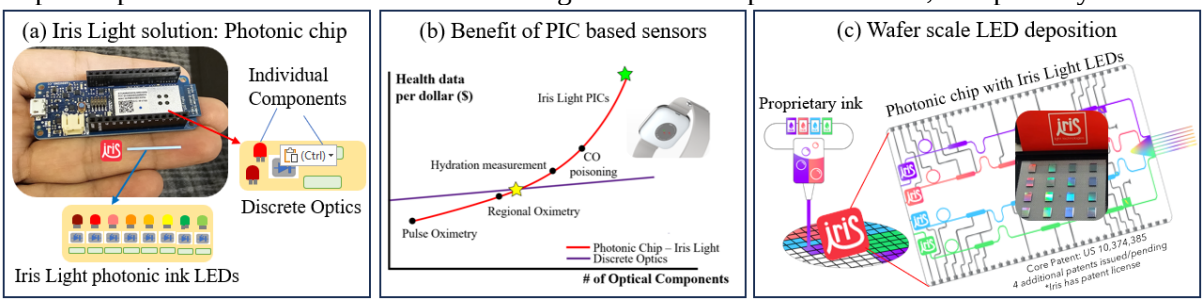

Figure 1: Illustrating the advantage of silicon photonics over discrete optics. (a) Image comparing an Iris Light SiP chip (20 x 1 mm) with *integrated* LEDs to large traditional *discrete* opto-electronics PCB board on proposer Pradeep Subedi's hand. (b) Societal benefits enabled by a silicon photonic chip medical sensor platform. (c) Wafer scale printing of sensors on chip enabled by Iris Light photonic ink.

Figure 1(a) shows a schematic of the current discrete optics approach for various medical wearable sensors. These devices consist of separate LEDs, photodiodes, filters, and packaging. Light absorption is used to measure patient physiological data. Signal processing takes place using off-chip electronics, posing additional signal-to-noise issues beyond the scope of this proposal.

Figure 1(b) illustrates how silicon photonics will enable the medical sensor industry to grow. A major drawback of the current approach based on discrete optics is that each individual sub-component has to be individually packaged, adding cost and complexity, **and in turn making them unaffordable to the general populace.** The economics simply do not work for the traditional approach to reach broad impact. As devices become more complex, photonic chips rapidly overtake discrete optics in terms of the key metric: *health data per dollar*. This transition point, marked by a yellow star in **Figure 1(b)**, occurs when devices consist of four or more LEDs. With our approach, additional LEDs can simply be printed onto a photonic chip as shown in **Figure 1(c)** which adds nominal device cost to the photonic chip but delivers expanded functionality and significantly richer patient data. The low-cost photonic ink

can be printed on-chip using commercially available, wafer-scale printing techniques including inkjet printing (IJP) and aerosol jet printing (AJP).

The 'why' for silicon photonics: solving the need for on-chip light sources

Although myriad industries (e.g. optical communications, LIDAR, immunoassays, quantum) recognize the revolutionary potential of silicon photonics, a major obstacle hampering its growth is the lack of a suitable gain material for silicon. The main method for coupling light into silicon today is to bond a separate III-V laser to the surface of the photonic integrated circuit (PIC), which is cumbersome and comprises >20% of product cost for a *single component*. In contrast, the PIC itself with *hundreds of components* at about 30% of cost. Integrating the laser onto the chip would drastically simplify the manufacturing process. **Figure 1(c) shows the Iris Light solution consisting of wafer scale printing of the actives on chip.** Our ink can be printed onto the surface of pre-patterned wafers with more than four LEDs per PIC. To address the need for multiple spectral bands, our semiconductor ink consists of nanoflakes that can be thickness-tuned to emit light covering 550-4000 nm (visible to near-infrared). We have already demonstrated proof-of-concept hybrid light sources at 1550 nm that couple ink gain material with silicon resonators [2].

Objective

The overall objective of the proposal is to develop a new class of printed photonic inks for LED light sources. These devices will be based on nanoscale black phosphorus (BP), a material that exhibits desirable opto-electronic properties including direct-gap light emission and high conductivity. The specific technical objectives are:

(1) Purification of nanomaterial BP inks for 1450 nm wavelength (four layer (4L)).
(2) Characterization of the opto-electronic properties of the 1450 nm ink, and
(3) Fabrication of printed LED at 1450 nm needed for skin hydration measurement.

This advance will be the first printed BP photonic ink LEDs on silicon photonic chips. In brief, the low-cost, on-chip light sources developed here will open the possibility of an entire new class of optical medical sensors and expand the reach beyond today's devices. It is likely that many emerging applications in human health monitoring have not even been conceived of because of the limitations of the current approach. In summary, the traditional platform that has been used to date cannot scale to meet the present and future needs of the $20 billion non-invasive medical sensor industry.

Literature Review – Non-invasive medical sensing and the need for silicon photonics.

Non-invasive medical sensing is currently achieved with methods that are either unreliable or very expensive. Here, we focus on skin hydration measurements since our minimum viable product (MVP) will be a skin hydration sensor. It is important to note that the on-chip optical sensors we are developing can be adapted for use in other high-volume medical sensing applications like blood pressure.

Currently, commercial skin hydration sensors rely on electrical measurements, such as capacitance or conductance of sweat. These kinds of devices do not directly measure the parameter of interest and are susceptible to environmental changes [3]. A more direct and reliable measurement is to detect skin hydration through optical absorption because water only absorbs at specific wavelengths. NIR wavelengths are most commonly used because of the high intensity OH and HOH vibration bands of water at 1450 nm and 1920 nm [4]. Water also absorbs at other wavelengths, such as 1200 nm. The most accurate optical sensor will operate using as many of these wavelengths as possible.

The largest players in the non-invasive medical industry (Medtronic, Edwards, Nonin) are shifting toward optical sensing to take advantage of its improved accuracy. Yet, these companies are still using discrete optics technology that are bulky and expensive. They are only beginning to explore photonic chips. Medtronic appears to be the early leader with their involvement in the EU project CARDIS (R&D) and their investment in Rockley Photonics in 2021. However, they have not released a product using silicon photonics. In addition, the product being worked on by Rockley targets smart watches, not medical sensors. This approach is expensive, and consequently not affordable to everyone, especially people from developing countries. Emerging companies like SiPhox (US) and MEEP (Belgium) are working on introducing photonics to point-of-need and at-home diagnostic sensors. However, their approach relies on two separate pieces, a consumable test, and a reader unit containing the light source and additional components. This is only *partial* integration and limited in potential reach.

The Optica Foundation Challenge grant will enable us to produce printed LEDs that operate at 1450 nm. We will achieve this through refinement of our existing black-phosphorus-based semiconducting inks. These LEDs would represent a large step toward our MVP of a fully-on-chip hydration sensor.

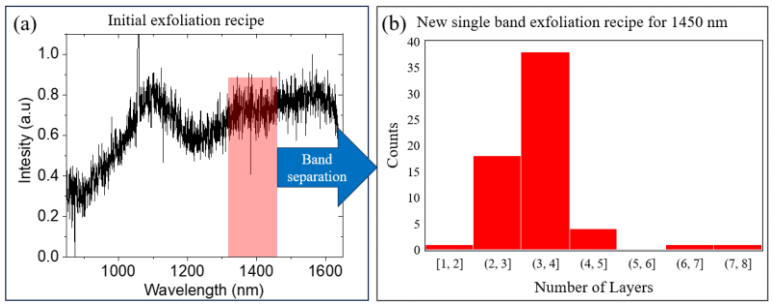

Figure 2: Separation of layers using Iris Light proprietary exfoliation method and centrifugation. (a) Photoluminescence of multi-layer BP ink. (b) AFM histogram of nearly-single spectrum flakes for 1450 nm (4L).

Black Phosphorus (BP) Photonic Devices and Inks: Nanomaterial BP was first isolated as an important 2D layered material in 2014 [5]. Semiconductor BP exhibits desirable opto-electronic properties including direct-band gap light emission and high conductivity. The optical properties of BP *can be engineered* because its bandgap *can be tuned by the number of 2D layers that comprise a BP flake* [5]. As a result, BP can achieve emission at broad range of wavelengths from visible 550 nm (1L) to infrared 4000 nm (bulk). Other 2D materials like graphene and transition metal dichalcogenides (TMDs) are not suitable for these applications. Graphene lacks a band gap, does not exhibit optical gain, and is too noisy for detectors. TMDs are only direct band gap in the monolayer and are also not efficient light emitters for many wavelengths of interest.

In recent years, the research community has demonstrated several examples of opto-electronic devices (LEDS and photodetectors) that demonstrate the immense potential of BP [6,7]. Bulk BP (no nanomaterial) was used to show electroluminescence with limited efficiency (<0.03%) with unoptimized device parameters, doping profile, and metallic contacts [8]. These LEDs are fabricated by a mechanical exfoliation (PVC tape) method that is not scalable. Additionally, they use >20 nm thickness BP flakes, resulting in emission near 3500 nm that is too far into the mid IR range for many applications. It should be possible to increase the quantum efficiency by at least an order of magnitude by changing the device parameters, such as the BP doping level [8]. Literature p-n junctions using BP have also demonstrated photo response. However, these devices suffer from the same issues (e.g. lack of scalability) as the LEDs. As a result, *no commercial deployment of BP has been achieved to date.* We are developing BP photonic ink using a method that was previously commercialized for graphene, highlighting a scalable path forward [9].

Printed electronics is a relatively young field and most inks in this industry are metallic (silver). To our knowledge, there is only one commercial graphene ink, and in low volumes [10]. BP inks have only been demonstrated recently for *polydisperse* materials (containing many different flake thicknesses) with unoptimized parameters [11]. Overall, there is a need for *monodisperse* BP inks to target specific optical properties. Beyond the immediate impact for medical sensors, our success will fulfill a key need for semiconductor inks for emerging printed electronics and opto-electronics.

Previous Results:

Iris Light Technologies has achieved to following milestones to date:

1. **BP-Silicon light emitters - proof of concept**: first demonstration of hybrid Si-BP light source [12].
2. **Demonstrated scalability of photonic chips:** Designed, taped out, and optically characterized custom silicon photonics Bragg grating chips using the 300 mm silicon line at AIM Photonics [13].
3. **Demonstrated scalability of printed nanomaterial inks:** Developed a polydisperse ink (BP flakes with range of layers) and printed on AIM Photonics chips using aerosol jet printing. Demonstrated 550-2200 nm light emission and electrical conduction.
4. **Opto-electronic devices:** We achieved chip-scale BP passivation [12], characterized electrical contact resistance to identify the optimal contact metal [unpublished]. Currently, we are working on characterization of photodetectors using unpurified (polydisperse) ink.

Since joining Iris Light in June 2022 Pradeep Subedi has achieved the following:

1. **Developed exfoliation recipes for 1450 nm and 1920 nm ink (Figure 2).**

Photoluminescence of the multi-layer ink in **Figure 2(a)** with preliminary AFM histogram results of single-layer ink in **Figure 2(b)**. Layer purification of exfoliated BP is necessary to achieve wavelengths relevant for specific devices. Our method has shown promising results for exfoliating 1450 nm BP **(Figure 2b)** as well as 1920 nm.

2. **Printed BP-based P-N photodiode displaying state-of-the-art 0.8 A/W at 980 nm (Figure 3).** BP is a native p-type material. **Figure (3)** show our successfully development of an prototype P-N photodiode combining our BP ink with a n-type substrate (Funded by NSF SBIR). The electrical properties and photocurrent response of these devices can be seen in **Figures 3(a) and (b)**.
3. **Achieved world record conductivity from printed 2D semiconductor ink (Figure 3)** Error! Reference source not found.**(c)** compares the conductivity of Iris Light printed BP films (9 Ω -cm) to the literature, highlighting orders of magnitude higher performance than other printed semiconductor films in the literature [14]. Error! Reference source not found.**(d)** shows a typical e lectrical conductivity characterization device (TLM) device made with multilayer BP ink deposited by aerosol jet printing (AJP).

Outline of tasks/Work plan

The overall technical goal of this proposal is to demonstrate printed LEDS from our BP photonic inks. As shown in **Figure 2**, we have achieved two inks to date, one tailored to 1450 nm emission (4L), and one tailored to 1920 nm emission (8L). Currently, the 1920 nm ink has higher conductivity and better yield. For the Optica Foundation Challenge, we will focus on achieving an LED from the 1450 nm ink. This is because it is a more monodisperse ink and because it is much easier for us to measure 1450 emission than 1920 nm. Further effort to make a 1920 nm LED will be investigated in the future which is known to show more intense water absorption band.

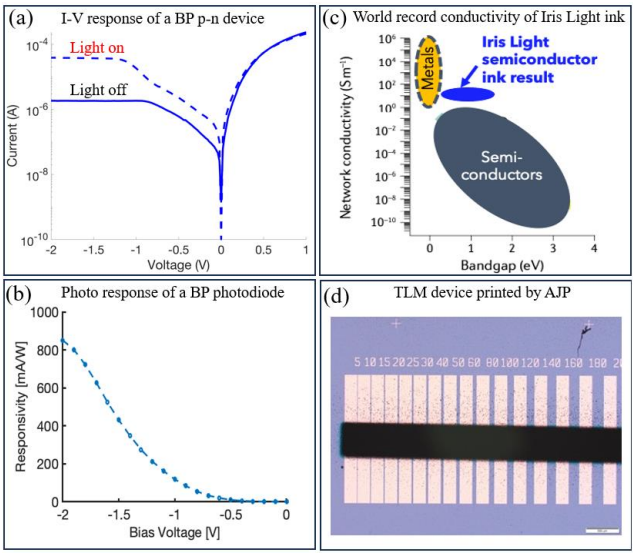

Figure 3: Electrical measurements of BP devices printed with aerosol jet printing. (a) I-V response of a BP p-n device. (b) Photo response of printed photodiode at 980 nm (c) World-record conductivity achieved by Iris compared to literature [14] (d) Typical conductivity characterization device printed with BP ink.

Specific technical objectives include: (1) Improving the yield of nanomaterial inks based on 1450 nm (4L) BP, (2) optimizing the opto-electronic properties of the 1450 nm inks, and (3) Fabrication of printed LEDs at 1450 nm that is needed for skin hydration measurements. These objectives will be achieved through the following tasks:

Task 1: Improving the yield of 1450 nm (4L) BP ink.

There are several variables that must be optimized to improve the material yield to a point where it is sufficient for printing on chips. A combination of change in exfoliation recipe and centrifugation parameters will be investigated to separate the 1450 nm BP with maximum yield. **Milestone/Success metrics:** Yield will be doubled from approximately 10% to 20%

Task 2: Optimization of the opto-electronic performance of purified 1450 nm (4L) BP inks.

Milestone/Success metrics: We will take photoluminescence spectra that shows emission peaking at 1450 nm. Exfoliation and centrifugation conditions will be altered until achieving PL that peaks at 1450 nm. Photodetector measurements will be carried out to determine the responsivity of printed 1450 nm ink at NIR wavelengths with a broadband supercontinuum source ranging from 1310 to 1550 nm.

Task 3: Demonstrate prototype LEDS at 1450 nm suitable for hydration measurement.

After preparing the 1450 nm (4L) ink, we will print LEDs onto silicon substrates with pre-patterned metal electrodes. **Milestone/Success metrics:** Measurements of LED optical spectra with emission at 1420 nm. Target quantum efficiency (EQE) of 1% (literature value is ~0.03%).

		PROJECT MONTH											
OBJECTIVE	TASK	1	2	3	4	5	6	7	8	9	10	11	12
Synthesis of 1450 nm nanomaterial inks based on 2D black phosphorus (BP) to achieve 20% yield.	1	M1											
Achieve desirable optoelectronic properties of 1450 nm photonic inks.	2				M2								
Demonstrate printed LEDs with response at 1450 nm.	3							M3					
Project Reporting							**						**

Outcome(s)

The following are the expected outcomes of this project:

- A novel recipe for a commercial, photonic ink operating at 1450 nm for printed electronics.
- Demonstration of a printed LED that emits at 1450 nm.

Impact

At scale, our solution developed with support from the Optica Foundation Challenge offers the potential for broad societal and economic benefit shared globally. The on-chip medical sensor platform will enable access to state-of-the-art medical care for people all over the world. Reduction of packaging costs compared to legacy optics will facilitate affordability so that people will benefit from accurate, non-invasive devices. While the initial application cited here is hydration measurement related, there is a vast range of applications that will benefit including cardiovascular diseases, continuous glucose monitoring for diabetes patients, diagnostic assays, and breath analysis. In terms of photonic innovation, the demonstration of low-cost integration of a novel gain medium based on printed photonic inks into silicon chips would mark a major path forward for the field. Indeed, getting light into silicon chips has been a longstanding issue and continues to inspire R&D and commercial efforts (see Integrated Photonic Systems Roadmap – IPSR). Our techno-economic analysis of the ink-based approach demonstrates the potential to be orders of magnitude lower cost compared to current and emerging approaches and offers a fresh perspective to the challenge.

References:

1. W. R. Mower, G. Myers, E. L. Nicklin, K. T. Kearin, L. J. Baraff, and C. Sachs, "Pulse Oximetry as a Fifth Vital Sign in Emergency Geriatric Assessment," Acad. Emerg. Med. **5**, 858–865 (1998).
2. C. Husko, J. Kang, G. Moille, J. D. Wood, Z. Han, D. Gosztola, X. Ma, S. Combrié, A. De Rossi, M. C. Hersam, X. Checoury, and J. R. Guest, "Silicon-Phosphorene Nanocavity-Enhanced Optical Emission at Telecommunications Wavelengths," Nano Lett. **18**, 6515–6520 (2018).
3. I. M. Gidado, M. Qassem, I. F. Triantis, and P. A. Kyriacou, "Review of Advances in the Measurement of Skin Hydration Based on Sensing of Optical and Electrical Tissue Properties," Sensors **22**, (2022).
4. Y. Tzabari Kelman, S. Asraf, N. Ozana, N. Shabairou, and Z. Zalevsky, "Optical tissue probing: human skin hydration detection by speckle patterns analysis," Biomed. Opt. Express **10**, 4874 (2019).
5. H. Liu, Y. Du, Y. Deng, and P. D. Ye, "Semiconducting black phosphorus: Synthesis, transport properties and electronic applications," Chem. Soc. Rev. **44**, 2732–2743 (2015).
6. N. Youngblood, C. Chen, S. J. Koester, and M. Li, "Waveguide-integrated black phosphorus photodetector with high responsivity and low dark current," Nat. Photonics **9**, 247–252 (2015).
7. J. Wang, A. Rousseau, M. Yang, T. Low, S. Francoeur, and S. Kéna-Cohen, "Mid-infrared Polarized Emission from Black Phosphorus Light-Emitting Diodes," Nano Lett. **20**, 3651–3655 (2020).
8. H. Kim, S. Z. Uddin, D. H. Lien, M. Yeh, N. S. Azar, S. Balendhran, T. Kim, N. Gupta, Y. Rho, C. P. Grigoropoulos, K. B. Crozier, and A. Javey, "Actively variable-spectrum optoelectronics with black phosphorus," Nature **596**, 232–237 (2021).
9. A. A. Green and M. C. Hersam, "Solution Phase Production of Graphene with Controlled Thickness via Density Differentiation," Nano Lett. **9**, 4031–4036 (2009).
10. E. B. Secor, P. L. Prabhumirashi, K. Puntambekar, M. L. Geier, and M. C. Hersam, "Inkjet Printing of High Conductivity, Flexible Graphene Patterns," J. Phys. Chem. Lett. **4**, 1347–1351 (2013).
11. H. Y. Jun, S. O. Ryu, S. H. Kim, J. Y. Kim, C. Chang, S. O. Ryu, and C. Choi, "Inkjet Printing of Few-Layer Enriched Black Phosphorus Nanosheets for Electronic Devices," Adv. Electron. Mater. **7**, 2100577 (2021).
12. J. Kang, S. A. Wells, J. D. Wood, J.-H. Lee, X. Liu, C. R. Ryder, J. Zhu, J. R. Guest, C. A. Husko, and M. C. Hersam, "Stable aqueous dispersions of optically and electronically active phosphorene," Proc. Natl. Acad. Sci. **113**, 11688–11693 (2016).
13. C. Husko, A. Ducharme, N. M. Fahrenkopf, and J. R. Guest, "Phase-shifted Bragg gratings in a foundry silicon nitride platform," OSA Contin. **4**, 933 (2021).
14. A. G. Kelly, D. O. Suilleabhain, C. Gabbett, and J. N. Coleman, *The Electrical Conductivity of Solution-Processed Nanosheet Networks* (Springer US, 2022).

Executive Summary for

Compact Computational Flat-Optical Bronchoscopes for Image-guided Cancer Therapies Under Respiratory Deformation of Lungs

Praneeth Chakravarthula

cpk@cs.unc.edu, UNC Chapel Hill, Department of Computer Science

Problem Statement and Objectives

Over 200,000 new cases of lung cancer are diagnosed annually in the United States alone, resulting in about 150,000 deaths, making lung cancer the most lethal of all forms of cancer. Only 1 in 6 lung cancers are diagnosed at an early stage and over half are diagnosed with distant metastasis. For effective and early diagnosis, adequate and representative biopsy sample collection is the key which will help in better management and improve patient outcomes. However, accessing inner nodules of the lung is challenging due to the large size of the bronchoscope compared to the bronchial airways of the lungs. Adding to this, the lungs deform intraoperatively due to respiratory motion making it further difficult to visualize the lesions towards the periphery of the lung. Given that existing solutions do not address this problem and a standard scope can only reach up to 4-5th generation of bronchi – in a typical 23 generation bronchial tree of lung – we aim to develop a compact bronchoscope based on computationally designed flat meta-optical elements that will significantly reduce the size while still allowing for full color real-time imaging and guided therapies.

Impact of Proposed Research

The development and implementation of thin bronchoscopes will have a transformative impact on respiratory medicine. These ultra-compact and agile instruments have the ability to revolutionize the landscape of minimally invasive operations and experimental surgeries, offering improved diagnostic capabilities and therapeutic interventions. The reduced rigid tip length of the proposed bronchoscope allows for enhanced maneuverability, facilitating smoother navigation through narrow and tortuous ducts with minimized patient discomfort and risk of complications. By reaching peripheral lung regions more effectively, the proposed thinner bronchoscope promises to enable more extensive visualization and sampling of lesions that were previously challenging to access, resulting in higher diagnostic yield and more accurate staging of lung cancer. Furthermore, integrating with the computational optimization techniques will improve image resolution thereby improving real-time guidance during procedures. Overall, the proposed research can significantly advance respiratory medicine and interventional pulmonology, enhancing patient outcomes.

Why should this proposal be granted?

The proposed technique represents a significant advancement in imaging optics for respiratory medicine and serves as a crucial initial step towards realizing the PI's long-term research vision. The project's success is pivotal in establishing the foundation for larger and more extensive grants in the future, which could further support the development of the bronchoscope demonstration over multiple years.

A Proposal to Optica Foundation Challenge Program

Compact Computational Flat-Optical Bronchoscopes for Image-guided Cancer Therapies Under Respiratory Deformation of Lungs

Praneeth Chakravarthula
cpk@cs.unc.edu
UNC Chapel Hill, Department of Computer Science
Chapel Hill, NC 27599-3175

Abstract

Bronchoscopy is a crucial minimally invasive diagnostic and therapeutic tool in respiratory medicine allowing direct visualization and sampling of the airways for the evaluation and management of various lung conditions. The size of bronchoscopes directly impacts the patient's comfort and tolerability during the procedure. A thinner and less rigid bronchoscope enables higher agility, larger accessibility especially for the peripheral pulmonary areas, and induce less stress on the surrounding tissues especially when the lung is deforming during respiration. The size of the imaging optics poses a major limitation in miniaturization of the bronchoscope as well as increasing the size of the working channel for procedures including taking cancer biopsy samples. Moreover, the size of the bronchoscope limits diagnostic and therapeutic approaches only to the central pulmonary regions, reaching only up to fourth-order bronchi in the best case.

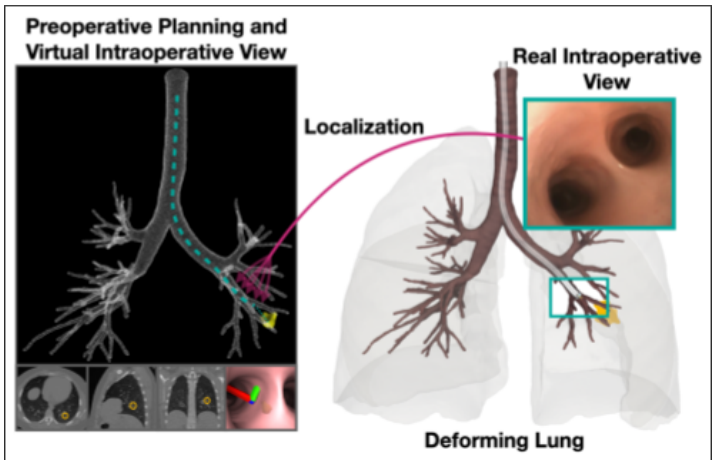

Figure 1. During bronchoscopy, a physician deploys a bronchoscope through the airways (right) to target a suspicious lung nodule (yellow) for biopsy or treatment, from a reference generated from the reconstruction of a preoperative CT scan (left).

In this project, we will explore the use of meta-optics to drastically miniaturize optics while achieving similar functionalities with significantly reduced size. We propose an inverse-designed meta-optic that will be computationally optimized and combined with a coherent fiber bundle to achieve an imaging device that will enable at least 60% reduction over traditional imaging optics used in bronchoscopes. The size of the meta-optic lens will be miniaturized to under 1mm in diameter and under 2mm in rigid tip length, compared to a few centimeters in standard bronchoscopes, allowing for significantly improved maneuverability into higher order (up to ninth-order) peripheral bronchi while maintaining image quality to visualize pulmonary airways. We will build an experimental prototype bronchoscope and demonstrate full color real-time video capture.

Problem Statement and Objectives

Over 200,000 new cases of lung cancer are diagnosed annually in the United States alone, resulting in about 150,000 deaths, making lung cancer the most lethal of all forms of cancer [1].

Only 1 in 6 lung cancers are diagnosed at an early stage and over half are diagnosed with distant metastasis. For effective and early diagnosis, adequate and representative biopsy sample collection is the key which will help in better management and improve patient outcomes. However, accessing inner nodules of the lung is challenging due to the large size of the bronchoscope compared to the bronchial airways of the lungs. Adding to this, the lungs deform intraoperatively due to respiratory motion making it further difficult to visualize the lesions towards the periphery of the lung. Given that existing solutions do not address this problem and a standard 5.9 mm scope[1] can only reach up to 4-5th generation of bronchi – in a typical 23 generation bronchial tree of lung – we aim to develop a compact bronchoscope based on computationally designed flat meta-optical elements that will significantly reduce the diameter as well as the rigid tip length of the bronchoscope while still allowing for full color real-time imaging and guided therapies.

Description of Proposed Work and Expected Outcomes

We aim to build a thin and compact bronchoscope, reducing the footprint of the imaging optics by replacing conventional bulky imaging lens stack with a computational flat-optical metalens. Conventional bronchoscopes, and endoscopes in general, use a bulky stack of refractive optical elements that are designed to reduce the aberrations and maximize the image quality. However, the size of these optical elements result in thicker imaging scopes with rigid tips, which fundamentally limits the device agility, especially within smaller ducts such as higher order bronchial branches. Solutions that reduce the rigid tip length and compact the bronchoscope are in fact urgently needed.

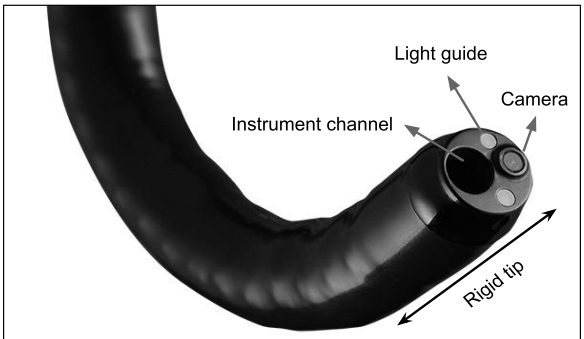

Figure 2. Standard 5.9mm Therapeutic Bronchoscope. The imaging optics restricts the size and flexibility of the bronchoscope, limiting the diagnosis only to the central airways, up to third or fourth order pulmonary nodules.

Flat meta-optics is an emerging technology that enables creating miniaturized optical elements using subwavelength structures that allow precise control over the behavior of light, such as its propagation, polarization, phase and amplitude. Metasurfaces are composed of arrays of nanoscale scatterer elements that interact with light in unconventional ways. Such ultrathin flat optics not only dramatically shrink the size of traditional optics, but can also enable functionalities that were not achievable previously, such as bending light at sharp angles, focusing light into subwavelength spots, and creating artificial optical phenomena, all on a single surface. However, meta-optics traditionally suffer from strong aberrations (both chromatic and Seidel) making large field-of-view and full-color imaging challenging. As such, a full-color meta-optic endoscope for 400-700 nm spectrum and a fractional bandwidth of ~0.54 with acceptable field-of-view, depth-of-field and a large enough aperture has not yet been achieved to the best of our knowledge.

[1] Fujifilm EB-580 T Therapeutic Bronchoscope

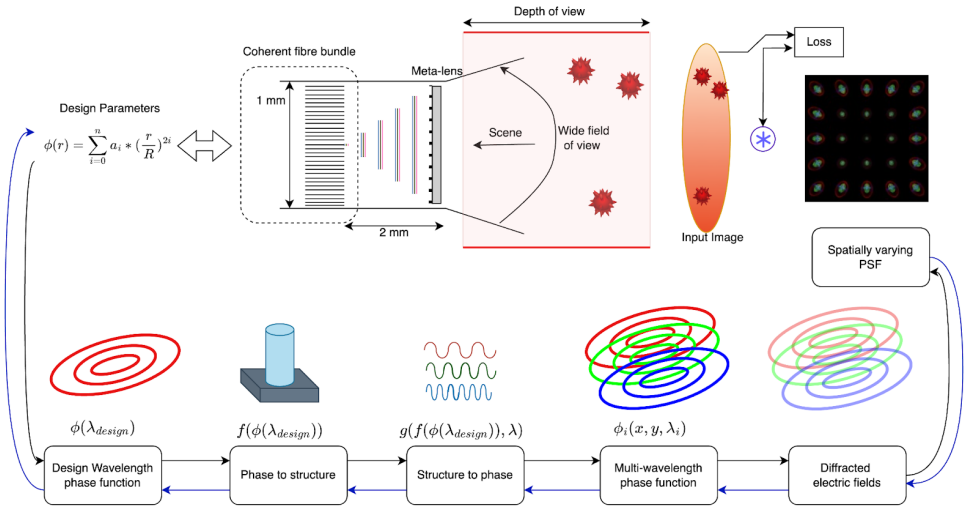

Figure 3. Overview of the metalens design pipeline. We circumvent computational FDTD methods via differentiable fast approximation of RCWA which allows us to perform gradient-based optimization.

In this proposal, we aim to achieve an inverse-designed meta-optic, optimized to capture in real-time full-color scenes in the visible spectrum. The metalens will be designed in conjunction with a coherent fiber bundle of 1mm diameter, keeping the overall size of the bronchoscope imaging area and the rigid tip length to the minimum, and significantly increasing its working channel as well as the flexibility to access higher-order peripheral bronchi of the lung, see Figure 2. To this end, we will build fully differentiable forward models via deep neural networks to model the wave effects of nano scatterers on the metalens, and optimize for the metalens phase as an optimization parameter to minimize any aberrations under broadband illumination.

Differentiable rendering for metasurface optics.
We will build deep learning models for efficiently determining the optical response of the metalens-based imaging system as a function of the design parameters (e.g. tip length, incident wavelength, nano scatter shape). Specifically, we can learn the imaging response as

$$y = f(x, p),$$

where y is the PSF of the optical system, x is the input wavefront, and p are the system design parameters. Imaging optics usually deviate from the paraxial regime where the imaging system can be described by a single, spatially-invariant PSF. We will fully quantify chromatic and Seidel aberrations (coma, distortion, astigmatism, spherical), and compute spatially-varying PSFs as

$$y(\theta) = f(x(\theta), p),$$

where θ is the angle of incidence for the incoming wavefront.

Modeling the millions of sub-wavelength scatterers on a meta-surface is challenging and requires full electromagnetic simulation to accurately model the wave effects of meta-optic. Traditionally, metasurfaces are simulated using finite-difference time-domain methods which result in high computational complexity, making them impractical for optimization-based inverse-design of metasurfaces beyond a few micrometers in aperture. Therefore, we will use rigorous coupled-wave analysis (RCWA) and build a proxy function using deep neural networks

to approximate the effects of nano structures on the meta-optic. This technique will allow for faster differentiable simulation. Specifically, we will approximate the phase response of the metasurface as

$$\phi(\lambda) = g(f(\phi(\lambda_{design})), \lambda),$$

where f is a function that converts the wavefront at the design wavelength λ_{design} into a metasurface nano-structure and g is a function that determines the phase response at an arbitrary wavelength λ for a given nano-structure design. Both f and g are built as fast and fully differentiable functions closely approximating RCWA techniques. An overview of the pipeline for designing the flat meta-optic is illustrated in Figure 3. Once designed, we will fabricate the metalens and combine it with a thin coherent fiber bundle to complete a thin bronchoscope for evaluation.

Evaluation Plan

We will analyze the optical performance of the proposed meta-optic bronchoscope both quantitatively via its modulation transfer function (MTF[2]) and qualitatively by comparing it with existing standard bronchoscopes. For qualitative comparison, we first plan to conduct a comparison of images that are displayed on an OLED screen and images that are captured with the newly designed metalens fiber optic imager and the in-built camera of a typical endoscope. Next, we plan to insert the metalens fiber-optic imager into the working channel of an existing bronchoscope, Ambu aScope 5 Broncho[3], and compare the image quality of the airways within the lungs. To this end, we will collaborate with Prof. Ron Alterovitz at UNC Chapel Hill who has prior experience with operating with bronchoscopes on experimental lungs, and real pig and human lungs.

We have already conducted a few preliminary evaluations in simulation for the proposed approach for designing the metalens-based bronchoscope, optimized for broadband illumination across the visible spectrum. Our preliminary results suggest that the metalens with 1mm aperture will reduce the tip length significantly, down to 2mm, compared to a few centimeters in standard 5.9mm bronchoscope. The imager will maintain a total field-of-view of 45 deg. We calculated the MTF of our proposed design and Figure 3 compares it to the recent design from Tseng et al.[1], which is reported to achieve a total FoV of about 40 deg.

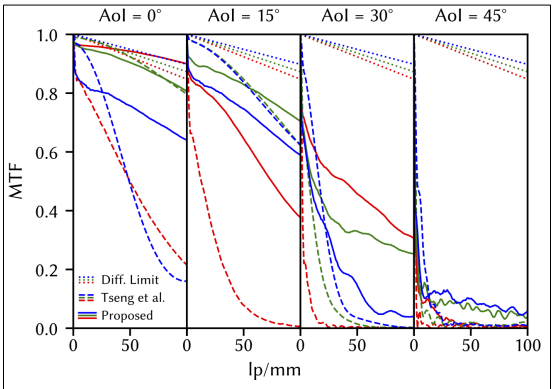

Figure 4. The calculated MTF for various angle of incidence (AoI). Thick solid lines correspond to the diffraction limit. Dashed lines correspond to calculated MTF curves for Tseng et al.[1]. Full thin lines correspond to the meta-optic proposed in this work.

[2] MTF is the ability of the optic to transfer contrast at a given spatial frequency (resolution) from the object to the imaging sensor.

[3] https://www.ambuusa.com/endoscopy/pulmonology/bronchoscopes/product/ascope-5-broncho

Impact of Proposed Research

The development and implementation of thin bronchoscopes will have a transformative impact on respiratory medicine. These ultra-compact and agile instruments have the ability to revolutionize the landscape of minimally invasive operations and experimental surgeries, offering improved diagnostic capabilities and therapeutic interventions. The reduced rigid tip length of the proposed bronchoscope allows for enhanced maneuverability, facilitating smoother navigation through narrow and tortuous ducts with minimized patient discomfort and risk of complications. By reaching peripheral lung regions more effectively, the proposed thinner bronchoscope promises to enable more extensive visualization and sampling of lesions that were previously challenging to access, resulting in higher diagnostic yield and more accurate staging of lung cancer. Furthermore, integrating with the computational optimization techniques will improve image resolution thereby improving real-time guidance during procedures. Overall, the proposed research can significantly advance respiratory medicine and interventional pulmonology, enhancing patient outcomes.

Prior Work

Solutions explored for thin endoscopy involve lensless and computational imaging with single fibers [2-4] or coherent fiber bundles [5-8]. However, these approaches are often restricted by short working distances and vulnerability to bending and twisting of the optical fibers, hindering real-time image capture. Additionally, research has been conducted on optimizing, and fabricating compact optical elements, including 3D printed elements directly on fibers [10] or freeform mirror optics for side-viewing endoscopes [11]. While these alternatives offer high optical performance, the scalability of 3D printed or freeform optical elements remains a challenge, particularly for bronchoscopy, where disposable optics are preferred to prevent cross-contamination between patients. Meta-optics [12,13], on the other hand, not only dramatically shrink the size of traditional optics, but also can combine multiple functionalities in a single surface [14,15]. Moreover, flat meta-optics are compatible with high-volume semiconductor manufacturing technologies [16,17], and thus can create disposable optics.

References

[1] Katsis et al: "Bronchoscopic biopsy of peripheral pulmonary lesions in 2020: a review of existing technologies." Journal of Thoracic Disease. 2020.

[2] Caramazza et al: "Transmission of natural scene images through a multimode fiber." Nature Communications, 2019.

[3] Liu et al: "All-fiber high-speed image detection enabled by deep learning." Nature Communications 2022.

[4] Wang et al: "High-speed all-Fiber micro-imaging with large depth of field." Laser Photonics 2022.

[5] Shin et al: "A minimally invasive lens-free computational microendoscope." Science Advances 2019.

[6] Badt and Katzl: "Real-time holographic lensless micro endoscopy through flexible fibers via fiber bundle distal holography." Nature Communications 2022.

[7] Orth et al: "Optical fiber bundles: ultra-slim light field imaging probes." Science Advances 2019.

[8] Choi et al: "Flexible-type ultrathin holographic endoscope for microscopic imaging of unstained biological tissues." Nature Communications 2022.

[10] Gissibl et al: "Two-photon direct laser writing of ultracompact multi-lens objectives." Nature Photonics 2016..

[11] Li et al: "Ultrathin monolithic 3D printed optical coherence tomography endoscopy for preclini- cal and clinical use." Light Science and Applications 2020.

[12] Yu and Capassol: "Flat optics with designer metasurfaces." Nature Materials 2014.

[13] Chen et al: "Principles, functions, and applications of Optical Meta-Lens" Advanced Optical Materials 2021.

[14] Munley et al: "Inverse-designed meta-optics with spectral-spatial engineered response to mimic color perception." Advanced Optical Materials 2022.

[15] Piccardo et al: "Roadmap on multimode light shaping" Advanced Optical Materials 2022.

[16] Colburn et al: "Broadband transparent and CMOS-compatible flat optics with silicon nitride metasurfaces." Optical Materials Express 2018.

[17] Zhang et al: "High-Efficiency, 80 mm aperture Metalens Telescope." Nano Letters 2023.

Silicon photonic biosensors for low-cost, portable, data-rich measurements of hormone biomarkers relevant to women's health and the menopausal transition

Executive Summary for Health Challenge

Dr. Samantha M. Grist, The University of British Columbia, Vancouver, Canada

What is the unmet need? There have historically been significant gender inequities in healthcare and medical research, with many women's health issues, including symptoms of the menopausal transition, neglected and underfunded. Women's gonadal (sex) hormones can be key indicators of health and impact many conditions beyond fertility, including cardiovascular conditions and neurological disorders. These hormones also fluctuate significantly during the menstrual cycle, requiring frequent monitoring to fully understand the levels and fluctuations. Gonadal hormones are critical during the menopausal transition, with levels of more than 10 hormones linked with perimenopausal symptoms including sleep and mood disruption, brain fog, and hot flashes. These symptoms present a significant societal burden – 25% of people experiencing perimenopause symptoms consider leaving the workforce – but people experiencing them and the physicians treating them have limited tools and data to understand and predict symptoms or monitor and improve the impact of treatment. To provide insightful, impactful data, the ideal monitoring tool would provide quantitative, accurate, and data-rich measurement of at least 4-10 hormones and hormone metabolites, and it would be able to provide these measurements quickly (in minutes) at low cost, in a form factor suitable for people to conveniently use at home at least multiple times per week. This kind of solution does not currently exist: centralized lab-based assays are expensive, slow, and inconvenient for daily testing, while existing point-of-need solutions like lateral flow assays do not provide the required quantitative, accurate, and multiplexed (measurement of multiple hormones) data.

What is being proposed to meet this need? Silicon photonic integrated circuits containing biosensors are well-suited to performing quantitative, accurate, data-rich measurements, and tens to hundreds of sensors can be integrated on a single millimeter-scale chip for multiplexed measurements. They are fabricated with scalable semiconductor manufacturing technologies, facilitating low costs at high volume. A key limitation of these types of sensors has historically been the size and cost of the readout system (e.g., the Genalyte platform for doctors' offices), because an expensive ($40,000-$100,000), bulky tunable laser and light coupling system are required to read out the data, precluding their use for at-home testing applications like hormone monitoring. We have invented a new sensor architecture that addresses this challenge, allowing us to use a tiny (<1 mm), inexpensive (<$1), fixed-wavelength laser for readout. In this project, we propose to validate this new silicon photonic technology, create a bench-scale portable readout system, and demonstrate urine-based detection of an initial panel of two hormone biomarkers relevant to menopause (expandable to tens in the future).

What are the expected outcomes? Through this work plan we will develop our new silicon photonic sensor and quantify its photonic performance metrics (to provide data-rich measurements at 1000× lower cost than traditional photonic biosensors), compare performance with gold-standard measurements, and also quantify detection of two biomarkers relevant to the menopausal transition: pregnanediol (PdG) and follicle-stimulating hormone (FSH). We will also demonstrate a portable system suitable for demonstration at Optica conferences and to collaborators.

What will be the real-world impact of this project? This project will use innovation in photonics to address a critical unmet need in women's healthcare by validating a portable, low-cost technology for decentralized, multiplexed monitoring of hormone markers in urine. With this project, we will build a tool that has the potential to drastically improve health and quality-of-life during the menopausal transition, and also lay the foundation for future development of tests for additional conditions for broader potential impact of the technology on human health.

Proposal - Ultra-low loss and broadband all-fiber acousto-optic circulators (FiberCircl)

Literature review

Non-reciprocal devices, such as isolators and circulators, constitute an important part of any optical setup and find application in simple tasks such as protecting a laser from back-reflections to more demanding operations as signal routing and processing in optical networks. Most off-the-shelf devices rely on the Faraday effect, an approach not easy to implement in integrated devices, may they be based on fiber-optics or photonic circuits, due to fabrication complexity, large material losses and difficulty in handling magnetic fields. For these reasons, extensive effort has been devoted to identify alternative ways to break Lorentz reciprocity, as for instance using non-linear optics [1], electro-optics [2], chirally coupled atoms [3] and acousto-optics. The latter has been particularly successful because of the strong coupling between light and acoustic vibration that can be achieved, when both waves are confined to small volumes, as for instance in tapered [4] and photonic-crystal fibers [5] or in photonic circuits [6-8] and whispering gallery mode resonators [9]. From a practical perspective, to date this approach is certainly the most promising for the next generation of magnetic-field-free non-reciprocal devices as it potentially allows low insertion loss, broadband operations and electrical actuation.

The best acousto-optic non-reciprocal devices in the literature roughly all rely on the same working principle. Let us consider the configuration in Fig. 1(a), in which light (frequency ω and wavevector β_{FM}) propagates along a waveguide in its fundamental optical mode (FM). Let us now assume that an acoustic wave of frequency Ω also co-propagates along the waveguide, causing a periodic modulation of its refractive-index. If phase-matching occurs, i.e., if the acoustic wavelength matches the beat-length between the FM and the first higher order mode (HOM), an energy transfer occurs between the two optical modes (see Fig. 1(a,b)). Notably, trying to use the same acoustic wave to couple backward propagating light fields (Fig.1(b)) results in a total phase mismatch [10]: $\Delta\varphi = \Delta\beta\, L = (\beta_{FM} + \beta_{HOM})\, L\, \Omega/\omega$, where L indicates the waveguide length. Non-reciprocal acousto-optic interaction occurs if $\Delta\varphi >> 2\pi$ and, since for most experimental systems $L \lesssim 10$ cm, it is only possible if the acoustic frequency Ω is large enough (e.g., $\Omega \gtrsim 10$ GHz). For a long time, exciting such high frequency waves required the use of auxiliary intense laser fields, which made the resulting devices unsuited for further applications [5, 10]. In the field of photonic circuits, electrical actuation of GHz acoustic waves has been reported only very recently [6-8], however, due to large in- and out-coupling loss, these state-of-the-art devices are not suited for low-loss fiber networks. **Electrical actuation** of **GHz acoustic waves** in **fiber-based systems** remains an **outstanding challenge** and to the best of my knowledge, no strategy to overcome this limitation has been demonstrated or proposed so far.

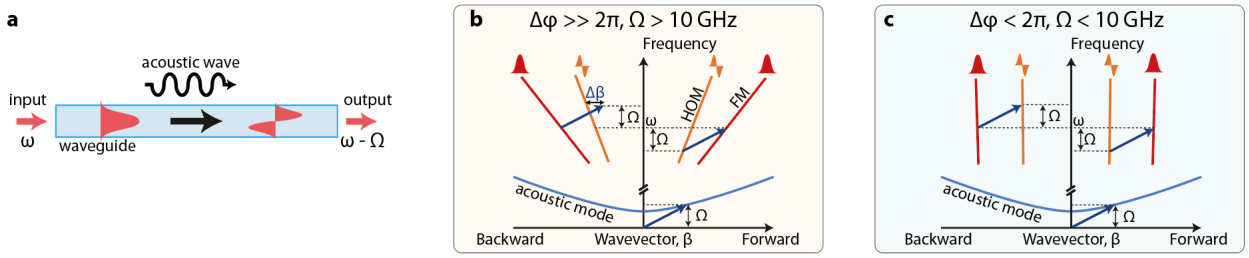

Fig. 1 (a) Diagram of acousto-optic interaction in optical waveguides: ω is the light frequency and Ω the acoustic frequency. (b,c) Dispersion diagram for optoacoustic intermodal coupling. (b) For large acoustic frequencies: $\Delta\varphi >> 2\pi$. The acoustic mode only phase-matches intermodal coupling in the forward direction ($\beta>0$). The wavevector mismatch in the backward direction is indicated with $\Delta\beta$. (c) In state-of-the-art electrically actuated all-fiber devices the achievable mechanical frequencies are usually small (1-50 MHz), therefore $\Delta\varphi \approx 0$. The same acoustic can mediate intermodal coupling both in forward and backward direction. The resulting device are completely reciprocal.

Problem Statement/Objective

The main objective of this project is to provide a concrete and robust solution to this issue by the proof-of-principle demonstration of electrically actuated all-fiber circulators with ultra-low loss (<0.1 dB), high

extinction ratios (>20 dB) and broadband operations (bandwidth > 100 GHz). Fabricated exclusively with standard single-mode fibers, these devices will rely on low frequency (~ MHz) acoustic waves and will be compatible with any existing or future fiber network. Beyond the intrinsic interest of extending acousto-optic non-reciprocity to fiber optics, the demonstration of ultra-low loss fiber-based circulators will have a profound impact the development of future quantum networks [11, 12], for which loss represents a highly undesired additional source of decoherence.

The key ingredient of this proposal is a particular type of fiber coupler known as **null-coupler**, first introduced by Birks et al. [4]. A standard fiber coupler is fabricated by heating and fusing together two identical fibers. Controlling the coupler length and degree of fusion allows any coupling ratio between 0% and 100%. However, if the fibers have different starting diameters, the maximum achievable coupling is less than 100%. A null-coupler is a fiber coupler made with fibers so dissimilar that the maximum coupling is approximately zero. In this case, adiabatic propagation along the coupler ensures that light launched into the larger fiber excites the FM of the coupler waist, eventually emerging from the same fiber at the other end of the coupler. The same occurs for light launched into the thinner fiber, which, instead, excites the HOM of the coupler waist (see Fig. 2(a,b)).

Acousto-optic interaction can transform a null-coupler in an **arbitrary splitting-ratio coupler** [4]. Let us consider the configuration in Fig. 2(c), in which a piezo transducer is employed to excite along the coupler waist acoustic waves, whose frequency and wavevector fulfills phase-matching between the FM and the HOM. As a result, light will couple from the FM to the HOM in an amount given by amplitude of the acoustic wave (see Fig. 2(c,d)). Figure 2(e) shows a preliminary measurement of this process for a null-coupler fabricated in our self-built fiber tapering rig. For a fixed acoustic frequency Ω, the phase-matching condition is fulfilled over an optical bandwidth of a few nm and by changing Ω, phase-matching can be achieved for any frequency over the entire working bandwidth of the selected optical fiber (see Fig. 2(f)).

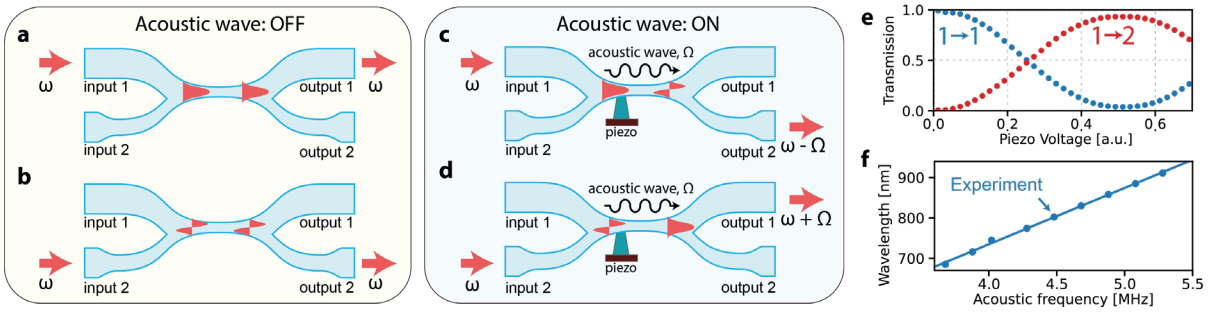

Fig. 2 (a-d) Schematic representation of the working principle of a null-coupler. (e) Measured coupling ratio between the input and output port of a null-coupler as a function of the amplitude of the voltage applied to the piezo transducer (Ω ≈ 4.9 MHz). The blue and red dots refer to the transmission measured from input 1 to output 1 and from input 1 to output 2, respectively. (f) Measured phase-matching wavelength as a function of the acoustic frequency, Ω. The device was fabricated with standard SM800 optical fiber.

Null-couplers work at acoustic frequencies, Ω, in the range 1 - 50 MHz and therefore, as already mentioned, they do not exhibit non-reciprocal light re-routing capabilities. However, light that is coupled across a null-coupler via acousto-optic interaction is subject to a **non-reciprocal frequency shift**, whose sign depends on the relative direction of propagation of the light and acoustic wave (see Fig. 1(c) and Fig. 2(c, d)). This equals −Ω if the light and acoustic wave are co-propagating and +Ω in the opposite case. To use this to our advantage let us consider the **non-linear interferometer** shown in Fig. 3 (a), where two null-couplers are cascaded in a Mach-Zehnder configuration. Let us assume that both null-couplers are set to a splitting ratio of 50 % (see Fig. 2 (e)) and operate at the same acoustic frequency. As depicted in Fig. 3(a), when light is launched from port 1, acousto-optic interaction in the first null-couplers shifts the frequency of the light field propagating in the lower arm of the interferometer by +Ω. This shift is later compensated at the second null-coupler, such that the light at port 2 exhibits no frequency shift and its intensity is given by:

$$I_{1\to 2} = \frac{1}{2} I_0 \left[1 + \cos(\Delta\varphi_{1\to 2})\right], \text{ where } \Delta\varphi_{1\to 2} = \frac{n\,\omega}{c}\,\Delta L - \frac{n\,\Omega}{c}\,L_2. \qquad (1)$$

Here, I_0 is the intensity of the input light and $\Delta L = L_1 - L_2$, where L_1 and L_2 are the lengths of the two arms of the interferometers. Instead, if light is launched from port 2 (see Fig. 3(b)), light propagating in the lower arm of the interferometer experiences a frequency shift of $-\Omega$ and the intensity of the light reaching port 1 is given by:

$$I_{2\to1} = \frac{1}{2} I_0 \left[1 + \cos(\Delta\varphi_{2\to1})\right], \text{ where } \Delta\varphi_{2\to1} = \frac{n\,\omega}{c}\Delta L + \frac{n\,\Omega}{c} L_2. \quad (2)$$

Comparing Eqs. (1) and (2) it is possible to derive a **non-reciprocal phase shift**, $\Delta\varphi_{NR}$:

$$\Delta\varphi_{NR} = \Delta\varphi_{2\to1} - \Delta\varphi_{1\to2} = 2\frac{n\,\Omega}{c} L_2 \quad (3)$$

An **optical circulator** can be realized by satisfying the condition: $\boldsymbol{\Delta\varphi_{NR} = \pi}$. In this case, operating the interferometer so that light launched from port 1 constructively interferes at port 2 (see Fig. 3(a)) ensures that light back-reflected from port 2 is completely re-routed to port 3 (see Fig. 3(b)). This mechanism also works when light is launched from ports 3 and 4, i.e., the proposed device is a **4 ports circulator**. Furthermore, in a Mach-Zehnder interferometer the intensity at each of the output ports is independent from the frequency of the input light if the lengths of the two arms are equal: $\boldsymbol{L_1 = L_2}$ (see Eqs. (1, 2)). In other words, satisfying this second condition ensures **broadband operations**, only limited by the bandwidth of null-couplers, which can easily exceed 100 GHz. From a practical perspective, given a standard working frequency Ω = 10 MHz, non-reciprocal operations require $L_1 = L_2$ = 5.2 m. Over these moderate lengths, optical fibers exhibit propagation losses of less than 0.01 dB. Hence, the total insertion losses of the proposed device will be comparable to those of the null-couplers, which in our laboratories are on average below 0.05 dB. Finally, we note that the working point of the interferometer can be easily stabilized by gently stretching one of its arms with a piezo actuator [13].

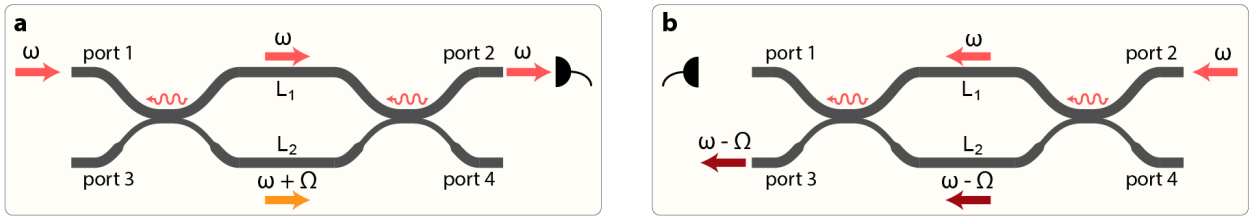

Fig. 3 Schematic of a null-coupler based non-linear interferometer for (a) forward and (b) backward light propagation. Due to acousto-optics interaction in the null-couplers, the light in the lower arm of the interferometer is subject to a direction-dependent frequency shift. This enables the use of the interferometer as a 4 port circulator, if the system parameters are such that $\boldsymbol{\Delta\varphi_{NR} = \pi}$ (see main text).

Outline of tasks/Work Plan

The route to the fabrication of technologically relevant non-reciprocal devices will require to address a number of challenges, which are schematically listed below in work points (WP).

WP 1: Proof-of-principle demonstration of all-fiber acousto-optic circulators

In this WP, we will test the main idea behind this proposal by building a prototype of the proposed device and assembling an optical setup to systematically study and characterize its optical properties. In particular, the demonstration of the proposed circulator relies on the fabrication of two high-quality and low-loss null-couplers operating at the same acoustic frequency. In practice, this only requires moderate control over the geometrical properties of the null-couplers because the acoustic frequency at which phase matching occurs can be widely tuned by stretching the null-coupler waist using a piezo actuator [4]. For this reason, I do not see any major obstacle for this WP.

WP 2: Demonstration of polarization independent operations

Acousto-optic non-reciprocal devices usually exhibit polarization dependent operations. In fact, the prototype of WP1 is likely to shown excellent performance, but only for a single input polarization state. This is certainly an issue that should be addressed for applications in quantum information processing.

Remarkably, polarization independent null-couplers have been demonstrated [14]. The idea is to precise control of the degree of fusion of the coupler waist, so that the geometrical birefringence perfectly compensates the one resulting from intermodal optic coupling via the acoustic wave. This is currently beyond the capabilities of our fiber tapering rig, which has been designed for the fabrication of optical nanofibers. For this project, it will be necessary to significantly improve the level of control offered by our setup by: (i) updating our rig with a more refined fabrication algorithm; (ii) assembling an imaging system for real-time inspection of the coupler shape and degree of fusion; (iii) systematically characterization of the dependency of the degree of fusion on the various parameters of the tapering process. This is certainly the most challenging WP, but its outcome will be the demonstration of an all-fiber circulator with polarization independent operations, a unique feature for any kind of sound-driven non-reciprocal device.

WP 3: Fabrication of ready-to-use devices for scientific collaborations

In this WP we will address a few practical issues that will facilitate the integration of the proposed devices in existing experimental setups. First, we will work to ensure a long service life. In a null-coupler light is guided at the interface between glass and air, which makes it sensitive to pollutants that might deposit on the glass surface over time. Thus, we will design air-tight enclosures for operations under vacuum or in high-purity nitrogen. Lifetime of >10 years has been demonstrated for optical nanofibers in this case. As a more elegant alternative, one could surround the coupler waist by a fluorine-doped low-index cladding during the tapering process, as routinely done for photonic lanterns [15]. This would protect the devices from pollutants without affecting their optical properties. Secondly, we will design and assembly a compact electronic module based on, e.g., the low-cost STEMLAB 125-14 FPGA boards, able to drive the acoustic wave and lock the working point of the interferometer. With these upgrades, it will be possible to easily integrate the circulators in the setups of the interested scientific collaborators (see below for further details).

WP 4: Market research and technological transfer

In this final WP, I will assess the potential of the proposed devices for commercial applications. This will be done with the help of Humboldt Innavation GmbH (https://humboldt-innovation.de/en), a subsidiary-company of the host institution, who will assist me in conducting market research and technology transfer to interested companies or institutions.

Working team and duration of the project

This project has an expected duration of **2 years** and relies on the extensive background in the **fabrication** and **post-processing** of **glass fibers**, that I acquired during my education [16, 17]. From the beginning, I will be assisted by a **PhD student**, who will work with me on all WPs and whose salary will be covered by the project budget. At the end of the project, the student will continue their studies, partially under my supervision, in the group of **Prof. Arno Rauschenbeutel** (Humboldt University of Berlin, Germany), with the long term goal of integrating one of the realized circulators into a cold atoms experiment [18, 19] and demonstrate novel protocols for quantum information processing.

	Year 1				Year 2			
WP 1: Proof of principle demonstration								
WP 2: Polarization independent operations								
WP 3: Ready-to-use devices for scientific collaborations								
WP 4: Market research and technological transfer								

Outcomes

The major outcome of this project will be the **demonstration of all-fiber ultra-low loss optical circulators**. After checking that the **intellectual property** is secured, the working principle, the fabrication technique and the experimental results will be **published** in an open access journal. Being able to fabricate such a unique device will be a splendid opportunity to **establish scientific collaborations:** we will partner with several research groups to discuss design constraints and possible use cases.

For instance, **Prof. Gerhard Rempe** (Max Planck Institute for Quantum Optics, Munich, Germany) already exhibited interest in integrating an ultra-low loss fiber circulator in his quantum networks prototypes. We are also in contact with **Dr. Andreas Wicht** of the Ferdinand Braun Institute (FBH) in Berlin, who is currently considering alternative solutions to on-chip acousto-optics isolators due to their extremely large power consumption (few orders of magnitude larger than what required for a standard null-coupler [7, 4]). The FBH is one of the world leading institution in the fabrication of integrated quantum photonics components and its collaboration would be highly beneficial for us. Furthermore, **Prof. Nicolas Joly** of the Max Planck Institute for the Science of Light (Erlangen, Germany) would be interested in collaborating with us, as null-couplers represent an ideal platform for the long-sought-after generation of photon triplets in the field of quantum optics [20] and we are one of the few groups in the world able to fabricate them.

Last but not least, succeeding in this proposal would represent **a major step in my scientific career** and a unique opportunity to establish myself as a leader in my research field.

Impact

Currently, the lack of all-fiber low-loss non-reciprocal devices represents the most striking flaw in existing fiber networks and one important ingredient still missing in the processing of quantum information stored in optical photons [11]. Succeeding in this project will represent a substantial and concrete step in solving this issue. From a more fundamental perspective, the proposed scheme demonstrates an additional and advantageous way to break Lorentz reciprocity, which could be easily extended to other platforms (e.g., photonic circuits). In addition, I would like to mentioned that, beyond non-reciprocity, this technology could be employed for the fabrication of ultra-narrow, low-loss and electronically reconfigurable filters, with linewidth from hundreds of GHz down to several hundred kHz, an ideal too for a large number of applications in quantum optics and quantum technologies.

Finally, given their compact size (few tens of cm^3) and relatively simple and low-cost fabrication procedure, I believe that there is a concrete possibility that, in a time-span of few years, the proposed devices can become a commercially available tool for experiments in optics and phonics and set new standards in terms of low-loss in optical non-reciprocity.

References:

[1] L. Del Bino et al., "Microresonator isolators and circulators based on the intrinsic nonreciprocity of the Kerr effect", Optica, 5, 279 (2018)

[2] H. Lira, "Electrically Driven Nonreciprocity Induced by Interband Photonic Transition on a Silicon Chip", Phys. Rev. Lett., 109, 033901 (2012)

[3] M. Scheucher et al., "Quantum optical circulator controlled by a single chirally coupled atom", Science, 354 (2016)

[4] T. Birks et al., "The acousto-optic effect in single-mode fiber tapers and couplers", J. Light. Technol., 14 (1996)

[5] M. S. Kang, "Reconfigurable light-driven opto–acoustic isolators in photonic crystal fibre", Nat. Photonics, 5 (2011)

[6] E. A. Kittlaus et al., "Electrically driven acousto-optics and broadband non-reciprocity in silicon photonics", Nat. Photonics, 15 (2021)

[7] D. B. Sohn et al., "Electrically driven optical isolation through phonon-mediated photonic Autler–Townes splitting", Nat. Photonics, 15 (2021)

[8] H. Tian et al., "Magnetic-free silicon nitride integrated optical isolator", Nat. Photonics, 15 (2021)

[9] J. Kim, S. Kim and G. Bahl, "Complete linear optical isolation at the microscale with ultralow loss", Scientific Reports, 7 (2017)

[10] E. A. Kittlaus et al., "Non-reciprocal interband Brillouin modulation", Nat. Photonics, 12 (2018)

[11] D. Niemietz et al., "Nondestructive detection of photonic qubits", Nature, 591 (2021)

[12] D. Witthaut et al., "Photon sorters and QND detectors using single photon emitters", Europhysics Letters, 97, 50007 (2012)

[13] A. Johnson et al., "Observation of Collective Superstrong Coupling of Cold Atoms to a 30-m Long Optical Resonator", Phys. Rev. Lett., 123, 243602 (2019)

[14] S. Farwell, "2x2 fused fiber null couplers with asymmetric waist cross sections for polarization independent (<0.01 dB) switching", J. Light. Technol., 16 (1998)

[15] A. M. Velazquez-Benitez et al., "Six mode selective fiber optic spatial multiplexer", Opt. Lett., 40 (2015)

[16] R. Pennetta et al., "Tapered Glass-Fiber Microspike: High-Q Flexural Wave Resonator and Optically Driven Knudsen Pump", Phys. Rev. Lett., 117, 273901 (2016)

[17] Xie et al., "Self-alignment of glass fiber nanospike by optomechanical back-action in hollow-core photonic crystal

[18] R. Pennetta et al., "Collective Radiative Dynamics of an Ensemble of Cold Atoms Coupled to an Optical Waveguide", Phys. Rev. Lett., 128, 073601 (2022)

fiber", Optica, 3, 3 (2016)

[19] R. Pennetta et al., "Observation of Coherent Coupling between Super- and Subradiant States of an Ensemble of Cold Atoms Collectively Coupled to a Single Propagating Optical Mode", Phys. Rev. Lett., 128, 203601 (2022)

[20] Cavanna et al, "Progress toward third-order parametric down-conversion in optical fibers", Phys. Rev. A, 101, 033840 (2020)

Name of the proposal:
Ultra-low loss and broadband all-fiber acousto-optic circulators (FiberCircl)

Category: Information

Applicant: Riccardo Pennetta, Humboldt University of Berlin

Executive summary

The introduction of low-loss optical fibers probably represents the single most important advance in the growth of our current global telecommunication system, which, in turn, fostered the rapid development of all kind of novel and more efficient fiber-based optical components. To meet our growing demand for secure communication and to interconnect future quantum computers, it is likely that our "classical network" will soon operate side by side of a so-called "quantum network", which, extremely sensitive to loss, poses new constraints and challenges to the performance of existing fiber devices. In particular, already demonstrated quantum networks prototypes explicitly pointed out a surprising flaw in our current fiber technology, namely the absence of low-loss non-reciprocal fiber components (i.e., isolators and circulators). To date, the best commercially available fiber-coupled circulators rely on free-space optics and feature high insertion-loss of approximately 1 dB at telecom wavelengths, which only increases for NIR and visible light.

Proposed project

In this project, I propose a solution to this pressing technological challenge by designing and fabricating novel all-fiber non-reciprocal devices based on acousto-optic interaction. These devices will combine ultra-low insertion loss (< 0.1 dB), large extinction ratio (at least 20 dB) and an extraordinary large bandwidth (> 100 GHz), considering the underlying physical mechanisms. They will be built from standard single-mode fiber and therefore could be readily integrated into existing fiber networks. Furthermore, they will be electrically switchable and reconfigurable within a response-time smaller than 100 μs.

The elementary units of my proposal are so-called fiber null-couplers. In brief these are fiber couplers, whose splitting ratio can be controlled via acoustic waves traveling along the coupler waist. It is well known that the acousto-optic effect breaks Lorentz reciprocity if the acoustic frequency is large enough, i.e., greater than 10 GHz for fiber-based devices. However, in practice, it is really challenging (and not yet demonstrated) to excite such high frequency waves in optical fibers via electrical actuation, an imperative requirement for any technologically relevant device. In this proposal, I show that cascading nearly identical null-couplers in a non-linear interferometer would allow us to break Lorentz non-reciprocity with acoustic waves of any frequency. As a consequence, I demonstrate how this concept can be applied to the design of novel electrically-actuated all-fiber circulators with ultra-low loss.

Intended outcomes

The most striking feature of the proposed devices is their ultra-low insertion loss, which is comparable to the one of standard fused couplers (< 0.1 dB). For this reason, these non-reciprocal devices could become a new technological standard for all optical systems in which low-loss are key, as in particular for future quantum networks, for which loss represents a highly undesired source of decoherence. Indeed, after an initial phase of careful design and parameters optimization, the future of these devices could go beyond the pure research environment, due to the relatively simple and potentially low-cost fabrication procedure.

Quantum Cellular Automata for fluid simulations on photonic quantum computers.

—By discovering and adapting quantum cellular automata (QCA) models for photonic quantum computers (PQC), our goal is to develop foundational work in the simulation of classical fluids. This research will pave the way for multiphysics simulations, ultimately providing a quantum advantage in real-world applications.

Classical fluid simulation is a challenging problem that has been approached from two main directions. The first approach is to discretize the continuous fluid equations, such as the Navier-Stokes equations. This approach is typically more accurate, but it can be computationally expensive. Second approach is based on cellular automata (**CA**) models, with the main idea of representing the fluid as a collection of discrete particles that interact with each other according to simple rules. This approach is less accurate than the first approach, but it is often much faster due to its highly parallelizable structure.

Regarding classical fluid simulation using CA, two main approaches have been proposed: *lattice gas cellular automata* (**LGCA**)[1] and the *lattice Boltzmann method* (**LBM**)[2]. The LGCA rely on cells with integer degrees of freedom, while interactions/collisions are stochastic in the majority of algorithms. In the LBM, the Boltzmann distribution is approximate over a discrete set of velocities, with continuous density distributions of the particles per velocity direction, then interaction and relaxation dynamics of the fluid are adjusted through collisions among distributions amplitudes and streaming is performed over discrete velocities. This approach has achieved maturity in specific fluid simulation at engineering level.

Cellular automaton models are expected to simulate a large number of complex phenomena [3], so it brings **flexibility** as first gain. A second advantage for fluid simulations comes from the successful application of the LBM for exceedingly different flows [2,4], being a **well-known** field. For the latter reasons, we recognize that research on capabilities of quantum computing implementations deserves more attention, and our contribution within CA models belong to *quantum native*—algorithms that encodes the physics or process into a quantum computing variables such that a clear analogy exist between the model and the evolution of the quantum system—.

On the downside, CA fluids simulations have some disadvantages in terms of flows through complex geometries and accuracy just for low-speed flows. But in these models it is also clear that solutions for complex problems, in general, will grow linearly with the mesh size or number of particles. Then becoming intractable for large-scales models; for example climate modeling or multiphysics flow simulations. In this sense CA models are promising, but another approach is

needed to extend CA models to reach specific flow regimes and computing efficiency for large-scale problems.

In the quantum domain, general purpose quantum computing is a well-established field of research with a rapidly growing industry, mainly oriented towards the circuit-gate model of computing. In the circuit-gate model, the algorithms are implemented by unitary operations (gates) in a certain order to perform initialization, processing and measurements to obtain results. Quantum devices primarily utilize superconducting qubits, cold atoms, or trapped ions as their physical building blocks.

Recently, quantum photonics has proven it can also provide a general quantum computing framework. With a distinct approach relying on initially entangled photon modes (cluster states), PQC can provide deterministic quantum computations, within the model known as one-way computing [5] or measurement-based quantum computing (**MBQC**)[6]. The main difference of MBQC and circuit-gate model is that MBQC rely on building first temporal entangled photons (cluster) with ancillary degrees of freedom, and then by measuring these ancillary resources it effectively implements quantum gates.

The aforementioned scheme for PQC has been successfully used on different sampling algorithms [7]. However, there are still challenges in scaling the photon sources for more demanding algorithms. It is also important to note that CA is based on basic operations that can lead to quantum advantage in certain LBM quantum implementations [8,9].

—**Proof that implementations of simple CA models in a quantum-native way are valuable, and represents a reliable approach for solving diverse real-world problems that can take advantage of increasing capabilities of photonic quantum computers [7]. In our case, quantum simulations of classical fluids.**

Based in our previous experience implementing quantum algorithms in the gate-based model [8,9], we have recognized the resources needed for large-scale CA, which coincides with the possibility of quantum computers to provide quantum advantage over two aspects: **linearity** of operation for specific CA models and the exponential capabilities for states encoding to get **massive parallel operations** [10]. Building on this, we propose to extend our expertise to PQC devices.

As a starting point, we will focus on the one-dimensional cellular automata (**1D-CA**) models. The main task will be to find appropriate encodings of CA variables for PQC. Once the encoding is clear, this will enable our first attempt at QCA, for both methods: QLBM and QLGCA. Our previous experiences will help in this regard, since the QLBM, our flagship method, has been demonstrated as a proof-of-concept (PoC) on real quantum devices [11]. The QLGCA model has recently been researched in our group to simulate classical fluids on the circuit-gate quantum computing model, and found similar properties are shared with QLBM.

In a second stage, the research will focus on exploring current photonics architectures and then adjusting our models to run on real devices. The main tasks will consist of evaluating different hardware capabilities, analyzing the precision, scaling, and flexibility of each of them. Then, we will establish a collaborative plan to execute our main goal, a **PoC for simpler QCA models**.

—**Main research goal will be to establish the cluster states needed to run 1-step of 1D-CA models (G1). By knowing how our algorithms will scale, we will estimate hardware resources to reach quantum advantage. Then build specific device-specific algorithms to be tested on PQC (PsiQuantum, Quandela) in a joint collaboration (G2).**

Our plan to achieve main goals **G1** and **G2** will be carried out using the budget for hiring a postdoctoral researcher, and for computational resources on PQC devices. In terms of human resources, we will directly collaborate within the quantum team of Quanscient:

- Dr. Valtteri Lahtinen (Quantum team lead)
- Prof. Ljubomir Budinski (Quantum senior algorithm researcher)
- Dr. Ossi Niemimäki (Quantum algorithm researcher)

Externally, we will collaborate with a world-leading **LBM** specialist, Prof. Pierre Sagaut from Aix-Marseille University.

The profile of the postdoctoral candidate will be as open as possible, but his/her familiarity with photonic platforms and quantum computing could be desirable. In our experience, a good candidate with a strong background in quantum physics and interest for quantum computing is enough.

I will be sharing workload with the postdoctoral research who will be hired for the quantum team of Quanscient. To achieve our objectives, we plan to break down the main goals **G1** and **G2** into simpler tasks. We propose a timetable as shown in **Table 1,** with following task and goals:

- **G1** Find appropriate encoding scheme and an algorithm for QCA models within the 1-way computing model. Alternatively, propose our computing model compatible with PQC.
    - G1.1 Research on cluster states and generate a clear picture of advantages and disadvantages, as well as the resources needed in current photonic quantum computing hardware (G2.1). This will involve a **review stage**.
    - G1.2 Once the review process is complete, a set of restrictions over our QCA models, and now should be clear which cluster states are appropriate to implement **QLBM** or **QLGCA**. Alternatively, another scheme could be proposed, such as the one studied in [12].
    - G1.3 Finally with the appropriate encoding and the needed operations, we will use different frameworks to implement our **photonic-aware quantum algorithm** and perform the **scaling analysis**. Finally a research paper will be submitted.

- **G2** Collaborating with a photonic quantum computing research group to make a PoC for the developed 1D-QCA models. Alternatively, use free resources as the ones developed by Quandela [13].
    - G2.1 At the same time the work for **G1** begins, we will actively search for and meet with different PQC manufacturers to establish a collaboration. By the end of G1.1, the pros and cons of different platforms and frameworks will be clear. Once our algorithms for PQC are in place, we will start getting to know real platforms and start to run on real PQC.
    - G2.2 Once a minimal example (PoC) is implemented on real devices, we will explore other alternatives to solve and optimize our algorithms. We will ask and rely on advice from our collaborators. A second task will be to extrapolate our algorithms for more realistic scenarios in 2D or 3D, and estimate the resources needed for quantum useful advantage.
    - G2.3 Finally, we will report our optimized algorithm results from real-devices runs to relevant journals. This will achieve **G2.** But more importantly, we will answer the scaling properties of QCA models for simulation of classical flows.

Month — Goals	1	2	3	4	5	6	7	8	9	10	11	12
G1.1												
G1.2												
G1.3							**G1**					
G2.1												
G2.2												
G2.3												**G2**

Table 1. Timetable for our one-year working plan. Two major goals will be output as a research paper G1 and a joint collaboration paper G2.

Providing solid examples of real-device applicable quantum algorithms with novel quantum advantages is the main expected result from our research on QLBM and QLGCA in photonic context. But as we have mentioned, to achieve **G2**, we need a previous step **G1,** consisting on establishing a theoretical framework to efficiently encode the models QLGCA and QLBM for photonic quantum computers. Having the expertise within our quantum team at Quanscient, we expect to achieve really good scaling properties for our quantum-native algorithms and justify our claims about useful quantum advantage.

As a result, we expect this research will achieve low- to mid-scale useful quantum computation in NISQ photonic devices. In the long term, we believe that this research has the potential to impact a range of different scientific fields for large-scale multiphysics problems.

The impact of our research on the quantum information community could be made in two ways:

- ☐ Scientifically: by exporting or adapting to PQC our quantum native algorithms we have been intensively researching at Quanscient. We anticipate that future QCA models implemented on PQC will be able to solve a variety of large-scale multiphysics problems.
- ☐ Industrially: by conducting proof-of-concept demonstrations in which the academic community, our company Quanscient, and quantum photonic partners collaborate to implement QCA models. Due to the early stage of PQC, we anticipate that we will have a greater impact on hardware development by using our flagship methods and justify the hardware requirements necessary to achieve useful quantum advantage.

—In brief, our impact will be to attract well-motivated research to CA models and to develop an alternative approach for useful quantum advantage on photonic quantum computers. We expect to also have a co-design hardware roadmap with our collaborators.

References

1. Brosl Hasslacher, *Discrete Fluids*, Los Alamos Science No. 15, (1987) link
2. *The Lattice Boltzmann Method*, Springer Cham (2017) doi
3. Schiff, J.L. (2007). Front Matter. *In Cellular Automata*, J.L. Schiff (Ed.) doi
4. *Lattice Boltzmann Modeling*, Springer Berlin, (2006) doi
5. C. Reimer *et. al.*, *High-dimensional one-way quantum processing implemented on d-level cluster states.* Nat. Phys. 15(2), 148–153 (2019) doi
6. Taira Giordani *et. al.*,*Integrated photonics in quantum technologies*, La Rivista del Nuovo Cimento, 46 (2023) doi
7. Dominik Hangleiter and Jens Eisert, *Computational advantage of quantum random sampling*, Rev. Mod. Phys., 95, 035001 doi
8. Budinski Ljubomir, *Quantum algorithm for the advection–diffusion equation simulated with the lattice Boltzmann method.* Quantum Inf Process 20, 57 (2021) doi
9. Budinski Ljubomir, *Quantum algorithm for the Navier–Stokes equations by using the stream function-vorticity formulation and the lattice Boltzmann method*, International Journal of Quantum Information (2022) doi
10. Budinski Ljubomir, *Efficient parallelization of quantum basis state shift*, (2023) doi
11. Lahtinen V. *et. al.*, Quanscient's Blog link
12. Wael Itani, *et. al.*, *Quantum Algorithm for Lattice Boltzmann (QALB) Simulation of Incompressible Fluids with a Nonlinear Collision Term*, doi
13. Nicolas Heurtel *et. al.*, *Perceval: A Software Platform for Discrete Variable Photonic Quantum Computing*, Quantum 7, 931 (2023) doi

Company Name: **Quanscient**

Challenge:

Simulation of classical fluids is an intensively researched and computationally demanding problem with direct impact on engineering and multidisciplinary fields such as climate modeling and automotive efficient design. We take on the challenge of efficient, low-energy consumption simulations by providing a novel way to provide quantum advantage through the development of quantum algorithms for photonic quantum computers (PQCs).

Proposed Research:

We aim to develop one-year fundamental research in the simulation of classical fluids by discovering and adapting quantum cellular automaton (QCA) models for photonic quantum computers. By enabling quantum speedup for cellular automata models we anticipate, in the long-term, our quantum native approach will revolutionize large-scale classical fluid simulation. We center our research over two main goals:

G1. Establish resources needed (theory and hardware) for implementation of QCA on PQC. Sustain our claim for quantum useful advantage throughout an scaling analysis in the photonic context.

G2. Collaborate with PQCs manufacturers to run on real-devices our developed algorithms obtained in G1. Open a collaborative channel to explore co-design to optimize hardware for algorithms, if possible.

Intended Outcomes:

The intended outcomes of this project are to:

- Research article in collaboration with Quanscient quantum team (7-months)
- Joint research article for the real-device implementation of QCA models (9-months)

Benefits:

The benefits of this project include:

- Attract well-motivated research to quantum cellular automaton models.
- Develop an alternative approach for useful quantum advantage on photonic quantum computers
- Establishing the first demonstration of QCA on photonics quantum computers.
- Produced the first milestone on quantum algorithms research for large-scale multiphysics problems.

Conclusion:

Proof that implementations of simple cellular automata models are valuable and represents a reliable approach for solving diverse real-world problems that can take advantage of increasing capabilities of photonic quantum computers.

Contact Information:

Dr. Roberto Antonio Zamora Zamora
Quantum Scientist
roberto.zamora-zamora@quanscient.com
+358 401903328

Silicon photonic biosensors for low-cost, portable, data-rich measurements of hormone biomarkers relevant to women's health and the menopausal transition

Proposal for Health Challenge

Dr. Samantha M. Grist, The University of British Columbia, Vancouver, Canada

Literature Review

There have been significant historical gender-based inequities in healthcare and medical research[1] that continue into the present day[2]. Clinical trial data have historically been collected using male participants and generalized[3,4]; this gender gap in medical research leads to disparities in clinical outcome since not all findings are translatable across gender[4]. Although progress has been made, this inequity persists in the 21st century[2], in part because of complexity introduced by fluctuating gonadal hormone levels during the menstrual cycle[5]. These fluctuations can impact expression of other biomarkers (e.g., in cardiovascular disease), resulting in misinterpretation of results and the need to monitor and control for gonadal hormone levels in clinical trials[5]. Although it has been neglected, monitoring of hormones relevant to women's health has wide-ranging application from fertility and contraception[6,7], to understanding pregnancy loss[8], to improving the menopausal transition[9]. This neglect creates an unmet need and is partly due to measurement limitations, since high sensitivity and frequent measurement is required to distinguish important trends from cycle fluctuations.

Although the menopausal transition affects all females (~50% of the population) as they reach midlife, there are pervasive issues with its standard of care. The menopausal transition (perimenopause) typically begins between ages 40-55 and lasts 7-14 years[10]. This significant period of life coincides with a time when the risk of several diseases (e.g., cancer, cardiovascular disease) increases. The body goes through drastic changes, and the perimenopausal experience is highly variable between individuals, with wide measured variation in hormone levels that can impact both perimenopausal symptoms and life-threatening health issues[11–15]. Menopause exerts a significant burden on individuals, healthcare, and the economy; as such, improving treatment options as well as measuring hormone levels during this period would confer significant benefit. Perimenopause negatively impacts quality of life and both physical and mental health[16,17] as well as increases risk of suicidal ideation[18,19]. Although there remains stigma associated with discussing menopause, recent surveys reveal that 59% of those experiencing symptoms report a negative impact on their work[20], and 25% consider leaving the workforce early[21,22]. Menopause increases the risk of conditions like osteoporosis[23] and cardiovascular disease[24], so though menopause itself is not a disease, diagnosing menopausal stages is important for screening. Perimenopausal symptoms can also be similar to those of diseases like cancer and neurodegenerative disease[25–27], potentially resulting in delayed diagnosis of those conditions[28] and resulting impact on mortality, morbidity, and healthcare cost. Despite these critical impacts on health, quality of life, and the economy, only 7% of physicians in US residency programs feel adequately prepared to provide menopausal care, and 80% feel "barely comfortable" discussing or treating menopause[29].

Predicting the duration of a patient's menopausal transition confers several benefits[9,30], but the current clinical practice for diagnosing menopause (12 months since the last menstrual period), an indication of when many symptoms may end, is by definition retrospective. This type of diagnosis does not give clinicians and patients the information they need to make treatment decisions[9]. A *prospective diagnosis* requires frequent measurement of hormones (e.g., follicle-stimulating hormone and estrogen) and hormone metabolites (e.g., pregnanediol, a progesterone metabolite)[9]. There are known correlations between >10 hormones and disruptive symptoms[12–15]. Hormone levels are also associated with development of cardiovascular disease[11], in addition to confounding biomarker measurements used for diagnostics[5]. Measuring these hormones could thus provide benefits of symptom prediction, treatment efficacy monitoring, and new insight into links between hormone levels and a suite of other conditions, leading to more effective diagnostics for a large population segment with needs that are currently underserved or neglected. Addressing these needs requires quantification of ≥4 hormones[9] ≥2×/week with immediate results, in a setting and at a cost point that does not make this testing burdensome to the user. Providing actionable data requires real-time correlation of symptoms and hormone levels with at-home testing and immediate results — not possible with current testing technologies.

Commercial-grade platforms today are subject to trade-offs including cost, time-to-result, sensitivity, and specificity. While the enzyme-linked immunosorbent assay (ELISA) is a quantitative gold-standard biomarker test it requires centralised laboratory analysis, trained technicians, long time-to-result, and expensive equipment. Surface plasmon resonance (SPR)-based testing (e.g., GE Biacore) offers quantitative label-free detection but also typically requires costly, lab-scale equipment[31]. Rapid, low-cost assays like lateral-flow strips (e.g., pregnancy tests, Mira Fertility hormone monitoring system) tend to be semi-quantitative and low-sensitivity and are not able to meet the multiplexing requirements (measuring enough hormones simultaneously) for this application[32].

One promising technology to meet this open need is based on silicon photonic integrated circuits (PICs)[33]. This technology leverages semiconductor manufacturing economies of scale[34], with multiple sensors on a single chip[35]. Each sensor can have its own chemistry for multiplex detection[36], enabling many high-sensitivity assays in a single compact device[37]. These sensors (Fig. 1a) measure changes in optical refractive index introduced by analytes binding to specific receptor chemistries immobilized on the surface of the sensor (e.g., by reading out changes in resonance wavelength of a resonator device in a fluid sample)[38]. Genalyte Inc. commercially produces multiplexed silicon photonics (SiP) diagnostics instruments using resonator-based sensors[39]; however, due to the large cost and size of the picometre-resolution swept-tunable laser ($40,000-$100,000) their systems cannot be widely deployed for the kind of at-home testing needed to improve the standard of menopause care.

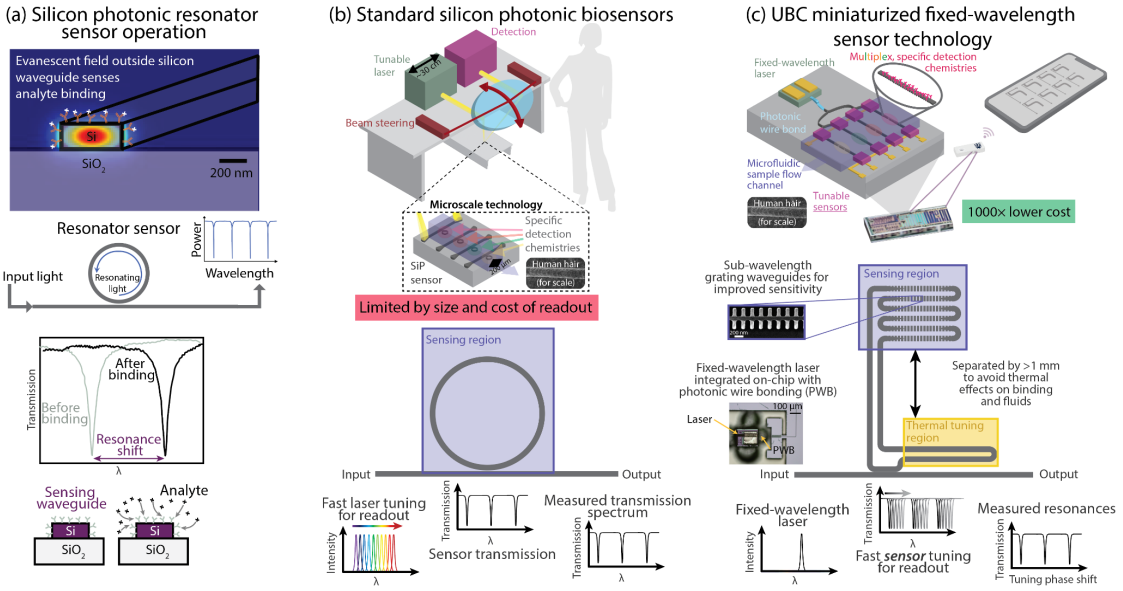

Fig. 1. Our technology drastically improves size and cost compared with the state of the art. (a) Silicon photonic (SiP) resonators use nanoscale silicon waveguides to sense analytes (biomarkers) of interest binding to the surface of the device by tracking shifts in resonance wavelength. (b) Standard SiP resonators require expensive, bulky tunable laser systems for readout, limiting their applicability to at-home testing. (c) Our proposed sensor architecture addresses this challenge by integrating controlled tunability into the sensor itself, allowing the use of tiny, inexpensive fixed-wavelength lasers on-chip to read out the same kind of resonance peak shifts as traditional SiP resonators.

Proposed Breakthrough Technology Building upon a decade of research[35,38,40–56], we have recently invented a unique sensor architecture that uses fixed-wavelength lasers. Unlike tunable lasers, fixed-wavelength lasers are cheaper (<$1 in high volume) and compact (<1 mm). Our compact, low cost biosensor will offer improvements in both size (100×) and cost (1000×) compared to existing SPR and SiP commercial systems (Fig. 1), promising laboratory-grade diagnostics in a portable form factor. Two key innovations will facilitate this technology: (1) electronic-photonic circuits to obviate the expensive (>$40,000) and bulky (100s of mm) tunable lasers required for readout of traditional SiP sensors, and (2) photonic wire bonding, a new technique suitable for high-volume manufacturing that allows us to integrate components like lasers onto photonic chips with low loss and high performance. With a thin glass surface (silicon native oxide) like commercial sensors, our sensor will be compatible with established functionalization chemistries to specifically detect various biomarkers[34,56–60].

Core Idea: "Sweep the sensor instead of the laser" Our novel sensor's mechanism of operation is shown and compared to typical SiP resonator sensors (like Genalyte) in Fig. 1. Rather than the full

passive resonator being used for sensing (Fig. 1b, requiring readout with the precise tunable laser), our resonator (Fig. 1c) is segmented into two regions: a sensing region containing high-sensitivity (due to increased overlap between the optical mode and the analyte) sub-wavelength grating waveguides[55] (blue), and a tuning region to facilitate readout (yellow). The tuning region integrates a thermal phase shifter[61,62] into the resonator to introduce precise, reproducible changes in refractive index and thus sensor resonance wavelength, using electronic control. These controlled changes in resonance wavelength allow us to controllably sweep the resonance wavelengths past the fixed-wavelength laser, *reading out similar spectra (e.g., Fig. 2d) to those quantified by sweeping the laser wavelength across a fixed transmission spectrum*. The two regions of the sensor are separated by >1 mm, to avoid any deleterious impact of electric field or temperature on the fluids or analyte binding in the sensing region. This technology holds potential to open the door to next-generation multiplexed biochemical urinalysis, particularly for women's hormones and metabolites – accessible for future at-home monitoring.

Problem Statement/Objective

Sensor development must be approached step-by-step, with rigorous validation during each stage of development and for each analyte. In this 1-year project we will demonstrate the first proof-of-concept of our proposed SiP technology to meet the critical needs for analytical hormone-monitoring to help support people experiencing symptoms of the menopausal transition. The 1-year deliverables will jump-start the development of our urinalysis platform, forming the basis for future work to advance the technology towards multiplexed, accessible at-home hormone monitoring.

Outline of Tasks/Work Plan to Demonstrate Portable, Multiplexed SiP Sensor Technology

Having demonstrated the preliminary working concept of the new architecture (Fig. 2, single sensor replicate), we aim to evaluate the performance of the full sensor architecture for photonic sensing, and develop functionalization assays to specifically detect the hormones relevant to monitoring of menopausal health. Therefore, we propose parallel development of two Aims.

Aim 1: Quantify the intrinsic sensor performance, fluidic stability, replicability, and system limit of detection of our multiplexed fixed-wavelength biosensor technology.

- *Hypothesis:* By harnessing electronic-photonic integration for readout, the performance of our novel sensor will meet/exceed that of traditional SiP biosensors requiring large, expensive readout systems.
- *Challenge:* To validate our paradigm-shifting sensor architecture's suitability for hormone monitoring and other biomedical applications, we must rigorously characterize its photonic and sensing performance and compare critical performance metrics with state-of-the-art SiP sensors.
- *Approach:* Building upon our pilot single-sensor demonstration of the novel architecture (Fig. 2), we will demonstrate the utility of our sensor by rigorously characterizing performance across multiple PICs, each with multiple sensors. Specifically, we will quantify the following established metrics of photonic sensor performance and stability, and compare our 1000× lower-cost sensor architecture against the state-of-the-art passive SiP biosensors using tunable laser readout:
  - Key performance metrics for resonator-based sensors[44]: quality factor Q, bulk refractive index sensitivity S_{bulk}, intrinsic and system limits of detection (*ILoD* and *sLoD*) in aqueous solutions.
  - Important metrics of stability and reproducibility: noise in resonance wavelength over time, variability (e.g., coefficient of variation, CV) in S_{bulk} between multiple trials/sensors.
  - Demonstration of analyte sensing performance, involving functionalization of the sensor surface with specific detection receptors as well as real-time measurement of analyte binding.
- *Activities:* We will demonstrate the capability of our new architecture in comparison to state-of-the-art traditional SiP sensors by validating critical sensor specifications in a *multiplexed* sensor design. We will design and fabricate (e.g., through AIM Photonics) electronic-photonic integrated circuits containing multiple instances of our new sensor architecture for differential and multiplexed sensing. We will then integrate these chips with electronic readout systems (electrical wire bonding to a custom printed circuit board, integrated with a source-measure unit and function generator) and microfluidics (fabricated using 3D printing, direct-write laser lithography, and soft lithography) to deliver fluids (aqueous NaCl refractive index standard solutions and a demonstration binding assay like that shown in Fig. 2g) to the sensor surface for sensor performance characterization. Pilot

sensor testing yields an experimental *ILoD* of 3.5×10^{-4} RIU (Fig. 2) – an ILoD among the best silicon photonic biosensors, and critical fixed-wavelength sensor characteristics like the quality factor and sensor-tuning performance have been demonstrated on a single sensor in our pilot work (Fig. 2). Building upon these pilot results, we will characterize the sensing performance of the multiplexed fixed-wavelength architecture both with and without on-chip DFB lasers and photonic wire bond optical integration. We will assess the multiplexed sensors' performance metrics as well as stability and reproducibility between sensors on the same photonic chip, across trials, and across photonic chips. We will improve noise and variability by reducing thermal drift and employing differential detection with control sensors. We will first characterize the sensors using a lab-scale test setup. We will subsequently build a desktop-scale system suitable for demonstration to collaborators and at Optica conferences, with a custom readout PCB containing ADCs, DACs, TIAs, laser diode and thermal controllers, and a microcontroller – a step towards the eventual miniaturization of the readout system into a handheld device. Sensor performance in both systems will be quantified and compared.

- *Quantitative target specifications for equivalence to standard SiP biosensors*: S_{bulk} > 50 nm/RIU; *ILoD* < 1×10^{-3} RIU; *sLoD* <2×10^{-5} RIU[49]; inter-assay and intra-assay CVs of sensor S_{bulk} < 20%.

Aim 2: Develop robust, multiplexed sensor functionalization strategies to detect a pilot set of hormone targets relevant to menopause urinalysis: pregnanediol (PdG) and follicle-stimulating hormone (FSH).

- *Hypothesis:* By facilitating quantitative, data-rich digital readout of both steady-state binding and binding kinetics, SiP biosensor performance will meet or exceed that of the lateral-flow assays used in current-generation hormone monitoring platforms.
- *Challenge:* Towards proof-of-concept of a multiplexed hormone-quantification platform, we must individually and quantitatively validate the technology's capability to detect each relevant hormone, and develop approaches for multiplexed functionalization and multiplexed detection.
- *Approach:* We will adapt established immunoassay chemistries for hormone quantification (e.g., via ELISA) to functionalize SiP biosensors and quantify hormone detection performance. Here, we will demonstrate detection of a pilot set of two hormone markers (PdG and FSH), with the ability to scale up to >10 targets in the future. We will benchmark assay performance against gold-standard ELISAs and LFAs. Finally, we will utilize silicon photonics' capabilities for multimodal measurement to integrate normalization controls within the same sensor chips to improve measurement robustness.
- *Activities*: Custom SiP integrated circuits will be designed and fabricated to multiplex ≥9 sensors per measurement (2 groups of 3 replicate sensors to measure two different hormone biomarkers, plus 3-6 replicate control sensors for normalization and nonspecific binding and temperature controls. Normalization controls will be implemented by precisely measuring the bulk refractive index of the urine (related to specific gravity, widely used for critical normalization in urinalysis)[63]. We will use commercial antibody pairs from third-party suppliers, and covalently link them to the sensor surface using established silane-crosslinker chemistry (APTES and BS3)[64,65]. We will first evaluate detection performance separately for each biomarker, and subsequently use pipette-spotting for multiplexed functionalization[57]. We will use lab-scale microfluidics readout systems to run the detection assays[48]. For analytical validation, we will quantify the sensors' lower and upper limits of detection (LLoD and ULoD), limits of quantification (LLoQ and ULoQ), and specificity from sample matrices of increasing complexity (e.g., starting with protein spiked into simple saline buffer solutions, adding confounding proteins, and moving to synthetic urine). We choose detection targets on the order of pg/mL, clinically relevant for urinalysis. In order to increase the dynamic range of our sensors, we will analyze the slope of the initial stage of the binding curve, which is proportional to analyte concentration with appropriate functionalization[66]; with this approach the measurable concentrations can span several orders of magnitude[58]. We will optimize functionalization, blocking, and flow protocols to improve LoQs and reduce nonspecific signal. We will assess cross-reactivity by spiking in confounding proteins (e.g., albumins, globulins), and analyzing more complex samples. We will use control sensors to correct for nonspecific binding and thermal drift via differential detection.
- *Quantitative target specifications for menopause relevance*: Upper/lower LoD & LoQ quantified and relevant for hormone urinalysis (PdG LLoQ < 100 pg/mL, ULoQ >32 μg/mL[67,68]; FSH LLoQ <

0.3 mIU/mL, ULoQ > 185 mIU/mL[69]). Sensor LoD CVs <15%. Stable >1 week under appropriate storage conditions[64]. < 15% uncertainty & inaccuracy compared to gold-standard measurements.

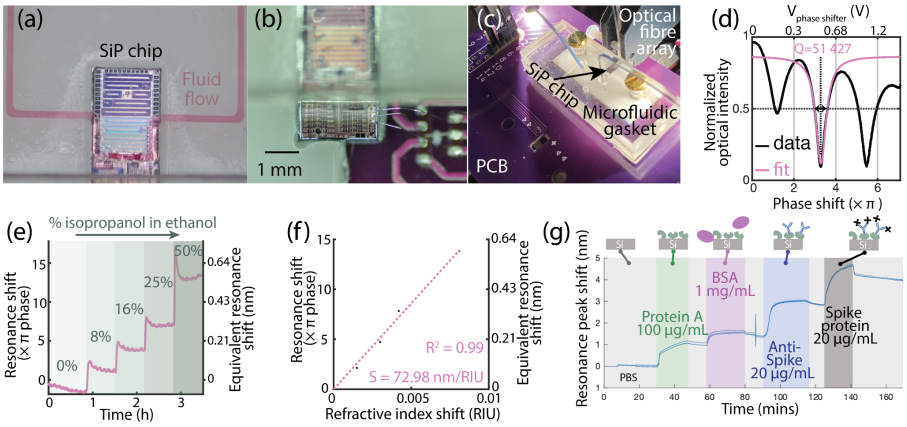

Fig. 2. Preliminary characterization of the fixed-wavelength sensor architecture. (a) Integration of the single-sensor silicon photonic (SiP) chip with a multilayer microfluidic gasket to deliver fluids to the sensor surface. (b) Electrical wire bonding of the sensor chip to the PCB, outside of the area covered by the gasket. (c) Lab-scale readout of the sensor chip by coupling to an optical fibre array. (d) Tuning the resonators for fixed-wavelength sensor operation reveals the resonance peak positions and allows the quality factor to be quantified. (e-f) Exposing the sensor to alcohol solutions with different refractive indices through the fluidic gasket allows us to monitor the resonance shift over time (e) and calculate the bulk refractive index sensitivity (f). (g) Example binding assay on n=3 traditional SiP resonators with tunable laser readout (not fixed-wavelength architecture), showing the binding shift and kinetics of adsorption during functionalization (protein A, anti-SARS-CoV-2 spike antibody) and detection of SARS-CoV-2 spike protein (as well as non-specific signal from BSA during the blocking step). In the finalized assay, the duration will be much shorter as functionalization & blocking are pre-performed (detection in minutes).

Outcome(s)

This project will take impactful concrete steps towards an at-home platform for monitoring hormone levels relevant to the menopausal transition and other women's health conditions. We will demonstrate (1) a new, low-cost SiP sensor technology for quantitative, data-rich detection in a portable form factor, benchmarking against state-of-the-art SiP sensors; (2) specific detection of hormone biomarkers relevant to the menopausal transition. Through these two Aims we will demonstrate a cutting-edge photonic sensor technology, and apply it to the historically neglected field of women's health.

Impact

Although biomarker-based testing provides critical evidence for physicians' diagnostic decisions, there is a constant need to decentralize diagnostic testing from expensive, slow laboratory assays to rapid diagnostics at the point of need – this need is particularly crucial for diagnostics in remote and rural communities, and applications where frequent monitoring and fast time-to-result are critical. Current rapid, portable diagnostics, however, do not provide the kind of robust, data-rich, and accurate results that physicians rely on from laboratory assays. Data-rich diagnostics like SiP sensors promote more accurate, reliable sensing because a suite of controls and error checks can be implemented within the device, and thus more accurate data can be reported. This project will address a critical unmet need in women's healthcare by validating a portable, low-cost technology for decentralized, multiplexed monitoring of hormone markers in urine. We anticipate that this project will lay the groundwork for an at-home urinalysis system with impact in improving symptom management and treatment as well as generating the kind of data needed to better diagnose and treat life-threatening conditions during the menopausal transition. Just like how the introduction of home glucose monitoring in 1980 revolutionized how we manage diabetes[70], home *hormone* monitoring could revolutionize midlife female health. Beyond menopause, quantification of hormones and hormone metabolites has broader impact in human health, including fertility and contraception and better understanding the relationships between premenopausal gonadal hormone fluctuations and expression of other biomarkers – addressing key gender disparities in healthcare. The outcomes of this work could also lead to a positive impact in diagnostics of other conditions, including in cardiology, oncology, neurology, and infectious diseases.

References

1 G. Sen and P. Ostlin, *Glob Public Health*, 2008, **3 Suppl 1**, 1–12.
2 R. Wilson, M. L. Adams and K. E. Pyke, *Appl. Physiol. Nutr. Metab.*, 2020, **45**, 911–914.
3 A. Holdcroft, *J. R. Soc. Med.*, 2007, **100**, 2–3.
4 L. Merone, K. Tsey, D. Russell and C. Nagle, *Womens Health Rep (New Rochelle)*, 2022, **3**, 49–59.
5 T. Huang, F. M. Howse, N. S. Stachenfeld and C. W. Usselman, *Am. J. Physiol. Heart Circ. Physiol.*, 2023, **324**, H33–H46.

6 A. K. Wegrzynowicz, A. Beckley, A. Eyvazzadeh, G. Levy, J. Park and J. Klein, *Medicina (Kaunas)*, , DOI:10.3390/medicina58121853.
7 R. E. Leach, et al., *Fertility and sterility*, 1997, **68**, 413–420.
8 L. Foo, S. Johnson, L. Marriott, T. Bourne, P. Bennett and C. Lees, *Paediatr. Perinat. Epidemiol.*, 2020, **34**, 495–503.
9 N. Santoro, et al., *Menopause*, 2007, **14**, 415–424.
10 What Is Menopause? | National Institute on Aging, https://www.nia.nih.gov/health/what-menopause#, (accessed July 21, 2023).
11 L. Newson, *Post Reprod. Health*, 2018, **24**, 44–49.
12 G. E. Hale, X. Zhao, C. L. Hughes, H. G. Burger, D. M. Robertson and I. S. Fraser, *J. Clin. Endocrinol. Metab.*, 2007, **92**, 3060–3067.
13 A. Allshouse, J. Pavlovic and N. Santoro, *Obstet. Gynecol. Clin. North Am.*, 2018, **45**, 613–628.
14 M. de Zambotti, I. M. Colrain and F. C. Baker, *J. Clin. Endocrinol. Metab.*, 2015, **100**, 1426–1433.
15 N. F. Woods, K. Smith-Dijulio, D. B. Percival, E. Y. Tao, H. J. Taylor and E. S. Mitchell, *J Womens Health (Larchmt)*, 2007, **16**, 667–677.
16 G. D. Mishra, W. J. Brown and A. J. Dobson, *Qual. Life Res.*, 2003, **12**, 405–412.
17 N. Santoro, C. N. Epperson and S. B. Mathews, *Endocrinol. Metab. Clin. North Am.*, 2015, **44**, 497–515.
18 J. Usall, et al., *J. Affect. Disord.*, 2009, **116**, 144–147.
19 S. Y. An, et al., *Epidemiol. Psychiatr. Sci.*, 2022, **31**, e60.
20 Majority of working women experiencing the menopause say it has a negative impact on them at work | CIPD, (accessed July 20, 2023).
21 *Menopause in the Workplace: Impact on Women in Financial Service*, The Fawcett Society, 2021.
22 Quarter of women going through menopause "considered leaving work" | ITV News, (accessed July 20, 2023).
23 M.-X. Ji and Q. Yu, *Chronic Diseases and Translational Medicine*, 2015, **1**, 9–13.
24 S. R. El Khoudary, et al., *Circulation*, 2020, **142**, e506–e532.
25 Can Cancer Symptoms Be Mistaken for Menopause? | Cancer.Net, (accessed July 20, 2023).
26 Menopause or a Thyroid Problem | The North American Menopause Society, NAMS, (accessed July 20, 2023).
27 Conditions with Similar Symptoms as Menopause | Complementary and Alternative Medicine | St. Luke's Hospital, (accessed July 20, 2023).
28 S. D. Cochran, N. F. Hacker and J. Berek, *Journal of Psychosomatic Obstetrics & Gynecology*, 1986, **5**, 245–252.
29 J. Wolff, What Doctors Don't Know About Menopause, (accessed July 6, 2023).
30 L. A. Bastian, C. M. Smith and K. Nanda, *JAMA*, 2003, **289**, 895–902.
31 P. Singh, *Sensors and Actuators B: Chemical*, 2016, **229**, 110–130.
32 K. M. Koczula and A. Gallotta, *Essays Biochem.*, 2016, **60**, 111–120.
33 L. Chrostowski and M. Hochberg, *Silicon Photonics Design*, Cambridge University Press, Cambridge, 2015.
34 M. Iqbal, et al., *IEEE J. Select. Topics Quantum Electron.*, 2010, **16**, 654–661.
35 L. Laplatine, et al., *Sensors and Actuators B: Chemical*, 2018, **273**, 1610–1617.
36 J. T. Kirk, G. E. Fridley, J. W. Chamberlain, E. D. Christensen, M. Hochberg and D. M. Ratner, *Lab Chip*, 2011, **11**, 1372–1377.
37 M. C. Estevez, M. Alvarez and L. M. Lechuga, *Laser & Photon. Rev.*, 2012, **6**, 463–487.
38 L. Chrostowski, S. Grist, et al., *SPIE Laser Resonators, Microresonators, and Beam Control Xiv*.
39 United States Food and Drug Administration, *Maverick™ SARS-CoV-2 Multi-Antigen Serology Panel v2 01030ART-01*, US FDA, 2020.
40 J. Flueckiger, S. M. Grist, E. Ouellet, L. Chrostowski and K. C. Cheung, 2011, pp. 565–567.
41 X. Wang, J. Flueckiger, S. Schmidt, S. Grist, et al., *Journal of Biophotonics*, 2013, **6**, 821–828.
42 S. T. Fard, S. M. Grist, et al., *SPIE Silicon Photonics Viii*.
43 S. M. Grist, et al., *Opt. Express*, 2013, **21**, 7994–8006.
44 S. Schmidt, J. Flueckiger, W. X. Wu, S. M. Grist, et al., *SPIE Biosensing and Nanomedicine Vii*.
45 V. Donzella, A. Sherwali, J. Flueckiger, S. M. Grist, S. T. Fard and L. Chrostowski, *Opt. Express*, 2015, **23**, 4791–4803.
46 V. Donzella, A. Sherwali, J. Flueekiger, S. T. Fard, S. M. Grist and L. Chrostowski, *Optics Express*, 2014, **22**, 21037–21050.
47 E. Luan, H. Yun, M. Ma, D. M. Ratner, K. C. Cheung and L. Chrostowski, *Biomed. Opt. Express*, 2019, **10**, 4825–4838.
48 L. Chrostowski, et al., in *Optical Interconnects XXI*, eds. H. Schröder and R. T. Chen, SPIE, 2021, vol. 11692.
49 J. Flueckiger, et al., *Opt. Express*, 2016, **24**, 15672–15686.
50 S. T. Fard, V. Donzella, S. A. Schmidt, J. Flueckiger, S. M. Grist, et al. *Opt. Express*, 2014, **22**, 14166–14179.
51 S. T. Fard, K. Murray, M. Caverley, V. Donzella, J. Flueckiger, S. M. Grist, et al., *Opt. Express*, 2014, **22**, 28517–28529.
52 E. Luan, et al., in *Integrated Optics: Devices, Materials, and Technologies XXII*, SPIE, 2018, p. 15.
53 E. Luan, et al., *IEEE J. Select. Topics Quantum Electron.*, 2019, **25**, 1–11.
54 L. Dias, et al., in *Conference on Lasers and Electro-Optics*, OSA, Washington, D.C., 2019, p. ATu4K.5.
55 L. S. Puumala, S. M. Grist, et al., *Biosensors (Basel)*, DOI:10.3390/bios12100840. 2022.
56 L. S. Puumala, S. M. Grist, et al., *Biosensors (Basel)*, DOI:10.3390/bios13010053. 2023.
57 H. M. Robison and R. C. Bailey, *Curr. Protoc. Chem. Biol.*, 2017, **9**, 158–173.
58 A. L. Washburn, L. C. Gunn and R. C. Bailey, *Anal. Chem.*, 2009, **81**, 9499–9506.
59 A. L. Washburn, M. S. Luchansky, A. L. Bowman and R. C. Bailey, *Anal. Chem.*, 2010, **82**, 69–72.
60 R. M. Graybill, M. C. Cardenosa-Rubio, H. Yang, M. D. Johnson and R. C. Bailey, *Anal. Methods*, 2018, **10**, 1618–1623.
61 Y. Xie, et al., *IEEE J. Select. Topics Quantum Electron.*, 2020, **26**, 1–20.
62 L. Chrostowski, et al., *IEEE J. Select. Topics Quantum Electron.*, 2019, **25**, 1–26.
63 R. C. Miller, E. Brindle, D. J. Holman, J. Shofer, N. A. Klein, M. R. Soules and K. A. O'Connor, *Clin. Chem.*, 2004, **50**, 924–932.
64 E. Valera, W. W. Shia and R. C. Bailey, *Clin. Biochem.*, 2016, **49**, 121–126.
65 S. Mudumba, et al., *J. Immunol. Methods*, 2017, **448**, 34–43.
66 R. B. M. Schasfoort, in *Handbook of surface plasmon resonance*, Royal Society of Chemistry, Cambridge, 2017, pp. 1–26.
67 N. Santoro, et al., *J. Clin. Endocrinol. Metab.*, 2017, **102**, 2218–2229.
68 ZRT Laboratory, *Urinary Progesterone Metabolites in Postmenopausal Women Not Supplementing with Progesterone*, 2014.
69 T. Yasui, Y. Ideno, Y. Onizuka, J. Nakajima-Shimada, H. Shinozaki and K. Hayashi, *J. Med. Invest.*, 2019, **66**, 297–302.
70 R. S. Weinstock, et al., *The role of blood glucose monitoring in diabetes management*, American Diabetes Association, Arlington, 2020. doi: 10.2337/db2020-31

Silicon photonic biosensors for low-cost, portable, data-rich measurements of hormone biomarkers relevant to women's health and the menopausal transition

Executive Summary for Health Challenge

Dr. Samantha M. Grist, The University of British Columbia, Vancouver, Canada

What is the unmet need? There have historically been significant gender inequities in healthcare and medical research, with many women's health issues, including symptoms of the menopausal transition, neglected and underfunded. Women's gonadal (sex) hormones can be key indicators of health and impact many conditions beyond fertility, including cardiovascular conditions and neurological disorders. These hormones also fluctuate significantly during the menstrual cycle, requiring frequent monitoring to fully understand the levels and fluctuations. Gonadal hormones are critical during the menopausal transition, with levels of more than 10 hormones linked with perimenopausal symptoms including sleep and mood disruption, brain fog, and hot flashes. These symptoms present a significant societal burden – 25% of people experiencing perimenopause symptoms consider leaving the workforce – but people experiencing them and the physicians treating them have limited tools and data to understand and predict symptoms or monitor and improve the impact of treatment. To provide insightful, impactful data, the ideal monitoring tool would provide quantitative, accurate, and data-rich measurement of at least 4-10 hormones and hormone metabolites, and it would be able to provide these measurements quickly (in minutes) at low cost, in a form factor suitable for people to conveniently use at home at least multiple times per week. This kind of solution does not currently exist: centralized lab-based assays are expensive, slow, and inconvenient for daily testing, while existing point-of-need solutions like lateral flow assays do not provide the required quantitative, accurate, and multiplexed (measurement of multiple hormones) data.

What is being proposed to meet this need? Silicon photonic integrated circuits containing biosensors are well-suited to performing quantitative, accurate, data-rich measurements, and tens to hundreds of sensors can be integrated on a single millimeter-scale chip for multiplexed measurements. They are fabricated with scalable semiconductor manufacturing technologies, facilitating low costs at high volume. A key limitation of these types of sensors has historically been the size and cost of the readout system (e.g., the Genalyte platform for doctors' offices), because an expensive ($40,000-$100,000), bulky tunable laser and light coupling system are required to read out the data, precluding their use for at-home testing applications like hormone monitoring. We have invented a new sensor architecture that addresses this challenge, allowing us to use a tiny (<1 mm), inexpensive (<$1), fixed-wavelength laser for readout. In this project, we propose to validate this new silicon photonic technology, create a bench-scale portable readout system, and demonstrate urine-based detection of an initial panel of two hormone biomarkers relevant to menopause (expandable to tens in the future).

What are the expected outcomes? Through this work plan we will develop our new silicon photonic sensor and quantify its photonic performance metrics (to provide data-rich measurements at 1000× lower cost than traditional photonic biosensors), compare performance with gold-standard measurements, and also quantify detection of two biomarkers relevant to the menopausal transition: pregnanediol (PdG) and follicle-stimulating hormone (FSH). We will also demonstrate a portable system suitable for demonstration at Optica conferences and to collaborators.

What will be the real-world impact of this project? This project will use innovation in photonics to address a critical unmet need in women's healthcare by validating a portable, low-cost technology for decentralized, multiplexed monitoring of hormone markers in urine. With this project, we will build a tool that has the potential to drastically improve health and quality-of-life during the menopausal transition, and also lay the foundation for future development of tests for additional conditions for broader potential impact of the technology on human health.

Wafer-scale, transfer-free hetero-integrated photonic circuits using confined growth of single-crystalline 2D materials

1. Literature Review and Motivation

The heterogeneous integration of functional optical materials has not only proven a backbone in prototyping massive optoelectronic applications with excellent performance, but also a driving engine to explore novel nanophotonic phenomena in diverse heterostructures[1]. Featured with broad bandwidth and ultrafast speed, photonic integrated circuits (PIC) are poised to circumvent the electrical bottleneck in integrated electronics, relying on a wide spectrum of devices such as lasers, optical modulators, and photodetectors[2]. However, despite the successes of silicon (Si) and silicon nitride photonics, single material platform still has varying intrinsic shortcomings that can hardly meet the increasing demand for and multifunctional high-performance PIC devices[2]. Moreover, conventional heteroepitaxy approaches to this end involve stringent lattice-matching requirements, severely limiting the available choices of hetero-integrated photonic devices.

Featured with van der Waals (vdW) surfaces, two-dimensional (2D) materials as transferrable vdW building blocks showcasing unprecedented degrees of freedom to integrate and mix with arbitrary photonic templates without lattice-matching constraints[1,3]. These atomically thin materials have attracted tremendous research interest in the photonics and optoelectronics, owing to their intriguing and salient optoelectronic attributes[4,5]. Including graphene[6], transition-metal dichalcogenides (TMDs), black phosphorus (BP), hexagonal boron nitride (h-BN), and emergent candidates like quasi-2D halide perovskites[7], a big family of 2D materials show abundant optical functionalities, covering light emission, modulation, detection, and nonlinear optics. Various endeavors have thus been devoted to incorporating 2D materials to optical waveguides to develop high-performance integrated photonic devices. For instance, graphene-transferred Si waveguides are used to develop optical polarizers, and integrated optical amplitude or phase modulators[8] with broad optical bandwidth. All-optical graphene plasmonic switches are also proposed with ultrafast operation speed and low power consumption[9]. Compared to graphene that lack an electronic bandgap, 2D BP and TMDs are more promising for active photonic applications such as nano-lasers[10], amplifiers, and photodetectors with miniaturized device footprint and excellent CMOS compatibility. Besides graphene, broadband photo-detectors were also demonstrated with high responsivity and wide bandwidth using BP[11], or 2D TMDs[12]. They can also be assembled into artificial vdW heterostructures with diverse designer photonic structures for drastically enhanced light-matter interactions.

2. Problem Statement/Objectives

Despite prior exciting progress on 2D integrated photonics, most proposed 2D-integrated devices remain lab explorations, making real-word practical products still a distinct vision[5]. For nearly the last two decades since the debut of graphene, intensive efforts have been put in 2D material synthesis and 2D-photonics integration optimization at large-scale to prototype new functional devices. Nevertheless, **significant progress towards commercialization of 2D material-based technology is still largely elusive**.

Large-scale graphene monolayers were successfully synthesized via chemical vapor deposition (CVD)[5]. However, to make functional integrated photonic devices, the graphene sheets need to be transferred to prefabricated optical waveguides made of, for instance, Si or silicon nitride[8,13]. The PMMA- or metal-handlers-based 2D transfer process will inevitably induce polymer residues and defects like wrinkles or cracks, which can crucially deteriorate device performance[6]. In terms of 2D TMDs-based optical applications, the majority of previous demonstrations rely on exfoliated flakes[12-14], because the growth of continuous 2D TMD monolayers over wafer-scale is still challenging. Although mechanical exfoliations can produce 2D flakes with the best quality for on-chip lasers, modulators[15], and photodetectors[12], it remains a trial-and-error heavy labor work with very small-sized, irregular-shaped 2D film and extremely low yield[1,5]. Even with the perspectives of robotics-aided film exfoliation, the 2D transfer-based approaches still require precise control over the delicate 2D films well-aligned to target photonic structures and it unavoidably induces defects on 2D with degraded device performance and rising cost, faltering most current research far away from robust and scalable mass-production required in 2D commercialization[1].

To summarize, currently **3 outstanding challenges exist** in 2D-materials-based integrated photonics. **(1) Lack of robust and high-throughput 2D material growth method** with high material quality over wafer-

scale. **(2) Reliance of 2D film transfer** that inevitably induce material defects and transfer residues. **(3) Lack of system level demonstration of 2D-based integrated photonic chips**, as current papers majorly centered on only single device. For the first challenge, the realization of single-crystalline 2D monolayers (such as 2D TMDs and h-BN, except graphene) continuous over wafer-scale is still under investigation. This is mainly because kinetic control of few atomic monolayers has proven extremely challenging, caused by 3 critical issues: (i) monolayer-by-monolayer 2D material growth, (ii) single-crystalline 2D material growth, and (iii) 2D materials growth at a wafer-scale. So far, a few reports have tried to address one among the three issues. However, no single report has been made to tackle all three at the same time, although 2D commercialization becomes possible only after all issues are solved. Monolayer single-domain TMDs were grown on laser-pre-damaged areas, but this method cannot realize 2D heterostructures in wafer-scale due to the unconfined growth scheme, low laser-scanning yield, and damaged bottom seedings[16]. Large-scale layer-by-layer growth of 2D heterostructures were also reported, by with poly-crystalline 2D quality of compromised performance[17]. For the second challenge, transfer-free heteroepitaxy was explored to grow MoTe2 on arbitrary surfaces[18]. However, except certain single-crystalline substrates, most photonic templates, especially the post-fabricated optical waveguides and cavity structures are not suitable for 2D material growth, leading to drastically deteriorated 2D material quality. Moreover, the demonstrated 2D TMDs remains bulk (>10 layers), the extraordinary optoelectronic properties of 2D TMDs only reveal at a few monolayers[4]. For the reported growth of bulk 2D TMDs, they are no longer direct bandgap material, losing the suitability for most active optoelectronic applications[1]. For the third challenge, MIT researchers have proposed chalcogenide glass-on-graphene as a handy platform to make various integrated photonic devices of modulators, photodetectors, and polarizers[19]. However, it still remains discrete device level demonstration and drawbacks of graphene transfer is still necessitated.

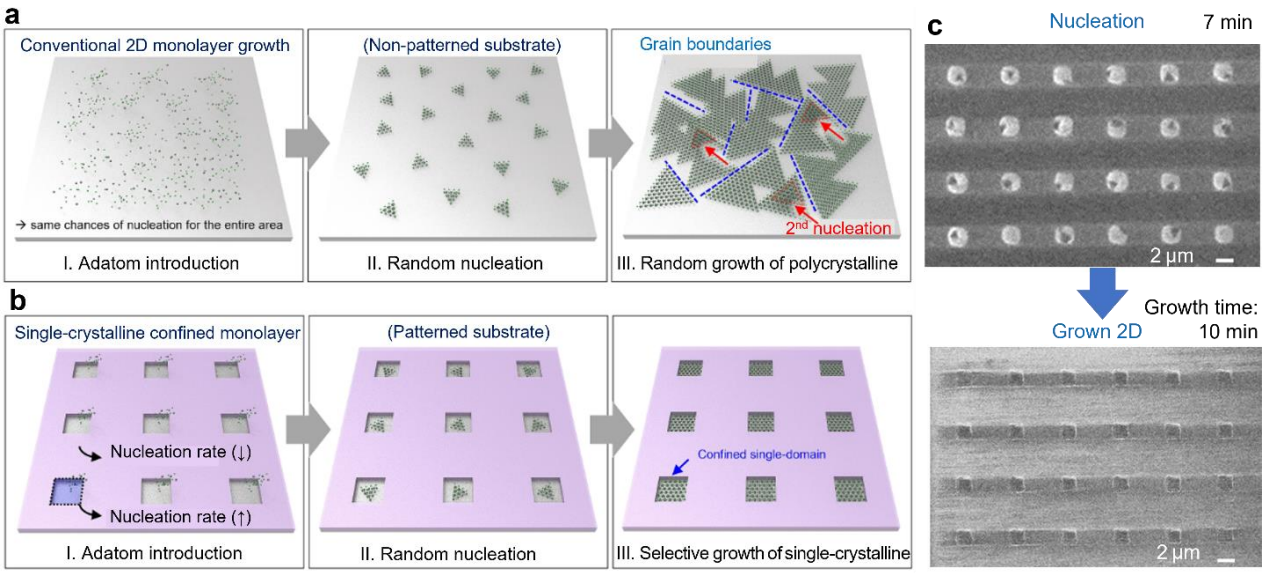

Figure 1. (a) Conventional CVD yields uniform polycrystalline 2D films with grain boundaries. (b) Confined CVD for location-selective single-domain 2D material synthesis strategy. (c) SEM of grown WSe_2 with verified 100% single-domain 2D monolayers on sapphire pockets with prefabricated a-SiO_2 trenches.

Objectives (proposed research): Here we propose a transfer-free and scalable approach to produce single-crystalline 2D material monolayers, bilayers, and their heterostructures via engineered CVD on judiciously pre-patterned optical substrates with designed growth pockets. This approach can make a **remarkable leap towards practical commercialization of 2D integrated photonics by simultaneously solving all the three challenges above**: **(1)** highly robust confined CVD growth of single-crystalline 2D materials for low-cost foundry mass-production. **(2)** Direct and controlled layer-by-layer growth of 2D monolayers on arbitrary pre-defined locations and on almost arbitrary industrial wafers. **(3)** Capable of making 2D-based integrated photonic systems with excellent process compatibility by modified device fabrication process. We will focus on integrated photonic devices and circuity based on 2D semiconductors such as 2D TMDs (e.g., WSe_2, MoS_2) and 2D metal halide perovskites for on-chip photodetectors and optical modulators, as

compared to graphene, wafer-scale growth of 2D TMDs with monolayer and single-crystallinity is still an open challenge with greater impact. The objectives above will be made reality based on the following three crucial technologies that we have already successfully achieved.

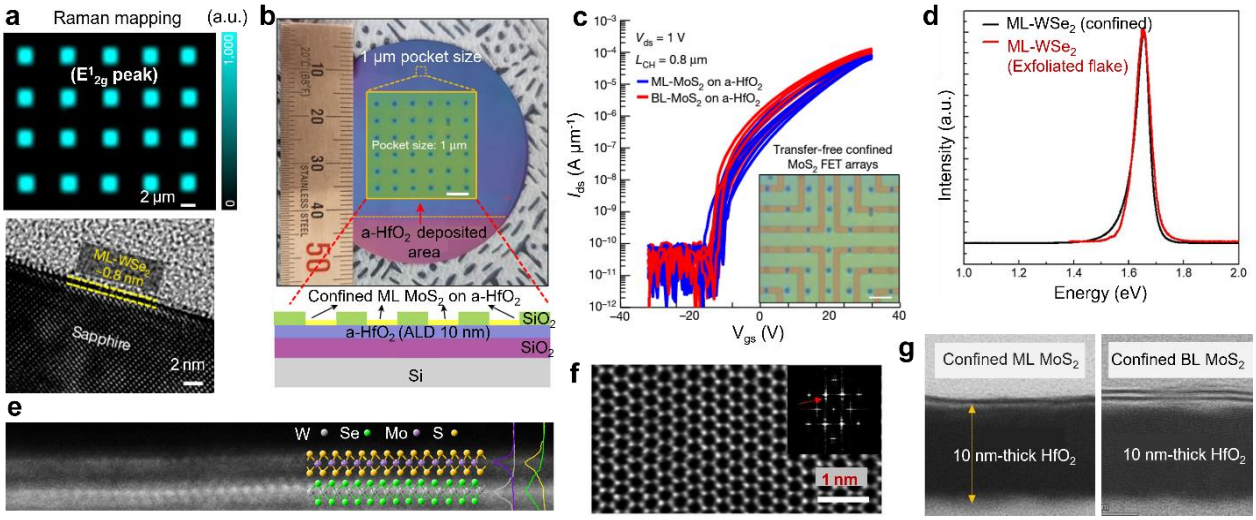

Figure 2. (a) Raman mapping & TEM of confined monolayer (ML) WSe_2 on sapphire. (b) Photo & schematic of confined growing ML-TMD on HfO_2-covered SiO_2/Si substrate. (c) Measured electrical I-V curve made by confined grown ML-bilayer (BL) MoS_2. (d) Photoluminescence spectra of confined grown ML-WSe_2 and exfoliated WSe_2 flakes. (e) and (f) HAADF-STEM of confined-grown WSe_2/MoS_2 vdW heterostructures, and ML-single-crystal WSe_2 on HfO_2. (g) Cross-sectional STEM of ML & BL MoS_2 grown on patterned HfO_2.

(i) Wafer-scale layer-by-layer controlled epitaxy of single-crystal 2D materials by geometrically confined CVD. In our previous work[1,20] (Nature 614, 88-94, 2023), we have solved multiple critical issues including monolayer-by-monolayer growth controllability (both homo- and hetero-structures) with single crystallinity at pre-designated locations in wafer-scale. Compared with conventional CVD that yields spatially ununiform (hybrid with 0~2 monolayers) polycrystalline 2D materials (**Fig. 1a**), crystalline sapphire substrates (c-plane Al_2O_3) patterned by deposited amorphous SiO_2 mask are applied as CVD growth templates. As the binding energies of the 2D adatoms on a-SiO2 is significantly higher than c-Al_2O_3, nucleation will preferably take place at the predefined growth pockets (i.e. c-Al_2O_3 substrate without SiO_2 coverage). The first set of nuclei is thus geometrically confined to predesignated locations (**Fig. 2b**). By judiciously controlling the growth pocket size (2~10 μm) and growth time, uniform single-crystalline 2D WSe_2 monolayers are formed (before starting the 2nd layer nucleation).

(ii) Monolayer-controllable non-epitaxial single-crystal 2D TMD growth on amorphous oxides by geometrically confined CVD. Despite the excellent 2D material quality realized on patterned c-sapphire, the substrate is not suitable for integrated photonic applications. On-chip integrated photonic devices typically require waveguide structures, such as Si-on-insulator, with thick buried low-index oxides (like SiO_2) to avoid leakage of guided electromagnetic waves[2]. Therefore, to realize a transfer-free method to fabricate 2D PICs, we need to directly growth 2D monolayers on optical templates with thick SiO_2 layer. Leveraging ALD HfO_2-covered oxide layers, growth selectivity is theoretically confirmed by density functional theory (DFT) calculations[20] and experimentally verified by Raman mapping (**Fig. 2a**), XPS, and AFM characterizations[20]. Single-domain controlled growth of monolayer (ML) to bilayer (BL) MoS_2 on a-HfO_2/ SiO_2/Si optical substrate (**Fig. 2b**) is experimentally verified with excellent optoelectronic properties (**Figs. 2b & 2c**), even comparable to mechanically exfoliated ML 2D TMD flakes (**Fig. 2d**). The primal single-crystallinity of the ML, BL, and vdW heterostructures of WSe_2 and MoS_2 are also verified by the High-angle annular dark-field STEM images (**Figs. 2e-2g**)[20].

(iii) Modified hybrid bottom-up fabrication process of 2D integrated photonic devices. Instead of growing 2D on prefabricated structures like optical waveguides and resonators[18], which have massive fabrication-induced defects and contained interfaces, we propose forming high-quality ML 2D materials first by confined CVD. Then proceed with electrical contact fabrication and lastly do the waveguide (WG)

fabrication (**Figs. 3a, 3b**) via e-beam lithography (EBL). This approach does not necessitate any 2D material transfer and consists of all-standard nanofabrication processes compatible for scalable manufacture at foundry with reduced cost. We have tested the fabrication of various SU-8 photonic structures (**Fig. 3c**) with low optical loss, such as the SU-8 polymer micro-ring resonator with quality factor Q~8×10^4 (**Fig. 3d**). The SU-8 polymer waveguides are beneficial with low optical loss, moderate refractive index, low-cost, and can be formed directly after EBL and development without involving expensive etching tools like RIE towards practical commercialization.

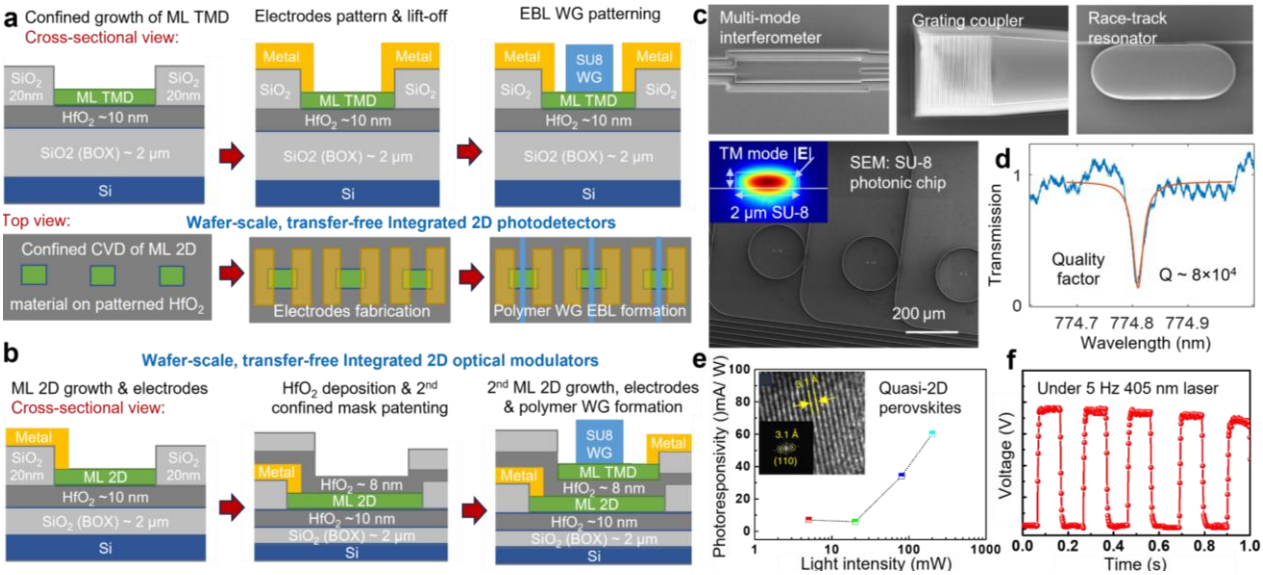

Figure 3. (a) and (b) Modified hybrid fabrication method for waveguide-integrated 2D photodetectors and modulators respectively. (c) SEM of various photonic components made by SU-8 polymer photonics. Inset: simulated |**E**| distribution of TM_{00} mode in a 2×0.6 μm SU-8 waveguide. (d) Transmission spectrum of a SU-8 micro-ring. (e), (f) Photo-responsivity of crystalline quasi-2D perovskite film. Inset: perovskite STEM image.

3. Outline of tasks/Work Plan

Tasks & milestones: We target the following 2D-integrated devices/systems. **(1)** Transfer-free, scalable fabrication of waveguide-coupled integrated photodetectors will be demonstrated levering confined-CVD-grown ML~BL WSe_2 or MoS_2, by following fabrication steps shown in **Fig. 3a**. **(2)** scalable fabrication of integrated optical amplitude or phase modulators based on confined CVD ML 2D TMDs (**Fig. 3b**). **(3)** A proof-of-concept demonstration of integrated photonic system with integrated optical modulators and photodetectors on the same photonic chip.

To realize the targets above, the following tasks will be addressed. **(T1) Optimized HfO_2 deposition and SiO_2 growth pattern design for optical applications**. Firstly, in our previous work, a-HfO_2 was deposited on ~ 30 nm thin SiO_2 substrate. To realize integrated optical waveguides without substrate light leakage, we will firstly optimize the atomic layer deposition (ALD) of ultra-flat a-HfO_2 on SiO_2 (2 μ-thick)/Si substrate. Also, our prior confined growth pocket size and pattern design were for electronic applications of 2D (**Fig. 2**): the growth pockets for 2D were too small in size (~ 2×2 μm) and too dense for optical applications. For integrated photonic devices such as modulators, lasers, and photodetectors, the desired size of ML 2D material (same as the growth pocket size) would be around 4~20 μm depending on applications. The spacing of the growth pockets is also desired to be larger to accommodate electrodes and avoid the evanescent coupling between adjacent waveguides[1,6]. Thus, we will re-design the growth pattern (the growth condition will be also changed) to guarantee high-quality monolayer (ML) 2D TMD growth first. Then further optimize the confined CVD condition to target ML~BL 2D TMD (WSe_2) with low multi-domain portion to even single-crystalline quality. **(T2) Dual-layer confined growth of ML 2D materials**. After achieving Task (T1), the proposed 2D integrated photodetectors can be realized by all standard process of photolithography, e-beam evaporate of Pt/Au electrodes, metal lift-off, and EBL process without challenge (**Fig. 3a**). However, for modulators, capacitor structures need to be formed in order to electrically

tune the carrier density/optical absorption of the 2D materials[15,19]. Thus, after the 1st confined growth, we will ALD HfO_2 as the spacing layer, followed by 2nd patterning of SiO_2 growth mask for 2nd confined CVD. **(T3) Confined growth of quasi-2D metal-halide perovskite (PVSK) & system optimization**. Besides 2D WSe_2 and MoS_2, we will also test confined CVD of 2D PVSK (**Figs. 3e, 3f**) for photodetection and laser applications. System optimization of photonic chip with 2D modulators & detectors will also be performed.

Schedule: **Month 1-2**: Optimize ALD HfO_2; Design confined growth mask pattern for optical applications.
Month 2-4: Optimize confined CVD growth condition for ML 2D WSe_2 on $HfO_2/SiO_2/Si$ with new patterns.
Month 4-5: Integrated 2D photodetectors array fabrication and optical measurement.
Month 5-8: Dual-layer confined growth of ML 2D WSe_2 or MoS_2 (with $2D/HfO_2/2D$ capacitor structure).
Month 9-10: Integrated optical modulators based on dual-ML 2D TMD and SU-8 polymer waveguides.
Month 10-12: Integrated 2D photonic chip with 2D modulator & photodetector: fabrication & measurement.

4. Outcomes and Impact

By implementing the tasks above, we embody an exciting leap towards the commercialization and advancement of 2D materials-based integrated photonics. A potentially revolutionary paradigm can be established by using confined CVD growth of ML single-crystalline 2D materials (TMDs, PVSK) for wafer-scale, transfer-free 2D integrated photonic devices manufacture with excellent quality, which simultaneously solving three previously long-standing challenges (2D quality, transfer issues, and system integration) in 2D integrated photonics society. We will demonstrate broadband integrated 2D photodetectors from 500 nm to 1 μm (responsivity > 0.3 $A \cdot W^{-1}$), broadband 2D modulators from visible to near infrared (> 5 GHz bandwidth), and proof-of-principle integrated 2D photonic chip via low-loss (<2 dB/cm) SU-8 waveguides with light modulation and photodetection, opening a new avenue for practical 2D hetero-integrated photonics towards commercialization to viable technology.

References

1. Meng, Y. et al. Photonic van der Waals integration from 2D materials to 3D nanomembranes. Nature Reviews Materials, doi:10.1038/s41578-023-00558-w (2023).
2. Tran, M. et al. Extending the spectrum of fully integrated photonics. Nature 610, 54–60 (2022).
3. Liu, Y., et al. Van der Waals integration before and beyond 2D materials. Nature 567, 323-333, (2019).
4. Xia, F., et al, A. Two-dimensional material nanophotonics. Nature Photonics 8, 899-907, (2014).
5. Kong, W. Path towards graphene commercialization from lab to market. Nat. Nanotechnol. 14, 927 (2019).
6. Romagnoli, M. et al. Graphene-based integrated photonics for next-generation datacom and telecom. Nature Reviews Materials 3, 392-414, (2018).
7. Ricciardulli, A. G., at al. Emerging perovskite monolayers. Nature Materials 20, 1325-1336 (2021).
8. Sorianello, V. et al. Graphene-Si phase modulators with gigahertz bandwidth. Nat. Photon. 12, 40-44 (2018).
9. Ono, M. et al. Ultrafast and energy-efficient all-optical switching with graphene-loaded deep-subwavelength plasmonic waveguides. Nature Photonics 14, 37-43 (2020).
10. Li, Y. et al. Room-temperature continuous-wave lasing from monolayer molybdenum ditelluride integrated with a silicon nanobeam cavity. Nature Nanotechnology 12, 987-992 (2017).
11. Youngblood, N., et al. Waveguide-integrated black phosphorus photodetector with high responsivity and low dark current. Nature Photonics 9, 247-252 (2015).
12. Maiti, R. et al. Strain-engineered high-responsivity MoTe2 photodetector for silicon photonic integrated circuits. Nature Photonics 14, 578-584 (2020).
13. Sun, Z., et al. Optical modulators with 2D layered materials. Nature Photonics 10, 227-238 (2016).
14. Sung, J. et al. Room-temperature continuous-wave indirect-bandgap transition lasing in an ultra-thin WS2 disk. Nature Photonics 16, 792-797 (2022).
15. Datta, I. et al. Low-loss composite photonic platform based on 2D semiconductor monolayers. Nature Photonics 14, 256-262 (2020).
16. Li, J. et al. General synthesis of 2D van der Waals heterostructure arrays. Nature 579, 368-374 (2020).
17. Jin, G. et al. Heteroepitaxial vdW semiconductor superlattices. Nature Nanotechnology 16, 1092 (2021).
18. Pan, Y. et al. Heteroepitaxy of semiconducting 2H-MoTe2 thin films on arbitrary surfaces for large-scale heterogeneous integration. Nature Synthesis 1, 701-708 (2022).
19. Lin, H. et al. Chalcogenide glass-on-graphene photonics. Nature Photonics 11, 798-805 (2017).
20. Kim, K. et al. Non-epitaxial single-crystal 2D material growth by geometrical confinement. Nature (2023).

References (Full-editable by Endnote)

1 Meng, Y. *et al.* Photonic van der Waals integration from 2D materials to 3D nanomembranes. *Nature Reviews Materials*, doi:10.1038/s41578-023-00558-w (2023).

2 Tran, M. *et al.* Extending the spectrum of fully integrated photonics. *Nature* **610**, 54–60 (2022).

3 Liu, Y., Huang, Y. & Duan, X. Van der Waals integration before and beyond two-dimensional materials. *Nature* **567**, 323-333, doi:10.1038/s41586-019-1013-x (2019).

4 Xia, F., Wang, H., Xiao, D., Dubey, M. & Ramasubramaniam, A. Two-dimensional material nanophotonics. *Nature Photonics* **8**, 899-907, doi:10.1038/nphoton.2014.271 (2014).

5 Kong, W. *et al.* Path towards graphene commercialization from lab to market. *Nature Nanotechnology* **14**, 927-938, doi:10.1038/s41565-019-0555-2 (2019).

6 Romagnoli, M. *et al.* Graphene-based integrated photonics for next-generation datacom and telecom. *Nature Reviews Materials* **3**, 392-414, doi:10.1038/s41578-018-0040-9 (2018).

7 Ricciardulli, A. G., Yang, S., Smet, J. H. & Saliba, M. Emerging perovskite monolayers. *Nature Materials* **20**, 1325-1336 (2021).

8 Sorianello, V. *et al.* Graphene–silicon phase modulators with gigahertz bandwidth. *Nature Photonics* **12**, 40-44 (2018).

9 Ono, M. *et al.* Ultrafast and energy-efficient all-optical switching with graphene-loaded deep-subwavelength plasmonic waveguides. *Nature Photonics* **14**, 37-43 (2020).

10 Li, Y. *et al.* Room-temperature continuous-wave lasing from monolayer molybdenum ditelluride integrated with a silicon nanobeam cavity. *Nature Nanotechnology* **12**, 987-992 (2017).

11 Youngblood, N., Chen, C., Koester, S. J. & Li, M. Waveguide-integrated black phosphorus photodetector with high responsivity and low dark current. *Nature Photonics* **9**, 247-252, doi:10.1038/nphoton.2015.23 (2015).

12 Maiti, R. *et al.* Strain-engineered high-responsivity MoTe2 photodetector for silicon photonic integrated circuits. *Nature Photonics* **14**, 578-584, doi:10.1038/s41566-020-0647-4 (2020).

13 Sun, Z., Martinez, A. & Wang, F. Optical modulators with 2D layered materials. *Nature Photonics* **10**, 227-238 (2016).

14 Sung, J. *et al.* Room-temperature continuous-wave indirect-bandgap transition lasing in an ultra-thin WS2 disk. *Nature Photonics* **16**, 792-797, doi:10.1038/s41566-022-01085-w (2022).

15 Datta, I. *et al.* Low-loss composite photonic platform based on 2D semiconductor monolayers. *Nature Photonics* **14**, 256-262, doi:10.1038/s41566-020-0590-4 (2020).

16 Li, J. *et al.* General synthesis of two-dimensional van der Waals heterostructure arrays. *Nature* **579**, 368-374, doi:10.1038/s41586-020-2098-y (2020).

17 Jin, G. *et al.* Heteroepitaxial van der Waals semiconductor superlattices. *Nature Nanotechnology* **16**, 1092-1098, doi:10.1038/s41565-021-00942-z (2021).

18 Pan, Y. *et al.* Heteroepitaxy of semiconducting 2H-MoTe2 thin films on arbitrary surfaces for large-scale heterogeneous integration. *Nature Synthesis* **1**, 701-708, doi:10.1038/s44160-022-00134-0 (2022).

19 Lin, H. *et al.* Chalcogenide glass-on-graphene photonics. *Nature Photonics* **11**, 798-805, doi:10.1038/s41566-017-0033-z (2017).

20 Kim, K. S. *et al.* Non-epitaxial single-crystal 2D material growth by geometrical confinement. *Nature* (2023).

Wafer-scale, transfer-free hetero-integrated photonic circuits using confined growth of single-crystalline 2D materials – Summary

Sang-Hoon Bae, Washington University in St. Louis

The integration of two-dimensional (2D) materials for on-chip photonic applications has attracted immense research interest, thanks to their prominent optoelectronic attributes and the unprecedented degrees of freedom to create heterogeneous integrated photonic layouts and van der Waals (vdW) heterostructures without the lattice-matching constraints that apply to heteroepitaxy. Abundant useful properties are shown in 2D materials of graphene and transition metal dichalcogenides (TMDs), encompassing vital optical functionalities from light emission, modulation, photodetection, and nonlinear optics. However, most reported 2D-materials-based integrated photonic devices to date still largely remain lab demonstrations, far faltering the surging vision of practical 2D-photonics commercialization in real-word.

Before fledging into fully viable technology, 3 long-standing challenges exist for integrated photonics based on 2D materials. (1) Most reported devices use transferred 2D materials. This is because substrates that are suitable for 2D material growth (such as sapphire) cannot be directly used for integrated optical applications (typically require thick SiO_2 BOX layer). Consequently, 2D materials are later transferred to prefabricated photonic templates such as waveguides and micro-cavities using PMMA or metal handler after growth. However, the transfer process inevitably induces residues and defects (cracks, holes, wrinkles) to 2D that significantly deteriorate material optical property and performance. Transfer of delicate 2D films is also incompatible with standard foundry mass-production process. (2) Lack of robust scalable synthesis method of high-quality 2D materials, especially 2D TMDs. Conventional mechanical exfoliation and transfer approaches can produce 2D flakes with high quality, but it remains a trial-and-error process with heavy labor work and extremely low yield. For scalable manufacture methods such as chemical vapor deposition (CVD), it was an open challenge to obtain controlled monolayer-by-monolayer (ML) single-crystalline uniform 2D material growth over wafer-scale, especially for 2D TMDs. (3) Due to the above two reasons, currently reported works are still restrained to single-device demonstration of 2D materials.

Here we propose a novel strategy to simultaneously solve the abovementioned issues, by providing a transfer-free approach to fabricate integrated 2D photonic devise at wafer-scale with high robustness, high throughput, and low-cost. The proposed project will be based on our modified CVD on patterned thin HfO_2/SiO_2 substrates that have judiciously engineered growth pockets to spatially confine the nucleation of 2D materials. Using this confined CVD method with spatial growth selectivity, we have priorly successfully achieved single-crystalline 2D TMD (WSe_2, MoS_2) controlled growth (ML, bilayer/BL, and BL 2D vdW heterostructures) on sapphire or HfO_2/Si templates. Here, we will use optical substrates (2 μm-thick SiO_2/Si) deposited with very thin (< 10 nm) HfO_2 to realize integrated photonic applications including 2D TMD (WSe_2, MoS_2) or quasi-2D metal-halide perovskites-based waveguide-integrated photodetectors and 2D ML-TMDs-based optical modulators. The growth patterns will be re-designed for optical devices followed by re-optimized confined CVD growth conditions. Compared to conventional Si or SiN photonic platforms that either necessitate 2D transfer or can hardly realize good waveguide quality on 2D, we propose a new hybrid bottom-up nanofabrication strategy, by using SU-8 polymer waveguides to directly make the as-grown 2D monolayers into integrated photonic devices without any layer transfer. This method completely solved the residue and defect problems in conventional approaches. The SU-8 polymer waveguides also have the benefit of low-loss (~2 dB/cm), low-cost, and easy-to-fabrication.

Wafer-scale hetero-integrated photodetectors array will be demonstrated without 2D transfer, by first doing confined CVD of ML 2D WSe_2 and/or MoS_2, followed by aligned photolithography and metal lift-off for electrodes and e-beam lithography (EBL) for SU-8 waveguides with high responsivity. Dual confined CVD of ML TMD will be developed to form 2D/HfO_2/2D structure to electrically modulate the absorption of the 2D material for broadband (visible to near infrared) integrated optical modulators. A proof-of-concept demonstration of scalable integrated 2D photonic nano-system with 2D modulators and photodetectors will be delivered as well, following the research steps/schedules detailed in proposal. By simultaneously solving the prior outstanding challenges in 2D integrated photonics community, we envisage this transfer-free scalable strategy to integrate single-crystalline 2D monolayers to photonic chip can offer a crucial leap towards the practical commercialization of 2D photonics into a viable and worthy technology.

Executive Summary:
Quantum-enhanced nonlinear optical learning machine

Category: Information
Saroch Leedumrongwatthanakun
Division of Physical Science, Faculty of Science, Prince of Songkla University, Thailand

In the current information era, the pressing demand for information processing systems with high-capacity, high-speed, and energy-efficient capabilities is of considerable significance. To address this challenge, we propose the development of a programmable optical circuit capable of high-performance computing - the “quantum-enhanced nonlinear optical learning machine”. It consists of a sequence of high-dimensional spatially entangled light sources, interspersed with a programmable linear optical circuit and reconfigurable optical phase arrays (see Figure 1).

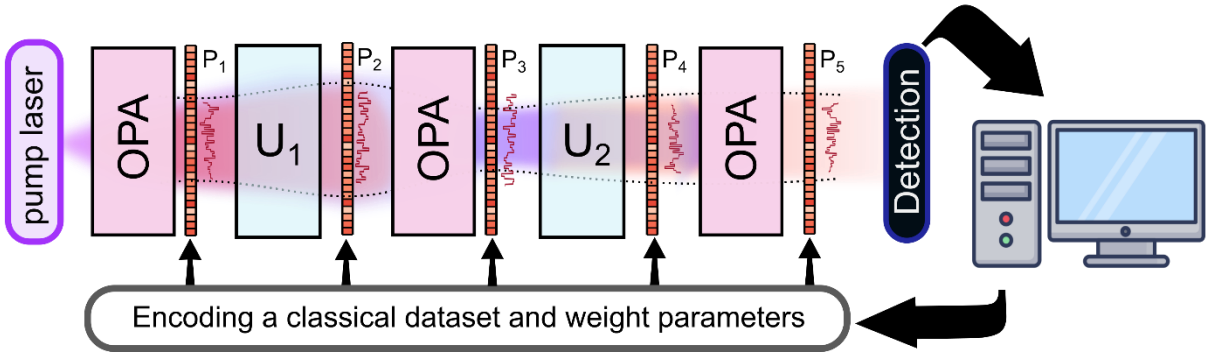

Figure.1 The conceptual schematic of quantum-enhanced nonlinear optical learning machine: It consists of a series of high-dimensional entangled light sources generated from the optical parametric amplification (OPA) process, and a programmable linear circuit, U_i, constructed from a cascade of random unitary transforms and reconfigurable optical phase arrays, P_i. The optical phase arrays, implemented by a spatial light modulator, are used to encode classical data and weight parameters onto the optical circuit where all pump, signal, and idler fields are manipulated to control de/amplification process in the cascade OPAs.

One layer of the optical machine, known as the multimode nonlinear SU(1,1) interferometer, has garnered significant attention for its sensing applications due to its sub-shot-noise sensitivity, even in the presence of external optical loss. Our research further explores the intricate interference between signal and idler radiations, paving the way for computing functionalities. Through the implementation of linear optical circuits, one can adjust the relative phases and amplitudes between the optical pump, signal, and idler fields of each mode of optical parametric amplifiers. This enables us to control the de/amplification and quantum correlation of parametric downconversion light throughout the entire circuit.

By harnessing the quantum optical process, we aim to investigate the learning capability and trainability of the optical machine through statistical learning theory. Additionally, we aspire to showcase its practicality for large-scale real-world data classifications and time-series predictions, all achieved at high speeds while consuming minimal energy. One highlight advantage of the optical machine is its independence from intricate lithography, precise designs of nonlinear optical components, and the requirement for a sophisticated mesh of reconfigurable Mach-Zehnder interferometers. These characteristics simplify the implementation process, making the optical machine more accessible and feasible for practical applications, catering to the ever-increasing demands of the modern information-driven world.

Proposal Submission
Quantum-enhanced nonlinear optical learning machine
Category: Information

Saroch Leedumrongwatthanakun
Division of Physical Science, Faculty of Science, Prince of Songkla University, Thailand

The collection of vast amounts of data has become primary, driven by our recognition of the immense potential in extracting and learning valuable information through AI-driven algorithms. Such knowledge could help enrich our quality of life and deepen our understanding of nature. The global demand for data storage and traffic as well as information processing via electronic computers has consequently increased. To meet the escalating requirements of training larger AI models, a transition towards more parallel processing using Graphics and Tensor Processing Units has been realized. The progression leads to even more acceleration in the demand for computations and necessitates the development of more efficient computing hardware capable of large-scale data processing while minimizing energy consumption. Addressing these challenges, our research proposal aims to investigate and demonstrate the capability of an alternative optical platform for computing. This platform is based on a programmable sequence of optical parametric amplifiers, offering a way for advancing quantum optical technologies and possibly overcoming the limitations of conventional electronic computing.

Literature Review

The development of diverse computing architectures has regained attention over the recent decade as the quest for alternative information processing units has been rapidly increasing. Examples include analog computing, neuromorphic computing, reservoir computing, extreme learning machines, and quantum computing [Wetzstein2020, Marković2020, Shastri2021].

Light is a good candidate for such computing paradigms because of its advantages in high bandwidth, high speed, low energy consumption, and low latency [Hamerly2019, Wetzstein2020]. As such, many researchers and startups have been advancing optical platforms both in bulk and integrated optics in many directions [Lin2018, Cartlidge2023]. For instance, in terms of energy consumption, an optical neural network has been shown to use less than 1 photon per multiplication to obtain about 90% accuracy on handwritten-digit classification [Wang2022]. In terms of high speed and large bandwidth, the recent development of the optical parallel convolutional processing unit has demonstrated 11 trillion operations per second, enabling the convolution of images with 2.5×10^5 pixels [Xu2020]. Besides, the idea based on large-scale optical random reservoir computing demonstrated the ability to predict spatiotemporal signals of chaotic systems [Rafayelyan2020].

Despite the recent progresses in optical computing, the incorporation of nonlinearity, a pivotal resource in deep neural networks, is the major problem and has been long considered commonly to be the main drawback of optical computing due to a high energy requirement of a nonlinear optical process [Farhat1985, Shen2017, Hughes2018, Wang2023]. Nevertheless, recent advancements have demonstrated promising results, for example, by harnessing the nonlinear effect in a multimode optical fiber and multiple scattering process, the accuracy of classification has been shown to be better than the device relying solely on linear optical transforms [Teğin2021, Xia2023, Yildirim2023].

In parallel, the emergence of quantum machine learning (QML) has opened a compelling avenue of research. In this context, our interest is in a specific scenario wherein a part of an information processing unit operates using quantum effects. The quantum device typically uses to process a computationally difficult subroutine and/or learn from classical data. We here referred to such a device as a *quantum-enhanced learning machine.* Various models

of such machines have been proposed, for example, variational quantum circuits and quantum Boltzmann machines [Cerezo2021, Amin2018, Mitarai2018, Steinbrecher2019]. To my knowledge, the questions about the advantage and performance of quantum-enhanced learning machines, in comparison to classical counterparts, are still unclear and continue to be actively investigated. Addressing challenges such as encoding large classical information into a small quantum system, and evaluating the learning capacity, trainability, and expressivity have been key areas of research [Schuld2022]. Additionally, the implementation of the quantum-enhanced learning machine within an optical platform remains in its infancy, with significant potential for future developments.

In our recent works, the implementation of programmable linear optical circuits within complex scattering processes was successfully demonstrated [Goel2022]. The circuit is utilized for the controllability of two-photon interferences [Leedumrongwatthanakun2020] as well as for the certification of high-dimensional entanglements [Goel2022]. Furthermore, our programmable optical circuit, known as the multi-plane light conversion device, was effectively utilized to achieve quantum state discrimination in high dimensions [Goel2023]. These results showcase the potential of our programmable optical circuit for manipulating entangled qudits, offering exciting possibilities to extend the implementation of quantum machine learning beyond a traditional qubit quantum circuit.

Building upon these advancements and using our expertise, we introduce the concept of the *quantum-enhanced nonlinear optical learning machine*. This machine is a reconfigurable optical circuit capable of generating high-dimensional entangled states from a cascade of multimodal optical parametric amplifiers (OPAs), interspersed with a programmable linear optical circuit and reconfigurable optical phase arrays. The idea is to generalize the traditional multimodal nonlinear SU(1,1) interferometer [Yurke1986, Frascella2019] to the cascade and reconfigurable configuration. Leveraging the programmability of spatial light modulators, we gain the manipulation over the relative complex amplitudes of the optical pump, signal, and idler fields in each circuit layer. This enables the control of de/amplification and quantum correlation of the cascade OPAs, feasibly unlocking a possibility for quantum-enhanced learning in nonlinear optical systems.

Objective

1. To build the quantum-enhance nonlinear optical learning machine.
2. To study the learning capability and trainability of the quantum-enhance nonlinear optical learning machine.
3. To explore the quantum interference between pump, signal, and idler fields and the control of de/amplification process of OPAs for information processing tasks.

Outline of tasks/Work plan

1. Determine the key design parameters of the optical circuit, e.g., optical gain of optical parametric amplification (OPA), the optical loss in the system, number of spatial entangled modes, target fidelity of programmable linear circuit, number of circuit layers, the sensitivity of a camera, phase stability of the setup. Place an order of the essential equipment, e.g., a pump laser, spatial light modulator, camera, nonlinear crystals, and optical components.
2. Advertise a position for a research assistant.
3. Develop integrated programming codes for interfacing and controlling the optical circuit and finalize the optical design.
4. Construct the optical learning machine from a cascade of the OPA process and the randomization-based programmable linear circuit [Goal2022].
    - Characterize and calibrate the functionalities of each circuit layer including the stability of the pump laser, the phase matching condition of OPA, the properties

of signal and idler beams, and the fidelity and programmability of linear circuits for pump, signal, and idler beams.
    - Inspect the properties of the entire optical circuit, e.g., synchronization, phase stability, misalignments, mode matching, aberrations, and loss.
5. Conduct the proof-of-principle experiment to study the effect of the cascade OPAs on the enhancement of phase sensitivity.
6. Analyze the experimental result.
7. Visit my collaborators in Europe for a month to discuss theoretical ideas and a detection scheme and attend a conference or a workshop on a topic related to quantum machine learning.
8. Hire a research assistant or graduate student who has or wants to develop skills in quantum nonlinear optics, optical engineering, data science, and statistical learning theory for a 1-year job contract.
9. Design and study an efficient encoding technique for embedding a classical dataset and weight parameters onto the generated quantum states.
10. Perform the experiment to investigate the learning capacity and trainability using the statistical learning theory.
11. Demonstrate a classification task using the developed circuit with different datasets and sizes.
12. Demonstrate time series analysis and forecasting.
13. Analyze the experimental results and estimate the performance of the developed optical machine.
14. Prepare the manuscripts for publication.

Work Plan	Month											
	2	4	6	8	10	12	14	16	18	20	22	24
1												
2												
3												
4												
5												
6												
7												
8												
9												
10												
11												
12												
13												
14												

Outcomes

1. Underlying physics of the programable cascade of optical parametric amplification.
2. Understanding the learning capability and trainability of the optical machine.
3. The optical machine that has the capability for high-performance computing
4. Training one research assistant and a few students
5. At least two publications

Impact

The research project holds the potential to have an impact on various aspects of information processing and artificial intelligence. If successful, the proposed investigation could lead to several significant advancements. It could contribute to our broader scientific understanding of quantum phenomena, that occurred in the cascade of multimodal optical parametric amplifications, interspersed with a programmable linear optical circuit. This control of amplifications and quantum correlation over multiple optical modes allows us to engineer a quantum state, particularly for sensing applications. For instance, it facilitates quantum-enhanced widefield imaging and a generation of high-dimensional multipartite entangled states for multiple observers.

We anticipate that the phenomena can be exploited for optical computing, the findings may put forwards the understanding of a quantum resource used in computing and the role of quantum measurements, i.e., the interface of the hybrid quantum(optic)/classical(electronic) information encoding. If true, the practical utility of the proposed optical machine in large-scale real-world data classifications and predictions could have far-reaching implications. Furthermore, the independence of the optical machine from intricate fabrication processes and specific designs of optical components presents an attractive feature for practical applications. This simplicity in implementation could lead to more accessible deployment of optical computing technologies.

Overall, the impact of the research proposal could lead to significant advancements in optical computing, quantum-enhanced technologies, and artificial intelligence, paving the way for a more energy-efficient approach to large-scale information processing in the modern era.

References

Amin, M. H., Andriyash, E., Rolfe, J., Kulchytskyy, B., & Melko, R. (2018). *Quantum Boltzmann Machine*. *Physical Review X*, **8**(2), 021050.

Cao, H. and Eliezer, Y., (2022). Harnessing disorder for photonic device applications. *Applied Physics Reviews*, **9**(1), p.011309.

Cartlidge, E. (January 2023) Optics & Photonics News - Photonic Computing for Sale. p.26-33.

Cerezo, M., Arrasmith, A., Babbush, R., Benjamin, S. C., Endo, S., Fujii, K., McClean, J. R., Mitarai, K., Yuan, X., Cincio, L., & Coles, P. J. (2021). Variational quantum algorithms. *Nature Reviews Physics*, **3**(9), 625–644.

Farhat, N. H., Psaltis, D., Prata, A., & Paek, E. (1985). Optical implementation of the Hopfield model. *Applied Optics*, **24**(10), 1469.

Feldmann, J., Youngblood, N., Karpov, M., Gehring, H., Li, X., Stappers, M., Gallo, M. L., Fu, X., Lukashchuk, A., Raja, A. S., Liu, J., Wright, C. D., Sebastian, A., Kippenberg, T. J., Pernice, W. H. P., & Bhaskaran, H. (2021). Parallel convolutional processing using an integrated photonic tensor core. *Nature*, **589**(7840), 52–58.

Frascella, G., Mikhailov, E. E., Takanashi, N., Zakharov, R. V., Tikhonova, O. V., & Chekhova, M. V. (2019). Wide-field SU(1,1) interferometer. *Optica*, **6**(9), 1233.

Goel, S., Leedumrongwatthanakun, S., Valencia, N. H., McCutcheon, W., Conti, C., Pinkse, P. W. H., & Malik, M. (2022). Inverse-design of high-dimensional quantum optical circuits in a complex medium. arXiv:2204.00578.

Goel, S., Tyler, M., Zhu, F., Leedumrongwatthanakun, S., Malik, M., & Leach, J. (2023). Simultaneously Sorting Overlapping Quantum States of Light. *Physical Review Letters*, **130**(14), 143602.

Hamerly, R., Bernstein, L., Sludds, A., Soljačić, M., & Englund, D. (2019). Large-Scale Optical Neural Networks Based on Photoelectric Multiplication. *Physical Review X*, **9**(2), 021032

Hughes, T. W., Minkov, M., Shi, Y., & Fan, S. (2018). Training of photonic neural networks through in situ backpropagation and gradient measurement. *Optica*, **5**(7), 864.

Leedumrongwatthanakun, S., Innocenti, L., Defienne, H., Juffmann, T., Ferraro, A., Paternostro, M., & Gigan, S. (2020). Programmable linear quantum networks with a multimode fibre. *Nature Photonics*, **14**(3), 139–142.

Lin, X., Rivenson, Y., Yardimci, N. T., Veli, M., Luo, Y., Jarrahi, M., & Ozcan, A. (2018). All-optical machine learning using diffractive deep neural networks. *Science*, **361**(6406), 1004–1008.

Marković, D., Mizrahi, A., Querlioz, D., & Grollier, J. (2020). Physics for neuromorphic computing. *Nature Reviews Physics*, **2**(9), 499–510.

Mitarai, K., Negoro, M., Kitagawa, M., & Fujii, K. (2018). Quantum circuit learning. *Physical Review A*, **98**(3), 032309.

Rafayelyan, M., Dong, J., Tan, Y., Krzakala, F. and Gigan, S., (2020). Large-scale optical reservoir computing for spatiotemporal chaotic systems prediction. *Physical Review X*, **10**(4), p.041037.

Schuld, M., & Killoran, N. (2022). Is Quantum Advantage the Right Goal for Quantum Machine Learning? *PRX Quantum*, **3**(3), 030101.

Shastri, B.J., Tait, A.N., Ferreira de Lima, T., Pernice, W.H., Bhaskaran, H., Wright, C.D. and Prucnal, P.R., (2021). Photonics for artificial intelligence and neuromorphic computing. *Nature Photonics*, **15**(2), pp.102-114.

Shen, Y., Harris, N. C., Skirlo, S., Prabhu, M., Baehr-Jones, T., Hochberg, M., Sun, X., Zhao, S., Larochelle, H., Englund, D., & Soljačić, M. (2017). Deep learning with coherent nanophotonic circuits. *Nature Photonics*, **11**(7), 441–446.

Steinbrecher, G. R., Olson, J. P., Englund, D., & Carolan, J. (2019). Quantum optical neural networks. *Npj Quantum Information*, **5**(1), 1–9.

Teğin, U., Yildirim, M., Oğuz, İ., Moser, C., & Psaltis, D. (2021). Scalable optical learning operator. *Nature Computational Science*, **1**(8), 542–549.

Wang, T., Ma, S.-Y., Wright, L. G., Onodera, T., Richard, B. C., & McMahon, P. L. (2022). An optical neural network using less than 1 photon per multiplication. *Nature Communications*, **13**(1), 123.

Wang, T., Sohoni, M. M., Wright, L. G., Stein, M. M., Ma, S.-Y., Onodera, T., Anderson, M. G., & McMahon, P. L. (2023). Image sensing with multilayer nonlinear optical neural networks. *Nature Photonics*, **17**(5), 408–415.

Wetzstein, G., Ozcan, A., Gigan, S., Fan, S., Englund, D., Soljačić, M., Denz, C., Miller, D. A. B., & Psaltis, D. (2020). Inference in artificial intelligence with deep optics and photonics. *Nature*, **588**(7836), 39–47.

Xia, F., Kim, K., Eliezer, Y., Shaughnessy, L., Gigan, S., & Cao, H. (2023). Deep Learning with Passive Optical Nonlinear Mapping. arXiv: 2307.08558.

Xu, X., Tan, M., Corcoran, B., Wu, J., Boes, A., Nguyen, T. G., Chu, S. T., Little, B. E., Hicks, D. G., Morandotti, R., Mitchell, A., & Moss, D. J. (2020). 11 TOPS photonic convolutional accelerator for optical neural networks. *Nature*, **589**(7840), 44–51.

Yildirim, M., Dinc, N. U., Oğuz, I., Psaltis, D., & Moser, C. (2023). Nonlinear Processing with Linear Optics. arXiv: 2307.08533.

Yurke, B., McCall, S. L., & Klauder, J. R. (1986). SU(2) and SU(1,1) interferometers. *Physical Review A*, **33**(6), 4033–4054.

Executive Summary (Category: Information, Period of project: 2 years)

Title: Electrically driven lasers based on two-dimensional materials

Moore's law observes that computing power doubles every 1.5–2 years. This will soon end as we reach the physical limits of traditional computing, yet demand for increased information processing capacity is surging. Researchers are investigating new, atomically thin, 2D materials, which can be used to build very small and highly energy efficient devices.

In the past decade, significant progress has been made in the field of optically driven 2D lasers, with the first successful demonstration occurring in 2015. These lasers have the advantage of being able to operate at room temperature due to the large exciton binding energy. However, there are several challenges that need to be addressed. These include improving the environmental stability of these lasers, expanding their lasing capabilities to the near infrared range, and developing electrically driven devices for 2D lasers.

This proposal aims to fill aforementioned research gap in the field of 2D material photonics. The primary objective is to showcase the first-ever electrically driven laser using 2D materials. Achieving electrically driven semiconductors is crucial but quite challenging. The main hurdle lies in designing electrodes that can efficiently guide electrical current to the specific section of the optical cavity where population inversion occurs. Furthermore, the electrode design should minimize any degradation in the Q-factor. To address these challenges, the project will investigate optical cavity and electrode designs that have proven successful in semiconductor nanolasers.

The proposed optical cavity will be entirely made from 2D materials, where the 2D gain medium is sandwiched between wide-bandgap 2D materials. It is known that a 2D dielectric material, hBN, increase the optical stability of other 2D semiconducting materials due to reduced surface defects, which result in reduced inhomogeneous broadening. This will effectively address the issue of poor instability in 2D material lasers. Additionally, for the first time, this project will utilize GaSe and InSe as the gain materials. These 2D materials maintain a direct bandgap in their bulk form, enabling the design of active material layers with various thicknesses to maximise the confinement factor.

The project's desired outcomes involve gaining valuable research insights in the advancement of integrated photonic circuits based on 2D materials. Through this investigation, we aim to identify the most suitable 2D material for various 2D optical systems and determine whether 2D material lasers can surpass traditional on-chip lasers in performance. The successful demonstration of an electrically driven 2D laser would not only contribute to a prestigious journal publication but also facilitate the practical implementation of 2D materials in on-chip lasers. The applications of 2D material lasers span across various fields, including LiDAR, biosensors, AI, and data centres.

The principal investigator possesses a strong track record and expertise in both 2D materials photonics and semiconductor lasers, as evidenced by her first-authored lasing papers and extensive work with various 2D materials. Her previous research experience at Prof. Yong-Hee Lee's group at KAIST, where they developed the first electrically driven photonic crystal laser, further strengthens her capabilities.

The project is highly relevant and timely, given the emerging field of 2D light sources, evident from the increasing number of publications in this area. A successful application would not only ensure the project's completion but also contribute significantly to the advancement of 2D material photonics. Securing funding for this research topic is critical as this topic currently has no external financial support. If successful, this funding opportunity will be the first external funding for the Principal Investigator, Dr Kim. Additionally, the PI's department has played a vital role in supporting Dr. Kim in establishing her research lab, which is equipped with a comprehensive micro-PL setup featuring various functionalities such as lifetime measurement and photon correlation measurement. The successful completion of this project will realise ultrafast, energy efficient lasers that will be critical for next generation optical computing technology.

Title: Electrically driven lasers based on two-dimensional materials

1. Background

Moore's law, an observation that states the number of transistors on a single chip doubles every two years, has been a key driving force behind the rapid advancement of electronics over the past few decades. However, with the size of transistors approaching its limits, it has become increasingly difficult to continue shrinking their size. Photonics provides an alternative solution to this challenge by using light instead of electrons to transmit information. By leveraging the unique properties of light, photonics can offer higher data transfer rates, lower energy consumption, and greater computational power, paving the way for a new era of high-speed, low-power computing. Now, researchers are exploring the use of new materials and manufacturing techniques to develop superior photonic devices.

Two-dimensional (2D) materials have taken a central role in contemporary research and recent technological development. Because of their exceptional physical and chemical properties (Figure 1a), numerous areas have benefited from their rise, with potential applications in virtually all fields of electronics and photonics. Using 2D materials not only reduces the size of the device but also removes the major limitation that is posed to conventional materials: lattice matching requirement. The emerging opportunities in photonics using a such new class of materials are especially promising. 2D light-emitting materials cover a wide range of wavelengths from UV to mid-infrared, where the type of light sources includes LEDs, lasers and quantum light sources. Unique experiments such as stacking different 2D materials or controlling the angle between layers, provide additional degrees of freedom to engineer material properties.

This project aims to push the boundaries of integrated photonics by developing high-quality nanolasers using 2D materials. As one of the essential building blocks of optical components in integrated photonic circuits, nanolasers hold immense promise for a wide range of applications in fields such as communications, sensing, and imaging. While traditional nanolasers were created using semiconductor quantum well, recent advances have shown that 2D materials can serve as a viable gain medium for lasers. Despite this, the integration of 2D materials into foreign optical cavities has presented a formidable obstacle, often resulting in degraded performance. Furthermore, the lack of demonstrated electrically driven 2D lasers has prevented the practical application.

To address these challenges, this project proposes to develop an all-2D material platform that will unlock the full potential of integrated 2D material devices (Figure 1b and 1c). The project will extend the goal to achieve the first electrically driven 2D laser.

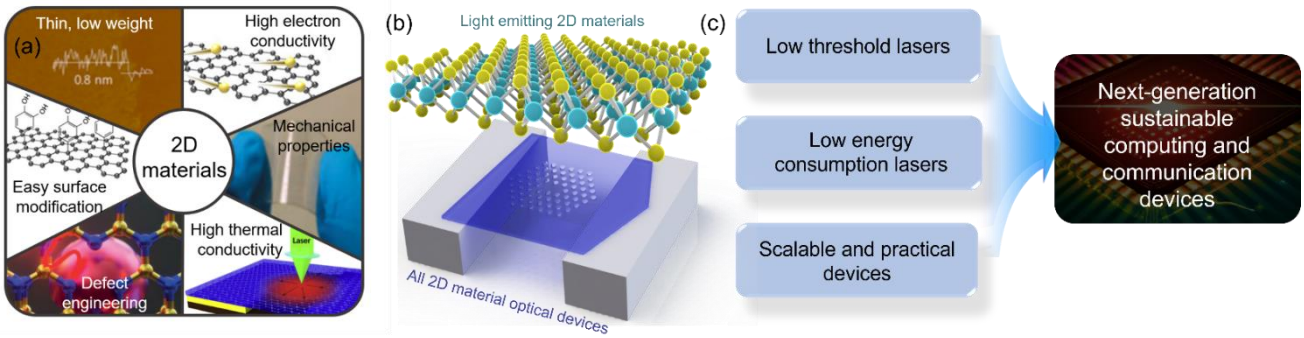

Figure 1 (a) Various advantages of using 2D materials for nanophotonics. (b) Integrating 2D light emitting materials into all-2D material optical systems to produce (c) low-threshold, low energy consumption lasers that are scalable for next-generation devices.

2. Literature review

• **The necessity of small lasers**. The progress of electronics has been primarily fuelled by the reduction in transistor size, and similarly, in integrated optical technology, minimizing optical components plays a vital role. Lasers, being a fundamental element of optical devices, necessitates the development of small lasers, which enable energy-efficient, ultrafast computing devices. Prospect applications of photonic integrated circuits (PICs) with laser sources includes LiDAR, biosensor, AI and data centre.[1]

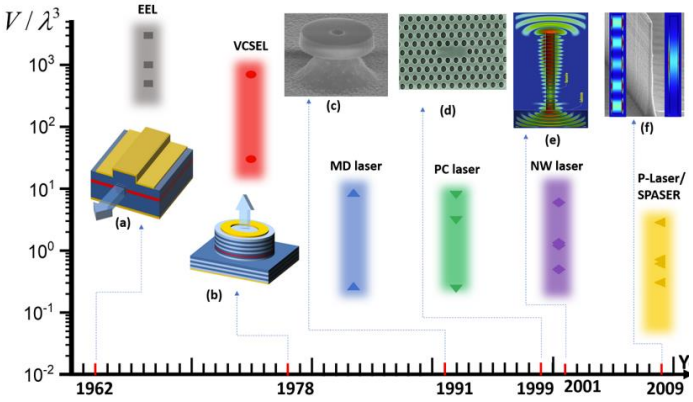

Figure 2. Device volume for several types of semiconductor lasers: edge emitting lasers (EEL), microdisk (MD), plasmonic lasers (P-Laser). Coloured bars indicate the ranges of values found in the literature.[2]

The size of the semiconductor has been reduced over five decades since the first demonstration of semiconductor lasers (Figure 2a).[2] Especially, advancement of fabrication technology, *i.e.*, electron beam lithography, allowed sophisticated fabrication of photonic crystal lasers and plasmonic lasers.

• **Important parameters for small lasers.** An efficient small laser should preferably consider all three factors: small device footprint, small active region, and large confinement factor.[2] As the active region gets smaller, optical cavity design to maximise the confinement factor is critical. The quality factor (Q factor) and spontaneous emission factor (β factor) are crucial parameters employed to assess the performance of lasers. A high Q factor ensures that photons remain within the laser cavity for a long time. Nanostructures have successfully achieved photon confinement through various methods such as total internal reflection, Fabri-Perot resonators, and photonic crystal bandgaps. The higher β factor enable an ultralow-threshold or threshold laser.

• **Ideal on-chip sources.** In general, ideal on-chip sources should satisfy the following criteria.[1] (1) The laser should be electrically powered. (2) The laser should operate with minimal energy consumption, having a low threshold and providing sufficient output power. (3) It is preferable for the laser to operate at a wavelength within the Telecom-wavelength bands, enabling seamless integration with fibre-optic networks. (4) The laser fabrication should not only be CMOS-compatible but also enable seamless integration onto the silicon platform.

• **Successful demonstration of 2D material lasers.** 2D materials provide feasible solution for the miniaturisation of small lasers. They also provide excellent optical properties such as high emission through small material volumes. Photoluminescence of 2D materials can be easily manipulated through a variety of ways, including strain engineering[3], chemical treatments and thickness adjustments[4].

After the 2010 Nobel Prize was awarded for the discovery and characterisation of graphene, there was a profound expectation of achieving the lasing experiment with 2D materials as a laser gain medium. The first report, using WSe_2 as a gain medium and gallium phosphide as a cavity material, was published in Nature in 2015,[5] and several papers have followed. So far, 2D material lasers have been demonstrated utilising the gain medium and cavity systems listed below: WS_2 with Si_3N_4 microdisk[6], MoS_2 with SiO_2 microdisk[7], and WS_2 itself as both gain and cavity medium[8].

3. Problem statement

Electrically driven lasers are critical for the device to practically implemented for the optoelectronic applications. Although optically pumped 2D material lasers are demonstrated, electrically driven 2D material lasers have not been demonstrated yet. This goal has been challenging for the entire photonics field, even for conventional materials, with the main difficulty lying in designing and fabricating electrodes for high-Q photonic cavities. Specifically, introducing electrodes degrades the Q-factor of photonic cavities, and so only a limited number of papers have been published on this topic.

This project aims to achieve the first electrically driven 2D material lasers. The project will create microdisk lasers that utilise a layer or layers of 2D semiconducting material sandwiched between 2D dielectric materials. These microdisk lasers will feature a top electrode made of graphene and a bottom electrode in the form of a micro post positioned at the centre of the disk. The project will also develop entirely 2D material-based lasers, wherein both the gain medium and the passive cavities will be fabricated using 2D materials exclusively. By successfully achieving these goals, this project will create low-threshold, energy efficient nanolasers for future integrated photonic circuits.

4. Objectives

• Objective 1. Finding the best wide bandgap 2D materials for passive optical devices. The effect of hexagonal boron nitride (hBN) as a substrate for some transition metal dichalcogenides (TMDs) has been studied recently. We will expand the material search and test wide bandgap materials, such as Mica and MoO_3. For light-emitting 2D materials we will investigate a wide range of materials, including InSe for near-IR and GaSe for near-UV.

• Objective 2. Demonstrating high-quality 2D material lasers. We will create lasers that are entirely made of 2D materials. A mono- or a few layered 2D materials will be encapsulated by 2D dielectric materials to demonstrate high-quality lasers, *i.e.*, low-threshold lasers.

• Objective 3. Achieving electrically driven 2D material lasers. The electrode contacts will be created to inject a current into the lasers to achieve electrically driven 2D material lasers. A cavity with electrodes that can sustain a high Q-factor will be carefully designed.

5. Capability and Feasibility

The main tasks of the proposed project focus on the advanced photonic functionalities of 2D materials in an integrated 2D platform, particularly the demonstration of low-threshold lasing and electrically driven 2D lasers. To achieve these aims, the device design, fabrication, experimental procedure, and data analysis are all essential. The investigator has strong track record and expertise in both 2D materials photonics and semiconductor lasers. Dr Kim published multiple lasing papers as a first author, showing her hands-on expertise in this research domain. Furthermore, she worked with various 2D materials in the last six years and has already produced multiple papers on photonic devices made of wide bandgap 2D materials.

Dr Kim also comes with knowhows in electrically driven lasers from her previous PhD study at Prof. Yong-Hee Lee's group at KAIST, Korea. Prof. Lee's research group has achieved a significant breakthrough by developing the first electrically driven photonic crystal laser, as published in Science. Furthermore, the project will also benefit from the expertise of existing collaborators, such as Dr Kwang-Yong Jeong, who has previously demonstrated the first electrically driven one-dimensional photonic crystal lasers. Additionally, Dr Su-Hyun Gong, known for their recent demonstration of an indirect bandgap laser, will also contribute valuable insights as a collaborator. Leveraging these collaborations, the chief investigator will bring a wealth of expertise and knowledge to the project, significantly bolstering its feasibility and chances of success.

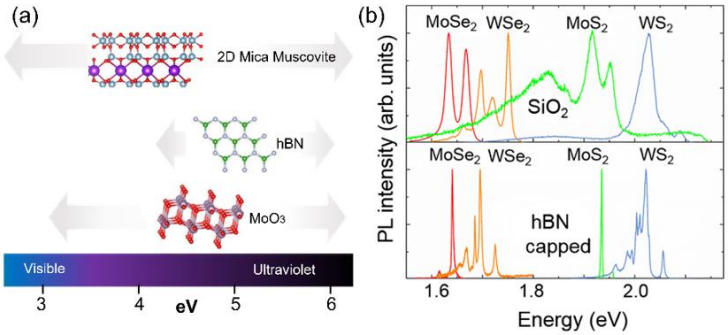

Figure 3. (a) Wide bandgap 2D materials. This image has been modified, and adopted.[3] (b) PL spectra for various light emitting 2D materials when directly placed on SiO_2 (Top) versus capped by hBN. Task 1 aims to observe the linewidth narrowing effect using various wide bandgap 2D materials.

6. Work Plan

Task 1. Test wide bandgap 2D materials. 2D materials with wide energy bandgap are ideal for passive optical components which require low absorption. The top three 2D materials that have wide bandgap are 2D mica, MoO_3 and hBN as shown in Figure 3a. More recent study reported that hBN enhance the optical quality of other TMDs material.[9] Figure 3b shows reduced linewidth when TMDs are encapsulated with hBN. This is due to reduced surface defects, which result in reduced inhomogeneous broadening. This task will test other promising 2D materials, mica and MoO_3 and measure linewidth change at both room temperature and cryogenic temperature.

Task 2. Develop fabrication protocols for wide bandgap 2D materials. 2D materials are rarely used for monolithic photonic devices, indeed, the first photonic components from 2D material were reported by Dr Kim in 2018. Therefore, this task builds directly upon Dr Kim's studies covering the fabrication of free-standing photonic nanostructures from hBN. This task will focus on optimising the drying etching process of hBN (mica, MoO_3 depending on the result from Task 1) utilising inductively coupled plasma reactive ion etching (ICP-RIE).

Task 3 Hybrid all-2D material cavities and lasing. This task will focus on integrating light-emitting 2D materials in-between two wide-bandgap 2D materials (each with ~ 100 nm thickness) using a stamp transfer setup. Furthermore, the integration of a light-emitting 2D material encapsulated within high-quality, wide-bandgap 2D materials diminishes detrimental interactions of the material with the substrate, and a significant increase in the quantum yield and linewidth reduction can then be observed. Therefore, by improving the surrounding environment, the excitonic light emission improves, which implies that the lasing threshold is pushed towards lower limits. This enables us to observe low-threshold lasers within 2D materials. To confirm lasing operation of our device, we will demonstrate the following properties, (i) linewidth narrowing of the mode, (ii) polarised emission, (iii) input vs. output power measurement, and (iv) second-order intensity correlation measurement.

Task 4 Electrically driven lasing of integrated 2D TMDs. The complexity of this task is given by the nanoscale arrangement and integration of the electronic supply to drive the emission of the material electrically. To be more detailed, we plan to test two geometries: first, stacking two different TMD materials, which feature intrinsic p- or n-type properties. By overlapping these materials, the recombination will be akin to an interlayer exciton recombination, where an electron of the n-type and a hole of the p-type material recombine. Such recombination has also been shown to be driven electronically in a p-n junction. Second, we will test the TMDs/hBN laser with top Graphene electrode. These hetero stacks could be assembled by means of a pick and place technique.

7. Novelty of this work

The project encompasses two novel approaches aimed at creating low-threshold lasers. The first novely lies in the utilisation of a special 2D material as the gain medium. Previous works were limited to using TMDs, such as WS_2 and WSe_2, which only work as effective light emitting materials when their thickness approaches that of a monolayer. This limitation hampers the confinement factor since the active layer's thickness is much smaller than the effective

wavelength (λ/n). To overcome this constraint, the project will employ 2D materials such as GaSe and InSe, which possess a direct bandgap even in bulk form. This characteristic allows for greater flexibility in cavity design by accommodating active layer thicknesses of varying sizes. The second novelty revolves around the use of hexagonal boron nitride (hBN) as a passive cavity, a concept yet to be explored in the context of 2D material lasers. Introducing hBN as a passive cavity element presents an innovative approach to enhancing laser performance. By incorporating these two novel approaches, the project significantly increases the likelihood of successfully demonstrating electrically driven lasers with the lowest possible thresholds.

8. Outcomes

This project will answer multiple research questions that will provide valuable insights into the development of 2D material-based integrated photonic circuits. While hBN has gained popularity as a substrate for other 2D materials including graphene and TMDs, other wide bandgap materials like Mica and MoO_3 are rarely investigated. We will investigate these materials as potential passive optical devices such as photonic waveguides and resonators. This investigation will help us to determine the best 2D material for all 2D optical systems. The next research question we will address is whether 2D material lasers can outperform classical on-chip lasers. Currently, there are only a limited number of papers reporting lasing action using 2D materials. The outcomes of this project have the potential for publication in high-impact journals.

The outcomes of this project have the potential to deliver substantial benefits in three ways. First, the project will help advance nanotechnology and related industries. Second, the project will create valuable know-how and patents. This project will offer excellent training opportunities in an emerging research field and future industries.

9. Impact

This project will resolve one of the main criticisms being directed at this field: None of the lasing papers published so far has satisfied all the conditions for lasing from direct bandgap emission.[10] In this project, the lasing operation will be confirmed by measuring intensity correlation, along with other essential measurements, including input vs. output intensity and input power vs. linewidth. Additionally, this project aims to achieve one of the long-sought-after goals in the field, an electrically driven 2D materials laser. So far, all 2D lasers have been only optically pumped, and there has been a race to achieve an electrically driven device operation. The successful demonstration of electrically driven 2D material lasers will mark a significant milestone with practical implications.

References

1 Yang, J., Tang, M., Chen, S. & Liu, H. From past to future: on-chip laser sources for photonic integrated circuits. *Light: Science & Applications* **12**, 16 (2023).

2 Ning, C.-Z. Semiconductor nanolasers and the size-energy-efficiency challenge: a review. *Advanced Photonics* **1**, 014002-014002 (2019).

3 Chaves, A. *et al.* Bandgap engineering of two-dimensional semiconductor materials. *npj 2D Materials and Applications* **4**, 29 (2020).

4 Kim, H.-C. *et al.* Engineering optical and electronic properties of WS2 by varying the number of layers. *ACS nano* **9**, 6854-6860 (2015).

5 Wu, S. *et al.* Monolayer semiconductor nanocavity lasers with ultralow thresholds. *nature* **520**, 69-72 (2015).

6 Ye, Y. *et al.* Monolayer excitonic laser. *Nature Photonics* **9**, 733-737 (2015).

7 Salehzadeh, O., Djavid, M., Tran, N. H., Shih, I. & Mi, Z. Optically pumped two-dimensional MoS2 lasers operating at room-temperature. *Nano letters* **15**, 5302-5306 (2015).

8 Sung, J. *et al.* Room-temperature continuous-wave indirect-bandgap transition lasing in an ultra-thin WS2 disk. *Nature Photonics* **16**, 792-797 (2022).

9 Cadiz, F. *et al.* Excitonic linewidth approaching the homogeneous limit in MoS 2-based van der Waals heterostructures. *Physical Review X* **7**, 021026 (2017).

10 Reeves, L., Wang, Y. & Krauss, T. F. 2D material microcavity light emitters: to lase or not to lase? *Advanced Optical Materials* **6**, 1800272 (2018).

Proposal title: Miniature extreme-ultraviolet light sources
Category: Health
Sub-category: Advancing biomedical imaging.

This project aims to develop new light sources with ultra-short wavelengths for next-gen optical diagnostics. The project aims to develop novel approaches to generate high harmonics – source of light in vacuum-ultraviolet and extreme-ultraviolet ranges. Currently, such sources are large and expensive. But recent research suggests practical all-solid-state sources are feasible to develop with the concepts of nanostructured solids. The project intends to develop theory and computation, nanofabrication, and experimental characterisation. Short-term outcomes include demonstrations of vacuum- and extreme-ultraviolet imaging that employs all-solid-state nanoscale sources of high harmonics. Long-term outcomes will be the development of new diagnostics techniques for medical imaging.

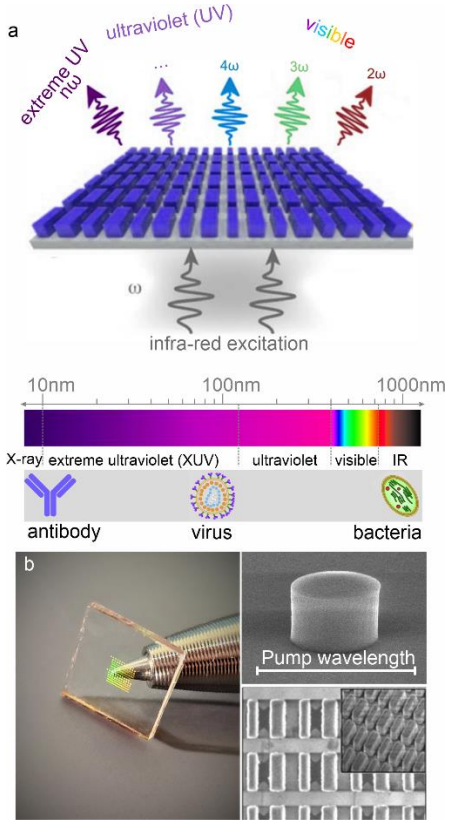

Figure 1. (a) Concept image of a nanostructure generating high harmonics – multiples of the incident frequency of light (top) and the scale of anticipated harmonics wavelength (bottom). (b) Examples of my preliminary nanostructures for harmonics generation [Sci Adv 9, eadg2655 (2023); Zograf, G. et al. ACS Photonics 9, 567–574 (2022)]

The project will facilitate the development of new technology capable of observing tiniest objects in living mater such as individual viruses and organelles inside cells. This will open up new insights into how cells sense, move and self-organize in context to tissue injury, pathogen invasion and cancer metastasis.

High-resolution biological imaging of such small objects is impossible with conventional optical microscopy due to Abbe diffraction limit. Typically, direct observations are done with electron microscopy (EM; TEM or SEM). However, electron microscopes impose substantial limitations: they cannot be used for imaging live cells, require sample fixation and freezing, and they continuously degrade sample during the observation. EMs are large and costly initially and in service and cannot be portable. Another currently available technology is confocal optical microscopy of fluorescent labels attached to sub-cell objects. It is more practical and faster, also being more biologically compatible. However, due to the resolution limitations they yield much less structural information. HHG-based imaging proposed here is poised to occupy the currently unexploited niche between the EMs and confocal microscopy. The EM market is valued at ~AUD 6 billion [Allied Market Research, Report A16756, p204] with a quarter of the market being driven by life and medical science. Confocal microscopy market is valued at ~AUD 1.5 billion, and it is dominated by life science.

The project is at the confluence of nanophotonics with medical imaging, and the research will be supported by a collaboration with the School of Medical Research at the Australian National University.

MINIATURE EXTREME-ULTRAVIOLET LIGHT SOURCES

LITERATURE REVIEW

Innovative engineering of optical materials at the nanoscale has led to breakthroughs in the fabrication of optical components. Nanoscale optical resonators in their two-dimensional layouts, known as metasurfaces, have progressed from fundamental concepts[1] to mass-fabricated consumer products[2]. My past research has demonstrated that multifunctional optical metasurfaces hundreds of times thinner than a human hair can match the performance, and even outperform, conventional bulky optics in the areas of holography[3], optical fibre communications[4] and quantum cryptography[5]. The physics behind interactions of light with optically active materials depends on the intensity of light. It can be divided into several categories: linear optics (low-intensity light), perturbative nonlinear optics (moderately high intensities) and nonperturbative nonlinear optics (high intensities).

Linear optics of nanostructures and metasurfaces has already resulted in a new generation of optical components[1-5].

Perturbative nonlinear optics has seen extensive developments including my own research[6,7] as I overviewed recently[8], and the focus is shifting from fundamental towards applied research.

Nonperturbative nonlinear optics at the nanoscale is a new direction of research underpinned by a phenomenon of high harmonics generation with promising applications in novel extreme-UV light sources. My group is among the first contributors to HHG in nanostructured solids[9]. This area is recognized by Optica as emerging and strategically important as evidenced by the organized *Optica Incubator on On-Chip High-Field Nanophotonics* (2022, Washington DC, USA) in which I was an invited participant. Current international efforts are focused on applications in semiconductor industry and in nanofabrication[10]. I propose to steer the field towards a conceptually new range of applications in medical imaging to address global health challenges.

My progress in this direction to date includes refs.[9,14,15] (see also Fig. 1b,c). My overview of the subject: Ref [8]. International progress on HHG in nanostructures includes Refs [11,16,17].

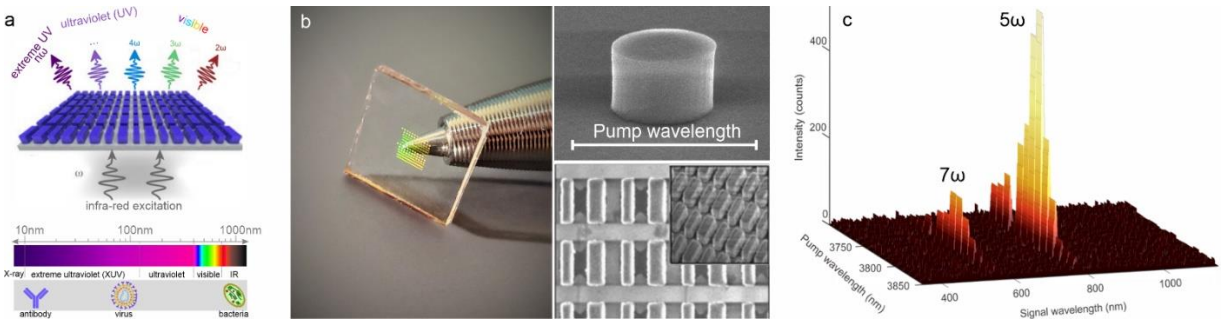

Figure 1. (a) Concept image of a nanostructure generating high harmonics – multiples of the incident frequency of light (top) and the scale of anticipated harmonics wavelength (bottom). (b) Examples of nanostructures for harmonics generation fabricated by my team[9,15]. (c) My recent proof-of-concept observation of up to 7th harmonic from a single nanoresonator[9]. My broad-audience description of this line of research: ref. [22].

PROBLEM STATEMENT

The project aims to deliver compact all-solid-state sources of extreme-UV light.

Short-wavelength extreme-UV sources are of a great practical interest for life science as they enable high-resolution medical imaging down to direct observations of objects much smaller than regular cells (such as intracellular molecular structures with sub-100 nm sizes and individual viruses). Such short-wavelength sources do not exist in nature, and presently available engineered sources (synchrotrons, free electron lasers, discharge plasma, gas-phase HHG – see Fig. 2) find limited applications due to their size and cost. Nanostructured solids generating HHG offer an opportunity to miniaturise sources of extreme-UV and to reduce the cost of such sources.

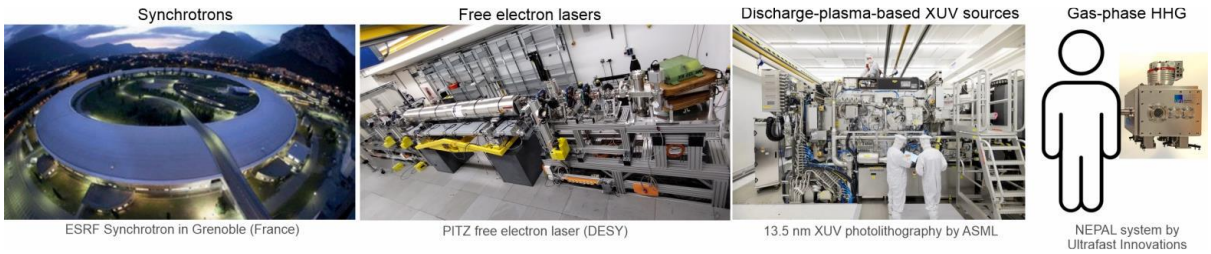

Figure 2. Examples of systems emitting light in the extreme-UV spectral region. Contemporary XUV sources are large and expensive.

OBJECTIVES

Objective 1 (new knowledge) To pursuit a new frontier of contemporary optics: *nonperturbative nonlinear optics* at the nanoscale. This is a new and rapidly growing area of research, and my recent results[9] are among the pioneering contributions to the field. The focus of the research will be on high harmonics generation (see Figure 1a).

Objective 2 (applied research). To achieve generation of high harmonics from nanostructured solids in the extreme-ultraviolet part of spectrum with average intensity of micro-Watts. The research aims to develop new sources of light in the extreme-UV spectral range. All-solid-state sources of HHG represent a practical pathway towards a wide adoption of extreme-UV light. While bulk solids are unsuitable for extreme-UV light generation due to material absorption, ultra-thin nanostructured solids mitigate this problem. Short wavelength of such sources should increase resolution of optical microscopy and metrology.

Objective 3 (contribution to strategic priority in health). **To deliver first proof-of-concept demonstration of biological/medical imaging of living matter using the developed short-wavelength source of light.** First proof-of-concept demonstrations of medical imaging are anticipated within the project lifetime in collaboration with medical researchers at the John Curtin School of Medical Research, the Australian National University. Strategic importance of this collaboration was recognized and supported recently by the Australian National University MEC grant. Trials of the new light sources for medical imaging will allow to assess the scope of applications of the new technology.

WORK PLAN

The project will be based on four main pillars: theoretical calculations, nanofabrication, optical diagnostics of the fabricated sources, and their use in medical imaging.

Theory: computational physics in this research will go beyond the conventions of perturbative nonlinear optics and will include such effects as generation of electron plasma via multiphoton absorption and tunnelling. Supercomputer simulations based on quantum-mechanics of electron dynamics at the nanoscale[19] will be applied.

Nanofabrication: the project will develop novel fabrication protocols for materials that feature (i) wide bandgaps and (ii) high refractive indices. Such materials (HfO_2, Ta_2O_5 and AlN_x) are unconventional in nanophotonics.
Optical diagnostics. Nanophotonics research will be established in the ultraviolet spectral ranges and will merge with strong-field laser physics. Experiments will be carried out in ambient and nitrogen atmosphere as well as in vacuum.
Medical imaging. The new light sources will be utilized for the extreme-UV imaging of living matter at sub-cellular level. Most practically important objects to study will be identified collaboratively with the School of Medical Research.

OUTLINE OF TASKS
Task 1. To design nanostructured solids that support high-quality factor resonances in the regime of excitation with strong optical fields (in the regime when the incident beam of light changes material properties and thus resonant response to such an extent that linear and perturbative nonlinear calculations fail to predict experimental observations)

I will conduct theoretical and experimental studies of the three types of resonant nanostructures: supporting Mie modes, Fano resonances and resonances associated with the bound states in the continuum. I will incorporate into the design of such structures information about spatially and temporary inhomogeneous electron-hole density distribution generated in the nonperturbative nonlinear regime alongside both direct and cascaded perturbative responses. This research will rely partially on first principle supercomputer simulations to account for the response of the material on the atomic level in the nonperturbative regime.

Task 2. To identify the most promising material platforms for the extreme-UV light sources considering both nonlinear material properties and the current status of development of nanofabrication technologies.

I will experimentally test several material platforms, some of which are not conventional for contemporary nanophotonics. Their nonlinear material properties remain largely unknown and will need to be characterised experimentally during the project. Nanofabrication protocols for such materials remain immature and they will need to be developed during the project. Materials that will be explored include wide-bandgap dielectrics: hafnia, tantala, gallium phosphite and aluminium nitride.

Task 3. To establish approaches to control parameters of extreme-UV beams at the generation stage (wavefront, polarisation, orbital angular momentum).

Nanostructured arrays of resonators – metasurfaces – open-up an untapped potential to tailor beams of light by shaping individual nanoresonators. Nonlinear metasurfaces allow us to incorporate functionalities of optical components directly into the generation of optical harmonics[8]. Ability of metasurfaces to arbitrarily structure optical beams during their generation process is of particular practical interest for the extreme-UV spectral regions, where many optical components are either not available or expensive and more complicated to use. The ability to configure the output beam immediately at the generation stage gives another key advantage to the metasurface-based sources of extreme-UV over all other available sources. I plan to incorporate three different functionalities into the metasurfaces generating HHG which have practical importance for imaging: a lens (beam focusing), a vortex beam generator (phase singularity), and a vector beam generator (polarisation singularity).

Task 4. To design, fabricate and experimentally test nanostructured solids generating extreme-UV light with brightness sufficient for imaging applications.

HHG from nanostructured solids in comparison to its gas phase and plasma counterparts may rely on less excitation power thus requiring cheaper and more compact pump lasers. The combination of a nanoscale source with a comparatively small and inexpensive pump laser will significantly reduce the overall footprint and cost of such extreme-UV system in comparison to any presently available alternative. Indeed, a typical configuration for HHG in gases relies on nonlinear interactions in a capillary over a distance of millimetres**.** For plasma-based HHG systems, a centimetre-long interaction length is typical. In a striking contrast, a typical length (the material thickness) over which nonlinear interactions take place in solids would be of the order of 100 nm -1 μm. The length of the interaction distance dictates the depth of focus and hence the beam waist of the pump laser. Thus, a smaller length allows for tighter focusing drastically reducing the requirements for output pump power for a required power density. The pump power requirements are further reduced for solids in comparison to gases and plasma thanks to their higher density. Finally, and most importantly, optical resonances incorporated into the nanoscale resonators and metasurfaces via careful design of their geometries will lead to multifold enhancement of the internal pump field confinement compared to the incident field. These factors enable extreme-UV generation with sufficient brightness in nanostructured solid in more compact and cheaper settings compared to gas- and plasma-phase counterparts.

Task 5. To deliver first proof-of-concept imaging results of sub-cellular objects obtained with the new light sources.

The project will facilitate the development of new technology capable of observing tiniest objects in living mater such as individual viruses and organelles inside cells. This will open up new insights into how cells sense, move and self-organize in context to tissue injury, pathogen invasion and cancer metastasis. First imaging will be demonstrated in collaboration with medical researchers at the Australian National University

IMPACT

The economic impact of compact and cheap extreme-UV sources can be significant. High-resolution biological imaging of objects much smaller than regular cells (such as intracellular molecular structures and viruses) is impossible with conventional optical microscopy due to the Abbe diffraction limit and relatively long wavelength of light from conventional sources. Typically, direct observation of such objects is achieved with electron microscopy. However, electron microscopes impose substantial limitations on the sample, cannot be used for imaging live cells or native molecules, require sample fixation and freezing and continuously degrade samples during observation. Electron microscopes are large, costly in purchase and service and are not portable. Optical microscopy, such as confocal microscopy of fluorescent labels attached to sub-cell objects are more practical and faster and biologically more compatible. However, due to the resolution limitation, they yield much less structural information. Extreme-UV-based imaging [23] is poised to occupy the currently unfilled niche between EMs and OMs. The EM market is valued at ~$6 billion [24], with a quarter of the market being driven by life sciences. The confocal microscopy market is valued at ~$1.5 billion [25], and it is dominated by life sciences. Compact all-solid-state sources of HHG proposed in this project may become central elements of extreme-UV based medical and biological imaging with a market share reaching similar values.

REFERENCES

[1] S. S. Kruk and Y. S. Kivshar, “Functional Meta-Optics and Nanophotonics Governed by Mie Resonances,” ACS Photonics, vol. 4, no. 11, pp. 2638–2649, Nov. 2017

[2] “What are Meta-Optics? - Metalenz.” https://metalenz.com/what-are-meta-optics/ (accessed Jul 4, 2023).

[3] L. Wang et al., “Grayscale Transparent Metasurface Holograms,” Optica, vol. 3, no. 12, pp. 1504–1505, 2016

[4] S. Kruk et al., “Transparent Dielectric Metasurfaces for Spatial Mode Multiplexing,” Laser & Photonics Review, vol. 12, no. 8, p. 1800031, Aug. 2018

[5] K. Wang et al., “Quantum Metasurface for Multiphoton Interference and State Reconstruction.,” Science, vol. 361, no. 6407, pp. 1104–1108, Sep. 2018

[6] S. Kruk et al., “Nonlinear Light Generation in Topological Nanostructures,” Nature Nanotechnology, vol. 14, pp. 126–130, Dec. 2019

[7] S. S. Kruk et al., “Asymmetric Parametric Generation of Images with Nonlinear Dielectric Metasurfaces,” Nature Photonics 2022 16:8, vol. 16, no. 8, pp. 561–565, Jun. 2022

[8] V. Zubyuk, L. Carletti, M. Shcherbakov, and S. Kruk, “Resonant Dielectric Metasurfaces in Strong Optical Fields,” APL Materials, vol. 9, no. 6, p. 060701, Jun. 2021

[9] A. Zalogina et al., “High-Harmonic Generation from a Subwavelength Dielectric Resonator,” Science Advances, vol. 9, no. 17, p. eadg2655, Apr. 2023

[10] S. D. C. Roscam Abbing et al., “Extreme-Ultraviolet Shaping and Imaging by High-Harmonic Generation from Nanostructured Silica,” Physical Review Letters, vol. 128, no. 22, p. 223902, Jun. 2022

[11] H. Liu et al., “Enhanced High-Harmonic Generation from an All-Dielectric Metasurface,” Nature Physics, vol. 14, no. 10, pp. 1006–1010, Oct. 01, 2018

[12] S. S. Kruk, W. Gao, D.-Y. Choi, T. Zentgraf, S. Zhang, and Y. Kivshar, “Nonlinear Imaging of Nanoscale Topological Corner States,” Nano Letters, vol. 21, no. 11, pp. 4592–4597, Jun. 2021

[13] P. R. Sharapova, S. S. Kruk, and A. S. Solntsev, “Nonlinear Dielectric Nanoresonators and Metasurfaces: Toward Efficient Generation of Entangled Photons,” Laser & Photonics Review, p. 2200408, Jan. 2023

[14] P. Tonkaev, K. Koshelev, M. A. Masharin, S. V Makarov, S. S. Kruk, and Y. Kivshar, “Observation of Enhanced Generation of a Fifth Harmonic from Halide Perovskite Nonlocal Metasurfaces,” ACS Photonics, vol. 10, no. 5, pp. 1367–1375, May 2023

[15] G. Zograf et al., “High-Harmonic Generation from Resonant Dielectric Metasurfaces Empowered by Bound States in the Continuum,” ACS Photonics, vol. 9, no. 2, pp. 567–574, Feb. 2022

[16] S. Han et al., “High-Harmonic Generation by Field Enhanced Femtosecond Pulses in Metal-Sapphire Nanostructure,” Nature Communications, vol. 7, Oct. 2016

[17] M. R. Shcherbakov et al., “Generation of Even and Odd High Harmonics in Resonant Metasurfaces using Single and Multiple Ultra-Intense Laser Pulses,” Nature Communications 2021 12:1, vol. 12, no. 1, pp. 1–6, Jul. 2021

[18] K. Koshelev et al., “Subwavelength Dielectric Resonators for Nonlinear Nanophotonics,” Science (1979), vol. 367, no. 6475, 2020

[19] “Introduction — SALMON software manual v.2.0.1 documentation.” https://salmontddft.jp/webmanual/v_2_0_1/html/introduction.html (accessed Jul 4, 2023).

[20] A. Zalogina, L. Wang, E. Melik-Gaykazyan, Y. Kivshar, I. Shadrivov, and S. Kruk, “Mid-Infrared Cylindrical Vector Beams Enabled by Dielectric Metasurfaces,” APL Materials, vol. 9, no. 12, p. 121113, Dec. 2021

[21] A. Tripathi et al., “Metasurface-Controlled Photonic Rashba Effect for Upconversion Photoluminescence,” Nano Letters, vol. 23, Mar. 2022

[22] “New nanoparticle source generates high-frequency light”, The Conversation https://theconversation.com/new-nanoparticle-source-generates-high-frequency-light-204618#:~:text=The%20nanoparticle%20absorbs%20energy%20from,harmonics%20of%20the%20emitted%20light. (accessed Jul 4, 2023)

[23] M. W. Zürch, Thesis “High-Resolution Extreme Ultraviolet Microscopy,” 2015, doi: 10.1007/978-3-319-12388-2.

[24] “Electron Microscopy Market Size, Share and Analysis | Forecast - 2031.” https://www.alliedmarketresearch.com/electron-microscopy-market-A16756

[25] “Confocal Microscope Market Analysis - Industry Report - Trends, Size & Share.” https://www.mordorintelligence.com/industry-reports/confocal-microscope-market

2023 Optica Foundation Challenge
Category: Health

Title: Combining Multispectral Imaging with Artificial Intelligence for Technology-driven Cancer Care

One of the major challenges in providing timely, holistic, and personalized care to the growing number of cancer patients around the world is our lack of understanding of how this disease develops, progresses, and alters the body's ecosystem. There are several molecular and physiological changes that together govern the course of the disease. Current clinical approaches rely on the physical changes in cells by investigating biopsy samples, whereas genetic tests rely on the average molecular expression of key biomarkers. None of these technologies captures the simultaneous alterations in the spatial-molecular profile of the disease and the surrounding microenvironment. This is crucial in individualized patient care rather than utilizing a one treatment fits all approach. The underlying mechanisms of the microenvironment (extracellular matrix + stromal cells + immune cells) drive tumor invasion and migratory patterns. We will address this need with a combination of artificial intelligence and multispectral imaging to investigate the structural, molecular, and biochemical signatures of cancer cells and the associated tumor microenvironment. Here, we will focus on breast cancer (the second leading cause of cancer deaths for women in the U.S.). However, this work can be extended to other types of cancers. The work is guided by two specific aims:

Aim 1. Integrating Artificial Intelligence with Multispectral Imaging for Disease Evaluation. Many high-resolution and multispectral tissue imaging technologies have been developed recently, powered by the recent advancements in the field of optics. However, there is a significant gap in integrating artificial intelligence (AI) tools with the emerging tissue imaging techniques that limits their potential for high-throughput diagnostic decision making. In this aim, we will integrate machine learning methods with multispectral images of breast cancer biopsies for high throughput evaluation of molecular markers. Additionally, we will combine information from the Hematoxylin and Eosin (H&E) stained images (most commonly used in clinics for cancer diagnosis) with multispectral imaging to get spatially registered molecular maps. The developed analytical pipeline will spectrally unmix the acquired data, divide tissue into different histological groups, segment cells of interest (tagged molecular markers) and models for diagnostic and prognostic analysis. Further, we will carry out validation and robustness studies to facilitate clinical translation of our developed methods.

Aim 2. Spatial and multiplexed analysis of the tumor-immune-microenvironment complex. It is now well known that the study of just the tumor is not enough to understand the disease profile of a patient and subsequently utilize the emerging treatments in cancer care. In this aim, we will investigate tumor cells along with their immune signatures and alterations in the microenvironment (particularly stromal cells). The underlying hypothesis is that stromal alterations and the different immune networks will elicit a unique tumor-immune signaling, providing new insights into personalized patient assessment. High resolution images along with machine learning models will enable spatial analysis across cell types in a tissue specimen. Abundance and spatial distribution of different immune cells will be correlated diagnostic profile of the tumor.The findings would then be combined across tissue specimens using statistical analysis.

Outcomes: The proposed work will extend our understanding of the tumor-immune heterogeneity with desired molecular and structural resolution. It will provide a pipeline to integrate AI with multispectral imaging for enhanced understanding of breast cancer. This pipeline can then be extended to any other cancers analyzed using multispectral imaging. It will be crucial in understanding tumor outcomes, and tailoring treatment strategies for different patient groups.

Key Deliverables: (1) Digital toolbox for cancer and microenvironment characterization using multispectral images. (2) Data and model standardization across patient samples. (3) All tools, particularly code developed in this proposal will be made open source to the community for further development and use.

BACKGROUND:

Breast cancer is diagnosed via histopathology, which involves biopsy, tissue staining followed by a manual examination by a pathologist. Breast tissue has a rich diversity of functional units, including epithelial cells, lymphocytes, blood vessels, fibroblasts, myofibroblasts, basal cells, and different types of extracellular matrices. This leads to a diversity of disease progression(*1*). While carcinomas start in the epithelial cells(*2*), it is now well understood that a multitude of stromal changes aid in cancer progression(*3*–*7*). It has been shown that genetic changes in the stroma are critical to predicting clinical outcome(*8*). The limited use of multiple tissue compartments in observing, understanding, and treating cancer arises from the lack of technology to capture its detailed morphological and biochemical signatures.

Manually utilizing pattern information from multiple cell types is impossible, and computerized pattern recognition has been reported to be effective(*7*, *9*–*11*). Currently, many immunohistochemical biomarkers are used to investigate breast tumors and determine their prognosis. These attempts that use simple structural data have been limited in information, and multiplexed molecular measurements are highly desirable(*12*–*19*). Multispectral imaging techniques based on multiplexed immunofluorescence (mIF) are increasingly being utilized for multidimensional characterization of diseases(*20*, *21*). However, standardized, fast and accurate artificial intelligence approaches are needed to fully utilize the exponential growing imaging datasets and correlate co-expression of markers with disease states(*22*).

A.1. Integration of Artificial Intelligence with Multispectral Imaging: The lack of standardized assessment of tumor and its microenvironment limits its use for patient prognostication. The evaluation is confounded by ill-defined tumor borders and the presence of a multitude of stromal and immune cells. Therefore, accurate and rapid protocols for characterizing the tumor and the associated stroma are needed to overcome the challenges of tumor-immune profiling in the current standards of patient care. Multispectral imaging of multiplexed stained samples offers a multidimensional and high-resolution view of the disease. However, large data sizes due to rapid and high-resolution data acquisition, lack of open source platforms for post-processing the images and classification models limits its widespread use for disease evaluation. An end-to-end pipeline for spectrally unmixing the signals, processing the images, segmenting tissue components, and cell characterization is needed for the seamless integration of multispectral imaging with diagnostic pathology. For some of the above-mentioned tasks like spectral unmixing and cell segmentation, existing softwares are available, however it can be expensive or inefficient for large-scale application. Additionally, there is a lack of a standardized pipeline to implement emerging models on multispectral imaging data.

A.2. Spatial and multiplexed analysis of the tumor-immune-microenvironment (TIME) complex: Risk stratification in patients has been a challenge as there are no clinical factors, histopathologic features, or molecular markers that permit reliable assessment of recurrence risk. This can result in potential short-term and long-term morbidities as well as increased healthcare costs. Some recent studies suggest the encouraging signs of using the TIME for modeling patient prognosis(*7*, *8*, *23*, *24*). These cells play an essential role in tumor progression, and their dynamic interactions with the tumor will give insights into the tumor-immune interactions and evasion mechanisms. Even though many studies have investigated the role of immune subpopulations for favorable disease prognosis, especially for aggressive tumor subtypes like triple-negative breast cancer (TNBC) and HER2+ tumors(*25*, *26*), there is still a gap in understanding the effect of these cells and their interactions across breast cancer subtypes(*27*, *28*).

OBJECTIVES:

The overall goal of this proposal is to use data analysis particularly artificial intelligence (AI) based models for extending the capabilities of multispectral imaging and providing a framework for spatial characterization of TIME complexes. This will not only enhance our understanding of tumor heterogeneity but also enable the widespread use of this technology for clinical translation.

A.1. In this aim, we will build AI tools for rapid, standardized, and accurate analysis of tumor samples using multispectral imaging. We will also register multispectral data with Hematoxylin and Eosin (H&E) stained images to get a multimodal view of the disease and provide easy integration of pathological analysis with molecular characterization. The same tissue sample will be labeled for multiple cancer related biomarkers and imaged on a high-resolution multispectral microscope. The developed analytical pipeline will spectrally unmix the acquired data, divide tissue into different histological groups, segment cells of interest (tagged molecular markers), and model for diagnostic and prognostic analysis. We will test our pipelines on data coming from different sources to ensure the generalizability of our models. We will use a suite of conventional digital approaches like random forests, clustering, logistic regression, and emerging methods like convolutional neural networks and deep learning (DL) to enhance the ability of digital algorithms to parse and identify complex cytological and architectural variants in breast cancer.

A.2. In this aim, multiplexed maps of molecular markers will be estimated and combined with histological segmentation maps to capture their interactions simultaneously with the tumor and the associated microenvironment. We will particularly investigate tumor heterogeneity in the context of stromal alterations [dense, loose, desmoplastic] and immune profile. Spatial networks of TIME complexes across tumor specimens will be generated to correlate relative abundance and cellular architectures with disease states.

WORK PLAN:

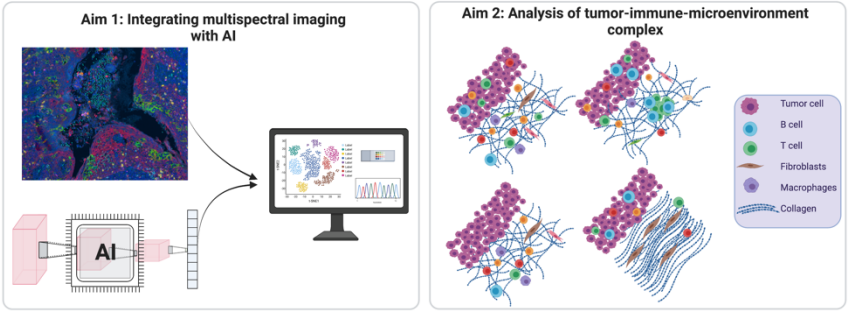

Figure 1: Overview of the proposed research plan.

The proposed research plan will utilize breast tissue biopsy samples, primarily formalin-fixed and paraffin-embedded (FFPE) for digital segmentation of the tumor, immune cells, and the microenvironment. We will utilize both state-of-the-art AI modeling and multispectral imaging (Aim1) and build spatial patterns of immune cells + tumor + associated microenvironment (Aim 2). To develop clinically relevant models, continuous feedback from clinicians will be incorporated. We will utilize both pre-existing collaborations with the UIC Department of Pathology and new collaborations with the University of Washington (UW) School of Medicine, particularly the Department of Pathology, for validation studies.

<u>Detailed Tasks</u>

The focus of this proposal is to accurately determine molecular maps and provide color-coded images segmenting different tumor components that are easy to visualize and interpret by clinicians. We will combine the power of knowledge-guided morphometric analysis (using

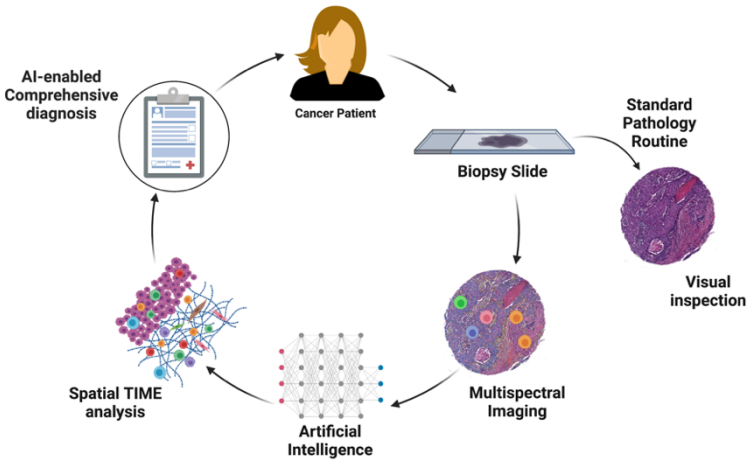

Figure 2: Overview of the deep learning-based framework for digital tumor and immune signature mapping.

textural features like adaptive thresholding, multi-step size filters, solidity variants, and morphological dilation) with automated architectural pattern analysis using deep learning to capture tumor heterogeneity, immune signatures, and microenvironment profiling (**Figure 2**). Ongoing models (**Figure 3)** in PI's lab to identify microenvironment changes on the H&E images will be customized and combined with multispectral imaging data. First, a simple deep learning model (previously developed by Mittal et al. (*29*)) is utilized to digitally segment the epithelial and stromal compartments on the H&E stained image. Next, these compartments are individually segmented using clustering and image segmentation to identify the different populations of the cells. In the stromal areas, the model captures various pockets of the collagen (altered density and polarization) and the intermixed cellular components. To further illustrate the new opportunities provided by this digital framework for TME analysis, stromal samples with accompanying fibrosis were investigated.

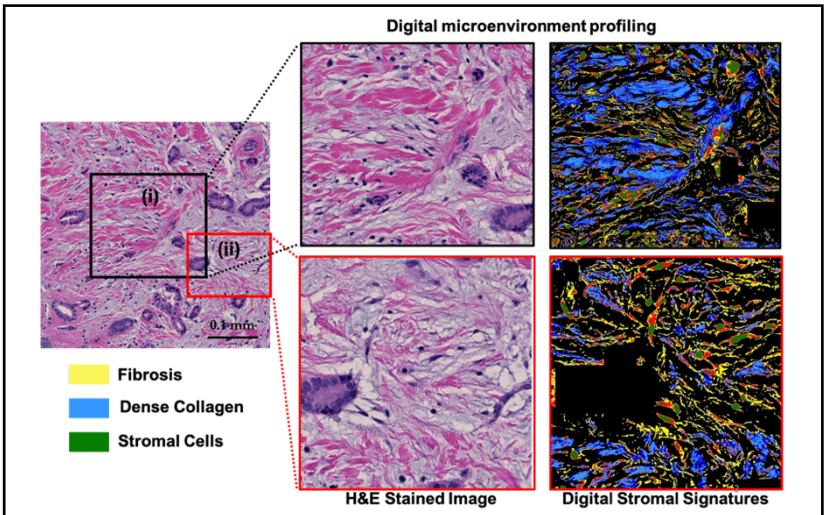

Figure 3: Digital stromal segmentation into dense, fibrotic, and cellular components with the H&E stained images on the left and the digitally segmented images on the right.

Conventionally, additional stains like Trichome blue or Picrosirius red are needed to visualize the alterations in the collagen. Our digital framework can provide clinicians with enhanced collagen visualization/segmentation (**Figure 3)**. Combining these approaches with multispectral imaging will provide a quantitative, rapid, and digital visualization of tumor subpopulations, stromal signatures, fibrosis, and immune cells allowing clinicians to determine a comprehensive disease profile in the context of the different histological and pathological components. Initially, some of the previously trained deep learning networks and algorithms developed by the PI (described above) will be tuned and adapted to the task to avoid the need for large training datasets. New methods for spectral unmixing will be investigated to avoid the large processing times that are needed for high-plex multispectral images. We will simultaneously map the interactions of immune cells with tumor and the microenvironment by utilizing multispectral imaging of a variety of cluster differentiation (CD) markers. This will be carried out by opal staining and imaging using the Vectra Polaris imaging system (in our lab) using nine-color fluorescence imaging and spectral unmixing. A set of algorithms will also be developed to process the spectral populations and phenotyping. Co-registered multiplexed maps will be analyzed using unsupervised (deep embedded clustering) and supervised (convolutional neural networks) learning using archival patient slides. Finally, a specialized

model will be cascaded to the previously tuned models to achieve cell segmentation and tumor-immune analysis.

Challenges and alternative approaches:

One of the challenges in the development of digital methods is selecting robust features that truly model disease alterations. We will identify conserved features across a wide variety of hand-crafted and automated models. Additionally, various samples will be utilized to identify pure features of tumor heterogeneity while minimizing within-patient variations or differences due to sample preparation. Additionally, while carrying out a spatial analysis of the tumor-immune cells, we might encounter huge variability in the performance of different cell segmentation approaches. We will implement a high throughput evaluation screening pipeline of multiple nuclear segmentation platforms including customizable deep learning models to inform the choice of platform for usage. Carrying out this evaluation pipeline on a sample of a dataset and choosing the best possible cell segmentation platform can aid in getting more accurate spatial correlations, phenotype mapping, and other mIF insights downstream.

OUTCOMES:

The proposed work will extend our understanding of the tumor-immune heterogeneity with desired molecular and structural resolution. It will provide a pipeline to integrate AI with multispectral imaging for an enhanced understanding of breast cancer. This pipeline can then be extended to any other cancers analyzed using multispectral imaging. It will be crucial in understanding tumor outcomes and tailoring treatment strategies for different patient groups. The key deliverables of this work will be (1) Digital toolbox for cancer and microenvironment characterization using multispectral images. (2) Data and model standardization across patient samples. (3) All tools, particularly code developed in this proposal will be made open source to the community for further development and use.

IMPACT:

Artificial Intelligence (AI) applied on the extensive biochemical and morphologic data acquired with multispectral imaging will provide novel insights into cell-cell interactions. AI algorithms will be integrated with data acquisition and typically take a few seconds to classify images. These algorithms will provide rapid, objective, and quantitative prognostic information for clinicians to improve patient care upon extensive validation. It will also address the long-recurring need to reduce pathological inter and intra- observer variability, impacting surgical treatment and patient outcomes. The collective mapping of the tumor-immune interactions and microenvironment characterization will reveal new insights for individualized disease progression, especially distal metastasis and outcome models. Immune and microenvironment profiling of the tumors will provide indicators to tailor immunotherapy for specific patient groups, especially triple-negative breast cancers, where other hormone-based targeted therapies are not available.

REFERENCES:

1. L. G. Martelotto, C. K. Y. Ng, S. Piscuoglio, B. Weigelt, J. S. Reis-Filho, Breast cancer intra-tumor heterogeneity. *Breast Cancer Research*. **16** (2014), pp. 1–11.
2. P. P. Rosen, *Rosen's Breast Pathology* (Lippincott Williams & Wilkins, 2001).
3. M. Hu *et al.*, *Nature genetics*. **37**, 899–905 (2005).
4. D. Hanahan, L. M. Coussens, *Cancer Cell*. **21**, 309–322 (2012).
5. A. Bergamaschi *et al.*, *Journal of Pathology*. **214**, 357–367 (2008).

6. J. Winkler, A. Abisoye-Ogunniyan, K. J. Metcalf, Z. Werb, Concepts of extracellular matrix remodelling in tumour progression and metastasis. *Nature Communications*. **11** (2020), pp. 1–19.

7. A. H. Beck *et al.*, *Sci Transl Med*. **3**, 108ra113-108ra113 (2011).

8. G. Finak *et al.*, *Nature Medicine*. **14**, 518–527 (2008).

9. A. Janowczyk, A. Madabhushi, *J Pathol Inform*. **7**, 29 (2016).

10. G. Litjens *et al.*, A survey on deep learning in medical image analysis. *Med Image Anal*. **42** (2017), pp. 60–88.

11. B. Ehteshami Bejnordi *et al.*, *JAMA*. **318**, 2199 (2017).

12. B. Heijs *et al.*, *Analytical chemistry*. **87**, 11978–11983 (2015).

13. N. C. Blessin *et al.*, *Cellular Oncology 2021*, 1–11 (2021).

14. P. Savas *et al.*, *Nature Medicine*. **24**, 986–993 (2018).

15. W.-L. Liu *et al.*, *Tumor Biology 2015 37:4*. **37**, 5013–5024 (2015).

16. S. Black *et al.*, *Nature Protocols 2021*, 1–36 (2021).

17. S. Cai, M. Allam, A. F. Coskun, *Trends in Cancer*. **6**, 813–818 (2020).

18. T. Z. Tien *et al.*, *Histopathology*. **79**, 139–159 (2021).

19. S. Mittal *et al.*, *Proc Natl Acad Sci U S A*. **115**, E5651–E5660 (2018).

20. D. Locke, C. C. Hoyt, *Front Mol Biosci*. **10**, 1051491 (2023).

21. E. R. Parra *et al.*, *Nature Communications 2023 14:1*. **14**, 1–16 (2023).

22. S. Berry *et al.*, *Science (1979)*. **372** (2021), doi:10.1126/SCIENCE.ABA2609/SUPPL_FILE/ABA2609_BERRY_REPRODUCIBILITY-CHECKLIST.PDF.

23. M. Hu *et al.*, *Nature genetics*. **37**, 899–905 (2005).

24. M. W. Conklin, P. J. Keely, *Cell adhesion & migration*. **6**, 249–260 (2012).

25. E. Parra, A. Francisco-Cruz, I. Wistuba, *Cancers*. **11**, 247 (2019).

26. M. Surace, L. Rognoni, J. Rodriguez-Canales, K. E. Steele, in *Methods in Enzymology* (Academic Press Inc., 2020), vol. 635, pp. 33–50.

27. B. Hellwig, *EXCLI journal*. **18**, 129–131 (2019).

28. X. Tekpli *et al.*, *Nature Communications*. **10**, 1–14 (2019).

29. S. Mittal, C. Stoean, A. Kajdacsy-Balla, R. Bhargava, *Front Bioeng Biotechnol*. **7**, 246 (2019).

Asymmetric Pharmaceutical Synthesis with Molecular Hall Effect

Shoufeng Lan, Texas A&M Engineering Experiment Station, Texas A&M University

Overview: More than 80% of U.S. Food and Drug Administration or FDA-approved commonplace pharmaceuticals such as ibuprofen carry an inherent flaw, pairing the active and beneficial ingredient with an ineffective or toxic counterpart. The underline mechanism is chirality, which discerns the dissimilarities between objects and mirror images. One prominent example is human hands because the left hand is the mirror image of the right hand, but they are not superimposable. Each handedness or so-called enantiomer of chiral objects should have the same probability of occurring, like the left hand and right hand always appearing in a pair. Unfortunately, the pairing of left- and right-handed chiral materials might not be favorable or often detrimental in the pharmaceutical industry, for example, the thalidomide tragedy that led to more than 10,000 birth deformities in the 1960s. Therefore, asymmetric synthesis, or selecting/sorting one enantiomeric handedness over the other, is a pressing need yet a grand challenge for human health and the pharmaceutical industry. According to the symmetry principle, the asymmetric synthesis should have a fundamental force (i.e., electromagnetic, gravitational, strong, and weak) to break the symmetry. The only one that breaks the parity-inversion symmetry is weak interaction. That is why all atoms are slightly left-handed, and indeed it results in enantiomeric excess, however, on the level of thermal fluctuation. Emulating the weak interaction using light and magnetism, we found a new magneto-chiral effect (MChE) that is several orders of magnitude stronger. Although the MChE could lead to enantiomeric excess in principle, implementing it for practical applications in asymmetric synthesis is a daunting task, which is also the challenge we will address. To that end, we have three specific objectives based on our recently published works on the MChE. (**1**) Electromagnetically induce enantiomeric excess by developing a plasmonic magneto-chiral system. (**2**) Dramatically enhance the plasmonic MChE with nanostructures to achieve an unprecedented spatial separation of chiral pharmaceuticals, which we named the molecular Hall effect. (**3**) Obtain enantiopure pharmaceutical molecules with on-demand handedness fully controlled by light and magnetism. Like the electronic Hall effect that lays the foundation of modern electronics, the molecular Hall effect could contribute to asymmetric synthesis, hence the pharmaceutical industry and human health.

Outcomes and Unique Aspects: Our proposed research will produce a universal physical means to separate chiral objects for asymmetric synthesis – in stark contrast to current techniques that use existing chiral objects (e.g., catalysis for the 2001 and 2021 Nobel prizes in Chemistry) to biologically and chemically transfer handedness. These chemical and biological methods are expensive, may only apply to specific molecules near the asymmetric center (proximity effect), or may damage more complex molecules with multiple chiral centers. Due to its physical rather than chemical or biological nature, our proposed method can enable all chiral species to be selectively sorted by their inherent handedness, potentially achieving absolute enantioselectivity. Also, the research will generate a molecular Hall effect from our proposed plasmonic magneto-chiral technique, providing the elusive spatial separation of chiral molecules favorable for asymmetric synthesis in pharmaceutical manufacturing.

Potential Impact: To the scientific community, the proposed research will introduce a relatively unknown phenomenon called plasmonic MChE, enhanced by momentum matching and directionally controlled by the polarization of light. With broader impacts, it can also lead to the cost-effective production of a wide range of enantiopure drugs. As 80% of FDA-approved drugs are chiral, our technique can play a role in the pharmaceutical industry and human health in general. Also, since the predicted global market for asymmetric synthesis is ~133 billion dollars by 2030, our research can contribute to the U.S. and the world economy.

Asymmetric Pharmaceutical Synthesis with Molecular Hall Effect

Shoufeng Lan, Texas A&M Engineering Experiment Station, Texas A&M University

1. Literature Review: One of the most fundamental mysteries is the homochirality of life, in which all living organisms on the Earth contain exclusively left-handed amino acids and right-handed sugars, not their mirrored counterparts. Scientists have spent endless efforts understanding the origin of such absolute enantiomeric excess ever since Louis Pasteur's great discovery of the molecular asymmetry of tartrates in the 1840s. From a physical point of view, a result of asymmetry (i.e., homochirality) must have a physical force to break the symmetry, according to Pierre Curie's fundamental symmetry principle. In 1956 [*Phys. Rev.* 104, 254–258 (1956)], Tsung-Dao Lee and Chen Ning Yang discovered that weak interaction, albeit small, is the only one that breaks parity-inversion symmetry among the four fundamental forces (i.e., electromagnetic, gravitational, strong, and weak interactions). Four decades later, Rikken *et al*. found an optical analogous of weak interactions named the magneto-chiral effect (MChE) that is several orders of magnitude stronger [*Nature* 390, 493–494 (1997)]. Indeed, the same group observed an enantiomeric excess of ~0.01% induced by the MChE in chemical reactions under a strong external magnetic field (~10 Tesla or about 100,000 times of the Earth's magnetic field) [*Nature* 405, 932–935 (2000)]. Recently, we obtained a record-strong MChE (~40 times Rikken's work) with the spontaneous magnetic moment of a ferromagnetic substrate while eliminating the need for an external magnetic field [*Nature Communications* 12, 2088 (2021)]. Despite the excellent work on the enantiomeric excess generation, scholars have not addressed the grand challenge of spatially separating chiral objects by physical means, which hampers applications in asymmetric synthesis with desired electromagnetic control. We propose to tackle the problem by combining the MChE with surface plasmon polariton (SPP) so that the left- and right-handed chiral objects experience different forces depending on the propagation direction of the SPP (**Figure 1**).

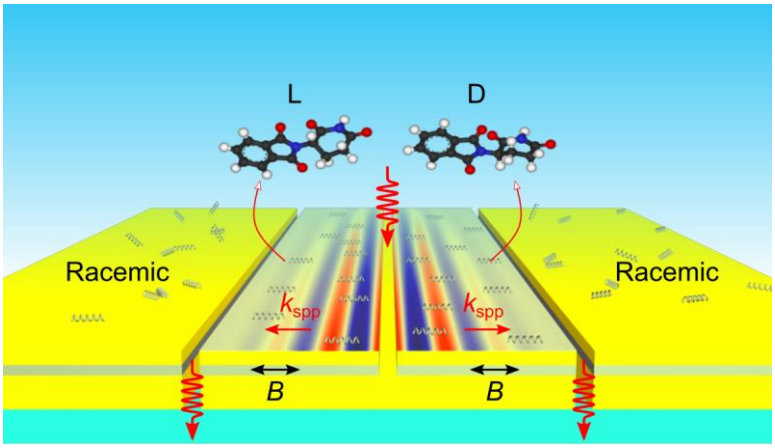

Figure 1. Schematic of a plasmonically induced universal asymmetric synthesis with electromagnetic control for selectively separating left- and right-handed (L and D) chiral objects from racemic mixtures. The layers of the structure are gold/cobalt/gold/glass. **B**: magnetic field, $\mathbf{k}_{SPP}$: wavevector of the excited surface plasmon polariton (SPP).

2. Background and Technical Methodology: A phenomenological description of electro- and magneto-optical effects is the expansion of the natural dielectric susceptibility, ε_N, with vectors and tensors that characterize either the wave itself or an external force. With the terms related to this work, the expansion is the following: $\varepsilon_{\pm}(\omega, \mathbf{B}, \mathbf{k}) = \varepsilon_N(\omega) \pm \varepsilon_M(\mathbf{B}) \pm \varepsilon_{Ch}(\mathbf{k}) + \varepsilon_{MCh}(\mathbf{B}, \mathbf{k})$, where ω is the angular frequency of the right (+) and left (−) circularly polarized light, **B** is a magnetic field, and **k** is a wavevector; the subscription of M, Ch, and MCh are the magnetically induced rotation, chirality, and magneto-chiral effect, respectively. For a general isotropic medium, the well-known magnetically induced rotation, Faraday or magnetic Kerr effect, results from a Larmor precession of electrons with the angular velocity $\Omega_L = -e\mathbf{B}/2m\mathbf{c}$, where e is the negative electron charge, m is the mass, and **c** is the velocity of light

in vacuum. Therefore, the right and left circularly polarized light experiences the dielectric susceptibility, not at the frequency of ω but a shifted frequency of $\omega_{\pm} = \omega \pm \Omega_{\mathrm{L}}$. And hence, the dielectric susceptibility for the magneto-optical effect writes as:

$$\varepsilon_{\pm}(\omega \pm \Omega_{\mathrm{L}}) = \varepsilon_{\mathrm{N}}(\omega) \pm \frac{|e|}{2mc} \cdot \frac{\partial \varepsilon_{\mathrm{N}}}{\partial \omega} \mathbf{B} \quad (1)$$

On the other hand, the dielectric susceptibility of a chiral medium is described by $\varepsilon_{\pm}(\omega) = \varepsilon_{\mathrm{N}}(\omega) \pm \alpha_{\mathrm{Ch}}(\omega)\mathbf{k}$. Similarly, light waves in a chiral medium under an externally applied magnetic field experience a new dielectric susceptibility:

$$\varepsilon_{\pm}(\omega, \mathbf{B}, \mathbf{k}) = \varepsilon_N \pm \frac{|e|}{2mc} \cdot \frac{\partial \varepsilon_{\mathrm{N}}}{\partial \omega} \mathbf{B} \pm \alpha_{\mathrm{Ch}} \mathbf{k} + \frac{|e|}{2mc} \cdot \frac{\partial \alpha_{\mathrm{Ch}}}{\partial \omega} (\mathbf{B} \cdot \mathbf{k}) \quad (2)$$

where the last term signifies the MChE that depends on the inner product of the magnetic field and wavevector together with the derivative of the chirality-induced dielectric susceptibility.

We can understand the underline mechanism of physically induced asymmetric synthesis by the fundamental symmetry principle. Although the theory of Nobel Prize-awarded weak interactions by Lee and Yang is particularly complicated, we can use a simplified equation, possibly oversimplified but not losing physical picture, to illustrate the violation of parity conservation. S(**σ**·**p**) = S(**σ**)·S(**p**) = −**σ**·**p**, where the parity symmetry operator S operates on the weak interaction proportional to **σ**·**p**, and the parity symmetry is no longer conserved (−**σ**·**p**). The key is the time-even pseudoscalar or the inner product between an axial vector (i.e., the spin **σ**) and a linear vector (i.e., the momentum **p**), both being either time-even or time-odd. Similarly, the MChE is proportional to **B**·**k**, in which **B** and **k** are the magnetic field (axial vector) and wavevector (linear vector), both time-odd. As **B**·**k** is a pseudoscalar, mimicking weak interactions, the MChE must violate the parity symmetry conservation or S(**B**·**k**) = −**B**·**k**. Following Pierre Curie's symmetry principle, it should also lead to absolute enantiomeric excess with the handedness depending on the relative direction between **B** and **k**.

3. Problem Statement and Objectives: Although the MChE could lead to enantiomeric excess in principle, it is a daunting task to implement for practical applications in asymmetric synthesis. The first challenge we have to address is that the MChE is relatively weak, even if it is already serval orders stronger than the weak interaction. We plan to follow our previous strategy to replace the external magnetic field with a spontaneous magnetic moment from a widely accessible ferromagnetic material - cobalt. Furthermore, we will dramatically increase the optical length for light-matter interaction using SPPs propagating along the in-plane direction. Also, SPPs have a strongly enhanced density of states and Purcell factor by confining light at the metal-dielectric interface, further elevated by purposely designed surface structures. With all these aspects in mind, we expect to obtain an enantiomeric excess of ~99%. The second challenge for asymmetric synthesis is the electromagnetic control, which we automatically solve by adopting the MChE proportional to a magnetic field and light. The third challenge is the spatial separation of chiral objects, which we will achieve by the excitation of SPPs because the sign of the plasmonic MChE is opposite on the two sides of the groove (**Figure 1**). Such physically induced asymmetric synthesis and spatial separation of chiral objects with built-in electromagnetic control have been long looked for but are still elusive. The long-term goal is to develop a physically induced asymmetric synthesis that is universal and cost-effective. To that end, we have three specific objectives based on our recently published works on the MChE. (**1**) Electromagnetically induce enantiomeric excess by developing a plasmonic magneto-chiral system. (**2**) Dramatically enhance the plasmonic MChE with nanostructures to obtain the molecular Hall effect. (**3**) Obtain enantiopure pharmaceutical molecules with on-demand handedness fully controlled by light and magnetism.

4. Outline of Tasks and Work Plan: Due to the nature of universality, physically induced spatial separation of chiral objects or the molecular Hall effect holds strong potential for cost-effective asymmetric synthesis. For unlocking its full potential, the foremost and essential step

is to find a physical force to induce enantiomeric excess. To do that, we will implement the MChE, emulating weak interactions, to violate the conservation of parity-inversion symmetry. We then plan to leverage the MChE by coupling it to SPPs to achieve a desirable yet challenging task of enantiomeric spatial separation (**Figure 1**). We will further enhance the plasmonic molecular Hall effect using grating couplers to provide the necessary momentum mismatched between free-space light and SPPs (**Figure 2**). We then plan to obtain enantiopure molecules through the polarization-controlled unidirectional excitation of SPPs (**Figure 3**).

4.1 A new plasmonic magneto-chiral system for enantioselective separation (**Months 1-8**)

We found a new path for MChE with record-high magneto-chiral anisotropy in atomic crystals that sustain excitons [*Nature Communications* 12, 2088 (2021)]. However, the atomic-scale thickness inevitably only affords a short distance for photons to interact with matter in the out-of-plane direction. We thus propose a plasmonic magneto-chiral system (**Figure 1**), in which photons interact with electrons forming SPPs that propagate along the surface in the in-plane direction. Also, instead of the previous thulium iron garnet (TIG, $Tm_3Fe_5O_{12}$), we plan to use cobalt as the ferromagnet with an in-plane magnetic moment. The schematic of the structure that contains layers of gold-cobalt-gold on a glass substrate is in **Figure 1**. In stark contrast to the well-studied magneto-plasmonic applications that use similar devices with a perpendicular magnetic field [*Nature Photonics* 4, 107–111 (2010)], our magnetic field is in-parallel to SPPs, leading to a relatively unknown phenomenon of plasmonic MChE.

As an initial step, we will use nanogroove (~100 nm) for free-space light in water to couple to SPPs (middle nanogroove) and back to water (left and right nanoslits) through the glass substrate. On the two sides of the middle nanogroove, the wavevectors of the SPPs (k_{spp}) are opposite. Because the MChE is proportional to the inner product between the magnetic field and wavevector, the generated force by the plasmonic MChE is also the opposite, provided with a fixed magnetic field. From the magneto-chiral theorem, a positive (negative) MChE preferably interact with the right- (left-) handed or D- (L-) enantiomer. As a result, the handedness of the chiral materials adsorbed on the two sides must also be different, achieving the molecular Hall effect. Another outstanding feature of the proposed plasmonic magneto-chiral system is that we can detect the chirality of the materials by analyzing the left/right circular polarization (LCP/RCP) of the out-coupling SPPs in the device. This effect is because the chirality will lead to different responses to LCP and RCP light or the so-called circular dichroism. Meanwhile, since only a tiny part of the scattered light by the groove can couple to SPPs, we expect the plasmonic MChE to be relatively weak at this stage.

4.2 Significant enhancement of plasmonic MChE using nanostructures (**Months 9-16**)

To enhance the plasmonic MChE, we will use grating couplers instead of a single groove for more light to couple to SPPs while keeping the magnetic field constant. Specifically, we will design gratings to provide the necessary momentum for efficient coupling between free-space light and SPPs, as shown in **Figure 2a**. Light shining on a metal surface at an angle of θ will have an in-plane wavevector component $k_{\mathrm{in,x}} = k_{\mathrm{in}} \sin\theta$, manifesting in the light line (solid gray). Similarly, SPPs propagate at the metal-dielectric interface have a wavevector of k_{SPP}. For light to couple to SPPs, the two in-plane momenta must be the same. At the specific frequency, for example, ω_{+1}, the in-plane wavevectors $k_{in,x}$ and k_{SPP} at the green and red circles are, unfortunately, not equal. This wavevector or momentum-mismatch prevents an efficient coupling between free-space light and SPPs. The scattering of light from a nanogroove in Section 4.1 enables part of the input light to match the momentum with SPPs, which can partially address the problem but with relatively low efficiency.

We plan to use grating couplers because their periodic structures provide an extra wavevector k_g in the reciprocal space. As a result, the light line shifts with a total wavevector

of $k_{\mathrm{in,x}} + k_{\mathrm{g}}$ (dotted line) that matches $k_{\mathrm{SPP}(+1)}$ at the red circle. Since the k_{g} can be in the opposite direction (−1 order), the total wavevector can also be $k_{\mathrm{in,x}} - k_{\mathrm{g}}$ or $k_{\mathrm{SPP}(-1)}$ at a different frequency of ω_{-1}. **Figures 2b** and **2c** clearly show the excited first-order SPPs propagating in positive and negative directions, accordingly. There will be higher orders of waves but with much lower efficiency. In addition, the analysis uses an oblique input light, but it also works for gratings under normal incidence (blue lines). As part of the preliminary results, we show in **Figure 2d** a scanning electron microscopy (SEM) image of the fabricated grating sample. We also provide the simulated electric field distribution (**Figure 2e**) using a full-wave simulation software of COMSOL for the grating at normal incidence. We should note that the current preliminary results are silver gratings on the glass in the air. We will optimize the operating conditions with gold, cobalt, water, and an extended nonpatterned area. Nevertheless, the wavevector of SPPs on the two sides of the grating will be opposite, leading to opposite plasmonic MChE selecting the handedness.

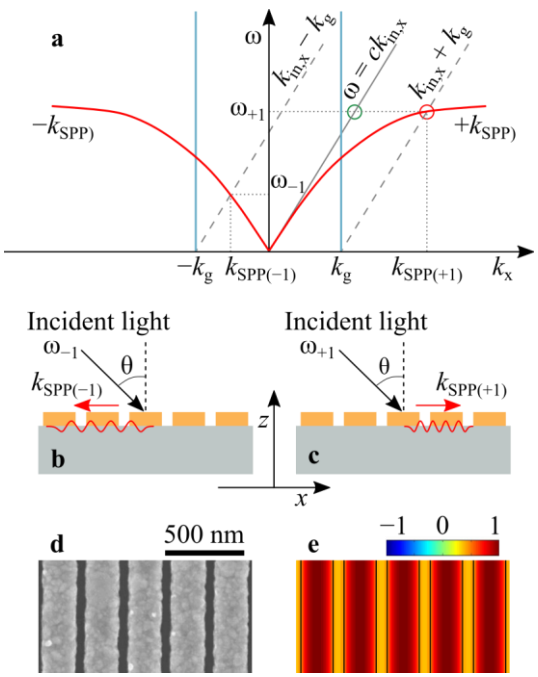

Figure 2. Grating coupler to enhance the plasmonic magneto-chiral effect. (**a**) The mechanism of grating coupler to excite backward (**b**) and forward (**c**) propagating SPPs. (**d**) SEM image of a grating coupler. (**e**) The simulated electric field under normal incidence using COMSOL.

Unidirectional excitation of plasmonic MChE for enantiopure molecules (**Months 17-24**)

The enantiomeric spatial separation of chiral molecules from racemic mixtures that contain an equal amount of L- and D-molecules could contribute to cost-effective asymmetric pharmaceutical synthesis. A higher-level challenge is to produce enantiopure molecules, not their enantiomeric counterparts. To do that, we will continue to use SPPs but only excite them in one direction under normal incidence. It is not an easy task because, under normal incidence, a plasmonic structure, including nanogroove and gratings, will excite an equal amount of SPPs in both directions. With oblique incidence at a specific frequency, on the other hand, plasmonic gratings can partially excite directional SPPs, as shown in **Figure 2a**. However, there will always be some scattering of the incident light, albeit small, to excite SPPs in the opposite direction, not to mention that the oblique incidence is not favorable for practical applications.

To eliminate the SPPs in the undesirable direction, we plan to manipulate the resonant scattering of nanostructures under the interference mechanism. In this context, Capasso's group at Harvard University demonstrated fantastic and inspiring work using plasmonic metasurfaces that contain an array of double-column apertures (**Figure 3**). When $W \ll L < \lambda_{\mathrm{SPP}}$, where λ_{SPP} is the wavelength of SPP, each one of the apertures selectively scatters incident light with polarization perpendicular to the elongated direction, giving rise to SPPs. We can treat the excited SPPs by a column of such apertures as a plane wave with electric fields E_1 and E_2. With the arrangement of the two columns shown in **Figure 3a**, i.e., $\theta_1 = 45°$, $\theta_2 = 135°$, separated by a distance of $S = \lambda_{\mathrm{SPP}}/2$, they will excite SPPs in the + and − directions as the following:

$$I_{\pm} \propto C[(E_1^2 + E_2^2) \pm 2E_1E_2\sin(\delta)] \quad (3)$$

where δ is the relative phase difference between E_1 and E_2 by the coupling process and transferred to the SPPs. Unidirectional excitation of SPPs occurs when the incident light has a

circular polarization ($E_1 = E_2$), with the direction determined by the handedness ($I_- = 0$, $\delta = \pi/2$ for LCP and $I_+ = 0$, $\delta = -\pi/2$ for RCP), as shown in **Figures 3c** to **3e** for the structures in **3b**. In this project, we will leverage the unidirectional SPPs by coupling them to the magnetic field of cobalt so that the plasmonic MChE will also happen in one direction. We note that the use of polarization for unidirectional SPPs is by no means contradictory to the fact that MChE is independent of polarization.

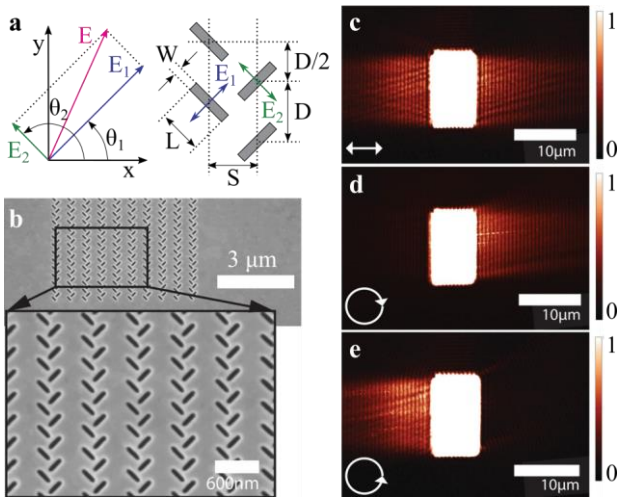

Figure 3. Polarization-controlled directional coupling of SPPs. (**a**) Illustration of the coupling of waves from two columns of apertures. (**b**) SEM images of the samples. (**c** to **e**) Near-field images with illumination by linear polarization (**c**), RCP (**d**), and LCP (**e**). Figure modified from [*Science* 340, 331-334 (2013)].

5. Outcomes: The proposed research will produce a universal physical means to create/sort chiral seeds for asymmetric synthesis – in stark contrast to current techniques that use existing chiral objects to biologically and chemically transfer handedness (e.g., the 2001 and 2021 Nobel Prizes). These chemical/biological methods are expensive, may only apply to specific molecules near the asymmetric center (proximity effect), or may damage more complex molecules with multiple chiral centers. Due to its physical rather than chemical or biological nature, the proposed method can enable all chiral species to be selectively sorted by their inherent handedness, achieving absolute enantioselectivity with electromagnetic control. The research will also generate the first spatial separation of chiral molecules depending on the handedness (molecular Hall effect) using the plasmonic MChE, further enhanced by grating couplers with momentum matching. Moreover, the research will create a unidirectional plasmonic MChE that only interacts with one handedness of chiral molecules, not the other.

6. Impact: While magneto-plasmonics has a magnetic field perpendicular to SPPs, our magnetic moment from a ferromagnetic substrate is in- or anti-parallel to the SPPs, leading to a relatively unknown phenomenon called plasmonic MChE. By providing the necessary momentum mismatched between free-space light and SPPs, our research will also introduce a general technique of grating coupling for enhancing plasmonic MChE. Moreover, our research will develop a unidirectional plasmonic MChE, leveraging the unidirectional SPPs. Beyond the scientific importance to the community, the proposed project can also have much broader impacts. The successful execution of this research can lead to the cost-effective production of a wide range of enantiopure drugs and bio/chemical products. As 80% of small-molecule drugs approved by the U.S. Food and Drug Administration or FDA were chiral, and 75% were enantiopure, our technique can play a role in the biomedical, pharmaceutical industries, and human health in general. Also, since the predicted global market for asymmetric synthesis is ~133 billion dollars by 2030, our research can contribute to the U.S. and the world economy.

7. The PI's Qualifications: The PI has in-depth experience in light-matter interactions, including plasmonics, chirality, and metamaterials. His research has consistently contributed to advancing the field with solid results in well-regarded journals, such as **6** in *Nature*-sister journals, **4** in *Advanced Materials*, and **4** in *Nano Letters*. Recognizing his accomplishments, he has received many awards, such as the SPIE Lovell scholarship. He also shows significant leadership by organizing conferences, serving on reviewer panels, and as an Associate Editor.

Pushing the limits of live-tissue multiplex imaging

Optica Challenge - Health

Significance and challenge of live-tissue multiplexing

Abnormal cell compositions, reorganization, and interactions play a central role in the initiation and progression of numerous diseases. Current gold-standard methods to evaluate cellular changes include flow cytometry, iterative immunolabeling, and multiplexed confocal laser scanning microscopy. However, these multiplexing (or cell phenotyping) methods are fundamentally limited by their incompatibility with thick and/or living samples. Multiplex (or multicolor, multimodal) multiphoton microscopy (mMPM) circumvents these limitations by its unique combination of deep penetration, 3D subcellular resolution, and relatively low phototoxicity while maintaining multiplexed tissue and cellular contrast. To date, mMPM has played an essential role in mapping neural circuits, immune systems, and tumor microenvironments. However, nontrivial technology limitations have restricted mMPM to few-type cell imaging in the superficial layers of organisms, which hamper its application to studying complex multicellular dynamics in living organisms. There is a significant unmet need for novel mMPM technologies to better understand the multicellular tissue architecture of intact/living organisms.

Multiplexed deep tissue imaging by a programmable, high-power, visible-to-SWIR source

Our preliminary studies achieved label-free cell phenotyping in living tissues by fiber-source-enabled multimodal nonlinear imaging. These studies form the basis for our proposed research to advance the proof-of-concept technology to a more versatile, gentle, and fast working prototype for live-cell multiplexing through innovations in the fiber source, excitation engineering, and demixing strategies. To overcome the limitations of current multiplex imaging technologies and enhance the accessibility and functionality of mMPM in biomedical research, we propose to develop:

Aim 1: Ultrabroadband source for flexible excitation of wide-ranging contrast in deep tissue
Aim 2: Simultaneous mMPM for imaging multicellular dynamics *in vivo* and *in vitro*
Aim 3: High-throughput mMPM for large-volume mapping of multicellular tissue architectures

Outcomes: This project will enable transformative imaging capacities of deep tissue microscopy. It overcomes the limitations of the current state of the art imaging techniques in three ways: 1) by deploying the visible-to-SWIR high-power fiber source, this technique will enable deep excitation of many endogenous and exogeneous contrast, making it an ultra-flexible tool for versatile deep-tissue multiplexed microscopy; 2) by incorporating high-speed spectral shaping devices, we will allow simultaneous and flexible imaging of multicellular dynamics in thick and moving organisms; 3) by joint design of excitation encoding hardware and decoding algorithms, we will enable fast time-lapse imaging, rapid tiling of large areas, and volumetric mapping of multicellular dynamics. Our work will lead to a paradigm shift in a new class of light generation and shaping tools that enables highly multiplexed imaging in deep and living tissues with higher versatility, lower phototoxicity, and greater sensitivity.

Impact: The technology development will have an important *positive impact* on *human health* because it will advance our understanding of complex multicellular processes in deep tissues such as organ functions, disease progression, and therapeutic mechanisms. The light source and imaging platforms developed in this project will enable new research in the broad area of biology, clinical imaging, and tissue engineering. **Application to real-world issues:** The proposed work will provide a new imaging platform for biologists and clinicians to probe and diagnose complex diseases. Specifically, this project will initiate a collaboration with Professor Linda Griffith and Dr. Keith Isaacson on the study and diagnosis of endometriosis. Label-free visualization and differentiation of lesions and glands will be a major advance in understanding of disease mechanism and diagnosis of endometriosis. In addition, our simultaneous label-free imaging platform will initiate a collaboration with Professor Fan Wang on *in vivo* whisker pad imaging for dissecting neural circuits and Professor Roger Kamm on *in vitro* imaging of dense organoids for understanding vascular network dynamics. Visualization of multiple cells noninvasively in dense disease-modeling organoids will be a major contribution to tissue engineering and drug screening.

Pushing the limits of live-tissue multiplex imaging

Introduction and Motivation

Importance of Multiplexing. Abnormal cell compositions, reorganization, and interactions play a central role in the initiation and progression of numerous diseases. Current gold-standard methods to evaluate cellular changes include flow cytometry, iterative immunolabeling, and multiplexed confocal laser scanning microscopy. However, these multiplexing (or cell phenotyping) methods are fundamentally limited by their incompatibility with thick and/or living samples. Multiplex (or multicolor, multimodal) multiphoton microscopy (mMPM) circumvents these limitations by its unique combination of deep penetration, 3D subcellular resolution, and relatively low phototoxicity while maintaining multiplexed tissue and cellular contrast. This makes mMPM an emerging deep-tissue cellular imaging tool for in vitro microphysiological systems and in vivo/in situ tissue microenvironments.

Imaging Technology Gap. To date, mMPM has played an essential role in mapping neural circuits, immune systems, and tumor microenvironments. However, nontrivial technology limitations have restricted mMPM to few-type cell imaging in the superficial layers of organisms, which hamper its application to studying complex multicellular dynamics in living organisms. The first is the limited bandwidth for deep-tissue excitation of popular fluorophores, which impedes the adoption of mMPM as a routine deep-tissue multiplexing technology. The second is slow sequential imaging, which prevents real-time monitoring of dynamic multicellular events. The third is insufficient contrast channels, which inhibits high-throughput cell phenotyping in deep tissues. Many cell dynamics that contain disease pathology are in deeper layers, rendering them inaccessible by existing imaging modalities due to the longstanding tradeoff between multiplexing, depth, and resolution. There is a significant unmet need for novel mMPM technologies to better understand the multicellular tissue architecture of intact/living organisms.

Proposed Solution: Multiplexed Deep Tissue Imaging by A Programmable, High-Power, Visible-to-SWIR Source

Our preliminary studies achieved label-free cell phenotyping in living tissues by fiber-source-enabled multimodal nonlinear imaging. These results demonstrate the importance and the feasibility of a spectrally flexible, high-throughput, and high-speed mMPM for multicellular imaging within living organisms for understanding disease models and organ functions. These studies form the basis for our proposed research to advance the proof-of-concept technology to a more versatile, gentle, and fast working prototype for live-cell multiplexing through innovations in the fiber source, excitation engineering, and demixing strategies.

To overcome the limitations of current multiplex imaging technologies and enhance the accessibility and functionality of mMPM in biomedical research, we propose to 1) build on our prior work[1–3] and prelim results[4] on broadband high-peak-power fiber sources to enable deep excitation of all popular endogenous and exogenous contrast, making it an ultra-flexible tool for versatile deep-tissue multicolor microscopy (Aim 1); 2) develop excitation engineering[5] and demixing strategies to allow high-throughput multiplex imaging with high speed, high multiplexing capability, and low phototoxicity, which will enable fast time-lapse imaging, rapid tiling of large areas, and volumetric mapping of multicellular dynamics in living organisms (Aim 2 and 3). By filling the technical gaps between multiplexing techniques and multiphoton microscopy (MPM) techniques, the proposed mMPM techniques will allow highly multiplexed, submicron-resolved, dynamic cell phenotyping in intact organoids and tissue samples.

Outcomes. This project will enable transformative imaging capacities of deep tissue microscopy. It overcomes the limitations of the current state of the art imaging techniques in three ways:
1) by deploying the visible-to-SWIR high-power fiber source, this technique will enable deep *in-vivo* excitation of many endogenous and exogeneous contrast, making it an ultra-flexible tool for versatile deep-tissue multiplexed microscopy;
2) by incorporating high-speed spectral shaping devices, we will allow simultaneous and flexible imaging of multicellular dynamics in thick and moving organisms;

3) by joint design of excitation encoding hardware and decoding algorithms, we will enable fast time-lapse imaging, rapid tiling of large areas, and volumetric mapping of multicellular dynamics in living organisms.

Our work will lead to a paradigm shift in developing a new class of light generation and shaping tools that enables highly multiplexed imaging in deep and living tissues with higher versatility, lower phototoxicity, and greater sensitivity. The proposed research will lead to a prototype of multiplexed nonlinear microscopy that will enable deep, 3D, high-resolution, versatile, fast, and gentle multiplexing in living organisms. The technology development will have an important *positive impact* on *human health* because it will advance our understanding of complex multicellular processes in deep tissues such as organ functions, disease progression, and therapeutic mechanisms.

Impact. The light source and imaging platforms developed in this project will enable new research in the broad area of biology, clinical imaging, and tissue engineering. For instance, the proposed work will provide a new label-free imaging platform for biologists and clinicians to probe and diagnose complex diseases. Specifically, this project will initiate a collaboration with Professor Linda Griffith and Dr. Keith Isaacson on the study and diagnosis of endometriosis. Label-free visualization and differentiation of lesions and glands will be a major advance in understanding of disease mechanism and diagnosis of endometriosis. In addition, our simultaneous label-free imaging platform will initiate a collaboration with Professor Fan Wang on *in vivo* whisker pad imaging for dissecting neural circuits and Professor Roger Kamm on *in vitro* imaging of dense organoids for understanding vascular network dynamics. Visualization of multiple cells noninvasively in dense disease-modeling organoids will be a major contribution to tissue engineering and drug screening.

Research Approach

Overall Strategy. Understanding multicellular changes in the context of tissue in disease progression and potential therapies requires tools for ultra-flexible, high-sensitivity, and high-speed interrogation of living organisms at the cellular level. Although existing mMPM has demonstrated substantial potential for imaging multicellular dynamics in living organisms[6–8], it suffers from several key barriers including the limited types of contrast, shallow imaging depth, and low signal throughput, which limits the technology to static few-type cell imaging or in the superficial layers of tissues. Our preliminary studies achieved label-free cell phenotyping in living tissues by fiber-source-enabled and AI (artificial intelligence)-assisted multimodal nonlinear imaging[9–16]. These results demonstrate the importance and the feasibility of a spectrally flexible, high-throughput, and high-speed mMPM for multicellular imaging within living organisms for better understanding of disease models and organ functions. These preliminary studies form the basis for our proposed research to advance the proof-of-concept technology to a more versatile, gentle, and fast working prototype for live-cell multiplexing through innovations in the fiber source, excitation engineering, and demixing strategies.

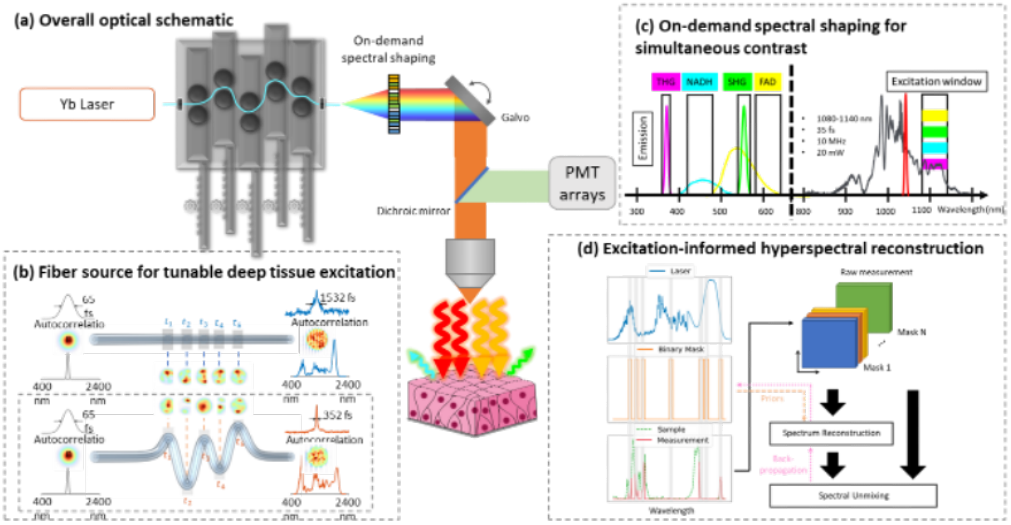

Fig. 1 (a) Overall optical schematic of the proposed computational nonlinear microscope for deep multiplex imaging. (b) Programmable high-peak-power broadband fiber source for deep-tissue excitation of wide array of endogenous contrast. (c) Simultaneous imaging of multicellular dynamics by on-demand spectral shaping. (d) Computational framework of excitation-informed hyperspectral reconstruction for highly multiplexed deep tissue imaging.

Our goal (Fig. 1) is to overcome the limitations of current multiplex imaging technologies and enhance the accessibility and functionality of mMPM in biomedical research. In Aim 1, we will build on our recent work[9,17] to develop a broadband (650 nm to 1700 nm) high-peak-power (> 1 MW) fiber source to significantly extend the excitation range of existing two-photon and three-photon microscopy (350 nm to 800 nm), covering almost all popular endogenous and exogenous contrast and making it an ultra-flexible tool for **versatile** deep-tissue multicolor microscopy. In Aim 2, we will leverage our preliminary studies (four modalities could be simultaneously acquired using parallel detection) and extend the simultaneous multiplexing capacity from fixed four colors to configurable six colors, allowing **simultaneous** and flexible mMPM imaging of multicellular dynamics in thick and moving organisms. In Aim 3, we will develop excitation-informed demixing strategies to allow **high-throughput** multiplex imaging with high speed (>10x higher sensitivity), high multiplexing capability (> 10 channels), and low phototoxicity, which will enable fast time-lapse imaging, rapid tiling of large areas, and volumetric mapping of multicellular dynamics in living organisms. We aim to achieve significant technical advancements over the existing state of the art by the completion of three high-level aims and corresponding three measurable objectives as detailed below.

Aim 1. Ultrabroadband source for flexible excitation of wide-ranging contrast in deep tissue

Although existing multicolor multiphoton microscopy has demonstrated substantial potential for imaging multicellular dynamics in living organisms, it suffers from several key barriers including the limited range of fluorophores, the imaging depth, and low signal throughput. These barriers could be effectively addressed by the development of an ultrabroadband high-peak-power femtosecond light source. The rapid advances in femtosecond laser sources have stimulated the dissemination of two-photon microscopy. However, existing laser sources lack the broad bandwidth (650 nm -1700 nm) and high peak power (>1 MW within 60-nm bandwidth) to enable multicolor imaging from violet to NIR, hindering the ability of researchers to adopt mMPM as a live-cell multiplexing technology. Our prior technique uses a custom-designed fiber source to introduce color diversity to mMPM, which enables unprecedented label-free deep-tissue cell phenotyping with a single compact source[9,12,18]. In this aim, we propose to advance our existing approach and synergistically combine the advances in large-core multimode fiber and our experiences of supercontinuum-based nonlinear microscopy to overcome the longstanding technological challenges of laser sources for mMPM (Fig. 2)[4].

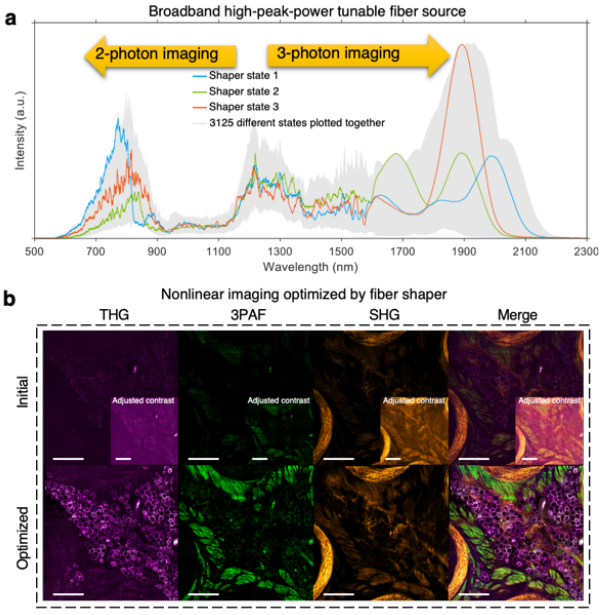

Fig. 2 a, Demonstration of full spectral coverage for 2- and 3-photon imaging with tunable spectral band energy. b, Example images produced by the adaptive fiber source.

Aim 2. Simultaneous mMPM for imaging multicellular dynamics *in vivo* and *in vitro*

Simultaneous contrast is a crucial aspect in order to capture fast multicellular dynamics in living and moving (or perfusing) organisms. Fig. 3 illustrates the results of label-free immune cell trafficking in the blood vessels of a living rat model, made possible by our previous parallel detection scheme[9,18]. This advancement is particularly valuable as it allows for the

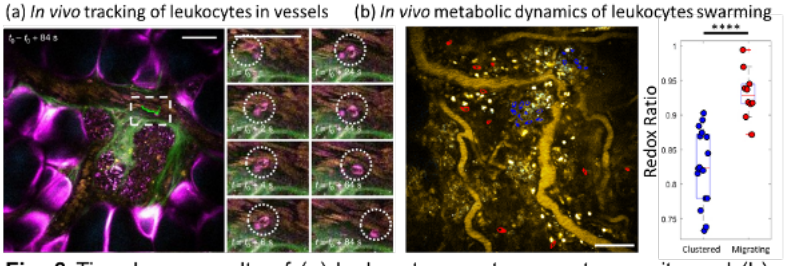

Fig. 3 Time-lapse results of (a) leukocyte arrest near a tumor site and (b) leukocyte metabolic dynamics in swarming behavior *in vivo* by simultaneous multimodal structural and metabolic imaging. Scale bar: 50 μm.

simultaneous analysis of different redox metabolic products and lipid granules within the same leukocytes. In order to extend its utility to general live-cell multiplexing, simultaneous access to increased contrast with configurable spectral flexibility is needed.

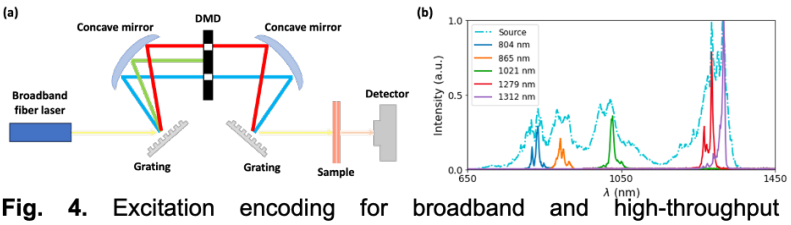

Fig. 4. Excitation encoding for broadband and high-throughput hyperspectral imaging. (a) System schematic of a DMD-based spectral shaper. (b) Exemplary spectral outputs at different designed wavelengths.

The integration of multiple contrasts is commonly obtained by sequential acquisitions. This constraint poses major challenges for live-cell imaging because sequential acquisitions slow down the imaging speed and are prone to motion artifacts. Simultaneous metabolic and structural imaging was demonstrated by the PI's and colleagues' previous work by acquiring co-registered three-photon autofluorescence of NADH and FAD, SHG of collagen fibers, and THG of tissue interfaces (e.g. myelin sheath, immune cells, and extracellular vesicles)[9,15,16]. However, the use of single-band 1110-nm excitation limits simultaneous label-free autofluorescence-multiharmonic (SLAM) microscopy to this fixed set of four contrasts. Many biological applications will benefit from a simultaneous multicolor imaging technique that supports an even larger number of simultaneous contrasts with greater flexibility in the choice of the contrasts. In this Aim, we will advance our previous excitation and detection strategies (Fig. 4) to extend the number of contrasts that's simultaneously available, and improve the flexibility of the choice of the contrasts. The overall strategy is to design and implement multi-band excitation and parallel detection to maximize the number of contrast while minimizing the crosstalk between detection channels. Compared to existing sequential multicolor imaging technologies, this will allow fast time-lapse imaging of multicellular dynamics in living organism with lower phototoxicity and higher speed.

Aim 3. High-throughput mMPM for large-volume mapping of multicellular tissue architectures

In addition to depth and multiplexing capacity, high-throughput multiplex imaging in deep tissues holds great significance for mapping tissue architectures at large volumes, such as organ-level imaging. Fig. 5 demonstrates the results of multimodal multiphoton imaging of different organs, made possible by the expansive field of view and versatile contrast offered by the multimodal imaging system[9]. This development is particularly valuable as it enables a comprehensive understanding of organs by mapping the circuits of multiple cells throughout the 3D volume. However, extending this approach to encompass entire organs presents challenges due to the decreasing multiplexing capacity and throughput as we delve deeper into the tissue, which will be addressed by the high-throughput mMPM (Aim 3).

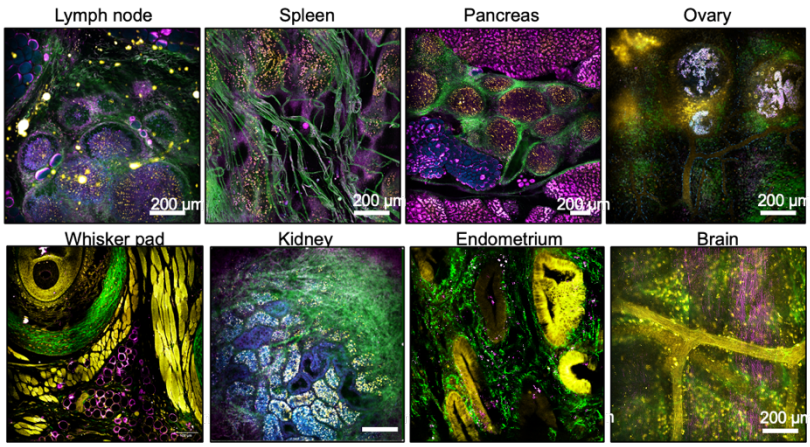

Fig. 5 Multiplexed label-free microscopy of various bulky tissue/organs.

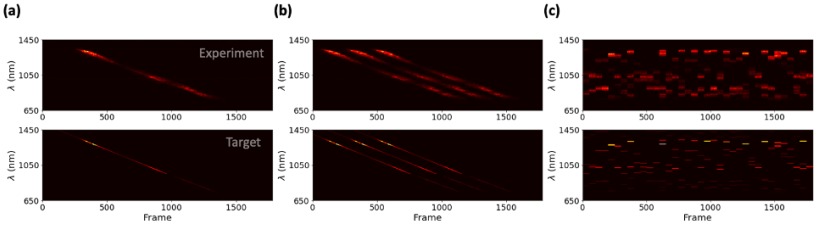

Fig. 6. Versatile excitation configurations enabled by the DMD-based spectral shaper. (a) Wavelength-swept source. (b) Multi-band excitation. (c) Spectral random access. The top and bottom figures are the experimental outputs of the spectral shaper and target spectral profiles, respectively.

In Aim 1, our objective is to advance ultrabroadband mMPM by deploying an advanced fiber source to excite a broad range of fluorophores in deep tissue. Another major bottleneck of mMPM is the detection and resolving of the multiplexed signals of the weak fluorescence. This

limitation arises from the tradeoff between signal throughput and spectral resolution in existing parallel detection approaches (e.g. spectrometer), as well as the decreasing signal throughput with depth and nonlinearity in two-photon and three-photon microscopy. To address this longstanding tradeoff, we propose utilizing excitation encoding (Fig. 6) as a promising solution to enhance sensitivity without sacrificing signal throughput. Excitation encoding offers two key advantages: sub-channel spectral resolution by excitation modulation and resistance to emitted light scattering. Therefore, our focus in this aim is to develop a high-throughput multiphoton microscopy (mMPM) system and apply it to the large-volume mapping of tissue architectures as evaluation experiments.

Reference

1. You S, Chaney EJ, Tu H, Sun Y, Sinha S, Boppart SA. Label-free deep profiling of the tumor microenvironment. *Cancer Res*. 2021;81(9):2534-2544. doi:10.1158/0008-5472.CAN-20-3124
2. You S, Tu H, Chaney EJ, et al. Intravital imaging by simultaneous label-free autofluorescence-multiharmonic microscopy. *Nat Commun*. 2018;9(1). doi:10.1038/s41467-018-04470-8
3. You S, Barkalifa R, Chaney EJ, et al. Label-free visualization and characterization of extracellular vesicles in breast cancer. *Proceedings of the National Academy of Sciences*. 2019;116(48):09243. doi:10.1073/pnas.1909243116
4. Qiu T, Cao H, Liu K, Lendaro E, Wang F, You S. Spatiotemporal control of nonlinear effects in multimode fibers for two-octave high-peak-power femtosecond tunable source. Published online 2023.
5. Yu LY, You S. High-Fidelity and High-Speed Wavefront Shaping through Complex Media via Sparsity-Constrained Optimization. Published online February 20, 2023. doi:10.48550/ARXIV.2302.10254
6. Choe K, Hontani Y, Wang T, et al. Intravital three-photon microscopy allows visualization over the entire depth of mouse lymph nodes. *Nat Immunol*. 2022;23(2):330-340. doi:10.1038/s41590-021-01101-1
7. Bares AJ, Mejooli MA, Pender MA, et al. Hyperspectral multiphoton microscopy for in vivo visualization of multiple, spectrally overlapped fluorescent labels. *Optica*. 2020;7(11):1587-1601. doi:10.1364/OPTICA.389982
8. Abdeladim L, Matho KS, Clavreul S, et al. Multicolor multiscale brain imaging with chromatic multiphoton serial microscopy. *Nat Commun*. 2019;10(1):1662. doi:10.1038/s41467-019-09552-9
9. You S, Tu H, Chaney EJ, et al. Intravital imaging by simultaneous label-free autofluorescence-multiharmonic microscopy. *Nat Commun*. 2018;9(1). doi:10.1038/s41467-018-04470-8
10. Sun Y, You S, Du X, et al. Real-time three-dimensional histology-like imaging by label-free nonlinear optical microscopy. *Quant Imaging Med Surg*. 2020;10(11):2177. doi:10.21037/QIMS-20-381
11. You S, Sun Y, Yang L, et al. Real-time intraoperative diagnosis by deep neural network driven multiphoton virtual histology. *NPJ Precis Oncol*. 2019;3(1):1-8. doi:10.1038/s41698-019-0104-3
12. You S, Chaney EJ, Tu H, Sun Y, Sinha S, Boppart SA. Label-free deep profiling of the tumor microenvironment. *Cancer Res*. 2021;81(9):2534-2544. doi:10.1158/0008-5472.CAN-20-3124/673679/AM/LABEL-FREE-DEEP-PROFILING-OF-THE-TUMOR
13. You S, Barkalifa R, Chaney EJ, et al. Label-free visualization and characterization of extracellular vesicles in breast cancer. *Proc Natl Acad Sci U S A*. 2019;116(48):24012-24018. doi:10.1073/PNAS.1909243116/SUPPL_FILE/PNAS.1909243116.SM09.AVI
14. Sun Y, You S, Tu H, et al. Intraoperative visualization of the tumor microenvironment and quantification of extracellular vesicles by label-free nonlinear imaging. *Sci Adv*. 2018;4(12). doi:10.1126/sciadv.aau5603
15. You S, Sun Y, Chaney EJ, et al. Slide-free virtual histochemistry (Part II): detection of field cancerization. *Biomedical Optics Express, Vol 9, Issue 11, pp 5253-5268*. 2018;9(11):5253-5268. doi:10.1364/BOE.9.005253
16. You S, Sun Y, Chaney EJ, et al. Slide-free virtual histochemistry (Part I): development via nonlinear optics. *Biomedical Optics Express, Vol 9, Issue 11, pp 5240-5252*. 2018;9(11):5240-5252. doi:10.1364/BOE.9.005240
17. Qiu T, Cao H, Liu K, Lendaro E, Wang F, You S. Spatiotemporal control of nonlinear effects in multimode fibers for two-octave high-peak-power femtosecond tunable source. *https://www.rle.mit.edu/yougroup/publications/*. Published online 2023.
18. Tu H, Liu Y, Turchinovich D, et al. Stain-free histopathology by programmable supercontinuum pulses. *Nat Photonics*. 2016;10(8). doi:10.1038/nphoton.2016.94

Scanning probe nano-optical investigation of biomolecule nanoparticle corona

Background & Challenge

The biomolecule nanoparticle (NP) corona is a hybrid structure that emerges when NPs interact with biological environments, leading to the absorption of biomolecules on their surfaces. The composition and conformation of coronas can vary depending on the specific NP properties and the surrounding biological milieu. Remarkably, the corona conformation plays a critical role in shaping the properties of NPs, granting them unique biological identities. As a result, studying coronas presents exciting prospects for a wide range of applications, including drug delivery, precise therapies, disease diagnosis, and environmental remediation. The successful development of corona-based applications necessitates a comprehensive understanding of corona characteristics at the nanoscale, where fundamental physical, chemical, and biological processes take place. However, current infrared (IR) spectroscopy-based analysis of corona composition and conformation, although highly productive, faces a limitation imposed by the diffraction law, which restricts the spatial resolution to > 10 μm. Consequently, a knowledge gap persists regarding the *nanoscale* features of biomolecule NP coronas, hindering a deeper scientific understanding and limiting engineering opportunities at the ultimate length scales.

Research Objectives & Outcomes

We aim to fill the knowledge gap of *nanoscale* characteristics in biomolecule NP coronas by unveiling their composition and conformation at < 50 nm length scales. To this end, we propose s-SNOM nano-imaging, spectroscopy, and manipulation of biomolecule NP coronas. Specifically, we will explore the nanoscale composition and conformation across a wide range of coronas with diverse parameters. These parameters include biomolecules and NP type, size, shape, and ratio, along with time, temperature, and pH during the incubation process. Moreover, we will study local properties and interactions between biomolecules and NPs in the corona, delving into aspects like local conductivity, plasmonic response, and charge transfer. Furthermore, we will manipulate coronas using the scanning probe to engineer on-demand functionalities. Specific objectives and outcomes include:

Objective 1: Unveil the *nanoscale* characteristics of biomolecule NP coronas
Outcomes 1: Unprecedented & comprehensive information on the composition, conformation, and spatial heterogeneity across diverse coronas, with a coverage down to < 50 nm

Objective 2: Study local properties & interactions between biomolecules and NPs in coronas
Outcomes 2: Nanoscale optical, electronic, and mechanical properties, their dynamics, as well as various interactions between NPs and biomolecules in coronas

Outcomes 3: Manipulate & engineer biomolecule NP coronas with scanning probes
Outcomes 3: Novel biomolecule NP coronas with delicately altered and engineered structures and conformations, leading toward desired functionalities

Impact

Unprecedented understanding & insights: Our proposal will uncover the nanoscale composition, conformation, and properties of biomolecule NP coronas. It is transformative since it will revolutionize our fundamental understanding of nano-bio systems, particularly coronas, and inspire nano-engineering of biomedical and healthcare devices from previously unexplored yet ultimate length scales.

Promising biomedical applications: The nanoscale characteristics and manipulation of coronas will facilitate corona nano-engineering for targeted drug delivery and precise immune responses. Revealed local properties and interactions between NPs and biomolecules in coronas offer tremendous potential for tailored therapies and nanophotonic biosensing for early, rapid, and accurate disease diagnosis.

New knowledge: Exploring nanoscale characteristics and manipulation in biomolecule NP coronas will complement current knowledge in nanobiotechnology, optics & photonics, physics, and mechanics with the understanding of corona structure, properties, and biomolecule NP interactions in nanoscales.

Career development: This proposal is a crucial step toward one of the PI's research visions in biophotonics, nano-optical investigation, and engineering biomedical materials and devices. Building upon the nano-optical study of coronas, the PI plans to explore other important biomedical systems and further develop the scanning probe nano-optics for biomedical and healthcare research. The PI envisions promising opportunities in photonic biomedical research leveraging his unique nano-optical expertise.

Scanning probe nano-optical investigation of biomolecule nanoparticle corona

1. Literature Review

1.1 Biomolecule nanoparticle corona

Materials' surfaces possess higher free energy than their bulk counterparts. Due to this fundamental characteristic, surfaces of nanoparticles (NPs) will adsorb biomolecules, such as proteins, lipids, and nucleic acids, in biological environments. As a result, the biomolecule NP corona (Fig. 1a) is formed at the NP-biomolecule interface. This formation process involves a combination of electrostatic interactions, van der Waals forces, and hydrogen bonding between NP and surrounding biomolecules[1]. The corona structure and conformation can vary depending on the NP properties and the composition of biological surroundings. It may comprise a heterogeneous mixture of biomolecules that can undergo conformational changes upon binding to the NP surface[2]. Importantly, the corona structure and conformation significantly affect NP's properties, endowing them with unique biological identities.

Because of these fascinating advances, studying biomolecule NP corona has opened up exciting opportunities for a wide range of important applications. One of the most significant applications is drug delivery. The corona formed on NP surfaces is crucial in determining their biodistribution, cellular uptake, cytotoxicity, and overall efficacy as drug carriers[3]. By engineering the corona to be selective toward specific cell types or tissues, it is possible to enhance the targeted delivery of drugs, reducing side effects and improving therapeutic outcomes[1]. Moreover, understanding the corona's interactions with the immune system allows for the development of immunomodulatory therapies, thereby enabling precise immune responses to combat a variety of diseases[3]. Furthermore, the research on biomolecule NP corona has significant implications in environmental science, as it plays a vital role in determining NP behavior in natural environments and biological systems[3]. This knowledge can aid in designing eco-friendly and efficient NP-based solutions for environmental remediation and pollution control. Overall, the applications of biomolecule NP corona are diverse and promising, paving the way for innovative advancements in healthcare, medicine, nanotechnology, and environmental conservation.

1.2 Mid-infrared spectroscopy to unveil composition and conformation information

Understanding the composition and conformation of biomolecule NP corona is pivotal in determining their unique characteristics and functionalities. To this end, mid-infrared (mid-IR)[4] spectroscopy emerges as an efficient technique to reveal composition and conformation information based on the interaction of specific wavelengths of mid-IR light with materials' chemical bonds. In essence, mid-IR light with the wavelength λ = 20–3 μm (frequency ω = 500–3333 cm^{-1}) excites vibrations and rotations of covalent bonds classified by chemical groups. Each chemical group interacts with mid-IR light at specific wavelengths characteristic of that chemical moiety. The versatility of mid-IR spectroscopy allows for the identification of functional groups in materials ranging from natural samples[5] to food, biomedical devices[6], and many others. This fingerprinting technique has been used in food and healthcare research, where the mid-IR spectra of biomolecules (e.g., proteins) exhibit prominent features known as the Amide I (ω = 1600–1700 cm^{-1}) and Amide II (ω ~ 1540 cm^{-1}) bands, associated with N–H bending and C=O and C–N stretching vibrations of the peptide backbone. Notably, the Amide I band spectra are sensitive to secondary structure changes, such as α-helices and β-sheets, making it particularly useful in food inspection and disease diagnosis, including Alzheimer's research[7].

For biomolecule NP corona, mid-IR spectroscopy has proven to be valuable in various aspects. It has been employed to study protein adsorption onto NP surfaces[8], monitor conformational changes of adsorbed proteins resulting from NP binding[9], investigate adsorption kinetics[10], analyze protein's secondary structure, explore NP-protein interactions[11], and examine surface properties of the corona.

1.3 Challenge and Knowledge Gap: *nanoscale* characteristics of corona

Despite a wealth of valuable results on composition and conformation identification, conventional mid-IR spectroscopy faces a fundamental limitation in its spatial resolution (> 10 μm). This limitation arises from the diffraction law due to the wave-like nature of light: the diffraction of light waves limits the smallest distance between two resolvable points to be about the wavelength of light. In the mid-IR, this limitation is > 10 μm. As a result, this spatial limit poses a significant challenge

when studying the biomolecule nanoparticle corona, although coronas' characteristic length scales and potential heterogeneities suggest promising science and engineering opportunities at the nanoscale.

2. Technical Approach: s-SNOM for nano-IR spectroscopy and imaging of corona

Studying nanoscale composition and conformation of biomolecule NP corona requires special optical characterizations at the subdiffractional length scales. Scattering-type scanning near-field optical microscopy (s-SNOM, Fig 1) is one prominent technique[12] to provide sample optical responses (reflection, absorption, etc.) with a spatial resolution of ~ 10 nm. This nanoscale IR resolution is independent of the free space light wavelength and surpasses conventional IR microscopy by more than a hundredfold. In the experiments, samples are scanned under the nanoscale sharp atomic force microscope (AFM) tip while being illuminated by the IR light. The illuminated AFM tip acts as the antenna, significantly enhancing the signal solely beneath the tip apex (tip radius: ~10 nm) due to the local (near-field) optical response of the sample. The AFM is operated in tapping mode to offer compatibility with soft materials and, more importantly, the lock-in amplification of the local optical signal. This amplified local optical signal can be isolated from the sample's global reflection by demodulating at the tip-tapping frequency.

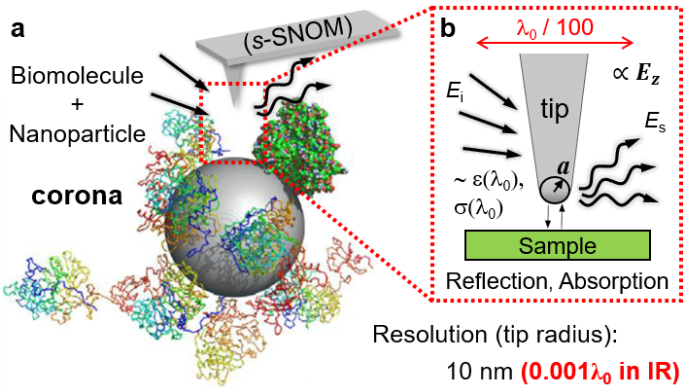

Fig. 1. (a), The s-SNOM study of biomolecule NP corona. (b), Zoom-in of the s-SNOM imaging schematic.

The s-SNOM output signal ($\propto E_z$) is related to the sample reflection and absorption (Fig. 1b), featuring same spectroscopic characteristics as the conventional IR spectroscopy. Moreover, by integrating s-SNOM with other measurements, nano-resolution can be achieved for properties such as conductivity, photocurrent, electron & lattice dynamics, work function, elasticity, and sample nanomanipulation. Furthermore, with proper feedback control of the scanning probe, s-SNOM can be performed in liquids and more complicated environments[13].

The PI's group possesses an s-SNOM for nano-IR imaging and spectroscopy, covering the mid-IR, near-IR, and visible frequencies. The PI has pioneered s-SNOM nano-imaging and spectroscopy with representative publications in both previous trainings[14-16] and his own group[17-19] at Auburn.

3. Objective

We aim to fill the knowledge gap (1.3) of *nanoscale* characteristics in biomolecule NP coronas by revealing their composition and conformation at < 50 nm length scales. To achieve this, we propose s-SNOM nano-imaging, spectroscopy, and manipulation of biomolecule NP coronas. Specifically, we will explore the nanoscale composition and conformation across a wide range of coronas with diverse parameters. These parameters include NP type, size, and shape; biomolecule type; time, temperature, pH, biomolecule concentration, and NP-biomolecule ratio during the incubation. Moreover, we will study local properties and interactions between biomolecules and NPs in the corona, such as the local conductivity, plasmonic response, and charge transfer. Further, we will manipulate coronas using the scanning probe to engineer on-demand functionalities. Specific objectives and outcomes include:

Objective 1: Unveil the *nanoscale* characteristics of biomolecule NP coronas
Outcomes 1: Unprecedented & comprehensive information on the composition, conformation, and spatial heterogeneity in various coronas, with a coverage down to < 50 nm (5.1)

Objective 2: Study local properties & interactions between biomolecules and NPs in coronas
Outcomes 2: Nanoscale optical, electronic, and mechanical properties, their dynamics, as well as various interactions between NPs and biomolecules in coronas (5.2)

Outcomes 3: Manipulate & engineer biomolecule NP coronas with scanning probes
Outcomes 3: Novel biomolecule NP coronas with delicately altered and engineered structures and conformations, leading toward desired functionalities (5.3)

4. Preliminary Results

The proposed research on nano-imaging, spectroscopy, and manipulation of NP biomolecule coronas is supported by our preliminary results on s-SNOM identification of nanoscale secondary structures in protein NP corona (Fig. 2) and successful scanning probe manipulation of NPs (Fig. 3).

4.1 Nanoscale secondary structure information in protein NP corona

We have preliminarily studied the nanoscale characteristics of coronas by examining the local distribution of secondary structures in Bovine Serum Albumin (BSA) protein Au NP coronas (Fig. 2) using the s-SNOM nano-IR imaging. We observed the nano-IR features of β-sheets at ω = 1639 cm^{-1} (Fig. 2b) and α-helices at 1671 cm^{-1} (Fig. 2c) inside the Amide I band, while no protein resonances were found at 1740 cm^{-1} (Fig. 2d). Our s-SNOM images reveal the nanoscale distribution of secondary structures over BSA and BSA Au NP corona (Fig. 2b–c). Notably, we obtained remarkable sensitivity in detecting IR responses of secondary structures in BSA, even with a thickness of just a few nanometers (Fig. 2c). Moreover, our results indicate the unique nanoscale conformation in the corona: while the α-helices exist evenly in BSA and BSA Au NP corona (Fig. 2c), β-sheets were primarily observed in the corona (Fig. 2b). These intriguing nano-IR results suggest the potential functionality of coronas in rendering specific protein secondary structures, such as β-sheets, which can be further investigated and developed.

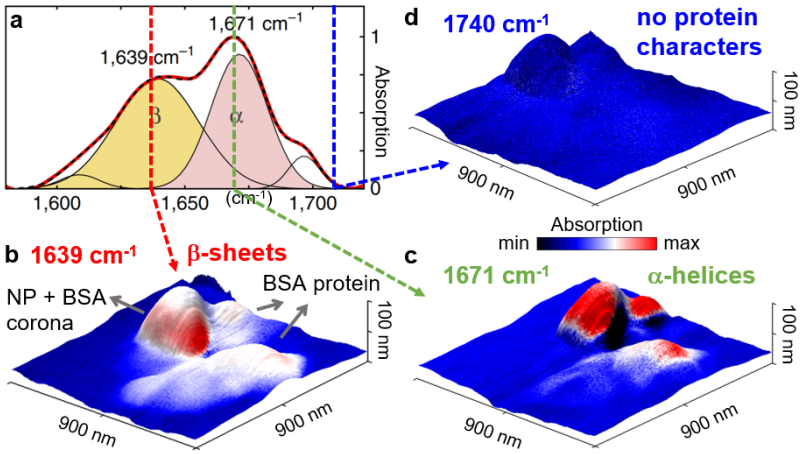

Fig. 2. Preliminary s-SNOM study of secondary structures in BSA Au NP corona. a) The standard IR spectra of protein Amide I band. (b)–(d), Combined topography (3D structure) and nano-IR images at ω = 1639 cm^{-1} (b), 1671 cm^{-1} (c), and 1740 cm^{-1} (d), revealing the secondary structure distribution in single Au NP with BSA protein.

4.2 Scanning probe manipulation of NPs

In addition to nano-IR imaging and spectroscopy, we have successfully carried out proof-of-principle experiments demonstrating the scanning probe manipulation of Au NPs (Fig. 3). The results demonstrate the precise and reversible assembly and relocation of NP clusters (white circles, size ~ 200 nm) by the scanning probe (Fig. 3b–c). By controlling the feedback of the scanning probe, we achieved NP assembly, showing an increased size from Fig. 3a to Fig. 3b. Moreover, the NPs were pushed by the scanning probe, relocating about 600 nm (Fig. 3b), and were even capable of returning to their original location (Fig. 3c).

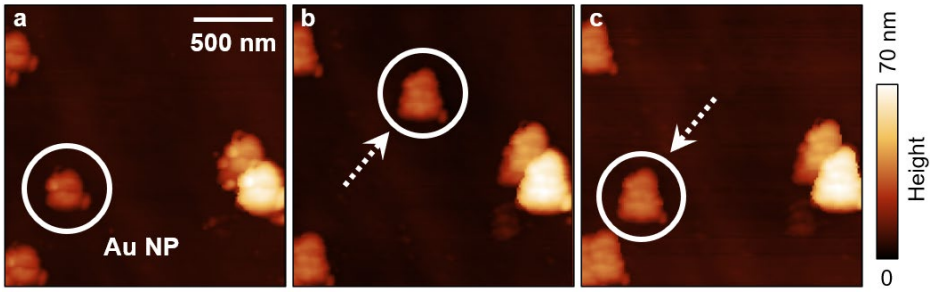

Fig. 3. AFM topography images show the precise and reversible scanning probe manipulation of Au NPs.

5. Work Plan

Building upon the support of our preliminary results (4.1 and 4.2), we propose a comprehensive exploration of nanoscale composition, conformation, heterogeneity, properties, and scanning probe manipulation & engineering of biomolecule NP coronas.

5.1 Unveil nanoscale composition and conformation of biomolecule NP coronas

We plan to comprehensively explore the nanoscale composition, conformation, and heterogeneity of a diverse range of biomolecule NP coronas. Our research will cover various NPs, including metals (e.g., Au, FeO_x), semiconductors (e.g., Si, quantum dots), lipids, polymers (e.g., PEG, PS), carbon-based (e.g., carbon nanotubes, graphene oxides), ceramic and magnetic NPs, with varying size, shape, and spatial distributions (e.g., separation or cluster). We will involve representative biomolecules, such as proteins (e.g., albumin, IgG, fibrinogen), lipids, nucleic acids (e.g., DNA, RNA), and antibodies. During the incubation, time, temperature, pH, biomolecule concentration, and NP-biomolecule ratio will be carefully controlled to produce a diverse range of biomolecule NP coronas.

Subsequently, these biomolecule NP coronas will be characterized by s-SNOM, similar to 4.1. We will perform single-ω nano-imaging and point spectroscopy of the coronas. Initially, we will select specific areas of interest based on topography and a coarse single-ω s-SNOM image. Point spectroscopy will then be conducted over these chosen areas, spanning ω = 800–3000 cm^{-1}. Around the spectral resonance frequencies, fine-area single-ω nano-imaging will be performed to unveil nanoscale information regarding the composition, conformation, and heterogeneity of the biomolecule NP coronas (like Fig. 2b-d). During the s-SNOM scan, the sample topography will be recorded simultaneously, thereby allowing the analysis of nano-IR responses overlaid with the corona topography (like Fig. 2).

5.2 Study local properties and interactions between biomolecules and NPs in coronas

In addition to the nano-optical image contrast and spectroscopic features, quantitative analysis of the s-SNOM signal ($\propto E_z$) can reveal samples' local properties. A representative property is conductivity. For example, the s-SNOM signal of metals is usually higher than insulators since metals are more conductive. We will examine the NP conductivity and its nanoscale distribution in coronas. The extracted conductivity nano-map may also reveal local interactions, such as the charge transfer, between NPs and biomolecules. In addition, we will explore other properties, including elasticity and adhesion, that can be extracted during the s-SNOM scan. These local properties can reveal nanoscale mechanical interactions between NPs and biomolecules in coronas.

Moreover, we will utilize s-SNOM to investigate the nanophotonic responses of NPs in coronas, especially around the plasmonic (metal NP), phononic (insulator NP), excitonic and interband (semiconductor NP) resonances. We aim to study how these intrinsic NP resonances are affected upon bonding with biomolecules in the corona. In addition, we will perform pump-probe s-SNOM[20] to examine the electron, lattice, and exciton dynamics of NPs in the corona. A systematic study of NP nanophotonic resonances in coronas will benefit biosensing and corona nanophotonic engineering.

For the proposed research in this section, we will work on a diverse range of coronas, as detailed in 5.1. Complementary to the experimental efforts, we will perform Finite Element Method simulations of the local properties to elucidate the experimental data and gain deeper insights from our observations.

5.3 Scanning probe manipulation and engineering of biomolecule NP coronas

Supported by our preliminary results in 4.2, we aim to systematically explore the nanomanipulation and engineering of biomolecule NP coronas using the scanning probe. By carefully controlling the mechanical feedback of the scanning probe, we plan to manipulate and reassemble a diverse range of coronas produced in 5.1. We will first independently manipulate NPs and biomolecules to establish reliable procedures and effective strategies. Subsequently, we will manipulate NPs and biomolecules in coronas and engineer them into designed conformations, potentially for on-demand functionalities. During the experiments, we will perform in situ nano-IR characterizations (as in 5.1 and 5.2) of the coronas to monitor their nanoscale characteristics in real-time, which can guide our nanomanipulation. In addition, we may explore various scanning probes, such as tips with tailored size, shape, sharpness, or stiffness, based on the specific aims of the nanomanipulation.

6. Outcomes

- Unprecedented and comprehensive *nanoscale* insights into the composition, conformation, and spatial heterogeneity across diverse biomolecule NP coronas, with a coverage down to < 50 nm

- Nanoscale optical, electronic, and mechanical properties, their dynamics, as well as various interactions between NPs and biomolecules in coronas.
- Novel biomolecule NP coronas with delicately altered and engineered structures and conformations, leading toward desired functionalities in various aspects

7. Impact

A *knowledge gap* of biomolecule NP coronas lies in their *nanoscale* characteristics (1.3), thereby limiting scientific understandings and engineering opportunities at the ultimate length scales.

- Unprecedented understanding & insights: Our proposal will *fill the scientific gap* of nanoscale characteristics in biomolecule NP coronas by unveiling their composition, conformation, heterogeneity, and various properties at < 50 nm length scales. This proposal is transformative since it will revolutionize our fundamental understanding of nano-bio systems, particularly coronas, and inspire nano-engineering of biomedical and healthcare devices from previously unexplored yet ultimate length scales.
- Promising biomedical & healthcare applications: The nanoscale characteristics and manipulation capability revealed in our research will facilitate the corona nano-engineering toward targeted drug delivery for specific cells or tissues, precise immune responses for disease treatment, and functional biomedical devices. Understanding local properties and interactions between NPs and biomolecules in coronas offers tremendous potential for NP-assisted tailored therapies and corona-based nanophotonic biosensing for early, rapid, accurate, and convenient (integrated with barcodes in cell phones or other devices) disease diagnosis.
- New knowledge: Exploring nanoscale characteristics and manipulation capability in biomolecule NP coronas will complement current knowledge in nanobiotechnology, optics & photonics, solid-state physics, and nano-mechanics with the understanding of biomolecule structure, biomolecule NP interactions, and manipulation & manufacturing in nanoscales.
- Career development: This proposal serves as a crucial stepping stone toward one of the PI's research visions in biophotonics, nano-optical investigation, and engineering biomedical materials and devices. Building upon the nano-optical study of coronas, the PI plans to delve deeper by exploring other important biomedical systems and further develop the scanning probe nano-optics for biomedical and healthcare research. The PI envisions promising opportunities in photonic biomedical research leveraging his unique nano-optical expertise (Section 2).

Reference

1. Lundqvist, M. et al. *Proceedings of the National Academy of Sciences* **105**, 14265 (2008).
2. Walkey, C.D. & Chan, W.C.W. *Chemical Society Reviews* **41**, 2780 (2012).
3. Mahmoudi, M. et al. *Nature Reviews Materials* **8**, 422 (2023).
4. Majid Ebrahim-Zadeh, I.T.S. (Springer Dordrecht, 2008).
5. Carvalho, V.V. et al. *Fuel* **210**, 514 (2017).
6. López-Lorente, Á.I. & Mizaikoff, B. *Analytical and Bioanalytical Chemistry* **408**, 2875 (2016).
7. Berriman, J. et al. *Proceedings of the National Academy of Sciences* **100**, 9034 (2003).
8. Mbeh, D.A. et al. *Journal of Biomedical Nanotechnology* **11**, 828 (2015).
9. Ma, Z. et al. *ACS Applied Materials & Interfaces* **6**, 2431 (2014).
10. Lehman, S.E. et al. *Environmental Science: Nano* **3**, 56 (2016).
11. Wang, M. et al. *Nanoscale* **7**, 15191 (2015).
12. Hillenbrand, R., Taubner, T. & Keilmann, F. *Nature* **418**, 159 (2002).
13. Virmani, D. et al. *Nano Letters* **21**, 1360 (2021).
14. Dai, S. et al. *Science* **343**, 1125 (2014).
15. Dai, S. et al. *Nature Communications* **6**, 6963 (2015).
16. Dai, S. et al. *Nature Nanotechnology* **10**, 682 (2015).
17. Chen, M. et al. *Nature Materials* **19**, 1307 (2020).
18. Dai, S. & Ma, Q. *Nature Materials* **22**, 805 (2023).
19. Chen, M. et al. *Nature Communications*, In press (2023).
20. Sternbach, A.J. et al. *Science* **371**, 617 (2021).

Compact laser-plasma very high-energy electron (VHEE) accelerator for cancer therapy

Executive summary - Health

According to World Health Organisation, cancer is a leading cause of death worldwide, accounting for nearly 10 million deaths in 2020, or almost one in six deaths. Roughly 60% of cancer patients receive radiation therapy, which is effective at causing remission in specific cancers. More than 90% of radiotherapy, however, is currently performed using megaelectron volt (MeV) X-rays. These sources are highly detrimental as their radiation severely harms healthy tissues on its way while reaching the deep tumor. By contrast, the use of very-high-energy electrons provides a much more uniform dose deposition depth, which could significantly reduce the harmful impact of the radiation on healthy tissues. Protecting healthy tissue is critical to the patient's recovery; thus, using energetic electrons could be a game changer for cancer radiotherapy. The challenge lies in the machinery needed to produce electrons in the energy range of hundreds of MeV suitable for deep tumor treatment. Machines that achieve such energetic electrons with conventional radio-frequency technology are considerably more complex, large, and expensive than the widely used photon guns used to produce MeV photons for standard X-ray radiotherapy. Therefore, access to high-quality radiotherapy for deep tumors is very limited in many parts of the world, especially in low- and middle-income countries.

This project aims to experimentally demonstrate a proof-of-principle of compact laser-plasma accelerator that delivers high-energy electrons up to 100 MeV at a kilo-Hertz (kHz) repetition rate. The accelerator utilizes an intense ultrashort pulse to generate and propel a plasma structure known as a wakefield. While this technology has already shown promise in achieving compact accelerators, it still encounters certain inherent limitations. One significant limitation is the disparity between the group velocity of the laser in the plasma and the relativistic electron bunch, which moves near the speed of light. Consequently, the faster electrons surpass the acceleration structure created by the wake, resulting in a termination of their acceleration. This limitation, known as "dephasing," constrains the maximum energy that can be attained by the electron bunches generated by the accelerator.

Optically shaping the driver laser in space and time at the focus will allow control of the dynamics of laser-plasma acceleration, mitigating the dephasing that limits the final electron energy. I aim to increase the electron energy by one order of magnitude compared to the current state-of-the-art kHz laser-plasma accelerators using the same driver-laser parameters. This source's unique beam properties, high energy, narrow energy spread, and high dose and dose rate will allow for the developing of next-generation radiotherapy treatments with precise dose control.

With current laser technology, the final size of this accelerator could be no larger than an optical table, making it cheap and accessible to many hospitals around the world. Moreover, a radiotherapy unit based on such technology could fit into a truck. This mobility and cost-effectiveness can allow this technology to permeate the economic and geographical periphery. This access will stand in contrast to techniques like proton beam therapy, whose massive sophistication and cost limit its use to the best-funded and most central cancer centers.

In conclusion, the development of this novel laser-plasma electron source technology, which relies on precise optical laser sculpting in space and time, offers promising prospects. It not only enables the creation of innovative and cost-effective radiotherapy sources but also unlocks opportunities for high-energy, high repetition rate table-top electron sources. This advancement holds the potential to drive significant advancements in medicine, biology, chemistry, and physics, which could lead to groundbreaking discoveries and transformative breakthroughs.

Proposal: Compact laser-plasma very high-energy electron (VHEE) accelerator for cancer therapy

Introduction

In a laser-plasma accelerator (LPA) [ESL09], an intense ultrashort laser pulse is focused on gas, causing ionization and forming a plasma (Fig. 1: Left). The laser pulse along the focus can be visualized as a flying sphere with a diameter of several microns. As the "laser sphere" moves, it expels electrons from the optical axis, creating a plasma wake or cavity-free region (Fig. 1: Right). Within this cavity, electric fields of remarkable magnitude, three orders of magnitude greater than those in standard radio-frequency (RF) accelerators, are generated. As a result, LPAs can accelerate electrons to energies as high as hundreds of MeV within a few millimeters. Conventional accelerators would require tens of meters to achieve the same electron energies.

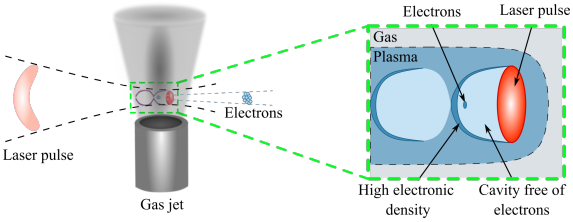

Figure 1: Left: Concept of a laser-plasma accelerator. Right: Zoomed region of the wake formation and electron acceleration.

The clear advantage of LPA is its substantial reduction in the facility's size and cost. In addition, the intrinsic properties of the LPA-generated electron bunches, such as durations of several femtoseconds (fs) and lateral dimensions on the order of a micron, have advantages over bunches obtained in conventional accelerators.

Many experiments are currently dedicated to pursuing laser-plasma acceleration of electrons to GeV energies. These efforts hope to use LPA to drive advanced light sources such as free electron lasers and as a new paradigm for the next generation of linear colliders for high-energy physics. Such experiments rely on petawatt scale laser systems that are large-scale lab facilities that operate, at best, at repetition rates on the order of one Hertz (Hz). Many high-impact societal applications, however, do not require such high-energy electrons. Radiotherapy of deep tissues, for example, needs electron beams with energies of around one hundred MeV. New near-single-optical-cycle duration, millijoule (mJ), kHz repetition rate lasers promise to deliver electrons at such energies. These laser systems are particularly attractive due to their tabletop size and competitive cost. The compact nature of this technology enables a radiotherapy unit to be housed within a truck, offering enhanced mobility and cost-effectiveness. This advantageous feature allows the technology to reach economic and geographical peripheries that previously lacked access to advanced radiotherapy treatments. In contrast to expensive and highly sophisticated techniques such as proton beam therapy, which are predominantly limited to well-funded and centrally located cancer centers, this technology has the potential to provide broader accessibility to effective cancer treatment.

Electron beams from LPAs have unique properties: they provide femtosecond electron bunches and dose rates as high as 10^8 Gy/s, compared to 10 Gy/min for conventional radiotherapy. Therefore, LPA could enable the study of the effect of extreme dose rates on ionizing radiation toxicity. Practically, this means that LPAs could be used to study the effect of the temporal fractionation of the dose on tissues [Bay+19] – to study how tumoral tissues react to the way the dose is deposited temporally. Such studies are motivated by the recently discovered FLASH effect [Fav+14], which shows that a very fast delivery (<500 ms) of therapeutic doses reduces the toxicity of healthy tissues while preserving the radiobiological effects on the tumor. Therefore, this project's ultra-compact electron source is a very promising tool for exploring innovative protocols for treating cancer.

Literature Review

Only a few kHz repetition rate LPAs are currently operational globally and have emerged recently. The leading kHz rate LPAs typically accelerate electrons within the energy range of 5-15 MeV [Gué+17; Hui+22; Sal+21], with some reaching up to 50 MeV [Laz+23]. The impressive stability exhibited during hands-off operation over a long period [Rov+20] stands a testament to the maturity of kHz LPA technology and its readiness for use in real-world applications. High repetition rate sources of electrons in the range of 10 MeV are excellent devices for radiobiology experiments of thin samples *in-vitro* [Cav+21].

However, they are unsuitable for irradiation of deep tissue, as is the case with cancer treatment in human adults. LPA experiments operating at 1 Hz have demonstrated that acceleration to energies of around 120 MeV provides electrons that deposit radiation doses at penetration depths of interest for electron beam radiotherapy of deep-seated tumors [Lun+12]. Thus, to bring the stability and high average dose rate advantages of kHz LPA machines to cancer therapy, a boost of around one order of magnitude in electron energy is required.

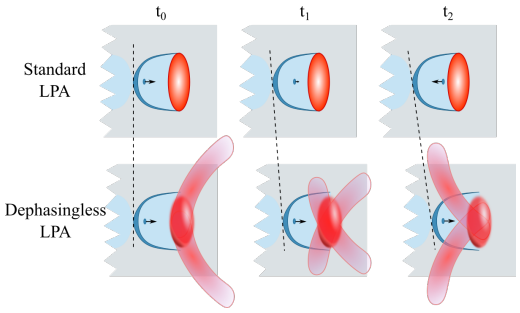

Figure 2: Top: Illustration of dephasing process LPA using a standard laser. Bottom: Illustration of dephasingless LPA with shaped laser. Arrows mark the acceleration direction of the electrons.

One of the processes which limit the maximal energy in LPAs is dephasing. In this process, trapped electrons reach the ion cavity's decelerating region in the cavity's forward part (Fig. 2: Top). It occurs because the laser group velocity in the plasma, and hence the cavity (or wakefield) velocity, are smaller than the electron beam velocity, which approaches (but never reaches) the speed of light.

I propose to mitigate the dephasing process by sculpting the laser in space and time along the focal depth. The laser front is shaped with special optics so that a focal spot "appears" due to constructive interference of the fronts coming from the sides (Fig. 2: Bottom). While the fronts have group velocities smaller than that of the electrons, the "appearance" velocity of the focal spot and hence the wake velocity could be matched with the velocity of the electrons. In this dephasingless LPA [Cai+20; Pal+20], electrons are accelerated during the whole process and gain much higher energy compared to standard LPA. According to a theoretical study [Cai+20], the expected electron energy for the project's laser parameters (3.4 fs, 2.5 mJ) is up to 200 MeV. This is an upper value with perfect beam shaping. Including possible optical aberrations, which cannot be corrected, and not having all freedom for shaping the laser in space and time, we will probably produce lower-energy electrons in the 50-100 MeV range.

Finally, this acceleration scheme can be combined with proven techniques for achieving high-quality mono-energetic bunches. Considering the practical and technical constraints, I propose developing a compact laser-plasma electron accelerator that delivers high-quality electrons up to 100 MeV at kHz. This significant energy gain would pave the way for groundbreaking tabletop experiments and applications benefiting cancer radiotherapy.

Problem Statement/Objectives

Main objective: Develop and obtain experimental proof-of-principle of a unique electron source that delivers high-quality mono-energetic electrons with energies up to 100 MeV at a kHz rate. The accelerator development will progress employing the following objectives, each covered by a Work Package (WP): WP1: Develop a theoretical foundation for dephasingless laser-plasma acceleration using few cycles, few mJ lasers at a kHz rate; WP2: Measure the intrinsic laser parameters and design an optical system for dephasingless acceleration, taking into account simulations/theory predictions (WP1); WP3: Design gas nozzles for the experiment considering simulations/theory predictions for the optimal density profiles. WP4: Ultimately obtain a working accelerator prototype, which delivers high-quality mono-energetic electrons with up to 100 MeV energy at a kHz rate.

Outline of tasks/Work Plan

To reach the desired kHz, 100 MeV monoenergetic electron source, three main components are required:

The laser which drives the acceleration of the electrons. The current research team and infrastructure at Laboratoire d'Optique Appliquée (France) possess expertise in developing and operating a TW-class laser system that delivers 2.5 mJ in 3.4 fs at kHz repetition rates [Oui+20]. This unique laser system, one of the few worldwide, is routinely used for kHz laser-plasma acceleration of stable electrons with MeV energy and picocoulomb charges. To achieve the desired pulse front curvature for dephasingless acceleration, I will implement a refractive beam shaper in the laser chain.

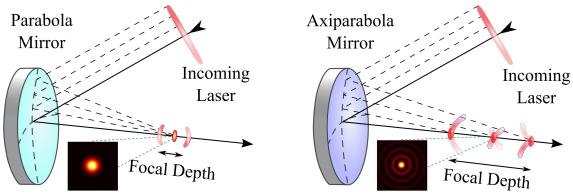

Figure 3: Left: Parabola mirror focuses rays to a single point, coupling spot size, and focal depth. Right: Axiparabola enables focusing rays from different radial positions to different focal planes, resulting in a small lateral spot and extended focal depth (quasi-Bessel beams).

The second ingredient needed to boost the energy of the electrons is a unique focusing optic that shapes the laser pulse at the focus to get more efficient acceleration. An ideal candidate is the aspherical reflective element known as the axiparabola (of which I am a co-inventor), which stretches the focal depth without increasing the lateral size of the beam [Sma+19; Oub+22]. This is done by generating quasi-Bessel beams, which are known for their diffraction-free features. The axiparabola effectively increases the acceleration length by focusing rays from different radial positions to different focal planes (Fig. 3: Right), while a standard parabolic mirror focuses all the rays to one point (Fig. 3: Left). The dynamics of the laser energy deposition on the optical axis are also critical, as the laser and trailing wake need to propagate at pace with the electrons in order to achieve efficient acceleration. The dynamics of the focal spot are controlled by manipulating the pulse front curvature before focusing on the axiparabola. With a curved front, the arrival time of different radial beam slices will be earlier than with a flat front, increasing the appearance velocity of the focal spot (Fig. 4). Together, this process is known as dephasingless acceleration. As shown in theoretical papers [Cai+20; Pal+20], the benefit of using such a method scales inversely with the pulse duration. Thus, significant energy gain is expected for the near-single-optical-cycle laser that will be used in this project. According to the theoretical models, we can expect up to 200 MeV electrons from the 2.5 mJ, 3.4 fs laser, while only 10-15 MeV have been achieved with standard parabolic focusing optics using a similar laser [Sal+21; Hui+22].

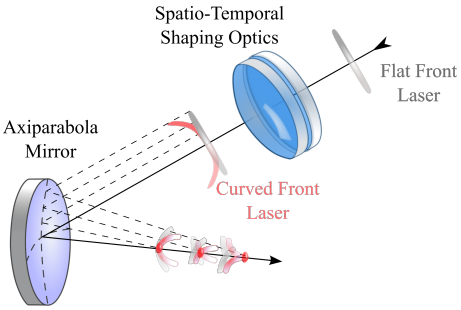

Figure 4: Spatiotemporal shaping optics initially transforms a flat (grey color) laser front to a curved one (rose color). It allows controlling the focal spot appearance velocity when used with an axiparabola. Curved fronts arrive faster to generate the necessary appearance velocity of the focal spot along the optical axis.

The final component of the project is the gas target. It is well known from LPA experiments that to achieve high-quality, monoenergetic electron beams; it is necessary to utilize controlled injection schemes. The main methods are (i) ionization injection which produces stable electrons with a broad spectrum (for the intermediate acceleration tests), and (ii) density gradient injection, which produces stable quasi-monoenergetic beams required for the ultimate goal of the project. Ionization injection is a relatively simple technique that requires only the installation of a particular gas mixture. Density gradient injection, meanwhile, requires precise shaping of the density of the gas target, achieved by specially designed supersonic nozzles. The group I work with has the expertise and academic collaborations to design and manufacture nozzles for the project [Rov+21].

The computational modeling for the WP1 phase will utilize Particle-in-Cell (PIC) simulations. In these simulations, the Maxwell equations for the electromagnetic field of the laser pulse are solved self-consistently with the equations of motion for macro-particles (ions and electrons) representing a large number of physical particles. First, I will introduce a quasi-Bessel laser beam into the code (M1.1). Then, I plan to introduce more complexity to the PIC simulation (M1.2) as the project progresses, bringing it closer to fully modeling the experimental conditions. The first simulation aims to obtain dephasingless acceleration in a uniform plasma. I will then model the plasma obtained from firing onto several standard supersonic nozzles (conical and slit nozzles), which I will use in the experiment (WP4). In parallel, I will work on a phenomenological theoretical model (M1.3), which will provide essential scalings (electron energy, charge, etc.) as a function of relevant input parameters of laser and plasma density.

To properly design the pulse shaping optics, I will measure the intrinsic properties of the experimental laser system (M2.1). Then using the OpticStudio ray tracing software, I will design an optical system that

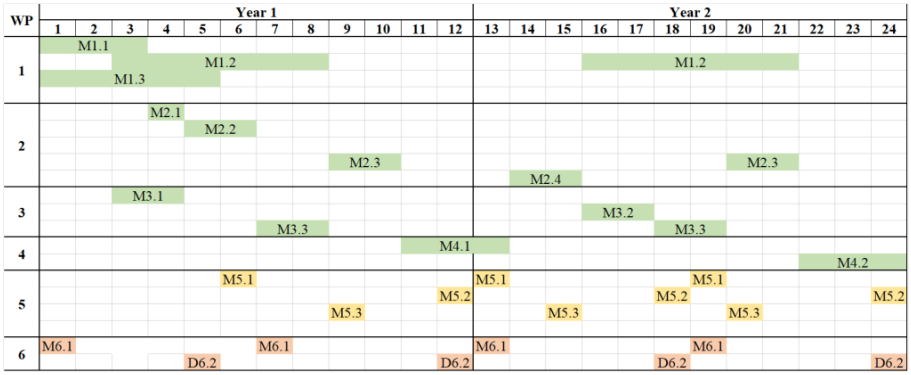

Figure 5: Gantt chart specifying the timing of the milestones (M) of the different work packages (WP), as well as the deliverables (D).

WP1	**Theory and simulations**
M1.1	Preparation for PIC simulations with shaped laser
M1.2	PIC simulations
M1.3	Analytical model development
WP2	**Optical design**
M2.1	Laser intrinsic properties measurements
M2.2	Optical design (spherical optics)
M2.3	Shaped beam measurement
M2.4	Optical design (aspherical/non-continous optics)
WP3	**Gas target design**
M3.1	Design a standard nozzle (conical or slit)
M3.2	Design a shock nozzle
M3.3	Interferometric gas/plasma density measurement
WP4	**Main experimental campaign**
M4.1	Phase-locked acceleration with spherical optics
M4.2	Phase-locked acceleration with **aspherical/non-continous** optics
WP5	**Exploration, dissemination and communication**
M5.1	Submit paper to Optica open-access journal
M5.2	Present results at Optica-organized symposium
M5.3	Lectures/workshops/seminars
WP6	**Project management**
M6.1	Meeting with the Optica Challenge Committee
D6.2	Progress report

Figure 6: Contents of the Work Packages, Milestones, and Deliverables.

sculpts lasers in space and time (M2.2) as required by the simulations in WP1. The shaping optics consist of a spherical refractive doublet (or triplet) and the axiparabola. Experimentally, I will first measure the spatial properties of the axiparabola focal line by taking focal spot diagnostics at different points along the optical axis (M2.3). Using a spatiotemporal measurement technique [Sma+22] I developed in my doctorate, I will measure the energy distribution in space and its velocity over the interaction region in a vacuum (M2.4).

The gas target development is contained in WP3. The nozzles for the experiment will be designed using the computational hydrodynamic simulation software Ansys Fluent. First, I will design and manufacture standard conical and slit nozzles that provide nearly uniform axial density (M3.1). Then I will design more complicated, in terms of geometry, shocked nozzles (M3.2). For both cases, using an interferometric measurement device, I will measure the gas and plasma density of the nozzles that will be used in the experiment (M3.2).

The final experimental part of the project will be performed in ascending complexity during two primary campaigns. First, I will perform a dephasingless acceleration experiment with an axiparabola and a spherical refractive system using standard nozzles (M4.1). Then I will use a more advanced, aspheric refractive beam shaping system or non-continuous surface axiparabola (M4.2). Finally, in the same campaign, I will use a specially designed shock nozzle to accelerate and achieve a quasi-monoenergetic electronic beam (M4.2).

I emphasize the significance of communication and sharing of project outcomes. To address this, I have incorporated a specialized work package, WP5, which involves several activities. These include submitting papers to open-access journals, preferably Optica (M5.1), delivering lectures at Optica-organized symposiums (M5.2), as well as participating in other workshops and seminars (M5.3).

Lastly, the final work package, WP6, focuses on project management. This includes engaging in meetings with the Optica Challenge committee (M6.1) to provide updates on the project's progress and learn from the expertise of committee members. Regular progress reports (D6.2) will also be submitted to ensure effective project management.

Outcome(s)

In this project, I propose to develop a compact laser-plasma accelerator delivering very-high-energy electrons (up to 100 MeV electrons) at a kilo-Hertz (kHz) rate. I aim to increase the electron energy by

one order of magnitude compared to the current state-of-the-art kHz laser-plasma accelerators using the same driver-laser parameters.

Impact

Radiotherapy is one of the primary cancer treatments. The project will develop accelerators for more uniform and less toxic dose deposition radiotherapy sources. With current laser technology, the final size of this accelerator could be no larger than an optical table, making it cheap and accessible to many hospitals around the world. The technology developed in the project can also be used in many other societal applications. It includes medical and industrial screening with X-rays that are a secondary outcome of the acceleration and innovative sterilization in which fast electrons kill off all bacteria and parasites in food products or medical equipment but do not cause any harm to vital properties of the irradiated substance or package.

Particle accelerators are essential tools in modern science and technology. They are used in medical and commercial applications but also for scientific research. In this project, I will demonstrate a proof of concept of a compact electron accelerator. I will use intricate sculpting of laser pulses in space and time to boost the resultant electron energy to 100 MeV, one order of magnitude greater than the state-of-the-art LPAs operating at kHz rates. Once implemented, these compact and affordable accelerators and their associated technology will boost advances in biology, chemistry, and physics research.

References

[ESL09] E. Esarey, C. B. Schroeder, and W. P. Leemans. "Physics of laser-driven plasma-based electron accelerators". In: *Rev. Mod. Phys.* 81 (3 Aug. 2009), pp. 1229–1285.

[Lun+12] O. Lundh et al. "Comparison of measured with calculated dose distribution from a 120-MeV electron beam from a laser-plasma accelerator". In: *Medical Physics* 39.6Part1 (2012), pp. 3501–3508.

[Fav+14] V. Favaudon et al. "Ultrahigh dose-rate FLASH irradiation increases the differential response between normal and tumor tissue in mice". In: *Science Translational Medicine* 6.245 (2014), 245ra93–245ra93.

[Gué+17] D. Guénot et al. "Relativistic electron beams driven by kHz single-cycle light pulses". In: *Nature Photonics* 11.5 (May 2017), pp. 293–296.

[Bay+19] E. Bayart et al. "Fast dose fractionation using ultra-short laser accelerated proton pulses can increase cancer cell mortality, which relies on functional PARP1 protein". In: *Scientific Reports* 9.1 (July 2019), p. 10132.

[Sma+19] S. Smartsev et al. "Axiparabola: a long-focal-depth, high-resolution mirror for broadband high-intensity lasers". In: *Opt. Lett.* 44.14 (July 2019), pp. 3414–3417.

[Cai+20] C. Caizergues et al. "Phase-locked laser-wakefield electron acceleration". In: *Nature Photonics* 14.8 (Aug. 2020), pp. 475–479.

[Oui+20] M. Ouillé et al. "Relativistic-intensity near-single-cycle light waveforms at kHz repetition rate". In: *Light: Science & Applications* 9.1 (Mar. 2020), p. 47.

[Pal+20] J. P. Palastro et al. "Dephasingless Laser Wakefield Acceleration". In: *Phys. Rev. Lett.* 124 (13 Mar. 2020), p. 134802.

[Rov+20] L. Rovige et al. "Demonstration of stable long-term operation of a kilohertz laser-plasma accelerator". In: *Phys. Rev. Accel. Beams* 23 (9 Sept. 2020), p. 093401.

[Cav+21] M. Cavallone et al. "Dosimetric characterisation and application to radiation biology of a kHz laser-driven electron beam". In: *Applied Physics B* 127.4 (Mar. 2021), p. 57.

[Rov+21] L. Rovige et al. "Symmetric and asymmetric shocked gas jets for laser-plasma experiments". In: *Review of Scientific Instruments* 92.8 (Aug. 2021), p. 083302.

[Sal+21] F. Salehi et al. "Laser-Accelerated, Low-Divergence 15-MeV Quasimonoenergetic Electron Bunches at 1 kHz". In: *Phys. Rev. X* 11 (2 June 2021), p. 021055.

[Hui+22] J. Huijts et al. "Waveform Control of Relativistic Electron Dynamics in Laser-Plasma Acceleration". In: *Phys. Rev. X* 12 (1 Feb. 2022), p. 011036.

[Oub+22] K. Oubrerie et al. "Axiparabola: a new tool for high-intensity optics". In: *Journal of Optics* 24.4 (Mar. 2022), p. 045503.

[Sma+22] S. Smartsev et al. "Characterization of spatiotemporal couplings with far-field beamlet cross-correlation". In: *Journal of Optics* 24.11 (Oct. 2022), p. 115503.

[Laz+23] C. M. Lazzarini et al. *50 MeV electron beams accelerated by a terawatt scalable kHz laser*. 2023.

Quantum-enhanced Raman imaging of hyperthermia-treated cancer cells

Cancer remains a leading cause of death and a barrier to increasing life expectancy worldwide, despite decades of efforts to develop reliable treatment procedures. According to the Global Cancer Incidence, Mortality and Prevalence report, **the number of cancer cases is expected to reach 28.4 million worldwide in 2040**. Hence, it is of vital importance to develop innovative treatments and investigate new therapeutic targets - which is the focus of this proposal.

Healthy cells become cancerous as a result of mutations accumulated in the various genes responsible for cell proliferation. Various carcinogens can generate reactive oxygen species (ROS) during their metabolism causing a reduction of molecular oxygen. Therefore, it is crucial to define the control mechanisms of ROS production. Throughout this project, I will **develop an innovative approach for quantum-enhanced biosensing of tumour cells aiming to understand the conditions of their vitality. Plasmonic-coupled quantum-enhanced Raman imaging of tumour cells will pave the way for a better understanding of hyperthermia efficiency for cancer treatment.**

The scientific novelty will bring the combination of quantum-squeezed light with surface-enhanced Raman spectroscopy to scan the intercellular environment. I will merge the above-mentioned physical phenomena and boost both sensitivity and Raman imaging to provide a new modality for quantum imaging of cancerous cells. With the outcome of this research, we aim at understanding the mechanisms of hyperthermia in stopping ROS production in tumour cells, thus understanding the not-viable conditions for tumour cells. Beyond cancer treatment, ROS detection and its quantification are critical in cardiovascular diseases, translatology, inflammation, organ injuries, and ageing. Hence, the impact of this research goes well beyond the development of a new quantum imaging modality and will aid in an “all-around” ROS analysis, thus contributing to the increase of our life expectancy.

Quantum-enhanced Raman imaging of hyperthermia-treated cancer cells

Cancer remains a leading cause of death and a barrier to increasing life expectancy worldwide despite the enormous efforts to develop novel treatment procedures. According to the Global Cancer Incidence, Mortality, and Prevalence report published in 2020, **the number of cancer cases is expected to reach 28.4 million worldwide in 2040**[1]. Hence, it is of vital importance to have a deep understanding of cancer treatment mechanisms, develop innovative treatments, and investigate new therapeutic targets.

In this research project, I will develop an innovative approach for quantum-enhanced biosensing of tumour cells aiming to understand the conditions of their vitality. Plasmonic-coupled quantum-enhanced Raman imaging of tumour cells will pave the way for a better understanding of hyperthermia efficiency for cancer treatment. The schematic of the proposed approach is shown in Figure 1.

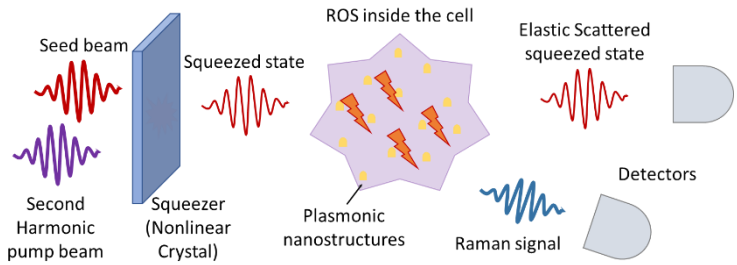

Fig.1 Schematic representation of the sensing mechanism: detection of plasmonic-enhanced elastic and Raman scattered signals excited by the generated squeezed beam.

Healthy cells become cancerous[2] as a result of mutations accumulated in the various genes responsible for cell proliferation. Various carcinogens can generate reactive oxygen species (ROS), such as H_2O_2[3], during their metabolism causing a reduction of molecular oxygen[4]. Oxidative damage to cellular DNA can yield mutations and may play an important role in the initiation and progression of multistage carcinogenesis[5]. ROS elevated in the tumor microenvironment are associated with tumor-induced immune response[6]. Therefore, it is crucial to define the control mechanisms of ROS production. Certain cancer treatment techniques, such as chemotherapy, immunotherapy, or hyperthermia target control over ROS production in tumour cells, resulting in the latter's irreparable damage and death. **Accurate quantification and characterization of ROS can be revolutionary for cancer treatment, but current methods cannot achieve proper analysis.**

Currently, standard ROS measurements use various molecular indicators such as fluorescent dyes or a fluorogenic CellROX probe[7], indicating oxidative stress in live cells and tissue. However, for in-vivo screening, it is desirable to use label-free techniques for ROS monitoring in cells. The use of fluorescent probes may alter the metabolic balance, influence cell life, and avoid further therapeutic applications. Therefore, as a label-free technique, Raman spectroscopy is the most frequently used to detect ROS, however, the signal is rather weak, and signal amplification techniques are required.

Among the different approaches, there is one to enhance the non-elastic scattered Raman signal based on surface plasmon resonance (SPR). SPR produces tightly confined, enhanced, and highly intense local electric fields resulting in a near-field enhancement in the vicinity of the structures which are utilized to enhance the performance of different physical effects[8] yielding signal enhancement as in surface-enhanced Raman spectroscopy (SERS). The correct architecture of nanoplasmonic surfaces can play a crucial role in the enhancement of Raman scattering excitation and emission cross-sections[9].

To further improve the SNR in bioimaging applications, current biosensing research bends towards the quantum properties of light. The microscopic and sensing techniques that utilize optical readout are approaching their absolute limits of detection as defined by the Heisenberg uncertainty principle in both, differential intensity and phase readout[10]. Yet, the use of more general minimum uncertainty states in the form of squeezed light can push the noise floor in these sensors below the shot noise limit (SNL)[11] associated with the noise of the coherent

state[12]. Very recently quantum-squeezed states of light are also becoming popular in cell research. The so-called quantum microscopy relies on the theoretical prediction that biological imaging can be improved without increasing the light intensity by using quantum photon correlations[13]. In 2021, C. A. Casacio et al. demonstrated for the first time quantum squeezing for the Raman imaging of molecular bonds within a cell with a 35% improved SNR compared to conventional microscopy, corresponding to a 14% improvement in concentration sensitivity[14].

Nanoplasmonic effects can play a fundamental role in further improving the SNR in Raman imaging, as well as in other microscopic techniques. Therefore, the combination of plasmonics and quantum-correlated states can establish new fundamental limits for biosensing and bioimaging applications. It is, however, important to understand whether the plasmonic effect influences quantum correlation or not. The first experimental observation of quantum optical effects in a plasmonic structure has shown that their entanglement survives[15] and the benefits of achieving a better SNR are conserved. Further research showed that the use of quantum correlated states in plasmonic sensing can enhance the sensor's sensitivity by up to 56%[16]. Although squeezing-enhanced Raman spectroscopy has already been reported[19], the latter has not yet been studied for SERS. Here, I will put together all the knowledge from the above-mentioned scientific approaches and gain information from biological samples such as ROS production in tumour cells. I will **develop a surface-enhanced Raman microscope coupled with a quantum-squeezed excitation source to study ROS concentration change in cells that undergo heat treatment yielding the death of tumour cells.**

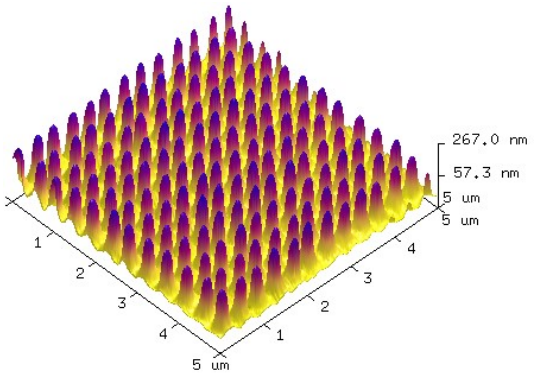

Fig. 2 Atomic Force Microscope 3D image of homogenously distributed periodic conical nanostructures fabricated at B-PHOT.

Problem Statement/Objectives

To address hyperthermia treatment influence on cancer cells, I will **develop a quantum-limited sensitivity-based Raman microscope to study the mechanisms of ROS production in tumour cells. This will yield an understanding of the conditions when tumour cells get damaged (apoptosis) or die (necrosis) after heat treatment.**

This multidisciplinary project has several objectives that will be fulfilled step-by-step in two years based on the work distribution listed below through the work packages (WPs). The whole project is divided into three main parts: Development of cell treatment and monitoring protocols; fabrication and optimization of nanoplasmonic structures for SERS measurements of ROS; quantum squeezed light coupling with plasmonics for Raman imaging.

WP1: Determine the effects of heat treatment on tumour cells by studying changes in the Raman signal of ROS variation.

Within the WP1 we will first determine the correlation between morphological changes in human liver cancer cells caused by extra heat, measured through an optical signal.

There are several ways to harm the tumour cells such as applying drugs, heating, and radiation, which are at the core of cancer treatment methods. ***Within the two years of this project, our focus will be on treating tumour cells under the temperature of 45°C for approximately one hour corresponding to a temperature used in hyperthermia cancer treatment[17] and monitoring changes in ROS production behavior leading to cell death.*** In this study, we will make use of HepG2 cells which come from a human liver cancer cell line that was derived from the liver tissue of a 15-year-old Caucasian male with hepatocellular carcinoma[18]. The effect of hyperthermia on HepG2 cell viability and ROS production mechanisms is still not fully understood and requires further investigation[19].

The feasibility of this WP1 is critical and is high given my existing expertise at Brussels Photonics (B-PHOT). In 2021 in B-PHOT at Vrije Universiteit Brussel we established a cell bio lab dedicated to HepG2 cell research. Currently, I am supervising a Ph.D. student who works on the development of a combined Raman and fluorescence microscopic system for drug-induced liver injury research on HepG2 cells. Consequently, the experience obtained with Raman measurements as well as cell growth and treatment techniques will be used in this project.

WP2: Development of a nanoplasmonic surface.

To achieve enhancement of weak Raman signal, in WP2 we will develop nanoplasmonic surfaces or so-called SERS substrates.

At B-PHOT we perform for a few years already intensive research on surface-enhanced Raman spectroscopy[20]. The gained expertise will be applied to this research. I, myself have recently demonstrated the use of two-photon polymerization (2PP) for SERS substrate fabrication[21] (see Figure 2) using Nanoscribe Photonic Professional GT+available at B-PHOT. This fabrication technique is ideal for proof-of-concept demonstration and fast prototyping since it does not require months of waiting time for lithographic nanofabrication. Therefore, the fabrication of the SERS substrates will be performed in-house by using a Nanoscribe system with optimized parameters. The structures will be fabricated on fused silica slides. The fabricated surfaces will be characterized with an Atomic Force Microscope available at our lab. Based on the obtained results, the tolerances of the fabrication will be used for the design of the final nanoplasmonic structures. The feasibility of this target is high since I am currently working on optimizing the nanofabrication of features with the smallest possible resolution of the device (≈200nm voxel diameter), pushing the system's boundaries. The first results on fabricated SERS substrates show a 10^4 enhancement factor of scattered Raman signal which is in line with commercially available SERS substrates. In addition, the possibility to develop the substrates in-house gives flexibility in design and adaptation to the cell geometries.

WP3: Generation of quantum-squeezed light.

The objective of the final WP3 is to build an optical system for quantum-squeezed light generation using an ultrafast pulsed laser[22] and to combine it with the SERS.

Single-mode squeezed light will excite the Raman signal of ROS in the cells and the collected SERS signal will be measured with a spectrum analyzer. To have a complete image of the cell morphology, we will perform sample scanning. In other words, the cell will be put on an XY translation stage and moved in the field of view of the squeezed light (see Figure 3). The first experiments to define the parameters of the quantum squeezer will be done at Joint Quantum Institution (JQI) at the University of Maryland, in collaboration with the group of Prof. Paul Lett, one of the pioneers in the field[23]. I will spend three months at JQI to perform Raman imaging of cells excited by squeezed light. In this work, we will benefit from the availability of a femtosecond laser with its second harmonic module (Ti:Sapphire and Second-Harmonic Generation (SHG) Module from Spectra-Physics) both at the JQI and Brussels Photonics at (VUB), to generate squeezed light with the parametric down-conversion (PDC) method[24] (Figure 3). Since JQI is specialized in squeezed light research, there are already setups available to perform initial tests on cells. I will generate squeezed light at the NIR wavelength range (between 700-800 nm) which is typically used in Raman spectroscopy. Next, the generated squeezed light will be used to excite the normal Raman of ROS in cells. Raman signal from H_2O_2 and the changes in the Raman signal of the cells will be studied. The

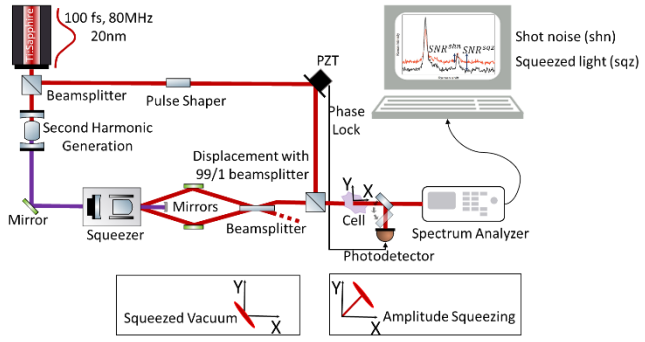

Fig. 3: Sketch of the amplitude squeezed states generation setup for cell spectroscopy.

former will show the variation in ROS levels caused by the heating and the latter will give information about cell mutation caused by the variation of ROS levels. The comparison between Raman signals excited with classical and quantum sources will give information about the quantum enhancement of the Raman signal.

As a final step, with the data collected at the University of Maryland, I will build a similar setup at VUB which will be the first quantum squeezer in Belgium. The performance of the squeezer will be benchmarked with the results obtained at the University of Maryland. Finally, SERS measurements will be performed for the first time with a quantum-squeezed excitation source.

The realization of these three work packages will lead to the establishment of a research topic at B-PHOT, Belgium focused on studying hyperthermia efficiency on cancer treatment by quantum-enhanced and plasmonic coupled Raman imaging.

Risks and mitigations

Risks (*Medium*) in WP1 and WP2 are mainly related to the weak Raman signal from the intercellular ROS. Although SERS substrates enhance the Raman scattered signal from cells, the background gets also enhanced and it can therefore be difficult to distinguish ROS's specific Raman peaks from other peaks coming from the cell. If required, Machine Learning (ML) algorithms for spectral data processing will be implemented. Our group already reported on the added values of ML techniques for Raman signal processing[25].

Risks (*High*) in WP3 are mainly experimental. Setting up the quantum squeezer process can face challenges because it is for the first time at our university that we will build such a system. To overcome this risk, I will get intensive training and preparation from pioneers in the field of quantum squeezing at the University of Maryland and can further rely on their expertise after my three-month stay.

A key point in this ambitious and novel research project is the fact that all the equipment needed for the experiments is in-house available for immediate use:

- Cell growth and treatment will be done in a fully equipped cell bio lab of the Photonics Innovation Center (PIC) at B-PHOT.
- B-PHOT owns a 2PP direct laser printer Nanoscribe GT+ to fabricate nanostructures.
- A gold coater is available in PIC for creating nanoplasmonic surfaces.
- The latter substrates will be characterized with AFM available at PIC.
- Raman measurements will be done using a Renishaw inVia confocal microscope.
- To realize quantum squeezing with a femtosecond laser, B-PHOT owns a Ti-Sapphire laser with a Second Harmonic Generation module.
- Finally, there is a Raman spectrum analyzer from Avantes (AvaSpec-HERO) available for the final measurements.

Outcome(s)

The scientific novelty of this project is the combination of quantum-squeezed light with surface-enhanced Raman spectroscopy to scan the intercellular environment. Whereas all three concepts are known and well understood on an individual basis, I will go beyond the state-of-the-art, by merging these 3 physical phenomena to obtain higher sensitivity and more than the reported 35% SNR in Raman imaging. As a result, this study paves the way for an increase in cancer detection rate in its early stages and treatment efficiency. Understanding the mechanism of tumour cells' damage while implementing heat will boost new possibilities for hyperthermia treatment, hence save lives.

After each WP is completed, I will write deliverables. The results will be published in open-access peer-reviewed journals, disseminating the research outcomes of the project to the public. Moreover, the project will be presented in outreach events often organized by B-PHOT. The establishment of the quantum squeezer at B-PHOT and coupling the quantum biosensing with plasmonics is a step forward in my career to prepare for a European Council Research Grant (ERC).

Impact(s)

- This research aims to bring a valuable impact on understanding the working principles of cancer treatment mechanism, such as hyperthermia on ROS production in tumour cells. This knowledge will next be used to expand the study of tumour cells' morphological changes after chemotherapy. I will collaborate with the university hospital (UZ-Brussel) to bring my research outcome to clinical benefit. Note, that I already have collaborations with the mentioned hospital.
- Beyond cancer treatment research ROS detection and quantification are of importance in the field of cardiovascular diseases, transplantology, inflammation and organ injuries, neuroscience, and ageing[26]. Hence all the mentioned fields will benefit from the development of a quantum-enhanced plasmonic excited nonlinear microscopic technique for more general ROS analyses.
- Developed two-photon polymerization-based fabrication technique for SERS substrates yields economic advantages to the project and further can be extended to other applications, hence polymer-based technologies are cheaper than traditionally used lithographic techniques.
- Startups bridging academic research with clinical personnel can take advantage of obtained knowledge from this project and develop miniaturized systems to use in the cancer treatment domain.

Project planning	MS - Milestone D - Deliverable M2 - Mobility to the University of Maryland (USA)							
	Year1				Year2			
	Q1	Q2	Q3	Q4	Q5	Q6	Q7	Q8
WP1		D1						
WP2				D2				
WP3								D3
Milestones	M1: SERS measurements of heat-treated HepG2 cells				M2: Development of Quantum squeezed light excitation system of plasmonic enhanced Raman imaging			

References

1. Sung, H. *et al.* Global Cancer Statistics 2020: GLOBOCAN Estimates of Incidence and Mortality Worldwide for 36 Cancers in 185 Countries.
2. O'Connor, C. M. & Adams, J. U. Essentials of Cell Biology.
3. Ray, P. D. et al. Reactive oxygen species (ROS) homeostasis and redox regulation in cellular signaling.
4. Zorov, D. B. et al. Mitochondrial Reactive Oxygen Species (ROS) and ROS-Induced ROS Release.
5. Waris, G. & Ahsan, H. Reactive oxygen species: role in the development of cancer and various chronic conditions.
6. Liu, R. *et al.* Oxidative Stress in Cancer Immunotherapy: Molecular Mechanisms and Potential Applications.
7. Rodrigues, M. B. An Efficient Technique to Detect Sperm Reactive Oxygen Species: The CellRox Deep Red® Fluorescent Probe.
8. Li, M., Cushing, S. K. & Wu, N. Plasmon-enhanced optical sensors: a review. *Analyst* **140**, 386–406 (2014).
9. Scott, R. *et al.* Two Photon Absorption in II–VI Semiconductors: The Influence of Dimensionality and Size.
10. Pooser, R. C. & Lawrie, B. Plasmonic trace sensing below the photon shot noise limit. 17.
11. Boyer, V., Marino, A. M., Pooser, R. C. & Lett, P. D. Entangled images from four-wave mixing.
12. Caves, C. M. Quantum-mechanical noise in an interferometer.
13. Taylor, M. A. & Bowen, W. P. Quantum metrology and its application in biology.
14. Casacio, C. A. *et al.* Quantum-enhanced nonlinear microscopy.
15. Altewischer, E., van Exter, M. P. & Woerdman, J. P. Plasmon-assisted transmission of entangled photons.
16. Dowran, M., Kumar, A., Lawrie, B. J., Pooser, R. C. & Marino, A. M. Quantum-enhanced plasmonic sensing.
17. Crezee, J., Franken, N. A. P. & Oei, A. L. Hyperthermia-Based Anti-Cancer Treatments.
18. Donato, M. T. et al. Culture and Functional Characterization of Human Hepatoma HepG2 Cells.
19. Wang, Q. *et al.* Sublethal hyperthermia enhances anticancer activity of doxorubicin in chronically hypoxic HepG2 cells through ROS-dependent mechanism.
20. Liu, Q. *et al.* SERS using two-photon polymerized nanostructures for mycotoxin detection.
21. Chalyan, T. et al. Two-Photon Polymerization based fabrication of SERS substrates for biosensing applications.
22. Xu, Z. *et al.* Quantum-enhanced stimulated Raman scattering microscopy in a high-power regime.
23. Lett, P. D. et al. Strong low-frequency quantum correlations from a four-wave-mixing amplifier.
24. Kouadou, T. Single-Pass Generation and Detection of Ultrafast Multimode Squeezed Light.
25. Chalyan T. et al. Benchmarking Spectroscopic Techniques Combined with Machine Learning to Study Oak Barrels for Wine Ageing.
26. Forrester, S. J. et al. Reactive Oxygen Species in Metabolic and Inflammatory Signaling.

Teerapat Rutirawut
Suranaree University of Technology, THAILAND

Executive Summary

"On-chip programable/controllable spatial light modulator for the next-generation quantum circuit using silicon nitride platform."

Quantum circuits are a fundamental concept in quantum computing and are essential as they provide a structured way to represent and manipulate quantum information using quantum gates, similar to classical circuits that use classical gates (like AND, OR, NOT gates) to manipulate classical bits. Quantum circuits facilitate the manipulation and processing of quantum information. They enable the encoding, transformation, and decoding of quantum states, which is crucial for performing quantum computations. The most startling and powerful future quantum technology is a quantum computer, which promises exponentially faster computation for particular tasks.

Spatial light modulators (SLM) are key components in the quantum optical circuit which will be further used to implement the gate in quantum computers. They are used to form optical wavefronts, generate hundreds of individually focused optical tweezers beams, and study new amplitude and phase modulation algorithms. As the quantum information processing tasks requires dense network connectivity, high dimensionality, and the possibility to actively reconfigure the network, nowadays techniques to fabricate the spatial light modulators are limited by the fabrication scalability, non-reconfigurable, and non-controllable.

In this research project, the invention of the optimal design of the programable/controllable SLM and the development of the fabrication process for the MMI and material integration will be performed. Based on the literature, the phase change material (PCM) is the material of use to manipulate the light in MMI showing as a reprogrammable SLM. The PCM reveal a low-power, but it is a passive wavefront shaping which require a reintegrate material to change the new- design wavefront shaping. Thus, in this research the integrated material of choice will be the liquid crystal (LC) with the SiN MMI to function a quantum linear transformation (two inputs to four outputs).

Material=> Liquid Crystal (LC)/Phase Change Material (PCM): Controllable/Programable SLM

=> Active Wavefront Shaping where the wavefront can be shaped real time by electrically changing the optical property of liquid crystal.

Design=> 2x2 MMI equipped with 2D-SLM (scalable up to NxM multiport MMI)

=> High-dimensional quantum operation in a small footprint

=> Easily scalable

Waveguide=> On-chip Silicon Nitride (SiN) MMI and Polarisation Beam Splitter (PBS)

=> Broad wavelength compatibility

=> Low losses and denser component architectures.

The simultaneous factors were established within the last decade which enabled this project in this timeline. (a) Advances in the field of photonics and nanotechnology, that enabled the controllable SLM proposed in this project. (b) The enormous leap in manufacturing techniques which enabled the fabrication of on-chip SLM and material integration to enable the next-generation quantum circuit. The on-chip programable/controllable spatial light modulator proposed in this project offers step change in both physical size, controllability and scalability limitation compared to existing SLM in quantum technology, making it an ideal candidate for SLM device in the next-generation quantum circuit.

Teerapat Rutirawut
Suranaree University of Technology, THAILAND

Project title: On-chip programable/controllable spatial light modulator for the next-generation quantum circuit using silicon nitride platform.

1. Literature Review

Over the past decades, quantum information science has emerged to consider as a powerful power and functionality which can be realized in the encoding, transmission, and processing of information by specifically harnessing quantum mechanical effects. The benefit of in quantum information technology to the new world‘s communication leading to the develpment in many quantum technologies include quantum key distribution which offers perfectly secure communication, quantum metrology which allows more precise measurements than could ever be achieved without quantum mechanics and quantum lithography which could enable fabrication of devices with features much smaller than the wavelength of light. The most startling and powerful future quantum technology is a quantum computer, which promises exponentially faster computation for particular tasks[1].

The search to develop a quantum computer require the fabrication of devices at the nano and possibly atomic scale, and precision control of their quantum mechanical states. The efficient implementation of quantum information processing tasks requires dense network connectivity, high dimensionality, and the possibility to actively reconfigure the network. Thus, linear optical networks are prominent candidates for practical quantum computing[2]. The requirements for realizing a quantum computer based a quantum optical circuit including a scalable physical qubit, two-photons state quantum systems that can be well isolated from the environment but also initialized, measured, and controllably interacted to implement a universal set of quantum logic gates. Currently, bulk and integrated linear optics are the most famous platforms which used to implement the linear optical networks. The general design of these networks is based on a cascade of beamsplitters and phase-shifters connected by single-mode waveguides [3, 4]. However, the scalability of bulk optics and the integrated linear optics is significantly limited by the construction process. The larger quantum optical circuit have been implement by uisng the integrated multimode waveguides and metasurfaces, but these technologies are not being reprogrammable after fabrication. Coupling spatial modes with many degrees of freedom such as polarization, time and frequency provides an alternative route to encoding and processing information with the larger dimension, but the engineering technique for these integrated optics required more improvement [5]. Therefore, the quest for a controllable high-dimensional optical network offering arbitrary connectivity is of interest.

2. Problem Statement/Objectives

Problem Statement

Quantum circuits are a fundamental concept in quantum computing and are essential as they provide a structured way to represent and manipulate quantum information using quantum gates, similar to classical circuits that use classical gates (like AND, OR, NOT gates) to manipulate classical bits. Quantum circuits facilitate the manipulation and processing of quantum information. They enable the encoding, transformation, and decoding of quantum states, which is crucial for performing quantum computations. The circuits are composed of quantum gates that perform specific quantum operations on quantum bits (qubits). These gates can create superpositions, entangle qubits, and apply unitary transformations. Moreover, the quantum circuits allow us to create and control superpositions and entanglement, two critical features of quantum mechanics that give quantum computers their unique power. Superposition enables qubits to exist in multiple states simultaneously, and entanglement allows the correlation of qubits, even when separated by long distances. Lastly, the quantum circuits are also used in quantum communication protocols, such as quantum teleportation and quantum key distribution, which offer secure and efficient ways of transmitting information.

Spatial light modulators (SLM) are key components in the quantum optical circuit which will be further used to implement the gate in quantum computers. They are used to form optical wavefronts, generate hundreds of individually focused optical tweezers beams, and study new amplitude and phase

Teerapat Rutirawut
Suranaree University of Technology, THAILAND

modulation algorithms. As the quantum information processing tasks requires dense network connectivity, high dimensionality, and the possibility to actively reconfigure the network, nowadays techniques to fabricate the spatial light modulators are limited by the fabrication scalability, non-reconfigurable, and non-controllable.

In 2012, the researcher at the department of physics of complex systems reported the use of the multimode waveguide to control the path of entangled two-photons. They experimentally show that two-photon path-entangled states can be coherently manipulated by multimode interference in multimode waveguides. This work reveals that multimode waveguides perform as a multiport beam splitter at the quantum level, creating a large variety of entangled and separable multipath [6]. In 2016, the scalable and reconfigurable all-optical spatial light modulator based on the silicon photonics circuits have been presented by the researcher from the University of Southampton. On-chip multimode interference (MMI) locally perturbed. This perturbation can redirect the propagation of light toward any specific output port and to evaluate the approach for all-optical routing purposes [7]. The use of an ultralow-loss phase change material with SLM in silicon photonic has been reported in 2021. The phase change material Sb_2Se_3 was used as the MMI cladding where the locally perturbation can be created on the phase change material. This work reveals the possibility to integrate the material on photonic chip for the benefit of the non-volatile programable modulation [8]. These SLM are reconfigurable and programable but not on use controllable. The use of on-chip photonic for generating heralded configurable, two-photon states in quantum optical circuit have been presented in 2021 [9]. While these techniques are widely used for the fabrication of SLM and the on-chip photonics became the need for scalable quantum circuit, there is no report on the use of on-chip controllable SLM for quantum optical circuit.

The above clearly illustrate the need to develop the scalable and programable/controllable spatial light modulators (SLM) is needed for the generation quantum circuit. Wavefront shaping by SLM equipped on multimode interference (MMI). The manipulation of a self-imaging effect in MMI can control the MMI output. As a solution to the challenge of compact and low-power integrated light modulation, nematic liquid crystal (LC), with strong birefringence at optical wavelengths, can be integrated into photonic platforms and used to manipulate the mode in photonic waveguides to induce a tunable phase shift. Integrated liquid-crystal-based devices on the silicon-nitride (SiN) waveguide for phase shift function showing the potential in using the integration of LC onto the photonic chip for the function of light modulation [10].

Silicon Nitride (SiN) is a common material in the electronics industry and is now becoming a choice of materials for the photonics industry as it is a fully CMOS (Complementary Metal Oxide Semiconductor) compatible platform for photonic integrated circuits. Therefore, SiN on silicon photonics technology allow an integration of electronic and optical system on the same chip by using the same fabrication techniques. Moreover, SiN is a material with a broadband transparent window, with low nonlinear losses, and a relatively low thermo-optic coefficient. These key properties of SiN are leading to a vast variety of applications covering from mid-infrared to ultra-violet regime. In quantum photonic technology, effective performance often relies on controlling individual photons. Because of this, it is especially important to control optical losses. This is where silicon nitride waveguides are outstanding. The broad transparency range SiN waveguides offers further advantages for quantum applications, enabling the integration of (single photon) light sources for schemes including spontaneous parametric down-conversion, spontaneous four-wave mixing sources and the integration of quantum dots.

Therefore, in this research project, the invention of the optimal design of the programable/controllable SLM and the development of the fabrication process for the MMI and material integration will be performed. Based on the literature, the phase change material (PCM) is the material of use to manipulate the light in MMI showing as a reprogrammable SLM. The PCM reveal a low-power, but it is a passive wavefront shaping which require a reintegrate material to change the new-design wavefront shaping. Thus, in this research the integrated material of choice will be the liquid crystal (LC) with the SiN MMI to function a quantum linear transformation (two inputs to four outputs).

Teerapat Rutirawut
Suranaree University of Technology, THAILAND

Liquid Crystal (LC): Controllable SLM

=> Active Wavefront Shaping where the wavefront can be shaped real time by eclectically changing the optical property of liquid crystal.

NxM multiport MMI equipped with 2D-SLM

=> High-dimensional quantum operation in a small footprint

=> Easily scalable

On-chip Silicon Nitride (SiN) MMI

=> Broad wavelength compatibility

=> Low losses and denser component architectures.

Objectives: A key task of this project is to design, create, and demonstrate the on-chip controllable spatial light modulator for the first time by using silicon nitride platform.

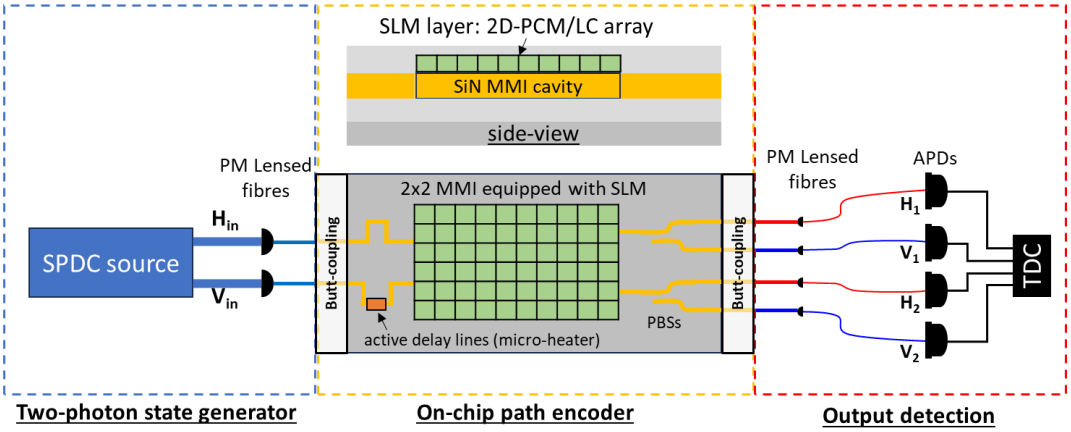

Figure1 : The design for an on-chip controllable spatial light modulator by using silicon nitride platform

Proposed research programme: The proposed on-chip programable/controllable spatial light modulator for the quantum circuit using silicon nitride platform will be designed, fabricated, and tested by separating into 3 working parts.

1. To design and fabricate the NxM multiport MMI equipped with 2D-SLM, both optical and electrical parameters have to be considered as they are affected to efficiency of the MMI. In this work, the designs of circuit and MMI dimension were optically and/or electrically simulated to optimise their performance. The optical simulations will be mainly performed by using FDTD solver. According to the optimal results from simulation, the layout of devices will be finally generated with Nazca software in order to create a lithography mask for the fabrication process.
2. The fabrication process will be performed in both THAILAND and UK. At Suranaree University of Technology, we have a great potential in the photonic chip fabrication facilities because there is the Synchrotron light research institute in the campus where they are sharing the facilities including the cleanroom with Suranaree University of Technology. So, the plan for fabrication process including the SiN photonic chip (w/ micro-heater), chip facets polishing for butt-coupling purpose via our collaborating research group, SLM integration by using a Phase change material (PCM) / Liquid Crystal (LC) at Suranaree University of Technology in Thailand. In case of using LC as SLM, electrode grid and electrical contacts prepared via our in-house cleanroom complex. In case of using PCM, SLM pattern will be written by using our in-house femtosecond laser writer.
3. The device characterization will be performed at Suranaree University of Technology and University of Southampton. I am now holding the visiting researcher position at University of Southampton where I did all the cleanroom fabrication when I was a PhD student and research fellow there.

Teerapat Rutirawut
Suranaree University of Technology, THAILAND

Therefore, some fabrication process and the characterization can be performed both in Thailand and in the UK. The University of Southampton can support this research work by sharing the facilities and exchange knowledge through the collaboration.

Equipment needed for the project

Activity	Equipment	Availability	
		Yes	Need to order
1. Two-photon state generator setting-up	Spontaneous Parametric Down Conversion (SPDC) source [1x]	✓	
	GRIN lens couples [2x]		✓
	Polarisation maintaining lensed fibres Array [2x]		✓
	3-axis micro stages for butt-coupling [1x]	✓	
2. APDs output detection setting-up	Avalanche Photodiodes (APD) [4x]		✓
	Time-Digital Converter (TDC) [1x]	✓	
	Polarisation maintaining lensed fibres Array [4x]		✓
	3-axis micro stages for butt-coupling [1x]		✓
3. SiN quantum photonic circuit simulation and design	Waveguide simulator for 2x2 MMI+SLM simulation [open-source]	✓	
	Circuitry mask design [open-source]	✓	
	SLM phase pattern calculator [open-source]	✓	
4. On-chip quantum photonic device preparation	SiN photonic chip (w/ micro-heater) ordered via a MPW project provided by a research SiP foundry		✓
	Chip facets polishing for butt-coupling purpose via our collaborating research group (cost of consumable materials e.g. polishing pads)		✓
	SLM integration by using a Phase change material (PCM) / Liquid Crystal (LC) via our collaborating research group in Thailand (cost of chemicals for preparing SLM material)		✓
	In case of using LC as SLM, electrode grid and electrical contacts prepared via our in-house cleanroom complex	✓	
	In case of using PCM, SLM pattern will be written by using our in-house femtosecond laser writer	✓	
5. Quantum circuit test - LC based SLM programming	SLM phase pattern display controller		✓

3. Outline of tasks/Workplan

Project workflow: The research group at the Suranaree University of Technology will be working on developing a prototype on-chip controllable spatial light modulator by using silicon nitride platform. This will include the simulation, mask design, and material integration.

Teerapat Rutirawut
Suranaree University of Technology, THAILAND

University of Southampton will be the collaborator to fabricate the NxM multiport MMI equipped with 2D-SLM .

Quantum consortium in Thailand and UK are the stake holder who will test the prototype of the on-chip controllable spatial light modulator by using silicon nitride platform both in Thailand and UK.

4. Outcomes

At the end of the first year, we expect to achieve the design and lab-scale prototype of the on-chip controllable spatial light modulator by using silicon nitride platform. The device and characterization of the device will be performed if the project can continue to the second year of this research work.

At least two publications are expected related to the design and the experimental validation of the prototype of the on-chip controllable spatial light modulator by using silicon nitride platform. The second publication will be about the applications in of the controllable SLM for quantum optical circuit.

5. Impact

The novel on-chip controllable spatial light modulator by using silicon nitride platform proposed in this project offers a step change in physical size, controllability and scalability limitation compared to existing SLM in quantum technology, making it an ideal candidate for SLM device in the next-generation quantum circuit. By collaborate this research project between Suranaree University of Technology and the Optoelectronics Research Centre (ORC), University of Southampton will allow the exchange of knowledge and know how through human resources, access to equipment and consumables which will be able to establish and maintain this collaboration.

The Optoelectronics Research Centre (ORC), University of Southampton has a long-established track of record for pioneering work in photonics and is now internationally recognised as a world leader in the field of silicon photonic. In 2008 the ORC moved into a new building incorporating a state-of-the-art (>100 million pound) clean room which is one of the premiere cleanrooms in Europe, ensuring that fabrication capabilities remain truly world class. Silicon photonics group at ORC currently has more than 50 research staff. This expertise has been consistently recognised by EPSRC and many European projects such as “PlasminiAC”, most recently when the ORC was selected to host Future Photonics Hub creating a bridge between industry and academia.

References

1. O'Brien, J.L., *Optical Quantum Computing.* Science, 2007. **318**(5856): p. 1567-1570.
2. Leedumrongwatthanakun, S., et al., *Programmable linear quantum networks with a multimode fibre.* Nature Photonics, 2019. **14**: p. 139-142.
3. Flamini, F., N. Spagnolo, and F. Sciarrino, *Photonic quantum information processing: a review.* Reports on Progress in Physics, 2019. **82**(1): p. 016001.
4. Matthews, J.C.F., et al., *Manipulation of multiphoton entanglement in waveguide quantum circuits.* Nature Photonics, 2009. **3**(6): p. 346-350.
5. Xu, Q., et al., *Electrically tunable optical polarization rotation on a silicon chip using Berry’s phase.* Nature Communications, 2014. **5**(1): p. 5337.
6. Poem, E., Y. Gilead, and Y. Silberberg, *Two-Photon Path-Entangled States in Multimode Waveguides.* Physical Review Letters, 2012. **108**(15): p. 153602.
7. Bruck, R., et al., *All-optical spatial light modulator for reconfigurable silicon photonic circuits.* Optica, 2016. **3**(4): p. 396-402.
8. Delaney, M., et al., *Nonvolatile programmable silicon photonics using an ultralow-loss Sb₂Se₃ phase change material.* Science Advances, 2021. **7**(25): p. eabg3500.
9. Hua, X., et al., *Configurable heralded two-photon Fock-states on a chip.* Optics Express, 2021. **29**(1): p. 415-424.
10. Notaros, M., et al., *Integrated visible-light liquid-crystal-based phase modulators.* Optics Express, 2022. **30**(8): p. 13790-13801.

LIGHTING RESEARCH SOLUTIONS LLC
Research • Education • Design • Development • Verification
www.**L**ighting**R**esearch**S**olutions.com | Philadelphia, PA 19122 USA

The Earth and its inhabitants require darkness

July 16, 2023

Executive Summary
Humans use electric light at night to illuminate our homes, our streets, sidewalks, outdoor sporting events, buildings, facades, landmarks, bridges, parks, parking lots, and commercial and industrial properties. Nearly everything we interact with at night is illuminated. Light at night has become essential to our feeling of security and to our ability to extend our activities into the evening.

But this is not without cost. Outdoor electric light sources placed by humans to illuminate the night—often called *artificial* or *anthropogenic* (i.e., "human generated") light at night (ALAN)—is seriously eroding natural light-dark cycles across the planet, having marked impacts on the biological functions and rhythms of humans, plants, and animals. This includes impacts on mortality (through light attraction or aversion), disruption of migratory and diurnal patterns, increasing or decreasing population size, altering natural competition, disturbing inter-species communication, and negative impacts on human health and well-being.

A significant portion of the Earth's population—especially in Europe and the Americas—now experiences light-polluted nights, which creates a sky glow that limits or eliminates our view of the night sky, poses significant problems for amateur and professional astronomical observations, negatively impacts animals in a myriad of ways, and wastes a significant amount of energy at great financial cost. The estimated cost of this wasted energy exceeds USD $7 Billion.

Without serious intervention, the problem is projected to get worse.

The objective of this project is to advance the science in architectural lighting with the goal of developing actionable guidance—for the lighting industry and local legislators—to reduce the negative impacts of ALAN, to disseminate research findings to spread awareness of these negative impacts, and to develop lightings standards and initiatives that minimize the negative impacts of ALAN (especially sky glow).

Corresponding to these objectives, the project will constitute three tasks.

Task 1 | advance research: the goal of this task is to advance research in the field of architectural lighting to provide actionable guidance for lighting professionals and local legislators. The work will study the barriers to use of promising emerging lighting technologies, such as phosphor-converted amber LEDs, and challenges faced by change-makers. The outcome of task 1 is a journal-quality research paper that will be submitted to an Optica journal, likely Optics Express. This work will provide actionable guidance for change-makers and influence standard ordinance language for local legislators being developed by DarkSky (formerly the International Dark Sky Association).

Task 2 | disseminate and advocate: to goal of task 2 is to spread awareness of the negative impacts of light at night by disseminating work at industry and industry-adjacent events. The outcome of this task is a series of educational presentations and scientific reports. The impact of this work is an increased awareness and sensitivity to the impacts of light at night.

Task 3 | reduce light pollution: the goal of this task is to develop new lighting standards and drive important changes to existing lighting standards. This includes an expansion of ANSI C78.377-2017 (an influential LED chromaticity standard) based on my previous research work, additional light pollution mitigation incentives in products from the International WELL Building Standard (where I am the *Director* of the *Lighting Concept*), and updated recommendations and standard ordinance language for local legislators from DarkSky, and organization with whom I liaise.

Thank you for your time and consideration. I am grateful for this potential opportunity. Thank you.

LIGHTING RESEARCH SOLUTIONS LLC
Research • Education • Design • Development • Verification
www.**L**ighting**R**esearch**S**olutions.com | Philadelphia, PA 19122 USA

The Earth and its inhabitants require darkness

July 16, 2023

Proposal

Background (and literature review)

Humans use electric light at night to illuminate our homes, our streets, sidewalks, outdoor sporting events, buildings, facades, landmarks, bridges, parks, parking lots, and commercial and industrial properties. Nearly everything we interact with at night is illuminated. Light at night has become essential to our feeling of security and to our ability to extend our activities into the evening.

But this is not without cost. Outdoor electric light sources placed by humans to illuminate the night—often called artificial or anthropogenic (i.e., "human generated") light at night (ALAN)—is seriously eroding natural light-dark cycles across the planet [Sanders 2020; Kyba et al 2017]. The negative impacts of ALAN are endless and have marked impacts on the biological functions and rhythms of living organism [Jagerbrand and Bouroussis 2021]. Here are some examples:

- It disrupts circadian rhythms (e.g., in humans [Tahkamo et al 2018])
- It suppresses melatonin—the "hormone of darkness"—in humans (e.g., Brainard 2001; Thapan 2001) and other vertebrates (e.g., Grubisic et al 2019)
- Decreases survivability and growth (e.g., in coral reef fish [Schligler et al 2021])
- Impacts hormone levels of animals, alters daily onset of activity in diurnal species and life history trats (e.g., number of offspring, predation, and cognition [Sanders et al 2020])
- It impacts cognition and sea finding in sea turtles [Berry et al 2013], a disorientation that causes them to wander significant distances from the ocean, leaving them susceptible to predators and accidental death by humans[1]
- Alters the balance of species, biodiversity, and predation in entire ecosystems [Spoelstra et al 2015]
- Produces physiological responses in plants, which impacts their seasonality, growth, and resource allocation [Bennie at al 2016]
- Disrupts visual signaling between flowers, pollinators, and predators (e.g., hawkmoths [Briolat et al 2021])
- Light attracts some organisms (moths, frogs, sea turtles), concentrating them as a food source to be preyed upon (or creating a trap which exhausts and kills them). Light repels some organisms, pushing them out of their habitat. Light alters the day/night patterns, resulting in insufficient sleep and associated consequences.[2]
- And many, many more.

ALAN is also a significant contributor to sky glow, which is described as "the brightening of the night sky that results from the scattering and reflection of light from the constituents of the atmosphere [of Earth]…in the direction of the observer" [IES 2021]. Sky glow limits or eliminates our view of space and the stars, poses significant problems for professional and amateur astronomy, has negative impacts on animal behavior patterns (e.g., on migratory species [UN 2021]), and wastes a significant amount of energy at great financial cost (estimates exceed USD $7 Billion [Gallaway et al. 2010]).

[1] https://myfwc.com/wildlifehabitats/wildlife/sea-turtle/lighting/disorientations/
[2] Paraphrased from: https://myfwc.com/conservation/you-conserve/lighting/criteria/

To add insult to injury, the problem is getting worse. Most of the world's population now experiences light polluted nights. Here, I will quote some of the world's experts to illustrate the severity and dire nature of the situation:

> "About two-thirds of the World population and 99 per cent of the population in the United States (excluding Alaska and Hawaii) and European Union live in areas where the night sky is above the threshold set for polluted status. …about one-fifth of the World population, more than two-thirds of the United States population and more than one half of the European Union population have already lost naked eye visibility of the MilkyWay." [Cinzano et al 2001]

> "…more than 80% of the world and more than 99% of the U.S. and European populations live under light-polluted skies. The Milky Way is hidden from more than one-third of humanity, including 60% of Europeans and nearly 80% of North Americans. Moreover, 23% of the world's land surfaces between 75°N and 60°S, 88% of Europe, and almost half of the United States experience light polluted nights." [Falchi et al 2016]

Without serious intervention, light pollution will get worse, wasting a significant amount of energy and increasing the negative impacts of ALAN on humans, plants, and animals.

Problem Statement/Objective

Humans light up the nighttime environment generating light pollution that wastes a significant amount of energy and causes a suite of deleterious impacts on humans, plants, and animals. This includes [Jagerbrand and Bouroussis 2021], but it not limited to, the following:

- **Mortality rates of species:** species attracted to light may be killed. As a concentrated food source for their predator(s), this may lead to an imbalance in the ecosystem
- **Migratory patterns:** light disrupts natural migratory patterns and disorients animals. This kills a significant number of migratory birds each year.
- **Increasing or decreases population size:** light can increase or decrease foraging of various species
- **Alters natural competition:** light may benefit some species at the expense of others
- **Communication:** light can disturb species-specific communication
- **Health and circadian rhythm:** ALAN impacts various physiological processes, such as hormone production and maintaining a normal circadian rhythm, which impacts human health and well-being.

Without serious intervention, the problem is expected to worsen. The objective of this project is to advance research in architectural lighting with the goal of developing strategies to reduce the negative impacts of anthropogenic light at night (specifically investigating the barriers to the implementation of emerging technologies and how to address the challenges of change-makers like local municipalities), to disseminate research findings to spread awareness of these negative impacts, and to develop lighting industry standards to minimize light pollution (especially sky glow).

Outline of Tasks/Work Plan

Task 1 | advance research: I recently co-authored a journal article published by LEUKOS, the journal of the Illuminating Engineering Society [Esposito and Radetsky 2023]. In that work, my co-author and I detail how light source spectral power distribution—i.e., the specific combination of wavelengths of radiation that a light source emits—impacts sky glow. We then provide a specification framework for architectural lighting practitioners to consider the impact of light sources on sky glow during the design phase of their lighting projects and provide actionable recommendations for choosing light sources that have the potential to reduce sky glow. We identified emerging lighting

technologies (such as very "warm" LEDs[3] or those based on phosphor-converted amber technology[4]) that have the potential to reduce sky glow and other negative impacts of light at night by providing a light source spectrum with reduced short wavelength ("blue") radiation. Concurrently, we also identified potential barriers these technologies face in entering the commercial market such as a lack of consumer education, concerns with visibility and safety, color confusion, misunderstanding of efficacy, lack of general awareness of these products, and a broader lack of knowledge that light at night is destroying ecosystems and negatively impacting human health. Studying the technologies and design practices that have the potential to reduce light pollution was recently identified as an important knowledge gap by the DarkSky (formerly the International Dark Sky Association).[5]

With Optica support, I will implement a research project that investigates these barriers more methodically. For this work, I will interview a range of stakeholders and change agents, including lighting product manufacturers (I have contacts at major semi-conductor manufacturers), product certification programs (such as LUNA from the DesignLights Consortium[6], with whom I also have close contact), and legislators in local government and municipalities. To date, there has not been a systematic investigation of the challenges that local legislators face in combatting light pollution. Understanding the challenges of these change agents is a necessary step in achieving real change, and is a current prerogative of DarkSky. I am amenable to publishing this work in one of Optica's journals. Optics Express is frequently used by authors in my industry. I have previously published there as well [e.g., Esposito and others 2022].

Task 2 | disseminate and advocate: To spread awareness of the negative impacts that light at night has on humans, plants, and animals, my current and future research findings will be presented at five (5) industry and industry-adjacent conferences and events. This includes the Annual Conference of the Illuminating Engineering Society, LightFair 2024/2025, The Enlighten Americas/Europe Conferences hosted by the International Association of Lighting Designers (IALD), and LEDucation (a lighting trade show for lighting equipment manufacturers whom this work will influence).

Task 3 | develop lighting standards: In the lighting industry, there are currently no lighting standards or actionable recommendations to reduce the negative impacts of light at night. Without lighting standards, lighting manufacturers, lighting designers, and building owners are left to figure it out on their own. There are three ways I can influence lighting standards, with support from Optica:

1. In my co-authored work described in Task 1 [Esposito and Radetsky 2023], my co-author and I propose a set of LED chromaticity definitions that expand the existing definitions of ANSI C78.377-2017,[7] a highly influential standard in the lighting industry. I have been in contact with the committee that publishes this standard. They have preliminarily agreed to modify the scope of the document and to incorporate my research work. Funding from Optica will support my contribution to the committee and to performing any additional analyses.
2. I currently serve at the *Director* of the Lighting Concept on the Standard Development team at the International WELL Building Institute (IWBI). Support from Optica will allow me to spend additional research time developing new features for the WELL Building Standard[8] and the WELL Community Standard[9] that incentive building owners to reduce light pollution.
3. I currently liaise with DarkSky (formerly the International Dark Sky Association), to maximize the impact of my research work on their Fixture Seal of Approval Program as well as their model lighting ordinance language for legislators. I will coordinate this research work with DarkSky to develop standard ordinance language and outline strategies to support local municipalities.

[3] https://led-ld.nichia.co.jp/en/product/lighting_lowcct.html
[4] Example: https://led-ld.nichia.co.jp/en/product/lighting_dmc.html
[5] https://zenodo.org/record/6903500
[6] https://www.designlights.org/our-work/luna/
[7] https://www.nema.org/standards/view/American-National-Standard-for-Electric-Lamps-Specifications-for-the-Chromaticity-of-Solid-State-Lighting-Products
[8] https://v2.wellcertified.com/en/wellv2/light
[9] https://v2.wellcertified.com/en/community/light

Outcomes

- **Outcome of Task 1**: This task will produce peer-reviewed research that advances the science of the negative impacts of anthropogenic light at night *with a focus on actionable advice for mitigating the problem* and implementable strategies for local governments and municipalities. This is a specific focus of the International Dark Sky Association ("DarkSky"),[10] with whom I directly liaise, and will be influential in their development of the successor to the Model Lighting Ordinance (MLO)[11] that they are currently developing for regulators.
- **Outcome of Task 2**: The architectural lighting industry is centrally poised to help mitigate the negative impacts of light at night through advanced design and advocacy strategies. The goal of Task 2 is to translate research work into lighting practice—including the findings of this project—to equip them with the knowledge and tools for doing so. This will include multiple lectures and paper presentations at industry conferences and meetings with change makers.
- **Outcome of Task 3**: The goal of Task 3 is to develop new lighting standards and drive important changes to existing lighting standards. To this end, this work will drive an important expansion to ANSI C78.377-2017, an influential LED chromaticity standard (for the purpose of reducing sky glow), provide support for developing new features in products from the International WELL Building Institute (where I am the *Director* of the lighting concept), and develop strategies and standard ordinance language for DarkSky (formerly the International Dark Sky Association).

Impact

- **Impacts of Task 1 | knowledge and lighting recommendations:** research work will address two questions in the pursuit of reducing the impact of light pollution: 1. What are the barriers to emerging lighting technologies (e.g., phosphor-converted amber LEDs)? and 2. What challenges do local municipalities and legislators face in combatting light pollution? This work will provide recommendations for lighting practice (including overcoming barriers for emerging technologies) and propose strategies and ordinance language for local legislators.
- **Impacts of Task 2 | awareness:** awareness inside and outside of the lighting industry is necessary to create broad change. Spreading awareness within the lighting industry is necessary for measurable change since lighting professionals are partially responsible for lighting up the night. Spreading awareness outside of the lighting industry is important since we lack a cultural awareness of the negative impacts of light at night; local legislators are important change-makers that will be much of the focus of this work.
- **Impacts of Task 3 | reduced impacts of light at night:** The lighting industry is currently missing lighting standards developed *on sound science that provide actionable guidance*. Developing such standards has the potential to profoundly reduce the negative impacts of light at night and drastically reduce sky glow, and I have a unique position in the industry to inform and influence these standards. For example, I have been invited to contribute my research work (see Esposito and Radetsky 2023] to expand ANSI C78.377-2017 (a highly influential chromaticity standard for LED light sources); I am the *Director and Light Concept Lead* at the International WELL Building Institute; and I directly liaise with Dark Sky to drive impactful change (such as developing strategies for local government and municipalities).

The negative impacts of human-generated light at night are vast and getting worse. Existing lighting standards are insufficient to reduce these negative impacts and not enough actionable guidance exists for members of the lighting industry and local legislators. Funding this project has the potential to set in motion a cascade of lighting standards development activity intended to darken our planet and minimize our impact on Earth's creatures.

[10] https://www.darksky.org/our-work/

[11] https://www.darksky.org/our-work/lighting/public-policy/mlo/

Acknowledgement

I want to thank Optica a funding opportunity for work that is important, but otherwise difficult to find support for. I am grateful for the potential opportunity to fight for nighttime darkness for Earth's inhabitants. I look forward to hearing the outcome of your decisions.

Thank you,

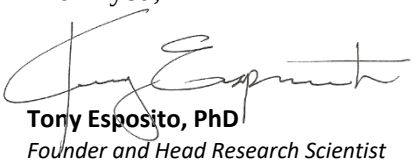

Tony Esposito, PhD
Founder and Head Research Scientist
Lighting Research Solutions LLC
tesposito@LightingResearchSolutions.com

Bibliography

Berry, M., Booth, D. T. & Limpus, C. J. Artificial lighting and disrupted sea-finding behaviour in hatchling loggerhead turtles (Caretta caretta) on the Woongarra coast, south-east Queensland, Australia. Aust. J. Zool. 61, 137–145 (2013).

Briolat, E.S., Gaston, K.J., Bennie, J. et al. Artificial nighttime lighting impacts visual ecology links between flowers, pollinators and predators. Nat Commun 12, 4163 (2021). https://doi.org/10.1038/s41467-021-24394-0

Brainard GC, Hanifin JP, Greeson JM, Byrne B, Glickman G, Gerner E, Rollag MD. Action spectrum for melatonin regulation in humans: evidence for a novel circadian photoreceptor. J Neurosci. 2001 Aug 15;21(16):6405-12. doi: 10.1523/JNEUROSCI.21-16-06405.2001. PMID: 11487664; PMCID: PMC6763155.

Conservation of migratory species (CMS). 2021. Impact of light pollution on different taxa of migratory species. Convention on the Conservation of Migratory Species of Wild Animals

Esposito T, Royer MP, Houser KW, "Measures of illuminant-induced metameric mismatch: theory, comparative analysis, and implications for application," Opt. Express 30, 14686-14708 (2022)

Esposito T, Radetsky LC. 2023. Specifying Non-White Light Sources in Outdoor Applications to Reduce Light Pollution. LEUKOS. 19(3): 269-293. DOI: 10.1080/15502724.2022.2121285

Gallaway T, Olsen RN, Mitchell DM. 2010. The economics of global light pollution. Ecol Econ. 69(3):658–665. https://doi.org/10.1016/j.ecolecon.2009.10.003

Grubisic, M.; Haim, A.; Bhusal, P.; Dominoni, D.M.; Gabriel, K.M.A.; Jechow, A.; Kupprat, F.; Lerner, A.; Marchant, P.; Riley, W.; Stebelova, K.; van Grunsven, R.H.A.; Zeman, M.; Zubidat, A.E.; Hölker, F. Light Pollution, Circadian Photoreception, and Melatonin in Vertebrates. Sustainability 2019, 11, 6400. https://doi.org/10.3390/su11226400

Kyba CCM, Kuester T, Sánchez de Miguel A, Baugh K, Jechow A, Hölker F, Bennie J, Elvidge CD, Gaston KJ, Guanter L. 2017. Artificially lit surface of Earth at night increasing in radiance and extent. Sci Adv. 3(11):e1701528. https://doi.org/10.1126/sciadv.1701528

Leena Tähkämö, Timo Partonen & Anu-Katriina Pesonen (2019) Systematic review of light exposure impact on human circadian rhythm, Chronobiology International, 36:2, 151-170, DOI: 10.1080/07420528.2018.1527773`

Sanders D, Frago E, Kehoe R, Patterson C, Gaston KJ. 2021. A meta-analysis of biological impacts of artificial light at night. Nat Ecol Evol. 5(1):74–81. https://doi.org/10.1038/s41559-020-01322-x

Schligler J, Cortese D, Beldade R, Swearer SE, Mills SC. Long-term exposure to artificial light at night in the wild decreases survival and growth of a coral reef fish. Proc Biol Sci. 2021 Jun 9;288(1952):20210454. doi: 10.1098/rspb.2021.0454. Epub 2021 Jun 9. PMID: 34102892; PMCID: PMC8187998.

Spoelstra, K., van Grunsven, R.H.A., Donners, M., et al. (2015) Experimental illumination of natural habitat – an experimental set-up to assess the direct and indirect ecological consequences of artificial light of different spectral composition. Philosophical Transactions Royal Society B. 370: 20140129. doi: 10.1098/rstb.2014.0129

Thapan K, Arendt J, Skene DJ. An action spectrum for melatonin suppression: evidence for a novel non-rod, non-cone photoreceptor system in humans. J Physiol. 2001 Aug 15;535(Pt 1):261-7. doi: 10.1111/j.1469-7793.2001.t01-1-00261.x. PMID: 11507175; PMCID: PMC2278766.

Jägerbrand, A.K.; Bouroussis, C.A. Ecological Impact of Artificial Light at Night: Effective Strategies and Measures to Deal with Protected Species and Habitats. Sustainability 2021, 13, 5991. https://doi.org/10.3390/su13115991

Label-free Widefield Multi-modal Interferometric-Raman Microscope for Exosome Imaging and Early Cancer Detection

Executive Summary:

Cancer remains a global health challenge, leading to the loss of millions of lives each year. Timely diagnosis plays a crucial role in increasing survival rates and improving patient outcomes. This project aims to address the urgent need for early cancer detection through the development of a multi-modal exosome imaging platform for liquid biopsy applications.

Exosomes, nanometer-sized extracellular vesicles found in body fluids, have emerged as potential biomarkers for various types of cancer. They carry a diverse array of molecules, including RNAs, DNA, proteins, and lipids, making them valuable indicators of disease progression. However, the translation of exosome research into clinical practice requires rapid and efficient exosome isolation methods, as well as sensitive and comprehensive characterization tools. Conventional isolation methods, such as ultracentrifugation, are labor-intensive and time-consuming. Standard analytical techniques, such as ELISA and western blot analysis, require large sample volumes and complex labeling procedures. These limitations hinder the development of high-throughput and clinically viable exosome analysis techniques.On the other hand, their heterogeneity requires the detection and analysis of individual exosomes to obtain comprehensive diagnostic information.

In this project, we propose the development of a complete label-free detection and quantification platform for exosome analysis in prostate cancer patients. The proposed platform combines an advanced interferometric microscope and a Raman module to enable label-free detection and quantification of exosomes at the single-particle level. By visualizing and characterizing individual exosomes, the platform overcomes the limitations of conventional ensemble-averaged methods and provides a more accurate representation of the exosome population's heterogeneity.The Interferometric module enables the visualization and size estimation of individual exosomes with high sensitivity and a large field of view. Novel data processing algorithms, including machine learning techniques, will be implemented to enhance resolution and accuracy. The Raman module provides chemical composition analysis, enabling the determination of the cellular origin of exosomes and the identification of tumor-derived exosomes.

The platform's validation will be conducted using clinical samples obtained from both healthy donors and prostate cancer patients. Through the multiparameter characterization of exosomes, including size distribution, concentration, and spectral signatures, we aim to differentiate exosomes derived from healthy cells and tumor cells. This validation process will demonstrate the clinical potential of the developed platform for early cancer detection.

The outcomes of this project will advance our understanding of exosomes as diagnostic markers for cancer, specifically prostate cancer. The label-free platform will provide accurate visualization and chemical characterization of exosomes, leading to improved diagnostic capabilities. By harnessing the power of exosomes, this research has the potential to revolutionize routine cancer patient monitoring, enabling the early detection of cancer-specific biomarkers and reducing the financial and economic burdens associated with advanced-stage treatments.

Moreover, the developed platform's adaptable nature allows for potential applications beyond cancer research. It can be utilized in the study of other diseases and viral infections, such as the detection and characterization of viral particles. This versatility paves the way for efficient virus detection, rapid diagnostics, and the development of targeted therapeutic interventions.

In summary, this project addresses the critical need for early cancer detection by developing a multi-modal exosome imaging platform. By focusing on the detection and analysis of individual exosomes isolated from the body fluids, the platform provides a more accurate representation of their heterogeneity. This advancement in exosome research has significant implications for cancer diagnostics, personalized medicine, and the broader understanding of disease biomarkers. The outcomes of this research will contribute to improved patient outcomes and pave the way for novel therapeutic approaches in the fight against cancer.

Label-free Widefield Multi-modal Interferometric-Raman Microscope for Exosome Imaging and Early Cancer Detection

1. Literature Review : Exosomes are nanometer sized (30-150 nm) extracellular vesicles, found in the body fluids such as blood, saliva and urine[1]. They are secreted from nearly all types of cells and contain various molecules including RNAs, DNA, proteins and lipids, which makes them critical for liquid biopsy applications. In recent years, exosomes emerged as potential biomarkers for cancer and neurodegenerative diseases[2]. Specifically, a variety of exosome-based biomarkers are discovered for cancer diagnostics such as pancreatic cancer[3], melanoma[4], lung cancer[5], and prostate cancer[6]. Although utilization of exosomes holds great potential for clinical applications in early diagnosis and treatment monitoring**, rapid, high-yield exosome isolation** and **robust, sensitive, high-throughput exosome characterization tools** are required to translate the exosome research into clinical practice.

Conventional isolation methods such as ultracentrifugation is labor intensive and time consuming. On the other hand, standard analytical characterization techniques such as ELISA or western blot analysis requires large volumes of sample and complex labeling procedures. Aside from increasing the complexity of the sample preparation protocols, labelling might also perturb the functionality of the particle of interest. Another characterization tool frequently used in the laboratories is Nanoparticle Tracking Analysis (NTA)[7] which measure the concentration and the size distribution of the particles. However, this technique doesn't provide any information about the content of the particles without using any labels. Moreover, all these methods provide only **ensemble averaged information**, making **single particle level characterization** is not possible.

Direct detection of a single exosome is challenging because of its size and low refractive index. Novel label-free platforms with single particle sensitivity have been demonstrated recently, using surface plasmon resonance[8], interferometry, whispering gallery mode resonators[9] or microchannel suspended resonators[10]. Among them nPLEX[8] is an SPR based device, in which sensor surface of the device is composed of complex periodic nanohole arrays. The sensor surface is functionalized with antibodies and the exosomes that bind to the surface is detected by monitoring the change in the optical transmission. Although the system is able to detect individual exosomes isolated from ovarian tumor cells, it doesn't provide any information on the size of each particle. Another label-free method that utilizes microtoroid resonators[11], provides single particle level exosome detection, however it requires complex fabrication and calibration steps, as the signal is highly dependent on the binding location.

Interferometric techniques offer robust and easy-to-implement solutions for nanosized particle visualization. Although different acronyms are introduced such as iSCAT[12], SP-IRIS[13] and COBRI[14] the basic mechanism is the same: the interference of the reference light and the scattered light emerging from the sample. Implementation of successful background removal methods in interferometric imaging enabled detection of individual viruses[15], exosomes[16] and even single proteins[17]. Particularly, iSCAT uses high-speed cameras to capture the interferometric images of the samples, and its background removal is based on subtracting consecutive frames to detect particle binding events. Due to requirement of high frame rate, its field of view is limited, which restricts its utilization as a biosensing platform. On the other hand, SP-IRIS[13] implements a microfabricated layered sensor surface as a sample substrate, which provides a relatively uniform background. Integration of Fourier filters to selectively remove the reference field enabled the detection of dielectric particles with 50 nm diameter. Recently we demonstrated that the utilization of defocused images in the data analysis pipeline improves the sensitivity of interferometric imaging[18]. We visualized dielectric particles as small as 30 nm in diameter, with a field of view of 300 µm x 200 µm.

2. Problem Statement/Objective: Although label-free interferometric techniques provide information on the size of individual particles or the concentration of the sample, captured images don't reveal any information about the chemical content. Sensor surface simply can be functionalized with antibodies to quantify surface protein content of the exosomes. Furthermore, by utilizing antibody microarrays multiplexed analysis can be performed. However, antibody immobilization has its own problems related to complex surface activation procedures. In general, protein microarrays exhibit huge spot-to-spot and sample-to-sample variation, which is the bottleneck for their clinical use. Moreover, the information is still limited by the type and the number of antibodies used. **Unfortunately, there is no single imaging technique that can provide both structural and chemical information at the same time.** Furthermore**,** the heterogeneous nature of exosomes requires **single-particle level characterization**.

In this project, we aim to design a complete label-free detection and quantification platform for exosome analysis. A custom multimodal Interferometric-Raman microscope will be developed. Interferometric images will be used to detect individual exosomes and determine their size. Chemical composition analysis will be provided by the Raman module of the system. Proposed imaging system will be combined with the novel exosome isolation chip ExoTIC[19], developed by our group at Stanford University, constituting a complete isolation and detection instrument. The developed system will be tested with the clinical samples from cancer patients and healthy donors to demonstrate the clinical potential of exosome characterization.

3. Outline of Tasks/Work Plan

Overview of the Work: In this project, we will develop a multimodal imaging platform for label-free characterization of exosomes at the single-particle level. The first task involves building an advanced interferometric microscope with the capability to visualize nanosized dielectric nanoparticles down to 10 nm across a large field of view exceeding 300 µm x 200 µm [WP1]. To enhance the imaging system's sensitivity, various optical enhancements such as wavefront engineering, Fourier phytography, and polarization-dependent illumination/collection will be incorporated. Additionally, novel data processing algorithms, including machine learning techniques utilizing scanning electron microscopy (SEM) images as a reference, will be implemented to improve resolution.

The second task will be design and integration of a Raman module into the imaging system to enable simultaneous chemical characterization of exosomes [WP2]. This feature will be instrumental in determining the cellular origin of the exosomes, particularly in distinguishing tumor-derived exosomes from non-tumor-derived ones, thus facilitating accurate diagnosis. To expedite spectral data acquisition, both modules will work in parallel, and only particles detected in the interferometric images will be scanning to obtain their spectral signatures.

The developed platform will be utilized for the multiparameter characterization of exosomes isolated from prostate cancer tumor cells [WP3]. Leveraging the expertise of our laboratory at Stanford University in cutting-edge exosome isolation technologies, the goal is to analyze exosomes at the single-particle level using the technologies developed in WP1 and WP2. This analysis will aid in identifying specific exosomal biomarkers associated with prostate cancer.

In the final phase of the project, validation of the system will be performed by characterizing exosomes isolated from both healthy donors and prostate cancer patients (~ 15 individuals per group). This comparative analysis will provide valuable insights into the distinctive characteristics of exosomes from different cohorts and further validate the effectiveness of the developed imaging platform.

By undertaking these outlined tasks, the project aims to advance our understanding of exosomes, their biomarkers, and their role in prostate cancer, ultimately contributing to improved diagnostic capabilities and potentially opening doors to novel therapeutic avenues.

WP 1: Development of Interferometric Microscope for Label-free Detection of Single Exosomes

Objectives	- Achieve discrete detection of unlabeled exosomes with a minimum diameter of 30 nm. - Estimate the size of each detected particle. - Develop a user-friendly control software.
Tasks	- Development of an interferometric scattering microscope for label-free visualization of exosomes (30-150 nm): Based on my previous expertise from my PhD studies, a custom common-path widefield interferometric microscope will be constructed. Novel data processing algorithms will be applied to enhance sensitivity and cover the entire range of exosome sizes. - Development of robust size estimation algorithms: The data analysis pipeline will utilize (i) Bayesian approach, taking advantage of prior knowledge about isolated exosomes on top of a layered substrate. A physical model, considering the point spread function of the imaging optics, will be incorporated using Markov Chain Monte Carlo (MCMC) analysis to estimate particle size. Initial trials will be conducted with reference dielectric nanoparticles prior to exosome experiments, and the results will be validated using electron microscopy. (ii) In the second step, electron microscopy images will be used as reference images and a neural network will be trained to estimate the particle size of nanoparticles. - Development of a GUI: Feedback from potential users, including technicians and clinicians, will be gathered to develop a user-friendly interface for microscope control (e.g., stages, camera) and result visualization. - Embedding the processing algorithms to a GPU: To improve computation speed, all processing algorithms will be implemented on a GPU.

Methodology: The heterogeneous nature of exosomes requires single-particle level characterization,A common-path widefield interferometric microscope will be constructed for label-free visualization of individual exosomes. A layered sensor chip (Au/SiO2/Si) will serve as the sample substrate, with layer thickness adjusted to optimize the interferometric signal. The Kohler scheme will be implemented to

achieve widefield illumination, focusing the light source onto the back focal plane of the objective lens. In this configuration, light scattered by the particles will be collected along with the reference wave reflected from the sample substrate using the same objective lens, and then imaged onto a CMOS camera to capture interferometric images (Fig.1a).

Nanoparticle images exhibit a unique defocusing response due to different angular components of the reference and scattering fields. This response can be utilized to enhance the visibility of nanoparticles. By acquiring z-stack images, correlation analysis will be implemented to improve the system's sensitivity limit and signal-to-noise ratio for nanosized particles. We demonstrated detection of polystyrene (PS) nanoparticles as small as 32 nm in diameter experimentally(Fig.1b-c). However, detecting exosomes poses a greater challenge due to their lower refractive index compared to PS nanoparticles.

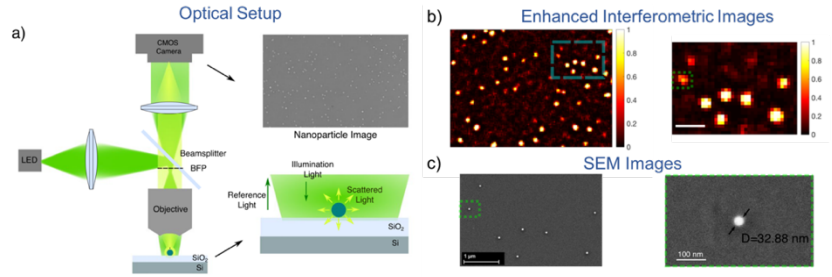

Figure 1: Optical Setup of Interferometric Microscope. b) our initial results of single polystyrene particles c) corresponding electron microscope image

To cover the entire range of exosome sizes, various optical modifications and data processing algorithms will be implemented. Electromagnetic simulations will be conducted to model the scattering fields caused by exosomes on a layered substrate, optimizing the layer thickness to maximize the mismatch between the angular distributions of the scattering and reference fields. Numerical aperture shaping filters will be designed based on simulation results to decrease the intensity of the reference wave and enhance the image contrast of exosomes.

The exosome detection problem is well-suited for a Bayesian approach, as exosomes have known size (30 nm-150 nm) and refractive index due to their isolation from biological fluids using predefined procedures. A physical model considering the point spread function of the imaging optics will be developed. The model, combined with experimental data, will enable discrimination of particles from the background and estimation of individual particle size.

By accomplishing the tasks outlined in this work package, we aim to develop an advanced interferometric scattering microscope capable of visualizing single exosomes and achieving accurate size estimation. This will lay the foundation for subsequent work packages and contribute to the overall goal of advancing exosome research for various applications, including early cancer detection.

WP2: Development of Raman Module for Label-free Characterization of Exosomes

Objectives	- Acquire Raman spectra between 400 cm-1 and 2000 cm-1. - Correlate operation with the interferometric imaging unit through smart scanning of the sample.
Tasks	- Development of Raman Microscope: Integrate a scanning illumination system based on galvo scanners, a collection path, and a NIR spectrometer into the interferometric imaging setup. -Implementation of Smart Scanning: Instead of scanning the entire sample, only the regions containing particles detected by interferometric images will be scanned, reducing the acquisition time.

Methodology: Raman spectroscopy is a label-free and noninvasive technique widely used for quantifying the chemical structure of samples, including in various biomedical applications. We demonstrated exosomes isolated from different cell lines can be discriminated using Raman signatures (Fig 2b). In the proposed work, we utilize gold thin films for surface enhancement, however, Raman signals are obtained through a nonlinear inelastic scattering process, which is weaker than elastic scattering. As a result, long integration times are necessary to obtain meaningful spectra, limiting the adaptation of Raman spectroscopy in clinical settings. Generating hyperspectral images with a high FOV is time-consuming. To address these challenges, multimodal imaging system have been proposed.

In this work package (WP2), our goal is to design and integrate a Raman imaging module into the label-free imaging platform developed in WP1 (Fig. 2a). The Raman module will consist of an

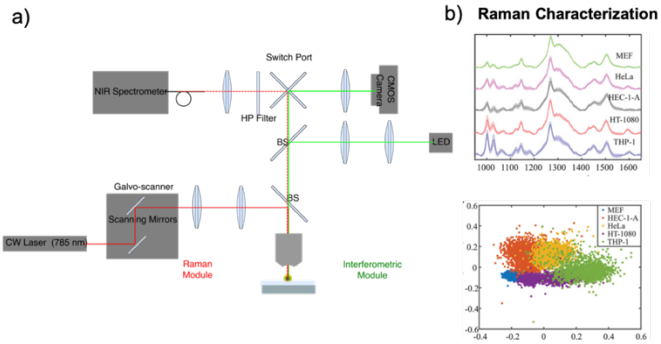

Fig. 2:a) Multimodal Imaging System b)Raman Characterization Results of Isolated Exosomes of different cancer cell origin(top), PCA Results (bottom)

illumination source (780 nm laser source), a galvo scanning unit, illumination and collection optics, and a NIR spectrometer. The same objective lens used in WP1 will be utilized for both.

Exosomes will be detected from the interferometric images, and instead of performing a raster scan, only regions containing exosomes will be analyzed by the Raman module. This selective scanning approach helps reduce acquisition time while focusing on the relevant areas of interest. By combining the strengths of interferometric imaging and Raman spectroscopy, we aim to achieve comprehensive chemical characterization of exosomes in a label-free manner. Our preliminary results of the Raman spectra demonstrate the identification of origin cells of exosomes (Fig 2b).

WP3: Validation of the Platform with Exosomes Isolated from Cell Lines and Patient Samples

Objectives	Demonstrate the detection and quantification capacity of the integrated system using exosome samples.
Tasks	- Spectral Quantification of Isolated Exosomes using Raman Module: Characterize the spectral variation among exosomes isolated from different sources. Quantify the chemical content, including cholesterol, phospholipids, and other potential disease signatures. - Physical Characterization of Exosomes using Interferometric Module: Determine the size distribution and concentration for each sample. - Determination of Exosomal Biomarkers: Characterize exosomes isolated from prostate cancer tumor cells and validate the diagnostic capability of the system.

In the exosome isolation process, an inexpensive, rapid, and effective exosome isolation tool called Exosome Total Isolation Chip (ExoTIC)[19] which is developed by the mentor's group at Stanford University. ExoTIC utilizes a filtration-based method that enables the purification of intact extracellular vesicles. This innovative approach offers a higher exosome yield and enables the detection of more proteins compared to traditional ultracentrifugation and commercial isolation kits. Notably, this work has revealed that the detected proteins, some of which are cancer biomarkers, vary depending on the exosome particle size. This finding underscores the importance of robust particle sizing and characterization techniques, similar to those proposed in this project, which will significantly contribute to the development of exosomal biomarkers for early cancer detection.

In the present work, exosomes from both tumor cell culture and human samples will be isolated and analyzed using the developed platform from WP1 and WP2. Key properties such as **size**, **concentration**, and **spectral signatures** (chemical content) will be thoroughly analyzed to determine the differences between exosomes derived from healthy cells and tumor cells. Additionally, the surface protein content of the exosomes will be characterized by activating the sensor surface with different capture antibodies targeting tetraspanins such as CD63, CD9, CD81, CD24, among others. This approach allows for the **label-free multiparameter characterization** of exosomes at the single-particle level, covering a large field of view. To validate the diagnostic capability of the system, exosomes isolated from both healthy donors (~15 individuals) and cancer patients (~15 individuals) will be analyzed using the developed platform.

We aim to advance our understanding of exosomes and their potential as diagnostic markers. The characterization of exosomes from different sources and the validation of the diagnostic capability of the developed platform will contribute significantly to the field of exosome research and pave the way for the translation of exosome-based diagnostics into clinical practice.

4. Outcomes: Our goal is to design a label-free detection and quantification platform for nanoparticle and nanovesicle such as exosome analysis. By integrating an advanced interferometric microscope with robust size estimation algorithms and a Raman module, we aim to achieve accurate visualization and chemical characterization of exosomes. The validation of the platform using samples from cancer patients and healthy donors will demonstrate its clinical potential. The outcomes of this project will advance our understanding of exosome biomarkers, and their role in diagnostics. Ultimately, this research will lead to improved diagnostic capabilities in early cancer detection.

5. Impact: Cancer is a global health challenge, responsible for the loss of millions of lives each year. Timely diagnosis plays a crucial role in increasing survival rates and improving patient outcomes. The objective of this project is to develop a liquid biopsy tool for exosome isolation, detection, and quantification, enabling early cancer diagnosis. This innovative non-invasive tool has the potential to revolutionize routine patient monitoring by detecting exosome-based biomarkers associated with various types of cancers. By utilizing this non-invasive tool, routine monitoring of patients can be performed to detect exosome-based biomarkers, leading to early detection and reducing the financial and economic burdens associated with advanced-stage treatments.

Furthermore, this tool can also be utilized to monitor the patient's response to treatment, enabling personalized and targeted therapy. This liquid biopsy tool enables monitor a patient's response to treatment, enabling personalized and targeted therapies. By regularly analyzing exosome profiles, healthcare providers can assess treatment efficacy, make informed decisions, and optimize patient care. This approach empowers clinicians with real-time information and facilitates the adjustment of treatment strategies to maximize effectiveness and minimize side effects. The significance of this project extends beyond cancer research. The label-free technology developed in this study offers a unique opportunity to acquire both structural and chemical information of single exosomes simultaneously. By better understanding the characteristics and functions of exosomes, researchers can uncover new opportunities for developing novel therapeutic approaches and diagnostic tools.

Moreover, the adaptable nature of this technology allows for potential applications beyond exosomes. For instance, given the similarities in physical and chemical properties between exosomes and viruses, such as SARS-CoV-2, the tools and methodologies developed in this project can be seamlessly translated to the study of viral particles. This paves the way for efficient virus detection, characterization, and the development of rapid diagnostic methods for emerging viral infections.

In summary, this project addresses the urgent need for early cancer detection using a comprehensive liquid biopsy tool. By leveraging optical detection and characterization with the unique properties of exosomes, it offers a non-invasive and efficient approach to identify cancer-specific biomarkers, exemplified by prostate cancer. Moreover, the research contributes to the advancement of scientific knowledge and holds significant potential for applications in cancer research, exosome-based therapeutics, viral detection, and personalized medicine. By harnessing the power of exosomes, we can enhance early diagnosis, improve treatment outcomes, and make substantial progress in the fight against specifically prostate cancer and potentially other diseases.

References

1. Denzer, K., Kleijmeer, M., Heijnen, H., Stoorvogel, W. & Geuze, H. Exosome: From Internal Vesicle of the Multivesicular Body to Intercellular Signaling Device. *J. Cell Sci.* **113**, 3365–3374 (2000).
2. Soung, Y. H., Ford, S., Zhang, V. & Chung, J. Exosomes in cancer diagnostics. *Cancers (Basel).* **9**, (2017).
3. Melo, S. A. *et al.* Glypican-1 identifies cancer exosomes and detects early pancreatic cancer. *Nature* **523**, 177–182 (2015).
4. Tucci, M. *et al.* Exosomes in melanoma: A role in tumor progression, metastasis and impaired immune system activity. *Oncotarget* **9**, 20826–20837 (2018).
5. Masaoutis, C., Mihailidou, C., Tsourouflis, G. & Theocharis, S. Exosomes in lung cancer diagnosis and treatment. From the translating research into future clinical practice. *Biochimie* **151**, 27–36 (2018).
6. Pan, J., Ding, M., Xu, K., Yang, C. & Mao, L. J. Exosomes in diagnosis and therapy of prostate cancer. *Oncotarget* (2017).
7. Bachurski, D. *et al.* Extracellular vesicle measurements with nanoparticle tracking analysis–An accuracy and repeatability comparison between NanoSight NS300 and ZetaView. *J. Extracell. Vesicles* **8**, (2019).
8. Im, H. *et al.* Label-free detection and molecular profiling of exosomes with a nano-plasmonic sensor. *Nat. Biotechnol.* **32**, 490–495 (2014).
9. Su, J. Label-Free Single Exosome Detection Using Frequency-Locked Microtoroid Optical Resonators. *ACS Photonics* (2015). doi:10.1021/acsphotonics.5b00142
10. Olcum, S. *et al.* Weighing nanoparticles in solution at the attogram scale. *Proc. Natl. Acad. Sci.* **111**, 1310–1315 (2014).
11. Su, J., Goldberg, A. F. & Stoltz, B. M. Label-free detection of single nanoparticles and biological molecules using microtoroid optical resonators. *Light Sci. Appl.* **5**, e16001 (2016).
12. Ortega-Arroyo, J. & Kukura, P. Interferometric scattering microscopy (iSCAT): new frontiers in ultrafast and ultrasensitive optical microscopy. *Phys. Chem. Chem. Phys.* **14**, 15625–36 (2012).
13. Avci, O., Ünlü, N., Özkumur, A. & Ünlü, M. Interferometric Reflectance Imaging Sensor (IRIS)—A Platform Technology for Multiplexed Diagnostics and Digital Detection. *Sensors* **15**, 17649–17665 (2015).
14. Hsieh, C. L. Label-free, ultrasensitive, ultrahigh-speed scattering-based interferometric imaging. *Opt. Commun.* **422**, 69–74 (2018).
15. Daaboul, G. G. *et al.* Enhanced light microscopy visualization of virus particles from Zika virus to filamentous ebolaviruses. *PLoS One* **12**, 1–15 (2017).
16. Daaboul, G. G. *et al.* Digital Detection of Exosomes by Interferometric Imaging. *Sci. Rep.* (2016). doi:10.1038/srep37246
17. Piliarik, M. & Sandoghdar, V. Direct optical sensing of single unlabelled proteins and super-resolution imaging of their binding sites. *Nat. Commun.* **5**, 4495 (2014).
18. Aygun, U., Urey, H. & Yalcin Ozkumur, A. Label-free detection of nanoparticles using depth scanning correlation interferometric microscopy. *Sci. Rep.* **9**, (2019).
19. Liu, F. *et al.* The Exosome Total Isolation Chip. *ACS Nano* **11**, 10712–10723 (2017).

Name: Development of low excess noise, ultra-high resolution, OCT system through the development of low intensity noise, continuous-wave, fiber Supercontinuum source.

Category: Health.

Problem: Excess intensity noise of broadband optical sources, such as supercontinuum (SC), used for spectral domain (SD) ultra-high resolution (UHR) Optical Coherence Tomography (OCT) forms the fundamental limitation to achieve shot-noise limited detection. The consequence of this is to lose the capability of early-stage detection of pathologies in ophthalmology, cardiology, cancer diagnosis etc. Existing solutions require either non-standard, complex, bulky sub 50 femtosecond pulse width, shot noise limited pump laser designs, and complex, patent protected optical fiber designs to generate low excess intensity noise supercontinuum. Such methods further elevate the cost and complexity of the already expensive (>100000$) UHR OCT systems that currently are limited to high-income developed countries. Further, the existing solutions fail if there is a small amount of intensity noise (0.5-1%) of pump (which is true with many practical pump lasers) used for SC generation.

Our Solution: The goal is to develop a low excess noise (ideally shot noise limited) UHR OCT system based on low intensity noise, fiber supercontinuum (SC) source. This will be achieved by following the essential requirements of low intensity noise SC generation. They are: 1) Low intensity noise of the pump that generates SC and 2) Low quantum noise amplification in the SC generated. Besides, both the above requirements should be met in a cost-efficient manner. This will be achieved, a) by developing, in-house, a low noise, continuous wave (CW) fiber-based pump laser, and b) by using standard off-the shelf telecom optical fibers for SC generation as shown in figure.

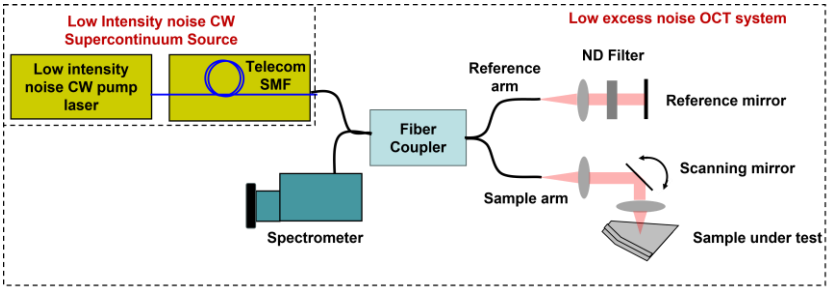

Figure: Schematic of proposed low excess noise SD UHR OCT system

Unique features: CW natures of the pump enable low quantum noise amplification (unlike femtosecond laser pumped SC generated), and the low intensity noise nature enables low intensity noise of the SC generated. Both CW pump and telecom fiber make the system cost-efficient by atleast an order of magnitude compared to the existing systems (based on complex, pulsed pump and, patent protected photonic crystal fibers), without compromising the excess noise performance of OCT. Same technique can be readily transferable to low intensity noise SC generation in other nonlinear optical fiber types such as photonic crystal fibers, highly nonlinear fibers etc., depending on the wavelength region of interest.

Outcomes: Publications and patents on these new methods for low noise nonlinear frequency generation to generate widely tunable wavelength and broadband SC sources in various nonlinear optical fiber media. Tabletop prototypes of low intensity noise widely tunable wavelength, broadband SC sources, and low excess noise OCT system. Technology transfer to a private Indian company for the first realization of UHR OCT system in India. Trained graduate students in research areas of fiber lasers, nonlinear fiber optics and OCT.

Impact: The proposed OCT system enables early-stage detection of multiple diseases in various categories of healthcare diagnostics such as Ophthalmology, Dermatology Cardiology etc. Due to the cost-efficient nature, the developed technology provides wide accessibility of UHR OCT technology to billions of underserved populations in low income developed countries. The SC source developed when used for other low-coherence interferometric applications such as contact-less, non-destructive testing and inspection of processes parameters in industrial manufacturing, oil, and gas sensing, can increase the signal to noise ratio, resolution, acquisition speed and sensitivity.

Development of low excess noise, ultra-high resolution, OCT system through the development of low intensity noise, continuous-wave, fiber Supercontinuum source.

1. Literature Review

Optical Coherence Tomography (OCT) uses low-coherence interferometry (LCI) technique to obtain cellular level resolution, 3D images of biological tissues in a non-invasive manner [1]. It is used in diagnosis of many diseases like Glaucoma, Skin cancer, Diabetic retinopathy, Coronary artery stenosis etc. [2]. Among various OCT modalities, Spectral/Fourier domain OCT (SD OCT) is most prevalent due to its higher sensitivity and image acquisition speeds [3]. Figure 1 shows the typical schematic of an SD OCT system. The achievable axial resolution of SD-OCT is inversely related to the spectral bandwidth of the source. Latest developments in the broadband optical sources with more than octave spanning bandwidth (called Supercontinuum), enabled SD-OCT to achieve ultra-high resolution (UHR-OCT) of few µm corresponding to a single cell dimension [4].

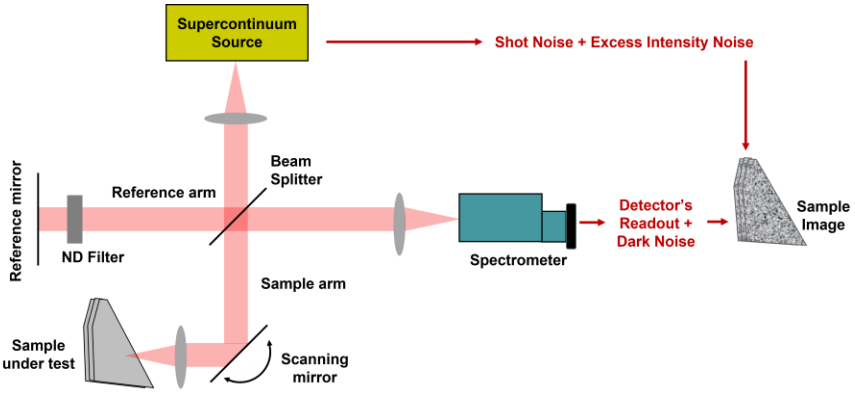

Fig. 1. Schematic of ultra-high resolution, spectral domain OCT system showing different components and noise sources.

A crucial figure of merit for an OCT system is the signal to noise ratio, (SNR). Signal corresponds to the detected spectral interference and is proportional to product of backscattered and reflected optical powers from SUT and the reference mirror. The noise corresponds to the background detected power. The noise degrades the achievable visibility of the spectral interference and hence the contrast of images. This significantly inhibits the early-stage detection of the diseases. As shown in figure 1, multiple noise sources originating from the input broadband source, and the detector, contribute to the SNR of OCT images. The goal of every OCT system is to achieve shot-noise limited detection [5], i.e., the noise in the detected image is limited by the fundamental random nature of detected photons, with negligible contribution from the noise of the detector and the optical source.

Towards this goal, OCT systems with bulky, expensive, cryogenically cooled superconducting, and high-internal gain photo detectors were demonstrated to avoid dark noise at low reference optical power levels [6]. On the other hand, the use of low-bandwidth sources such as superluminescent diodes (SLDs), can also achieve shot-noise limited OCT due to negligible excess intensity noise of SLDs [4]. However, owing to UHR capability and the availability of multiple spectral bands, SC sources are highly attractive to OCT systems. But the excess intensity noise arising from the SC source dominates the noise of detector in OCT images. This is due to various nonlinear optical processes involved in SC generation mechanism [7]. Therefore, there is a compromise between achieving UHR and the shot-noise limited detection in OCT imaging systems.

	Reference publication	Fiber Type	Pump Choice	Limitations
Anomalous Dispersion Regime	J M Dudley et al. Rev. Mod. Phy., (2006),	Standard Photonic Crystal Fiber (PCF)	<50fs shot noise limited pump lasers	**Non-standard, complex pump laser designs - Expensive**
Normal Dispersion Regime	A M Heidt et al., Optica, (2022)	PCFs with Low (<7ps^2/km), flat Dispersion profile	Standard Mode Locked (100fs – <1ps), shot noise limited pump lasers	**Non-standard, Complex, Research grade, patents protected fiber (PCF) designs - Expensive**

Fig. 2. Summary of current low excess noise SC generation methods in anomalous and normal dispersion regimes.

This has triggered a lot of research activity in the development of low excess intensity noise SC sources for OCT [8]. The methods, summarized in figure 2, include use of very short pulse (<50fsec) pump sources for SC generation in anomalous dispersion standard photonic crystal fibers (PCFs) [8], and the use of normal dispersion (ANDi) PCFs with low and flat dispersion profiles over a broad wavelength range for ANDi SC generation [9].

2. Problem Statement and Objective

The primary limitations of the existing low excess intensity noise UHR OCT systems shown in figure 2 are:

1. In anomalous dispersion, the pump pulse widths needed for low-noise, coherent SC generation are of sub 50fs [8]. Such non-standard pump lasers require complex, bulky designs and hence are expensive.
2. In normal dispersion, the fibers needed must have low (<7ps^2/km) [9], flat dispersion profiles. Such fibers require complex dispersion engineered refractive index profiles making them expensive and they are still in research phase with patents protection.
3. The above methods utilize seeded incoherent nonlinear optical processes in anomalous dispersion and coherent nonlinear optical processes in normal dispersion to obtain coherent and low-noise SC [8]. However, for OCT, only low-noise and low-coherence of SC is needed.
4. Further, it was shown that with small excess intensity noise of the pump source (~1%), the above SC generation methods completely fail due to pump noise induced SC de-coherence and noise amplification [10,11].
5. However, J. R. Taylor et. al, in 2004 demonstrated that the use of continuous-wave (CW) pump source rather than femtosecond pulsed pump for SC generation can significantly reduce intensity noise level of SC to the input pump noise level (unlike 50dB amplified intensity noise of femtosecond pulse pumped SC) due to low peak power (10s watts), Raman Soliton nature of the SC generated [12].

Therefore, what is desirable for low excess noise OCT system is

1. A CW pump source, but with ideally zero intensity noise (shot-noise limit) for low intensity noise SC generation.
2. A standard, conventional off the shelf optical fibers (e.g, SMF28e) for SC generation.
3. A low noise detection mechanism. This can be achieved with standard off-the-shelf spectrometers.

Therefore, the primary objective of this proposal is to develop a low excess noise (ideally shot noise limited) OCT system. The has been divided into subobjectives detailed below.

3. Work Plan/Tasks

3.1. Development of low excess intensity noise pump source for SC generation

In this objective, we aim to achieve wavelength tunable from 1µm to 1.5µm, low excess intensity noise (ideally shot noise limited) fiber laser with ~50W of optical power. This enables SC generation in standard telecom fibers with zero dispersion wavelength (ZDW) at 1.3µm and highly nonlinear fibers (HNLFs) with ZDW at 1.5µm. To achieve this, we will use the widely known tunable wavelength cascaded Raman fiber lasers architecture [13-15] shown in figure 3.

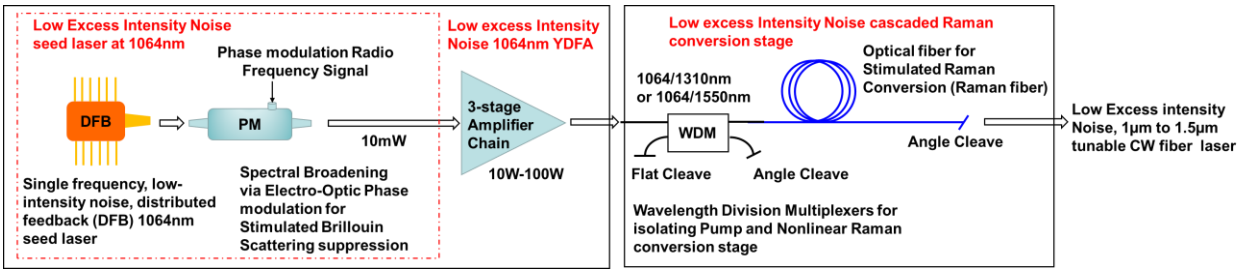

Fig. 3. Schematic of Tunable wavelength low excess intensity noise CW fiber laser.

A low excess intensity noise, ~100W class Ytterbium doped fiber amplifier (YDFA) based on multistage amplification of shot-noise limited, phase modulated single frequency distributed feedback (DFB) seed laser will be developed and used for pumping cascaded Raman conversion stage. This enables low excess intensity noise Raman fiber laser from 1µm to 1.5µm [15]. Theoretical/Numerical investigation will be performed to study and optimize the intensity noise performance.

3.2. Development of low excess intensity SC source

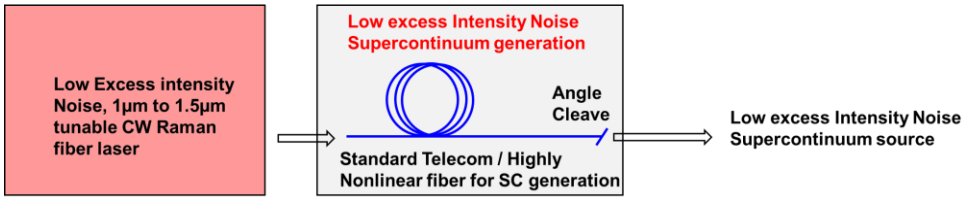

Fig. 4. Schematic of low excess intensity noise SC source

In this objective, the above developed tunable, low excess intensity noise Raman fiber laser will be utilized as pump for SC generation in telecom or HNLF optical fibers as shown in figure 4. The target optical bandwidth and relative intensity noise (RIN) of SC source are >300nm (1300 – 1700nm) and <-120dBc/Hz (0 – 10MHz RF frequencies). The >300nm optical bandwidth ensures UHR of ~1µm and <-120dBc/Hz RIN ensures low excess noise of OCT images. Theoretical/numerical investigations will be performed to optimize the RIN of SC generation.

3.3. Development of low excess noise UHR OCT system

In the final objective, low excess noise, UHR OCT system will be developed by utilizing the low excess intensity noise SC source developed above along with standard OCT components as shown in figure 5.

The noise performance will be evaluated by acquiring OCT images of various phantoms and will be compared with existing research grade and commercial OCT systems.

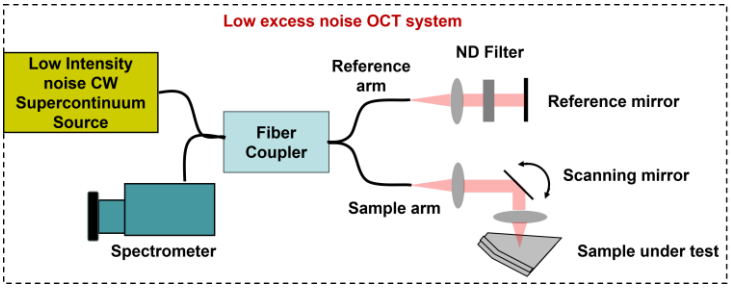

Fig. 5. Schematic of low excess noise UHR OCT system

Theoretical and Numerical analysis of SNR performance evaluation of the OCT system and the images will be performed.

Below is the summary of all the objectives with timelines to achieve the goal of this project.

Task	1-6 mos.	7-12 mos.	13-18 mos.	19-24 mos.
1. Development of low excess intensity noise, 50W class, 1-1.5µm tunable wavelength Raman fiber laser	■	■		
1.1. Purchase of all the components necessary for low excess intensity noise YDFA	■			
1.2. Purchase of components necessary for Raman conversion	■			
1.3. Development of low excess intensity noise, 100W class phase modulated single frequency YDFA		■		
1.4. Development of YDFA pumped tunable Raman fiber laser		■		
1.5. Theoretical and Numerical analysis of RF phase modulation schemes for RIN optimization of Raman fiber lasers	■	■		
2. Development of low excess intensity noise SC source using the above tunable Raman fiber laser.			■	
2.1. Purchase of components necessary for SC generation	■			
2.2. Theoretical and Numerical analysis of RF phase modulation schemes for RIN optimization of SC generation.			■	■
3. Development of low excess noise OCT system using the above SC source.				■
3.1. Purchase of components of OCT system except the optical source		■		
3.2. OCT experiments on the tissue phantoms using the above system				■
3.3. Theoretical and Numerical analysis of SNR performance evaluation of the OCT system and the images obtained			■	■

4. Intended Outcomes

1) Publications/Patents on low excess noise continuous wave (CW) tunable Raman fiber lasers based on low noise YDFAs.

2) Publications/Patents on low excess noise CW SC generations methods in conventional optical fibers.
3) Publications/Patents on the developed OCT system and its performance enhancements.
4) Protype of low excess noise, low-cost UHR OCT system using the developed SC source.
5) Transfer of this technology to an Indian company, Innovation Imaging Technologies Pvt Ltd (IITPL), for realization of the first UHR OCT system in India.
6) Trained graduate students with skills in fiber lasers analysis, design and development, nonlinear fiber optics etc. to either take industry or academic jobs.

5. Impact

(1) Research: It disseminates new knowledge and techniques on CW, low-noise nonlinear frequency generation through SC and it's RIN properties which has been least considered in the literature.
(2) Technology: It develops fiber-based low excess noise CW tunable wavelength and SC sources, low-complex, shot-noise limited OCT system for early-stage detection of many pathologies. Due to its low-cost nature, it enables wide accessibility of UHR OCT to billions of underserved populations in low-income, developing countries.

6. References

1. J. Fujimoto and E. Swanson, "The development, commercialization, and impact of optical coherence tomography," Invest. Ophthalmol. Visual Sci. 57(9), OCT1–OCT13 (2016).
2. Ali S, Gilani SBS, Shabbir J et al. Optical coherence tomography's current clinical medical and dental applications: a review, F1000Research 2021, 10:310 (https://doi.org/10.12688/f1000research.52031.1)
3. Johannes F. de Boer, Rainer Leitgeb, and Maciej Wojtkowski, "Twenty-five years of optical coherence tomography: the paradigm shift in sensitivity and speed provided by Fourier domain OCT [Invited]," Biomed. Opt. Express 8, 3248-3280 (2017).
4. A. Unterhuber, B. Považay, K. Bizheva, B. Hermann, H. Sattmann, A. Stingl, T. Le, M. Seefeld, R. Menzel, M. Preusser, H. Budka, C. Schubert, H. Reitsamer, P. K. Ahnelt, J. E. Morgan, A. Cowey, and W. Drexler, "Advances in broad bandwidth light sources for ultrahigh resolution optical coherence tomography," Phys. Med. Biol. 49, 1235–1246 (2004).
5. D. S. S. Rao, M. Jensen, L. Grüner-Nielsen, J. T. Olsen, P. Heiduschka, B. Kemper, J. Schnekenburger, M. Glud, M. Mogensen, N. M. Israelsen, and O. Bang, "Shot-noise limited, supercontinuum based optical coherence tomography," Light Sci. Appl. 10, 133 (2021).
6. Fathipour, V., Schmoll, T., Bonakdar, A. et al. Demonstration of Shot-noise-limited Swept Source OCT Without Balanced Detection. Sci Rep 7, 1183 (2017).
7. K. L. Corwin, N. R. Newbury, J. M. Dudley, S. Coen, S. A. Diddams, B. R. Washburn, K. Weber, and R. S. Windeler, "Fundamental amplitude noise limitations to supercontinuum spectra generated in a microstructured fiber," Appl. Phys. B 77, 269–277 (2003).
8. J. M. Dudley, G. Genty, and S. Coen, "Supercontinuum generation in photonic crystal fiber," Rev. Mod. Phys. 78, 1135–1184 (2006).
9. Benoît Sierro, Pascal Hänzi, Dirk Spangenberg, Anupamaa Rampur, and Alexander M. Heidt, "Reducing the noise of fiber supercontinuum sources to its limits by exploiting cascaded soliton and wave breaking nonlinear dynamics," Optica 9, 352-359 (2022).
10. N. R. Newbury, B. R. Washburn, K. L. Corwin, and R. S. Windeler, "Noise amplification during supercontinuum generation in microstructure fiber," Opt. Lett. 28, 944-946 (2003).
11. Etienne Genier, Patrick Bowen, Thibaut Sylvestre, John M. Dudley, Peter Moselund, and Ole Bang, "Amplitude noise and coherence degradation of femtosecond supercontinuum generation in all-normal-dispersion fibers," J. Opt. Soc. Am. B 36, A161-A167 (2019).
12. C. J. S. de Matos, S. V. Popov, and J. R. Taylor, "Temporal and noise characteristics of continuous-wave-pumped continuum generation in holey fibers around 1300nm", Appl. Phys. Lett. 85, 2706-2708 (2004).
13. V. R. Supradeepa, Y. Feng, and J. W. Nicholson, "Raman fiber lasers," J. Opt. 19, 023001 (2017).
14. Y. Feng and L. Zhang, "High power Raman fiber lasers" in Raman Fiber Lasers, Berlin, Germany:Springer, 2017.
15. Rashmita Deheri, Sarthak Dash, V. R. Supradeepa, and V. Balaswamy, "Cascaded Raman fiber lasers with ultrahigh spectral purity," Opt. Lett. 47, 3499-3502 (2022).

Name of the project: Design of a Modular system for Measuring Electric Field in plasmas oriented to Fusion (DEMOMEFF)

Category: ENVIRONMENT

Highlights:

- ✓ **Design, characterization, and construction of a modular system for the measurement of the electric field in plasmas oriented to fusion via second harmonic generation.**
- ✓ **Improving the generation of second harmonic generation via the generation of different polarization and optical vortexes, to improve the sensitivity of the electric field measurements.**
- ✓ **Adaptable to different types of discharges and experiments, thus facilitating the diagnosis of this type of devices**.
- ✓ **Generation of a scientific network on the electric filed measurements, that will serve as a consulting service, for the design of new set-ups and for monitoring measurement campaigns.**

This proposal presents the design and construction of a modular system to measure the electric field in plasmas, using the technique known as Electric Field Induced Second Harmonic (E-FISH). This method allows the generation of the second harmonic of a radiation when it passes through an external electric field. The project arises from the urgence of developing a clean source energy, where fusion plasmas play a key role.

Among many other techniques, laser spectroscopy has been a powerful characterization tool, providing a good spatial and temporal resolution. In this project, I propose a modular experiment to optimize the measurement of a crucial parameter when talking about plasmas: the electric field. Here, I propose the optimization of this measurement creating optical vortexes to improve the generation of the second harmonic; and also, to be able to detect the different components and orientations of the electric field.

At the end of the project, the following outcomes are expected:

- The generation of optical vortexes with nanosecond lasers for the detection and measurement of the different components and orientations of the electric field in a discharge.
- An electrical discharge built to simulate discharge conditions oriented to fusion devices, allowing the development of this and other types of photonics-based characterizations.
- Electric field measurements provided, being an important source of data for the scientific community. This data serve as a basis for new experiments, simulations, and development of theoretical models.
- Generation of a consulting network to provide solutions on the design of the electric field installation, and monitoring of electric filed measurement campaigns in real fusion-like devices.

This proposal will provide the community valuable data about fusion-like device behavior via photonic characterization, advancing in the control and knowledge of this technology called to be the source of clean energy the world needs.

Design of a Modular system for Measuring Electric Field in plasmas oriented to Fusion (DEMOMEFF)

1. Background and state of the art

Plasma physics has gained special relevance in the last few decades. The many applications developed in fields as diverse as medicine, industry, food analysis, etc., clearly show the strategic importance of this field, involving multiple lines of current and future development[1]. Nonetheless, the biggest and most promising work in plasma physics has been in fusion, an energy source that will be an increasingly necessary paradigm shift in the climate emergency that we are starting to experience.

The great challenge of fusion is the correct control and characterization of its nature: a complete study requires as many parameters as possible. Among the many parameters that characterize a plasma, such as the electronic density and temperature, the distribution of the electric field (EF) is of vital importance for its complete comprehension. Understanding the EF distribution within a plasma allows access to important parameters, since it determines the flows of charged particles, their energy distributions and charge densities, as well as conditioning to a large extent the structure of the discharge itself[2].

Despite the enormous interest in this parameter, it is extremely difficult to obtain quality experimental measurements, always claimed by the scientific community. Over the years, several strategies have been developed to measure the EF in different types of plasmas. The first ones were Langmuir probes, evolving to devices such as Pockels cells; both with good results, but very perturbative for the plasma at the local level, which hampered achieving a good spatial resolution. Optical diagnostics soon emerged as a powerful technique for characterizing plasmas. The advent of lasers allowed direct access to the interior of plasmas, providing a spatial resolution hitherto non-existent before[3]. Over the years, different strategies for measuring the EF have been developed with excellent results[4–8].

In the 1970s, the technique known as Electric Field Induced Second Harmonic (E-FISH) was discovered, based on the generation of the second harmonic (SH) of an original radiation when it passed through a region in which there is an externally applied EF[9,10]. The success of this technique relays in that is species independent, only requiring that the media is centrosymmetric, such as is air. In recent years this technique has been successfully applied to the measurement of the EF in different types of plasmas and discharges.

Most of the experiments exploring this technique employ high-power femtosecond lasers to reach the needed pulse energy to generate SH[11–14]. Nowadays, however, it has become apparent that this type of measurement can be performed with nanosecond lasers, which are often a more affordable and available option on the market [15–18], extending the laser focusing area to maximize the SH generation.

Although these configurations have proven to be feasible, there is still room for improvement in the generation of the SH for the measurement of the EF. It is demonstrated that the polarization of incident light plays a fundamental role in the generation of the SH[14,19]. Moreover, it is well known that the EF is sensitive to the polarization of incident light and optical vortexes[20–22], allowing to distinguish the different EF components, and certain light polarizations present stronger propagation into plasmas[23,24]

In view of all this, in this project I propose the design and construction of a modular system to measure the EF in discharges by means of the E-FISH technique, using as light source a nanosecond laser. Likewise, I will explore the generation of optical vortexes, to improve the detection of the different components of the EF present in discharges that can be assimilated as existing fusion-oriented experiments.

2. Objectives. Methodology and work plan

The main objectives (indicated as GO) and specific objectives of the project (indicated as SO) are specified below, detailing the procedure to achieve each of them.

GO1. Simulation and preliminary study of electric fields in air at atmospheric pressure.

SO1.1. Simulation of the expected electric field distribution for different geometrical discharge distributions

The distribution of the EF generated between the electrodes will be simulated using programs such as Quickfield and Matlab. In this way, it will be possible to test different configurations, and to proceed to the discharge construction in the most favorable conditions.

SO1.2. Simulation of expected second harmonic generation.

To choose the best discharge configuration, I will simulate at the same time the amount of second harmonic generated in those conditions, to optimize the experiment construction.

SO1.3. Simulation of the optical vortexes

In conjunction with the two previous sections, we will need to optimize the generation of the optical vortexes to improve the second harmonic generation, and with it the measurement of the electric field.

GO2. Construction of a discharge for electric field generation

SO2.1. Discharge design and installation

The first step will be the design of the most versatile discharge configuration, based on the simulations results obtained in GO1. The elements constituting the discharge will be carefully manufactured and installed, in conjunction with the high-power supplies, resistors, etc. All the safety elements (grounding, insulating screens, etc.) will be installed and checked.

SO2.2. Discharge characterization in different geometries and study of performances

The discharge installed will be carefully characterized based on the voltage-intensity characteristic curves, beyond other electrical diagnostics. That knowledge will allow a controlled functioning of the discharge, altogether with its characteristics and regimes.

GO3. Tuning of a nanosecond laser system for second harmonic generation

SO3.1. Laser characterization with different configurations

The experimental system will be modular, allowing different SH generation conditions, adapting the set-up to provide diverse spatial resolutions for adapting the design to different kind of plasma devices. For this purpose, I will characterize various laser beam configurations (focusing length, beam waist, fluence, etc.) for the SH generation.

SO3.2. Optical vortexes generation

Along with the beam characterization, I will explore the generation of optical vortexes to improve the incident light propagation into the discharge and the generation of the SH, upgrading in this way the sensitivity of the EF measurements. Furthermore, this will improve the detection of the EF measuring the different components and orientations available.

GO4. Electric field measurements.

SO4.1. Electric field measurements at different spatial resolutions

Once the different geometrical configurations and the optimal optical designs for each of them have been studied, the EF distribution in each of them will be measured exhaustively. This objective includes different measurement campaigns to test the set-up in conditions alike real fusion devices.

GO5. Generation of a consulting network on EF measurements

SO5.1. Consulting service on EF measurements

Establish a consulting network about the experimental measurement of the electric field in plasmas, in such a way that this type of consultation can be favored, and the researchers can state their needs, or the type of experiment they have, so that I can design a strategy in the system designed to suit their needs.

SO5.2. Monitoring EF measurement campaigns in real plasma devices

Using the network created in the SO5.1 objective, it will be possible to monitor measurement campaigns specifically designed for some experiments and devices in other laboratories, making use of the equipment available there or transferring part of the equipment of the present project.

3. Timeline

The project is intended to be developed over 24 months. The following schedule details the different phases of work over the duration of the project. The different colors indicate the general and specific objectives details in Section 2:

B0. Management. Project reports and documents related to the economic and scientific progress of the project. Publications of the results.

B1. Simulation of electric fields and SH generation

B2. Discharge design and construction

B3. Laser system set-up

B4. Electric field measurement

B5. Generation of an EF network

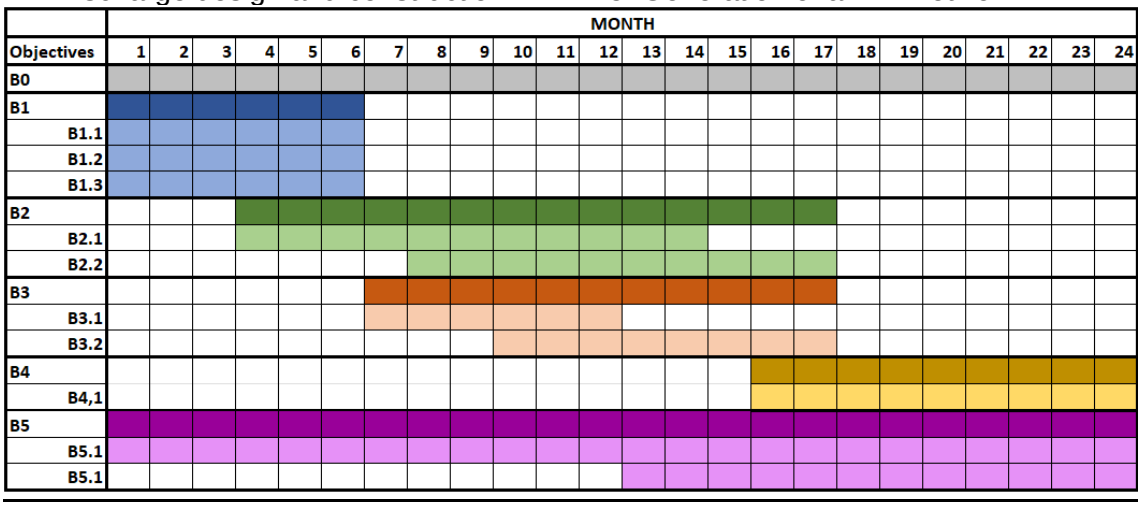

4. Viability of the project

The project proposed involves the design and construction of a modular system for the EF measurement via the E-FISH technique. It will open a new line of research in the Applied Optics Complutense Group at the Universidad Complutense de Madrid (UCM), specialized in the development of sensors and different optical characterizations, where I currently develop my professional activity.

I have an extensive experience in plasma physics and in the experimental measurement of the EF by means of different optical techniques developed in different institutions. My PhD thesis dealt with the measurement of the EF distribution in hydrogen and deuterium discharges by laser spectroscopy[25–28], and the subject of my postdoctoral research was the characterization of an argon plasma column by spectro-tomography[29]. Therefore, the needed experience to carry out successfully this proposal is proven.

Regarding the Risk assessment and contingency plan, I have identified some risks along the project. I have classified them into LOW, MEDIUM, planning a contingency plan when needed.

Task	Risk	Contingency plan
GO1	LOW	Not Necessary
GO2	MEDIUM	If it were not possible to make the designed discharge work, for various reasons, the objective of the project would not be hindered, since I could test the measurement of the electric field in a hollow cathode discharge located in the Plasma Spectroscopy Laboratory of the University of Valladolid, with which I currently maintain a collaboration.
GO3	MEDIUM	If the laser inevitably fails, the final objective of the project would not be compromised, since the measurement of the electric field could be transferred to a facility equipped with this type of laser. The facilities of the UCM's own Ultrafast Laser Center could be used, or the laboratories of the Institute of Optics of the CSIC could be used as well.
GO4	MEDIUM	Contingency plan explained in GO3 and GO4
GO5	LOW	Not Necessary

5. Expected impact of the results and outcomes

This project is focused in supporting the development of a clean, new safe and eco-responsible source of energy such is fusion. Furthermore, Photonics is identified as a key worldwide technology. In this project, I propose the combination of these two strategic areas to improve the EF measurements for fusion purposes via SH generation combined with optical vortexes.

It is expected that this project will generate at least three publications in high-quality scientific journals. In addition, the developed technology in optical vortexes and SH optimization justifies the possibility of exporting these results in the form of a patent.

At the end of the project, the following outcomes are expected:

- The generation of optical vortexes with nanosecond lasers for the detection and measurement of the different components and orientations of the electric field in a discharge.
- An electrical discharge will have been built to simulate discharge conditions oriented to fusion devices, allowing the development of this and other types of photonics-based characterizations.
- Electric field measurements will have been provided that will be an important source of data for the scientific community and will serve as a basis for new experiments, simulations, and development of theoretical models.
- Generation an EF measurement network, while monitoring the measurement of EF in plasmas devices present in other laboratories.

Regarding the social impact, as a community we must not lose sight of the gender issue in any team, and especially in Physics, where the female presence is a minority. Efforts are needed to unlock new opportunities focused on access to funding and access to the labor market. Therefore, the results of the project will only be awarded to companies that respect good gender practices.

6. ***Future perspectives***

The project I present here, opens more research lines either as a continuation or as new lines to be explored. I include some of the future lines that this proposal opens:

- Inclusion in the experiment of a vacuum chamber to generate discharges in different gases of interest for the plasma community.
- Development of other types of diagnostics based on optics and photonics, e.g. plasmonic measurements using fiber optic sensors.

7. References

1 Adamovich, I. *et al. J. Phys. D: Appl. Phys.* 50, (2017)

2 Bogaerts, A. *et al. Appl Phys B* 75, 731–738 (2002)

3 Gavrilenko, V. P. *Instruments and Experimental Techniques* 49, 149–156 (2006)

4 Lawler, J. E. *et al. Adv. At., Mol., Opt. Phys.* 34, 171–206 (1994)

5 Czarnetzki, U. *et al. Phys. Rev. Lett.* 81, 4592 (1998)

6 Booth, J. P. *et al. Appl. Phys. Lett.* 65, 819–821 (1994)

7 Hebner, G. A. *et al. J. Appl. Phys.* 76, 4036–4044 (1994)

8 Spasojević, Dj. *et al. J. Appl. Phys.* 119, 53301 (2016)

9 Godefroy, P. *et al. Appl Phys Lett* 68, 1981–1983 (1996)

10 Ward, F. *et al. Phys Rev Lett* 26, 285–289 (1970)

11 Nakamura, S. *et al. Phys Rev A (Coll Park)* 104, 1–6 (2021)

12 Guillet de Chatellus, H. *et al. Opt Express* 9, 586 (2001)

13 Fujii, T. *et al. Opt Lett* 46, 238 (2021)

14 Dogariu, A. *et al. Phys Rev Appl* 7, 1–7 (2017)

15 Chng, T. L. *et al. Opt Lett* 45, 1942 (2020)

16 Goldberg, B. M. *et al. Appl Phys Lett* 112, (2018)

17 Fujii, T. *et al. Opt Lett* 46, 238 (2021)

18 Cui, Y. *et al. Appl Phys Lett* 115, (2019)

19 Beresna, M. *et al. Appl Phys Lett* 95, (2009)

20 Horovitz, Y. *et al.* (1997)

21 Ahn, W. *et al. Nano Lett* 12, 219–227 (2012)

22 Mitryukovskiy, S. *et al. Phys Rev Lett* 114, (2015)

23 Sakai, K. *et al. Sci Rep* 5, 8431 (2015)

24 Ju, L. B. *et al. Phys Rev E* 94, (2016)

25 Gonzalez-Fernandez, V. *et al. Plasma Sources Sci Technol* 26, 105004 (2017)

26 Gonzalez-Fernandez, V. *et al. J Appl Phys* 124, (2018)

27 Gonzalez-Fernandez, V. *et al. Spectrochim Acta Part B At Spectrosc* 105972 (2020)

28 Gonzalez-Fernandez, V. *et al. Spectrochim Acta Part B At Spectrosc* 180, 106194 (2021)

29 Gonzalez-Fernandez, V. *et al. Sci Rep* 10, 1–12 (2020)

Executive summary of:

Stimulated Coherence Tomography for Fluorescent Imaging in Turbid Tissues

Vicente J. Parot
Institute for Biological and Medical Engineering
Pontificia Universidad Católica de Chile

Tracking of therapeutic agents inside the human body is a long-sought technology with potential to improve drug targeting and treatment response monitoring. Multiple approaches have been investigated using probably all imaging modalities including PET, MRI, and a variety of optical methods. While label-free optical techniques gather anatomical, dynamical, and spectroscopic information from tissues, they lack therapeutic specificity. Optical detection specificity can be greatly improved by using molecular markers that provide functional insights into biological processes. Fluorescence imaging is particularly effective in detecting both endogenous signals and external contrast agents, which are often clinically beneficial for assessing superficial tissues. Applications in routine clinical use include retinal vasculature angiography, diagnosis of corneal abrasions, and evaluation of cholecystitis and urethral obstructions. Fluorescence imaging is also under investigation in clinical trials for cancer surgery, especially for identifying sentinel lymph nodes and for intraoperative tumor margin delineation.

But the optically accessible region for fluorescence microscopy is fundamentally limited to only about the first tenth of a millimeter from the surface in scattering tissues. As light travels through biological tissues, it gets scattered, and beyond this distance it loses the sharp focusing that is typically necessary for imaging. Because the utility of current fluorescence microscopy is limited by depth, most clinical applications use bulk fluorescence or are applied only in the tissue surface.

In this project, we will develop a new technology to increase 10-fold the optically accessible region for fluorescence imaging, with the goal to expand the clinical utility of fluorescence-based molecular contrast agents. This could be achieved by stimulating fluorescence emission from a chromophore of interest, while using an Optical Coherence Tomography (OCT) system to perform interferometric detection of back reflected light after multiple scattering in tissue. The signal contributed by the fluorophore will be isolated by differentially modulating illumination in the chromophore excitation wavelength, which will be incoherent to the interferometry measurement. The interferometry detection normally isolates the back reflected signals from the randomly scattered light, thus typically imaging up to 10 times deeper than standard fluorescence microscopy. Enabling fluorescence detection by this method would allow fluorescence imaging at OCT depths. This work will build on our previous research developing computational microscopes for sensitive detection of fluorescent reporters and on our previous research investigating OCT contrast generated by multiply scattered light.

The availability of fluorescence contrast at 10-fold increased depths will enable imaging deeper inside tissues to expand the clinical utility of optical interrogation with functional and molecular specificity. New medical applications that could be enabled include precise monitoring of labeled cell therapies and deep tracking of diagnostic contrasts agents.

Stimulated Coherence Tomography for Fluorescent Imaging in Turbid Tissues

Vicente J. Parot
Institute for Biological and Medical Engineering
Pontificia Universidad Católica de Chile

Background:

To advance healthcare, biomedical research strives to develop methods that improve our understanding of diseases and our abilities to perform effective interventions. For example, in cancer diagnosis and treatment using optical methods, there is a need for precise imaging that can inform of metastasis progression and treatment monitoring. One key area of improvement is deep imaging, as traditional fluorescence microscopy is fundamentally limited to about the first 100 micrometers in scattering tissue. This limitation arises from the way light propagates through biological tissues. As light encounters multiscale changes in the refractive index caused by interfaces between water, lipids, and proteins, it gets scattered, and beyond a certain distance, it loses the sharp focus that is typically necessary for imaging. This distance is characterized by the mean free path, average distance that a photon would travel without being scattered.

In cancer treatment, surgical procedures require precision to surgically removing the entire cancerous tissue while sparing healthy tissue. The identification of tumor vs healthy tissue can be done accurately with time consuming biopsies and histopathology, but this method is not convenient for decision making during the surgery, when time is limited. Optical imaging methods and fluorescence imaging, which offers molecular contrast, are being investigated in clinical trials to enhance surgical precision by delineating tumor margins and identifying sentinel lymph nodes in situ in live tissues. Other clinical applications where fluorescence imaging of superficial tissues is routinely useful include retinal vasculature angiography, diagnosis of corneal abrasions, and evaluation for cholecystitis, and for urethral obstructions. As decisions must currently be made on the basis of superficial information, or bulk fluorescence from deeper tissues, increasing the optically accessible depth for high resolution fluorescent imaging could increase the effectiveness of these procedures by providing precise characterization of the molecular contrast of interest over larger clinically relevant volumes of live tissue.

Other existing medical imaging methods such as Computed Tomography (CT), Positron Emission Tomography (PET), Magnetic Resonance Imaging (MRI), and Ultrasound (US) have an excellent capacity to obtain information deep from the human body because they operate in regions of the electromagnetic spectrum where there is minimal or no scattering in biological tissues. Some of the fundamental properties of these methods are that PET resolution is limited to ~5 mm by detector size[1], whereas CT, MRI, and US provide detailed anatomical images but lack molecular specificity[2]. Thus, none of these methods provide an adequate combination of resolution, depth, speed, and molecular contrast that is required for surgical tumor delineation.

Optical Coherence Tomography[3] (OCT) is a label free reflectance imaging method that reaches up to 10 times deeper than fluorescence microscopy[4,5] by using interferometry to detect backscattered light that is coherently matched to a reference of the illumination. The intrinsic coherent detection mechanism of OCT precludes detection of conventional fluorescence, whose spontaneous emission is inherently incoherent[6]. OCT obtains deep images of microscopic tissue anatomy and is routinely used to characterize the 3D morphology of the retina. OCT is also under investigation for a number of other clinical applications including imaging of coronary artery walls, lung airways, and gastrointestinal mucosa.

Optical measurements that leverage the interaction of a pump and a probe beams enable the incoherent (non-interferometric) detection of fluorescence with very high sensitivity by stimulated emission[7]. In this process, a pump beam excites a fluorophore in its absorption wavelength, and a probe beam in the fluorophore emission wavelength is amplified by stimulated emission. High speed modulation and lock-in detection allow differential extraction of the stimulated emission signal with

rejection of low frequency noise sources to yield high sensitivity. We then consider if this process could be measured with interferometry and generate OCT contrast. Although pump-probe methods have also been used in OCT (interferometric) measurements to generate molecular contrast[8–11], none of them used stimulated emission that is reflected back from the sample. Understandably, as a coherent amplification process, stimulated emission has long been regarded to be indistinguishable from the probe beam for imaging, as occurs in the bulk stimulated emission that generates laser light amplification. However stimulated emission and scattering that occur in the excited state of a fluorophore have only recently been examined in detail for the context of biological imaging[12,13], providing a framework for future instrument design efforts. Another consideration is the availability of back reflected stimulated emission in epifluorescence detection mode, a configuration that would be necessary for practical medical applications. We find that coherent pump-probe experiments have demonstrated that a significant portion of backscattered light enables incoherent, non-interferometric detection in epi-illumination mode after multiple scattering[14]. On the other hand, the back scattered reflectance after multiple scattering had traditionally been considered a source of noise and image degradation in OCT[15,16], but has more recently been characterized in detail to show that multiply scattered light maintains a degree of coherence that allows interferometric detection and useful imaging contrast[17,18]. Taken together, these considerations indicate that an instrument designed to detect optical coherence amplification by stimulated emission should be able to report fluorescence from depths accessible through OCT measurement.

Problem and objectives:

Our goal is to develop a system that uses interferometric detection of backscattered light to measure stimulated emission from chromophores, aiming to achieve fluorescence imaging contrast with OCT depth penetration in turbid tissue. During this project we will seek to construct the minimal system that is able to demonstrate the working principle of this technology, and to perform validation experiments using scattering tissues. Additional objectives within this project include A) Establishing and providing training for a biomedical nonlinear optical research laboratory at our institution, and B) Conduct an analysis to optimize the detection sensitivity and molecular specificity of this system for target applications. This analysis will consider technical constraints from available light sources, interferometers, scanning and modulation methods, chromophores, wavelengths of interest, and co-design of computational methods with the hardware implementation.

Tasks and work plan:

Our technology development will be guided by the need for an OCT or similar low-coherence interferometry measurement ("probe") to be performed in spectral overlap with the fluorescence emission of the chromophore. A secondary illumination that excites the chromophore ("pump") should not contribute to the OCT signal either due to non-overlapping spectral band excitation of the chromophore, or due to lack of coherence with the probe. Instead, presence or absence of the pump will differentially modulate the OCT signal by coherent amplification of the probe due to stimulated emission from the chromophore. These differences will be analyzed by subtraction of measurements, or by high-speed modulation with lock-in detection.

Tasks will be organized in a 2-year schedule (4 semesters)

Task / Semester	1	2	3	4
System design	X	X		
Implement interferometer		X	X	
Implement modulation and lock in detection		X	X	
Validation experiments			X	X

The outcome of this project will be the demonstration of this new technology, together with information that will provide design principles for a clinically useful implementation.

Impact:

The availability of fluorescence contrast at 10-fold increased depths will enable imaging organs, cells and biosensors deeper inside intact live organisms. New applications that could be enabled include tracking of therapeutic agents noninvasively, thick imaging of scattering tissues, and deep probing of intact neurophysiology.

References

1. Moses, W. W. *Nucl. Instrum. Methods Phys. Res. Sect. Accel. Spectrometers Detect. Assoc. Equip.* **648 Supplement 1**, S236–S240 (2011).
2. Pysz, M. A., Gambhir, S. S. & Willmann, J. K. *Clin. Radiol.* **65**, 500–516 (2010).
3. Huang, D. *et al. Science* **254**, 1178–1181 (1991).
4. Badon, A. *et al. Sci. Adv.* **2**, e1600370 (2016).
5. Bouma, B. E. *et al. Nat. Rev. Methods Primer* **2**, 79 (2022).
6. Ntziachristos, V. *Nat. Methods* **7**, 603–614 (2010).
7. Min, W. *et al. Nature* **461**, 1105–1109 (2009).
8. Rao, K. D., Choma, M. A., Yazdanfar, S., Rollins, A. M. & Izatt, J. A. *Opt. Lett.* **28**, 340–342 (2003).
9. Bredfeldt, J. S., Vinegoni, C., Marks, D. L. & Boppart, S. A. *Opt. Lett.* **30**, 495–497 (2005).
10. Jacob, D., Shelton, R. L. & Applegate, B. E. *Opt. Express* **18**, 12399–12410 (2010).
11. Yu, C., Chung, S.-S. M., Kuo, W.-C. & Kao, F.-J. in (eds. Brown, T. G., Cogswell, C. J. & Wilson, T.) 93301G (2015). doi:10.1117/12.2077970.
12. Varma, S. R., Patange, S. & York, A. G. *Github.io* (2020) doi:10.5281/zenodo.3665824.
13. Wong-Campos, J. D., Porto, J. V. & Cohen, A. E. *J. Phys. Chem. A* **125**, 10667–10676 (2021).
14. Evans, C. L. *et al. Proc. Natl. Acad. Sci.* **102**, 16807–16812 (2005).
15. Wang, R. K. *Phys. Med. Biol.* **47**, 2281–2299 (2002).
16. Bilenca, A., Lasser, T., Bouma, B. E., Leitgeb, R. A. & Tearney, G. J. *IEEE Photonics J.* **1**, 119–127 (2009).
17. Parot, V., Cannon, T. M., Villiger, M., Uribe-Patarroyo, N. & Bouma, B. E. in *Biomedical Applications of Light Scattering XI* vol. 11657 116570A (International Society for Optics and Photonics, 2021).
18. Untracht, G. R. *et al. Sci. Adv.* **9**, eadh5435 (2023).

“ROD - The inclusive retina system”

“Inclusive Low-Cost Retinal Oximetry providing Diagnostic Imaging Systems for Retinopathy - Exploring the Links between Infectious & Non-Communicable Diseases in Limited Resource Settings”

What is proposed?

The proposal aims to create an inclusive low-cost retinal oximeter as a minimal viable product, to enable diagnostic imaging systems for retinopathy in low-resource, under-served community settings in the Global South. The tools will be used to explore the links between infectious & non-communicable diseases including for example diabetic retinopathy and malaria.

Why is this important? Over the last decades the field of retinal imaging has been under constant progress and improvement. However, under-represented vulnerable communities, with increased levels of melanin, have not been included in the design of such tools. The programme will lead to new optical design, algorithms that can cope with these differences in human biology, enabling the validation of the tool in retinal disease diagnosis amongst people of all skin colours.

What is the problem? There is currently a lack of low-cost retinal diagnostics systems in low resource community settings to identify disease in rural clinics. Exiting instruments are expensive and placed in centralised facilities. New optical retinal systems that work effectively despite pigmentation will in future be used to save lives and prevent loss of sight.

What is the solution? This proposal outlines new solutions based upon novel optical imaging methods and new algorithms to compensate for differences in signals amongst different individuals, and the use of deep-learning as a diagnostic decision support tool. The device itself will be based upon the implementation of a illumination technique, allowing us to obtain high quality images with ultra-low cost designs.

Who cares (impact)? The proposed technique/system will find broad application amongst rural clinics to collect data on different individual retinophathies including those caused by diabetes and by malaria. The tool will also help establish links between these two disparate diseases, developing a new field of clinical and epidemiological research. In the longer term, we aim to develop both industrial and clinical translational pathways such that these low cost sytems will enable such diagnostic data to be collected in community clinics in remote rural areas, guiding care pathways and treatment.

Why should this proposal be granted? The proposed technique advances the state-of- the-art in low-cost retinal imaging systems, that will have the potential to help populations living in remote, rural communities, particularly in Sub-Saharan Africa. The work also represents a critical first step to enable the PI to realise his research vision of creating new diagnostic tools based upon optical systems

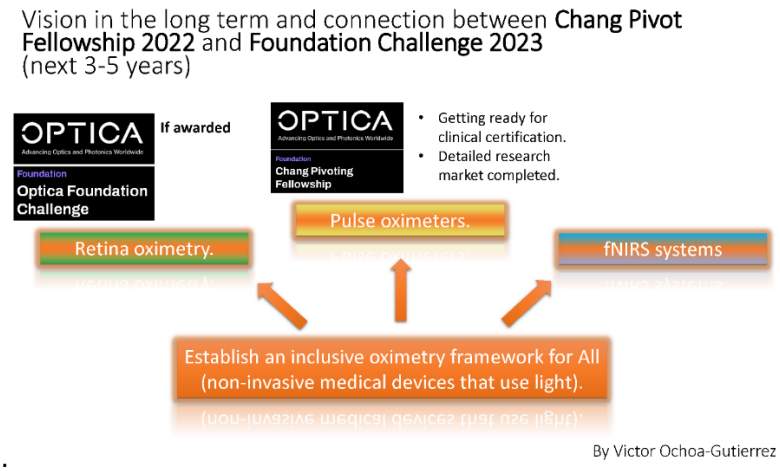

.

“ROD - The inclusive retina system”

“Inclusive Low-Cost Retinal Oximetry providing Diagnostic Imaging Systems for Retinopathy - Exploring the Links between Infectious & Non-Communicable Diseases in Limited Resource Settings”

Literature Review

Retina and Optics: There are around 2.2 billion visually-impaired people world-wide suffering from a wide range of retinal diseases, particularly aging population, such as blindness due to unaddressed refractive error (88.4 million), cataract (94 million), age-related macular degeneration (8 million), glaucoma (7.7 million), diabetic retinopathy (3.9 million), as well as near vision impairment caused by unaddressed presbyopia (826 million). Screening using retinal imaging devices is crucial for the 80% of these cases that are preventable or treatable to avoid or delay the loss of sight. Current screening and diagnosis employ retinal imaging methods ranging from simple low-cost, narrow-field handheld ophthalmoscopes, through benchtop retinal fundus cameras to ultra-widefield ophthalmoscopes such as the scanning laser ophthalmoscopes (SLO). These devices image typically 1%, 7% and 70% of the retina accordingly. However, the complexity of the optics required to image a larger area of the retina leads to higher manufacturing costs for example the wide-field SLO, in comparison to a narrow field-of-view hand-held instrument. In consequence the market for SLOs is restricted to high-income countries and this market is both highly competitive for manufacturers and growing relatively slowly.

Non-Communicable Diseases: There is a growing recognition that the relationship between communicable and non-communicable diseases (NCDs) in both low- and middle-income countries (LMICs) and high-income countries (HICs) is becoming increasingly important, particularly in low-resource settings, both in terms of the increasing risk of disease and also the wealth disparity in access to screening and management of these conditions (1), (2). Evidence shows that chronic and acute infections (e.g. viral, bacterial and parasitic diseases including tuberculosis, TB, malaria and HIV) interact strongly with non-communicable diseases such as diabetes mellitus, and vascular and chronic lung disease. Such multi-morbidities are emerging as major threats to local health and wellbeing in both HICs and LIMCs, with changing demographics and lifestyles.

There is now also compelling evidence that both neonatal NCDs e.g., cardiovascular disease and type II diabetes (3) can be strongly influenced by the infectious disease status of the foetus and/or the mother. Additional factors common in LMICs, such as malnutrition in pregnancy and infancy, coupled with stress arising from chronic inflammation following endemic infections (4) have also been linked both to early-life later-life health outcomes. Against this evolving backdrop of new understanding, within LMICs, healthcare provision for disease is frequently siloed into “vertical” activities in specialist donor-funded clinics, particularly in semi-urban or rural communities (5), creating a challenge around patient-level “horizontal” data linkages between disease, treatment and outcomes. Despite investments in LMIC healthcare, healthcare systems remain vertically integrated by disease group (5), (6), (7), such that, it is challenging for a clinician running malaria and diabetes clinics in a rural hospital to establish linkages, where records are still primarily held for single disease groups.

Underpinning my vision is the recognition of the tensions between vertical healthcare programmes (with specialist clinics, often donor-funded) and horizontal linkages, focused on the interplay between an individual’s multiple co-morbidities. This paradox is not new (5), (7), although as yet there are no optimised systems implemented that combine a blend of vertical and horizontal activity (a concept termed “diagonal diagnostics”). My aim is to develop new tools that will enable “a window into the eye” of type 2 diabetes and malaria, two very different and related diseases, both increasing in prevalence in LMICs. The strong interdependency between type 2 diabetes and malaria is already well established, with diabetes greatly increasing the risk of people catching malaria (8). This proposal is for the development of a device that effectively covers the “diagonal diagnostics” described above.

Problem Statement/Objective: “Looking into the window of the eye to save lives”.

Cerebral malaria is potentially fatal but can be diagnosed to inform treatment towards recovery, whilst diabetes is similarly better treated, the earlier it is detected. Both can be detected and diagnosed using retinal imaging, which is often better accepted than the alternative invasive tests, especially in infants and young children. Our aim is to use an inclusive low-cost retinal oximetry system to detect the characteristic discoloration, visual features, and oxygenation of the retinal vessels, associated with both diseases. Being able to detect malaria and diabetic retinopathy at the same time has the potential to make screening campaigns easier, thus leading to early detection, associated with better outcomes.

Malaria is still considered one of the most common and deadliest diseases. In 2019, malaria led to an estimated 229 million cases and ~409,000 deaths worldwide. In endemic countries, asymptomatic malarial parasitaemia is common, and may lead to neurological complications and death, if undiagnosed (13). Children under 5 years are the most vulnerable group affected accounting for 67% (274 000) of all malaria deaths (14). Amongst these individuals, many die from undiagnosed cerebral malaria, resulting from compromised perfusion of the brain due to parasites in the microvasculature (15). An early incluisive eye screen can however diagnose cerebral malaria (13), mitigating many of the complications associated with a poor prognosis.

The team have previously worked closely with both clinical and industrial experts (including Optos and Nikon) in the field of retinal imaging, examining the retinal vasculature to understand cerebral vascular diseases (16), (17), (18). It is now propose that by combining a low cost (fundus) retinal imaging as a new portable optical system, with artificial intelligence/deep learning (19), it will be able to detect the characteristic artefacts associated with the presence of either diabetic or malarial retinopathies in the microvascular network of the retinal tissue.

Figure 1 – Optics System Concept: The key element of the innovation is a multi-technique: multiple retina illumination points (trans-pars-planar, trans scleral illumination) can be independently optimised and controlled to prevent glares, and inconsistent brightness in the local area on the retina, but overall, completely cover a wide view. This alleviates optical constraints that have previously prevented ultra-wide view retinal imaging with conventional technology: mainly, a single objective lens that needs to correct for a wide view is substituted by an array of lenslets that are optimised for smaller local areas of the retina. The innovation thus enables a huge reduction in complexity, and will enable compact and lightweight solutions (envisaged at less than 12x9x9cm and 0.5kg), provide high usability and reducing the need for high-skilled user training, and operating without eye contact (figure illustrates previous efforts to be improved)

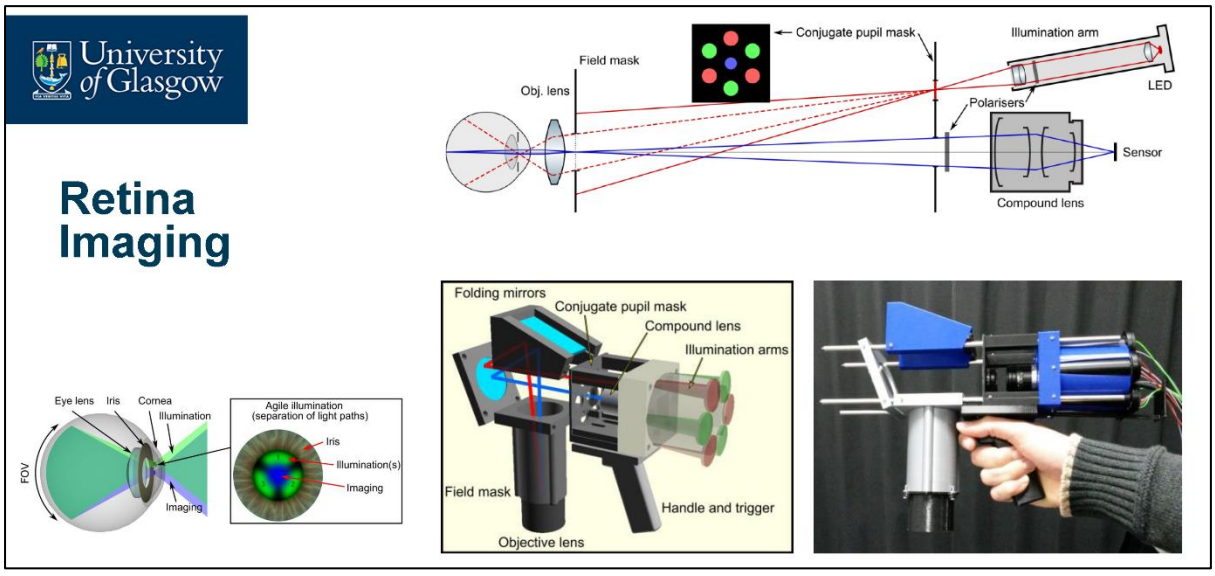

The novelty of our approach that differentiates us from other low-cost retinal imaging systems, and previously developed research tools includes:

(i) The use of ultra-lowcost optics, based on trans-pars-planar, trans scleral illumination, providing high quality images, at a cost of goods affordable in low-resource healthcare settings;

(ii) The exploration of new imaging modalities which include the potential for trans-pars-planar, trans scleral illumination for less-invasive collection of high-quality signals;

(iii) The development of a sophisticated image analysis tool, including an AI deep-learning diagnostic decision support, which will be validated in collaboration with clinical ophthalmologists in the UK, prior to being implemented in Tanzania. The tool includes training data collected from appropriate ethnic groupings ensuring (unlike other optical clinical devices, associated with blood oxygenation and temperature measurements) strong diagnostic efficacy across groupings with high colouration.

Outline of tasks/Work Plan

Phase I (month 1 – month 13) – platform development and laboratory validation

1.1 Optical design: Adapt the current retinal imaging device for pigmented retinas, it will consist in a re-design, measure of success will be around the resolution of the image, sufficient to detect artefacts in the retina (including discolouration) associated with cerebral malaria or diabetes. Safety assessment and demonstration of the modified camera on ex vivo rabbits and humans .

1.2 AI system model prediction: Using real images from public databases (20), (21), (22), the team will train deep-learning tool using a Convolution Neural Network (CNN).. As a proof-of-concept, the team have already shown the development of a blood vessel classification AI supported tool able to assign vascular architecture to retinal images (identifying veins and arteries). The tool will be adapted for measurement of retinal artefacts and colouration. A contribution to the state-of-art will be the result of using public data sets that does not provide information regarding retina melanin content in comparison to our retinal images that will provide melanin content information.

1.3 Privacy-enabled cloud communication: The team have recently developed a block-chain enabled end-to-end encryption (24), enabling medical images to be uploaded into cloud-based systems, providing entrusted keys to defined users. Images will be uploaded to improve our library/training sets, whilst providing trust and assurance around privacy of medical records.

1.4 Apply for ethical approval in Tanzania. The team have experience of working in the country and anticipate this process to take 3-6 months.

Deliverable Phase I (D1 month 13): a laboratory-validated prototype and analysis pipeline.

Phase II (month 14 – month 24) – field validation and route to deployment

2.1 Iterated optical design, the team will iterate on our initial low-cost design (deliverable D1) after a first short visit to Tanzania, which will include a co-creation workshop, with 3D-printed prototypes.

2.2 Using clinical expertise in KCRI, Tanzania, it will be performed a limited field validation study, comparing a new inclusive proof-of-concept system against standard of care reference techniques and data. Whilst malaria is endemic in rural communities and many children <5 years in sub-Saharan Africa (>60%) will have the disease during the course of a year, the prevalence of cerebral malaria is much less, ~2.5% in hospitalised children (25). Thus, whilst a statistically powered study falls beyond the scope of the project, the team will instead compare retinal images of hospitalised children, diagnosed with cerebral malaria against

control children, implementing retina oximetry as a main indicator for cerebral malaria detection.

2.3 Route to impact. Once the inclusive proof-of-concept is established, we will work with collaborators in Tanzania for wider validation leading to a clinical trial. We will also disseminate the results and the design using the principles of open innovation/open access to enable a more widespread development and adoption of our methods.

Deliverable Phase II *(D2 month 24)* – prototype designs disseminated and data published.

Gantt Chart

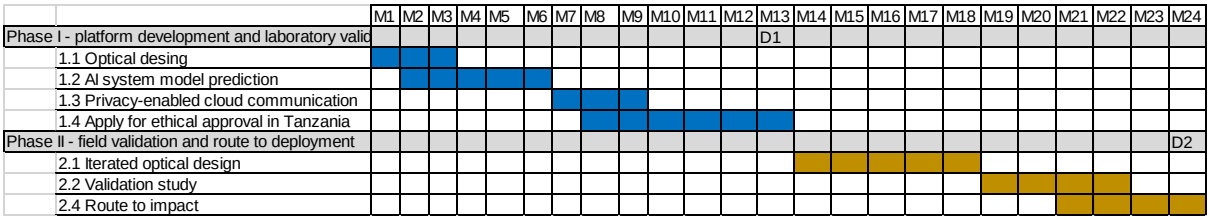

Risk/Project Management. The team will hold monthly meetings on project progress (remotely on Zoom) with all collaborators, in which risk management will form a standing agenda item. We have mitigated most technical risks in our experimental design (above) and initial proof-of-concept experiments, although gaining a useful illumination of the pupil will be important for obtaining high quality images. Should direct illumination reveal challenging to extract features linked with the diseases, the team will explore other illumination such as trans-pars-planar, trans scleral illumination.

Team

Dr. Victor Ochoa-Gutierrez	University of Glasgow (UoG)	ECR (**Project Lead**) – Retinal Imaging, oximetry, prototype development
Professor Jonathan Cooper	UoG	Research mentor - field-based experience on malaria diagnosis
Xin Guo	UoG	AI, Cloud Infrastructure and User Interface.
Dr. Ian MacCormick	University of Edinburgh	Clinical Lecturer – ophthalmology.
Dr. Blandina T. Mmbaga	KCRI Tanzania	Director of Institute (Kilimanjaro Clinical Research Institute), clinical expertise in malaria and diabetes.

Outcome(s)

I. The clinical use cases are: i) detection of any retinopathy from screening images (abnormal/normal), and/or ii) detection of diabetic retinopathy severe enough to require referral to ophthalmology according to SIGN guidelines (or other national guidelines such as Tanzania's National Diabetic Retinopathy Management Guidelines, 2018). Both outcomes will also reduce the workload of human graders.

II. Increased capacity in retinal health screening for LMICs. The team will ensure that our technologies perform across multiple ethnicities, particularly those involving darker skin pigmentations where retinal imaging quality can be different and often with lower signal-to-noise due to the strong absorption of light by melanin. Patient selection will follow best practice as per ethics approvals, in particular including a gender-balanced cohort.

Impact

- Promotion of inclusivity in research and technology development for retinal imaging;
- Supporting an informed and collaborative approach to the development, implementation, adoption and exploitation of research outcomes of new medical devices, including technologies, processes, evidence-based policy, community impact or creative outputs;
- To provide early-stage investment in a new medical technology with the potential for

commercialization, to support the de-risking of these opportunities;

- In the longer term, the project will contribute to reduction in patient morbidity (and mortality for malaria), in particular in children under 5, through early diagnosis of retinopathy, leading to sustained, inclusive and sustainable economic growth as well as resilient healthcare infrastructures.

References

1. Abbafati C et al. Global burden of 369 diseases and injuries in 204 countries and territories, 1990–2019: a systematic analysis for the Global Burden of Disease Study 2019. The Lancet.
2. The Malawi NCDI Poverty Commission Report — The NCDI Poverty Network. 2018.
3. Di Bernardo S et al. Assessing the consequences of gestational diabetes mellitus on offspring's cardiovascular health: MySweetHeart Cohort study, BMJ Open. 2017.
4. Ogoina D et al.. The role of infections in the emergence of non-communicable diseases (NCDs) J Infect Public Health 2009.
5. Marquez PV et al. No more disease silos for sub-Saharan Africa. BMJ 2012.
6. Huang F et al. Beyond pilotitis: Taking digital health interventions to the national level in China and Uganda. Global Health 2017.
7. Mills A. Mass campaigns versus general health services: What have we learnt in 40 years about vertical versus horizontal approaches? Bull World Health Organ. 2005.
8. Danquah I et al. Type 2 diabetes mellitus and increased risk for malaria infection. Emerging Infectious Diseases. 2010.
13. Newton CRJC, et al. Cerebral malaria. J. Neurol. Neurosurg. Psychiatry 2000.
14. WHO. Malaria report. 2022.
15. Ogwang R et al. Asymptomatic malaria parasitaemia and seizure control in children with nodding syndrome; A cross-sectional study. BMJ Open. 2018.
16. Moss HE. Retinal Vascular Changes are a Marker for Cerebral Vascular Diseases. Curr Neurol Neurosci Rep. 2015
17. Carles G et al. Wide-field, illumination-agile, oximetric retinal imaging with a handheld camera. OSA Imaging and Applied Optics Congress 2021 CTh4E.6.
18. Ochoa-Gutierrez VJ et al. Multi-spectral vascular oximetry of rat dorsal spinal cord. Optics and Biophotonics in Low-Resource Settings VI; 2020
19. Agustin T et al. Optimization Convolutional Neural Network for Classification Diabetic Retinopathy Severity. ICOIACT 2020.
20. Drive: Digital Retinal Images for Vessel Extraction - Data Set. 2012.
21. Clinical Data Sets - The Royal College of Ophthalmologists. 2022.
22. Kaggle Repository. 2022.
23. Guo X et al. Smartphone-based DNA diagnostics for malaria detection using deep learning for local decision support and blockchain technology for security. Nature Electronics. 2021
24. Singh R et al. Blockchain-enabled End-to-End Encryption for Instant Messaging Applications. In IEEE 23rd International Symposium on a World of Wireless; 2022
25. Nkhoma WAC et al. Cerebral malaria in Malawian children hospitalized with Plasmodium falciparum infection. Annals of Tropical Medicine and Parasitology. 1999.
26. Carles G et al. Wide-field, illumination-agile, oximetric retinal imaging with a handheld camera. Conference Papers; 2021 The Optical Society. CTh4E.6.

PROJECT NAME: SureVision. CATEGORY: Health.

Refractive errors (myopia, hyperopia, astigmatism, presbyopia) affect up to 67% of the global population, and 100% over 50 years. Furthermore, preventable refractive error affects 1 billion people worldwide, representing the 1st cause of visual impairment and the 2nd cause of visual loss according to WHO (UN), with dramatic consequences at social and economic levels and, impacting life quality for people. The evaluation of refractive error is the basic piece of information about the state of the eye and is the main test performed in eyecare clinics worldwide. The gold standard method for diagnosis is called **subjective refraction** and consists of identifying different letters through different lenses until achieving the best combination of lenses providing the best visual acuity. **This traditional approach is highly variable (0.27 D), time-consuming (>6 minutes), is affected by accommodation, and requires a clinician with years of experience to master the technique.**

We have developed a new method called **Direct Subjective Refraction (DSR)**, which uses a tunable lens to create fast and periodic defocus changes that, combined with the chromatic aberration of the eye and a bichromatic stimulus, creates a chromatic flicker perception which is minimum when the patient is perfectly compensated. The task of the patient in the DSR method is minimizing the chromatic flicker. We showed that the **DSR task is easy, barely requires supervision** (clinicians explains the task and patients perform it autonomously), **decreases measurement time by 5x, and increases precision by 2x compared to the traditional method.**

The first attempt of including this new method in the clinic is **SureVision**, a new ophthalmic device that uses the DSR method as working principle to obtain the visual the prescription of the patient. First clinical measurements have shown the potential of the new device and has allowed to acquire invaluable feedback from the clinicians, the final user. The DSR method brings **a revolution to the eyecare community** as the first subjective method that provides a prescription without identifying letters. The high precision and low measurement time make SureVision a potential candidate for replacing current paradigms, as their advantages overpass current devices and improve the stakeholders experience: patients, clinicians, clinics, manufacturers.

The main goal of this project proposal to the OPTICA Foundation Challenge is to **develop an industrial prototype** that can be used in a clinical environment, which includes the feedback obtained from clinicians. Particularly, the following key steps will be followed:

1. **Scientific advance**. Answer key questions regarding the DSR method such as accommodation response, theoretical simulation, chromatic components, and pupil size.
2. **Industrial prototype**. Refinement of the optical system. Design the prototype. Develop an app for performing measurements. Develop 1st industrial prototype. Reach TRL 8.
3. **R&D activities**. i) Develop a measurement of the angle of astigmatism, ii) including pupil alignment control, iii) design calibration system, iv) conceptualize the inclusion of objective measurement via aberrometer or light reflex, and v) include DSR in a conventional phoropter.
4. **Gather clinical evidence**. Clinical studies in i) general population (Hospital Clinico San Carlos Madrid) and ii) refractive surgery patients (Moorfields Eye Hospital, London).
5. **Business roadmap**. Full business and financial plan. Market study. Develop investment strategy (Caixa Impulse, Healthstart, CSIC Hackaton, FIPSE Estudios Viabilidad, investment forums, startup competitions) and investment pitch. Management and maintenance of IP portfolio.

In the long term, the project will be highly transformative, as it will represent a **disruptive method** to measure the refractive error. It will also serve as an incentive for the ophthalmic industry, as more precise prescriptions will require new expertise and resources. The potential launch of a spin-off company would create an impact in the community, generating value, high-skill jobs, and the return of the investment to society. Members of the SureVision project have already been part of successful spin-off companies, employing PhDs with multi-year post-doctoral international experience. We take this as an example and lesson to learn. Furthermore, given the large size of the market, a prospective license, and to a much larger extent, the success of the company, SureVision will have high business potential and financial viability. Therefore, the **successful completion of the project** (and of subsequent phases towards regulatory process and commercialization) **will bring a positive impact on the community at large, healthcare, economic growth, preventable blindness, and well-being in general**.

LITERATURE REVIEW

The evaluation of the visual prescription is probably the most common procedure followed in eye care exams, where clinicians measure the refractive error of the eye. **Refractive error** is the condition where the optics of the eye does not focus the light on the retina, resulting in blurred images and reduced visual performance. It is classified into myopia, hyperopia, astigmatism, and presbyopia. Refractive error affects 67% of the global population, and 100% of people over 50 years old, leading to >4 billion people using some type of visual correction. Furthermore, preventable refractive error affects 1 billion people worldwide, representing the 1st cause of visual impairment and the 2nd cause of visual loss according to the World Health Organization, with dramatic consequences at social and economic levels and impacting life quality for people[1]. A pesar de no ser una enfermedad mortal, es altamente discapacitante si no es diagnosticada y compensada, y que disminuye progresivamente la calidad de vida de las personas. Hence, determining refractive error stands as a pivotal aspect in eye care. Not only it guides the prescription of ophthalmic corrections, but it also serves as a fundamental means of obtaining basic information about the state of the patient's eyes, such as emmetropia, moderate or high myopia or hyperopia, and more. This preliminary assessment often precedes various other ophthalmic procedures.

There are numerous techniques available for measuring refractive error. **Objective refraction** techniques are typically rapid measurements that do not need active participation of the patient. On the other hand, **subjective refraction** techniques rely on the patient's responses in tasks such as letter identification, blur comparison, or blur minimization, which can be cumbersome. Despite advancements in objective refraction techniques, they are used as clinicians still consider the **traditional subjective refraction as the gold standard** for evaluating refractive error[2], using. This approach involves testing various lenses until maximum visual acuity, i.e., the smallest recognizable letters on a chart, is achieved. Traditionally, subjective refraction is performed using a trial frame and a set of trial lenses, or alternatively, a phoropter. Over time, stimuli for subjective refraction have evolved from static eyecharts to dynamic optotype projections and fully programmable digital displays controlled by software.

Accommodation, the ability of the eye to change the focusing position, has a strong influence in the subjective refraction procedure. During the procedure, accommodation can be activated and can typically lead to overcorrection of myopia or undercorrection of hyperopia, especially in young subjects, where the accommodation response is fully functional. To reduce the impact of accommodation, the **fogging** technique is the most used method to reach the best focus, which consists of adding positive power (myopic defocus, not possible to compensate for it with the accommodation of the eye) to blur the letter test, and then decrease said addition in small steps. This technique, although effective in reducing the influence of accommodation, entails a long detour in the evaluation, increasing measurement time and thus the fatigue of the patient.

Subjective refraction is a **time-consuming** procedure. It entails, for each patient's eye, the full dedication of a well-trained eye care professional for **>6 minutes**[3], and can be much more in some patients. For numerous eye care practitioners, subjective refraction comprises a significant portion of their daily workload. The limited presence of optometrists stands as a primary factor contributing to non-corrected refractive errors in developing regions, creating a bottleneck within eye care services. Time limitations in optometry practice restrict the extent of comprehensive eye examinations and visual tests.

The **high variability** of subjective refraction is closely related to the constrains in measurement time. The intraoptometrist repeatability, the deviation across repeated measurements by the same optometrist evaluating the same eye, reported values in the spherical component from **±0.20 to ±0.32 diopters (D)**[3]. The interoptometrist variability, the deviation across repeated measurements by different optometrists evaluating the same eye ranges from **±0.20 to ±0.38 D**[3]. These errors are significant, as reported by Atchinson et al.[4], where they reported that 0.25 D of difference can produce visual symptoms. Bist et al.[5] found that 50% of

---

[1] World Health Organization. World report on vision. Vol. 214, World health Organization. 2019. 1–160 p

[2] Elliott DB. Clinical procedures in primary eye care. 4th ed. London, United Kingdom; 2014. 68–111 p.

[3] Rodriguez-Lopez, Dorronsoro. Beyond traditional subjective refraction. Current Opinion in Ophthalmology. 3(3), 228-234 (2022).

[4] Atchison DA, Schmid KL, Edwards KP, et al. The effect of under and over refractive correction on visual performance and spectacle lens acceptance. Ophthalmic Physiol Opt. 2001;21(4):255–61.

[5] Bist J, Kaphle D, Marasini S, Kandel H. Spectacle non-tolerance in clinical practice – a systematic review with meta-analysis. Ophthalmic Physiol Opt. 2021;41(3):610–22.

intolerances to visual prescription comes from an inaccurate evaluation, and Freeman et al.[6] showed that most intolerances could be solved by modifying the prescription only 0.50 D. In summary, although the visual system can adapt, accurate prescriptions are still needed for comfortable and precise vision.

PROBLEM STATEMENT/OBJECTIVE

Over the years, efforts have been made to enhance efficiency by developing objective techniques that eliminate the subjective and iterative nature of traditional methods. Modern objective refraction instruments, many of which are open-field, wavefront-based, portable, or combined with keratometry, has become widespread in clinics. However, objective autorefractors are not considered to yield results that are directly interchangeable with subjective refraction. Instead, they serve as a valuable starting point for the subjective refraction procedure[2,3].

Attempts have been made to introduce new technologies aimed at simplifying the traditional method, such as Vision-R 800T (Essilor), i.Scription (Zeiss), Chronos (Topcon), NidekTS-610 (Nidek), Netra (EyeNetra), Easee eye test (Easee), VARS (VmaxVision), EyeRefract (Visionix), and VAO (Voptica)[3]. These instruments offer certain advantages such as automation, self-refraction, or a combination of subjective and objective techniques. However, these instruments are based on variations of the traditional subjective refraction, and, while they bring some improvements, they are still subject to the intrinsic limitations and constraints associated with the traditional method of identifying letters or minimize blur.

In the Institute of Optics from CSIC (Madrid, Spain), we have developed a new method to evaluate the refractive error called **Direct Subjective Refraction (DSR)**, which uses a disruptive working principle based on the use of quick defocus changes in combination with a bichromatic stimulus (made of blue and red components) to create a chromatic flicker. In short, the quick change in defocus produces a flicker perception on the stimulus, which affects more to blue components when the subject is myopic, to red components where is hyperopic, and it is minimum in the best prescription. This video shows the working principle. Therefore, the task of the subject in this method is to minimize the flicker, being the **first subjective method that does not use the letter identification** of the traditional method to find the refractive error. We have shown that this method **reduces measurement time by 5x** (from 6 to 1.2 minutes) and **increases repeatability** (from ±0.28 to ±0.17 D) compared to the traditional method[7]. The improvement of this method is explained because **the accommodation response barely influences**, which stays in a fixed position due to the impossibility of following the fast defocus change, largely eliminating the main issue of the traditional method. Besides, it is an **autonomous** procedure as patients can perform it by themselves (previous explanation of the task by the clinician). We have created a **portable** device called **SureVision**, that implements the DSR method, increasing the suitability of the technology for most environments.

The DSR method has been developed during the PhD thesis of the Project Leader, Victor Rodriguez Lopez[8]. A pilot study was carried out to test the proof-of-concept in 25 volunteers. It was proved that the DSR method is much faster (<1 minute) and more repeatable (±0.17 D) than the traditional method. Besides, the method was extended to provide a full prescription (both the spherical equivalent and the amount of astigmatism)[8] and its robustness against different stimuli configuration has been confirmed[9]. A first prototype (SureVision) was already developed using 3D modeling and 3D printing and custom electronics, and was tested in Hospital Clinico San Carlos (Madrid, Spain). Out of these measurements, we obtained precious feedback from real patients to iterate and pivot the prototype. We are currently implementing that feedback.

Many **scientific contributions** have been produced:

- 3 contributions to ARVO Annual Meetings (2019 -hot topic, among the 5% best contributions of the conference over 12.000-; 2021; and 2023), the most important conference in ophthalmology and vision

---

[6] Freeman CE, Evans BJW. Investigation of the causes of non-tolerance to optometric prescriptions for spectacles. Ophthalmic Physiol Opt. 2010;30(1):1–11.

[7] V. Rodríguez-Lopez, A. Hernandez, C. Dorronsoro. Defocus flicker deactivates accommodation. Biomed. Opt. Exp (2023) https://doi.org/10.1364/BOE.486466. Biomedical Optics Express 14, 3654-3670 (2023).

[8] V. Rodríguez-Lopez. Perception of static and dynamic blur for developing clinical instrumentation in optometry and ophthalmology. PhD in Biomedical Sciences and Technologies. Defended 25th November 2022.

[9] V. Rodríguez-Lopez, C. Sanchez-García, E. Esteban-Ibañez, N. Arejita, C. Dorronsoro. Robustness of the Direct Subjective Refraction method. Association for Research in Vision and Ophthalmology Conference (ARVO) New Orleans, 2023

science, and 2 more to other important international meetings in visual science (Summer Data Blast 2022 and Biophotonics Eye Research Conference 2023).

- 1 patent (P190451ES, CSIC owner) filled 4th March 2019 and accepted 7th April 2021, and PCT extended to Europe, US, and Japan.
- 3 papers published in high-impact journals: 1) *Beyond Traditional Subjective Refraction*, Current Opinion in Ophthalmology, 2) *Defocus flicker deactivates accommodation* in Biomedical Optics Express and 3) *The spatiotemporal defocus sensitivity function* in Biomedical Optics Express.
- 1 PhD thesis[8].
- 3 Master's Thesis.

The **commercial viability** of SureVision has been explored and the **innovative profile** of the project and the Project Leader (VRL) have also been validated:

- VRL was granted with 100,000€ with a Caixa Validate Research program from Fundación La Caixa, one of the most important grants for innovation in health from the Spanish ecosystem.
- VRL was granted with a Special Mention in the Best Patent of the Year by Young Inventors Award 2023 granted by the Spanish Patent Office with this patent.
- VRL has been selected as an MIT Innovator Under 35 Europe 2023.
- A Freedom To Operate (FTO) analysis was made by the patent firm Pons IP covering US, Europe, and Japan and it showed that there is no infringement of other intellectual property rights.
- Successful completion of 2 acceleration programs (CRAASH BCN 2021 by CIMIT and Biocat; winner of Healthstart 2023 -10.000€- and Special Incubation Award by Fundacion Madri+d) that have provided a thorough comprehension of the market and the development of an initial business plan.
- 3rd winner of Hackaton CSIC I 2022 and finalist of Hackaton CSIC II 2023.
- Prototype exhibition in CSIC Innovation Hub Converge presentation 2023 and Demo Day CSIC 2022.

SureVision is a **novel and disruptive ophthalmic instrument** that evaluates the refractive error faster and more accurately than the traditional gold-standard method of testing. SureVision is based on the patent-protected Direct Subjective Refraction method bringing a revolution to the eyecare community. The high precision and low measurement time of DSR make SureVision a potential candidate for replacing the current paradigms, as their advantages overpass current devices and improve the experience of all stakeholders implied: patients, clinicians, clinics, manufacturers. The **final goal** of this project is to create a spinoff company to exploit the technology and commercialize this new ophthalmic device.

OUTLINE OF TASKS/WORK PLAN

Work package (WP) 1. Scientific advance

- Build optical system to monitor accommodation response while performing DSR task to answer fundamental questions about accommodation and temporal blur perception.
- Develop a computational theory about the DSR method, as a framework for understanding and explaining theoretically the perceptual consequences and as a tool for improving the stimulus.

WP2. Product development

- Refinement of the optical system to optimize the psychophysical task.
- Design industrial prototype: conceptualization of the prospective product (head-mounted), 3D modeling and printing.
- First Industrial Prototype.
- Design an App to carry out the measurements.
- Iteration of the first prototype.

WP3. R&D developments

- General R&D efforts for refining psychophysical method and clinical protocol. Measurement of angle of astigmatism. Explore the effect of other parameters: pupil size, distance, overall luminance.
- R&D development I: Protocol for controlling pupil alignment using cameras and infrared illumination.
- R&D development II: Calibration system to ensure alignment of all optical elements.
- R&D development III: Inclusion of objective measurement using aberrometry or pupil light reflex.

- R&D development IV: include DSR method in a conventional phoropter by reengineering the device and including the psychophysical task.

WP4. Clinical studies

- Clinical study I. Conduct clinical study in normal (healthy) population for technology validation and regulatory approval. Obtain feedback from >20 clinical stakeholders and from >5 economic buyers and potential early adopters.
- Clinical study II. Conduct clinical study in refractive surgery population. Increase scientific evidence.

WP5. Business roadmap

- Develop full business plan and financial plan. Market analysis.
- Investment strategy (Caixa Impulse, FIPSE Viability Studies, OPTICA Foundation Challenge, Spanish National Projects RETOS-Colaboración, Technology Development in Health Carlos III Institute; investment forums, and startup competitions) and investment proposal (pitch).
- Management and maintenance of IP portfolio.
- Spin-off creation: Legal framework for shareholders agreement, CSIC involvement in the company, etc.

WP6. Dissemination

- Attendance to key conferences (ARVO, AAO, ESCRS, ASCRS, FiO, Photonic West) to share with the scientific and clinical with the latest updates and results. Scientific publications.
- Meetings with early adopters, users, and potential clients.
- SureVision brand: webpage, trademark, marketing material, sales strategy.

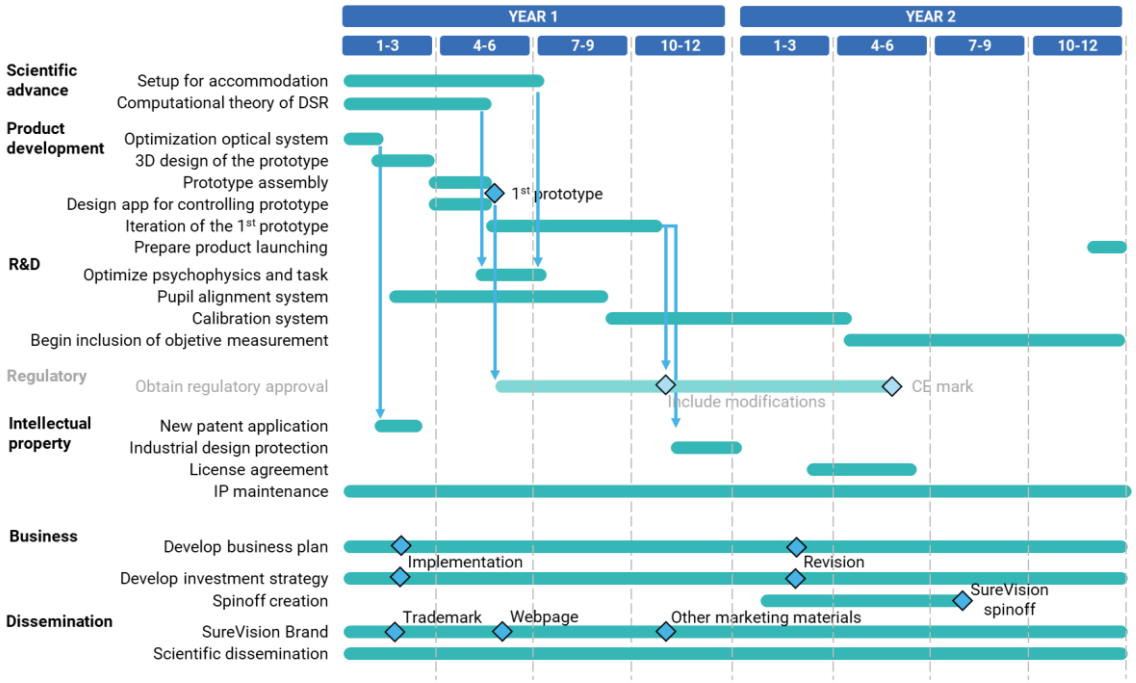

Figure 1. Gantt Chart of the activities of the project.

I differentiate between WP1 (scientific advance) and WP3 (R&D activities) because WP1 is devoted to advance in the scientific understanding of the project and WP3 is focused on activities to improve a future device. Also, regulatory activities (in gray in Figure 1) will be cofounded by other grants of the laboratory.

OUTCOME(S)

The disruptive nature of the technology makes the Direct Subjective Refraction the first subjective method that does not use letter identification as its working principle, like the traditional method, but chromatic flicker minimization. This project will allow the advance on the general knowledge of the method as well as ground scientific questions regarding the accommodative system of the human eye. The main expected results are:

- The main outcome of the project will be a novel ophthalmic device using the DSR method, ready for clinical use, and very close to the market.

- 2-3 scientific papers in high-impact journals (Optica, Eye, Biomedical Optics Express, BMC Ophthalmology, Ophthalmology, Current Biology, Nature Communications, among others).
- 1 patent application protecting the novel optical system, growing the family patent of the method, and considering PCT extension to other regions of interest.
- Incorporation of 1 junior engineer for carrying out the R&D developments described in the work plan.
- Participation in international conferences: Annual Meeting of the Association for Research in Vision and Ophthalmology, European Society of Cataract & Refractive Surgeons, American Society of Cataract & Refractive Surgeons, OPTICA-Frontiers in Optics, SPIE-Photonics West, or Visual and Physiological Optic meeting; all of them previously attended by the fellow or other team members.
- Website creation for promoting the technology and as a digital hub for clinical, business, and scientific accomplishments and for opening doors to new opportunities, collaborators, investors, and customers.

IMPACT

SureVision is a technology that enables a fast and accurate evaluation of refractive errors, significantly reducing measurement time while increasing precision. It represents a turning point in the way vision has been evaluated in the last decades, with the potential for transforming not only the eyewear industry but also society as a whole. As mentioned before, novel methods are mainly modifications of the traditional method and therefore maintain their disadvantages. This method is the first that uses a different subjective approach to provide a prescription, minimization of chromatic flicker. All agents involved are benefited:

- **For patients**. Reduces fatigue and measurement time associated with obtaining the prescription, providing an accurate prescription in a very short time. The suitability of the new method will increase access to a simple prescription to patients that currently do not have it. The patient can benefit from both more time to obtain a more complete visual exam as well as obtaining a *premium* prescription.
- **For clinicians**. It reduces measurement time, allowing them to use that extra time to perform more tests in a complete visual exam or to measure more patients while providing a very accurate prescription.
- **For clinics**. It improves overall efficiency and can pay back in a very short time the improvements SureVision provides, both in more accurate or *premium* prescriptions, as well as using the time savings on more patients or more vision tests.
- **For lens manufacturers**. Reduce returns by having a more accurate prescription. In addition, the current minimum lens pitch is ±0.25 D in most cases. SureVision stimulates technological progress by promoting the possibility of more accurate lens manufacturing.
- **Screening companies and NGOs** could benefit from the advantages of SureVision, as it provides an accurate and autonomous prescription with portable and accessible equipment.

Furthermore, SureVision potentially has a significant impact on the eyewear industry. The high precision of SureVision precision can lead to a reduction in the number of returns and exchanges, thereby reducing waste and CO_2 footprint and improving the sustainability of the industry. Additionally, the customization can provide the opportunity for more innovative and personalized eyewear designs, catering to individual needs and styles.

The project has a strong relationship with the **Sustainable Development Goals** of the United Nations, mainly with Goal 3 (Good health and well-being), 8 (Decent work and economic growth), and 10 (Reduced inequalities). RRI principles will be implemented and sustained in the long term. From the ethical perspective, the project will be carried out in accordance with ethical standards for research, national and EU regulations and will be submitted to CSIC's Ethical Committee for approval. We will also develop gender competence within the team to ensure gender-responsive implementation.

As a summary, transferring SureVision to society, which is the final goal of this project, will be highly transformative, revolutionizing how refractive error is measured with a disruptive approach. It will also serve as an incentive for the ophthalmic industry, as more precise prescriptions will require new expertise and resources. The successful completion of the project (phases towards regulatory approval, spinoff constitution, and commercialization) will produce a positive impact on the community at large, healthcare, economic growth, preventable blindness, and well-being in general, aligned with the Sustainable Development Goals of the United Nations.

Project summary

Challenge: Biomarkers are biological molecules present in the bodily fluids and tissues which provide critical knowledge on human health. Detecting and quantifying biomarkers are useful in disease diagnostics, prognosis, efficacy of therapy and treatment, and drug discovery and development. Current detection methodologies such as enzyme-linked immunosorbent assay (ELISA), polymerase chain reaction, western blotting, and electrochemical sensors lack either low limit of detection (i.e, quantifying attomolar concentrations) or long detection time or combination of both. This limits their use for detecting biomarkers that are found in low concentrations but provide valuable information on human health. Thus, to quantify these biomarkers, it is necessary to develop a new sensing methodology with low limit of detection and faster sensing time, that is also cost-effective and user-friendly.

Proposed project: The overarching goal of this project is to develop a digital, ultra-sensitive, cost-effective, and user-friendly sensor system for biomarkers. We aim to achieve this by employing an *advanced nanophotonic platform called as zero-mode waveguides (ZMWs) in combination with an optical dark-field microscopy*. In this project, we will develop our sensor targeted to Interleukin-6 (IL-6), one of the common cytokines to understand the condition of disease which is associated with several diseases including COVID-19, HIV, Alzheimer's and CAR-T cancer therapy. ZMWs are cylindrical or conical nanopores in a thin metal film (typically 100 – 200 nm) with a bottom pore diameter smaller than the wavelength of visible light, capable of confining excitation radiation within the nanopore with the intensity decaying exponentially along the axial direction. We will exploit this feature of the ZMW to quantify biomarkers with the plasmonic nanoparticle as a scattering readout mechanism. Imaging the ZMW substrate under dark-field mode blocks the trans-illumination but effectively captures the low angle light scattered by the individual nanopores. The inherent light scattering by the nanopore increases with the insertion of a plasmonic nanoparticles such as silver inside the nanopore due to their localized surface plasmon resonance (LSPR) property. Using this principle, we will quantify the biomarker concentration in two ways: 1) Construct molecular architecture to attract and hold IL-6 in the nanopores and use silver nanoparticles to specifically bind to the nanopores containing IL-6. By monitoring and counting the number of nanopores with the nanoparticles, we can quantify the IL6 concentration. 2) Immobilize IL-6 on the surface of silver nanoparticles using molecular architecture followed by releasing silver particles and microscopically counting them on the ZMW substrate and relate to IL-6 concentration. Further, we will improve the limit of detection and detection time by increasing the mass transport of silver nanoparticles inside the nanopores using a voltage gate.

Outcomes: We expect that the proposed nanophotonic based platform, zero-mode waveguides will quantify IL-6 in the atto molar range (~10-18 M) within 30 minutes including assay formation and readout. Naturally, the platform can be extended to quantify other biomarkers by forming suitable assay. Further, the approach can be transformed into multiplex sensing by co-functionalizing nanopores with multiple recognition elements targeting different analytes, which can be sensed by employing different size plasmonic nanoparticle to provide difference in the scattering intensity magnitude. Lastly, the dark-field microscopy can be implemented on a smartphone-based detection setup, making it an easily accessible POC platform.

Electrochemical Zero-mode Waveguides Based Digital Sensing of Biomarkers

PI: Vignesh Sundaresan, Assistant Professor of Chemistry and Biochemistry, University of Mississippi

Current state and problems. Cytokines are small proteins produced by cells in the immune system that regulate inflammatory responses, making them ideal biomarkers for various pathological states.[1, 2] Although cytokines typically guide healthy immune responses, pathogens can trigger excessive immune responses caused by the overproduction of proinflammatory cytokines ('cytokine storms'), which can rapidly escalate to multi-organ failure and eventually death.[3, 4] Treatment requires early detection and intervention. However, there is currently no reliable diagnostic test to detect the onset of cytokine storms. This is a critical issue with COVID-19 as well as a major side-effect of CAR-T cancer therapy, where physicians report the most severe cases, and a large number of deaths (20-30%) correlate with cytokine storms.[5-7] Recent studies suggest elevated levels of interleukin-6 (IL-6), an early-stage proinflammatory cytokine, is a reliable precursor to COVID-19 cytokine storms and adverse patient outcomes.[8, 9] IL-6 has also been shown to be an effective marker for a variety of diseases such as HIV, Alzheimer's, and cytokine release syndrome.[10-14]

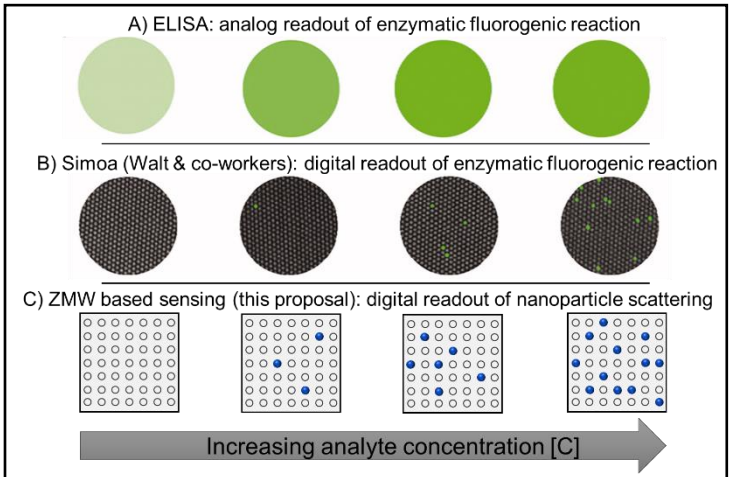

Figure 1. Detection method schematic of ELISA, Simoa, and ZMW based sensing. Panels A and B are from ref. 17

Currently, the existing "gold standard" method for quantifying IL-6 in patient samples is enzyme-linked immunosorbent assay (ELISA), where the IL-6 concentration is determined by the intensity of an enzymatic fluorogenic reaction (**Figure 1A**).[15] However, ELISA is not sensitive enough to detect the onset of cytokine storms (limit of detection, LOD - 5.24 fM), and is also time-consuming.[16] Walt and co-workers demonstrated ultra-sensitive detection of IL-6 (0.21 fM) using the single-molecule array (Simoa), where the enzymatic fluorogenic immunoassay is developed within microwells and the analyte concentration is determined by the number of microwells that exhibit fluorescence output (**Figure 1B**).[16, 17] Because Simoa is based on single-molecule fluorescence, it requires a large number of microwells (>50000) and utilizes enzymes, lasers, and ultra-sensitive detectors which makes it a costly assay. Moreover, at low analyte concentrations, the fluorescence is shot noise-limited which affects the Simoa sensitivity.

Research Objectives. The overarching goal of this proposal is to develop a digital, and ultra-sensitive sensor system for IL-6 that is also cost-effective and user-friendly. We aim to achieve this by employing **an advanced nanophotonic platform called zero-mode waveguides (ZMWs) in combination with optical dark-field microscopy** (**Figure 1C**). We envision that this nanophotonic platform will provide diagnostic and prognostic value by quantifying IL-6 digitally and lead to improved health care. The plan to achieve this is divided into three specific aims: 1) detect and determine IL-6 concentration directly by immobilizing nanoparticles (NPs) into ZMWs; 2) quantify IL-6 concentration indirectly by counting the number of captured NPs; 3) achieve rapid and ultra-sensitive detection by electric-field enhanced mass-transport of NPs. Analytical sensitivity, LOD, linear dynamic range, robustness to interferences, and reproducibility will be determined.

ZMWs and advantages. ZMWs which, at the most basic level, a cylindrical perforation (diameter < 150 nm) in a thin metal film, capable of trapping optical radiation (**Figure 2A**).[18, 19] The trapped radiation can interact with molecules contained in the zeptoliter-scale (1 zL = 10^{-21} L) volume bounded by the radiation field and enclosed within the nanopore (**Figure 2B**).[20] Although ZMWs have been previously used in single-molecule studies, in this proposal, we will push the boundaries of ZMWs by using them as a digital sensing platform, which can be directly applied in the healthcare setting.

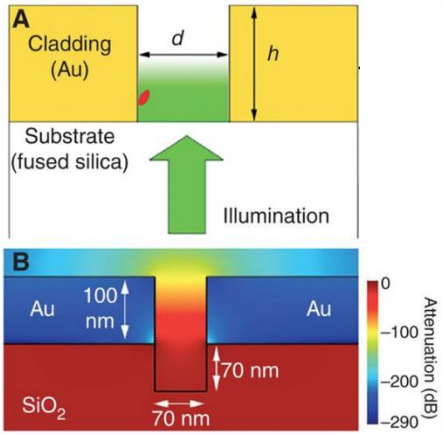

Figure 2. A) Schematic cross-section of a single E-ZMW illustrating Au film used both as an optical cladding layer and working electrode. Red ellipse represents single molecule. B) Cross-sectional illustration of single E-ZMW with optical field heat map showing evanescent field. From Ref. 20.

ZMWs based sensing platform offer several advantages:[21] (1) Ultra-low volume. The active volume of individual nanopores is in the order of femto- to attoliters (or 10^{-18} m^3 to 10^{-21} m^3) which helps to sequester single entities such as molecules or NPs even in relatively high concentrations (i.e., single molecule or NP per pore coverage for 11 aL nanopore can be achieved with 2 µM concentration). Additionally, the nanopore dimension can be easily tuned to accommodate one or a few NPs. (2) Chemical functionalization. The construction of ZMWs with Au cladding layer and a SiO_2 base can take advantage of the chemical orthogonality of these two materials, so the biorecognition elements can be directed to, and immobilized at either the base of the ZMWs (using organosilane linker chemistry) or the Au layer (using thiol based self-assembly strategies). (3) Control of local electric field. The gold optical cladding layer in each pore is connected to those in all the other pores which can be used as electrodes. Additionally, another Au layer or electrode can be added on top of the structure, which can be used to change the electric field locally by applying appropriate potentials (*vide infra, see Aim 3)*. (4) Massively parallel array and digitization. The capture of NPs can be studied simultaneously over an entire array and can obtain a digitized output using a simple algorithm. (5) Enhanced sensitivity. This sensor platform is based on NPs scattering, which are efficient scatterers, so it is not shot noise limited.

Research Plan.

Aim 1: Detect and determine IL-6 concentration directly by immobilizing NPs into ZMWs. The ZMWs will be fabricated using a combination of deposition and focused ion beam (FIB) techniques.[22, 23] Briefly, a gold layer (200 nm) will be deposited onto a clean glass coverslip using e-beam evaporation followed by the deposition of silicon dioxide (100 nm) using plasma-enhanced chemical vapor deposition (PECVD). Finally FIB will be used to mill an array of conical nanopores on the metal-insulator structure. A representative 21 × 21 nanopore array (pore diameter: top = ~200 nm and bottom = ~100 nm) is shown in **Figure 3A**. The optical dark-field image of the nanopore array (**Figure 3B**) shows an array of bright spots in which each bright

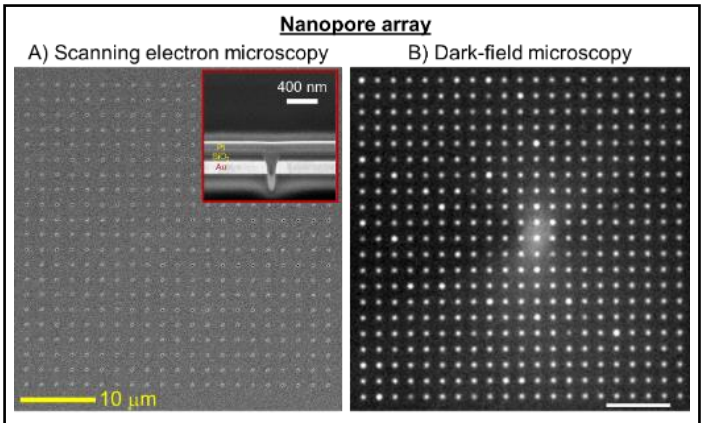

Figure 3. ZMW array imaged with two different microscopy methods. Inset shows cross-section of single nanopore.

spot corresponds to the light scattering from individual nanopores. The array size, the interpore distance, and the diameter of the nanopore can easily be optimized by adjusting FIB parameters.

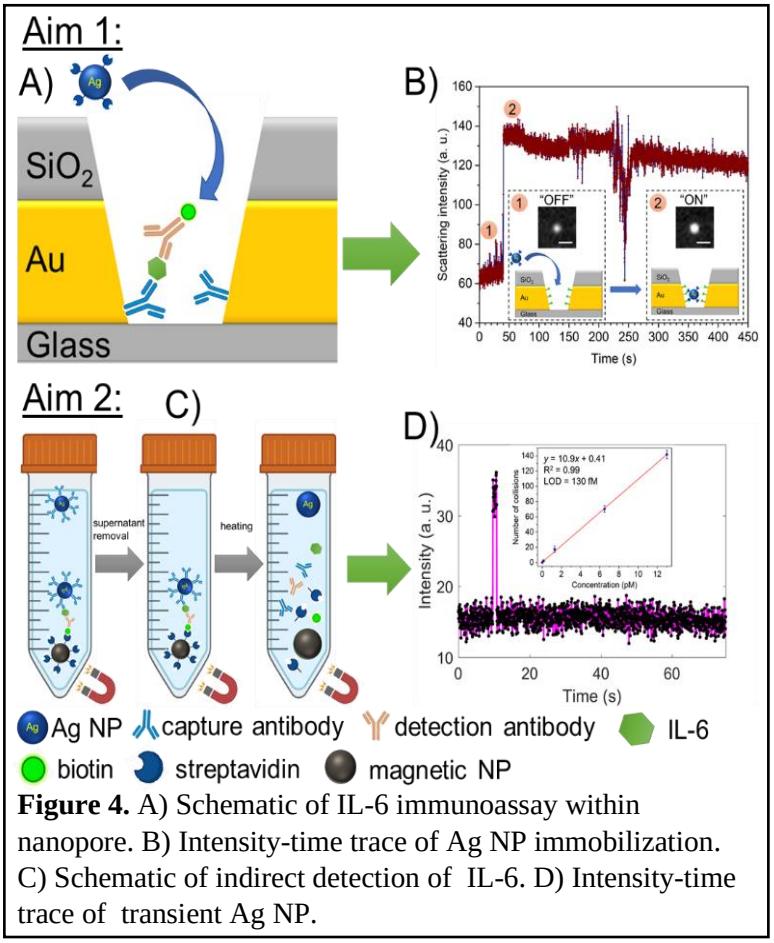

Figure 4. A) Schematic of IL-6 immunoassay within nanopore. B) Intensity-time trace of Ag NP immobilization. C) Schematic of indirect detection of IL-6. D) Intensity-time trace of transient Ag NP.

To detect IL-6 directly, we will immobilize a capture antibody in each nanopore (**Figure 4A**). First, the exposed gold surface within the nanopore will be functionalized with thiol/carbodiimide linker chemistry, followed by the immobilization of IL-6 capture antibodies. Ideally, we aim to have a single IL-6 molecule in each nanopore so finite-difference time-domain (FDTD) simulations can be carried out to optimize assay parameters such as incubation time and the number of pores for obtaining single molecule coverage. Then, the nanopore array substrate will be exposed to a standard solution of IL-6 analyte to allow binding to the capture antibody. After the formation of the antibody-antigen complex, a biotinylated secondary antibody will be introduced followed by streptavidin labeled Ag NP (S-Ag NP) and subsequently imaged with dark-field microscopy (**Figure 4A**). If a nanopore contains IL-6 and the recruited biotinylated detection antibody, S-Ag NPs can be captured within the nanopore because of the high-affinity binding of biotin to streptavidin.[24] Because the Ag NPs exhibit enhanced light scattering due to the localized surface plasmon resonance (LSPR), we expect the dark-field scattering intensity of the nanopore to increase due to the insertion of Ag NP. Preliminary results (**Figure 4B**) confirm that the S-Ag NP can be immobilized within the biotin functionalized nanopore as indicated by the step increase in scattering intensity. We will then image the dark-field array, digitize the output, and analyze the results by calculating the ratio of high intensity (with NP) to low intensity (without NP) pores, *i.e.* [ON/OFF]. The limit of detection and dynamic linear range will be obtained by creating a calibration curve relating [ON/OFF] to IL-6 concentration.

Aim 2: Quantify IL-6 concentration indirectly by counting the number of captured NPs. This aim focuses on the indirect sensing of IL-6 by quantifying the concentration of Ag NPs. To accomplish this, the IL-6 capture antibodies (described in Aim 1) will be assembled on the surface of Ag NP. After IL-6 recognition, they will be labeled by hybridization to streptavidin-labeled magnetic NPs and separated using a magnetic field (**Figure 4C**).[25] The Ag NPs without IL-6 will not be attracted by the magnetic field; thus, they will be removed with the supernatant. After supernatant removal, the solution will be heated to denature biomolecules that release Ag NPs, whose concentration will be quantified by introducing the solution containing released Ag NPs onto the unlabeled-nanopore array substrate. In these assays, Ag NPs will be allowed to diffuse in and out of the nanopore, and the resulting Ag NPs will be detected by transient

scattering increase, **Figure 4D**. The concentration of Ag NP released during heating is dictated by the IL-6 concentration, so we can calibrate the number of collisions *vs.* the Ag NP/IL-6 concentration. A preliminary experiment performed with citrate-capped Ag NPs on a 21 × 21 nanopore array showed several transient scattering events, proportional to the concentration of free Ag NPs (**Figure 4D**, *inset*). After creating the calibration curve (# of collisions *vs.* Ag NPs concentration), we determined the LOD as 130×10^{-15} M, and it should be possible to further improve the LOD simply by employing a larger nanopore array.

Aim 3: Achieve rapid and ultra-sensitive detection by electric-field enhanced mass-transport of NPs. This aim focuses on improving the speed and sensitivity of the nanophotonic sensor platform by introducing another hierarchical gold and silicon dioxide layer such that each pore supports two vertically spaced gold layers as schematically shown in **Figure 5A**.[19] The SEM image of our preliminary fabrication attempt is shown in **Figure 5B**, where the two gold layers (100 nm each) are separated by the silicon nitride insulator layer and the top gold layer is protected by the silicon dioxide layer. As discussed in Aim 1, the bottom gold layer will be used to functionalize biorecognition elements, whereas the top gold layer will be used to apply suitable potentials to control the transport of Ag NPs. For example, applying a small positive potential (+0.3 V) to a solution containing negatively charged citrate-capped Ag NPs enhances the capture of NPs by the nanopore because of the local increase in the electric field within the nanopore. Additionally, the same architecture can be used to improve the detection time for the approach described in Aim 2 without functionalizing the bottom gold layer. Previously, this architecture was used to study the oxidation of single Ag NPs electrochemically (**Figure 5C**).[26] In their experiments, the bottom gold layer was poised to +0.3 V to detect the oxidation of Ag NPs, and the potential of the top gold layer was increased from +0.1 to +0.7 V. The collision frequency of the Ag NPs increased with the potential at the top gold layer. Overall, their approach showed 5× improvement in NP transport to the nanopore, so it is reasonable to project that by applying an electric field and increasing the nanopore array size, we can achieve LODs in the ~10^{-18} M (aM) range, rendering this an ideal approach for IL-6 and other cytokines that must be measured at ~10^{-15} M concentrations.

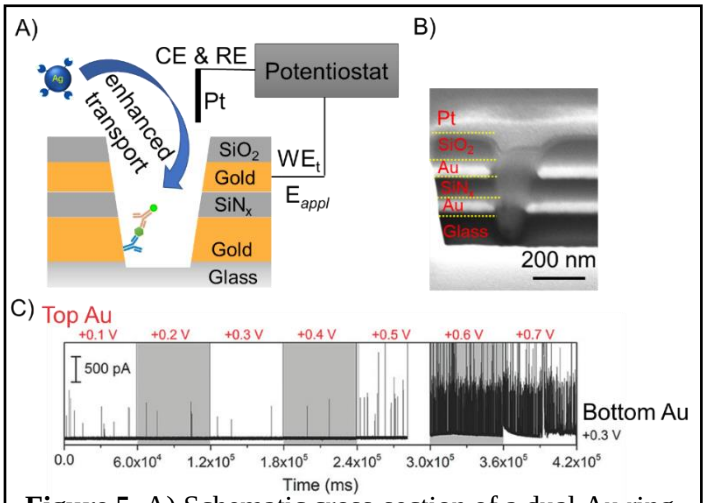

Figure 5. A) Schematic cross-section of a dual Au ring ZMW illustrating the top Au film used as a working electrode (WE), while the bottom Au is functionalized with the antibodies. B) Cross-section SEM image of dual Au ring ZMW. C) Current-time trace of the bottom Au layer poised at +0.3 V at different potentials of top Au layer (red). From ref. 26.

Outcomes and broader impact.

Milestones	Time (in months)			
	0 – 6	7 – 12	13 – 18	19 – 24
Aim 1: Detect and determine IL-6 concentration directly by immobilizing NPs into ZMWs				
Aim 2: Quantify IL-6 concentration indirectly by counting the number of captured NPs				
Aim 3: Achieve rapid and ultra-sensitive detection by electric-field enhanced mass-transport of NPs				

The main expected outcome of this project is an ultra-sensitive, user-friendly digital sensing nanophotonic platform – zero-mode waveguide - for quantifying biomarkers with LODs in the atto molar (~10^{-18} M) range. Additionally, the detection or sensing time of

the sensor is expected to be faster (<30 minutes) than traditional sensing methodologies enabling its use in point of care (POC) testing. In this proposal we used IL-6 as a model biomarker, naturally one can extend this approach to quantify other biomarkers by utilizing suitable recognition elements such as antibodies and aptamers. Additionally, this platform can be transformed for multiplex sensing by suitably functionalizing ZMWs and employing different size plasmonic NPs (each size targeted for a specific biomarker) to provide a difference in the scattering intensity magnitude (i.e., scattering intensity varies with the NP size).[27] Lastly, the IL-6 -specific assay (and by extension to other specific assays) can be pre-prepared on the nanopore array, and dark-field microscopy can be implemented on a smartphone-based detection setup,[28] making it an easily accessible POC platform.

References:

1. J.-M. Zhang and J. An, *International Anesthesiology Clinics*, 2007, **45**.
2. G. Arango Duque and A. Descoteaux, *Frontiers in Immunology*, 2014, **5**.
3. N. Mangalmurti and C. A. Hunter, *Immunity*, 2020, **53**, 19-25.
4. D. C. Fajgenbaum and C. H. June, *New England Journal of Medicine*, 2020, **383**, 2255-2273.
5. T. Kishimoto, *International Immunology*, 2021, DOI: 10.1093/intimm/dxab011.
6. T. Giavridis, S. J. C. van der Stegen, J. Eyquem, M. Hamieh, A. Piersigilli and M. Sadelain, *Nature Medicine*, 2018, **24**, 731-738.
7. S. Hojyo, M. Uchida, K. Tanaka, R. Hasebe, Y. Tanaka, M. Murakami and T. Hirano, *Inflammation and Regeneration*, 2020, **40**, 37.
8. C. A. Hunter and S. A. Jones, *Nature Immunology*, 2015, **16**, 448-457.
9. S. A. Jones and C. A. Hunter, *Nature Reviews Immunology*, 2021, **21**, 337-339.
10. J. M. Haissman, L. S. Vestergaard, S. Sembuche, C. Erikstrup, B. Mmbando, S. Mtullu, M. M. Lemnge, J. Gerstoft and H. Ullum, *JAIDS Journal of Acquired Immune Deficiency Syndromes*, 2009, **52**, 493-497.
11. E. Tackey, P. E. Lipsky and G. G. Illei, *Lupus*, 2004, **13**, 339-343.
12. W. Swardfager, K. Lanctôt, L. Rothenburg, A. Wong, J. Cappell and N. Herrmann, *Biological Psychiatry*, 2010, **68**, 930-941.
13. O. P. Kristiansen and T. Mandrup-Poulsen, *The Good, the Bad, or the Indifferent?*, 2005, **54**, S114-S124.
14. H. Murthy, M. Iqbal, J. C. Chavez and M. A. Kharfan-Dabaja, *Immunotargets Ther*, 2019, **8**, 43-52.
15. E. H. Cheteh, V. Sarne, S. Ceder, J. Bianchi, M. Augsten, H. Rundqvist, L. Egevad, A. Östman and K. G. Wiman, *Cell Death Discovery*, 2020, **6**, 42.
16. D. Wu, M. D. Milutinovic and D. R. Walt, *Analyst*, 2015, **140**, 6277-6282.
17. C. Wu, A. M. Maley and D. R. Walt, *Critical Reviews in Clinical Laboratory Sciences*, 2020, **57**, 270-290.
18. L. P. Zaino, D. A. Grismer, D. Han, G. M. Crouch and P. W. Bohn, *Faraday Discussions*, 2015, **184**, 101-115.
19. D. Han, Garrison M. Crouch, K. Fu, L. P. Zaino Iii and P. W. Bohn, *Chemical Science*, 2017, **8**, 5345-5355.
20. K. Fu, W. Xu, J. Hu, A. Lopez and P. W. Bohn, *Cold Spring Harb Perspect Med*, 2019, **9**.
21. K. Fu, S.-R. Kwon, D. Han and P. W. Bohn, *Accounts of Chemical Research*, 2020, **53**, 719-728.
22. V. Sundaresan and P. W. Bohn, *Chemical Science*, 2020, **11**, 10951-10958.
23. S. Baek, D. Han, S.-R. Kwon, V. Sundaresan and P. W. Bohn, *Analytical Chemistry*, 2022, **94**, 3970.
24. K. Aslan, C. C. Luhrs and V. H. Pérez-Luna, *The Journal of Physical Chemistry B*, 2004, **108**, 15631-15639.
25. T. Li, X. Xu, G. Zhang, R. Lin, Y. Chen, C. Li, F. Liu and N. Li, *Analytical Chemistry*, 2016, **88**, 4188
26. K. Fu, D. Han, G. M. Crouch, S.-R. Kwon and P. W. Bohn, *Small*, 2018, **14**, 1703248.
27. K. A. Willets and R. P. V. Duyne, *Annual Review of Physical Chemistry*, 2007, **58**, 267-297.
28. D. Sun and T. Y. Hu, *Biosensors and Bioelectronics*, 2018, **99**, 513-518.

Executive Summary

Title: Temperature Influence on Integrated Silicon-Germanium Electroabsorption Modulator for Optical Machine Learning Accelerator

PI: Weilu Gao, the University of Utah, Email: weilu.gao@utah.edu

Category: Information

Machine learning (ML) algorithms have seen unprecedented performance in broad applications, including computer vision, the discovery of materials and molecules, and electronic chip design. However, the execution of ML algorithms on hardware requires substantial computation and energy resources. The fundamental quantum mechanics limit leads to a bottleneck of further reducing the energy consumption and simultaneously increasing the integration density of electronic circuits to catch up with the increasing scale of modern large-scale ML models, thus urgently calling for new high-throughput and energy-efficient hardware ML accelerators. Recently, optical systems built upon silicon-on-insulator photonic integrated circuits (PICs) are emerging as high-performance hardware accelerators for executing the most computationally intensive matrix-vector multiplication (MVM) operations in large-scale ML models, thanks to their parallel and speed-of-light processing, and low static energy consumption. In addition, with the continuing advances of semiconductor foundry manufacturing, the integration density of PICs can reach thousands of devices in an area of $\sim$ mm^2 and the cost of PICs has reduced drastically. **The key to high-throughput and energy-efficient optical MVM calculations is the implementation of fast and energy-efficient electro-optic intensity modulators.**

Current modulation mechanisms implemented in the components of foundry Process Design Kits, such as GlobalFoundries and American Institute for Manufacturing Integrated Photonics (AIM Photonics), are mainly based on heat (e.g., thermal shifters) and carrier transport (e.g., p-n junctions) with limited modulation speeds (hundreds of kHz to a few GHz) and large energy consumptions (pJ to nJ/bit). In contrast, the electric field effects, such as the electroabsorption effects near the band edges of semiconductors including Franz-Keldysh (FK) and quantum-confined Stark effects, are ideal because they can deliver ultrafast response (> 100 GHz) and require little switching energy (10s fJ/bit). In particular, the latest photonics foundry technologies have prepared processes to involve high-speed electronics for high-speed optical modulators. For example, the GlobalFoundries just released its first-of-its-kind SiGe platform, GF Fotonix, laying the ground for the volume manufacturing of semiconductor FK electroabsorption optical modulators.

Despite the readiness of industry technologies and a few but limited prior works, there has been little attention paid to the temperature influence on FK electroabsorption modulators. **The goal of this 15-month project will be analyzing the temperature influence on the behaviors of devices, circuits, and ML systems based on FK modulators, and designing new temperature-insensitive circuits and chip tapeouts ready for future foundry manufacturing and testing**. Specifically, this project will **(i)** create a high-throughput, integrated simulation framework consisting of materials, devices, circuits, and ML systems based on SiGe FK modulators for analyzing temperature influence and **(ii)** design temperature-insensitive circuits and chip tapeouts based on AIM Photonics foundry processes for future manufacturing and testing. The deliverables of this project will have far-reaching implications in various aspects. For example, the developed integrated simulation framework will enable the co-design and end-to-end design of optical materials, devices, circuits, and systems. In addition, the designed temperature-insensitive FK modulators can be applied not only to next-generation high-speed, high-throughput, and energy-efficient optical ML hardware accelerators, but also many other application scenarios, such as optical communications and photonic quantum information processing.

Temperature Influence on Integrated Silicon-Germanium Electroabsorption Modulator for Optical Machine Learning Accelerator

PI: Weilu Gao, the University of Utah

1. Literature Review

Machine learning (ML) algorithms have seen unprecedented performance in broad applications, including computer vision [1], the discovery of materials and molecules [2], and electronic chip design [3]. However, the execution of ML algorithms on hardware requires substantial computation and energy resources. The fundamental quantum mechanics limit leads to a bottleneck of further reducing the energy consumption and simultaneously increasing the integration density of electronic circuits to catch up with the increasing scale of modern large-scale ML models [4, 5], thus urgently calling for new high-throughput and energy-efficient hardware ML accelerators. Recently, optical systems built upon silicon-on-insulator (SOI) photonic integrated circuits (PICs) are emerging as high-performance hardware accelerators for executing the most computationally intensive matrix-vector multiplication (MVM) operations in large-scale ML models [6–11], thanks to their parallel and speed-of-light processing, and low static energy consumption. In addition, with the continuing advances of semiconductor foundry manufacturing, the integration density of PICs can reach thousands of devices in an area of $\sim$ mm^2 and the cost of PICs has reduced drastically.

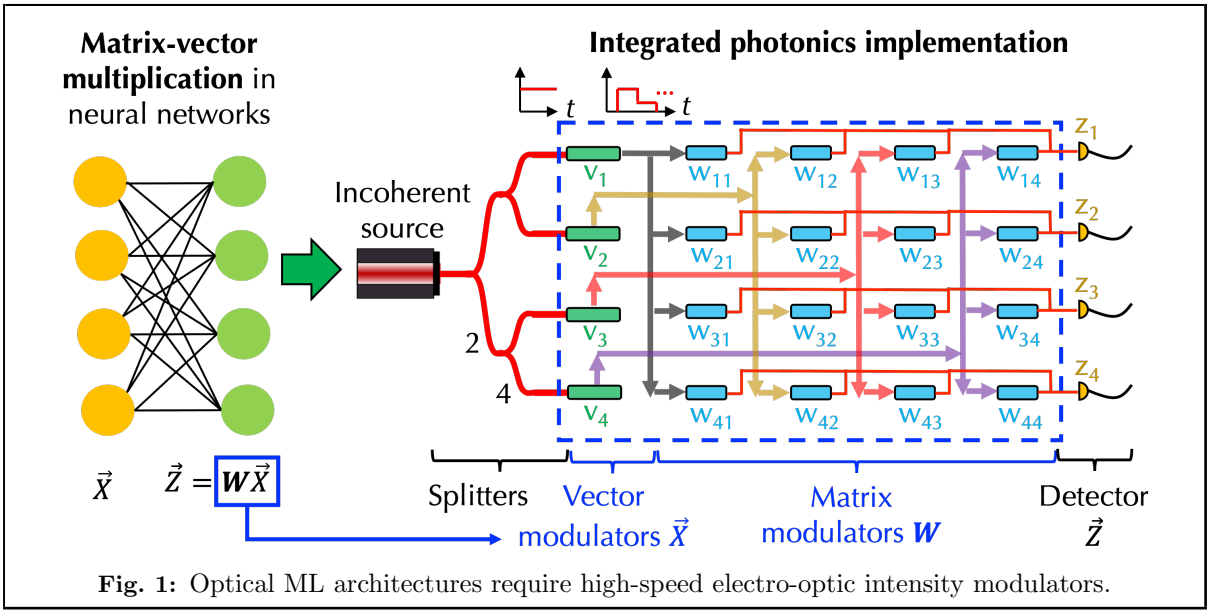

Fig. 1: Optical ML architectures require high-speed electro-optic intensity modulators.

Fig. 1 depicts an illustration of performing 4×4 MVM in PICs. An *incoherent* light source (e.g., superluminescent diode) equally splits its power through cascaded Y-junctions. The input vector $\vec{X}$, such as flattened images, and the matrix $\mathbf{W}$, such as neural network weights, are physically implemented by modulating light *intensity* with 1D and 2D arrays of modulators, respectively. The connection among modulators represents the calculation orders in MVM operations. The detector array converts the output vector $\vec{Z}$ signal from optical to electrical domains for post-processing, such as applying nonlinear functions. **Hence, the implementation of fast and energy-efficient electro-optic intensity modulators is one key to high-throughput and energy-efficient optical MVM calculations**.

Current modulation mechanisms implemented in the components of foundry Process Design Kits, such as GlobalFoundries and American Institute for Manufacturing Integrated Photonics (AIM Photonics), are mainly based on heat (e.g., thermal shifters) and carrier transport (e.g., *p*-*n* junctions) with limited modulation speeds (hundreds of kHz to a few GHz) and large energy consumptions (pJ to nJ/bit). In contrast, the electric field effects, such as the electroabsorption

effects near the band edges of semiconductors including Franz-Keldysh (FK) and quantum-confined Stark effects, are ideal because they can deliver ultrafast response ($> 100\,\text{GHz}$) and require little switching energy (10s fJ/bit) [12–14]. In particular, the latest photonics foundry technologies have prepared processes to involve high-speed electronics for high-speed optical modulators. For example, the GlobalFoundries just released its first-of-its-kind SiGe platform, GF Fotonix [15], laying the ground for the volume manufacturing of semiconductor FK electroabsorption optical modulators [16–20].

2. Problem Statement

Despite the readiness of industry technologies and a few but limited prior works [16–20], there has been little attention paid to the temperature influence on FK electroabsorption modulators. **Fig. 2a** displays the calculated spectra of absorption coefficient α of Ge under various applied electric fields. The detailed calculation approach is described in **Sec. 3**. At zero fields (blue line in **Fig. 2a**), there is a clear cutoff of absorption spectra at $\approx 1.59\,\mu\text{m}$, which corresponds to an interband transition gap in Ge. As the electric field increases, the subband absorption (i.e., in the region $> 1.59\,\mu\text{m}$) increases because of quantum tunneling between transition bands. There is also an oscillation in absorption spectra above the gap (i.e., in the region $< 1.59\,\mu\text{m}$, not shown in **Fig. 2a**). The subband absorption and above-gap absorption oscillation are two hallmark features of the FK effect [21]. Hence, the interband transition gap plays a crucial role in the FK effect. However, such gaps in any semiconductors have temperature dependence, which is typically described as Varshni equations (details in **Sec. 3**). **Fig. 2b** displays the calculated absorption spectra of Ge at two temperatures ($T = 300\,\text{K}$ and $315\,\text{K}$), showing a clear and strong temperature dependence with α change 40 % at $\approx 1.6\,\mu\text{m}$.

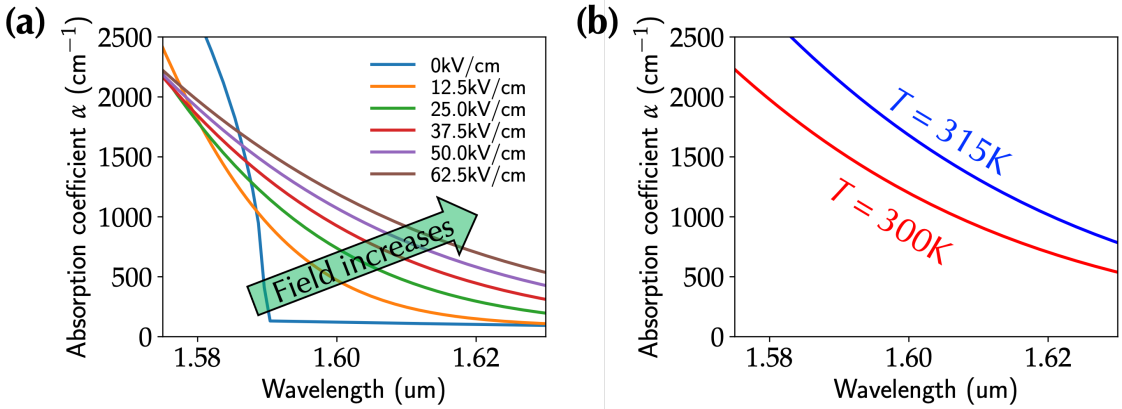

Fig. 2: Ge absorption spectra under **(a)** various electric fields and **(b)** $T = 300\,\text{K}$ and $350\,\text{K}$.

The goal of this 15-month project will be analyzing the temperature influence on the behaviors of devices, circuits, and ML systems based on FK modulators, and designing new temperature-insensitive circuits and chip tapeouts ready for future foundry manufacturing and testing. The specific tasks of this project will include:

- **(a)** Create a high-throughput, integrated simulation framework consisting of materials, devices, circuits, and ML systems based on SiGe FK modulators for analyzing temperature influence.
- **(b)** Design temperature-insensitive circuits and chip tapeouts based on AIM Photonics foundry processes for future manufacturing and testing.

3. Work Plan

3.1. PI's Qualifications

The PI is an expert on photonic and optoelectronic materials, devices, and systems. In total, the PI has authored > 70 peer-reviewed journal articles and accumulated citations are > 4700

(Google Scholar). Detailed publications can be found in the submitted CV. The PI has broad prior experience related to this project. For example, as a Ph.D. and postdoc at Rice University, the PI designed SOI-PICs using the OpSIS service and implemented graphene-loaded electro-optic modulators at telecommunication wavelengths through post-processing [22]. Furthermore, the PI has pioneered in creating an innovative solution-based self-assembly technique for preparing long-sought-after wafer-scale, highly aligned, densely packed carbon nanotube films [23–25]. With such materials, the PI observed microcavity exciton-polaritons with record-breaking ultrastrong coupling and exceptional points in their dispersions [26], and has implemented high-temperature hyperbolic thermal emitters [27]. These results have been published in high-impact journals, such as *Nature Photonics*, *Nature Nanotechnology*, *Nano Letters*, and *ACS Photonics*.

As a Photonics Designer in the company Lightmatter Inc., the PI was a core member of the photonics team and designed and tested large-scale integrated silicon photonic chips for accelerating ML calculations and interchip communication through optical interconnects. The PI worked with commercial photonics foundries including GlobalFoundries and AIM Photonics.

As a group leader at the University of Utah, the PI focuses on leveraging ML approaches for solving scientific problems and utilizing optical systems to accelerate ML operations [28–33]. For example, the PI recently developed an integrated simulation framework including device and system simulators for a free-space photonic matrix-vector multiplier and then utilized a reinforcement learning (RL) approach to directly optimize individual devices based on system performance. This RL-driven design in the integrated framework enabled end-to-end design automation without human supervision and domain knowledge [31]. These achievements lead to multiple publications in high-impact journals, such as *Nature Computational Science* and *Laser & Photonics Reviews*.

3.2. Detailed Plan

Task 1: High-throughput integrated simulation framework – **Fig. 3a** displays the proposed framework, which will consist of the following components implemented using Python and PyTorch framework.

(a) FK material module: This module will describe various physical models that are necessary to describe temperature-dependent optical properties from the FK effect. Specifically, the absorption coefficient $\alpha(\omega, F)$, where ω is angular frequency and F is applied electric field, will be calculated as described in Ref. [34]

$$\alpha(\omega, F) = (C\theta_F^{1/2}/\omega)[|d\mathrm{Ai}(\beta)/d\beta|^2 - \beta|\mathrm{Ai}(\beta)|^2]$$

with $\theta_F = (e^2F^2/2\mu\hbar)^{1/3}$ and $\beta = (\omega_1 - \omega)/\theta_F$. Here, e is electron charge, μ is the reduced mass of electron-hole pairs, $\hbar$ is reduced Planck constant, $\hbar\omega_1 = E_\Gamma$ corresponds to the interband transition between Γ points ($\approx 0.8\,\mathrm{eV}$ for Ge), C is a constant, and Ai is the Airy function. Furthermore, the corresponding refractive index $n(\omega, F)$ will be calculated based on *Kramers-Kronig* relationship as

$$n(\omega, F) = \frac{c}{\pi}\int_0^\infty \frac{\alpha(\omega', F)}{\omega'^2 - \omega^2}d\omega',$$

where c is the speed of light. The temperature dependence comes from E_Γ, which will be described by the Varshni equation as $E_\Gamma = E_{\Gamma_0} - 5.82 \times 10^{-4}T^2/(T + 296)$ in the unit of eV for Ge with T the temperature in the unit of Kelvin.

(b) FK device module: This module will perform photonic and electronic simulations of FK modulators to establish the connection between applied electric field F (the quantity in the *FK material module*) and the applied voltage in practical devices with realistic geometry and electronic doping profiles available in AIM Photonics processes. The overall device architecture will include a *p-i-n* Ge junction structure, where the guided light in Si waveguides will be

redirected to propagate in the Ge structure through tapers. The strong F will be generated when the Ge junction is under *reverse bias*, which will be applied through a *p-i-n* Si junction underneath. The highly doped p^+ and n^+ regions will be connected to metal electrodes for driving circuitry. The PI will utilize Ansys Lumerical FDTD and CHARGE solvers, which are available in PI's lab, for simulations.

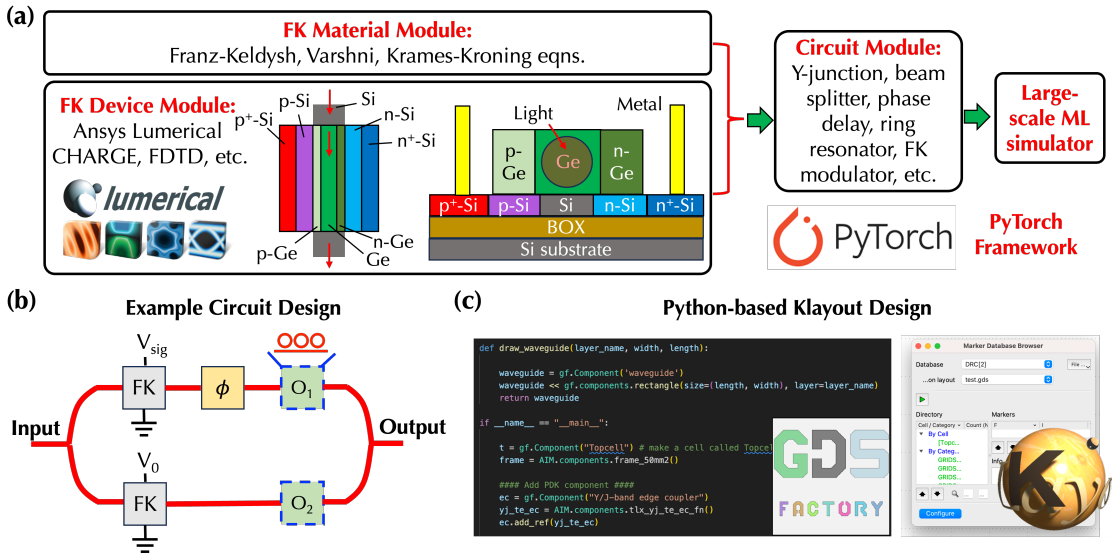

Fig. 3: **(a)** Simulation framework consisting of material, device, circuit, and ML simulators. **(b)** One example implementation of vector/matrix modulators based on FK modulators. **(c)** Design tools for AIM Photonics processes.

(c) Circuit module and large-scale ML simulator: This module will *integrate* both the FK material module and the field-voltage relationship from the FK device module to describe FK modulators, and also provide high-level descriptions of standard integrated photonic components such as Y-junction, beam splitter, phase delay, ring resonator, etc. These components will be connected as functional circuits for performing MVM operations. For example, one possible implementation of the modulator (green and blue rectangles in **Fig. 1**) can be an interferometer illustrated in **Fig. 3b** without two blue dashed blocks. The input light will be equally split through a Y-junction with an FK modulator analyzed in FK material and device modules on each arm. One FK modulator will be biased at a constant voltage (V_0) and the other will be biased at various signal voltages (V_{sig}) for modulation. Two arms will have a constant phase difference through a phase delay component (ϕ box in **Fig. 3b**), which can be simply a waveguide. The output light from two arms will be combined through the other Y-junction. All these interferometers based on FK modulators will be connected as an array following patterns illustrated in **Fig. 1** for MVM operations. Furthermore, the PI will implement a large-scale MVM simulator (e.g., 300 × 300) for evaluating multiple ML algorithms such as classifying handwritten digits from the Modified National Institute of Standards and Technology (MNIST) database. The PI has requested funds to purchase a computer server with high-performance CPU and GPU for integrating all modules (see *Budget*).

The developed integrated simulation framework will enable the analysis of temperature influence on the full stack of the system across materials, devices, circuits, and ML applications.

Task 2: Temperature-insensitive circuit design and chip tapeouts of FK modulators – Because of temperature-dependent band structures of Ge, functional circuits built upon FK modulators are expected to be temperature sensitive as well. In this task, the PI will further explore circuit designs to reduce temperature sensitivity. For example, depending on the operation wavelength, the modulated refractive index (Δn) and absorption coefficient

($\Delta\alpha$) of FK modulators in the circuit shown in **Fig. 3b** can have either positive or negative temperature coefficients. To compensate for such temperature dependence, the PI will employ ring resonators in each arm of the interferometer (blue dashed boxes O_1 and O_2 in **Fig. 3b**). In each dashed box (O_1 or O_2), there will be different combinations of multiple coupled rings so that their amplitude and phase responses under varying temperatures can be nearly arbitrarily engineered [35].

Finally, the PI will generate chip tapeouts based on previous designs following AIM Photonics processes using design tools, including GDS factory and KLayout (**Fig. 3c**). Note that because of the limited total budget (USD $100,000) of this project, the expensive multiple wafer project cost of AIM Photonics (USD $88,000 for customized chips), and long chip manufacturing turnover ($>$ 6 months), it is *not* feasible to manufacture and test designed chips within this project. However, the deliverables of this project will lay solid foundations for securing future funding resources (e.g., U.S. National Science Foundation) for chip manufacturing and testing after this project.

4. Outcome

The outcome of this project will mainly include:

- **(a)** A high-throughput, integrated simulation framework consisting of materials, devices, circuits, and ML systems based on SiGe FK modulators for analyzing temperature influence across the full stack.
- **(b)** The design and chip tapeouts of temperature-insensitive circuits based on AIM Photonics foundry processes for future manufacturing and testing.

5. Impact

The successful development of the integrated simulation framework will enable the co-design and end-to-end design of materials, devices, circuits, and systems. In addition, the successful demonstration of designed temperature-insensitive FK modulators can lead to next-generation high-speed, high-throughput, and energy-efficient optical ML hardware accelerators. Furthermore, the deliverables of this project can also be applied to many other application scenarios, such as optical communications and photonic quantum information processing.

References

1. LeCun, Y. *et al. Nature* **521,** 436–444 (2015).
2. Butler, K. T. *et al. Nature* **559,** 547–555 (2018).
3. Mirhoseini, A. *et al. Nature* **594,** 207–212 (2021).
4. Theis, T. N. *et al. Computing in Science & Engineering* **19,** 41–50 (2017).
5. Leiserson, C. E. *et al. Science* **368,** eaam9744 (2020).
6. Shen, Y. *et al. Nat. Photonics* **11,** 441 (2017).
7. Harris, N. C. *et al. Optica* **5,** 1623–1631 (2018).
8. Ying, Z. *et al. Nat. Commun.* **11,** 2154 (2020).
9. Wetzstein, G. *et al. Nature* **588,** 39–47 (2020).
10. Zhang, H *et al. Nat. Commun.* **12,** 457 (2021).
11. Feldmann, J *et al. Nature* **589,** 52–58 (2021).
12. Chuang, S. L. (John Wiley & Sons, 2012).
13. Reed, G. T. *et al. Nat. Photonics* **4,** 518–526 (2010).
14. Miller, D. A. *J. Light. Technol.* **35,** 346–396 (2017).
15. GlobalFoundries Announces Next Generation in Silicon Photonics Solution. `https://gf.com/gf-press-release/globalfoundries-announces-next-generation-silicon-photonics-solutions-and/`.
16. Chaisakul, P. *et al. Opt. Express* **20,** 3219–3224 (2012).
17. Gupta, S. *et al.* in *Optical Fiber Communication Conference* (2015), Tu2A–4.
18. Srinivasan, S. A. *et al. J. Light. Technol.* **34,** 419–424 (2016).
19. Chaisakul, P. *et al. Photonics* **6,** 24 (2019).
20. Wu, L. *et al. Opt. Express* **28,** 7585–7595 (2020).
21. Franz, W. *Zeitschrift für Naturforschung A* **13,** 484–489 (1958).
22. Qiu, C *et al. Nano Lett.* **14,** 6811–6815 (2014).
23. He, X. *et al. Nat. Nanotechnol.* **11,** 633–638 (2016).
24. Gao, W. *et al. R. Soc. Open Sci.* **6,** 181605 (2019).
25. Gao, W. *et al. J. Phys. D Appl. Phys.* **53,** 063001 (2020).
26. Gao, W. *et al. Nat. Photonics* **12,** 362–367 (2018).
27. Gao, W. *et al. ACS Photonics* **6,** 1602–1609 (2019).
28. Gao, W. *et al. Advanced Photonics Research,* 2100048 (2021).
29. Tang, Y. *et al. Nat. Comput. Sci.* **2,** 169–178 (2022).
30. Chen, R. *et al. Laser Photonics Rev.,* 2200348 (2022).
31. Tang, Y. *et al. Laser Photonics Rev.,* 2200381 (2022).
32. Zeng, H. *et al. Opt. Express* **30,** 12712–12721 (2022).
33. Lou, M. *et al. Opt. Lett.* **48,** 219–222 (2023).
34. Seraphin, B. *et al. Phys. Rev.* **139,** A560 (1965).
35. Teng, J. *et al. Opt. Express* **17,** 14627–14633 (2009).

Executive Summary of Proposal:

Real-time quadrupled resolution of ultrafast structured illumination microscopy by multi-constrained learning

Dr. Weisong Zhao (weisongzhao@hit.edu.cn)
Early-Career Member of Optica
Assistant Professor, School of Instrumentation Science and Engineering
Harbin Institute of Technology, China

The emergence of super-resolution (SR) fluorescence microscopy technologies has revolutionized biology and enabled previously unappreciated, intricate structures to be observed. However, many of these earlier experiments were conducted in fixed cells in which the dynamic structural and functional changes of cellular structures were lost. The reachable spatial resolutions of modern live-cell SR microscopes are ultimately limited by the maximum collected photon flux. To meet this challenge, we previously developed a sparse deconvolution algorithm that extends resolution beyond the physical limits posed by the hardware (***Weisong Zhao et al., Nat. Biotechnol. 40, 606–617, 2022***). As a result, sparse deconvolution-assisted structured illumination microscopy (Sparse-SIM) achieves ~60 nm resolution at a temporal resolvability of ~2 ms. However, with multiple constraints involved, the use of sparse deconvolution requires step-by-step parameter adjustment, with considering the experimental conditions and different organelle features. These complexities of use essentially restrict the method dissemination and high-throughput application.

In this proposal, we will use learning-based representations to eliminate the adjustable parameters of sparse deconvolution. A deep-learning engine is used to extract the pattern of parameter selections in a high-dimensional representation, enabling parameter-free and real-time sparse deconvolution reconstruction. Inputting raw SIM images with the optimally reconstructed images as ground-truth, the deep neural networks will automatically learn the complex expressions of low-to-high resolution transformations. Then, the well-trained DNNs can be frozen for direct SR reconstructions. This non-iterative form of reconstruction with the graphics processing unit (GPU) acceleration has the potential to achieve real-time SR imaging.

By integrating of ultrafast SIM imaging system with this real-time SR reconstruction module, we construct a smart bioimaging platform. There are several advantages of this platform. First, our platform has contained all advantages of ultrafast live-cell SIM for 564 Hz maximum imaging speed and is compatible with all fluorescence labels. Second, the spatial resolution is automatically doubled from 120 nm of SIM to 60 nm without parameter-tuning. Last, the SR reconstructions are in real-time at 30 Hz (in full data acquisition, analysis, and saving time), and this feature is particularly valuable for live-cell imaging.

Using this platform, biologists can dissect the sub-organelle interactions in real-time without the need for training or specific experience. It enables biologists to observe the ultra-microstructure and subcellular dynamics of cells, significantly facilitating live-cell imaging research. Beyond that, we also expect our smart platform to break the stereotype that SR microscopes are all difficult to use, making SR imaging easier.

Real-time quadrupled resolution of ultrafast structured illumination microscopy by multi-constrained learning

Dr. Weisong Zhao (weisongzhao@hit.edu.cn)
Early-Career Member of Optica
Assistant Professor, School of Instrumentation Science and Engineering
Harbin Institute of Technology, China

1. Background

The emergence of super-resolution (SR) fluorescence microscopy technologies has revolutionized biology[1] and enabled previously unappreciated, intricate structures to be observed, such as periodic actin rings in neuronal dendrites[2], nuclear pore complex structures [3], and the organization of pericentriolar materials surrounding the centrioles[4, 5]. However, many of these earlier experiments were conducted in fixed cells in which the dynamic structural and functional changes of cellular structures were lost. To temporally encode SR information via specific optics and fluorescent on-off indicators, the reachable spatial resolutions of modern live-cell SR microscopes are ultimately limited by the maximum collected photon flux.

Taking advantage of a priori knowledge of the sparsity and continuity of fluorescent structures, we previously developed a mathematical deconvolution algorithm[6] that extends resolution beyond physical limits posed by the hardware (**Fig. 1a**). As a result, sparse deconvolution-assisted structured illumination microscopy (Sparse-SIM)[6] achieves ~60 nm resolution at a temporal resolvability of ~2 ms, allowing it to resolve intricate structures, including small vesicular fusion pores and relative movements between the inner and outer membranes of mitochondria (IMM and OMM) in live cells.

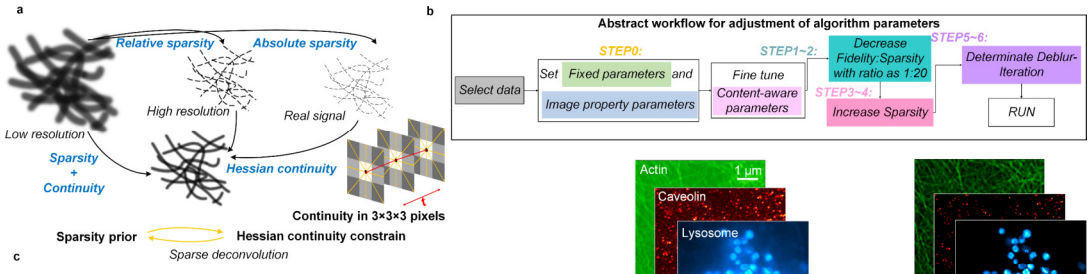

c

Data	Fidelity	continuity	Sparsity	Deblur-Iteration	Background (iteration)	Background (level)
Actin	150	0.5	10	5	5	7
Caveolin	600	0.1	100	80	3	7
Lysosome	30	0.1	1	3	5	7
OMM (t-axis)						
5s	50	0.05	10	10	3	7
300s	30	0.03	6	10	3	7

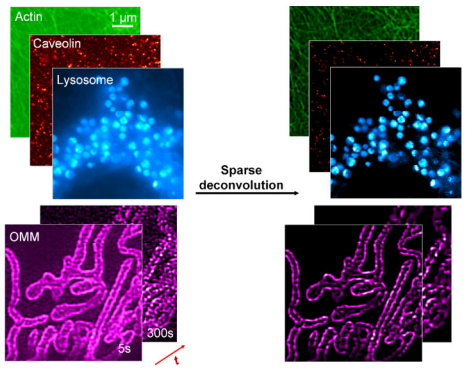

Fig1. Model, parameter tuning procedure, and examples of Sparse deconvolution. a) Reconstruction model of sparse deconvolution; b) The main parameter tuning steps of the sparse deconvolution algorithm; c) The representative parameter sets and the corresponding SIM and Sparse-SIM results.

However, with multiple constraints involved, the use of sparse deconvolution requires step-by-step parameter adjustment (**Fig. 1b**). The parameters are set by considering the corresponding experimental signal-to-noise ratio (SNR) and different organelle features (**Fig.**

1c). The parameter tuning is tricky and requires prior knowledge. The users should back-and-forth tune the weights of sparsity and continuity and iteration times case-by-case. For example, the optimal parameters of different datasets, i.e., the experiments of actin, caveolin, and lysosome, are very different (table in **Fig. 1c**). Moreover, because of the inevitable photobleaching effect, the SNR will vary over time in long-term live-cell imaging, leading to different optimal parameters even in the same dataset. These complexities of use essentially restrict the method dissemination and high-throughput application.

Overall, it is of great significance to eliminate the adjustable parameters of sparse deconvolution, enabling automatic resolution improvements and real-time live-cell imaging, which is the major motivation of this proposal. Combining with the ultrafast SIM, this smart real-time Sparse-SIM has many unexplored possibilities of revolutionizing current SR imaging for cell biology and biomedical research.

2. Statement of problem, objectives, and method

The major problems that we aim to solve are the automatic selections of sparse deconvolution parameters and real-time reconstruction. Fundamentally, there is no objective metric to evaluate the reconstruction performance of the SR images. The tuning of parameters requires the human subjective judgment of the experimental SNR and desired result. Furthermore, the iterative optimization used by sparse deconvolution is time-consuming, which is hard to realize a real-time data analysis.

Our proposed solution is to utilize a deep-learning engine to extract the pattern of parameter selections in a high-dimensional representation, enabling parameter-free and real-time sparse deconvolution reconstruction. Inputting raw SIM images with the optimally reconstructed images as ground-truth, the deep neural networks (DNNs) will automatically learn the complex expressions of low-to-high resolution transformations. Then, the well-trained DNNs can be frozen for direct SR reconstructions. This non-iterative form of reconstruction with the graphics processing unit (GPU) acceleration has the potential to achieve real-time SR imaging.

The overall technical route is shown in **Fig. 2**. First, we construct an ultrafast interference-based SIM system. Each SR-SIM image with doubled resolution is obtained by reassembling per nine structured illuminated images. Then, we apply sparse deconvolution to further boost SNR, contrast, and resolution, fulfilling the 4fold resolution improvements against diffraction-limit. At this stage, the parameters of sparse deconvolution are all selected by experts with the step-by-step protocol. By collecting SR images of different organelles under different SNRs, the generative adversarial network with multi-scale discriminators (PatchGAN) is employed to learn the transformation from the SIM image to its corresponding Sparse-SIM image. Then, we pre-trained the SR reconstruction network and pruned it to a lightweight model for acceleration. Finally, this frozen model will be integrated into the imaging system as a postprocessing step.

By integrating of ultrafast SIM imaging system with real-time SR reconstruction module, we construct a smart bioimaging platform. There are several advantages of our platform. First, our platform has contained all advantages of ultrafast live-cell SIM for 564 Hz temporal resolution and is compatible with all fluorescence labels. Second, the spatial resolution is automatically doubled from 120 nm of SIM to 60 nm without parameter-tuning. Last, the SR reconstructions are in real-time, and this feature is particularly valuable for live-cell imaging. Using this platform, biologists can dissect the sub-organelle interactions in real-time without

training or specific experience. We expect our smart platform to break the stereotype that SR microscopes are all difficult to use, making SR imaging easier.

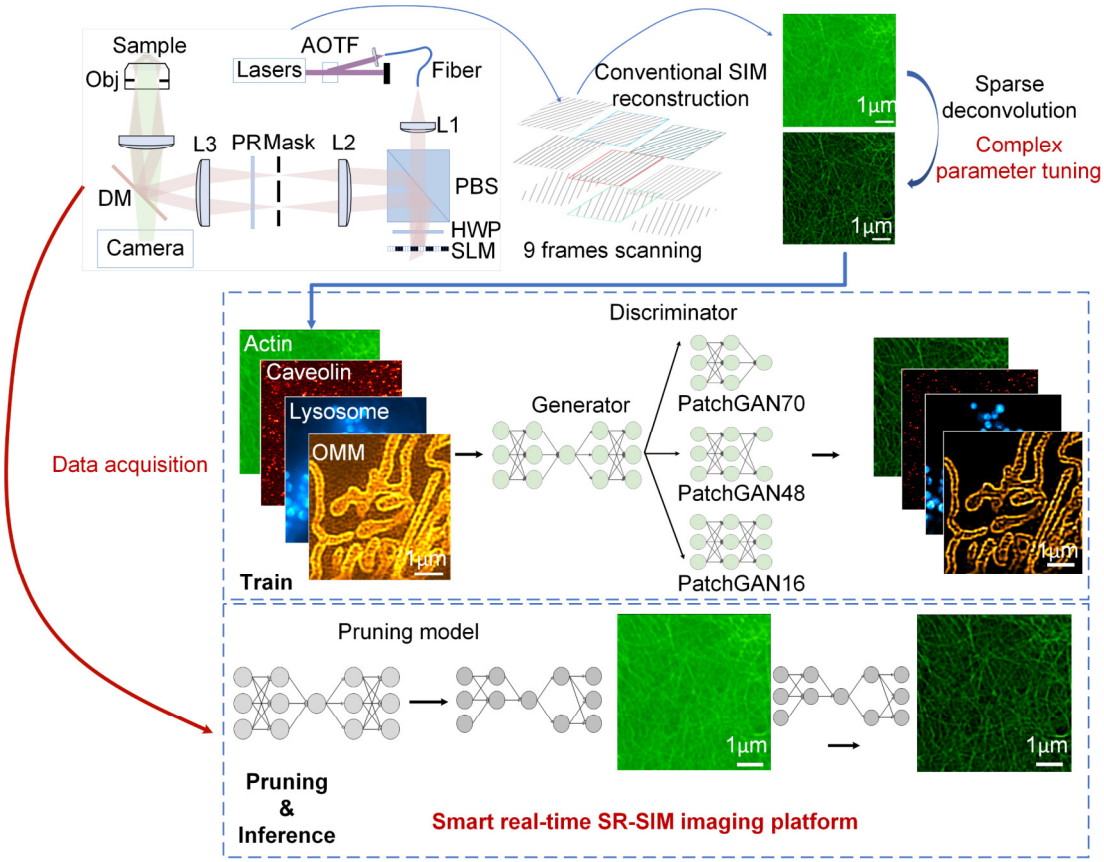

Fig 2. Smart real-time Sparse-SIM platform. PBS: polarization beam splitter; AOTF: acousto-optic tunable filters; HWP: half wave-plate; DM: dichroic mirror; SLM: spatial light modulator; PR: polarization rotator; L1–L5: lenses; Obj: Objective.

3. Outline of Work Plan

3.1 Optical setup of ultrafast SIM

The SIM system is based on a commercial inverted fluorescence microscope (IX83, Olympus) equipped with a TIRF (total internal reflection fluorescence) objective (100×/1.7 HI oil, APON, Olympus) and a multiband dichroic mirror (DM) as shown in **Fig. 2**[6]. In short, the output light from a polarization-maintaining single-mode fiber is collimated by an objective lens (L1) and diffracted by the pure phase grating that consisted of a polarizing beam splitter (PBS), a half-wave plate and the SLM (3DM-SXGA, ForthDD). The diffraction beams are then focused by another achromatic lens (L2) onto the intermediate pupil plane, where a carefully designed stop mask is placed to block the zero-order beam and other stray light and to permit passage of ±1 ordered beam pairs only. To maximally modulate the illumination pattern, a home-made polarization rotator is placed after the stop mask. Next, the light passes through another lens (L3) and a tube lens (L4) to focus on the back focal plane of the objective lens, which interferes with the image plane after passing through the objective lens. Emitted fluorescence collects by the same objective passed through a DM, an emission filter, and another tube lens (L5). Finally, the emitted fluorescence is split by an image splitter before being captured by an ultrafast sCMOS camera (Flash 4.0 V3, Hamamatsu, Japan).

With encoded high-frequency information from the nine acquired raw images, we use a Wiener-SIM reconstruction to achieve a twofold resolution improvement. Subsequently, the Wiener-SIM image is further processed by the Sparse deconvolution to fulfill a fourfold resolution improvement for 60 nm resolution SR imaging. To collect feature-rich enough data for training, we systematically perform the experiments for various organelles, including actin, microtubules, caveolin, lysosome, OMM/IMM, ER (endoplasmic reticulum), lipid droplet, and so on, under different SNRs. Such a data pool will effectively guide the DNNs to learn the authentic representation of the Sparse deconvolution with preventing the over-fitting effects.

3.2 Deep learning SR reconstruction method

Different from natural images containing various scales of features, the fluorescence images from the same targeted protein or organelle are commonly with similar features. Considering more efficient use of such mechanism, we specially design three Markovian patch discriminators with different receptive fields for the conditional generative adversarial networks (PatchGAN) to recover the high-frequency information (**Fig. 3**). Regarding the different discriminators, they effectively model the image as a Markov random field[7], assuming independence between pixels separated by more than a patch diameter. Specifically, we use the patch size as 70 pixels, 48 pixels, and 16 pixels for continuous actin structures, complex IMM, and small versicle-like CCPs, respectively. This configuration will derive more accurate local determination for the resulting SR reconstructions, ensuring the understanding of biological features. The generator is a U-shaped architecture (U-net)[8], which is composed of a contracting path and an expansive path. In the contracting path, the input layer is followed by a successive down-convolution block, consisting of 4 × 4 kernel convolution with a stride step of 2, batch normalization (BN), and a leaky rectified linear unit (LeakyReLU) function. The expansive pathway combines the feature and spatial information from the contracting path through a series of up-convolution blocks and concatenations with high-resolution features. The last layer is another convolutional layer that maps the 32 channels into one channel image.

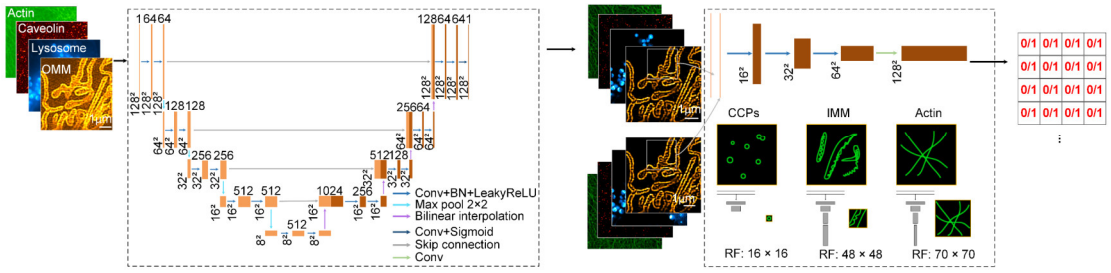

Fig 3 PatchGAN network architecture

3.3 Integration of smart real-time SR-SIM platform

The pre-trained model will be pruned to compress the models to run with significantly reduced energy cost and inference time. Since this compression removes redundant information, the prediction accuracy could even increase after pruning and it can also reduce the potential over-fitting effects. Then, with optimization of the linear and non-iterative Wiener-SIM reconstruction on a high-performance GPU, we further enable real-time SIM reconstructions. Integrated with the subsequent learning-based inference, we construct a fully automatic bioimaging platform that enables 60 nm spatial resolution with 30 Hz real-time imaging speed (containing acquisition, reconstruction, and saving time).

3.4 Timeline of implementing this work

	2023 (by quarter)				2024 (by quarter)			
	1st	2nd	3rd	4th	1st	2nd	3rd	4th
System construction and data acquisition	√	√	√					
Deep learning model construction and testing	√	√	√					
Deep learning model optimization and pruning			√	√	√			
Automatic bioimaging platform construction					√	√	√	
Publication and finalization							√	√

4. Outcome(s)

In this proposal, we will develop a fully automatic bioimaging platform that integrates SR-SIM imaging, high-speed data collection, and real-time analysis. Specific outcomes and deliverables include:

(1) An SR-SIM platform with 60nm resolution and frame rate of 30 Hz (containing full data collection time, data processing time, and data saving time).

(2) More than 2 high-impact publications (targeted in Optica and other journals);

(3) One optical scientist to be trained.

5. Impact

In summary, this proposal would enable the fusion of emerging learning-based techniques with our previously developed Sparse-SIM for new and paradigm-shift innovations. Specifically, we will construct a smart real-time Sparse-SIM for automatic bioimaging with 60 nm resolution and 30 Hz real-time imaging speed. It enables biologists to observe the ultra-microstructure and subcellular dynamics of cells, significantly facilitating live-cell imaging research.

6. Reference

1. Schermelleh, L. et al. Super-resolution microscopy demystified. ***Nature Cell Biology*** **21**, 72-84 (2019).
2. Xu, K., Zhong, G. & Zhuang, X. Actin, spectrin, and associated proteins form a periodic cytoskeletal structure in axons. ***Science*** **339**, 452-456 (2013).
3. Szymborska, A. et al. Nuclear pore scaffold structure analyzed by super-resolution microscopy and particle averaging. ***Science*** **341**, 655-658 (2013).
4. Lawo, S., Hasegan, M., Gupta, G.D. & Pelletier, L. Subdiffraction imaging of centrosomes reveals higher-order organizational features of pericentriolar material. ***Nature Cell Biology*** **14**, 1148-1158 (2012).
5. Mennella, V. et al. Subdiffraction-resolution fluorescence microscopy reveals a domain of the centrosome critical for pericentriolar material organization. ***Nature Cell Biology*** **14**, 1159-1168 (2012).
6. Weisong, Z. et al. Sparse deconvolution improves the resolution of live-cell super-resolution fluorescence microscopy. ***Nature Biotechnology*** **40**, 606–617 (2022).
7. Li, C. & Wand, M. in ECCV 2016 702-716 (Springer, 2016).
8. Ronneberger, O., Fischer, P. & Brox, T. in MICCAI 2015 234-241 (Springer, 2015).

Executive Summary

Cerebral blood flow (CBF) is an important biomarker for brain health which plays a crucial role in regulating oxygen delivery to the brain and facilitating the removal of metabolic waste like carbon dioxide. Alterations in CBF are closely associated with serious clinical conditions such as ischemic stroke, traumatic brain injury, and Alzheimer's disease. CBF can also be utilized to measure brain function due to neurovascular coupling, which has been done in functional magnetic resonance imaging (fMRI). Therefore, monitoring CBF is valuable in physiology and cognitive neuroscience research, as well as in clinical applications. Optics presents a convenient and non-invasive approach to continuously monitor CBF at the bedside. It is especially useful for populations and for studies for which other imaging modalities are limited, e.g. fMRI, including for children, infants, and studies that involve motion and interactions or require high temporal resolution. Diffuse correlation spectroscopy (DCS) is the state-of-the-art optical method that has already been used to measure CBF clinically. However, traditional DCS often has relatively low SNR, restricting the achievable source-detector separation (SDS) to shorter distances (~20 mm). Consequently, the scalp rather than the brain contributes primarily to the measured blood flow at such short SDSs. More temporal averaging can be utilized to improve SNR but at the expense of reduced temporal resolution. DCS also uses relatively expensive single photon counting devices, e.g. single photon avalanche diode (SPAD) detector (>$10,000), thus is financially challenging for wide adoptions.

Recently, we have proposed to use a fiber-based speckle contrast optical spectroscopy (SCOS) to measure human CBF. Compared to DCS, SCOS uses relatively low-cost complementary metal–oxide–semiconductor (CMOS) cameras as detectors. Our recent modeling and experimental work has demonstrated that the performance of SCOS can surpass that of DCS systems for human brain measurements in terms of signal to noise ratio (SNR) by *at least one and up to two orders of magnitude* at a high measurement rate of ~50 Hz with lower cost (~$500). SCOS also measures the optical density (OD) that is linearly related to cerebral blood volume (CBV) that is not measured by DCS. But our prototype SCOS system utilizes lenses and bulky cameras such that it needs to be established on the optical table in the lab environment. Therefore, the development of the next generation miniaturized SCOS system is key to extend its utility for everyday monitoring of brain health. We propose to miniaturize the SCOS system to construct a more portable and wearable device that measures CBF and CBV non-invasively in real time. This will be done by pursuing two specific aims:

Aim 1: Design the optics for the miniaturized SCOS device (Year 1). We will remove the lenses in both the illumination and detection side of the prototype SCOS system to improve wearability. A new cap will be built to hold the source fiber and CMOS detector on the human head.

Aim 2: Develop the hardware and software for real time displaying of brain hemodynamics and function (Year 2). We will improve the portability by connecting the CMOS detector to a mini-computer and develop the software for real time displaying of CBF and CBV time traces.

This success of this project will provide a miniaturized SCOS device to monitor human CBF and CBV in real time. It will provide great clinical values such as to monitor CBF for patients suffering from medical conditions as shock, stroke, cerebral edema, or traumatic brain injury. The portability and affordability also makes it an ideal solution for global health care, especially in rural areas where the access to medical resources, e.g. MRI scanner, is limited. It will also motivate the development of future generations of SCOS devices that feature wireless connections to tablets and cellphones, high density measurements that cover a larger area of the brain, and integration with functional near infrared spectroscopy (fNIRS) to enable measurements of hemoglobin concentrations and cerebral metabolic rate of oxygen ($CMRO_2$). These will shape the future of everyday recording of human brain health that responds to the stated goal of the *Optica Foundation Challenge* that calls for "*innovative and affordable technology solutions*" for the medical community.

Literature Review

Cerebral blood flow (CBF) is an important bio-marker of brain health as it regulates oxygen delivery to the brain and removes metabolic waste such as carbon dioxide. Alterations in CBF correlate with serious clinical conditions such as ischemic stroke[1,2], traumatic brain injury[3], and Alzheimer's disease[4,5]. CBF also provides information about brain function[6–9] as neural activation induces hemodynamic changes via neurovascular coupling[10]. Thus, monitoring CBF is important for physiology and cognitive neuroscience studies as well as clinical applications. Optics offers a convenient way to non-invasively and continuously monitor CBF at the bedside that cannot be accomplished with other techniques such as positron emission tomography and arterial spin labelling magnetic resonance imaging. When a scattering sample is illuminated by coherence light, speckle patterns with grainy appearances of bright and dark regions will arise from the interference of waves as illustrated in Fig. 1. A speckle pattern is very sensitive to any variation of the scattering sample and is often referred to as the fingerprint of the scattering medium[11]. Therefore, analysis of speckle pattern evolution can provide valuable information of the scattering particles, which can be used to measure, for instance, the speed of the red blood cells in biomedical applications.

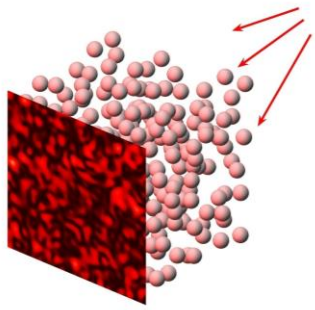

Figure 1. Speckle pattern. Speckle pattern arises from interference of scattered wave.

Diffuse correlation spectroscopy (DCS) is an existing state-of-the-art optical method to measure blood flow that has been widely used[12]. In DCS, coherence light is incident at one position on the surface of the sample and a detector is placed at another position to collect reemitted light with intensity $I(t)$ that changes over time due to speckle fluctuations. A blood flow index (BFi) is obtained from the decorrelation time τ_c of the intensity auto-correlation function $g_2(\tau) = \langle I(t)I(t+\tau)\rangle / \langle I(t)\rangle^2$. The depth of the measurement is determined by the source-detector separation (SDS). At a larger SDS, the penetration depth is larger but the collected photon flux is smaller resulting in poorer signal to noise ratio (SNR). But traditional DCS has relatively low SNR such that the achievable SDS is usually short (~20 mm), at which the main contribution to the measured blood flow arises from the scalp instead of the brain for adults, i.e., the brain-to-scalp sensitivity is low[13]. Thus, it is not feasible for brain function measurements in adults with applications such as brain-computer interfaces. It also has relatively low acquisition rate (<10 Hz), which is not desired when high temporal resolution is desired, and requires costly single photon counting devices as detectors. A new method that can achieve higher SNR and acquisition rate with lower cost, while also maintain the advantages of DCS including non-invasiveness, robustness, and wearability will be ideal for everyday monitoring of CBF and brain health.

Problem Statement/Objective

Recently, we have developed a fiber-based speckle contrast optical spectroscopy (SCOS) system to measure CBF. In SCOS, the spatial speckle contrast K defined as $K = std(I)/\langle I\rangle$ is calculated, where $std(I)$ is the standard deviation and $\langle I\rangle$ is the average of the speckle pattern intensity[14]. The optical density (OD) defined as $OD = log_{10}(I(0)/I(t))$, which is linearly related to cerebral blood volume (CBV), can also be measured in SCOS which cannot not measured in DCS. The contrast K is directly related to τ_c measured in DCS[15]. We have set up a first-generation SCOS system (Figs. 2a,b) and demonstrated measurements of human CBF

Abbreviations: ***BFi*** blood flow index; **CBF** cerebral blood flow; **CBV** cerebral blood volume; **CMOS** complementary metal–oxide–semiconductor; **$CMRO_2$** cerebral metabolic rate of oxygen; **CrCP** critical closing pressure; **DCS** diffuse correlation spectroscopy; **fNIRS** functional near infrared spectroscopy; **ICP** intracranial pressure; **OD** optical density; ROI region of interest; **SCOS** speckle contrast optical spectroscopy; **SDS** source-detector separation; **SNR** signal to noise ratio.

as well as OD at a large SDS of 33 mm[16,17] shown in Fig. 2c during a cognitive task of mental subtraction. We have also demonstrated a more than 10X improvement of SNR at a much higher measurement rate (~50 Hz) as compared to traditional DCS systems by taking the SCOS and DCS measurements simultaneously, which can be seen in Fig. 2d that the noise level of SCOS is much lower, and the cardiac pulse measured on human forehead is much cleaner. Unlike DCS which requires costly single photon counting devices, SCOS utilizes relatively low-cost complementary metal-oxide semiconductor (CMOS) cameras as detectors. These makes SCOS a perfect candidate for the task of everyday monitoring of CBF. But our prototype SCOS system utilizes lenses and bulky cameras such that it needs to be established on the optical table in the lab environment. Therefore, the development of the next generation miniaturized SCOS system is key to extend its utility for everyday monitoring of brain health.

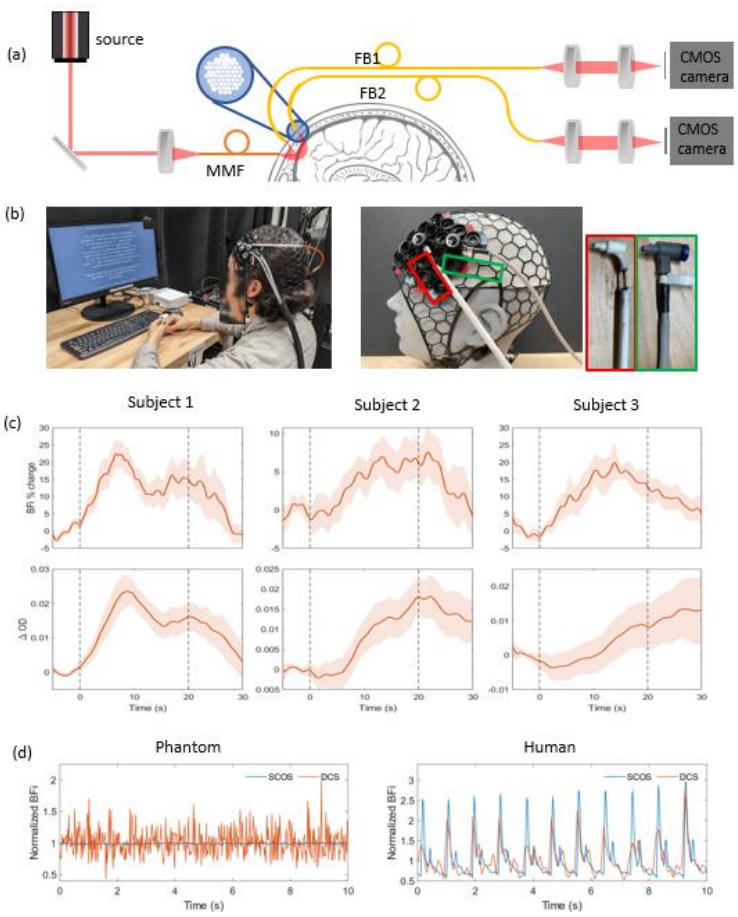

Figure 2. Demonstration of SCOS measurements. (a) Schematic of our existing prototype SCOS system. (b) Demonstration of the placement of the fiber on the subject head. (c) Results of the brain function measurements at a source-detector separation of 33 mm during a mental subtraction tasks. (d) Comparison between SCOS and DCS using a dynamic phantom sample (left) and human forehead measurement (right).

We propose to miniaturize the SCOS system to construct a more portable and wearable device that measures CBF and CBV non-invasively in real time. We will characterize the camera properties and set up the optics design that does not require lenses as shown in the prototype system in Fig. 1. We will then develop the hardware and software for real-time display of CBF, CBV, and other physiological parameters.

Outline of tasks/Work Plan

We will proceed by pursuing two specific aims in Year 1 and 2 respectively:

Aim 1: Design the optics for the miniaturized SCOS device (Year 1).

We will remove the lenses in both the illumination and detection side of the prototype SCOS system to improve wearability. On the illumination side, we will use a fiber-coupled laser source (Toptica iBeam, 850 nm, already exists in the Neurophotonics center of Boston University) that can be directly connected to the human head. We will attach a light pipe and a diffuser at the subject side of the multi-mode fiber to ensure that the average power per area is low enough to be in compliance with the ANSI safety limit for human measurements. On the detector side, we will use a low-cost, light weight, board level housing CMOS detector (Basler

daA1920-160um, 2.3 MP, 160 fps, $289) to be placed in direct contact with the subject's skin. Compare to the fiber-based system where there is photon loss due to the coupling efficiency with the fiber, our new design will maximize the photon-harvesting capability of the detection system. We will characterize the camera properties to calibrate the measured K using our established data processing stream[17]. In short, we will correct for the bias in K induced by shot, dark and read noise of the camera, which requires accurate measurements and validation of the camera gain and read noise. We will also redesign the 3D printed cap shown in Fig. 1b to hold and protect the source fiber and CMOS sensors to be placed on a subject's head. By the end of Year 1, we will demonstrate the measurements of human CBF, CBV and function during a cognitive task similar to that shown in Fig. 1c with the new optics design.

Aim 2: Develop the hardware and software for real time displaying of brain hemodynamics and function (Year 2).

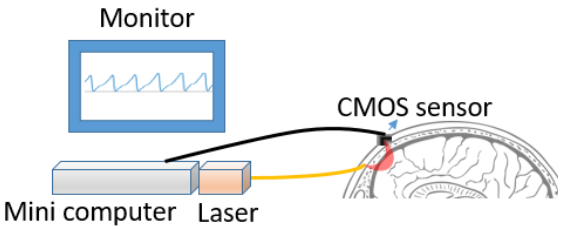

Figure 3. The schematic of the miniaturized SCOS system.

With the optical system designed and characterized in Aim 1, we will improve the portability by connecting the detector to a mini-computer (Intel NUC 13 Pro, $580) instead of the workstation that has been installed in the lab. We will preload the camera properties characterized in Year 1 and develop the software to process the raw speckle images to calculate the blood flow index (BFi) and optical density (OD). The results will be displayed in real time on a ~10 inch monitor. We will also offer an option to save the raw speckle images and the processed time traces of BFi, and OD for offline analysis. Other bio-markers that can be derived from pulsatile CBF and CBV measurements, including heartbeat rate and intracranial pressure (ICP), and critical closing pressure (CrCP, or zero flow pressure) will also be included in the options to be calculated in the software[18]. Some of these parameters requires connecting to another device such as a Finapres Nova device (Finapres Medical Systems, Netherland) to measure arterial blood pressure[18]. We will provide the interface but ensure that the SCOS device can be used alone without the Finapres Nova device. The laser source, the mini-computer, and the monitor will be contained in a box that connects to a fan to dissipate heat, which makes it convenient to translate the system. The illustration of the miniaturized SCOS device is shown in Fig. 3. By the end of Year 2, we will achieve this second generation SCOS device that can be used in various environments other than in the lab.

Pitfalls and alternative plans

We are proposing to use a low-cost CMOS detector to measure CBF, which has a relatively higher read noise (~2 e^-) as compared to the scientific CMOS camera (~ 1.4 e^-) used in our prototype system. But as we have mentioned earlier, since there is no fiber coupling required for the new detection design, we expect to achieve higher photon flux to compensate for the SNR loss due to the higher read noise. An alternative plan is to use a larger sensor with more pixels that can be used for averaging to improve SNR (e.g., Basler daA2448-70um, 5MP), or to average a few camera frames at the cost of reduced measurement rate. We will quantify SNR in Year 1 to determine the optimized strategy. At this stage we did not experience limitations in the data transfer and computing speed for real-time displaying. But if we experience a delay, we will improve the data streaming and processing pipeline so that it is capable to display the results for a smaller region of interest (ROI) of the speckle images, or to use machine learning for faster computations. The raw speckle images with full ROI can still be saved for offline analysis.

Outcome

Upon completion of these aims, we will develop the next-generation, miniaturized, low-cost SCOS device that is capable of measuring and displaying human brain hemodynamics and function in real time.

Impact

This miniaturized SCOS device will provide a convenient way for non-invasive and continuous monitoring of human CBF and CBV serving as bio-markers for brain health. The use of low-cost CMOS sensors makes it a more affordable solution compared to DCS which is the existing state-of-the-art optical technique to measure human CBF. It will provide great clinical values such as to monitor the ICP and CBF for patients suffering from medical conditions as shock, stroke, cerebral edema, or traumatic brain injury, where the cerebral autoregulation can be impaired leading to cerebral hyperperfusion, hypoperfusion, and ischemia. The portability also makes it an ideal solution for global health care, especially in rural areas.

The success of this project will also motivate the development of future generations of the SCOS devices. For the third generation SCOS device, we will integrate SCOS with functional near infrared spectroscopy (fNIRS)[19] to measure CBF, oxy- and deoxy-hemoglobin, and calculate the cerebral metabolic rate of oxygen ($CMRO_2$). This can be done by including a second wavelength (650 nm) channel in the SCOS device to measure ODs at both wavelengths. The advantage of developing a SCOS-fNIRS system is that ODs can be measured by SCOS such that no extra detectors are required, while DCS-fNIRS systems require different detectors for CBF and OD measurements. The fourth generation SCOS device will feature measurements for a larger area or the full head by implementing a multi-channel system to improve spatial resolution. The brain activation maps can be reconstructed[20,21] from the multi-channel measurements for applications such as brain-computer interfaces. The fifth generation SCOS device will be a helmet or cap with sources and detectors implemented on it. Wireless communications will be utilized using tablets or cell phones for easier recording and displaying. Our focus is to measure brain hemodynamics, but this technology can also be used to measure blood flow in other organs.

In summary, the development of the SCOS device will open up new opportunies to monitor brain health, detect disease that affects brain hemodynamics, and access the effectiveness of treatments. It does not require special training of medical staff to use so that patients can use it either in the clinics or at home. It can also be easily carried to communities that have limited access to medical resources such as magnetic resonance imaging (MRI) scanners. Therefore, this proposal responds to the stated goal of the *Health* category of the *Optica Foundation Challenge* that calls for "*innovative and affordable technology solutions*" for the medical community.

References

1. Bandera, E., Botteri, M., Minelli, C., Sutton, A., Abrams, K.R., and Latronico, N. (2006). Cerebral Blood Flow Threshold of Ischemic Penumbra and Infarct Core in Acute Ischemic Stroke. Stroke *37*, 1334–1339. 10.1161/01.STR.0000217418.29609.22.
2. Leigh, R., Knutsson, L., Zhou, J., and van Zijl, P.C. (2018). Imaging the physiological evolution of the ischemic penumbra in acute ischemic stroke. J. Cereb. Blood Flow Metab. *38*, 1500–1516. 10.1177/0271678X17700913.
3. Bouma, G.J., and Muizelaar, J.P. (1992). Cerebral blood flow, cerebral blood volume, and cerebrovascular reactivity after severe head injury. J. Neurotrauma *9 Suppl 1*, S333-348.
4. Korte, N., Nortley, R., and Attwell, D. (2020). Cerebral blood flow decrease as an early pathological mechanism in Alzheimer's disease. Acta Neuropathol. (Berl.) *140*, 793–810. 10.1007/s00401-020-02215-w.
5. Cruz Hernández, J.C., Bracko, O., Kersbergen, C.J., Muse, V., Haft-Javaherian, M., Berg, M., Park, L., Vinarcsik, L.K., Ivasyk, I., Rivera, D.A., et al. (2019). Neutrophil adhesion in brain capillaries reduces cortical blood flow and impairs memory function in Alzheimer's disease mouse models. Nat. Neurosci. *22*, 413–420. 10.1038/s41593-018-0329-4.

6. Durduran, T., Yu, G., Burnett, M.G., Detre, J.A., Greenberg, J.H., Wang, J., Zhou, C., and Yodh, A.G. (2004). Diffuse optical measurement of blood flow, blood oxygenation, and metabolism in a human brain during sensorimotor cortex activation. Opt. Lett. *29*, 1766–1768. 10.1364/OL.29.001766.
7. Jaillon, F., Li, J., Dietsche, G., Elbert, T., and Gisler, T. (2007). Activity of the human visual cortex measured non-invasively by diffusing-wave spectroscopy. Opt. Express *15*, 6643–6650. 10.1364/OE.15.006643.
8. Li, J., Ninck, M., Koban, L., Elbert, T., Kissler, J., and Gisler, T. (2008). Transient functional blood flow change in the human brain measured noninvasively by diffusing-wave spectroscopy. Opt. Lett. *33*, 2233–2235. 10.1364/OL.33.002233.
9. Liu, W., Qian, R., Xu, S., Chandra Konda, P., Jönsson, J., Harfouche, M., Borycki, D., Cooke, C., Berrocal, E., Dai, Q., et al. (2021). Fast and sensitive diffuse correlation spectroscopy with highly parallelized single photon detection. APL Photonics *6*, 026106. 10.1063/5.0031225.
10. Cheng, X., Sie, E.J., Naufel, S., Boas, D.A., and Marsili, F. (2021). Measuring neuronal activity with diffuse correlation spectroscopy: a theoretical investigation. Neurophotonics *8*, 035004. 10.1117/1.NPh.8.3.035004.
11. Goodman, J.W. (1975). Statistical Properties of Laser Speckle Patterns. In Laser Speckle and Related Phenomena Topics in Applied Physics., J. C. Dainty, ed. (Springer), pp. 9–75. 10.1007/978-3-662-43205-1_2.
12. Durduran, T., and Yodh, A.G. (2014). Diffuse correlation spectroscopy for non-invasive, micro-vascular cerebral blood flow measurement. NeuroImage *85*, 51–63. 10.1016/j.neuroimage.2013.06.017.
13. Zhou, W., Kholiqov, O., Zhu, J., Zhao, M., Zimmermann, L.L., Martin, R.M., Lyeth, B.G., and Srinivasan, V.J. Functional interferometric diffusing wave spectroscopy of the human brain. Sci. Adv. *7*, eabe0150. 10.1126/sciadv.abe0150.
14. Valdes, C.P., Varma, H.M., Kristoffersen, A.K., Dragojevic, T., Culver, J.P., and Durduran, T. (2014). Speckle contrast optical spectroscopy, a non-invasive, diffuse optical method for measuring microvascular blood flow in tissue. Biomed. Opt. Express *5*, 2769–2784. 10.1364/BOE.5.002769.
15. Boas, D.A., and Dunn, A.K. (2010). Laser speckle contrast imaging in biomedical optics. J. Biomed. Opt. *15*, 011109. 10.1117/1.3285504.
16. Zilpelwar, S., Zilpelwar, S., Sie, E.J., Postnov, D., Chen, A.I., Zimmermann, B., Marsili, F., Boas, D.A., Boas, D.A., Cheng, X., et al. (2022). Model of dynamic speckle evolution for evaluating laser speckle contrast measurements of tissue dynamics. Biomed. Opt. Express *13*, 6533–6549.
17. Kim, B., Zilpelwar, S., Sie, E.J., Marsili, F., Zimmermann, B., Boas, D.A., and Cheng, X. (2023). Measuring human cerebral blood flow and brain function with fiber-based speckle contrast optical spectroscopy system. bioRxiv, 2023–04.
18. Wu, K.C., Sunwoo, J., Sheriff, F., Farzam, P., Farzam, P.Y., Orihuela-Espina, F., LaRose, S.L., Monk, A.D., Aziz-Sultan, M.A., Patel, N., et al. (2021). Validation of diffuse correlation spectroscopy measures of critical closing pressure against transcranial Doppler ultrasound in stroke patients. J. Biomed. Opt. *26*, 036008. 10.1117/1.JBO.26.3.036008.
19. Ferrari, M., and Quaresima, V. (2012). A brief review on the history of human functional near-infrared spectroscopy (fNIRS) development and fields of application. NeuroImage *63*, 921–935. 10.1016/j.neuroimage.2012.03.049.
20. Dehghani, H., White, B.R., Zeff, B.W., Tizzard, A., and Culver, J.P. (2009). Depth sensitivity and image reconstruction analysis of dense imaging arrays for mapping brain function with diffuse optical tomography. Appl. Opt. *48*, D137–D143. 10.1364/AO.48.00D137.
21. Boas, D.A., and Yodh, A.G. (1997). Spatially varying dynamical properties of turbid media probed with diffusing temporal light correlation. JOSA A *14*, 192–215. 10.1364/JOSAA.14.000192.

Integrated Silicon Photonics with On-chip Quantum Dot Lasers

The rapid growth of artificial intelligence (AI)-driven services has created an unprecedented demand for compute capacity and speed. However, this surge is accompanied by a parallel increase in power consumption [>60 kWh per rack in extremely-dense AI workloads], as well as capital (CapEx) and operational (OpEx) expenditures [$154 billion globally on AI services in 2023]. The rate of progress in electronic hardware, doubling every 18 months, lags behind the doubling of machine learning computational demands every 3.5 months, resulting in a widening gap between compute requirements and hardware capacities.

Photonic integrated circuits (PICs) offer a promising solution by capitalizing on the inherent properties of photons, offering ultra-high bandwidth and processing frequency (>100GHz), ultra-low power consumption (projected sub-pJ/bit), and high parallelism through additional dimensions of division multiplexing. Notably, **optical neural networks (ONNs)** have emerged as hardware accelerators for AI workloads, particularly in matrix-vector-multiplication (MVM), which constitutes >80% of operations in modern AI models. For ONN implementation, **Silicon (Si) photonics** is an appealing platform due to its CMOS compatibility and high-density integration capacity. Prototypes of Si-based ONN hardware have been successfully verified using cascaded Mach-Zehnder interferometers (MZIs) and wavelength division multiplexing (WDM)-based microring resonator (MRR) arrays. However, *the inherent indirect bandgap of Si has impeded the progress of on-chip laser integration, thereby hindering the realization of a fully-integrated ONN system-on-chip (SoC)* that can further enhance system performance and address the computational acceleration demands of edge devices.

Leveraging Intel's silicon photonics platform, our team previously pioneered the heterogeneous integration of **quantum dot (QD) lasers** with Si PICs. In this project, we aim to further advance the development of a volume-manufacturable, fully integrated ONN system with high bandwidth and energy efficiency. We aim to achieve this by implementing QD mode-locked lasers (MLLs) as on-chip embedded sources through wafer-salce heterogeneous integration. This innovative approach deviates from conventional off-chip solutions, which require considerable power (approximately 2dB+6dB) for coupling and modulation. A key innovation also lies in utilizing QDs as active elements in the light sources to replace the commonly used quantum well (QW) active medium. QDs offer several favorable material properties over QW counterparts, including low threshold currents, high thermal durability, and excellent reliability. Moreover, QD-based lasers exhibit isolator-free stability, facilitating higher on-chip integration densities. By implementing QD MLLs as optical frequency on-chip comb sources for the ONN MVM system, our targets include reduced laser thresholds (< 200 A/cm^2), high thermal stability (>100°C), maximized output power (~20 wall-plug efficiency), multiwavelength emission (>8 modes at 25/50/100 GHz spacing), as well as demonstration of an **isolator-free system**.

At the ONN system level, we propose a novel architecture that employs hardware and software co-design approach for full integration on Si. The architecture utilizes an MRR crossbar design, which offers high scalability and parallelism by leveraging both spectral and spatial parallelism in optics, thereby maximizing the advantages of QD lasers. By employing an innovative, hardware-adapted algorithm to address the hardware modulation and operational speed mismatch, we aim to achieve increasingly complex tasks with a small hardware footprint. Initial simulation validation yielded a recognition accuracy of 91.313% on the MNIST dataset with mere 536 model parameters at high-speed (37 GHz) using Intel's standard 65 nm CMOS process line. By incorporating on-chip non-volatile memory and multi-cores scale-out framework, we project our hardware to theoretically increase in computing density by 70 times compared to Google's TPU electronic accelerator while reducing power consumption by 1000 times. Ultimately, the fabricated **QD MLL device and ONN system**, optimized and fine-tuned for this purpose, will be **co-integrated** using the state-of-the-art **heterogeneous integration technology** into a **holistic and isolator-free PIC** as a **compact and efficient SoC**. This transformative development is anticipated to unlock unprecedented advancements in energy efficiency, sustainability, and scalability and create new avenues for commercialization.

Integrated Silicon Photonics with On-chip Quantum Dot Lasers

I. Background and Literature Review

The advent of artificial intelligence (AI)-driven services has triggered an unprecedented increase in demand for processing capability and energy efficiency[1]. A prime example is the phenomenal growth of ChatGPT-3, which now boasts a staggering 175 billion parameters. Consequently, the cost of inference using ChatGPT-3 is tenfold higher than that of a standard search on conventional search engines like Google[2]. Industry estimates reveal that daily operating costs can reach up to $700,000[3]. These astonishing figures merely scratch the surface as the complexity and size of AI models continue to expand. While the computational demand of machine learning (ML) doubles every 3.5 months, advancements in electronic hardware, such as transistor density, clock speed, and power efficiency, lag behind with a doubling rate of approximately 18 months. This widening gap between the escalating compute demands, and the limited capacities of electronic hardware has emerged as a critical bottleneck in AI progress.

In this context, there is a rekindled interest in custom hardware designed to accelerate matrix-vector multiplication (MVM), a key operation that dominates modern AI models by constituting over 80% of their workloads. *Optical neural networks (ONNs)* provide a promising alternative by leveraging the inherent properties of photons, including ultra-high bandwidth and processing frequency (>100GHz), ultra-low power consumption (sub-pJ/bit), and high parallelism through additional dimensions of division multiplexing[4]. Among the various platforms, *silicon (Si) photonics* stands out due to its compatibility with complementary metal–oxide–semiconductor (CMOS) manufacturing and high-density integration capacity, making it an ideal candidate for hardware implementation of ONNs. Currently, mainstream ONN Si-based hardware solutions include cascaded Mach-Zehnder interferometers (MZIs) and wavelength division multiplexing (WDM)-based microring resonator (MRR) arrays. While the former has a more established process and structure, it suffers from higher computational complexity of $O(n^2)$ and requires a larger area[5]. In contrast, the directly mapped MRR architecture offers a more efficient solution with high parallelism and a smaller footprint, and has gained traction since the "broadcast-and-weight (B&W)" scheme was pioneered by Tait *et al.* in 2014[6]. However, the scalability of the B&W solution is limited due to the inevitable internal loop waveguide design. Consequently, attention has shifted to the crossbar configuration, which ensures high parallelism within a compact area, enhances scalability, and represents the most desirable large-scale ONN architecture. In 2021, Feldmann *et al.* achieved state-of-the-art ONN hardware that integrated non-volatile memory with an MRR crossbar, enabling trillions of multiply-accumulate operations per second[7]. However, their solution still relied on an off-chip laser co-packaged with a discrete optical comb, leading to substantial coupling losses. To further enhance system performance and fulfill the computational acceleration demands of edge devices, the development of **a fully integrated ONN hardware with an on-chip laser remains an essential objective.**

To overcome the inherent limitation of the indirect bandgap of Si for efficient on-chip light sources, our former team spearheaded a pioneering *heterogeneous integration process*. This groundbreaking technique enabled the seamless integration of InP-based quantum well (QW) material for light generation with Si waveguides for light guiding. By constructing III-V devices on Si with lithographically limited alignment to Si waveguides via wafer-scale processing, mass production of Si photonics-based optical modules was achieved within a decade through collaboration with Intel, generating revenue exceeding $1 billion. Ongoing efforts, spearheaded by the applicant, Dr. Yating Wan, focus on device design and process optimization to replace InP-based QW epitaxial material with GaAs-based *quantum dot (QD)* epitaxial material through the cooperation with *Intel® Research Center*. This strategic endeavor holds immense promise for improving performance and reducing costs by incorporating QD active regions, which offer benefits such as lower threshold currents, higher temperature stabilities, and, most importantly, *much-reduced sensitivity to reflections that obviates the need for bulky and costly isolators*[8].

II. Problem Statement and Objectives

In addressing the critical challenges associated with on-chip light sources and the AI computational bottleneck, our proposal aims to co-design hardware and software for a **fully integrated ONN Si photonic integrated circuit** (PIC). Leveraging **heterogeneous integration technology** and **Intel's Si photonics platform,** this project will **integrate multi-channel QD lasers** with an optimized **crossbar-based ONN hardware architecture** that exceeds the capabilities of traditional electronic architectures in terms of speed, power efficiency, and parallel processing capabilities. This stands in stark contrast to the bulky off-chip solution that requires substantial power consumption (approximately 2dB+6dB) for coupling and modulation alone.

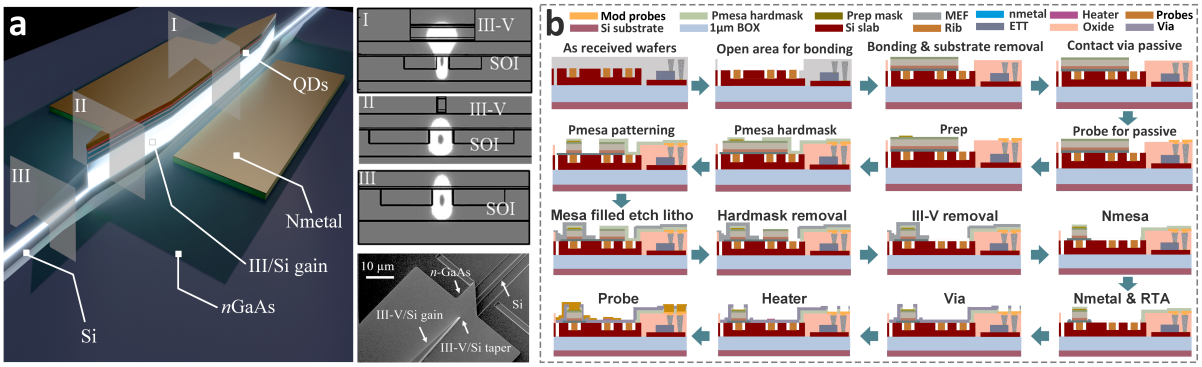

Fig. 1 (a) Schematic and (b) process flow to heterogeneously integrate the QD lasers with ONN PIC.

To achieve this, we will develop **robust, energy-efficient on-chip QD mode-locked lasers (MLLs)** capable of generating optical frequency combs for WDM ONNs. These lasers will be optimized to meet several key metrics. *Firstly*, we will focus on reducing losses in the cavity and lowering laser thresholds below 200 A/cm^2 to maximize energy efficiency. *Secondly*, we will achieve multi-wavelength emission by integrating multi-wavelength QD lasers on Si and progressing towards fixed 50 or 100 GHz channel spacing, with a channel count > 8 and power-per-line > 0 dBm. *Thirdly*, we will strive to maximize operation temperature by leveraging the 3D confinement and the large conduction band offset of InAs/GaAs QDs. Building upon our previous achievement of 120°C operation[9], we aim to further increase this parameter to >150°C through epi and device design optimization. *Fourthly*, drawing upon our previous achievement of reaching 185 mW continuous-wave optical power, we aim to achieve even higher optical power values by enhancing the gain region bonded on Si and minimizing the optical loss and series resistance via the optimization of device and epi designs, fabrication processes, and contact metallization. *Finally*, we will address the issue of laser sensitivity to reflections by leveraging the lower linewidth enhancement factor of QDs (0.4) compared to quantum QWs (approximately 4). Our group has previously demonstrated no sensitivity to reflection even with 100% off-chip feedback in Fabry-Perot lasers, and we aim to replicate this result in the QD MLLs.

In parallel, the **ONN will be designed and optimized for high efficiency and high parallelism** to fully leverage the advantages and superiorities of the on-chip MLL solution. We have chosen a compliant architecture of MRR crossbar as an MVM accelerator, incorporating a hardware-software co-design approach to improve computational density and energy consumption. *Firstly*, we aim to minimize the design's footprint and reduce crosstalk (both thermal and inter-channel) through simulation-based verification of individual device structure and system-level functionality. Our objective is to achieve a compact, high-precision hardware design with predicted performance parameters and packaging requirements. *Secondly*, we will develop an ONN algorithm that accomplishes as most-complex tasks as possible with the minimum number of parameters to ensure effective acceleration on edge devices. We will utilize training tools such as light weighting, noise perception, and quantization to further improve the generality and accuracy of the model on large datasets. *Thirdly*, we will fabricate and measure the designed ONN chip, followed by comprehensive testing of the fully integrated optoelectronic hardware. *Thereafter*, the fabricated **QD MLLs and ONN chip will be heterogeneously integrated into a single isolator-free package** confining all optical signals. This integration will enhance efficiency, stability, and scalability while eliminating unnecessary coupling and modulation losses (>8 dB) associated with external sources, endowing our circuits with unprecedented advantages in terms of cost, size, weight, and power (cSWaP).

III. Research Plan and Outcomes

The research plan for this project consists of three core tracks encompassing design, simulation, fabrication, co-integration, and characterization.

Track 1: Design and fabrication of QD lasers for heterogeneous integration. Our previous works provided initial demonstrations of integrated QD lasers on the Si-on-insulator (SOI) platform with exceptional performance. QD gain medium embraces multiple favorable material properties over QW counterpart, such as low transparency current density, excellent optical gain thermal stability, inhomogeneous dot size-resulted wide spectral gain bandwidth, low relative intensity noise, large tolerance to material/process defects and optical feedback. Through the low-loss evanescent coupling of the laser light to a Si waveguide, we successfully developed heterogeneous-integrated on-chip QD lasers with a threshold current of 4 mA, an SMSR of 60 dB, a fundamental linewidth of 26 kHz, and a 3-dB bandwidth of 13 GHz[8]. Building upon this foundation, we will now focus on fabricating *high-quality frequency combs using QD MLLs*. The unique broadband gain profiles and inhomogeneous broadening effects of QDs enable the engineering of MLLs to generate comb emissions with varying mode spacings. This characteristic is crucial to realize *compact and efficient sources of WDM signals in the ONN MVM implementation*. Fig. 1a shows a schematic of the laser evanescently coupled to low-loss Si waveguides. The critical goals in the *laser design* include optimizing the saturable absorber length, the electrical isolation distance, and the Sagnac loop mirror design. *Testing* will focus on extracting relevant characteristics for computing applications, including bandwidth, relative intensity noise (RIN), timing jitter, and total transmission capacity. Fig. 1b outlines the proposed *process flow* for the heterogeneous integration platform. Critical steps include post-wafer-bonding process to accommodate the prefabricated Si structures and protective measures to mitigate potential damage to the Si waveguides. To achieve this, we will implement a more restrictive mesa dry etch area and introduce a wet mesa filled etch step to selectively remove excess III–V materials near the protective oxides safeguarding the Si devices. Substrate removal conditions will be thoroughly investigated to ensure proper preservation of Si devices while maintaining high bonding strength and yield.

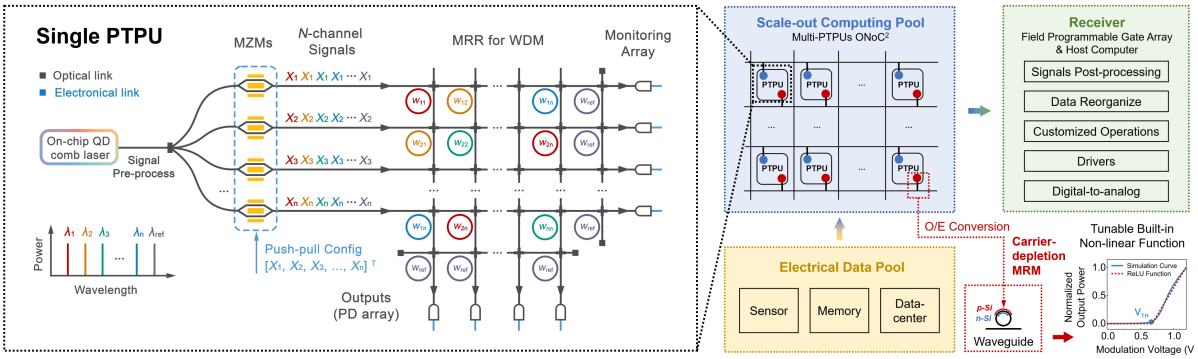

Fig. 2 Schematic of a typical N×N PTPU and its scaling solution.

Track 2: Hardware-software co-design for a fully integrated ONN architecture. To leverage the benefits of heterogeneously integrated MLL sources, we have devised a photonic tensor processing unit (PTPU) that incorporates a compact and scalable MRR crossbar architecture for parallel signal processing. Further introducing a broadband inter-core communication framework with an in-situ activation function, this system can be significantly scaled out through an on-chip optical network ($ONoC^2$) that interconnects multiple PTPUs (Fig. 2). In this architecture, the input signal is processed via broadband Mach-Zehnder modulators (MZMs), which reduce the peripheral refresh rate through simultaneous multi-channel encoding. The computed results in the MRR array then undergo optical/electrical (O/E) conversion, summation by photodetectors (PDs), and voltage signal readout. Within the multi-core framework, voltage signals from each PTPU are transferred via carrier-depletion microring modulators (MRMs) to waveguides, facilitating broadband interconnections. Considering the process and area overhead, the design includes a simplified layout for verifying the basic MVM function of the PTPU and MRMs devices based on Intel's standard 65 nm CMOS process line (Fig. 3a)[10]. System-level simulations, using the Lumerical INTERCONNECT, have assessed the transfer characteristics of individual MZMs and MRRs, as delineated in Fig. 3b and Fig. 3c, respectively.

Computation is executed within the highly linear regions to avoid undesired nonlinearities. By implementing a reference row/column, the weight matrix can effectively expand to the negative domain by a simple subtraction step in the electrical domain. A typical output signal and its post-processing result are depicted in Fig. 3d.

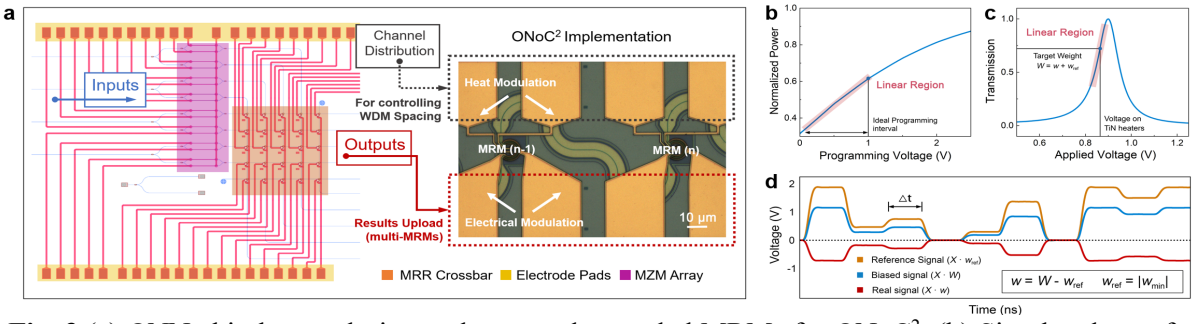

Fig. 3 (a) ONN chip layout design and prepared cascaded MRMs for ONoC^2, (b) Simulated transfer characteristic of the MZM, (c) Simulated transfer characteristic of the MRR and the weights mapping relationship, (d) A typical calculated output signal.

For algorithm development, we plan to adopt hardware-friendly optimization strategies encompassing data slicing and augmentation tailored to the scale and requirements of the devices. In our current hardware-adapted ONN model, we employed a reuse approach to reduce the number of model parameters and minimize the MRR modulation refresh rate, thereby eliminating the impact of thermal modulation speed limitations on the overall hardware operation. By deploying this model in a simulated edge device scenario, with a limited scale of MRR array and 8-bit quantization of weights, the hardware demonstrates a 91.313% recognition accuracy on the MNIST dataset. Building upon this model, we aim to further introduce advanced lightweight techniques, such as pruning, to enhance accuracy with fewer parameters and to achieve validation on larger datasets (*e.g.,* Cifar-10). Furthermore, we will explore efficient and scalable hardware-aware training methods that consider the control precision limitation to determine a set of ONN parameters with high noise robustness. By incorporating these techniques, we anticipate improved overall accuracy and reliability of our customized ONN model.

Track 3: Co-integration and characterization of the optoelectronic hardware. Heterogeneous integration technology will be utilized to merge the III-V QD lasers with the ONN passive chips. This integration process will yield fully integrated ONN acceleration hardware with a high-quality on-chip light source. Following this, we plan to complete the packaging of the optoelectronic I/O components and establish the peripheral control and testing platform concurrently. Ultimately, we will conduct a comprehensive functional verification and analysis of the optoelectronic hardware. According to our simulation data, we have carried out the performance estimation of our proposed fully integrated system. With a clock speed of 37 GHz (primarily dictated by the MZMs)[11], the theoretical computational density of a single PTPU reaches up to 4.5 TOP/mm^2. After including all peripheral overheads, the *overall computational density* for a 12×12 MRR array is anticipated to be ~0.37 TOP/mm^2, with an *energy consumption* of ~0.022 pJ/OP. These metrics outperform existing solutions reported in the literature. Further capitalizing on the ONoC^2 scale-out strategy, the performance metrics of the entire multi-core hardware will witness exponential improvement as the scale increases.

IV. Significance and Potential Impact

Successful development of this proposal can solve the efficiency and bandwidth capacity bottlenecks of electronic-based AI systems as well addressing the impending need for continued feasible scaling.

Impact towards Energy-efficiency and Sustainability: AI is swiftly becoming a major contributor to power consumption in data centers, with extreme-density AI workloads reaching up to 60 kW per rack while generating enormous amounts of heat and greenhouse emissions[12]. The electricity consumption of global data centers in 2021 was >400 billion kWh[13]. Conventional electronic interconnect technology, which relies on energy-intensive off-chip communication (>1 pJ/bit) and inter-system communication (up to 100 pJ/bit), exacerbates power consumption and thermal dissipation, thereby limiting the bandwidth density and scalability of data centers. Here, the successful development

of our photonic-based AI accelerators holds great promise in addressing these challenges and overcoming the bottlenecks in bandwidth, power consumption, and scalability. Based on preliminary simulations and by further leveraging on-chip non-volatile memory and our large-scale ONoC[2] framework, we project our hardware to theoretically increase in *computing density by 70 times compared to Google's TPU electronic accelerator*, while *reducing power consumption by 1000 times*. This breakthrough has the potential to revolutionize AI acceleration and enable more efficient and scalable data center architectures.

Commercialization potential: Heterogeneously integrated on-chip lasers, initially developed in a university lab (where the applicant conducted 5-year Postdoc research), have been successfully commercialized within a decade and have since generated over $1 billion in revenue by Intel[14]. However, the current packaging limitations pose challenges in accommodating bulky, lossy, expensive, and complex optical isolators. Our approach, leveraging QD lasers with their small LEF, offers a more compact and efficient solution by eliminating the need for these isolators, offering a more compact and efficient solution. In addition, realizing fully integrated ONN modules powered by on-chip QD lasers can potentially inspire patent innovations and foster the establishment of startups. The suitability of heterogeneous integration for scaling to larger wafer sizes, such as 300 mm or even 450 mm, enables high-volume manufacturability and further enhances the prospects of this technology.

Socioeconomic impact: Global spending on AI services and applications will reach $154 billion in 2023[15], with a compound annual growth rate (CAGR) of 27% expected over the 2022-2026 period, which is expected to reach $300 billion in 2026. This represents more than 4× the growth rate of the overall IT spending over the same timeframe[16]. Adopting such radical paradigms toward AI system implementation has the potential to alleviate expenditure and have far-reaching impacts in various industries, including autonomous driving, health care, telecommunication, and entertainment.

References

1. Shastri, B. J. *et al.* Photonics for artificial intelligence and neuromorphic computing. *Nature. Photonics* **15**, 102–114 (2021).
2. Dastin, J. *et al.* For tech giants, AI like Bing and Bard poses billion-dollar search problem, *Reuters* (2023).
3. Mok, A. ChatGPT could cost over $700,000 per day to operate. Microsoft is reportedly trying to make it cheaper. *Business Insider* (2023).
4. Feng, C. *et al.* A Compact Butterfly-Style Silicon Photonic–Electronic Neural Chip for Hardware-Efficient Deep Learning. *ACS Photonics* **9**, 3906–3916 (2022).
5. Zhang, H. *et al.* An optical neural chip for implementing complex-valued neural network. *Nature Communications* **12**, 457 (2021).
6. Tait, A. N., *et al.* Broadcast and Weight: An Integrated Network For Scalable Photonic Spike Processing. *Journal of Lightwave Technology* **32**, 3427–3439 (2014).
7. Feldmann, J. *et al.* Parallel convolutional processing using an integrated photonic tensor core. *Nature* **589**, 52–58 (2021).
8. Wan, Y. *et al.* High Speed Evanescent Quantum-Dot Lasers on Si. *Laser & Photonics Reviews* **15**, 2100057 (2021).
9. Shang, C. *et al.* Perspectives on Advances in Quantum Dot Lasers and Integration with Si Photonic Integrated Circuits. *ACS Photonics* **8**, 2555–2566 (2021).
10. Sun, J. *et al.* A 128 Gb/s PAM4 Silicon Microring Modulator With Integrated Thermo-Optic Resonance Tuning. *Journal of Lightwave Technology* **37**, 110–115 (2019).
11. Van Campenhout, J. *et al.* Silicon Photonics for 56G NRZ Optical Interconnects. in *2018 Optical Fiber Communications Conference and Exposition (OFC)* 1–3 (2018).
12. Su, L. Plenary: Innovation for the next decade of compute efficiency. (2023).
13. Hintemann, R. & Hinterholzer, S. *Data centers 2021: Data center boom in Germany continues - Cloud computing drives the growth of the data center industry and its energy consumption*. (2022).
14. Gazettabyte. *Intel details its 800-gigabit DR8 optical module* (2021).
15. Shirer, M. Worldwide Spending on AI-Centric Systems Forecast to Reach $154 Billion in 2023. (2023).
16. NRDC. *Data Center Efficiency Assessment* (2014).

Multi-modal photogrammetry for enhanced pathology documentation

Challenge

Contrary to the popular belief that anatomic pathology is primarily dependent on microscopy, many pathology evaluations today are actually performed at the macroscopic level by visual inspection, or “grossing.” Grossing can reveal the malignancy or severity of many diseases. It also helps pathologists to identify regions of interest for further microscopic analysis.

Grossing relies on good communication between surgeons and pathologists. Sample origin, orientation, and key landmarks must be explained precisely and accurately. Graphical data like sketches and photography facilitate communication, but tissue landmarks and orientations are still easily misrepresented in 2D images, leading to sampling errors, misdiagnosis, and wrong treatment plans. These shortfalls stress the need for a transition towards more accurate and comprehensive graphical communication methods.

The implications of grossing errors can be severe but are hard to gauge or recover. Surgical samples processed into microscope slides cannot be examined again. 2D images are often the only remaining visual evidence, but they cannot represent the entirety of the specimens in 3D. Sometimes, an image itself could be a source of error if not properly acquired. To prevent and catch errors in grossing, clinicians need a better method to acquire and preserve the graphical data of the specimens.

Proposed Project

Anatomic pathology heavily depends on graphics to document and describe cases, but 2D images miss 3D details and quality to provide complete visuals of surgical specimens. It is the root cause of the problem above. If surgeons can create a detailed 3D visualization of the tissue in the operating room (OR), digitally label and annotate, send it to pathologists, and keep it on record, all problems will be resolved. In fact, recent pilot studies suggested that 3D scans of surgical specimens can improve surgical pathology communication and leave extra evidence for post-surgical reviews. However, existing 3D scanners struggle to handle a large range of sample sizes, record high-resolution details, manage tissue physical properties, and provide a streamlined clinical experience. Clinicians are also concerned with extra costs and training, not to mention regulatory concerns and workflow changes.

In addressing these challenges, we aim to create an optical 3D scanner uniquely tailored to clinical specimens and users. The scanner is intended to be compact and user-friendly, readily adaptable to diverse sample properties such as texture, size, and resolution, and seamlessly integrated into clinical workflow. We determined photogrammetry is the ideal technology to satisfy these specifications and are prepared to tackle inherent technical hurdles, including variations in illumination and deformation during scanning. Integrating photogrammetry with novel optical contrasts, such as fluorescence and luminescence, will simplify illumination design and generate fresh perspectives on pathology. We will also develop a robust photogrammetry 3D reconstruction pipeline, automated 3D model optimization, and a user interface with features designed for medical professionals.

Intended Outcomes

The project will deliver a prototype photogrammetry 3D scanner comprising modules for illumination, imaging, mechanical manipulation, and data handling. This prototype shall let us engage our first users, create strategic partnerships with key stakeholders in academia and hospitals, start initial tests, build feedback channels, and enable continuous improvement of design and user experience. We aim to prove that a tissue 3D scanner is technically and clinically viable. We also anticipate that our work could bolster various medical photonic innovations, such as **enhanced slide-free pathology** and **fluorescence-guided surgery,** and provide new data support for advancements in **personalized medicine, virtual reality medical training, medical robotic applications, and novel AI medical insights**.

Multi-modal photogrammetry for enhanced pathology documentation

Personal Statement

During my transition from academia to entrepreneurship, the best thing I learned was the art of finding the most exciting problems to solve. The trick is talking to a lot of customers. Hear their needs. Last year, my research team interviewed 100+ key stakeholders in surgical pathology during an entrepreneurship training program. Our objective was to understand how enhanced pathology techniques, in particular, light sheet fluorescence microscopy, could be implemented in operating rooms (OR) and clinical pathology labs. However, we ended up identifying a new challenge in surgical pathology, a challenge to various clinical subspecialties, a challenge that our expertise in biomedical optics can readily address.

Literature Review

Miscommunication and human errors are the leading cause of quality issues in today's surgical pathology workflow, resulting in poor patient outcomes and increased costs of care. Many miscommunication and errors find their roots in the initial phase of pathology evaluation - grossing, the visual examination of surgical specimens. Grossing is responsible for direct diagnosis and accurate sampling for downstream histopathology evaluation. Misunderstanding, mislabeling, miscommunicating, and mis-sampling are common human mistakes and cause misdiagnosis [1]. A study even showed that 69% of labeling errors happen during the gross examination procedure [2].

Our interviews revealed more specific problems with the grossing under several clinical specialties. **Otolaryngology (ENT) surgery** deals with the most complex lesions in the head and neck. All ENT surgeon interviewees (n=11) suggested they frequently need to pause the surgery and meet pathologists in person to explain the tissue geometry and determine the sampling strategy for histopathology analysis [3]. The process can take a long time, increase OR charges to the patients, and reduce their bandwidth for research.

Mohs micrographic surgeries iteratively remove a layer of skin, analyze it for cancer cells using histopathology, and repeat until no cancer cells remain. The goal is to remove all cancerous tissue and preserve healthy tissue as much as possible. 63% (n=19) of Mohs surgeons expressed concerns with tissue stretching and wrapping during the handling process. Such deformations lead to the displacement of key tissue landmarks, uncertainties in subsequent micrographic surgery, and unnecessary tissue removal [4].

Lymph node biopsy's morphology is a key diagnostic and prognostic factor in many cancer surgeries. Detailed lymph node morphology is often poorly documented and difficult to recover after surgery [5]. With poor evidence, pathologists sometimes cannot even agree on the number of lymph node samples that are examed [6]. Several pathologist interviewees accepted that poor documentation may have caused undetectable issues.

The surgical pathology field continues to explore new technology to improve the quality and efficacy of grossing. Recently, several medical researchers tested optical 3D scanning in surgical procedures [7,8]. They found that digitalized surgical specimens improved intraoperative communication, facilitated post-surgical evaluation, and provided surgical guidance through augmented reality.

Although 3D scanners promise to improve the quality of care, no 3D scanners in the market are designed for clinical pathology or able to meet these niche medical user needs. Repurposing existing 3D scanners for medical use is challenging. In one study, the workflow can take more than 30 minutes, the sample size is limited to above 30 mm, and significant labor was involved in the process [7]. Cost, training, sample prep, tissue properties, image quality, data handling, and regulatory burdens are all viable concerns. Pathologists and surgeons need a 3D scanner designated for clinical specimens.

Problem Statement/Objectives

In summary of our findings above, miscommunication and efficiency bottlenecks are two common problems in pathology grossing [7]. Fundamentally, the issues arise from the extra efforts regarding tracking the sample origin, geometry, orientation, and key landmarks. Surgeons must precisely and accurately pass this information to pathologists, creating delays and room for errors. A common practice is to combine hand drawings with cutting/stitching/ink marks. In complex cases, surgeons must stop the surgery, leave the OR, physically meet the pathologists and help them with grossing. More time must be spent on the communication process to prevent miscommunication.

Insufficient graphic documentation (e.g., photos of the specimens) causes another problem in surgical pathology. Morphological features, such as size, shape, volume, and texture, provide valuable insights into potential malignancies and severity. Many diseases (e.g., breast cancers [9]) can be diagnosed and staged based solely on pathology grossing. However, pathologists only have one chance to examine the original specimen before it is permanently destroyed for microscopic analysis. Pathologists take digital photos of the sample before grossing. The images are useful for post-surgical evaluation, occasionally catching and correcting misdiagnoses or sampling errors during grossing [10]. Regardless, the 3D spatial details of the tissue are irretrievably lost, necessary information is missing, and the potential detriment of misdiagnosis remains indeterminable.

Imaging the specimen from all angles is a straightforward solution to this problem, but implementing it with human workers is impractical with expensive clinical labor. Optical 3D scanning technologies serve this purpose well. Besides, a new form of data could provide additional clinical insights. Regardless, no existing 3D scanners are designed for this new application. New solutions need to address more technical and design challenges. These challenges define our design objectives for the new pathology 3D scanner:

Illumination - Unlike common industry and consumer 3D objects, surgical specimens have challenging optical properties for 3D scanning. Soft tissue behaves like composite hydrogels. Translucency and specular highlights can interfere with 3D scanning. In conventional 3D scanning, users can solve the problem by applying a diffusive surface coating. The solution is impractical for clinical specimens because it completely alters critical tissue texture necessary for pathology assessment. Carefully engineered illumination is required.

Imaging - Surgical specimens have a wide range of sizes, varying from a peanut to a football. Ideally, the 3D scanner should accommodate a wide range of sample types. Some small gross anatomy features are also important to diagnosis. Therefore, the scanner should also provide high resolution beyond ordinary 3D scanners. To manage these requirements, we need an imaging system with balanced performance across various magnifications.

Mechanics - Mechanical deformation during data acquisition is another issue for 3D reconstruction. Many tissue samples are not firm and susceptible to elastic deformation during handling. The problem should be minimized during sample mounting and manipulation. Considering tissue samples naturally do not have a rigid shape, software correction can also help to remediate the problem.

Workflow - Finally, implementing 3D scanning in the clinical workflow is the most challenging step. The system must be small, portable, easy to deploy, and compliant with clinical regulations. R&D, regulatory, and manufacturing costs must also be managed. From a user experience perspective, the new procedure should minimally affect the existing clinical workflow. The additional time and labor required must be insignificant. Training and operation should be simple. The user interface should also be easy to use and provide pathology-specific features such as digital inking and simple deformation modeling.

Outline of tasks/Work Plan

There are three major types of optical 3D scanners: laser, structured light, and photogrammetry. We chose photogrammetry because all modules of a photogrammetry scanner can be found in the existing clinical workflow. This design decision drastically reduces regulatory uncertainties for potential market entry. It also handles a large range of sample sizes and imaging resolution, provides photographic surface textures, and is the most cost-effective among all optical 3D scanning modalities.

Task 1: Hardware design and integration. The proposed system comprises three main modules; each can function independently. The illumination module casts uniform light on the tissue. A highlight of our plan is to test fluorescence and luminescence as potential photogrammetry contrast. These novel photogrammetry contrasts can potentially remediate specular highlights and create new insights for pathology analysis. The imaging module will use consumer mirrorless cameras and macro lenses as the platform. The design should provide balanced performance at a large range of magnifications to handle surgical specimens of varying sizes and desired resolution. The mechanical module will facilitate sample mounting, centering, and rotation. Different modular mounting mechanisms will be provided to handle different sample sizes and mechanical properties. The principal investigator will lead a hardware engineering intern to perform the hardware development.

Task 2: Software development. The first step of the data pipeline is photogrammetry 3D reconstruction. We will evaluate multiple computational and neural 3D reconstruction methods and identify the most effective method for our data. Automated mesh optimization will be implemented as the second step to refine the 3D reconstructed data for rendering and visualization. Finally, a front-end user interface (UI) will be developed to facilitate image rendering and basic manipulations. The first two steps will be developed in-house. We will hire a freelance 3D mobile game developer contractor to build the front-end UI.

Task 3: Verification, validation, and continuous improvement. Our testing and validation strategy commences with a benchmarking phase for our hardware and software to ensure they meet outlined technical specifications in the Outcome(s) section. Following this, we will validate system functionality using livestock tissues mimicking clinical specimens. Confirmed functionality paves the way for external evaluators to scrutinize the system and offer feedback. This system will then undergo additional field testing in a simulated clinical environment at Case Western Reserve University. Finally, we'll engage potential partners, including University Hospitals, the Louis Stokes Cleveland VA Medical Center, and Vanderbilt University's surgical ENT group (who did the pilot 3D scanner study [8]), to conduct testing in clinical environments.

Outcome(s)

Illumination module - The illumination module will follow illumination system design principles to ensure sufficient intensity, high uniformity, and minimal shadows. Key tech specs will be defined according to the performance of the imaging module. The module comprises a mounting frame and numerous modular LED units. The LEDs will be evenly distributed on a hemispherical surface behind a diffuser layer. The frame can be attached to the imaging or the mechanical module during imaging. Modular LEDs can be easily replaced for different illumination needs.

Imaging module - For the prototype, we will use specialty consumer macro lenses (e.g., Venus Optics Laowa 25mm f/2.8 2.5-5X or 58 mm f/2.8 2X Ultra Macro Apo Lens) and a mirrorless camera as our primary imaging device. The optics have a variable field of view to cover common surgical specimens of all sizes. Using an unmodified consumer digital camera also better justifies the use of our device in clinical environments. As a side project, we will test the feasibility and performance of smartphone-based photogrammetry and LiDAR 3D scanning on large clinical specimens with the help of the mechanical module.

Mechanical module (static) - Two types of mounting mechanisms will be provided. For small samples, the specimens can be pieced with thin tungsten wires. For large samples, the specimens can be directly placed on top of a flat stage for large specimens. The static mounting mechanism can be attached to the mechanical gimbal.

Mechanical module (dynamics) - The sample will be rotated around two axes for positioning and one linear axis for focusing purposes. Two stepper motors with embedded drivers and encoders will facilitate this gimbaled motion. The encoders will provide absolute position feedback. The rest of the module will remain static. Low-power aiming lasers will be implemented and aligned to the rotating axes to facilitate sample positioning.

Resolution and field depth - The resolution and field depth depends on the aperture size of the imaging system. Given enough sampling, up to 1.5 um optical resolution can be achieved with an F2.8 macro lens. Focal stacking may be necessary to acquire a high-resolution image over an extended depth of field. Reducing the aperture size can improve the depth of focus at the cost of lowered resolution and prolonged exposure time.

Manage difficult tissue optical properties - The tissue translucency problem should be negligible for lower-resolution imaging of larger specimens. The system should be able to image fresh, large tissue samples without staining or coating procedures. Though, translucency can affect high-resolution imaging in smaller samples. To address the problem, We will use UV and deep UV illumination with high tissue absorbance. High absorption can reduce signal from the subsurface and prevents image contrast degradation. Staining the tissue with a UV-blocking reagent can further improve the effect. Fluorescence and luminescence dyes added to the stain formulation can convert light reflection into light emission, further reducing specular highlights and creating additional image contrast.

Footprint, portability, speed, and cost - Each module should have a < 2X2 sqft footprint and < 10 lb weight to deploy in a clinical workbench easily. Ideally, the integrated system will be installed on a clinical rolling cart to make it more portable. Each scanning session takes a total time equal to the sum of the setup time, imaging time, data transfer time, and data processing time. The setup time can vary depending on the complexity of the sample. A reasonable initial target of scan time is 1 fps image acquisition speed and 60 views per sample. A low-quality preview of the specimen should be immediately available to the user. Data transfer and high-definition 3D reconstruction should take less than 5 minutes on the cloud. The total scanning time for a sample should be less than 10 minutes. Based on our discussion with users, the material cost of a scanner should and can be limited to $10000.

Software features - Traditional photogrammetry computation should perform well using high-quality images with uniform intensity profiles. Newer neural-network-based methods (e.g., neural radiance fields) can tolerate higher image variabilities and provide higher reconstruction speed, although the quality of the result can be unstable. Both methods will be implemented to provide quality/performance redundancy. Data quality will also be verified both before and after 3D reconstruction. The data will be processed remotely to ensure process speed. Unnecessarily complex 3D models will be optimized before sending to the front-end UI. The UI should include basic 3D rendering features like object/camera motions and color correction. Pathology-specific features such as virtual inking and annotation will also be provided to facilitate graphical communication.

Training, operation, and workflow - The device includes an intuitive interface with minimal training required. By watching <15 min training videos, an average user should learn to prepare a sample, mount a sample, initiate scanning, and interact with data on a portable device. To maximize simplicity, the user only needs to press one button to activate the scan. We will first test the device in the OR environment. The tissue sample will be scanned in the OR. The OR personnel will review the data before releasing the sample to the pathology lab. Finally, pathologists and surgeons can visualize the data together in the app.

Impact

The project addresses the challenge of miscommunication and efficiency bottlenecks in surgical pathology by creating a 3D scanning platform specifically tailored to imaging clinical samples. 3D visualization will provide more detailed graphical documentation of surgical specimens, facilitate efficient communication between surgeons and pathologists, enable better quality control, prevent human errors, and ultimately improve patient outcomes.

We aim to provide medical professionals access to advanced optical imaging technologies positioned to revolutionize pathology. Expensive regulatory barriers hinder market penetration, limiting clinicians' exposure to these technologies. Our strategically planned project circumvents these obstacles, offering a practical, value-adding optical technology solution. It acquaints users with new optical technologies, 3D imaging, sample handling, and user interfaces. Ultimately, the 3D scanner will also be a versatile platform for integrating other cutting-edge medical photonic technologies, such as non-destructive slide-free histopathology, aligning with the long-term strategic goal of the startup.

A tissue 3D scanner can also stimulate the progression of numerous emerging photonic medical technologies. For instance, creating high-resolution 3D models of dissected tissue for fluorescence-guided surgeries can enhance the visualization of fluorescent markers in space. It offers the potential for a more precise delineation of tumor boundaries, improved surgical outcomes, and better prognosis. Our envisioned concept of a fluorescence 3D scanner will catalyze the evolution of this emerging surgical technique.

AR/VR and 3D models based on real clinical samples synergize in the medical field. While AR/VR translates abstract ideas into tangible experiences, 3D models of the tissue elevate visualization realism. The combo can simulate real-life medical challenges in medical training, fostering experiential learning. Patients can also benefit from these 3D models, as they simplify complex medical details, improving their grasp of health conditions.

3D scanning forms the basis for automating pathology grossing. As a first step, a digital collection of tissue 3D models must be created through a controlled process, enabling AI tools to understand gross anatomy in 3D. These AI-generated insights do more than just assist pathologists in improving or automating the existing grossing procedure—they also open possibilities for unveiling previously unrevealed knowledge. Our clinical 3D scanning platform represents the first move in this endeavor.

Finally, our ambition extends beyond the mere construction of a research prototype. We emphasize that every user should be able to access these technologies. With this in mind, we are committed to bringing optical 3D scanners to hospital benches. More importantly, we have the capability to turn this vision into a reality.

References

1. M. F. Santana and L. C. L. Ferreira, J. Bras. Patol. E Med. Lab. **53**, 124 (2017).
2. L. J. Layfield and G. M. Anderson, Am. J. Clin. Pathol. **134**, 466 (2010).
3. M. B. Happ, T. Roesch, and S. H. Kagan, Cancer Nurs. **27**, 1 (2004).
4. E. S. Gardner, W. T. Sumner, and J. L. Cook, Dermatol. Surg. **27**, 813 (2001).
5. K. Straalman, U. S. Kristoffersen, H. Galatius, and C. Lanng, The Breast **17**, 167 (2008).
6. V. Parkash, C. Bifulco, R. Feinn, and D. Jain, Am. J. Clin. Pathol. **134**, 42 (2010).
7. M. P. Saturno, M. Brandwein-Weber, L. Greenberg, A. Silberzweig, D. Buchbinder, E. M. Dowling, M. N. Khan, R. Chai, and M. L. Urken, Head Neck **45**, 10 (2023).
8. A. N. Perez, K. F. Sharif, E. Guelfi, S. Li, A. Miller, K. Prasad, R. J. Sinard, J. S. Lewis, and M. C. Topf, J. Pathol. Inform. **14**, 100186 (2023).
9. E. S. McDonald, A. S. Clark, and G. M. Freedman, J. Nucl. Med. **57**, 9S (2016).
10. R. Lott, J. Tunnicliffe, E. Sheppard, J. Santiago, C. Hladik, M. Nasim, K. Zeitner, T. Haas, S. Kohl, and S. Movahedi-Lankarani, Coll. Am. Pathol. 1 (2015).

High-power 2-µm frequency combs for rapid greenhouse gas sensing

20th Anniversary Challenge OPTICA Category: Environment

Applicant: Yicheng Wang

Carbon dioxide (CO_2), methane (CH_4), and nitrous oxide (N_2O) compose 98% of global greenhouse gas emissions, and significantly contribute to global warming. Despite their importance, effectively understanding and monitoring regional emissions through sensitive remote detection of these gases remains challenging today. Dual-frequency-comb based remote sensing has emerged as a unique tool for this purpose in the 'eye-safe' wavelength range of 1.6 µm. Despite the remarkable progress in Er-fiber-based laser systems at this wavelength for this application, the 1.9-2.4 µm wavelength region offers potential advantages due to stronger absorption lines of the greenhouse gas, making it attractive for sensitive tracking of small concentration variations. I propose here employing a **high-power Ho-laser based frequency-comb system (HoLa-Comb) for rapid greenhouse gas detection**.

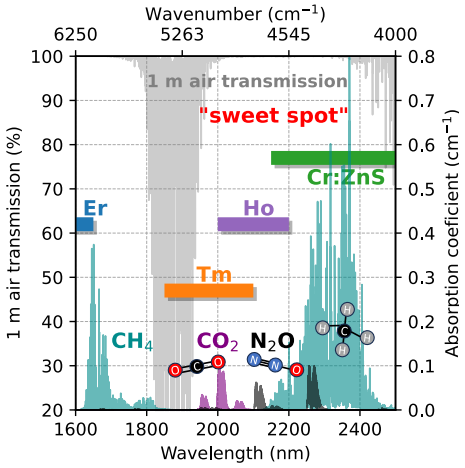

Laser emission range (1.6-2.5 µm) illustrated. Ho-laser operates at the 'sweet spot' for max. air transmission, covering both greenhouse gas lines.

The success of 2-µm rapid remote sensing relies on lasers meeting specific requirements: firstly, the air transmission at 2 µm is low due to water vapor in the atmosphere, necessitating **high average power** levels for long-distance remote sensing. Moreover, to cover the absorption band of the greenhouse gas (about 450 cm^{-1} from 2000-2200 nm), a sufficiently **broadband source** is needed. Additionally, **high repetition rate** is beneficial for measurement speed and detection sensitivity in dual-comb spectroscopy.

In this regard, Tm-, Ho-, and Cr-lasers emitting direct broadband pulses at 2-µm are desirable due to compactness, simplicity, and stability without nonlinear conversion stages or amplifiers. However, their average power is typically below Watt-scale, limiting long-distance remote detection. Ho-laser is operating at the “sweet spot” in this wavelength region, where air transmission is maximum, and the emission is possible to cover both gas absorption lines. Recently, we achieved significant milestones with Ho-laser, including a record-high average power mode-locked laser using all commercially available parts, as well as long-term stability and low-noise. Motivated by its outstanding performance and potential applications, I plan to develop a compact high-power single cavity dual-comb based on Ho-laser and polarization-multiplexing, named **HoLa-Comb**, and demonstrate the proof of concept for rapid greenhouse gas sensing.

The project’s impact extends beyond greenhouse gas sensing, benefiting various fields such as next-gen MIR-spectroscopy for environmental monitoring and medical diagnostics, exploring the 2-µm waveband for communications, and enhancing GHz-burst fs-laser ablation at 2-µm, advancing precise material processing on silicon and transparent materials. We are currently exploring the option of creating a spin-off with our Ho-laser, and funding from this proposal is crucial to fully explore its commercial potential, establish a strong foundation for market entry, and drive innovative solutions that benefit society.

High-power 2-µm frequency combs for rapid greenhouse gas sensing (HoLa-Comb)

Applicant: Yicheng Wang
Institution: Ruhr-University-Bochum, Germany
Email: yicheng.wang@ruhr-uni-bochum.de

Literature Review

Carbon dioxide (CO_2), methane (CH_4), and nitrous oxide (N_2O) compose 98% of global greenhouse gas emissions [1], and remote, sensitive detection of the concentrations of these gases is key for understanding and monitoring regional emissions. Dual frequency-comb-based remote sensing has proved to be a unique tool for kilometer open-air path remote monitoring of such gases in the 'eye-safe' wavelength range of 1.6 µm [2,3]. Despite the remarkable progress in Er-fiber based laser systems at this wavelength for this application, the 2-µm wavelength region – which is also 'eye-safe' - has many potential advantages, since strong absorption lines are present here, as shown in Figure 1. For instance, CO_2 exhibits nearly two times higher absorption coefficients in this range compared to 1.6 µm, presenting an attractive prospect for sensitive tracking of small concentration variations [4]. In this proposal, we suggest employing a **Ho-laser based frequency-comb system (HoLa-Comb) for rapid greenhouse gas detection**.

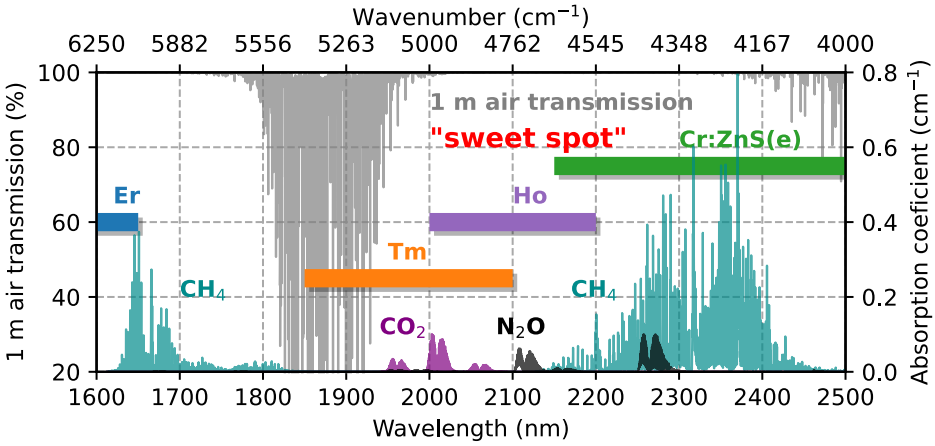

Figure 1. Laser emission range illustrated with 1-m air transmission and greenhouse gas absorption coefficient in the 1.6-2.5 µm wavelength range (from HITRAN database). Ho-Laser is operating at the maximum air transmission 'sweet spot'.

The successful application of 2-µm rapid remote sensing relies on lasers that meet specific requirements:

- The air absorption coefficient at 2 µm is significantly higher than at 1.6 µm due to water vapor in atmosphere (Grey lines in Figure 1), making **high average power** levels crucial for long-distance 2-µm remote sensing.
- To cover the absorption band of the 3 greenhouse gases (about 450 cm^{-1} from 2000 nm-2200 nm), a sufficiently **broadband source** is needed.
- For such a system, **high repetition rate** is beneficial since both measurement speed and bandwidth of dual-comb spectroscopy (DCS) quadratic scales with the fundamental repetition rate [5]. Furthermore, the power per comb line increases at high repetition rate such that higher detection sensitivity can be reached.

These requirements can be achieved in attractive and compact systems using mode-locked lasers emitting directly broadband pulses at this wavelength without needing nonlinear conversion stages or amplifiers. In fact, robustness as provided by simple, single-

oscillator designs is a key factor for environmental sensing since these are typically done outdoors in rough scenarios. In this regard, Tm, Ho, and Cr based lasers have generally attracted attention for broadband oscillators, however, their average power is typically well below Watt-scale, especially in the 2-3 µm region (Figure 2), which makes it difficult to apply such systems for remote detection at long distances.

Currently, 2-3 µm high repetition-rate mode-locked oscillators mainly rely on Tm- or Ho-doped fibers. However, the use of single-mode fibers with limited active media volume results in low average power and pulse energy levels. Although harmonic mode-locking techniques or amplifier stages can overcome these limits, fundamentally mode-locked oscillators are preferred for their simplicity and low noise. Cr:ZnS (known as MIR-Ti:Sapphire) shows promise for power-scaling GHz oscillators around 2.4 µm [6], but challenges remain due to specialized components and difficulties in scaling to higher powers. Commercialization is costly, hindering broader applications of such oscillators. Additionally, grain boundary diffusion poses challenges in scaling polycrystalline Cr:ZnS to higher powers [7].

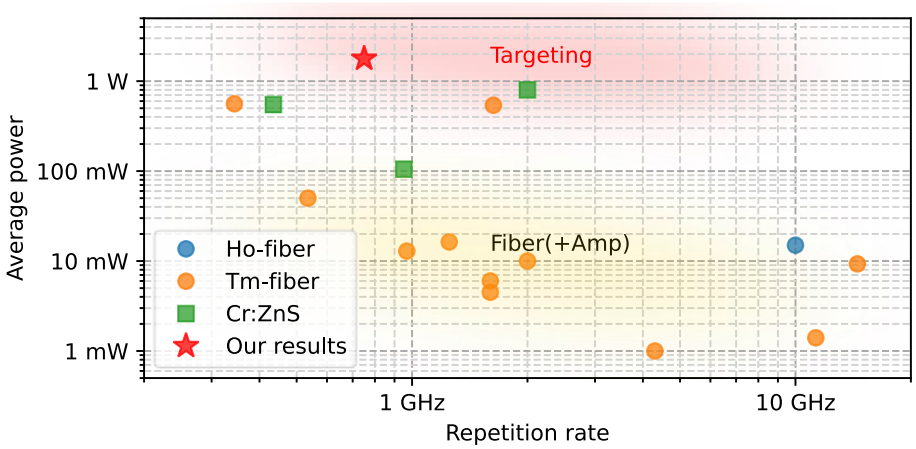

Figure 2. Overview of high repetition-rate mode-locked oscillators in the 2-3 µm wavelength range.

Ho:CALGO, is currently recognized as one of the best materials for ultrafast pulse generation in 2-µm due to its broad gain bandwidth and good thermal properties [8]. And the single crystal could be grown in a large volume by the standard Czochralski method. During my postdoc at the PULS group I was in charge of demonstrating the potential of this material for high-power mode-locking. Our group achieved significant milestones by demonstrating (1) a record-high average power mode-locked laser utilizing in-band-pumped Ho:CALGO, using off-the-shelf commercial components [9]. Additionally, we successfully implemented (2) Kerr-lens mode-locking (KLM) earlier this year, showcasing long-term stability and low noise [10]. Encouraged by these promising outcomes, the PULS group is currently exploring GHz repetition rate KLM, and the preliminary results have already exhibited superior performance compared to other reports within the same wavelength range. I propose here that a watt-level GHz Ho:CALGO laser is ideal for dual-comb operation and would like to explore this potential specifically for gas sensing. The 20th anniversary challenge grant would thus allow me to develop this application activity as an independent activity, with the goal of identifying potentially promising application fields for a spinoff company.

Problem Statement and Objective

Objective:

The primary goal of the project is to design and develop industrial-grade, robust, high-power high-repetition-rate mode-locked oscillator operating around the 2-µm wavelength range based on Ho:CALGO. The overall objectives are to create advanced systems capable of

effectively detecting greenhouse gases for environmental monitoring and research purposes. In the following section, I will address the challenges associated with this task and propose solutions to overcome them.

Problem 1: Q-switching instability.

Self-focusing introduced Q-switching instability is a well-known limit for high-repetition-rate oscillators. Ho:CALGO also has a rather long upper state life time compare with more standard gain material at other wavelength, which makes Q-switching instability more announced. It will be also enhanced if we apply undoped CaF_2 spacers inside the cavity.

Possible solutions:

- Optimizing cavity design. Specifically, optimizing a small beam radius in the gain medium and large beam radius inside the spacers and selecting spacer material with a smaller nonlinear refractive index such as CaF_2. In PULS group, we achieved these steps from 100 MHz cavity up to 750 MHz without Q-switching instability. To further increase repetition rate based on the current knowhow (both theoretically and practically) should be straightforward.
- Introduce self-defocusing mechanism. As presented in Ref [11], PPLN device can operate as a self-defocusing element with an effective negative n_2.
- Introduce self-phase modulation cancellation material. As discussed in Ref [12], SHG crystal can be used to cancel out the strong self-phase modulation.

Problem 2: Noise characterization and stabilization.

For spectroscopy applications for example frequency comb spectroscopy, low-noise laser sources are the key for high dynamic range and sensitive detection. There are mainly 3 types of noise need to be characterized and stabilized: Intensity noise, phase noise and carrier envelope phase (CEP) noise. For gas sensing applications, the first 2 noises are more critical.

Possible solutions:

- Utilizing the specific solid-state laser design including **high-Q cavity, KLM** and **mechanical design**. Current Ho:CALGO characterization already shows great performance in terms of low long-term and short-term noise. In particular, most of the noise in the free-running laser is concentrated at very low frequencies, which will be possible to stabilize in the future.
- To design **single cavity dual-comb.** Recently, the attractive possibility of a single-laser dual-comb source has confirmed its potential [13]. Ho:CALGO is naturally birefringent thus polarization-multiplexing can be used.
- Introducing **low n_2 spacers** inside the cavity. One of the project's ideas originated from a monolithic cavity design [14], where an undoped CaF_2 blank was introduced as spacer for the mode-locked cavity. The current project could benefit by replacing the air with spacers to reduce noise, avoid water vapor absorption, as well as introducing flat negative dispersion.

Furthermore, the current project will benefit from strong support provided by the PULS group and the ETIT department at Ruhr-University-Bochum. This support includes access to their extensive expertise and state-of-the-art equipment, encompassing a wide range of well-equipped characterization tools, from mode-locking characterization to noise analysis.

Outline of tasks and work plan

My primary work plan for the current project consists of two main parts:

Part I: HoLa-Comb Development

1. **Design of the GHz oscillator (Month 1-3)**: This involves creating a standard ABCD matrix cavity design and simulating it to analyze Q-switching instabilities.

Additionally, appropriate calculations and simulations need to be performed to determine the combination of nonlinear refractive index and material dispersion inside the cavity.

2. **Demonstrate of the GHz oscillator (Month 4-6)**: Build and showcase the mode-locked oscillator. Further characterization and optimization of the oscillator's phase noise and time jitter should be conducted to ensure its optimal performance.
3. **Design and demonstrate of the single cavity dual/comb (Month 7-10)**: With the knowledge and results from the GHz cavity research, we will focus on refining and developing the dual comb cavity. Figure 3 illustrates the schematic of the potential HoLa dual comb, as discussed in the previous section.
4. **Characterization and stabilization (Month 11-13):** including long- and short-term stability of the HoLa-Comb.

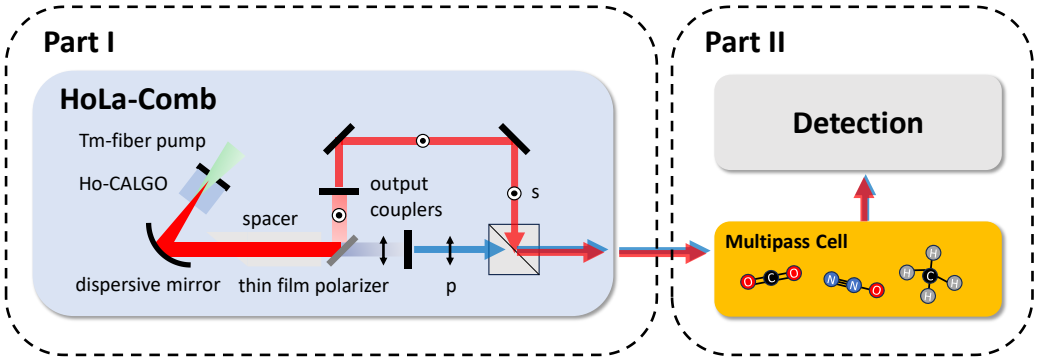

Figure 3. Schematic of the HoLa-Comb with the possible lab-based gas sensing diagram

Part II: Gas Sensing Experiment

The gas sensing experiment is conducted after successfully demonstrating the HoLa-Comb. This part involves the following steps:

1. **Lab-based proof of concept demonstration (Month 14-16)**: Use multipass gas cells to demonstrate greenhouse gas sensing in a controlled laboratory environment. The detection can be performed using either Fourier transform spectroscopy (FTS) or DCS.
2. **Utilize a detection algorithm with DCS (Month 17-18)**: Develop and apply a detection algorithm that utilizes DCS for rapid and sensitive gas detection.
3. **Field-based open-air path gas sensing experiment (after Month 19)**: Conduct a gas sensing experiment in real-world conditions, focusing on long-distance gas detection in an open-air environment.

Outcomes

- **Novel HoLa-Comb system development:** The key specifications I aimed to achieve with the high-power high-repetition-rate 2-µm oscillators are Watt-level average power, repetition rate >250 MHz, and nJ pulse energy.
- **Enhanced greenhouse gas detection**: Demonstrating the effectiveness of the HoLa-Comb system in rapidly detecting greenhouse gases can lead to publications highlighting the enhanced sensitivity, accuracy, and speed of the system compared to existing detection methods.
- **Scientific publications**: During the duration of the current project, I anticipate achieving 1-2 journal publications and submitting over 2 conference proceedings.
- **Training future experts**: One or two master's students will be actively involved in the current project, receiving comprehensive training in the field of ultrafast laser development and gas-sensing.
- **Interdisciplinary collaborations:** If the project involves collaboration with other frequency-comb groups, it could bridge Ruhr-Uni-Bochum's laser source

development expertise with spectroscopy research. Accelerate progress and innovation in the field through joint projects and knowledge exchange.

- **From research to product**: After the funding period, the research results will undergo further development to create a prototype with the support of 3rd party funding, establishing a startup to bring the prototype to market.

Impact

The current project's success is expected to significantly impact not only greenhouse gas sensing applications but also other fields:

- **Promoting next-gen MIR-spectroscopy**: The project's advancements in 2.1-µm oscillator seeded MIR-generation, utilizing non-oxide nonlinear crystals for generating MIR radiations, will benefit spectroscopy, environmental monitoring, and medical diagnostics [15].
- **Exploring the 2-µm waveband for communications:** The project's findings in the 2.1-µm waveband will promote its use in applications like lidar sensing, IoT, and fiber communications, potentially increasing communication capacity.
- **Enhancing GHz burst fs laser ablation at 2.1-µm**: Ruhr-University-Bochum possesses strong expertise in material processing, led by Prof. Andreas Ostendorf and Prof. F. Ömer Ilday. The 2-µm GHz source can significantly advance precise material processing on silicon and transparent materials, benefiting various industries.

In conclusion, the successful project completion will have significant impact on technology, environmental monitoring, and industrial innovation. We are currently already exploring the option of our MHz oscillator Ho:CALGO for spin-off creation, and this proposal's funding will be essential to fully explore its commercial potential and establish a strong foundation for market entry, driving transformative solutions and benefiting society.

Reference

1. Intergovernmental Panel On Climate Change, 1st ed. (Cambridge University Press, 2015).
2. G. B. Rieker, F. R. Giorgetta, W. C. Swann, J. Kofler, A. M. Zolot, L. C. Sinclair, E. Baumann, C. Cromer, G. Petron, C. Sweeney, P. P. Tans, I. Coddington, and N. R. Newbury, Optica **1**, 290 (2014).
3. S. Coburn, C. B. Alden, R. Wright, K. Cossel, E. Baumann, G.-W. Truong, F. Giorgetta, C. Sweeney, N. R. Newbury, K. Prasad, I. Coddington, and G. B. Rieker, Optica **5**, 320 (2018).
4. E. Baumann, E. V. Hoenig, E. F. Perez, G. M. Colacion, F. R. Giorgetta, K. C. Cossel, G. Ycas, D. R. Carlson, D. D. Hickstein, K. Srinivasan, S. B. Papp, N. R. Newbury, and I. Coddington, Opt. Express **27**, 11869 (2019).
5. I. Coddington, N. Newbury, and W. Swann, Optica **3**, 414 (2016).
6. A. Barh, B. Ö. Alaydin, J. Heidrich, M. Gaulke, M. Golling, C. R. Phillips, and U. Keller, Opt. Express **30**, 5019 (2022).
7. P. G. Schunemann and K. T. Zawilski, in *Laser Congress 2019 (ASSL, LAC, LS&C)* (OSA, 2019), p. ATu4A.2.
8. Y. Wang, P. Loiko, Y. Zhao, Z. Pan, W. Chen, M. Mero, X. Xu, J. Xu, X. Mateos, A. Major, M. Guina, V. Petrov, and U. Griebner, Opt. Express **30**, 7883 (2022).
9. W. Yao, Y. Wang, S. Tomilov, M. Hoffmann, S. Ahmed, C. Liebald, D. Rytz, M. Peltz, V. Wesemann, and C. J. Saraceno, Opt. Express **30**, 41075 (2022).
10. W. Yao, Y. Wang, S. Ahmed, M. Hoffmann, M. Van Delden, T. Musch, and C. J. Saraceno, Opt. Lett. **48**, 2801 (2023).
11. A. S. Mayer, C. R. Phillips, and U. Keller, Nat Commun **8**, 1673 (2017).
12. F. Saltarelli, A. Diebold, I. J. Graumann, C. R. Phillips, and U. Keller, Optica **5**, 1603 (2018).
13. R. Liao, H. Tian, W. Liu, R. Li, Y. Song, and M. Hu, J. Phys. Photonics **2**, 042006 (2020).
14. T. D. Shoji, W. Xie, K. L. Silverman, A. Feldman, T. Harvey, R. P. Mirin, and T. R. Schibli, Optica **3**, 995 (2016).
15. A. Schliesser, N. Picqué, and T. W. Hänsch, Nature Photon **6**, 440 (2012).

Monolithic III-V active devices in-plane coupled with Si for integrated Si-photonics

The relentless growth of data traffic is rapidly approaching the communication bottleneck of Si-based integrated circuits and systems, with further scaling down hindered by technological and economic viability. Si-photonics, leveraging the highly successful Si IC infrastructure, is regarded as the enabling technology for new-generation communications as well as emerging fields, including supercomputers, neural and quantum networks, microwave photonics, and sensing. While Si-photonics has been successful with Si-based passive components, integrating III-V lasers on Si has remained the major challenge for Si-photonics. Heterogeneous integration approaches such as wafer-bonding and micro-transfer printing have facilitated the integration of high-performance III-V lasers on Si-photonics platforms. However, their integration density, cost, and manufacturing yield are suboptimal compared to monolithic integration, thereby limiting the broad adoption of Si-photonics. In the past few years, our group, along with a few others worldwide produced III-V lasers on Si by blanket epitaxy of III-V thin films on Si and incorporation of quantum dot active region. Unfortunately, the thick III-V buffer layers for defect engineering severely impede the efficient coupling between III-V active devices and Si passive components. To address this dilemma, we have developed a novel selective epitaxy method named ***lateral aspect ratio trapping (LART)***. The core concept of LART involves the ***in-plane and intimate placement of Si and III-V***, eliminating the III-V buffers and providing an elegant solution for efficient coupling between III-V and Si. The wisdom of LART also lies in the ***unique feature of removing threading dislocations (TDs)***. Traditional blanket epitaxy methods only allow for the reduction of TD density to approximately 10^6 cm^{-2} for GaAs on Si and 10^8 cm^{-2} for InP on Si using 2 to 3 μm thick III-V buffer layers. In contrast, the LART method enables the complete removal of TDs, rendering the entire III-V devices TD-free, a feat not yet achieved on any other platform.

Building upon the LART method, we have achieved TD-free III-V crystals on SOI with excellent uniformity and flexible dimensions of up to hundreds of micrometers. Furthermore, on the versatile III-V/SOI platform, we have realized high-performance photodetectors (PDs), optically pumped lasing of telecom micro-lasers arrays and distributed feedback lasers and Si-waveguide-coupled III-V PDs. In this project, we propose to advance the field by developing monolithic integration of III-V electrically pumped lasers, PDs, modulators, and Si passive devices through efficient and in-plane coupling. This program will leverage our expertise in designing novel metal-organic chemical vapor deposition (MOCVD) growth procedures, as well as laser fabrication and characterization technologies. A primary focus will be addressing the specific challenges associated with coupling high-performance III-V lasers with Si passive components on SOI – a crucial requirement for the realization of Si-photonics that has not yet been achieved on any existing platform.

The results of this project will lead to *the placement of high-performance lasers exactly where they are needed in the photonic integrated circuit in an elegant, efficient, scalable, and low-cost manner*. This unique and versatile technology will significantly contribute to the development of energy-efficient Si-photonics, yielding benefits for both academia and industry. Furthermore, it will enable the integration of cost-effective electronics and power-efficient photonics on the same chip, unlocking the next generation of datacom and telecom, fostering advancements in novel computing systems, microwave photonics, optomechanics, sensing, and LIDAR, creating new opportunities for research and innovation.

Monolithic III-V active devices in-plane coupled with Si for integrated Si-photonics

I. Literature Review

The staggering growth in the volume of data traffic is pushing the performance limits of Si-based integrated circuits and systems in present computing nodes and datacenters. However, further scaling down is challenging in terms of technological and economic viability. In this context, photonic integrated circuit (PIC) is regarded as the enabling technology to conceive new-generation communications, owing to the intrinsic capability of light to transport information over long distances with large bandwidth and minimal power consumption. Si-photonics, leveraging the highly successful Si IC infrastructure and mature complementary metal-oxide-semiconductor (CMOS) technology, is the most powerful strategic pillar of this paradigm shift. Furthermore, Si-photonics is gaining momentum in various emerging applications and research areas, including supercomputers, neural and quantum networks, microwave photonics, sensing, etc. While Si-photonics has been underpinned by the success of Si-based passive components, the light emission necessitates the integration of III-V compound semiconductors due to the indirect bandgap nature of Si [1-3]. With the evolution of PICs, integrating efficient III-V lasers on Si has remained the major challenge for Si-photonics.

Practical applications in Si-photonics require these light sources to be electrically pumped, stably operated at elevated temperatures with a long lifetime, and efficiently coupled with Si-based passive components. Heterogeneous integration approaches such as wafer-bonding and micro-transfer printing have enabled the integration of high-performance III-V lasers on Si-photonics platforms using evanescent coupling strategies [1, 2, 4]. However, the integration density, cost and yield of manufacturing are less optimum than monolithic integration thereby restricting the widespread adoption of Si-photonics. In the past few years, our group, along with a few others worldwide, produced III-V lasers on Si by blanket epitaxy of III-V thin films on Si and incorporation of quantum dot/quantum dash active regions [5-7]. Unfortunately, the thick III-V buffer layers required for defect engineering severely impede the efficient coupling between III-V active devices and Si passive components as illustrated in Figure 1(a) and (b).

II. Problem statement/Objective

To fundamentally solve this dilemma, we have developed a selective epitaxy method named lateral aspect ratio trapping (LART) as shown in Figure 1(c) and (d). The main concept of this method is the in-plane and intimate placement of Si and III-V, eliminating the III-V buffer and enabling efficient coupling between III-V active devices and Si passive components [8-10]. The wisdom of this method also lies in the removal of TDs. For the traditional blanket epitaxy, the TD density can be only reduced to ~10^6 cm^{-2} for GaAs on Si and ~10^8 cm^{-2} for InP on Si, respectively, through the 2 to 3 μm thick III-V buffer layers. In contrast, the LART method enables the removal of TDs with the lateral epitaxy within a narrow width of only 350 nm at Si/III-V interface. The narrow defective region at Si/III-V interface will be easily removed during the later device fabrication, resulting in a TD-free device region, a feat not yet achieved on any other platform. Using this method, we have achieved high-quality III-V crystals on SOI with flexible dimensions and good uniformity as illustrated in Figure 2 (a) [unpublished]. The width of the epitaxial III-V is up to ~9 μm, and the length and thickness of the epitaxial III-V can vary from hundreds of nanometers to hundreds

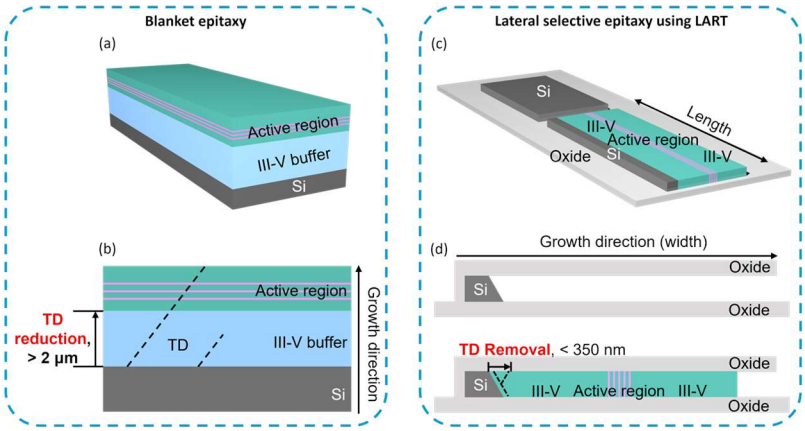

Figure 1. Comparison of traditional blanket epitaxy and our proposed lateral epitaxy using LART.

of micrometers and 220 nm to around 1 µm, respectively. The high-quality and TD-free characteristic are verified by the scanning transmission electron microscopy (STEM) characterizations along and perpendicular to the growth direction. On the versatile III-V/SOI platform, we have incorporated doping during epitaxy and demonstrated high-performance photodetectors (PDs) with novel device designs and fabrication techniques [10]. These PDs manifest low dark current, high responsivity spanning the entire telecom wavelength range, large bandwidth, and high data transmission rates exceeding 112 Gb/s as presented in Figure 2(b). Thanks to the III-V-on-insulator structure resulting from LART, tight optical confinement within the III-V devices is provided, thereby facilitating efficient lasers on SOI with various cavity designs, lasing wavelengths, and performance characteristics as depicted in Figure 2(c) and (d). Both

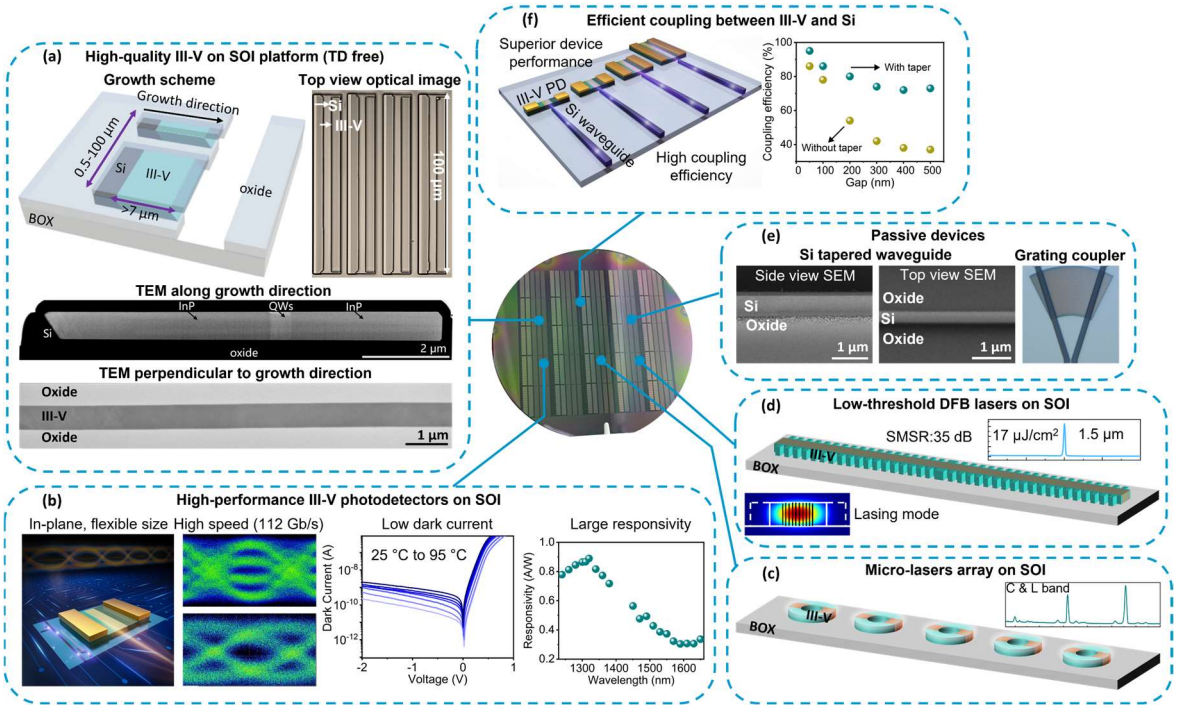

Figure 2. Summary of works based on the LART technique, including high-quality III-V on SOI platform, high-performance III-V PDs on SOI, micro-lasers array on SOI, low-threshold DFB lasers on SOI, passive devices on SOI and efficient light coupling between III-V and Si.

micro-lasers with small footprints [11] and distributed feedback (DFB) lasers with stable low-threshold single-mode emission were achieved [12]. Si-based passive components, including low-loss waveguides, Si inverse tapers, grating couplers, and edge couplers, have also been built on this platform for future integration. Furthermore, the epitaxial III-V material's co-planar configuration with the Si device layer leads to compact and efficient butt-coupling schemes as shown in Figure 2(f). Si waveguides coupled III-V PDs have been demonstrated with a high coupling efficiency between III-V and Si of over 75%, which can be further enhanced to over 95% with advanced lithography modules in the foundry [13].

The objective of this program is to investigate and explore the monolithic integration of III-V active devices and Si passive components on SOI through efficient in-plane light coupling. The III-V active devices include electrically pumped III-V lasers, PDs, and modulators, while the Si passive components mainly focus on Si tapered waveguides, grating couplers, and edge couplers.

III. Outline of tasks/Work plan

Building upon our capability of growing telecom optically pumped lasers with large material volume and designing and fabricating p-i-n photodetectors on industry-standard SOI wafers, we propose the development of monolithic integration and in-plane coupling of III-V active devices and Si passive components. As delineated in Figure 3, the project consists of three main tasks: 1) Electrically pumped lasers on SOI: We will optimize growth parameters for the large-area III-V on SOI, especially the nucleation layer, to achieve device-quality III-V crystals on SOI using LART. Then we will incorporate the doping and design lateral p-i-n structures for electrically pumped lasers based on our previous experience with high-performance III-V PDs on SOI and simulations. After that, we will fabricate electrically pumped Fabry-Perot (FP) lasers and DFB lasers on SOI according to the simulated structural design and well-established techniques including surface treatment, dry etchings, lithography, passivation, and metallization (see Figure 4(a)). 2) Si-waveguide-coupled III-V lasers: We will design a butt-coupling scheme with advanced couplers between III-V and Si to minimize reflections between III-V lasers and Si waveguides.

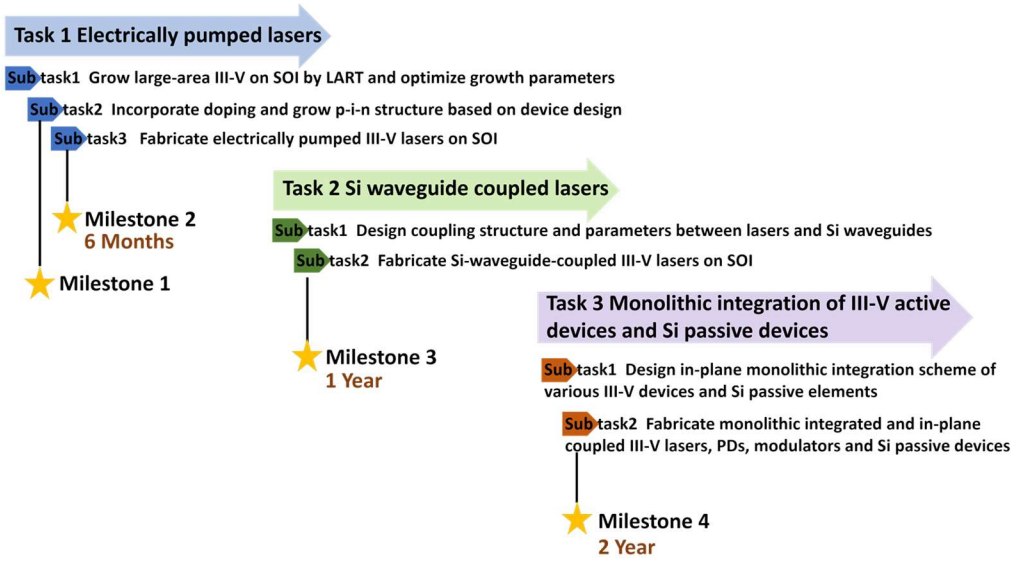

Figure 3. Gantt chart of the work plan and tasks.

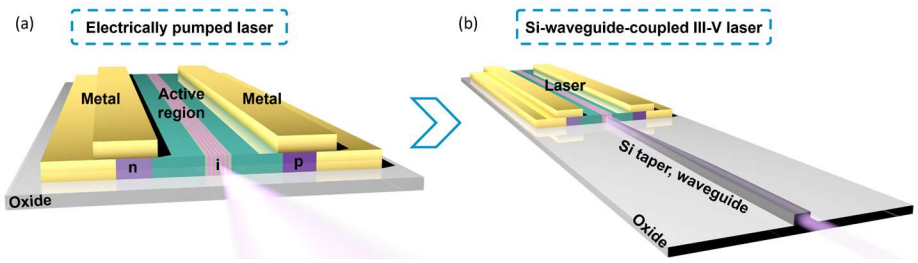

Figure 4. (a) Schematic of electrically pumped III-V laser on SOI using LART. (b) 3D architecture of Si-waveguide-coupled III-V laser on SOI with an in-plane structure.

The proposed approaches include sub-wavelength gratings, inverse tapers, and angled III-V end facets. Si-waveguide-coupled III-V lasers on SOI will be fabricated to enable the monolithic integration and in-plane efficient coupling of III-V lasers and Si waveguides, which is the key for fully integrated Si-photonics. The high coupling efficiency is guaranteed by the zero-misaligned coupling in the vertical direction and the tolerant coupling in the lateral direction as depicted in Figure 4(b). 3) Monolithic integration of III-V active devices and Si passive devices: We will develop III-V modulators on the same platform and design detailed coupling schemes between various III-V devices and Si passive components. III-V lasers, PDs, modulators, and Si waveguides will be fabricated on SOI with each building block placed at the desired position for monolithic integration as illustrated in Figure 5. Compared with the system using ring resonators and micro-disk resonators, the system proposed in this project is less sensitive to fabrication accuracies and temperature changes.

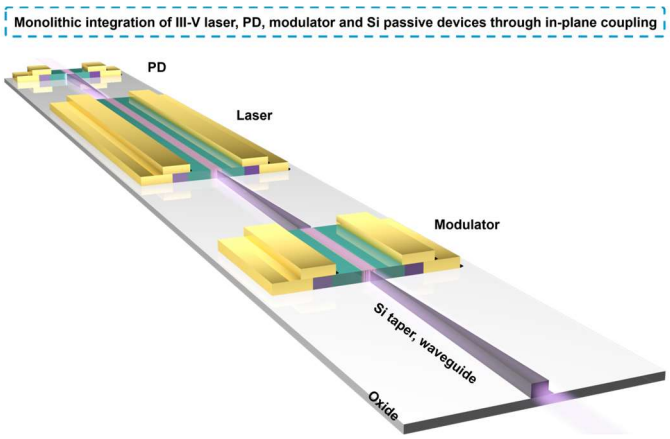

Figure 5. Monolithic integrated and in-plane coupled III-V lasers, PDs, modulators, and Si passive devices.

IV. Outcome

The overarching outcome is to design and experimentally demonstrate 1) In-plane electrically pumped III-V lasers on SOI in telecom band; 2) Si-waveguide-coupled III-V lasers on SOI; 3) Monolithic integration of III-V lasers, photodetectors, modulators, and Si passive devices through in-plane and efficient coupling. The in-plane configuration enables CMOS-compatible fabrication and high coupling efficiency. The III-V-on-insulator structure is similar to the integration platforms enabled by bonding or transfer printing techniques, making it easier to develop integration technology on this LART platform. This

program will allow us to combine the expertise of designing novel metal-organic chemical vapor deposition (MOCVD) growth procedures, as well as laser fabrication and characterization technologies. We will address specific issues of coupling high-performance III-V lasers with Si passive components on SOI, which is the key to Si-photonics and not available on any demonstrated platform. As schematically illustrated in Figure 5, the proposed system allows for high-speed data transmission, detection, and modulation using efficient coupling between III-V devices and Si passive components.

V. Impact

Integrating high-performance III-V light sources that can be coupled with Si passive components on the same platform is of paramount importance The results of this project will enable the placement of high-performance lasers exactly where they are needed in the photonic integrated circuit in an elegant, efficient, scalable, and low-cost manner. This is the most unique and versatile technology to support energy-efficient silicon photonics, which is of great significance for both academia and industry. This technology, by integrating cost-effective electronics and power-efficient photonics on the same chip, will unlock the next generation of datacom and telecom and enable new applications and research areas such as novel computing systems, microwave photonics, optomechanics, sensing and LIDAR.

References:

[1] M. Near, C. Xiang, Steven M. Bowers, A. Bjorlin, R. Blum, and John E. Bowers, "Perspective on the future of silicon photonics and electronics." Applied Physics Letters, 118(22), 220501, (2021).

[2] D. Thomson, A. Zilkie, John E Bowers, T. Komljenovic, Graham T Reed, L. Vivien, D. Marris-Morini, E. Cassan, L. Virot,Jean-Marc Fédéli, J. Hartmann, Jens H Schmid, D. Xu, F. Boeuf, P. O'Brien, Goran Z Mashanovich and M Nedeljkovic. "Roadmap on silicon photonics." Journal of Optics, 18(7), 073003, (2016).

[3] Y. Han, H. Park, J. Bowers, & K. M. Lau, "Recent advances in light sources on silicon." Advances in Optics and Photonics, 14(3), 404-454, (2022).

[4] Y. Hu, D. Liang, K. Mukherjee, Y. Li, C. Zhang, G. Kurczveil, X. Huang, and Raymond G. Beausoleil. "III/V-on-Si MQW lasers by using a novel photonic integration method of regrowth on a bonding template," Light: Science & Applications 8(1), 1-9, (2019).

[5] Y. Wan, C. Xiang, J. Guo, K. R.oscica, M.J. Kennedy, J. Selvidge, Z. Zhang, L. Chang, W. Xie, D. Huang, and A.C. Gossard, "High Speed Evanescent Quantum-Dot Lasers on Si," Laser & Photonics Reviews, 15(8), p.2100057, (2021).

[6] Y. Xue, W. Luo, S. Zhu, L. Lin, B. Shi, and K. M. Lau, "1.55 μm electrically pumped continuous wave lasing of quantum dash lasers grown on silicon", Optics Express, 28(12), pp.18172-18179, (2020).

[7] C. Shang, E. Hughes, Y. Wan, M. Dumont, R. Koscica, J. Selvidge, R. Herrick, A. C. Gossard, K. Mukherjee, and J. E. Bowers, "High-temperature reliable quantum-dot lasers on Si with misfit and threading dislocation filters," Optica 8, 749 (2021).

[8] Y. Han, Y. Xue, Z. Yan and K. M. Lau, "Selectively grown III-V lasers for integrated Si-photonics," Journal of Lightwave Technology, 39(4), pp.940-948, (2021).

[9] Z. Yan, Y. Han, L. Lin, Y. Xue, C. Ma, W. K. Ng, K. S. Wong, and K. M. Lau, "A monolithic InP/SOI platform for integrated photonics." Light: Science & Applications 10(1), 1-10, (2021).

[10] Y. Xue, Y. Han, Y. Tong, Z.hao Yan, Y. Wang, Z. Zhang, H. K. Tsang, and K. M. Lau, "High-performance III-V photodetectors on a monolithic InP/SOI platform." Optica 8(9), 1204-1209, (2021).

[11] J. Li, Y. Xue, L. Lin, Z. Xing, K. S. Wong and K. M. Lau, "Telecom InGaAs/InP quantum well lasers laterally grown on Silicon-on-Insulator," Journal of Lightwave Technology, vol. 40, no. 16, pp. 5631-5635 (2022).

[12] Y. Xue, J. Li, Y. Wang, K. Xu, Z. Xing, K. S. Wong, H. K. Tsang, and K. M. Lau, "In-plane 1.5 μm distributed feedback lasers selectively grown on (001) SOI", Laser & Photonics Reviews, DOI: 10.1002/lpor.202300549.

[13] Y. Xue, Y. Han, Y. Wang, J. Li, J. Wang, Z. Zhang, X. Cai, H. K. Tsang, and K. M. Lau, "High speed and low dark current Si-waveguide coupled III-V photodetectors selectively grown on SOI", Optica , 9(11), 1219-1226, (2022).

Optica Foundation Challenge 2023: Information

Spatiotemporal quantum metasurfaces for high-dimensional information processing

Challenge:

Single-photon sources are crucial for many optical and quantum technologies. Typical stand-alone quantum emitters (QEs) basically feature less brightness, low efficiency, and no polarization and phase priorities that prevent them being directly used in advanced photonic applications. The common way for changing the polarization and phase front of single-photon beams requires the use of bulky and slow-response optical components, unavoidably lowing the efficiency, tunability, and compactness. Alternatively, by carefully engineering the near-field environment around, e.g., coupling with nanocavity, the QE decay rate was domenstrated to be significantly enhanced. The investigation has been extended to modulate the direction, polarization, and phase front with QE coupling with planar surface nanostructures. However, on-chip generation of structured quantum emission, e.g., encoded with composite multichannel SAMs and OAMs, remains challenging. Moreover, most of state-of-the-art single-photon sources are set in stone with fixed modes once constructed, up to now, ***the realization of spatiotemporal single photon sources is still elusive***. Overcoming this challenge can potentially provide more channels for date transmission in optical and quantum information processing.

Proposed project:

In this project, I propose an approach using MEMS- integrated QE-coupled metasurfaces, i.e., spatiotemporal quantum metasurfaces, in a vertical cavity, in which the gap distance between QE-coupled metasurface and optical shaping metasurface is dynamically tunable. Remarkably, right- and left-circular SAM states ($|R\rangle$ and $|L\rangle$) and OAM states ($\pm\ell$) will be dynamically encoded with single photons. The main features of proposed spatiotemporal single-photon sources:

a. **Structured single-photon beams by QE-coupled metasurfaces (M1).** Solid-state QEs should be first selected and precisely positioned with prefabricated align markers on the substrate. M1 is then designed and fabricated around selected QEs to convert QE-excited surface plasmon polaritons into structured single-photon beams, i.e., with the "doughnut" patterns changing in *z* direction.
b. **Manipulation SAM and OAM by optical shaping metasurfaces (M2).** M2 have several annular areas, consisting of different azimuthally and radially arranged nanoelements, which can manipulate the polarization and phase of photon emission. With different sizes of emission pattern ("doughnut"), photon beams will interact with corresponding areas and thus will encode different SAMs and OAMs.
c. **Tunable gap distance of MEMS-controlled vertical cavity (C0).** M1 and M2 forms a vertical cavity. The pattern size of photon emission when arriving M2 is related to the distance between M1 and M2. This gap distance can be dynamically tunable by MEMS with a fast response (~0.1 millisecond) when changing the voltage. This can be viewed as one of the keys of the tunability of the proposed single photon sources.

Outcomes:

The overall goal of this project is to realize for the first time the spatiotemporal single-photon sources with ultrafast tunability. Reaching this goal means a great progress from currently inefficient and static single photon sources to tunable and efficient regime, opening a new perspective for quantum technologies especially with its dynamic tunability. Moreover, the tunability is not only realize on SAM (two states, $|L\rangle$ and $|R\rangle$) but also can be superpositioned with OAM (unlimited states, $\pm\ell$), which is crucial for exploiting full potential and freedom of single photons from QEs.

In the scientific side, one of the significant achievements is the on-chip generation of higher-dimensional structured single photons, beyond the state-of-the-art 2D single photon vortexes. In the technologic side, we will realize the integrated platform consisting of QE, metasurfaces, and MEMS, with scalable on-chip integration of complicated nanostructures around QEs in *x*, *y*, and *z* directions. Overall, we believe this project will provide a new toolkit by making significant impact not only on fundamental understanding of light-matter interactions but also on wide-ranging applications that benefit from ultracompact, ultrahigh-capacity, and ultrahigh-speed single-photon OAM systems-on-a-chip, which is crucial to advanced modern optical and quantum applications.

Optica Foundation Challenge 2023: Information

Spatiotemporal quantum metasurfaces for high-dimensional information processing

In a nutshell:

Twisting single photons with unbounded set of helical spatial modes is crucial to fundamental physics and modern quantum technologies, especially offering a new degree of freedom to boost optical and quantum information capacity. The common way for changing the polarization and phase front of single-photon beams requires the use of bulky and slow-response optical components, unavoidably lowing the efficiency, tunability, and compactness. In this project, I will conduct the investigation for answering this straightforward but fundamental and challenging question:

Can we dynamically twist single photons with spatiotemporal quantum metasurfaces?

This project aims to realize spatiotemporal quantum metasurfaces with dynamically tunable spin angular momentum (SAM) and twisted mode, i.e., carrying orbital angular momentum (OAM). It will demonstrate a versatile approach and platform for designing advanced single-photon sources, which is in demand for high-capacity optical information processing.

Introduction /The state-of-the-art/Problem statement:

Single-photon sources are crucial for many optical and quantum technologies, including quantum communications, quantum computation, and quantum-enhanced metrology.[1] Typical stand-alone (i.e., in homogenous environment) quantum emitters (QEs), such as quantum dots, molecules, and defect centers in diamonds basically feature less brightness, low efficiency, and no polarization and phase priorities that prevent them being directly used in advanced photonic applications.[2] Generally, there are two routes for modulating the polarization and phase of photon emission. Conventional far-field approach for shaping QE emission relies on bulky optical components, including polarizers, quarter-wave plates, and spatial light modulators, which is relatively clumsy and suffering low efficiency, tunability, and compactness. Alternatively, by carefully engineering the near-field dielectric environment around QEs, the QE emission characteristics also can be modified, e.g., via the Purcell effect.[3,4] One of the most straightforward approaches is to use QE-coupled nanocavities that significantly enhance the QE decay rate, while the polarization and direction of photon emission would be hard to control.[5,6] Flexibly molding QE emission with desired optical properties, e.g., encoding with angular momenta[7,8], including SAM (associated with photon circularly polarized states)[9,10] and OAM (associated with the wavefront helicity)[11,12], is highly desirable but calls for new designing strategies that should extend beyond traditional nanocavities or nanoattenans.

On-chip QE-coupled metasurfaces, consisting of extended planar surface nanostructures surrounding QEs, represent an attractive and rapidly developing approach for efficiently molding the photon emission by structuring the out-coupling of (diverging) surface plasmon polaritons (SPPs) that are non-radiatively excited by QEs.[13-15] SAM-encoded single-photon sources have been realized with dielectric width-gradient nanoridges encircling preselected QEs.[13] By properly displacing circular bullseye nano-ridges, the off-normal photon emission was achieved, though without polarization benefit.[14] Moreover, on-chip OAM single-photon sources have been demonstrated using Archimedean spiral nano-ridge gratings with different number of arms.[15] These configurations, representing extended surface nanostructures on-chip coupled with QEs, have shown a new avenue to modulate nonclassical single photon emission while getting rid of the bulky and clumsy optical components and systems. However, ***on-chip generation of multichannel and structured quantum emission, e.g., encoded with composite SAMs and OAMs, remains elusive.*** Moreover, unfortunately, ***all aforementioned single-photon sources are static with fixed modes once constructed.***

Up to now, ***the realization of spatiotemporal single-photon sources is still elusive***. Single photons with dynamically tunable angular momenta can potentially provide more channels for date transmission in optical communications and quantum information processing. Generally, to realize dynamically tunable single photon sources, one should leave at least one parameter unfixed during the design and fabrication. One of the potential ways is to use phase change materials to construct

nanostructures around QEs. However, this method has intrinsic issues for precisely and flexibly changing the material's permittivity [16], thus further manipulation of photon emission would be more difficult and relatively slow.

In this project, I propose an approach using MEMS- integrated QE-coupled metasurfaces, i.e., spatiotemporal quantum metasurfaces, in a vertical cavity, in which the gap distance between QE-coupled metasurface and optical shaping metasurface can be dynamically tunable. Remarkably, right- and left-circular SAM states ($|R\rangle$ and $|L\rangle$) and OAM states ($\pm\ell$) will be dynamically encoded with single photons, providing additional freedoms for advanced applications in high-dimensional and multiplexing quantum information processing.

Outline of tasks:

Proposed method:

The general idea is to utilize two metasurfaces, i.e., QE-coupled metasurface (M1) and optical shaping metasurface (M2), that are separated by a microcavity (C0) with a tunable gap distance (Fig. 1). The QE-coupled metasurface is used to generate structured single-photon beams that feature varied beam sizes in the propagation direction (*z*-direction). The optical shaping metasurface can mold incident photon beams with different polarizations and phases. The tunability of gap distance is ensured by MEMS.

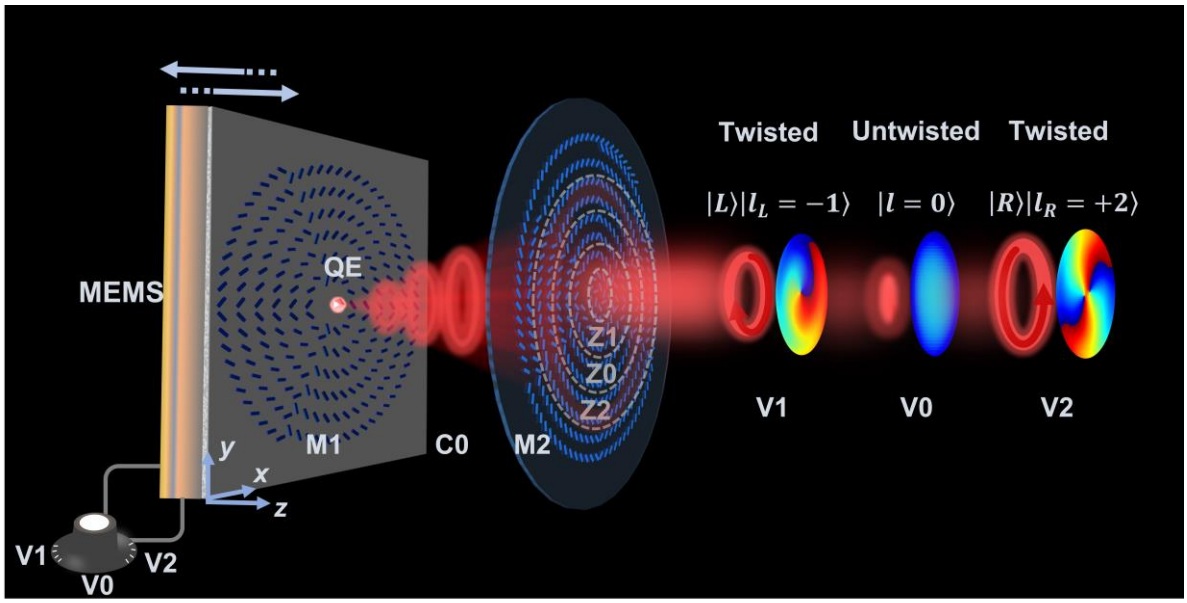

Fig. 1 Schematic of the spatiotemporal single-photon source.

The main features of proposed dynamically tunable single photon sources:

a. **Structured single-photon beams by QE-coupled metasurfaces (M1).** Solid-state QEs, e.g., nanodiamonds with color center, should be first selected and precisely positioned with prefabricated align markers on MEMS substrate. M1 is designed and fabricated around selected QEs to convert QE-excited radially diverging SPPs into structured single-photon beams, i.e., with the "doughnut" patterns varying in the propagation direction.
b. **Manipulation SAMs and OAMs by optical shaping metasurfaces (M2).** M2 have several annular areas (Z0, Z1, or Z2), consisting of different azimuthally and radially arranged nanoelements, which can manipulate the polarization and phase of photon emission with a high transmission efficiency. With different sizes of emission pattern ("doughnut"), photon beams will interact with corresponding areas and thus will encode different SAMs and OAMs.
c. **Tunable gap distance of MEMS-controlled vertical cavity (C0).** M1 and M2 forms a vertical cavity. The pattern size of photon emission when arriving M2 is related to the distance between M1 and M2. This gap distance can be dynamically tunable by MEMS with a fast

response (expect to be in scale of 0.1 milliseconds), when changing the voltage (V0, V1, and V2). This can be viewed as one of the keys of the tunability of the proposed single photon sources.

Research work plan:

1. **Metasurfaces design, fabrication, and characterization.**
   (1) QE-coupled metasurfaces (M1): Design M1 enabling generation of structed single-photon beams, e.g., Laguerre-Gaussian beams, with the targeting wavelength of 602 nm (germanium vacancy centers in nanodiamond); Fabricate M1 with QE precisely in the center of the configuration; Develop the experimental setup for characterizing M1 with structured single photon beams.
   (2) Optical shaping metasurfaces (M2): Design and fabricate M2 capable of molding incident radially polarized photon beams to left-hand and right-hand circular polarizations (LCP and RCP) with different vortex (e.g., topological charge of -1 and +2). Characterize M2 with different size of annular light incident by Supercontinuum Lasers (602 nm).
2. **Dynamically tunable single photon sources.**
   (1) Construction: M1 is adhered to the movable MEMS, M2 is mounted directly to the substate of the MEMS. M1 and M2 should be in good alignment, and the gap distance should be tunable and varied in a large range (1μm - 10μm).
   (2) Characterization: Characterize dynamical tunability of single photon sources with SAM shift between $|L\rangle$ and $|R\rangle$, and OAM shift between -1 and +2. Other properties of dynamically tunable single photon sources, such as second-order coherence, decay time, and spectrum, will also be characterized.

Major outcomes:

The overall goal of the project is to realize the first time the spatiotemporal single-photon sources with ultrafast tunability. Reaching this goal means a great progress from currently inefficient and static single-photon sources to tunable and efficient regime, opening a new perspective for advanced optical and quantum technologies especially with its dynamic tunability. Moreover, the tunability is not only realize on SAM (two states, $|L\rangle$ and $|R\rangle$) but also can be superpositioned with OAM (unlimited states, $\pm\ell$), which is crucial for exploiting full potential and freedom of single photons from QEs.

During the implement of the project, two challenges should be overcome. On the theory side, as it is still elusive for on-chip generation of structured single-photon beams, I should figure out the way of its generation and propagation, then correspondingly design optical shaping metasurfaces. On the technique side, I should develop a method to precisely align two metasurfaces (M1 and M2), which is important for leading single-photon beams incident on the expected areas of optical shaping metasurfaces.

Realization of spatiotemporal single-photon sources with SAM shift between $|L\rangle$ and $|R\rangle$, and OAM shift between 0, -1, and +2 can be viewed as criteria success of the first stage. After realizing the proposed idea, lots of other applications can benefit, for example, straightforwardly, it can be easily extended to tunable single-photon holography, high-dimensional single-photon detectors, and dynamic single-photon radars.

Impact:

Over the years, many efforts have been dedicated to generating single photons that constitute one of the crucial technologies for quantum communication and information systems. However, most of the proposed sources are set in stone during their fabrication, requiring complex set-ups to modulate photon emission with low efficiency and tunability. The project will address this issue and make a breakthrough in on-chip realization of integrated single-photon sources with more freedoms of dynamically modulating the SAMs and OAMs. The magnitude and importance of the project's contribution to the expected scientific, societal, and economic impacts are summarized as following:

Expected scientific impact:

Various of micro/nano structures, including nanoantennas and nanocavities, have been designed in recent years to enhance the photon emission from QEs by making use of the Purcell effect. However,

the underlying physics of the near-field coupling between QE and planner nanostructure arrays are still elusive, let alone the design approach for integrated spatiotemporal single-photon sources. In this project, we will introduce the design idea of simultaneously utilizing two different kinds of metasurfaces to manipulate the QE photon emission, which involves optics, material science, and computational electromagnetics. This thoroughly exploration of light-matter interaction in micro/nanoscale will enable a range of new physical phenomena that are distinctly different from those in conventional bulk optics. ***One of the significant achievements is the on-chip generation of higher-dimensional structured single photons, beyond the state-of-the-art 2D single-photon vortexes.*** It will not only benefit the designing of metasurfaces for single photon sources, but also will open a new avenue for designing other nanodevices in the emerging field of quantum nanophotonics.

Expected technological impact:

In recent years, with the development of nanofabrication techniques, metasurfaces have opened up a new era of the so-called flat optics which are increasingly used to replace whole sets of traditional optical elements. This project will develop a reliable and mature technology for precisely integrating QEs with metasurfaces in both the fabrication process (with the QE position error less than 20 nm) and mounted process (integrated QE-coupled metasurfaces and optical shaping metasurfaces). We consider the main challenges and key advantages of the platform, with a focus on scalable on-chip fabrication and integration of complicated nanostructures around QEs in *x*, *y*, and *z* directions. Therefore, metasurfaces themselves, which are realizable with current fabrication technologies, will become a novel type of enabling device for on-chip manipulating non-classical light, thereby opening the door to new possibilities for quantum nanotechnologies. Moreover, in many applications, it is beneficial to precisely integrate photon sources with other nanophotonic devices, including photonic cavities, filters, waveguides, resonators, and detectors.

Expected societal impact:

Photonic technologies are becoming increasingly prevalent in our daily lives. After decades of rapid advances, light sources - especially lasers and light-emitting diodes - have become high-performing, yet low-cost and reliable components, driving the internet and lighting cities. Single-photon sources, as one of the new light sources, offer the prospect of a quantum revolution with qualitative improvements in a wide range of technologies. The proposed method, together with the designed nanodevices, will provide broader functionalities and have a great potential to on-chip dynamically structure single photons and produce a wide variety of multiphoton entangled states, e.g., the orbital and spin degrees of freedom, whereas conventional optical components cannot. Furthermore, with these advances in photon sources, especially after adding dynamic tunability, it can be expected that their unique properties will allow to secure quantum optical internet, quantum enhanced optical sensing, and ultrafast quantum computation.

Overall, we believe this project will provide a new toolkit by making significant impact not only on fundamental understanding of light-matter interactions but also on wide-ranging applications that benefit from ultracompact, ultrahigh-capacity, and ultrahigh-speed single-photon OAM systems-on-a-chip, which is crucial to advanced modern optical and quantum applications.

Appropriateness:

This project fits the requirement of *Optica Foundation Challenge* well, while it may be not suitable for conventional grant programs as it is very challenging. Actually, it is a new research area for on-chip generation of structured single photons with desired SAMs and OAMs, which is still an unfinished target of state-of-the-art single photon sources even in static, let alone dynamically tunable SAMs and OAMs for higher-dimensional single-photon sources.

Although the project has high risk, realizing the proposed idea will also bring lots of benefit. On the one hand, it will not only miniaturize single-photon sources, getting rid of the bulky and expensive optical components, but also bring new degree of freedom to single photons. On the other hand, the exploration on both theoretical and technological sides as well as the platform proposed, will open a new avenue for diverse applications from conventional optics to quantum technologies.

References:

[1] J. Wang, F. Sciarrino, A. Laing, and M. G. Thompson, "Integrated photonic quantum technologies," Nat. Photonics **14**(5), 273–284 (2020).

[2] I. Aharonovich, D. Englund, and M. Toth, "Solid-state single-photon emitters," Nat. Photonics **10**, 631–641 (2016).

[3] L. Novotny and B. Hecht, *Principles of nano-optics* (Cambridge University, 2012).

[4] S. I. Bogdanov, O. Makarova, X. Xu, Z. O. Martin, A. S. Lagutchev, M. Olinde, D. Shah, S. N. Chowdhury, A. R. Gabidullin, I. A. Ryzhikov, I. A. Rodionov, A. V. Kildishev, S. I. Bozhevolnyi, A. Boltasseva, V. M. Shalaev, and J. B. Khurgin, "Ultrafast quantum photonics enabled by coupling plasmonic nanocavities to strongly radiative antennas," Optica **7**(5), 463 (2020).

[5] G. M. Akselrod, C. Argyropoulos, T. B. Hoang, C. Ciracì, C. Fang, J. Huang, D. R. Smith, and M. H. Mikkelsen, "Probing the mechanisms of large Purcell enhancement in plasmonic nanoantennas," Nat. Photonics **8**(11), 835–840 (2014).

[6] S. I. Bozhevolnyi and J. B. Khurgin, "Fundamental limitations in spontaneous emission rate of single-photon sources," Optica **3**(12), 1418 (2016).

[7] A. Forbes, M. de Oliveira, and M. R. Dennis, "Structured light," Nat. Photonics **15**(4), 253–262 (2021).

[8] J. Ni, C. Huang, L.-M. Zhou, M. Gu, Q. Song, Y. Kivshar, and C.-W. Qiu, "Multidimensional phase singularities in nanophotonics," Science **374**(6566), eabj0039 (2021).

[9] I. Söllner, S. Mahmoodian, S. L. Hansen, L. Midolo, A. Javadi, G. Kiršanskė, T. Pregnolato, H. El-Ella, E. H. Lee, J. D. Song, Søren Stobbe, and P. Lodahl, "Deterministic photon–emitter coupling in chiral photonic circuits," Nat. Nanotechnol. **10**(9), 775–778 (2015).

[10] Y. Ma, H. Zhao, N. Liu, Z. Gao, S. S. Mohajerani, L. Xiao, J. Hone, L. Feng, S. Strauf, "On-chip spin-orbit locking of quantum emitters in 2D materials for chiral emission," *Optica* **9**, 953-958 (2022).

[11] T. Stav, A. Faerman, E. Maguid, D. Oren, V. Kleiner, E. Hasman, and M. Segev, "Quantum entanglement of the spin and orbital angular momentum of photons using metamaterials," Science **361**(6407), 1101–1104 (2018).

[12] T. Santiago-Cruz, S. D. Gennaro, O. Mitrofanov, S. Addamane, J. Reno, I. Brener, and M. V. Chekhova, "Resonant metasurfaces for generating complex quantum states," Science **377**(6609), 991–995 (2022).

[13] Y. Kan, S. K. H. Andersen, F. Ding, S. Kumar, C. Zhao, and S. I. Bozhevolnyi, "Metasurface-enabled generation of circularly polarized single photons," Adv. Mater. **32**(16), 1907832 (2020).

[14] Y. Kan, F. Ding, C. Zhao, and S. I. Bozhevolnyi, "Directional off-normal photon streaming from hybrid plasmon-emitter coupled metasurfaces," ACS Photonics **7** (5) 1111–1116 (2020).

[15] C. Wu, S. Kumar, Y. Kan, D. Komisar, Z. Wang, S. I. Bozhevolnyi, and F. Ding, "Room-temperature on-chip orbital angular momentum single-photon sources," Sci. Adv. **8**(2), eabk3075 (2022).

[16] A. M. Shaltout, V. M. Shalaev, and M. L. Brongersma, "Spatiotemporal light control with active metasurfaces," Science **364**(6441), eaat3100 (2019).

Executive Summary

Project Title: A New Solution for Microwave Photonic Sensing by Laser Dynamics

Challenge: Microwave photonic (MWP) sensing and measurement are envisioned to be a promising alternate to the conventional pure electronic or optical solutions as MWP overcomes their critical limitations: the requirements of large instantaneous bandwidth and wide frequency coverage may not be achievable by pure electronic schemes or lead to extremely complicated and costly systems, and pure optical schemes are subject to small sensing range and limited by interrogation speed. However, most existing MWP sensing schemes require a microwave signal through an electro-optical modulator (EOM) to modulate an optical source for generating MWP signals, and a measurand is applied to the sensing system through EOM or an optical sensor such as optical interferometry, fibre sensor, etc. This leads to an MWP system that is large in size, making it difficult to integrate all key components onto a single chip, and consequently expensive in terms of cost.

To tackle the challenge, the project proposes a new sensing scheme and provides an innovative solution, where a laser serves as both an MWP source and a sensor, and MWP signals are directly generated by laser dynamics without external modulation (thus electro-optical conversion is not required), which can lead to: highly compact (minimum part-count) and cost effective implementation; a great potential to boost the sensing resolution, sensitivity and measurement range; more functionalities and more practical applications.

Expected outcomes: I, together with my colleagues at the University of Wollongong (UOW), Australia, have been working in the field of the proposed project with a set of findings. Based on the solid research background previously built, this project aims to

- Conduct theoretical investigations on a new MWP generation scheme and its relevant sensing mechanism. New theories on MWP sensing and measurement will be generated.
- Develop advanced signal processing algorithms to exploit the full potentials of the proposed new scheme and to efficiently extract the rich information on measurand contained in the MWP signals, thereby achieving high sensing performance.
- Investigate the mechanism of the generation and control of photonic microwave frequency comb (PMFC) using the new scheme, leading to a number of well-synchronized parallel chirp signals over a wide frequency band. Chirped PMFC will be developed to achieve high resolution and flexibility in microwave remote sensing.
- Develop an integrated sensing platform with optical sensing and microwave remote sensing sharing a common core optical configuration and explore their industrial applications.

The proposed project will be conducted in 'Sensing, Communications and Control Laboratory' within the Faculty of Engineering and Information, University of Wollongong, Australia, where I have been working since my PhD study. The research lab will provide both optical and electrical devices, and elements for the relevant experimental investigation.

The proposed project falls within one of the three categories: Information and aligns with Item 4"Exploring high-sensitivity optical sensors and detectors" and Item10 "Exploring new optical sensing technologies to improve various parameter monitoring capabilities", listed in the **Proposals of interest** of 2023 Optica Foundation Challenge.

Project Title: A New Solution for Microwave Photonic Sensing by Laser Dynamics

1. Literature Review

Our world is being changed by the fourth industrial revolution, whose foundation is paved by advances in sensing technologies. As one of the most important sensing technologies invented in the 20th century, laser interferometer finds wide applications to ultra-precision machining, manufacturing, positioning control, etc. Optical feedback interferometry (OFI) is a new class of laser interference sensing technology utilizing external optical feedback effect in a laser. OFI has been recognized as a promising non-contact sensing technology due to its merits of minimum part-count scheme, low cost in implementation and ease in optical alignment.

Numerous efforts have been devoted to exploring theories and applications of OFI sensing, and a multitude of applications have been reported, including the measurement of displacement, velocity, distance, acoustics, etc [1, 2]. The research on OFI has been led by researchers in Europe, the USA and Japan [1, 2]. OFI systems are conventionally based on semiconductor lasers (SL). Recent years, the lasers employed in OFI systems have been extended to THz lasers, leading to a variety of promising THz applications to imaging, materials analysis, etc [3]. In existing OFI sensing techniques, the laser operates at its steady state.

I have been working on OFI since my PhD work. What if a laser for OFI is pushed to operate beyond the steady state? This question was first explored recent years by me together with my research partners in UOW, Australia. We experimentally discovered that the capability of OFI sensing can be greatly enhanced when making a laser work at higher dynamic states, e.g., period-one (P1) [4-6]. We observed that, in this case, the laser intensity is modulated by a waveform in microwave frequencies, leading to the generation of microwave photonic (MWP) signals. Furthermore, we also discovered that, by making a laser operate at and quasi-period (QP), a photonic microwave frequency comb (PMFC) can be generated, and the PMFC is controllable. These discoveries open a new door for MWP sensing and measurement, which is an active and exciting emerging research area with numerous applications in advanced sensing, internet of things, 5G, etc [7, 8].

MWP sensing and measurement are envisioned to be a promising alternate to the conventional pure electronic or optical solutions. MWP overcomes their critical limitations: the requirements of large instantaneous bandwidth and wide frequency coverage may not be achievable by pure electronic schemes or lead to extremely complicated and costly systems [7, 9], and pure optical schemes are subject to small sensing range and limited by interrogation speed [10-12]. However, most existing MWP sensing schemes require a microwave signal through an electro-optical modulator (EOM) to modulate an optical source for generating MWP signals, and a measurand is applied to the sensing system through EOM or an optical sensor such as optical interferometry [13], fibre sensor [8], etc. This results in the system large in size and difficulties in the integration of all key components in a chip, and expensive in its cost. The scheme in this project provides an innovative solution, **where a laser serves as both an MWP source and a sensor, and MWP signals are directly generated by laser dynamics without external modulation** (and thus not requiring an electro-optical conversion), which leads to the following merits.

Firstly, the direct generation of MWP signals with lasers can make the sensor highly compact (minimum part-count) and cost effective. Secondly, due to the rich information carried by the MWP signals, the new scheme has a great potential to boost the sensing resolution, sensitivity and measurement range by designing advanced signal processing algorithms. Thirdly, the availability and ease of operation of semiconductor lasers, in a wide range of configurations, make the scheme very flexible, enabling more functionalities and more practical applications.

REFERENCES

[1] T. Taimre, M. Nikolić, K. Bertling, Y. L. Lim, T. Bosch, and A. D. Rakić, "Laser feedback interferometry: a tutorial on the self-mixing effect for coherent sensing," *Adv. Opt. Photon.,* vol. 7, no. 3, pp. 570-631, 2015/09/30 2015.

[2] S. Donati, "Developing self-mixing interferometry for instrumentation and measurements," *Laser & Photonics Reviews,* vol. 6, no. 3, pp. 393-417, 2012.
[3] P. Dean, A. Valavanis, J. Keeley, K. Bertling *et al.*, "Terahertz imaging using quantum cascade lasers—a review of systems and applications," *Journal of Physics D: Applied Physics,* vol. 47, no. 37, p. 374008, 2014/08/28 2014.
[4] **Y. Ruan**, B. Liu, Y. Yu, J. Xi, Q. Guo, and J. Tong, "High sensitive sensing by a laser diode with dual optical feedback operating at period-one oscillation," *Applied Physics Letters,* vol. 115, no. 1, p. 011102, 2019.
[5] B. Nie, **Y. Ruan**, Y. Yu, Q. Guo, J. Xi, and J. Tong, "Period-One Microwave Photonic Sensing by a Laser Diode With Optical Feedback," *Journal of Lightwave Technology,* vol. 38, no. 19, pp. 5423-5429, 2020.
[6] B. Liu, **Y. Ruan**, Y. Yu, Q. Guo, J. Xi, and J. Tong, "Modeling for optical feedback laser diode operating in period-one oscillation and its application," *Optics Express,* vol. 27, no. 4, pp. 4090-4104, 2019/02/18 2019.
[7] J. Capmany and D. Novak, "Microwave photonics combines two worlds," *Nature photonics,* vol. 1, no. 6, p. 319, 2007.
[8] J. Yao, "Optoelectronic Oscillators for High Speed and High Resolution Optical Sensing," *Journal of Lightwave Technology,* vol. 35, no. 16, pp. 3489-3497, 2017.
[9] X. Zou, B. Lu, W. Pan, L. Yan, A. Stöhr, and J. Yao, "Photonics for microwave measurements," *Laser & Photonics Reviews,* vol. 10, no. 5, pp. 711-734, 2016.
[10] G.-D. Kim, H.-S. Lee, C.-H. Park, S.-S. Lee *et al.*, "Silicon photonic temperature sensor employing a ring resonator manufactured using a standard CMOS process," *Optics Express,* vol. 18, no. 21, pp. 22215-22221, 2010/10/11 2010.
[11] C. L. Arce, K. D. Vos, T. Claes, K. Komorowska, D. V. Thourhout, and P. Bienstman, "Silicon-on-Insulator Microring Resonator Sensor Integrated on an Optical Fiber Facet," *IEEE Photonics Technology Letters,* vol. 23, no. 13, pp. 890-892, 2011.
[12] H. Yi, D. S. Citrin, and Z. Zhou, "Highly Sensitive Athermal Optical Microring Sensor Based on Intensity Detection," *IEEE Journal of Quantum Electronics,* vol. 47, no. 3, pp. 354-358, 2011.
[13] L. Li, X. Yi, S. X. Chew, S. Song, L. Nguyen, and R. A. Minasian, "Double-pass microwave photonic sensing system based on low-coherence interferometry," *Optics Letters,* vol. 44, no. 7, pp. 1662-1665, 2019/04/01 2019.
[14] R. Lang and K. Kobayashi, "External optical feedback effects on semiconductor injection laser properties," *IEEE journal of Quantum Electronics,* vol. 16, no. 3, pp. 347-355, 1980.

2. Problem Statement/Objectives

The traditional OFI sensing operates a laser at its steady state and produces an interferometric-like sensing signal with fringe resolution of half laser wavelength, and this technology is generally only used for short range optical sensing. It has been a challenge to enhance the sensing performance in terms of resolution, sensitivity and measurement range to fulfil the increasing demand on ultra-precision machining and manufacturing for industry 4.0, internet of things, etc. In the project, a laser operates at high dynamic states, leading to MWP sensing that brings together the worlds of optoelectronics and microwave engineering. The new scheme not only solves the problem with existing OFI but also contributes a new solution for MWP sensing. In particular, the capability of generating tuneable PMFC will result in novel solutions for remote sensing. With the new sensing scheme proposed, a series of powerful sensing functionalities based on a common core OFI structure can be developed. The following research questions are identified and will be investigated in this project:

- Investigate the fundamental theory for the generation of an MWP sensing signal by operating OFI at the P1 state (called MWP-P1 sensing signal in below).
- Explore and understand the sensing mechanism of MWP-P1 and its related application systems. This includes the characterization of the MWP-P1 sensing system, the optimisation of system configuration and operation condition, and design signal processing

algorithms to maximise its sensing capability in terms of sensitivity, resolution and measurement range.

- Investigate the mechanism of generation and control of PMFC and design advanced signal processing to achieve high performance remote sensing

3. Outline of tasks/Work Plan

Generally, an OFI configuration consists of a semiconductor laser (SL), a photodiode (PD), a focusing lens and an external target associated with the measurands. As the SL dynamics are highly dependent of the optical feedback (OF), varying the OF can make the OFI operate at steady state, period-one (P1) oscillation, quasi-period (QP) oscillation or chaos (C). In this project, two types of MWP sensing will be explored. In type 1, I will explore optical sensing with OFI operating at P1 state for fundamental displacement measurement, from which various sensing can be extended. In type 2, I will operate OFI at QP state to generate PMFC for remote sensing. And a sensing platform will be implemented for exploring various applications.

Task 1: Sensing by an OFI at P1 (time allocation: year 1)

Firstly, it needs to investigate the modelling for an SL with optical feedback and theoretically determine the operating conditions for the generation of an MWP-P1 signal. The investigation can be made by revising the L-K equations [14] to include dual-cavity feedback, varying cavity parameters, etc. The influence of the four controllable parameters (L: cavity length, J:injection current, α: Henry factor and k: feedback strength) on the P1 state will be studied. This will result in a set of rules for selecting the system parameters. Moreover, the optimal operating conditions will be studied to ensure that an OFI works at P1 region with high stability. Non-linear system dynamic analysis will be carried out to determine the stable region, with which methods will be developed to control and stabilize the system. As an MWP-P1 is a microwave modulated light signal, signal analysis and characterization will be performed in both optical domain and microwave domain.

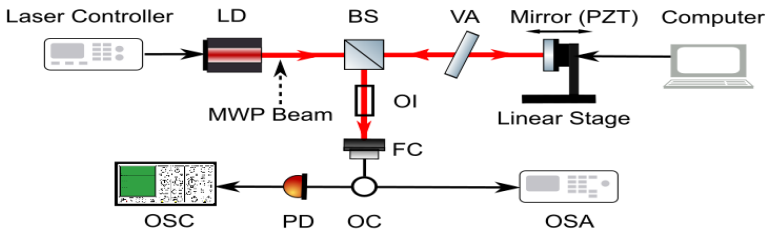

Fig. 1. Configuration for generation of an MWP-P1 sensing signal.

Extensive experiments will be conducted to verify the theoretical analysis by means of an experimental system shown in Fig. **1**. In this task, the following investigations will be conducted:

- According to the selection rules obtained from the theoretical analyses, suitable initial values will be selected and used for the system parameters. The generated MWP-P1 signal is directed to an FC, which is then separated into two beams by an optical coupler (OC). One beam is sent to OSA for optical spectrum analysis, and the other one is sent to PD to obtain microwave components to be recorded by OSC and then sent to the computer for analysis and processing.
- The optimal operating condition for the generation of the MWP-P1 signal will be verified experimentally to validate the theoretical analysis. In addition, the best operating point at which the system has the highest sensitivity will be experimentally determined with the guidance of the developed theory.

Task 2: MWP-P1 sensing with a large measurement range (time allocation: 2nd half of year 1 to 1st half of year 2)

Displacement sensors are extensively employed in industry for measuring the position and movement of objects and any physical quantities that can be converted into movement, such as pressure, acceleration, etc. It is always a challenge to achieve high resolution and simultaneously a large dynamic range. In my recent work [5], we found a linear relationship between the peak frequency of an MWP-P1 and external cavity displacement, which can be used to achieve displacement measurement with a resolution up to 0.36nm. However, the work in [5] only applies for a small measurement range of less than 1.5mm. In this task, I aim to make full use of the MWP-P1 area to achieve displacement sensing with remarkably larger measurement range. The following specific tasks will be carried out:

- Theoretical study will be conducted on the relationship between MWP-P1 oscillation frequency and displacement within a large displacement range applied on the external cavity (formed by a PZT installed on a linear stage). Approaches to deal with laser mode-hopping and frequency-hopping in MWP-P1 need to be developed.
- Investigation on the features of MWP-P1 signals (after PD) from both time domain and frequency domain. Develop algorithms to retrieve cavity displacement.
- Extension of displacement measurement to measurement of other physical quantities e.g velocity, vibration etc.. It needs to study the waveform and spectrum of the resultant MWP-P1 signal from its optical and microwave frequency band, and its relationship with the cavity displacement. Based on this, the relevant signal processing algorithms will be designed to retrieve various physical quantities and achieve multiple quantities measurement simultaneously.

Task 3: MWP-P1 sensing for super measurement resolution (time allocation: 2nd half of year 1 to 1st half of year 2)

The traditional OFI sensing operates a laser at its steady state and produce an interferometric-like signal with fringe resolution of half laser wavelength (λ_0). Therefore, $\lambda_0/2$ is the fundamental resolution for all existing OFI based displacement sensing. Over the years, researchers have put extensive efforts to increase the resolution by optical or electrical subdivision for OFI fringes.

In this task, a dual-cavity OFI will be designed with one cavity for adjusting laser states and one for measurement. With this configuration, the dependence among MWP-P1 signal, OFI fringe signal and the displacement applied on the target cavity will be studied. Optimal system design will enable us to make use of the MWP-P1 signal to achieve OFI fringe subdivision.

This is a complex non-linear system. Both the internal and external parameters of the laser will affect the response of the OFI system to the meaurand. I will analyse the impact of these parameters and characterise the system response mathematically, which will be crucial to the determination of the stable operation region and optimisation of the sensing system. Moreover, the features of the generated MWP-P1 signal and the relationship between the parameters of the MWP-P1 signal and the measurand will be studied.

The sub-tasks are specified in the following:

- Model the proposed dual-cavity OFI system and analyse the system response through studying the state diagrams of the dual-cavity OFI.
- Analyse the system stability and determine the stable P1 region, then develop the relevant system control rules.
- Develop new sub-division method to achieve super-high resolution sensing in nm scale. It is expected that making use of MWP-P1 signal to sub-divide the OFI fringe (corresponding to a half laser wavelength), can lead to a resolution in nm scale. A relevant signal processing algorithm will also be developed.
- Improve the sensing performance by applying advanced signal denoising techniques to remove/reduce various noises such as ambient noise, thermal noise in lasers, or noise induced through the two cavities,

Task 4: Photonic microwave frequency comb (PMFC) generation and implementation of a sensing platform (time allocation: year 2)

Microwave frequency comb (MFC) is a series of frequency components with the same frequency interval in the microwave frequency domain. It has gained a great interest for a variety of applications, including communications, radar, frequency metrology and spectroscopy, etc. The traditional way to generate MFC is based on electronic methods. However, the bandwidth of MFC is limited to a few gigahertz due to the electronic bottleneck. Alternatively, optical methods for MFC generation are more attractive.
In this task, I will propose a new optical approach for the generation of photonic MFC based on OFI operating at QP state. This approach is attractive due to its low-cost, all-optical components configuration and flexibility for tunable MFC generation with linearly chirp each comb tooth. This will offer a novel solution for remote sensing and achieve parallel coherent radar imaging with high resolution.
Our preliminary work has shown that the use of OFI at QP is able to generate PMFC with controllable comb teeth. The following theory and experiment studies will be conducted:

- Investigate the rules for selecting parameters on operating an OFI at QP to generate a PMFC with a minimal noise floor.
- Develop an approach for linear chirp control for the PMFC by designing a new modulation for both laser injection current and its external cavity length.
- Explore PMFC based radar imaging
- Implement a sensing platform that can be used to develop different application systems

4. Outcome(s)

- Develop a new scheme for MWP sensing based on optical feedback interferometry (OFI), where a laser is used to serve as both an MWP source and a sensor, and the MWP signals are generated directly by laser dynamics without external modulation. Conduct theoretical investigations on MWP signal generation and the relevant sensing mechanism, which will lead to new theory and technology on MWP sensing and measurement.
- Design advanced signal processing algorithms to exploit the full potentials of the proposed scheme and efficiently extract the information on measurands contained in MWP signals, thereby achieving high sensing performance.
- Investigate the generation of photonic microwave frequency comb (PMFC) using the proposed scheme with OFI operating at quasi-period state. In particular, the PMFC can be controlled by designing a joint modulation method, enabling the development of a multiband microwave sensing system with advanced signal processing algorithms to achieve high resolution and flexible remote imaging.
- Develop a new super-high subdivision method for OFI fringe signals to achieve nanometer scale displacement sensing with a dual-cavity OFI configuration operating at period-one state of the proposed scheme.

5. Impact

In this project, a new sensing scheme is proposed with a laser operating at high dynamic state to generate a MWP signal for sensing, which brings together the worlds of optoelectronics and microwave engineering. By making full use of the dual natures of MWP signals in both optics and microwave, both optical sensing with high performance and novel remote microwave sensing can be achieved. It is expected to open up new capabilities of sensing, which can offer small size, light weight, high resolution, high speed, high sensitivity, immunity to electromagnetic interference, and a variety of functionalities. The project will lead to significant advances in sensing technologies by successfully conducting this project.

- Super-high resolution and precise sensing technology is indispensable to advanced manufacturing, auto-driving vehicles, IoT, etc. Development of high performance sensors will contribute to the economic and social advancement.
- The project has great potential to create commercial opportunities that can translate into new employment/manufacturing opportunities on high quality MWP sensing technology and its relevant products developed by this project.

Accelerating Optical Edge Sensing with Photonic Deep Learning

PI: Zaijun Chen, University of Southern California, zaijunch@usc.edu

Category: Information

Abstract: Existing optical sensing networks rely on sensors deployed at the internet's edge and processing in the cloud. Data acquisition, transmission, and processing lead to large energy consumption, data traffic, and long latency that are unacceptable in the era of the Internet of Things (a self-driving car would require decision-making within <1 ms). Optical neural networks (ONNs) are emerging to process machine learning tasks with great potential to elevate the electronic bottleneck for both general-purpose computing (Z. Chen, et al, VCSEL-ONN, ***Nat. Photonics*** 2023) and decentralized photonic edge computing (Sludds, et al, ***Science*** 378, (2022)). In particular, incorporating ONN processors with optical sensing would lead to the development of *"smart optical sensors"* that can detect and process optical signals without the need of converting the signal to the electronic domain, thus reducing energy consumption, latency, data traffic, and sensor footprint by orders of magnitude.

Intended outcomes: 1. **first smart optical sensors** incorporating both sensing and processing in a single photonic integrated circuit. 2. **System integration** with laser frequency combs, electro-optic modulators, photonic memories, and long optical waveguides. 3. **state-of-the-art computing performance**: low-energy (10 fJ/MAC), low latency processing (<1 ns), high-density processing chip area 1 cm^2; 4. **On-chip optical sensing** with an optical neural network to retrieve sample information (sample existence, concentration, etc). 5. **Reduced data traffic** with in-sensor processing.

Capability and Impact:

As the global emergence of IoT will continue to explore optical sensing for real-time, high-sensitivity detection, pushing the demands on lower latency, lower energy consumption and footprint, smart optical sensors will play an essential role in addressing the response time, energy cost and data traffic issues, such as in autonomous driving.

For optical sensing, the implementation of neural network hardware (with custom-designed kernels) could enhance the sensitivity of a specific feature that might have been buried in a regular spectral measurement, which would lead to new breakthroughs in biosensing and disease monitoring.

Toward photonic integration, the success of the project will have a profound impact on miniaturized and low-power optoelectronic circuits (frequency combs, photonic memories, coherent detectors) for neuromorphic photonics.

For computing, the architecture allows MAC operations on both amplitude and phase information encoded with hundreds of comb modes in parallel, which might lead to the development of next-generation **ultralow-power optical tensor processors** with high throughput and low computing power in the post-Moore's age.

Accelerating Optical Edge Sensing with Photonic Deep Learning

PI: Zaijun Chen, University of Southern California, zaijunch@usc.edu

1. Literature Review

Optical neural networks (ONNs) are emerging to process machine learning tasks with high optical bandwidth and low-loss data movement [1–5]. Deep learning with photonic circuits has the potential to elevate the electronic bottleneck for next-generation high-speed, ultralow-energy processors. This proposal aims to exploit the processing power of ONNs in optical sensing, for the development of *"smart optical sensors"* that can detect and process optical signals without converting to electronic computers, thus reducing energy consumption, latency, data traffic, and sensor footprint by orders of magnitude.

Optical sensors have been widely deployed at the internet's edge, in applications ranging from real-time 3D light detection and ranging (LiDAR) for self-navigation cars, aircraft, and spacecraft, to spectroscopic sensing and imaging for environmental sensing and health monitoring (Fig. 1). The sensing techniques have been developed towards high precision, resolution, sensitivity and measurement speed. In recent years, the advent of optical frequency combs (OFCs) has revolutionized the field of optical metrology [6]. In spectroscopy sensing, OFCs directly interrogate a sample, providing broad spectra with a resolution up to the comb mode spacing (~1 pm) and a precision determined by an atomic clock, allowing to study, for instance, a small trace of gas in the earth's atmosphere and to diagnose the existence and concentration of a species in a biological sample in a rapid manner [7–9]. In combination with on-chip OFC sources, these spectrometers can be integrated for *lab-on-chip* detection [10,11]. Beyond spectroscopy, OFCs have been used for hyperspectral imaging [12,13] and LiDAR [14], enabling parallel detection with hundreds of wavelength channels for significantly reduced measurement times.

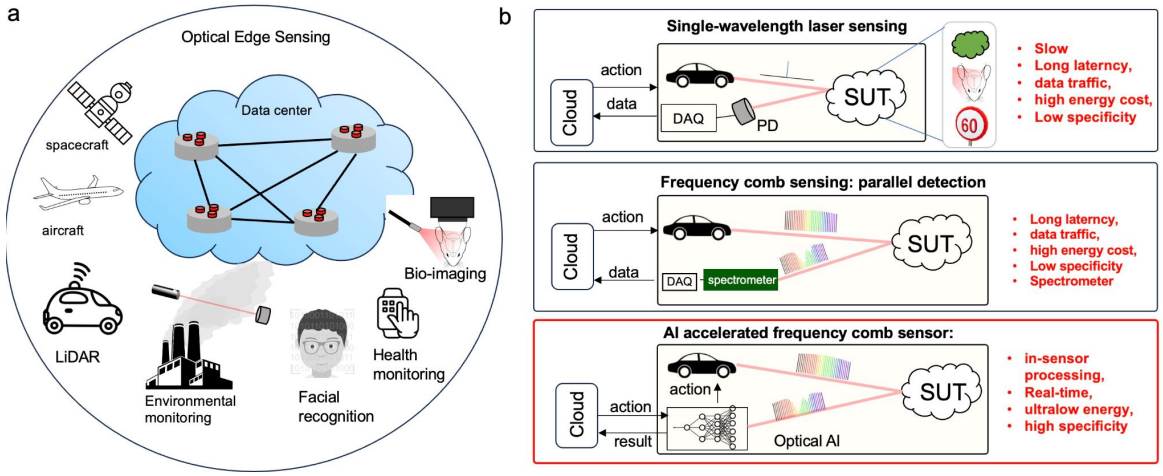

Fig. 1 Concept of optical edge sensing with photonic AI acceleration. (a). Billions of smart optical sensors at the edge. Relying on data center computing leads to long latency, data traffic, and energy consumption. (b) Comparison of state-of-the-art edge sensing techniques, single wavelength laser sensing, frequency comb sensing, and optical-AI-based frequency comb sensing. All three techniques can be adapted for laser spectroscopy, imaging, Lidar, etc. SUT: system under test. AI: artificial intelligence. DAQ: data acquisition

However, practical constraints emerge when deploying optical sensors for real-life applications, especially at scale in the new era of the Internet of Things (IoT). As shown in Fig. 1a, *billions of*

optical sensors in our life need "intelligence". Optical sensors constantly detect and monitor the surrounding environment, producing a massive amount of data. Due to the lack of processing power in the sensor, these data are transmitted, processed, and stored in the cloud, leading to large data traffic that pushes the network bandwidth requirements to their limit and leads to long response times and high energy consumption in processing (Fig. 1b), which are however critical for almost all the above-mentioned applications. In recent years, edge computing is emerging to empower sensors with 'intelligence', such as Google Edge TPU. However, these digital circuits are energy-consuming, bulky, and slow. It requires digitizers and high-speed data links to convert the optical signals for processing, leading to energy and latency constraints.

The performance of ONNs has been significantly advanced in recent years in terms of architecture design, device, and system development [1,2,4,15–18]. State-of-the-art ONNs, with an improvement of over 100-fold in energy efficiency and 25-fold in computing density over electronic computing, have been demonstrated in PI Chen's previous work [1]. This proposal aims to harness these optical AI processors in OFC-based sensors; in-sensor all-optical processing elevates the energy and latency bottlenecks. The advantages are listed in Fig. 1b.

2. Problem Statement/Objective

To develop smart optical sensors with high programmability, energy efficiency, and low latency, we propose to incorporate a frequency-encoded neural network model (W_{ij}^n) to process the sensing information (X^n) encoded in the phase or amplitude of an OFC (Fig. 2). Based on coherent homodyne detection with frequency modes, matrix-vector multiplications with multiple cascade layers (not shown) allows deriving gas parameters (line position, concentration, temperature, pressure, etc). This is achieved without the need of resolving the frequency comb spectrum, which has been a main goal as well as the difficulty in frequency comb spectroscopy.

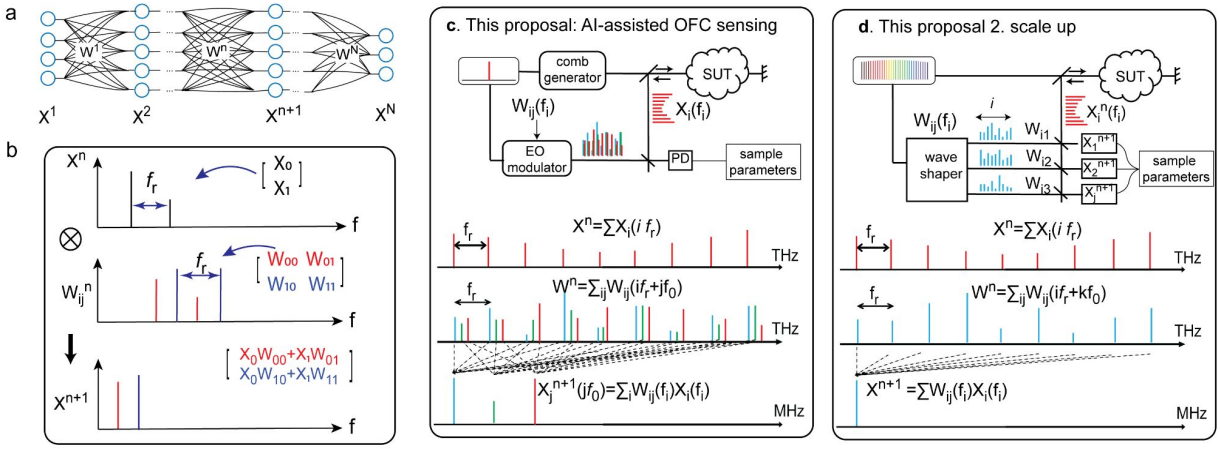

Fig. 2 Processing OFC-based signals with optical deep learning. **a**. a forward propagating optical neural network consisting of N layers, each layer computes an MVM. **b**. Principle of MVM operations. The sample-induced signal, $X_{(1xi)}=[X_0, X_1]$, is encoded to the amplitude of *i* comb lines, and the weight matrix W_{ij}^n is encoded to the *i*·*j* frequency modes. The interference of the two combs yields MVM. **c**. experimental implementation of the scheme in OFC sensing. The entire pre-trained weight matrix is encoded using Field Programmable Gate Arrays (FPGA). The MAC operation has been demonstrated in PI. Chen's prior work for radio-frequency signal processing [19] d. scale-up of the system. Spatial multiplexing extends computation bandwidth by a factor of *j*.

The objectives of this proposal include:

- Development of a training model (weight matrix) for retrieving spectral information.

- Development of a low energy, on-chip data modulation scheme to encode the trained weight matrix values to individual frequency modes.
- System and device fabrication: on-chip frequency comb generation with 100 comb lines in the 1.64 μm (methane absorption line). Single-side-band (SSB) modulators or microring weight banks for weight encoding. Sensing spiral waveguide for sample interaction.

3. Outline of tasks / Work Plan

PI Chen's prior work has demonstrated homodyne-based ONNs with coherent micron-scale laser arrays [1], decentralized photonic deep learning [2], radio-frequency-encoded homodyne ONNs [19], frequency comb spectroscopy and on-chip spectrometers for gas-phase sensing [7,8,10].

Our proposed new architecture to process sensing signals is shown in Fig. 2. The entire system will be integrated into thin-film Lithium Niobate (TFLN) photonic circuits. Fig. 2a-b illustrates the computing concept of frequency-mode MVM. The proposed scheme 1 (Fig. 2c) allows encoding arbitrary long matrix sizes (at the cost of computing bandwidth, limited by the FPGA). This FPGA bandwidth is sufficient for gas phase sensing as the linewidth of gas molecular transition under atmospheric pressure is about 5 GHz.

Training of machine learning models.

The team will train machine learning models to retrieve spectral parameters. The team has previously developed multiple models for image classification, and language processing using both fully connected layers and convolutional neural networks (CNNs), using the Pytorch training platform and implementing the trained weight matrix to the network. The team in collaboration with Prof. Wei Wu's group at USC has developed a machine-learning model for disease prediction [20]. The training spectrum data set will be achieved using the line parameters available in HITRAN database.

Device design

We aim to develop the two sensing schemes (Fig. 3) within the 1-year timeline. In Fig. 3a, a chip-based CW laser is split into two parts, one part is used to generate a frequency comb (detailed below), which interrogates the sample based on evanescent sensing in an air-clad spatial waveguide. The other part passes through a chirp-free amplitude modulator, which encodes the entire weight matrix using a waveform (inverse Fourier transform of the time trace) generated by the FPGA. This encoding format allows it to stream in arbitrarily large matrix sizes, within the bandwidth of the FPGA (64 GS/s in this proposal). Larger models lead to longer encoding times. We propose a spatial multiplexing to scale up the computing power,

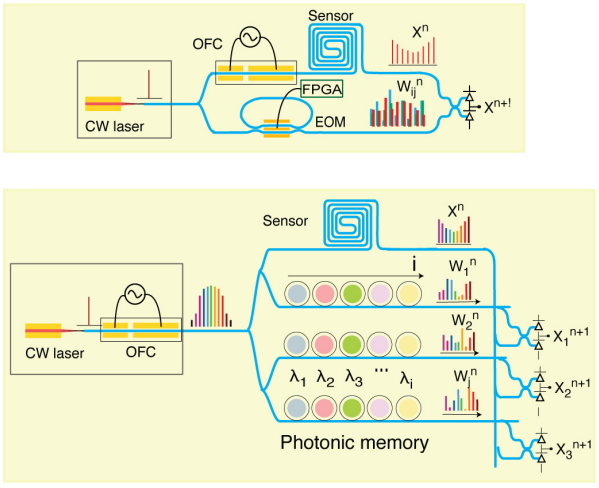

Fig. 3 Smart optical sensor layout using optical machine learning. Spectroscopic sensing using a spiral waveguide is under the scope of 1 year. Beyond spectroscopy, the comb in the sensing arm can be replaced with a grating/prism to detect objects and speed for Lidar [14]

technique, where each j-th spatial channel encodes a weight vector (size (1xi)) using i ring base modulator (Fig. 2b), each channel computes a signal beam in a parallel detection channel.

On-chip frequency comb generation

Integrated electro-optic (EO) frequency combs on TFLN offer the possibility of generating frequency comb with tunable repetition rates, determined by the microwave driving frequency. Such a source is ideal for spectroscopic sensing since it can be adapted to measure different samples due to the compelling advantages of frequency agility, robust operation, and comb efficiency. Fig.4 (center plot) shows the scheme of the device which consists of one amplitude modulator and a double-pass phase modulator. Such comb sources have been recently demonstrated at USC [21]. Prof. Chen's group has improved the design to reduce the jitters between amplitude modulation and phase modulation using a single electrode.

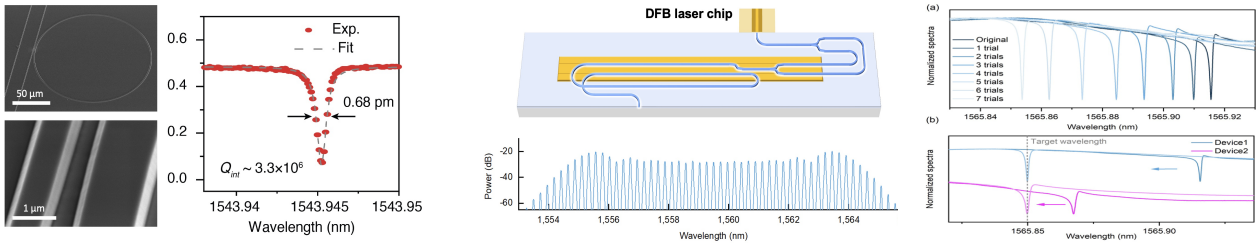

Fig 4. TFLN photonics fab at USC. Left: high-Q TFLN cavity and low-loss waveguides. An intrinsic Q of 3.3 m has been achieved. center: Flat-top frequency comb generation in Prof. Chen's group (unpublished). Right: nonvolatile cavity trimming using lithium niobate for static photonic memories (unpublished).

Encoding machine learning model with embedded photonic memory

A key difficulty of this work is developing a low-energy platform to encode the weight matrix to the optical field. In Fig. 3a approach, the key element is a chirp-free SSB modulator, which can operate at the electronic bandwidth limit (64 GS/s). Based on our TFLN platform, we have demonstrated phase and amplitude modulators, which have made the solid foundation for the SSB modulator. However, the final goal is to use the full bandwidth of optics using the scheme in Fig. 3b, which is achievable by using the Viener effect to have each microring resonate with a target comb mode. In reality, due to fabrication errors, the cavity resonance might vary. We have recently developed a photonic memory based on the pyroelectric and photorefractive effect in TFLN, which can trim the microring cavity resonance by multiple linewidth (Fig. 4c), introducing amplitude modulation to one ring per mode.

4. Outcomes

The outcome of this project is the first optical smart sensor incorporating both the sensing unit and optical processor for low-energy (10 fJ/OP), high-density computing (a chip area of less than 1 cm^2).

- The processing time can well be <1 ms for the proposed scheme 1 (Fig. 2c, limited by the AWG bandwidth) and <1 ns for the proposed scheme 2 (Fig. 2d).
- The energy consumption of MAC operation can be reduced significantly. In the proposed scheme 1, although the weight generation requires high driving voltages on EO modulators, the weight beams can be broadcast for parallel processing of N-distributed sensors. In the proposed scheme 2, the weights are static photonic memory; once it's set, it doesn't cost

energy. The overall power consumption comes from the optical power limit, which operates at the shot noise limit, at the 10's femtojoule per operation region.

5. Impact:

As the global emergence of IoT will continue to explore optical sensing for real-time, high-sensitivity detection, pushing the demands on lower latency, lower energy consumption and footprint, smart optical sensors will play an essential role in addressing the response time, energy cost and data traffic issues, such as in autonomous driving. For spectroscopic sensing, the implementation of neural network hardware (with custom-designed kernels) could enhance the sensitivity of a specific feature that might have been buried in a regular spectral measurement, which would lead to new breakthroughs in biosensing and disease monitoring. Beyond optical sensing, the architecture allows MAC operation on both amplitude and phase information encoded with hundreds of comb modes in parallel, which might lead to the development of next-generation ultralow-power optical tensor processors with high throughput and low computing power in the post-Moore's age. In addition, the success of the project will have a profound impact on miniaturized and low-power optoelectronic circuits (frequency combs, photonic memories, coherent detectors) for neuromorphic photonics.

References

[1] **Z. Chen** et al., *Deep Learning with Coherent VCSEL Neural Networks*, ***Nature Photonics*** (2023).

[2] A. Sludds, S. Bandyopadhyay, **Z. Chen**, et al., *Delocalized Photonic Deep Learning on the Internet's Edge*, Science **378**, 270 (2022).

[3] R. Hamerly, A. Sludds, S. Bandyopadhyay, **Z. Chen**, *Netcast: Low-Power Edge Computing with WDM-Defined Optical Neural Networks*, **IEEE Journal of Quantum Electronics** (2023).

[4] Y. Shen et al., *Deep Learning with Coherent Nanophotonic Circuits*, ***Nat. Photonics*** **11**, 441 (2017).

[5] G. Wetzstein, A. Ozcan, S. Gigan, S. Fan, D. Englund, M. Soljačić, C. Denz, D. A. B. Miller, and D. Psaltis, *Inference in Artificial Intelligence with Deep Optics and Photonics*, **Nature 588**, 39 (2020).

[6] T. W. Hänsch, *Nobel Lecture: Passion for Precision*, **Rev. Mod. Phys**. **78**, 1297 (2006).

[7] **Z. Chen**, M. Yan, T. W. Hänsch, and N. Picqué, *A Phase-Stable Dual-Comb Interferometer*, **Nat. Commun**. **9**, 3035 (2018).

[8] **Z. Chen**, T. W. Hänsch, and N. Picqué, *Mid-Infrared Feed-Forward Dual-Comb Spectroscopy*, **PNAS 116**, 3454 (2019).

[9] M. L. Weichman, P. B. Changala, J. Ye, **Z. Chen**, et al,, *Broadband Molecular Spectroscopy with Optical Frequency Combs*, J. Mol. Spectrosc. **355**, 66 (2019).

[10] A. Shams-Ansari*, M. Yu*, **Z. Chen***, et al, *Thin-Film Lithium-Niobate Electro-Optic Platform for Spectrally Tailored Dual-Comb Spectroscopy*, **Communications Physics 5**, 1 (2022).

[11] K. Van Gasse, **Z. Chen**, et al, *An on-Chip III-V-Semiconductor-on-Silicon Laser Frequency Comb for Gas-Phase Molecular Spectroscopy in Real-Time*, http://arxiv.org/abs/2006.15113.

[12] E. Vicentini, Z. Wang, K. Van Gasse, T. W. Hänsch, and N. Picqué, *Dual-Comb Hyperspectral Digital Holography*, **Nat. Photonics 15**, 890 (2021).

[13] P. Martín-Mateos, F. U. Khan, and O. E. Bonilla-Manrique, *Direct Hyperspectral Dual-Comb Imaging*, **Optica 7**, 199 (2020).

[14] J. Riemensberger, A. Lukashchuk, M. Karpov, W. Weng, E. Lucas, J. Liu, and T. J. Kippenberg, *Massively Parallel Coherent Laser Ranging Using a Soliton Microcomb*, **Nature 581**, 164 (2020).

[15] X. Xu et al., *11 TOPS Photonic Convolutional Accelerator for Optical Neural Networks*, **Nature 589**, 44 (2021).

[16] J. Feldmann et al., *Parallel Convolutional Processing Using an Integrated Photonic Tensor Core*, **Nature 589**, 52 (2021).

[17] T. Wang, M. M. Sohoni, L. G. Wright, M. M. Stein, S.-Y. Ma, T. Onodera, M. G. Anderson, and P. L. McMahon, *Image Sensing with Multilayer Nonlinear Optical Neural Networks*, **Nat. Photonics 17**, 408 (2023).

[18] X. Lin, Y. Rivenson, N. T. Yardimci, M. Veli, Y. Luo, M. Jarrahi, and A. Ozcan, *All-Optical Machine Learning Using Diffractive Deep Neural Networks*, **Science 361**, 1004 (2018).

[19] R. Davis III, **Z. Chen**, R. Hamerly, and D. Englund, *Frequency-Encoded Deep Learning with Speed-of-Light Dominated Latency*, arXiv Preprint arXiv (2022).

[20] Z. Liu et al., *Ultrafast Early Warning of Heart Attacks through Plasmon-Enhanced Raman Spectroscopy Using Collapsible Nanofingers and Machine Learning*, **Small 19**, e2204719 (2023).

[21] M. Yu et al., *Integrated Femtosecond Pulse Generator on Thin-Film Lithium Niobate*, ***Nature*** **612**, 252 (2022).